# ANTIVIRALS FOR EMERGING VIRUSES: VACCINES AND THERAPEUTICS

EDITED BY: Lijun Rong, Lu Lu and Christopher C. Broder
PUBLISHED IN: Frontiers in Microbiology

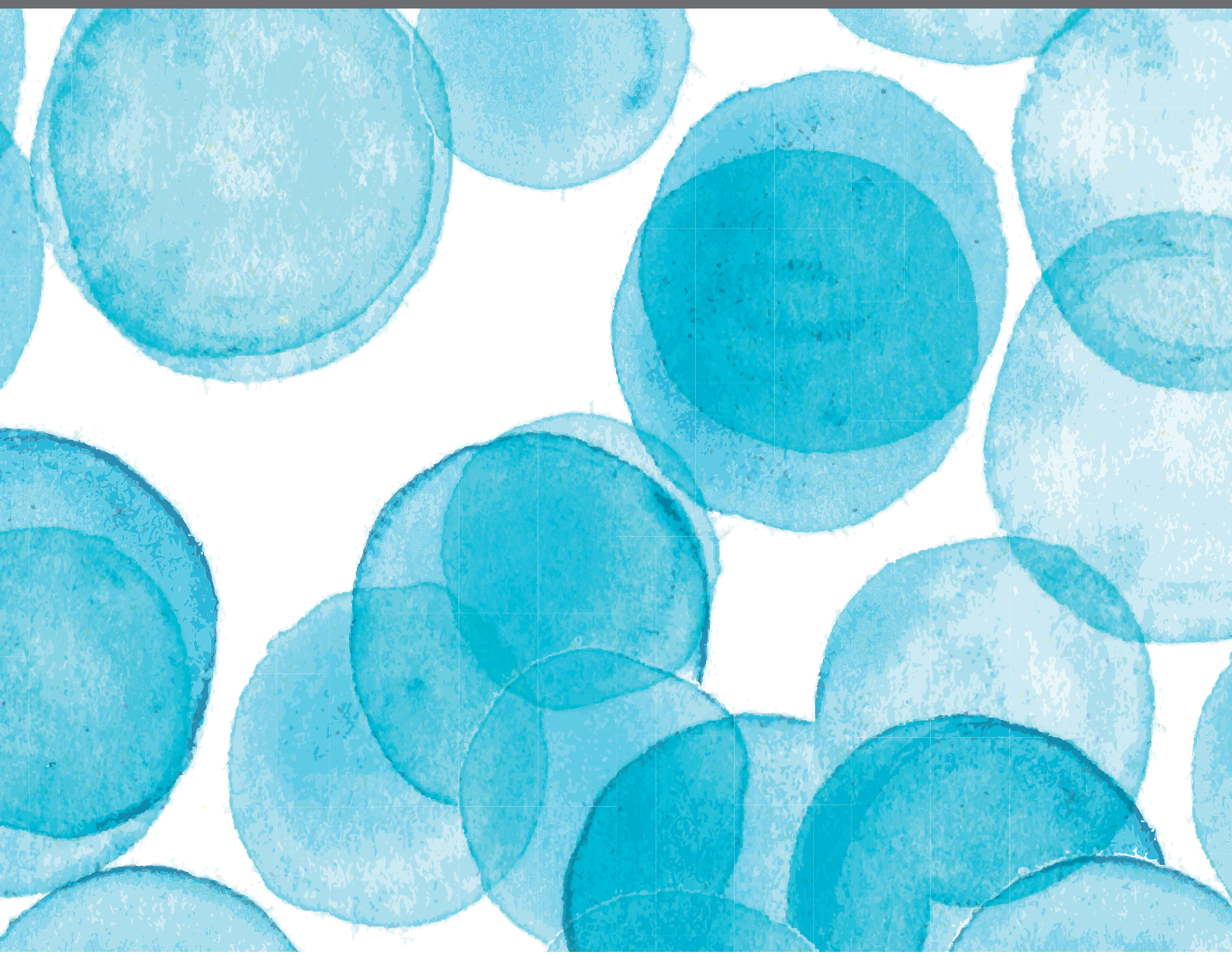

frontiers Research Topics

# frontiers

**Frontiers eBook Copyright Statement**

The copyright in the text of individual articles in this eBook is the property of their respective authors or their respective institutions or funders. The copyright in graphics and images within each article may be subject to copyright of other parties. In both cases this is subject to a license granted to Frontiers.

The compilation of articles constituting this eBook is the property of Frontiers.

Each article within this eBook, and the eBook itself, are published under the most recent version of the Creative Commons CC-BY licence. The version current at the date of publication of this eBook is CC-BY 4.0. If the CC-BY licence is updated, the licence granted by Frontiers is automatically updated to the new version.

When exercising any right under the CC-BY licence, Frontiers must be attributed as the original publisher of the article or eBook, as applicable.

Authors have the responsibility of ensuring that any graphics or other materials which are the property of others may be included in the CC-BY licence, but this should be checked before relying on the CC-BY licence to reproduce those materials. Any copyright notices relating to those materials must be complied with.

Copyright and source acknowledgement notices may not be removed and must be displayed in any copy, derivative work or partial copy which includes the elements in question.

All copyright, and all rights therein, are protected by national and international copyright laws. The above represents a summary only. For further information please read Frontiers' Conditions for Website Use and Copyright Statement, and the applicable CC-BY licence.

ISSN 1664-8714
ISBN 978-2-88966-252-4
DOI 10.3389/978-2-88966-252-4

## About Frontiers

Frontiers is more than just an open-access publisher of scholarly articles: it is a pioneering approach to the world of academia, radically improving the way scholarly research is managed. The grand vision of Frontiers is a world where all people have an equal opportunity to seek, share and generate knowledge. Frontiers provides immediate and permanent online open access to all its publications, but this alone is not enough to realize our grand goals.

## Frontiers Journal Series

The Frontiers Journal Series is a multi-tier and interdisciplinary set of open-access, online journals, promising a paradigm shift from the current review, selection and dissemination processes in academic publishing. All Frontiers journals are driven by researchers for researchers; therefore, they constitute a service to the scholarly community. At the same time, the Frontiers Journal Series operates on a revolutionary invention, the tiered publishing system, initially addressing specific communities of scholars, and gradually climbing up to broader public understanding, thus serving the interests of the lay society, too.

## Dedication to Quality

Each Frontiers article is a landmark of the highest quality, thanks to genuinely collaborative interactions between authors and review editors, who include some of the world's best academicians. Research must be certified by peers before entering a stream of knowledge that may eventually reach the public - and shape society; therefore, Frontiers only applies the most rigorous and unbiased reviews.
Frontiers revolutionizes research publishing by freely delivering the most outstanding research, evaluated with no bias from both the academic and social point of view. By applying the most advanced information technologies, Frontiers is catapulting scholarly publishing into a new generation.

## What are Frontiers Research Topics?

Frontiers Research Topics are very popular trademarks of the Frontiers Journals Series: they are collections of at least ten articles, all centered on a particular subject. With their unique mix of varied contributions from Original Research to Review Articles, Frontiers Research Topics unify the most influential researchers, the latest key findings and historical advances in a hot research area! Find out more on how to host your own Frontiers Research Topic or contribute to one as an author by contacting the Frontiers Editorial Office: researchtopics@frontiersin.org

# ANTIVIRALS FOR EMERGING VIRUSES: VACCINES AND THERAPEUTICS

Topic Editors:
**Lijun Rong,** University of Illinois at Chicago, United States
**Lu Lu,** Fudan University, China
**Christopher C. Broder,** Uniformed Services University of the Health Sciences, United States

**Citation:** Rong, L., Lu, L., Broder, C. C., eds. (2020). Antivirals for Emerging Viruses: Vaccines and Therapeutics. Lausanne: Frontiers Media SA.
doi: 10.3389/978-2-88966-252-4

# Table of Contents


06 ***Influenza Vaccine With Consensus Internal Antigens as Immunogens Provides Cross-Group Protection Against Influenza A Viruses***
Xinci Xie, Chen Zhao, Qian He, Tianyi Qiu, Songhua Yuan, Longfei Ding, Lu Liu, Lang Jiang, Jing Wang, Linxia Zhang, Chao Zhang, Xiang Wang, Dongming Zhou, Xiaoyan Zhang and Jianqing Xu

19 ***Recent Advances in the Vaccine Development Against Middle East Respiratory Syndrome-Coronavirus***
Chean Yeah Yong, Hui Kian Ong, Swee Keong Yeap, Kok Lian Ho and Wen Siang Tan

37 ***Crystal Structure of Refolding Fusion Core of Lassa Virus GP2 and Design of Lassa Virus Fusion Inhibitors***
Xuejiao Zhang, Cong Wang, Baohua Chen, Qian Wang, Wei Xu, Sheng Ye, Shibo Jiang, Yun Zhu and Rongguang Zhang

49 ***The Underlying Mechanism of 3-Hydroxyphthalic Anhydride-Modified Bovine Beta-Lactoglobulin to Block Human Papillomavirus Entry Into the Host Cell***
Chen Hua, Yun Zhu, Congquan Wu, Lulu Si, Qian Wang, Long Sui and Shibo Jiang

60 ***A Peptide-Based Virus Inactivator Protects Male Mice Against Zika Virus-Induced Damage of Testicular Tissue***
Lulu Si, Yu Meng, Fang Tian, Weihua Li, Peng Zou, Qian Wang, Wei Xu, Yuzhu Wang, Minjie Xia, Jingying Hu, Shibo Jiang and Lu Lu

73 ***Inhibition by Marine Algae of Chikungunya Virus Isolated From Patients in a Recent Disease Outbreak in Rio de Janeiro***
Claudio Cesar Cirne-Santos, Caroline de Souza Barros, Caio Cesar Richter Nogueira, Renata Campos Azevedo, Kristie Aimi Yamamoto, Guilherme Louzada Silva Meira, Zilton Farias Meira de Vasconcelos, Norman Arthur Ratcliffe, Valéria Laneuville Teixeira, Jonas Schmidt-Chanasit, Davis Fernandes Ferreira and Izabel Christina Nunes de Palmer Paixão

84 ***Interleukin-37 Ameliorates Influenza Pneumonia by Attenuating Macrophage Cytokine Production in a MAPK-Dependent Manner***
Feifei Qi, Mingya Liu, Fengdi Li, Qi Lv, Guanpeng Wang, Shuran Gong, Shunyi Wang, Yanfeng Xu, Linlin Bao and Chuan Qin

96 ***Anti-TGEV Miller Strain Infection Effect of* Lactobacillus plantarum *Supernatant Based on the JAK-STAT1 Signaling Pathway***
Kai Wang, Ling Ran, Tao Yan, Zheng Niu, Zifei Kan, Yiling Zhang, Yang Yang, Luyi Xie, Shilei Huang, Qiuhan Yu, Di Wu and Zhenhui Song

108 ***Development of Small-Molecule Inhibitors Against Zika Virus Infection***
Lili Wang, Ruiying Liang, Yaning Gao, Yanbai Li, Xiaoqian Deng, Rong Xiang, Yina Zhang, Tianlei Ying, Shibo Jiang and Fei Yu

129 ***Recent Progress in Vaccine Development Against Chikungunya Virus***
Shan Gao, Siqi Song and Leiliang Zhang

139 ***Montelukast, an Anti-asthmatic Drug, Inhibits Zika Virus Infection by Disrupting Viral Integrity***
Yongkang Chen, Yuan Li, Xiaohuan Wang and Peng Zou

153 ***Vaccines and Therapeutics Against Hantaviruses***
Rongrong Liu, Hongwei Ma, Jiayi Shu, Qiang Zhang, Mingwei Han, Ziyu Liu, Xia Jin, Fanglin Zhang and Xingan Wu

172 ***Broadly Protective Strategies Against Influenza Viruses: Universal Vaccines and Therapeutics***
Olivia A. Vogel and Balaji Manicassamy

186 ***Antiviral Drugs Against Severe Fever With Thrombocytopenia Syndrome Virus Infection***
Mutsuyo Takayama-Ito and Masayuki Saijo

196 ***Intradermal Immunization of EBOV VLPs in Guinea Pigs Induces Broader Antibody Responses Against GP Than Intramuscular Injection***
Ying Liu, Zhiyuan Wen, Ricardo Carrion Jr., Jerritt Nunneley, Hilary Staples, Anysha Ticer, Jean L. Patterson, Richard W. Compans, Ling Ye and Chinglai Yang

206 ***Subunit Vaccines Against Emerging Pathogenic Human Coronaviruses***
Ning Wang, Jian Shang, Shibo Jiang and Lanying Du

225 ***Identification of Chebulinic Acid and Chebulagic Acid as Novel Influenza Viral Neuraminidase Inhibitors***
Ping Li, Ruikun Du, Yanyan Wang, Xuewen Hou, Lin Wang, Xiujuan Zhao, Peng Zhan, Xinyong Liu, Lijun Rong and Qinghua Cui

234 ***Does Mucosal B1 Activation Result in the Accumulation of Peak IgM During Chronic Intrarectal SIVmac239 Exposure to Protect Chinese-Origin Rhesus Macaques From Disease Progression?***
Zhe Cong, Ling Tong, Yuhong Wang, Aihua Su, Ting Chen, Qiang Wei, Jing Xue and Chuan Qin

244 ***Defeat Dengue and Zika Viruses With a One-Two Punch of Vaccine and Vector Blockade***
Jin Sun, Senyan Du, Zhihang Zheng, Gong Cheng and Xia Jin

265 ***Virus-Like Particles Derived From a Virulent Strain of Pest des Petits Ruminants Virus Elicit a More Vigorous Immune Response in Mice and Small Ruminants Than Those From a Vaccine Strain***
Feihu Yan, Entao Li, Ling Li, Zachary Schiffman, Pei Huang, Shengnan Zhang, Guohua Li, Hongli Jin, Hualei Wang, Xinghai Zhang, Yuwei Gao, Na Feng, Yongkun Zhao, Chengyu Wang and Xianzhu Xia

279 ***Discovery of Retro-1 Analogs Exhibiting Enhanced Anti-vaccinia Virus Activity***
Lalita Priyamvada, Philip Alabi, Andres Leon, Amrita Kumar, Suryaprakash Sambhara, Victoria A. Olson, Jason K. Sello and Panayampalli S. Satheshkumar

290 ***The Current and Future State of Vaccines, Antivirals and Gene Therapies Against Emerging Coronaviruses***
Longping V. Tse, Rita M. Meganck, Rachel L. Graham and Ralph S. Baric

316 ***Tolcapone Potently Inhibits Seminal Amyloid Fibrils Formation and Blocks Entry of Ebola Pseudoviruses***
Mengjie Qiu, Zhaofeng Li, Yuliu Chen, Jiayin Guo, Wei Xu, Tao Qi, Yurong Qiu, Jianxin Pang, Lin Li, Shuwen Liu and Suiyi Tan

334 ***Protein- and Peptide-Based Virus Inactivators: Inactivating Viruses Before Their Entry Into Cells***
Xiaojie Su, Qian Wang, Yumei Wen, Shibo Jiang and Lu Lu

353 ***Contributions of HA1 and HA2 Subunits of Highly Pathogenic Avian Influenza Virus in Induction of Neutralizing Antibodies and Protection in Chickens***
Edris Shirvani, Anandan Paldurai, Berin P. Varghese and Siba K. Samal

364 ***Self-Assembly M2e-Based Peptide Nanovaccine Confers Broad Protection Against Influenza Viruses***
Qimin Wang, Yuling Zhang, Peng Zou, Meixiang Wang, Weihui Fu, Jialei She, Zhigang Song, Jianqing Xu, Jinghe Huang and Fan Wu

frontiers in Microbiology

ORIGINAL RESEARCH
published: 16 July 2019
doi: 10.3389/fmicb.2019.01630

# Influenza Vaccine With Consensus Internal Antigens as Immunogens Provides Cross-Group Protection Against Influenza A Viruses

*Xinci Xie[1], Chen Zhao[1], Qian He[1], Tianyi Qiu[1], Songhua Yuan[1], Longfei Ding[1], Lu Liu[1], Lang Jiang[1], Jing Wang[1], Linxia Zhang[1], Chao Zhang[2], Xiang Wang[2], Dongming Zhou[2]*, Xiaoyan Zhang[1]* and Jianqing Xu[1]**

[1] Shanghai Public Health Clinical Center and Institutes of Biomedical Science, Shanghai Medical College, Fudan University, Shanghai, China, [2] Vaccine Research Center, Key Laboratory of Molecular Virology and Immunology, Institut Pasteur of Shanghai, Chinese Academy of Sciences, Shanghai, China

OPEN ACCESS

**Edited by:**
Lijun Rong,
The University of Illinois at Chicago, United States

**Reviewed by:**
Di Liu,
Wuhan Institute of Virology (CAS), China
Youchun Wang,
National Institutes for Food and Drug Control, China
Bao Lin Lin,
Institute of Laboratory Animal Sciences (CAMS), China

***Correspondence:**
Dongming Zhou
dmzhou@sibs.ac.cn
Xiaoyan Zhang
zhangxiaoyan@shphc.org.cn
Jianqing Xu
xujianqing@shphc.org.cn

**Specialty section:**
This article was submitted to Virology, a section of the journal Frontiers in Microbiology

**Received:** 07 May 2019
**Accepted:** 02 July 2019
**Published:** 16 July 2019

**Citation:**
Xie X, Zhao C, He Q, Qiu T, Yuan S, Ding L, Liu L, Jiang L, Wang J, Zhang L, Zhang C, Wang X, Zhou D, Zhang X and Xu J (2019) Influenza Vaccine With Consensus Internal Antigens as Immunogens Provides Cross-Group Protection Against Influenza A Viruses. Front. Microbiol. 10:1630. doi: 10.3389/fmicb.2019.01630

Given that continuing antigenic shift and drift of influenza A viruses result in the escape from previous vaccine-induced immune protection, a universal influenza vaccine has been actively sought. However, there were very few vaccines capable of eliciting cross-group ant-influenza immunity. Here, we designed two novel composite immunogens containing highly conserved T-cell epitopes of six influenza A virus internal antigens, and expressed them in DNA, recombinant adenovirus-based (AdC68) and recombinant vaccinia vectors, respectively, to formulate three vaccine forms. The introduction of the two immunogens via a DNA priming and viral vectored vaccine boosting modality afforded cross-group protection from both PR8 and H7N9 influenza virus challenges in mice. Both respiratory residential and systemic T cells contributed to the protective efficacy. Intranasal but not intramuscular administration of AdC68 based vaccine was capable of raising both T cell subpopulations to confer a full protection from lethal PR8 and H7N9 challenges, and blocking the lymphatic egress of T cells during challenges attenuated the protection. Thus, by targeting highly conserved internal viral epitopes to efficiently generate both respiratory and systemic memory T cells, the sequential vaccination strategy reported here represented a new promising candidate for the development of T-cell based universal influenza vaccines.

**Keywords: universal influenza vaccine, consensus sequence, CD8+ T cell epitope, cross-protection, lung residential T cells**

## INTRODUCTION

Influenza A virus (IAV) has continued to be a major threat to human health (Horimoto and Kawaoka, 2005; Gostin et al., 2014). The need for cross-protective IAV vaccines has arisen in recent years after several global outbreaks of IAV strains such as avian H5N1, swine H1N1, canine H3N2, and avian H7N9 (Gao et al., 2013). However, the licensed influenza vaccines, the majority of which act by inducing antibody against the viral hemagglutinin surface protein, only induce strain-specific immunity and could not provide efficient protection against mismatched epidemic and pandemic

influenza variants which have continually emerged by antigenic drift or shift (Hannoun, 2013; Houser and Subbarao, 2015).

Alongside the humoral response, cellular response is the other arm of human immunity battling against influenza infection. A recent study on the victims of 2013 H7N9 outbreak revealed that patients making faster recovery exhibited earlier prominent H7N9-specific CD8+ T-cell responses than those who required longer hospitalization (Wang et al., 2015). There was also evidence supporting the important protective role of CD8+ T-cell response in human adults upon pandemic H1N1 infection (Sridhar et al., 2013). Notably, unlike the surface viral proteins which evolve fast in response to the pressure of human neutralizing antibodies, the internal IAV structural proteins, as exampled by matrix protein (Fan et al., 2004; Valkenburg et al., 2014), nuclear protein (Lamere et al., 2011; Pica and Palese, 2013), and polymerase protein (Cox and Dewhurst, 2015; Uddback et al., 2016) are more conserved and the derived conserved epitopes have shown potential to induce broad-spectrum cellular responses and provide cross-protection (Jaiswal et al., 2013). It's also worth mentioning that tissue-resident memory CD8 T cells have been reported to be indispensable for cross-protection against different strains of influenza virus (Brown and Kelso, 2009).

A variety of approaches have been attempted to development universal influenza vaccines. The vaccination approaches using attenuated and inactivated influenza viruses have been most popular but the lack of effectiveness and productivity has always been of concern (Holloway et al., 2014). A growing number of novel strategies have been also explored including DNA vaccines, viral vector-based vaccines and combinatorial strategies with DNA vaccine as prime and viral vector-based vaccine or purified protein subunit as boost (Draper and Heeney, 2010), some of which have even been evaluated in clinical trials (Stanekova and Vareckova, 2010). Among all the viral vector-based platforms, adenovirus-based vector holds great promise because of its broad cell tropism, strong genetic stability, high transduction efficiency, and high gene expression. The most common adenovirus vector is human Ad serotype 5 (AdHu5); however, it has already elicited neutralizing antibodies in a large number of people, which greatly limits its clinical application (Wang et al., 2014). In this regard chimpanzee adenovirus serotype 68 (AdC68) has been recently identified as a potential candidate vaccine vector more suitable for human use than AdHu5, owing to its significantly lower seropositivity rate in humans (Zhang et al., 2013; Xing et al., 2016). Another viral vector-based platform of interest is attenuated, replication-competent TIANTAN vaccinia (TTV) virus which has the ability to infect many cell types, and induce both antigen-specific antibody titers and cellular response. The potential of TTV virus for vaccine development is substantiated by the finding that the administration of this virus is safe in human, including people with compromised immune systems (Huang et al., 2007a,b).

In this study, we utilized different vector-based platforms to develop influenza vaccines which are tailored to elicit broad T cell response targeting conserved viral epitopes by expressing conserved sequences of influenza internal proteins. Specifically, we deduced the consensus amino acid sequence of six conserved internal proteins-M1, M2, NP, PA, PB1, and PB2 from approximately 40,000 IAV strains. Consequently, two vaccine sequences were designed according to computation-based prediction of conservative CD8+ T cell epitopes, and used to generate vaccines based on different vector-based platforms, including DNA vaccines, recombinant chimpanzee adenovirus-based vaccines and a recombinant TIANTAN vaccinia vaccine. The immunogenicity and efficacy of these vaccines as well as their combined administration were evaluated in mouse models. The results revealed that both AdC68 vaccine and TTV vaccine, in conjunction with priming of DNA vaccine, were able to elicit significant protective CD8+ T cell response, although the potency and breadth of such responses differs between the two types of vaccine. Further exploration of sequential vaccinations and administration route identified the regimen of DNA priming followed by consecutive boosting with AdC68 vaccine via intranasal route and TTV vaccine via intramuscular route as the most efficient regimen in conferring protection against lethal challenges of H1N1 and H7N9 influenza virus. Together, these data demonstrated DNA prime-novel viral vector boost to deliver conserved CD8+ T cell epitopes of viral proteins as a promising strategy to develop universal influenza vaccines capable of cross-group protection.

# MATERIALS AND METHODS

## Immunogen Design and Optimization

The protein sequences of approximately 40,000 IAV strains were downloaded from Genbank database, and multiple sequence alignment was conducted using CLUSTAL X program to identify the consensus amino acid at each position. The consensus protein sequence was synthesized by combining individual consensus amino acid; only partial sequences of PA, PB1, and PB2 were encompassed on the basis of CD8+ T cell epitope prediction through online tools (Singh and Raghava, 2003; Moutaftsi et al., 2006). The sequences were optimized with respect to mammalian codon usage.

## Vaccine Construction and Validation

The PAPB1M1 and NPPB2M2 immunogens were cloned into three types of vectors for vaccine construction. For DNA vaccine, pSV1.0 vector was used as the backbone vector. For adenovirus-based vaccine, the immunogen sequences were first cloned into p-Shuttle vector and subsequently subcloned into the E1/E3 deleted AdC68 vector. The resulting vectors, namely AdC68-PAPB1M1 and AdC68-NPPB2M2, were linearized and transfected into HEK293 cells to generate adenoviruses which were purified from the supernatant by CsCl gradient centrifugation followed by determination of virus particle number by UV absorbance. For TTV vaccinia-based vaccines, the immunogen sequences were cloned into pSC65 shuffle vector and then transfected into TK143 cells. The transfected cells were subsequently infected with recombinant wild-type Tiantan virus followed by BrdU screening, yielding recombinant virus which was amplified using Vero cells. For validation of vaccines in immunogen expression, the

DNA-based vaccine vectors were transfected into HEK293 cells and the AdC68-based and TTV vaccinia-based virus vaccines were used to infect HEK293 and Vero cells, respectively. The transfected or infected cells were harvested 24 or 48 h late and the immunogens presented in the resulting lysates were detected by immunobloting using anti-M1 monoclonal antibody (abcam, ab22396) or anti-M2 monoclonal antibody (Santa Cruz, sc-52026).

## Mouse Immunization

Six- to eight-week-old female C57BL/6 mice were purchased from the B&K Universal Group Ltd. (Shanghai, China) and housed under specific pathogen-free (SPF) conditions at the animal facilities of Shanghai Public Health Clinical Center, Fudan University (Shanghai, China). For immunization, two doses of pSV1.0-PAPB1M1 (50 μg) and pSV1.0-NPPB2M2 (50 μg) were used as prime and AdC68-PAPB1M1 ($5 \times 10^{10}$ vp)/AdC68-NPPB2M2 ($5 \times 10^{10}$ vp) or TTV-2a ($1 \times 10^{7}$ pfu) was used individually or in sequential combination as boost(s). The mice were immunized following the indicated schedules and route. For sham control, either only the priming vector was substituted by empty vector or both the priming and boosting vectors were replaced with empty vectors. Four weeks after vaccination, mice were sacrificed for immunogenicity evaluation including IFN-γ ElISpot assay and intracellular cytokine staining.

## T-Cell Response Determination

Immunogenicity evaluation was performed 4 weeks after last vaccination. Control or vaccinated mice were sacrificed for isolating splenocytes and bronchoalveolar lavage cells. A total of $2 \times 10^5$ isolated cells were plated in triplicate in 96-well plates pre-coated with 5 μg/ml of purified anti-mouse IFN-γ and subsequently stimulated with a peptide specific for one of the six viral immunogens (M2, M1, NP, PA, PB1, and PB2) at a final 5 μg/ml concentration (**Table 1**). A total of 16 peptides were used with one for M2 and three each for the rest five immunogens. After 24 h stimulation, the cells were washed with deionized water and exposed to 100 μl biotinylated anti-mouse IFN-γ (2 μg/ml) for 2 h at room temperature, followed by extensive washing prior to the addition of 100 μl Streptavidin-HRP. After 1 h incubation at room temperature, the cells were washed and 100 μl of substrate solution was added to develop spots. The reaction was stopped with water and the number of spot-forming cells (SFCs) was determined using an automated ELISPOT software (Saizhi, Beijing, China). For intracellular staining of cytokines, $2 \times 10^6$ immune cells were stimulated for 1 h with a peptide pool consisting of equal amount of all the 16 peptides described in **Table 1** in the presence of anti-mouse CD107a-PE (BioLegend) antibody, followed by exposure to 1 μl/ml Brefeldin (BD Bioscience) for 6 h. The cells were then washed, and stained with the surface-specific mouse antibodies, LIVE/DEAD-AmyCan, CD3-PerCP-cy5.5, CD8-PB (BioLegend). Cells were subsequently permeabilized using the BD Cytofix/Cytoperm Kit and stained for the intracellular cytokines by FITC anti-mouse IFNγ antibody and PECy7 anti-mouse TNFα antibody (BioLegend). Samples were measured using Fortessa Flow cytometer (BD Bioscience), and the data were analyzed with FlowJo 10.0.6 software (Tree Star).

**TABLE 1 |** Influenza A virus-specific peptides employed to stimulate splenocytes for the quantification of T cell responses.

| Protein | Amino acid sequence of peptides |
|---|---|
| M1 | 58–66:GILGFVFTL (Halstead et al., 2002)<br>128–135:MGLIYNRM (Lawrence et al., 2005)<br>99–107:LYRKLKREI |
| M2 | 2–24:SLLTEVETPIRNEWGCRCNDSSD |
| NP | 146–155:ATYQRTRALV (Turner et al., 2004)<br>366–374:ASNENMDTM (Tussey et al., 1995)<br>383–391:SRYWAIRTR (Belz et al., 2001) |
| PB1 | 703–711:SSYRRVPGI (Chen et al., 2001)<br>415–424:VSGVNESADM<br>494–502:DGGPNLYNI |
| PB2 | 198–206:ISPLMVAYM (Zhu et al., 2013)<br>344–352:VLTGNLQTL<br>544–553:SVLVNTYQWI |
| PA | 509–518:SHLRNDTDVV<br>515–523:TDVVNFVSM<br>601–609:VEEGSIGKV |

## Influenza A Virus Challenge

Four weeks after vaccination, mice were challenged with either IAV/PR8(H1N1) virus or IAV/Shanghai/4664T/2013(H7N9) virus. The dosage for lethal challenge for both viruses was 500 50% tissue culture-infective dose (TCID50), while a dosage of 100 TCID50 of H7N9 virus was employed for sub-lethal challenge. For assaying the impact of FTY720, experimental groups were split into two halves, one of which was *ad libitum* exposed to drinking water containing 2 μg/ml FTY720 during the whole duration of virus challenge. The body weight and survival rate were daily monitored for 14 days. Lung viral loads were determined on day 5 post infection by quantification of viral RNA: total RNA was extracted from lung tissues and subjected to TaqMan real-time reverse transcription-PCR (RT-PCR) using influenza virus-specific primers for determination of relative levels of viral loads. For normalization, glyceraldehyde phosphate dehydrogenase were used as the reference gene. The used primers were: For H7N9 virus detection, end primer pair as of GAAGAGGCAATGCAAAATAGAATACA and CCCGAAG CTAAACCARAGTAT CA, probe as of CCAGTCAAACTAAG CAGYGGCTACAAA; for PR8 virus detection, end primer pair as of GACCGATCCTGTCACCTCTGA and AGGGCAT TCTGGACAAA GCG TCTA, probe as of TGCAGTCCTC GCTCACTGGGCACG -3′; for GAPDH reference detection, end primer pair as of CAATGTGTCCGTCGTGGA TCT and GTCCTCAGTGTAGCCCAAGATG, probe as of CGTGCC GCCTGGAGAA ACCTGCC. The animal studies were carried out in accordance with the "Guide for the Care and Use of Laboratory Animals of the Institute of Laboratory Animal Science (est. 2006)." Mice that lost over 30% of their initial body weight were scored dead and humanely euthanized. All other mice were humanely euthanized after 14-day observation period. The H7N9 virus-related experiments were conducted in a biosafety level 3 laboratory following protocols approved by

the Institutional Biosafety Committee at Shanghai Public Health Clinical Center.

## Statistical Analysis

All statistical analyses were performed using GraphPad Prism 6.0 (GraphPad Software, Inc.). Mantel-Cox log rank test and two-way ANOVA test were applied to evaluate difference in survival and weight loss, respectively. In other cases, *t*-test was used. Significant difference was defined as $p < 0.05$.

# RESULTS

## Construction of Influenza Internal Gene Based Vaccines

As the first step to develop new cross-protective IAV vaccine, we sought to identify new immunogens that have a broad coverage of conserved CD8+ T cell epitopes of IAV antigens. To this end, we deduced the consensus amino acid sequences of influenza M1, M2, NP, PA, PB1, and PB2 proteins from approximately 40,000 IAV strains available in Genebank database. To be more efficient in immunogen design, we only included partial sequences of PA, PB1, and PB2 enriched with CD8+ T cell epitopes as predicted by online tools (Singh and Raghava, 2003; Moutaftsi et al., 2006). Consequently, we generated two immunogen sequences, denoted as PAPB1M1 and PB2NPM2, whose protein composition were schematically illustrated in **Figure 1A** and amino sequences were included in the **Supplementary Material**.

We thus constructed vaccines to express the two immunogens in three platforms including DNA vector, E1/E3-deleted replication-deficient chimpanzee Adenovirus (AdC68), and recombinant Tiantan vaccinia virus (TTV). For the first two platforms, two immunogens were expressed separately, resulting in two DNA-based vaccines (pSV1.0-PAPB1M1 and pSV1.0-PB2NPM2) and two AdC68-based vaccines (AdC68-PAPB1M1 and AdC68-PB2NPM2); for TTV platform, two immunogens were expressed from a single vaccinia vaccine, namely TTV-2a. The resulting vaccines were introduced into cultured cells by either transfection or infection, and their expressions of encoded immunogens in the cells were validated by immunoblotting using antibodies specific for IAV M1 or M2 protein (**Figure 1B**). Thus, all three platforms were capable of expressing PAPB1M1 and PB2NPM2 immunogens efficiently.

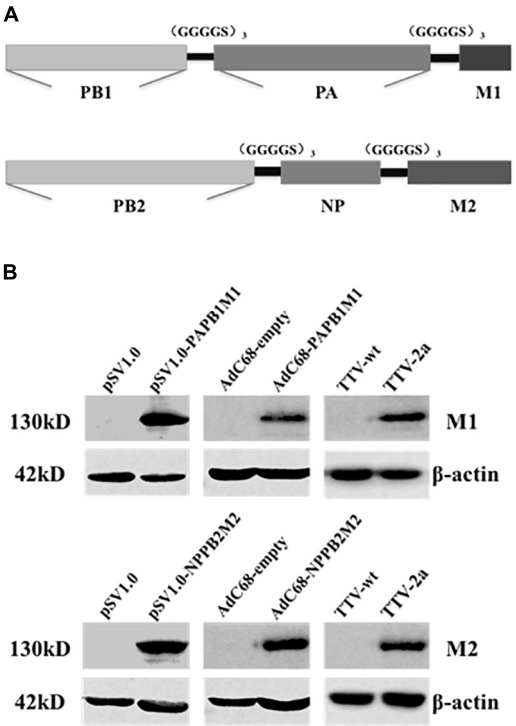


**FIGURE 1 |** Immunogen design and expression through three different vaccine platforms. **(A)** Schematic diagram of two synthetic immunogens, PB1PAM1 and PB2NPM2, which were designed on the basis of amino acid conservation and CD8+ T cell epitope prediction of influenza M1, M2, NP, PA, PB1, and PB2 sequences. **(B)** Validation of vaccine-generated PAPB1M1 and PB2NPM2 protein expression in cultured cells. HEK293 cells were used for the transfection of pSV1.0-based vectors or the infection with AdC68-based vectors, while Vero cells were used for TTV infections. The resulting cell lysates were resolved by denaturing electrophoresis followed by western blotting using antibodies against influenza M1 or M2 protein, or anti-β-actin antibodies as internal control. The cell lysates yielded from transfection or infection of corresponding empty vector were used as negative controls.

## DNA Prime and Viral Vectored Boost Efficiently Mounted Influenza-Specific CD8+ T Cell Responses

We next examined the capability of our newly developed vaccines in a DNA prime-viral vectored boost modality to induce influenza-specific cellular immune responses in mice. The mice were divided into three groups: the control group was immunized intramuscularly with two doses of control vector pSV1.0 (100 ug) and one dose of control vector AdC68-empty ($1 \times 10^{11}$ vp); the two experimental groups, namely DNA+AdC68 and DNA+TTV group, were immunized intramuscularly twice with pSV1.0-PAPB1M1 (50 μg)/pSV1.0-NPPB2M2 (50 μg), followed by intramuscularly boosting with AdC68-PAPB1M1 ($5 \times 10^{10}$ vp)/AdC68-NPPB2M2 ($5 \times 10^{10}$ vp) or TTV-2a ($1 \times 10^{7}$ pfu), respectively (**Figure 2A**). Four weeks after vaccination, three mice in each group were euthanized and splenocytes were isolated for measuring influenza-specific CD8+ T cell response by IFN-γ ELISpot assay (**Figure 2B**) and intracellular cytokine staining (ICS) assay (**Figures 2C,D**).

The data showed that, among the 16 influenza-specific epitope peptides examined (**Table 1**), NP-2 and PB2-1 peptides were dominant in inducing IFN-γ-producing immune cells for both experimental groups. However, DNA+AdC68 group exhibited a noticeably higher response to either of these two peptides than DNA+TTV group (**Figure 2B**). In addition, significantly more IFN-γ+/TNF-α+, IFN-γ+ cells, and CD107a+ cells appeared in DNA+AdC68 group as compared to DNA+TTV group after stimulation with a peptide pool composed of all the 16 peptides (**Figures 2C,D**). In contrast, DNA+TTV group exhibited a broader cellular response, as was indicated by more peptides, e.g., M2, NP-3, PB1-1, PB1-3, PA-1, and PA-3, eliciting modest

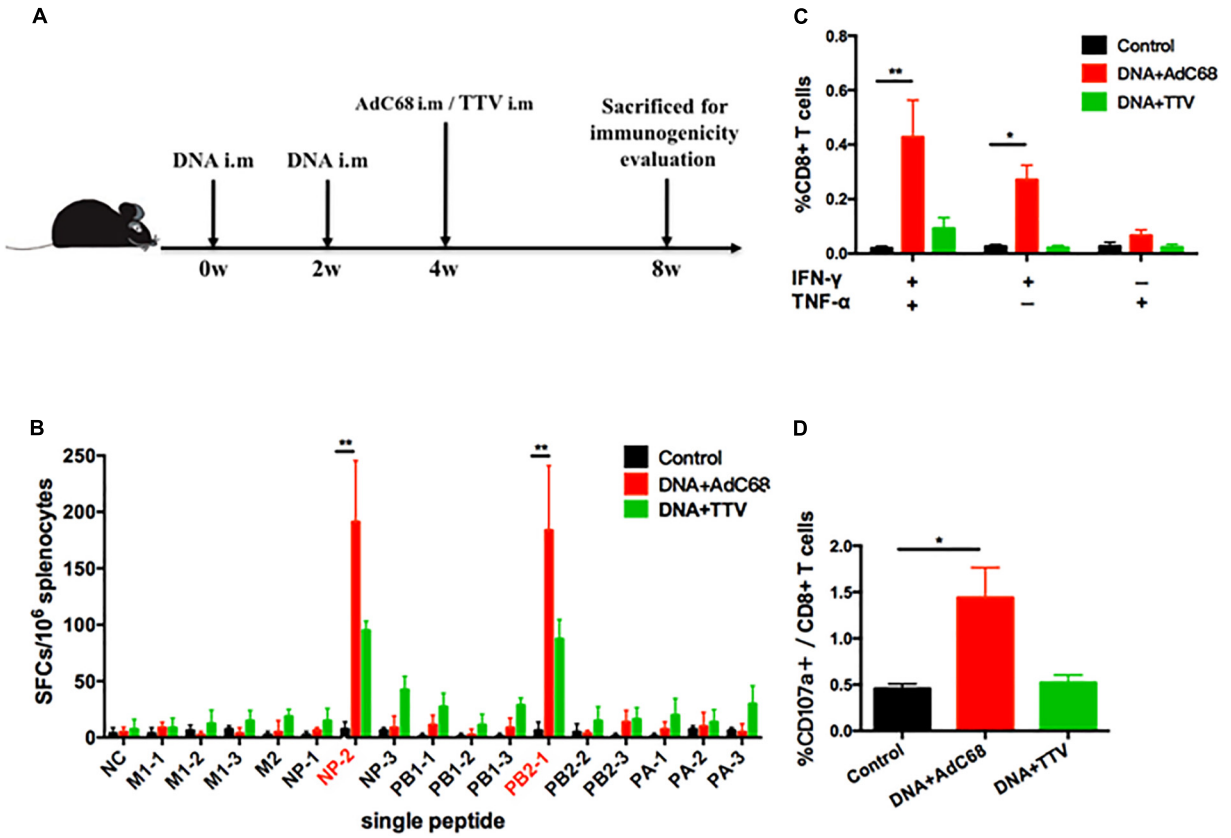


**FIGURE 2 |** Influenza-specific T-cell immune responses raised by DNA prime-viral vectored vaccine boost. **(A)** Schematic representation of immunization regimens. **(B–D)** Cellular responses elicited in vaccinated mice. Splenocytes of vaccinated C57 mice were isolated 4 weeks after vaccination and subjected to both IFN-γ ELISpot assay **(B)** and intracellular cytokine staining assay **(C,D)**. The IFN-γ ELISpot assays were performed in response to stimulation with a single IAV virus-specific peptide and described as numbers of spot forming cells (SFCs) per $10^6$ splenocytes. A total of 16 peptides were tested (**Table 1**). The intracellular cytokine staining assays were performed upon stimulation with a peptide pool composed of all the 16 peptides, and represented as the percentage of CD8+ T cells that were single positive or double positive for IFN-γ, TNF-α, and CD107a expression. All experiments were carried out in triplicate; the error bars are represented as SDs. $^{**}p < 0.01$; $^{*}p < 0.05$, *t*-test.

but detectable IFN-γ induction in immune cells from this group (**Figure 2B**). Thus, DNA+AdC68 regimen was more effective in raising immunodominant T-cell responses whereas DNA+TTV regimen appeared to perform better in eliciting sub-immunodominant T-cell responses. We also compared the serum levels of anti-M2 and anti-NP IgG between immunized and sham groups. The results showed that the two immunogens were ineffective in raising significant antibody response to either of the two viral proteins, which were also true for other vaccination regimens we later examined (**Supplementary Appendix 1**).

## DNA Prime/Viral Vectored Boost Regimens Afforded Protection Against Heterologous Influenza Virus Challenges in Murine Model

To determine the protective efficacy of the DNA prime/viral vectored boost regimens, we utilized a murine model of influenza challenge. Mice were immunized following schedule as described in **Figure 2A** and, split into two groups, which were respectively challenged with either A/PR8(H1N1) (a group 1 IAV) or A/Shanghai/4664T/2013(H7N9) (a group 2 IAV) 4 weeks later.

After a fatal challenge with A/PR8 (H1N1) virus, mice in sham control rapidly and continuously lost their weights (**Figure 3A**). Consequently, they went to death between day 7 and 12 (**Figure 3B**). In contrast, although the body weights of the two vaccinated groups also experienced an initial decrease, they reached a nadir on day 8 and then rebound afterward (**Figure 3A**). Accordingly, all the mice survived (**Figure 3B**). Furthermore, vaccinated mice showed reduced lung viral loads as compared to control group (**Figure 3E**). Interestingly, DNA+TTV group underwent a slower and less decrease in their body weights in comparison with DNA-AdC68 group (**Figure 3A**), which was in line with slightly lower viral loads (**Figure 3E**), suggesting that DNA+TTV regimen may provide a better protection. Hence, our newly designed T-cell vaccine is capable of affording efficient protection against fatal PR8 challenge.

In the case of H7N9 challenge, both regimens were found to be ineffective in protection from a lethal infection (data not shown).

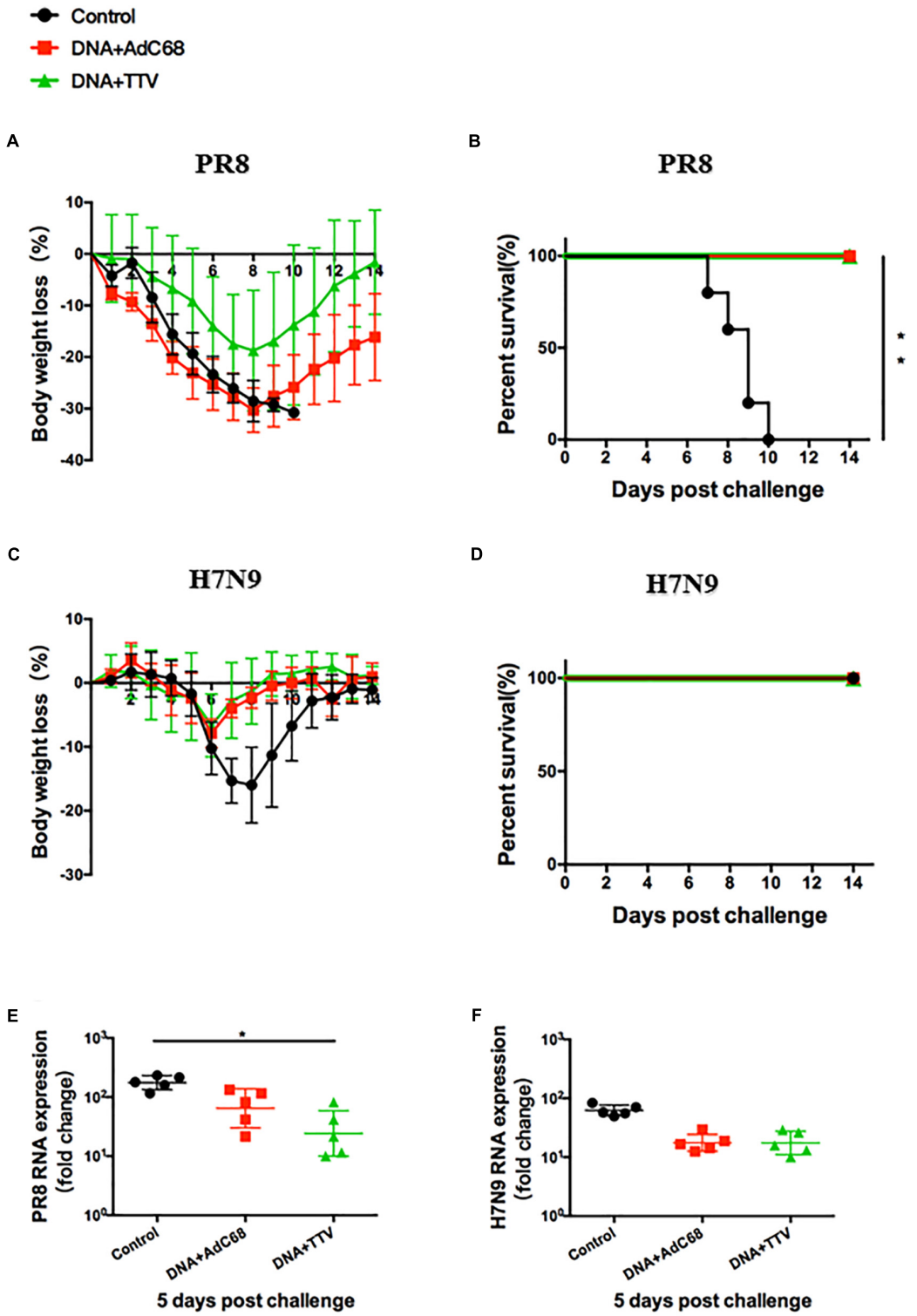


**FIGURE 3 |** DNA prime-viral vectored vaccine boost strategies conferred protection against PR8/(H1N1) and H7N9 viruses in vaccinated mice. Mice were immunized following schedule outlined in **Figure 2A**, and 4 weeks later challenged with either 500 50% tissue culture-infective dose (TCID50) of A/PR8(H1N1) or 100 TCID50 A/Shanghai/4664T/2013(H7N9) influenza virus. After infection, mice ($n$ = 5 in each group) were monitored daily for body weight **(A,C)** or survival **(B,D)**. Five mice in each group were sacrificed on day 5 post infection to isolate lung tissues for RNA extraction, followed by RT-PCR quantification of viral RNA to determine the relative viral loads **(E,F)**. The error bars represent the SDs. Two-way ANOVA test, Mantel–Cox log rank test and $t$-test were used to determine difference in weight loss, lethality, and viral load, respectively. $^{**}p < 0.01$; $^{*}p < 0.05$.

However, they did show protective effects against a non-lethal challenge (**Figure 3D**), as indicated by less initial loss and earlier recovery of body weights in comparison to control group ($p < 0.05$ during the period of day 6 to day 10 after infection) (**Figure 3C**). This was in agreement with discernible, although not statistically significant, inhibition of viral replication in lung (**Figure 3F**). Thus both DNA+AdC68 and DNA+TTV regimens were able to mount some protection from H7N9 infection in murine models.

## Intranasal Administration of Adenoviral Vectored Vaccine Elicits Vigorous Respiratory Residential T-Cell Responses in a Combinatory Regimen

To further optimize our vaccination strategy to improve cross-protection, we evaluated the effect of second boost as well as administration route on the vaccine-induced immune responses. Specifically, AdC68 was either intranasally or intramuscularly administered before or after TTV intramuscular inoculation in a combinatorial regimen with a DNA intramuscular priming (**Figure 4A**). The IFN-γ ELISpot assay of splenocytes isolated from vaccinated mice showed that, among the four tested groups, DNA+TTV+AdC68 group mounted significantly higher systemic cellular responses to immunodominant NP-2 and PB2-1 epitope peptides than the other three groups (**Figure 4B**). In contrast, the regimens of DNA+AdC68+TTV and DNA+AdC68 i.n.+TTV raised more potent T-cell immune responses against subdominant epitopes than those of the other two regimens (**Figure 4B**). We further analyzed the T-cell functionalities by measuring the production of intracellular cytokine after stimulation with the peptide pool. As shown in **Figure 4D**, the intramuscular administration of AdC68 induced more influenza-specific IFN-γ+, TNF-α+ and IFN-γ+TNF-α+ double positive T cells than their intranasal counterparts. Among all the four groups, DNA+TTV+AdC68 group exhibited the highest induction of CD107a+ cells ($p = 0.049$) (**Figure 4E**).

Given the potential important role that lung-resident T cells play in anti-influenza immunity, we extended our IFN-γ ELISpot analysis to bronchoalveolar lavage (BAL) lymphocytes. Strikingly, only the two intranasal groups showed robust BAL T-cell immune response upon stimulation with NP-2 and PB2-1 epitope peptides (**Figure 4C**). Thus, intranasal administration of AdC68 appeared to have a pronounced advantage over intramuscular administration in the induction of respiratory resident T cells.

## Intranasal Administration of AdC68-Based Vaccine Afforded a Better Protection From Lethal Influenza Challenge in Mice

We next evaluated the *in vivo* protective efficacy of prime-boost-boost immunization regimens against PR8 and H7N9 challenges. In response to lethal PR8 challenge, the two AdC68 intranasal immunization groups experienced similar weight losses that were less severe than the two intramuscular immunization groups (**Figure 5A**). This was marked by a slower initial loss and an earlier rebound of weights on day 9 as compared to day 10 in the later groups, resulting in a higher nadir weight before rebounding. Consequently, all the mice from the two intranasal immunization groups survived whereas the two intramuscular immunization groups only attained 60–80% survival rate. In contrast, all the mice from the sham control group died (**Figure 5B**). We further found that intranasal administration appeared to result in more reduced lung vial loads, which was especially obvious with the DNA+Adc68 i.n.+TTV group ($p = 0.046$) (**Figure 5E**). Thus, although all the four combinatorial immunization regimens were able to confer protection against PR8 infection, the two regimens with intranasal AdC68 vaccination were more effective.

Our studies on lethal H7N9 challenge models further supported that the intranasal route was superior to intramuscular route in protection. In particular, both DNA+Adc68 i.n.+TTV and DNA+TTV+Adc68 i.n. groups exhibited a body weight loss curve similar to that observed in PR8 challenge with the body weight reaching a nadir at day 9 and then rebounding afterward, differing significantly from DNA+Adc68+TTV, DNA+TTV+Adc68 and control groups which all suffered more rapidly and continuous weight loss without recovery (**Figure 5C**). Consequently, the two intranasal immunization groups all survived whereas the majority of the two intramuscular immunization groups died (**Figure 5D**). Interestingly, the measured lung viral load at day 5 after challenge revealed only modest advantage of intranasal vaccination over intramuscular vaccination (**Figure 5F**). Collectively, these data demonstrated that intranasal route is an optimal route for Adc68-based vaccine to achieve cross-group influenza protection in prime-boost-boost modality.

## Both Respiratory Residential and Systemic Memory T Cells Are Essential for Fully Protection

Our above results indicated that DNA+AdC68 i.n.+TV and DNA+TTV+Adc68 i.n. regimens were capable of raising both respiratory residential and systemic memory T cells. To dissect the contributions of these two T cell subpopulations to the protective immunity, we took advantage of Fingolimod (FTY720), an immunosuppressant which prevents T cell egress from lymph nodes or spleen by antagonizing sphingosine-1-phosphate while unaffects the residential memory T cells (Masopust et al., 2010). For the sake of reducing animal usage, the experiments presented in **Figures 5**, **6** were performed in parallel, sharing the sham control and the two intranasal groups without FTY720 treatment.

When exposed to FTY720 during lethal PR8 challenge, both intranasal groups were significantly less protected, showing more rapid body weight loss and much delayed regain of body weight (**Figure 6A**). Consequently, the survival rate dropped from 100 to 80% and 60% for DNA+AdC68 i.n +TTV group and DNA+TTV+AdC68 i.n., respectively (**Figure 6B**), concomitant with less suppression of viral replication (**Figure 6E**). Similar impact of FTY720 treatment was

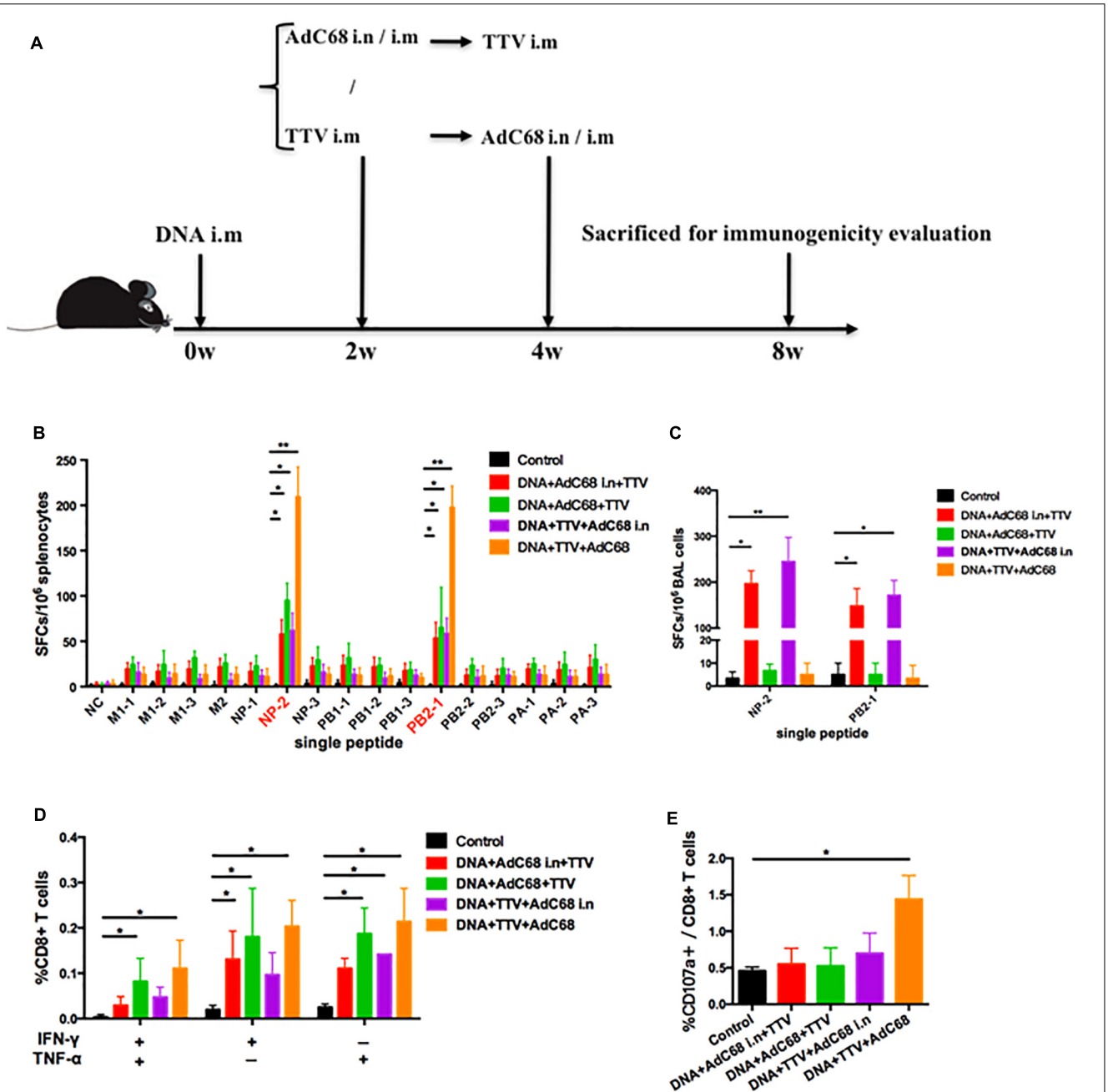


**FIGURE 4 |** Intranasal administration of AdC68 elicits significantly more potent respiratory residential and less systemic memory T cell responses. **(A)** Schematic illustration of immunization regimens. Control group were immunized with one dose of control pSV1.0 vector (100 ug) via intramuscular (i.m) route and two doses of control AdC68 empty vector ($1 \times 10^{11}$ vp) separately via intramuscular (i.m) and intranasal (i.n.) route. Experimental groups were sequentially immunized with DNA, AdC68, and TTV in the indicated order, the intramuscular route was treated as default to be left undenoted whereas the intranasal administration was labeled as i.n. Splenocytes and bronchoalveolar lavage (BAL) were isolated 4 weeks after vaccination for measurement of influenza-specific immune responses. **(B)** IFNγ ELISpot assay of splenocytes in response to stimulation with a single indicated influenza-specific epitope peptide. **(C)** IFNγ ELISpot assay of BAL in response to stimulation with NP-1 and PB2-1 peptides. **(D,E)** Intracellular cytokine staining assay to determine the percentage of CD8+ splenocytes secreting IFN-γ, TNF-α, or both, and CD107a-positive cells after stimulation with the peptide pool. All determinations were carried out in triplicate and the error bars represent the SDs. $^{**}p < 0.01$; $^{*}p < 0.05$, *t*-test.

also observed in protection against H7N9 challenge, despite that DNA+TTV+AdC68 i.n. group suffered even a bigger drop in survival (**Figures 6C,D,F**). Taken together, these data suggest that the protection conferred by our intranasal immunization strategy were attributed to the action of both respiratory residential and systemic T cells.

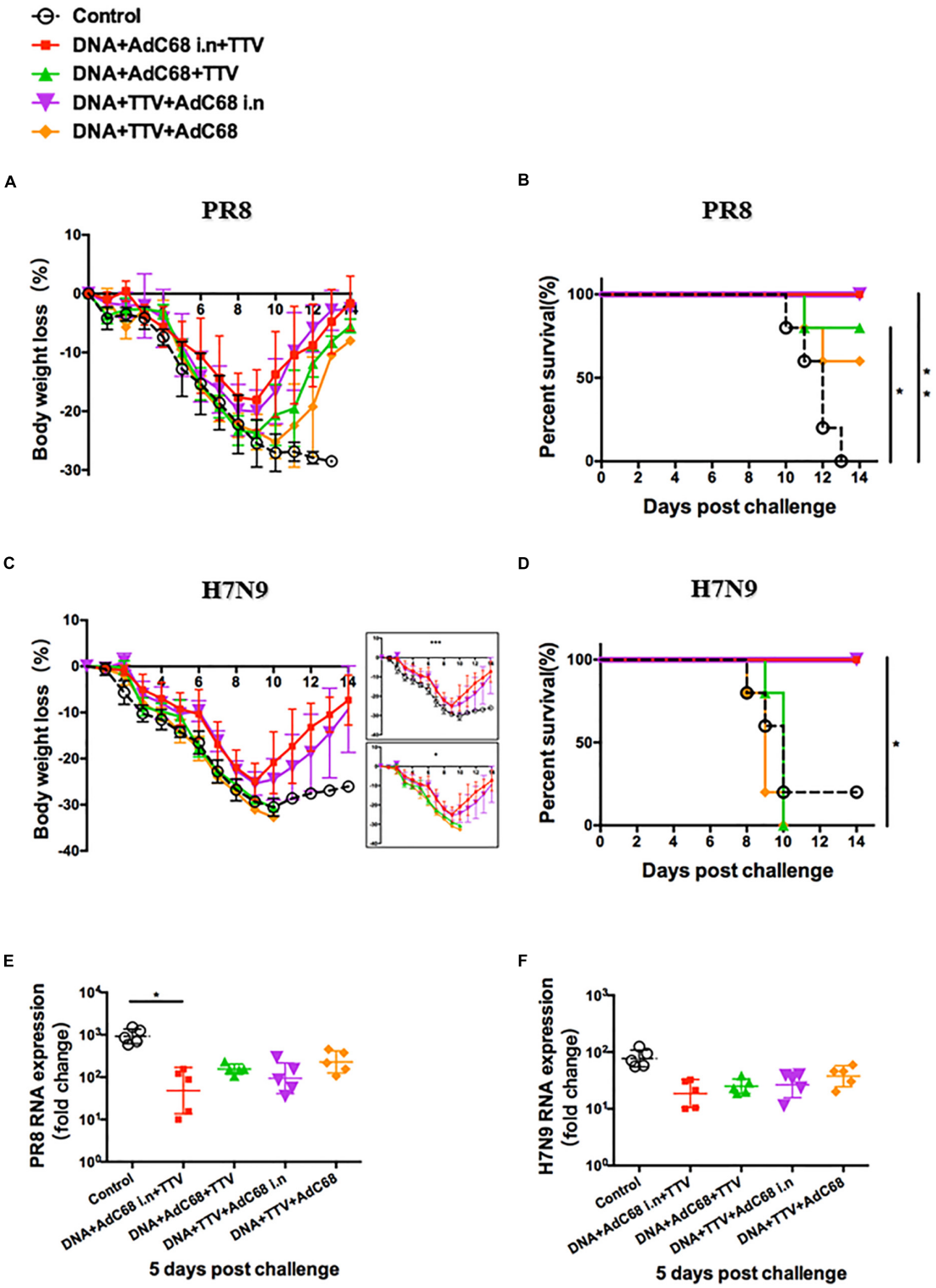


**FIGURE 5 |** Intranasal administration of AdC68 afforded a better protection from lethal challenge of influenza. Mice were subjected to different combinatorial immunizations following schemes outlined in **Figure 4A**, and 4 weeks later challenged with lethal doses of PR8 or H7N9 IAV virus. Shown are: **(A,C)** Body weight curves of virus-challenged mice. **(B,D)** Survival curve of virus-infected mice. **(E,F)** Relative lung viral loads at day 5 after virus challenge as measured by RT-PCR quantifications of influenza-specific RNA. The error bars represent the SDs. Two-way ANOVA test, Mantel–Cox log rank test and *t*-test were used to determine difference in weight loss, lethality, and viral load, respectively. $^{**}p < 0.01$; $^{*}p < 0.05$; $n = 5$. Weight loss in the two intranasal immunization groups were significantly different from both the two non-intranasal immunization groups and control group with $p < 0.001$ and $p < 0.05$, respectively.

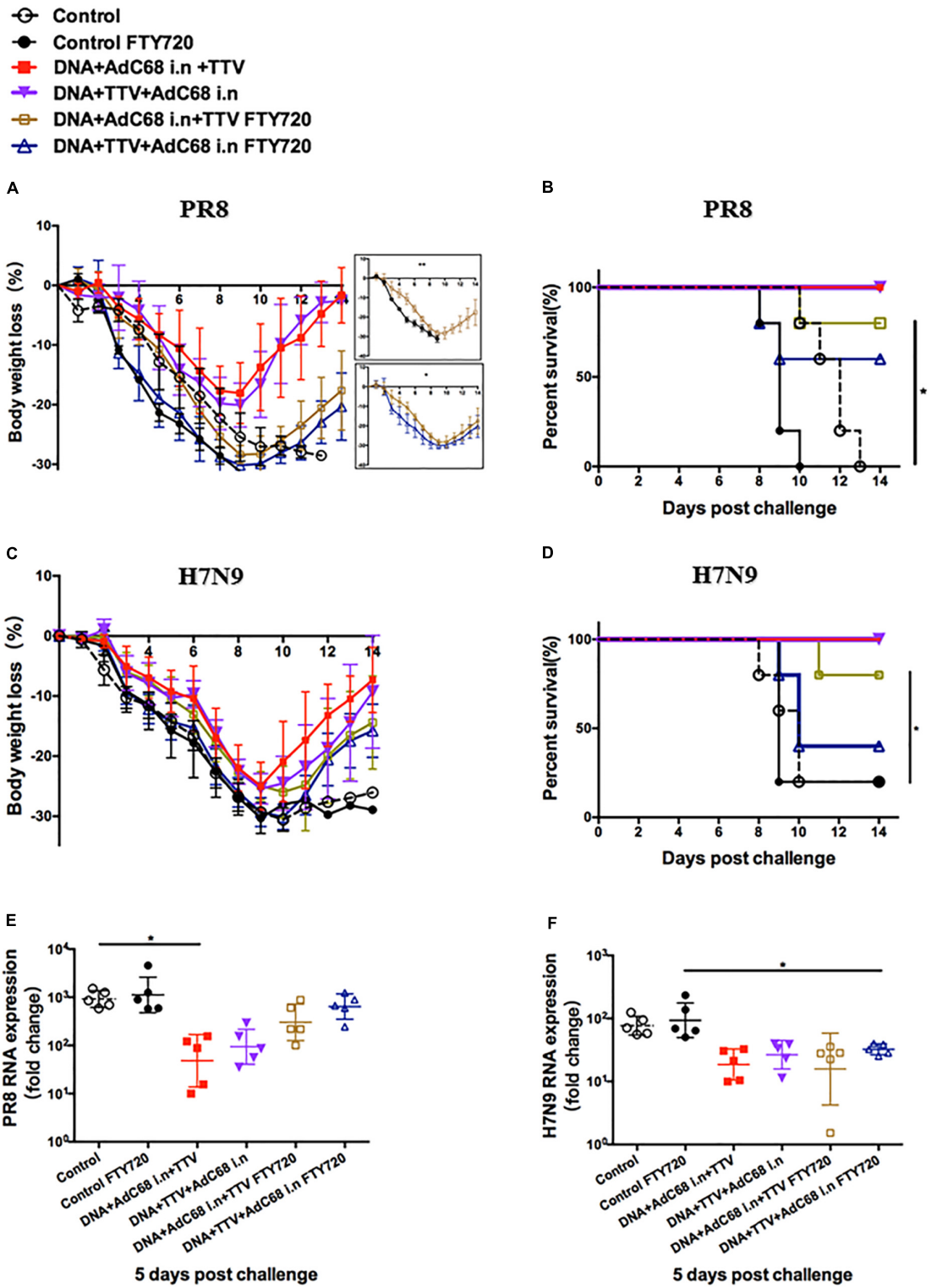


**FIGURE 6 |** Both respiratory residential and systemic T cells are essential for fully protection. The sequential immunizations and virus challenges of vaccinated mice were essentially performed as described in **Figure 5A**, except that, where indicated, the mice were exposed *ad libitum* to drinking water containing 2 μg/ml of dissolved FTY720 during challenge. Shown are: **(A,C)** Body weight curve of virus-challenged mice. **(B,D)** Survival curve of virus-challenged mice. **(E,F)** Relative lung viral loads in infected mice at day 5 after virus challenge as measured by RT-PCR quantifications of influenza-specific RNA. The error bars represent the SDs. Two-way ANOVA test, Mantel–Cox log rank test and *t*-test were used to determine difference in weight loss, lethality, and viral load, respectively. $^{**}p < 0.01$; $^{*}p < 0.05$; $n = 5$.

## DISCUSSION

Current influenza vaccines function by raising humoral immunity against strain-specific HA and NA glycoproteins. Consequently, they failed to confer cross-protection in human and must be re-formulated every year to match the circulating influenza strains (Steel et al., 2010). There has been growing urgency to develop universal IAV vaccines that are capable of affording cross-protection (Grant et al., 2013). The development of cross-reactive influenza vaccines has been explored on both the humoral arm of the immune response directing against the conserved HA stem or M2e, and its cellular arm targeting the internal viral proteins which are much more conserved than surface viral glycoproteins (Saletti et al., 2018). The potential of T-cell based vaccine was further supported by our recent studies of H7N9-infected patients revealing the pivotal role of an effective and timely CD8+ T cell response in overcoming H7N9 infection in human (Wang et al., 2015). Here, we presented new vaccination strategies focusing on the effective delivery of cross-conserved influenza-specific epitopes to induce broad spectrum T-cell response.

We would expect that our newly designed PAPB1M1 and PB2NPM2 immunogens together should provide a close to full coverage of conserved T-cell epitopes internally on IAV. Importantly, the co-introduction of the two immunogens in a modality of DNA prime followed by AdC68 or TTV viral vectored boost elicited not only strong T cell response to immunodominant epitopes but also discernible T cell response to sub-immunodominant epitopes, which was more evident when TTV served as the boost. In current study, we have not yet dissected the respective protective contributions of immune responses to the two immunodominant epitopes, NP-2 and PB2-1, and the subdominant epitopes. This will be only accomplished by future examination of the protective efficacy of mutated immunogens in which NP-2 and PB2-1 epitopes are eliminated in comparison to that of the original immunogens in mouse infection model. Even if the subdominant epitopes were found to be insufficient for raising effective protection against influenza challenge in vaccinated mice, their contribution in broadening the T cell repertoire may be important for a vaccine being effective in a human setting. One of the major challenges in the development of T cell-based universal influenza vaccine is that the T cell response to the same influenza infection or vaccine might vary considerably between individuals, primarily owing to the possession of diverse HLA alleles that restricted the number of viral peptides displayed to T cells for recognition (Clemens et al., 2018). With HLA restriction, an influenza vaccine incorporating a multitude of conserved viral epitopes would more likely provide better population coverage than that concentrated on specific conserved epitopes. Thus, the new vaccines we engineered have the potential to overcome the HLA challenge in human settings, fitting one important criterion of universal influenza vaccines.

Our construction of three types of vaccines to express the PAPB1M1 and PB2NPM2 immunogens enabled us to test a sequential immunization strategy combining the three vaccines. It is a rare opportunity as, for viral vectored vaccine, the second boost with the same vaccine would usually not be beneficial due to the pre-existing vector immunity raised by the first boost. The sequential use of different viral platform-based boost also allows the integration of individual advantages of different viral vectored vaccine to induce potent broad-spectrum T-cell immunity.

In light of recent findings that influenza-specific lung resident T cells is critical for anti-influenza immunity (Wu et al., 2014; Zens et al., 2016), we utilized either intramuscular or intranasal route for administering AdC68 based vaccine and analyzed the impact on induction of memory T cells alongside protective efficacy. Our results demonstrated that, although intramuscular immunization was more effective in triggering systemic CD8+ T cell response, only intranasal immunization was capable of evoking lung-resident CD8+ T cells. Consequently, full protection from lethal PR8 and H7N9 challenges was only observed in intranasal immunization groups. One interesting observation was that the level of lung viral load at early phase of infection was marginally correlated with the protective efficacy in terms of weight loss and survival rate. This might be explained by the polyfunctionality of tissue-residing T cells, engaged in duties other than directly clearing virus-infected cells to provide protection, e.g., secreting cytokines to create a virus-hostile local environment, and/or facilitating recruitment of circulating immune cells into lesioned tissues (Schenkel et al., 2013; Ariotti et al., 2014).

Although intranasal administration of adenovirus vectors has been extensively shown to induce potent immune responses in mice, its use in primates has been much less documented in literature precedence. Given the large difference in oropharyngeal immune system between mice and primates, there is concern whether our promising results in mice can be fully translated to humans. However, a recent study reported intranasal application of adenovirus vector being part of a vector prime-protein boost vaccination modality to afford effective protection in African green monkey model against respiratory syncytial virus (RSV) infection (Eyles et al., 2013). Nevertheless, future studies in non-human primates will be needed to justify our notion that, for T-cell based adenovirus vaccine, intranasal route can achieve better efficacy than intramuscular route via establishing lung-resident CD8 memory cells.

Finally, we discovered that systemic T cell response also mediate the protection afforded by our new intranasal immunization strategy. FTY720 treatment, which prevents homing of circulated T cells to periphery tissues, significantly reduced the protective efficacy. Interestingly, a number of recent studies revealed that circulating T cells can be recruited into lung tissues to convert into residing cells (Slutter et al., 2017; Pizzolla et al., 2018). Thus, systemic and respiratory residential T cell might not act independently, but rather orchestrate together in mounting an effective protection against influenza infection.

As compared to other current available vaccination approaches, our new approach is advantageous in expanding the breadth of induced immune response. According to a position statement regarding universal influenza vaccine recently published by National Institute of Allergy and Infectious Diseases (NIAID), one critical qualification element of a universal influenza virus vaccine is to be effective against both group 1 and group 2 influenza A viruses. Most if not

all of the current available vaccination approaches will not meet the criterion. For example, one most recent preclinical study identified live attenuated influenza vaccine (LAIV) in combination with sequential immunization strategy as the most promising vaccination regimen to confer broad protection against group 1 influenza viruses (Liu et al., 2019). However, it is uncertain whether the same approach can achieve similar protective efficacy against group 2 influenza viruses, and if yes whether it is feasible to design right immunogens and regimen for attaining effective cross-group protection. The efficacy of LAIV as well as other vaccines lies in their ability to raise potent influenza-specific antibody response, especially against surface HA protein. Such antibody response was missed in the immunity raised by our new vaccine, possibly accounting for less inhibition of viral replication as compared to other vaccines shown in previous studies. How to modify our strategy to engage the B cell response will await further research. Nevertheless, starting with a demonstration of its ability to confer cross-group protection against lethal IAV challenges in vaccinated mice, the novel vaccine described in this study might open new avenue to tackle the challenge of universal influenza vaccine.

## DATA AVAILABILITY

All datasets generated for this study are included in the manuscript and/or the **Supplementary Files**.

## ETHICS STATEMENT

This study was carried out in accordance with the "Guide for the Care and Use of Laboratory Animals" of the Institute of Laboratory Animal Sciences (est. 2006). The protocol was approved by the Institutional Biosafety Committee at Shanghai Public Health Clinical Center.

## AUTHOR CONTRIBUTIONS

JX, XZ, and DZ conceived, designed, and supervised the study. XX performed most of the experiments, analyzed the data, and wrote the original draft. CZ (2nd Author) analyzed the data. TQ helped design the immunogen sequences. QH, SY, LD, LL, LJ, JW, LZ, CZ (11th Author), and XW conducted some experiments. CZ (2nd Author), JX, XZ, and DZ edited the manuscript. All authors reviewed and approved the manuscript.

## FUNDING

This work was supported by the National Natural Science Foundation of China (8161101262, 81430030, and 81672018), National Key Project for Infectious Disease Prevention and Control (2017zx10304402-002-007), the Leading Academic Discipline Project of Shanghai (2016-035), the Leading Medical Discipline Project of Shanghai, and intramural funding from Shanghai Public Clinical Health Center.

## SUPPLEMENTARY MATERIAL

The Supplementary Material for this article can be found online at: https://www.frontiersin.org/articles/10.3389/fmicb.2019.01630/full#supplementary-material

## REFERENCES

Ariotti, S., Hogenbirk, M. A., Dijkgraaf, F. E., Visser, L. L., Hoekstra, M. E., Song, J. Y., et al. (2014). T cell memory. Skin-resident memory CD8(+) T cells trigger a state of tissue-wide pathogen alert. *Science* 346, 101–105. doi: 10.1126/science.1254803

Belz, G. T., Xie, W., and Doherty, P. C. (2001). Diversity of epitope and cytokine profiles for primary and secondary influenza a virus-specific CD8+ T cell responses. *J. Immunol.* 166, 4627–4633. doi: 10.4049/jimmunol.166.7.4627

Brown, L. E., and Kelso, A. (2009). Prospects for an influenza vaccine that induces cross-protective cytotoxic T lymphocytes. *Immunol. Cell Biol.* 87, 300–308. doi: 10.1038/icb.2009.16

Chen, W., Norbury, C. C., Cho, Y., Yewdell, J. W., and Bennink, J. R. (2001). Immunoproteasomes shape immunodominance hierarchies of antiviral CD8(+) T cells at the levels of T cell repertoire and presentation of viral antigens. *J. Exp. Med.* 193, 1319–1326. doi: 10.1084/jem.193.11.1319

Clemens, E. B., Van De Sandt, C., Wong, S. S., Wakim, L. M., and Valkenburg, S. A. (2018). Harnessing the power of T cells: the promising hope for a universal influenza vaccine. *Vaccines* 6:E18. doi: 10.3390/vaccines6020018

Cox, A., and Dewhurst, S. (2015). A single mutation at pb1 residue 319 dramatically increases the safety of PR8 live attenuated influenza vaccine in a murine model without compromising vaccine efficacy. *J. Virol.* 90, 2702–2705. doi: 10.1128/JVI.02723-15

Draper, S. J., and Heeney, J. L. (2010). Viruses as vaccine vectors for infectious diseases and cancer. *Nat. Rev. Microbiol.* 8, 62–73. doi: 10.1038/nrmicro2240

Eyles, J. E., Johnson, J. E., Megati, S., Roopchand, V., Cockle, P. J., Weeratna, R., et al. (2013). Nonreplicating vaccines can protect african green monkeys from the memphis 37 strain of respiratory syncytial virus. *J. Infect. Dis.* 208, 319–329. doi: 10.1093/infdis/jit169

Fan, J., Liang, X., Horton, M. S., Perry, H. C., Citron, M. P., Heidecker, G. J., et al. (2004). Preclinical study of influenza virus A M2 peptide conjugate vaccines in mice, ferrets, and rhesus monkeys. *Vaccine* 22, 2993–3003. doi: 10.1016/j.vaccine.2004.02.021

Gao, R., Cao, B., Hu, Y., Feng, Z., Wang, D., Hu, W., et al. (2013). Human infection with a novel avian-origin influenza A (H7N9) virus. *N. Engl. J. Med.* 368, 1888–1897. doi: 10.1056/NEJMoa1304459

Gostin, L. O., Phelan, A., Stoto, M. A., Kraemer, J. D., and Reddy, K. S. (2014). Virus sharing, genetic sequencing, and global health security. *Science* 345, 1295–1296. doi: 10.1126/science.1257622

Grant, E., Wu, C., Chan, K. F., Eckle, S., Bharadwaj, M., Zou, Q. M., et al. (2013). Nucleoprotein of influenza A virus is a major target of immunodominant CD8+ T-cell responses. *Immunol. Cell Biol.* 91, 184–194. doi: 10.1038/icb.2012.78

Halstead, E. S., Mueller, Y. M., Altman, J. D., and Katsikis, P. D. (2002). In vivo stimulation of CD137 broadens primary antiviral CD8+ T cell responses. *Nat. Immunol.* 3, 536–541. doi: 10.1038/ni798

Hannoun, C. (2013). The evolving history of influenza viruses and influenza vaccines. *Expert Rev. Vaccines* 12, 1085–1094. doi: 10.1586/14760584.2013.824709

Holloway, R., Rasmussen, S. A., Zaza, S., Cox, N. J., and Jernigan, D. B. (2014). Updated preparedness and response framework for influenza pandemics. *MMWR Recomm. Rep.* 63, 1–18.

Horimoto, T., and Kawaoka, Y. (2005). Influenza: lessons from past pandemics, warnings from current incidents. *Nat. Rev. Microbiol.* 3, 591–600. doi: 10.1038/nrmicro1208

Houser, K., and Subbarao, K. (2015). Influenza vaccines: challenges and solutions. *Cell Host Microbe* 17, 295–300. doi: 10.1016/j.chom.2015.02.012

Huang, X., Liu, L., Ren, L., Qiu, C., Wan, Y., and Xu, J. (2007a). Mucosal priming with replicative Tiantan vaccinia and systemic boosting with DNA vaccine raised strong mucosal and systemic HIV-specific immune responses. *Vaccine* 25, 8874–8884. doi: 10.1016/j.vaccine.2007.08.066

Huang, X., Xu, J., Qiu, C., Ren, L., Liu, L., Wan, Y., et al. (2007b). Mucosal priming with PEI/DNA complex and systemic boosting with recombinant TianTan vaccinia stimulate vigorous mucosal and systemic immune responses. *Vaccine* 25, 2620–2629. doi: 10.1016/j.vaccine.2006.12.020

Jaiswal, V., Chanumolu, S. K., Sharma, P., Chauhan, R. S., and Rout, C. (2013). EpiCombFlu: exploring known influenza epitopes and their combination to design a universal influenza vaccine. *Bioinformatics* 29, 1904–1907. doi: 10.1093/bioinformatics/btt304

Lamere, M. W., Moquin, A., Lee, F. E., Misra, R. S., Blair, P. J., Haynes, L., et al. (2011). Regulation of antinucleoprotein IgG by systemic vaccination and its effect on influenza virus clearance. *J. Virol.* 85, 5027–5035. doi: 10.1128/JVI.00150-11

Lawrence, C. W., Ream, R. M., and Braciale, T. J. (2005). Frequency, specificity, and sites of expansion of CD8+ T cells during primary pulmonary influenza virus infection. *J. Immunol.* 174, 5332–5340. doi: 10.4049/jimmunol.174.9.5332

Liu, W. C., Nachbagauer, R., Stadlbauer, D., Solorzano, A., Berlanda-Scorza, F., Garcia-Sastre, A., et al. (2019). Sequential immunization with live-attenuated chimeric hemagglutinin-based vaccines confers heterosubtypic immunity against influenza a viruses in a preclinical ferret model. *Front. Immunol.* 10:756. doi: 10.3389/fimmu.2019.00756

Masopust, D., Choo, D., Vezys, V., Wherry, E. J., Duraiswamy, J., Akondy, R., et al. (2010). Dynamic T cell migration program provides resident memory within intestinal epithelium. *J. Exp. Med.* 207, 553–564. doi: 10.1084/jem.20090858

Moutaftsi, M., Peters, B., Pasquetto, V., Tscharke, D. C., Sidney, J., Bui, H. H., et al. (2006). A consensus epitope prediction approach identifies the breadth of murine T(CD8+)-cell responses to vaccinia virus. *Nat. Biotechnol.* 24, 817–819. doi: 10.1038/nbt1215

Pica, N., and Palese, P. (2013). Toward a universal influenza virus vaccine: prospects and challenges. *Annu. Rev. Med.* 64, 189–202. doi: 10.1146/annurev-med-120611-145115

Pizzolla, A., Nguyen, T. H., Sant, S., Jaffar, J., Loudovaris, T., Mannering, S. I., et al. (2018). Influenza-specific lung-resident memory T cells are proliferative and polyfunctional and maintain diverse TCR profiles. *J. Clin. Invest.* 128, 721–733. doi: 10.1172/JCI96957

Saletti, G., Gerlach, T., and Rimmelzwaan, G. F. (2018). Influenza vaccines: 'tailor-made' or 'one fits all'. *Curr. Opin. Immunol.* 53, 102–110. doi: 10.1016/j.coi.2018.04.015

Schenkel, J. M., Fraser, K. A., Vezys, V., and Masopust, D. (2013). Sensing and alarm function of resident memory CD8(+) T cells. *Nat. Immunol.* 14, 509–513. doi: 10.1038/ni.2568

Singh, H., and Raghava, G. P. (2003). ProPred1: prediction of promiscuous MHC Class-I binding sites. *Bioinformatics* 19, 1009–1014. doi: 10.1093/bioinformatics/btg108

Slutter, B., Van Braeckel-Budimir, N., Abboud, G., Varga, S. M., Salek-Ardakani, S., and Harty, J. T. (2017). Dynamics of influenza-induced lung-resident memory T cells underlie waning heterosubtypic immunity. *Sci. Immunol.* 2:eaag2031. doi: 10.1126/sciimmunol.aag2031

Sridhar, S., Begom, S., Bermingham, A., Hoschler, K., Adamson, W., Carman, W., et al. (2013). Cellular immune correlates of protection against symptomatic pandemic influenza. *Nat. Med.* 19, 1305–1312. doi: 10.1038/nm.3350

Stanekova, Z., and Vareckova, E. (2010). Conserved epitopes of influenza A virus inducing protective immunity and their prospects for universal vaccine development. *Virol. J.* 7:351. doi: 10.1186/1743-422X-7-351

Steel, J., Lowen, A. C., Wang, T. T., Yondola, M., Gao, Q., Haye, K., et al. (2010). Influenza virus vaccine based on the conserved hemagglutinin stalk domain. *MBio* 1, e18–e10. doi: 10.1128/mBio.00018-10

Turner, S. J., La Gruta, N. L., Stambas, J., Diaz, G., and Doherty, P. C. (2004). Differential tumor necrosis factor receptor 2-mediated editing of virus-specific CD8+ effector T cells. *Proc. Natl. Acad. Sci. U.S.A.* 101, 3545–3550. doi: 10.1073/pnas.0307347101

Tussey, L. G., Rowland-Jones, S., Zheng, T. S., Androlewicz, M. J., Cresswell, P., Frelinger, J. A., et al. (1995). Different MHC class I alleles compete for presentation of overlapping viral epitopes. *Immunity* 3, 65–77. doi: 10.1016/1074-7613(95)90159-0

Uddback, I. E., Steffensen, M. A., Pedersen, S. R., Nazerai, L., Thomsen, A. R., and Christensen, J. P. (2016). PB1 as a potential target for increasing the breadth of T-cell mediated immunity to Influenza A. *Sci. Rep.* 6:35033. doi: 10.1038/srep35033

Valkenburg, S. A., Li, O. T., Mak, P. W., Mok, C. K., Nicholls, J. M., Guan, Y., et al. (2014). IL-15 adjuvanted multivalent vaccinia-based universal influenza vaccine requires CD4+ T cells for heterosubtypic protection. *Proc. Natl. Acad. Sci. U.S.A.* 111, 5676–5681. doi: 10.1073/pnas.1403684111

Wang, X., Xing, M., Zhang, C., Yang, Y., Chi, Y., Tang, X., et al. (2014). Neutralizing antibody responses to enterovirus and adenovirus in healthy adults in China. *Emerg. Microbes Infect.* 3:e30. doi: 10.1038/emi.2014.30

Wang, Z., Wan, Y., Qiu, C., Quinones-Parra, S., Zhu, Z., Loh, L., et al. (2015). Recovery from severe H7N9 disease is associated with diverse response mechanisms dominated by CD8(+) T cells. *Nat. Commun.* 6:6833. doi: 10.1038/ncomms7833

Wu, T., Hu, Y., Lee, Y. T., Bouchard, K. R., Benechet, A., Khanna, K., et al. (2014). Lung-resident memory CD8 T cells (TRM) are indispensable for optimal cross-protection against pulmonary virus infection. *J. Leukoc Biol.* 95, 215–224. doi: 10.1189/jlb.0313180

Xing, M., Wang, X., Chi, Y., and Zhou, D. (2016). Gene therapy for colorectal cancer using adenovirus-mediated full-length antibody, cetuximab. *Oncotarget* 7, 28262–28272. doi: 10.18632/oncotarget.8596

Zens, K. D., Chen, J. K., and Farber, D. L. (2016). Vaccine-generated lung tissue-resident memory T cells provide heterosubtypic protection to influenza infection. *JCI Insight* 1:85832. doi: 10.1172/jci.insight.85832

Zhang, S., Huang, W., Zhou, X., Zhao, Q., Wang, Q., and Jia, B. (2013). Seroprevalence of neutralizing antibodies to human adenoviruses type-5 and type-26 and chimpanzee adenovirus type-68 in healthy Chinese adults. *J. Med. Virol.* 85, 1077–1084. doi: 10.1002/jmv.23546

Zhu, Z., Yang, Y., Feng, Y., Shi, B., Chen, L., Zheng, Y., et al. (2013). Infection of inbred BALB/c and C57BL/6 and outbred Institute of Cancer Research mice with the emerging H7N9 avian influenza virus. *Emerg. Microbes Infect.* 2:e50. doi: 10.1038/emi.2013.50

**Conflict of Interest Statement:** Shanghai Public Health Clinical Center has filed a patent application with PCT Application No. PCT/CN2018/105020, which covers the PAPB1M1 and PB2NPM2 immunogens and the derived influenza vaccines. XX, XZ, and JX have been listed as inventors of PCT/CN2018/105020.

The remaining authors declare that the research was conducted in the absence of any commercial or financial relationships that could be construed as a potential conflict of interest.

*Copyright © 2019 Xie, Zhao, He, Qiu, Yuan, Ding, Liu, Jiang, Wang, Zhang, Zhang, Wang, Zhou, Zhang and Xu. This is an open-access article distributed under the terms of the Creative Commons Attribution License (CC BY). The use, distribution or reproduction in other forums is permitted, provided the original author(s) and the copyright owner(s) are credited and that the original publication in this journal is cited, in accordance with accepted academic practice. No use, distribution or reproduction is permitted which does not comply with these terms.*

frontiers in Microbiology

REVIEW
published: 02 August 2019
doi: 10.3389/fmicb.2019.01781

# Recent Advances in the Vaccine Development Against Middle East Respiratory Syndrome-Coronavirus

*Chean Yeah Yong[1,2], Hui Kian Ong[3], Swee Keong Yeap[4], Kok Lian Ho[3] and Wen Siang Tan[1,2]**

[1] Department of Microbiology, Faculty of Biotechnology and Biomolecular Sciences, Universiti Putra Malaysia, Serdang, Malaysia, [2] Laboratory of Vaccines and Immunotherapeutics, Institute of Bioscience, Universiti Putra Malaysia, Serdang, Malaysia, [3] Department of Pathology, Faculty of Medicine and Health Sciences, Universiti Putra Malaysia, Serdang, Malaysia, [4] China ASEAN College of Marine Sciences, Xiamen University Malaysia, Sepang, Malaysia

Middle East respiratory syndrome (MERS) is a deadly viral respiratory disease caused by MERS-coronavirus (MERS-CoV) infection. To date, there is no specific treatment proven effective against this viral disease. In addition, no vaccine has been licensed to prevent MERS-CoV infection thus far. Therefore, our current review focuses on the most recent studies in search of an effective MERS vaccine. Overall, vaccine candidates against MERS-CoV are mainly based upon the viral spike (S) protein, due to its vital role in the viral infectivity, although several studies focused on other viral proteins such as the nucleocapsid (N) protein, envelope (E) protein, and non-structural protein 16 (NSP16) have also been reported. In general, the potential vaccine candidates can be classified into six types: viral vector-based vaccine, DNA vaccine, subunit vaccine, nanoparticle-based vaccine, inactivated-whole virus vaccine and live-attenuated vaccine, which are discussed in detail. Besides, the immune responses and potential antibody dependent enhancement of MERS-CoV infection are extensively reviewed. In addition, animal models used to study MERS-CoV and evaluate the vaccine candidates are discussed intensively.

**Keywords: Middle East respiratory syndrome, coronavirus, animal model, vaccine, antibody dependent enhancement**

OPEN ACCESS

***Edited by:***
*Lu Lu,*
*Fudan University, China*

***Reviewed by:***
*Jincun Zhao,*
*Guangzhou Medical University, China*
*Vincent Munster,*
*National Institutes of Health (NIH), United States*
*Jasper Fuk Woo Chan,*
*The University of Hong Kong, Hong Kong*

***Correspondence:**
*Wen Siang Tan*
*wstan@upm.edu.my*

***Specialty section:***
*This article was submitted to Virology, a section of the journal Frontiers in Microbiology*

***Received:*** *10 May 2019*
***Accepted:*** *18 July 2019*
***Published:*** *02 August 2019*

***Citation:***
*Yong CY, Ong HK, Yeap SK, Ho KL and Tan WS (2019) Recent Advances in the Vaccine Development Against Middle East Respiratory Syndrome-Coronavirus. Front. Microbiol. 10:1781. doi: 10.3389/fmicb.2019.01781*

## INTRODUCTION

Camel flu, or more commonly known as the Middle East respiratory syndrome (MERS), is a respiratory disease caused by MERS-coronavirus (MERS-CoV). MERS-CoV was first identified in Saudi Arabia in 2012 (Zaki et al., 2012). As of February 2019, 27 countries worldwide have reported cases of MERS-CoV infection, with 2,374 reported viral infection and 823 associated deaths, which corresponds to ∼35% fatality in identified cases (World Health Organization [WHO], 2019b), although the actual fatality rate of the viral infection is most likely below 35% due to some unidentified, mild, or asymptomatic cases. Majority of these cases occurred in Saudi Arabia, amounting to 1,983 of reported cases, with 745 associated deaths or ∼37.5% fatality (World Health Organization [WHO], 2019a).

Majority of the identified MERS-CoV cases are nosocomially acquired via direct close contact with infected patients (Chowell et al., 2015; Cauchemez et al., 2016), whereas cases of zoonotic transmission from dromedary camels to humans were reported primarily in Saudi Arabia, where

human-camel interaction is frequent (Gossner et al., 2016). Hitherto, no specific treatments and vaccines are available for MERS-CoV infections. Although MERS-CoV is currently not listed as a potential pandemic threat, a recent outbreak in South Korea which demonstrated virus emergence in second and third generation contacts, has immediately raised concern that multiple mutations of MERS-CoV might cause enhanced human-to-human transmission (Wang et al., 2015b; Oh et al., 2018). Recently, MERS-CoV was added to the NIAID's pathogen priority list as Category C Priority Pathogens due to its potential applications in biological warfare (Du et al., 2016b). Preventive measures against MERS-CoV infection, particularly vaccine development, are crucial to avoid deadly and unexpected future pandemics.

Middle East respiratory syndrome-coronavirus, the causative agent of MERS, is a positive sense, single-stranded RNA *Betacoronavirus* which belongs to the family of *Coronaviridae*. Its viral genome is about 30 kb in length, flanked by a 5'-terminal cap and 3'-poly(A) tail (van Boheemen et al., 2012; Scobey et al., 2013). MERS-CoV genome contains at least 10 open reading frames (ORFs), which encodes for 4 structural proteins: spike (S) protein, envelope (E) protein, membrane (M) protein, nucleocapsid (N) protein, 16 non-structural proteins (NSP1-NSP16), and 5 accessory proteins (ORF3, ORF4a, ORF4b, ORF5, and ORF8b) (van Boheemen et al., 2012; Du et al., 2017). Of all these viral proteins, S and N proteins are of particular interest in the development of vaccines against MERS-CoV, although other proteins such as E protein and NSP16 are potential immunogens as live attenuated vaccines (Almazan et al., 2013; Menachery et al., 2017).

## CRITERIA FOR AN EFFECTIVE MERS-CoV VACCINE

Two viral proteins of MERS-CoV, S and N proteins, were demonstrated to be highly immunogenic and capable of eliciting T-cell responses. However, only S protein was shown to induce neutralizing antibodies, the critical effectors against MERS-CoV (Agnihothram et al., 2014). Notably, N protein had also been proposed to be a potential protective immunogen for both neutralizing antibodies and T-cell immune responses through *in silico* approaches (Shi et al., 2015). Despite the prediction, no biological data have been presented thus far. Another potential B cell epitope of the MERS-CoV E protein was identified recently using *in silico* methods, yet similarly, no biological data were presented (Xie et al., 2018). Therefore, most of the MERS-CoV vaccine candidates are still based on the full length or part of the S protein.

Ideally, an effective MERS-CoV vaccine is required to induce both robust humoral and cell-mediated immunities, particularly antibody responses are crucial for the survival of the vaccinated hosts (Du et al., 2016b). Previous studies indicated that the level of serum neutralizing antibodies correlated positively with the reduction of lung pathogenesis, which increased the survival of animals challenged with MERS-CoV (Zhao et al., 2015; Zhang et al., 2016). In general, most of the potential MERS-CoV vaccine candidates were able to elicit systemic antibody responses, producing high titer of serum IgG upon immunization, but many failed to generate sufficient mucosal immunity unless the vaccines were administered via a mucosal or intranasal route. Activation of mucosal immunity is heavily dependent on the route of immunization, and this is a common challenge in vaccine development for many respiratory pathogens (Ma et al., 2014a; Guo et al., 2015). Pre-existing neutralizing mucosal antibodies are important as a first line of defenses against MERS-CoV infection (Guo et al., 2015). All neutralizing antibodies elicited by vaccines based on S protein could bind to the receptor binding domain (RBD) of the protein thereby inhibiting viral internalization and membrane fusion (Du et al., 2017). Little is known about the memory B-cell responses against MERS-CoV, apart from a recent study which demonstrated the persistence of anti-MERS-CoV antibodies in MERS survivors up to 34 months (Payne et al., 2016). On the other hand, antibody responses against another closely related coronavirus, SARS-CoV, were not persistent, whereby a 6-year follow-up study did not detect memory B-cell responses in SARS survivors (Tang et al., 2011). It is likely that some of the B-cells differentiate into MERS-CoV-specific memory B-cells following infection or vaccination, but the longevity and protective efficacy of these memory B-cells against MERS-CoV infection or re-challenge remain unresolved questions (Du et al., 2016b; Perlman and Vijay, 2016).

T-cell responses elicited by MERS-CoV vaccines also play important roles in protection against MERS. This is supported by the fact that viral clearance was impossible in T-cell deficient mice, but was possible in mice lacking B-cells (Zhao et al., 2014). Although T-cells are demonstrated to be a critical effector in acute viral clearance, protection for subsequent MERS-CoV infection is largely mediated by humoral immunity (Zhao et al., 2014). Several animal studies also demonstrated activation of T-cell responses following immunization with a MERS-CoV vaccine candidate, resulting in the elevated secretion of Th1 and Th2 cytokines (Lan et al., 2014; Ma et al., 2014a; Malczyk et al., 2015; Muthumani et al., 2015). It is also noteworthy to mention that adjuvants could be co-administered with MERS-CoV vaccines to tailor and possibly enhance the immune responses elicited by the vaccines. One study has indicated that co-administration of the MERS-CoV vaccine based on the S protein with Alum in mice resulted in a Th2 biased immunity, whereas a more robust Th1 and Th2 mixed immune response was produced when an additional adjuvant, cysteine-phosphate-guanine (CpG) oligodeoxynucleotides (ODN) was included in the formulation (Lan et al., 2014). To date, no detail investigation on MERS-CoV vaccine-induced memory T-cell responses is reported. However, MERS-CoV infection was shown to induce memory CD4+ and CD8+ T-cells responses in MERS survivors, at least up to 24 months (Zhao et al., 2017). There is little understanding about the biological function of memory CD4+ T-cells but they are likely to contribute to direct virus inhibition via cytokine production, particularly IFN-γ, and enhance the effector functions of CD8+ T-cells and B-cells (MacLeod et al., 2010). Although subsequent MERS-CoV infection is generally antibody mediated, memory CD8+ T cells are believed to facilitate virus clearance by eliminating

infected cells (Kaech and Ahmed, 2001; Zhao et al., 2017). MERS survivors who later demonstrated strong virus-specific memory CD8+ T-cell responses were also shown to experience mitigated morbidity during the hospitalization period (Zhao et al., 2017). Similarly, the importance of T-cell responses against SARS-CoV was also highlighted in many studies (Channappanavar et al., 2014; Chu H. et al., 2014; Zhao et al., 2016). Interestingly, unlike SARS-CoV, MERS-CoV can infect both the CD4+ and CD8+ T cells in human, resulting in the downregulation of hDPP4, and induced intrinsic and extrinsic caspase-dependent apoptosis in T cells, which may lead to severe immunopathology (Chu et al., 2016). In addition, Chu et al. (2016) demonstrated the capability of MERS-CoV in infecting the T cells of common marmosets.

It is critical for a potential MERS-CoV vaccine to induce robust humoral and cell-mediated immunities. Although the protection against MERS-CoV is mainly mediated by humoral immunity, T-cell responses are crucial for acute viral clearance. Mucosal route is recommended for MERS-CoV vaccine delivery to induce the mucosal immunity in addition to the systemic responses. Persistence of the virus-specific antibodies induced by MERS-CoV vaccine is not thoroughly studied but represents a major challenge. An effective MERS-CoV vaccine is also required to induce immunological memory to provide a long-lived protection which in turn reduces the need of boosters, and in the long run will bring down the cost of vaccinations. Lastly, different adjuvants may also be used to improve the immunogenicity of MERS-CoV vaccines but would require detail studies on the interactions between them to ensure optimal vaccine efficacy and safety. So far, three potential MERS-CoV vaccines: a DNA vaccine and two viral vector-based vaccines have advanced into clinical trials (National Institutes of Health [NIH], 2016, 2018b,c).

## POTENTIAL ANTIBODY DEPENDENT ENHANCEMENT (ADE) OF MERS-CoV INFECTION

Antibody dependent enhancement (ADE) is a condition whereby non-neutralizing antibodies are produced following an infection or a vaccination, which enhance the infectivity of the subsequent infection (Kuzmina et al., 2018). ADE of viral infections have been reported for dengue virus, human immunodeficiency virus, influenza virus, other alpha and flaviviruses, SARS-CoV, and Ebola virus (Dutry et al., 2011; Kuzmina et al., 2018). Thus, ADE is a critical issue that should be considered seriously in designing a MERS-CoV vaccine.

Attributed to the taxonomic and structural similarities between SARS-CoV and MERS-CoV, the processes involved in development of new vaccines against these two viruses, to a large extent, are similar. Vaccine candidates against SARS-CoV were initially developed based on the full-length S protein. However, these vaccines were later demonstrated to induce non-neutralizing antibodies which did not prevent MERS-CoV infection, and the immunized animals were not protected from the viral challenge instead they experienced adverse effects like enhanced hepatitis, increased morbidity, and stronger inflammatory responses (Weingartl et al., 2004; Czub et al., 2005). Many potential vaccines against MERS-CoV were also mainly focused on the same full-length S protein, raising a safety concern on the practical application of these vaccines (Du et al., 2016b).

To date, no ADE has been observed in MERS-CoV. Indeed, the ADE of SARS-CoV infection in human cells was only discovered 8 years after the virus was first identified in 2003 (Yip et al., 2011). Jaume et al. (2012) demonstrated that non-neutralizing antibodies induced by the full-length S protein of SARS-CoV facilitated the viral entry into host cells via a FcγR-dependent pathway. Our understanding about MERS-CoV is relatively lesser compared to SARS-CoV, mainly due to the fact that the former was discovered less than 7 years, thus it is unsurprising that the ADE of MERS-CoV has yet to be reported (Du et al., 2016b). Nevertheless, by employing appropriate strategies and methods, the ADE of MERS-CoV infection could be revealed in the future.

Two approaches have been suggested to mitigate the adverse effects of ADE. The first approach involves shielding the non-neutralizing epitopes of the S proteins by glycosylation, whereas the second approach, namely immunofocusing, aims to direct the adaptive immune responses to target only the critical neutralizing epitope to elicit a more robust protective immunity (Du et al., 2016a; Okba et al., 2017). A supporting evidence for the latter is that a MERS-CoV vaccine candidate based on a shorter S1 domain induced slightly stronger neutralizing activity than that based on the full-length S protein. In addition, a vaccine candidate based on the even shorter RBD induced the highest neutralizing immune responses (Okba et al., 2017).

## CURRENT ANIMAL MODELS EMPLOYED FOR EVALUATION OF MERS-CoV VACCINES

Animal models available for evaluation of MERS-CoV vaccines are highly limited, thus representing a huge challenge for vaccine development. MERS-CoV infects the human (Zaki et al., 2012), non-human primates-rhesus macaques (de Wit et al., 2013; Munster et al., 2013) and marmosets (Falzarano et al., 2014), and dromedary camels (Alagaili et al., 2014; Chu D.K. et al., 2014; Memish et al., 2014). The first animal model adopted for the development of MERS-CoV vaccine was rhesus macaques (de Wit et al., 2013; Munster et al., 2013). They demonstrated clinical symptoms of MERS-CoV infection including an increase in respiratory rate and body temperature, hunched posture, piloerection, cough, and reduced food intake. Radiographic imaging analysis also revealed varying degree of pulmonary diseases following infection. Although the viral RNA of MERS-CoV was detected in most of the respiratory tissues, but viral tropism was restricted primarily to the lower respiratory tract. Rhesus macaques infected with MERS-CoV experienced transient, mild to moderate disease severity (van Doremalen and Munster, 2015; Du et al., 2016b). It is noteworthy that the pathological changes induced in rhesus macaques infected by MERS-CoV were

the results of the host inflammatory responses triggered by the virus instead of the direct viral cytolytic activity (Prescott et al., 2018).

The common marmoset is another frequently used animal model to evaluate MERS-CoV vaccines (Falzarano et al., 2014). Similar to rhesus macaques, humoral and cell-mediated immunities could be detected in these animals following MERS-CoV vaccination. The common marmosets infected with MERS-CoV developed moderate to severe acute pneumonia and increased viral load in the respiratory tract in addition to other clinical symptoms experienced by rhesus macaques (van Doremalen and Munster, 2015; Yu et al., 2017). Intriguingly, the common marmoset also demonstrated signs of renal damage as in human cases following MERS-CoV infection, and the viral RNA could be detected in other non-respiratory organs contrary to rhesus macaques (van Doremalen and Munster, 2015; Yeung et al., 2016). Falzarano et al. (2014) also reported that the common marmoset could serve as a partially lethal animal model. Similarly, Chan et al. (2015) demonstrated that marmosets challenged with MERS-CoV developed severe diseases, leading to fatality. Thereafter, marmosets have been successfully used as a moderate and severe model to study MERS-CoV (Baseler et al., 2016; Yeung et al., 2016; Chen et al., 2017; van Doremalen et al., 2017; Yu et al., 2017; de Wit et al., 2019).

The dromedary camels serve as a natural reservoir for MERS-CoV, and are responsible for zoonotic transmission of the virus to humans. Mild clinical symptoms such as increase in body temperature and rhinorrhea were observed in the dromedary camels infected with MERS-CoV (Adney et al., 2014). Interesting, MERS-CoV tropism in dromedary camels is limited to the upper respiratory tract, and is less apparent in the lower respiratory tract, contrary to rhesus macaques (Adney et al., 2014). The viral RNAs of MERS-CoV are detectable in the respiratory tract, lymph node and the excreted breath of the infected dromedary camels. Viral shedding from the upper respiratory tract of the dromedary camels may explain the efficiency of virus transmission among the camels, and from camels to humans (Adney et al., 2014). The dromedary camels immunized with MERSV-CoV vaccines were also shown to activate both the B-cell and T-cell responses (Muthumani et al., 2015; Haagmans et al., 2016; Adney et al., 2019).

Although camels are the natural reservoirs of MERS-CoV, whilst macaques and marmosets are closely related to the human, the handling of these large mammals is laborious and costly. The lack of small animal models for the initial screening of potential vaccine candidates greatly hampers the development of MERS-CoV vaccines. Unlike SARS-CoV, MERS-CoV does not readily infect smaller rodents such as mice or hamsters due to the substantial differences in the viral binding receptors, dipeptidyl peptidase 4 (DPP4) (Goldstein and Weiss, 2017). Nevertheless, considerable amount of efforts have been devoted to produce MERS-CoV-permissive small rodents for evaluation of MERS-CoV vaccines. Mice transduced by a viral vector to express human DPP4 (hDPP4) were shown to be susceptible to MERS-CoV infection, manifested by the development of pneumonia and histopathological changes in the lungs. However, viral clearance in these infected mice was observed at day-8 post-infection, failing to recapitulate severe human diseases (Zhao et al., 2014). Later, a more established transgenic mouse model expressing hDPP4 globally was developed, and it was the first lethal animal model available to evaluate MERS-CoV vaccines. Mortality was noted in these mice within days post-infection, and virus dissemination to other organs was observed with exceptionally high titer detected in the lung and brain (Agrawal et al., 2015). Recently, a transgenic mouse model was produced by replacing the full-length mouse *DPP4* gene with the human equivalent. However, these transgenic mice did not demonstrate any sign of diseases following the MERS-CoV infection, and no virus dissemination to other organs was observed (Pascal et al., 2015). CRISPR/Cas9 was also previously employed to sensitize the mice to MERS-CoV infection by substituting two amino acids at positions 288 and 230 of the mouse DPP4. Although these genetically engineered mice allowed viral replication in the lungs, they did not experience apparent morbidity following infection by the wild-type MERS-CoV. Severe diseases were observed only when the mice were infected by mouse-adapted MERS-CoV generated via 15 serial lung passages (Cockrell et al., 2016). As mouse DPP4 is vital to normal glucose homeostasis and immunity, altering the mouse DPP4 could have unforeseen complications to the mouse model (Fan et al., 2018). Therefore, another transgenic mouse model has been introduced, in which the *hDPP4* gene was inserted into the genome of C57BL/6-mouse at Rosa26 locus using the CRISPR/Cas9 technology. This mouse model, namely R26-hDPP4, when infected by MERS-CoV at low dose, developed severe lung diseases related to acute respiratory symptoms (ARDS) and central nervous system (CNS). In addition, the R26-hDPP4 is also susceptible to infection by a MERS-CoV pseudovirus, serving as an alternative to test MERS-CoV vaccines in the absence of BSL-3 facility (Fan et al., 2018). All of the animal models described above are summarized in **Table 1**.

Apart from the mouse model, rabbits were also reported to be asymptomatically infected by MERS-CoV. By extensive research, these animals could represent another potential animal model to evaluate MERS-CoV vaccines (Haagmans et al., 2015). Smaller animal models are more economically available to vaccine evaluations in addition to the ease of animal manipulation and readily available methods in testing vaccine efficacy.

## CURRENT MERS-CoV VACCINE PLATFORMS

As of now, SARS-CoV and MERS-CoV are the only coronaviruses known to cause severe diseases in human. Development of SARS vaccines was mainly focused on the S protein of SARS-CoV (Bukreyev et al., 2004; Weingartl et al., 2004; Yang et al., 2004; Czub et al., 2005; Kam et al., 2007; Lin et al., 2007; Fett et al., 2013). To date, no vaccine has been licensed to prevent MERS-CoV infection. Although several vaccine candidates are currently in clinical trials, many still remained in the pre-clinical stage. Current approaches for the

**TABLE 1 |** Animal models used for vaccine development against Middle East respiratory syndrome-coronavirus.

| Animal models | Results | Advantages/Limitations | References |
|---|---|---|---|
| Rhesus macaques | The animals manifested clinical signs within 24 h following infection, including increase in respiratory rate and body temperature, hunched posture, piloerection, cough, reduced food intake and varying degree of pneumonia. No mortality was observed in the infected animals throughout the study. The increase in white blood cell counts was early and transient, and viral-load was reported to be higher in lower respiratory tract and decreased overtime. | | Munster et al., 2013 |
| Rhesus macaques | The animals experienced early increase in neutrophil at day-1 post-infection (P.I.), and restored at day-3 P.I. Development of pneumonia in the animals was rapid after the infection but short-lived. No mortality or virus dissemination to other non-respiratory tissue was observed in the infected animals. Infection is restricted primarily at lower respiratory tract. | – Genetically closer to human<br>– Do not recapitulate severe diseases in human<br>– Expensive model due to high husbandry requirement | de Wit et al., 2013 |
| Rhesus macaques | The rectal temperature of the animals increased at 1 to 2 days P.I. and restored thereafter. Extensive lung lesions and varying degree of inflammation were observed in the lungs of the animals collected at day-3 P.I. Other pathological changes of the infected lungs include interstitial pneumonia, pulmonary edema, hemorrhaging, degeneration and necrosis of pneumocytes and bronchial epithelial cells. No sign of damage in other non-respiratory organs was observed. | | Yu et al., 2017 |
| Immunosuppressed rhesus macaques | The immunosuppressed animals developed rapid pneumonia but less severe than the non-immunosuppressed monkey. Higher viral load, viral shedding, and virus dissemination to other non-respiratory organs were observed in the immunosuppressed animals following infection. | – Potential model for mimicking MERS-CoV infection in immunocompromised patients<br>– Expensive model due to high husbandry requirement<br>– Additional treatment is required to produce immunosuppressed animals | Prescott et al., 2018 |
| Common marmosets | Most of the infected animals developed progressive severe pneumonia characterized by interstitial infiltration. Some animals were euthanized because of diseases severity. Extensive lung lesions were observed in all the infected animals at different necropsies time points. Viral RNA could be detected in blood, respiratory organs and other non-respiratory organs including kidney, suggesting virus dissemination. | – Severe, partially lethal animal model<br>– Able to manifest renal damage<br>– Expensive model due to high husbandry requirement | Falzarano et al., 2014 |
| Common marmosets | Infected animals developed severe pneumonia at day-3 P.I. characterized by exudative pathological changes with widespread pulmonary edema, hemorrhaging, and huge number of inflammatory cells. | | Yu et al., 2017 |
| Common marmosets | *In vitro* analysis using lung and kidney cells showed that hyperexpression of Smad7 or FGF2 induced by MERS-CoV led to an immense apoptotic response. Common marmosets infected with MERS-CoV demonstrated acute respiratory distress and disseminated infection in kidneys and other organs. | | Yeung et al., 2016 |
| Dromedary camels | The animals infected experimentally with MERS-CoV developed mild symptoms such as increase in body temperature and rhinorrhea. Symptoms of the infected animals lasted less than 2 weeks. Shedding of infectious virus was detected in less than 7 days P.I. but viral RNA remained detectable up to 35 days P.I. in the nasal swabs. Viral RNA, but not infectious virus, was detected in the exhaled breath of the infected animals at day-3 and -5 P.I. The Infection was restricted to upper-respiratory tract. | – Potential model for pathogenesis studies of MERS-CoV and transmission to human<br>– Do not recapitulate severe diseases in human<br>– Expensive model due to high husbandry requirement | Adney et al., 2014 |
| hDPP4-transduced mice | Mice transduced with adenoviral vector to express hDPP4 in lungs were susceptible to MERS-CoV infection. Following the infection, mice developed interstitial pneumonia in addition to reduced weight gain in young mice and weight loss in aged mice. No mortality was observed in all infected animals, and virus clearance was detected at day-6 to -8 P.I. Expression of hDPP4 in the animals' lungs lasted for 17 to 22 days after transduction. | – Ease of manipulation<br>– Low husbandry requirement<br>– Readily available methods in testing vaccine efficacy<br>– Do not recapitulate severe diseases in human | Zhao et al., 2014 |

*(Continued)*

**TABLE 1 |** Continued

| Animal models | Results | Advantages/Limitations | References |
|---|---|---|---|
| Transgenic mice expressing hDPP4 globally | Following the infection, the transgenic animals developed severe pneumonia, and 100% mortality was detected at day-6 P.I. Virus dissemination to other non-respiratory organs was detected with significantly high viral RNA in the brains and lungs. No viral RNA could be detected in the kidney or the liver of the infected mice. | – Lethal animal model<br>– Ease of manipulation<br>– Low husbandry requirement<br>– Readily available methods in testing vaccine efficacy<br>– Lack physiological expression pattern because all mouse cells express hDPP4 | Agrawal et al., 2015 |
| hDPP4-humanized transgenic mice | Humanized mice can be infected with MERS-CoV but do not demonstrate clinical sign of diseases. Pathological changes including peri-bronchiolar inflammation, interstitial infiltration, and minimal peri-vascular inflammation were observed at 2 to 4 days P.I. Viral RNA was detected in the lungs, and no virus dissemination to other organs was observed | – Ease of manipulation<br>– Low husbandry requirement<br>– Readily available methods in testing vaccine efficacy<br>– Correct physiological expression pattern<br>– Little to no clinical sign | Pascal et al., 2015 |
| CRISPR/Cas9-engineered mice | Mice genome was modified to incorporate human codons at amino acid positions 288 and 330 in the mouse *DPP4* gene causing them to become susceptible to MERS-CoV infection. The infected mice did not demonstrate any sign of diseases but supported viral replication in the lungs. Inflammation of the infected lungs was moderate. Severe disease could be induced in these mice by infecting them with mouse-adapted MERS-CoV. | – Severe, partially lethal animal model (challenged with mouse-adapted MERS-CoV only)<br>– Ease of manipulation<br>– Low husbandry requirement<br>– Readily available methods in testing vaccine efficacy | Cockrell et al., 2016 |
| hDPP4-knockin mice using CRISPR/Cas9 | hDPP4-knockin mice were susceptible to MERS-CoV infection. The mice experienced drastic weight loss above the typical euthanization endpoint (20%) by day-5 P.I. Lesions and virus load were detected in the brains and the lungs of the mice but not in the kidneys or livers. | – Lethal animal model<br>– Ease of manipulation<br>– Low husbandry requirement<br>– Readily available methods in testing vaccine efficacy<br>– Lack physiological expression pattern because all mouse cells express hDPP4 | Fan et al., 2018 |

*MERS-CoV, Middle East respiratory syndrome-coronavirus; DPP4, dipeptidyl peptidase 4; hDPP4, human dipeptidyl peptidase 4; P.I., post-infection.*

development of MERS-CoV vaccines are mostly referred to the methods used for the development of SARS-CoV vaccines during the past two decades, which include: viral vector-based vaccine, DNA vaccine, subunit vaccine, virus-like particles (VLPs)-based vaccine, inactivated whole-virus (IWV) vaccine and live attenuated vaccine.

In general, IWV vaccine is the most rapid approach for vaccine production following a new outbreak. However, the use of IWV as a vaccine in MERS was reported to be associated with hypersensitivity-type lung immunopathologic reaction in the mouse model (Agrawal et al., 2015), thereby limiting its potential. Subunit vaccine is by far the most popular method in the development of MERS vaccine, mostly focusing on the recombinant RBD of the S protein produced in heterologous expression systems. Subunit vaccines, however, are often administered along with adjuvants to boost the immunogenicity of the recombinant antigens. Nanoparticles such as VLPs-based vaccines are similar to subunit vaccines, in which only specific viral proteins are expressed. Unlike subunit vaccines, VLPs-based vaccines are comprised of recombinant viral proteins capable of self-assembling into larger particles resembling viruses. Although the immunogenicity of VLPs-based vaccines could be enhanced by adjuvants, the VLPs themselves can serve as adjuvants which increase the immunogenicity of displayed epitopes, particularly those of smaller ones (Murata et al., 2003; Quan et al., 2008). Live attenuated vaccines are composed of live viruses, which have been modified to remove or reduce their virulence. This type of vaccine is often very immunogenic, whereby a single administration without an adjuvant is sufficient to induce protective immunity. However, the risk of reversion to a virulent virus has limited its usage as MERS vaccine. Viral vector-based vaccine is one of the most popular approaches in developing MERS vaccines. Two out of the three candidate vaccines which have entered the clinical phase are viral vector vaccines. This approach utilizes well-studied virus replication system to display MERS-CoV antigen, thereby inducing protective immunity against MERS-CoV. Another candidate vaccine currently in phase I/II clinical trial is a DNA vaccine. Unlike other types of vaccines, DNA vaccine production does not involve virus replication, protein expression and purification, therefore reduce the cost of production. However, administration of DNA vaccines often requires an external device such as electroporator or gene gun, which eventually increases the cost of immunization. **Table 2** summarizes the vaccine candidates against MERS-CoV infection, which are further discussed intensively in the following sections.

**TABLE 2 |** Potential vaccine candidates against Middle East respiratory syndrome-coronavirus.

| Vaccine type | Vector and antigen | Administration route | Results | References |
|---|---|---|---|---|
| Viral-vector | rAd5 encoding S1 protein | IM | Immunization with rAd5 constructs expressing CD40-targeted S1 fusion protein (rAd5-S1/F/CD40L) offered complete protection to hDPP4 transgenic mice against MERS-CoV challenge and prevented pulmonary perivascular hemorrhage. | Hashem et al., 2019 |
| | rAd5 or rAd41 encoding S protein | IM or IG | IG administration of rAd5-S or rAd41-S elicited antigen-specific IgG and neutralizing antibody in serum, but T-cell responses were not detected. A single IM injection of Ad5-S or Ad41-S induced systemic humoral response in addition to the functional antigen-specific T-cell responses in the spleen and pulmonary lymphocytes of the mice, which persisted for several months. | Guo et al., 2015 |
| | rAd5 encoding S protein or S1 | IM and later boosted with IN | Immunized mice demonstrated antibody responses against spike protein, which neutralized MERS-CoV *in vitro*. Stronger neutralizing antibody responses were observed in the mice vaccinated with the vector encoding the shorter S1 protein than the full-length S protein. | Kim et al., 2014 |
| | ChAdOx1 encoding S protein* | IM or IN | Single dose intranasal or intramuscular immunization protected transgenic BALB/c mice against lethal virus challenge. Immunogenicity and efficacy were comparable between immunization routes. | Munster et al., 2017 |
| | ChAdOx1 encoding S protein* | IM | Single dose immunization with ChAdOx1 MERS vaccine with tPA induced 5 logs of neutralizing antibodies in BALB/c mice. | Alharbi et al., 2017 |
| | MVA encoding S protein | IM | Immunization with MVA MERS vaccine containing tPA regulated by F11 promoter induced 4.7 logs of neutralizing antibodies in BALB/c mice. | Alharbi et al., 2017 |
| | MVA encoding S protein** | IM or SC | Both immunization routes induced neutralizing antibodies and CD8+ T-cell responses in mice. Vaccinated mice were protected against MERS-CoV challenge infection after transduction with the hDPP4 receptor. | Volz et al., 2015 |
| | MVA encoding S protein** | IM | Neutralizing antibody responses were induced in immunized mice. | Song et al., 2013 |
| | MVA encoding the N-protein | IM or IP | CD8+ T-cell response was elicited in the immunized mice in both immunization routes. | Veit et al., 2018 |
| | NDV encoding S protein | IM | Recombinant NDV expressing MERS-CoV S protein induced neutralizing antibodies in BALB/c mice and Bactrian camels. | Liu et al., 2017 |
| Viral-vector and nanoparticle | rAd5 and MERS-CoV S nanoparticle | IM | Heterologous prime-boost vaccination with rAd5-S protein and alum-adjuvanted recombinant S protein induced both Th1 and Th2 immune responses in SPF BALB/c mice. | Jung et al., 2018 |
| DNA | DNA encoding S protein*** | IM followed by EP | The DNA vaccine was immunogenic in mice, camels and rhesus macaques. When the immunized macaques were challenged with MERS-CoV, characteristic clinical symptoms including pneumonia were reduced. | Muthumani et al., 2015 |
| | DNA encoding S or S1 protein | IM | DNA encoding S1 protein elicited stronger antibody and cellular immune responses in mice than that encoding the S protein. Both DNAs encoding S1 and S proteins induced neutralizing antibodies that cross-reacted with MERS-CoV strains of human and camel origins. | Al-Amri et al., 2017 |
| | DNA encoding S1 protein | IM | Immunization with DNA encoding S1 protein and passive transfer of immune sera from the vaccinated mice protected hDPP4-transduced-mice from MERS-CoV infection. | Chi et al., 2017 |

*(Continued)*

**TABLE 2 |** Continued

| Vaccine type | Vector and antigen | Administration route | Results | References |
|---|---|---|---|---|
| Subunit | MERS-CoV S1 protein | SC | Adjuvanted (MF59) MERS-CoV S1 protein protected hDPP4 transgenic mice against lethal MERS-CoV challenge, where the protection correlated well with the neutralizing antibody titer. | Wang et al., 2017c |
| | MERS-CoV S1 protein | IM | Immunization with adjuvanated (Advax HCXL adjuvant and Sigma Adjuvant System) S1 protein reduced and delayed virus shedding in the upper respiratory tract of dromedary camels and provided complete protection in alpaca against MERS-CoV challenge. | Adney et al., 2019 |
| | MERS-CoV S protein trimer on Fd | IM | Recombinant prefusion trimeric MERS-CoV S protein induced high titer of neutralizing antibodies in BALB/cJ mice. | Pallesen et al., 2017 |
| | RBD trimer on Fd | SC or IM | Adjuvanted (alum) RBD-Fd induced neutralizing antibodies in BALB/c mice and protected (83%) hDPP4 transgenic mice against lethal MERS-CoV challenge. | Tai et al., 2016 |
| | RBD fused to Fc | SC | Adjuvanted RBD-Fc induced high titer of neutralizing antibodies in BALB/c mice and New Zealand white rabbits. | Ma et al., 2014b |
| | RBD fused to Fc | SC | Mice immunized with the vaccine and Montanide ISA 51 adjuvant produced neutralizing antibodies which inhibited binding of the RBD to DPP4 receptor, neutralizing MERS-CoV infection. | Du et al., 2013 |
| | RBD fused to Fc | IN or SC | Mice vaccinated with both immunization routes in the presence of adjuvants (Montanide ISA 51 adjuvant for SC and Poly(I:C) for IN) elicited systemic humoral immune responses. Stronger systemic cellular immune responses and local mucosal immune responses were observed in mice immunized via IN route. | Ma et al., 2014a |
| | RBD fused to Fc | IM | hCD26/DPP4 transgenic mice immunized with the vaccine in the presence of adjuvant, AddaVax elicited neutralizing antibodies and were protected against MERS-CoV infection. | Nyon et al., 2018 |
| | RBD fused to Fc | SC | Mice immunized with the vaccine alone produced detectable neutralizing antibodies and cellular immune responses. Immunogenicity of the vaccine improved when the adjuvants such as Freund's adjuvant, alum, monophosphoryl lipid A, Montanide ISA51 or MF59 was included in the formulation. MF59 was demonstrated to be superior in enhancing the vaccine immunogenicity and protection against viral challenge. | Zhang et al., 2016 |
| | Recombinant RBD | IM or SC | When the subunit vaccine was administered together with combination of alum and CpG ODN, optimized RBD-specific humoral and cellular immunity were elicted. Robust RBD-specific antibody and T-cell responses were induced in mice immunized with the vaccine in combination with IFA and CpG ODN, but low level of neutralizing antibodies were induced. | Lan et al., 2014 |
| | Recombinant RBD | IM | Rhesus macaques immunized with the subunit vaccine and alum adjuvant produced neutralizing antibodies and experienced mitigated clinical symptoms when challenged with MERS-CoV. | Lan et al., 2015 |
| | rNTD of S protein | IM | Immunization with rNTD of MERS-CoV S protein adjuvanted with alum induced neutralizing antibodies and reduced the respiratory tract pathology of BALB/c mice challenged with MERS-CoV. | Jiaming et al., 2017 |

*(Continued)*

**TABLE 2 |** Continued

| Vaccine type | Vector and antigen | Administration route | Results | References |
|---|---|---|---|---|
| VLPs | MERS-CoV VLPs | IM | Co-administration of the VLPs-based vaccine and alum activated RBD specific humoral and cellular immune responses in rhesus macaques. | Wang et al., 2017b |
| | S protein nanoparticles | IM | S protein produced in the baculovirus insect cells expression system assembled into nanoparticles of approximately 25 nm. Mice immunized with these nanoparticles in the presence of alum produced high titer of neutralizing antibody. | Coleman et al., 2014 |
| | S protein nanoparticles | IM | The vaccine together with Matrix M1 adjuvant activated S protein specific humoral immune responses, and protected hDPP4 transduced mice against viral challenge. | Coleman et al., 2017 |
| | CPV VLP displaying RBD | IM | Immunization of the mice with the chimeric VLPs displaying RBD in the presence of adjuvants [alum or Poly(I:C)] elicited neutralizing antibody responses as well as cellular immune responses. | Wang et al., 2017a |
| | Influenza A VLP displaying S protein | IM | Immunization of the mice with the chimeric VLPs displaying RBD in the presence of a combination of adjuvants (alum and CpG ODN) elicited neutralizing antibody responses. | Lan et al., 2018 |
| Nanoparticle | Ferritin displaying RBD | IM | Immunization with chaperna-mediated ferritin nanoparticle displaying MERS-CoV RBD adjuvanted with MF59 induced RBD-specific antibodies in BALB/c mice which inhibited RBD binding to hDPP4 receptor protein. | Kim et al., 2018 |
| Inactivated whole -virus | MERS-CoV | IM | Mice immunized with the inactivated vaccine in the presence of a combination of adjuvants (alum and CpG ODN) elicited neutralizing activity but not cell-mediated immunity. This vaccine also protected hDPP4 transduced mice against MERS-CoV challenge. | Deng et al., 2018 |
| | MERS-CoV | IM | Gamma radiation-inactivated MERS-CoV induced neutralizing antibodies and reduced viral load in hDPP4 transgenic mice but may cause hypersensitivity-type lung immunopathologic reaction upon MERS-CoV challenge. | Agrawal et al., 2016 |
| | Chimeric RABV displaying S1 protein | IM | The inactivated vaccine induced high titer of neutralizing antibodies in mice, and protected hDPP4-transduced-mice against MERS-CoV infection. | Wirblich et al., 2017 |
| Live-attenuated | MERS-CoV mutant | - | The mutant was produced by deleting the *E* gene of the MERS-CoV. This mutant lacked infectivity but was single-cycle replicative. | Almazan et al., 2013 |
| | MERS-CoV mutant | IN | Attenuated MERS-CoV through mutation of NSP16 (D130A) protected CRISPR-Cas9-targeted 288–330$^{+/+}$ C57BL/6 mice from mouse-adapted MERS-CoV challenge. | Menachery et al., 2017 |
| | MV expressing full-length or truncated, soluble variant of S protein | IP | The recombinant MV was replication competent. Immunization of the type I interferon receptor-deficient (IFNAR$^{-/-}$) CD46Ge mice with the recombinant MV induced both MV and S protein specific neutralizing antibodies as well as cellular immune responses. The recombinant MV protected hDPP4-transduced-mice against viral challenge. | Malczyk et al., 2015 |
| | MV expressing N protein | IP | Recombinant MV expressing MERS-CoV N protein induced N-specific T cell responses in IFNAR$^{-/-}$-CD46Ge mice. | Bodmer et al., 2018 |

*(Continued)*

**TABLE 2** | Continued

| Vaccine type | Vector and antigen | Administration route | Results | Reference |
|---|---|---|---|---|
| | Recombinant VSV expressing S protein | IN or IM | Recombinant VSV was produced by replacing the glycoprotein of VSV with the S protein of MERS-CoV. The recombinant virus induced neutralizing antibodies and T cell responses in rhesus macaques after a single intramuscular or intranasal immunization dose. | Liu et al., 2018 |

*MERS-CoV, Middle East respiratory syndrome-coronavirus; rAd5, recombinant human adenovirus type-5; rAd41, recombinant human adenovirus type-41; MVA, modified vaccinia virus Ankara; ChAdOx1, chimpanzee adenovirus, Oxford University #1; NDV, Newcastle disease virus; MV, measles virus; CPV, canine parvovirus; RABV, rabies virus; VLP, virus-like particle; NSP, non-structural protein; S protein, spike protein; S1 protein, spike protein receptor binding subunit; RBD, receptor-binding domain in S1; N protein, nucleocapsid protein; rNTD, recombinant N-terminal domain; Fd, foldon trimerization motif; Fc, Fc region of human IgG; tPA, leader sequence of the human tissue plasminogen activator gene; IFNAR$^{-/-}$-CD46Ge mice, genetically modified mice deficient of type I IFN receptor and transgenically expressing human CD46; SPF, specific-pathogen-free; IM, intramuscular; IN, intranasal; IP, intraperitoneal; SC, subcutaneous; IG, intragastric; EP, electroporation. Vectors and antigens marked with "*" have entered phase I clinical trial (*MERS001; **MVA-MERS-S; ***GLS-5300).*

## VIRAL VECTOR-BASED VACCINE

The first viral vector-based vaccine was reported by Moss et al. (1984) who developed a potential hepatitis B vaccine using the vaccinia viral vector. Unlike subunit or inactivated vaccines, which generally function as extracellular antigens, a viral vector works by carrying a DNA encoding immunogenic components into host cells, followed by intracellular antigen expression, thereby activating a broad spectrum cell-mediated immunity in addition to the humoral immune responses. Majority of the viral-vector based vaccines do not require adjuvant for optimum efficacy (Ura et al., 2014). Adenovirus and modified vaccinia virus Ankara (MVA) are the two most common viral vectors used in the development of MERS-CoV vaccines.

Mice immunized intramuscularly with the recombinant human adenoviral (type 5 or 41) vector encoding the full-length S protein were shown to induce systemic neutralizing antibodies and mucosal T-cells immunity. Intriguingly, no mucosal T-cell response was detected when the vaccine was administered via an intragastric route, contrary to previous findings which suggested the importance of mucosal vaccination in activating the mucosal immunity (Guo et al., 2015). A recombinant human adenovirus type 5 (rAd5) vector encoding the shorter S1 extracellular domain of the S protein was reported to elicit slightly stronger neutralizing antibody responses than that encoding the full-length, suggesting the effect of immunofocusing (Kim et al., 2014). A recent study by Hashem et al. (2019) demonstrated that rAd5 constructs expressing CD40-targeted S1 fusion protein (rAd5-S1/F/CD40L) offered a complete protection to hDPP4 transgenic mice against MERS-CoV challenge, and prevented pulmonary perivascular hemorrhage. Additionally, Jung et al. (2018) showed that heterologous prime-boost vaccination with rAd5-S protein and alum-adjuvanted recombinant S protein nanoparticle successfully induced both the Th1 and Th2 immune responses in specific-pathogen-free BALB/c mice.

Pre-existing immunity against human adenovirus in human population is widespread, hampering its clinical application as a vector for vaccine development (Fausther-Bovendo and Kobinger, 2014). Recent developments of new adenovirus vectors for vaccine antigen delivery focus on the serotype to which human population is less exposed. Chimpanzee adenovirus (ChAdOx1) represents an attractive alternative to the human adenoviral vector due to its good safety profile and lack of pre-existing immunity in human population (Dicks et al., 2012), and has since been employed in the vaccine development against MERS-CoV infection. The recombinant ChAdOx1 encoding full-length S protein (ChAdOx1 MERS) was shown to be immunogenic in mice, and lethal virus challenge using hDPP4 transgenic mouse model further demonstrated its high protective efficacy against MERS-CoV (Alharbi et al., 2017; Munster et al., 2017). It is noteworthy that the immunogenicity of S protein could be improved by insertion of a gene encoding the signal peptide of human tissue plasminogen activator (tPA) upstream of the *S* gene of MERS-CoV, in both ChAdOx1 and MVA vectors (Alharbi et al., 2017). Currently, a candidate MERS-CoV vaccine known as MERS001, which contains the ChAdOx1 encoding the S protein of MERS-CoV is at phase I clinical trial. The trial is estimated to be completed by December 2019, in which the safety and immunogenicity of MERS001 at different dosage are being studied in healthy adult volunteers recruited and sponsored by the University of Oxford, United Kingdom (National Institutes of Health [NIH], 2018b).

Recombinant MVA encoding the full-length S protein represents another potential MERS-CoV vaccine candidate due to its good safety profile, decent immunogenicity, and high protective efficacy against MERS-CoV (Song et al., 2013; Volz et al., 2015; Alharbi et al., 2017). Another candidate vaccine currently in phase I clinical trial is MVA-MERS-S. The trial is being performed by the University Medical Center Hamburg-Eppendorf, Germany, in which the safety and immunogenicity of MVA-MERS-S in healthy adult volunteers are being assessed (National Institutes of Health [NIH], 2018c). Apart from the S protein, the highly conserved N protein of MERS-CoV was inserted into MVA, and inoculated into mice. Although the recombinant MVA encoding the N-protein elicited CD8+ T-cell response in the immunized mice, its protective efficacy was not investigated (Veit et al., 2018).

Apart from adenovirus and MVA, Newcastle disease virus (NDV) was also used as a viral-vector for displaying MERS-CoV S protein. The NDV-based vaccine candidate induced neutralizing antibodies in BALB/c mice and Bactrian camels (Liu et al., 2017). Although viral vector-based vaccines are able

to induce robust immune responses, they are not free from drawbacks, which include pre-existing immunity against viral vector, risk of pathogenesis, low viral titer production, and potential tumorigenesis (Ura et al., 2014).

## DNA VACCINE

DNA vaccine is composed of a recombinant plasmid encoding immunogens. This vaccine is typically delivered via direct injection, gene gun, or electroporation into host cells, where the immunogens can be expressed and prime the immune system (Ferraro et al., 2011). DNA vaccine offers two distinct advantages over the subunit or protein-based vaccine: the ease of DNA manipulation and low cost of production (Leitner et al., 1999).

Similarly, all DNA vaccines developed against MERS-CoV target the S protein or the shorter S1 domain of MERS-CoV. DNA encoding the full-length S protein was shown to induce neutralizing antibodies and robust cell-mediated immunity in mice, macaques, and camels. When the immunized macaques were challenged with MERS-CoV, characteristic clinical symptoms including pneumonia were mitigated (Muthumani et al., 2015). GLS-5300 is one of the three candidate vaccines currently in a clinical trial. Sponsored by the GeneOne Life Science, Inc., Korea, a phase I clinical trial to test the vaccine's safety profile in human volunteers was completed in the Walter Reed Army Institute of Research, United States (National Institutes of Health [NIH], 2016). Currently, the phase I and phase II clinical trials are being performed in the International Vaccine Institute, Korea, to further evaluate the safety and immunogenicity of GLS-5300, as well as a device for electroporation (CELLECTRA® 2000 Electroporation) (National Institutes of Health [NIH], 2018a).

To avoid the possible adverse effects induced by the full-length S protein, other researchers revealed that immunization with a DNA encoding the S1 domain, and passive transfer of immune sera from the vaccinated mice protected hDPP4-transduced-mice from MERS-CoV infection (Chi et al., 2017). The DNA encoding the S1 domain was also demonstrated to be more superior than that encoding the full-length S protein in eliciting antibody and cellular responses. Both DNAs encoding the S1 and S proteins were shown to induce neutralizing antibodies that cross-reacted with MERS-CoV strains of human and camel origins (Al-Amri et al., 2017). Despite the effectiveness of DNA vaccines, spontaneous plasmid integration into host genomes represents a potential risk, but the probability is extremely low (Ledwith et al., 2000).

## SUBUNIT VACCINE

In general, subunit vaccines have the highest safety profile among all current vaccines despite their low immunogenicities (Du et al., 2016b). Precautions should be taken during the development of MERS-CoV vaccines based on the S protein to avoid induction of non-neutralizing antibodies. Unlike the full-length S protein, RBD of MERS-CoV comprises the critical neutralizing domains but lacking the non-neutralizing immunodominant region. Therefore, upon immunization, the RBD-based vaccines are restricted to produce RBD-specific neutralizing immune responses, thus are incapable of inducing non-neutralizing antibodies that may potentially contribute to harmful pathological effects (Du and Jiang, 2015; Wang et al., 2015a). From the safety and effectiveness perspectives, the RBD is a more promising candidate in the development of MERS-CoV vaccines over the full-length S protein.

The RBD of MERS-CoV was reported to induce neutralizing antibodies against multiple strains of MERS-CoV due to the presence of several conformational neutralizing epitopes (Du et al., 2016b). Any MERS-CoV strains with a single mutation in an epitope may not suffice to escape the RBD-specific neutralizing antibodies. Wang et al. (2015a) demonstrated that an amino acid mutation at position 509 (aspartic acid to glycine substitution) in RBD rendered the mutated strain resisted to neutralization by a RBD-specific monoclonal antibody, F11, but susceptible to another RBD-specific monoclonal antibody, D12. Both of these antibodies could bind to different regions of the RBD of MERS-CoV. Similarly, the RBD of SARS-CoV also consists of multiple neutralizing domains that are capable of inducing broad neutralizing immune responses against many SARS-CoV strains (He et al., 2006). Development of antibody escape mutants may require a mutation in two or more epitopes in the RBD of MERS-CoV, which is less likely to take place, and if developed, may exhibit reduced viral fitness (Tang et al., 2014; Tai et al., 2017).

It was demonstrated that the MERS-CoV S1 protein with MF59 adjuvant protected hDPP4 transgenic mice against lethal MERS-CoV challenge, where the protection correlated well with the neutralizing antibody titer (Wang et al., 2017c). In addition, adjuvanted recombinant S1 proteins (Advax HCXL adjuvant and Sigman Adjuvant System) reduced and delayed virus shedding in the upper respiratory tract of dromedary camels (MERS-CoV animal reservoir), and provided complete protection in alpaca (a surrogate infection model) against MERS-CoV challenge (Adney et al., 2019).

In general, MERS-CoV subunit vaccines based on the S1 domain require the use of adjuvant or fusion with an immune enhancer to heighten immunogenicity. Several studies have indicated that RBD fused with Fc fragment of human IgG (RBD-Fc) elicited strong systemic neutralizing antibody and cellular immune responses in vaccinated mice (Du et al., 2013; Ma et al., 2014a; Tang et al., 2015; Nyon et al., 2018) and New Zealand white rabbits (Ma et al., 2014b). hDPP4-transduced-mice immunized with RBD-Fc were also protected from viral challenge (Ma et al., 2014a). Other adjuvants such as Freund's adjuvant, alum, monophosphoryl lipid A, Montanide ISA51 and MF59 were also reported to further improve the immunogenicity and protection of RBD-Fc in mice, particularly MF59 is superior among these adjuvants (Zhang et al., 2016). In addition, co-administration of multiple adjuvants together with RBD antigen could synergistically improve the immunogenicity of the RBD-based subunit vaccine. Mice immunized with RBD antigen together with alum and CpG ODN produced stronger humoral and cellular immune responses than those immunized with RBD

antigen and alum or CPG ODN alone (Lan et al., 2014). RBD-based subunit vaccine was also previously tested in the rhesus macaque model in the presence of alum. This vaccine formulation was shown to induce robust and sustained humoral and cellular immunities, and partially protected rhesus macaques from viral challenge (Lan et al., 2015).

As native spikes of MERS-CoV exist in the form of trimers, vaccine designs mimicking the native viral S proteins have also been reported (Tai et al., 2016; Pallesen et al., 2017). Through the use of foldon (Fd), a T4 fibritin trimerization domain, Pallesen et al. (2017) synthesized a recombinant prefusion trimeric MERS-CoV S protein, which induced high titer of neutralizing antibodies in BALB/cJ mice. Similarly, Tai et al. (2016) expressed RBD trimers on Fd, and demonstrated the vaccine's protective efficacy (83% survival) in hDPP4 transgenic mice against lethal MERS-CoV challenge.

Although most of the subunit vaccine studies focused on the RBD of the S protein, a recent study by Jiaming et al. (2017) proposed the use of recombinant N-terminal domain (rNTD) of the S protein as another potential vaccine candidate. The rNTD, when used to immunize BALB/c mice, induced neutralizing antibodies and reduced the respiratory tract pathology of mice in a non-lethal MERS-CoV challenge.

Apart from focusing on the S protein, multivalent vaccines designed using *in silico* methods which contain the B cell and T cell epitopes of S, E, M, N and NSPs have been proposed (Srivastava et al., 2018). However, until now, no biological data have been presented for these multivalent vaccines. In addition, the N protein and S2 domain of S protein are more conserved among coronaviruses, representing other attractive targets in the development of a broad-spectrum coronavirus vaccine (Schindewolf and Menachery, 2019). Nevertheless, it is crucial to ensure that these proteins do not contribute to the ADE of MERS-CoV infection.

## VIRUS-LIKE PARTICLES (VLPs)-BASED VACCINE

Virus-like particles are nanoscale particles similar to the native viral particles but devoid of infectious genetic materials. They are composed of repetitive viral structural proteins with inherent self-assembly properties. VLPs are non-replicative and non-infectious. VLPs can be produced by expressing the viral structural proteins in a suitable expression system (Yong et al., 2015a,b; Ong et al., 2017). In general, VLPs-based vaccine is similar to the whole inactivated virus vaccine, but it does not require the viral inactivation step which may alter the antigenicity and immunogenicity of a viral protein. Because no live virus is involved in the manufacturing process, VLPs can be easily generated in a low-containment manufacturing environment (DeZure et al., 2016).

Virus-like particles of MERS-CoV were previously produced in baculoviral expression system by co-expressing the S, E and M proteins of MERS-CoV. The VLPs generated were indistinguishable from the authentic viral particle when observed under an electron microscope. These VLPs, when administered with alum induced neutralizing antibodies and a Th1-biased immunity in rhesus macaques (Wang et al., 2017b). Intriguingly, when the S protein of MERS-CoV was expressed alone, it self-assembles into nanoparticles of approximately 25 nm, about a quarter of the diameter of the authentic viral particle. Immunogenicity studies in mice demonstrated that these nanoparticles elicited antibody responses in the presence of alum, and when the adjuvant was replaced with Matrix M1 adjuvant, they induced a significantly higher titer of neutralizing antibodies (Coleman et al., 2014). Viral challenge in hDPP4-transduced-mice which had been immunized with Matrix M1 and S protein nanoparticles further proven the protective efficacy of this vaccine formulation against MERS-CoV (Coleman et al., 2017). As mentioned earlier under the viral vector-based vaccine, adjuvanted S protein nanoparticles as boosters in mice primed with rAd-5 S have also yielded promising Th1 and Th2 immune responses (Jung et al., 2018).

Advancement in genetic engineering enables VLPs to display different epitopes of viruses, producing chimeric VLPs (cVLPs) (Ong et al., 2017). Expression of the RBD of MERS-CoV fused to the VP2 structural protein of canine parvovirus (CPV) produced cVLPs displaying the RBD of MERS-CoV. These cVLPs were morphologically similar to native CPV and elicited both RBD-specific humoral and cell-mediated immunities in mice (Wang et al., 2017a). The cVLPs displaying the S protein of MERS-CoV and matrix 1 protein of influenza A virus were also developed, and shown to be immunogenic in mouse models. However, the actual protective efficacy of these cVLPs against MERS-CoV has yet to be investigated *in vivo* (Lan et al., 2018).

In addition to vaccines based on VLPs, non-viral nanoparticle such as ferritin has also been reported as a potential carrier for MERS-CoV antigen (Kim et al., 2018). Kim et al. (2018) utilized a chaperna-mediated ferritin nanoparticle to display MERS-CoV RBD. When adjuvanted with MF59, the ferritin-based nanoparticle induced RBD-specific antibodies in BALB/c mice, which inhibited RBD binding to hDPP4 receptor protein, suggesting its potential use as MERS-CoV antigen carrier (Kim et al., 2018).

## INACTIVATED WHOLE-VIRUS VACCINE

Inactivated whole-virus comprises the entire disease causing virion which is inactivated physically (heat) or chemically. IWV offers several advantages, including relatively low cost of production, good safety profile, and does not involve laborious genetic manipulation (DeZure et al., 2016). Nevertheless, production of IWV requires the live virus to be grown under a high-level containment, and the antigenicity of the immunogen could be altered in the viral inactivation step (DeZure et al., 2016).

Formaldehyde-inactivated-MERS-CoV induced neutralizing antibodies in mice, but not T-cell response. Supplementing this IWV with a combined adjuvant (alum and CpG ODN) was reported to enhance its protective immunity against MERS-CoV in mice transduced with hDPP4 (Deng et al., 2018). On the other hand, an inactivated bivalent whole virus vaccine

that targets rabies virus (RABV) and MERS-CoV was recently developed using a recombinant vector encoding a fusion protein comprising the MERS-CoV S1 domain fused to the C-terminus of RABV G protein. Following expression, the S1 domain was incorporated into RABV particles (BNSP333-S1). When the mice were immunized with the chemically inactivated BNSP333-S1, robust neutralizing antibody responses against S1 and G proteins were detected. Inactivated BNSP333-S1 also protected hDPP4-transduced-mice against MERS-CoV challenge (Wirblich et al., 2017). Despite the benefits associated with IWV-based vaccines, inactivated MERS-CoV vaccine was reported to potentially cause a hypersensitivity-type lung immunopathologic reaction upon MERS-CoV challenge, even though it induced neutralizing antibodies and reduced the viral load in hDPP4 transgenic mice, similar to those observed in SARS-CoV (Agrawal et al., 2016).

## LIVE ATTENUATED VACCINE

Live attenuated vaccine is one of the most effective vaccines due to its capability to induce immunity similar to the natural infection. This vaccine contains viable but attenuated virus. Common approaches to develop a live attenuated vaccine include deletion of the viral genes that confer virulence, and via reverse genetic. In general, live attenuated vaccines are highly immunogenic, thus do not require adjuvant for optimal efficacy, and single immunization is usually sufficient to induce protective immunity. Nevertheless, live attenuated vaccines come with some unwanted limitations, particularly the risk of reversion to a virulent strain, and the absolute need for vaccine cold chain. Live attenuated vaccine is also not suitable for infants, immunocompromised individuals, and elderly people (Lauring et al., 2010).

A live attenuated vaccine against MERS-CoV was previously developed by deleting the *E* gene of MERS-CoV (rMERS-CoV-ΔE). This engineered virus lacked infectivity and replicated in a single cycle. Vaccines based on the live attenuated viruses could pose biosafety problems associated with the risk of virulence reversion, whereas rMERS-CoV-ΔE is propagation defective in the absence of E protein, preventing a straightforward reversion to virulence, thus providing a safer alternative (Almazan et al., 2013). More recently, a live attenuated MERS-CoV was generated through mutation of NSP16 (D130A), where the attenuated virus protected CRISPR-Cas9-targeted 288–330$^{+/+}$ C57BL/6 mice from a mouse-adapted MERS-CoV challenge (Menachery et al., 2017).

Other than MERS-CoV, a replication competent recombinant measles virus (MV) was used as a platform for the development of live attenuated MERS-CoV vaccine. The recombinant MV was engineered to express the full-length S protein (MV$_{vac2}$-CoV-S) or its truncated version (MV$_{vac2}$-CoV-solS). Both MV$_{vac2}$-CoV-S and MV$_{vac2}$-CoV-solS were shown to induce neutralizing antibodies and cell-mediated immune responses against MV and MERS-CoV, and protected hDPP4-transduced-mice from MERS-CoV challenge (Malczyk et al., 2015). Three years later, Bodmer et al. (2018) compared the MV$_{vac2}$-CoV-S with its UV-inactivated derivative, and showed that the inactivated version did not induce any specific immune response against both the MV and MERS-CoV. Concurrently, Bodmer et al. (2018) constructed a live attenuated recombinant MV expressing MERS-CoV N protein (MV$_{vac2}$-MERS-N), and its administration into IFNAR$^{-/-}$-CD46Ge mice (genetically modified mice deficient of type I IFN receptor and transgenically expressing human CD46) induced N-specific T cell responses, although not as strong as those of MV$_{vac2}$-CoV-S. Similarly, in another study, a viable recombinant vesicular stomatitis virus (VSV) with its G protein replaced with the S protein of MERS-CoV also elicited both humoral and cell-mediated immunities in rhesus macaques (Liu et al., 2018).

## OBSTACLES IN BRINGING MERS VACCINES TO THE MARKET

Development of MERS vaccines started immediately following the discovery of MERS-CoV in 2012. Pre-clinical trials on animal models capable of recapitulating the clinical signs and symptoms in the human are a must prior to clinical trials and licensing of a vaccine (Gerdts et al., 2007). The choice of an animal model is generally preferable to be as phylogenetically closer as possible to the human (Swearengen, 2018). Therefore, majority of the vaccine candidates will be evaluated in non-human primates such as chimpanzees, rhesus macaques (Sibal and Samson, 2001) or marmosets (Carrion and Patterson, 2012). Employing these animal models in experiments, however, is extremely costly (Gerdts et al., 2015). Before involving non-human primates in a vaccine evaluation, strong justification or supporting evidence from *in vitro* analysis, or more preferable from animal studies such as small rodents are often required (Gerdts et al., 2015). However, MERS-CoV cannot infect smaller rodents naturally, representing a huge challenge in initial vaccine developments (Goldstein and Weiss, 2017). Although transgenic mouse models for evaluation of MERS-CoV vaccines have been successfully developed, the costs of these transgenic animals are not affordable by many research groups, especially those from the less affluent parts of the world. This issue consequently delayed the development of an effective vaccine, and its advancement into clinical trial.

Funding is the primary drivers in any vaccine developments. Many vaccines demonstrating promising results at the pre-clinical stage require additional investments from the government or the private industry to advance into clinical trials (Hakoum et al., 2017). However, government funding for clinical trials is rather restricted, whereas private industry is generally profit oriented, of which the market size and potential profits are of priority (Smith, 2000). Unlike other widespread diseases such as hepatitis and influenza, MERS cases are primarily reported in Saudi Arabia apart from the Korea outbreak (Gossner et al., 2016). Its relatively low occurrence is likely to limit the market size of MERS vaccines, leading to lower interest by the private funding bodies. Although three potential MERS vaccine candidates have advanced into clinical trials, they are currently

in phase I/II. As completing the entire trials often take 10 years and above, they are unlikely to be commercially available in the coming 3–5 years.

## CONCLUSION

Despite having a low occurrence of recorded human-to-human transmission, the recent MERS outbreak in South Korea which demonstrated virus emergence in second and third generation contacts has reignited public awareness regarding the danger of MERS-CoV. As no effective treatment against MERS is currently available, therefore the best solution is to develop a functional MERS vaccine to prevent MERS-CoV infection. Amongst the six types of vaccines discussed above, more studies are focused on the viral vector-based and subunit vaccines. Even though many promising vaccine candidates have been proposed and reported, as of now, only three potential MERS-CoV vaccine candidates have progressed to phase I clinical trials: a DNA vaccine (GLS-5300) and two viral vector-based vaccines (MVA-MERS-S and MERS001. It is still very likely that no MERS vaccine will be available in the market for human in the near future. Therefore, considerable efforts should be given to minimize delays in executing clinical trials, such as better understanding and coordination between sponsors, primary investigators, investigators, participants and stakeholders.

## AUTHOR CONTRIBUTIONS

CY and HO wrote the manuscript. SY, KH, and WT reviewed, edited, and approved its final version.

## FUNDING

This work was supported by the Universiti Putra Malaysia (Grant No: GP-IPS/2018/9602500).

## REFERENCES

Adney, D. R., van Doremalen, N., Brown, V. R., Bushmaker, T., Scott, D., de Wit, E., et al. (2014). Replication and shedding of MERS-CoV in upper respiratory tract of inoculated dromedary camels. *Emerg. Infect. Dis.* 20, 1999–2005. doi: 10.3201/eid2012.141280

Adney, D. R., Wang, L., van Doremalen, N., Shi, W., Zhang, Y., Kong, W. P., et al. (2019). Efficacy of an adjuvanted middle east respiratory syndrome coronavirus spike protein vaccine in dromedary camels and alpacas. *Viruses*11:E212. doi: 10.3390/v11030212

Agnihothram, S., Gopal, R., Yount, B. L., Jr., Donaldson, E. F., Menachery, V. D., Graham, R. L. (2014). Evaluation of serologic and antigenic relationships between middle eastern respiratory syndrome coronavirus and other coronaviruses to develop vaccine platforms for the rapid response to emerging coronaviruses. *J. Infect Dis.* 209, 995–1006. doi: 10.1093/infdis/jit609

Agrawal, A. S., Garron, T., Tao, X., Peng, B. H., Wakamiya, M., Chan, T. S., et al. (2015). Generation of a transgenic mouse model of middle east respiratory syndrome coronavirus infection and disease. *J. Virol.* 89, 3659–3670. doi: 10.1128/JVI.03427-3414

Agrawal, A. S., Tao, X., Algaissi, A., Garron, T., Narayanan, K., Peng, B. H., et al. (2016). Immunization with inactivated middle east respiratory syndrome coronavirus vaccine leads to lung immunopathology on challenge with live virus. *Hum. Vaccin. Immunother.* 12, 2351–2356. doi: 10.1080/21645515.2016.1177688

Al-Amri, S. S., Abbas, A. T., Siddiq, L. A., Alghamdi, A., Sanki, M. A., Al-Muhanna, M. K., et al. (2017). Immunogenicity of candidate MERS-CoV DNA vaccines based on the spike protein. *Sci. Rep.* 7:44875. doi: 10.1038/srep44875

Alagaili, A. N., Briese, T., Mishra, N., Kapoor, V., Sameroff, S. C., Burbelo, P. D., et al. (2014). Middle east respiratory syndrome coronavirus infection in dromedary camels in Saudi Arabia. *MBio* 5:e00884-e14. doi: 10.1128/mBio.00884-14

Alharbi, N. K., Padron-Regalado, E., Thompson, C. P., Kupke, A., Wells, D., Sloan, M. A., et al. (2017). ChAdOx1 and MVA based vaccine candidates against MERS-CoV elicit neutralising antibodies and cellular immune responses in mice. *Vaccine* 35, 3780–3788. doi: 10.1016/j.vaccine.2017.05.032

Almazan, F., DeDiego, M. L., Sola, I., Zuniga, S., Nieto-Torres, J. L., Marquez-Jurado, S., et al. (2013). Engineering a replication-competent, propagation-defective middle east respiratory syndrome coronavirus as a vaccine candidate. *MBio* 4:e00650-13. doi: 10.1128/mBio.00650-13

Baseler, L. J., Falzarano, D., Scott, D. P., Rosenke, R., Thomas, T., Munster, V. J., et al. (2016). An acute immune response to middle east respiratory syndrome coronavirus replication contributes to viral pathogenicity. *Am. J. Pathol.* 186, 630–638. doi: 10.1016/j.ajpath.2015.10.025

Bodmer, B. S., Fiedler, A. H., Hanauer, J. R. H., Prufer, S., and Muhlebach, M. D. (2018). Live-attenuated bivalent measles virus-derived vaccines targeting middle east respiratory syndrome coronavirus induce robust and multifunctional T cell responses against both viruses in an appropriate mouse model. *Virol* 521, 99–107. doi: 10.1016/j.virol.2018.05.028

Bukreyev, A., Lamirande, E. W., Buchholz, U. J., Vogel, L. N., Elkins, W. R., St Claire, M., et al. (2004). Mucosal immunisation of African green monkeys (*Cercopithecus aethiops*) with an attenuated parainfluenza virus expressing the SARS coronavirus spike protein for the prevention of SARS. *Lancet* 363, 2122–2127. doi: 10.1016/s0140-6736(04)16501-x

Carrion, R., Jr., and Patterson, J. L. (2012). An animal model that reflects human disease: the common marmoset (*Callithrix jacchus*). *Curr. Opi. Virol.* 2, 357–362. doi: 10.1016/j.coviro.2012.02.007

Cauchemez, S., Nouvellet, P., Cori, A., Jombart, T., Garske, T., Clapham, H., et al. (2016). Unraveling the drivers of MERS-CoV transmission. *Proc. Natl. Acad. Sci. U.S.A.* 113, 9081–9086. doi: 10.1073/pnas.1519235113

Chan, J. F., Yao, Y., Yeung, M. L., Deng, W., Bao, L., Jia, L., et al. (2015). Treatment with lopinavir/ritonavir or interferon-beta1b improves outcome of MERS-CoV infection in a nonhuman primate model of common marmoset. *J. Infect. Dis.* 212, 1904–1913. doi: 10.1093/infdis/jiv392

Channappanavar, R., Zhao, J., and Perlman, S. (2014). T cell-mediated immune response to respiratory coronaviruses. *Immunol. Res.* 59, 118–128. doi: 10.1007/s12026-014-8534-z

Chen, Z., Bao, L., Chen, C., Zou, T., Xue, Y., Li, F., et al. (2017). Human neutralizing monoclonal antibody inhibition of middle east respiratory syndrome coronavirus replication in the common marmoset. *J. Infect. Dis.* 215, 1807–1815. doi: 10.1093/infdis/jix209

Chi, H., Zheng, X., Wang, X., Wang, C., Wang, H., Gai, W., et al. (2017). DNA vaccine encoding middle east respiratory syndrome coronavirus S1 protein induces protective immune responses in mice. *Vaccine* 35, 2069–2075. doi: 10.1016/j.vaccine.2017.02.063

Chowell, G., Abdirizak, F., Lee, S., Lee, J., Jung, E., Nishiura, H., et al. (2015). Transmission characteristics of MERS and SARS in the healthcare setting: a comparative study. *BMC Med.* 13:210. doi: 10.1186/s12916-015-0450-450

Chu, D. K., Poon, L. L., Gomaa, M. M., Shehata, M. M., Perera, R. A., Abu Zeid, D., et al. (2014). MERS coronaviruses in dromedary camels, Egypt. *Emerg. Infect. Dis.* 20, 1049–1053. doi: 10.3201/eid2006.140299

Chu, H., Zhou, J., Wong, B. H., Li, C., Chan, J. F., Cheng, Z. S., et al. (2016). Middle east respiratory syndrome coronavirus rfficiently infects human primary T lymphocytes and activates the extrinsic and intrinsic apoptosis pathways. *J. Infect. Dis.* 213, 904–914. doi: 10.1093/infdis/jiv380

Chu, H., Zhou, J., Wong, B. H., Li, C., Cheng, Z. S., Lin, X., et al. (2014). Productive replication of middle east respiratory syndrome coronavirus

in monocyte-derived dendritic cells modulates innate immune response. *Virol* 454-455, 197–205. doi: 10.1016/j.virol.2014.02.018

Cockrell, A. S., Yount, B. L., Scobey, T., Jensen, K., Douglas, M., Beall, A., et al. (2016). A mouse model for MERS coronavirus-induced acute respiratory distress syndrome. *Nat. Microbiol.* 2:16226. doi: 10.1038/nmicrobiol.2016.226

Coleman, C. M., Liu, Y. V., Mu, H., Taylor, J. K., Massare, M., Flyer, D. C., et al. (2014). Purified coronavirus spike protein nanoparticles induce coronavirus neutralizing antibodies in mice. *Vaccine* 32, 3169–3174. doi: 10.1016/j.vaccine.2014.04.016

Coleman, C. M., Venkataraman, T., Liu, Y. V., Glenn, G. M., Smith, G. E., Flyer, D. C., et al. (2017). MERS-CoV spike nanoparticles protect mice from MERS-CoV infection. *Vaccine* 35, 1586–1589. doi: 10.1016/j.vaccine.2017.02.012

Czub, M., Weingartl, H., Czub, S., He, R., and Cao, J. (2005). Evaluation of modified vaccinia virus ankara based recombinant SARS vaccine in ferrets. *Vaccine* 23, 2273–2279. doi: 10.1016/j.vaccine.2005.01.033

de Wit, E., Feldmann, F., Horne, E., Okumura, A., Cameroni, E., Haddock, E., et al. (2019). Prophylactic efficacy of a human monoclonal antibody against MERS-CoV in the common marmoset. *Antiviral. Res.* 163, 70–74. doi: 10.1016/j.antiviral.2019.01.016

de Wit, E., Rasmussen, A. L., Falzarano, D., Bushmaker, T., Feldmann, F., Brining, D. L., et al. (2013). Middle east respiratory syndrome coronavirus (MERS-CoV) causes transient lower respiratory tract infection in rhesus macaques. *Proc. Natl. Acad. Sci. U.S.A.* 110, 16598–16603. doi: 10.1073/pnas.1310744110

Deng, Y., Lan, J., Bao, L., Huang, B., Ye, F., Chen, Y., et al. (2018). Enhanced protection in mice induced by immunization with inactivated whole viruses compare to spike protein of middle east respiratory syndrome coronavirus. *Emerg. Microbes. Infect.* 7:60. doi: 10.1038/s41426-018-0056-57

DeZure, A. D., Berkowitz, N. M., Graham, B. S., and Ledgerwood, J. E. (2016). Whole-Inactivated and virus-like particle vaccine strategies for chikungunya virus. *J. Infect. Dis.* 214(suppl. 5), S497–S499. doi: 10.1093/infdis/jiw352

Dicks, M. D. J., Spencer, A. J., Edwards, N. J., Wadell, G., Bojang, K., Gilbert, S. C., et al. (2012). A novel chimpanzee adenovirus vector with low human seroprevalence: improved systems for vector derivation and comparative immunogenicity. *PLoS One* 7:e40385. doi: 10.1371/journal.pone.0040385

Du, L., and Jiang, S. (2015). Middle east respiratory syndrome: current status and future prospects for vaccine development. *Exp. Opin. Biol. Ther.* 15, 1647–1651. doi: 10.1517/14712598.2015.1092518

Du, L., Kou, Z., Ma, C., Tao, X., Wang, L., Zhao, G., et al. (2013). A truncated receptor-binding domain of MERS-CoV spike protein potently inhibits MERS-CoV infection and induces strong neutralizing antibody responses: implication for developing therapeutics and vaccines. *PLoS One* 8:e81587. doi: 10.1371/journal.pone.0081587

Du, L., Tai, W., Yang, Y., Zhao, G., Zhu, Q., Sun, S., et al. (2016a). Introduction of neutralizing immunogenicity index to the rational design of MERS coronavirus subunit vaccines. *Nat. Commun.* 7:13473. doi: 10.1038/ncomms13473

Du, L., Tai, W., Zhou, Y., and Jiang, S. (2016b). Vaccines for the prevention against the threat of MERS-CoV. *Expert. Rev. Vaccines* 15, 1123–1134. doi: 10.1586/14760584.2016.1167603

Du, L., Yang, Y., Zhou, Y., Lu, L., Li, F., and Jiang, S. (2017). MERS-CoV spike protein: a key target for antivirals. *Expert. Opin. Ther. Targets* 21, 131–143. doi: 10.1080/14728222.2017.1271415

Dutry, I., Yen, H. L. Lee, H., Peiris, M., and Jaume, M. (2011). Antibody-dependent enhancement (ADE) of infection and its possible role in the pathogenesis of influenza. *BMC Proc.* 5(Suppl. 1):P62. doi: 10.1186/1753-6561-5-S1-P62

Falzarano, D., de Wit, E., Feldmann, F., Rasmussen, A. L., Okumura, A., Peng, X., et al. (2014). Infection with MERS-CoV causes lethal pneumonia in the common marmoset. *PLoS Pathog.* 10:e1004250. doi: 10.1371/journal.ppat.1004250

Fan, C., Wu, X., Liu, Q., Li, Q., Liu, S., Lu, J., et al. (2018). A human DPP4-knockin mouse's susceptibility to infection by authentic and pseudotyped MERS-CoV. *Viruses* 10:E448. doi: 10.3390/v10090448

Fausther-Bovendo, H., and Kobinger, G. P. (2014). Pre-existing immunity against Ad vectors: humoral, cellular, and innate response, what's important? *Hum. Vaccines Immunother.* 10, 2875–2884. doi: 10.4161/hv.29594

Ferraro, B., Morrow, M. P., Hutnick, N. A., Shin, T. H., Lucke, C. E., and Weiner, D. B. (2011). Clinical applications of DNA vaccines: current progress. *Clin. Infect. Dis.* 53, 296–302. doi: 10.1093/cid/cir334

Fett, C., DeDiego, M. L., Regla-Nava, J. A., Enjuanes, L., and Perlman, S. (2013). Complete protection against severe acute respiratory syndrome coronavirus-mediated lethal respiratory disease in aged mice by immunization with a mouse-adapted virus lacking E protein. *J. Virol.* 87, 6551–6559. doi: 10.1128/jvi.00087-13

Gerdts, V., Littel-van den Hurk, S. V. D., Griebel, P. J., and Babiuk, L. A. (2007). Use of animal models in the development of human vaccines. *Future Microbio.* 2, 667–675. doi: 10.2217/17460913.2.6.667

Gerdts, V., Wilson, H. L., Meurens, F., van Drunen Littel-van den Hurk, S., Wilson, D., Walker, S., et al. (2015). Large animal models for vaccine development and testing. *ILAR J.* 56, 53–62. doi: 10.1093/ilar/ilv009

Goldstein, S. A., and Weiss, S. R. (2017). Origins and pathogenesis of middle east respiratory syndrome-associated coronavirus: recent advances. *F1000Res* 6:1628. doi: 10.12688/f1000research.11827.1

Gossner, C., Danielson, N., Gervelmeyer, A., Berthe, F., Faye, B., Kaasik Aaslav, K., et al. (2016). Human-dromedary camel interactions and the risk of acquiring zoonotic middle east respiratory syndrome coronavirus infection. *Zoonoses Public Health* 63, 1–9. doi: 10.1111/zph.12171

Guo, X., Deng, Y., Chen, H., Lan, J., Wang, W., Zou, X., et al. (2015). Systemic and mucosal immunity in mice elicited by a single immunization with human adenovirus type 5 or 41 vector-based vaccines carrying the spike protein of Middle East respiratory syndrome coronavirus. *Immunology* 145, 476–484. doi: 10.1111/imm.12462

Haagmans, B. L., van den Brand, J. M., Provacia, L. B., Raj, V. S., Stittelaar, K. J., Getu, S., et al. (2015). Asymptomatic middle east respiratory syndrome coronavirus infection in rabbits. *J. Virol.* 89, 6131–6135. doi: 10.1128/JVI.00661-615

Haagmans, B. L., van den Brand, J. M., Raj, V. S., Volz, A., Wohlsein, P., Smits, S. L., et al. (2016). An orthopoxvirus-based vaccine reduces virus excretion after MERS-CoV infection in dromedary camels. *Science* 351, 77–81. doi: 10.1126/science.aad1283

Hakoum, M. B., Jouni, N., Abou-Jaoude, E. A., Hasbani, D. J., Abou-Jaoude, E. A., Lopes, L. C., et al. (2017). Characteristics of funding of clinical trials: cross-sectional survey and proposed guidance. *BMJ Open* 7:e015997. doi: 10.1136/bmjopen-2017-015997

Hashem, A. M., Algaissi, A., Agrawal, A., Al-Amri, S. S., Alhabbab, R. Y., Sohrab, S. S., et al. (2019). A highly immunogenic, protective and safe adenovirus-based vaccine expressing MERS-CoV S1-CD40L fusion protein in transgenic human DPP4 mouse model. *J. Infect. Dis.* 26:jiz137. doi: 10.1093/infdis/jiz137

He, Y., Li, J., Li, W., Lustigman, S., Farzan, M., and Jiang, S. (2006). Cross-neutralization of human and palm civet severe acute respiratory syndrome coronaviruses by antibodies targeting the receptor-binding domain of spike protein. *J. Immunol.* 176, 6085–6092. doi: 10.4049/jimmunol.176.10.6085

Jaume, M., Yip, M. S., Kam, Y. W., Cheung, C. Y., Kien, F., Roberts, A., et al. (2012). SARS CoV subunit vaccine: antibody-mediated neutralisation and enhancement. *Hong Kong Med. J.* 18 (Suppl. 2), 31–36.

Jiaming, L., Yanfeng, Y., Yao, D., Yawei, H., Linlin, B., Baoying, H., et al. (2017). The recombinant N-terminal domain of spike proteins is a potential vaccine against Middle East respiratory syndrome coronavirus (MERS-CoV) infection. *Vaccine* 35, 10–18. doi: 10.1016/j.vaccine.2016.11.064

Jung, S. Y., Kang, K. W., Lee, E. Y., Seo, D. W., Kim, H. L., Kim, H., et al. (2018). Heterologous prime-boost vaccination with adenoviral vector and protein nanoparticles induces both Th1 and Th2 responses against middle east respiratory syndrome coronavirus. *Vaccine* 36, 3468–3476. doi: 10.1016/j.vaccine.2018.04.082

Kaech, S. M., and Ahmed, R. (2001). Memory CD8+ T cell differentiation: initial antigen encounter triggers a developmental program in naïve cells. *Nat. Immunol.* 2, 415–422. doi: 10.1038/87720

Kam, Y. W., Kien, F., Roberts, A., Cheung, Y. C., Lamirande, E. W., Vogel, L., et al. (2007). Antibodies against trimeric S glycoprotein protect hamsters against SARS-CoV challenge despite their capacity to mediate FcgammaRII-dependent entry into B cells *in vitro*. *Vaccine* 25, 729–740. doi: 10.1016/j.vaccine.2006.08.011

Kim, E., Okada, K., Kenniston, T., Raj, V. S., AlHajri, M. M., Farag, E. A., et al. (2014). Immunogenicity of an adenoviral-based middle east respiratory Syndrome coronavirus vaccine in BALB/c mice. *Vaccine* 32, 5975–5982. doi: 10.1016/j.vaccine.2014.08.058

Kim, Y. S., Son, A., Kim, J., Kwon, S. B., Kim, M. H., Kim, P., et al. (2018). Chaperna-mediated assembly of ferritin-based middle east respiratory syndrome-coronavirus nanoparticles. *Front. Immunol.* 9:1093. doi: 10.3389/fimmu.2018.01093

Kuzmina, N. A., Younan, P., Gilchuk, P., Santos, R. I., Flyak, A. I., Ilinykh, P. A., et al. (2018). Antibody-dependent enhancement of ebola virus infection by human antibodies isolated from survivors. *Cell Rep.* 24, 1802.e5–1815.e5. doi: 10.1016/j.celrep.2018.07.035

Lan, J., Deng, Y., Chen, H., Lu, G., Wang, W., Guo, X., et al. (2014). Tailoring subunit vaccine immunity with adjuvant combinations and delivery routes using the middle east respiratory coronavirus (MERS-CoV) receptor-binding domain as an antigen. *PLoS One* 9:e112602. doi: 10.1371/journal.pone.0112602

Lan, J., Deng, Y., Song, J., Huang, B., Wang, W., and Tan, W. (2018). Significant spike-specific IgG and neutralizing antibodies in mice induced by a novel chimeric virus-iike particle vaccine candidate for middle east respiratory syndrome coronavirus. *Virol. Sin.* 33, 453–455. doi: 10.1007/s12250-018-0064-68

Lan, J., Yao, Y., Deng, Y., Chen, H., Lu, G., Wang, W., et al. (2015). Recombinant receptor binding domain protein induces partial protective immunity in rhesus macaques against middle east respiratory syndrome coronavirus challenge. *EBioMedicine* 2, 1438–1446. doi: 10.1016/j.ebiom.2015.08.031

Lauring, A. S., Jones, J. O., and Andino, R. (2010). Rationalizing the development of live attenuated virus vaccines. *Nat. Biotechnol.* 28, 573–579. doi: 10.1038/nbt.1635

Ledwith, B. J., Manam, S., Troilo, P. J., Barnum, A. B., Pauley, C. J., Griffiths, T. G., et al. (2000). Plasmid DNA vaccines: assay for integration into host genomic DNA. *Dev. Biol.* 104, 33–43.

Leitner, W. W., Ying, H., and Restifo, N. P. (1999). DNA and RNA-based vaccines: principles, progress and prospects. *Vaccine* 18, 765–777. doi: 10.1016/s0264-410x(99)00271-6

Lin, J. T., Zhang, J. S., Su, N., Xu, J. G., Wang, N., Chen, J. T., et al. (2007). Safety and immunogenicity from a phase I trial of inactivated severe acute respiratory syndrome coronavirus vaccine. *Antivir. Ther.* 12, 1107–1113.

Liu, R. Q., Ge, J. Y., Wang, J. L., Shao, Y., Zhang, H. L., Wang, J. L., et al. (2017). Newcastle disease virus-based MERS-CoV candidate vaccine elicits high-level and lasting neutralizing antibodies in Bactrian camels. *J. Integrat. Agri.* 16, 2264–2273. doi: 10.1016/S2095-3119(17)6166061665

Liu, R., Wang, J., Shao, Y., Wang, X., Zhang, H., Shuai, L., et al. (2018). A recombinant VSV-vectored MERS-CoV vaccine induces neutralizing antibody and T cell responses in rhesus monkeys after single dose immunization. *Antiviral. Res.* 150, 30–38. doi: 10.1016/j.antiviral.2017.12.007

Ma, C., Li, Y., Wang, L., Zhao, G., Tao, X., Tseng, C. T. K., et al. (2014a). Intranasal vaccination with recombinant receptor-binding domain of MERS-CoV spike protein induces much stronger local mucosal immune responses than subcutaneous immunization: implication for designing novel mucosal MERS vaccines. *Vaccine* 32, 2100–2108. doi: 10.1016/j.vaccine.2014.02.004

Ma, C., Wang, L., Tao, X., Zhang, N., Yang, Y., Tseng, C. K., et al. (2014b). Searching for an ideal vaccine candidate among different MERS coronavirus receptor-binding fragments–the importance of immunofocusing in subunit vaccine design. *Vaccine* 32, 6170–6176. doi: 10.1016/j.vaccine.2014.08.086

MacLeod, M. K. L., Kappler, J. W., and Marrack, P. (2010). Memory CD4 T cells: generation, reactivation and re-assignment. *Immunology* 130, 10–15. doi: 10.1111/j.1365-2567.2010.03260.x

Malczyk, A. H., Kupke, A., Prufer, S., Scheuplein, V. A., Hutzler, S., Kreuz, D., et al. (2015). A highly immunogenic and protective middle east respiratory syndrome coronavirus vaccine based on a recombinant measles virus vaccine platform. *J. Virol.* 89, 11654–11667. doi: 10.1128/JVI.01815-1815

Memish, Z. A., Cotten, M., Meyer, B., Watson, S. J., Alsahafi, A. J., Al Rabeeah, A. A., et al. (2014). Human infection with MERS coronavirus after exposure to infected camels, Saudi Arabia, 2013. *Emerg. Infect. Dis.* 20, 1012–1015. doi: 10.3201/eid2006.140402

Menachery, V. D., Gralinski, L. E., Mitchell, H. D., Dinnon, K. H., 3rd, Leist, S. R., Yount, B. L., et al. (2017). Middle east respiratory syndrome coronavirus nonstructural protein 16 Is necessary for interferon resistance and viral pathogenesis. *mSphere* 2:e00346-17.

Moss, B., Smith, G. L., Gerin, J. L., and Purcell, R. H. (1984). Live recombinant vaccinia virus protects chimpanzees against hepatitis B. *Nature* 311, 67–69. doi: 10.1038/311067a0

Munster, V. J., de Wit, E., and Feldmann, H. (2013). Pneumonia from human coronavirus in a macaque model. *N. Engl. J. Med.* 368, 1560–1562. doi: 10.1056/NEJMc1215691

Munster, V. J., Wells, D., Lambe, T., Wright, D., Fischer, R. J., Bushmaker, T., et al. (2017). Protective efficacy of a novel simian adenovirus vaccine against lethal MERS-CoV challenge in a transgenic human DPP4 mouse model. *NPJ Vaccines* 2:28. doi: 10.1038/s41541-017-0029-21

Murata, K., Lechmann, M., Qiao, M., Gunji, T., Alter, H. J., and Liang, T. J. (2003). Immunization with hepatitis C virus-like particles protects mice from recombinant hepatitis C virus-vaccinia infection. *Proc. Natl. Acad. Sci. U.S.A.* 100, 6753–6758. doi: 10.1073/pnas.1131929100

Muthumani, K., Falzarano, D., Reuschel, E.L., Tingey, C., Flingai, S., Villarreal, D.O., et al. (2015). A synthetic consensus anti-spike protein DNA vaccine induces protective immunity against middle east respiratory syndrome coronavirus in nonhuman primates. *Sci. Trans. Med.* 7:301ra132. doi: 10.1126/scitranslmed.aac7462

National Institutes of Health [NIH] (2016). *Phase I, Open Label Dose Ranging Safety Study of GLS-5300 in Healthy Volunteers*. Available at: https://clinicaltrials.gov/ct2/show/NCT02670187?term=GLS-5300 (accessed February 25, 2019).

National Institutes of Health [NIH] (2018a). *Evaluate the Safety, Tolerability and Immunogenicity Study of GLS-5300 in Healthy Volunteers*. Available at: https://clinicaltrials.gov/ct2/show/NCT03721718 (accessed June 2019).

National Institutes of Health [NIH] (2018b). *Safety and Immunogenicity of a Candidate MERS-CoV Vaccine (MERS001)*. Available at: https://clinicaltrials.gov/ct2/show/study/NCT03399578 (accessed February 25, 2019).

National Institutes of Health [NIH] (2018c). *Safety, Tolerability and Immunogenicity of Vaccine Candidate MVA-MERS-S*. Available at: https://clinicaltrials.gov/ct2/show/NCT03615911#outcomemeasures (accessed February 25, 2019).

Nyon, M. P., Du, L., Tseng, C. K., Seid, C. A., Pollet, J., Naceanceno, K. S., et al. (2018). Engineering a stable CHO cell line for the expression of a MERS-coronavirus vaccine antigen. *Vaccine* 36, 1853–1862. doi: 10.1016/j.vaccine.2018.02.065

Oh, M. -D., Park, W. B., Park, S. -W., Choe, P. G., Bang, J. H., Song, K. -H., et al. (2018). Middle east respiratory syndrome: what we learned from the 2015 outbreak in the Republic of Korea. *Korean J. Int. Med.* 33, 233–246. doi: 10.3904/kjim.2018.031

Okba, N. M., Raj, V. S., and Haagmans, B. L. (2017). Middle east respiratory syndrome coronavirus vaccines: current status and novel approaches. *Curr. Opin. Virol.* 23, 49-58. doi: 10.1016/j.coviro.2017.03.007

Ong, H. K., Tan, W. S., and Ho, K. L. (2017). Virus like particles as a platform for cancer vaccine development. *PeerJ* 5:e4053. doi: 10.7717/peerj.4053

Pallesen, J., Wang, N., Corbett, K. S., Wrapp, D., Kirchdoerfer, R. N., Turner, H. L., et al. (2017). Immunogenicity and structures of a rationally designed prefusion MERS-CoV spike antigen. *Proc. Natl. Acad. Sci. U.S.A.* 114, E7348–E7357. doi: 10.1073/pnas.1707304114

Pascal, K. E., Coleman, C. M., Mujica, A. O., Kamat, V., Badithe, A., Fairhurst, J., et al. (2015). Pre- and postexposure efficacy of fully human antibodies against spike protein in a novel humanized mouse model of MERS-CoV infection. *Proc. Natl. Acad. Sci. U.S.A.* 112, 8738–8743. doi: 10.1073/pnas.1510830112

Payne, D. C., Iblan, I., Rha, B., Alqasrawi, S., Haddadin, A., Al Nsour, M., et al. (2016). Persistence of antibodies against middle east respiratory syndrome coronavirus. *Emerg. Infect. Dis.* 22, 1824–1826. doi: 10.3201/eid2210.160706

Perlman, S., and Vijay, R. (2016). Middle east respiratory syndrome vaccines. *Int. J. Infect. Dis.* 47, 23–28. doi: 10.1016/j.ijid.2016.04.008

Prescott, J., Falzarano, D., de Wit, E., Hardcastle, K., Feldmann, F., Haddock, E., et al. (2018). Pathogenicity and viral shedding of MERS-CoV in immunocompromised rhesus macaques. *Front. Immunol.* 9:205. doi: 10.3389/fimmu.2018.00205

Quan, F. S., Compans, R. W., Nguyen, H. H., and Kang, S. M. (2008). Induction of heterosubtypic immunity to influenza virus by intranasal immunization. *J. Virol.* 82, 1350–1359. doi: 10.1128/jvi.01615-1617

Schindewolf, C., and Menachery, V. D. (2019). Middle east respiratory syndrome vaccine candidates: cautious optimism. *Viruses* 11:E74. doi: 10.3390/v11010074

Scobey, T., Yount, B. L., Sims, A. C., Donaldson, E. F., Agnihothram, S. S., Menachery, V. D., et al. (2013). Reverse genetics with a full-length infectious cDNA of the middle east respiratory syndrome coronavirus. *Proc. Natl. Acad. Sci. U.S.A.* 110, 16157–16162. doi: 10.1073/pnas.1311542110

Shi, J., Zhang, J., Li, S., Sun, J., Teng, Y., Wu, M., et al. (2015). Epitope-based vaccine target screening against highly pathogenic MERS-CoV: an *in silico* approach applied to emerging infectious diseases. *PLoS One* 10:e0144475. doi: 10.1371/journal.pone.0144475

Sibal, L. R., and Samson, K. J. (2001). Nonhuman primates: a critical role in current disease research. *ILAR J.* 42, 74–84. doi: 10.1093/ilar.42.2.74.

Smith, R. (2000). Vaccines and medicines for the world's poorest. Public-private partnerships seem to be essential. *BMJ* 320, 952–953. doi: 10.1136/bmj.320.7240.952

Song, F., Fux, R., Provacia, L. B., Volz, A., Eickmann, M., Becker, S., et al. (2013). Middle east respiratory syndrome coronavirus spike protein delivered by modified vaccinia virus Ankara efficiently induces virus-neutralizing antibodies. *J. Virol.* 87, 11950–11954. doi: 10.1128/JVI.01672-1613

Srivastava, S., Kamthania, M., Singh, S., Saxena, A. K., and Sharma, N. (2018). Structural basis of development of multi-epitope vaccine against middle east respiratory syndrome using *in silico* approach. *Infect. Drug Resist.* 11, 2377–2391. doi: 10.2147/idr.s175114

Swearengen, J. R. (2018). Choosing the right animal model for infectious disease research. *Animal Model Exp. Med.* 1, 100–108. doi: 10.1002/ame2.12020

Tai, W., Wang, Y., Fett, C. A., Zhao, G., Li, F., Perlman, S., et al. (2017). Recombinant receptor-binding domains of multiple middle east respiratory syndrome coronaviruses (MERS-CoVs) induce cross-neutralizing antibodies against divergent human and camel MERS-CoVs and antibody escape mutants. *J. Virol.* 91:e01651-16. doi: 10.1128/JVI.01651-1616

Tai, W., Zhao, G., Sun, S., Guo, Y., Wang, Y., Tao, X., et al. (2016). A recombinant receptor-binding domain of MERS-CoV in trimeric form protects human dipeptidyl peptidase 4 (hDPP4) transgenic mice from MERS-CoV infection. *Virol* 499, 375–382. doi: 10.1016/j.virol.2016.10.005

Tang, F., Quan, Y., Xin, Z. T., Wrammert, J., Ma, M. J., Lv, H., et al. (2011). Lack of peripheral memory B cell responses in recovered patients with severe acute respiratory syndrome: a six-year follow-up study. *J. Immunol.* 186, 7264–7268. doi: 10.4049/jimmunol.0903490

Tang, J., Zhang, N., Tao, X., Zhao, G., Guo, Y., Tseng, C. T., et al. (2015). Optimization of antigen dose for a receptor-binding domain-based subunit vaccine against MERS coronavirus. *Hum. Vaccin. Immunother.* 11, 1244–1250. doi: 10.1080/21645515.2015.1021527

Tang, X. -C., Agnihothram, S. S., Jiao, Y., Stanhope, J., Graham, R. L., Peterson, E. C., et al. (2014). Identification of human neutralizing antibodies against MERS-CoV and their role in virus adaptive evolution. *Proc. Natl. Acad. Sci. U.S.A.* 111:E2018. doi: 10.1073/pnas.1402074111

Ura, T., Okuda, K., and Shimada, M. (2014). Developments in viral vector-based vaccines. *Vaccines* 2, 624–641. doi: 10.3390/vaccines2030624

van Boheemen, S., de Graaf, M., Lauber, C., Bestebroer, T. M., Raj, V. S., Zaki, A. M., et al. (2012). Genomic characterization of a newly discovered coronavirus associated with acute respiratory distress syndrome in humans. *MBio* 3:e00473-12. doi: 10.1128/mBio.00473-412

van Doremalen, N., Falzarano, D., Ying, T., de Wit, E., Bushmaker, T., Feldmann, F., et al. (2017). Efficacy of antibody-based therapies against middle east respiratory syndrome coronavirus (MERS-CoV) in common marmosets. *Antiviral Res.* 143, 30–37. doi: 10.1016/j.antiviral.2017.03.025

van Doremalen, N., and Munster, V. J. (2015). Animal models of middle east respiratory syndrome coronavirus infection. *Antiviral Res.* 122, 28–38. doi: 10.1016/j.antiviral.2015.07.005

Veit, S., Jany, S., Fux, R., Sutter, G., and Volz, A. (2018). CD8+ T cells responding to the middle east respiratory syndrome coronavirus nucleocapsid protein delivered by vaccinia virus MVA in mice. *Viruses* 10:718. doi: 10.3390/v10120718

Volz, A., Kupke, A., Song, F., Jany, S., Fux, R., Shams-Eldin, H., et al. (2015). Protective efficacy of recombinant modified vaccinia virus ankara delivering middle east respiratory syndrome coronavirus spike glycoprotein. *J. Virol.* 89, 8651–8656. doi: 10.1128/JVI.00614-615

Wang, C., Zheng, X., Gai, W., Wong, G., Wang, H., Jin, H., et al. (2017a). Novel chimeric virus-like particles vaccine displaying MERS-CoV receptor-binding domain induce specific humoral and cellular immune response in mice. *Antiviral Res.* 140, 55–61. doi: 10.1016/j.antiviral.2016.12.019

Wang, C., Zheng, X., Gai, W., Zhao, Y., Wang, H., Wang, H., et al. (2017b). MERS-CoV virus-like particles produced in insect cells induce specific humoural and cellular imminity in rhesus macaques. *Oncotarget* 8, 12686–12694.

Wang, L., Shi, W., Joyce, M. G., Modjarrad, K., Zhang, Y., Leung, K., et al. (2015a). Evaluation of candidate vaccine approaches for MERS-CoV. *Nat. Commun.* 6:7712. doi: 10.1038/ncomms8712

Wang, Y., Liu, D., Shi, W., Lu, R., Wang, W., Zhao, Y., et al. (2015b). Origin and possible genetic recombination of the middle east respiratory syndrome coronavirus from the rirst imported case in China: phylogenetics and coalescence analysis. *MBio* 6, e1280-15. doi: 10.1128/mBio.01280-1215

Wang, Y., Tai, W., Yang, J., Zhao, G., Sun, S., Tseng, C. K., et al. (2017c). Receptor-binding domain of MERS-CoV with optimal immunogen dosage and immunization interval protects human transgenic mice from MERS-CoV infection. *Hum. Vaccin. Immunother.* 13, 1615–1624. doi: 10.1080/21645515.2017.1296994

Weingartl, H., Czub, M., Czub, S., Neufeld, J., Marszal, P., Gren, J., et al. (2004). Immunization with modified vaccinia virus ankara-based recombinant vaccine against severe acute respiratory syndrome is associated with enhanced hepatitis in ferrets. *J. Virol.* 78:12672. doi: 10.1128/JVI.78.22.12672-12676.2004

World Health Organization [WHO] (2019a). *MERS Situation Update*. Available at: http://applications.emro.who.int/docs/EMROPub_2019_EN_22346.pdf?ua=1&ua=1 (accessed May 2019).

World Health Organization [WHO] (2019b). *Middle East Respiratory Syndrome Coronavirus (MERS-CoV)*. Available at: https://www.who.int/emergencies/mers-cov/en/ (accessed May 2019).

Wirblich, C., Coleman, C. M., Kurup, D., Abraham, T. S., Bernbaum, J. G., Jahrling, P. B., et al. (2017). One-Health: a safe, efficient, dual-use vaccine for humans and animals against middle east respiratory syndrome coronavirus and rabies Virus. *J. Virol.* 91, e02040-16

Xie, Q., He, X., Yang, F., Liu, X., Li, Y., Liu, Y., et al. (2018). Analysis of the genome sequence and prediction of B-Cell epitopes of the envelope protein of middle east respiratory syndrome-coronavirus. *IEEE/ACM Trans. Comput. Biol. Bioinf.* 15, 1344–1350. doi: 10.1109/tcbb.2017.2702588

Yang, Z. -Y., Kong, W. -P., Huang, Y., Roberts, A., Murphy, B. R., Subbarao, K., et al. (2004). A DNA vaccine induces SARS coronavirus neutralization and protective immunity in mice. *Nature* 428, 561–564. doi: 10.1038/nature02463

Yeung, M. L., Yao, Y., Jia, L., Chan, J. F., Chan, K. H., Cheung, K. F., et al. (2016). MERS coronavirus induces apoptosis in kidney and lung by upregulating Smad7 and FGF2. *Nat. Microbiol.* 1:16004. doi: 10.1038/nmicrobiol.2016.4

Yip, M. S., Cheung, C. Y., Li, P. H., Bruzzone, R., Peiris, J. S. M., and Jaume, M. (2011). Investigation of antibody-dependent enhancement (ADE) of SARS coronavirus infection and its role in pathogenesis of SARS. *BMC Proc.* 5(Suppl. 1):P80.

Yong, C. Y., Yeap, S. K., Goh, Z. H., Ho, K. L., Omar, A. R., and Tan, W. S. (2015a). Induction of humoral and cell-mediated immune responses by hepatitis B virus epitope displayed on the virus-Like particles of prawn nodavirus. *Appl. Environ. Microbiol.* 81, 882–889. doi: 10.1128/AEM.03695-3614

Yong, C. Y., Yeap, S. K., Ho, K. L., Omar, A. R., and Tan, W. S. (2015b). Potential recombinant vaccine against influenza A virus based on M2e displayed on nodaviral capsid nanoparticles. *Int. J. Nanomed.* 10, 2751–2763. doi: 10.2147/IJN.S77405

Yu, P., Xu, Y., Deng, W., Bao, L., Huang, L., Xu, Y., et al. (2017). Comparative pathology of rhesus macaque and common marmoset animal models with middle east respiratory syndrome coronavirus. *PLoS One* 12:e0172093. doi: 10.1371/journal.pone.0172093

Zaki, A. M., Van Boheemen, S., Bestebroer, T. M., Osterhaus, A. D., and Fouchier, R. A. (2012). Isolation of a novel coronavirus from a man with pneumonia in Saudi Arabia. *N. Engl. J. Med.* 367, 1814–1820. doi: 10.1056/NEJMoa1211172

Zhang, N., Channappanavar, R., Ma, C., Wang, L., Tang, J., Garron, T., et al. (2016). Identification of an ideal adjuvant for receptor-binding domain-based subunit vaccines against middle east respiratory syndrome coronavirus. *Cell Mol. Immunol.* 13, 180–190. doi: 10.1038/cmi.2015.03

Zhao, J., Alshukairi, A. N., Baharoon, S. A., Ahmed, W. A., Bokhari, A. A., Nehdi, A. M., et al. (2017). Recovery from the middle east respiratory syndrome is associated with antibody and T-cell responses. *Sci. Immunol.* 2:eaan5393. doi: 10.1126/sciimmunol.aan5393

Zhao, J., Li, K., Wohlford-Lenane, C., Agnihothram, S. S., Fett, C., Zhao, J., et al. (2014). Rapid generation of a mouse model for middle east respiratory

syndrome. *Proc. Natl. Acad. Sci. U.S.A.* 111, 4970–4975. doi: 10.1073/pnas.1323279111

Zhao, J., Perera, R. A., Kayali, G., Meyerholz, D., Perlman, S., and Peiris, M. (2015). Passive immunotherapy with dromedary immune serum in an experimental animal model for middle east respiratory syndrome coronavirus infection. *J. Virol.* 89, 6117–6120. doi: 10.1128/JVI.00446-415

Zhao, J., Zhao, J., Mangalam, A. K., Channappanavar, R., Fett, C., Meyerholz, D. K., et al. (2016). Airway Memory CD4(+) T cells mediate protective immunity against emerging respiratory coronaviruses. *Immunity* 44, 1379–1391. doi: 10.1016/j.immuni.2016.05.006

**Conflict of Interest Statement:** The authors declare that the research was conducted in the absence of any commercial or financial relationships that could be construed as a potential conflict of interest.

*Copyright © 2019 Yong, Ong, Yeap, Ho and Tan. This is an open-access article distributed under the terms of the Creative Commons Attribution License (CC BY). The use, distribution or reproduction in other forums is permitted, provided the original author(s) and the copyright owner(s) are credited and that the original publication in this journal is cited, in accordance with accepted academic practice. No use, distribution or reproduction is permitted which does not comply with these terms.*

frontiers in Microbiology

ORIGINAL RESEARCH
published: 13 August 2019
doi: 10.3389/fmicb.2019.01829

# Crystal Structure of Refolding Fusion Core of Lassa Virus GP2 and Design of Lassa Virus Fusion Inhibitors

*Xuejiao Zhang[1,2†], Cong Wang[3†], Baohua Chen[1†], Qian Wang[3], Wei Xu[3], Sheng Ye[1,4], Shibo Jiang[3,5*], Yun Zhu[1*] and Rongguang Zhang[1,6*]*

[1] National Laboratory of Biomacromolecules, Institute of Biophysics, Chinese Academy of Sciences, Beijing, China, [2] College of Life Sciences, University of Chinese Academy of Sciences, Beijing, China, [3] Key Laboratory of Medical Molecular Virology of MOE/MOH/CAMS, School of Basic Medical Sciences and Shanghai Public Health Clinical Center, Fudan-Jinbo Joint Research Center, Fudan University, Shanghai, China, [4] Interdisciplinary Innovation Institute of Medicine and Engineering, Beijing Advanced Innovation Center for Big Data-Based Precision Medicine, School of Biological Science and Medical Engineering, Beihang University, Beijing, China, [5] Lindsley F. Kimball Research Institute, New York Blood Center, New York, NY, United States, [6] National Center for Protein Science Shanghai, Shanghai Institute of Biochemistry and Cell Biology, Shanghai Institutes for Biological Sciences, Chinese Academy of Sciences, Shanghai, China

OPEN ACCESS

**Edited by:**
*Lijun Rong,*
*The University of Illinois at Chicago, United States*

**Reviewed by:**
*Jinsong Liu,*
*Guangzhou Institutes of Biomedicine and Health (CAS), China*
*Yechiel Shai,*
*Weizmann Institute of Science, Israel*

***Correspondence:**
*Shibo Jiang*
*shibojiang@fudan.edu.cn*
*Yun Zhu*
*zhuyun@ibp.ac.cn*
*Rongguang Zhang*
*rzhang@ibp.ac.cn*

*† These authors have contributed equally to this work*

**Specialty section:**
*This article was submitted to Virology, a section of the journal Frontiers in Microbiology*

**Received:** *04 June 2019*
**Accepted:** *25 July 2019*
**Published:** *13 August 2019*

**Citation:**
*Zhang X, Wang C, Chen B, Wang Q, Xu W, Ye S, Jiang S, Zhu Y and Zhang R (2019) Crystal Structure of Refolding Fusion Core of Lassa Virus GP2 and Design of Lassa Virus Fusion Inhibitors. Front. Microbiol. 10:1829. doi: 10.3389/fmicb.2019.01829*

The envelope glycoproteins GP1 and GP2 of Lassa virus (LASV) bind to the host cell receptors to mediate viral infection. So far, no approved vaccines and specific treatment options against LASV exist. To develop specific fusion inhibitors against LASV, we solved the crystal structure of the post-fusion 6 helix bundle (6-HB) formed by two heptad repeat domains (HR1 and HR2) of GP2. This fusion core contains a parallel trimeric coiled-coil of three HR1 helices, around which three HR2 helices are entwined in an antiparallel manner. Various hydrophobic and charged interactions form between HR1 and HR2 domains to stabilize the overall conformation of GP2 fusion core. Based on the structure, we designed several peptides spanning the HR2 domain and tested their antiviral activities. We found that the longer HR2 peptides were effective in inhibiting LASV GPC protein-mediated cell–cell fusion under low pH condition. These results not only suggest that LASV infects the target cell mainly through endocytosis, including micropinocytosis, and membrane fusion at low pH, but also provide an important basis for rational design of LASV fusion inhibitors.

**Keywords: Lassa virus, GP2, fusion core, crystal structure, viral entry**

## INTRODUCTION

Lassa fever is an acute viral hemorrhagic illness occurring in West Africa, having posed a serious public health threat in many countries (Sogoba et al., 2012; Shaffer et al., 2014). Its case-fatality rate is 1% for overall infection and 15∼20% for severe cases among patients hospitalized. This mortality rate will increase sharply during epidemics or in pregnant women (Asogun et al., 2012). The etiologic agent of Lassa fever is Lassa virus (LASV), belonging to the arenavirus family. Arenavirus has more than 30 members divided into two groups: the New World viruses (or Tacaribe complex) and the Old World viruses (or LCM-Lassa complex). The New World family mainly contains Venezuelan hemorrhagic fever (VHF), Junín virus (JUNV), Machupo virus (MACV), and Bolivian hemorrhagic fever (BHF), while the Old World viruses includes, for example Lujo virus (LUJV), Lymphocytic choriomeningitis virus (LCMV), Morogoro virus (MORV), and LASV. These arenaviruses have both geographical and genetic differences.

Lassa virus is an enveloped, single-stranded RNA virus. The two RNA segments in its genome encode four viral proteins, including zinc-binding protein (Z), RNA polymerase (L), nucleoprotein (NP), and the surface glycoprotein precursor (GP, or spike protein). GP is cleaved into envelope glycoproteins GP1 and GP2 (Cao et al., 1998). GP1 that is responsible for receptor binding (including α-dystroglycan, heparin sulfate, DC-SIGN, etc.) and GP2 that mediates membrane fusion interact with each other to form a stable trimer complex on the LASV viral envelope (Li et al., 2016; Hastie et al., 2017). Upon receptor binding, LASV enters the target cell via clathrin- and dynamin-independent endocytosis with subsequent transport to late endosomal compartments, where fusion occurs at low pH (Vela et al., 2007; Rojek et al., 2008). A recent study has also found that after GP1 binds to cell receptor α-dystroglycan, LASV enters into the target cell through the unusual micropinocytosis pathway and membrane fusion under low pH condition (Oppliger et al., 2016).

So far, no approved vaccines and specific treatment modalities against LASV are available. Given that the first peptide-based antiviral drug enfuvirtide (T20) inhibits human immunodeficiency virus (HIV) fusion with and entry into the target cell by targeting the heptad repeat domain in the viral envelope glycoprotein gp41 (Qi et al., 2017; Su et al., 2017), the heptad repeat domain in GP2 of LASV may also serve as a target for the design of LASV fusion inhibitors. We have previously demonstrated that the N-terminal heptad repeat 1 (HR1) domain binds to C-terminal heptad repeat 2 (HR2) domain to form a stable six-helix bundle (6-HB) to mediate viral entry; therefore, peptides derived from HR2 should specifically bind to the homotrimeric HR1, interfering with the formation of 6-HB and, hence, blocking viral entry (Zhu et al., 2015, 2016; Xia et al., 2019). Therefore, it is essential to determine the 6-HB core structure and characterize the interaction sites in the HR1 and HR2 domains, in order to design the HR2-derived peptides against LASV infection. Here, we solved the crystal structure of the post-fusion 6-HB formed by LASV HR1 and HR2 domains. Based on the structure, we designed several peptides spanning the HR2 domain and tested their antiviral activities. Concurrent with the preparation of the present manuscript, another group reported a post-fusion structure of LASV using the insect baculovirus expression system (Shulman et al., 2019), which allows us to compare the structural differences of 6-HB cores formed by the HR1 and HR2 domains in their truncated version of LASV GP2 spanning residues 306–421 with those in our LASV HR1-T-loop-HR2 construct. These comparisons provide more comprehensive knowledge for better understanding the entry mechanism of LASV and designing of peptide-based LASV fusion inhibitors.

# MATERIALS AND METHODS

## Cells, Peptides, and Plasmids

The 293T cell line was obtained from ATCC (Manassas, VA, United States), and the Huh-7 cell line was from the Cell Bank of the Chinese Academy of Sciences (Shanghai, China). These two cell lines were propagated in Dulbecco's Modified Eagle's Medium (DMEM) supplemented with 10% fetal bovine serum (FBS). Peptides (LASV/HR2-1, LASV/HR2-2, LASV/HR2-3, LASV/HR2-4, and LASV/HR2-5) were synthesized by solid-phase peptide synthesis at SYN Inc. (Shanghai, China). Recombinant plasmids encoding the LASV GPC protein were synthesized by SYN Inc.

## Protein Expression and Renaturation

The gene coding for HR1-T-loop-HR2 construct of LASV GP2 (residues 306–432, with a C310S mutation and $\Delta_{378}GK_{379}$ truncation) was amplified by PCR and cloned into vector pET-28a with an artificially introduced PreScission Protease cleavage site at its N-terminus for stable expression. The fusion protein was overexpressed in *Escherichia coli* BL21. Cells were grown to OD600 $\approx$ 0.6 in lysogeny broth (LB) media supplemented with 1 μg/mL kanamycin at 37°C and were induced by 1 mM IPTG for 16 h at 37°C for expression. Cells were harvested by centrifugation at 4500 × *g* for 15 min at 4°C and were lysed by high pressure homogenizer twice after resuspension in buffer containing 25 mM Tris–HCl, pH 8.0, and 200 mM NaCl. The inclusion body was harvested by centrifugation at 18,000 x *g* for 30 min and resuspended in buffer containing 50 mM Tris–HCl, 200 mM NaCl, pH 8.0, 8 M Urea, and 50 mM DTT. Then the trimeric LASV 6-HB protein was refolded using limit dilution method. Briefly, the denatured protein was diluted at 1:100 volume ratio into renaturation buffer (25 mM Tris–HCl, 200 mM NaCl, pH 8.0, 100 mM Arginine, 1 mM GSH and 0.1 mM GSSG) very slowly (0.02 mL/min), and stored for 1 week at 4°C. Refolded protein was isolated by Ni-affinity chromatography and purified by anion exchange chromatography (HiTrap Q Fast Flow 5 mL, GE Healthcare), as well as gel filtration chromatography (Superdex 200 10/300 GL, GE Healthcare), and then concentrated to 15 mg/mL for crystallization or storage at −80°C for further use.

## Crystallization

Crystals were obtained at 16°C for 7 days using the hanging drop vapor diffusion method by mixing equal volume of protein solution [LASV-6-HB: 6 mg/mL] and reservoir solution, [0.17 M Ammonium Acetate, 0.085 M Sodium Citrate: HCl, pH 5.6, 25.5% (w/v) PEG 4000, and 15% (v/v) Glycerol]. Then crystals were flash-frozen after immersing in paraffin oil for about 10 s, followed by transfer to liquid nitrogen for further data collection.

## Data Collection, Structure Determination, and Refinement

The datasets were collected at beamline BL-18U1, Shanghai Synchrotron Radiation Facility, at a wavelength of 0.97930 Å. The crystals were kept at 100 K during X-ray diffraction data collection. Data were indexed and scaled with HKL2000 (Otwinowski and Minor, 1997). Phases were solved by the molecular replacement method using PHENIX.phaser (Mccoy, 2007). All refinement procedures were carried out with PHENIX.refine (Zwart et al., 2008) and COOT (Emsley and Cowtan, 2004). **Table 1** shows the detailed statistics of data collection and refinement.

**TABLE 1 |** Data collection and refinement statistics.

| | LASV 6-HB PDB ID: 6JGY |
|---|---|
| **Data collection** | |
| Space group | H32 |
| **Cell dimensions** | |
| a, b, c (Å) | 58.7, 58.7, 268.6 |
| α, β, γ (°) | 90, 90, 120 |
| Wavelength (Å) | 0.97930 |
| Resolution (Å) | 3.39–38.04 (3.39–3.48)† |
| $R_{merge}$ | 0.118 (0.080) |
| Mean I/σ(I) | 19.2 (3.4) |
| Completeness (%) | 98.1 (100.0) |
| Redundancy | 6.3 (6.4) |
| **Refinement** | |
| Resolution (Å) | 3.39–38.04 |
| No. of reflections | 2839 |
| Reflections in test set | 135 |
| $R_{work}/R_{free}$ | 0.233/0.274 |
| **No. of atoms** | |
| Protein | 873 |
| Water | 0 |
| **R.m.s. deviations** | |
| Bond lengths (Å) | 0.010 |
| Bond angles (°) | 1.214 |
| Average *B*-factor (Å$^2$) | 103.01 |

†*Values in parentheses are for the highest resolution shell.*

## Accession Numbers

Coordinates and structure factors have been deposited in the Protein Data Bank with accession number 6JGY for crystal structure of fusion core of LASV GP2 protein.

## Biolayer Interferometry

Biolayer interferometry (BLI) is a common technique for detecting interactions between substances. The working principle of this method is that the molecules are immobilized on the surface of the sensor to form a biolayer, thereby causing interference against light waves passing through the sensor, which was then detected in the form of phase displacement, so that any change in the number of molecules on the surface of the sensor can be detected. Based on this principle, the mobile phase cannot have a non-specific combination with the sensor. The sensor type selected in this experiment was Super Streptavidin (SSA) Biosensor, and all the tests were performed using Octet RED96.

The biotinylation of protein for immobilization onto SSA was carried out according to the following procedure. The activated biotin reagent was prepared in DMSO at a concentration of 5 mg/mL. The peptides were mixed with biotin reagent, and the molar ratio of peptide to biotin reagent was 2:1. The reactions were incubated at room temperature for 1 h. Then free biotin was removed by dialysis. Biotinylation of protein for immobilization onto SSA was at a concentration of 80 μg/mL. The loading time was 300 s. The concentration of mobile phase in the initial test was 50 μM. The concentration gradient in the further test was 30, 15, 7.5, and 3.75 μM. The association time was 300 s, and the dissociation time was 600 s.

## CD Spectroscopy

The secondary structure of peptides LASV/HR2-1 (residues 385–432) and LASV/HR1 (residues 296–345), as well as their mixture, were determined by CD spectroscopy. Briefly, the peptides were diluted in phosphate-buffered saline (PBS) (pH 7.2). After incubating at 37°C for 30 min, CD spectra were acquired on a Jasco spectropolarimeter (model J-815; Jasco, Inc., Easton, MD, United States) from 195 to 260 nm at room temperature, using the optical path length of 0.1 cm and bandwidth of 1 nm. The baseline was determined using PBS. The α-helical content was calculated from the CD signal by dividing the mean residue ellipticity [θ] at 222 nm by the value expected for 100% helical formation (−33,000 degrees cm$^2$ dmol$^{-1}$).

## Production of Pseudoviruses

Lassa virus pseudoviruses were constructed as described previously (Li et al., 2017; Wang et al., 2017). Briefly, 293T cells were seeded in a 10-cm tissue culture dish. When 293T cells grown in a 10-cm dish reached 80% confluence, cells were cotransfected with plasmids pcDNA3.1-LASV-GPC (encoding GPC protein of LASV) and pNL4-3.luc.RE (encoding Env-defective, luciferase-expressing HIV-1 capsid protein) at a ratio of 1:1 using VigoFect (Vigorous Biotechnology, Beijing, China). The supernatant was replaced with fresh DMEM at 8–10 h post-transfection and harvested after incubation for an additional 72 h. Cell debris was removed by centrifuging at 3000 rpm for 10 min, followed by filtration through a 0.45 μm filter.

## Inhibition of LASV Pseudovirus Entry Into the Target Cells

A LASV pseudovirus inhibition assay was performed in a manner similar to other envelope virus assays (Lu et al., 2014; Channappanavar et al., 2015; Xia et al., 2018). Briefly, Huh-7 cells were placed ($10^4$ cells/well) into a 96-well plate and incubated overnight at 37°C. LASV pseudovirus was incubated with serially diluted peptides for 30 min at 37°C, followed by the addition of Huh-7 cells. The cells were incubated with or without pseudovirus as virus control and cell control, respectively. At 12 h post-infection, the culture was replaced with fresh medium, followed by an additional incubation for 72 h. Cells were lysed, and cell lysates were transferred to a 96-well Costar flat-bottom luminometer plate (Corning Costar, New York, NY, United States), followed by the addition of luciferase substrate (Promega) to measure luminescence using an Infinite M200 PRO (Tecan, GröDig, Austria).

## Inhibition of LASV GPC Protein-Mediated Cell–Cell Fusion

Lassa virus GPC protein-mediated cell–cell fusion was performed as previously described (Cosset et al., 2009). Briefly, plasmid pAAV-IRES-LASV-EGFP encoding the LASV GPC protein

was transfected into 293T cells (293T/LASV/EGFP) using the transfection reagent VigoFect (Vigorous). When GFP was obviously expressed on most 293T cells, 293T/LASV/EGFP cells were digested and mixed with Huh-7 cells at ratio of 1:1. The mixture was incubated at $2 \times 10^4$ cells/well in wells of a 96-well plate for 12 h. The peptides were serially diluted with low pH (pH5) DMEM and then added to the mixture of 293T/LASV/EGFP cells and Huh-7 cells. After 20 min of exposure in the low pH medium for triggering the fusion between the 293T/LASV/EGFP cells and Huh-7 cells, the cells were restored to neutral medium and cultured for 1 to 2 h at 37°C. The 293T/LASV/EGFP cells fused or unfused with Huh-7 cells were fixed with 4% PFA and counted under an inverted fluorescence microscope (Nikon, Tokyo, Japan). The fused cells showed much larger size and weaker fluorescence intensity than the unfused cells because of the diffusion of EGFP from one cell to more cells.

# RESULTS

## Overall Structure of LASV Fusion Core

The GP2 protein contains a N-terminal fusion peptide (FP) (residues 258-295), a N-terminal HR1 domain (residues 295-363), a linker T-loop domain (residues 363-386), a C-terminal HR2 domain (residues 386-431), a transmembrane domain (residues 431-453), and an intracellular domain (residues 454-491) (**Figure 1A**). By multiple sequence alignment with other representative arenaviruses, like LCMV, JUNV, and MACV, LASV showed a highly conserved T-loop domain and a variable HR2

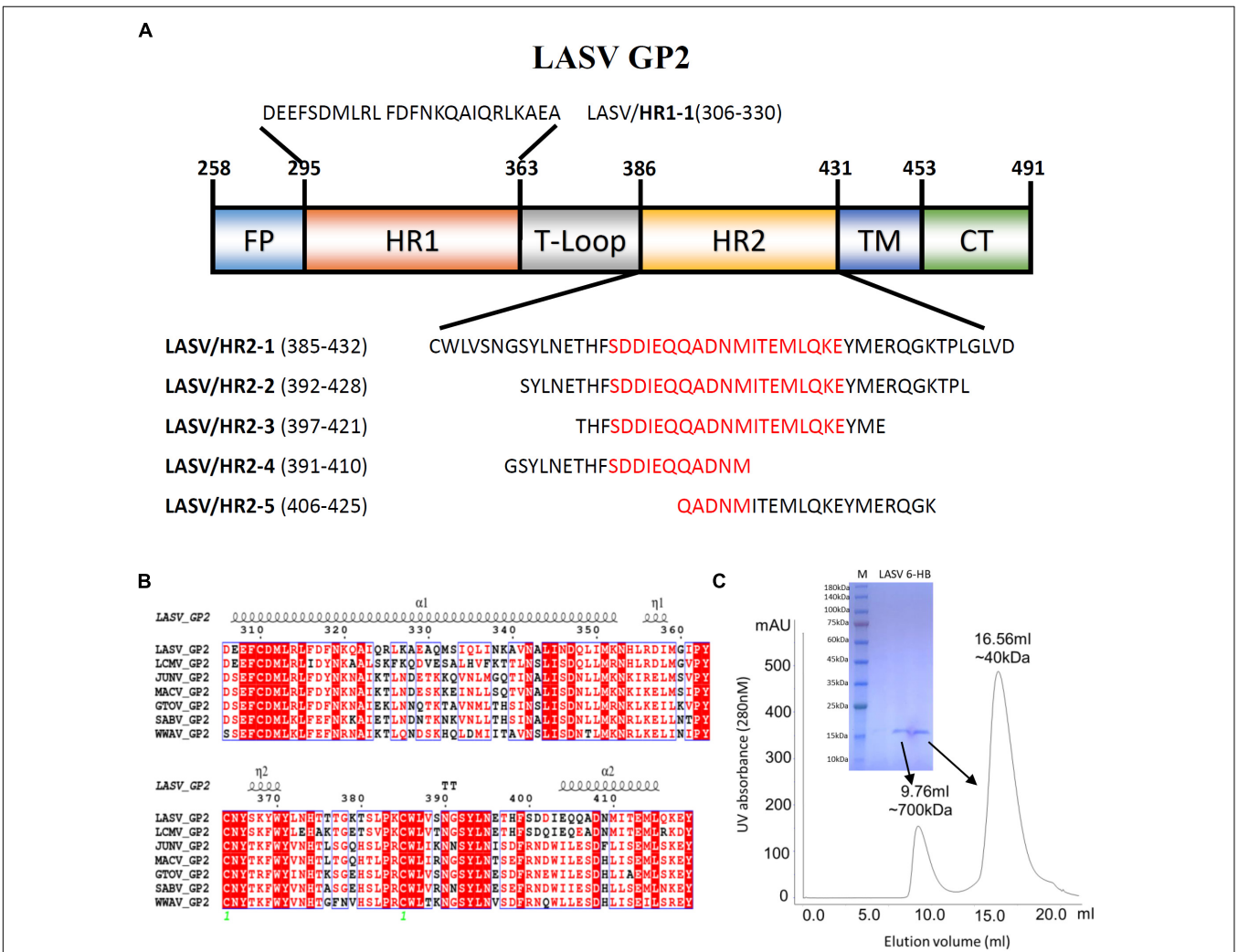


**FIGURE 1 |** The amino acid sequence and purification of LASV fusion core. **(A)** The division of different domains of LASV GP2 protein, including fusion peptide (FP), first heptad repeat domain (HR1), linker of T-loop domain, second heptad repeat domain (HR2), transmembrane domain (TM) and C-terminal intracellular domain (CT). The designed peptides are also listed. **(B)** Sequence alignment of GP2 from representative arenaviruses, like LASV (*Lassa virus*, Taxon ID: 11622), LCMV (*Lymphocytic choriomeningitis virus*, Taxon ID: 11624), JUNV (*Junin mammarenavirus*, Taxon ID: 2169991), MACV (*Machupo virus*, Taxon ID: 11628), GTOV (*Guanarito mammarenavirus*, Taxon ID: 45219), SABV (*Sabia mammarenavirus*, Taxon ID: 2169992), and WWAV (*Whitewater Arroyo mammarenavirus*, Taxon ID: 46919). **(C)** The size exclusion chromatography and SDS–PAGE result of refolded LASV GP2 6-HB proteins.

domain (**Figure 1B**). Two ends of the HR1 domain are conserved, but its middle region is relatively unique, which may be helpful to adapt the variable HR2 domain of LASV GP2.

To reveal the interaction between HR1 and HR2 domains of LASV, stable 6-HB covering HR1, T-loop and HR2 domains (residues 306–432), was constructed for crystallographic study. The denaturation and renaturation were used to acquire stable 6-HB from inclusion body to mimic its post-fusion state. During refolding process, the wild type LASV 6-HB protein mainly formed precipitations or high polymers. After the single mutation of C310S was introduced, the trimeric LASV 6-HB protein was obtained (**Figure 1C**). However, the large-scale of crystal screening for this protein could not yield high-quality crystals. Then we continued to try different truncations and deletions in 6-HB, and finally found that a deletion of Gly378 and Lys379 in the T-loop region could yield protein crystal with enough quality for structure determination.

The overall structure of the HR1-T-loop-HR2 domain showed a canonical 6-HB structure (**Figure 2A**). Taking a rod-like shape with a length of ∼75 Å and a diameter of ∼40 Å, the LASV fusion core contains a parallel trimeric coiled-coil of three HR1 helices (gray in **Figure 2A**), around which three HR2 helices are entwined (green in **Figure 2A**) in an antiparallel manner. Between these two domains, the T-loop forms a $3_{10}$ helix linker hovering outside (cyan in **Figure 2A**).

## Comparison of the Fusion Core Structure of LASV With Those of LCMV, HIV, Middle East Respiratory Syndrome Coronavirus (MERS-CoV), and Mouse Hepatitis Virus (MHV)

According to the structure shown in electrostatic potential surface (**Figure 2B**), the HR2 region of LASV can be divided into

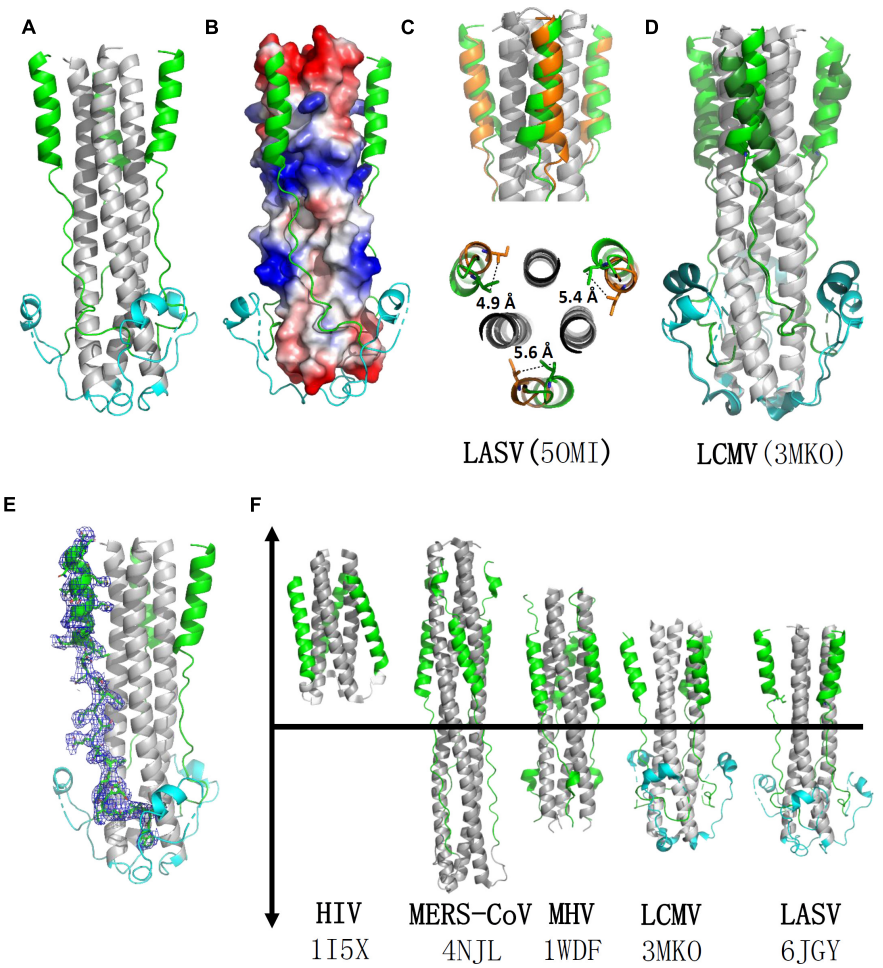


**FIGURE 2 |** Crystal structure of LASV fusion core. **(A)** The overall structure of HR1-T-loop-HR2 domains of LASV is shown in cartoon representation. HR1 domain is colored in gray, T-loop is in cyan and HR2 is in green. **(B)** The HR1 trimer core is shown as electrostatic potential surface. **(C)** Comparing the structure with another reported LASV 6-HB structure (PDB: 5OMI), the HR2 domain of which is colored in orange. **(D)** Comparing the structure with fusion core structure of LCMV (PDB: 3MKO), the T-loop domain and HR2 domain of which are colored in dark green. **(E)** The electron density map of HR2 domain are shown as blue mesh. **(F)** Structural comparison of different fusion cores, including HIV (PDB: 1I5X), MERS-CoV (4NJL), MHV (PDB: 1WDF), LCMV (PDB: 3MKO), and LASV (PDB: 6JGY). Their HR1 domains are colored in gray, HR2 in green, and T-loop in cyan.

two parts: a linear N-terminal region and a helical C-terminal region. The linear N-terminal region binds to two adjacent HR1 helices through hydrophobic interactions, consistent with other fusion core structures, as previously determined (Lu et al., 2014). Some obvious charged interactions take place between the helical C-terminal region of HR2 and HR1 trimer core, and these will be discussed later. Another group deposited a post-fusion structure of LASV in PDB (entry code 5OMI), using a baculovirus expression system, instead of our renaturation method. Compared with this structure, the HR2 helical region in our structure exhibited a significant shift of 4.9∼5.6 Å toward the hydrophobic grooves of two adjacent HR1 helices, showing much stronger hydrophobic interaction (**Figures 2C,E**).

Lymphocytic choriomeningitis virus and LASV both belong to the Old World family and have high sequence homology (**Figure 1B**). Comparing the fusion core structure of LCMV (PDB entry 3MKO) with that of LASV, we found that their HR1 domains overlap with each other very well, but their T-loop and HR2 helical regions have obvious differences (**Figure 2D**). The T-loop region of LCMV fusion core moves closer to the HR2 region, and its HR2 helical region slopes away from HR2 of LASV. When further comparing the 6-HB structures of LCMV and LASV with those of other viruses, we found several unique features for arenavirus GP2 protein (**Figure 2F**). The HR1 and HR2 regions of HIV form a short regular α-helix structure, while coronaviruses, like MERS-CoV and MHV, have a short helical HR2 region, but longer helical HR1 region. For arenavirus of LASV or LCMV, a special T-loop region is situated between HR1 and HR2 domains, packing along the linear HR2 region.

## Interactions in LASV 6-HB Fusion Core

The three HR1 helices of LASV are closely packed against each other by hydrophobic force in a parallel manner. The buried area for each HR1 domain reaches 1584 $Å^2$, indicating a much stronger interaction (**Figure 3A**). At the C-terminal of HR1, it is interesting that two hydrophilic interactions occur among the HR1 trimers. The Asp347 and Lys352 of one HR1 domain bind to the residues with opposite charges in other two HR1 domains. As shown in **Figure 1B**, these two residues are highly conserved among different arenaviruses, suggesting that this additional charged interaction may play an important role in enhancing the stability at the end of HR1 trimer.

The T-loop region and HR2 domain are well packed against the hydrophobic grooves of a central three-helical coiled coil with an interface of 2143 $Å^2$ (**Figure 3B**). Leu355, Ile358, and Ile361 of T-loop bind to the C-terminal end of HR1 trimer. In the linear HR2 domain, Trp386, Val388, Leu394, and Phe399 are deeply buried in the HR1 hydrophobic groove. Even in the helical HR2 domain, many hydrophobic residues with long side chains are involved in binding to HR1, including Ile403, Met410, Ile411, Met414, and Leu415 (**Figure 3B**). Moreover, at the junction region between linear and helical parts of HR2, several strong hydrogen bonds and salt bridges are noted. For hydrogen bonds, the hydroxyl group of Ser400 in HR2 interacts with Glu329 in one HR1 helix (∼2.5 Å distance), while its carbonyl oxygen interacts with Lys327 in another HR1 helix (∼2.2 Å distance) (**Figure 3B**). For salt bridges, Asp402 interacts with Arg325 (∼2.9 Å distance), and Glu404 interacts with Lys320 and Gln324 (∼3.2 Å and 3.6 Å distances, respectively). These relatively concentrated hydrophilic interactions constitute an anchoring point in the middle of HR2 domain, stabilizing the linear and helical region of HR2 and also the whole 6-HB conformation.

To confirm the secondary structure before and after the formation of fusion core, the α-helical ratios of HR1 peptide, HR2 peptide, and their mixture were analyzed by circular dichroism. In solution, the single HR1 and HR2 peptides showed relatively low α-helical ratio of 17 and 28%, respectively. However, when they were mixed together to form 6-HB, the α-helical ratio largely increased to 68% (**Figure 3C**), which is consistent with the crystal structure. It suggests that the two peptides undergo a significantly conformational change when they interact with each other to form 6-HB fusion core.

## Biophysical Characterization of HR2-Derived Peptides

To elucidate the interactions between HR1 and HR2 regions of LASV, as observed in the crystal structure, the HR1-derived peptide (HR1-1) and HR2-derived peptides (HR2-1∼HR2-5) were synthesized to measure their binding affinities using BLI. HR2-1 peptide showed a significant non-specific adsorption on the sensor, making it impossible to measure affinity data. All other peptides showed weak non-specific binding to the sensor at the concentration of 60 μM. Then, HR1-1 was used as the immobilized molecule to detect the affinity between HR1-1 and HR2-2 ∼ HR2-5. The results showed that HR2-2 and HR2-3 peptides could strongly bind to HR1-1 peptides in a dose-dependent manner (**Figure 4A**), while HR2-4 and HR2-5 could not.

Both hydrophobic and hydrophilic interactions between HR2-4 and HR1-1 peptide are seen in the crystal structure (**Figure 4B**). The major hydrophobic interactions in HR2-4 peptide (391-410) include Phe399, Ile403, and Met410, which were buried in the hydrophobic groove of HR1-1 trimeric core. Several hydrogen bonds were also observed between HR2-4 and HR1-1. The side chain oxygen of Ser400 binds to Glu329 in one HR1 helix, while its main chain oxygen binds to Lys327 in another HR1 helix (**Figure 3B**). Then Asp402 binds to Arg325, and Glu404 interacts with Lys320 and Gln324. However, despite these potential interactions, BLI results showed weak interaction between HR2-4 and HR1-1 peptides. It is possible that a short peptide like HR2-4 may not form the right conformation to bind to its target; otherwise, the missing hydrophobic interactions mediated by Met414 and Leu415 might reduce the binding affinity.

Almost no hydrophilic interaction occurs between the HR2-5 peptide and HR1-1 peptide in the structure. Their hydrophobic interactions are mainly provided by Met410, Ile411, Met414, and Leu415 (**Figure 3B**). Based on BLI testing, no strong interactions were found between HR2-5 and HR1-1 peptides. Therefore, the missing hydrogen bonds and hydrophobic residues largely reduce HR2-5′s interactions with viral HR1 core.

In the BLI test, both HR2-2 and HR2-3 peptides exhibited interactions with HR1-1 peptide. The structure also showed many strong hydrophobic and hydrophilic interactions between HR2-2 and HR2-3 peptides, both of which have identical residues providing hydrophobic interactions with HR1-1, including Phe399, Ile403, Met410, Ile411, Met414, and Leu415 (**Figure 3B**). They also share the same amino acids involved in hydrophilic interactions, including Ser400, Asp402, and Glu404. Compared with HR2-4 and HR2-5, longer peptides like HR2-2 and HR2-3 exhibited the optimal conformation folding and

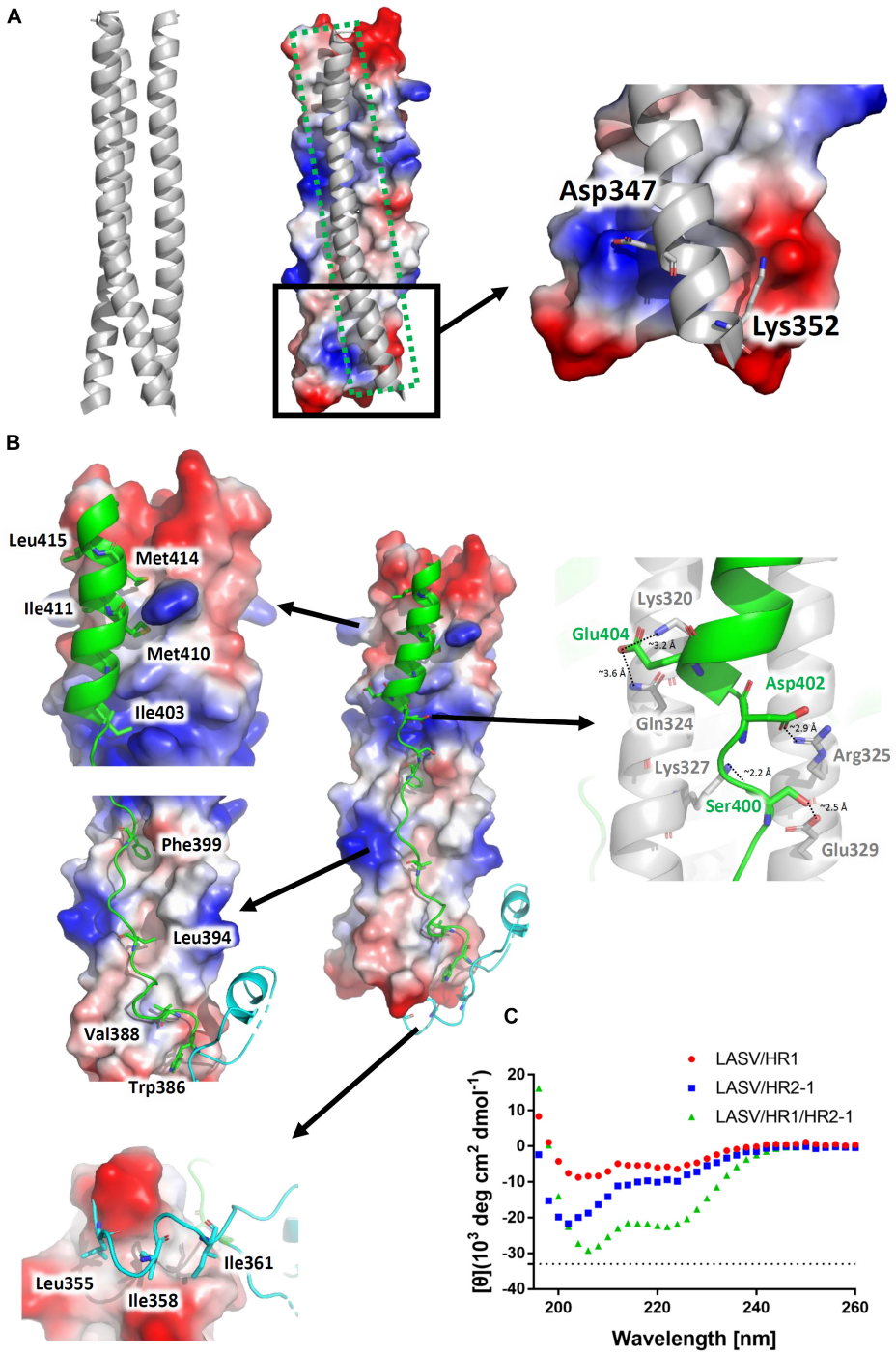


**FIGURE 3 |** Interactions within the LASV 6-HB fusion core. **(A)** Three HR1 helices are tightly packed together in the fusion core with a buried interface of 1584 Å$^2$ for each HR1. Hydrophilic interactions are also at the end of the trimers. **(B)** Interactions for T-Loop or HR2 domain against HR1 trimer core. The buried interface for each HR2 domain with HR1 core is 2143 Å$^2$. Important hydrophobic and hydrophilic residues are indicated. **(C)** The circular dichroism spectroscopy of HR peptides.

had sufficient key residues for interaction with the HR1-1 trimer.

## The Longer HR2-Peptides Could Not Block LASV Pseudovirus Entry Into the Target Cell, but Were Effective in Inhibiting LASV GPC Protein-Mediated Cell–Cell Fusion

Because of the strict restriction on the use of highly pathogenic viruses in our BSL-3 facilities, we were not able to get live LASV for testing the anti-LASV activity of the HR2-peptides. We thus tested the potential inhibitory activity of these peptides against LASV pseudovirus entry into the target cells. Unexpectedly, none of the HR2-derived peptides exhibited significant inhibitory activity on the entry of the LASV pseudovirus into the target cell at the concentration as high 100 μM (**Figure 5A**). These results suggest that the HR2-peptides may not interact with the GP1 protein, which mediates the attachment of LASV to the target cell, the first step of viral entry, and that LASV may not get into the cell through the cytoplasm membrane fusion under neutral pH condition, the second step of entry of some class I enveloped viruses, such as HIV and MERS-CoV (Qi et al., 2017; Su et al., 2017; Xia et al., 2019).

Next, we assessed the potential inhibitory activities of these HR2-derived peptides against LASV GPC protein-mediated cell–cell fusion under low pH condition. At 20 μM, peptide HR2-1 could completely inhibit the cell–cell fusion, while peptides HR2-2 and HR2-3 could inhibit about 30–40% and 20% cell–cell fusion, respectively, and the peptides HR2-4 and HR2-5 showed no inhibitory activity (**Figure 5Ba**). Further analysis indicated that the peptides HR2-1 and HR2-2 inhibited cell–cell fusion in a dose-dependent manner with the $IC_{50}$ (the half maximal inhibitory concentration) values of 0.37 and 26.45 μM, respectively (**Figure 5Bb**), while other HR2-derived peptides had no detectable inhibitory activity. These results suggest that the

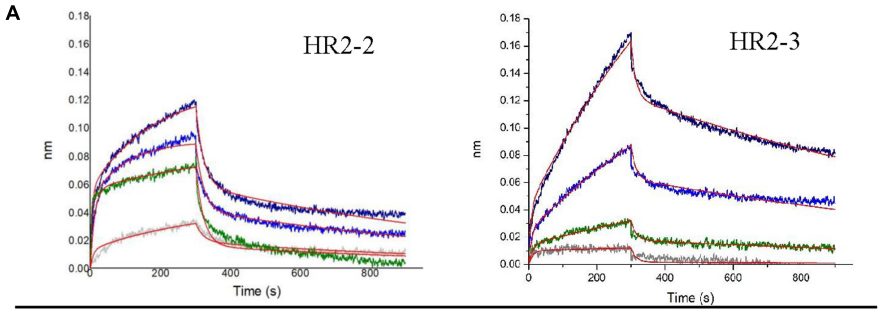


| Immobilized molecule | Mobile phase | Concentration (μM) | Response (nm) | KD (M) | Kon (1/Ms) | Kdis (1/ s) |
|---|---|---|---|---|---|---|
| HR1-1 | HR2-2 | 30 | 0.119 | 1.62E-05 | 5.73E+02 | 6.77E-02 |
| | | 15 | 0.0958 | | | |
| | | 7.5 | 0.0743 | | | |
| | | 3.75 | 0.0341 | | | |
| | HR2-3 | 30 | 0.1668 | 6.69E-05 | 1.42E+03 | 8.23E-02 |
| | | 15 | 0.0857 | | | |
| | | 7.5 | 0.0307 | | | |
| | | 3.75 | 0.0104 | | | |

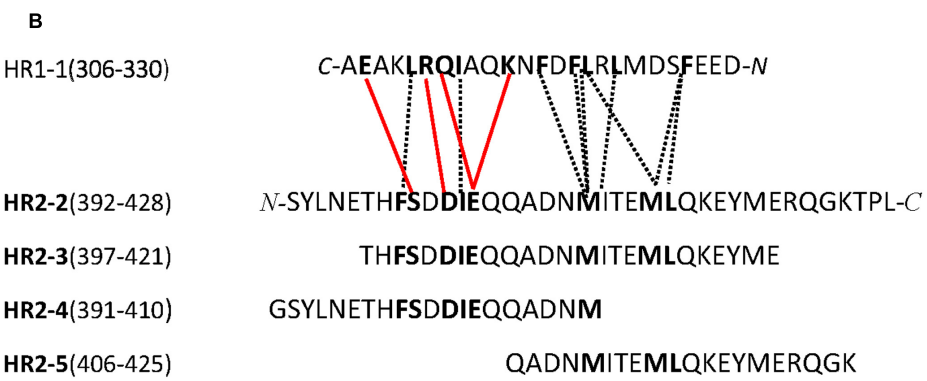


**FIGURE 4 |** Binding affinity between HR1 and HR2 peptides was measured by BLI. **(A)** Binding curve of HR2-2 or HR2-3 peptide in concentration gradient (30 μM, 15 μM, 7.5 μM, and 3.75 μM) against HR1-1 peptide. The red curves represent the fitting line. The KD values are also shown. **(B)** The interaction residues between HR1- and HR2-derived peptides. The hydrophobic interactions are shown in black dashed lines, while the hydrophilic interactions are shown in red lines.

longer HR2 peptides could inhibit cell–cell fusion because of their higher affinity to bind with the HR1 groove (**Figure 3B**) and that LASV may enters into the target cell through micropinocytosis and membrane fusion under low pH condition.

## DISCUSSION

We solved the crystal structure of the post-fusion 6-HB formed by HR1 and HR2 domains of LASV GP2 protein and then designed several HR2-derived peptides to study their binding affinities against HR1 peptide and inhibitory activities for viral entry. We found that the longer HR2 peptides, HR2-2 (37-mer: 392-428), and HR2-3 (25-mer: 397-421), had higher binding affinity with HR1 peptide than the shorter HR2 peptides, HR2-4 (20-mer: 391-410), and HR2-5 (20-mer: 406-425), possibly owing to their rich hydrophobic and hydrophilic interactions (**Figure 4**). Moreover, the longer peptides of HR2-1 (48-mer: 385–432) and HR2-2 exhibited more obvious inhibitory activities against LASV G protein-mediated cell–cell fusion. These results suggest that the longer HR2-derived peptides, which have stronger affinity against the HR1 domain, also have more potent inhibitory activity. On the contrary, the shorter HR2 peptides, HR2-4 and HR2-5, do not interact with HR1 peptide, thus showing no cell–cell fusion inhibitory activity. In the cell–cell fusion process, the GP1 protein of LASV binds to its target receptor to expose the GP2 subunit. Then, the HR2 domain binds to the HR1 domain to form the 6-HB fusion core to mediate the formation of membrane fusion pores. At this time, the HR1 domain becomes a very exposed target for binding and blocking by an HR2-derived peptide. Therefore, the binding affinity of HR2 peptides is positively related to the inhibitory activity against LASV GPC protein-mediated cell–cell fusion under low pH condition.

However, all these HR2-derived peptides showed weak or no inhibitory activity against LASV pseudovirus entry into the target cell. It confirms that the HR2-peptides do not interact with the GP1 protein to block its interaction with the receptor on the target cell, the first step of viral entry. These findings also suggest that LASV enters the target cell using the fusion pathway different from that utilized by some other class I enveloped viruses, such as HIV and MERS-CoV (Qi et al., 2017; Su et al., 2017; Xia et al., 2019), which get into the host cells via cytoplasm membrane fusion under neutral pH condition. Several groups have shown that LASV enters the host cell via clathrin- and dynamin-independent endocytosis and membrane fusion occurs at low pH (Vela et al., 2007; Rojek et al., 2008). Oppliger and coworkers (Oppliger et al., 2016) have recently reported that LASV enters the target cell through macropinocytosis. Since our results are consistent with those in the reports above, we proposed an infection model of LASV (**Figure 6**). Specifically, LASV enters

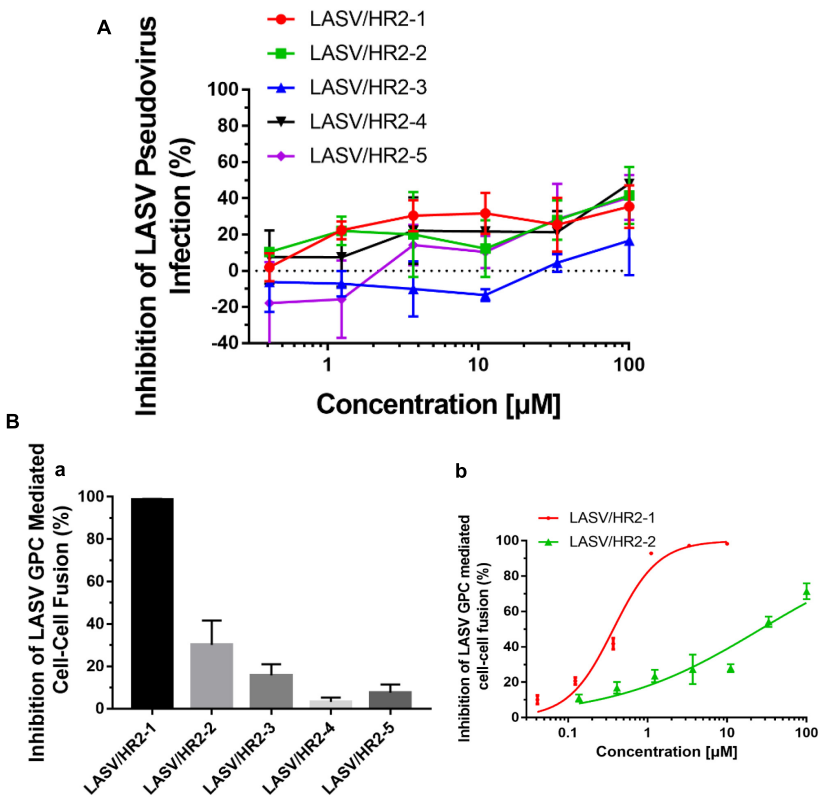


**FIGURE 5 |** The inhibitory activity of LASV HR2-derived peptides on LASV pseudovirus into the target cell and LASV G protein-mediated cell–cell fusion. **(A)** Inhibition of HR2-derived peptides on the entry of LASV pseudovirus into the host cell. **(B)** Inhibition of five HR2 peptides at 20 μM **(a)** or different concentrations **(b)** against LASV GPC protein-mediated cell–cell fusion.

the target cells via endocytosis, including macropinocytosis. In the membrane fusion process as revealed by the cell–cell fusion assay, the GP1 trimer of LASV binds to its receptor(s), e.g., α-Dystroglycan, to trigger the conformational change of GP2. Then HR1 is exposed to bind with HR2 to form 6-HB, resulting in the fusion between viral envelope and endosomal membrane. Under these conditions, HR2-derived peptides could bind to the HR1 target to block viral infection. However, during the entry process of live and pseudotyped LASV, the HR1 domain of viral GP2 can only be exposed in the endosomal compartment and interacts with the HR2 domain of viral GP2 to mediate membrane fusion under low pH condition, making it impossible for HR2 peptides to enter the endosomal compartment to block membrane fusion there (**Figure 6**). Therefore, HR2 peptides must be modified, for example, by adding TAT cell penetration sequence (Miller et al., 2011) or hydrocarbon stapling motif (Wang et al., 2018), so that they can enter into the endosomal compartment inside the cell to interact with HR1 domain of the viral GP1 domain and inhibit the membrane fusion at low pH there.

In the BLI test, HR2-2 and HR2-3 peptides exhibited different binding affinity with HR1-1 peptide, even though they shared the same hydrophilic and hydrophobic residues to interact with NHR fusion core in the structure (**Figure 4**). HR2-2 peptide

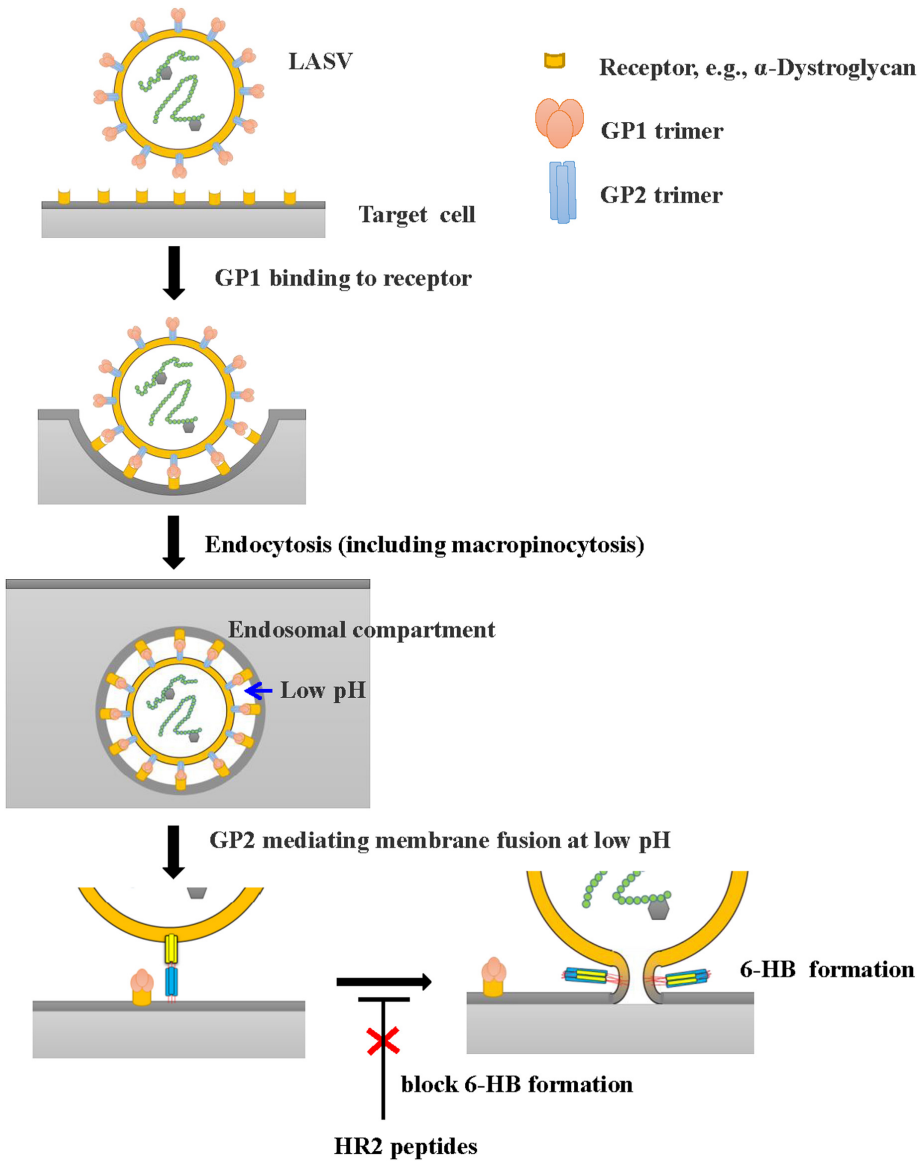


**FIGURE 6 |** Proposed infection model of LASV. LASV can enter the target cell via endocytosis, including macropinocytosis, and membrane fusion at low pH. HR2-peptides or their analogs, if they can enter the endosomal compartment inside the host cell, can interact with the HR1 domain in viral GP2 and block the 6-HB formation, thereby inhibiting membrane fusion at low pH. Their fusion inhibitory activity can be assessed using the LASV GPC protein-mediated cell–cell fusion assay under low pH condition (**Figure 5B**).

has several additional residues in both N-terminus (SYLNE) and C-terminus (RQGKTPL) compared with the HR2-3 peptide. Although these residues are not involved in the NHR-CHR interactions in the crystal structure, they may help stabilize the overall structure of the entire HR2 peptide. Thus, compared with the HR2-3 peptide, the more stable HR2-2 peptide has higher affinity in binding HR1-1 peptide (**Figure 4**), as well as higher inhibitory activity in cell–cell fusion (**Figure 5B**). Therefore, the HR2-2 peptide will be modified for further development as an anti-LASV drug candidate.

## DATA AVAILABILITY

The datasets generated for this study can be found in the Protein Data Bank with accession number 6JGY for crystal structure of fusion core of LASV GP2 protein.

## AUTHOR CONTRIBUTIONS

YZ, SJ, and SY designed the experiments. YZ, SJ, and RZ wrote the manuscript. XZ and BC performed the protein purification and crystallization. CW, QW, and WX participated in the viral experiments.

## FUNDING

This work was supported by grants from the National Natural Science Foundation of China (31400638 to YZ, 81630090 to SJ, 81701998 to QW, and 81703571 to WX) and the Strategic Priority Research Program of the Chinese Academy of Sciences (Grant No. XDB08030102).

## ACKNOWLEDGMENTS

We are very grateful to the staff of the Structural Biology Core Facility (Institute of Biophysics, University of Chinese Academy of Sciences) for their technical assistance, especially to Ms. Ya Wang, Mr. Yi Han, Ms. Xiaoxia Yu, Zhenwei Yang, Bingxue Zhou, and Ms. Yuanyuan Chen. We are also grateful to Ye Fan (Institute of Microbiology, Chinese Academy of Sciences) for technical help with BLI experiments and to Ms. Min Wang for her kind help with laboratory affairs.

## REFERENCES

Asogun, D. A., Adomeh, D. I., Ehimuan, J., Odia, I., Hass, M., Gabriel, M., et al. (2012). Molecular diagnostics for lassa fever at irrua specialist teaching hospital, Nigeria: lessons learnt from two years of laboratory operation. *PLoS Negl. Trop. Dis.* 6:e1839. doi: 10.1371/journal.pntd.0001839

Cao, W., Henry, M. D., Borrow, P., Yamada, H., Elder, J. H., Ravkov, E. V., et al. (1998). Identification of α-dystroglycan as a receptor for lymphocytic choriomeningitis virus and lassa fever virus. *Science* 282, 2079–2081. doi: 10.1126/science.282.5396.2079

Channappanavar, R., Lu, L., Xia, S., Du, L., Meyerholz, D. K., Perlman, S., et al. (2015). Protective effect of intranasal regimens containing peptidic middle east respiratory syndrome coronavirus fusion inhibitor against MERS-CoV infection. *J. Infect. Dis.* 212, 1894–1903. doi: 10.1093/infdis/jiv325

Cosset, F. L., Marianneau, P., Verney, G., Gallais, F., Tordo, N., Pecheur, E. I., et al. (2009). Characterization of *Lassa virus* cell entry and neutralization with *Lassa virus* pseudoparticles. *J. Virol.* 83, 3228–3237. doi: 10.1128/JVI.01711-08

Emsley, P., and Cowtan, K. (2004). Coot: model-building tools for molecular graphics. *Acta Crystallogr. D Biol. Crystallogr.* 60, 2126–2132. doi: 10.1107/s0907444904019158

Hastie, K. M., Zandonatti, M. A., Kleinfelter, L. M., Heinrich, M. L., Rowland, M. M., Chandran, K., et al. (2017). Structural basis for antibody-mediated neutralization of *Lassa virus*. *Science* 356, 923–928. doi: 10.1126/science.aam7260

Li, Q., Liu, Q., Huang, W., Wu, J., Nie, J., Wang, M., et al. (2017). An LASV GPC pseudotyped virus based reporter system enables evaluation of vaccines in mice under non-BSL-4 conditions. *Vaccine* 35, 5172–5178. doi: 10.1016/j.vaccine.2017.07.101

Li, S., Sun, Z., Pryce, R., Parsy, M. L., Fehling, S. K., Schlie, K., et al. (2016). Acidic pH-induced conformations and LAMP1 binding of the *Lassa Virus* glycoprotein spike. *PLoS Pathog.* 12:e1005418. doi: 10.1371/journal.ppat.1005418

Lu, L., Liu, Q., Zhu, Y., Chan, K. H., Qin, L., Li, Y., et al. (2014). Structure-based discovery of middle east respiratory syndrome coronavirus fusion inhibitor. *Nat. Commun.* 5, 3067. doi: 10.1038/ncomms4067

Mccoy, A. J. (2007). Solving structures of protein complexes by molecular replacement with Phaser. *Acta Crystallogr. D Biol. Crystallogr.* 63, 32–41. doi: 10.1107/s0907444906045975

Miller, E. H., Harrison, J. S., Radoshitzky, S. R., Higgins, C. D., Chi, X., Dong, L., et al. (2011). Inhibition of *Ebola virus* entry by a C-peptide targeted to endosomes. *J. Biol. Chem.* 286, 15854–15861. doi: 10.1074/jbc.M110.207084

Oppliger, J., Torriani, G., Herrador, A., and Kunz, S. (2016). *Lassa Virus* cell entry via dystroglycan involves an unusual pathway of macropinocytosis. *J. Virol.* 90, 6412–6429. doi: 10.1128/JVI.00257-16

Otwinowski, Z., and Minor, W. (1997). Processing of X-ray diffraction data collected in oscillation mode. *Methods Enzymol.* 276, 307–326. doi: 10.1016/s0076-6879(97)76066-x

Qi, Q., Wang, Q., Chen, W., Du, L., Dimitrov, D. S., Lu, L., et al. (2017). HIV-1 gp41-targeting fusion inhibitory peptides enhance the gp120-targeting protein-mediated inactivation of HIV-1 virions. *Emerg. Microbes Infect.* 6, e59. doi: 10.1038/emi.2017.46

Rojek, J. M., Sanchez, A. B., Nguyen, N. T., De La Torre, J. C., and Kunz, S. (2008). Different mechanisms of cell entry by human-pathogenic old world and new world arenaviruses. *J. Virol.* 82, 7677–7687. doi: 10.1128/JVI.00560-08

Shaffer, J. G., Grant, D. S., Schieffelin, J. S., Boisen, M. L., Goba, A., Hartnett, J. N., et al. (2014). Lassa fever in post-conflict sierra leone. *PloS Negl. Trop. Dis.* 8:e2748. doi: 10.1371/journal.pntd.0002748

Shulman, A., Katz, M., Cohen-Dvashi, H., Greenblatt, H. M., Levy, Y., and Diskin, R. (2019). Variations in core packing of GP2 from old world mammarenaviruses in their post-fusion conformations affect membrane-fusion efficiencies. *J. Mol. Biol.* 43, 2095–2111. doi: 10.1016/j.jmb.2019.04.012

Sogoba, N., Feldmann, H., and Safronetz, D. (2012). Lassa fever in West Africa: evidence for an expanded region of endemicity. *Zoonoses Public Health* 59(Suppl. 2), 43–47. doi: 10.1111/j.1863-2378.2012.01469.x

Su, S., Wang, Q., Xu, W., Yu, F., Hua, C., Zhu, Y., et al. (2017). A novel HIV-1 gp41 tripartite model for rational design of HIV-1 fusion inhibitors with improved antiviral activity. *AIDS* 31, 885–894. doi: 10.1097/QAD.0000000000001415

Vela, E. M., Zhang, L., Colpitts, T. M., Davey, R. A., and Aronson, J. F. (2007). Arenavirus entry occurs through a cholesterol-dependent, non-caveolar, clathrin-mediated endocytic mechanism. *Virology* 369, 1–11. doi: 10.1016/j.virol.2007.07.014

Wang, C., Xia, S., Zhang, P., Zhang, T., Wang, W., Tian, Y., et al. (2018). Discovery of Hydrocarbon-stapled short alpha-helical peptides as promising middle east respiratory syndrome coronavirus (MERS-CoV) fusion inhibitors. *J. Med. Chem.* 61, 2018–2026. doi: 10.1021/acs.jmedchem.7b01732

Wang, X., Zou, P., Wu, F., Lu, L., and Jiang, S. (2017). Development of small-molecule viral inhibitors targeting various stages of the life cycle of emerging

and re-emerging viruses. *Front. Med.* 11:449–461. doi: 10.1007/s11684-017-0589-5

Xia, S., Xu, W., Wang, Q., Wang, C., Hua, C., Li, W., et al. (2018). Peptide-Based membrane fusion inhibitors targeting HCoV-229E spike protein HR1 and HR2 domains. *Int. J. Mol. Sci.* 19:E487. doi: 10.3390/ijms19020487

Xia, S., Yan, L., Xu, W., Agrawal, A. S., Algaissi, A., Tseng, C.-T. K., et al. (2019). A pan-coronavirus fusion inhibitor targeting the HR1 domain of human coronavirus spike. *Sci. Adv.* 5:eaav4582. doi: 10.1126/sciadv.aav4580

Zhu, X., Zhu, Y., Ye, S., Wang, Q., Xu, W., Su, S., et al. (2015). Improved pharmacological and structural properties of HIV fusion inhibitor ap3 over enfuvirtide: highlighting advantages of artificial peptide strategy. *Sci. Rep.* 5:13028. doi: 10.1038/srep13028

Zhu, Y., Su, S., Qin, L., Wang, Q., Shi, L., Ma, Z., et al. (2016). Rational improvement of gp41-targeting HIV-1 fusion inhibitors: an innovatively designed Ile-Asp-Leu tail with alternative conformations. *Sci. Rep.* 6:31983. doi: 10.1038/srep31983

Zwart, P. H., Afonine, P. V., Grosse-Kunstleve, R. W., Hung, L. W., Ioerger, T. R., Mccoy, A. J., et al. (2008). Automated structure solution with the PHENIX suite. *Methods Mol. Biol.* 426, 419–435. doi: 10.1007/978-1-60327-058-8_28

**Conflict of Interest Statement:** The authors declare that the research was conducted in the absence of any commercial or financial relationships that could be construed as a potential conflict of interest.

*Copyright © 2019 Zhang, Wang, Chen, Wang, Xu, Ye, Jiang, Zhu and Zhang. This is an open-access article distributed under the terms of the Creative Commons Attribution License (CC BY). The use, distribution or reproduction in other forums is permitted, provided the original author(s) and the copyright owner(s) are credited and that the original publication in this journal is cited, in accordance with accepted academic practice. No use, distribution or reproduction is permitted which does not comply with these terms.*

frontiers in Microbiology

ORIGINAL RESEARCH
published: 26 September 2019
doi: 10.3389/fmicb.2019.02188

# The Underlying Mechanism of 3-Hydroxyphthalic Anhydride-Modified Bovine Beta-Lactoglobulin to Block Human Papillomavirus Entry Into the Host Cell

*Chen Hua[1†], Yun Zhu[2*], Congquan Wu[3†], Lulu Si[1], Qian Wang[1], Long Sui[3*] and Shibo Jiang[1*]*

[1]*Key Laboratory of Medical Molecular Virology (MOE/NHC/CAMS), School of Basic Medical Sciences, Fudan-Jinbo Functional Protein Joint Research Center, Fudan University, Shanghai, China,* [2]*National Laboratory of Biomacromolecules, Institute of Biophysics, Chinese Academy of Sciences, Beijing, China,* [3]*Medical Center for Diagnosis and Treatment of Cervical Disease, Obstetrics and Gynecology Hospital, Fudan University, Shanghai, China*

OPEN ACCESS

**Edited by:**
*Lijun Rong,*
*University of Illinois at Chicago, United States*

**Reviewed by:**
*Young Bong Kim,*
*Konkuk University, South Korea*
*Yang Xiang,*
*Peking Union Medical College Hospital (CAMS), China*

***Correspondence:**
*Yun Zhu*
*zhuyun@ibp.ac.cn*
*Long Sui*
*suilong@fudan.edu.cn*
*Shibo Jiang*
*shibojiang@fudan.edu.cn*

[†]*These authors have contributed equally to this work*

**Specialty section:**
*This article was submitted to Virology, a section of the journal Frontiers in Microbiology*

**Received:** *13 July 2019*
**Accepted:** *05 September 2019*
**Published:** *26 September 2019*

**Citation:**
*Hua C, Zhu Y, Wu C, Si L, Wang Q, Sui L and Jiang S (2019) The Underlying Mechanism of 3-Hydroxyphthalic Anhydride-Modified Bovine Beta-Lactoglobulin to Block Human Papillomavirus Entry Into the Host Cell. Front. Microbiol. 10:2188. doi: 10.3389/fmicb.2019.02188*

We have previously demonstrated that 3-hydroxyphthalic anhydride (3HP)-modified bovine beta-lactoglobulin (3HP-β-LG) is highly effective in inhibiting entry of pseudovirus (PsV) of high- and low-risk human papillomavirus (HPV) into the target cell. Intravaginally applied 3HP-β-LG-containing vaginal gel could significantly inhibit HPV infection and reduce viral load in the cervical region. However, we still do not understand the underlying molecular mechanism by which 3HP-β-LG is able to inhibit HPV infection. Here, though, we showed that 3HP-β-LG did not inactivate HPV PsV, but rather blocked entry of HPV PsV into the target cell *via* its interaction with virus, not cell. It bound to the positively charged region in the HPV L1 protein, suggesting that 3HP-β-LG binds to HPV L1 protein through the interaction between the negatively charged region in 3HP-β-LG and the positively charged region in HPV L1 protein, thus competitively blocking the binding of HPV to the receptor on the basement membrane in vaginal mucosa. Although 3HP-modified chicken ovalbumin (3HP-OVA) also carries high net negative charges, it exhibited no anti-HPV activity, suggesting that the interaction between 3HP-modified protein and HPV L1 protein relies on both electrostatic and matchable conformation of the binding sites in both proteins. When topically applied, 3HP-β-LG did not enter the host cell or blood circulation. These findings suggest that 3HP-β-LG targets HPV L1 protein and blocks HPV entry into the host cell, thus being safe and effective for topical application in the treatment of HPV infection.

**Keywords: 3HP-β-LG, human papillomavirus, virus entry inhibition, L1 protein, mechanism of action**

## INTRODUCTION

Cervical cancer is the second most common cancer among women in China (Chen et al., 2016). Almost all these cases result from the persistent infection of human papillomavirus (HPV) (Bosch et al., 2002). HPVs are a large viral family consisting of about 200 different types (Bernard et al., 2010). Among them, 18 types have high oncogenic properties, and these

are regarded as the high-risk types, such as HPV16, HPV18, and HPV58. The high-risk types of HPV have relatively low self-clearance rate compared to the low-risk types of HPV (Safaeian et al., 2008). To prevent the infection of these high-risk HPVs and the occurrence of cervical cancer, several prophylactic vaccines, like Cervarix, Gardasil, and Gardasil 9 (Deschuyteneer et al., 2010; McCormack, 2014), have been developed and approved for marketing in many countries. However, no therapeutic vaccines or drugs have been approved for clinical use to treat HPV-infected patients.

HPV is a non-enveloped, double-stranded DNA virus. Its capsid is made up of two proteins, major protein L1 and minor protein L2. They are both involved in receptor binding and viral entry. Analysis of the atomic structure of native $T = 7$ HPV virus-like particle (VLP) reveals that 72 L1 pentamers form the icosahedral shell of HPV (Baker et al., 1991; Li et al., 2016). The L1 pentamer strongly binds to HPV receptors, such as heparan sulfate proteoglycans (HSPGs), on the basement membrane to mediate viral entry and infection (Kines et al., 2009). The highly potent neutralizing antibodies elicited by HPV vaccines were found to bind to the L1 protein and prevent HPV infection (Li et al., 2018). Thus, the L1 pentamer is regarded as the most important target for development of antiviral agents against HPV infection.

Viral entry inhibitors represent a class of antiviral agents that inhibit virus infection by blocking virus entry into the host cells. Jiang et al. reported the first peptide-based HIV entry inhibitor, SJ-2176, in 1993 (Jiang et al., 1993) and the first HIV entry inhibitor-based anti-HIV drug, enfuvirtide, was approved by U.S. FDA for clinical use in 2003 (Dando and Perry, 2003). Later, Jiang and colleagues have reported that anhydride-modified proteins such as 3-hydroxyphthalic anhydride (3HP)-modified proteins are potent virus entry inhibitors against a number of enveloped viruses, such as HIV (Neurath et al., 1996), herpes simplex virus (HSV) (Neurath et al., 1996), and Ebola virus (EBOV) (Li et al., 2017). In 2012, Jiang's group reported that 3HP-modified bovine beta-lactoglobulin (3HP-β-LG) could also inhibit entry into the target cell of the pseudovirus (PsV) of non-enveloped virus, HPV (high-risk HPV16 and HPV18, and low-risk HPV6) (Lu et al., 2013). In the clinical trial, the topical application of vaginal gel containing 3HP-β-LG was proven to be very safe and highly effective in suppressing HPV infection and reducing viral load in vaginal mucosa (Guo et al., 2016a,b). However, we still do not understand the molecular mechanism by which 3HP-β-LG inhibits HPV infection. In this study, we found that while 3HP-β-LG could not inactivate HPV PsV, it was effective in inhibiting HPV PsV entry into the host cell *via* its interaction with virus, not the cell. Unlike β-LG, 3HP-β-LG could bind with L1 protein and the peptides derived from the positively charged region in the HPV L1 protein, suggesting that 3HP-β-LG inhibits HPV infection by binding, *via* its negatively charged region, to L1 protein, and thus competitively blocking HPV binding to the receptor on the basement membrane in vaginal mucosa, which then inhibits HPV from entering and replicating in the host cell. We have also shown that topically applied 3HP-β-LG does not enter the host cell and blood circulation. Therefore, the 3HP-β-LG-containing formulations can be safely used in vagina for treatment of HPV infection and prevention of cervical cancer development.

# MATERIALS AND METHODS

## Reagents

3-Hydroxyphthalic anhydride (HP), 2,4,6-trinitrobenzenesulfonic acid (TNBS), human serum albumin (HSA), β-lactoglobulin (β-LG), chicken ovalbumin (OVA), and bovine serum albumin (BSA) were purchased from Sigma. Horseradish peroxidase (HRP)-conjugated goat anti-human IgA and IgE antibodies were purchased from Abcam (UK). HRP-conjugated rabbit anti-mouse IgG antibody was purchased from Dako (Denmark). The HPV16- and HPV-58-L1/L2-expressing plasmids and Luciferase pCLucf plasmid were kindly provided by Dr. John Schiller at the Laboratory of Cellular Oncology, National Cancer Institute, NIH, MD, USA.

## Chemical Modification and Characterization of Anhydride-Modified Proteins

Anhydride-modified proteins were produced as previously described (Lu et al., 2013). Briefly, each kind of protein was dissolved with 0.1 M phosphate buffer (pH 8.5) at a final concentration of 20 mg/ml. Afterward, protein solutions were mixed with anhydrides (HP at 1 M in DMSO) to a final concentration of 60 mM by the addition of five equal aliquots at 20-min intervals, while the pH was adjusted to 9.0 with 4 M NaOH after each mixing. All mixtures were kept at 25°C for two more hours and then dialyzed against PBS.

## 3-Hydroxyphthalic Anhydride Modified Bovine Beta-Lactoglobulin-Mediated Inhibition Against Human Papillomavirus Pseudovirus Entry Into HeLa or HaCaT Cells

The HPV pseudovirus was produced as previously described[1]. Briefly, 293 T cells, which had been seeded in a 10-cm culture dish ($4 \times 10^6$ cells) at 16 h before transfection, were transfected with a mixture of HPV16-L1/L2-expressing plasmid (p16sheLL) and pCLucf plasmid for HPV16 PsV, or a mixture of HPV58-L1/L2-expressing plasmid (p58sheLL) and pCLucf plasmid for HPV58 PsV, using VigoFect (Vigorous Biotechnology Corp.). The cells were suspended in 0.5 ml of lysis buffer and incubated for 24 h at 37°C with slow rotation. The lysate was cooled on ice for 5 min, mixed with 5 M NaCl solutions to adjust the concentration of NaCl to 0.85 M, and further kept on ice for 10 min. Then, the lysate was centrifuged at 5,000 × *g* for 10 min at 4°C, and quantified for the concentration of L1/L2 capsid protein levels. To remove aggregates, the pseudovirion stock was filtered before use for the neutralization assay. The

[1]http://home.ccr.cancer.gov/lco/default.asp

inhibitory activity of 3HP-β-LG against HPV PsV entry into HeLa or HaCaT cells was detected as previously described (Surviladze et al., 2012; Kwak et al., 2014). Briefly, HeLa or HecCatT cells were seeded at $1.5 \times 10^4$ cells in 100 μl of 10% FBS DMEM (DMEM-10) per well in a 96-well plate, followed by a culture at 37°C overnight. 3HP-β-LG or β-LG was serially diluted in DMEM and incubated with 100 μl of HPV PsV (equal to 35 ng L1). Mixtures were added to HeLa or HaCaT cells and incubated at 37°C for 16 h. After replacement of the culture supernatants with free medium and culture for additional 72 h, cells were lysed for measurement of luciferase activity, according to the manufacturer's manual (Promega, Madison, WI, USA).

## Enzyme-Linked Immunosorbent Assay

3HP-β-LG diluted in PBS was coated onto all wells of a 96-well polystyrene plate (Corning, USA) at 4°C overnight. After blocking with protein-free blocking buffer (Thermo Fisher Scientific, USA), HPV L1 (type16 or 18) protein at 1 μg/ml was added into the wells for 50 μl/well, and the plate was incubated at 37°C for 1 h. After washing with PBST three times, mouse anti-HPV L1 (type16 or 18) antibody (Abcam, UK) was added at a 1: 1,000 dilution. After incubation at 37°C for 1 h and washing again, HRP-conjugated rabbit anti-mouse IgG antibody (Dako, Denmark) was added for 1 h. After washing and adding tetramethylbenzidine (Sigma, USA), the absorbance was measured at 450 nm. Similar protocols were used for detection of 3HP-β-LG in the serum of rhesus monkeys and 3HP-β-LG-specific IgA and IgE in the vaginal swab eluates, which were leftover samples from the clinical trials for evaluating the *in vivo* safety and efficacy of the intravaginally applied 3HP-β-LG-containing vaginal gels (Registry No.: ChiCTR-TRC-12002016) (Guo et al., 2016a,b).

## Isothermal Titration Calorimetry for Measurement of the Binding Ability of 3-Hydroxyphthalic Anhydride Modified Bovine Beta-Lactoglobulin and Beta-Lactoglobulin to Peptides

Two positively charged peptides of HPV L1 protein, L1-I (residues 474–488: LKAKPKFTLGKRKAT) and L1-II (residues 493–505: STSTTAKRKKRKL), were synthesized by a standard solid-phase Fmoc method as previously reported (He et al., 2007). The peptide solution (1 mM) was prepared in 50 mM phosphate buffer (pH 7.4) and added into the titration sample cells. 3HP-β-LG and β-LG were also dissolved in phosphate buffer to 50 μM and then added to the titration needle. Isothermal titration calorimetry (ITC) analysis was carried out at constant temperature of 18°C with stirring speed of 1,000 rev/min. Each titration volume was 2 μl, and the titration interval was 60 s for the first drop and 120 s for the others.

## Time-of-Addition Assay

HeLa cells were plated in a 96-well plate (for $1.0 \times 10^5$/well) overnight. Then, cells were incubated with 3HP-β-LG at a final concentration of 15 μg/ml at 0.5 h before or 0, 0.5, 1, 2, 4, 8, 12, 24, and 48 h after addition of HPV PsV (equal to 36 ng L1), followed by an incubation at 37°C for 16 h. After replacement of culture supernatant with fresh medium and an incubation for additional 72 h, cells were lysed to determine the entry inhibition ratio, according to the manufacturer's manual (Promega).

## Cell Wash Assay

HeLa cells in 96-well plates were preincubated with 100 μl of 3HP-β-LG (5 μM) or β-LG (5 μM) at 37°C for 1 h and then washed with DMEM three times before addition of HPV PsV. For the control, 3HP-β-LG- or β-LG-pretreated HeLa cells were not washed before HPV PsV was added. HPV PsV entry into HeLa cells was detected as described above.

## Temperature Shift Assay

The plated HeLa cells and 3HP-β-LG mixture were both prechilled at 4°C for 30 min. Then, the cells were incubated with the 3HP-β-LG mixture at 4°C for 12 h. After washing with cold PBS buffer twice, the cells were further incubated at 37°C for 72 h. Then the cells were lysed to determine luciferase activity, according to the luciferase assay system manual (Promega, USA).

## Experiment on Rhesus Macaques

The experiment on rhesus macaques was conducted under ethical guidelines and approved by the Ethics Committee of the Institute of Laboratory Animal Science, Chinese Academy of Medical Sciences and Peking Union Medical College (approval number: ILAS-VL-2015-001). In brief, the rhesus macaques were randomly divided into treatment group and control group. In the treatment group, vaginal gel containing 3HP-β-LG (1.8 mg per dose) was dispersed into carbomer gel and administered intravaginally or rectally. In the control group, only carbomer gel was applied. Then, 2 ml of blood was collected before or after injection at −1 h, 0 h, 30 min, 1 h, 2 h, 3 h, 6 h, 12 h, and 24 h. The serum was separated after condensation.

## Immunofluorescence Staining

To determine whether 3HP-β-LG could enter into HeLa or 293 T cells, cells ($1 \times 10^5$) were seeded onto coverslips in a 6-well plate. Then, 3HP-β-LG (0.5 μg/ml) was added for 12 h. Then, the supernatant was replaced with DMEM containing 2% FBS. After 24 days, the cells were fixed by 4% paraformaldehyde (PFA; Sigma-Aldrich, St. Louis, MO), perforated by 0.2% Triton X-100, and blocked with 3% BSA (Amresco, LLC, Solon, OH). Next, cells were incubated overnight with anti-3HP-β-LG mAb or anti-β-actin mAb (1:1,000) at 4°C. After five washes, the cells were incubated with Alexa Fluor 488-labeled donkey anti-mouse IgG (1, 1,000, Thermo Fisher Scientific, Wilmington, DE, USA) at room temperature for 1 h. After five washes, the coverslips were sealed with Prolong Gold Antifade reagent with 4,6-diamidino-2-phenylindole (Thermo Fisher Scientific) and scanned with the Leica SP8 confocal microscope.

## RESULTS

### 3-Hydroxyphthalic Anhydride Modified Bovine Beta-Lactoglobulin Is the Most Potent Anhydride-Modified Protein Against Human Papillomavirus Entry Into the Target Cell

Our previous studies have shown that 3-hydroxyphthalic anhydride-modified bovine beta-lactoglobulin (3HP-β-LG) is a promising HPV entry inhibitor against entry of PsV of both high-risk and low-risk HPV types (Lu et al., 2013). This inhibitory activity was attributed to the interaction of the increased net negative charges on β-LG after 3-hydroxyphthalic anhydride modification (Lu et al., 2013). One may ask whether all proteins with increased net negative charges can inhibit HPV entry into the target cell. To answer this question, we compared the inhibitory activity of 3HP-β-LG with that of 3-hydroxyphthalic anhydride-modified human serum albumin (3HP-HSA) and 3-hydroxyphthalic anhydride-modified chicken ovalbumin (3HP-OVA) against entry of HPV16 PsV into HeLa cells, using the unmodified β-LG, HSA, and OVA as controls. As shown in **Figure 1A**, 3HP-β-LG exhibited potent anti-HPV activity in a dose-dependent manner with an $IC_{50}$ (the half maximal inhibitory concentration) of 0.59 μg/ml, which is more potent than that of 3HP-HSA ($IC_{50}$: 2.28 μg/ml). 3HP-OVA and all three unmodified proteins at the concentration as high as 10 μg/ml showed no significant inhibitory activity against HPV16 PsV entry into the target cell. These results confirm that not all, just some, proteins, such as β-LG and HSA, modified by 3-hydroxyphthalic anhydride gain the ability to inhibit HPV infection.

In our previous studies, we proved the antiviral activity of 3HP-β-LG against entry of the high-risk HPV types 16 and 18 and low-risk HPV type 6 into the target cell (Lu et al., 2013). Aside from these three representative HPV types worldwide, another important high-risk type, HPV58, is found with high incidence in China. To determine whether 3HP-β-LG is also effective against HPV58, we constructed the HPV58 pseudovirus and tested its sensitivity to 3HP-β-LG (control: β-LG). As shown in **Figure 1B**, 3HP-β-LG could also inhibit HPV58 PsV entry into the target cell in a dose-dependent manner ($IC_{50}$ of 0.28 μg/ml), confirming that 3HP-β-LG has broad-spectrum anti-HPV activity.

Considering that the HaCaT cells express abundant integrin and heparan sulfate proteoglycan (HSPG), the receptors for HPV (Aksoy et al., 2014; Kumar et al., 2014) and act as target cells for HPV infection, we also evaluated the inhibitory activity of 3HP-β-LG against HPV16 and HPV58 PsV entry into HaCaT cells. As shown in **Figures 1C,D**, 3HP-β-LG was also effective

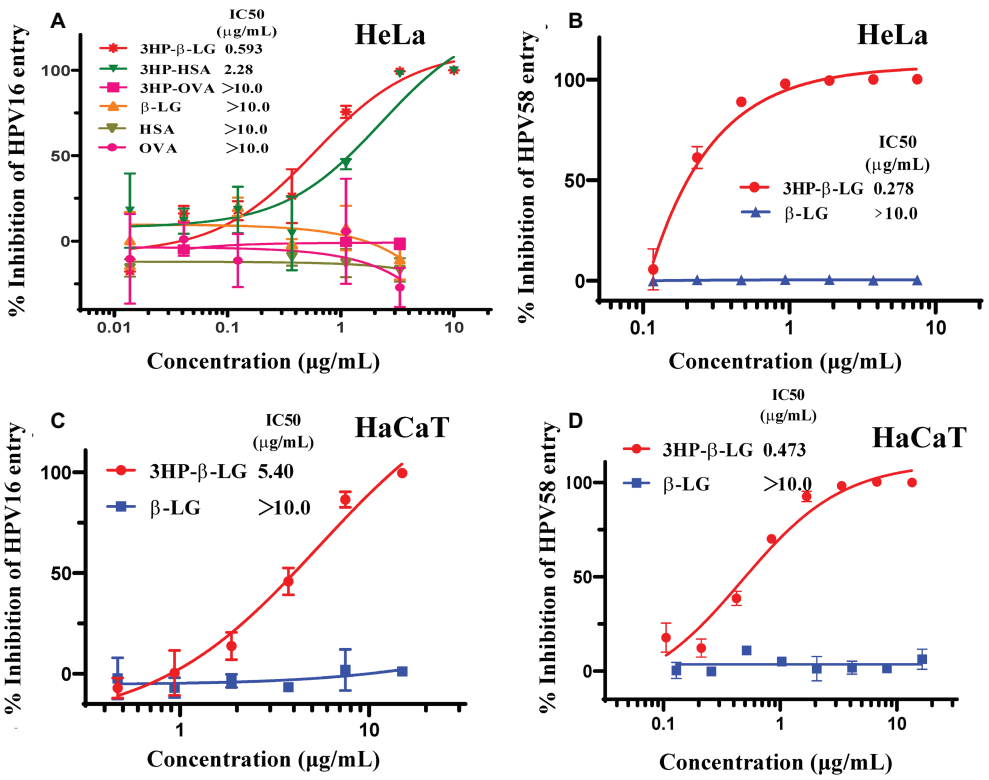


**FIGURE 1 |** Anti-HPV activities of anhydride-modified proteins. **(A)** Inhibition of anhydride-modified proteins on entry of HPV16 PsV into HeLa cells. Protein candidates include human serum albumin (HSA), β-lactoglobulin (β-LG), and chicken ovalbumin (OVA). **(B)** Inhibition of 3HP-β-LG on entry of HPV58 PsV into HeLa cells. **(C)** Inhibition of 3HP-β-LG on entry of HPV16 PsV into HaCaT cells. **(D)** Inhibition of 3HP-β-LG on entry of HPV58 PsV into HaCaT cells. Each sample was tested in triplicate, and the experiment was repeated twice. Data from a representative experiment are presented as mean ± standard deviation (SD).

against entry of HPV16 and HPV58 PsV into HaCaT cells, suggesting that 3HP-β-LG acts on the virus, rather than the target cell.

## 3-Hydroxyphthalic Anhydride Modified Bovine Beta-Lactoglobulin Binds to the L1 Protein and the Peptides Derived From the Positively Charged Residue-Enriched Region in Human Papillomavirus L1 Protein

As we proposed before, 3HP-β-LG inhibited HPV PsV entry into the target cell possibly through the binding of the negatively charged residues in 3HP-β-LG with the positively charged residues in a protein on the surface of the viral particle, thereby blocking the interaction between viral protein and receptor on the target cell (Lu et al., 2013). However, it is still unclear which protein on the virus surface may be involved in this interaction. The most abundant protein on the HPV particle is L1 protein. Here we detected the interaction between 3HP-β-LG and HPV L1 protein by ELISA. As shown in **Figures 2Aa,Ab**, 3HP-β-LG could strongly bind to the L1 protein of both HPV16 and HPV18, while the unmodified β-LG protein could not.

The C-terminal positively charged region of HPV L1 was proved to regulate the binding of HPV to the receptor (Sibbet et al., 2000; Bousarghin et al., 2003). This region was exposed on the viral surface, and involved in the binding to cell surface receptors or neutralizing antibodies. Therefore, we synthesized two positively charged peptides in this region of L1 protein, L1-I (residues 474–488) and L1-II (residues 493–505). The binding ability of 3HP-β-LG and β-LG to these peptides was measured by isothermal titration calorimetry (ITC). As shown in **Figure 2B**, β-LG had no obvious binding to L1-I or L1-II peptide, while 3HP-β-LG showed high binding ability against both L1-I (binding constant $K_\alpha$ value equals $2.31 \times 10^5$/M) and L1-II (binding constant $K_\alpha$ value equals $1.04 \times 10^5$/M). These results suggested that 3HP-β-LG may bind to the positively charged sites in the C-terminal region of L1 protein on the HPV surface to block the interaction between the viral particle and cell receptor.

## 3-Hydroxyphthalic Anhydride Modified Bovine Beta-Lactoglobulin Did Not Inactivate Human Papillomavirus Pseudovirus, but, Instead, Blocked Entry of Human Papillomavirus Pseudovirus Into the Target Cell *via* Its Inaction With Virus, Not Cells

To determine whether 3HP-β-LG could inactivate HPV PsV, we incubated HPV PsV with 3HP-β-LG at room temperature

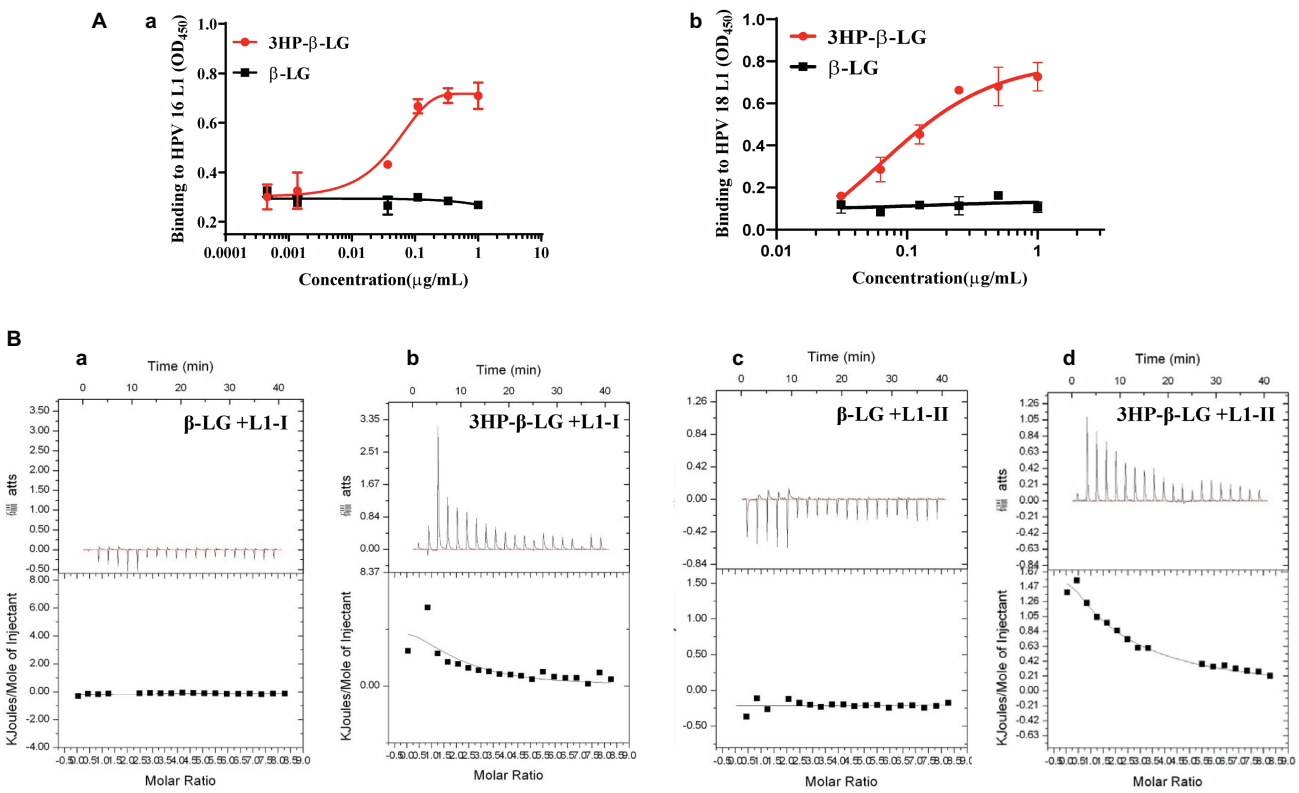


**FIGURE 2 |** Interaction of 3HP-β-LG with HPV L1 protein and with peptides derived from the positively charged region in the HPV L1 protein. **(A)** Binding of 3HP-β-LG (control: β-LG) with L1 protein of HPV16 **(a)** and HPV18 **(b)** in ELISA. Each sample was tested in triplicate, and the experiment was repeated twice. Data from a representative experiment are presented as mean ± SD. **(B)** Binding of 3HP-β-LG (control: β-LG) with L1–1 peptide **(a** and **b)** or L1-II peptide **(c** and **d)** derived from the region of residues 474–488 (LKAKPKFTLGKRKAT) or region of residues 493–505 (STSTTAKRKKRKL) of HPV16, respectively, in ITC.

for 2 h and then removed 3HP-β-LG by PEG-8000 precipitation. As shown in **Figure 3A**, the treated virus could still infect the target host cell with no reduced activity, compared the control virus (DMEM- or β-LG-treated), suggesting that the binding between 3HP-β-LG and HPV PsV may be noncovalent and reversible so that 3HP-β-LG cannot permanently inactive the virus.

HPV entry into the host cell takes more than 10 h, a relatively slow process compared to other viruses (Aksoy et al., 2017), which provides a long window period for an entry inhibitor to bind with the viral protein responsible for interaction with the receptor on the target cell and block viral entry. Here, we performed a time-addition assay to pinpoint the window of functional 3HP-β-LG blocking of HPV entry into the target cell. As shown in **Figure 3B**, 3HP-β-LG (15 μg/ml) could fully inhibit HPV16 PsV entry when it was added to the cells 0.5 h before and 0.5, 1, 2, 4, and 8 h after addition of HPV16 PsV, respectively, while about 70, 10, and 5% of HPV16 PsV entry were blocked when 3HP-β-LG was added to the cells 12, 24, and 48 h after addition of HPV16 PsV, respectively (**Figure 3B**). This result suggests that during this relatively long period of entry process (Aksoy et al., 2017), the entry inhibitor 3HP-β-LG remains sufficiently active to inhibit HPV PsV entry into the target cell.

To confirm the functional stage of 3HP-β-LG in blocking viral entry, we used a temperature shift assay to slow down the viral infection process. At 4°C, HPV PsV could bind to cell receptors, but could not fully enter the cytoplasm because the speeds of membrane fusion and cytoskeletal transformation are largely reduced at such low temperature. We incubated HPV PsV and HeLa cells at 4°C for 12 h so that HPV could bind to the cell surface. Then we washed away the unbound HPV before shifting the cells to 37°C for further 72 h of incubation. When 3HP-β-LG was added into the cells at the beginning and then removed by washing, no viral entry occurred (**Figure 3C**). This proved that 3HP-β-LG blocked the attachment between PsV and cell receptor at the earliest stage of infection. To determine whether 3HP-β-LG could also bind to the receptor on the target cell surface to block HPV entry, we incubated HeLa cells with 3HP-β-LG (control: β-LG) at 37°C for 1 h. The cells were washed with DMEM to remove the unbound proteins, or not washed (as control), before addition of HPV PsV. Under the washing conditions, HPV PsV entry into the HeLa cells was not blocked, while under the non-washing conditions, HPV PsV entry into the HeLa cells was effectively blocked. No inhibition was observed in the β-LG control groups, no matter whether the β-LG-treated HeLa cells were

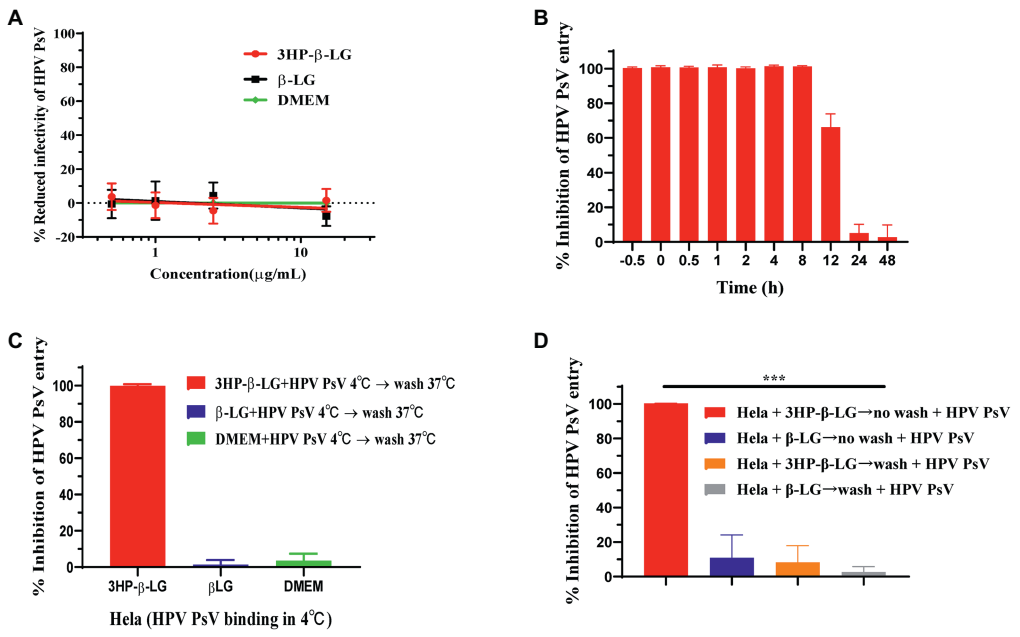


**FIGURE 3 |** 3HP-β-LG inhibited HPV PsV entry by targeting virus, not cells. **(A)** 3HP-β-LG was unable to inactivate HPV PsV. HPV PsV was incubated with 3HP-β-LG (control: β-LG) at room temperature for 2 h and then separated by PEG-8000 to analyze its entry activity. The DMEM-treated virus was taken as negative control. **(B)** 3HP-β-LG blocked HPV PsV entry into the target cell. HeLa cells were incubated with HPV PsV, while 3HP-β-LG (15 μg/ml) was added at different time points (–0.5, 0, 0.5, 1, 2, 4, 8, 12, 24, and 48 h) to analyze the inhibitory activity. **(C)** 3HP-β-LG blocked HPV PsV entry by targeting virus. Temperature shift assay for anti-HPV activity of 3HP-β-LG (control: β-LG). Diluted 3HP-β-LG or β-LG at 15 μg/ml was mixed with HPV PsV and prechilled at 4°C for 30 min; then they were added to HeLa cells for 12 h. After washing twice, the cells were further incubated at 37°C for 72 h and then analyzed for fluorescent integrated density. **(D)** 3HP-β-LG inhibited HPV PsV entry by targeting the virus, not the host cell. HeLa cells were incubated with 3HP-β-LG (control: β-LG) at 37°C for 1 h with/without washing by DMEM before addition of HPV PsV. Each sample was tested in triplicate, and the experiment was repeated twice. Data from a representative experiment are presented as mean ± SD. Asterisks represent significant differences. ***$p < 0.001$.

washed or not washed (**Figure 3D**). These results suggest that 3HP-β-LG inhibition of HPV PsV entry into HeLa cells does not result from its binding to HPV's receptor on the host cell.

### 3-Hydroxyphthalic Anhydride Modified Bovine Beta-Lactoglobulin Could Not Penetrate Into the Cell and the Vaginally Applied 3-Hydroxyphthalic Anhydride Modified Bovine Beta-Lactoglobulin Did Not Enter Into the Blood Circulation

To determine whether intravaginally applied 3HP-β-LG could enter into epithelial cells, we incubated HeLa cells and 293 T cells with 3HP-β-LG for 24 h and then washed the cells three times using PBS. The cells were stained with mouse anti-3HP-β-LG antibody or anti-β-actin antibody, as a control, and Alexa Fluor 488-labeled donkey anti-mouse IgG. Different from the anti-β-actin antibody-treated cells that showed strong fluorescence signals, anti-3HP-β-LG antibody-treated cells displayed no significant fluorescence signals inside or outside the cells (**Figure 4**). These results indicate that 3HP-β-LG could neither enter into the cell nor bind the cell surface proteins, including the receptor(s) for HPV.

To investigate whether the topically applied 3HP-β-LG enters the blood circulation, a carbomer gel with or without 3HP-β-LG was topically administered in the vagina or anus of rhesus macaques. Their blood samples were collected at different time points before and after gel application. The concentration of 3HP-β-LG in the blood samples and that in the gel (as positive control) were quantified with ELISA using anti-3HP-β-LG mAb. As shown in **Figure 5**, no 3HP-β-LG was detected in the blood samples of rhesus macaques vaginally or rectally administered with carbomer gel with or without 3HP-β-LG, confirming that the topically applied 3HP-β-LG does not enter the blood circulation.

## DISCUSSION

About 10–20% of acute HPV infections become persistent, leading to various forms of cancer (Shanmugasundaram and You, 2017), such as the cervical cancer. Although several multivalent prophylactic HPV vaccines have been used in clinics to prevent HPV infection and cervical cancer development, they have no effect against pre-existing HPV infection in middle-aged and elderly women, the population at high risk for cervical cancer. Therefore, it is essential to develop effective and safe therapeutic agents for treatment of HPV infection in order to reduce the morbidity of cervical cancer.

Viral entry inhibitors have been proven effective and safe for the treatment of viral infections (Jiang et al., 1993; Dando and Perry, 2003; Lu et al., 2016; Li et al., 2017; Su et al., 2019). We have previously reported that an HPV entry inhibitor, 3HP-β-LG, is highly effective in blocking the entry of HPV, both high- and low-risk types, into the host cell (Lu et al., 2013). In a randomized clinical trial, topical application of the vaginal gel containing 3HP-β-LG has shown excellent efficacy and safety to treat high-risk HPV infections (Guo et al., 2016a,b). However, how 3HP-β-LG inhibits HPV entry into the target cell is still unclear.

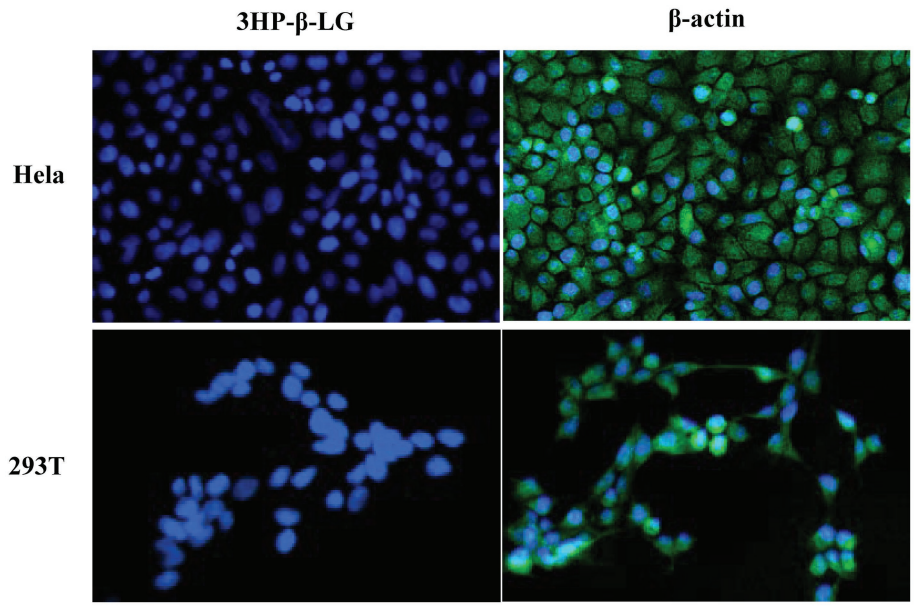


**FIGURE 4 |** 3HP-β-LG could not enter into the target cell. After incubation with HeLa and 293 T cells, 3HP-β-LG in the cells was detected by immunofluorescence assay using anti-3HP-β-LG mAb (green). β-actin was used as positive control. Cell nuclei were stained by 4,6-diamidino-2-phenylindole (blue).

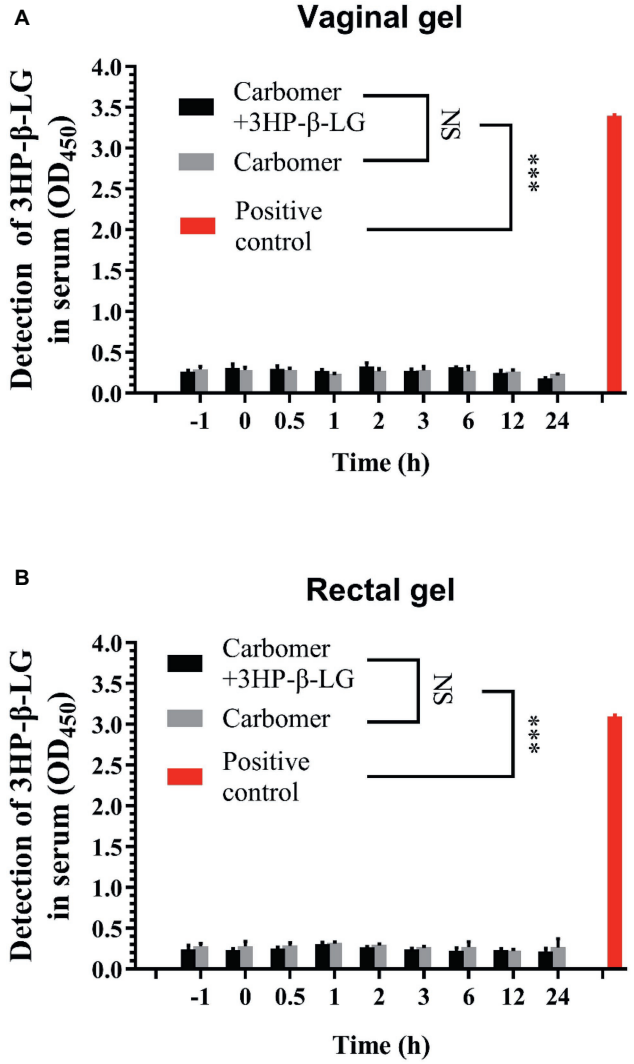


**FIGURE 5 |** 3HP-β-LG could not enter into blood circulation when applied through the vagina or anus. **(A)** Concentration of 3HP-β-LG in sera of monkeys through vaginal administration. **(B)** Concentration of 3HP-β-LG in sera of monkeys through rectal administration. 3HP-β-LG was formulated in a carbomer gel (1.8 mg/each) and administered through the vagina or anus of rhesus macaques. Their blood samples were collected at different time points before and after the application (–1 to 24 h). 3HP-β-LG in the blood samples was analyzed by ELISA. Each sample was tested in triplicate, and the experiment was repeated twice. Data from a representative experiment are presented as mean ± SD. The asterisks represent significant differences: $^{*}p < 0.05$; $^{**}p < 0.01$; $^{***}p < 0.001$.

In our previous study, we demonstrated that the inhibitory activity of 3HP-β-LG on HPV PsV entry into the target cell is closely correlated with the number of the positively charged lysine and arginine residues in 3HP-β-LG, as modified, *i.e.*, the net negative charges on 3HP-β-LG (Lu et al., 2013), suggesting that the negatively charged residues on 3HP-β-LG play an important role in 3HP-β-LG-mediated inhibition of HPV infection. As shown in **Figure 6A**, the unmodified bovine β-LG contains 18 positively charged residues (15 Lys and 3 Arg) and 26 negatively charged residues (16 Asp and 10 Glu) (Qin et al., 1999), thus having a net charge of −8. In 3HP-β-LG, 14 out of the 15 Lys and all 3 Arg were modified by 3HP at 6 mM (Lu et al., 2013), resulting in the neutralization of 17 of the 18 positive charges. Therefore, the net charge of 3HP-β-LG becomes −25, making 3HP-β-LG be active in binding to a viral protein with high positive net charges and inhibiting virus infection.

In this study, we demonstrated that 3HP-β-LG could strongly bind to the L1 protein on the HPV16 PsV, while the unmodified β-LG protein could not (**Figure 2A**). Using ITC analysis, we showed that unlike β-LG, 3HP-β-LG could strongly interact with the positively charged residue-enriched C-terminal regions (residues 474–488 and 493–505) of L1 protein, which is responsible for the attachment of the HPV particle to the host cell, possibly through its interaction with the cellular receptor(s).

One may argue that 3HP-β-LG may bind to any virus with high net positive charges on its surface protein and inhibit its infection. Indeed, 3HP-β-LG can also inhibit infection of simian immunodeficiency virus (SIV) (Wyand et al., 1999) and HSV (Neurath et al., 1996), but it is not effective against infection of MERS-CoV and VSV (unpublished data). In this study, we showed that 3HP-modified HSA (3HP-HSA) was also effective, while 3HP-modified OVA (3HP-OVA) was not effective in inhibiting HPV PsV entry (**Figure 1**), even though 3HP-OVA also contains high net negative charges on its surface. Thus, aside from having high net negative charges, these results suggest that the active site in 3HP-β-LG for binding to the viral protein must possess a conformation that fits with that in the corresponding site in the viral protein (**Figure 6B**), enabling 3HP-β-LG to strongly and closely interact with the viral protein to block HPV entry into the host cell. Indeed, the molecular docking analysis indicated that 3HP-β-LG could strongly bind to the positively charged region of HPV L1 protein, which is the binding site for the negatively charged HSPG receptor for HPV (**Figure 6B**). 3HP-β-LG has many more negative charges on the surface, and the interface between 3HP-β-LG and HPV-L1 is much larger than the HSPG molecule. Therefore, 3HP-β-LG can competitively bind to HPV L1 to block the binding of the HSPG receptor.

Based on the results obtained from this study, we proposed a mechanistic model of 3HP-β-LG for inhibiting HPV infection in the cervical mucosa (**Figure 6C**). The newly invaded HPV accesses the basal cell layer through micro lesions or breaks in the cervical epithelium and binds to the HSPG receptor on the basement membrane through interaction between the positively charged region in L1 protein of HPV and the negatively charged region in HSPG. This interaction results in a series of conformational changes in the capsid, which leads to protease digestion of L2 and exposure of its N terminus, thus initiating entry of HPV into to the epithelial cells (Kines et al., 2009; Pyeon et al., 2009). After HPV infects the epithelial cell, it gradually matures along with the host cell cycles and moves toward the top layer of epithelia, followed by eventual release from the epidermal cells. The newly released

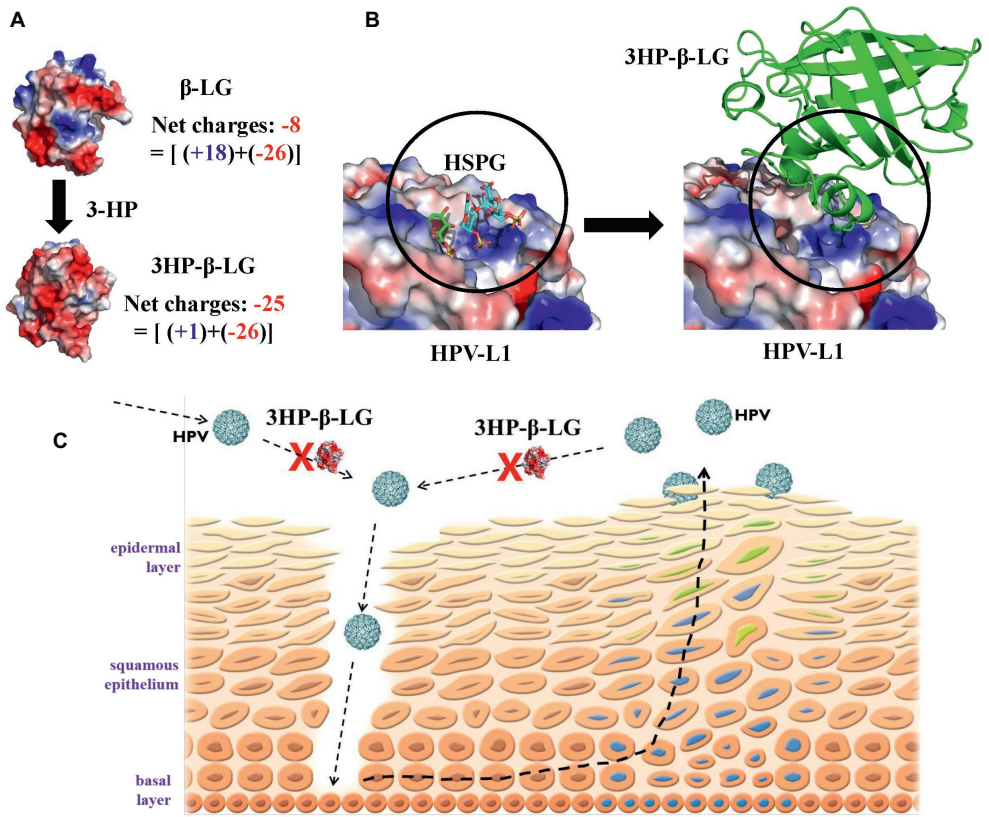


**FIGURE 6 |** Proposed mechanism by which 3HP-β-LG inhibits HPV infection in cervical mucosa. **(A)** The increased net negative charges on β-lactoglobulin after modification of the protein with 3-hydroxyphthalic anhydride. The structure of 3HP-β-LG was modeled by COOT (Emsley et al., 2010) using the crystal structure of β-LG (PDB entry: 1BEB). The structures were shown as an electrostatic surface by Pymol (Alexander et al., 2011). **(B)** Predicted interactions between HPV L1 pentamer and 3HP-β-LG. Crystal structure of HSPG-bound HPV L1 pentamer (PDB entry: 5W1O) was shown as electrostatic surface (Dasgupta et al., 2011), and the docking structure between HPV L1 and 3HP-β-LG was generated by AutoDock (Trott and Olson, 2010). **(C)** Schematic illustration showing how 3HP-β-LG inhibits HPV entry and infection. The newly invaded or newly released HPV particles access the basal layer through the mucosal lesion, or breaks, and bind to the HSPG receptor on the basement membrane, resulting in the entry of HPV into and replication in mucosal epithelial cells. 3HP-β-LG can bind with HPV L1 protein, through the electrostatic interaction between the negatively charged region in 3HP-β-LG and the positively charged region in L1 protein, to block the attachment of HPV to the HSPG receptor, resulting in inhibition of HPV infection in vaginal mucosa.

HPV particles access the basement membrane through micro lesions of the cervical epithelium and start another infection and replication cycle, gradually establishing persistent infection and promoting the development of cervical cancer.

3HP-β-LG that is topically applied in the vagina can bind to the L1 protein of the newly invaded or the newly released HPV and block the attachment of HPV to the basement membrane, thereby inhibiting the entry of HPV into the host cells for replication. After treatment with 3HP-β-LG for a certain period of time (e.g., 2 months), the newly produced HPV-free epithelial cells in the lower part of the mucosal epithelium are expected to move upward and push the HPV-infected cells away from the vaginal mucosa (this movement is accelerated during the menstrual period), making all layers of mucosal epithelium free of HPV infection.

Considering that the presence of micro lesions or breaks in the cervical epithelium, possibly caused by sexual activity, is the requirement for HPV to access the HSPG receptor on basement membrane (Bousarghin et al., 2003), combinational use of some biocompatible materials for mucosa wound healing, such as human collagen proteins (Hua et al., 2019), may have synergistic or complementary effects against HPV infection.

The results from the time-of-addition assay, cell washout assay, and virus inactivation indicate that 3HP-β-LG could interact with the virions, rather than the cells, to effectively block the entry of HPV PsV into the target cell, but could not inactivate the virions (**Figure 3**). These biological properties of 3HP-β-LG make it an ideal anti-HPV agent for topical application to treat HPV infection because it can interact with HPV particles on the vaginal mucosa and block the virions binding to the receptor, e.g., HSPG, on basement membrane. Since 3HP-β-LG cannot enter into the cell or the blood circulation, it is not expected to cause systemic toxicity to human or induce harmful 3HP-β-LG-specific antibodies. Therefore, the topical formulations containing 3HP-β-LG can be safely used to treat local HPV infection.

## DATA AVAILABILITY STATEMENT

All datasets generated for this study are included in the manuscript/supplementary files.

## ETHICS STATEMENT

The animal study was reviewed and approved by Institute of Laboratory Animal Science, Chinese Academy of Medical Sciences and Peking Union Medical College (approval number: ILAS-VL-2015-001).

## AUTHOR CONTRIBUTIONS

SJ, LSu, and YZ conceived and designed the experiments. CH, CW, LSi, and QW conducted the experiments. YZ performed the computer modeling and analysis of the interaction between 3HP-β-LG and HPV L1 protein. CH, YZ, LSu, and SJ analyzed the data and wrote the manuscript. All authors have read and approved the final manuscript.

## FUNDING

This work was supported by an intramural fund of Fudan-Jinbo Functional Protein Joint Research Center, Fudan University.

## ACKNOWLEDGMENTS

We thank Dr. Jing Xue at the Institute of Laboratory Animal Science, Chinese Academy of Medical Sciences and Peking Union Medical College for performing the experiments on rhesus macaques; Dr. John Schiller at the Laboratory of Cellular Oncology, National Cancer Institute, NIH, MD, USA for providing plasmids for constructing HPV PsV; and Yuhong Fu for assistance in preparing anhydrate-modified proteins.

## REFERENCES

Aksoy, P., Abban, C. Y., Kiyashka, E., Qiang, W., and Meneses, P. I. (2014). Hpv16 infection of HaCaTs is dependent on beta4 integrin, and alpha6 integrin processing. *Virology* 449, 45–52. doi: 10.1016/j.virol.2013.10.034

Aksoy, P., Gottschalk, E. Y., and Meneses, P. I. (2017). Hpv entry into cells. *Mutat. Res. Rev. Mutat. Res.* 772, 13–22. doi: 10.1016/j.mrrev.2016.09.004

Alexander, N., Woetzel, N., and Meiler, J. (2011). Bcl::cluster: a method for clustering biological molecules coupled with visualization in the Pymol molecular graphics system. *IEEE Int. Conf. Comput. Adv. Bio. Med. Sci.* 2011, 13–18. doi: 10.1109/ICCABS.2011.5729867

Baker, T. S., Newcomb, W. W., Olson, N. H., Cowsert, L. M., Olson, C., and Brown, J. C. (1991). Structures of bovine and human papillomaviruses. Analysis by cryoelectron microscopy and three-dimensional image reconstruction. *Biophys. J.* 60, 1445–1456. doi: 10.1016/S0006-3495(91)82181-6

Bernard, H. U., Burk, R. D., Chen, Z., van Doorslaer, K., zur Hausen, H., and de Villiers, E. M. (2010). Classification of papillomaviruses (Pvs) based on 189 Pv types and proposal of taxonomic amendments. *Virology* 401, 70–79. doi: 10.1016/j.virol.2010.02.002

Bosch, F. X., Lorincz, A., Munoz, N., Meijer, C. J., and Shah, K. V. (2002). The causal relation between human papillomavirus and cervical cancer. *J. Clin. Pathol.* 55, 244–265. doi: 10.1136/jcp.55.4.244

Bousarghin, L., Touze, A., Combita-Rojas, A. L., and Coursaget, P. (2003). Positively charged sequences of human papillomavirus type 16 capsid proteins are sufficient to mediate gene transfer into target cells via the heparan sulfate receptor. *J. Gen. Virol.* 84, 157–164. doi: 10.1099/vir.0.18789-0

Chen, W., Zheng, R., Baade, P. D., Zhang, S., Zeng, H., Bray, F., et al. (2016). Cancer statistics in China, 2015. *CA Cancer J. Clin.* 66, 115–132. doi: 10.3322/caac.21338

Dando, T. M., and Perry, C. M. (2003). Enfuvirtide. *Drugs* 63, 2755–2766; discussion 67-8. doi: 10.2165/00003495-200363240-00005

Dasgupta, J., Bienkowska-Haba, M., Ortega, M. E., Patel, H. D., Bodevin, S., Spillmann, D., et al. (2011). Structural basis of oligosaccharide receptor recognition by human papillomavirus. *J. Biol. Chem.* 286, 2617–2624. doi: 10.1074/jbc.M110.160184

Deschuyteneer, M., Elouahabi, A., Plainchamp, D., Plisnier, M., Soete, D., Corazza, Y., et al. (2010). Molecular and structural characterization of the L1 virus-like particles that are used as vaccine antigens in Cervarix, the As04-adjuvanted Hpv-16 and -18 cervical cancer vaccine. *Hum. Vaccin.* 6, 407–419. doi: 10.4161/hv.6.5.11023

Emsley, P., Lohkamp, B., Scott, W. G., and Cowtan, K. (2010). Features and development of Coot. *Acta Crystallogr. D Biol. Crystallogr.* 66, 486–501. doi: 10.1107/S0907444910007493

Guo, X., Qiu, L., Wang, Y., Wang, Y., Meng, Y., Zhu, Y., et al. (2016a). Safety evaluation of chemically modified beta-lactoglobulin administered intravaginally. *J. Med. Virol.* 88, 1098–1101. doi: 10.1002/jmv.24439

Guo, X., Qiu, L., Wang, Y., Wang, Y., Wang, Q., Song, L., et al. (2016b). A randomized open-label clinical trial of an anti-Hpv biological dressing (Jb01-Bd) administered intravaginally to treat high-risk Hpv infection. *Microbes Infect.* 18, 148–152. doi: 10.1016/j.micinf.2015.10.004

He, Y., Liu, S., Jing, W., Lu, H., Cai, D., Chin, D. J., et al. (2007). Conserved residue Lys574 in the cavity of HIV-1 Gp41 coiled-coil domain is critical for six-helix bundle stability and virus entry. *J. Biol. Chem.* 282, 25631–25639. doi: 10.1074/jbc.M703781200

Hua, C., Zhu, Y., Xu, W., Ye, S., Zhang, R., Lu, L., et al. (2019). Characterization by high-resolution crystal structure analysis of a triple-helix region of human collagen type iii with potent cell adhesion activity. *Biochem. Biophys. Res. Commun.* 508, 1018–1023. doi: 10.1016/j.bbrc.2018.12.018

Jiang, S., Lin, K., Strick, N., and Neurath, A. R. (1993). HIV-1 inhibition by a peptide. *Nature* 365:113. doi: 10.1038/365113a0

Kines, R. C., Thompson, C. D., Lowy, D. R., Schiller, J. T., and Day, P. M. (2009). The initial steps leading to papillomavirus infection occur on the basement membrane prior to cell surface binding. *Proc. Natl. Acad. Sci. USA* 106, 20458–20463. doi: 10.1073/pnas.0908502106

Kumar, A., Jacob, T., Abban, C. Y., and Meneses, P. I. (2014). Intermediate heparan sulfate binding during Hpv-16 infection in Hacats. *Am. J. Ther.* 21, 331–342. doi: 10.1097/MJT.0000000000000054

Kwak, K., Jiang, R., Wang, J. W., Jagu, S., Kirnbauer, R., and Roden, R. B. (2014). Impact of inhibitors and L2 antibodies upon the infectivity of diverse alpha and beta human papillomavirus types. *PLoS One* 9:e97232. doi: 10.1371/journal.pone.0097232

Li, Z., Song, S., He, M., Wang, D., Shi, J., Liu, X., et al. (2018). Rational design of a triple-type human papillomavirus vaccine by compromising viral-type specificity. *Nat. Commun.* 9:5360. doi: 10.1038/s41467-018-07199-6

Li, Z., Yan, X., Yu, H., Wang, D., Song, S., Li, Y., et al. (2016). The C-terminal arm of the human papillomavirus major capsid protein is immunogenic and involved in virus-host interaction. *Structure* 24, 874–885. doi: 10.1016/j.str.2016.04.008

Li, H., Yu, F., Xia, S., Yu, Y., Wang, Q., Lv, M., et al. (2017). Chemically modified human serum albumin potently blocks entry of Ebola pseudoviruses and viruslike particles. *Antimicrob. Agents Chemother.* 61. doi: 10.1128/AAC.02168-16

Lu, L., Yang, X., Li, Y., and Jiang, S. (2013). Chemically modified bovine beta-lactoglobulin inhibits human papillomavirus infection. *Microbes Infect.* 15, 506–510. doi: 10.1016/j.micinf.2013.03.003

Lu, L., Yu, F., Cai, L., Debnath, A. K., and Jiang, S. (2016). Development of small-molecule HIV entry inhibitors specifically targeting Gp120 or Gp41. *Curr. Top. Med. Chem.* 16, 1074–1090. doi: 10.2174/1568026615666150901114527

McCormack, P. L. (2014). Quadrivalent human papillomavirus (types 6, 11, 16, 18) recombinant vaccine (Gardasil®): a review of its use in the prevention of premalignant anogenital lesions, cervical and anal cancers, and genital warts. *Drugs* 74, 1253–1283. doi: 10.1007/s40265-014-0255-z

Neurath, A. R., Jiang, S., Strick, N., Lin, K., Li, Y. Y., and Debnath, A. K. (1996). Bovine beta-lactoglobulin modified by 3-hydroxyphthalic anhydride blocks the Cd4 cell receptor for HIV. *Nat. Med.* 2, 230–234. doi: 10.1038/nm0296-230

Neurath, A. R., Li, Y. Y., Strick, N., and Jiang, S. (1996). A herpesvirus inhibitor from bovine whey. *Lancet* 347, 1703–1704. doi: 10.1016/S0140-6736(96)91539-1

Pyeon, D., Pearce, S. M., Lank, S. M., Ahlquist, P., and Lambert, P. F. (2009). Establishment of human papillomavirus infection requires cell cycle progression. *PLoS Pathog.* 5:e1000318. doi: 10.1371/journal.ppat.1000318

Qin, B. Y., Bewley, M. C., Creamer, L. K., Baker, E. N., and Jameson, G. B. (1999). Functional implications of structural differences between variants A and B of bovine beta-lactoglobulin. *Protein Sci.* 8, 75–83. doi: 10.1110/ps.8.1.75

Safaeian, M., Kiddugavu, M., Gravitt, P. E., Gange, S. J., Ssekasanvu, J., Murokora, D., et al. (2008). Determinants of incidence and clearance of high-risk human papillomavirus infections in rural Rakai, Uganda. *Cancer Epidemiol. Biomark. Prev.* 17, 1300–1307. doi: 10.1158/1055-9965.EPI-07-2678

Shanmugasundaram, S., and You, J. (2017). Targeting persistent human papillomavirus infection. *Viruses* 9, 229. doi: 10.3390/v9080229

Sibbet, G., Romero-Graillet, C., Meneguzzi, G., and Saveria Campo, M. (2000). Alpha6 integrin is not the obligatory cell receptor for bovine papillomavirus type 4. *J. Gen. Virol.* 81:1629. doi: 10.1099/0022-1317-81-2-327

Su, S., Rasquinha, G., Du, L., Wang, Q., Xu, W., Li, W., et al. (2019). A peptide-based HIV-1 fusion inhibitor with two tail-anchors and palmitic acid exhibits substantially improved in vitro and ex vivo anti-HIV-1 activity and prolonged in vivo half-life. *Molecules* 24, 1134. doi: 10.3390/molecules24061134

Surviladze, Z., Dziduszko, A., and Ozbun, M. A. (2012). Essential roles for soluble virion-associated heparan sulfonated proteoglycans and growth factors in human papillomavirus infections. *PLoS Pathog.* 8:e1002519. doi: 10.1371/journal.ppat.1002519

Trott, O., and Olson, A. J. (2010). AutoDock Vina: improving the speed and accuracy of docking with a new scoring function, efficient optimization, and multithreading. *J. Comput. Chem.* 31, 455–461. doi: 10.1002/jcc.21334

Wyand, M. S., Manson, K. H., Miller, C. J., and Neurath, A. R. (1999). Effect of 3-hydroxyphthaloyl-beta-lactoglobulin on vaginal transmission of simian immunodeficiency virus in rhesus monkeys. *Antimicrob. Agents Chemother.* 43, 978–980. doi: 10.1128/AAC.43.4.978

**Conflict of Interest:** The authors declare that the research was conducted in the absence of any commercial or financial relationships that could be construed as a potential conflict of interest.

*Copyright © 2019 Hua, Zhu, Wu, Si, Wang, Sui and Jiang. This is an open-access article distributed under the terms of the Creative Commons Attribution License (CC BY). The use, distribution or reproduction in other forums is permitted, provided the original author(s) and the copyright owner(s) are credited and that the original publication in this journal is cited, in accordance with accepted academic practice. No use, distribution or reproduction is permitted which does not comply with these terms.*

frontiers in Microbiology

ORIGINAL RESEARCH
published: 27 September 2019
doi: 10.3389/fmicb.2019.02250

# A Peptide-Based Virus Inactivator Protects Male Mice Against Zika Virus-Induced Damage of Testicular Tissue

*Lulu Si[1†], Yu Meng[1†], Fang Tian[2], Weihua Li[2], Peng Zou[1], Qian Wang[1], Wei Xu[1], Yuzhu Wang[2], Minjie Xia[2], Jingying Hu[2]*, Shibo Jiang[1,2,3]* and Lu Lu[1]**

[1] Key Laboratory of Medical Molecular Virology (MOE/NHC/CAMS), School of Basic Medical Sciences and Shanghai Public Health Clinical Center, Fudan University, Shanghai, China, [2] NHC Key Laboratory of Reproduction Regulation (Shanghai Institute of Planned Parenthood Research), Fudan University, Shanghai, China, [3] Lindsley F. Kimball Research Institute, New York Blood Center, New York, NY, United States

OPEN ACCESS

**Edited by:**
Lijun Rong,
University of Illinois at Chicago, United States

**Reviewed by:**
Tian Wang,
University of Texas Medical Branch at Galveston, United States
David Ojcius,
University of the Pacific, United States

***Correspondence:**
Jingying Hu
hujingying@aliyun.com
Shibo Jiang
shibojiang@fudan.edu.cn
Lu Lu
lul@fudan.edu.cn

† These authors have contributed equally to this work

**Specialty section:**
This article was submitted to Virology, a section of the journal Frontiers in Microbiology

**Received:** 15 August 2019
**Accepted:** 17 September 2019
**Published:** 27 September 2019

**Citation:**
Si L, Meng Y, Tian F, Li W, Zou P, Wang Q, Xu W, Wang Y, Xia M, Hu J, Jiang S and Lu L (2019) A Peptide-Based Virus Inactivator Protects Male Mice Against Zika Virus-Induced Damage of Testicular Tissue. Front. Microbiol. 10:2250. doi: 10.3389/fmicb.2019.02250

Zika virus (ZIKV) was a re-emerging arbovirus associated with Guillain–Barré Syndrome in adult and congenital Zika syndrome in fetus and infant. Although ZIKV was mainly transmitted by mosquito bites, many sexual transmission cases have been reported since the outbreak in 2015. ZIKV can persist in testis and semen for a long time, causing testicular tissue damage and reducing sperm quality. However, no drug has been approved for prevention or treatment of ZIKV infection, especially infection in male testicular tissue. Previously reported peptide Z2 could inactivate ZIKV, inhibiting ZIKV infection *in vitro* and *in vivo*. Importantly, Z2 could inhibit vertical transmission of ZIKV in pregnant mice, reducing ZIKV infection in fetus. Here we showed that intraperitoneally administered Z2 could also be distributed to testis and epididymis, resulting in the reduction of ZIKV RNA copies in testicular tissue and protection of testis and epididymis against ZIKV-induced pathological damage and poor sperm quality in type I interferon receptor-deficient A129 mice. Thus, Z2, a ZIKV inactivator, could serve as an antiviral agent for treatment of ZIKV infection and attenuation of ZIKV-induced testicular tissue damage.

**Keywords: inactivator, peptide, Zika virus, testicular tissue damage, sperm**

## INTRODUCTION

Zika virus was a re-emerging arbovirus (Gao, 2018; Pettersson and Bohlin, 2018), like dengue virus (DENV) and Japanese encephalitis virus (JEV), belonging to *Flavivirus* genus in the *Flaviviridae* family. Since the outbreak in Brazil in 2015, ZIKV has rapidly spread to 87 countries and territories[1] (Baud et al., 2017a; Gorshkov et al., 2018), attracting global attention. About 80% of those infected with ZIKV presented with asymptomatic, or only mild illness (Petersen E. et al., 2016; Pierson and Diamond, 2018). However, ZIKV infection has been associated with more severe complications: Guillain–Barré Syndrome in adult (Brasil et al., 2016; Peixoto et al., 2019) and congenital Zika syndrome in fetus and infant (Baud et al., 2017b; Gurung et al., 2019).

[1] https://www.who.int/emergencies/diseases/zika/epidemiology-update/en/

ZIKV is mainly transmitted through mosquito bites (Petersen L.R. et al., 2016), while it can also be transmitted via *in utero* from mother to fetus (Besnard et al., 2014), blood transfusion (Tai et al., 2019) and intercourse (Duggal et al., 2017; Mead et al., 2018; Sakkas et al., 2018). It is reported that ZIKV was transmitted through sexual contact, perhaps up to 41 days after the onset of symptoms (Turmel et al., 2016), and infective virions were still isolated from semen 69 days after infection (Arsuaga et al., 2016; Garcia-Bujalance et al., 2017). The viral load in semen was 100,000 times that in the blood at 2 weeks post-infection (Mansuy et al., 2016), and viral RNA was still detected up to 370 days after illness onset (Barzon et al., 2018). It is also reported that ZIKV infection caused patients to have a decreasing total sperm count in the acute phase of infection (Joguet et al., 2017) and abnormal spermogram results 1 year after infection (Avelino-Silva et al., 2018), suggesting ZIKV was harmful to human spermatozoa production. Testis explants from uninfected donors were also proven to be susceptible to ZIKV infection (Matusali et al., 2018). As determined from an *in vitro* human testicular organoid culture system, ZIKV-infected testicular organoids may lead to multiple kinds of cell death (Strange et al., 2018). Although little was known about ZIKV infection in human testis and epididymis, except for semen, many murine models were used to study damage to testicular tissue. Govero et al. (2016) performed a study in wild-type C57BL/6 mice in the presence of the anti-Ifnar1 antibody and revealed that ZIKV preferentially infected spermatogonia and Sertoli cells in the testis. This led to cell death and destruction of the seminiferous tubules in association with testis damage and poor sperm quality (Govero et al., 2016). Ma et al. (2017) also established a mouse model using IFNα/β receptor-deficient mice (*Ifnar1*$^{-/-}$ knockout mice), and demonstrated that ZIKV infection induced inflammation in the testis and epididymis, leading to severe damage to testes at 60 days post-infection. Taken together, these findings suggested that ZIKV could persist in testicular tissue for a long time, causing severe damage to testis and epididymis and reducing sperm quality.

Currently, no approved drug is available to inhibit ZIKV infection (da Silva et al., 2018), especially infection in testicular tissue. Ebselen (EBS), an antioxidant in clinical trials, was reported to alleviate testicular pathology in ZIKV-infected mice by reducing the level of oxidative stress and proinflammatory cytokines. However, it only had a weak effect on ZIKV directly, and its safety for pregnant women was unknown (Simanjuntak et al., 2018). This calls for the development of safe and effective drugs to prevent ZIKV-induced testicular damage. The testis is a male reproductive organ, mainly producing spermatozoa and androgen. Specifically, spermatogenesis is a complex cellular event taking place in the seminiferous epithelium of seminiferous tubules and protected by Sertoli cells that form the blood–testes barrier (BTB) by tight junction protein (Su et al., 2011). The BTB provides a specialized microenvironment for spermatogenesis by preventing harmful agents from entering the seminiferous tubule, but this was found to pose a major obstacle to the delivery of therapeutic drugs to the seminiferous epithelium (Cheng and Mruk, 2012). Therefore, any drug able to prevent ZIKV-induced damage in testicular tissue should be able to cross the BTB into seminiferous tubules, or reach the testicular tissue, to inhibit ZIKV from entering into seminiferous tubules. The most promising anti-ZIKV drugs so far include small-molecule compounds (Deng et al., 2016a; Chan et al., 2017; Li et al., 2017), antibodies (Zhang et al., 2016; Wang et al., 2017, 2019), and peptides (Yu et al., 2017; Jackman et al., 2018). Compared with small-molecule compounds, peptides were safer, especially for pregnant women. As a macromolecular substance, passing through the BTB was challenging for antibodies, and it is reported that the concentration of specific IgG entering into the rete testis was 0.6% of that in blood serum (Knee et al., 2005). Therefore, the safer and cheaper peptide drugs, which consisted of dozens of amino acids, began to gain gradual acceptance. We previously demonstrated that an amphipathic peptide Z2, derived from the stem region of ZIKV E protein (**Figure 1A**), inhibited ZIKV infection *in vivo* and *in vitro*, suggesting its promise as an anti-ZIKV candidate drug. What's more, Z2 had a protective effect in pregnant mice and their fetuses, suggesting it was able to cross the placental barrier (Yu et al., 2017). However, whether Z2 could enter the seminiferous tubules and protect testicular tissue against ZIKV infection remained unknown.

In this work, we showed that intraperitoneally injected Z2 could be distributed in the testicular tissue. It then inhibited ZIKV infection, resulting in significant reduction of viral loads and protection of testis, epididymis, and sperm from ZIKV-induced pathological damage. These results suggest that Z2 has the potential to be further developed as an anti-ZIKV agent for treatment and prevention of ZIKV-induced damage in testicular tissue.

# MATERIALS AND METHODS

## Ethics Statement and Mice

All animal experiments were carried out according to ethical guidelines and approval by Shanghai Public Health Clinical Center Animal Welfare and Ethics Committee (2016-A021-01) and Institutional Laboratory Animal Care and Use Committee at Fudan University (20160927-2). The type I interferon receptor-deficient mice A129 (male, 6–7 weeks old) were bred at the Animal Experiment Department of Shanghai Public Health Clinical Center. Experiments using A129 mice infected by ZIKV were conducted in a Biosafety Level 2 (BSL2) facility at Shanghai Public Health Clinical Center. Specific pathogen-free BALB/c mice (male, 6–7 weeks old) were bought from Shanghai Lingchang BioTech, Co., Ltd. (Shanghai, China) and bred at the Department of Laboratory Animal Science of Fudan University.

## Cells, Viruses, and Peptides

Baby Hamster Kidney (BHK-21) cells and Cercopithecus Aethiops Kidney (Vero-E6) cells were obtained from ATCC (Manassas, VA, United States). Cells were cultured in Dulbecco's modified Eagle's medium (DMEM, meilunbio, Shanghai, China) supplemented with 10% fetal bovine serum (FBS) at 37°C and 5% $CO_2$. Mouse Testis Sertoli (TM4) cells were purchased from Zhong Qiao Xin Zhou BioTech, Co., Ltd. (Shanghai, China) and cultured in Dulbecco's modified Eagle's medium/Nutrient

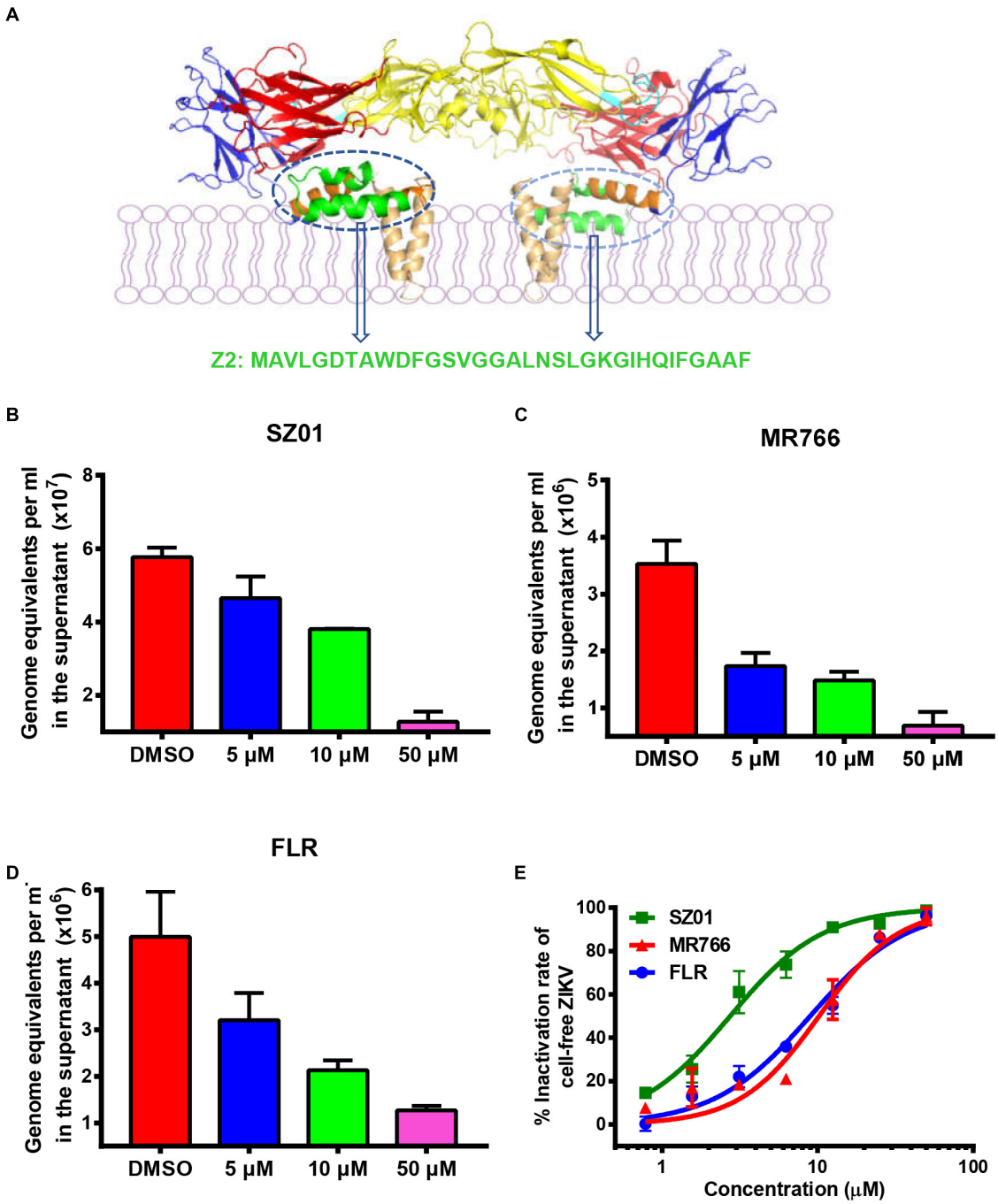


**FIGURE 1 |** Z2 inhibited infection of ZIKV strains with Asian and African lineages in TM4 cells. **(A)** Sequence and location of Z2 in ZIKV E dimer. Side view of ZIKV E protein in the dimeric conformation is shown [Protein Data Bank: 5IRE (Sirohi et al., 2016)]; DI, DII, DIII, stem and transmembrane domain are shown in red, yellow, blue, orange, and wheat, respectively; the fusion peptide is shown in cyan, and Z2 (421–453) is shown in green. TM4 cells were infected with ZIKV strain SZ01 **(B)**, MR766 **(C)** and FLR **(D)**, treated with Z2 at different concentration, and then viral copies in the supernatant at 48 h were measured by qRT-PCR. Data were presented as means ± SD. **(E)** Z2-treated ZIKV of different strain lost infectivity on TM4 cells irreversibly. After incubation with Z2 at 37°C for 2 h, ZIKV particles were separated from the unbound Z2 by PEG 8000 to measure their infectivity on TM4 cells. Each sample was tested in triplicate and the experiments were repeated at least once. The data from two independent experiments were presented as mean ± SD.

Mixture F-12 (DMEM/F12, Thermo Fisher Scientific, Waltham, MA, United States) supplemented with 5% Horse Serum and 2.5% FBS at 37°C and 5% $CO_2$.

Zika virus (ZIKV) strain SZ01/2016 (GenBank No. KU866423) was kindly provided by Dr. Cheng-Feng Qin (Deng et al., 2016b) and preserved in our laboratory. ZIKV

strains MR766 (#VR1838) and FLR (#VR1844) were obtained from ATCC. ZIKV was propagated in Vero-E6 cells. Briefly, Vero-E6 cells were infected with the virus at multiplicity of infection (MOI) of 0.01. The supernatants were harvested at 5 days post-infection, centrifuged at 4,000 rpm for 30 min to remove cellular debris, and stored at −80°C as stock.

Peptides Z2 (MAVLGDTAWDFGSVGGALNSLGKGIHQIFG AAF), Z2-Cy5 and scrambled peptide (LDIIAGLSAGFQ GGATFVDAHGMVKASFLGGNW) were synthesized at Kangbei Bio, Co., Ltd. (Ningbo, China) with 95% purity. Peptides were solubilized in dimethyl sulfoxide (DMSO) at 10 mM and stored at −20°C.

## Plaque Forming Assay

Virus titer was detected by plaque forming assay as shown below. BHK-21 cells were seeded onto a 12-well plate with $2 \times 10^5$ cells per well and cultured overnight at 37°C and 5% $CO_2$. Serially 10-fold diluted virus were added to each well and incubated for 2 h at 37°C. Then the supernatant was replaced with 1 ml DMEM containing 1% low melting agarose and 2% FBS. After agarose solidification, the cells were cultured at 37°C and 5% $CO_2$ for 6 days. Then cells were fixed with 4% formalin and stained with 1% crystal violet overnight. Finally, the plaque forming units were counted, and virus titer was calculated.

## *In vivo* Small Animal Optical Imaging

Six male A129 mice (7–8 weeks old) were randomly divided into two groups. Mice in each group ($n$ = 3) were injected intraperitoneally with Z2-Cy5 (100 μg in 100 μl PBS) or PBS (vehicle in 100 μl PBS) as control. After anesthetization with pentobarbital sodium, mice were imaged by the IVIS Lumina K series III *in vivo* imaging system from PerkinElmer (Waltham, MA, United States) for 1 h. To determine the distribution of Z2-Cy5 in the testicular tissue, mice were sacrificed using pentobarbital sodium, and all testes and epididymides were removed for imaging. The radiant efficiency ($ps^{-1}cm^{-2}sr^{-1}$) ($\mu W^{-1}cm^{-2}$) in mouse body and testis and epididymis was calculated by Living Image 4.5.5 software.

## Assay for Assessing Protective Effect of Z2 Against ZIKV Infection in Testicular Tissue of Male A129 Mice

To determine the protection of Z2 against ZIKV-induced testis damage, male A129 mice (7–8 weeks old) were randomly divided into three groups ($n$ = 5): Z2-treated group, vehicle-treated group, and mock-infected group. Mice in the Z2- or vehicle-treated group were intraperitoneally injected (i.p.) with 200 PFU ZIKV with Z2 (15 mg/kg) or vehicle on day 0, followed by i.p. administration of Z2 (15 mg/kg) or vehicle once daily for six consecutive days, respectively. Mice in the mock-infected group only received PBS as normal control. The body weight was monitored daily for 14 days, and blood was collected at 1, 3, 7, 11, and 16 days post-infection (d.p.i.) for detection of ZIKV copies in sera. At 16 d.p.i., mice were euthanized by $CO_2$ inhalation, and the testes and epididymides were removed. The weight and size of testes were measured as previously described (de La Vega et al., 2018). After imaging, the left testes and epididymides were immersed in Bouin's for hematoxylin-eosin (H&E) staining. The right testes and epididymides were soaked in RNAiso Plus reagent at −80°C for further detection of ZIKV copies.

## Safety Analysis of Z2 in Testicular Tissue of Male BALB/c Mice

For safety analysis of Z2 in testicular tissue, 10 male BALB/c mice (7–8 weeks old) were randomly divided into two groups. Five mice in each group were i.v. administered with Z2 at 100 mg/kg of body weight or PBS control for 3 days. The body weight of mice was monitored every other day for 30 days. Blood was collected at 4 h, as well as 1, 14, and 30 days post-injection and sera were separated from the blood samples for use in ELISA to detect the concentration of testosterone and inhibin B as well as the titer of Z2-specific antibody. At 30 days, mice were sacrificed, and the testes and epididymides were removed for histological examination.

## Computer-Assisted Sperm Analysis (CASA)

Mature sperm in the cauda epididymis of the three groups of male A129 mice were collected and placed in 1 ml PBS (preincubated at 37°C) immediately after euthanasia. The sperm suspension was analyzed for total sperm count and motility by computer-assisted sperm analysis (CASA), as previously described (Goodson et al., 2011), using Hamilton Thorne IVOS II (Beverly, MA, United States). Then, after smear, desiccation and fixation, remaining sperm were stained by the Papanicolaou staining method for manual morphological analysis. Sperm morphology was observed in each mouse.

## qRT-PCR for Detection of ZIKV RNA

ZIKV-infected mice were euthanized at 16 days post-infection. Testes and epididymides were homogenized with beads in 1 ml RNAiso Plus reagent (TaKaRa, Japan) using Tissuelyser-48 (Jingxin, Shanghai, China) after weighing. Homogenized tissue were centrifuged for 15 min at 14,000 rpm at 4°C, then total RNA in tissues was extracted according to the operating manual and stored at −80°C for the next step. Sperm collected in PBS were placed in RNAiso to extract total RNA under the same procedure. Viral RNA in sera samples on specific days was extracted using the EasyPure® Viral DNA/RNA Kit (TransGen, China) and stored at −80°C for the next step. ZIKV RNA was examined by one-step real-time quantitative reverse transcription PCR (qRT-PCR) using the Mastercycler® ep realplex Real-time PCR System (Eppendorf, Germany). ZIKV RNA copies were calculated based on the standard curve which was determined by plasmid containing specific sequence. The following primers were used: ZIKV-F: 5′-TTGGTCATGATACTGCTGATTGC-3′; ZIKV-R: 5′-CCTTCCACAAAGTCCCTATTGC-3′; ZIKV-probe: 5′-FAM-CGGCATACAGCATCAGGTGCATAGGAG-BHQ1-3′.

## ELISA for Measuring the Concentration of Testosterone and Inhibin B in Mouse Sera

The concentration of testosterone and inhibin B in the sera of BALB/c mice was detected by Mouse Testosterone (ml001948, mlbio, Shanghai, China) and Inhibin B ELISA kit (ml301823, mlbio, Shanghai, China), respectively. According to the manual, 50 μl standard or testing samples were added to a 96-well plate, which was coated with purified mouse testosterone or inhibin B antibody combined with HRP labeling. HRP-conjugate reagent was added to each well, except blank well (no sample; HRP-conjugate reagent added as background). The plate was closed with closure plate membrane and incubated at 37°C for 60 min. After washing, chromogen solution was added and incubated for 15 min at 37°C. Stop solution was added to each well, and absorbance was read at 450 nm.

## Assay to Detect the Inhibitory Activity of Z2 on ZIKV Infection in TM4 Cells

Peptide Z2 was dissolved in DMSO and diluted to different concentration by DMEM/F12. Then 125 μl of different ZIKV strains were incubated with Z2 for 2 h at 37°C. The mixture was added to $5 \times 10^4$ cells seeded into a 24-well plate and incubated at 37°C for 2 h. After the culture supernatant was replaced by DMEM/F-12 with 2% horse serum, cells were cultured for 48 h at 37°C. Then the culture supernatant was collected to detect ZIKV RNA copies by qRT-PCR, as described above.

## Assay to Detect Z2-Mediated Inactivation of ZIKV

The ability of Z2 to inactivate different ZIKV strains was determined as follows. Briefly, 100 μl Z2 or Z2-scr, at graded concentration were added to 100 μl ZIKV ($5 \times 10^3$ PFU/ml), followed by incubation at 37°C for 2 h. Then, PEG-8000 and NaCl were added to the treated virus at final concentration of 10% and 0.67M, respectively. After incubation on ice for 2 h, the mixture was centrifuged at 13,000 rpm for 1 h. The supernatants were removed, and the pellet was resuspended in 200 μl DMEM with 2% FBS. The infectivity of the ZIKV particles in the pellet was determined by CCK-8 on BHK-21 cells or qRT-PCR on TM4 cells.

## Histopathological Analysis

The testis and epididymidis of Z2- or vehicle-treated ZIKV-infected mice and mock-infected mice were all collected post mortem. Tissues were fixed in Bouin's overnight, dehydrated, embedded in paraffin and sectioned. Then the sections (4 μm thick) were stained by H&E. Subsequently, observation was made *via* panoramic scanner (3D HISTECH Pannoramic MIDI, Hungary).

## Statistical Analysis

Student's unpaired two-tailed *t*-test was used to monitor the distribution of Z2 in male A129 mouse body and testicular tissue and to analyze the difference of viral RNA level in sera or tissues between Z2- and vehicle-treated A129 mice. One-way ANOVA was used to examine the effect of Z2 on the weight, length and width of testes, as well as sperm count, sperm motility and progressive sperm motility among the three groups. *P*-value was calculated by GraphPad Prism software, v. 7.00, and significant difference was achieved with *P*-value less than 0.05. $^*P < 0.05$; $^{**}P < 0.01$; $^{***}P < 0.001$; $^{****}P < 0.0001$.

# RESULTS

## Z2 Inhibited Infection of ZIKV Strains of Asian and African Lineages in TM4 Cells

To determine the protective effect of Z2 on ZIKV infection of testicular tissue, we tested if Z2 could inhibit infection by different ZIKV strains of Asian and African lineages in mouse Sertoli TM4 cells, which are nurse-like cells that support spermatogenesis (Wei et al., 2018) and important target cells for ZIKV testicular infection. ZIKV SZ01 (Asian lineage), FLR (Asian lineage), or MR766 (African lineage) was pretreated with Z2 at different concentration before addition of TM4 cells and incubation at 37°C for 2 h. After replacement of culture medium and further incubation for 48 h, the viral copies in the supernatant were examined by qRT-PCR. As shown in **Figures 1B–D**, Z2 treatment resulted in a decrease of ZIKV copies in a dose-dependent manner. Considering that Z2-mediated inhibition of ZIKV infection is possibly attributed to its viral inactivation activity (Yu et al., 2017), different strains of ZIKV were incubated with Z2 at different concentration for 2 h at 37°C, followed by separating virions from the unbound free peptide by PEG 8000 and detecting the infectivity of Z2-treated ZIKV in TM4 cells (**Figure 1E**) and BHK-21 cells (**Supplementary Figure S1**). We found that Z2-treated ZIKV strains lost their infectivity in a dose-dependent manner with 50% effective concentration ($EC_{50}$) of 2.74 ± 0.44 μM (for SZ01), 10.21 ± 1.00 μM (for MR766) and 8.96 ± 0.95 μM (for FLR), respectively, suggesting that Z2 inhibits infection of ZIKV strains of both Asian and African lineages in TM4 and BHK-21 cells *via* inactivation of virions.

## Z2 Could Be Distributed in the Testis and Epididymis of Mice

To determine whether Z2 entered testicular tissue of male mice, we employed Cy5-conjugated Z2 peptide (Z2-Cy5) to detect the distribution of Z2 in the organs of male mice. As shown in **Figure 2A**, the bodies of the Z2-Cy5-treated mice showed a strong fluorescence signal with average radiant efficiency of about $3.05 \times 10^8$ ($ps^{-1}cm^{-2}sr^{-1}$) ($\mu W^{-1}cm^{-2}$), which is significantly higher than that in PBS-treated mice ($P = 0.0269$, Student's two-tailed *t*-test; **Figure 2B**). Then, the testes and epididymides were collected for examination of the fluorescence signal in the testicular tissue. As expected, both testes and epididymides of mice treated with Z2-Cy5 showed a strong fluorescence signal, while those in the PBS-treated mice displayed no significant fluorescence signal (**Figure 2C**). The average radiant efficiency in testes and epididymides of Z2-Cy5-treated mice was significantly

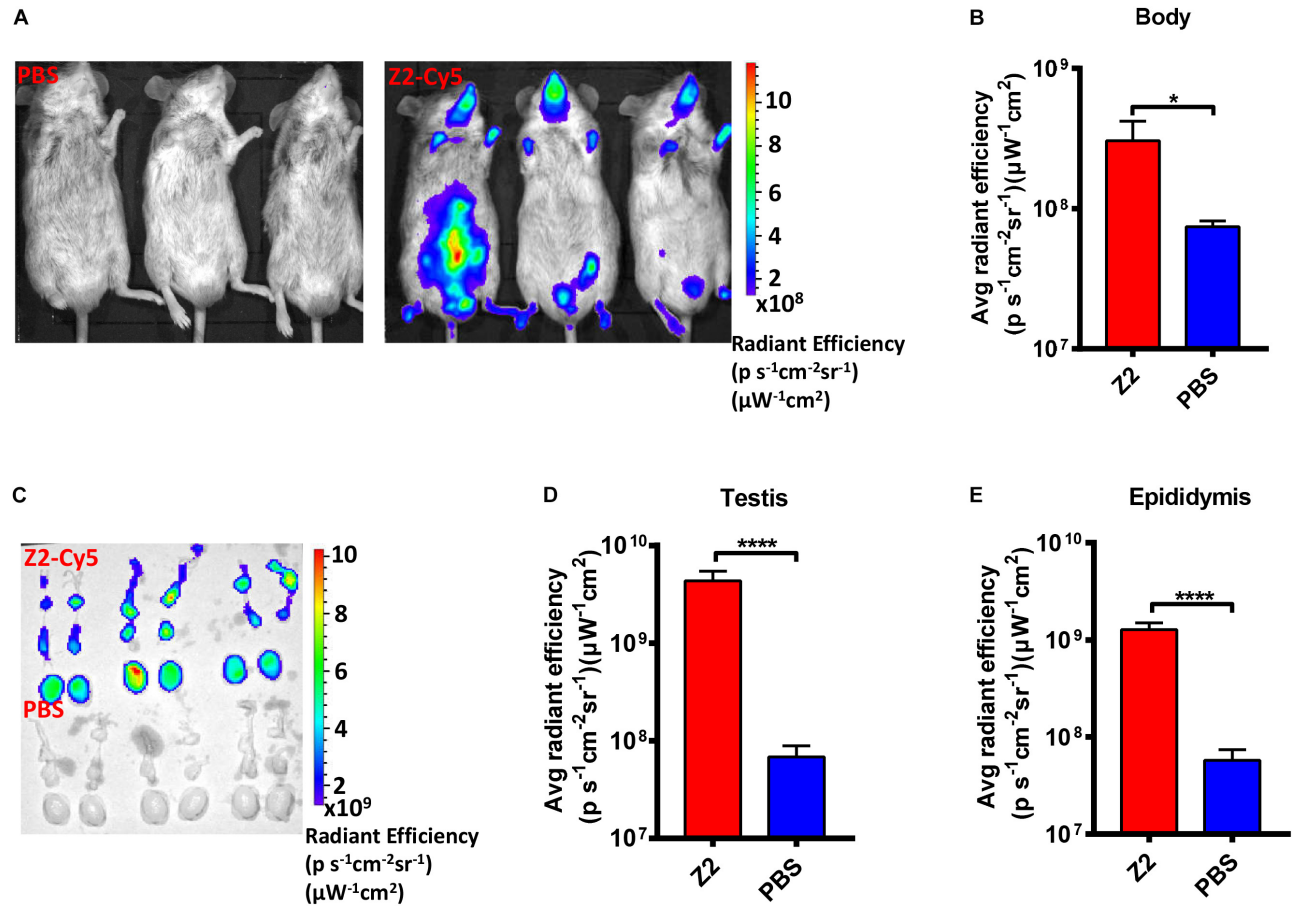


**FIGURE 2 |** Distribution of Z2 in the testicular tissue of male A129 mice. **(A)** Imaging of male A129 mice treated with Z2-Cy5 or PBS by the IVIS Lumina K Series III from PerkinElmer. Male A129 mice were injected intraperitoneally with 100 μg Z2-Cy5 ($n$ = 3) or PBS ($n$ = 3) as control, followed by imaging analysis. **(B)** The statistical analysis of fluorescence signal intensity in mouse body. Data were presented as means ± SD. **(C)** Imaging of the testes and epididymides from male A129 mice. **(D)** Statistical analysis of fluorescence signal intensity in testis. Each sample was tested in triplicate and the data were presented as mean ± SD. **(E)** Statistical analysis of fluorescence signal intensity in epididymis. Data were presented as means ± SD. *$P$ < 0.05; ****$P$ < 0.0001, Student's two-tailed $t$-test.

higher than that of PBS-treated mice ($P$ < 0.0001, Student's two-tailed $t$-test; **Figures 2D,E**). These results suggest that Z2 peptide can be distributed in the testis and epididymis of male mice.

## The Protective Effect of Z2 on Male A129 Mice Challenged With ZIKV

To determine the protective effect of Z2 against ZIKV infection of male mice, 200 PFU ZIKV were intraperitoneally injected into male A129 mice (type I interferon receptor-deficient). The infected mice were i.p. administered with Z2 at 15 mg/kg of body weight or vehicle, respectively, daily for 7 days (**Figure 3A**). Mice in the mock-infected group received PBS as normal control. Results showed that the Z2-treated mice had neither weight loss (**Figure 3B**) nor obvious clinical symptoms, consistent with mice in the mock-infected group (data not shown). However, in the vehicle-treated group, mouse body weight began to decline from the fifth day post-infection (d.p.i.) (**Figure 3B**), and some symptoms, like hunched posture and ruffled fur, appeared. We then examined viral copies in sera of Z2- or vehicle-treated mice at different time points by qRT-PCR. A high level of viral load was detected in sera of vehicle-treated mice, e.g., about $10^{10}$ copies/ml at 3 d.p.i. (**Figure 3C**). However, viral load in sera of Z2-treated mice (**Figure 3C**) was as low as $10^4$ copies/ml at all time points tested, significantly lower than that of vehicle-treated mice. These results suggest that Z2 can exert protection against ZIKV infection of male mice.

## Z2 Protects Mice Against ZIKV-Induced Damage of Testicular Tissue

To further evaluate the protective effect of Z2 against ZIKV-induced damage of testicular tissue in male mice, all mice were sacrificed at 16 d.p.i. and their testes were collected for analysis of weight and size. We found that testis weight in vehicle-treated mice was around 50 mg, which was significantly lower than that in Z2-treated mice (∼100 mg) ($P$ < 0.0001, one-way ANOVA, **Figure 4A**). The length and width of testes in vehicle-treated mice were both significantly decreased compared with those of testes in Z2-treated mice

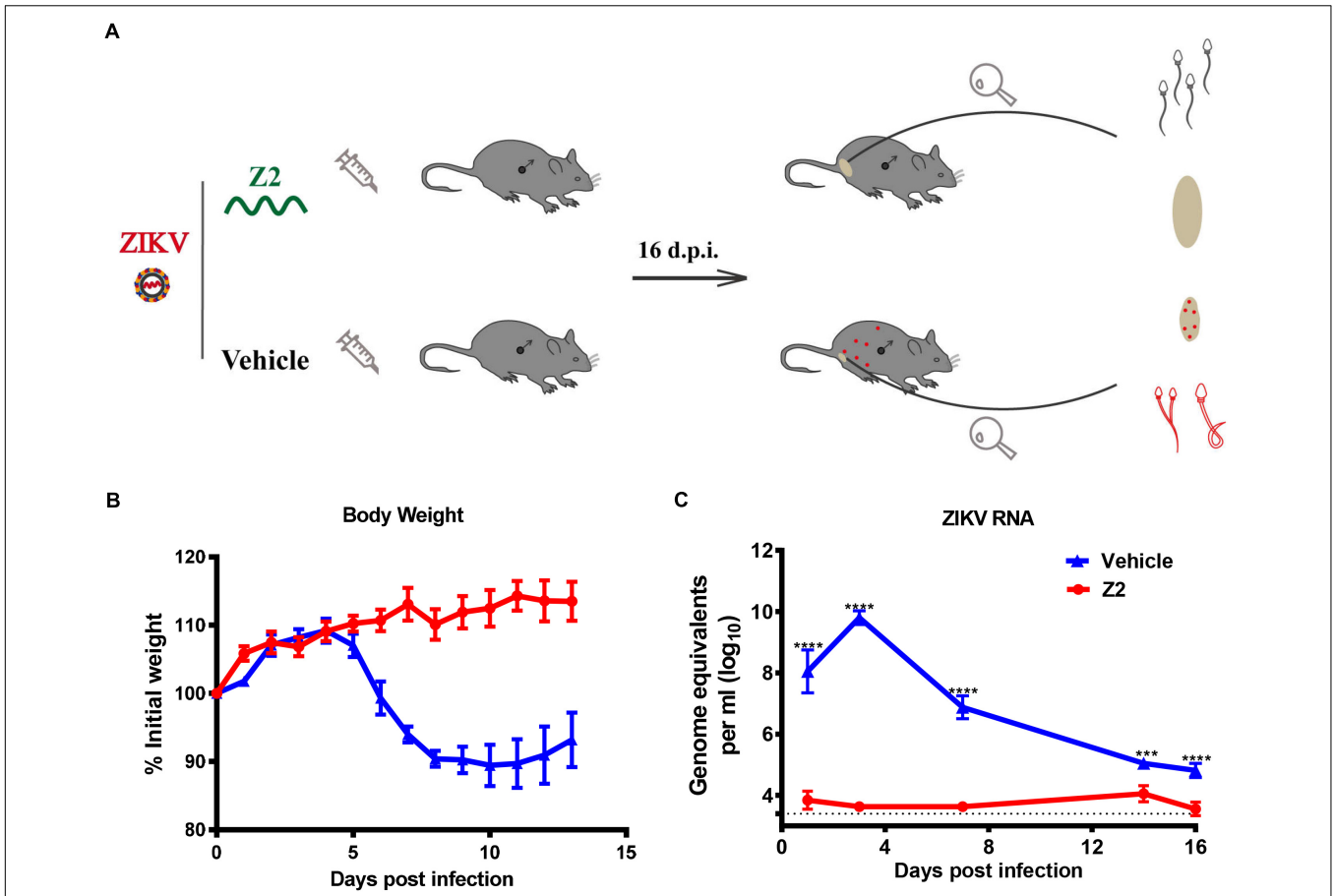


**FIGURE 3 |** Protective effect of Z2 against ZIKV infection in male A129 mice. **(A)** Schematic diagram of animal experiment. **(B)** The change of mouse body weight was monitored daily for 14 days. **(C)** The change of ZIKV RNA level in mouse sera were detected by qRT-PCR at days 1, 3, 7, 14, and 16 after ZIKV infection. Male A129 mice were intraperitoneally injected with 200 PFU ZIKV with Z2 (15 mg/kg) or vehicle on day 0, followed by daily injection of Z2 (15 mg/kg) or vehicle for six consecutive days. Each sample was tested in triplicate and the data were presented as mean ± SEM, ***$P < 0.001$; ****$P < 0.0001$, Student's two-tailed *t*-test.

($P = 0.0022$ and $P < 0.0001$, one-way ANOVA, **Figures 4B,C**). No significant difference in weight ($P > 0.5$, one-way ANOVA, **Figure 4A**), as well as length ($P > 0.5$, one-way ANOVA, **Figure 4B**), and width ($P > 0.5$, one-way ANOVA, **Figure 4C**) of testes were noted between Z2-treated ZIKV-infected mice and mock-infected mice. The representative image of testes from the three groups of mice were shown in **Figure 4D**.

Subsequently, we examined the testes and epididymides for histopathological changes. The results of H&E staining of testes in vehicle-treated mice revealed that the normal architecture of the seminiferous tubule was seriously destroyed and replaced with an infiltrate of mixed inflammatory cells and necrotic debris, accompanied by degeneration of the spermatogenic lineage (**Figure 4E**, upper panel). The connective tissue areas surrounding the seminiferous tubule had also been infiltrated by a large number of inflammatory cells (**Figure 4E**, upper panel). However, the architecture of the seminiferous tubule in the testes of both Z2-treated and mock-infected mice was intact and clear. Spermatogenic cells at different stages were organized tightly and identified clearly (**Figure 4E**, upper panel).

Histological analysis of epididymis showed that epididymides from mice in the vehicle-treated group were also damaged. Sperm in the lumen of caput epididymides decreased precipitously, only to be replaced by secretions and numerous necrotic epithelial cells (**Figure 4E**, middle panel). The lumens of cauda epididymis contained degenerating spermatozoa and a small number of normal spermatozoa, accompanied by scattered necrotic epithelial cells and inflammatory cells (**Figure 4E**, lower panel). However, histological analysis of the caput epididymis and cauda epididymis showed no apparent microscopic differences between Z2-treated and mock-infected mice (**Figure 4E** middle, lower panel). The architecture of the caput epididymis and cauda epididymis in these two groups was normal with no obvious morphological damage, suggesting that Z2 protected testicular tissue against ZIKV-induced pathological damage.

## Z2 Protects Mice Against ZIKV-Induced Spermatic Damage

We used CASA to evaluate the protective effect of Z2 on the count and motility of mouse sperm. As shown in **Figure 5**, the

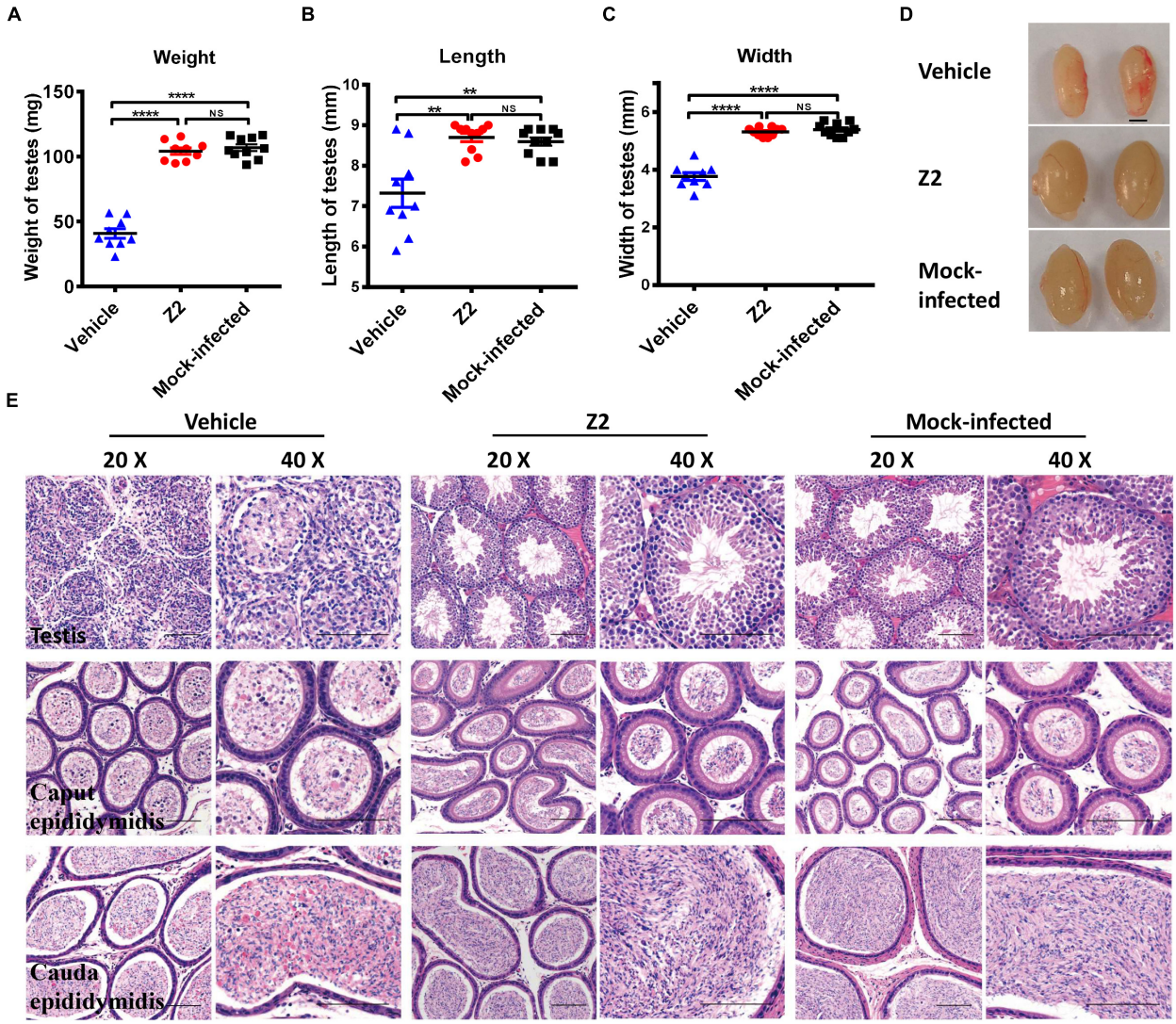


**FIGURE 4 |** Z2 effectively attenuated damage to testes and epididymides of ZIKV- infected male A129 mice. **(A)** The weight, **(B)** length, and **(C)** width of testes from Z2- or vehicle-treated ZIKV-infected and mock-infected male A129 mice at day 16. Each symbol represents one testis; all horizontal bars indicate mean, and error bars reflect SEM. **(D)** The representative image of testes from Z2- or vehicle-treated ZIKV-infected and mock-infected male A129 mice at day 16. Scale bar, 2 mm. **(E)** Histopathological analyses of testes and epididymides collected from Z2- or vehicle-treated ZIKV- infected male A129 mice and mock-infected mice used as a control. Scale bar: 100 μm. Upper panel, testes; middle panel, caput epididymides; lower panel, cauda epididymides. $^{**}P < 0.01$; $^{****}P < 0.0001$; one-way analysis of variance with Tukey's multiple comparison *post hoc* tests.

sperm count of Z2-treated mice was significantly higher than that of the vehicle-treated group ($P = 0.0124$, one-way ANOVA; **Figure 5A**). Meanwhile, the percentages of total (**Figure 5B**) and progressively (**Figure 5C**) motile sperm in Z2-treated mice were dramatically higher than those in the vehicle-treated group ($P = 0.0055$ and $P = 0.0075$, one-way ANOVA), but similar to that in the mock-infected mouse group ($P > 0.05$, one-way ANOVA). Papanicolaou staining of morphological spermatic features revealed more noticeable teratogenesis of sperm in vehicle-treated mice compared to the other groups (**Figure 5D**).

To investigate whether the protective effect of Z2 on testicular tissue results from the reduction of local viral load, we examined the viral copies in different testicular tissues. Results showed a high level of viral RNA ($10^{10}$–$10^{13}$ equivalents per g) detected in the testis and epididymis of vehicle-treated mice at 16 d.p.i., much higher than that ($10^{5}$–$10^{7}$ equivalents per g) in Z2-treated mice (**Figures 6A,B**). Notably, ZIKV RNA was also detected (up to $10^{8}$ equivalents per ml) in the mature sperm collected from cauda epididymis in vehicle-treated mice, which was significantly higher than that in Z2-treated mice ($P = 0.0002$, Student's two-tailed *t*-test; **Figure 6C**).

## Z2 Is Safe for Male BALB/c Mice

Finally, to examine the safety of Z2 for male mice, male BALB/c mice were injected intravenously with Z2 at 100 mg/kg of

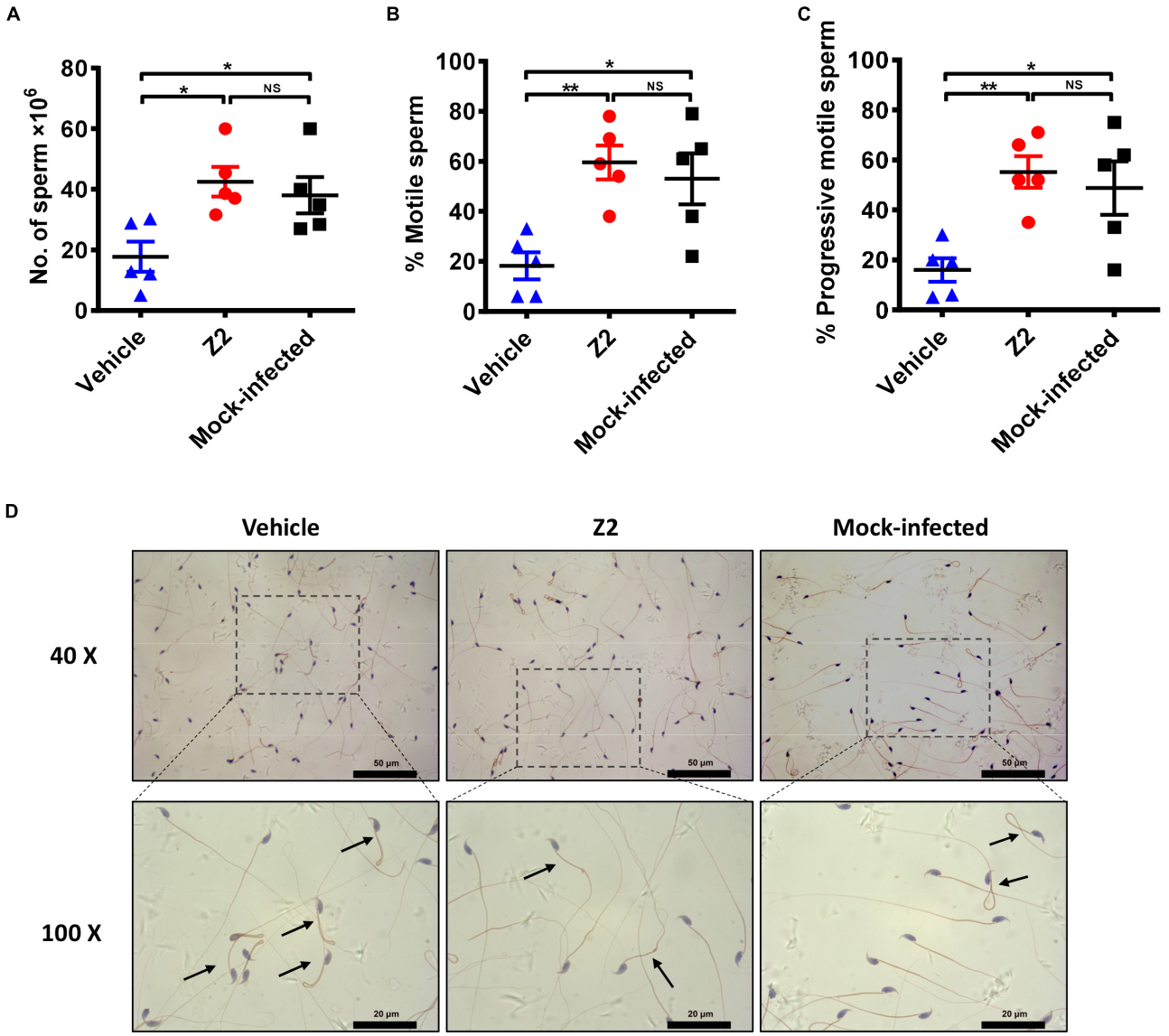


**FIGURE 5 |** Sperm characterization in Z2-treated ZIKV-infected male A129 mice. **(A)** Sperm count; percentage of **(B)** total motile sperm and **(C)** progressive motile sperm was analyzed by CASA. Each symbol represents data from individual mice; all horizontal bars indicate mean, and error bars reflect SEM. **(D)** Morphological features of sperm from vehicle- (left) or Z2- (middle) treated ZIKV-infected and mock-infected (right) mice. Mature sperm collected from cauda epididymides were stained by Papanicolaou, and the images were taken at 40 and 100× magnification. Black arrows indicated abnormal sperm. $^{*}P < 0.05$; $^{**}P < 0.01$, one-way analysis of variance with Tukey's multiple comparison *post hoc* tests.

body weight ($n$ = 5) or PBS ($n$ = 5). Results showed that body weight change of mice was nearly consistent in the two groups (**Figure 7A**), indicating that Z2 peptide did not cause significant harm to the male mice. Since the levels of testosterone and inhibin B reflect testicular function and sperm count, the concentration of these hormones in mouse sera at the indicated time points was measured. We found no significant difference between the Z2- and PBS-treated groups at all time points tested (**Figures 7B,C**), suggesting Z2 may not affect the function of testis or sperm. We then compared the potential histopathological changes between the two groups. As shown in **Figure 7D**, H&E analysis of testis and epididymis revealed no obvious pathological abnormality in mice treated with Z2 compared with the PBS group. Besides, the titer of Z2-specific antibody in sera of mice at 14 and 30 days post-injection was detected. As shown in **Figures 7E,F**, no significant level of Z2-specific antibody was detected in the sera of mice that were intravenously injected with high doses of Z2 peptide, consistent with the finding from our previous report for studying anti-MERS-CoV peptides (Xia et al., 2019). This result suggests that Z2 peptide consisting of 33 amino acids is unable to elicit a significant Z2-specific antibody response after it is intravenously administered in the absence of

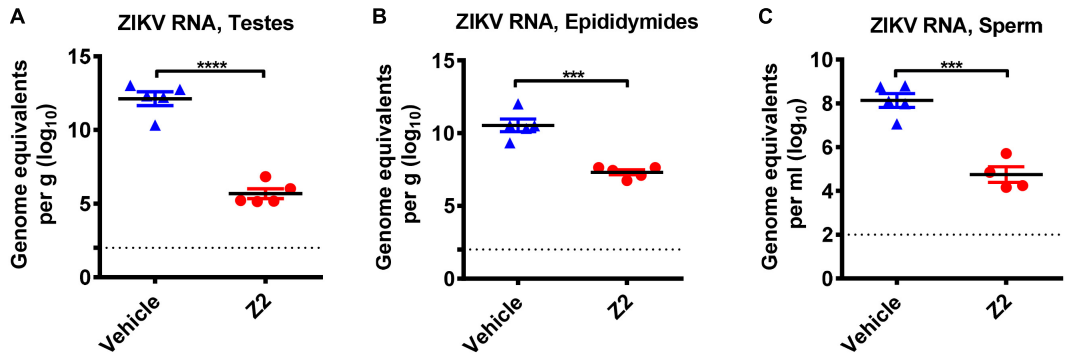


**FIGURE 6 |** Z2 inhibited ZIKV replication in testes, epididymides and sperm. ZIKV RNA copies in **(A)** testes, **(B)** epididymides, and **(C)** sperm of Z2- or vehicle-treated ZIKV-infected male A129 mice at day 16 were detected by qRT-PCR. Each symbol represents data from individual mice; all horizontal bars indicate mean, and error bars reflect SEM. Experiment was repeated at least twice. ***$P < 0.001$ or ****$P < 0.0001$ respectively, Student's two-tailed $t$-test.

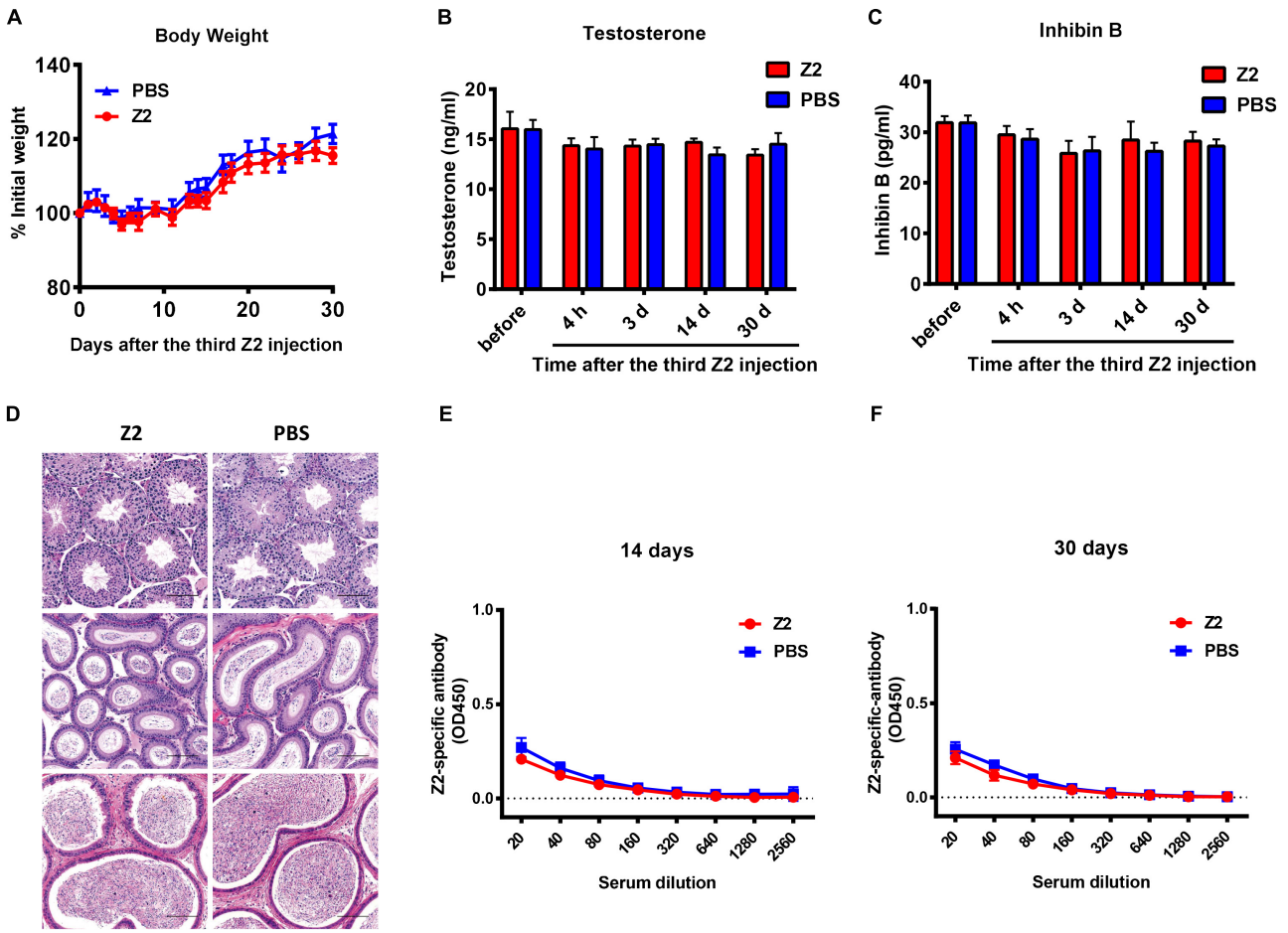


**FIGURE 7 |** Safety analysis of Z2 for male BALB/c mice. BALB/c mice were injected with Z2 (100 mg/kg/day, i.v.) for 3 days ($n = 5$), and another group of mice ($n = 5$) received PBS as a control. **(A)** Body weight change of BALB/c mice at different time points. Data were presented as means ± SEM. Concentration of **(B)** testosterone and **(C)** inhibin B in sera before and after Z2 injection. Data were presented as means ± SEM of triplicate experiments. **(D)** Histological analysis of the testis and epididymis collected from Z2- or PBS-treated male BALB/c mice. Scale bar: 100 μm. **(E)** Z2-specific antibody response in mice 14 days after i.v. administration of Z2 or PBS. **(F)** Z2-apecific antibody response in mice 30 days after i.v. administration of Z2 or PBS. Each sample was tested in triplicate and the data were presented as mean ± SD.

adjuvant. Therefore, Z2 is safe for male mice, especially for their testicular tissue.

## DISCUSSION

Currently, many studies have reported the deleterious effects of ZIKV on male testicular tissue, causing severe damage of testis and epididymis, even leading to infertility (Ma et al., 2017; Uraki et al., 2017). Two DNA vaccines were reported to reduce ZIKV persistence in the testicular tissue and ZIKV-associated pathological lesion (Griffin et al., 2017), or partially prevent infertility of male mice (de La Vega et al., 2018). However, no effective and safe antiviral agent has ever been reported to prevent or treat ZIKV infection in testicular tissue. Our previous study has demonstrated that Z2 peptide is highly effective in inhibiting ZIKV infection *in vivo* and *in vitro* (Yu et al., 2017). Noticeably, it can penetrate the placental barrier to inhibit vertical transmission of ZIKV in pregnant mice. However, whether Z2 could cross the BTB and protect testicular tissue against ZIKV infection remained unknown.

Several studies have reported that Sertoli cells play an important role in the entry of ZIKV into the seminiferous tubules and support long-term replication of ZIKV in the testicular tissue (Siemann et al., 2017; Kumar et al., 2018). We found that Z2 peptide possesses potent antiviral activity against ZIKV infection in BHK-21 and Vero cells (Yu et al., 2017). In this study, we found that Z2 was also highly effective in inhibiting infection of divergent ZIKV strains with Asian and African lineages in TM4 cells, the mouse Sertoli cell line. Particularly, Z2 treatment *via* intraperitoneal injection resulted in dramatically decreased ZIKV RNA level in the testis of A129 mice, suggesting that Z2 can protect testis against ZIKV infection in Sertoli cells.

Meanwhile, we employed Z2-Cy5 to examine whether Z2 could enter seminiferous tubule, and we found that intraperitoneally injected Z2 could be distributed in the testicular tissue of male A129 mice, consistent with the observation in mice intravenously administered with Z2 (Yu et al., 2017). However, because of the intricate structure of capillary vessel and seminiferous tubule in mouse testis, we could not obtain sufficient evidence to prove that Z2 crossed BTB into seminiferous tubule. H&E analysis showed no obvious pathological damage in the testicular tissue of Z2-treated mice, but it did reveal severe pathological damage in the testis and epididymis of vehicle-treated mice, consistent with the findings of other studies (Govero et al., 2016; Ma et al., 2017). When combined with evidence that viral load in mature sperm of Z2-treated A129 mice was significantly decreased, we speculate that Z2 may, indeed, cross the BTB and enter seminiferous tubule to inhibit ZIKV infection in the sperm.

Zika virus infection in the testicular tissue not only damages male testicular tissue, resulting in pathological lesion of testes and epididymides, but also produces ZIKV-infected semen, causing infertility. In addition, ZIKV in semen of an infected male can be sexually transmitted to his pregnant partner (Russell et al., 2017; Nelson et al., 2018), who can further pass the virus to her fetus, causing congenital Zika syndrome in the newborn (Yarrington et al., 2019). Sexual transmission may also contribute to the spread of ZIKV in regions where the *Aedes mosquito* is not endemic (Rowland et al., 2016). Here we found that Z2 treatment could significantly reduce viral load in sperm of ZIKV-infected A129 mice and improve the number and motility of sperm, implying that application of Z2 can limit the damage to testicular tissue and sperm caused by ZIKV infection and reduce the risk of sexual transmission of ZIKV.

## CONCLUSION

Z2 administered *via* intraperitoneal or intravenous injection could be distributed in mouse testicular tissue, protect the tissue against ZIKV infection and ZIKV-induced pathological damage and poor sperm quality, suggesting that Z2 peptide has the potential to be further developed as an anti-ZIKV therapeutic for treatment of ZIKV infection and attenuation of ZIKV-induced damage in the testicular tissue.

## DATA AVAILABILITY STATEMENT

All datasets generated for this study are included in the manuscript/**Supplementary Files**.

## ETHICS STATEMENT

The animal study was reviewed and approved by Shanghai Public Health Clinical Center Animal Welfare and Ethics Committee Institutional Laboratory Animal Care and Use Committee at Fudan University.

## AUTHOR CONTRIBUTIONS

LL, SJ, and JH conceived and designed the experiments. LS, YM, PZ, QW, and WX performed the experiments. FT, YW, MX, and WL carried out the CASA and H&E staining analysis about A129 mice. LS and YM analyzed the data. LL, SJ, JH, and LS wrote the manuscript.

## FUNDING

This work was supported by the National Megaprojects of China for Major Infectious Diseases (2018ZX10301403 to LL), the National Natural Science Foundation of China (81661128041, 81672019, and 81822045 to LL; 81630090 to SJ; 81701998 to QW; and 81703571 to WX), the Sanming Project of Medicine in Shenzhen (to SJ), the National Key Research and Development Program of China (2016YFC1000905), and the Shanghai Municipal Science and Technology Committee (18431900200).

## ACKNOWLEDGMENTS

We are very grateful to the staff at the Animal Experiment Department of Shanghai Public Health Clinical Center for their contribution to this study.

## SUPPLEMENTARY MATERIAL

The Supplementary Material for this article can be found online at: https://www.frontiersin.org/articles/10.3389/fmicb.2019.02250/full#supplementary-material

## REFERENCES

Arsuaga, M., Bujalance, S. G., Diaz-Menendez, M., Vazquez, A., and Arribas, J. R. (2016). Probable sexual transmission of Zika virus from a vasectomised man. *Lancet Infect. Dis.* 16:1107. doi: 10.1016/s1473-3099(16)30320-6

Avelino-Silva, V. I., Alvarenga, C., Abreu, C., Tozetto-Mendoza, T. R., Canto, C., Manuli, E. R., et al. (2018). Potential effect of Zika virus infection on human male fertility? *Rev. Inst. Med. Trop Sao Paulo* 60:e64. doi: 10.1590/s1678-9946201860064

Barzon, L., Percivalle, E., Pacenti, M., Rovida, F., Zavattoni, M., Del Bravo, P., et al. (2018). Virus and antibody dynamics in travelers with acute Zika virus infection. *Clin. Infect. Dis.* 66, 1173–1180. doi: 10.1093/cid/cix967

Baud, D., Gubler, D. J., Schaub, B., Lanteri, M. C., and Musso, D. (2017a). An update on Zika virus infection. *Lancet* 390, 2099–2109. doi: 10.1016/s0140-6736(17)31450-2

Baud, D., Musso, D., Vouga, M., Alves, M. P., and Vulliemoz, N. (2017b). Zika virus: a new threat to human reproduction. *Am. J. Reprod. Immunol.* 77:e12614. doi: 10.1111/aji.12614

Besnard, M., Lastere, S., Teissier, A., Cao-Lormeau, V., and Musso, D. (2014). Evidence of perinatal transmission of Zika virus, French Polynesia, december 2013 and february 2014. *Euro Surveill.* 19:20751. doi: 10.2807/1560-7917.es2014.19.13.20751

Brasil, P., Sequeira, P. C., Freitas, A. D., Zogbi, H. E., Calvet, G. A., de Souza, R. V., et al. (2016). Guillain-Barre syndrome associated with Zika virus infection. *Lancet* 387:1482. doi: 10.1016/s0140-6736(16)30058-7

Chan, J. F., Chik, K. K., Yuan, S., Yip, C. C., Zhu, Z., Tee, K. M., et al. (2017). Novel antiviral activity and mechanism of bromocriptine as a Zika virus NS2B-NS3 protease inhibitor. *Antivir. Res.* 141, 29–37. doi: 10.1016/j.antiviral.2017.02.002

Cheng, C. Y., and Mruk, D. D. (2012). The blood-testis barrier and its implications for male contraception. *Pharmacol. Rev.* 64, 16–64. doi: 10.1124/pr.110.002790

da Silva, S., Oliveira Silva Martins, D., and Gomes Jardim, A. C. (2018). A review of the ongoing research on Zika virus treatment. *Viruses* 10:E255. doi: 10.3390/v10050255

de La Vega, M. A., Piret, J., Griffin, B. D., Rheaume, C., Venable, M. C., Carbonneau, J., et al. (2018). Zika-induced male infertility in mice is potentially reversible and preventable by deoxyribonucleic acid immunization. *J. Infect. Dis.* 219, 365–374. doi: 10.1093/infdis/jiy336

Deng, Y. Q., Zhang, N. N., Li, C. F., Tian, M., Hao, J. N., Xie, X. P., et al. (2016a). Adenosine analog NITD008 is a potent inhibitor of Zika virus. *Open Forum Infect. Dis.* 3:ofw175. doi: 10.1093/ofid/ofw175

Deng, Y. Q., Zhao, H., Li, X. F., Zhang, N. N., Liu, Z. Y., Jiang, T., et al. (2016b). Isolation, identification and genomic characterization of the Asian lineage Zika virus imported to China. *Sci. China Life Sci.* 59, 428–430. doi: 10.1007/s11427-016-5043-4

Duggal, N. K., Ritter, J. M., Pestorius, S. E., Zaki, S. R., Davis, B. S., Chang, G. J., et al. (2017). Frequent Zika virus sexual transmission and prolonged viral RNA shedding in an immunodeficient mouse model. *Cell Rep.* 18, 1751–1760. doi: 10.1016/j.celrep.2017.01.056

Gao, G. F. (2018). From "A"IV to "Z"IKV: attacks from emerging and re-emerging pathogens. *Cell* 172, 1157–1159. doi: 10.1016/j.cell.2018.02.025

Garcia-Bujalance, S., Gutierrez-Arroyo, A., De la Calle, F., Diaz-Menendez, M., Arribas, J. R., Garcia-Rodriguez, J., et al. (2017). Persistence and infectivity of Zika virus in semen after returning from endemic areas: report of 5 cases. *J. Clin. Virol.* 96, 110–115. doi: 10.1016/j.jcv.2017.10.006

Goodson, S. G., Zhang, Z., Tsuruta, J. K., Wang, W., and O'Brien, D. A. (2011). Classification of mouse sperm motility patterns using an automated multiclass support vector machines model. *Biol. Reprod.* 84, 1207–1215. doi: 10.1095/biolreprod.110.088989

Gorshkov, K., Shiryaev, S. A., Fertel, S., Lin, Y. W., Huang, C. T., Pinto, A., et al. (2018). Zika virus: origins, pathological action, and treatment strategies. *Front. Microbiol.* 9:3252. doi: 10.3389/fmicb.2018.03252

Govero, J., Esakky, P., Scheaffer, S. M., Fernandez, E., Drury, A., Platt, D. J., et al. (2016). Zika virus infection damages the testes in mice. *Nature* 540, 438–442. doi: 10.1038/nature20556

Griffin, B. D., Muthumani, K., Warner, B. M., Majer, A., Hagan, M., and Audet, J. (2017). DNA vaccination protects mice against Zika virus-induced damage to the testes. *Nat. Commun.* 8:15743. doi: 10.1038/ncomms15743

Gurung, S., Reuter, N., Preno, A., Dubaut, J., Nadeau, H., Hyatt, K., et al. (2019). Zika virus infection at mid-gestation results in fetal cerebral cortical injury and fetal death in the olive baboon. *PLoS Pathog.* 15:e1007507. doi: 10.1371/journal.ppat.1007507

Jackman, J. A., Costa, V. V., Park, S., Real, A., Park, J. H., Cardozo, P. L., et al. (2018). Therapeutic treatment of Zika virus infection using a brain-penetrating antiviral peptide. *Nat. Mater.* 17, 971–977. doi: 10.1038/s41563-018-0194-2

Joguet, G., Mansuy, J. M., Matusali, G., Hamdi, S., Walschaerts, M., Pavili, L., et al. (2017). Effect of acute Zika virus infection on sperm and virus clearance in body fluids: a prospective observational study. *Lancet Infect. Dis.* 17, 1200–1208. doi: 10.1016/s1473-3099(17)30444-9

Knee, R. A., Hickey, D. K., Beagley, K. W., and Jones, R. C. (2005). Transport of IgG across the blood-luminal barrier of the male reproductive tract of the rat and the effect of estradiol administration on reabsorption of fluid and IgG by the epididymal ducts. *Biol. Reprod.* 73, 688–694. doi: 10.1095/biolreprod.105.041079

Kumar, A., Jovel, J., Lopez-Orozco, J., Limonta, D., Airo, A. M., Hou, S., et al. (2018). Human Sertoli cells support high levels of Zika virus replication and persistence. *Sci. Rep.* 8:5477. doi: 10.1038/s41598-018-23899-x

Li, C., Deng, Y. Q., Wang, S., Ma, F., Aliyari, R., Huang, X. Y., et al. (2017). 25-hydroxycholesterol protects host against Zika virus infection and its associated microcephaly in a mouse model. *Immunity* 46, 446–456. doi: 10.1016/j.immuni.2017.02.012

Ma, W., Li, S., Ma, S., Jia, L., Zhang, F., Zhang, Y., et al. (2017). Zika virus causes testis damage and leads to male infertility in mice. *Cell* 168:542. doi: 10.1016/j.cell.2017.01.009

Mansuy, J. M., Dutertre, M., Mengelle, C., Fourcade, C., Marchou, B., Delobel, P., et al. (2016). Zika virus: high infectious viral load in semen, a new sexually transmitted pathogen? *Lancet Infect. Dis.* 16:405. doi: 10.1016/s1473-3099(16)00138-9

Matusali, G., Houzet, L., Satie, A. P., Mahe, D., Aubry, F., Couderc, T., et al. (2018). Zika virus infects human testicular tissue and germ cells. *J. Clin. Invest.* 128, 4697–4710. doi: 10.1172/jci121735

Mead, P. S., Hills, S. L., and Brooks, J. T. (2018). Zika virus as a sexually transmitted pathogen. *Curr. Opin. Infect. Dis.* 31, 39–44. doi: 10.1097/qco.0000000000000414

Nelson, E. J., Luetke, M. C., McKinney, C., and Omodior, O. (2018). Knowledge of the sexual transmission of Zika virus and preventive practices against Zika virus among U.S. travelers. *J. Community Health.* 44, 377–386. doi: 10.1007/s10900-018-0594-x

Peixoto, H. M., Romero, G. A. S., de Araujo, W. N., and de Oliveira, M. R. F. (2019). Guillain-Barre syndrome associated with Zika virus infection in Brazil: a cost-of-illness study. *Trans. R. Soc. Trop. Med. Hyg.* 113, 252–258. doi: 10.1093/trstmh/trz010

Petersen, E., Wilson, M. E., Touch, S., McCloskey, B., Mwaba, P., Bates, M., et al. (2016). Rapid spread of Zika virus in the americas–implications for public health preparedness for mass gatherings at the 2016 Brazil Olympic Games. *Int. J. Infect. Dis.* 44, 11–15. doi: 10.1016/j.ijid.2016.02.001

Petersen, L. R., Jamieson, D. J., Powers, A. M., and Honein, M. A. (2016). Zika virus. *N. Engl. J. Med.* 374, 1552–1563. doi: 10.1056/NEJMra1602113

Pettersson, J. H., and Bohlin, J. (2018). Re-visiting the evolution, dispersal and epidemiology of Zika virus in Asia. *Emerg. Microb. Infect.* 7:79. doi: 10.1038/s41426-018-0082-5

Pierson, T. C., and Diamond, M. S. (2018). The emergence of Zika virus and its new clinical syndromes. *Nature* 560, 573–581. doi: 10.1038/s41586-018-0446-y

Rowland, A., Washington, C. I., Sheffield, J. S., Pardo-Villamizar, C. A., and Segars, J. H. (2016). Zika virus infection in semen: a call to action and research. *J. Assist. Reprod. Genet.* 33, 435–437. doi: 10.1007/s10815-016-0684-6

Russell, K., Hills, S. L., Oster, A. M., Porse, C. C., Danyluk, G., Cone, M., et al. (2017). Male-to-female sexual transmission of Zika virus-United States. January-april 2016. *Clin. Infect. Dis.* 64, 211–213. doi: 10.1093/cid/ciw692

Sakkas, H., Bozidis, P., Giannakopoulos, X., Sofikitis, N., and Papadopoulou, C. (2018). An update on sexual transmission of Zika virus. *Pathogens* 7:E66. doi: 10.3390/pathogens7030066

Siemann, D. N., Strange, D. P., Maharaj, P. N., Shi, P. Y., and Verma, S. (2017). Zika virus infects human Sertoli cells and modulates the integrity of the in vitro blood-testis barrier model. *J. Virol.* 91:e00623-17. doi: 10.1128/jvi.00623-17

Simanjuntak, Y., Liang, J. J., Chen, S. Y., Li, J. K., Lee, Y. L., Wu, H. C., et al. (2018). Ebselen alleviates testicular pathology in mice with Zika virus infection and prevents its sexual transmission. *PLoS Pathog.* 14:e1006854. doi: 10.1371/journal.ppat.1006854

Sirohi, D., Chen, Z., Sun, L., Klose, T., Pierson, T. C., Rossmann, M. G., et al. (2016). The 3.8 Å resolution cryo-EM structure of Zika virus. *Science* 352, 467–470. doi: 10.1126/science.aaf5316

Strange, D. P., Zarandi, N. P., Trivedi, G., Atala, A., Bishop, C. E., Sadri-Ardekani, H., et al. (2018). Human testicular organoid system as a novel tool to study Zika virus pathogenesis. *Emerg. Microb. Infect.* 7:82. doi: 10.1038/s41426-018-0080-7

Su, L., Mruk, D. D., and Cheng, C. Y. (2011). Drug transporters, the blood-testis barrier, and spermatogenesis. *J. Endocrinol.* 208, 207–223. doi: 10.1677/joe-10-0363

Tai, W., Voronin, D., Chen, J., Bao, W., Kessler, D. A., Shaz, B., et al. (2019). Transfusion-transmitted Zika virus infection in pregnant mice leads to broad tissue tropism with severe placental damage and fetal demise. *Front. Microbiol.* 10:29. doi: 10.3389/fmicb.2019.00029

Turmel, J. M., Abgueguen, P., Hubert, B., Vandamme, Y. M., Maquart, M., Le Guillou-Guillemette, H., et al. (2016). Late sexual transmission of Zika virus related to persistence in the semen. *Lancet* 387:2501. doi: 10.1016/s0140-6736(16)30775-9

Uraki, R., Hwang, J., Jurado, K. A., Householder, S., Yockey, L. J., Hastings, A. K., et al. (2017). Zika virus causes testicular atrophy. *Sci. Adv.* 3:e1602899. doi: 10.1126/sciadv.1602899

Wang, J., Bardelli, M., Espinosa, D. A., Pedotti, M., Ng, T. S., Bianchi, S., et al. (2017). A human bi-specific antibody against Zika virus with high therapeutic potential. *Cell* 171:229-241.e15. doi: 10.1016/j.cell.2017.09.002

Wang, L., Wang, R., Wang, L., Ben, H., Yu, L., Gao, F., et al. (2019). Structural basis for neutralization and protection by a Zika virus-specific human antibody. *Cell Rep.* 26:3360-3368.e5. doi: 10.1016/j.celrep.2019.02.062

Wei, X., Li, K., Zhang, G., Huang, Y., Lv, J., Li, M., et al. (2018). B7-H3 promoted proliferation of mouse spermatogonial stem cells via the PI3K signaling pathway. *Oncotarget* 9, 1542–1552. doi: 10.18632/oncotarget.23457

Xia, S., Yan, L., Xu, W., Agrawal, A. S., Algaissi, A., Tseng, C. K., et al. (2019). A pan-coronavirus fusion inhibitor targeting the HR1 domain of human coronavirus spike. *Sci. Adv.* 5:eaav4580. doi: 10.1126/sciadv.aav4580

Yarrington, C. D., Hamer, D. H., Kuohung, W., and Lee-Parritz, A. (2019). Congenital Zika syndrome arising from sexual transmission of Zika virus, a case report. *Fertil. Res. Pract.* 5:1. doi: 10.1186/s40738-018-0053-5

Yu, Y., Deng, Y. Q., Zou, P., Wang, Q., Dai, Y., Yu, F., et al. (2017). A peptide-based viral inactivator inhibits Zika virus infection in pregnant mice and fetuses. *Nat. Commun.* 8:15672. doi: 10.1038/ncomms15672

Zhang, S., Kostyuchenko, V. A., Ng, T. S., Lim, X. N., Ooi, J. S. G., Lambert, S., et al. (2016). Neutralization mechanism of a highly potent antibody against Zika virus. *Nat. Commun.* 7:13679. doi: 10.1038/ncomms13679

**Conflict of Interest:** The authors declare that the research was conducted in the absence of any commercial or financial relationships that could be construed as a potential conflict of interest.

*Copyright © 2019 Si, Meng, Tian, Li, Zou, Wang, Xu, Wang, Xia, Hu, Jiang and Lu. This is an open-access article distributed under the terms of the Creative Commons Attribution License (CC BY). The use, distribution or reproduction in other forums is permitted, provided the original author(s) and the copyright owner(s) are credited and that the original publication in this journal is cited, in accordance with accepted academic practice. No use, distribution or reproduction is permitted which does not comply with these terms.*

frontiers in Microbiology

ORIGINAL RESEARCH
published: 24 October 2019
doi: 10.3389/fmicb.2019.02426

# Inhibition by Marine Algae of Chikungunya Virus Isolated From Patients in a Recent Disease Outbreak in Rio de Janeiro

*Claudio Cesar Cirne-Santos[1,2], Caroline de Souza Barros[1], Caio Cesar Richter Nogueira[1,3], Renata Campos Azevedo[4], Kristie Aimi Yamamoto[4], Guilherme Louzada Silva Meira[4], Zilton Farias Meira de Vasconcelos[5], Norman Arthur Ratcliffe[6], Valéria Laneuville Teixeira[3,7], Jonas Schmidt-Chanasit[8], Davis Fernandes Ferreira[4,9]*† and Izabel Christina Nunes de Palmer Paixão[1]*†*

[1] Laboratório de Virologia Molecular e Biotecnologia Marinha, Programa de Pós-graduação em Ciências e Biotecnologia, Departamento de Biologia Celular e Molecular, Instituto de Biologia, Universidade Federal Fluminense, Niterói, Brazil, [2] Departamento de Ensino, Curso de Farmácia na Universidade Salgado de Oliveira, Niterói, Brazil, [3] Laboratório de Produtos Naturais de Algas Marinhas (ALGAMAR), Departamento de Biologia Marinha, Instituto de Biologia, Universidade Federal Fluminense, Niterói, Brazil, [4] Instituto de Microbiologia Paulo de Góes (IMPPG), Departamento de Virologia, Universidade Federal do Rio de Janeiro, Rio de Janeiro, Brazil, [5] Instituto Fernandes Figueira (IFF), Fundação Oswaldo Cruz (Fiocruz), Rio de Janeiro, Brazil, [6] Department of Biosciences, College of Science, Swansea University, Swansea, United Kingdom, [7] Laboratório de Biologia e Taxonomia de Algas (LABIOTAL), Programa de Pós-graduação em Biodiversidade Neotropical, Instituto de Biociencias, Universidade Federal do Estado do Rio de Janeiro, Rio de Janeiro, Brazil, [8] Bernhard Nocht Institute for Tropical Medicine, WHO Collaborating Centre for Arbovirus and Haemorrhagic Fever Reference and Research, Hamburg, Germany, [9] Department of Molecular and Structural Biochemistry, North Carolina State University, Raleigh, NC, United States

Chikungunya virus (CHIKV) infection is one of the most challenging re-emergent diseases caused by a virus, and with no specific antiviral treatment it has now become a major public health concern. In this investigation, 25 blood samples were collected from patients with characteristic CHIKV symptoms and submitted to a virus isolation protocol, which detected 3 CHIKV isolates. These samples were evaluated by sequencing for the characterization of the strains and any homology to viruses circulating in Brazil during a recent outbreak. These viruses were used for the development of antiviral assays. Subsequently, the inhibitory effects of seaweed extracts on CHIKV replication were studied. The marine species of algae tested were *Bryothamnion triquetrum, Caulerpa racemosa, Laurencia dendroidea, Osmundaria obtusiloba*, *Ulva fasciata*, and *Kappaphycus alvarezii,* all of which are found in different countries including Brazil. The results revealed high levels of CHIKV inhibition, including extracts of *O. obtusiloba* with inhibition values of 1.25 μg/mL and a selectivity index of 420. Viral inhibition was dependent on the time of addition of extract of *O. obtusiloba* to the infected cells, with the optimal inhibition occurring up to 16 h after infection. Neuron evaluations with *O. obtusiloba* were performed and demonstrated low toxicity, and in infected neurons we observed high inhibitory activity in a dose-dependent manner. These results indicate that the algal extracts may be promising novel candidates for the development of therapeutic agents against CHIKV infections.

**Keywords: chikungunya, arbovirus, seaweed, antiviral, crude extracts**

OPEN ACCESS

***Edited by:***
*Lijun Rong,*
*University of Illinois at Chicago, United States*

***Reviewed by:***
*Adam Taylor,*
*Griffith University, Australia*
*Emi E. Nakayama,*
*Osaka University, Japan*

***Correspondence:**
*Davis Fernandes Ferreira*
*davisf@micro.ufrj.br*
*Izabel Christina Nunes de Palmer Paixão*
*izabeluff@gmail.com*

*† These authors have contributed equally to this work*

***Specialty section:***
*This article was submitted to Virology, a section of the journal Frontiers in Microbiology*

***Received:*** *22 May 2019*
***Accepted:*** *08 October 2019*
***Published:*** *24 October 2019*

***Citation:***
*Cirne-Santos CC, Barros CdS, Nogueira CCR, Azevedo RC, Yamamoto KA, Meira GLS, Vasconcelos ZFMd, Ratcliffe NA, Teixeira VL, Schmidt-Chanasit J, Ferreira DF and Paixão ICNdP (2019) Inhibition by Marine Algae of Chikungunya Virus Isolated From Patients in a Recent Disease Outbreak in Rio de Janeiro. Front. Microbiol. 10:2426. doi: 10.3389/fmicb.2019.02426*

## INTRODUCTION

First described in Tanzania in the African continent in 1952 and later definitively identified in Thailand in 1958, Chikungunya virus (CHIKV) has become a serious public health problem. CHIKV is a reemerging arbovirus infection, with significant human morbidity, and until now one million suspected cases have occurred worldwide (Burt et al., 2012; Presti et al., 2014; Brasil, 2018). CHIKV is mainly transmitted by *Aedes albopictus* and *Aedes aegypti*. Infection causes a self-limited febrile illness known as chikungunya fever with symptoms that include myalgia, fever, rash and debilitating joint symptoms such as persistent polyarthritis, which has been reported to last for many months or even years (Schilte et al., 2013). During a mild course of infection, symptoms usually appear after 4–7 days incubation and disappear after about 1 week from onset of symptoms (Grischott et al., 2016; Purpura et al., 2016).

Although CHIKV had not yet been considered a neurotropic virus, there is evidence now of its involvement as a cause of neurological diseases at different ages, although the maternal-child stage has been described as the main target in the manifestations of encephalopathy by this virus. Further studies are needed for the neurotropic correlation of CHIKV, although there is evidence of some probable neurological complications including encephalitis, myelopathy, peripheral neuropathy, melopoeia, and myopathy (Arpino et al., 2009; Chandak et al., 2009).

Arboviruses have symptoms that may be very difficult to differentiate because of their high overlapping characteristics, and thus clinical diagnosis has become a major challenge, mainly due to the current lack of effective methodologies for more accurate diagnosis. Some tests may be more decisive for CHIKV characterization, such as the reduction of platelet numbers and the presence of eruptions. However, the clinical signs and symptoms of CHIKV are indistinguishable from those of dengue fever, and both diseases are transmitted by *Aedes* mosquitoes (Rudolph et al., 2014). Therefore, steps should be taken to minimize misleading diagnosis during patient examination.

Arbovirus outbreaks, mainly of Zika virus (ZIKV), CHIKV, and dengue (DENV), have been frequently reported. In Thailand, CHIKV outbreaks were first documented in the early 1960s, and the latest outbreak was reported in 2008–2009 (Dash et al., 2007; Montagnier, 2010). Studies have shown that CHIKV was transmitted to Europe, in south-eastern France, between 2010 and 2014. However, in 2013, the first cases of autochthonous transmission in the French Caribbean were reported. Throughout 2018, the distribution of CHIKV in the Americas was also observed, reaching more than one million people (Leparc-Goffart et al., 2014; Powers, 2015).

The first autochthonous cases of CHIKV infection in Brazil were confirmed in 2014, in Oiapoque, Amapá (Rudolph et al., 2014). In 2017, there were 161,346 probable cases of CHIKV fever. In 2018, as of June 23, there were 53,089 probable cases of chikungunya fever in this country. Until this latter date, 11 deaths were confirmed from CHIKV while in the same period of 2017, 160 deaths were recorded (Brasil, 2018). To date, four CHIKV genotypes have been described, namely, East-Central-South African (ECSA), Asian, Indian Ocean, and West African (Weaver and Forrester, 2015). The Asian genotype was first detected in the Caribbean region in late 2013 and then spread throughout Central America. Nine months later, the first autochthonous cases in Brazil were detected in Oiapoque City, Amapá State and also in Feira de Santana, Bahia State, which are more than 2,000 Km from each other. Curiously, the ECSA genotype may be circulating in Feira de Santana and this has been shown to be from an individual who had recently returned from Angola and had a symptomatic contact in Feira de Santana (Nunes et al., 2015).

Chikungunya virus is an alphavirus of the Togaviridae family and has an 11.8 kb genome positive-sense single-stranded RNA. Alphavirus particles are enveloped, have a diameter of 70 nm, tend to be spherical (though slightly pleomorphic) and have an isometric nucleocapsid of 40 nm. The central region of the nucleocapsid has about 240 copies of the capsid protein that surrounds the viral genome. In addition, studies have shown that a number of host factors can be added to the nucleocapsid (Sokoloski et al., 2013). The lipid bilayer is strictly from the host and the source of the viral budding site (Strauss and Strauss, 1994; Lu and Kielian, 2000). Alphaviruses encode four non-structural proteins (nsp1, nsp2, nsp3, and nsp4), which are fundamental for viral genome replication, and also the structural proteins that include the capsid, and are related to the viral assembly process (Strauss and Strauss, 1994).

There are no vaccines or specific treatments available for the high morbidity rate caused by CHIKV. The most effective treatments are only symptomatic and use analgesics or anti-inflammatories. Therefore, new compounds are urgently required that can act on the CHIKV infection, reducing the high morbidity and mortality rates resulting from this virus. In this present study, natural products derived from marine algae have been tested against CHIKV as a new strategy since, previously, these extracts have been shown to have high activity against different microorganisms and also to be non-toxic for mammalian cells (Bourjot et al., 2012; Abdelnabi et al., 2015; Ching et al., 2015).

## MATERIALS AND METHODS

### Seaweed Material and Extraction

The project obtained a permit for scientific purposes on 01/07/2012 at SISBIO/IBAMA number 3534 (VLT) and access to genetic heritage (register SISGEN – IBAMA) from the Universiade Federal Fluminense number A05E653 (VLT) in 01/11/2018.

The seaweeds were collected by snorkeling at a depth 1–3 m in various sites from the Brazilian coast. *Bryothamnion triquetrum* (S. G. Gmelin) M. Howe was collected at Atol das Rocas reef, Rio Grande do Norte State (lat. 03° 51′03″, long. 33° 40′29″), *Caulerpa racemosa* (Forsskål) J. Agardh was collected at Baía da Ribeira, Angra dos Reis, Rio de Janeiro State (lat. 22° 98′33″, long. 44° 38′33″), *Kappaphycus alvarezii* (Doty) Doty ex P. C. Silva was harvested from mariculture at Praia Grande, Paraty, Rio de Janeiro State (lat. 23° 16′15″, long. 44° 34′48″), *Laurencia*

*dendroidea* J. Agardh was collected at Orla Bardot, Armação de Búzios, Rio de Janeiro State (lat. 22° 05′03″, long. 41° 53′ 01″), *Osmundaria obtusiloba* (C. Agardh) R. E. Norris was collected at Rasa Beach, Armação de Búzios, Rio de Janeiro State (lat. 22° 45′40″, long. 41° 54′ 32″) and *Ulva fasciata* Delile was collected at Itaipú Beach, Niterói, Rio de Janeiro State (lat. 22o 58′26″, long. 43° 02′ 46″).

The seaweeds were separated from sediments, epiphytes and other associated organisms, washed with sea water and air-dried (approximate temperature 28–30°C for 7–10 days) until the total evaporation of any water.

Air-dried seaweeds (approximately 100 g) were powdered and exhaustively extracted three times using different organic solvents (PA.) each time for 72 h. *Bryothamnion triquetrum* was extracted with dichloromethane, *Caulerpa racemosa* was extracted with acetone, *Kappaphycus alvarezii* was extracted with ethanol, *Laurencia dendroidea* was extracted with hexane, and *Osmundaria obtusiloba* and *Ulva fasciata* were extracted with ethanol.

The extracts were evaporated under reduced pressure, yielding crude extracts of each species (15–20 mg), of which 2–5 mg were used in tests against the CHIKV. The extracts were chosen according to their chemical composition, and by the presence of different classes of active substances (terpenes, sterols, fatty acids, polysaccharides, alkaloids, aromatic compounds) from these algae as indicated by previous studies (Santos et al., 2010; de Souza Barros et al., 2016; Lira et al., 2016). Analytical TLC was performed on Merck Kieselgel $GF_{254}$ plates, spot detection was obtained by spraying with a 2% solution of Ce(SO4) in 2N $H_2S0_4$ followed by heating for 5 min at 150°C. The extracted compounds were examined by $^1$H NMR for detection of the majority of substances in each extract. $^1$H NMR was determined on a Varian-VNMRS apparatus at 300 and 500 MHz. Spectra were recorded in $CDCl_3$ solutions using TMS as internal standard.

The thin layer chromatographic (TLC) used silica gel $GF_{254}$ and various solvents systems as eluents and Nuclear Magnetic Resonance Proton ($^1$H NMR) analyses demonstrated the majority presence of fatty acids and sterols in *B. triquetrum,* the caulerpin; a pigment bis-indole alkaloid from *C. racemosa;* the sterols, mainly cholesterol, from *K. alvarezii;* elatol, a halogenated sesquiterpene from *Laurencia dendroidea*; bromo-phenols from *Osmundaria obtusiloba*; and palmitic acid and other fatty acids from *U. fasciata.* All the products mentioned were obtained in previous studies (Rocha et al., 2007).

For the *in vitro* experiments the crude extracts were diluted in 100% DMSO and then added with culture medium to the final concentration of 0.01% DMSO.

## Cell Lines

VERO cells (African green monkey kidney) VERO-ATCCCCL81 were plated in Eagle's minimum essential medium (MEM) (GIBCO) supplemented with 5% Fetal Bovine Serum (FBS). C6/36 mosquito cell line from *Aedes albopictus*, adapted to grow at 33 °C, was cultured in L-15 Medium (Leibovitz) supplemented with 0.3% tryptose phosphate broth, 0.02% glutamine, 1% MEM non-essential amino acids solution and 5% FBS. Purified cultures of retinal neurons were prepared according to earlier descriptions (Mejía-García and Paes-de-Carvalho, 2007). Retinas of 8-day-old chicken embryos were excised, incubated with 0.1% trypsin and then the cells were dissociated in medium with the help of a conical Pasteur pipette. Subsequently, the cells were seeded on 24 well plastic plates coated with poly-L-ornithine at a density of 830 cells/mm in BME containing 2.5% fetal calf serum, 100 U/ml penicillin, 100 mg/ml streptomycin and 2 mM glutamine and incubated at 37°C for 3 days in a 5% CO2 atmosphere. These purified cultures of retinal neurons were firstly described by Adler et al. (1984). In this work, they showed that almost 100% of the cells possess a neuronal identity using techniques such as phase-contrast microscopy, lectin staining and electron microscopy. After that, some groups have been working with this kind of culture to study different effects on neuronal cells, such as (Ferreira and Paes-de-Carvalho, 2001; Paes-de-Carvalho et al., 2003; Mejía-García et al., 2013) among others. More recently, Anccasi et al. (2013) demonstrated by immunocytochemistry assays that these cells are positive to Tuj1 (beta-tubulin III), which is a protein only found in neurons and considered as a neuronal marker, but negative to a glial marker 2M6.

## Virus Isolation

Between the months of March and April 2016, 25 samples of 5 mL venous whole blood were collected in a tube containing EDTA anticoagulant. Samples were taken from selected patients who had clear clinical symptoms of arbovirus infections, mainly joint symptoms and fever, and were treated at a hospital in Niteroi, RJ. The patients were interviewed and agreed to blood collection by signing the free and informed consent form, approved by the ethics committee with approved registration – CAAE: 61845416.0.0000.5289. After collection, all samples were submitted to RT-PCR analysis to determine if the patients had other viral infections, either Flavivirus or Alfavirus, and not only CHIKV. Samples were centrifuged for 5 min, and the leukocyte pellet was removed and added to 24-well plates at 90% confluence in VERO cells. After 24 h, the blood cells were removed from the VERO cell monolayer, fresh media was added, containing 5% FBS, and incubated in an atmosphere of 5% $CO_2$ at 37°C for 3 to 5 days. The cell culture plates were evaluated daily in order to determine any cytopathic effect as a result of viral infection.

## RNA Detection by RT-qPCR and Virus Sequence

RNA from samples presenting cytopathic effects was extracted using the commercial kit QIAamp viral RNA mini (QIAGEN, Valencia, CA, United States) according to the manufacturer's instructions. Isolation was confirmed by reverse transcription real-time PCR (RT-PCR) using primers targeting the structural polyprotein (forward TATCCTGACCATCCGACCCT/reverse GGCTCTTGTCCTTGCACTCT) and Superscript III One-Step RT PCR Kit (Invitrogen Carlsbad, CA, United States), according to the manufacturer's instructions. Amplification was performed in the PeqStar (PeqLab, Erlangen, Germany). PCR conditions were as follows: 60°C for 1 min, 50°C for 45 min, 94°C for 2 min followed by 45 cycles of 95°C for 15 s, 55°C for 30 s and 68°C for 60 s.

The resulting amplicons were sequenced in the ABI 3730 genetic analyzer (Applied Biosystems) following the manufacturer's protocol. Raw sequence data were aligned, edited and assembled using the Assembler tool Bioedit Sequence Aligner Editor. The identity was confirmed by using the Basic Local Alignment Search Tool (Blast) and compared to other CHIKV sequences. Phylogenetic tree was constructed using MEGA 7 program. The sequences were deposited in GenBank under accession numbers MK910738 (BRA/RJ/1F), MK910739 (BRA/RJ/18), and MK910740 (BRA/RJ/23). For the antiviral activity assays the strain with deposit number MK910739 was used.

## Plaque Reduction Assay

VERO cells were cultured in growth medium DMEM. The cells were then incubated with CHIKV for 2 h, washed with PBS and a mixture of 2% (w/v) carboxymethylcellulose (Sigma-Aldrich) and DMEM supplemented with 5% FCS, 5 mM L-glutamine and 0.20% sodium bicarbonate was added. Serial dilutions of compounds without overlap medium were done. Cells were fixed with 10% formaldehyde subsequently stained with 1% violet crystal. The infectious virus titer (PFU/ml) was determined using the following formula: plaque count × dilution factor × (1/inoculation volume).

## Antiviral Assay

Antiviral activity was evaluated using a virus plaque reduction assay. Vero cells and Neurons were grown in 24-well plates, as described above, and subsequently infected with MOI of 0.1 CHIKV in the absence or presence of different concentrations of the compounds. After 1 h of adsorption at 37°C, the residual inoculum was replaced by MEM containing 1% methyl-cellulose and the corresponding dose of each compound. Plaques were counted after 5–10 days of incubation at 37°C, at 5% $CO_2$. Uninfected and treated neurons were incubated for 48 to 72 h, and the cells were evaluated daily for cytopathic effects and the culture supernatant was collected to determine the reduction of viral RNA production by RT-PCR. For VERO cells, the inhibitory concentration 50% ($EC_{50}$) was calculated as the compound concentration reducing virus plaques by 50%. The Selective Index (SI) is derived from the relationship between the $CC_{50}$ and the $EC_{50}$ and reflects the potency and possible future selectivity for future drug development. All determinations were performed twice and each in triplicate.

## Time of Addition

VERO cells were infected with CHIKV at a MOI of 0.1 and incubated for 2 h. Afterward, the viruses were removed and the medium was replaced. In addition, 2.5 mg/mL of *C. racemosa* and *O. obtusiloba* crude extracts were added at different points of virus replication at 3, 2 or 1 h before infection, time 0 (immediately after virus added) or 1, 2, 4, 8, 12, 16, 20 or 24 h after infection. These cells were incubated in 5% $CO_2$ atmosphere at 37°C for 72 h, and then viral replication was measured by plaque assay. Titration at all times was performed at the end of the experiment.

## Virucidal Effect

A CHIKV suspension containing $10^6$ PFU/mL was incubated with different concentrations of *C. racemosa*, *O. obtusiloba*, and *K. alvarezii* (2.5, 5 or 10 μg/mL) for 2 h at 37°C. The CHIKV suspension was also incubated with the same volume of solvent in the extracts (0.01% DMSO). Then, the samples were diluted in MEM and the remaining infectivity was titrated by plaque formation after 48 h. The important point about the extracts is that the sample dilution effectively reduced the drug concentration incubated with the cells by at least 200-fold to confirm that the titer reduction was only due to cell-free virion inactivation. The 50% relative virucidal effect defined inactivation compared to the controls.

## Statistical Analysis

The data were analyzed by the Tukey test or Dunnett test comparing all with the controls (ribavirin and DMSO) using the GraphPad Instat version 3 program. A $p$-value of $<0.05$ was considered statistically significant. The values of $p < 0.05$ and $p < 0.01$ are shown in the figures.

# RESULTS

## RT-PCR of the Isolated Samples and Sequencing

C6/36 mosquito cell line from *Aedes albopictus* was exposed to blood samples from patients suspected of infection by ZIKV or CHIKV and observed daily. At each passage in the C6/36 cells, 50 μL of the supernatant was removed and added into VERO cell cultures in which, at the fourth passage after the supernatant was added, the cytopathic effect was observed after 48 h. Of the 25 samples evaluated from patients who exhibited symptoms characteristic of CHIKV, such as fever, rash, muscular pains, joint pains, and headache, 3 presented cytopathic effects so that the culture supernatants were removed and analyzed by RT-PCR. All 3 samples were positive for CHIKV by PCR, but in order to confirm identity, nucleotide sequencing was performed to characterize the chikungunya strains. Phylogenetic Analysis confirmed the presence of the ECSA genotype in Rio de Janeiro. All viral infection experiments were performed with only one isolate as we determined in an initial experiment that there was no difference in the results obtained for each isolate. The isolates were closely related to strains previously detected in Bahia, Pernambuco and Rio de Janeiro (**Figure 1**).

## Cytotoxicity in VERO and Neuron Cells

The cytotoxicity ($CC_{50}$) of algae extracts in Vero and neuron cells was assessed by MTT [3-(4,5-dimethylthiazole-2-yl)-2,5-diphenyltetrazolium bromide] (Sigma-Aldrich), as previously described (Mosmann, 1983) using $10^5$ cells in 96-well plates. Vero cells were exposed to increasing concentrations of the compounds (50, 100, 200, 400, 800, and 1000 μg/mL) and incubated for 72 h to determine cell viability. The results in **Table 1** show that in Vero cells the $CC_{50}$ values for the extracts ranged from 178 to 732 μg/mL. In the

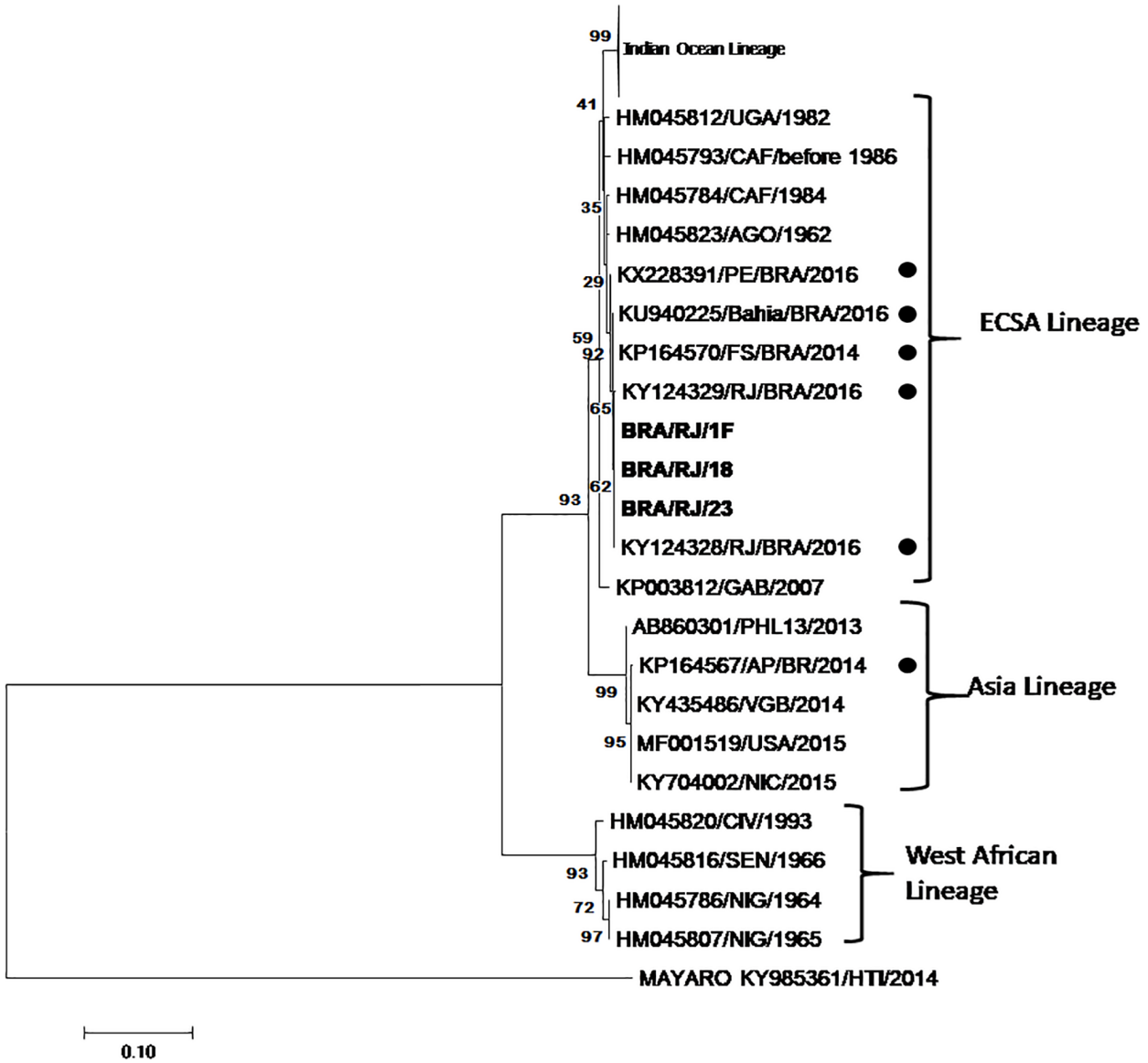


**FIGURE 1 |** Phylogenetic tree was construct for partial non-structural protein (710 pb). Performed by using the Maximum Likelihood method based on the Kimura 2-parameter model. The analysis involved 69 nucleotide sequences. One fragment of sequences described in this studied is in bold, BRA/RJ/1F, BRA/RJ/18, and BRA/RJ/23 (GenBank access numbers MK910738; MK910739; MK910740). Dots mark the Brazilian isolates.

neurons exposed to the *O. obtusiloba* extracts, there was low cytotoxicity with high viability maintained in concentrations up to 200 μg/mL. In contrast, ribavirin presented cytotoxicity from 100 μg/mL (**Figure 2**).

## Inhibition of Chikungunya Virus by Marine Algae

To evaluate the potential of the extracts to inhibit CHIKV replication, Vero cells and neurons were infected in 96-well plates with 0.1 CHIKV MOI, incubated for 1 h for viral adsorption and, subsequently, treated with increasing concentrations of algae extracts. **Figure 3** shows that all the extracts inhibited the replication of CHIKV in a dose-dependent manner. *C. racemosa*, *O. obtusiloba* and *K. alvarezii* inhibited 30 to 98% of CHIKV replication at concentrations from 1.25 to 50 μg/ml. However, the *O. obtusiloba* extract had the highest $EC_{50}$ value (viral inhibition) at 1.25 μg/mL and had a $CC_{50}$ of 525 μg/mL ± 3.11, generating a selectivity index (SI) of 420. In contrast, *C. racemosa* and *K. alvarezii* had lower SIs at 174.2 and 130.1, respectively. Ribavirin, which was used as a control, had an $EC_{50}$ value of 1.73 ± 0.55 μg/mL and was less potent than *O. obtusiloba* extract in inhibiting CHIKV replication (**Table 1**). In infected neurons treated with *O. obtusiloba* extract, there was a significant reduction in the production of copies of viral RNA, demonstrating a

**TABLE 1 |** Cytotoxicity ($CC_{50}$) in Vero Cells, anti-CHIKV profile ($EC_{50}$) and selectivity index (SI) of crude extracts from six seaweeds and ribavirin.

| Crude extracts | $CC_{50}$[a] (μg/mL) | $EC_{50}$[b] (μg/mL) | *SI*[c] |
|---|---|---|---|
| *C. racemosa* | 732 ± 18.1 | 4.2 ± 0.83 | 174.2 |
| *L. dendroidea* | 178 ± 8.2 | 7.78 ± 1.1 | 22.9 |
| *U. fasciata* | 245 ± 11.6 | 18.9 ± 3.8 | 12.9 |
| *O. obtusiloba* | 525 ± 15.4 | 1.25 ± 0.36 | 420 |
| *K. alvarezii* | 423 ± 19.4 | 3.25 ± 0.9 | 130.1 |
| *B. triquetrum* | 400 ± 13.5 | 3.30 ± 0.82 | 121.2 |
| Ribavirin | 118 ± 5.88 | 1.73 ± 0.55 | 68 |

*Data represented as mean ± SD from three independent experiments. [a]Concentration that reduced the cytotoxic concentration in Vero cells by 50% when compared to untreated controls. [b]Concentration that reduced the CHIKV replication by 50% when compared to infected controls. [c]Selectivity index was defined as the ratio between $CC_{50}$ and $EC_{50}$ and represents the safety for in vitro assays.*

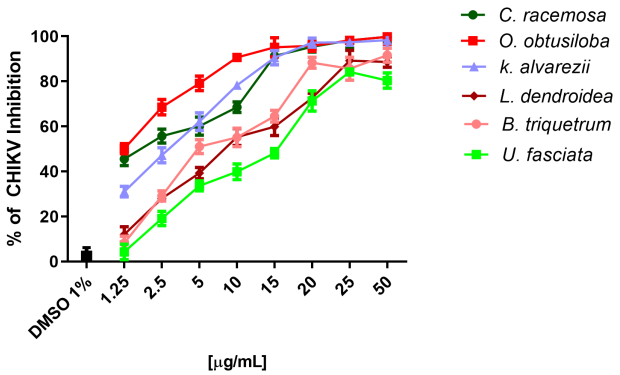


**FIGURE 3 |** Effect of six seaweeds crude extracts on CHIKV replication. Vero cells were infected with CHIKV ($10^6$ PFU/mL) at MOI of 0.1 and treated with different concentrations of the extracts, namely, 1.25, 2.5, 5, 10, 15, 20, 25, and 50 μM. The results were evaluated by plaque assay. Error bars indicate the standard deviation and experiments were performed in triplicate. DMSO used as solvent remained at the final concentration of 0.01% showing no activity on CHIKV replication.

strong inhibitory effect of the replication of CHIKV by these compounds (**Figure 4**).

## Virucidal Effect

The extracts exhibiting the highest inhibition profiles of CHIKV were selected to test for virucidal effects. To this end, the virus was subjected to three concentrations of the compounds (10, 5, and 2.5 μg/ml) for 2 h at 37°C. **Figure 5** shows that the extracts tested had limited virucidal potentials. However, *O. obtusiloba* was able to inhibit about 40% of CHIKV replication in the highest concentration of extract used (10 μg/mL). In contrast,

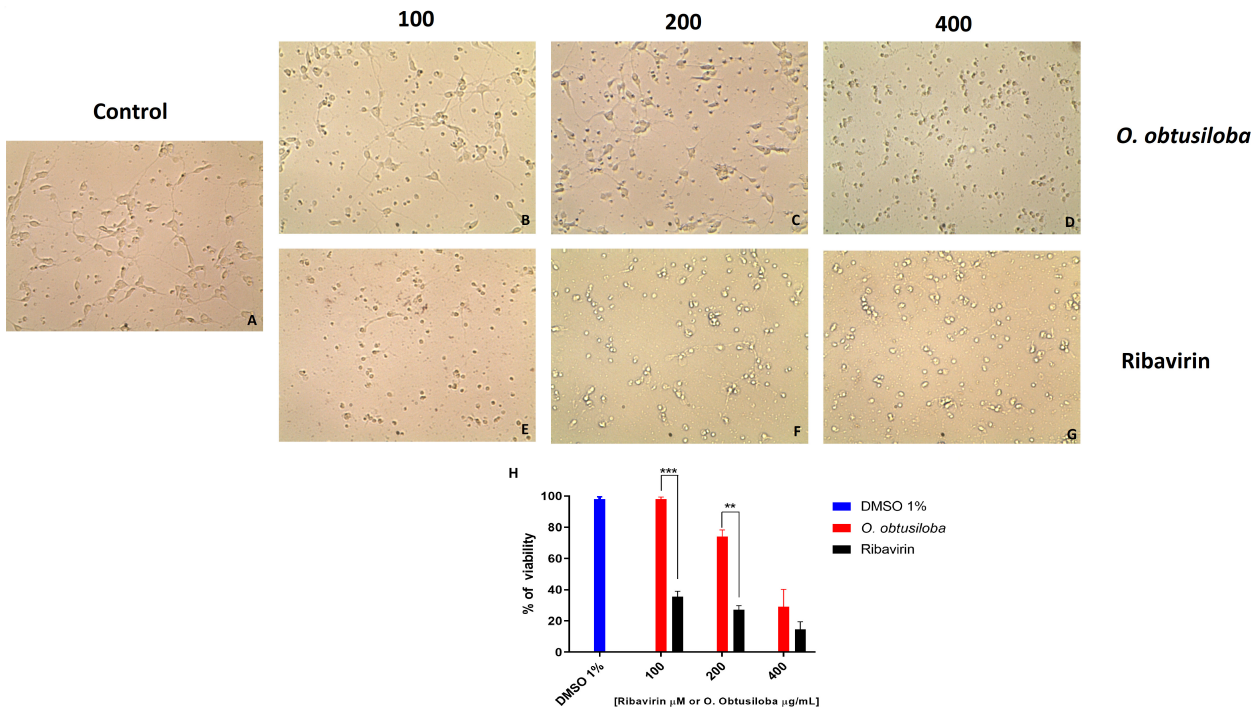


**FIGURE 2 |** Cytotoxicity of *O. obtusiloba* extract and ribavirin in chick retina neurons in 4-day-old purified cultures. **(A)** Control culture. **(B,C,D)** Cultures incubated with *O. obtusiloba* at concentrations of **(B)** 100 μg/mL, **(C)** 200 μg/mL and **(D)** 400 μg/mL. **(E,F,G)** Cultures incubated with *ribavirin* at concentrations of **(E)** 100 μM, **(F)** 200 μM and **(G)** 400 μM. **(H)** Graphical representation showing the percentage of viability of treated cells with *O. obtusiloba* (blue bar) and percentage of viability of treated cells with ribavirin (dark bar). The results were evaluated by MTT assay and showed that the exposure to the *O. obtusiloba* extract presented low cytotoxicity maintaining high viability in concentrations up to 200 μg/mL. Error bars indicate the standard deviation and experiments were performed in triplicate. $^{**}p < 0.01$; $^{***}p < 0.001$ in Tukey test.

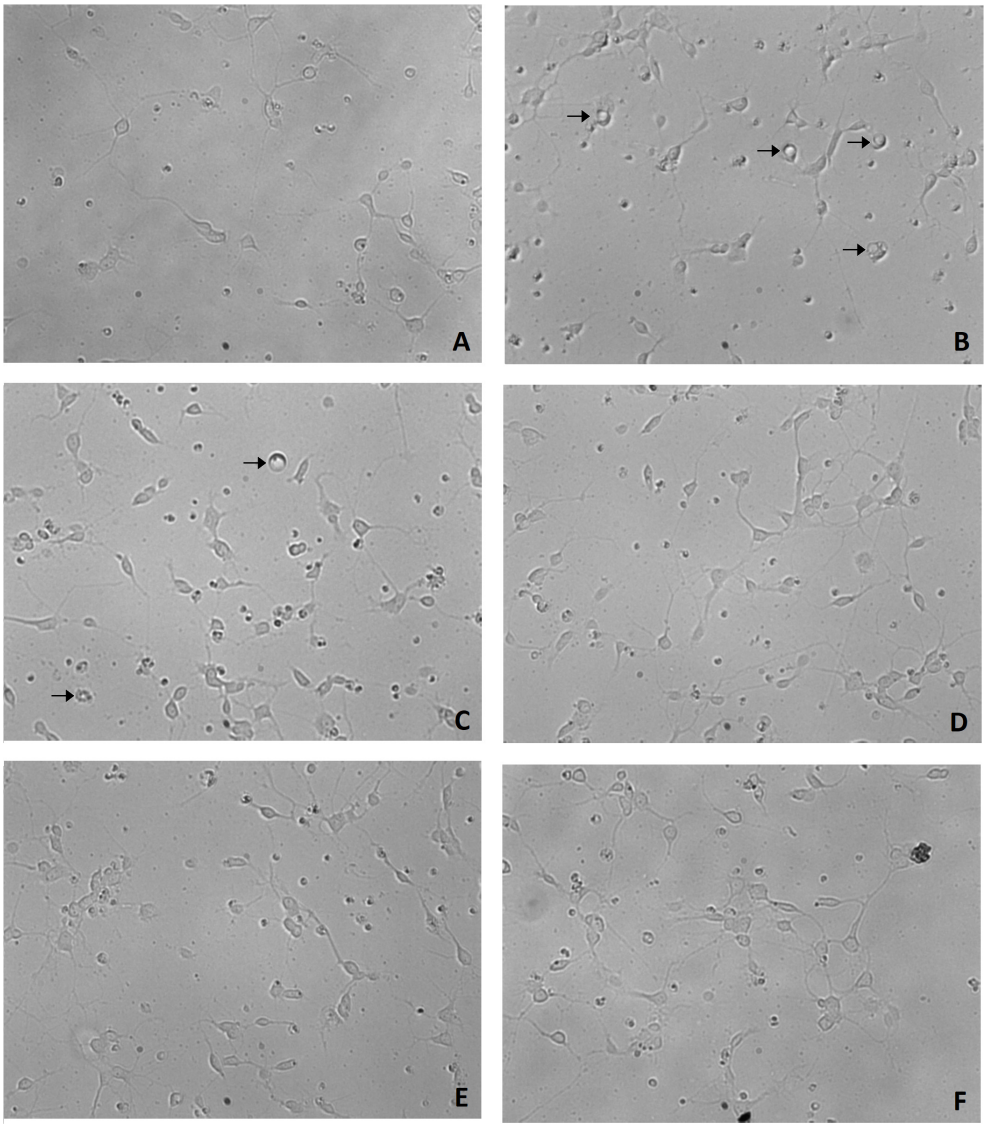


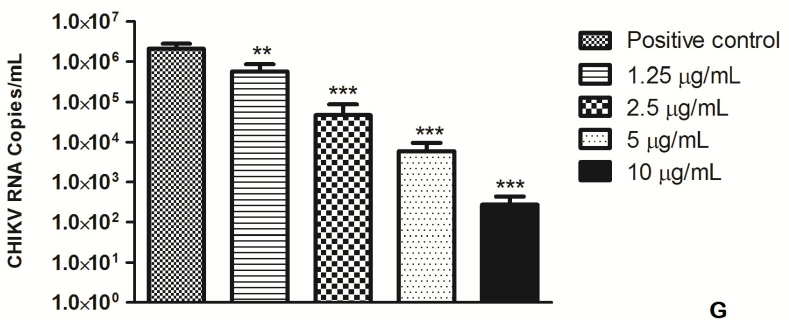


**FIGURE 4 |** Effect of *O. obtusiloba* extract on CHIKV replication in chick retina neurons in 4-day-old purified cultures. **(A)** Uninfected culture with normal morphology. **(B)** CHIKV-infected culture presenting cytopathic effect (arrow). **(C)** CHIKV-infected culture incubated with 1.25 μg/mL of *O. obtusiloba* presenting cytopathic effect (arrow). **(D)** CHIKV-infected culture incubated with 2.5 μg/mL of *O. obtusiloba* with normal morphology. **(E)** CHIKV-infected culture incubated with 5 μg/mL of *O. obtusiloba* with normal morphology. **(F)** CHIKV-infected culture incubated with 10 μg/mL of *O. obtusiloba* with normal morphology. Chick retina neurons were infected with CHIKV ($10^6$ PFU/mL) at MOI of 0.1. **(G)** Graphical representation showing the effect of *O. obtusiloba* extract at concentrations of 1.25, 2.5, 5, and 10 μg/mL on CHIKV genomic RNA by quantitative PCR. The results showed that all treatments with the extract showed a significant reduction of RNA copies. Error bars indicate the standard deviation and experiments were performed in triplicate. $^{**}p < 0.01$; $^{***}p < 0.001$ in Tukey test.

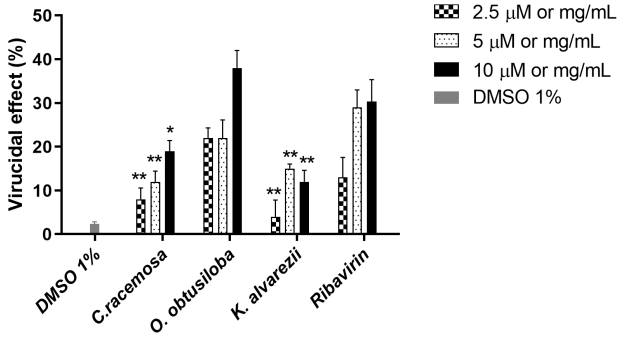


**FIGURE 5 |** Effect of C. racemosa, O. obtusiloba and K. alvarezii crude extracts on infectivity of CHIKV. To assess potential virucidal activity, we incubated stock CHIKV [CHIKV (106 PFU/mL) at MOI of 0.1] directly with each compound separately at different concentrations for 1 h or with vehicle/DMEM, after which we determined virus titers by standard plaque assays in Vero cells. Experiments were performed independently in triplicate with duplicate plate assays. Error bars indicate the standard deviation and experiments were performed in triplicate. $*p < 0.05$; $**p < 0.01$ in Dunnett test vs. control (Ribavirin). DMSO used as solvent remained at the final concentration of 0.01%, showing no virucidal activity on CHIKV.

Ribavirin used as a control at the same concentration, only inhibited 29% of the production of viral plaques. DMSO used as solvent remained at the final concentration of 0.01%, showing no virucidal activity on CHIKV.

## Time of Drug Addition

In order to investigate the mechanism of action of the tested compounds, a time of addition assay was performed using extracts of *C. racemosa* or *O. obtusiloba*, which showed more promising results. For this, VERO cells were treated with *C. racemosa* or *O. obtusiloba* using the antiviral drug Ribavirin, as a control. **Figure 6** shows that when *C. racemosa* or *O. obtusiloba* extracts were added prior to infection of the cells, they produced a pretreatment effect inhibiting about 40% of viral replication. However, when added at time 0, we observed an effect greater than 60% for *C. racemosa* and above 90% for *O. obtusiloba* and Ribavirin. Although Ribavirin was more effective in inhibiting the virus than seaweed extracts between −3 and −1 h, its effect decreased steadily within 2 h after infection, greatly reducing its effects on post infection. In contrast, the effect of *O. obtusiloba* persisted for at least 16 h after infection, slowly reducing to 60% at 20 and 24 h and was significantly greater ($p < 0.01$) than the Ribavirin controls.

# DISCUSSION

There are no effective antivirals or vaccines against CHIKV, and as a result this infection has had a significant public health impact, particularly in Brazil and the Americas between 2014 and 2015 (Tan et al., 2018), affecting large numbers of people (Ching et al., 2015; Ahmadi et al., 2016). Numerous studies have been undertaken to discover effective drugs to control this infection, and as a result certain drugs with inhibitory potential for the replication of CHIKV replication, such as Ribavirin, Favipiravir and chloroquine, were developed (Delang et al., 2014; Lani et al., 2015; Ahmadi et al., 2016; Varghese et al., 2016). In the present study, *O. obtusiloba* showed promising results in inhibiting the replication of CHIKV compared to Ribavirin, which has been described as a potential choice for the treatment of CHIKV infection and was used as a control for our studies (Rothan et al., 2015).

The experiments evaluated blood samples of patients suspected of CHIKV infection in the second half of 2016 and who did not travel during this period. This allowed the identification of patients who had been infected by the CHIKV that was circulating in Rio de Janeiro. Samples were collected from 25 patients from Rio de Janeiro who had characteristic chikungunya symptoms and, after extensive attempts, successfully isolated the CHIKV from three patients. RT-PCR and sequencing confirmed that these CHIKV were the same as those in circulation in Brazil and that were initially identified in Bahia to later migrate to Rio de Janeiro (Nunes et al., 2015). This CHIKV were used for *in vitro* studies to test the inhibition of viral replication using seaweed extracts.

Marine organisms, including algae, have undergone many demographic studies as well as analyses of their antimicrobial, antifungal, antiviral, anti-inflammatory activities, and are sources of new therapeutic agents. More recently, the promising antiviral potential of algal derivatives has been targeted in pharmaceutical research, especially for HIV infections (Cirne-Santos et al., 2008; Ahmadi et al., 2015; Pérez et al., 2016).

In the present study, the algal extracts studied had low cytotoxicity in VERO cells with $CC_{50}$ at concentrations higher than 170 μg/mL. The extracts of the algae, *C. racemosa* and *O. obtusiloba,* clearly showed particularly promising results with $CC_{50}$ of 732 and 525 μg/mL, respectively. In relation to the inhibitory effect on CHIKV replication, the $EC_{50}$ of *O. obtusiloba* extract was 1.25 μg/mL, considerably lower than the result obtained with the *C. racemosa* extract, which was 4.2 μg/mL. Comparing the SI levels of both (*C. racemosa* of 174.2 and *O. obtusiloba* of 420) also confirms their potential as possible candidates for further investigation in the discovery of novel anti-CHIKV drugs. Taking into account the inhibitory effects of Ribavirin, which has been inserted in several studies as a control and given results similar to those presented by the extracts, we can see a strong potential for further studies of the mechanism of action as well as the determination of the respective active compounds present in algae.

Some evidence of compounds derived from algae has been well described in the literature, showing significant effects on various viruses such as *Caulerpa racemosa* extract, where alkaloids and terpenoids are found, and in the acetonic extract the main component is caulerpine, which has antiviral activity against HSV-1 (Macedo et al., 2012; Pinto et al., 2012). Antiviral activity against HSV-1 and HSV-2 has also been described for glycolipids extracted from *O. obtusiloba* with $EC_{50}$ values of 42 μg/mL and 12 μg/mL, respectively (de Souza et al., 2012). *O. obtusiloba* ethanolic extract also showed potent antiviral activity against ZIKV ($EC_{50}$ = 1.82) (Cirne-Santos Claudio et al., 2018). De Alencar et al. (2016) showed that the 70%

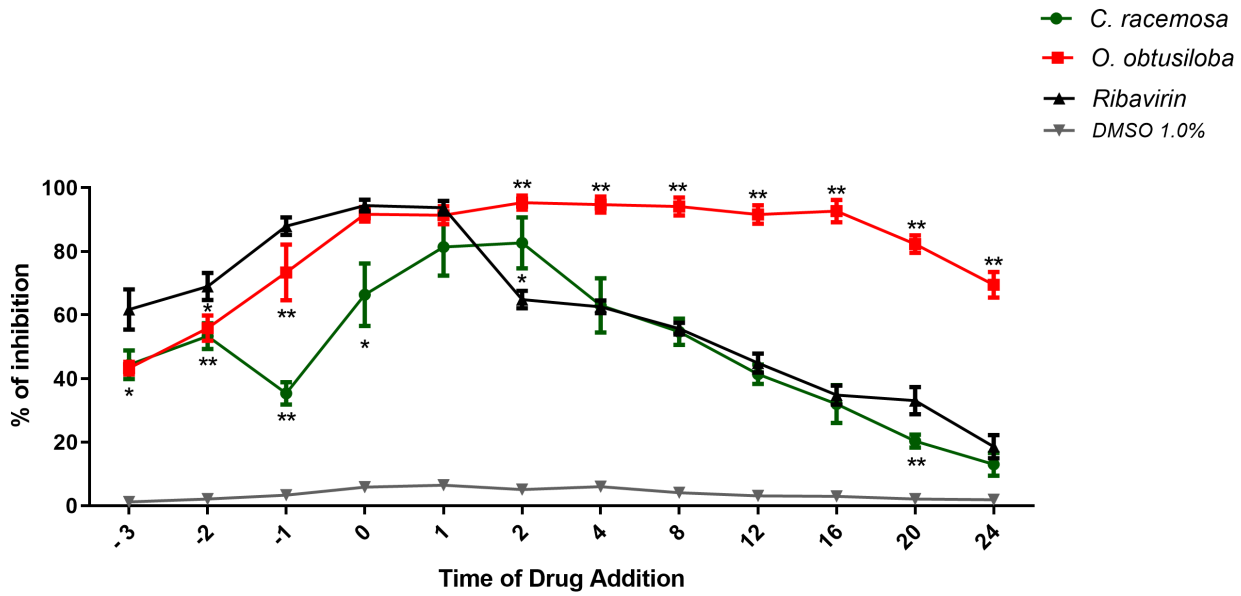


**FIGURE 6 |** Time of drug addiction studies with *C. racemosa*, *O. obtusiloba*, and *K. alvarezii* crude extracts on CHIKV replication. Vero cells were infected with CHIKV ($10^6$ PFU/mL) on MOI of 0.1 following each treatment (before the infection, –3, –2, and –1 h; during the infection, 0h; and after the infection, +1, +2, +4, +8, +12, +16, +20, and +24 h), the results were evaluated by plaque assay. Experiments were performed in triplicate. Ribavirin (5 μM) was used as a positive control. $^*p < 0.05$; $^{**}p < 0.01$ in Dunnett test vs. control (Ribavirin). DMSO used as solvent remained at the final concentration of 0.01% showing no activity on CHIKV replication.

EtOH was the most effective solvent for extracting phenolic compounds from red seaweeds when compared to hexane, and *O. obtusiloba* EtOH extract presented high antioxidant activity. Seven substances were identified in Brazilian *O. obtusiloba*: three sulfated bromophenols, two bromophenols, one sterol and one glyceride (Carvalho et al., 2006). Given that *O. obtusiloba* ethanolic extract is rich in bromophenols, it is possible that these compounds may be responsible for the inhibitory effects of CHIKV replication.

The extract-tested compounds also had low virucidal potentials (**Figure 5**), with only *O. obtusiloba* resulting in about 40% virucidal activity at 10 μg/mL, although it was superior to the effect of the same concentration of Ribavirin that was used as a control. The study of compounds with this activity is highly relevant because virucidal compounds are chemicals that attack and inactivate viral particles outside the cell (virions), although it is possible that damage to the viral structure occurs (Galabov, 2007).

Several studies have also demonstrated the ability of CHIKV to infect neurons and glial cells with associated neurological complications, suggesting the neurotropic nature of the virus (Chandak et al., 2009; Das et al., 2010; Dhanwani et al., 2012). The results demonstrated that the CHIKV cytopathic effects on infected neurons can be reduced by treatment with *O. obtusiloba* (**Figure 4**). Increasing concentrations of *O. obtusiloba* have higher antiviral activity so that treatment with this compound should be more widely studied, as this may contribute to the reduction of morbidity and mortality of the clinical conditions such as encephalopathies and bone and joint disorders related to CHIKV. Thus, the observation of the reduction in viral RNA production demonstrated by O. obtusiloba tells us the important role of this compound in inhibiting CHIKV replication not only in summer cells but also in primary neurons (**Figure 4**).

Finally, the virus replication inhibition assays by varying the time of extract addition (**Figure 6**) showed that the addition of *O. obtusiloba* at time zero, at the same time as the virus, inhibited viral replication at a rate greater than 80%. This effect was maintained even if the extracts were added up to 16 h after CHIKV infection. There was a small decline in the inhibitory effect after this time, but the extract still inhibited CHIKV replication above 60% if the compound was added within 24 h post-infection. This demonstrates a protective effect even after prolonged contact of the VERO cells with the virus. Pretreatment with these same algal compounds exhibits inhibition of viral replication (approximately 40%), emphasizing the possibility of a virucidal and somewhat protective effect. Importantly, as observed in the time of drug addiction assays, the *O. obtusiloba* extract inhibited viral replication for a longer time than the Ribavirin used as control and also maintains its inhibitory effect for long periods post-infection. This may be vital in many clinical settings where the diagnosis takes some time.

Considering the promising results of the *O. obtusiloba* extract and the previous work of our group demonstrating the low toxicity of this extract administered orally in BALB/c mice (Barros et al., 2018), the extract of this alga becomes a good candidate for further studies. In addition, the possibility of oral treatment with the extract, or the active ingredient isolated from the extract, can also be tested, as was done with

dolabelladienetriol (20 mg/Kg/dose; twice a day) against HSV-1 in BALB/c (Garrido et al., 2017).

## DATA AVAILABILITY STATEMENT

The raw data supporting the conclusion of this manuscript will be made available by the authors, without undue reservation, to any qualified researcher.

## ETHICS STATEMENT

This project was submitted to the research ethics committee of ASSOCIACAO SALGADO DE OLIVEIRA DE EDUCACAO E CULTURA and obtained the registration approval – CAAE: 61845416.0.0000.5289.

## AUTHOR CONTRIBUTIONS

CC-S, CB, KY, GM, and CN performed the experiments and wrote the manuscript. RA, ZV, and JS-C worked on the implementation of methodologies and data review. VT worked on the supply of natural product. NR worked on the revision of English and in writing. DF and IP worked as job coordinators.

## FUNDING

The authors are grateful to CNPq (Conselho Nacional de Desenvolvimento Científico e Tecnológico) for financial support and for Productivity Fellowships to IP and VT (443930/2014-7 and 304070/2014-9). IP and VT (E-26/201.442/2014) also thank the FAPERJ (Fundação de Amparo à Pesquisa do Estado do Rio de Janeiro) for the Cientista do Nosso Estado Fellowship. CC-S thanks CAPES (Coordenação de Aperfeiçoamento de Pessoal de Nível Superior) for the Postdoc fellowship and CB thanks FAPERJ for the Postdoc fellowship (E-26/201.344/2016). Support also came from the postgraduate program in sciences and biotechnology of UFF (PPBI-UFF).

## ACKNOWLEDGMENTS

The authors would like to acknowledge for the technical support of Thereza Elizabeth P. P. Garcia.

## REFERENCES

Abdelnabi, R., Neyts, J., and Delang, L. (2015). Towards antivirals against chikungunya virus. *Antiviral Res.* 121, 59–68. doi: 10.1016/j.antiviral.2015.06.017

Adler, R., Lindsey, J. D., and Elsner, C. L. (1984). Expression of cone-like properties by chick embryo neural retina cells in glial-free monolayer cultures. *J. Cell Biol.* 99, 1173–1178. doi: 10.1083/jcb.99.3.1173

Ahmadi, A., Hassandarvish, P., Lani, R., Yadollahi, P., Jokar, A., Bakar, S. A., et al. (2016). Inhibition of chikungunya virus replication by hesperetin and naringenin. *RSC Adv.* 6, 69421–69430. doi: 10.1039/c6ra16640g

Ahmadi, A., Zorofchian Moghadamtousi, S., Abubakar, S., and Zandi, K. (2015). Antiviral potential of algae polysaccharides isolated from marine sources: a review. *BioMed Res. Int.* 2015:825203. doi: 10.1155/2015/825203

Anccasi, R. M., Ornelas, I. M., Cossenza, M., Persechini, P. M., and Ventura, A. L. M. (2013). ATP induces the death of developing avian retinal neurons in culture via activation of P2X7 and glutamate receptors. *Purinergic Signal.* 9, 15–29. doi: 10.1007/s11302-012-9324-5

Arpino, C., Curatolo, P., and Rezza, G. (2009). Chikungunya and the nervous system: what we do and do not know. *Rev. Med. Virol.* 19, 121–129. doi: 10.1002/rmv.606

Barros, C. D. S., Gomes, M. W. L., Gomes, R. D. S. P., Melchiades, V., Nogueira, C. C. R., Cirne-Santos, C. C., et al. (2018). Acute toxicity evaluation of ethanol extract of red algae, Osmundaria obtusiloba, in BALB/c mice. *J. Med. Plants Res.* 12, 217–221. doi: 10.5897/jmpr2018.6582

Bourjot, M., Delang, L., Nguyen, V. H., Neyts, J., GuéRitte, F. O., Leyssen, P., et al. (2012). Prostratin and 12-O-tetradecanoylphorbol 13-acetate are potent and selective inhibitors of chikungunya virus replication. *J. Nat. Prod.* 75, 2183–2187. doi: 10.1021/np300637t

Brasil. (2018). *Boletim epidemiológico*. Brazil: Ministério da Saúde.

Burt, F. J., Rolph, M. S., Rulli, N. E., Mahalingam, S., and Heise, M. T. (2012). Chikungunya: a re-emerging virus. *Lancet* 379, 662–671. doi: 10.1016/s0140-6736(11)60281-x

Carvalho, L. R. D., Guimarães, S. M., and Roque, N. F. (2006). Sulfated bromophenols from Osmundaria obtusiloba (C. Agardh) RE Norris (*Rhodophyta*, *Ceramiales*). *Braz. J. Bot.* 29, 453–459.

Chandak, N. H., Kashyap, R. S., Kabra, D., Karandikar, P., Saha, S. S., Morey, S. H., et al. (2009). Neurological complications of Chikungunya virus infection. *Neurol. India* 57, 177–180. doi: 10.4103/0028-3886.51289

Ching, K.-C., Kam, Y.-W., Merits, A., Ng, L. F., and Chai, C. L. (2015). Trisubstituted thieno [3, 2-b] pyrrole 5-carboxamides as potent inhibitors of alphaviruses. *J. Med. Chem.* 58, 9196–9213. doi: 10.1021/acs.jmedchem.5b01047

Cirne-Santos, C. C., Souza, T. M. L., Teixeira, V. L., Fontes, C. F. L., Rebello, M. A., Castello-Branco, L. R. R., et al. (2008). The dolabellane diterpene dolabelladienetriol is a typical noncompetitive inhibitor of HIV-1 reverse transcriptase enzyme. *Antiviral Res.* 77, 64–71. doi: 10.1016/j.antiviral.2007.08.006

Cirne-Santos Claudio, C., Souza Barros Caroline, D., Richter Nogueira Caio, C., Santos Correa Amorim Leonardo, D., Mendonca Campos Renata, D., Ratcliffe Norman, A., et al. (2018). Antiviral effect of the seaweed osmundaria obtusiloba against the Zika virus. *J. Med. Plants Res* 12, 387–395. doi: 10.5897/JMPR2018.6624

Das, T., Jaffar-Bandjee, M. C., Hoarau, J. J., Trotot, P. K., Denizot, M., Lee-Pat-Yuen, G., et al. (2010). Chikungunya fever: CNS infection and pathologies of a re-emerging arbovirus. *Prog. Neurobiol.* 91, 121–129. doi: 10.1016/j.pneurobio.2009.12.006

Dash, P., Parida, M., Santhosh, S., Verma, S., Tripathi, N., Ambuj, S., et al. (2007). East Central South African genotype as the causative agent in reemergence of Chikungunya outbreak in India. *Vector Borne Zoonotic Dis.* 7, 519–528. doi: 10.1089/vbz.2007.7272

De Alencar, D. B., De Carvalho, F. C. T., Rebouças, R. H., Dos Santos, D. R., Dos Santos Pires-Cavalcante, K. M., De Lima, R. L., et al. (2016). Bioactive extracts of red seaweeds pterocladiella capillacea and osmundaria obtusiloba (*Floridophyceae*: *Rhodophyta*) with antioxidant and bacterial agglutination potential. *Asian Pac. J. Trop. Med.* 9, 372–379. doi: 10.1016/j.apjtm.2016.03.015

de Souza, L. M., Sassaki, G. L., Romanos, M. T. V., and Barreto-Bergter, E. (2012). Structural characterization and anti-HSV-1 and HSV-2 activity of glycolipids from the marine algae osmundaria obtusiloba isolated from Southeastern Brazilian coast. *Mar. Drugs* 10, 918–931. doi: 10.3390/md10040918

de Souza Barros, C., Garrido, V., Melchiades, V., Gomes, R., Gomes, M. W. L., Teixeira, V. L., et al. (2016). Therapeutic efficacy in BALB/C mice of extract from marine alga Canistrocarpus cervicornis (*Phaeophyceae*) against herpes simplex virus type 1. *J. Appl. Phycol.* 29, 769–773. doi: 10.1007/s10811-016-0865-9

Delang, L., Segura Guerrero, N., Tas, A., Quérat, G., Pastorino, B., Froeyen, M., et al. (2014). Mutations in the chikungunya virus non-structural proteins cause

resistance to favipiravir (T-705), a broad-spectrum antiviral. *J. Antimicrob. Chemother.* 69, 2770–2784. doi: 10.1093/jac/dku209

Dhanwani, R., Khan, M., Bhaskar, A., Singh, R., Patro, I., Rao, P., et al. (2012). Characterization of Chikungunya virus infection in human neuroblastoma SH-SY5Y cells: role of apoptosis in neuronal cell death. *Virus Res.* 163, 563–572. doi: 10.1016/j.virusres.2011.12.009

Ferreira, J. M., and Paes-de-Carvalho, R. (2001). Long-term activation of adenosine A2a receptors blocks glutamate excitotoxicity in cultures of avian retinal neurons. *Brain Res.* 900, 169–176. doi: 10.1016/s0006-8993(01)02279-x

Galabov, A. S. (2007). Virucidal agents in the eve of manorapid synergy®. *GMS Krankenhaushyg. Interdiszip.* 2, 1–8.

Garrido, V., Barros, C., Melchiades, V. A., Fonseca, R. R., Pinheiro, S., Ocampo, P., et al. (2017). Subchronic toxicity and anti-HSV-1 activity in experimental animal of dolabelladienetriol from the seaweed, dictyota pfaffii. *Regul. Toxicol. Pharmacol.* 86, 193–198. doi: 10.1016/j.yrtph.2017.03.007

Grischott, F., Puhan, M., Hatz, C., and Schlagenhauf, P. (2016). Non-vector-borne transmission of Zika virus: a systematic review. *Travel Med. Infect. Dis.* 14, 313–330. doi: 10.1016/j.tmaid.2016.07.002

Lani, R., Hassandarvish, P., Chiam, C. W., Moghaddam, E., Chu, J. J. H., Rausalu, K., et al. (2015). Antiviral activity of silymarin against chikungunya virus. *Sci. Rep.* 5, 11421. doi: 10.1038/srep11421

Leparc-Goffart, I., Nougairede, A., Cassadou, S., Prat, C., and De Lamballerie, X. (2014). Chikungunya in the Americas. *Lancet* 383:514.

Lira, M.-L. F., Lopes, R., Gomes, A. P., Barcellos, G., Verícimo, M., Osako, K., et al. (2016). Anti-leishmanial activity of Brazilian green, brown, and red algae. *J. Appl. Phycol.* 28, 591–598. doi: 10.1007/s10811-015-0538-0

Lu, Y. E., and Kielian, M. (2000). Semliki forest virus budding: assay, mechanisms, and cholesterol requirement. *J. Virol.* 74, 7708–7719. doi: 10.1128/jvi.74.17.7708-7719.2000

Macedo, N. R. P. V., Ribeiro, M. S., Villaça, R. C., Ferreira, W., Pinto, A. M., Teixeira, V. L., et al. (2012). Caulerpin as a potential antiviral drug against herpes simplex virus type 1. *Rev. Bras. Farmacogn.* 22, 861–867. doi: 10.1590/s0102-695x2012005000072

Mejía-García, T., and Paes-de-Carvalho, R. (2007). Nitric oxide regulates cell survival in purified cultures of avian retinal neurons: involvement of multiple transduction pathways. *J. Neurochem.* 100, 382–394. doi: 10.1111/j.1471-4159.2006.04244.x

Mejía-García, T. A., Portugal, C. C., Encarnação, T. G., Prado, M. A. M., and Paes-De-Carvalho, R. (2013). Nitric oxide regulates AKT phosphorylation and nuclear translocation in cultured retinal cells. *Cell. Signal* 25, 2424–2439. doi: 10.1016/j.cellsig.2013.08.001

Montagnier, L. (2010). 25 years after HIV discovery: prospects for cure and vaccine. *Virology* 397, 248–226.

Mosmann, T. (1983). Rapid colorimetric assay for cellular growth and survival: application to proliferation and cytotoxicity assays. *J. Immunol. Methods* 65, 55–63. doi: 10.1016/0022-1759(83)90303-4

Nunes, M. R. T., Faria, N. R., De Vasconcelos, J. M., Golding, N., Kraemer, M. U., De Oliveira, L. F., et al. (2015). Emergence and potential for spread of Chikungunya virus in Brazil. *BMC Med.* 13:102. doi: 10.1186/s12916-015-0348-x

Paes-de-Carvalho, R., Maia, G., and Ferreira, J. (2003). Adenosine regulates the survival of avian retinal neurons and photoreceptors in culture. *Neurochem. Res.* 28, 1583–1590.

Pérez, M. J., Falqué, E., and Domínguez, H. (2016). Antimicrobial action of compounds from marine seaweed. *Mar. Drugs* 14:E52.

Pinto, A. M. V., Leite, J. P. G., Ferreira, W. J., Cavalcanti, D. N., Villaça, R. C., Giongo, V., et al. (2012). Marine natural seaweed products as potential antiviral drugs against bovine viral diarrhea virus. *Rev. Bras. Farmacogn.* 22, 813–817. doi: 10.1590/s0102-695x2012005000060

Powers, A. M. (2015). Risks to the Americas associated with the continued expansion of chikungunya virus. *J. Gen. Virol.* 96, 1–5. doi: 10.1099/vir.0.070136-0

Presti, A. L., Lai, A., Cella, E., Zehender, G., and Ciccozzi, M. (2014). Chikungunya virus, epidemiology, clinics and phylogenesis: a review. *Asian Pac. J. Trop. Med.* 7, 925–932. doi: 10.1016/S1995-7645(14)60164-4

Purpura, L. J., Choi, M. J., and Rollin, P. E. (2016). Zika virus in semen: lessons from Ebola. *Lancet Infect. Dis.* 16, 1107–1108. doi: 10.1016/s1473-3099(16)30330-9

Rocha, F. D., Soares, A. R., Houghton, P. J., Pereira, R. C., Kaplan, M. A. C., and Teixeira, V. L. (2007). Potential cytotoxic activity of some Brazilian seaweeds on human melanoma cells. *Phytother. Res.* 21, 170–175. doi: 10.1002/ptr.2038

Rothan, H. A., Bahrani, H., Mohamed, Z., Teoh, T. C., Shankar, E. M., Rahman, N. A., et al. (2015). A combination of doxycycline and ribavirin alleviated chikungunya infection. *PLoS One* 10:e0126360. doi: 10.1371/journal.pone.0126360

Rudolph, K. E., Lessler, J., Moloney, R. M., Kmush, B., and Cummings, D. A. (2014). Incubation periods of mosquito-borne viral infections: a systematic review. *Am. J. Trop. Med. Hyg.* 90, 882–891. doi: 10.4269/ajtmh.13-0403

Santos, A. O. D., Veiga-Santos, P., Ueda-Nakamura, T., Sudatti, D. B., Bianco, ÉM., Pereira, R. C., et al. (2010). Effect of elatol, isolated from red seaweed Laurencia dendroidea, on Leishmania amazonensis. *Mar. Drugs* 8, 2733–2743. doi: 10.3390/md8112733

Schilte, C., Staikovsky, F., Couderc, T., Madec, Y., Carpentier, F., Kassab, S., et al. (2013). Chikungunya virus-associated long-term arthralgia: a 36-month prospective longitudinal study. *PLoS Neg.l Trop. Dis.* 7:e2137. doi: 10.1371/journal.pntd.0002137

Sokoloski, K. J., Snyder, A. J., Liu, N. H., Hayes, C. A., Mukhopadhyay, S., and Hardy, R. W. (2013). Encapsidation of host-derived factors correlates with enhanced infectivity of Sindbis virus. *J. Virol.* 87, 12216–12226. doi: 10.1128/JVI.02437-13

Strauss, J. H., and Strauss, E. G. (1994). The alphaviruses: gene expression, replication, and evolution. *Microbiol. Rev.* 58, 491–562.

Tan, Y., Pickett, B. E., Shrivastava, S., Gresh, L., Balmaseda, A., Amedeo, P., et al. (2018). Differing epidemiological dynamics of Chikungunya virus in the Americas during the 2014-2015 epidemic. *PLoS Negl. Trop. Dis.* 12:e0006670. doi: 10.1371/journal.pntd.0006670

Varghese, F. S., Kaukinen, P., Gläsker, S., Bespalov, M., Hanski, L., Wennerberg, K., et al. (2016). Discovery of berberine, abamectin and ivermectin as antivirals against chikungunya and other alphaviruses. *Antiviral Res.* 126, 117–124. doi: 10.1016/j.antiviral.2015.12.012

Weaver, S. C., and Forrester, N. L. (2015). Chikungunya: evolutionary history and recent epidemic spread. *Antiviral Res.* 120, 32–39. doi: 10.1016/j.antiviral.2015.04.016

**Conflict of Interest:** The authors declare that the research was conducted in the absence of any commercial or financial relationships that could be construed as a potential conflict of interest.

*Copyright © 2019 Cirne-Santos, Barros, Nogueira, Azevedo, Yamamoto, Meira, Vasconcelos, Ratcliffe, Teixeira, Schmidt-Chanasit, Ferreira and Paixão. This is an open-access article distributed under the terms of the Creative Commons Attribution License (CC BY). The use, distribution or reproduction in other forums is permitted, provided the original author(s) and the copyright owner(s) are credited and that the original publication in this journal is cited, in accordance with accepted academic practice. No use, distribution or reproduction is permitted which does not comply with these terms.*

frontiers in Microbiology

ORIGINAL RESEARCH
published: 30 October 2019
doi: 10.3389/fmicb.2019.02482

# Interleukin-37 Ameliorates Influenza Pneumonia by Attenuating Macrophage Cytokine Production in a MAPK-Dependent Manner

*Feifei Qi[1,2†], Mingya Liu[1,2†], Fengdi Li[1,2], Qi Lv[1,2], Guanpeng Wang[1,2], Shuran Gong[1,2], Shunyi Wang[1,2], Yanfeng Xu[1], Linlin Bao[1,2*] and Chuan Qin[1,2*]*

[1]NHC Key Laboratory of Human Disease Comparative Medicine, The Institute of Laboratory Animal Sciences, Peking Union Medical College Hospital (CAMS), Beijing, China, [2]Beijing Key Laboratory for Animal Models of Emerging and Reemerging Infectious, The Institute of Laboratory Animal Sciences, Peking Union Medical College Hospital (CAMS), Beijing, China

Viral pneumonitis caused by influenza A (H1N1) virus leads to high levels of morbidity and mortality. Given the limited treatment options for severe influenza pneumonia, it is necessary to explore effective amelioration approaches. Interleukin-37 (IL-37) has been reported to inhibit excessive immune responses and protect against a variety of inflammatory diseases. In this study, by using BALB/c mice intranasally infected with A/California/07/2009 (H1N1), we found that IL-37 treatment increases the survival rate and body weight, and reduces the pulmonary index, impaired the lung injury and decreased production of pro-inflammatory cytokines in the BALF and lung tissue. Moreover, IL-37 administration enhanced not only the percentage of macrophages, but also the percentage of IL-18Rα$^+$ macrophages, suggesting that enhancing the macrophages function may improve outcomes in a murine model of H1N1 infection. Indeed, macrophages depletion reduced the protective effect of IL-37 during H1N1 infection. Furthermore, IL-37 administration inhibited MAPK signaling in RAW264.7 cells infected with H1N1. This study demonstrates that IL-37 treatment can ameliorate influenza pneumonia by attenuating cytokine production, especially by macrophages. Thus, IL-37 might serve as a promising new target for the treatment of influenza A-induced pneumonia.

**Keywords: A/California/07/2009 (H1N1), Interleukin-37, viral pneumonia, macrophages, inflammation**

OPEN ACCESS

***Edited by:***
*Lu Lu,*
*Fudan University, China*

***Reviewed by:***
*Ji Wang,*
*Sun Yat-sen University, China*
*Jianqing Xu,*
*Fudan University, China*

****Correspondence:***
*Linlin Bao*
*baoll@cnilas.org*
*Chuan Qin*
*qinchuan@pumc.edu.cn*

*†These authors have contributed equally to this work*

***Specialty section:***
*This article was submitted to Virology, a section of the journal Frontiers in Microbiology*

***Received:*** *18 September 2019*
***Accepted:*** *15 October 2019*
***Published:*** *30 October 2019*

***Citation:***
*Qi F, Liu M, Li F, Lv Q, Wang G, Gong S, Wang S, Xu Y, Bao L and Qin C (2019) Interleukin-37 Ameliorates Influenza Pneumonia by Attenuating Macrophage Cytokine Production in a MAPK-Dependent Manner. Front. Microbiol. 10:2482. doi: 10.3389/fmicb.2019.02482*

## INTRODUCTION

Influenza H1N1 infection induced "flu"-like illness or pneumonia depends on the infecting strain, host immune system, and environmental factors (Rice et al., 2012; Daoud et al., 2019). H1N1 pneumonia may progress rapidly, resulting in severe respiratory distress syndrome or refractory hypoxemia, is associated with a longer hospital stay with higher mortality compared to bacterial pneumonia (Perez-Padilla et al., 2009; Rello et al., 2009; Hermann et al., 2017). Thus, H1N1 infection is considered a more life-threatening disease (Ramsey and Kumar, 2013; Liu et al., 2016).

Increasing evidence has demonstrated that it is an excessively activated immune response, not a direct viral infection that leads to the increasing influenza pneumonia severity (Morita et al., 2013; Uematsu et al., 2015). Although various prevention and treatment methods have been used for viral diseases, the limited treatment options for severe influenza pneumonia prioritize the need for the discovery of effective therapies.

Interleukin-37 (IL-37), a novel member of the IL-1 family, inhibits systemic and local inflammation by reducing the levels of pro-inflammatory mediators (Nold et al., 2010; Boraschi et al., 2011; Al-Anazi et al., 2019). IL-37 binds to the IL-18Rα chain, and then recruits TIR-8/IL-1R8/SIGIRR to execute its anti-inflammatory effects (Kumar et al., 2002; Boraschi and Tagliabue, 2013; Dinarello and Bufler, 2013; Lunding et al., 2015; Nold-Petry et al., 2015). IL-37 has been shown to increase the survival rate and body weight, and downregulated the production of IL-6 and IL-17A in a coxsackievirus B3-induced model of murine viral myocarditis (An et al., 2017). In addition, comparing with wild-type (WT) mice, a low dose of mouse-adapted H1N1-induced morbidity and the decreases in body weight are significantly attenuated in IL-37tg mice, which express human IL-37 isoform b precursor transgene (Davis et al., 2017). Moreover, IL-37 significantly attenuates pulmonary eosinophilia, CCL11 production and airway hyper-reactivity in a murine asthma model (Lv et al., 2018). Increasing evidence suggests that IL-37 can inhibit excessive immune responses and protect against a variety of inflammatory diseases, autoimmune diseases, and tumors. However, little is known about the function of IL-37 in the influenza-infected murine model, particularly the regulatory role in viral pneumonia induced by A/California/07/2009 (H1N1) infection. Thus, in the present study, we focused on IL-37 treatment in H1N1-infected mice, to investigate the therapeutic effect and the mechanisms by which IL-37 treatment ameliorates influenza pneumonia.

# MATERIALS AND METHODS

## Animals and Viruses

Specific pathogen-free, 4- to 6-week-old female BALB/c mice were obtained from Vital River Laboratories (Beijing, China). The seasonal influenza A virus strain A/California/07/2009 (H1N1) was provided by the Institute of Laboratory Animal Science, Peking Union Medical College, China. All experiments were performed in biosafety level 2 facilities in compliance with governmental and institutional guidelines. The experimental protocol was evaluated and approved by the Institute of Animal Use and Care Committee of the Institute of Laboratory Animal Science, Peking Union Medical College (BLL19004).

## Therapeutic Treatments

Oseltamivir phosphate capsules were purchased from Roche Pharmaceutical Co., Ltd. (Shanghai, China). The pGEM-T-IL-37b plasmid was kindly supplied by Dr. RF. Wei., Institute of Laboratory Animal Science, Peking Union Medical College, China. Individual mice were anesthetized with tribromoethanol and inoculated intranasally with 50 μl ($10^{4.3}$ $TCID_{50}$) of allantoic fluid containing influenza A/California/07/2009 (H1N1) virus. Subsequently, the mice were chronically intragastrically administered oseltamivir phosphate (30 mg/kg) for 5 days, and the animals were inoculated with IL-37 (12.5 μg/kg) *via* intravenous or intranasal administration at three separate time points (2, 24, and 48 h post infection). Seven mice were selected randomly from each group for monitoring the disease signs, weight loss, and mortality daily up to 14 days post inoculation (d.p.i.). The remaining mice in each group were euthanized at 6 d.p.i. and blood samples, bronchoalveolar lavage fluid (BALF), and lung tissues were collected for the assessment of lung histology, pro-inflammatory cytokines, and immune cell counts.

## Preparation of Single Cell Suspensions From the Lung

Mice were anesthetized and the lung was flushed *in situ* with 20 ml of phosphate-buffered saline (PBS) *via* cannulation of the heart to remove the intravascular blood pool. Minced lung tissues were incubated at 37°C for 1 h on a rocker with 200 μg/ml collagenase D and 40 μg/ml DNase I (Roche Molecular Biochemicals) in 10 ml of DMEM supplemented with 10% FBS. Single cell suspensions from the digested lung were filtered through a 75-μm strainer and then collected through density-gradient centrifugation with lymphocyte separation solution. The immune cells were washed twice with Hank's solution and suspended in Hank's solution.

## Flow Cytometry Analysis

Cells were pre-incubated with Zombie Aqua™ Fixable Viability Kit (Biolegend) and purified rat anti-mouse CD16/CD32 (Mouse BD Fc Block™, 2.4G2, BD Pharmingen™) ice for 15 min at room temperature. For the extracellular cell marker analysis, the cells were incubated with the following fluorescein-conjugated antibodies for 30 min: BV421-anti-CD11b (M1/70, Biolegend), FITC-anti-CD45 (30-F11, Biolegend), BV605-anti-F4/80 (BM8, Biolegend), PE-anti-IL-18Rα (Miltenyi Biotec), AF647-anti-SIGIRR (Santa Cruz), BV421-anti-CD3ε (145-2C11, Biolegend), PE-Cy7-anti-CD4 (RM4-5, BD Biosciences), and PerCP-Cy5.5-anti-CD8a (53-6.7, BD Biosciences). Finally, samples were acquired using a fluorescence-activated cell sorting (FACS) Aria II system (BD Biosciences). The data were analyzed using a Kaluza analysis and FlowJo 10.1 software.

## Preparation of Lung Homogenate Supernatant

Lung homogenates were prepared by homogenizing perfused whole lung tissue using an electric homogenizer for 2 min 30 s in 1 ml of PBS. The homogenates were centrifuged at 3,000 rpm for 10 min at 4°C. The supernatant was collected and stored at −80°C.

## Analysis of Bronchoalveolar Lavage Fluid

Bronchoalveolar lavage fluid (BALF) was collected by washing the lungs of sacrificed mice twice with 1 ml PBS. The PBS was then recovered after 1 min and centrifuged at 1,500 rpm for 10 min at 4°C. The supernatant was collected and stored at −80°C. Total cellular infiltration in the BALF was assessed using a hemocytometer; cytosine slides were fixed and stained with Wright-Giemsa stain, and the composition was assessed in a blinded manner by counting 200 or more cells using a light microscope.

## Clodronate Treatment

To deplete macrophages, ready-made clodronate liposomes and control liposomes (FormuMax; CA, USA) were intranasally

administered to mice using the manufacturer's recommending dose 1 day before and 1 day after A/California/07/2009 (H1N1) infection. Mice were monitored for signs of disease, weight loss, and mortality upto 14 d.p.i.

## Quantification of Cytokines

The concentrations of granulocyte colony-stimulating factor (G-CSF), granulocyte-macrophage colony-stimulating factor (GM-CSF), interferon-γ (IFN-γ), monokine induced by IFN-γ (MIG), interleukin (IL)-1α, IL-1β, IL-4, IL-5, IL-6, IL-10, IL-12/IL-23p40, IL-13, IL-17A, RANTES, monocyte chemoattractant protein 1 (MCP-1), macrophage inflammatory protein 1α (MIP-1α), MIP-1β, and tumor necrosis factor (TNF) in the serum and BALF samples were determined by flow cytometry (FACS Aria II, BD, USA) using the Cytometric Beads Array (CBA) Kits, according to the manufacturers' instructions (BD, USA). Briefly, 50 μl of each testing sample were labeled in duplicate with equal volumes of diluted FlexSet capture beads at room temperature for 1 h and treated with PE-conjugated detection reagent. After washing, the captured cytokines and chemokines were analyzed by flow cytometry.

## Hematoxylin and Eosin Staining

For each mouse, the whole right lung was fixed in 10% formalin for 24 h and then embedded in paraffin for histological examination. The lung tissue sections (4 μm) were deparaffinized and hydrated using xylene and an alcohol gradient and then, stained with Hematoxylin and Eosin (H&E). The histopathology of the lung tissue was observed by light microscopy.

## Quantitative Real-Time Polymerase Chain Reaction Analysis

Total RNA was isolated from individual samples using an RNeasy Mini kit, according to the manufacturer's instructions (Qiagen, Hilden, Germany). The RNA was reversely transcribed into cDNA using random primers and a SuperScript II reverse transcriptase reaction mixture (Invitrogen). The target gene mRNA transcripts were determined by RT-PCR using SYBR Green PCR Master Mix, specific primers, and a 7500 PCR system (ABI, USA). Primer sets for individual genes are shown in **Table 1**.

**TABLE 1** | Primer sequences used for RT-PCR analysis.

| Gene | Forward (5′-3′) | Reverse (5′-3′) |
|---|---|---|
| β-actin | CAACGAGCGGTTCCGATG | GCCACAGGATTCCATACCCA |
| IL-6 | TCTATACCACTTCACAAGTCGGA | GAATTGCCATTGCACAACTCTTT |
| IL1α | TCTCAGATTCACAACTGTTCGTG | AGAAAATGAGGTCGGTCTCACTA |
| IL-1β | CAACCAACAAGTGATATTCTCCATG | GATCCACACTCTCCAGCTGCA |
| RANTES | GCTGCTTTGCCTACCTCTCC | TCGAGTGACAAACACGACTGC |
| IP10 | CCAAGTGCTGCCGTCATTTTC | GGCTCGCAGGGATGATTTCAA |
| MCP1 | AGTAGGCTGGAGAGCTACAA | GTATGTCTGGACCCATTCCTTC |
| MIP1α | TTCTCTGTACCATGACACTCTGC | CGTGGAATCTTCCGGCTGTAG |
| MIP1β | TTCCTGCTGTTTCTCTTACACCT | CTGTCTGCCTCTTTTGGTCAG |
| MIG | TCCTTTTGGGCATCATCTTCC | TTTGTAGTGGATCGTGCCTCG |
| IFN-γ | TATCTGGAGGAACTGGCAAA | GGTGTGATTCAATGACGCTT |
| IL18Rα | TCACCGATCACAAATTCATGTGG | TGGTGGCTGTTTCATTCCTGT |

*The results are normalized to β-actin expression and presented as the fold change in mRNA expression (fold change = $2^{-\triangle\triangle CT}$).*

## Cells

Murine macrophage cell lines (RAW264.7) were maintained in Dulbecco's modified Eagle's medium (Gibco, Life Technologies, New York) supplemented with 10% FBS, 100 IU/ml penicillin, and 100 μg/ml streptomycin and were incubated at 37°C with 5% $CO_2$. RAW264.7 cells in six-well plates were infected with H1N1 at a multiplicity of infection (MOI) of 0.01 for 1 h absorption at 37°C. Then, the cells were washed and cultured with 2 ml of serum-free DMEM containing TPCK-treated trypsin (0.5 mg/ml) antibiotics and 70 μM oseltamivir phosphate with or without IL-37b for 72 h. The cells were collected at 0, 12, and 24 h post infection to detect the expression of cytokines such as IL-6, MCP-1, TNF-α, IL-1β, and IL-1α. The protein levels of MAPKs and NLRP3 were detected by western blot assay at 0, 30, and 60 min after infection.

## Western Blot Assay

The expression of GAPDH, p38, phospho-p38 (p-p38), ERK, phospho-ERK (p-ERK), NF-κB, JNK, phospho-JNK (p-JNK), and NLRP3 (Cell Signaling, Boston, MA, USA) was assessed by western blotting. Protein bands were detected with a chemiluminescent imaging system (Amersham, Freiburg, Germany). The expression of a target protein was normalized to that of GAPDH.

## Statistical Analysis

The data are presented as the mean ± SEM. Analysis of variance (ANOVA) was used to analyze the differences between three or more groups, and *t* tests were used to analyze the differences between two groups. Statistical graphs were obtained using GraphPad Prism 5 software. Differences were considered statistically significant at values of $p < 0.05$.

# RESULTS

## Interleukin-37 Treatment Reduces the Body Weight Recovery Time and Improves the Survival Rate in H1N1-Infected Mice

To explore the efficacy of the recombinant IL-37 protein, BALB/c mice challenged intranasally with 50 μl H1N1 were treated with oseltamivir phosphate for 5 days with/without recombinant IL-37 for 7 days at 2 h.p.i. As shown in **Figure 1A**, the body weights of mice treated for 7 days (oseltamivir+IL-37 7d) were not obviously different from those of mice in the oseltamivir phosphate group. Nevertheless, in this study, we extended the IL-37 administration time to 9 days (oseltamivir+IL-37 9d), and the death and body weight changes in the mice ($n = 7$) were monitored for 14 d.p.i. The results showed that the body weights of mice began to increase from 7 d.p.i., which was 2 days earlier than the body weights of mice in the oseltamivir phosphate group began to increase (**Figure 1A**). A total of 71% of the mice from the oseltamivir+IL-37 9d group survived, whereas the survival rate in the oseltamivir phosphate group was 57% survival. All of the mice in the model group died (**Figure 1B**), suggesting that IL-37 treatment for 9 days advanced the onset of body weight recovery and improves the survival rate in H1N1-infected mice.

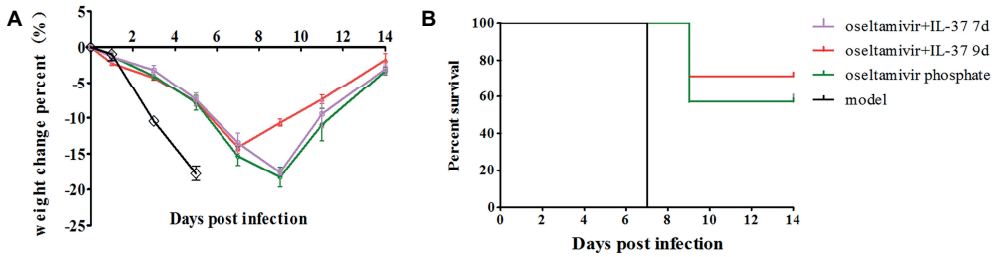


**FIGURE 1 |** IL-37 treatment reduces the time to body weight recovery onset and decreases mortality in mice during influenza infection. Mice were infected intranasally with $10^{4.6}$ $TCID_{50}$ of influenza A (H1N1) virus; body weight **(A)** and mortality rates **(B)** were recorded at two different time points of intravenous IL-37 administration. Data are presented as the average values from three independent experiments ± SD (*n* = 7 per group).

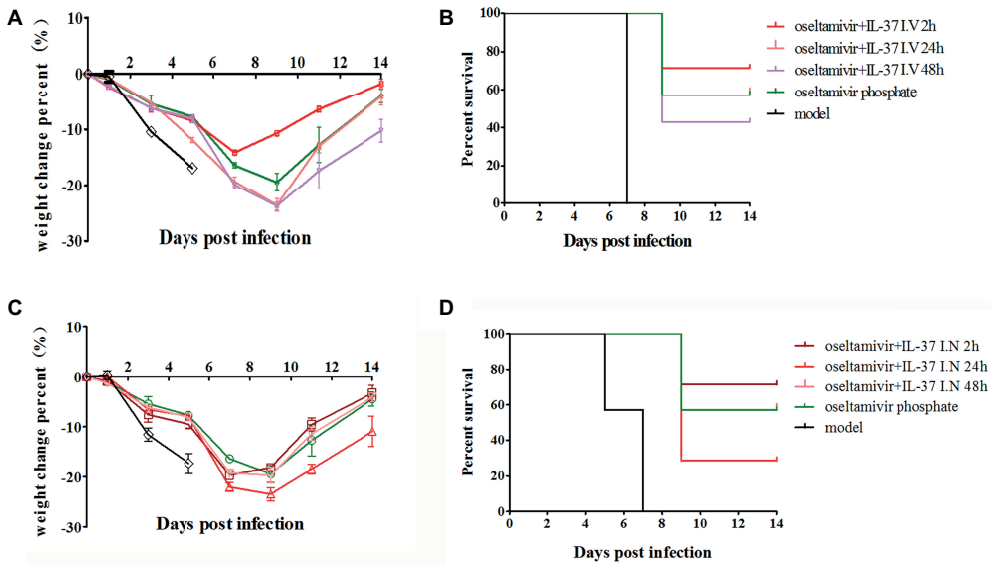


**FIGURE 2 |** IL-37 intravenous administration offers enhanced protection against influenza challenge in mice. BALB/c mice (*n* = 7 in each group) treated with or without IL-37 were divided into eight groups: the H1N1-infected group (model) and oseltamivir phosphate, intravenous oseltamivir phosphate combined with IL-37 at three separate time points (oseltamivir+IL-37 I. V 2 h, oseltamivir+IL-37 I. V 24 h, oseltamivir+IL-37 I. V 48 h) or intranasal oseltamivir phosphate combined with IL-37 at three separate time points (oseltamivir+IL-37 I. N 2 h, oseltamivir+IL-37 I. N 24 h, oseltamivir+IL-37 I. N 48 h) treatment groups. The body weights **(A,C)** and mortality rates **(B,D)** of mice treated *via* intravenous or intranasal routes were monitored. Data are presented as the average values from two independent experiments ± SD (*n* = 7 per group).

## Intravenous Interleukin-37 Administration in Mice Enhances the Protection Against Influenza Challenge

To further explore the best time point and route of administration for IL-37, after infection, the BALB/c mice were divided into eight groups: H1N1 infection (model), oseltamivir phosphate, oseltamivir phosphate combined with intravenous IL-37 administration at three separate time points (oseltamivir+IL-37 I. V 2 h, oseltamivir+IL-37 I. V 24 h, and oseltamivir+IL-37 I. V 48 h) or oseltamivir phosphate combined with intranasal IL-37 administration at three separate time points (oseltamivir+IL-37 I. N 2 h, oseltamivir+IL-37 I. N 24 h, and oseltamivir+IL-37 I. N 48 h). A model group was also administered PBS. Seven mice were selected randomly from each group, and mortality rates and body weight changes in the mice were monitored for 14 d.p.i. Treatment with IL-37 protein in combination with oseltamivir phosphate reduced the time to the onset of body weight recovery, and this reduction varied based on the different administration times. As shown in **Figure 2A**, the body weights of mice infected with H1N1 decreased and began to increase from the 7th day of IL-37 plus oseltamivir phosphate treatment at 2 h.p.i. (oseltamivir+IL-37 I.V 2 h), whereas the body weights of mice in the oseltamivir phosphate group began to increase on the 9th day; in the model group, the body weight continued to decrease until death. Moreover, animals that received PBS succumbed to infection 5–7 days after viral challenge. When therapeutic treatment was started at 24 h.p.i, 57% of the infected mice survived, which was the same rate as the mice treated with oseltamivir phosphate only. The administration of IL-37 at 2 h.p.i. increased the mouse survival rate to 71%. However, in the group administered IL-37 at 48 h.p.i, the mortality rate increased (**Figure 2B**).

Similar to the results shown in **Figure 2**, the survival rate of mice intranasally administered IL-37 at 2 h.p.i., was significantly enhanced compared to that of mice in the oseltamivir phosphate group (**Figure 2D**). However, the body weight in the intranasal IL-37 treatment group was not significantly increased compared with that in the oseltamivir phosphate group; however, the body weight decrease time was shortened and remained stable at 7–9 d.p.i (**Figure 2C**). These results demonstrate that intravenous IL-37 administration at 2 h.p.i significantly decreases the mortality of mice infected with H1N1 and shortens the recovery time of infected mice, so intravenous IL-37 administration at 2 h.p.i offers enhanced protection against influenza challenge in mice.

## Interleukin-37 Treatment Reduces Lung Damage in Mice Infected With H1N1 Virus

In addition, to further validate the therapeutic effect of IL-37, lung tissue was collected to monitor the pulmonary indexes and lung histology. As expected, the IL-37 combined with oseltamivir phosphate administration group had significantly lower pulmonary index values than the other groups (**Figure 3A**). The BAL fluid was gathered 6 days after infection or IL-37 treatment. The total cell number in the BALF was increased significantly after infection (**Figure 3B**). However, IL-37 treatment evidently diminished H1N1-induced neutrophilic and eosinophilic airway inflammation (**Figure 3C**). Additionally, H&E staining of the lung tissue samples showed that the lungs in the model group exhibited many merged, inflated, or enlarged alveoli as well as an increase in the exudation of inflammatory proteins in the alveolar spaces at 6 d.p.i., which was largely decreased in the IL-37-treated group (**Figure 3D**). These results further indicate that IL-37 could be a useful therapeutic agent in mice with H1N1 infection.

## Interleukin-37 Inhibits the Production of Inflammatory Cytokines in H1N1-Infected Mice

IL-37, as a potent inhibitor of innate immunity, can shift the cytokine equilibrium away from excessive inflammation (Teng et al., 2014). Thus, to more accurately assess the efficacy

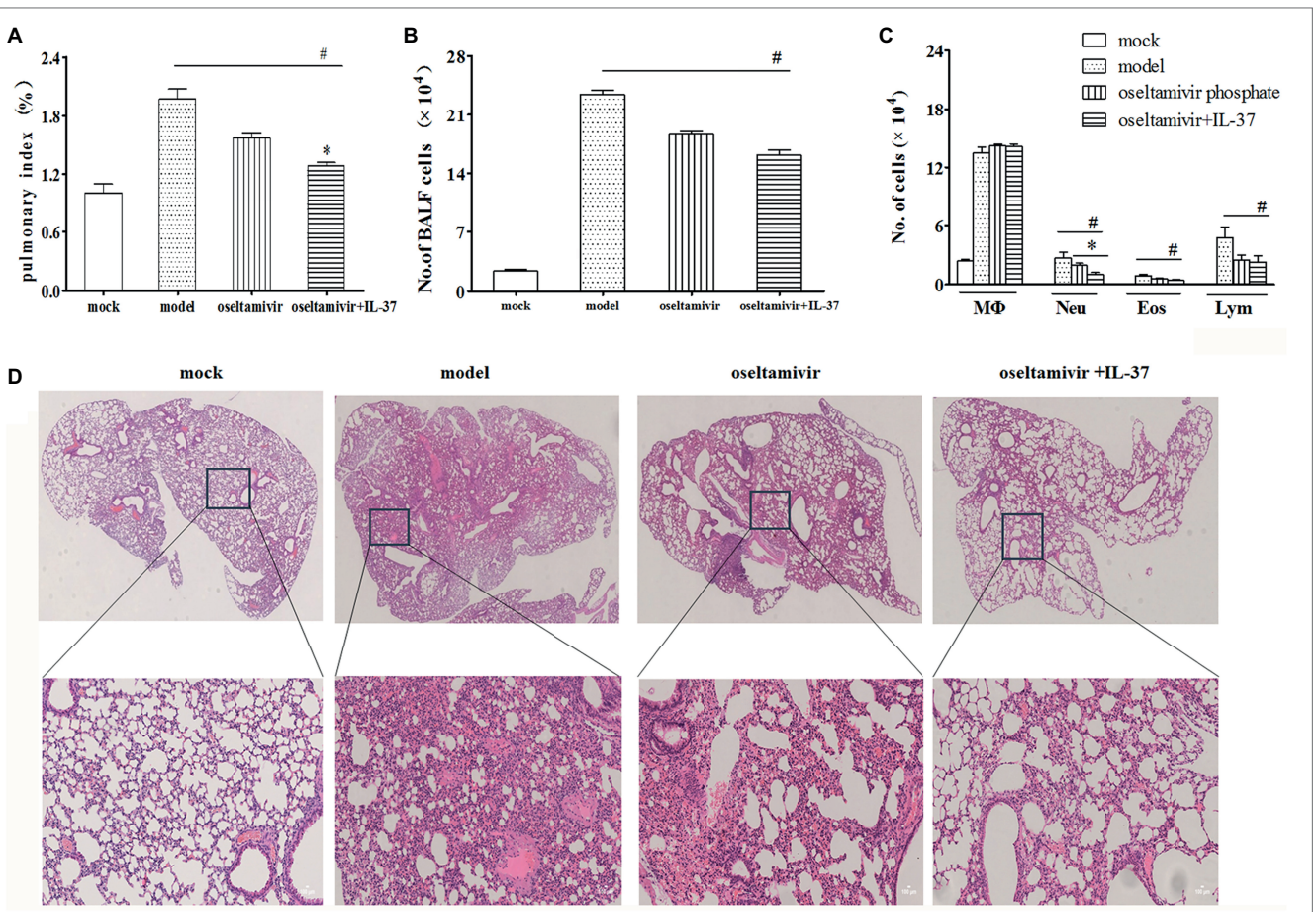


**FIGURE 3 |** IL-37 treatment attenuates H1N1-induced lung tissue damage *in vivo*. Lungs were obtained from different groups of mice, and the pulmonary index on day 6 post infection was monitored **(A)**. The BALF was harvested on day 6 d.p.i, the number of total BALF cells **(B)** and the proportions of different leukocyte subtypes in the BALF **(C)** were calculated. **(D)** Mouse lung tissues were stained with H&E. Data are representative of three independent experiments with three mice per group (100× magnification). Data are representative of three independent experiments with three mice for each group. *Significant difference ($p < 0.05$), compared with oseltamivir-inoculated mice. #Significant difference ($p < 0.05$), compared with H1N1-infected mice.

of IL-37 during H1N1 infection, the mRNA expression and the protein production levels of IL-6, TNF-α, MCP-1, IL-1α, IL-1β, MIP-1α, MIP-1β, IP-10, MIG, RANTES, IFN-γ and IL-10 were detected by RT-PCR and CBA in the lung tissue, BALF and serum samples on day 6 after H1N1 infection. As expected, IL-37 treatment inhibited the increase in levels of MCP-1, IL-1β, MIP-1α, MIP-1β, MIG, IFN-γ and RANTES in the lungs of the model group (**Figure 4A**). Paralleling the decreased production of cytokines, the upregulation of MCP-1, IL-1β, IL-6, IP-10, MIG, and RANTES mRNA expression was markedly reduced in the IL-37 treatment group (**Figure 4D**). In addition, it is worth mentioning that the expression of MCP-1 and IL-1β, especially the level of MCP-1 in the oseltamivir group, was higher than that in the model group; however, oseltamivir plus IL-37 treatment corrected the increase in MCP-1 expression (**Figure 4D**). Moreover, the mRNA expression of the anti-inflammatory cytokine IL-10 was downregulated in the IL-37-treated group (**Figure 4D**); however, the production of IL-10 protein in the lungs was not significantly changed (data not shown).

Furthermore, compared with that in the model and oseltamivir groups, the upregulated production of MCP-1, IL-6 and IFN-γ in the BALF (**Figure 4B**) and serum (**Figure 4C**) was markedly reduced in the IL-37 treatment group. These results indicate that IL-37 exerts a protective effect by regulating the levels of inflammatory cytokines, particularly by regulating macrophage cytokine production.

## Macrophage Percentages Are Increased in Interleukin-37 Treated Mice

To evaluate the roles of immune cells in the IL-37-mediated protection against influenza A (H1N1) infection, the changes in the numbers of macrophages and T cells in the lungs of different groups at multiple time points were analyzed using flow cytometry. In fact, the percentages of $CD4^+$ and $CD8^+$, $IL\text{-}18R\alpha^+CD4^+$ or $CD8^+$ T cells in the IL-37 treatment group were not obviously different compared with those in the model group (**Supplementary Figure S1**). However, an increase in the percentage of macrophages, which were identified as $CD45^+F4/80^+CD11b^+$ cells, was observed in the lungs of mice in the IL-37 administration group, peaking at day 6 post infection (**Figure 5A**). Paralleling the augmented macrophage percentage, the percentage of $IL\text{-}18R\alpha^+$ macrophages was markedly enhanced in the lungs of IL-37-treated mice (**Figure 5B**). These results show that IL-37 administration impairs the decrease in the macrophage population in the lungs, indicating that macrophages may exert immunoprotective effects in mice treated with IL-37 during H1N1 infection.

## Depleting Macrophages Reduces the Protective Effect of Interleukin-37 During Influenza Virus Infection

As macrophages may exert immunoprotective effects in H1N1-infected mice treated with IL-37, we intranasally administered clodronate liposomes, which have been shown to deplete macrophages in the lungs (Tate et al., 2010; Wong and Smith, 2017), to mice during influenza virus infection to test the dependency of the IL-37 treatment-induced reduction in mortality on macrophages. As expected, under the same conditions, the clodronate liposome administration group reached its lowest weight at 9 d.p.i. and the body weight change did not recover in the control liposome group (**Figure 6A**). Moreover, clodronate liposome treatment significantly increased the mortality rate (**Figure 6B**). These data further demonstrate that macrophages are critical for the protective effect of IL-37 during influenza virus infection.

## Interleukin-37 Inhibits the Expression of Inflammatory Cytokines in a MAPK-Dependent Manner *in vitro*

To clearly demonstrate the anti-inflammatory efficacy of IL-37, following H1N1 infection, murine macrophage RAW264.7 cells were treated with IL-37 for different times (12 and 24 h). The levels of inflammatory factors in the cells were determined by real-time PCR. As shown in **Figure 7A**, IL-6 mRNA expression at all time points was obviously downregulated in the IL-37 treatment groups compared with the oseltamivir group. Similar inhibitory effects were also observed on TNF-α, IL-1β and MIP-1β expression (**Figure 7A**).

To further explore the underlying mechanisms of IL-37, we examined the expression of PRR-related protein phosphorylation. For this purpose, western blot analyses were performed using the cell lysates of RAW264.7 cells treated with or without IL-37 to analyze the phosphorylation of MAPKs and GAPDH. In addition, NLRP3 protein production was detected. As shown in **Figure 7B**, compared with that in the infection and oseltamivir groups, the phosphorylation of ERK1/2 and p38 MAPK was significantly reduced in the IL-37 treated RAW264.7 cell group. Similarly, the ratio of NLRP3 in the IL-37-treated group was significantly decreased *in vitro*. These results show that IL-37 treatment inhibits the production of macrophage inflammatory cytokines induced by H1N1 infection in a MAPK-dependent manner.

# DISCUSSION

Influenza viruses cause seasonal epidemics and sporadic pandemics, and are a major burden on human health. The rapid development of viral pneumonitis induced by aggressive inflammation resulting in high morbidity and mortality, emphasizing the importance of exploring effective approaches to ameliorate the viral pneumonia during H1N1 infection (Morita et al., 2013). IL-37 has been shown to block the deleterious effects of pro-inflammatory stimuli or conditions in numerous models (Barbier et al., 2019; Theoharides et al., 2019), it is essential for the inhibition of innate immunity and inflammation and plays a role in the inhibition of cytokine and chemokine production, and inflammatory cell infiltration (Theoharides et al., 2019). Increasing evidence suggests that the anti-inflammatory cytokine IL-37, improve functional outcomes in combination, including neuroprotection and reduced of lung infection burden (Zhang et al., 2019).

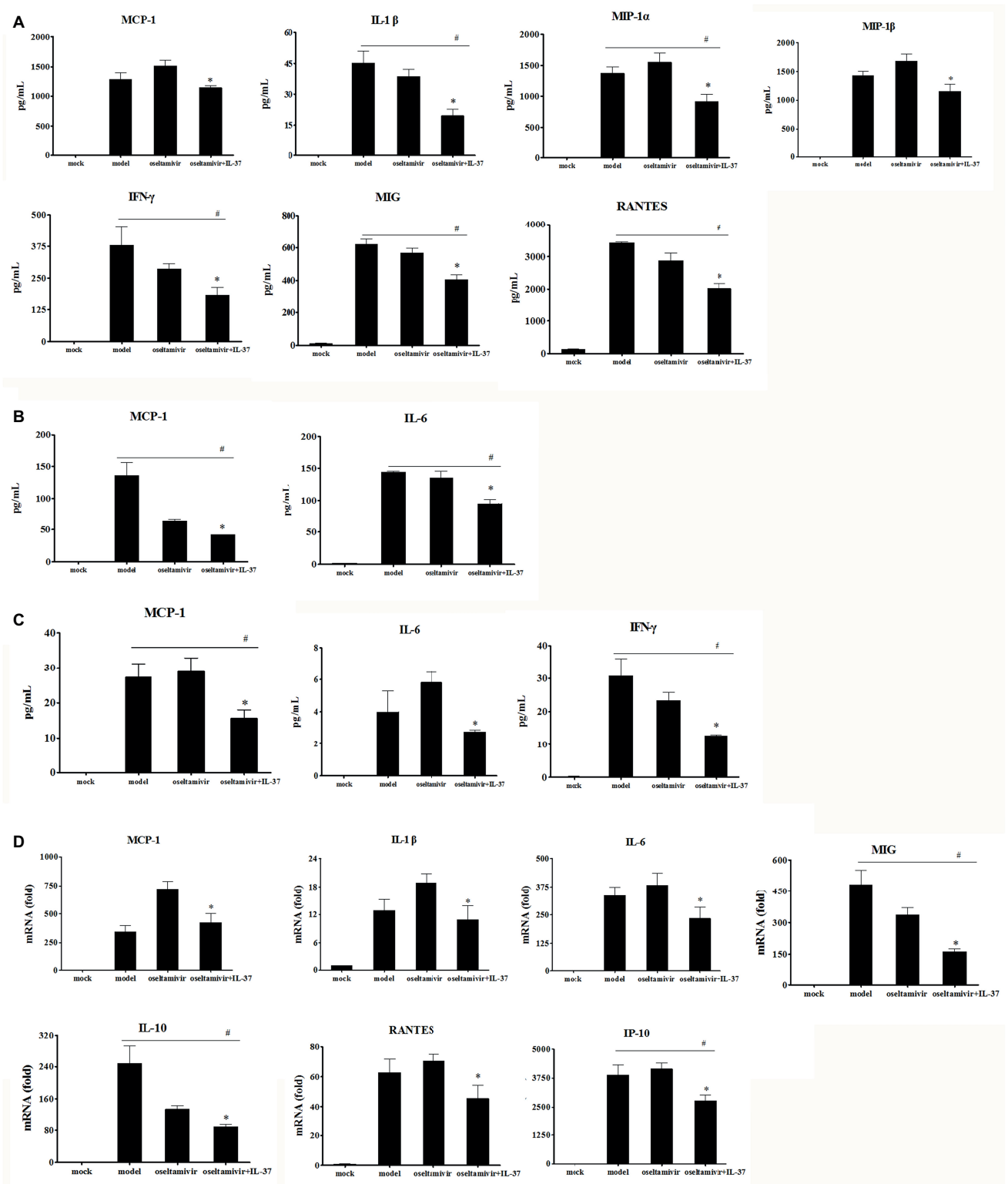


**FIGURE 4 |** IL-37 treatment modulates immune responses to H1N1 infection. BALF, serum and lung homogenates were harvested 6 d.p.i. following IL-37 treatment. The levels of G-CSF, GM-CSF, IFN-γ, MIG, IL-1α, IL-1β, IL-4, IL-5, IL-6, IL-10, IL-12p70, IL-13, IL-17A, RANTES, MCP-1, MIP-1α, MIP-1β, and TNF, in lung homogenates **(A)**, BAL fluid **(B)** as well as serum samples **(C)** were measured quantitatively using a Cytometric Beads Array. There were no significant differences in the concentrations of other cytokines and chemokines tested (data not shown). **(D)** The relative mRNA expression of cytokines in lung tissues were detected by real-time RT-PCR. Data are representative of three independent experiments with three mice for each group. *Significant difference ($p < 0.05$), compared with oseltamivir-inoculated mice. # Significant difference ($p < 0.05$), compared with H1N1-infected mice.

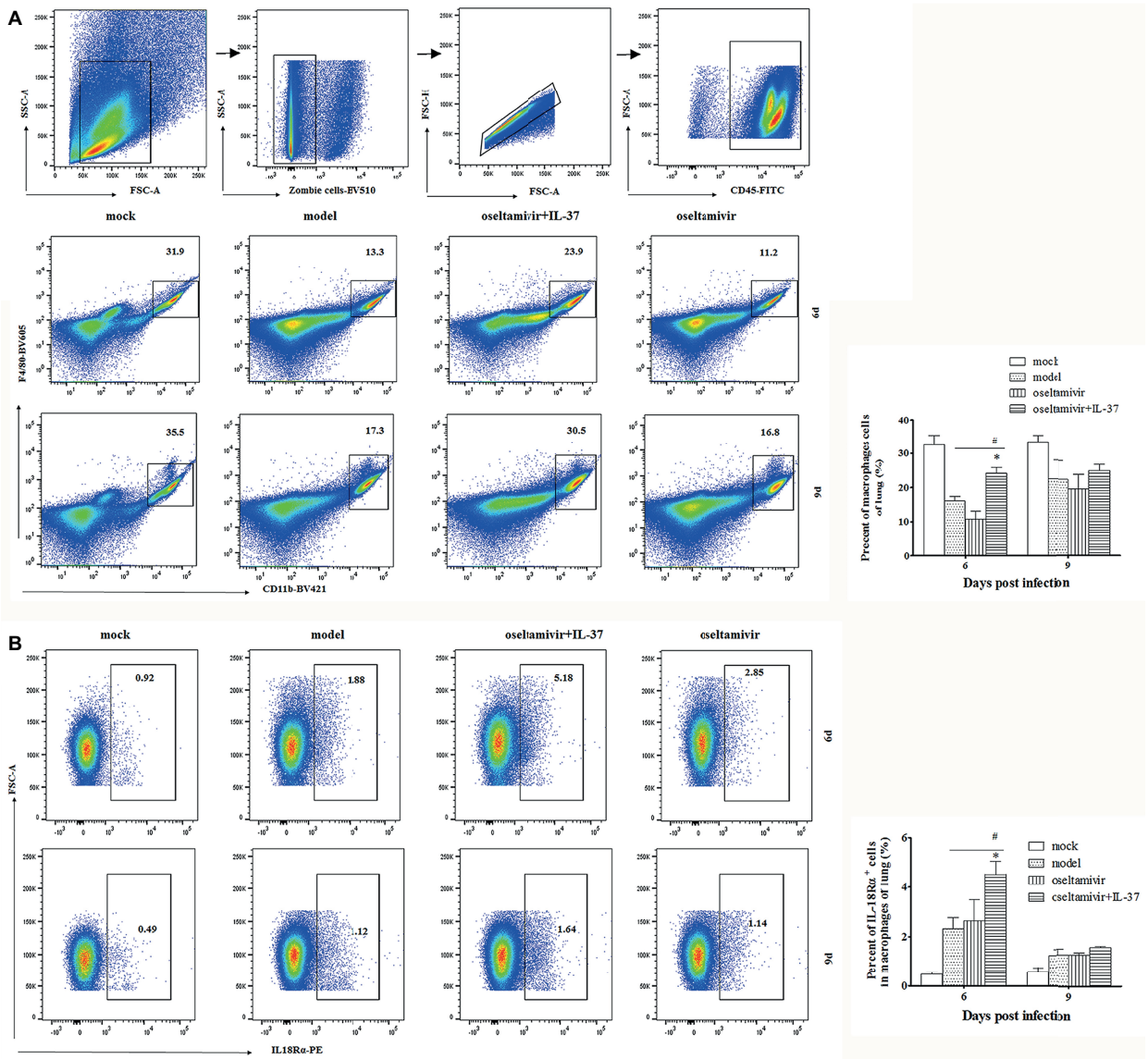


**FIGURE 5 |** The macrophage percentages are increased in IL-37-treated mice. The percentage of $CD45^+F4/80^+CD11b^+$ macrophages **(A)** and IL-18Rα$^+$ macrophages **(B)** in the lungs of mice was determined by flow cytometry at the indicated time points. Data are representative of three independent experiments with three mice for each group. *Significant difference ($p < 0.05$), compared with oseltamivir-treated mice. #Significant difference ($p < 0.05$), compared with H1N1-infected mice.

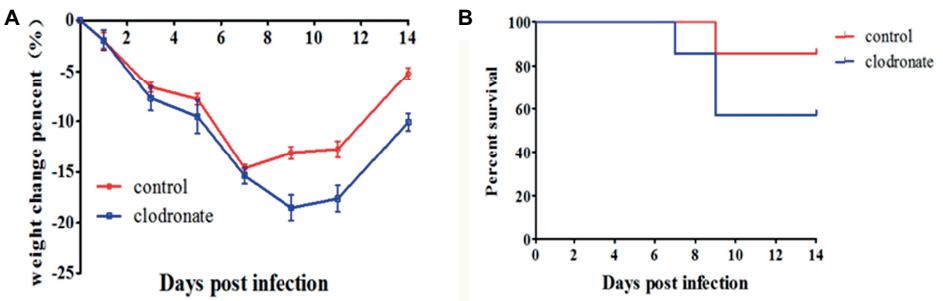


**FIGURE 6 |** Macrophage depletion reduces the protective effect of IL-37 during influenza virus infection. Body weights **(A)** and survival rates of **(B)** mice treated with clodronate liposomes or control liposomes during IL-37 administration. Data are presented as the average values from two independent experiments ± SD ($n = 7$ per group).

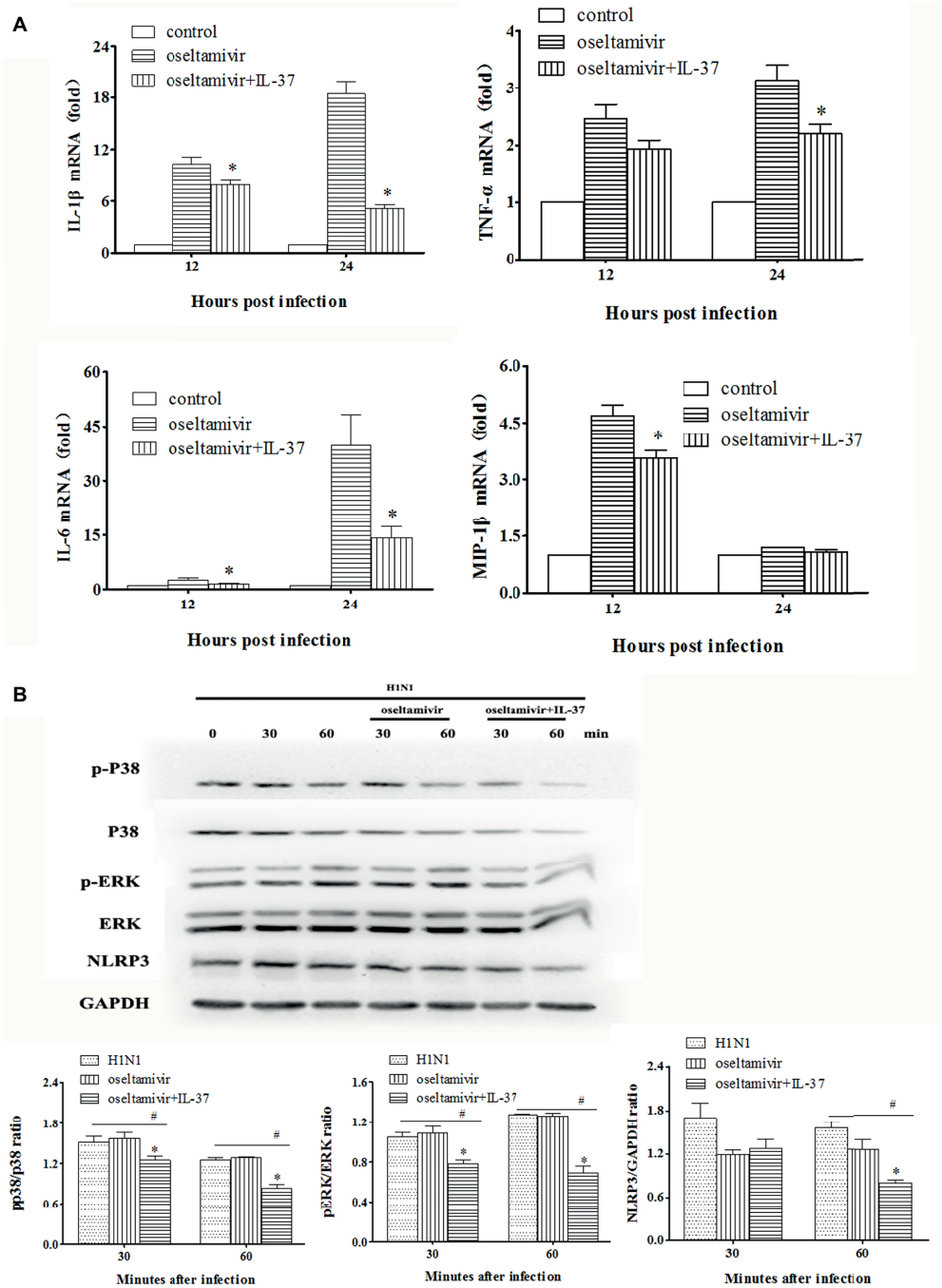


**FIGURE 7 |** IL-37 inhibited the expression of inflammatory cytokines in MAPK-dependent pathway *in vitro*. **(A)** Effects of IL-37 on the mRNA expression of MCP-1, IL-6, MIP-1α, MIP-1β, TNF-α, etc. in RAW264.7 cells on 12, and 24 h after infection. **(B)** Representative photographs of western blot in protein expressions of the phosphorylated and non-phosphorylated forms of ERK1/2, P38 MAPK, NLRP3 and GAPDH in RAW264.7 cells with or without IL-37 treatment during H1N1 infection. The data are representative of three independent experiments. *Significant difference ($p < 0.05$), compared with oseltamivir-inoculated mice. #Significant difference ($p < 0.05$), compared with H1N1-infected cells.

In the present study, by using H1N1-infected BALB/c mice, we found that intravenous IL-37 treatment advanced the time to body weight recovery onset, improved the survival rate (**Figures 1, 2**), and ameliorated the increase in the exudation of inflammatory proteins in the alveoli (**Figure 3**). These results demonstrate that IL-37 treatment can ameliorate viral pneumonia and afford a better protection from A/California/07/2009 (H1N1) infection in the murine model. Furthermore, IL-37 treatment significantly reduced the production of the inflammatory cytokines and chemokines MCP-1, IL-1β, MIP-1, IFN-γ, MIG and RANTES,

meanwhile the increased mRNA expression of MCP-1, IL-1β, IP-10, IL-10, MIG and RANTES in the lungs of the IL-37-treatment group was obviously decreased compared with that in the oseltamivir group (**Figure 4**). Interestingly, most of the cytokines obviously decreased at both the transcriptional and translational levels were macrophage cytokines.

Indeed, IL-37 administration impaired the decrease in the percentage of macrophages in the lungs of H1N1-infected mice (**Figure 5**), and depleting macrophages reduced the protective effect of IL-37 during influenza virus infection (**Figure 6**). The anti-inflammatory endogenous ligand annexin A1 has been shown to attenuate pathology upon subsequent influenza A virus infection, and reduction in lung damage severity is associated with an increase in the number of alveolar macrophages (AMs) in the murine model of influenza A virus infection (Schloer et al., 2019). Numerous literatures have demonstrated that macrophage are critical for host defense in mice during influenza viral infection (He et al., 2017; Wong and Smith, 2017). Our results are consistent with the results of these reports, showing that macrophages may exert immune protective effects in H1N1-infected mice treated with IL-37.

IL-37 can strongly regulate macrophages to restrain the autoimmune response (Ye and Huang, 2015; Toulmin et al., 2017; Wang et al., 2018; Yang et al., 2019). It has been reported that IL-37 can promote macrophage polarization from the pro-inflammatory subtype (M1) to the anti-inflammatory subtype (M2) in atherosclerosis (McCurdy and Baumer, 2017). Moreover, IL-37 induces a phenotypic shift in THP1-derived macrophages toward a $CD206^{+high}$ and $CD86^{+low}$ macrophage subtype and enhanced the mRNA levels of IL-10, which are characteristic hallmarks of M2 macrophages (Huang et al., 2015). In summary, these results indicate that IL-37 treatment ameliorates the lung damage by polarizing macrophages from an M1 to an M2 phenotype. Further research regarding the mechanisms of the inhibitory effect of IL-37 is needed.

To further confirm that macrophages play an important role in the anti-inflammatory effect of IL-37, RAW264.7 cells were infected with H1N1, and treated with oseltamivir in combination with/without IL-37. At the indicated intervals, macrophages were collected, and the expression of cytokine mRNA in the cells was detected. As shown in **Figure 7A**, compared with that in the oseltamivir group, the mRNA expression of IL-1β, IL-6, TNF-α and MIP-1 was obviously downregulated in the IL-37 treatment group. These results are consistent with those of pulmonary studies, which further indicates that IL-37 treatment can ameliorate H1N1-induced inflammation by reducing macrophage cytokine production.

The activity of IL-37 has been reported to largely depend upon IL-18Rα and SIGIRR for the extracellular activation of the anti-inflammatory pathway (Lunding et al., 2015; Zeng et al., 2017). Herein, we found that paralleling the augmented macrophages percentage, the $IL\text{-}18R\alpha^{+}$-macrophages percentage was enhanced markedly in the lungs of IL-37-treated mice (**Figure 5**), indicating that IL-37 down-regulates the increased production of pro-inflammatory cytokines in an IL-18Rα activation-dependent manner. Then, by using the RAW264.7 cell line, the underlying mechanisms of the IL-37 effect in macrophages were further investigated. Studies have shown that MAPK-related signaling can be inhibited by IL-37 in activated mast cells (Gallenga et al., 2019). In addition, the intraperitoneal injection of IL-37 significantly decreases the expression of NLRP3 in the mouse lung aspergillosis model (Moretti et al., 2014; Jia and Liu, 2018). Indeed, our results showed that the increased phosphorylation of ERK1/2 and p38 MAPK was significantly downregulated in RAW264.7 cells treated with IL-37; furthermore, the ratio of NLRP3 in the IL-37-treated group was decreased *in vitro* (**Figure 7**). In contrast, treatment with IL-37 did not inhibit the production of JNK protein in influenza A virus-infected RAW 264.7 cells (data not shown). These results confirm that IL-37 ameliorates influenza pneumonia by attenuating macrophage cytokine production in a MAPK pathway-dependent manner, especially the ERK1/2 and p38 pathways.

In conclusion, these data provide evidence that IL-37 inhibits the pathogenesis of influenza pneumonia by decreasing the production of essential pro-inflammatory cytokines, indicating a new and promising therapeutic approach for excessively activated immune responses in influenza A infection-induced pneumonia. However, the function of IL-37 in other viral infections, especially serious emergent and re-emerged infectious diseases, remains unclear. Further detailed research remains necessary to fully determine the possible functions of IL-37 in viral infections.

## DATA AVAILABILITY STATEMENT

All datasets generated for this study are included in the article/**Supplementary Material**.

## ETHICS STATEMENT

The animal study was reviewed and approved by The Institute of Animal Use and Care Committee of the Institute of Laboratory Animal Science, Peking Union Medical College.

## AUTHOR CONTRIBUTIONS

CQ, LB, and FQ conceived, designed, and supervised the experiments. FQ and ML performed most experiments, analyzed the data, and wrote the original draft. LB, FQ, and ML analyzed the data. FL, QL, GW, SG, SW, and YX conducted some experiments. FQ and ML edited the manuscript. All authors reviewed and approved the manuscript.

## FUNDING

This work was supported by the National Megaprojects of China for Major Infectious Diseases (2018ZX10301403-004), the Chinese National Major S & T Project (2017ZX10304402-001), the CAMS Innovation Fund for Medical Sciences (2016-I2M-1-014, 2016-12 M-006), and the Fundamental Research Funds for the Central Universities (3332018108).

## SUPPLEMENTARY MATERIAL

The Supplementary Material for this article can be found online at: https://www.frontiersin.org/articles/10.3389/fmicb.2019.02482/full#supplementary-material

**SUPPLEMENTARY FIGURE S1 |** Percentages of lymphocytes were detected in IL-37-treated mice. **(A)** The percentages of different lymphocytes that were identified as $CD3^+CD4^+$ or $CD3^+CD8^+$ as well as IL-$18R\alpha^+$ lymphocytes in the lungs of IL-37 treated mice were determined by flow cytometry on day 6 during H1N1 infection. Data are representative of three independent experiments with three mice for each group. *Significant difference ($p < 0.05$), compared with oseltamivir-treated mice.

## REFERENCES


Al-Anazi, M. R., Matou-Nasri, S., Al-Qahtani, A. A., Alghamdi, J., Abdo, A. A., Sanai, F. M., et al. (2019). Association between IL-37 gene polymorphisms and risk of HBV-related liver disease in a Saudi Arabian population. *Sci. Rep.* 9:7123. doi: 10.1038/s41598-019-42808-4

An, B., Liu, X., Li, G., and Yuan, H. (2017). Interleukin-37 ameliorates coxsackievirus B3-induced viral myocarditis by modulating the Th17/regulatory T cell immune response. *J. Cardiovasc. Pharmacol.* 69, 305–313. doi: 10.1097/FJC.0000000000000476

Barbier, L., Ferhat, M., Salame, E., Robin, A., Herbelin, A., Gombert, J. M., et al. (2019). Interleukin-1 family cytokines: keystones in liver inflammatory diseases. *Front. Immunol.* 10:2014. doi: 10.3389/fimmu.2019.02014

Boraschi, D., Lucchesi, D., Hainzl, S., Leitner, M., Maier, E., Mangelberger, D., et al. (2011). IL-37: a new anti-inflammatory cytokine of the IL-1 family. *Eur. Cytokine Netw.* 22, 127–147. doi: 10.1684/ecn.2011.0288

Boraschi, D., and Tagliabue, A. (2013). The interleukin-1 receptor family. *Semin. Immunol.* 25, 394–407. doi: 10.1016/j.smim.2013.10.023

Daoud, A., Laktineh, A., Macrander, C., Mushtaq, A., and Soubani, A. O. (2019). Pulmonary complications of influenza infection: a targeted narrative review. *Postgrad. Med.* 131, 299–308. doi: 10.1080/00325481.2019.1592400

Davis, C. J., Zielinski, M. R., Dunbrasky, D., Taishi, P., Dinarello, C. A., and Krueger, J. M. (2017). Interleukin 37 expression in mice alters sleep responses to inflammatory agents and influenza virus infection. *Neurobiol. Sleep Circadian Rhythms* 3, 1–9. doi: 10.1016/j.nbscr.2016.11.005

Dinarello, C. A., and Bufler, P. (2013). Interleukin-37. *Semin. Immunol.* 25, 466–468. doi: 10.1016/j.smim.2013.10.004

Gallenga, C. E., Pandolfi, F., Caraffa, A., Kritas, S. K., Ronconi, G., Toniato, E., et al. (2019). Interleukin-1 family cytokines and mast cells: activation and inhibition. *J. Biol. Regul. Homeost. Agents* 33, 1–6. https://www.ncbi.nlm.nih.gov/pubmed/30656901

He, W., Chen, C. J., Mullarkey, C. E., Hamilton, J. R., Wong, C. K., Leon, P. E., et al. (2017). Alveolar macrophages are critical for broadly-reactive antibody-mediated protection against influenza A virus in mice. *Nat Commun.* 8:846. doi: 10.1038/s41467-017-00928-3

Hermann, B., Lehners, N., Brodhun, M., Boden, K., Hochhaus, A., Kochanek, M., et al. (2017). Influenza virus infections in patients with malignancies – characteristics and outcome of the season 2014/15. A survey conducted by the infectious diseases working party (AGIHO) of the German Society of Haematology and Medical Oncology (DGHO). *Eur. J. Clin. Microbiol. Infect. Dis.* 36, 565–573. doi: 10.1007/s10096-016-2833-3

Huang, Z., Gao, C., Chi, X., Hu, Y. W., Zheng, L., Zeng, T., et al. (2015). IL-37 expression is upregulated in patients with tuberculosis and induces macrophages towards an M2-like phenotype. *Scand. J. Immunol.* 82, 370–379. doi: 10.1111/sji.12326

Jia, H., and Liu, J. (2018). Reviews of Interleukin-37: functions, receptors, and roles in diseases. *Biomed. Res. Int.* 2018:3058640. doi: 10.1155/2018/3058640

Kumar, S., Hanning, C. R., Brigham-Burke, M. R., Rieman, D. J., Lehr, R., Khandekar, S., et al. (2002). Interleukin-1F7B (IL-1H4/IL-1F7) is processed by caspase-1 and mature IL-1F7B binds to the IL-18 receptor but does not induce IFN-gamma production. *Cytokine* 18, 61–71. doi: 10.1006/cyto.2002.0873

Liu, L., Oza, S., Hogan, D., Chu, Y., Perin, J., Zhu, J., et al. (2016). Global, regional, and national causes of under-5 mortality in 2000-15: an updated systematic analysis with implications for the sustainable development goals. *Lancet* 388, 3027–3035. doi: 10.1016/S0140-6736(16)31593-8

Lunding, L., Webering, S., Vock, C., Schroder, A., Raedler, D., Schaub, B., et al. (2015). IL-37 requires IL-18Ralpha and SIGIRR/IL-1R8 to diminish allergic airway inflammation in mice. *Allergy* 70, 366–373. doi: 10.1111/all.12566

Lv, J., Xiong, Y., Li, W., Cui, X., Cheng, X., Leng, Q., et al. (2018). IL-37 inhibits IL-4/IL-13-induced CCL11 production and lung eosinophilia in murine allergic asthma. *Allergy* 73, 1642–1652. doi: 10.1111/all.13395

McCurdy, S., and Baumer, Y. (2017). Macrophage-specific expression of IL-37 in hyperlipidemic mice attenuates. *Atherosclerosis* 199, 3604–3613. doi: 10.4049/jimmunol.1601907

Moretti, S., Bozza, S., Oikonomou, V., Renga, G., Casagrande, A., Iannitti, R. G., et al. (2014). IL-37 inhibits inflammasome activation and disease severity in murine aspergillosis. *PLoS Pathog.* 10:e1004462. doi: 10.1371/journal.ppat.1004462

Morita, M., Kuba, K., Ichikawa, A., Nakayama, M., Katahira, J., Iwamoto, R., et al. (2013). The lipid mediator protectin D1 inhibits influenza virus replication and improves severe influenza. *Cell* 153, 112–125. doi: 10.1016/j.cell.2013.02.027

Nold, M. F., Nold-Petry, C. A., Zepp, J. A., Palmer, B. E., Bufler, P., and Dinarello, C. A. (2010). IL-37 is a fundamental inhibitor of innate immunity. *Nat. Immunol.* 11, 1014–1022. doi: 10.1038/ni.1944

Nold-Petry, C. A., Lo, C. Y., Rudloff, I., Elgass, K. D., Li, S., and Gantier, M. P. (2015). IL-37 requires the receptors IL-18Ralpha and IL-1R8 (SIGIRR) to carry out its multifaceted anti-inflammatory program upon innate signal transduction. *Nat. Immunol.* 16, 354–365. doi: 10.1038/ni.3103

Perez-Padilla, R., De La Rosa-Zamboni, D., Ponce De Leon, S., Hernandez, M., Quinones-Falconi, F., Bautista, E., et al. (2009). Pneumonia and respiratory failure from swine-origin influenza A (H1N1) in Mexico. *N. Engl. J. Med.* 361, 680–689. doi: 10.1056/NEJMoa0904252

Ramsey, C. D., and Kumar, A. (2013). Influenza and endemic viral pneumonia. *Crit. Care Clin.* 29, 1069–1086. doi: 10.1016/j.ccc.2013.06.003

Rello, J., Rodriguez, A., Ibanez, P., Socias, L., Cebrian, J., Marques, A., et al. (2009). Intensive care adult patients with severe respiratory failure caused by influenza a (H1N1)v in Spain. *Crit. Care* 13:R148. doi: 10.1186/cc8044

Rice, T. W., Rubinson, L., Uyeki, T. M., Vaughn, F. L., John, B. B., Miller, R. R. 3rd, et al. (2012). Critical illness from 2009 pandemic influenza A virus and bacterial coinfection in the United States. *Crit. Care Med.* 40, 1487–1498. doi: 10.1097/CCM.0b013e3182416f23

Schloer, S., Hubel, N., Masemann, D., Pajonczyk, D., Brunotte, L., Ehrhardt, C., et al. (2019). The annexin A1/FPR2 signaling axis expands alveolar macrophages, limits viral replication, and attenuates pathogenesis in the murine influenza A virus infection model. *FASEB J.* 33:fj201901265R. doi: 10.1096/fj.201901265R

Tate, M. D., Pickett, D. L., Van Rooijen, N., Brooks, A. G., and Reading, P. C. (2010). Critical role of airway macrophages in modulating disease severity during influenza virus infection of mice. *J. Virol.* 84, 7569–7580. doi: 10.1128/JVI.00291-10

Teng, X., Hu, Z., Wei, X., Wang, Z., Guan, T., Liu, N., et al. (2014). IL-37 ameliorates the inflammatory process in psoriasis by suppressing proinflammatory cytokine production. *J. Immunol.* 192, 1815–1823. doi: 10.4049/jimmunol.1300047

Theoharides, T. C., Tsilioni, I., and Conti, P. (2019). Mast cells may regulate the anti-inflammatory activity of IL-37. *Int. J. Mol. Sci.* 20:3701. doi: 10.3390/ijms20153701

Toulmin, E., Lee, B. H., and Boisvert, W. A. (2017). Macrophage-specific expression of IL-37 in hyperlipidemic mice attenuates atherosclerosis. *J. Immunol.* 199, 3604–3613. doi: 10.4049/jimmunol.1601907

Uematsu, T., Iizasa, E., Kobayashi, N., Yoshida, H., and Hara, H. (2015). Loss of CARD9-mediated innate activation attenuates severe influenza pneumonia without compromising host viral immunity. *Sci. Rep.* 5:17577. doi: 10.1038/srep17577

Wang, L., Quan, Y., Yue, Y., Heng, X., and Che, F. (2018). Interleukin-37: a crucial cytokine with multiple roles in disease and potentially clinical therapy. *Oncol. Lett.* 15, 4711–4719. doi: 10.3892/ol.2018.7982

Wong, C. K., and Smith, C. A. (2017). Aging impairs alveolar macrophage phagocytosis and increases influenza-induced mortality in mice. *J. Immunol.* 199, 1060–1068. doi: 10.4049/jimmunol.1700397

Yang, Z., Kang, L., Wang, Y., Xiang, J., Wu, Q., Xu, C., et al. (2019). Role of IL-37 in cardiovascular disease inflammation. *Can. J. Cardiol.* 35, 923–930. doi: 10.1016/j.cjca.2019.04.007

Ye, L., and Huang, Z. (2015). IL-37 restrains autoimmune diseases. *Oncotarget* 6, 21775–21776. doi: 10.18632/oncotarget.4887

Zeng, Q., Song, R., Fullerton, D. A., Ao, L., Zhai, Y., Li, S., et al. (2017). Interleukin-37 suppresses the osteogenic responses of human aortic valve interstitial cells *in vitro* and alleviates valve lesions in mice. *Proc. Natl. Acad. Sci. USA* 114, 1631–1636. doi: 10.1073/pnas.1619667114

Zhang, S. R., Nold, M. F., Tang, S. C., Bui, C. B., Nold, C. A., Arumugam, T. V., et al. (2019). IL-37 increases in patients after ischemic stroke and protects from inflammatory brain injury, motor impairment and lung infection in mice. *Sci. Rep.* 9:6922. doi: 10.1038/s41598-019-43364-7

**Conflict of Interest:** The authors declare that the research was conducted in the absence of any commercial or financial relationships that could be construed as a potential conflict of interest.

*Copyright © 2019 Qi, Liu, Li, Lv, Wang, Gong, Wang, Xu, Bao and Qin. This is an open-access article distributed under the terms of the Creative Commons Attribution License (CC BY). The use, distribution or reproduction in other forums is permitted, provided the original author(s) and the copyright owner(s) are credited and that the original publication in this journal is cited, in accordance with accepted academic practice. No use, distribution or reproduction is permitted which does not comply with these terms.*

frontiers in Microbiology

ORIGINAL RESEARCH
published: 06 November 2019
doi: 10.3389/fmicb.2019.02540

# Anti-TGEV Miller Strain Infection Effect of *Lactobacillus plantarum* Supernatant Based on the JAK-STAT1 Signaling Pathway

*Kai Wang[1†], Ling Ran[1†], Tao Yan[2], Zheng Niu[1], Zifei Kan[1], Yiling Zhang[1], Yang Yang[1], Luyi Xie[1], Shilei Huang[1], Qiuhan Yu[1], Di Wu[1] and Zhenhui Song[1*]*

[1] Department of Microbiology and Immunology, College of Animal Science, Southwest University, Chongqing, China,
[2] Department of Preventive Veterinary Medicine, Medical College of Animals, Xinjiang Agricultural University, Ürümqi, China

OPEN ACCESS

**Edited by:**
*Lu Lu,*
*Fudan University, China*

**Reviewed by:**
*Harish Changotra,*
*Jaypee University of Information Technology, India*
*Gabriela Del Valle Perdigon, National Council for Scientific and Technical Research (CONICET), Argentina*

***Correspondence:**
*Zhenhui Song*
*szh7678@126.com*

*[†]These authors have contributed equally to this work*

**Specialty section:**
*This article was submitted to Virology, a section of the journal Frontiers in Microbiology*

**Received:** *25 July 2019*
**Accepted:** *21 October 2019*
**Published:** *06 November 2019*

**Citation:**
*Wang K, Ran L, Yan T, Niu Z, Kan Z, Zhang Y, Yang Y, Xie L, Huang S, Yu Q, Wu D and Song Z (2019) Anti-TGEV Miller Strain Infection Effect of Lactobacillus plantarum Supernatant Based on the JAK-STAT1 Signaling Pathway. Front. Microbiol. 10:2540. doi: 10.3389/fmicb.2019.02540*

Transmissible gastroenteritis (TGE), caused by transmissible gastroenteritis virus (TGEV), is one many gastrointestinal inflections in piglets, characterized by diarrhea, and high mortality. Probiotics are ubiquitous bacteria in animal intestines, which have many functions, such as promoting intestinal peristalsis and maintaining the intestinal balance. We found that the supernatant of the Lp-1 strain of *Lactobacillus plantarum*, isolated in our laboratory, and named Lp-1s had marked anti-TGEV effect on IPEC-J2 cells. Lp-1s could induce large amounts of interferon-β in IPEC-J2 cells in the early stage (6 h) of infection with TGEV, and increased the level of phosphorylated signal transducer and activator of transcription and its nuclear translocation in the late stage (24–48 h) of infection. This resulted in upregulated expression of interferon-stimulated genes, and increased the transcription and protein expression of antiviral proteins, resulting in an anti-TGEV effect.

**Keywords: transmissible gastroenteritis virus, *Lactobacillus plantarum*, interferon-beta, STAT1, interferon-stimulating genes**

## INTRODUCTION

Transmissible gastroenteritis virus (TGEV) is the pathogenic agent of porcine transmissible gastroenteritis (TGE), which causes vomiting, diarrhea, and high mortality in suckling piglets (Masters, 2006), resulting in heavy losses to the pig breeding industry (Zhao et al., 2014). In particular, viral diarrhea diseases are more serious because of limited treatment options. Probiotics comprise microorganisms that have beneficial activities to the host, and mainly comprise *Clostridium butyricum*, *Lactobacillus*, *Bifidobacteria*, Actinomycetes, and yeasts. They usually occupy the human gut and reproductive system, and can improve the balance of the host micro-ecology (Fuller, 1989; Maragkoudakis et al., 2010; da Silva Sabo et al., 2017; Stofilova et al., 2017). There is growing interest in the oral administration of appropriate probiotics to reduce the pressure in the intestines and produce an effective innate immune response (Pollmann et al., 2005; Maragkoudakis et al., 2010). In recent years, probiotic animal feed supplements have been developed as viable alternatives to antibiotics because of the ban on antibiotics in feed (Scharek et al., 2007). The addition of probiotic feed can prevent the infection of pathogens causing intestinal diseases, directly benefiting the animal host (Villena et al., 2014), or can indirectly enhance the

host's immune response by balancing the disordered microbiota (Lee et al., 2018). In addition, many basic and clinical studies have confirmed that probiotic strains have antiviral effects (Lee et al., 2011; Yuan et al., 2018). Studies have shown that *Lactobacillus plantarum* can stimulate the body's innate and acquired immunity, and contributes to the production of inflammatory factors that inhibit the replication of the virus in the body. For example, *L. plantarum* strain YU (LpYU) not only has high interleukin (IL)-12-inducing activity mediated by Toll-like receptor (TLR) 2 in mouse peritoneal macrophages, but also communicates with natural killer cells (NK) in the spleen to stimulate the production of IgA to enhance the body's anti-H1N1 virus activity (Kawashima et al., 2011). In addition, *L. plantarum* L-137 can stimulate the production of type I interferon (IFN-1) to effectively inhibit the proliferation of H1N1 (Maeda et al., 2009). TGEV is an important gastrointestinal diarrhea virus; therefore, research and exploration into the antiviral mechanism of probiotics could lead to the development of oral probiotics to prevent and treat TGEV infection.

The body reacts rapidly to viral invasion by synthesizing and secreting type I interferon IFN-1 (IFN-α/β), which plays a key role in the host antiviral response. The binding of IFN-1 to its receptor (interferon α/β receptor, IFNAR) leads to activation of the Janus family kinase (JAK) and subsequent signal transduction and transcriptional activator (STAT) signaling cascade, resulting in the activation and upregulation of interferon-stimulating genes (*ISGs*), ultimately activating IFN to exert its antiviral effects (Zhao et al., 2016; Chen et al., 2017).

A strain of *L. plantarum* was successfully isolated and named Lp-1 (Song Han et al., 2017). We wondered whether the IPEC-J2 cells treated by Lp-1 could induce an antiviral mechanism through the IFN-β/JAKs/STAT/*ISGs* pathway after TGEV infection. In the present study, we found that the supernatant of *L. plantarum* Lp-1 (Lp-1s) could significantly inhibit TGEV infection. By detecting the replication of TGEV N gene in porcine intestinal epithelial cells treated with Lp-1s at different time points, we confirmed that Lp-1s had a preventive effect against TGEV. Then, by detecting the levels of IFN, p-STAT and *ISGs*, we further confirmed that Lp-1s exerts its anti-TGEV role by upregulating the expression of IFN-β.

# MATERIALS AND METHODS

## Cells, Viruses, and Reagents

Porcine kidney cells (ST) to amplify the virus and the experimental model pig jejunal cells (IPEC-J2 cells) were both cultured in Roswell Park Memorial Institute (RPMI) 1640 medium (Gibco, Grand Island, NY, United States) containing 10% fetal bovine serum (FBS, Gibco), under 37°C and 5% $CO_2$. IPEC-J2 cells and ST cells were purchased from the Shanghai Sur Biotech Co., Ltd (Shanghai, China). *L. plantarum* LP-1 was isolated and stored in our laboratory. Its 16S ribosomal gene sequence has been submitted to GenBank (MH727586). Lp-1s was isolated from a culture of *L. plantarum* LP-1 after shaking for 14 h at 37°C. The TGEV Miller strain (Yang et al., 2018) was preserved in our laboratory. Viral fluid was collected from ST cells after replication for approximately 72 h when the cells showed obvious cytopathic effects (CPEs).

## Primer Design and Synthesis

The GenBank sequences of the TGEV N gene (GQ-374566.1) coding sequence (CDS) conserved region, the porcine MX1 CDS (MX dynamin like GTPase 1; AH015318.2), the MX2 CDS (MX dynamin like GTPase 2; AY897395.1), the ISG15 CDS (interferon-stimulated protein, 15 KDa; NM_214303.2), the OASL CDS (2′-5′-oligoadenylate synthetase like; NM_214303.2), the PKR CDS (double stranded RNA-dependent protein kinase; AB104654.1), the ZAP CDS (zeta-chain associated protein; GU_563332.1), and internal reference pig β-Actin gene (ACTB; XM_003124280.2) were obtained and pairs of specific primers were designed using Primer 5.0 software for quantitative real-time PCR [performed using SYBR Premix EX Taq II (Takara, Shiga, Japan)] as follows: TGEV-N (Forward: 5′-TTCAACCCC ATAACCCTCCAACAA-3′ and Reverse: 5′-GGCCCTTCAC CAT GCGATAGC-3′), MX1 (Forward: 5′-ATCTGTAAGCAGG AGACCATCAACTT G-3′ and Reverse: 5′-CTCGCCACGTCCA CTATCTTGTC-3′), MX2 (Forward: 5′-TTCACTCGCATCCGC ACTTCAG-3′ and Reverse: 5′-AGCTCCTCTGTCGCACTC TGG-3′), ISG15 (Forward: 5′-GGCAGCACAGTCCTGTT GATGG-3′ and Reverse: 5′-TGCGTCAGCCAGACCTCAT AGG-3′), OASL (Forward: 5′-CGTTGGTGGTGG AGACACA TACAG-3′ and Reverse: 5′-TCAGGCGACACCTTCCAGG ATC-3′), PKR (Forward: 5′-ACAGGACCTGCACATAACT TGAGG-3′ and Reverse: 5′-TGCTGTCGGCAGTGATGAAGA AC-3′), ZAP (Forward: 5′-GCTCAGTGCGAAC ACCTGGA TG-3′ and Reverse: 5′-TGACAGATGAAGGCGTGGAG AGG-3′), and ACTB (Forward: 5′-CTCTTCCAGC CCTCCT TCC-3′ and Reverse: 5′-GGTCCTTG CGGATGTCG-3′). The designed primers were synthesized by Shanghai Shenggong Biotechnology Service Co., Ltd. (Shanghai, China).

## Assessment of Cellular Toxicity of Lp-1s by the CPE Effect and the MTT Assay

After centrifugation of Lp-1 with an $OD_{600}$ of 1.8 at 4000 rpm/min for 10 min, the obtained supernatant was filtered through a 0.22-μm filter, and then diluted with RPMI 1640 high sugar medium to six gradients at two times ratio, i.e., Lp-1s was diluted to obtain $OD_{600}$ values of 0.9, 0.45, 0.225, 0.113, 0.056, and 0.028, respectively. IPEC-J2 cells were seeded at $1 \times 10^5$/mL in 96-well plates and incubated overnight in 5% $CO_2$ at 37°C. The medium was discarded when the cells reached 90% confluence in the 96-well plate, and then 100 μL of each gradient dilution of Lp-1s was added to each well. The medium in the control group was replaced with RPMI 1640. After incubating for 90 min, the supernatant was discarded, and the cells were washed twice with phosphate-buffered saline (PBS). Culture was continued and the cytopathic effect (CPE) was observed daily. The maximum non-toxic dose of Lp-1s to the cells was detected using the 3-(4,5-dimethylthiazol-2-yl)-2,5-diphenyltetrazolium bromide (MTT) reagent (BBI, Shanghai, China), when 80% of the cells in the negative control group were damaged. MTT assays for each dilution were repeated three times independently.

## Optimal Concentration of Lp-1s for Anti-TGEV Activity

Lp-1s was prepared as above and then diluted to an $OD_{600}$ of 0.45, 0.225, 0.113, and 0.056 with RPMI 1640 high-sugar medium. IPEC-J2 cells were seeded at $1.8 \times 10^6$/mL in 6-well plates and cultured in 5% $CO_2$ at 37°C. At 90% confluence, the medium was discarded, the cells were washed three times with PBS, 1 mL of each gradient dilution of Lp-1s was added to each well, and the cells incubated at 37°C in 5% $CO_2$ for 90 min. The medium in the control group was replaced with RPMI 1640. For the other wells, the supernatant was discarded, TGEV (multiplicity of infection (MOI) = 0.1) in RPMI 1640 medium was added to Lp-1s-treated IPEC-J2, and incubated at 37°C in 5% $CO_2$ for 1.5 h. The supernatants were discarded and incubation continued in RPMI 1640 high glucose medium. After 48 h of culture, proteins were extracted for western blotting to detect the levels of the TGEV N protein after treatment with different concentrations of Lp-1s.

## Median Tissue Culture Infectious Dose (TCID50) Analysis

IPEC-J2 cells treated with Lp-1s for 1.5 h were exposed to TGEV (MOI = 0.1). The IPEC-J2 cells treated with Lp-1s were sampled at 12 h post infection (hpi), 24 hpi, and 48 hpi and then frozen and thawed three times to collect virus particles in the cells and supernatants. Gradient dilution of IPEC-J2 cells was performed from $10^{-1}$ and $10^{-7}$, respectively. TGEV titers of IPEC-J2 cells treated with Lp-1s for different times were detected using ST cells in 96-well plates. Each dilution gradient was assayed in 12 replicate wells. The $TCID_{50}$ of the virus in the different groups was calculated by Reed and Muench methods.

## Detection of TGEV-N Gene Copy Number and Protein Expression

IPEC-J2 cells were inoculated into 6-well plates at $1.8 \times 10^6$/mL. The IPEC-J2 cells treated with Lp-1s for 1.5 h were exposed to TGEV (MOI = 0.1) for RNA extraction and protein sampling. When the cells reached 90% confluence, RNA was extracted and reverse transcribed into cDNA and quantified at 500 ng/mL. Absolute fluorescence quantitative PCR was performed using fluorescence quantitative PCR. The reaction parameters were as follows: Pre-denaturation at 95°C for 3 min, followed by 40 cycles of denaturation at 94°C for 30 s, annealing at 60°C for 30 s, and prolongation at 72°C for 30 s. The reaction for each sample was repeated three times. The Bio-Rad CFX Manager random matrix method was used to analyze the linear relationship between cycle threshold (CT) value and the copy number to calculate the copy number of the TGEV-N gene. Protein samples were also extracted at the same time point and detected using western blotting. The primary antibody was a mouse monoclonal antibody against TGEV-N, and the secondary antibodies were horseradish peroxidase (HRP)-conjugated goat anti-mouse antibodies (Proteintech,Wuhan,China). The immunoreactive protein bands were visualized using a Vilber fusion FX5 chemiluminescent imager.

## Effect of Lp-1s on IFN-β Induction in IPEC Cells

IPEC-J2 cells were inoculated into 6-well plates at $1.8 \times 10^6$/mL. When they reached 90% confluence, three experimental groups were established: An Lp-1s optimal concentration treatment group infected TGEV, a TGEV single infection group, and the uninfected control group. Cell samples at 6, 12, 24, and 48 hpi were centrifuged at 4000 rpm for 10 min, and the supernatant subjected to an enzyme linked immunosorbent assay (ELISA) to detect IFN-β.

## Western Blotting Analysis

Transmissible gastroenteritis virus (MOI = 0.1) was infected to IPEC-J2 cells that had been treated with Lp-1s for 1.5 h, and then cell samples at 12, 24, and 48 hpi were collected to produce protein lysates. In addition, TGEV (MOI = 0.1) was infected into IPEC-J2 cells cultured in RPMI 1640 for 1.5 h as the TGEV control group and the proteins were extracted at the same time points as the Lp-1s group. The protein concentration was determined using the bicinchoninic acid method and subjected to sodium dodecyl sulfate polyacrylamide gel electrophoresis. The separated proteins were transferred to a nitrocellulose membrane (Bio-Rad). The membranes were blocked using 5% skimmed milk and incubated with the following primary antibodies: Anti-STAT1 rabbit polyclonal antibodies (British Biorbyt Company), anti-phospho-(p)STAT1 (Tyr701) rabbit polyclonal antibodies (Biorbyt), anti-ZAP rabbit polyclonal antibodies (Abcam), anti-PKR rabbit polyclonal antibodies (Abcam), anti-(p)PKR (T446) rabbit polyclonal antibodies (Abcam), and anti-β-tubulin rabbit polyclonal antibodies (Proteintech). Secondary antibodies comprised goat anti-rabbit immunoglobulin (H + L). The immunoreactive protein bands were visualized using the Vilber fusion FX5 imaging system (VILBER), and the grayscale values of each band were analyzed by GraphPad Prism.

## Indirect Immunofluorescence Detection of Nuclear Displacement

IPEC-J2 cells were seeded at a density of $1.5 \times 10^6$ in cell slides in 24-well culture dishes. These cells were set as three experimental groups comprising an Lp-1s optimal concentration treatment group, a TGEV alone infection group, and a blank (uninfected) control group, when they reached 90% confluence. The cells were sampled at 12, 24, and 48 hpi; washed three times with PBS; fixed with 4% paraformaldehyde at 37°C for 1.5 h; washed three times with PBS; permeated by 0.3% Triton-X-100 for 10 min; washed three times with PBS; and blocked by 1% bovine serum albumin for 30 min at room temperature. Primary antibodies comprising anti-p-STAT1 protein rabbit polyclonal antibodies and anti-TGEV-N mouse monoclonal antibodies were added and incubated overnight in 4°C in a wet box. The cells were then washed three times with PBS, proportionally added CY3-goat anti-rabbit fluorescence and fluorescein isothiocyanate (FITC)-labeled goat anti-mouse fluorescent secondary antibodies were then added, the cells were incubated for 1 h in a dark room at 37°C, incubated with 2-(4-amidinophenyl)-1H-indole-6-carboxamidine (DAPI) for 5 min, rinsed with PBS. Laser

confocal microscopy was then used to observe p-STAT1, its nuclear translocation, and the TGEV N protein. The protein levels were analyzed using the ZEN software.

## Quantitative Real-Time Reverse Transcription Polymerase Chain Reaction (qRT-PCR)

IPEC-J2 cells were seeded at $1.8 \times 10^6$/mL in 6-well plates, grown to 90% confluence, and then divided into three groups: Cells treated with Lp-1s for 1.5 h and then infected with TGEV (MOI = 0.1), TGEV infection alone, and the blank control (uninfected cells). The IPEC-J2 cells were sampled at 12, 24, and 48 hpi for qRT-PCR. Total RNA was extracted using the RNAiso plus reagent (Takara), and then single-stranded RNA was isolated using an RNA PCR (AMV) ver 3.0 kit (Takara). cDNA was then synthesized via reverse transcription. Quantitative real-time PCR was then performed using the SYBR premix EX Taq II (Takara) to detect the mRNA levels of ZAP, PKR, OASL, and ISG15 (fluorescent primers were synthesized by Shanghai Shenggong Bioengineering Technology Service Co., Ltd.).

## Small Interfering RNA (siRNA) Assays

Small interfering RNA (siRNA) targeting STAT1, 5′-GGAACAGAAATACACCTAT-3′ (produced by RIBO, China). Transfected with the STAT1-specific siRNA using LipofectamineTM 3000 (Invitrogen, United States), according to the manufacturer's instructions, to the TGEV-infected groups treated with Lp-1s and TGEV infection alone groups, respectively, in IPEC-J2 cells. ConsiRNA transfected as control groups. The collected samples were analyzed by Western blotting using a rabbit pAb recognizing STAT1 as the primary antibody and HRP-conjugated goat anti-rabbit IgG as the secondary antibody.

## Statistical Analyses

All results were plotted and analyzed using GraphPad Prism 6 software (GraphPad Inc., La Jolla, CA, United States). The data were presented as the mean ± standard deviation (SD) of three independent experiments. Data were statistically compared using the *t* test. A $p$ value $< 0.05$ ($^*p < 0.05$ and $^{**}p < 0.01$) was considered statistically significant.

# RESULTS

## MTT Cytotoxicity Test and Lp-1s Concentration Screening

The MTT assay (**Figure 1**) showed that the higher dilution ratio of Lp-1s, the higher the cell viability. The maximum non-toxic dose toward the cells was greater than 50% $OD_{490}$; therefore, the maximum non-toxic dose of Lp-1s to IPEC-J2 cells is $OD_{600}$ 0.45 (**Figure 1A**). The TGEV inhibition rate of Lp-1s decreased with increasing dilution factor and was thus concentration dependent. The results showed that amount of TGEV Miller strain (MOI = 0.1) was reduced by 1/4-fold by Lp-1s, i.e., the $OD_{600}$ was 0.45, and the treated IPEC-J2 cells received the highest non-toxic dose of Lp-1s (**Figure 1B**).

## Results of $TCID_{50}$ Experiment

The experimental data (**Figure 2**) showed that the TGEV titers at 12, 24, and 48 hpi after TGEV infection of IPEC-J2 cells treated with Lp-1s were $10^{2.5}$ $TCID_{50}$/mL, $10^{2.55}$ $TCID_{50}$/mL, and 103.3 $TCID_{50}$/mL, respectively. Compared with the TGEV control group, the amount of viral of lesions decreased by 1.1, 1.9, and 1.8-fold at 12, 24, and 48 hpi, respectively, in the Lp-1s group and no lesions appeared in the blank control group. Therefore, Lp-1s has a significant anti-TGEV effect ($^{**}p < 0.01$) and is optimal for antiviral activity at 24 hpi.

## TGEV-N Gene Copy Number and Protein Expression Levels in Response to Lp-1s

We found that the TGEV N gene copy number in IPEC-J2 cells treated with Lp-1s was lower than that in cells infected with TGEV only ($^*p < 0.05$, $^{**}p < 0.01$). In addition, the viral N gene copy number in the TGEV infection group was positively correlated with the infection duration (**Figure 3A**). Western blotting showed that the level of the TGEV N protein in the Lp-1s group was lower than that in the TGEV group at all three time points. No expression of TGEV N protein was observed in the blank control group (**Figures 3B,C**). These results demonstrated that Lp-1s could inhibit the transcription and protein expression of TGEV N.

## Lp-1s Induces IFN-β

The results in **Figure 4** indicate that IFN-β levels gradually increased in IPEC-J2 cells during TGEV infection. However, compared with the TGEV-infected group, the IFN-β level of the TGEV (MOI = 0.1)-infected group treated with Lp-1s increased significantly with infection time ($^{**}p < 0.01$). Therefore, Lp-1s can significantly increase the level of intracellular IFN-β during TGEV infection.

## Lp-1s Stimulates the Phosphorylation of STAT1

The results in **Figure 5** show that there was almost no change in the total expression of STAT1 in IPEC-J2 cells under different treatments and at different time points; however, the amount of phosphorylated STAT1 changed significantly. The amount of phosphorylated STAT1 in the Lp-1s group was higher than that in the TGEV group at the different time points ($^*p < 0.05$ and $^{**}p < 0.01$), while only a small amount of phosphorylated STAT1 was detected in the blank control group at the different time points. Therefore, although TGEV infection could significantly increase the amount of phosphorylated STAT1, Lp-1s could further significantly increase the amount of phosphorylated STAT1 in cells after TGEV infection.

## Lp-1s Activates Nuclear Translocation of p-STAT1

The results in **Figure 6** show that the amount of p-STAT1 (red fluorescence) in the nuclei of TGEV infected cells treated with Lp-1s at different time points was significantly higher than that in the nuclei of cells in TGEV infected group. At the same time, the amount of p-STAT1 correlated positively with the duration

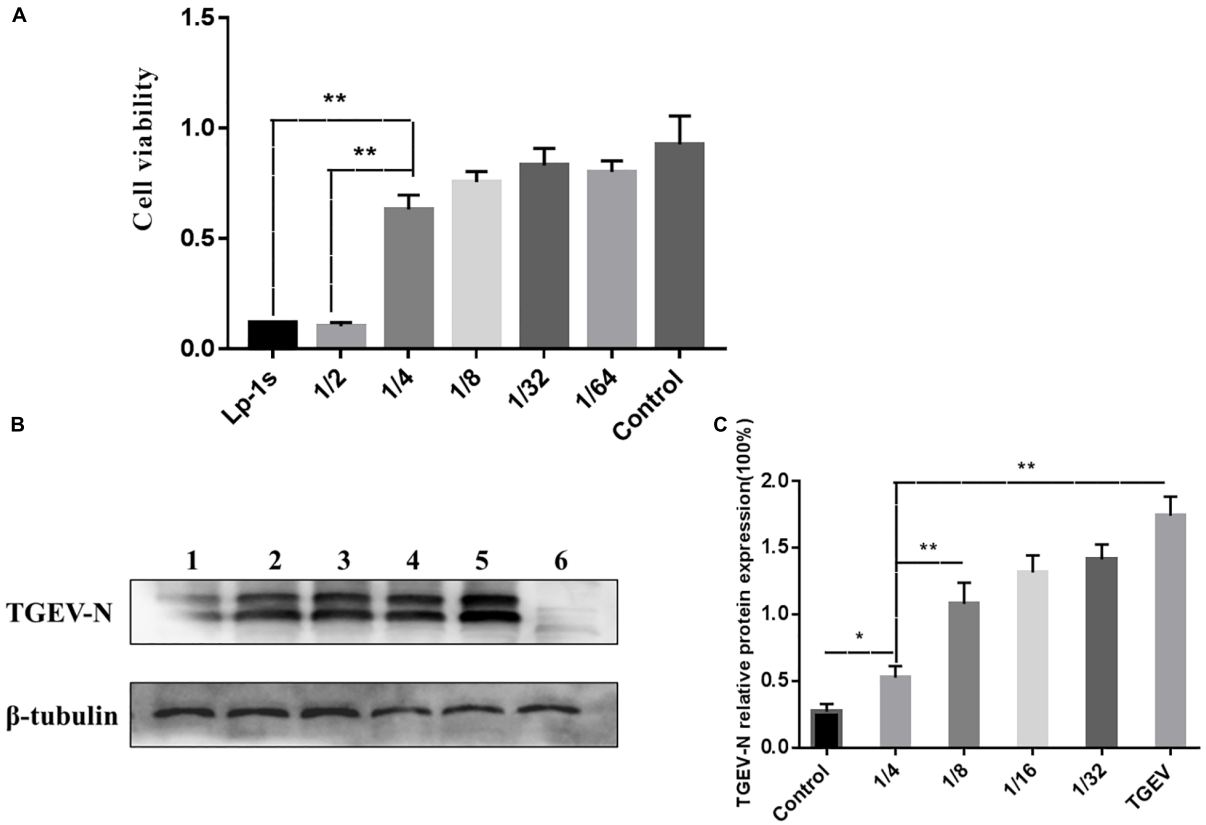


**FIGURE 1 |** MTT cytotoxicity test and Lp-1s concentration screening. **(A)** Results of Lp-1s cytotoxicity as detected using the MTT method on 1/4, 1/8, 1/32, and 1/64 times dilutions of Lp-1s acting on IPEC-J2 cells. The cell adherence state remained basically unchanged. According to the experimental data, the Lp-1s undiluted group, the 1/2-fold dilution group and the 1/4-fold dilution group showed significantly difference in cytotoxicity (**$P < 0.01$), and the 1/4-fold dilution group showed no significant difference compared with that of the control group ($P > 0.05$). **(B)** The expression of the TGEV N protein in IPEC-J2 cells treated with Lp-1s at different dilutions was detected by western blotting. Lane 1, infected TGEV group after Lp-1s 1/4 dilution pretreatment; Lane 2, infected TGEV group after Lp-1s 1/8 dilution pretreatment; Lane 3, infected TGEV group after Lp-1s 1/16 dilution pretreatment; Lane 4, infected TGEV group after Lp-1s 1/32 dilution pretreatment; Lane 5, TGEV infection group; and Lane 6, uninfected control cells (normal group). **(C)** Grayscale analysis of the relative expression of TGEV N in IPEC-J2 cells infected with Lp-1s at different dilutions showing that TGEV N protein levels were decreased in the 1/4-fold dilution of Lp-1s treatment group after 48 h, compared with the 1/8-fold dilution and TGEV infection group, there was a significant difference (**$P < 0.01$), which was significantly different from the control group (*$P < 0.05$).

of infection after Lp-1s-treatment of IPEC-J2 cells infected with TGEV. However, the amount of red fluorescence emitted by p-STAT1 labeled with Cy3 correlated negatively with the amount of green fluorescence emitted by FITC-labeled TGEV N protein. We found that when TGEV was directly infected into IPEC-J2 cells, the red fluorescence of p-STAT1 was mainly gathered around the cell wall and only a small amount appeared in the nucleus; the green fluorescence and red fluorescence of the blank control group were not obvious. Meanwhile, the signal intensity of p-STAT1 in the nuclei of the Lp-1s treatment group correlated positively with time (**Figure 6**). Therefore, Lp-1s could significantly increase the level of p-STAT1 and promoted its translocation into the nucleus, while simultaneously inhibiting the expression of TGEV N.

## Transcriptional Expression of *ISGs*

We found that the mRNA expression levels of *ZAP*, *MX2*, *MX1*, *PKR*, *OASL*, and *ISG15* were significantly higher in the Lp-1s treated group than in the TGEV infected group at various points after infection. The expression levels of *ZAP*, *PKR*, *OASL*, and *ISG15* in each experimental group increased with time. The expression levels of *MX1* and *MX2* peaked at 24 h and then decreased at 48 h (**Figures 7A–F**). The results showed that the best time to STAT1-siRNA targeting gene silencing STAT1 was 48 h (**Figure 7G**), and the best interference fragment was STAT1-siRNA1 (**Figure 7H**). After gene silencing STAT1, we found that the expression of ISGs decreased compared to the groups which no knock down STAT1, and the expression ISGs of Lp-1s-treated TGEV infected group was higher than that of TGEV infected alone group (**Figures 7I–N**). The results showed that TGEV infection of IPEC-J2 cells treated with Lp-1s could stimulate the expression of *ISGs* in cells to inhibit viral replication.

## Proteins Levels of ZAP, PKR, and p-PKR

As expected, the protein levels of ZAP, PKR, p-PKR (**Figures 8A–D**) at 24, and 48 hpi in the Lp-1s group were significantly higher than those in negative control group and TGEV group (ZAP, *$P < 0.05$ and PKR, **$P < 0.01$). There was

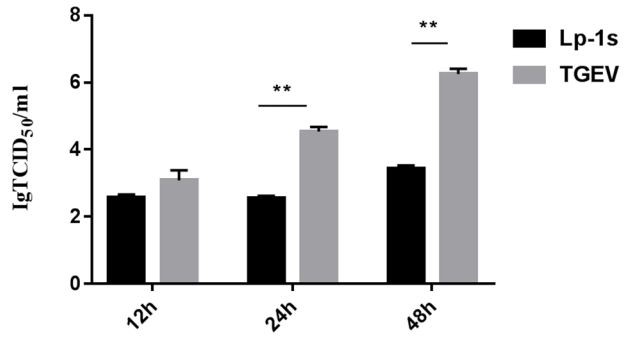


**FIGURE 2 |** $TCID_{50}$ analysis. The results of statistical analysis showed that the 24 h and 48 h Lp-1s supernatant treatment groups had significantly different $TCID_{50}$ values compared with that of the simultaneous TGEV challenge group (**$P < 0.01$) demonstrating that IPEC-J2 had a reduced viral titer of the TGEV Miller strain after treatment with Lp-1s.

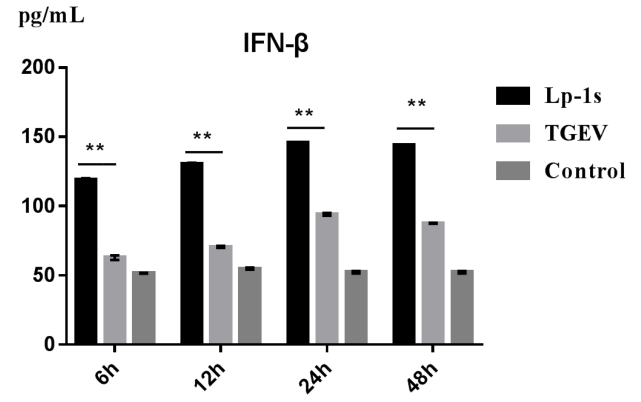


**FIGURE 4 |** Changes in IFN-β levels induced by cells in different groups. Lp-1s, Lp-1s pretreatment of IPEC-J2 cells infected with TGEV; TGEV, cells directly infected with TGEV; Con, uninfected cells (normal group). There were significant differences in IFN-β levels between the TGEV group and the Lp-1s group at different time points (**$P < 0.01$).

no significant change in the relative expression of p-PKR/PKR, however, the expression level of p-PKR protein varied with the amount of PKR protein. The level of STAT-1 in **Figure 8E** where the expression of this gene was knocked down using siRNA is significantly lower than the level of unknocked down STAT1 in **Figure 5A**. After gene silencing STAT1, the protein levels of STAT1, p-STAT1 ZAP, PKR, p-PKR (**Figures 8E–H**) at 12, 24, and 48 hpi in the Lp-1s group were significantly higher than TGEV group (p-STAT1/STAT1, *$P < 0.05$; ZAP, *$P < 0.05$; and p-PKR/PKR, *$P < 0.05$). The results showed that Lp-1s could

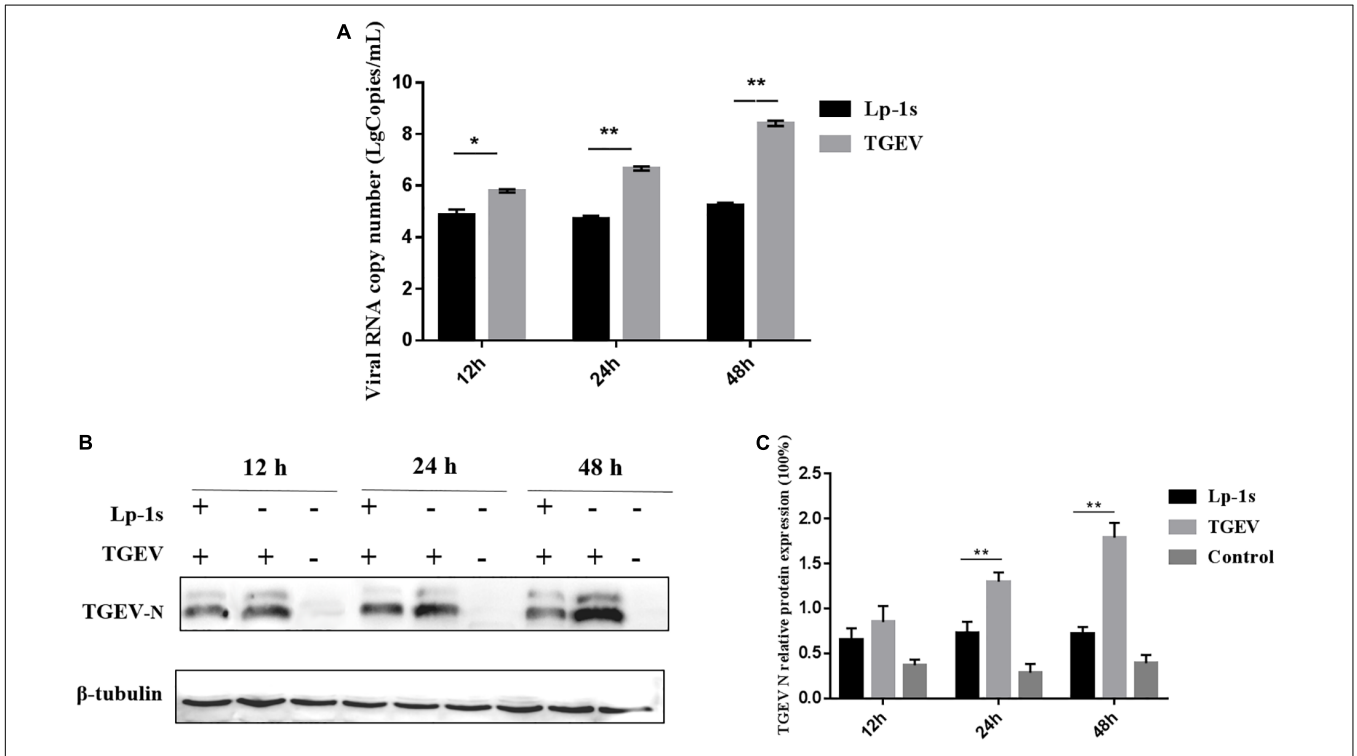


**FIGURE 3 |** Time course of TGEV N gene and protein expression. **(A)** TGEV N gene copy number in different groups of cells infected with TGEV for 12, 24, and 48 h. The TGEV N gene copy number was significantly different between the TGEV group and the TGEV group after treatment with Lp-1s for 12 h (*$P < 0.05$). The TGEV group and the TGEV group with Lp-1s treatment infected for 24 and 48 h showed a significant difference (**$P < 0.01$). **(B)** Western blotting detection of TGEV N protein levels at different time points after infection of TGEV in Lp-1s-treated cells. **(C)** Grayscale analysis of TGEV N protein levels at different time points after infection of TGEV by Lp-1s treated cells. There was no significant difference between the two groups ($P > 0.05$) at 12 h; however, the difference was extremely significant at 24 and 48 h (**$P < 0.01$). Lp-1s, Lp-1s pretreatment of IPEC-J2 cells infected with TGEV; TGEV, cells directly infected with TGEV.

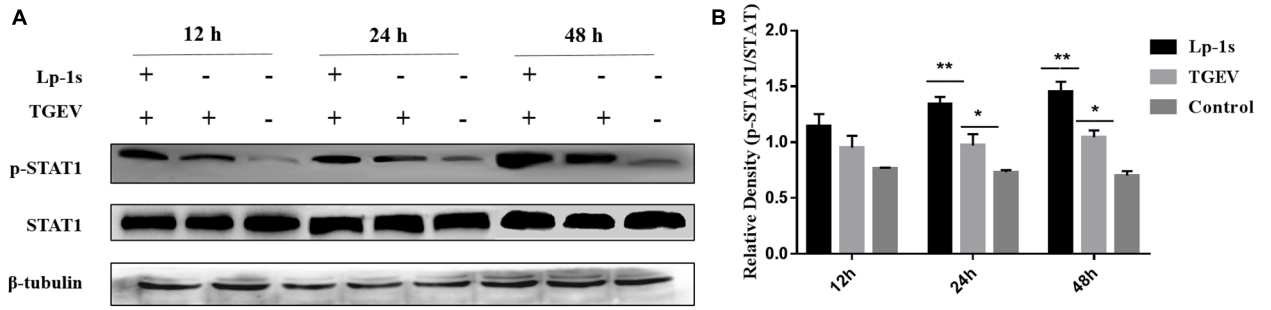


**FIGURE 5 |** Western blotting detection of p-STAT1 and STAT1 levels in different groups. Lp-1s, Lp-1s pretreatment of IPEC-J2 cells infected with TGEV; TGEV, cells directly infected with TGEV; Con, uninfected cells (normal group). **(A)** STAT1 total protein levels and phosphorylated STAT1 levels at 12–48 h. **(B)** Grayscale analysis of the levels of phosphorylated STAT1 in the different groups. Statistical analysis showed that the level of phosphorylated STAT1 was higher in the Lp-1s group than in the TGEV group after 12 h ($P > 0.05$); after 24 h of Lp-1s treatment, the level of phosphorylated STAT1 in the Lp-1s group was significantly higher than that in the TGEV group (**$P < 0.01$); after 48 h of Lp-1s treatment, the level of phosphorylated STAT1 in the Lp-1s group was significantly higher than that in the TGEV group (*$P < 0.05$). The results showed that treatment of TGEV-infected IPEC-J2 cells with Lp-1s (24–48 h), induced increased of levels of phosphorylated intracellular STAT1.

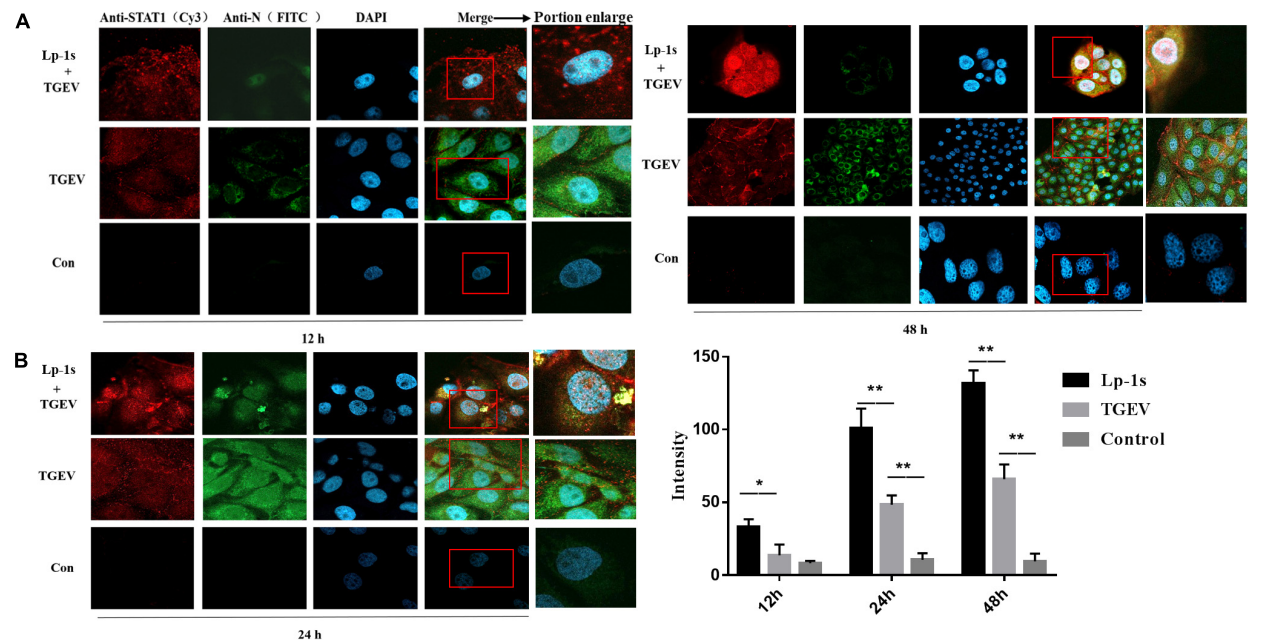


**FIGURE 6 |** Identification of nuclear translocation in porcine p-STAT by IFA (magnification: 63×). Lp-1s, Lp-1s pretreatment of IPEC-J2 cells infected with TGEV; TGEV, cells directly infected with TGEV; Con, uninfected cells (normal group). **(A)** Anti-pSTAT1 (Cy3), goat anti-rabbit IgG Cy3 labeled p-STAT1 protein; Anti-TGEV N (FITC), goat anti-mouse IgG FITC labeled TGEV N protein; DAPI, DAPI nuclear staining; Merge, fused image of the three fluorescent images. **(B)** The nucleus was identified using Zen blue software and the intensity of red fluorescence emitted by Cy3-labeled p-STAT1 was analyzed. The statistical results showed that the fluorescence intensity of Cy3 in IPEC-J2 cells treated with Lp-1s was significantly higher than that in the TGEV group after 12 h (*$P < 0.05$). In the late stage of TGEV infection (24–48 h), the fluorescence signal intensity of p-STAT1 in the nucleus of this group was significantly higher than that in TGEV group (**$P < 0.01$).

increase the expression of *ISGs* and inhibit the replication of TGEV in IPEC-J2 cells, which was basically consistent with the expression trend of the *PKR* and *ZAP* genes.

## DISCUSSION

Previous studies have found that many lactic acid bacteria can inhibit the infection of diarrhea-causing viruses (such as RV and PEDV) in the host through a variety of methods (Hou et al., 2007; Kawakami et al., 2010). Some lactic acid bacteria can be recognized by Toll like receptor (TLR)-2 or TLR-9 to enhance their response to stimulation by the interferon inducer poly (I: C) and induce a large amount of IFN-I (Maeda et al., 2009; Kanmani and Kim, 2018; Lee et al., 2019). At the same time, they can also upregulate the transcription of *IL6* and *TNFA* (Reyes-Diaz et al., 2018). In addition, some lactic acid bacteria can enhance the expression of surface molecules and cytokines in intestinal

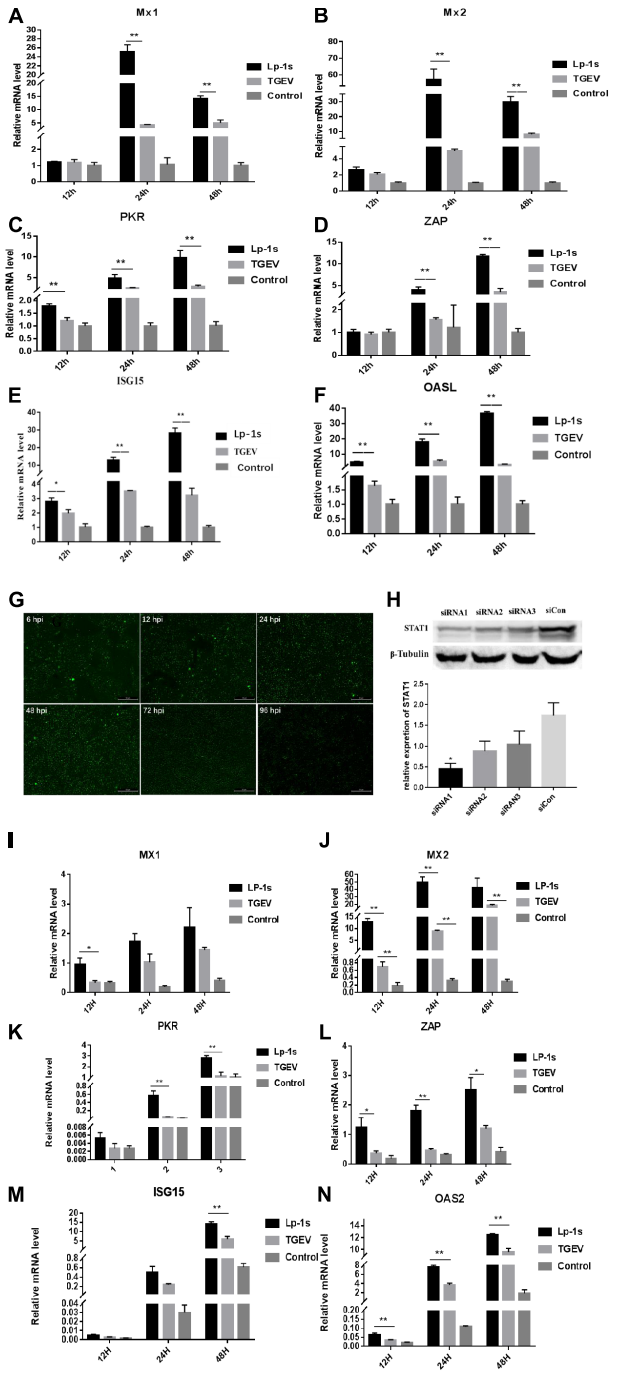


**FIGURE 7 |** Relative mRNA expression levels of *ISGs* in different experimental groups. Lp-1s, Lp-1s pretreatment of IPEC-J2 cells infected with TGEV; TGEV, cells directly infected with TGEV; Con, uninfected cells (normal group). **(A–F)** Relative mRNA expression levels of *MX1*, *MX2*, *PKR*, *ZAP*, *ISG15*, and *OASL*, respectively. The expression levels of *ZAP*, *MX2*, and *MX1* in Lp-1s group after 12 h were not significantly different from those in the TGEV group ($P > 0.05$). The expression level of *ISG15* was significantly higher in the Lp-1s group than in the TGEV group (*$P < 0.05$). The expression levels of *PKR* and *OASL* were significantly higher in the Lp-1s group than in the TGEV group (**$P < 0.01$). The expression levels of *ZAP*, *MX2*, *MX1*, *PKR*, *OASL*, and *ISG15* in the Lp-1s group after 24 and 48 h were significantly higher than *(Continued)*

**FIGURE 7 |** Continued
those in the TGEV group (**$P < 0.01$). **(G,H)** Screening of siRNA targeting STAT1 optimal treatment time and gene silencing efficiency fragment. As shown in the figure, the optimal time for siRNA targeting STAT1 is 48 h, and the best gene silencing siRNA fragment is siRNA1 (*$P < 0.05$). **(I–N)** Relative mRNA expression levels of *MX1*, *MX2*, *PKR*, *ZAP*, *ISG15*, and *OASL*, respectively, after targeting gene silencing STAT1. The expression levels of *PKR* and *OASL* in Lp-1s group after 12 h were not significantly different from those in the TGEV group ($P > 0.05$). The expression level of *MX2*, *PKR*, *ZAP*, *ISG15*, and *OASL* was significantly higher in the Lp-1s group after 24 h than in the TGEV group (*$P < 0.05$ and **$P < 0.01$). The expression levels of *ZAP*, *ISG15* and *OASL* were significantly higher in the Lp-1s group after 48 h than in the TGEV group (*$P < 0.05$ and **$P < 0.01$).

antigen presenting cells (APC), and enhance the molecular expression of MHC-II and IL-1β (Villena et al., 2014). In addition, other lactic acid bacteria can also stimulate the response level of TLR-3 to poly (I: C) (Hosoya et al., 2011). They can also regulate the role of TLR-2, TLR-4, and TLR negative regulators in the immune response, further enhancing the production of IFN-I induced by cells, and upregulate the transcription level of related antiviral factors (such as *MXA* and *OASL*) (Castillo et al., 2011). Other studies have shown that probiotics can inhibit TGEV infection by adsorbing virus particles and stimulating cells to produce innate immunity (Chai et al., 2013).

Recent studies have shown that the main reasons why the body's interferon-beta (IFN-β) cannot fully exert its antiviral effect after TGEV infection are as follows: First, the cells do not respond in time to the immune response because of the level of viral replication and the virus titer of TGEV in the early stage of infection, resulting in lower levels of IFNs, which is the main cause of the short burst of TGEV latency (Zhu et al., 2017). Second, IFN-β does not play a direct antiviral role. Its antiviral function is produced by activating the IFN-mediated JAK-STAT signaling pathway to stimulate downstream interferon-stimulating genes *(ISGs)* (Saha and Pahan, 2006; Li, 2008; Proia et al., 2011). And, activation of the JAK-STAT1 signaling pathway requires Phosphorylated STAT1 (Tyr 701) enters the nucleus to activate interferon-stimulating factors *ISGs* (including MX1, MX2, PKR, OAS, ISG15, and ZAP) (Hovanessian, 1991; Zhu et al., 1997; Shi et al., 2010; Goujon et al., 2013; Amici et al., 2015; Li et al., 2015; Nigg and Pavlovic, 2015). ZAP can bind viral RNA directly and prevent the accumulation of viral RNA in the cytoplasm. It can also recruit RNA exosomes to degrade target viral RNA (Li et al., 2015). PKR-mediated inhibition of viral replication is activated by the formation of dsRNA during the replication of single-stranded RNA after viruses invade cells. The main reason is that the amino terminus of PKR can recognize the dsRNA domain and the carboxyl terminus has the kinase domain. When the viral double-stranded RNA is recognized, the inactive PKR protein located in the cytoplasm is phosphorylated. On the other hand, it can also regulate the cell immune response and autophagy caused by virus invasion to inhibit the virus. At the same time, PKR can activate the nuclear factor kappa B (NF-kB) signaling pathway via phosphorylation and further induce IFN production in cells (Sudhakar et al., 2000; Amici et al., 2015).

In the present study, we found that IPEC-J2 cells still produced IFN-β after infection with TGEV, which increased with time,

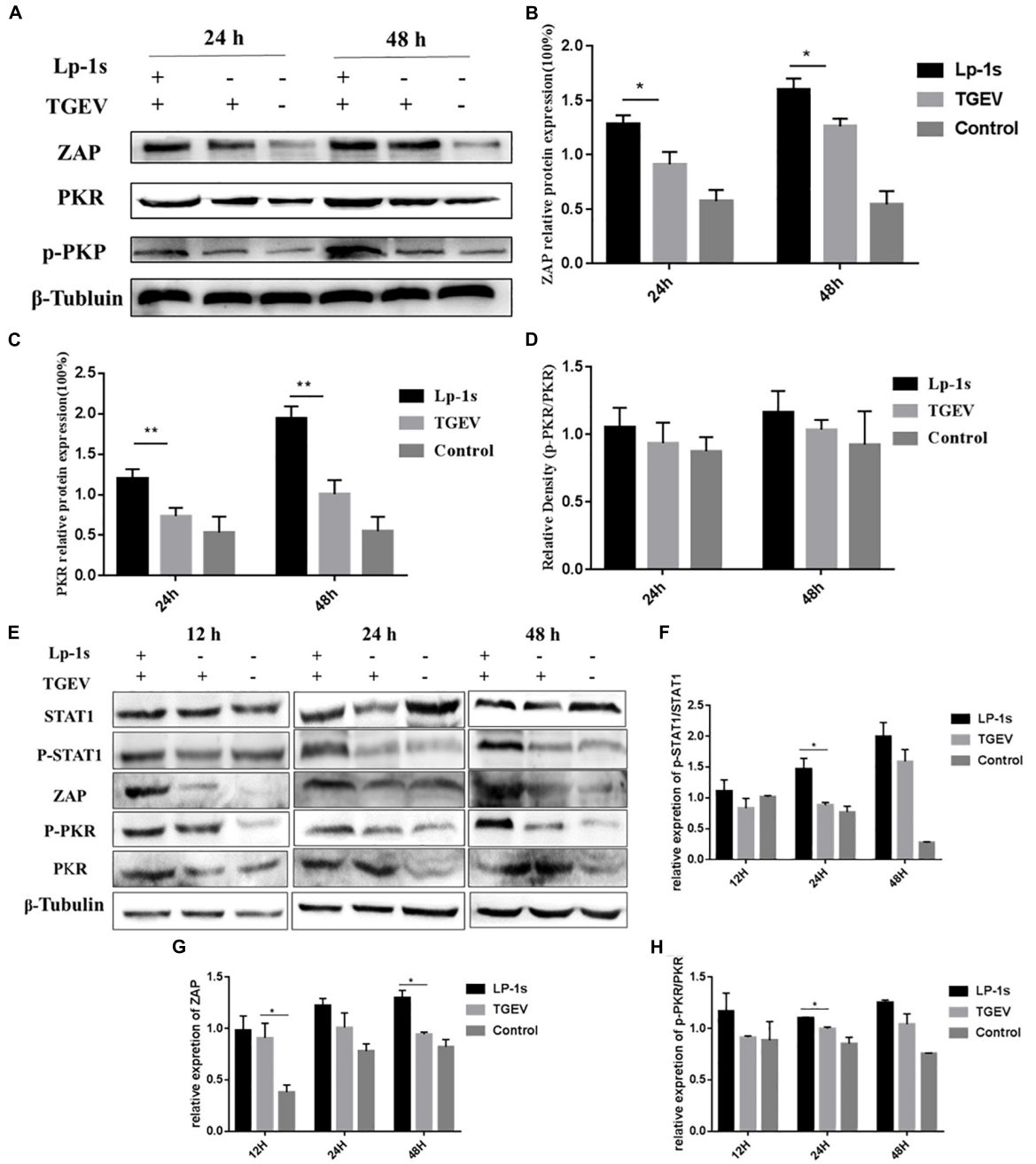


**FIGURE 8 |** Protein levels of ZAP, PKR and p-PKR in different experimental groups. Lp-1s, Lp-1s pretreatment of IPEC-J2 cells infected with TGEV; TGEV, cells directly infected with TGEV; Con, Uninfected cells (normal group). **(A)** The expression of ZAP, PKR, p-PKR, and β-Tubulin protein. **(B)** Grayscale analysis of the ZAP/β-Tubulin results. The ZAP level of Lp-1s treatment group was significantly higher than TGEV infected alone at 24 and 48 h (*$P < 0.05$). **(C)** Grayscale analysis of the PKR/β-Tubulin ratio. The ratio of PKR/β-Tubulin in the Lp-1s group was significantly higher after 48 h compared with that in the TGEV group (**$P < 0.01$). **(D)** Grayscale analysis of the p-PKR/PKR ratio. There was no significant difference in the p-PKR/PKR ratio at the different time points ($P > 0.05$). **(E–H)** The expression of STAT1, p-STAT1, ZAP, PKR, and p-PKR proteins after silencing STAT1. **(E)** The expression of STAT1, p-STAT1, ZAP, PKR, p-PKR, and β-Tubulin protein. **(F)** Relative expression of p-STAT1/STAT1 in Lp-1s treatment group was significantly higher than TGEV infected alone at 24 h (*$P < 0.05$). **(G)** Relative expression of ZAP in Lp-1s treatment group was significantly higher than TGEV infected alone at 48 h (*$P < 0.05$). **(H)** Relative expression of p-PKR/PKR in Lp-1s treatment group was significantly higher than TGEV infected alone at 24 h (*$P < 0.05$).

reaching a peak at 24 h and no longer increased at 48 h. At the corresponding time points, the level of infection, viral titer, and replication of TGEV on IPEC-J2 cells showed an increasing trend.

After Lp-1s treatment, IPEC-J2 cells produced a large amount of IFN-β at the early stage of TGEV infection (6 h), which was significantly higher than that of cells infected with TGEV only.

The induced level of IFN-β in Lp-1s-treated IPEC-J2 cells was significantly different from that in the TGEV infected group at the same time point. The induction level of IFN-β in the Lp-1s treated group was significantly higher than that in TGEV infected group at the different time points. The level of IFN-β induction correlated positively with time, peaking at 24 h before decreasing toward 48 h. The early boost in IFN-β production in IPEC-J2 cells treated with Lp-1s might be one of the reasons for its inhibition of TGEV.

In addition, although TGEV delayed the expression of IFN-β in the early stage of infection, it promoted the expression of IFN-β at the peak of viral replication. The expression of IFN-β was parallel to the increase of viral RNA replication level at 24–48h, which demonstrated that TGEV replication remained high in the late stage of infection when IFN-β was produced in large quantities. This might be caused by the inhibitory effect of TGEV on IFN-β-mediated signaling pathways, resulting in the inability of IFN-β to regulate the transcription and expression of downstream target cytokines and exert an antiviral role.

Although there was no significant difference in the levels of p-STAT1 between the Lp-1s group and the TGEV group at 12 hpi, the level of p-STAT1 in the Lp-1s group was significantly higher than that in the TGEV group at the later stages (24 and 48 h). The level of p-STAT1 in the Lp-1s group correlated positively with time from 12–48 h. The results showed that IPEC-J2 cells treated with Lp-1s could effectively increase STAT1 phosphorylation in the late stage of virus infection. At the same time, the level of p-STAT1 changed slightly from 12–48 h after infection with TGEV. The results were quite different from those reported in previous studies on the infection of ST cells by TGEV. In addition, the level of p-STAT1 in IPEC-J2 cells infected with TGEV from 24–48 h was significantly lower than that in ST cells infected with TGEV from 24–48 h, which might reflect the difference between the cell lines and viruses used.

Further experiments showed that the level p-STAT1 nuclear translocation in the Lp-1s group was significantly higher than that in the TGEV group at the same time points, and p-STAT1 nuclear accumulation correlated positively with time. In TGEV-infected cells, p-STAT1 at the late stage of infection (24–48 h) accumulated in large amounts near the cell membrane and only a few nuclear translocations occurred. We speculated that the reason might be that the intracellular STAT1 protein is activated by IFN-β after IPEC-J2 cells are directly infected with TGEV to form a homologous or heterodimer, and the virus interacts with its receptor IRF9. The interaction resulted in the inability of activated STAT1 to undergo nuclear translocation through receptor-induced endocytosis, and could only dissociate around IFNAR, which reduced the JAK-STAT signaling pathway cascade response and antagonized the antiviral effect of IFN-β. The fluorescence value of activated STAT1 was significantly higher than that of blank control group. This indicated that TGEV could not completely escape the immune mechanism of IFN-β

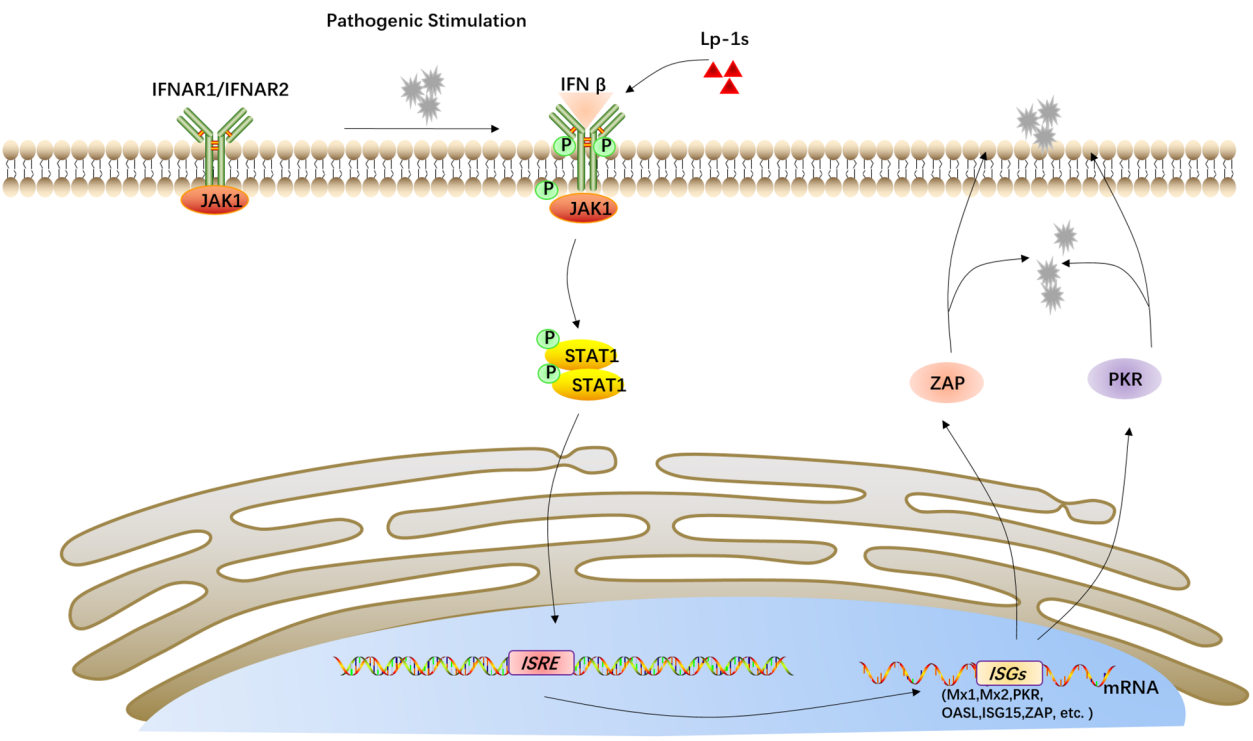


**FIGURE 9 |** Proposed mechanism of the anti-TGEV effect of Lp-1s. Lp-1s increases IFN-β expression, and the binding of IFN-β to its receptor IFNAR leads to activation of the Janus family kinase (JAK) and subsequent activation of signal transduction and transcriptional activator 1 (STAT1) signaling cascades. These signaling pathways upregulate downstream interferon-stimulated genes (*ISGs*), including *MX1*, *MX2*, *PKR*, *OAS*, *ISG15*, and *ZAP*), which produce the corresponding antiviral proteins, e.g., ZAP and PKR, ultimately activating IFN-β to exert an antiviral effect.

production in IPEC-J2 cells. At the same time, the fluorescence intensity of p-STAT in the nucleus of the cells in the Lp-1s treatment group correlated positively with time, and the intensity of FITC-labeled TGEV N protein was significantly lower than that in the TGEV treatment group at the same time point. These results showed that IPEC-J2 cells treated with Lp-1s could indeed activate the JAK-STAT1 signaling pathway when infected with TGEV, and the intensity of JAK-STAT1 signaling pathway was significantly higher in the Lp-1s-treated cells than in the cells directly infected with TGEV. As the signaling pathway cascade response increased, the replication level of TGEV in IPEC-J2 cells was further inhibited.

Finally, the transcriptional levels of *ISGs* in the Lp-1s treatment group were different at different time points. *MX1* and *MX2* reached their peak at 24 h, while the transcriptional levels of the two *ISGs* decreased at 48 h after TGEV infection. The transcription levels of *PKR*, *ZAP*, OASL and *ISG15* were positively correlated in groups. We speculated that the decrease in *MX1* and *MX2* mRNA transcription levels within 48 h after Lp-1s treatment might be related to the cycle of infected cells. The expression of *ISGs* of gene silenced STAT1 decreased as a whole compared to the groups which no knock down STAT1, indicating that STAT1 could affect downstream *ISGs*. While the *ISGs* of TGEV infected group treated with Lp-1s showed an upward trend, which further confirmed that Lp-1s could activate downstream *ISGs*. To further explore the difference in the intracellular response of Lp-1s treated IPEC-J2 cells to TGEV infection, we detected the changes in ZAP and PKR protein levels. The level of the ZAP protein in the Lp-1s and TGEV groups was consistent with its transcription level at the time point. Although the level of the ZAP protein in Lp-1s treated cells was significantly higher than that in the TGEV infection group, the difference in the transcription level of *ZAP* was significantly lower than that in the TGEV infection group. These results suggested that after Lp-1s treatment, the IFN-β and JAK-STAT1 signaling pathways induced in the cells are enhanced, and the expression of the ZAP protein is still limited, suggesting that other factors have an impact on the transcriptional regulation of ZAP. The protein level of PKR was consistent with its mRNA transcription level. There was no significant difference in the p-PKR/PKR values between the two groups at 24 and 48 h; however, the p-PKR/β-tubulin protein values were in line with our expectations. The results showed that the p-PKR level in the Lp-1s group was significantly higher than that in the TGEV group, and correlated positively with time. Therefore, we believe that the increase in p-PKR is mainly determined by the expression of the PKR protein.

Based on the above results, Lp-1s plays an antiviral role by stimulating the IFN-β-mediated JAK1/STAT pathway, resulting in upregulation interferon-stimulating genes, which induce the synthesis of antiviral proteins such as ZAP and PKR (**Figure 9**).

## DATA AVAILABILITY STATEMENT

The datasets generated for this study are available on request to the corresponding author.

## AUTHOR CONTRIBUTIONS

KW and ZS conceived and designed the experiments. KW, LR, and TY performed the experiments. ZN, ZK, YZ, YY, LX, SH, QY, and DW analyzed the data. LR and ZS wrote the manuscript.

## FUNDING

This work was supported by the Fundamental Research Funds for the Central Universities (XDJK2018B023), and the Chongqing Basic Research Program (CYS19137).

## ACKNOWLEDGMENTS

The authors gratefully acknowledge Peng Yuan, Zhou Yang, and other veterinary medicine students from the Southwest University for their valuable suggestions and assistance.

## REFERENCES

Amici, C., La Frazia, S., Brunelli, C., Balsamo, M., Angelini, M., and Santoro, M. G. (2015). Inhibition of viral protein translation by indomethacin in vesicular stomatitis virus infection: role of eIF2alpha kinase PKR. *Cell Microbiol.* 17, 1391–1404. doi: 10.1111/cmi.12446

Castillo, N. A., Perdigon, G., and de Moreno de Leblanc, A. (2011). Oral administration of a probiotic *Lactobacillus* modulates cytokine production and TLR expression improving the immune response against *Salmonella enterica* serovar Typhimurium infection in mice. *BMC Microbiol.* 11:177. doi: 10.1186/1471-2180-11-177

Chai, W., Burwinkel, M., Wang, Z., Palissa, C., Esch, B., Twardziok, S., et al. (2013). Antiviral effects of a probiotic *Enterococcus* faecium strain against transmissible gastroenteritis coronavirus. *Arch. Virol.* 158, 799–807. doi: 10.1007/s00705-012-1543-0

Chen, J., Xu, W., Chen, Y., Xie, X., Zhang, Y., Ma, C., et al. (2017). Matrix metalloproteinase 9 facilitates hepatitis B virus replication through binding with type I interferon (IFN) receptor 1 to repress IFN/JAK/STAT signaling. *J. Virol.* 91:e1824-16. doi: 10.1128/JVI.01824-16

da Silva Sabo, S., Perez-Rodriguez, N., Dominguez, J. M., and de Souza Oliveira, R. P. (2017). Inhibitory substances production by *Lactobacillus plantarum* ST16Pa cultured in hydrolyzed cheese whey supplemented with soybean flour and their antimicrobial efficiency as biopreservatives on fresh chicken meat. *Food Res. Int.* 99, 762–769. doi: 10.1016/j.foodres.2017.05.026

Fuller, R. (1989). Probiotics in man and animals. *J. Appl. Bacteriol.* 66, 365–378. doi: 10.1111/j.1365-2672.1989.tb05105.x

Goujon, C., Moncorge, O., Bauby, H., Doyle, T., Ward, C. C., Schaller, T., et al. (2013). Human MX2 is an interferon-induced post-entry inhibitor of HIV-1 infection. *Nature* 502, 559–562. doi: 10.1038/nature12542

Hosoya, S., Villena, J., Shimazu, T., Tohno, M., Fujie, H., Chiba, E., et al. (2011). Immunobiotic lactic acid bacteria beneficially regulate immune response triggered by poly(I:C) in porcine intestinal epithelial cells. *Vet Res.* 42, 111. doi: 10.1186/1297-9716-42-111

Hou, X. L., Yu, L. Y., Liu, J., and Wang, G. H. (2007). Surface-displayed porcine epidemic diarrhea viral (PEDV) antigens on lactic acid bacteria. *Vaccine.* 26, 24–31. doi: 10.1016/j.vaccine.2007.10.065

Hovanessian, A. G. (1991). Interferon-induced and double-stranded RNA-activated enzymes: a specific protein kinase and 2′,5′-oligoadenylate synthetases. *J. Interferon Res.* 11, 199–205. doi: 10.1089/jir.1991.11.199

Kanmani, P., and Kim, H. (2018). Protective effects of lactic acid bacteria against TLR4 induced inflammatory response in hepatoma HepG2 cells through modulation of toll-like receptor negative regulators of mitogen-activated protein Kinase and NF-kappaB signaling. *Front. Immunol.* 9:1537. doi: 10.3389/fimmu.2018.01537

Kawakami, S. I., Yamada, T., Nakanishi, N., and Cai, Y. M. (2010). Feeding of lactic acid bacteria and yeast on growth and diarrhea of Holstein Calves. *J. Anim. Vet. Adv.* 9, 1112–1114. doi: 10.3923/javaa.2010.1112.1114

Kawashima, T., Hayashi, K., Kosaka, A., Kawashima, M., Igarashi, T., Tsutsui, H., et al. (2011). *Lactobacillus plantarum* strain YU from fermented foods activates Th1 and protective immune responses. *Int. Immunopharmacol.* 11, 2017–2024. doi: 10.1016/j.intimp.2011.08.013

Lee, B. M., Han, Y. W., Kim, S. B., Rahman, M. M., Uyangaa, E., Kim, J. H., et al. (2011). Enhanced protection against infection with transmissible gastroenteritis virus in piglets by oral co-administration of live attenuated *Salmonella enterica* serovar Typhimurium expressing swine interferon-alpha and interleukin-18. *Comp. Immunol. Microbiol. Infect Dis.* 34, 369–380. doi: 10.1016/j.cimid.2011.05.001

Lee, E. S., Song, E. J., Nam, Y. D., and Lee, S. Y. (2018). Probiotics in human health and disease: from nutribiotics to pharmabiotics. *J. Microbiol.* 56, 773–782. doi: 10.1007/s12275-018-8293-y

Lee, J., Jung, I., Choi, J. W., Lee, C. W., Cho, S., Choi, T. G., et al. (2019). Micronized and heat-treated *Lactobacillus plantarum* LM1004 stimulates host immune responses Via the TLR-2/MAPK/NF-kappaB signalling pathway in vitro and in vivo. *J. Microbiol. Biotechnol.* 29, 704–712. doi: 10.4014/jmb.1812.12059

Li, M., Yan, K., Wei, L., Yang, J., Lu, C., Xiong, F., et al. (2015). Zinc finger antiviral protein inhibits coxsackievirus B3 virus replication and protects against viral myocarditis. *Antiviral. Res.* 123, 50–61. doi: 10.1016/j.antiviral.2015.09.001

Li, W. X. (2008). Canonical and non-canonical JAK-STAT signaling. *Trends Cell Biol.* 18, 545–551. doi: 10.1016/j.tcb.2008.08.008

Maeda, N., Nakamura, R., Hirose, Y., Murosaki, S., Yamamoto, Y., Kase, T., et al. (2009). Oral administration of heat-killed *Lactobacillus plantarum* L-137 enhances protection against influenza virus infection by stimulation of type I interferon production in mice. *Int. Immunopharmacol.* 9, 1122–1125. doi: 10.1016/j.intimp.2009.04.015

Maragkoudakis, P. A., Chingwaru, W., Gradisnik, L., Tsakalidou, E., and Cencic, A. (2010). Lactic acid bacteria efficiently protect human and animal intestinal epithelial and immune cells from enteric virus infection. *Int. J. Food Microbiol.* 141(Suppl. 1), S91–S97. doi: 10.1016/j.ijfoodmicro.2009.12.024

Masters, P. S. (2006). The molecular biology of coronaviruses. *Adv. Virus Res.* 66, 193–292. doi: 10.1016/S0065-3527(06)66005-3

Nigg, P. E., and Pavlovic, J. (2015). Oligomerization and GTP-binding requirements of MxA for viral target recognition and antiviral activity against influenza a virus. *J. Biol. Chem.* 290, 29893–29906. doi: 10.1074/jbc.M115.681494

Pollmann, M., Nordhoff, M., Pospischil, A., Tedin, K., and Wieler, L. H. (2005). Effects of a probiotic strain of *Enterococcus* faecium on the rate of natural chlamydia infection in swine. *Infect Immun.* 73, 4346–4353. doi: 10.1128/IAI.73.7.4346-4353.2005

Proia, D. A., Foley, K. P., Korbut, T., Sang, J., Smith, D., Bates, R. C., et al. (2011). Multifaceted intervention by the Hsp90 inhibitor ganetespib (STA-9090) in cancer cells with activated JAK/STAT signaling. *PLoS One.* 6:e18552. doi: 10.1371/journal.pone.0018552

Reyes-Diaz, A., Mata-Haro, V., Hernandez, J., Gonzalez-Cordova, A. F., Hernandez-Mendoza, A., Reyes-Diaz, R., et al. (2018). Milk fermented by specific *Lactobacillus* strains regulates the serum levels of IL-6, TNF-alpha and IL-10 cytokines in a LPS-stimulated murine model. *Nutrients* 10, E691. doi: 10.3390/nu10060691

Saha, R. N., and Pahan, K. (2006). Regulation of inducible nitric oxide synthase gene in glial cells. *Antioxid Redox Signal.* 8, 929–947. doi: 10.1089/ars.2006.8.929

Scharek, L., Guth, J., Filter, M., and Schmidt, M. F. (2007). Impact of the probiotic bacteria *Enterococcus* faecium NCIMB 10415 (SF68) and Bacillus cereus var. toyoi NCIMB 40112 on the development of serum IgG and faecal IgA of sows and their piglets. *Arch. Anim. Nutr.* 61, 223–234. doi: 10.1080/17450390701431540

Shi, H. X., Yang, K., Liu, X., Liu, X. Y., Wei, B., Shan, Y. F., et al. (2010). Positive regulation of interferon regulatory factor 3 activation by Herc5 via ISG15 modification. *Mol. Cell Biol.* 30, 2424–2436. doi: 10.1128/MCB.01466-09

Song Han, T. L., Li, W., Wei, D., Peng, Y., Zhou, Y., and Zhenhui, S. (2017). Identification of a intestinal probiotic strain from piglets and preliminary study on the strain against the proliferation of TGEV in vitro. *Heilongjiang Animal Husbandry and Veterinary* 17, 178–181.

Stofilova, J., Langerholc, T., Botta, C., Treven, P., Gradisnik, L., Salaj, R., et al. (2017). Cytokine production in vitro and in rat model of colitis in response to *Lactobacillus plantarum* LS/07. *Biomed Pharmacother.* 94, 1176–1185. doi: 10.1016/j.biopha.2017.07.138

Sudhakar, A., Ramachandran, A., Ghosh, S., Hasnain, S. E., Kaufman, R. J., and Ramaiah, K. V. A. (2000). Phosphorylation of serine 51 in initiation factor 2 alpha (eIF2 alpha) promotes complex formation between eIF2 alpha(P) and eIF2B and causes inhibition in the guanine nucleotide exchange activity of eIF2B. *Biochemistry.* 39, 12929–12938. doi: 10.1021/bi0008682

Villena, J., Chiba, E., Vizoso-Pinto, M. G., Tomosada, Y., Takahashi, T., Ishizuka, T., et al. (2014). Immunobiotic *Lactobacillus* rhamnosus strains differentially modulate antiviral immune response in porcine intestinal epithelial and antigen presenting cells. *BMC Microbiol.* 14:126. doi: 10.1186/1471-2180-14-126

Yang, Z., Ran, L., Yuan, P., Yang, Y., Wang, K., Xie, L., et al. (2018). EGFR as a negative regulatory protein adjusts the activity and mobility of NHE3 in the cell membrane of IPEC-J2 cells With TGEV infection. *Front. Microbiol.* 9:2734. doi: 10.3389/fmicb.2018.02734

Yuan, L., Zhang, S., Wang, Y., Li, Y., Wang, X., and Yang, Q. (2018). Surfactin inhibits membrane fusion during invasion of epithelial cells by enveloped viruses. *J. Virol.* 92, e809–e818. doi: 10.1128/JVI.00809-18

Zhao, S., Gao, Q., Qin, T., Yin, Y., Lin, J., Yu, Q., et al. (2014). Effects of virulent and attenuated transmissible gastroenteritis virus on the ability of porcine dendritic cells to sample and present antigen. *Vet. Microbiol.* 171, 74–86. doi: 10.1016/j.vetmic.2014.03.017

Zhao, Y., Valbuena, G., Walker, D. H., Gazi, M., Hidalgo, M., DeSousa, R., et al. (2016). Endothelial cell proteomic response to rickettsia conorii infection reveals activation of the janus kinase (JAK)-signal transducer and activator of transcription (STAT)-interferon stimulated gene (ISG)15 pathway and reprogramming plasma membrane integrin/cadherin signaling. *Mol. Cell Proteomics.* 15, 289–304. doi: 10.1074/mcp.M115.054361

Zhu, L., Yang, X., Mou, C., and Yang, Q. (2017). Transmissible gastroenteritis virus does not suppress IFN-beta induction but is sensitive to IFN in IPEC-J2 cells. *Vet. Microbiol.* 199, 128–134. doi: 10.1016/j.vetmic.2016.12.031

Zhu, X., Wen, Z., Xu, L. Z., and Darnell, J. E. Jr. (1997). Stat1 serine phosphorylation occurs independently of tyrosine phosphorylation and requires an activated Jak2 kinase. *Mol. Cell Biol.* 17, 6618–6623. doi: 10.1128/mcb.17.11.6618

**Conflict of Interest:** The authors declare that the research was conducted in the absence of any commercial or financial relationships that could be construed as a potential conflict of interest.

*Copyright © 2019 Wang, Ran, Yan, Niu, Kan, Zhang, Yang, Xie, Huang, Yu, Wu and Song. This is an open-access article distributed under the terms of the Creative Commons Attribution License (CC BY). The use, distribution or reproduction in other forums is permitted, provided the original author(s) and the copyright owner(s) are credited and that the original publication in this journal is cited, in accordance with accepted academic practice. No use, distribution or reproduction is permitted which does not comply with these terms.*

frontiers in Microbiology

REVIEW
published: 06 December 2019
doi: 10.3389/fmicb.2019.02725

# Development of Small-Molecule Inhibitors Against Zika Virus Infection

*Lili Wang[1†], Ruiying Liang[2†], Yaning Gao[3†], Yanbai Li[2], Xiaoqian Deng[2], Rong Xiang[2], Yina Zhang[2], Tianlei Ying[4*], Shibo Jiang[4*] and Fei Yu[2*]*

*[1] Research Center of Chinese Jujube, Hebei Agricultural University, Baoding, China, [2] College of Life and Science, Hebei Agricultural University, Baoding, China, [3] Department of Natural Medicines, School of Pharmaceutical Sciences, Peking University, Beijing, China, [4] MOE/NHC/CAMS Key Laboratory of Medical Molecular Virology, School of Basic Medical Sciences, Shanghai Medical College, Fudan University, Shanghai, China*

In recent years, the outbreak of infectious disease caused by Zika virus (ZIKV) has posed a major threat to global public health, calling for the development of therapeutics to treat ZIKV disease. Here, we have described the different stages of the ZIKV life cycle and summarized the latest progress in the development of small-molecule inhibitors against ZIKV infection. We have also discussed some general strategies for the discovery of small-molecule ZIKV inhibitors.

**Keywords: Zika virus, life cycle, small-molecule inhibitor, treatment, mechanism**

OPEN ACCESS

***Edited by:***
*Lijun Rong,*
*University of Illinois at Chicago, United States*

***Reviewed by:***
*Gong Cheng,*
*Tsinghua University, China*
*Liying Ma,*
*China CDC NAIDS, China*

****Correspondence:***
*Tianlei Ying*
*tlying@fudan.edu.cn*
*Shibo Jiang*
*shibojiang@fudan.edu.cn*
*Fei Yu*
*shmyf@hebau.edu.cn*

*[†] These authors have contributed equally to this work*

***Specialty section:***
*This article was submitted to Virology, a section of the journal Frontiers in Microbiology*

***Received:*** *29 September 2019*
***Accepted:*** *08 November 2019*
***Published:*** *06 December 2019*

***Citation:***
*Wang L, Liang R, Gao Y, Li Y, Deng X, Xiang R, Zhang Y, Ying T, Jiang S and Yu F (2019) Development of Small-Molecule Inhibitors Against Zika Virus Infection. Front. Microbiol. 10:2725. doi: 10.3389/fmicb.2019.02725*

## INTRODUCTION

Zika virus (ZIKV) is an arthropod-borne virus (arbovirus) belonging to the family Flaviviridae and genus Flavivirus. As a single-stranded positive RNA virus, the genome of ZIKV is approximately 10 kb and encodes three structural proteins and seven non-structural proteins (Wang et al., 2016). In 1947, ZIKV was discovered and isolated from a sentinel Rhesus monkey in the Zika Forest of Uganda (Dick et al., 1952). However, it was only in 2015 that the first outbreak of ZIKV-caused diseases was reported in Brazil (Petersen et al., 2016) with more than one million cases. Since then, it rapidly spread to 84 countries around world, particularly in South America, rendering ZIKV a public health threat (Han and Mesplede, 2018; **Figure 1**).

Mild symptoms include fever, rash, headache, and joint pain, but the major concern involves the potential for severe neurological disorders, such as microcephaly, neurological disorders in newborns, meningo-encephalitis, Guillain–Barré syndrome, myelitis, and ocular abnormalities (Barros et al., 2018). Until now, neither a specific antiviral drug nor a vaccine has been developed to prevent or cure ZIKV infection. However, several well-characterized drug targets encoded by the virus, or presented in host cells, may help us prevent or treat ZIKV infection. In this review, we focus on current progress on the research and development of small-molecule ZIKV inhibitors, either viral or host cell inhibitors, targeting different stages of the ZIKV life cycle. Such data are essential to the design of drugs and drug delivery modalities against ZIKV and related viruses.

## ZIKV LIFE CYCLE AND POTENTIAL TARGETS FOR THE DEVELOPMENT OF SMALL-MOLECULE INHIBITORS AGAINST ZIKV INFECTION

The life cycle of ZIKV can be divided into four stages, including virus entry, genome replication, virus assembly, and release. Mature ZIKV particles first adhere to host cells by interacting with

**FIGURE 1 |** Summary of ZIKV morbidity statistics with country- and quarter-level panel data. The deeper the color, the higher the number of infected people.

specific receptors on host cells, such as DC-SIGN, AXL, Tyro, and TIM-1 (Musso and Gubler, 2016; Nowakowski et al., 2016; Meertens et al., 2017). Several proteins, including DC-SIGN and TIM as well as some TAM proteins that belong to the phosphatidylserine receptor family, have been reported to act as receptors for entry of dengue virus (DENV)(Lozach et al., 2005; Meertens et al., 2012; Perera-Lecoin et al., 2013). To determine whether these receptors are also involved in ZIKV entry, a series of transfected HEK293T cells expressing DC-SIGN, TIM-1, or a TAM family member (AXL or Tyro3) could be infected by ZIKV at varying degrees (Hamel et al., 2015). DC-SIGN consists of group II (calcium-dependent with single carbohydrate recognition domain) transmembrane C-type lectins that can interact through their carbohydrate recognition domains to bind carbohydrates to viral protein E (Zelensky and Gready, 2005; Cruz-Oliveira et al., 2015). DC-SIGN also plays an important role in flavivirus binding and the infection of myeloid cells (Navarro-Sanchez et al., 2003) as it mediates attachment of viral particles on the cell surface and facilitates their interaction with primary receptors on the host cell (Chen et al., 1997; Germi et al., 2002). Tyro3 and AXL belong to the TAM family, a group of three receptor protein tyrosine kinases that mediate the clearance of apoptotic cells (Lemke and Rothlin, 2008). AXL is expressed in astrocytes and microglia in the human brain development and mediates ZIKV infection of glial cells (Nowakowski et al., 2016; Meertens et al., 2017). AXL consisting of two different Gas6-binding epitopes, including the N-terminal Ig-like domain, and a second Ig domain exists in the dimeric form. Gas6, which is the ligand of AXL, connects ZIKV to glial cells. TIM-1, which is abundant on Th-2 T cells, mucosal epithelial cells, and mast cells, mediates the attachment of ZIKV particles on the cell surface to facilitate their interaction with AXL as well as the subsequent infection (Hamel et al., 2015). The availability of different entry receptors is likely to provide an evolutionary advantage for the virus, and, as a result, the virus is able to infect a wide range of human host cells.

After binding with host cells, ZIKV is internalized by clathrin-mediated endocytosis and traffics to $Rab5^{+}$ endosomes (Wang X. et al., 2017; Mottin et al., 2018). In the process of entering the host cell, AXL kinase activity is activated by the ZIKV/Gas6 complex, which downregulates interferon signaling and promotes infection. Then, the endosome membrane and virus envelope (E) are fused under the acidic environment of the endosome. The viral genomic RNA is then released into the cytoplasm (Wang X. et al., 2017; Mottin et al., 2018). In the process of virus entry, some inhibitors can block viral attachment, endocytosis, and fusion. The proteins E on ZIKV and the DC-SIGN, AXL, Tyro, and TIM-1 entry/adhesion factors on the host cell are involved in viral attachment, endocytosis, fusion, and entry (Hasan et al., 2017; Heinz and Stiasny, 2017; Shi and Gao, 2017). They all therefore serve as targets for the development of small molecule inhibitors. After virus entry, the genome of ZIKV is translated and cleaved into three structural proteins, including Capsid (C), Precursor of the

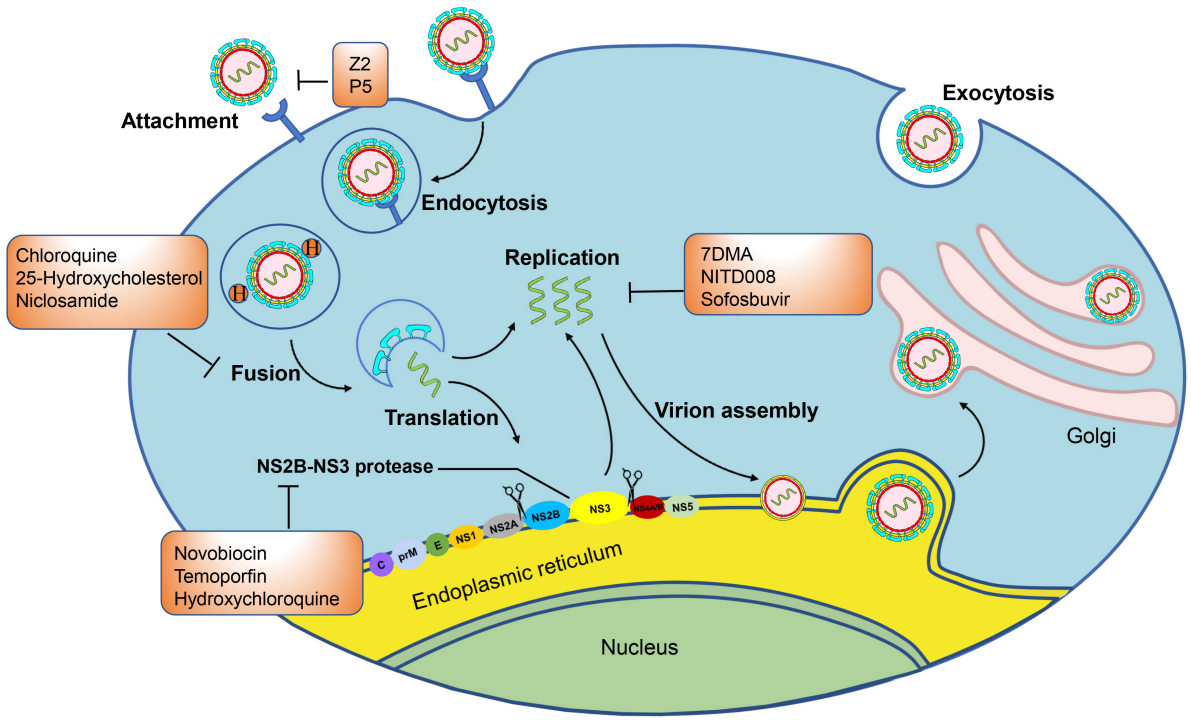


**FIGURE 2 |** Zika virus infectious life cycle: Host cell membrane receptors bind the E protein of the mature Zika virion, triggering endocytosis. The acidic environment of the endosome induces fusion of the host endosome membrane with the viral envelope and the release of the RNA genome. The RNA is translated into a polyprotein complex, which is cleaved by the host and viral proteases in the ER lumen and cytoplasm, respectively. Following translation, a replication complex is assembled and associated with virus induced membranes where viral replication takes place. The methylated (+) ssRNA, C, E, and prM proteins assemble to form immature virions in the endoplasmic reticulum (ER). The immature virions bud out of the ER into the Golgi apparatus, and they then mature in the trans-Golgi network that are released by exocytosis. In the orange boxes are the names of the compounds that can inhibit the marked steps of the virus lifecycle and that are evaluated in animal models or clinical trials.

membrane protein (prM)/membrane protein (M), Envelope (E), as well as seven non-structural proteins (NS1, NS2A, NS2B, NS3, NS4A, NS4B, and NS5). The NS1 protein is related to flavivirus replication and virion maturation. The NS2B protein activates the active region of the NS3 protein and forms an NS2B-NS3 complex with the NS3 protein to exert proteolytic enzyme activity. The NS4A and NS4B proteins comprise the endoplasmic reticulum (ER)-associated replication complex. The NS5 protein contains the C-terminal RNA-dependent RNA polymerase domain and the N-terminal methyltransferase domain, which cooperate during the initiation and extension of RNA synthesis. In addition, the NS5 protein is the largest NS protein in molecular weight and the most highly conserved. Then RNA is replicated with the actions of NS1, NS2B-NS3 proteinase and NS3 helicase, NS5 methyltransferase, and NS5RdRp. Viruses encode their own essential proteases in the viral replication process, which can serve as targets for therapeutic intervention. The methylated (+) ssRNA, C, E, and prM proteins are assembled to form immature virions in the ER. Then, the ER vesicles transport the virus particles to Golgi apparatus, and the virus particles undergo surface polysaccharide modification, prM-E protein trimer rearrangement, and Furin protease cleavage prM while mature virus particles with a smooth surface are produced, finally leaving the host cell by exocytosis as mature virus (**Figure 2**; Wang X. et al., 2017; Mottin et al., 2018). Some small molecule inhibitors that target the C protein or inhibit viral capsid formation are able to affect viral assembly and release. Meanwhile, correct expression and processing of nascent proteins in host cells are essential for efficient viral replication. Several host proteins, such as ER membrane complex, α-glucosidase, cyclophilin, and proteasome elements, are responsible for monitoring proper protein synthesis, folding, and degradation. Impairment of these functions results in reduced viral assembly and budding. Therefore, these host proteins may also serve as targets for the development of small molecule ZIKV inhibitors.

Most antiviral drugs are small-molecule inhibitors that target different stages of the viral life cycle by interacting with virus or host proteins critical for virus replication (De Clercq and Li, 2016). For example, inhibiting AXL function can protect cells from infection and, thus, may be a potential target for the production of entry inhibitors. However, destroying AXL function may also have many adverse consequences (Nowakowski et al., 2016). In addition, the proteases crucial for ZIKV replication are potential targets for developing ZIKV replication inhibitors. Therefore, more effective and appropriate targets need to be developed by researchers.

# CURRENT SMALL-MOLECULE INHIBITORS AGAINST ZIKV INFECTION AND THEIR MECHANISMS OF ACTION

## ZIKV Entry Inhibitors

### ZIKV Inhibitors Targeting Viral E Protein

The structure of ZIKV envelope protein (E protein) is similar to that of other flaviviruses, and it has three characteristic domains: a central β-barrel-shaped domain I, a Slender finger-like domain II, and a C-terminal immunoglobulin-like domain III (Dai et al., 2016). The recognition and binding of ZIKV E proteins to host cell receptors mark the beginning of ZIKV infection; therefore, some inhibitors designed for envelope proteins can effectively inhibit virus infection (Byrd et al., 2013).

Small molecule inhibitors that specifically target the ZIKV E protein have been reported. Peptide Z2 (**Table 1**), derived from the stem region of the ZIKV E protein, inhibits vertical transmission of ZIKV in pregnant C57BL/6 mice and protects type I or type I/II interferon receptor-deficient mice against lethal ZIKV challenge (Yu et al., 2017). Peptide Z2 can interact with viral E proteins to form a membrane pore and disrupt the integrity of the viral membrane (Yu et al., 2017). ZINC33683341 [**Figure 3**(1); Fernando et al., 2016], which can bind with the ZIKV E protein, is preferential when compared with glycan and can block the formation of glycoside bonds between ZIKV and host Vero cells at the concentration of 100 μM (**Table 2**; Fernando et al., 2016).

Some small molecule inhibitors that non-specifically target the ZIKV E protein were also active against other medically relevant viruses that use a similar route of entry. P5, a peptide extracted from the stem of Japanese encephalitis virus E protein, can inhibit ZIKV entry into host cells by changing the conformation of the E protein under low pH. The hydrophobicity of the last seven amino acid residues is also considered to be the key to the binding of the viral membrane (**Table 1**; Chen et al., 2017). *In vivo* experiments in mice highly sensitive to ZIKV showed that P5 can inhibit spermatic tubule disorder and reproductive epithelial cell degeneration while also alleviating the circulatory constriction of blood vessels (Chen et al., 2017).

The molecular tweezer CLR01, which has potent inhibition activity to envelope viruses, can inhibit ZIKV strains in Vero E6 cells [**Figure 3**(2) and **Table 2**] by destroying the intact membrane structure that is enriched with high levels of sphingolipid and cholesterol (Bavari et al., 2002; Chazal and Gerlier, 2003; Brugger et al., 2006; Lorizate et al., 2013; Rocker et al., 2018). In addition, it can inhibit ZIKV infection in semen, urine, saliva, cerebrospinal fluid, and other body fluids, but lose activity in serum (Rocker et al., 2018). Some studies have attributed this effect to the relatively high protein content in serum (Rocker et al., 2018).

Baicalin [**Figure 3**(3)], which has high affinity to the virus E protein and low toxicity to cells, can inhibit ZIKV from entering cells (**Table 2**; Oo et al., 2019). (-)-Epigallocatechin gallate (EGCG), a polyphenol from green tea, was shown to inhibit many viruses [**Figure 3**(4) and **Table 2**; Isaacs et al., 2008; Nance et al., 2009; Calland et al., 2012]. Accordingly, EGCG can bind to the ZIKV E protein to block ZIKV entry into host cells (Song et al., 2005). However, EGCG contains the catechol group that may non-specifically inhibit many different targets (Mottin et al., 2018). Curcumin can inhibit ZIKV infection in a dose-dependent manner [**Figure 3**(5)]. It is not only a replication inhibitor of ZIKV, but also prevents the viral E protein from

**TABLE 1 |** Zika virus peptide inhibitors.

| Inhibitor | Sequence | Testing model | Cell lines | $IC_{50}$ (μM) | $CC_{50}$ (μM) | References |
|---|---|---|---|---|---|---|
| Peptide Z2 | MAVLGDTAWDF<br>GSVGGALNSLG<br>KGIHQIFGAAF | *in vitro* | BHK21 cells<br><br>Vero cells | 1.75 ± 0.13<br>3.69 ± 0.27 | – | Yu et al. (2017) |
| P5 | GQASNGVFVIH<br>WGKFDSFGIAV | *in vitro* | Vero cells | 3.27 | – | Chen et al. (2017) |
| Ev37 | GLINEKKVQQYLDE<br>KLPNGVVKGALKSL<br>VHKAAKNQNLCAF<br>NVDTVGMCDADCK<br>RQGKAKGVCHGT<br>KCKCDVELSYKK | *in vitro* | Huh-7 cells | – | – | Li et al. (2019) |
| Aprotinin | – | *in vitro* | – | 0.07 ± 0.012 | – | Shiryaev et al. (2017) |
| Acyl-KR-aldehyde | – | – | – | 0.208 | – | Li et al. (2017d) |
| AH-D peptide | SGSWLRDVWDWIC<br><br>TVLTDFKTWLQSKL | *in vivo* | In mouse | 0.0119 | – | Cho et al. (2009), Jackman et al. (2018) |
| FFAAP | FFAAP | *in vitro* | Human JEG-3 cells<br>Vero cells | | – | Margueron and Reinberg (2011), Di Croce and Helin (2013), Kim et al. (2015), Vasireddi et al. (2019) |
| ZMP STE24 | – | *in vitro* | T98-G cells | – | – | Fu et al. (2017) |

binding to the cell surface (Mounce et al., 2017; Roy et al., 2017). In Vero cells, the $IC_{50}$ and $CC_{50}$ value of curcumin inhibiting ZIKV is 1.90 and 11.6 μM, respectively (**Table 2**; Mounce et al., 2017). Nanchangmycin [**Figure 3**(6)], produced by Streptomyces nanchang fermentation, can inhibit gram-positive bacteria and has insecticidal and antibacterial activities against poultry *in vitro* (Rausch et al., 2017). For Zika virus, Nanchangmycin can inhibit ZIKV infection by blocking clathrin-mediated endocytosis with $IC_{50}$s between 0.1 and 0.4 μM, and it has low toxicity in this range (**Table 2**) in human U2OS cells, human brain microvascular endothelial cells (HBMEC), and human Jeg-3 cells, respectively (Rausch et al., 2017).

### ZIKV Inhibitors Targeting Endosome

Endosomes provide a transport route for ZIKV to enter host cells. Ev37 (**Table 1**), an endosomal scorpion peptide inhibitor, can effectively inhibit ZIKV infection at a non-cytotoxic concentration (Li et al., 2019). Ev37 is a broad-spectrum and specific antiviral peptide, which can alkalize the pH value of endosomes, inhibit the release of a viral genome, and prevent it from entering the cytoplasm, thus blocking ZIKV infection (Li et al., 2019). In Huh-7 cells, Ev37 can reduce 87% of ZIKV infection at a concentration of 10 μM (Li et al., 2019). Chloroquine (Li et al., 2017a), Suramin (Albulescu et al., 2017), and 25-hydroxycholesterol [**Figure 3**(7–9) and **Table 2**; Li et al., 2017a) demonstrated their ability to inhibit ZIKV internalization *in vitro*. Niclosamide is an FDA-approved drug broadly used in the treatment of intestinal helminthiasis [**Figure 3**(10) and **Table 2**]. It can prevent endosomal acidification, but the mechanism is not fully elucidated (Fonseca et al., 2012; Jurgeit et al., 2012).

### ZIKV Inhibitors Targeting AXL

AXL is a tyrosine kinase receptor (TKR), which can mediate viral attachment to host cells. Therefore, it is necessary to inhibit primary cells with high AXL content (Nowakowski et al., 2016). Cabozantinib and BMS-777607 are two kinase inhibitors that inhibit AXL [**Figure 3**(11,12); Rausch et al., 2017]. In human U2OS cells, their $IC_{50}$ values are 0.2 and 0.6 μM, respectively, and the $CC_{50}$ values are greater than 10 μM (**Table 2**; Rausch et al., 2017). However, the experiments showed that AXL inhibitors were effective only on AXL-rich cells (Rausch et al., 2017), indicating that the effect is cell-type specific.

Although several studies proclaimed that AXL is a receptor for ZIKV entry *in vitro*, a few reports showed the opposite results. The genetic ablation of AXL has no significant effect on ZIKV entry or ZIKV-mediated cell death in human-induced pluripotent stem cell (iPSC)-derived NPCs or cerebral organoids (Nyboe Andersen et al., 2017; Rausch et al., 2017) reported that Jeg-3 cells that show no detectable AXL expression were highly permissive to ZIKV infection, suggesting that AXL may not be essential for ZIKV infection. This hypothesis is corroborated by an *in vivo* study (Wang Z. Y. et al., 2017). Notably, the AXL receptor supports neural stem cell survival, proliferation and neurogenesis (Ji et al., 2014), and signaling; the AXL also regulates blood–brain barrier (BBB) integrity in the context of viral infections (Miner et al., 2015). Therefore, while blocking AXL may protect against ZIKV infecting or viral replication, perturbation of AXL function may also have multiple adverse consequences. Therefore, the use of the AXL receptor as an idea target for the inhibition of Zika virus infection remains to be confirmed. Efforts to elucidate the molecular mechanism for ZIKV infection, through both targeted TAM receptor knockout studies and unbiased screening for other binding factors that render cells resistant to ZIKV, will lead to the identification of new targets for development of anti-ZIKV therapeutics.

## ZIKV Replication Inhibitors

### ZIKV Inhibitors Targeting NS2B-NS3 Protease

NS2B-NS3 protease of Zika virus plays an essential role in ZIKV replication and maturation. NS2B-NS3 processes the viral non-structural proteins from the viral polyprotein into individual proteins. NS2B-NS3 is a serine protease that consists of the N-terminal domain of NS3 and a short cofactor from the hydrophilic core sequence of NS2B. Like the NS4A cofactor of the HCV protease, Flavivirus NS3 is inactive without the NS2B co-factor (Erbel et al., 2006).

Three different ZIKV NS2B-NS3 protease (ZIKVpro) constructs have been proposed. First, a covalent $G_4SG_4$ linker peptide between NS2B and NS3 (gZiPro) construct was adopted based on previous West Nile and DENV protease constructs (Lei et al., 2016). The other two constructs include one bivalent protease consisting of two separate polypeptide NS2B and NS3 (bZiPro) (Zhang et al., 2016) and one with its own NS2B C-terminal peptide (TGKR) binding NS2B to NS3 (eZiPro) (Phoo et al., 2016). Remarkably, the single-chain enzyme gZiPro with an artificial linker that is commonly applied for the constructs of other flaviviruses has been widely used for screening inhibitors. Aprotinin, a 58 amino acid bovine trypsin inhibitor, inhibits ZIKV NS2B-NS3 protease with an $IC_{50}$ of 70 nM by blocking the interactions of NS3 and NS2B, as predicted by molecular modeling studies (**Table 1**; Shiryaev et al., 2017). By using structure-based virtual screening, novobiocin and lopinavir-ritonavir can inhibit ZIKV NS2B-NS3 protease activity by using molecular docking analysis [**Figure 3**(13–15); Yuan et al., 2017]. Novobiocin, an aminocoumarin antibiotic, inhibited protease activity by highly stable binding with ZIKV NS2B-NS3 protease to diminish its catalytic efficiency (Kirby et al., 1956; Yuan et al., 2017). It can inhibit ZIKV replication with an $IC_{50}$ of 26.12 ± 0.33 μg/ml and $CC_{50}$ of 850.50 μg/ml in Vero cells and an $IC_{50}$ of 38.14 ± 4.53 μg/ml and $CC_{50}$ of 1103.18 μg/ml in Huh-7 cells (**Table 3**; Yuan et al., 2017). Lopinavir-ritonavir can inhibit protease activity of ZIKV replication with an $IC_{50}$ of 4.78 ± 0.41 μg/ml and $CC_{50}$ of 30.00 μg/ml in Vero cells and an $IC_{50}$ of 3.31 ± 0.36 μg/ml $CC_{50}$ of 32.12 μg/ml in Huh-7 cells (**Table 3**; Yuan et al., 2017).

Recently, Phoo et al. have shown that the glycine-rich artificial linker or "TGKR" peptide could introduce steric hindrance, resulting in the change of the inhibitor-binding mechanism (Phoo et al., 2016). The wide-type NS2B and NS3pro domain are not covalently linked (Kim et al., 2013). bZiPro, which is closer to the native state, has higher activity and is more suitable

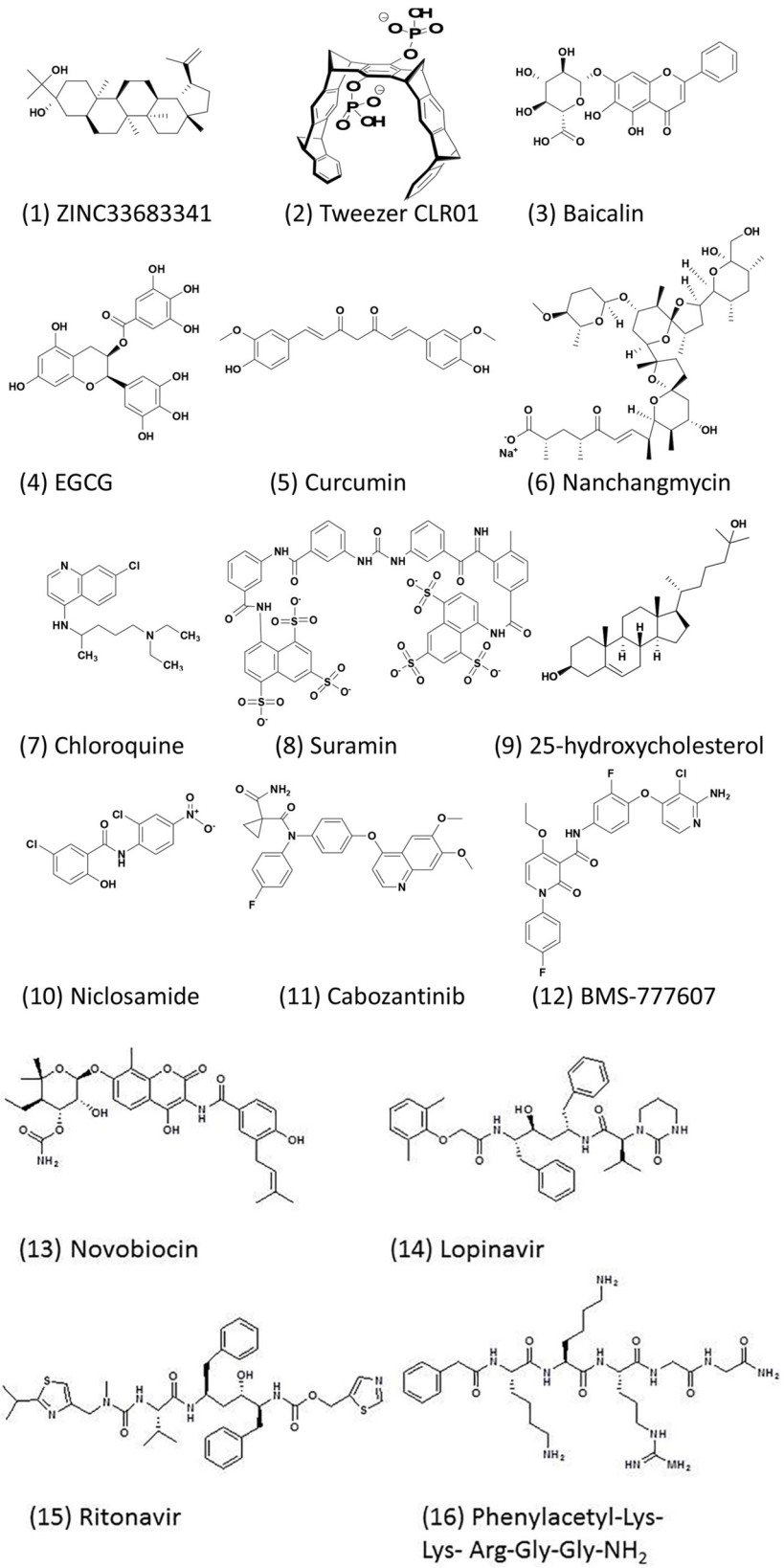


**FIGURE 3 |** Continued

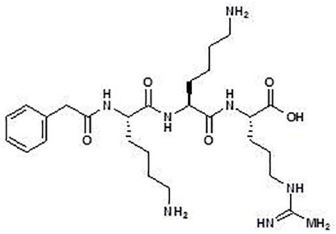

(17) 4-guanidinomethyl-phenylacetyl- Lys-Lys-Arg-$NH_2$

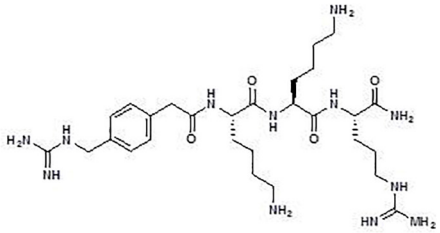

(18) 4-guanidinomethyl-phenylacetyl-Arg-Arg-Arg-4-amidinobenzylamide

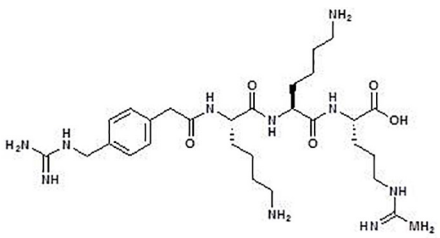

(19) Hydrolysis product of phenylacetyl-Lys-Lys-Arg-Gly-Gly-$NH_2$

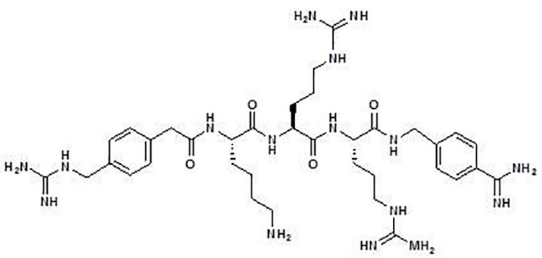

(20) Hydrolysis product of 4-guanidinomethyl-phenylacetyl-Lys-Lys-Arg-$NH_2$

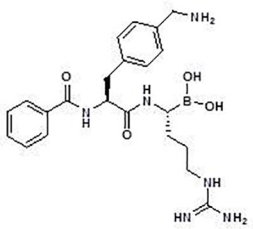

(21) Bz-[4-(CH2NH2)]Phe-Arg-$B(OH)_2$

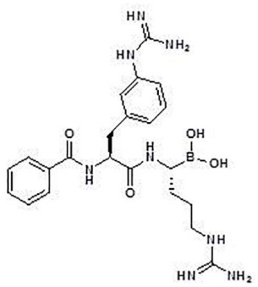

(22) B(OH)2Bz-(3-guanidinyl) Phe-Arg-$B(OH)_2$

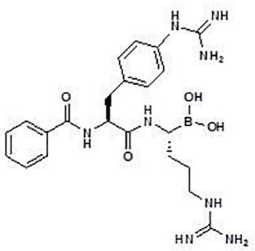

(23) $B(OH)_2$Bz-(4-guanidinyl) Phe-Arg-$B(OH)_2$

**FIGURE 3 |** Continued

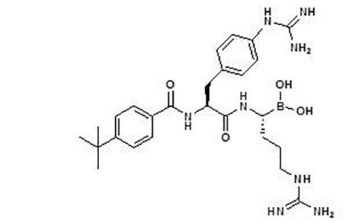

(24) 4-tBuBz-(4-guanidinyl) Phe-Arg-$B(OH)_2$

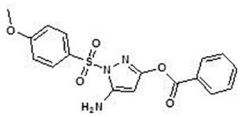

(25) 5-amino-1-((4-methoxyphenyl)sulfonyl)-1H-pyrazol-3-yl

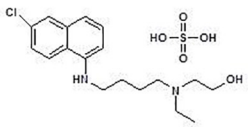

(26)Hydroxychloroquine

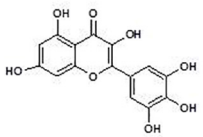

(27) Myricetin

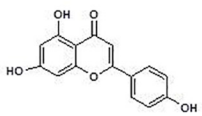

(28) Apigenin

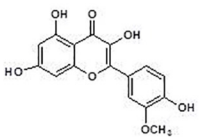

(29) Isorhamnetin

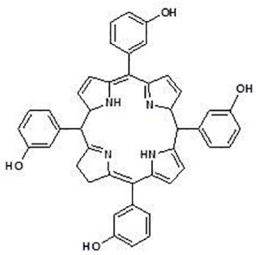

(30) Temoporfin

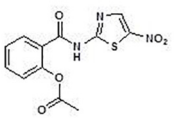

(31) Nitazoxanide

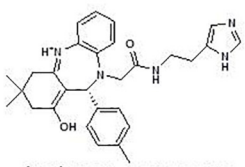

(32) BAS 19192837

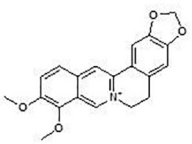

(33) Berberine

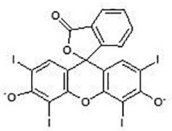

(34) Erythrosin B

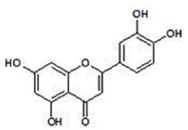

(35) Luteolin

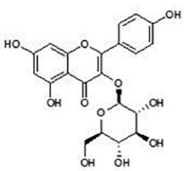

(36) Astragalin

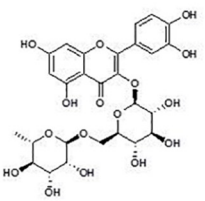

(37) Rutin

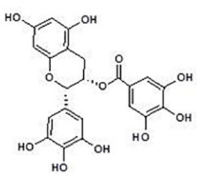

(38) Epigallocatechin gallate

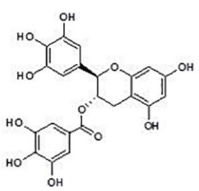

(39) Gallocatechin gallate

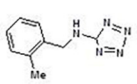

(40) ZINC64717952

**FIGURE 3 |** Continued

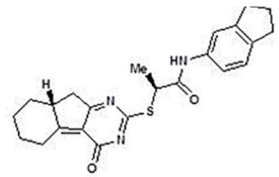

(41) ZINC39563464

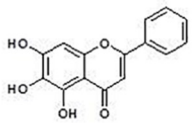

(42) Baicalein

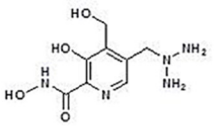

(43) DMB213

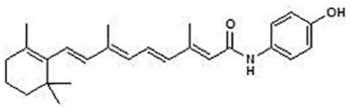

(44) N-(4-hydroxyphenyl) retinamide

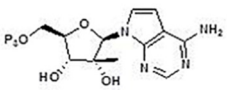

(45) 7DMA

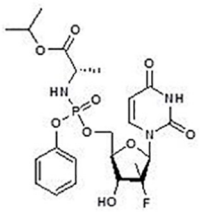

(46) Sofosbuvir

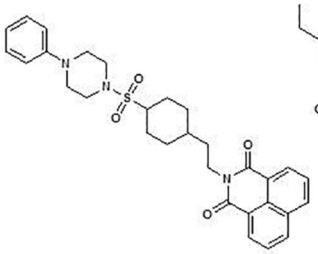

(47) F3043-0013

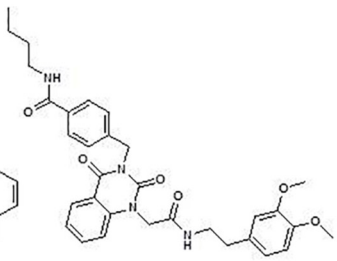

(48) F0922-0796

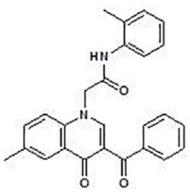

(49) F1609-0442

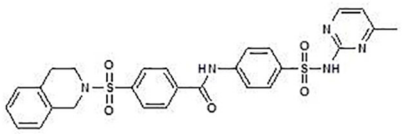

(50) F1750-0048

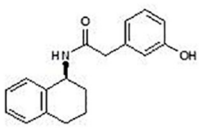

(51) ZINC50166190

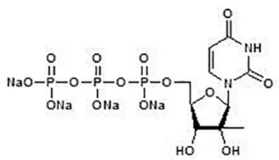

(52) 2′-C-Me-UTP

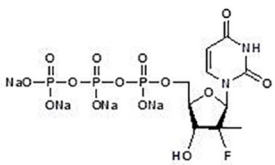

(53) 2′-F-2′-C-Me-UTP

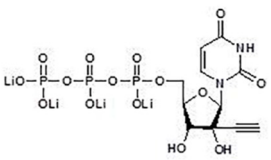

(54) 2′-C-ethynyl-UTP

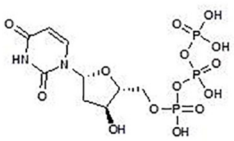

(55) 3′-dUTP

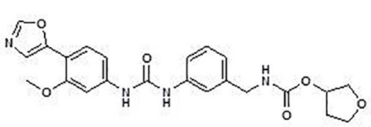

(56) Merimepodib

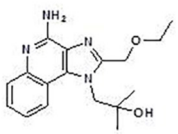

(57) Resiquimod

**FIGURE 3 |** Continued

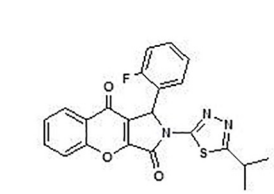

(58) AV-C

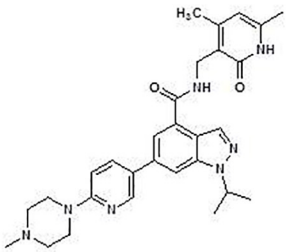

(59) GSK926

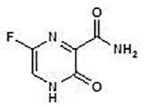

(60) T-705

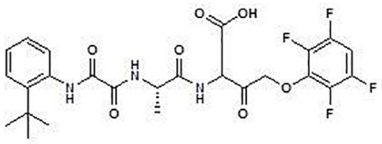

(61) Emricasan

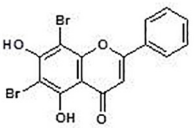

(62) FV13

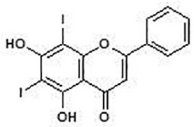

(63) FV14

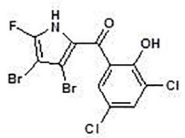

(64) Compound 1

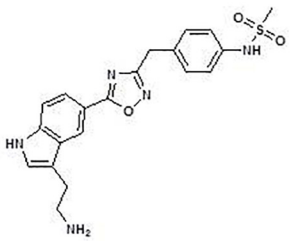

(65) PKI 14-22

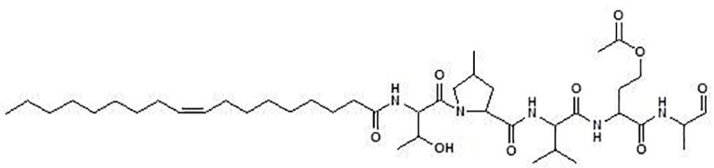

(66) Cavinafungin

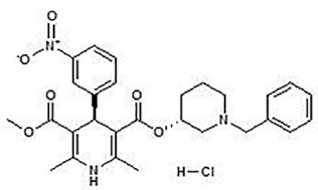

(67) benidipine hydrochloride

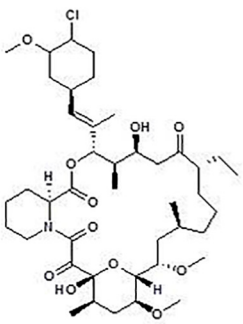

(68) Pimecrolimus

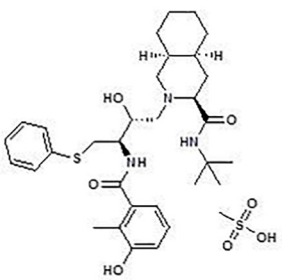

(69) nelfinavir mesylate

**FIGURE 3 |** Continued

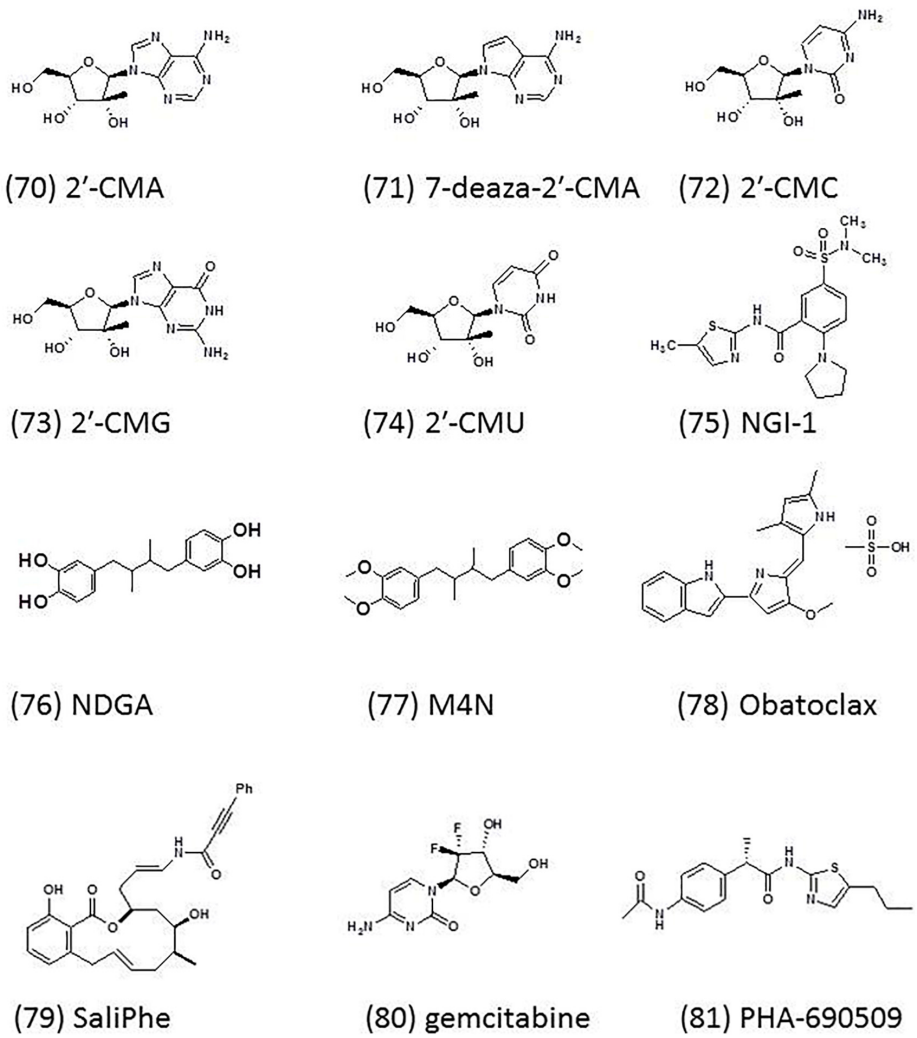


**FIGURE 3 |** Chemical structures of ZIKV small-molecule inhibitors.

for inhibitor screening than gZiPro and eZiPro because of its free active site being accessible to substrates or inhibitors (de la Cruz et al., 2011; Phoo et al., 2016; Shannon et al., 2016). Acyl-KR-aldehyde, a dipeptide, can form a covalent bond with the Ser135 residue of NS3 and the KR residues occupy the S1 and S2 sites of NS3 (Li et al., 2017d). Acyl-KR-aldehyde can inhibit the bZiPro construct of NS2B-NS3 protease with an $IC_{50}$ of 208 nM (**Table 1**; Li et al., 2017d). Nuclear magnetic resonance (NMR) spectroscopy demonstrated that the bZiPro construct of NS2B-NS3 and Acyl-KR-aldehyde can form a stable complex (Li et al., 2017c). The peptidomimetic inhibitors composed of a P1-P4 segment and different P1' residues, including Phenylacetyl-Lys-Lys-Arg-Gly-Gly-$NH_2$, 4-guanidinomethyl-phenylacetyl-Lys-Lys-Arg-$NH_2$, 4-guanidinomethyl-phenyl-acetyl-Arg-Arg-Arg-4-amidinobenzylamide, a hydrolysis product of phenylacetyl-Lys-Lys-Arg-Gly-Gly-NH2, and a hydrolysis product of 4-guanidinomethyl-phenylacetyl-Lys-Lys-Arg-NH2 [**Figure 3**(16–20)], can inhibit ZIKV replication against the NS2B-NS3 protease of ZIKV with an $IC_{50}$ of 1.2 ± 0.14, 1.6 ± 0.14, 1.1 ± 0.07 μM, and 18.4 ± 1.9, 5.9 ± 0.55 μM, respectively (**Table 3**; Phoo et al., 2018). As non-competitive inhibitors, five macrocyclic peptides can act as ligands with high affinity and can be rapidly isolated for nearly any target by using display screening approaches, such as an mRNA display or phage display (Passioura et al., 2014). These peptides can inhibit bZiPro constructs of NS2B-NS3 protease activity with an $IC_{50}$ from 0.24 to 4.9 μM (Nitsche et al., 2019). AH-D peptide, a 27-mer amphipathic α-helical peptide, protects against lethal ZIKV infection with $IC_{50}$ = 0.012 μM in primary neuronal cells, inhibits ZIKV infection in mouse brains, and preserves BBB integrity (**Table 1**; Cho et al., 2009; Jackman et al., 2018). The AH-D peptide also significantly reduced viral loads in the serum, brain, spleen, and optical nerve throughout the course of infection (Jackman et al., 2018). Four dipeptidic inhibitors have a C-terminal boronic acid moiety, including Bz-[4-(CH2NH2)]Phe-Arg-$B(OH)_2$,

**TABLE 2 |** Zika virus entry inhibitors.

| Number of chemical structures in Figure 3 | Inhibitor | Testing model | Cell lines | $IC_{50}$ (μM) | $CC_{50}$(μM) | References |
|---|---|---|---|---|---|---|
| 1 | Tweezer CLR01 | *in vitro* | Vero E6 cells | 8.2 | – | Bavari et al. (2002), Chazal and Gerlier (2003), Brugger et al. (2006), Lorizate et al. (2013), Rocker et al. (2018) |
| 2 | ZINC33683341 | *in vitro* | Vero cells | – | – | Fernando et al. (2016) |
| 3 | Baicalin | *in vitro* | Vero cells | 14 | 553 | Oo et al. (2019) |
| 4 | EGCG | *in vitro* | Vero E6 cells | – | – | Song et al. (2005), Isaacs et al. (2008), Nance et al. (2009), Calland et al. (2012), Carneiro et al. (2016) |
| 5 | Curcumin | *in vitro* | Huh-7 cells | 1.90 | 11.6 | Song and Ni (1998), Mounce et al. (2017), Nitsche et al. (2017), Roy et al. (2017) |
| 6 | Nanchangmycin | *in vitro* | Human U2OS cells | 0.1 | 7 | Liu et al. (2008), Pierson and Kielian (2013), Rausch et al. (2017) |
| | | | Human HBMEC cells | 0.4 | >10 | |
| | | | Human JEG-3 cells | 0.97 | 6.10 | |
| 7 | Chloroquine | *in vitro* | Huh-7 cells | 1.72 | – | Li et al. (2017b) |
| | | *in vivo* | Vero cells; BALB/c mice and A129 mice | 4.15 | | |
| 8 | Suramin | *in vitro* | Vero cells | 39.8 | 1900 | Albulescu et al. (2017), Coronado et al. (2018) |
| 9 | 25-hydroxycholesterol | *in vitro* *in vivo* | Vero cells; BALB/c mice and A129 mice | 0.188 | – | Li et al. (2017a) |
| 10 | Niclosamide | *in vitro* | A549 cells SNB-19 cells | 12.3 ± 0.6 1.72 | 4.8 ± 1.0 | Baell and Holloway (2010), Li et al. (2017d), Xu et al. (2016), Li et al. (2017d) |
| 11 | Cabozantinib | *in vitro* | Human U2OS cells | 0.2 | >10 | Rausch et al. (2017) |
| 12 | BMS-777607 | *in vitro* | Human U2OS cells | 0.6 | >10 | Rausch et al. (2017) |

Bz-(3-guani-dinyl)Phe-Arg-$B(OH)_2$, Bz-(4-guani-dinyl)Phe-Arg-$B(OH)_2$, and 4-tBuBz-(4-guanidinyl)Phe-Arg-$B(OH)_2$ [**Figure 3**(21–24)]. These compounds can inhibit ZIKV NS2B-NS3 protease activity with $IC_{50}$ from 0.25 to 2.1 μM (**Table 3**; Nitsche et al., 2017).

Li Y. et al. have found that a pyrazole ester derivative, 5-amino-1-((4-methoxyphenyl)sulfonyl) -1H-pyrazol-3-yl benzoate [**Figure 3**(25)], can inhibit ZIKV replication with an $IC_{50}$ of 1.5 μM when benzoyl-Nle-Lys-Arg-Arg-aminomethylcoumarin (BznKRR-AMC) was used as a substrate (**Table 3**; Li Y. et al., 2018). The benzoyl group of this inhibitor forms a covalent bond with the side chain of catalytic residue S135 to stabilize the closed conformation of the ZIKV bZiPro construct of NS2B-NS3 protease (Li Y. et al., 2018). In addition, a derivative of pyrazole ester, 5-amino-1-((4-methoxyphenyl)sulfonyl)-1H-pyrazol-3-yl benzoate, with an $IC_{50}$ of 0.1 μM can interact in a manner similar to the compound [**Figure 3**(25)] and strongly inhibit binary ZIKV bZiPro construct of NS2B-NS3 protease (Li Y. et al., 2018). Hydroxychloroquine [**Figure 3**(26)], a drug already approved and used in pregnancy, can inhibit the bZiPro construct of NS2B-NS3 protease activity with an inhibition constant (Ki) of 92.34 ± 11.91 μM (**Table 3**; Kumar et al., 2018).

Some natural products from edible plants, like myricetin, can inhibit ZIKV infection with an $IC_{50}$ of 1.26 μM and an inhibitory constant of ZIKV NS2B-NS3 protease activity with *Ki* of 0.77 μM by establishing six hydrogen bonds with four Zika NS3pro residues: Lys73, Asn152, Gln74, and Gly124 [**Figure 3**(27) and **Table 3**; Roy et al., 2017]. Apigenin inhibits ZIKV infection with an $IC_{50}$ of 56.32 μM and inhibitory constant *Ki* of 34.02 μM [**Figure 3**(28) and **Table 3**; Roy et al., 2017]. Isorhamnetin, also

**TABLE 3 |** Zika virus replication inhibitors.

| Number of chemical structures in Figure 3 | Inhibitor | Testing model | Cell lines | $IC_{50}$ (μM) | $CC_{50}$ (μM) | References |
|---|---|---|---|---|---|---|
| **Inhibitors targeting NS2B-NS3 protease** | | | | | | |
| 13 | Novobiocin | *in vitro* | Vero cells | 26.12 ± 0.33 | 850.50 | Kirby et al. (1956), Yuan et al. (2017) |
| | | | Huh-7 cells | 38.14 ± 4.53 | 1103.18 | |
| 14,15 | Lopinavir-ritonavir | *in vitro* | Vero cells | 4.78 ± 0.41 | 30.00 | Yuan et al. (2017) |
| | | | Huh-7 cells | 3.31 ± 0.36 | 32.12 | |
| 16 | Phenylacetyl-Lys-Lys-Arg-Gly-Gly-NH2 | *in vitro* | – | 1.2 ± 0.14 | – | Passioura et al. (2014), Phoo et al. (2018), Nitsche et al. (2019) |
| 17 | 4-guanidinomethyl-phenylacetyl-Lys-Lys-Arg-NH2 | *in vitro* | – | 1.6 ± 0.14 | – | Passioura et al. (2014), Phoo et al. (2018), Nitsche et al. (2019) |
| 18 | 4-guanidinomethyl-phenylacetyl-Arg-Arg-Arg-4-amidinobenzylamide | *in vitro* | – | 1.1 ± 0.07 | – | Passioura et al. (2014), Phoo et al. (2018), Nitsche et al. (2019) |
| 19 | Hydrolysis product of phenylacetyl-Lys-Lys-Arg-Gly-Gly-NH2 | *in vitro* | – | 18.4 ± 1.9 | – | Passioura et al. (2014), Phoo et al. (2018), Nitsche et al. (2019) |
| 20 | Hydrolysis product of 4-guanidinomethyl-phenylacetyl-Lys-Lys-Arg-NH2 | *in vitro* | – | 5.9 ± 0.55 | – | Passioura et al. (2014), Phoo et al. (2018), Nitsche et al. (2019) |
| 21 | Bz-[4-(CH2NH2)]Phe-Arg- B(OH)2 | *in vitro* | – | 0.25 | – | Nitsche et al. (2017) |
| 22 | Bz-(3-guanidinyl)Phe-Arg- B(OH)2 | *in vitro* | – | 1.9 | – | Nitsche et al. (2017) |
| 23 | Bz-(4-guanidinyl)Phe-Arg- B(OH)2 | *in vitro* | – | 0.83 | – | Nitsche et al. (2017) |
| 24 | 4-tBuBz-(4-guanidinyl)Phe-Arg- B(OH)2 | *in vitro* | – | 2.1 | – | Nitsche et al. (2017) |
| 25 | 5-amino-1-((4-methoxyphenyl)sulfonyl)-1H-pyrazol-3-yl benzoate | *in vitro* | BznKRR-AMC | 1.5<br>0.1 | – | Zhao and Tan (2015) |
| 26 | Hydroxychloroquine | *in vitro* | JEG3 cells | – | – | Kumar et al. (2018) |
| 27 | Myricetin | *in vitro* | – | 1.26 | – | Lim et al. (2017), Roy et al. (2017) |
| 28 | Apigenin | *in vitro* | – | 56.32 | – | Roy et al. (2017) |
| 29 | Isorhamnetin | *in vitro* | – | 15.46 | – | Roy et al. (2017) |
| 30 | Temoporfin | *in vitro* | A549 cells | 1.1 ± 0.1 | 40.7 ± 0.7 | Baell and Holloway (2010), Li et al. (2017d) |
| 31 | Nitazoxanide | *in vitro* | A549 cells | 15.9 ± 0.9 | 77 ± 7.2 | Baell and Holloway (2010), Li et al. (2017d) |
| 32 | BAS 19192837 | – | – | – | – | Rohini et al. (2019) |
| 33 | Berberine | *in vitro* | – | – | – | Sahoo et al. (2016) |
| 34 | Erythrosin B | *in vitro* | A549 cells | 0.62 ± 0.12 | – | Lee et al. (2017), Li Z. et al. (2018) |
| 35 | Luteolin | *in vitro* | – | 53 ± 1.3 | – | Lim et al. (2017) |
| 36 | Astragalin | *in vitro* | – | 112 ± 5.5 | – | Lim et al. (2017) |
| 37 | Rutin | *in vitro* | – | 104 ± 2.9 | – | Lim et al. (2017) |
| 38 | Epigallocatechin gallate | *in vitro* | – | 87 ± 1.2 | – | Lim et al. (2017) |
| 39 | Gallocatechin gallate | *in vitro* | – | 99 ± 1.8 | – | Lim et al. (2017) |

*(Continued)*

**TABLE 3** | Continued

| Number of chemical structures in Figure 3 | Inhibitor | Testing model | Cell lines | $IC_{50}$ (μM) | $CC_{50}$ (μM) | References |
|---|---|---|---|---|---|---|
| **Inhibitors targeting NS5** | | | | | | |
| 40 | ZINC64717952 | *in vitro* | – | – | – | Ramharack and Soliman (2018) |
| 41 | ZINC39563464 | *in vitro* | – | – | – | Ramharack and Soliman (2018) |
| 42 | Baicalein | *in vitro* | Vero cells | 0.004 | – | Zandi et al. (2012), Moghaddam et al. (2014), Jin et al. (2018), Oo et al. (2018, 2019) |
| 43 | DMB213 | *in vitro* | Huh-7 cells | 5.2 | – | Xu et al. (2017) |
| 44 | *N*-(4-hydroxyphenyl) retinamide | *in vitro* | Vero cells | 1.1 ± 0.4<br>1.2 ± 0.1 | – | Wang C. et al. (2017) |
| 45 | 7DMA | *in vitro* | Vero cells | 20 ± 15<br>9.6 ± 2.2 | >357 | Olsen et al. (2004), Zmurko et al. (2016) |
| 46 | Sofosbuvir | *in vitro* | Huh-7 cells<br>Jar human placental choriocarcinoma cells | 1 ∼ 5 | >200 | Lee et al. (2017), Li Z. et al. (2018) |
| 47 | F3043-0013 | *in vitro* | Vero cells | 4.8 ± 2.3 | – | Stephen et al. (2016) |
| 48 | F0922-0796 | *in vitro* | Vero cells | 12.5 ± 7.4 | – | Stephen et al. (2016) |
| 49 | F1609-0442 | *in vitro* | Vero cells | 17.5 ± 8.4 | – | Stephen et al. (2016) |
| 50 | F1750-0048 | *in vitro* | Vero cells | 17.6 ± 3.1 | – | Stephen et al. (2016) |
| 51 | ZINC50166190 | *in vitro* | – | – | – | Singh and Jana (2017) |
| 52 | 2′-C-Me-UTP | *in vitro* | – | 5.78 | – | Lu et al. (2017) |
| 53 | 2′-F-2′-C-Me-UTP | *in vitro* | – | 90.76 | – | Lu et al. (2017) |
| 54 | 2′-C-ethynyl-UTP | *in vitro* | – | 0.46 | – | Lu et al. (2017) |
| 55 | 3′-dUTP | *in vitro* | – | 0.67 | – | Lu et al. (2017) |
| 56 | Merimepodib (MMPD, VX-497) | *in vitro* | Huh-7 cells | 0.6 ± 0.2 | >10 | Tong et al. (2018) |
| 57 | Resiquimod | *in vitro* | CHME3 cells. | – | – | Vanwalscappel et al. (2018) |

called 3′-Methylquercetin, can inhibit ZIKV infection with $IC_{50}$ of 15.46 μM and *Ki* of 6.22 μM as well as Quercetin with $IC_{50}$ of 2.42 μM and *Ki* of 1.12 μM [**Figure 3**(29) and **Table 3**; Roy et al., 2017). Structurally, isorhamnetin is a derivative of quercetin with a very similar molecular structure (Roy et al., 2017). In addition, curcumin [**Figure 3**(5) and **Table 2**], a natural phenol with two aromatic rings linked by a heptadiene group, can inhibit ZIKV infection with $IC_{50}$ of 3.45 μM and *Ki* of 2.61 μM, most likely by having bivalent binding sites (Song and Ni, 1998; Roy et al., 2017). The introduction of a C-terminal boronic acid moiety into dipeptidic inhibitors can raise the affinity to target by a 1000-fold (Nitsche et al., 2017). However, curcumin, quercetin, and other flavonoids have shown themselves to be promiscuous inhibitors, e.g., via colloidal aggregation (McGovern et al., 2002; Duan et al., 2015; Tritsch et al., 2015). Curcumin also contains reactive Michael acceptors, and quercetin has a catechol, a well-known PAINS substructure, which might make these compounds less favorable (Mottin et al., 2018).

A total of 2,816 approved and investigational drugs were screened using a high-throughput screening (HTS) assay (Li et al., 2017d). Among these, 23 compounds were confirmed to possess an $IC_{50}$ below 15 μM. Three of them, including temoporfin, niclosamide, and nitazoxanide, could inhibit with an $IC_{50}$ of 1.1 ± 0.1, 12.3 ± 0.6, 15.9 ± 0.9 μM and $CC_{50}$ of 40.7 ± 0.7, 4.8 ± 1.0, 77 ± 7.2 μM in A549 cells, respectively [**Figure 3**(10,30,31) and **Table 3**; Baell and Holloway, 2010).

Temoporfin was tested in a viremia mouse model and a lethal mouse model, and it was able to inhibit viremia and protect 83% of the mice; the mice that survived did not present any signs of neurological disorder (Li et al., 2017d). These compounds inhibit the interaction between NS3 and the NS2B N-terminal fragment. By using an e-pharmacophore-based virtual screening assay, BAS 19192837 was chosen as a potent Zika NS2B-NS3 protein inhibitor [**Figure 3**(32)]. However, the experimental data of the $IC_{50}$ about this inhibitor was not shown (**Table 3**; Rohini et al., 2019).

Berberine, an FDA-approved drug against DENV, has shown high binding affinity of 5.8 kcal/mol, and it binds around the active site of the receptor [**Figure 3**(33) and **Table 3**; Sahoo et al., 2016]. Niclosamide, an FDA-approved category B anthelmintic drug for treating worm infections in both humans and domestic livestock, inhibited all three strains of ZIKV, which was measured by intracellular ZIKV RNA levels with $IC_{50}$ values of 1.72 μM in SNB-19 cells (Xu et al., 2016). PHA-690509, an investigational compound that functions as a cyclin-dependent kinase inhibitor (CDKi), inhibited three stains with $IC_{50}$ values of 0.37 μM as measured by intracellular ZIKV RNA levels in SNB-19 cells (Xu et al., 2016). According to experimental results, the mechanism of these two compounds occurs at post-entry stage, likely at the viral RNA replication step (Xu et al., 2016). Suramin [**Figure 3**(8)], an approved polyanion antiparasitic drug, can be a potential inhibitor of Zika virus complex NS2B/NS3 proteinase with $IC_{50}$ of 47 μM (**Table 2**; Coronado et al., 2018). Computational analysis showed that suramin suppressed NS2B/NS3 proteinase activity by blocking catalytical Ser135 residue and interacting with the catalytical histidine residue (Coronado et al., 2018). Erythrosin B [**Figure 3**(34)], a pregnancy category B food additive, inhibited ZIKV replication by targeting NS2B-NS3 proteases with an $IC_{50}$ of 0.62 ± 0.12 μM in A549 cells (**Table 3**) via a non-competitive mechanism by enzymatic kinetic experiments (Li Z. et al., 2018). Erythrosin B can also inhibit ZIKV RNA synthesis and protein expression in ZIKV-relevant neural progenitor and human placental cells (Li Z. et al., 2018).

Two inhibitors were tested to inhibit NS2B-NS3 protease activity with $IC_{50}$ values of 5.2 and 4.1 μM by blocking the active site of ZIKV NS2B-NS3 protease in docked conformation (Lee et al., 2017). Five polyphenol compounds, including luteolin, astragalin, rutin, epigallocatechin gallate, and gallocatechin gallate from flavone and flavonol, inhibited ZIKV replication with $IC_{50}$ values ranging from 22 ± 0.2 to 112 ± 5.5 μM [**Figure 3**(35–39) and **Table 3**; Lim et al., 2017].

## ZIKV Inhibitors Targeting NS5

Zika virus NS5 is a relative conserved large protein among members of the genus, containing an MTase domain and an RNA polymerase (RdRp) domain connected by a 10 residues linker. ZIKV NS5 can be used as a template for genome replication with an efficiency similar to that of an RNA template (Lu et al., 2017). In one study, ZIKV NS5 could extend an RNA primer annealed to an RNA template in an $Mn^{2+}$-dependent manner, as opposed to $Mg^{2+}$ (Lu et al., 2017). ZINC64717952 and ZINC39563464 can interact with NS5 by enzyme–ligand interactions under virtual conditions to inhibit ZIKV propagation, but no clear data about $IC_{50}$ and $CC_{50}$ have been reported [**Figure 3**(40,41) and **Table 3**; Ramharack and Soliman, 2018].

Baicalein [**Figure 3**(42)], a flavonoid analog, could downregulate ZIKV replication up to 10 h post-infection, while prophylactic effects were evident in pretreated Vero cells with $IC_{50} \approx 0.004$ μM and selectivity index (SI) ≈ 105,000 (**Table 3**; Oo et al., 2019). It also has antiviral activity against DENV, chikungunya virus (CHIKV), and influenza virus (Zandi et al., 2012; Moghaddam et al., 2014; Jin et al., 2018; Oo et al., 2018). DMB213 [**Figure 3**(43) and **Table 3**] is a pyridoxine-derived non-nucleoside small-molecule inhibitor with an $IC_{50}$ of 5.2 μM (Xu et al., 2017). This compound inhibits ZIKV by blocking RNA synthesis reactions catalyzed by recombinant ZIKV NS5 polymerase (Xu et al., 2017). A nuclear import inhibitor, *N*-(4-hydroxyphenyl) retinamide [**Figure 3**(44) and **Table 3**], can block the interaction between high nanomolar affinity ZIKV NS5 and the host cell importin α/β1 heterodimer (Wang S. et al., 2017). 7-deaza-2′-C-methyladenosine (7DMA) [**Figure 3**(45)], an inhibitor of hepatitis C virus polymerase (Olsen et al., 2004), could inhibit ZIKV strain MR766 with $CC_{50} > 357$ μM and an $IC_{50}$ of 20 ± 15 μM in a CPE reduction assay and 9.6 ± 2.2 μM in a virus yield reduction assay in Vero cells (African Green monkey kidney cells; ECACC) (**Table 3**; Zmurko et al., 2016). *In vivo*, 7DMA also reduced viremia (between day 3 and 8 post infection) and delayed virus-induced morbidity and mortality in AG129 (IFN-α/β and IFN-γ receptor knockout) mice infected with ZIKV (Zmurko et al., 2016). Sofosbuvir [**Figure 3**(46)], an FDA-approved nucleotide polymerase inhibitor, can efficiently inhibit replication and infection of several ZIKV strains, including African and American isolates, with $IC_{50}$ values of 1–5 μM and $CC_{50} > 200$ μM in Huh-7 and Jar human placental choriocarcinoma cells (**Table 3**; Bullard-Feibelman et al., 2017). In addition, oral treatment with sofosbuvir also protected against ZIKV-induced death in 5-week-old C57BL/6J mice (Li Z. et al., 2018).

Using virtual screening, Stephen et al. identified four top-scoring ligands from the 28,341 compounds, including F3043-0013, F0922-0796, F1609-0442, and F1750-0048, against ZIKV with $IC_{50}$ values of 4.8 ± 2.3, 12.5 ± 7.4, 17.5 ± 8.4, and 17.6 ± 3.1 μM, respectively, by plaque reduction assay (PRA) [**Table 3** and **Figure 3**(47–50); Stephen et al., 2016]. These compounds may cooperatively interact with the hydrophobic binding pocket, extending to the S-adenosyl homocysteine (SAH) binding pocket (Stephen et al., 2016). Based on the modeling of the catalytic domain of ZIKV RNA-dependent RNA polymerase (RdRpC), Ligand 6 [(S)-2-(3-hydroxyphenyl)-*N*-(1,2,3,4-tetrahydronaphthalen-1yl)acetamide] (ZINC50166190) was chosen as potentially having inhibitory activity against ZIKV RdRpC protein by acting as a GTP-nucleotide analog to prevent initiation of ZIKV RNA polymerization [**Figure 3**(51) and **Table 3**; Singh and Jana, 2017). Some ribonucleotide 5′-triphosphate analogs like 2′-C-Me-UTP, 2′-F-2′-CMe-UTP, 2′-C-ethynyl-UTP, and 3′-dUTP inhibit ZIKV replication with $IC_{50}$s of 5.78, 90.76, 0.46, and 0.67 μM [**Figure 3**(52–55) and **Table 3**], respectively, as measured in the presence of 1 μM competing UTP by an alternative non-radioactive

coupled-enzyme assay (Lu et al., 2017). One of the major inhibitory mechanisms of ribonucleotide 5′-triphosphate against ZIKV infection is its direct termination of viral RNA polymerases (Lu et al., 2017). Merimepodib (MMPD, VX-497) [**Figure 3**(56)], a potent inhibitor of inosine-5′-monophosphate dehydrogenase (IMPDH), inhibited ZIKV RNA replication with an $IC_{50}$ of 0.6 ± 0.2 μM and $IC_{90}$ of 1.0 ± 0.2 μM in Huh7 cells. In the cytotoxicity assay, the $CC_{50}$ was determined to be >10 μM, which resulted in the selective index > 17 μM (**Table 3**; Tong et al., 2018). TLR7/8 agonist R848 (resiquimod) (toll-like receptor (TLR) agonists) inhibited ZIKV RNA synthesis in CHME3, a transformed microglial cell-line [**Figure 3**(57) and **Table 3**; Vanwalscappel et al., 2018).

## Other Small-Molecule Inhibitors With Undefined Mechanisms

AV-C(1-(2-fluorophenyl)-2-(5-isopropyl-1,3,4-thiadiazol-2-yl)-1,2-dihydrochromeno[2,3-c]pyrrole-3,9-dione) [**Figure 3**(58)], an interferon-activating agonist of the TRIF pathway, inhibited replication of ZIKV ($IC_{90}$) of 5.815 μM by activating innate- and interferon-associated responses, and the $CC_{50}$ values are well below dosages observed to induce detectable cytotoxicity of THF cells (**Table 4**; Pryke et al., 2017). Along with Selenium, a free-form amino acid sequence (FFAAP) comprising glycine, cystine, and a glutamate source inhibited ZIKV replication with an $ED_{90}$ (effective dose at which 90% of a dose of Zika virus was inhibited) of 2.5 mM in human JEG-3 cells and 4 mM in Vero cells (**Table 1**; Vasireddi et al., 2019). Histone H3K27 methyltransferases EZH2 and EZH1 (EZH2/1) can suppress gene transcription via propagation of repressive H3K27me3-enriched chromatin domains (Margueron and Reinberg, 2011; Di Croce and Helin, 2013; Kim et al., 2015). GSK926 [**Figure 3**(59)], an inhibitor of histone methyltransferases EZH2/1 (Verma et al., 2012), can suppress not only DNA viruses, like herpes simplex virus (HSV) and human cytomegalovirus (adenovirus) infection, but also an RNA virus, like ZIKV replication, in human foreskin fibroblast (HFF) cells (**Table 4**; Arbuckle et al., 2017). However, no $IC_{50}$ was reported. T-705 (favipiravir) [**Figure 3**(60)], a broad-spectrum antiviral with effects against many viruses, and a structural analog, T-1105, inhibited ZIKV strain SZ01 with an $IC_{50}$ of 110.9 ± 13.1 and 97.5 ± 6.8 μM, respectively, and $CC_{50}$ > 3000 μM in Vero cells (**Table 4**; Cai et al., 2017). Emricasan [**Figure 3**(61)], a pan-caspase inhibitor, inhibited ZIKV-induced increases in caspase-3 activity with $IC_{50}$ values of 0.13–0.9 μM in SNB-19 cells against three ZIKV strains: FSS13025 (2010 Cambodian strain), MR766 (1947 Ugandan strain), and PRVABC59 (2015 Puerto Rican strain; **Table 4**; Xu et al., 2016). In addition, in Caspase-3/7 assay, Emricasan also reduced the total number of active (cleaved) caspase-3-expressing forebrain-specific hNPCs (human cortical neural progenitor cells) in both the monolayer and 3-dimensional organoid cultures infected by ZIKV FSS13025 strain (Xu et al., 2016). Two halogenated chrysins, FV13 and FV14 [**Figure 3**(62,63)], inhibited ZIKV infection with an $IC_{50}$ of 1.65 ± 0.86 and 1.39 ± 0.11 μM in LLC/MK2 cells, respectively (Suroengrit et al., 2017). The $CC_{50}$s to the LLC/MK2 cell-based system of FV13 and FV14 were 44.28 ± 2.90 and 42.51 ± 2.53 μM, respectively (**Table 4**; Suroengrit et al., 2017). The investigations into the mechanism of these two halogenated chrysin actions suggested multiple targets, but maximal efficiency was achieved with early post-infection treatment (Suroengrit et al., 2017). Compound 1 was confirmed with an inhibitor of ZIKV-induced cytopathic effect (CPE) with an $IC_{50}$ of 5.95 μM and a $CC_{50}$ of 100 μM in human fetal neural stem cells (NSCs) [**Figure 3**(64) and **Table 4**; Bernatchez et al., 2018). PKI 14-22 (PKI) [**Figure 3**(65)], a PKA inhibitor, could act as a potent inhibitor of Asian/American and African lineages of ZIKV replication with an $IC_{50}$ of about 20 μM in endothelial cells and astrocytes by minimal cytotoxicity (**Table 4**; Cheng et al., 2018). Cavinafungin [**Figure 3**(66)], targeting ER signal peptidase by binding on SEC11, inhibited ZIKV replication with an $IC_{50}$ of 150 nM and $CC_{50}$ of 1650 nM in A549 cells (**Table 4**; Estoppey et al., 2017). Manidipine and cilnidipine, voltage-gated $Ca^{2+}$ channel (VGCC) inhibitors, could inhibit ZIKV infection by 100% with no plaque formation observed at a concentration of 10 μM in Vero cells (Wang S. et al., 2017). According to accumulating data, benidipine hydrochloride, pimecrolimus, and nelfinavir mesylate can also inhibit ZIKV replication with a concentration of 10 μM in Vero cells [**Table 4** and **Figure 3**(67–69); Wang S. et al., 2017]. Five 2′-C–methylated derivatives of nucleoside analog [nucleosides with a methyl moiety at the 2′-C position of the ribose ring, including 2′-CMA,7-deaza-2′-CMA, 2′-CMC, 2′-CMG, and 2′-CMU [**Figure 3**(70–74)], can reduce the viral titer with an $IC_{50}$ of 5.26 ± 0.12 μM for 2′-CMA, 8.92 ± 3.32 μM for 7-deaza-2′-CMA, 10.51 ± 0.02 μM for 2′-CMC, 22.25 ± 0.03 μM for 2′-CMG, and 45.45 ± 0.64 μM for 2′-CMU in Vero cells (**Table 4**; Eyer et al., 2016). All these nucleoside analogs showed weak or no cytotoxic effects at a concentration of 100 μM on cell proliferation (Eyer et al., 2016). NGI-1 [**Figure 3**(75)], an aminobenzamide-sulfonamide compound targeting both oligosaccharyltransferase OST isoforms, can block viral RNA replication significantly to inhibit viral particle formation with an $IC_{50}$ of 2.2 μM in HEK293 cells (**Table 4**; Puschnik et al., 2017). Nordihydroguaiaretic (NDGA) and its methylated derivative, tetra-*O*-methyl nordihydroguaiaretic acid (M4N), disturbed lipid metabolism and sterol regulatory element-binding proteins (SREBP) [**Figure 3**(76–77)], thereby inhibiting ZIKV PA259459 isolated from a patient with an $IC_{50}$ of 9.1 μM and SI of 17.8 and $IC_{50}$ of 5.7 μM and SI of 187.9, respectively (**Table 4**; Merino-Ramos et al., 2017). Obatoclax, SaliPhe, and gemcitabine affected ZIKV-mediated transcription [**Figure 3**(78–80) and **Table 4**], translation, and posttranslational modifications as well as metabolic pathways, by different mechanisms of action, inhibiting ZIKV infection at non-cytotoxic concentrations (Kuivanen et al., 2017). ZMP STE24, when complexed with proteins of the interferon-induced transmembrane protein (IFITM) family by co-immunoprecipitation studies, inhibited ZIKV viral titer in T98-G cells (**Table 1**; Fu et al., 2017). PHA-690509 [**Figure 3**(81)], an investigational compound that functions as a CDKi, inhibited three ZIKV stains with $IC_{50}$ values of 0.37 μM, as measured

**TABLE 4 |** Other small-molecule inhibitors with undefined mechanisms.

| Number of chemical structures in Figure 3 | Inhibitor | Testing model | Cell lines | $IC_{50}$ (μM) | $CC_{50}$ (μM) | References |
|---|---|---|---|---|---|---|
| 58 | AV-C | *in vitro* | THF cells | – | – | Pryke et al. (2017) |
| 59 | GSK926 | *in vitro* | HFF cells | – | – | Verma et al. (2012) |
| 60 | T-705 | *in vitro* | Vero cells | 110.9 ± 13.1 | >3000 | Cai et al. (2017) |
| 61 | Emricasan | *in vitro* | SNB-19 cells | 0.13 ∼ 0.9 | – | Xu et al. (2016) |
| 62 | FV13 | *in vitro* | LLC/MK2 cells | 1.65 ± 0.86 | 44.28 ± 2.90 | Suroengrit et al. (2017) |
| 63 | FV14 | *in vitro* | LLC/MK2 cells | 1.39 ± 0.11 | 42.51 ± 2.53 | Suroengrit et al. (2017) |
| 64 | Compound 1 | *in vitro* | Human fetal neural stem cells | 5.95 | 100 | Bernatchez et al. (2018) |
| 65 | PKI 14-22 | *in vitro* | Endothelial cells | 20 | – | Cheng et al. (2018) |
| 66 | Cavinafungin | *in vitro* | A549 cells | 150 | 1650 | Estoppey et al. (2017) |
| 67 | Benidipine hydrochloride | *in vitro* | Vero cells | – | – | Wang S. et al. (2017) |
| 68 | Pimecrolimus | *in vitro* | Vero cells | – | – | Wang S. et al. (2017) |
| 69 | Nelfinavir mesylate | *in vitro* | Vero cells | – | – | Wang S. et al. (2017) |
| 70 | 2′-CMA | *in vitro* | Vero cells | 5.26 ± 0.12 | – | Eyer et al. (2016) |
| 71 | 7-deaza-2′-CMA | *in vitro* | Vero cells | 8.92 ± 3.32 | – | Eyer et al. (2016) |
| 72 | 2′-CMC | *in vitro* | Vero cells | 10.51 ± 0.02 | – | Eyer et al. (2016) |
| 73 | 2′-CMG | *in vitro* | Vero cells | 22.25 ± 0.03 | – | Eyer et al. (2016) |
| 74 | 2′-CMU | *in vitro* | Vero cells | 45.45 ± 0.64 | – | Eyer et al. (2016) |
| 75 | NGI-1 | *in vitro* | HEK293 cells | 2.2 | – | Puschnik et al. (2017) |
| 76 | NDGA | *in vitro* | Vero cells | 9.1 | – | Merino-Ramos et al. (2017) |
| 77 | M4N | *in vitro* | Vero cells | 5.7 | – | Merino-Ramos et al. (2017) |
| 78 | Obatoclax | *in vitro* | RPE cells | 0.04 ± 0.01 | 2.6 ± 0.4 | Kuivanen et al. (2017) |
| 79 | SaliPhe | *in vitro* | RPE cells | 0.05 ± 0.02 | >10 | Kuivanen et al. (2017) |
| 80 | Gemcitabine | *in vitro* | RPE cells | 0.01 | >10 | Kuivanen et al. (2017) |
| 81 | PHA-690509 | *in vitro* | SNB-19 cells | 0.37 | – | Xu et al. (2016) |

by intracellular ZIKV RNA levels in SNB-19 cells (**Table 3**; Xu et al., 2016).

## STRATEGIES FOR DEVELOPING SMALL-MOLECULE ZIKA INHIBITORS

The development of anti-ZIKV drugs requires effective strategies. For example, using existing drug libraries to screen drug molecules that inhibit new targets is an effective method to develop new drugs (Yang et al., 2017; Kumar et al., 2018). In silicon-based drug modeling, it is another economical and useful strategy to identify candidate drugs in a short amount of time (Pal et al., 2017; Kumar et al., 2018). In addition, virtual screening and electronic pharmacokinetic modeling also facilitate the discovery of effective drug molecules (Rohini et al., 2019). First, the virtual screening method based on electronic pharmacodynamics was adopted to screen effective inhibitors of ZIKV NS2B-NS3 protein from the ASINE database (including 467,802 molecules) (Rohini et al., 2019). Then, the complexes of known NS2B-NS3 protein and its inhibitor were used to establish a five-featured pharmacophore hypothesis, ADDRR, which consists of one hydrogen bond acceptor (A), two hydrogen bond donors (D), and two aromatic rings (R) (Rohini et al., 2019). The pharmacophore model was verified by enrichment analysis before the virtual screening process (Rohini et al., 2019).

Active development of screening methods to assess the antiviral activity of compounds is a key step in the discovery of new drugs (Ekins et al., 2016). Virus replication relies on cellular mechanisms, which means that *in vitro* experiments use host cells for culture and virus replication. Since ZIKV can infect many different cells, multiple cell lines should be used to study ZIKV infection. The screening of effective drugs using multiple cells provides a good framework for drug discovery (Barr et al., 2016). Other strategies include RNA interference, long non-coding RNAs, miRNAs, interfering peptides, and compounds targeting viral RNA (Han and Mesplede, 2018), underexplored building blocks, and elements introducing into medicinal chemistry (Nitsche et al., 2017).

## CONCLUSION

As an arthropod-borne single-stranded positive RNA virus, ZIKV utilizes a number of host viral proteins and cellular components to accomplish its replication cycle, including the steps of viral entry, genomic replication, structural and non-structural protein processing, assembly, and budding of virions. Such actions result in a series of congenital abnormities like

Guillain–Barré syndrome in adults, microcephaly in newborns, and fetal demise during pregnancy (Dick et al., 1952), and the viral and host proteins involved in the virus life cycle can serve as targets for development of small-molecule ZIKV inhibitors. For example, the ZIKV E protein is responsible for the binding of the virus to host cell receptors and mediating viral entry into the host cell; therefore, some small molecule inhibitors targeting the ZIKV E protein are effective in inhibiting virus attachment and entry (Byrd et al., 2013; Fernando et al., 2016; Oo et al., 2019). AXL expressed on human glial cells can permit ZIKV binding and entry into the host glial cells (Nowakowski et al., 2016; Meertens et al., 2017) and small molecule compounds targeting AXL may be effective in inhibiting ZIKV infection (Rausch et al., 2017). However, any compounds targeting host proteins may affect their normal functions and cause adverse effects.

Study has shown that, since the stem region of the ZIKV E protein has high sequence similarity to that of other flaviviruses, such as DENV and yellow fever virus (YFV), the ZIKV inhibitor targeting this region is also highly effective against DENV and YFV infection (Yu et al., 2017). Therefore, it is essential to develop small molecule compounds with broad flavivirus inhibitory activity. Another important strategy is to develop small molecule ZIKV inhibitors targeting the different steps of ZIKV replication cycle with a synergistic antiviral effect when they are used in combination.

Numerous cases of ZIKV sexual transmission have been reported during recent ZIKV outbreaks, and studies have shown that ZIKV also replicates in human prostate cells (Spencer et al., 2018). However, little is known about what viral protein(s) and host factor(s) are involved in this event. Therefore, it is essential to identify these proteins as targets for development of small-molecular inhibitors for preventing sexual transmission of ZIKV.

With the increasing understanding of viral protein structure, tremendous progresses have been made in structure-based discovery of inhibitors targeting the structure and non-structure protein of ZIKV, such as the E protein, three NS2B-NS3 proteinase constructs and helicase, NS5 methyltransferase and polymerase. Several series of small-molecule ZIKV inhibitors targeting these proteins have been reported. However, most of them were tested *in vitro* while only a small percentage of these compounds have been evaluated in animal models *in vivo*, and very few have advanced into clinical trials. Therefore, further studies should focus on exploiting novel strategies to identify new anti-ZIKV compounds, elucidating their mechanisms of action, improving the efficacy of anti-ZIKV compounds, and evaluating the *in vivo* efficacy and safety of these compounds in suitable animal models and patients. Further development of small-molecule ZIKV inhibitors with high-efficiency and low toxicity will bring promise for clinic treatment of ZIKV infection and related diseases in the near future.

## AUTHOR CONTRIBUTIONS

LW, RL, YG, YL, XD, RX, YZ, and FY drafted the manuscript. TY, SJ, and FY revised and edited the manuscript.

## FUNDING

This work was supported by grants from the National Natural Science Foundation of China (81974302 and 81601761), Hebei Province's Program for Talents Returning from Studying Overseas (CN201707), a starting grant from Hebei Agricultural University (ZD2016026 and YJ201843), and the Program for Youth Talent of Higher Learning Institutions of Hebei Province (BJ2018045).

## REFERENCES

Albulescu, I. C., Kovacikova, K., Tas, A., Snijder, E. J., and van Hemert, M. J. (2017). Suramin inhibits Zika virus replication by interfering with virus attachment and release of infectious particles. *Antiviral Res.* 143, 230–236. doi: 10.1016/j.antiviral.2017.04.016

Arbuckle, J. H., Gardina, P. J., Gordon, D. N., Hickman, H. D., Yewdell, J. W., Pierson, T. C., et al. (2017). Inhibitors of the histone methyltransferases EZH2/1 induce a potent antiviral state and suppress infection by diverse viral pathogens. *mBio* 8:e01141-17. doi: 10.1128/mBio.01141-17

Baell, J. B., and Holloway, G. A. (2010). New substructure filters for removal of pan assay interference compounds (PAINS) from screening libraries and for their exclusion in bioassays. *J. Med. Chem.* 53, 2719–2740. doi: 10.1021/jm901137j

Barr, K. L., Anderson, B. D., Prakoso, D., and Long, M. T. (2016). Working with Zika and Usutu Viruses in vitro. *PLoS Negl. Trop. Dis.* 10:e0004931. doi: 10.1371/journal.pntd.0004931

Barros, J. B. S., da Silva, P. A. N., Koga, R. C. R., Gonzalez-Dias, P., Carmo Filho, J. R., Nagib, P. R. A., et al. (2018). Acute Zika virus infection in an endemic area shows modest proinflammatory systemic immunoactivation and cytokine-symptom associations. *Front. Immunol.* 9:821. doi: 10.3389/fimmu.2018.00821

Bavari, S., Bosio, C. M., Wiegand, E., Ruthel, G., Will, A. B., Geisbert, T. W., et al. (2002). Lipid raft microdomains: a gateway for compartmentalized trafficking of Ebola and Marburg viruses. *J. Exp. Med.* 195, 593–602. doi: 10.1084/jem.20011500

Bernatchez, J. A., Yang, Z., Coste, M., Li, J., Beck, S., Liu, Y., et al. (2018). Development and validation of a phenotypic high-content imaging assay for assessing the antiviral activity of small-molecule inhibitors targeting Zika virus. *Antimicrob. Agents Chemother.* 62:AAC.00725-18, doi: 10.1128/AAC.00725-18

Brugger, B., Glass, B., Haberkant, P., Leibrecht, I., Wieland, F. T., and Krausslich, H. G. (2006). The HIV lipidome: a raft with an unusual composition. *Proc. Natl. Acad. Sci. U.S.A.* 103, 2641–2646. doi: 10.1073/pnas.0511136103

Bullard-Feibelman, K. M., Govero, J., Zhu, Z., Salazar, V., Veselinovic, M., Diamond, M. S., et al. (2017). The FDA-approved drug sofosbuvir inhibits Zika virus infection. *Antiviral Res.* 137, 134–140. doi: 10.1016/j.antiviral.2016.11.023

Byrd, C. M., Dai, D., Grosenbach, D. W., Berhanu, A., Jones, K. F., Cardwell, K. B., et al. (2013). A novel inhibitor of dengue virus replication that targets the capsid protein. *Antimicrob. Agents Chemother.* 57, 15–25. doi: 10.1128/AAC.01429-12

Cai, L., Sun, Y., Song, Y., Xu, L., Bei, Z., Zhang, D., et al. (2017). Viral polymerase inhibitors T-705 and T-1105 are potential inhibitors of Zika virus replication. *Arch. Virol.* 162, 2847–2853. doi: 10.1007/s00705-017-3436-8

Calland, N., Albecka, A., Belouzard, S., Wychowski, C., Duverlie, G., Descamps, V., et al. (2012). (-)-Epigallocatechin-3-gallate is a new inhibitor of hepatitis C virus entry. *Hepatology* 55, 720–729. doi: 10.1002/hep.24803

Carneiro, B. M., Batista, M. N., Braga, A. C. S., Nogueira, M. L., and Rahal, P. (2016). The green tea molecule EGCG inhibits Zika virus entry. *Virology* 496, 215–218. doi: 10.1016/j.virol.2016.06.012

Chazal, N., and Gerlier, D. (2003). Virus entry, assembly, budding, and membrane rafts. *Microbiol. Mol. Biol. Rev.* 67, 226–237. doi: 10.1128/mmbr.67.2.226-237.2003

Chen, L., Liu, Y., Wang, S., Sun, J., Wang, P., Xin, Q., et al. (2017). Antiviral activity of peptide inhibitors derived from the protein E stem against Japanese encephalitis and Zika viruses. *Antiviral Res.* 141, 140–149. doi: 10.1016/j.antiviral.2017.02.009

Chen, Y., Maguire, T., Hileman, R. E., Fromm, J. R., Esko, J. D., Linhardt, R. J., et al. (1997). Dengue virus infectivity depends on envelope protein binding to target cell heparan sulfate. *Nat. Med.* 3, 866–871. doi: 10.1038/nm0897-866

Cheng, F., Ramos, da Silva, S., Huang, I. C., Jung, J. U., and Gao, S. J. (2018). Suppression of Zika virus infection and replication in endothelial cells and astrocytes by PKA inhibitor PKI 14-22. *J Virol* 92:e02019-17. doi: 10.1128/JVI.02019-17

Cho, N. J., Dvory-Sobol, H., Xiong, A., Cho, S. J., Frank, C. W., and Glenn, J. S. (2009). Mechanism of an amphipathic alpha-helical peptide's antiviral activity involves size-dependent virus particle lysis. *ACS Chem. Biol.* 4, 1061–1067. doi: 10.1021/cb900149b

Coronado, M. A., Eberle, R. J., Bleffert, N., Feuerstein, S., Olivier, D. S., de Moraes, F. R., et al. (2018). Zika virus NS2B/NS3 proteinase: a new target for an old drug - Suramin a lead compound for NS2B/NS3 proteinase inhibition. *Antiviral Res.* 160, 118–125. doi: 10.1016/j.antiviral.2018.10.019

Cruz-Oliveira, C., Freire, J. M., Conceicao, T. M., Higa, L. M., Castanho, M. A., and Da Poian, A. T. (2015). Receptors and routes of dengue virus entry into the host cells. *FEMS Microbiol. Rev.* 39, 155–170. doi: 10.1093/femsre/fuu004

Dai, L., Song, J., Lu, X., Deng, Y. Q., Musyoki, A. M., Cheng, H., et al. (2016). Structures of the Zika Virus envelope protein and its complex with a flavivirus broadly protective antibody. *Cell Host. Microbe* 19, 696–704. doi: 10.1016/j.chom.2016.04.013

De Clercq, E., and Li, G. (2016). Approved antiviral drugs over the Past 50 Years. *Clin. Microbiol. Rev.* 29, 695–747. doi: 10.1128/CMR.00102-15

de la Cruz, L., Nguyen, T. H., Ozawa, K., Shin, J., Graham, B., Huber, T., et al. (2011). Binding of low molecular weight inhibitors promotes large conformational changes in the dengue virus NS2B-NS3 protease: fold analysis by pseudocontact shifts. *J. Am. Chem. Soc.* 133, 19205–19215. doi: 10.1021/ja208435s

Di Croce, L., and Helin, K. (2013). Transcriptional regulation by Polycomb group proteins. *Nat. Struct. Mol. Biol.* 20, 1147–1155. doi: 10.1038/nsmb.2669

Dick, G. W., Kitchen, S. F., and Haddow, A. J. (1952). Zika virus. I. Isolations and serological specificity. *Trans. R. Soc. Trop. Med. Hyg.* 46, 509–520. doi: 10.1016/0035-9203(52)90042-4

Duan, D., Doak, A. K., Nedyalkova, L., and Shoichet, B. K. (2015). Colloidal aggregation and the in vitro activity of traditional Chinese medicines. *ACS Chem. Biol.* 10, 978–988. doi: 10.1021/cb5009487

Ekins, S., Mietchen, D., Coffee, M., Stratton, T. P., Freundlich, J. S., Freitas-Junior, L., et al. (2016). Open drug discovery for the Zika virus. *F1000Res* 5:150. doi: 10.12688/f1000research.8013.1

Erbel, P., Schiering, N., D'Arcy, A., Renatus, M., Kroemer, M., Lim, S. P., et al. (2006). Structural basis for the activation of flaviviral NS3 proteases from dengue and West Nile virus. *Nat. Struct. Mol. Biol.* 13, 372–373. doi: 10.1038/nsmb1073

Estoppey, D., Lee, C. M., Janoschke, M., Lee, B. H., Wan, K. F., Dong, H., et al. (2017). The natural product cavinafungin selectively interferes with Zika and Dengue virus replication by inhibition of the host signal peptidase. *Cell Rep.* 19, 451–460. doi: 10.1016/j.celrep.2017.03.071

Eyer, L., Nencka, R., Huvarova, I., Palus, M., Joao Alves, M., Gould, E. A., et al. (2016). Nucleoside inhibitors of Zika virus. *J. Infect. Dis.* 214, 707–711. doi: 10.1093/infdis/jiw226

Fernando, S., Fernando, T., Stefanik, M., Eyer, L., and Ruzek, D. (2016). An approach for Zika virus inhibition using homology structure of the envelope protein. *Mol. Biotechnol.* 58, 801–806. doi: 10.1007/s12033-016-9979-1

Fonseca, B. D., Diering, G. H., Bidinosti, M. A., Dalal, K., Alain, T., Balgi, A. D., et al. (2012). Structure-activity analysis of niclosamide reveals potential role for cytoplasmic pH in control of mammalian target of rapamycin complex 1 (mTORC1) signaling. *J. Biol. Chem.* 287, 17530–17545. doi: 10.1074/jbc.M112.359638

Fu, B., Wang, L., Li, S., and Dorf, M. E. (2017). ZMPSTE24 defends against influenza and other pathogenic viruses. *J. Exp. Med.* 214, 919–929. doi: 10.1084/jem.20161270

Germi, R., Crance, J. M., Garin, D., Guimet, J., Lortat-Jacob, H., Ruigrok, R. W., et al. (2002). Heparan sulfate-mediated binding of infectious dengue virus type 2 and yellow fever virus. *Virology* 292, 162–168. doi: 10.1006/viro.2001.1232

Hamel, R., Dejarnac, O., Wichit, S., Ekchariyawat, P., Neyret, A., Luplertlop, N., et al. (2015). Biology of Zika virus infection in human skin cells. *J. Virol.* 89, 8880–8896. doi: 10.1128/JVI.00354-15

Han, Y., and Mesplede, T. (2018). Investigational drugs for the treatment of Zika virus infection: a preclinical and clinical update. *Expert Opin. Investig. Drugs* 27, 951–962. doi: 10.1080/13543784.2018.1548609

Hasan, S. S., Miller, A., Sapparapu, G., Fernandez, E., Klose, T., Long, F., et al. (2017). A human antibody against Zika virus crosslinks the E protein to prevent infection. *Nat. Commun.* 8:14722. doi: 10.1038/ncomms14722

Heinz, F. X., and Stiasny, K. (2017). The antigenic structure of Zika Virus and its relation to other flaviviruses: implications for infection and immunoprophylaxis. *Microbiol. Mol. Biol. Rev.* 81:AAC.1967-1916. doi: 10.1128/MMBR.00055-16

Isaacs, C. E., Wen, G. Y., Xu, W., Jia, J. H., Rohan, L., Corbo, C., et al. (2008). Epigallocatechin gallate inactivates clinical isolates of herpes simplex virus. *Antimicrob. Agents Chemother.* 52, 962–970. doi: 10.1128/AAC.00825-07

Jackman, J. A., Costa, V. V., Park, S., Real, A., Park, J. H., Cardozo, P. L., et al. (2018). Therapeutic treatment of Zika virus infection using a brain-penetrating antiviral peptide. *Nat. Mater.* 17, 971–977. doi: 10.1038/s41563-018-0194-2

Ji, R., Meng, L., Jiang, X., Cvm, N. K., Ding, J., Li, Q., et al. (2014). TAM receptors support neural stem cell survival, proliferation and neuronal differentiation. *PLoS One* 9:e115140. doi: 10.1371/journal.pone.0115140

Jin, J., Chen, Y. J., Wang, D. C., Ma, L. M., Guo, M., Zhou, C. L., et al. (2018). The inhibitory effect of sodium baicalin on oseltamivir-resistant influenza A virus via reduction of neuraminidase activity. *Arch. Pharm. Res.* 41, 664–676. doi: 10.1007/s12272-018-1022-6

Jurgeit, A., McDowell, R., Moese, S., Meldrum, E., Schwendener, R., and Greber, U. F. (2012). Niclosamide is a proton carrier and targets acidic endosomes with broad antiviral effects. *PLoS Pathog.* 8:e1002976. doi: 10.1371/journal.ppat.1002976

Kim, J. M., Kim, K., Punj, V., Liang, G., Ulmer, T. S., Lu, W., et al. (2015). Linker histone H1.2 establishes chromatin compaction and gene silencing through recognition of H3K27me3. *Sci. Rep.* 5:16714. doi: 10.1038/srep16714

Kim, Y. M., Gayen, S., Kang, C., Joy, J., Huang, Q., Chen, A. S., et al. (2013). NMR analysis of a novel enzymatically active unlinked dengue NS2B-NS3 protease complex. *J. Biol. Chem.* 288, 12891–12900. doi: 10.1074/jbc.M112.442723

Kirby, W. M., Hudson, D. G., and Noyes, W. D. (1956). Clinical and laboratory studies of novobiocin, a new antibiotic. *AMA Arch. Intern. Med.* 98, 1–7.

Kuivanen, S., Bespalov, M. M., Nandania, J., Ianevski, A., Velagapudi, V., De Brabander, J. K., et al. (2017). Obatoclax, saliphenylhalamide and gemcitabine inhibit Zika virus infection in vitro and differentially affect cellular signaling, transcription and metabolism. *Antiviral Res.* 139, 117–128. doi: 10.1016/j.antiviral.2016.12.022

Kumar, A., Liang, B., Aarthy, M., Singh, S. K., Garg, N., Mysorekar, I. U., et al. (2018). Hydroxychloroquine inhibits Zika virus NS2B-NS3 protease. *ACS Omega* 3, 18132–18141. doi: 10.1021/acsomega.8b01002

Lee, H., Ren, J., Nocadello, S., Rice, A. J., Ojeda, I., Light, S., et al. (2017). Identification of novel small molecule inhibitors against NS2B/NS3 serine protease from Zika virus. *Antiviral Res.* 139, 49–58. doi: 10.1016/j.antiviral.2016.12.016

Lei, J., Hansen, G., Nitsche, C., Klein, C. D., Zhang, L., and Hilgenfeld, R. (2016). Crystal structure of Zika virus NS2B-NS3 protease in complex with a boronate inhibitor. *Science* 353, 503–505. doi: 10.1126/science.aag2419

Lemke, G., and Rothlin, C. V. (2008). Immunobiology of the TAM receptors. *Nat. Rev. Immunol.* 8, 327–336. doi: 10.1038/nri2303

Li, C., Deng, Y. Q., Wang, S., Ma, F., Aliyari, R., Huang, X. Y., et al. (2017a). 25-Hydroxycholesterol protects host against Zika virus infection and its associated microcephaly in a mouse model. *Immunity* 46, 446–456. doi: 10.1016/j.immuni.2017.02.012

Li, C., Zhu, X., Ji, X., Quanquin, N., Deng, Y. Q., Tian, M., et al. (2017b). Chloroquine, a FDA-approved Drug, Prevents Zika virus infection and its associated congenital microcephaly in mice. *EBioMedicine* 24, 189–194. doi: 10.1016/j.ebiom.2017.09.034

Li, Y., Zhang, Z., Phoo, W. W., Loh, Y. R., Wang, W., Liu, S., et al. (2017c). Structural dynamics of Zika virus NS2B-NS3 protease binding to dipeptide inhibitors. *Structure* 25:1242-1250.e3. doi: 10.1016/j.str.2017.06.006

Li, Z., Brecher, M., Deng, Y. Q., Zhang, J., Sakamuru, S., Liu, B., et al. (2017d). Existing drugs as broad-spectrum and potent inhibitors for Zika virus by targeting NS2B-NS3 interaction. *Cell Res.* 27, 1046–1064. doi: 10.1038/cr.2017.88

Li, F., Lang, Y., Ji, Z., Xia, Z., Han, Y., Cheng, Y., et al. (2019). A scorpion venom peptide Ev37 restricts viral late entry by alkalizing acidic organelles. *J. Biol. Chem.* 294, 182–194. doi: 10.1074/jbc.RA118.005015

Li, Y., Zhang, Z., Phoo, W. W., Loh, Y. R., Li, R., Yang, H. Y., et al. (2018). Structural insights into the inhibition of Zika virus NS2B-NS3 protease by a small-molecule inhibitor. *Structure* 26:555-564.e3. doi: 10.1016/j.str.2018.02.005

Li, Z., Sakamuru, S., Huang, R., Brecher, M., Koetzner, C. A., Zhang, J., et al. (2018). Erythrosin B is a potent and broad-spectrum orthosteric inhibitor of the flavivirus NS2B-NS3 protease. *Antiviral Res.* 150, 217–225. doi: 10.1016/j.antiviral.2017.12.018

Lim, H. J., Nguyen, T. T., Kim, N. M., Park, J. S., Jang, T. S., and Kim, D. (2017). Inhibitory effect of flavonoids against NS2B-NS3 protease of ZIKA virus and their structure activity relationship. *Biotechnol. Lett.* 39, 415–421. doi: 10.1007/s10529-016-2261-6

Liu, T., Lin, X., Zhou, X., Deng, Z., and Cane, D. E. (2008). Mechanism of thioesterase-catalyzed chain release in the biosynthesis of the polyether antibiotic nanchangmycin. *Chem. Biol.* 15, 449–458. doi: 10.1016/j.chembiol.2008.04.006

Lorizate, M., Sachsenheimer, T., Glass, B., Habermann, A., Gerl, M. J., Krausslich, H. G., et al. (2013). Comparative lipidomics analysis of HIV-1 particles and their producer cell membrane in different cell lines. *Cell Microbiol.* 15, 292–304. doi: 10.1111/cmi.12101

Lozach, P. Y., Burleigh, L., Staropoli, I., Navarro-Sanchez, E., Harriague, J., Virelizier, J. L., et al. (2005). Dendritic cell-specific intercellular adhesion molecule 3-grabbing non-integrin (DC-SIGN)-mediated enhancement of dengue virus infection is independent of DC-SIGN internalization signals. *J. Biol. Chem.* 280, 23698–23708. doi: 10.1074/jbc.M504337200

Lu, G., Bluemling, G. R., Collop, P., Hager, M., Kuiper, D., Gurale, B. P., et al. (2017). Analysis of ribonucleotide 5'-triphosphate analogs as potential inhibitors of Zika virus RNA-Dependent RNA polymerase by using nonradioactive polymerase assays. *Antimicrob. Agents Chemother.* 61:AAC.01967-16. doi: 10.1128/AAC.01967-16

Margueron, R., and Reinberg, D. (2011). The Polycomb complex PRC2 and its mark in life. *Nature* 469, 343–349. doi: 10.1038/nature09784

McGovern, S. L., Caselli, E., Grigorieff, N., and Shoichet, B. K. (2002). A common mechanism underlying promiscuous inhibitors from virtual and high-throughput screening. *J. Med. Chem.* 45, 1712–1722. doi: 10.1021/jm010533y

Meertens, L., Carnec, X., Lecoin, M. P., Ramdasi, R., Guivel-Benhassine, F., Lew, E., et al. (2012). The TIM and TAM families of phosphatidylserine receptors mediate dengue virus entry. *Cell Host. Microbe* 12, 544–557. doi: 10.1016/j.chom.2012.08.009

Meertens, L., Labeau, A., Dejarnac, O., Cipriani, S., Sinigaglia, L., Bonnet-Madin, L., et al. (2017). Axl mediates ZIKA virus entry in human glial cells and modulates innate immune responses. *Cell Rep.* 18, 324–333. doi: 10.1016/j.celrep.2016.12.045

Merino-Ramos, T., Jimenez, de Oya, N., Saiz, J. C., and Martin-Acebes, M. A. (2017). Antiviral activity of nordihydroguaiaretic acid and its derivative Tetra-O-methyl nordihydroguaiaretic acid against west nile virus and Zika virus. *Antimicrob. Agents Chemother.* 61:AAC.00376-17, doi: 10.1128/AAC.00376-17

Miner, J. J., Daniels, B. P., Shrestha, B., Proenca-Modena, J. L., Lew, E. D., Lazear, H. M., et al. (2015). The TAM receptor Mertk protects against neuroinvasive viral infection by maintaining blood-brain barrier integrity. *Nat. Med.* 21, 1464–1472. doi: 10.1038/nm.3974

Moghaddam, E., Teoh, B. T., Sam, S. S., Lani, R., Hassandarvish, P., Chik, Z., et al. (2014). Baicalin, a metabolite of baicalein with antiviral activity against dengue virus. *Sci. Rep.* 4:5452. doi: 10.1038/srep05452

Mottin, M., Borba, J., Braga, R. C., Torres, P. H. M., Martini, M. C., Proenca-Modena, J. L., et al. (2018). The A-Z of Zika drug discovery. *Drug Discov. Today* 23, 1833–1847. doi: 10.1016/j.drudis.2018.06.014

Mounce, B. C., Cesaro, T., Carrau, L., Vallet, T., and Vignuzzi, M. (2017). Curcumin inhibits Zika and chikungunya virus infection by inhibiting cell binding. *Antiviral Res.* 142, 148–157. doi: 10.1016/j.antiviral.2017.03.014

Musso, D., and Gubler, D. J. (2016). Zika Virus. *Clin. Microbiol. Rev.* 29, 487–524. doi: 10.1128/CMR.00072-15

Nance, C. L., Siwak, E. B., and Shearer, W. T. (2009). Preclinical development of the green tea catechin, epigallocatechin gallate, as an HIV-1 therapy. *J. Allergy Clin. Immunol.* 123, 459–465. doi: 10.1016/j.jaci.2008.12.024

Navarro-Sanchez, E., Altmeyer, R., Amara, A., Schwartz, O., Fieschi, F., Virelizier, J. L., et al. (2003). Dendritic-cell-specific ICAM3-grabbing non-integrin is essential for the productive infection of human dendritic cells by mosquito-cell-derived dengue viruses. *EMBO Rep.* 4, 723–728. doi: 10.1038/sj.embor.embor866

Nitsche, C., Passioura, T., Varava, P., Mahawaththa, M. C., Leuthold, M. M., Klein, C. D., et al. (2019). De novo discovery of nonstandard macrocyclic peptides as noncompetitive inhibitors of the Zika virus NS2B-NS3 protease. *ACS Med. Chem. Lett.* 10, 168–174. doi: 10.1021/acsmedchemlett.8b00535

Nitsche, C., Zhang, L., Weigel, L. F., Schilz, J., Graf, D., Bartenschlager, R., et al. (2017). Peptide-boronic acid inhibitors of flaviviral proteases: medicinal chemistry and structural biology. *J. Med. Chem.* 60, 511–516. doi: 10.1021/acs.jmedchem.6b01021

Nowakowski, T. J., Pollen, A. A., Di Lullo, E., Sandoval-Espinosa, C., Bershteyn, M., and Kriegstein, A. R. (2016). Expression analysis highlights AXL as a Candidate Zika virus entry receptor in neural stem cells. *Cell Stem Cell* 18, 591–596. doi: 10.1016/j.stem.2016.03.012

Nyboe Andersen, A., Nelson, S. M., Fauser, B. C., Garcia-Velasco, J. A., Klein, B. M., Arce, J. C., et al. (2017). Individualized versus conventional ovarian stimulation for in vitro fertilization: a multicenter, randomized, controlled, assessor-blinded, phase 3 noninferiority trial. *Fertil. Steril.* 107, 387-396.e4. doi: 10.1016/j.fertnstert.2016.10.033

Olsen, D. B., Eldrup, A. B., Bartholomew, L., Bhat, B., Bosserman, M. R., Ceccacci, A., et al. (2004). A 7-deaza-adenosine analog is a potent and selective inhibitor of hepatitis C virus replication with excellent pharmacokinetic properties. *Antimicrob. Agents Chemother.* 48, 3944–3953. doi: 10.1128/AAC.48.10.3944-3953.2004

Oo, A., Rausalu, K., Merits, A., Higgs, S., Vanlandingham, D., Abu Bakar, S., et al. (2018). Deciphering the potential of baicalin as an antiviral agent for Chikungunya virus infection. *Antiviral Res.* 150, 101–111. doi: 10.1016/j.antiviral.2017.12.012

Oo, A., Teoh, B. T., Sam, S. S., Bakar, S. A., and Zandi, K. (2019). Baicalein and baicalin as Zika virus inhibitors. *Arch. Virol.* 164, 585–593. doi: 10.1007/s00705-018-4083-4

Pal, P., Misra, G., and Mathur, P. (2017). In silico screening of small molecule modulators of Zika virus proteins . Noida: IEEE.

Passioura, T., Katoh, T., Goto, Y., and Suga, H. (2014). Selection-based discovery of druglike macrocyclic peptides. *Annu. Rev. Biochem.* 83, 727–752. doi: 10.1146/annurev-biochem-060713-035456

Perera-Lecoin, M., Meertens, L., Carnec, X., and Amara, A. (2013). Flavivirus entry receptors: an update. *Viruses* 6, 69–88. doi: 10.3390/v6010069

Petersen, L. R., Jamieson, D. J., Powers, A. M., and Honein, M. A. (2016). Zika Virus. *N. Engl. J. Med.* 374, 1552–1563. doi: 10.1056/NEJMra1602113

Phoo, W. W., Li, Y., Zhang, Z., Lee, M. Y., Loh, Y. R., Tan, Y. B., et al. (2016). Structure of the NS2B-NS3 protease from Zika virus after self-cleavage. *Nat. Commun.* 7:13410. doi: 10.1038/ncomms13410

Phoo, W. W., Zhang, Z., Wirawan, M., Chew, E. J. C., Chew, A. B. L., Kouretova, J., et al. (2018). Structures of Zika virus NS2B-NS3 protease in complex with peptidomimetic inhibitors. *Antiviral Res.* 160, 17–24. doi: 10.1016/j.antiviral.2018.10.006

Pierson, T. C., and Kielian, M. (2013). Flaviviruses: braking the entering. *Curr. Opin. Virol.* 3, 3–12. doi: 10.1016/j.coviro.2012.12.001

Pryke, K. M., Abraham, J., Sali, T. M., Gall, B. J., Archer, I., Liu, A., et al. (2017). A novel agonist of the TRIF pathway induces a cellular state refractory to replication of Zika, Chikungunya, and dengue viruses. *mBio* 8:e00452-17. doi: 10.1128/mBio.00452-17

Puschnik, A. S., Marceau, C. D., Ooi, Y. S., Majzoub, K., Rinis, N., Contessa, J. N., et al. (2017). A small-molecule oligosaccharyltransferase inhibitor with pan-flaviviral activity. *Cell Rep.* 21, 3032–3039. doi: 10.1016/j.celrep.2017.11.054

Ramharack, P., and Soliman, M. E. S. (2018). Zika virus NS5 protein potential inhibitors: an enhanced in silico approach in drug discovery. *J. Biomol. Struct. Dyn.* 36, 1118–1133. doi: 10.1080/07391102.2017.1313175

Rausch, K., Hackett, B. A., Weinbren, N. L., Reeder, S. M., Sadovsky, Y., Hunter, C. A., et al. (2017). Screening bioactives reveals nanchangmycin as a broad spectrum antiviral active against Zika Virus. *Cell Rep.* 18, 804–815. doi: 10.1016/j.celrep.2016.12.068

Rocker, A. E., Muller, J. A., Dietzel, E., Harms, M., Kruger, F., Heid, C., et al. (2018). The molecular tweezer CLR01 inhibits Ebola and Zika virus infection. *Antiviral Res.* 152, 26–35. doi: 10.1016/j.antiviral.2018.02.003

Rohini, K., Agarwal, P., Preethi, B., Shanthi, V., and Ramanathan, K. (2019). Exploring the lead compounds for Zika Virus NS2B-NS3 protein: an e-pharmacophore-based approach. *Appl. Biochem. Biotechnol.* 187, 194–210. doi: 10.1007/s12010-018-2814-3

Roy, A., Lim, L., Srivastava, S., Lu, Y., and Song, J. (2017). Solution conformations of Zika NS2B-NS3pro and its inhibition by natural products from edible plants. *PLoS One* 12:e0180632. doi: 10.1371/journal.pone.0180632

Sahoo, M., Jena, L., Daf, S., and Kumar, S. (2016). Virtual screening for potential inhibitors of NS3 protein of Zika Virus. *Genomics Inform.* 14, 104–111. doi: 10.5808/GI.2016.14.3.104

Shannon, A. E., Pedroso, M. M., Chappell, K. J., Watterson, D., Liebscher, S., Kok, W. M., et al. (2016). Product release is rate-limiting for catalytic processing by the Dengue virus protease. *Sci. Rep.* 6:37539. doi: 10.1038/srep37539

Shi, Y., and Gao, G. F. (2017). Structural Biology of the Zika Virus. *Trends Biochem. Sci.* 42, 443–456. doi: 10.1016/j.tibs.2017.02.009

Shiryaev, S. A., Farhy, C., Pinto, A., Huang, C. T., Simonetti, N., Elong Ngono, A., et al. (2017). Characterization of the Zika virus two-component NS2B-NS3 protease and structure-assisted identification of allosteric small-molecule antagonists. *Antiviral Res.* 143, 218–229. doi: 10.1016/j.antiviral.2017.04.015

Singh, A., and Jana, N. K. (2017). Discovery of potential Zika virus RNA polymerase inhibitors by docking-based virtual screening. *Comput. Biol. Chem.* 71, 144–151. doi: 10.1016/j.compbiolchem.2017.10.007

Song, J., and Ni, F. (1998). NMR for the design of functional mimetics of protein-protein interactions: one key is in the building of bridges. *Biochem. Cell Biol.* 76, 177–188.

Song, J. M., Lee, K. H., and Seong, B. L. (2005). Antiviral effect of catechins in green tea on influenza virus. *Antiviral Res.* 68, 66–74. doi: 10.1016/j.antiviral.2005.06.010

Spencer, J. L., Lahon, A., Tran, L. L., Arya, R. P., Kneubehl, A. R., Vogt, M. B., et al. (2018). Replication of Zika Virus in human prostate cells: a potential source of sexually transmitted virus. *J. Infect. Dis.* 217, 538–547. doi: 10.1093/infdis/jix436

Stephen, P., Baz, M., Boivin, G., and Lin, S. X. (2016). Structural insight into NS5 of Zika virus leading to the discovery of MTase inhibitors. *J. Am. Chem. Soc.* 138, 16212–16215. doi: 10.1021/jacs.6b10399

Suroengrit, A., Yuttithamnon, W., Srivarangkul, P., Pankaew, S., Kingkaew, K., Chavasiri, W., et al. (2017). Halogenated chrysins inhibit dengue and Zika virus infectivity. *Sci. Rep.* 7:13696. doi: 10.1038/s41598-017-14121-5

Tong, X., Smith, J., Bukreyeva, N., Koma, T., Manning, J. T., Kalkeri, R., et al. (2018). Merimepodib, an IMPDH inhibitor, suppresses replication of Zika virus and other emerging viral pathogens. *Antiviral Res.* 149, 34–40. doi: 10.1016/j.antiviral.2017.11.004

Tritsch, D., Zingle, C., Rohmer, M., and Grosdemange-Billiard, C. (2015). Flavonoids: true or promiscuous inhibitors of enzyme? The case of deoxyxylulose phosphate reductoisomerase. *Bioorg. Chem.* 59, 140–144. doi: 10.1016/j.bioorg.2015.02.008

Vanwalscappel, B., Tada, T., and Landau, N. R. (2018). Toll-like receptor agonist R848 blocks Zika virus replication by inducing the antiviral protein viperin. *Virology* 522, 199–208. doi: 10.1016/j.virol.2018.07.014

Vasireddi, M., Crum, A., May, H., Katz, D., and Hilliard, J. (2019). A novel antiviral inhibits Zika virus infection while increasing intracellular glutathione biosynthesis in distinct cell culture models. *Antiviral Res.* 161, 46–52. doi: 10.1016/j.antiviral.2018.09.004

Verma, S. K., Tian, X., LaFrance, L. V., Duquenne, C., Suarez, D. P., Newlander, K. A., et al. (2012). Identification of Potent, Selective, Cell-active inhibitors of the histone lysine methyltransferase EZH2. *ACS Med. Chem. Lett.* 3, 1091–1096. doi: 10.1021/ml3003346

Wang, C., Yang, S. N. Y., Smith, K., Forwood, J. K., and Jans, D. A. (2017). Nuclear import inhibitor N-(4-hydroxyphenyl) retinamide targets Zika virus (ZIKV) nonstructural protein 5 to inhibit ZIKV infection. *Biochem. Biophys. Res. Commun.* 493, 1555–1559. doi: 10.1016/j.bbrc.2017.10.016

Wang, S., Liu, Y., Guo, J., Wang, P., Zhang, L., Xiao, G., et al. (2017). Screening of FDA-approved drugs for inhibitors of Japanese encephalitis virus infection. *J Virol* 91:e01055-17. doi: 10.1128/JVI.01055-17

Wang, X., Zou, P., Wu, F., Lu, L., and Jiang, S. (2017). Development of small-molecule viral inhibitors targeting various stages of the life cycle of emerging and re-emerging viruses. *Front. Med.* 11:449–461. doi: 10.1007/s11684-017-0589-5

Wang, Z. Y., Wang, Z., Zhen, Z. D., Feng, K. H., Guo, J., Gao, N., et al. (2017). Axl is not an indispensable factor for Zika virus infection in mice. *J. Gen. Virol.* 98, 2061–2068. doi: 10.1099/jgv.0.000886

Wang, Z., Wang, P., and An, J. (2016). Zika virus and Zika fever. *Virol. Sin.* 31, 103–109. doi: 10.1007/s12250-016-3780-y

Xu, H. T., Hassounah, S. A., Colby-Germinario, S. P., Oliveira, M., Fogarty, C., Quan, Y., et al. (2017). Purification of Zika virus RNA-dependent RNA polymerase and its use to identify small-molecule Zika inhibitors. *J. Antimicrob. Chemother.* 72, 727–734. doi: 10.1093/jac/dkw514

Xu, M., Lee, E. M., Wen, Z., Cheng, Y., Huang, W. K., Qian, X., et al. (2016). Identification of small-molecule inhibitors of Zika virus infection and induced neural cell death via a drug repurposing screen. *Nat. Med.* 22, 1101–1107. doi: 10.1038/nm.4184

Yang, H. T., Ju, J. H., Wong, Y. T., Shmulevich, I., and Chiang, J. H. (2017). Literature-based discovery of new candidates for drug repurposing. *Brief Bioinform.* 18, 488–497. doi: 10.1093/bib/bbw030

Yu, Y., Deng, Y. Q., Zou, P., Wang, Q., Dai, Y., Yu, F., et al. (2017). A peptide-based viral inactivator inhibits Zika virus infection in pregnant mice and fetuses. *Nat. Commun.* 8:15672. doi: 10.1038/ncomms15672

Yuan, S., Chan, J. F., den-Haan, H., Chik, K. K., Zhang, A. J., Chan, C. C., et al. (2017). Structure-based discovery of clinically approved drugs as Zika virus NS2B-NS3 protease inhibitors that potently inhibit Zika virus infection in vitro and in vivo. *Antiviral Res.* 145, 33–43. doi: 10.1016/j.antiviral.2017.07.007

Zandi, K., Teoh, B. T., Sam, S. S., Wong, P. F., Mustafa, M. R., and Abubakar, S. (2012). Novel antiviral activity of baicalein against dengue virus. *BMC Complement. Altern. Med.* 12:214. doi: 10.1186/1472-6882-12-214

Zelensky, A. N., and Gready, J. E. (2005). The C-type lectin-like domain superfamily. *FEBS J.* 272, 6179–6217. doi: 10.1111/j.1742-4658.2005.05031.x

Zhang, Z., Li, Y., Loh, Y. R., Phoo, W. W., Hung, A. W., Kang, C., et al. (2016). Crystal structure of unlinked NS2B-NS3 protease from Zika virus. *Science* 354, 1597–1600. doi: 10.1126/science.aai9309

Zhao, Y., and Tan, W. (2015). [Advances in the researches of genomic characterization and molecular detection of Middel East respiratory syndrome coronavirus]. *Zhonghua Yu Fang Yi Xue Za Zhi* 49, 461–464.

Zmurko, J., Marques, R. E., Schols, D., Verbeken, E., Kaptein, S. J., and Neyts, J. (2016). The Viral Polymerase inhibitor 7-Deaza-2′-C-Methyladenosine Is a Potent inhibitor of In Vitro Zika virus replication and delays disease progression in a robust mouse infection model. *PLoS Negl. Trop. Dis.* 10:e0004695. doi: 10.1371/journal.pntd.0004695

**Conflict of Interest:** The authors declare that the research was conducted in the absence of any commercial or financial relationships that could be construed as a potential conflict of interest.

*Copyright © 2019 Wang, Liang, Gao, Li, Deng, Xiang, Zhang, Ying, Jiang and Yu. This is an open-access article distributed under the terms of the Creative Commons Attribution License (CC BY). The use, distribution or reproduction in other forums is permitted, provided the original author(s) and the copyright owner(s) are credited and that the original publication in this journal is cited, in accordance with accepted academic practice. No use, distribution or reproduction is permitted which does not comply with these terms.*

frontiers in Microbiology

REVIEW
published: 19 December 2019
doi: 10.3389/fmicb.2019.02881

# Recent Progress in Vaccine Development Against Chikungunya Virus

*Shan Gao[1], Siqi Song[1,2] and Leiliang Zhang[1]**

[1] Institute of Basic Medicine, Shandong First Medical University & Shandong Academy of Medical Sciences, Jinan, China,
[2] School of Basic Medicine, Qingdao University, Qingdao, China

Chikungunya fever (CHIKF) is an acute infectious disease that is mediated by the mosquito-transmitted chikungunya virus (CHIKV). People infected with CHIKV may experience high fever, severe joint pain, skin rash, and headache. In recent years, this disease has become a global public health problem. However, there is no licensed vaccine available for CHIKV. Accumulating research data have provided novel approaches and new directions for the development of CHIKV vaccines. Our review focuses on recent progress in CHIKV vaccine studies. The potential vaccine candidates are classified into seven types: inactivated vaccine, subunit vaccine, live-attenuated vaccine, recombinant virus-vectored vaccine, virus-like particle vaccine, chimeric vaccine, and nucleic acid vaccine. These studies will provide important insights into the future development of CHIKV vaccines.

**Keywords: chikungunya fever, CHIKV, live-attenuated vaccine, VLP, chimeric vaccine**

OPEN ACCESS

***Edited by:***
*Lu Lu,*
*Fudan University, China*

***Reviewed by:***
*Rong Zhang,*
*Shanghai Medical College of Fudan University, China*
*Qiang Ding,*
*Tsinghua University, China*

****Correspondence:***
*Leiliang Zhang*
*armzhang@hotmail.com*

***Specialty section:***
*This article was submitted to Virology, a section of the journal Frontiers in Microbiology*

***Received:*** *30 September 2019*
***Accepted:*** *29 November 2019*
***Published:*** *19 December 2019*

***Citation:***
*Gao S, Song S and Zhang L (2019) Recent Progress in Vaccine Development Against Chikungunya Virus. Front. Microbiol. 10:2881. doi: 10.3389/fmicb.2019.02881*

## INTRODUCTION

Chikungunya fever (CHIKF) is a recurrent infectious disease caused by the chikungunya virus (CHIKV). The main clinical symptoms are arthritis and fever. Patients may also suffer from headache, myalgia, and rash. The mortality of CHIKF is below 0.5%, lower than dengue fever, which has similar clinical symptoms. For infants under 1 year old and people over 60 years old, the mortality will significantly increase (Langsjoen et al., 2018). The acute symptoms usually disappear within about 1–2 weeks, but patients may endure long-lasting joint pain and fatigue (Elsinga et al., 2017). Since CHIKV was first isolated in 1952 from Tanzania, it has induced several outbreaks, mainly in Africa and Asia. However, after re-emerging in 2004 in Kenya, the epidemic area expanded from the tropical zone to even Europe and America (Enserink, 2007). The unprecedentedly rapid and wide spread of this disease calls for efficient preventive measures.

Belonging to the genus Alphavirus of the *Togaviridae* family, CHIKV is an enveloped arthropod-borne virus (arbovirus) with *Aedes aegypti* and *Aedes albopictus* as its primary vectors. The genome of CHIKV consists of a positive-sense RNA approximately 11.5 kb in length. The CHIKV genome comprises two open reading frames (ORFs) that encode four non-structural proteins (nsPs) and one structural polyprotein (**Figure 1**). The nsPs function as a replicase complex, which not only replicates genomic RNA for progeny but also transcribes subgenomic RNA to express structural proteins (Ljungberg and Liljestrom, 2015). As for the structural polyprotein, it will be further cleaved to capsid and E3-E2-6K/TF-E1 (**Figure 1**). The latter is important for virion assembly and virus entry. E1/E2 glycoprotein in the envelope was reported to mediate cell binding at the early stage of infection (Strauss and Strauss, 1994).

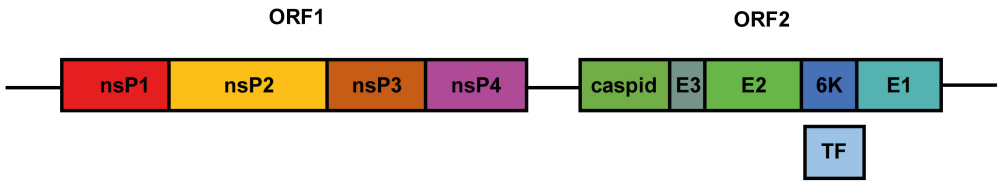


**FIGURE 1 |** Schematic diagram of the CHIKV genome. The genome of CHIKV is a single-strand RNA compromising two ORFs. ORF1 encodes four nsPs. Translation and further processing of ORF2 produce structural proteins capsid, E3, E2, 6K, and E1. During translation, ribosome shifts to –1 reading frame in 6K, leading to the production of TF protein.

The large-scale resurgence of CHIKV is, to some extent, due to social and economic developments, such as the increased number of overseas tourists, the high population density brought about by urbanization, and the changes in mosquito distribution caused by global warming. A lot of antiviral compounds have shown valuable therapeutic efficacies, especially during CHIKF outbreak. Since it is one of the most cost-benefit public strategies to prevent infectious disease, vaccine is an indispensable means for preventing CHIKF. Considering that the CHIKV antigen variety is limited and infection may lead to lifelong immunity, the advantage of vaccination is particularly prominent.

The attempt to develop a CHIKV vaccine started from the 1960s, not long after the virus was isolated. Since then, researchers have continued to develop CHIKV vaccine candidates that balance immunogenicity and safety. However, there is no licensed CHIKV vaccine available for use. Researchers have taken advantage of progress in biochemical and molecular methods and have utilized various strategies to develop vaccines, which can be classified as inactivated viral vaccine, subunit vaccine, live-attenuated virus (LAV) vaccine, recombinant virus-vectored vaccine, chimeric vaccine, virus-like particle (VLP) vaccine, and nucleic acid vaccine. In the majority of this review, we focus on novel CHIKV vaccine development and progress in the evaluation of vaccine candidates since 2016.

## INACTIVATED VACCINE

The first attempts to develop a CHIKV vaccine emerged shortly after the first CHIKF outbreak in the 1960s. Early studies adopted inactivated vaccine as the preferred strategy. By inactivating the virus via heating or chemical treatment (formalin), researchers generated vaccines that could stimulate the immune response without risk of infection, which conferred inactivated vaccine with high safety.

Researchers first infected mouse brains with an African genotype strain of CHIKV and successfully collected neutralizing antibodies 15 days post infection (Kitaoka, 1967). The most prominent achievements in early CHIKV vaccine development were made at the Walter Reed Army Institute of Research, based on a series of platforms including chicken embryos, suckling-mouse brains, and African green monkey kidney cells. The first evaluation of inactivated vaccine in humans was reported in 1971 (Harrison et al., 1971). Two groups of healthy volunteers were vaccinated twice (day 0 and 28) with 0.5 or 1 mL, respectively. Both groups developed neutralizing antibodies within 2 weeks without adverse effects.

In the following 40 years, many vaccine candidates based on inactivation have been developed and have entered the clinical phase. One inactivated vaccine, which was produced in Vero cells, stimulated both cellular and humoral immune responses, with the peak titer of neutralizing antibodies appearing at 6–8 weeks post-vaccination (Tiwari et al., 2009). Kumar et al. (2012) evaluated the protective efficacy of an E2 protein-based recombinant vaccine and whole-virus inactivated vaccine. When measuring the virus load in serum and tissues, both vaccines were verified to protect mice from CHIKV infection. Recently, the means of inoculation has also been improved. Rudd et al. (2015) introduced Foroderm for the delivery of inactivated CHIKV vaccine using cylindrical silica microparticles. This needle-free strategy greatly improves the convenience of vaccination.

The stability and safety of inactivated vaccine come at the expense of efficacy and production cost, which, to a certain extent, impedes its accessibility. The development of inactivated vaccines shows a less prosperous trend than vaccines based on other strategies.

## SUBUNIT VACCINE

Subunit vaccine, like inactivated vaccine, is an early mature strategy for vaccine preparation. The viral envelope or capsid is obtained through chemolysis or proteolysis to prepare the vaccine. By using individual viral proteins, subunit vaccines elicit an immune response without inducing the production of antibodies against unrelated antigens or infectious viral particles. This method not only ensures the safety of the vaccine but also makes large-scale manufacturing possible.

The CHIKV envelope glycoproteins E1 and E2 have been selected to develop CHIKV subunit vaccines in different expression systems. Metz et al. (2011) first expressed E1 and E2 in insect cells. Both proteins were N-glycosylated and membrane-targeting, consistent with the maturation of E1 and E2 in whole CHIKV virion. E2 antibody generated by this baculovirus expression system was able to neutralize CHIKV in rabbits. Next, they compared the immunogenicity of three recombinant baculoviruses: E1, E2, and CHIKV VLPs. Although all three baculoviruses induced neutralizing antibodies, the titers of the subunits were not as high as that of VLP. When challenging AG129 mice with infectious CHIKV, VLP

protected all animals, while only half of the mice vaccinated by the subunits finally survived. These results suggested that the efficacy of subunit vaccine was not as good as that of other strategies (Metz et al., 2013). This was partially confirmed by other studies that identified the important role of adjuvants in subunit vaccine application (Khan et al., 2012; Kumar et al., 2012). Also, subunits based on CHIKV E1 and E2 were alternatively generated in bacterial expression systems. E1 and E2 proteins from bacteria successfully neutralized CHIKV and completely protected BALB/c mice from disease induced by CHIKV. However, the efficacies varied with different adjuvants, indicating that the immune response to subunit vaccine largely depended on adjuvants.

## LAV

Live-attenuated virus is generated by modifying the structure of a virus to significantly weaken its virulence while retaining its immunogenicity. Compared with inactive vaccine, which is a fully inactive pathogen, LAV can stimulate a stronger and long-term immune response. However, higher immunogenic ability is a trade-off for lower safety. In this regard, the safety of LAV should be cautiously evaluated during animal model and clinical trials (Plante et al., 2015). Owing to its high immunogenic potency, LAV is the platform with the best prospects. It can also be combined with other strategies such as vector vaccine, which further extends its application.

After CHIKV enters cells, early immune response is activated by nsPs. Thus, several LAVs have been designed that target nsPs. By the use of the concept well established in the Semliki Forest virus (SFV), Chan et al. (2019) introduced point mutation to generate three CHIKV mutants. The specific mutation sites and corresponding vaccine candidates were as follows: RH-CHIKV, with R532H substitution in the cleavage region between nsP1 and nsP2; EV-CHIKV, with E515V substitution in nsP2; RHEV-CHIKV, with combinational double mutations of R532H and E515V. Researchers characterized the activity of the three mutants *in vitro* and found that the viral RNA titers of both RH-CHIKV and RHEV-CHIKV were lower than that of WT-CHIKV. Consistent with this result, RH-CHIKV and RHEV-CHIKV induced high levels of IFN-α and IFN-γ. To clarify whether the reduced activity exhibited in mouse tail fibroblasts affected symptoms *in vivo*, WT and mutant CHIKV were injected into adult mice. Acute viremia was largely alleviated in RH-CHIKV and RHEV-CHIKV infected mice. Mutant CHIKV also changed the cytokine pathway toward anti-inflammatory response. When challenged by the closely related O'nyong-nyong virus, no obvious viremia was detected in nsP-mutant-infected mice, indicating broad cross-protection by the vaccines.

Another LAV targeting nsP was Δ5nsP3, in which 180 nucleotides in the replicase region of nsP3 were deleted. Single-dose immunization with Δ5nsP3 generated high titers of neutralizing antibodies that lasted until the day of virus challenge (LR2006-OPY1 strain, day 123). It also induced IFN-γ T-cell responses. By determining the viral load in plasma and measuring hematological parameters, Δ5nsP3 vaccination showed protective efficacy in cynomolgus macaques against CHIKV infection. In this study, researchers evaluated another two LAVs. One was a DNA-launched replicon vaccine, DREP-E, in which the capsid of CHIKV was deleted. The other was a recombinant modified vaccinia virus that encoded the full CHIKV C-E3-E2-6K-E1. Both vaccine candidates showed similar results as Δ5nsP3, indicating good prospects for the future application of LAV (Roques et al., 2017).

Capsid was another potential target for LAV development. Recently, a novel vaccine candidate against CHIKV was generated in which the capsid was completely deleted (Zhang et al., 2019). Researchers found that capsid was dispensable for ΔC-CHIKV virion assembly. Consistent with this, ΔC-CHIKV successfully propagated in BHK-21 cells and had similar antigenic activity to WT-CHIKV. Single-dose vaccination ($10^4$ PFU) of C57BL/6 mice and immunocompromised IFNAR$^{-/-}$ mice protected them from subsequent CHIKV (ECSA strain) challenge. ΔC-CHIKV efficiently induced neutralizing antibodies, comparably with WT CHIKV. No footpad swelling was observed in ΔC-CHIKV immunized mice. The attenuated infection in IFNAR$^{-/-}$ mice indicated that ΔC-CHIKV could be a potential vaccine. The researchers specially assessed the stability of ΔC-CHIKV, since it was an important concern for all LAVs. After five passages, no detectable genomic change was reported. The efficacy and safety of ΔC-CHIKV suggested that it is a promising vaccine candidate.

Taylor et al. (2017) found a nuclear localization sequence (NoLS) in the N-terminal region of capsid protein that was important for virus replication and developed a vaccine candidate by site-directed mutagenesis. Mechanistically, they discovered that the attenuated replication resulted from reduced nuclear import of capsid protein. Attenuation was confirmed by measuring the virus copy number in the supernatants of cultured BHK-21 and C6/36 cells. Mice administered a subcutaneous injection of CHIKV-NoLS showed no disease symptoms. Cross-protection was monitored when CHIKV-NoLS-immunized mice were challenged by another alphavirus, Ross River virus (RRV). The attenuation and stability of CHIKV-NoLS were further evaluated by histological and flow cytometric analysis (Abeyratne et al., 2018). Mice inoculated with CHIKV-NoLS exhibited minimal inflammation in the footpad compared with a CHIKV-WT infected group. When stored at −20°C and −80°C for up to 56 days, the titer of CHIKV-NoLS remained stable. Besides, CHIKV-NoLS showed no loss of infectivity after freeze and thaw. These results confirmed the preclinical safety and stability of CHIKV-NoLS.

Recently, a novel genomic rationale was adopted by Carrau et al. (2019). Multiple replacements of synonymous codons were made in the CHIKV genome to reduce the mutational robustness of the virus and led to a deleterious evolutionary direction (Carrau et al., 2019). Synonymous codons that had the highest likelihood of becoming stop codons ("1-to-Stop," one mutation away from stop) were examined. They constructed two candidates. Specifically, the STOP virus had 151 "1-to-Stop" synonymous codons for all Leu and Ser, while the SuperStop virus had 285 "1-to-Stop" synonymous codons for leucine, serine, arginine, and glycine in the structural-protein-coding region of

the CHIKV genome. In experiments on mice, attenuated virus infectivity and diminished disease symptoms were observed. One prominent advantage of this approach was its safety. Since hundreds of synonymous mutations were generated, the reversion risk was greatly reduced.

## RECOMBINANT VIRUS-VECTORED VACCINE

Recombinant virus-vectored vaccine is obtained by inserting genes encoding exogenous protective antigen into the vector virus genome. Recombinant vector vaccine offers the advantages of safety and easy inoculation. A variety of virus vectors, such as poxvirus, herpesvirus, adenovirus, and paramyxovirus, have been used in vaccine development.

Recombinant measles virus vector is widely used to develop CHIKV vaccines and performed well in phase I and II clinical trials. Rossi et al. (2019) tested the immunogenicity and efficacy of their new developed measles virus-vectored vaccine on cynomolgus macaques. Serum was examined by plaque reduction neutralization test and enzyme-linked immunosorbent assay (ELISA). The results indicated that a robust immune response was elicited by measles virus-vectored vaccine. There was no obvious difference in hematology and clinical chemical indicators between control and the vaccinated group. The clinical symptoms of the disease, mainly referring to fever here, were not observed either after vaccination or after virus challenge. Macaques were also protected from viremia. The efficacy and safety of this vaccine were confirmed by the outcome of clinical trials. In a randomized, double-blind Phase I clinical trial, the seroconversion rate was 44–92% with a single dose and reached 100% after a second vaccination (Ramsauer et al., 2015). Recently, a double-blind, randomized, placebo-controlled and active-controlled phase II trial was carried out and reported (Reisinger et al., 2019). Participants aged 18–55 respectively received control vaccine ($n$ = 34), MV-CHIK ($n$ = 195), or measles prime and MV-CHIK ($n$ = 34) by intramuscular injections between August 17, 2016, and May 31, 2017. Neutralizing antibodies specifically against CHIKV were detected in MV-CHIK treatment groups, with no serious adverse events reported. Due to its good safety and immunogenicity, MV-CHIK is a promising vaccine candidate for CHIKV.

Most CHIKV vaccine candidates are delivered through injection subcutaneously at the wrist or intramuscularly in the quadriceps muscles. Taking advantage of their platform based on adenovirus 5, the researchers developed an oral CHIKV vaccine (Dora et al., 2019). Preservation in tablets promoted further processing, facilitated non-sterile packaging, shortened the production time, and reduced the economic cost. Oral administration also alleviated the discomfort of vaccination. A replication-deficient 5 type adenovirus (rAd) with a lack of E1 and E3 allowed for the expression of different antigens concurrently, which made it an ideal platform for vaccine development. The researchers have constructed three vaccine candidates with different combinations of CHIKV structural proteins: Ad-CHIKV-SG (expressing C-E3-E2-6K/TF-E1), Ad-CHIKV-E3/E2/E1, and Ad-CHIKV-E3/E2/6K (Dora et al., 2019). All three vaccines induced high IgG titers against CHIKV at week 7, while the former two candidates showed significantly higher titers than Ad-CHIKV-E3/E2/6K. C57BL/6 mice were adopted to test immunogenicity and protection against CHIKV disease. A single dose of $10^8$ IU administration intranasally gave rise to neutralizing antibodies and protected mice from viremia and footpad swelling.

Another adenovirus-based study utilized replication-deficient chimpanzee adenovirus. Due to the induction of anti-adenovirus immune response, human adenoviral-vectored vaccines are not suitable for humans. Chimpanzee adenovirus overcomes this problem to maintain vaccine efficacy (Lopez-Camacho et al., 2019). In this study, the full length or capsid-deleted structural proteins of CHIKV were expressed at the adenoviral platform to generated vaccines ChAdOx1 sCHIKV and ChAdOx1 sCHIKV ΔC. A single dose of the two kinds of ChAdOx1 vaccines was injected in BALB/c mice. Two weeks after vaccination, mice that had received either of the two vaccines showed a high T-cell response frequency. ChAdOx1 sCHIKV and ChAdOx1 sCHIKV ΔC also induced a robust humoral response, indicated by a high level of CHIKV-specific IgG. The above results also highlighted that ChAdOx1 sCHIKV did not require an adjuvant to achieve efficacy. Having confirmed the immunogenicity of ChAdOx1 sCHIKV, further studies will be needed to promote preclinical trials.

Vectors are also suitable for bivalent vaccine. ZIKV, an enveloped positive-stranded RNA virus, shares similarities with CHIKV in clinical symptoms and transmission route. Chattopadhyay et al. previously developed a CHIKV vaccine based on VSV vector (VSVΔG-CHIKV), in which the G protein of VSV was replaced by CHIKV E3-E2-6K-E1 envelope polyprotein (Chattopadhyay et al., 2013). They went further to additionally express ZIKV envelope glycoproteins on that platform (VSVΔG-CHIKV-ZIKV) (Chattopadhyay et al., 2018). Vaccination with VSVΔG-CHIKV-ZIKV induced neutralizing antibody in immunocompetent BALB/c mice and type-I IFN receptor-deficient A129 mice. The immune response was sufficient to protect immunized animals from ZIKV and CHIKV infection, with no viremia detectable. Additionally, the deletion of the G protein also eliminated the neurotropism of VSV, making it safer and more efficient.

## VLP

Virus-like particle is assembled by expressing viral structural proteins that possess self-assembly capacity. With antigenic epitopes similar to wild-type virus, VLP can induce high neutralizing antibody titer. VLP has high safety due to its deficiency in replicative and infectious ability (DeZure et al., 2016). Although the development of VLP vaccine started later than that of traditional strategies, several prominent VLP vaccine candidates have been developed recently.

Virus-like particle vaccines have shown prospective applications, but the mammalian expression systems in

which VLP vaccines have been produced limited productivity and increased cost. *Pichia pastoris*, an ideal platform for protein expression, has been adopted to produce VLP for many viruses. The *Pichia* system not only supplied native circumstance for protein expression but also increased the performance-to-price ratio to a large extent (Vogl et al., 2013). Saraswat et al. (2016) have made a good attempt to utilize a yeast expression system for developing CHIKV VLP vaccine. They successfully introduced the gene expressing CHIKV whole structural proteins into the *Pichia* expression system and confirmed the morphological identity of VLPs with CHIKV by electron microscopy. Next, the potential of this product (CHIK-VLPs) to be a vaccine candidate was extensively evaluated. ELISA and plaque reduction neutralization testing showed that CHIK-VLPs induced high-titered antibodies with super specificity and neutralizing activity. Elevated levels of TNF-α and IL-10 indicated a robust cellular response, which combined with restricted levels of IL-2, IL-4, and IFN-γ to make a balanced response. The humoral and cellular immune response elicited by CHIK-VLPs was consistent with the protection of CHIK-VLP-immunized BALB/c mice against CHIKV pathogenesis.

In another study, researchers evaluated the efficacies of different VLP formulations with or without an adjuvant in protecting adult and aged mice (Arevalo et al., 2019). Although VLP alone was able to protect adult mice against CHIKV disease, the disease was even more serious in aged mice vaccinated by VLP alone or VLP plus QuilA adjuvant. ELISA and microneutralization assays showed that immunization elicited a high level of neutralizing antibody titer specifically against CHIKV in adult mice. However, for aged mice, negligible antibody was detected. This research implied that specific vaccines suitable for the elderly should be developed in the future.

## CHIMERIC VACCINE

Chimeric vaccine links the genome or genome fragments of at least two pathogens by genetic engineering to express antigens from multiple pathogens simultaneously. The most attractive advantage of chimera vaccines is a high immune response against multiple pathogens. Besides, since it is constructed by genomic methods, chimeric vaccines are more stable than traditional LAV.

The ideal vaccine would balance safety and immunogenicity; low performance in one or the other is the disadvantage of LAV and inactivated vaccine, respectively. To overcome this issue, Erasmus et al. (2017) creatively used an insect-specific alphavirus, Eilat virus (EILV), to contain CHIKV structural proteins. Its deficiency of replication gave this chimera virus a high level of safety. However, the entry and delivery of RNA during the early stage of virus replication resembled that of wild-type CHIKV. They first identified that EILV/CHIKV virus had an identical structure to wild-type CHIKV. They then chose immunocompetent C57BL/6 mice, immunocompromised A129 IFNα/βR$^{-/-}$ mice, and cynomolgus macaques to conduct *in vivo* experiments. A single dose elicited rapid seroconversion 4 days post-vaccination (DPV). Meanwhile, antigen-specific IFN-γ-producing CD8$^{+}$ T cells were induced. Challenged by CHIKV at 30 DPV, all C57BL/6 mice vaccinated by EILV/CHIKV were protected from viremia. For IFNα/βR$^{-/-}$ mice, which were utilized for long-term efficacy assessment, EILV/CHIKV vaccination also protected them from weight loss, footpad swelling, viremia, and death. Finally, EILV/CHIKV vaccination was tolerated in cynomolgus macaques. The body temperature remained at baseline level, and viremia was not detectable after CHIKV challenge. In addition, EILV/CHIKV exhibited cross-neutralization against three different strains from the Asian, West African, and Indian Ocean lineages (Erasmus et al., 2017). Another alphavirus, Sindbis virus (SINV), is commonly used as the genetic backbone for chimeric vaccine and successfully protected cynomolgus macaques against lethal eastern equine encephalitis virus (EEEV). However, the Eilat virus is hosted only by insects, further ensuring the safety of the chimeric vaccine.

## NUCLEIC ACID VACCINE

DNA vaccine is a novel platform that has been developed in recent years. By introducing exogenous DNA into the host, antigen proteins are synthesized by the host expression system. The obvious advantage of DNA vaccine is its simplicity of production. Additionally, DNA vaccine is stable at low temperature, which makes it convenient to store and transport across long distances (Powers, 2018). However, there are several drawbacks to this strategy. Integrating exogenous DNA may elicit an autoimmune response in the host. The immunogenicity is low in humans, and thus vaccination needs repeated boosters as well as adjuvants (Powers, 2018). Addressing these concerns will enable breakthroughs in DNA vaccine design.

Hidajat et al. have developed a new method called iDNA® infectious clone technology, which generates vaccine from plasmid DNA both *in vitro* and *in vivo* (Hidajat et al., 2016). It is distinct from traditional infectious clone technology, which needed *in vitro* RNA transcription and *in vitro* transfection involving bacteriophage polymerase, in that an iDNA® infectious clone uses a CMV promoter to transcribe genomic RNA from a plasmid in eukaryotic cells (Tretyakova et al., 2013). Taking advantage of this novel technology, they developed a DNA-launching vaccine for CHIKV (pCHIKV-7) that encoded the full-length cDNA of 181/25 vaccine. *In vivo* experiments showed that single-dose vaccination with pCHIKV-7 protected mice from CHIKV disease, with neutralizing antibodies being detectable in all animals (Tretyakova et al., 2014). In 2016, researchers analyzed its genetic stability by next-generation sequencing (NGS) (Hidajat et al., 2016). Illumina HiSeq2000 sequencing revealed that overall pCHIKV-7 was more stable than 181/25. As for E2-12 and E2-82 residues, two previously identified attenuating mutations, the frequencies of reversion in pCHIKV-7 were 0.064 and 0.086%, respectively, much lower than that of 181/25 (0.179 and 0.133%).

Conventional vaccines require a lag phase to allow enough antibody generation, which is not suitable for urgent protective need in response to a virus outbreak. Passive immunotherapy such as monoclonal antibody (mAb) prophylaxis provides effective short-term protection. However, repeated injection

**TABLE 1 |** Recently developed vaccine candidates against CHIKV.

| Type | Vaccine | Antigen/target | Animal model | Dosage | Route | Results | References |
|---|---|---|---|---|---|---|---|
| LAV | RH-CHIKV<br>EV-CHIKV<br>RHEV-CHIKV | R532H-nsP1<br>E515V-nsP2 | Adult C57BL/6J mice | $10^6$ PFU, single injection | Injection in the metatarsal region of the footpad | RH-CHIKV and RHEV-CHIKV reduced CHIKV infectivity and alleviated viremia and joint symptoms. Cross-protection against ONNV | Chan et al. (2019) |
| LAV | Δ5nsP3<br>DREP-E<br>MVA-CE | nsP3 envelope and capsid | Cynomolgus macaques | $10^5$ PFU, single injection | Subcutaneous injection in the shoulder and in the upper part of the left wrist | Δ5nsP3 did not induce fever, lymphopenia, or increase in cytokine | Roques et al. (2017) |
| LAV | ΔC-CHIKV | Capsid deletion | 6-week C57BL/6J and IFNAR$^{-/-}$ mice | $10^4$ PFU, single injection | Subcutaneous injection | Preserves infectivity in BHK-21 cells. Single-dose injection elicited strong protection against CHIKV in both WT and IFNAR$^{-/-}$ mice, without footpad swelling or weight loss | Zhang et al. (2019) |
| LAV | CHIKV-NoLS | N-terminal region of capsid protein | 21-day C57BL/6 mice | $10^4$ PFU, single injection | Subcutaneous injection | No sign of footpad welling, viremia reduced, and expression of proinflammatory factors decreased. Cross-protection against RRV. Vaccine thermo-stable, and minimal inflammation and tissue damage | Taylor et al. (2017); Abeyratne et al. (2018) |
| LAV | Stop CHIKV<br>SuperStop CHIKV | Multiple synonymous mutations in genome to reduce mutational robustness | 5-week C57BL/6 mice | $10^4$ PFU, single injection | Footpad injection | No footpad swelling, low viremia, high level of neutralizing antibody | Carrau et al. (2019) |
| Vector virus | MV-CHIK | Measles-vectored CHIKV structural proteins | 18–55-year-old healthy volunteers | $5 \times 10^4$, $5 \times 10^5$ TCID50, twice injection; measle-primed group accepted additional injection at −28 day | Intramuscular injection | Safety and tolerance similar to measle vaccine | Reisinger et al. (2019) |
| Vector virus | MV-CHIK | Measles-vectored CHIKV structural proteins | Adult cynomolgus macaques | 0.35 mL single measle vaccine dose, twice injection at day 0 and day 28 | Intramuscular injection in the quadriceps muscles | Viremia low. No signs of disease. Cross-protection against other CHIKV strains | Rossi et al. (2019) |
| Vector virus | Ad-CHIKV-SG<br>Ad-CHIKV-E3/E2/6K<br>Ad-CHIKV-E3/E2/E1 | Structural proteins | 6–8-week BALB/c mice<br>4-week C57BL/6 mice | $10^7$ infectious units (BALB/c) $10^8$ infectious units (C57BL/6) | Intranasal administration | Induced high tighter of CHIKV-specific IgG antibodies | Dora et al. (2019) |
| Vector virus | ChAdOx1 sCHIKV<br>ChAdOx1 sCHIKV ΔC | Structural polyprotein | 6–8-week BALB/c mice | $10^8$ infectious units with or without adjuvant | Intramuscular injection | High immunogenicity | Lopez-Camacho et al. (2019) |

*(Continued)*

**TABLE 1 |** Continued

| Type | Vaccine | Antigen/target | Animal model | Dosage | Route | Results | References |
|---|---|---|---|---|---|---|---|
| Vector virus | VSVΔG-CHIKV | CHIKV: E3-E2-6K-E1 envelope polyprotein ZIKV: envelope glycoproteins | 6–8-week BALB/c mice 7-week A129 mice | $10^7$ PFU, single injection | Intramuscular injection | Induced neutralizing antibody responses to both CHIKV and ZIKV. Protected from both CHIKV- and ZIKV-induced diseases | Chattopadhyay et al. (2018) |
| Chimeric virus | EILV/CHIKV | EILV cDNA clone containing CHIKV structural proteins | 4-week C57BL/6 mice; 6-week IFNα/βR$^{-/-}$ mice Cynomolgus macaques | 8.8 log10 PFU (C57BL/6) or 8.5 log10 PFU (IFNα/βR$^{-/-}$mice) of live EILV/CHIKV, single injection | Subcutaneous injection | Protected from viremia and footpad swelling when challenged by virus on day 30 post-vaccination. Exhibited long-term efficacy in IFNα/βR$^{-/-}$ mice. For cynomolgus macaques, held normal, baseline diurnal body temperatures 31 DPC | Erasmus et al. (2017) |
| VLP | CHIK-VLP | C-E proteins | 6–8-week (adult), 18–24-month (aged) C57BL/6 mice | 30 μg VLPs with different adjuvants Three-time vaccination with or without adjuvants | Intramuscular injection | CHIK VLP without adjuvant elicited immune responses and protected adult mice but exacerbated disease on aged mice | Arevalo et al. (2019) |
| VLP | CHIK-VLPs | Structural proteins introduced into yeast expression system | 4-week BALB/c mice | 10, 20, and 40 μg of yeast-derived CHIK-VLPs (in Freund's adjuvant); boosted at day 14 and day 28 | Subcutaneous injection | High level of specific antibody with high neutralization activity. Induced robust humoral and cell-mediated response | Saraswat et al. (2016) |
| DNA vaccine | dMAb | CHIKV envelope | B6. Cg-Foxn1nu/J mice | 100 μg CVM1-Fab plus 25 μg CHIKV Env plasmid injected three times at 2-week intervals | Intramuscular injection | One injection produced antibodies rapidly and neutralized diverse CHIKV clinical isolates | Muthumani et al. (2016) |
| DNA vaccine | pCHIKV-7 | Full-length cDNA of 181/25 vaccine | – | – | – | Genetic stable | Hidajat et al. (2016) |
| RNA vaccine | CHKV-24 | Lipid-encapsulated neutralizing human mAbs | AG129 mice Cynomolgus macaques | 10, 2, or 0.4 mg/kg, single injection | Intravenous injection | Protected mice from arthritis, musculoskeletal tissue infection, and lethality and reduced viremia to undetectable levels | Kose et al. (2019) |

*LAV, live-attenuated virus; VLP, virus-like particles; –, not mentioned.*

is necessary due to the short half-life of immunoglobulins. Muthumani et al. (2016) combined the advantages of a passive antibody and vaccination by an *in vivo* delivery method. DNA encoding the biologically active mAb (dMAb) targeting CHIKV envelope was delivered by plasmid rather than virus vector through electroporation. This strategy also circumvented the risk of inducing an immune response against the vector. Immunizing animals by intramuscular injection of dMAb induced antibodies much more rapidly than conventional vaccination methods. Footpad swelling was not observed in immunized animals challenged by the virus. These dMAbs were able to neutralize diverse CHIKV clinical isolates. In conclusion, this study highlighted the advantages of DNA vaccine, which could be combined with other platforms for vaccine development.

A design based on mRNA is one of the newest strategies for CHIKV vaccine. The vaccine can be designed to deliver mAb just like the DNA vaccine introduced above. Kose et al. (2019) isolated neutralizing human mAbs from the B cells of a survivor of CHIKV infection. They introduced the mAb-encoding sequences into lipid-encapsulated mRNA, which was then delivered by infusion. Among all the mAbs being examined, CHKV-24 showed most prominent inhibitory effect in neutralization assay. *In vivo* experiments revealed that infusion of CHKV-24 succeeded in inducing human IgG in both mice and macaques, the latter of which peaked at 24 h after immunization with the dosage varied from 10.1 to 35.9 μg/mL. Compared with proteins, nucleic acids encoding antibodies are easy to produce and cost less. Another strategy for using an mRNA platform is to instruct host cells to express viral antigens for generating antibodies accordingly. A biotech company named Moderna Therapeutics developed an mRNA CHIKV vaccine (mRNA-1388) and made it through to phase I clinical trial, using engineered mRNA that encoded CHIKV structural polyprotein. With a single dose of this mRNA vaccine, a strong immune response was elicited, and 100% protection was achieved in mice (Goyal et al., 2018). This innovation avoided an immune response against engineered mRNA and ensured sufficient protein synthesis.

## ANIMAL MODELS

Apart from extensive *ex vivo* studies, *in vivo* experiments are important for developing vaccines. Different animal models have provided platforms for evaluating the efficacy and security of potential CHIKV vaccines. The studies summarized in this paper used cynomolgus macaques and mice of multiple strains involving C57BL/6, BALB/c, and A129.

C57BL/6 mice are immunocompetent animals. Because they are easy to breed and their traits are stable, C57BL/6 mice are widely used to evaluate vaccines. Live-attenuated vaccines evaluated in C57BL/6 mice have included CHIKV-NoLS, RH-CHIKV, EV-CHIKV, RHEV-CHIKV, ΔC-CHIKV, "STOP," and "SuperStop." C57BL/6 mice have also been used to assess CHIK-VLP.

BALB/c mice are easy to breed and display little gender difference in body weight. BALB/c mice have been widely employed to develop DNA vaccines and recombinant vector vaccines (ChOdAx1 sCHIKV, ChOdAx1 sCHIKV ΔC, Ad-CHIKV-SG, Ad-CHIKV-E3/E2/6K, and Ad-CHIKV-E3/E2/E1).

Another murine model used in CHIKV infection is A129. Since they lack type I interferon receptors, A129 mice are deficient in the innate immune response. However, their adaptive immunity is retained so that they are tolerant to virus challenging (Couderc et al., 2008). A129 mice have been involved in immunogenicity studies of the EILV/CHIKV, VSVΔG-CHIKV, and CHKV-24 mRNA vaccines.

The cynomolgus macaque, as a non-human primate, is particularly suitable for studying the pathogenesis of viral infection. Compared with murine models, non-human primates share more similarities with humans in physiology, metabolism, and immunity (Labadie et al., 2010), making them highly effective for predicting the efficacy of human treatment. Despite the high cost and complexity of breeding them, macaques remain an irreplaceable model in vaccine development. Non-human primates have been proved to be susceptible to CHIKV infection (Labadie et al., 2010). Studies on LAV vaccine Δ5nsP3, vector vaccine MV-CHIK, mRNA vaccine CHKV-24, and chimeric vaccine EILV/CHIKV have set cynomolgus macaque as an animal model for immunogenicity assessment.

## CONCLUSION

As a rapidly spreading recurrent infectious disease, CHIKF has attracted wide attention. Vaccination is a powerful means to control epidemic diseases including CHIKF, but there is no commercial vaccine against CHIKV at present. The re-outbreak of CHIKF since 2004 boosted CHIKV vaccine development. Researchers have applied a variety of strategies to develop vaccine candidates, some of which have entered the Phase-I or Phase-II stage of clinical trials and show promising application prospects. In this paper, the latest progress in the development and testing of CHIKV vaccine, especially since 2016, was reviewed. The development strategies, immunogenicity evaluation, and protective efficacy against diseases were introduced; the key information is summarized in **Table 1**.

Future studies should pay more attention to the following aspects: (1) Comprehensive consideration of both safety and immunogenicity. This is a common concern for all vaccine production. On the premise of keeping a low rate of revertant mutation of the virus, the vaccine titer should be enhanced to achieve better protection efficacy. (2) Convenience of production and use. Vaccines should be thermostable and easy to produce, transport, and store. In addition, their administration should be convenient, and the discomfort of vaccination should be alleviated. Bivalent and multivalent chimeric vaccines can immunize against more than one virus at one time, which will greatly improve the immune response. (3) Long-term and short-term protection. Vaccines should provide long-term protection. However, acute protection is needed in local areas in times of outbreak. From this point of view, DNA vaccine with both long-term and short-term protective efficacies is a good choice (Muthumani et al., 2016). (4) Different performance in different

populations. In one study involving adult and aged mice, vaccines that showed protective efficacies in adult mice exaggerated the symptoms of disease in aged mice (Arevalo et al., 2019). This result suggests that the populations had a significant difference in response to the vaccine. Attention should be paid to the complexity of the social population, especially when determining the dose of vaccine to use. Broadly speaking, most vaccine studies are based on animal models, whether the developed vaccine is suitable for humans has yet to be evaluated. Clinical trials need to be promoted. It is believed that with the progress of new strategies and studies, commercial CHIKV vaccine with high safety, strong immunogenicity, convenient development, and moderate cost can be developed in the near future.

## AUTHOR CONTRIBUTIONS

LZ and SS provided the concept. SG drafted the manuscript. SG and LZ revised the manuscript. All authors approved the final version for publication.

## FUNDING

This work was supported by grants from the National Key Plan for Research and Development of China (2016YFD0500300), the National Natural Science Foundation of China (81871663 and 81672035), and the Academic Promotion Program of Shandong First Medical University.

## REFERENCES

Abeyratne, E., Freitas, J. R., Zaid, A., Mahalingam, S., and Taylor, A. (2018). Attenuation and stability of CHIKV-NoLS, a live-attenuated chikungunya virus vaccine candidate. *Vaccines* 7:E2. doi: 10.3390/vaccines7010002

Arevalo, M. T., Huang, Y., Jones, C. A., and Ross, T. M. (2019). Vaccination with a chikungunya virus-like particle vaccine exacerbates disease in aged mice. *PLoS Negl. Trop. Dis.* 13:e0007316. doi: 10.1371/journal.pntd.0007316

Carrau, L., Rezelj, V. V., Noval, M. G., Levi, L. I., Megrian, D., Blanc, H., et al. (2019). Chikungunya virus vaccine candidates with decreased mutational robustness are attenuated in vivo and have compromised transmissibility. *J. Virol.* 93:e00775-19. doi: 10.1128/JVI.00775-19

Chan, Y. H., Teo, T. H., Utt, A., Tan, J. J., Amrun, S. N., Abu Bakar, F., et al. (2019). Mutating chikungunya virus non-structural protein produces potent live-attenuated vaccine candidate. *EMBO Mol. Med.* 11:e10092. doi: 10.15252/emmm.201810092

Chattopadhyay, A., Aguilar, P. V., Bopp, N. E., Yarovinsky, T. O., Weaver, S. C., and Rose, J. K. (2018). A recombinant virus vaccine that protects against both Chikungunya and Zika virus infections. *Vaccine* 36, 3894–3900. doi: 10.1016/j.vaccine.2018.05.095

Chattopadhyay, A., Wang, E., Seymour, R., Weaver, S. C., and Rose, J. K. (2013). A chimeric vesiculo/alphavirus is an effective alphavirus vaccine. *J. Virol.* 87, 395–402. doi: 10.1128/JVI.01860-12

Couderc, T., Chretien, F., Schilte, C., Disson, O., Brigitte, M., Guivel-Benhassine, F., et al. (2008). A mouse model for Chikungunya: young age and inefficient type-I interferon signaling are risk factors for severe disease. *PLoS Pathog.* 4:e29. doi: 10.1371/journal.ppat.0040029

DeZure, A. D., Berkowitz, N. M., Graham, B. S., and Ledgerwood, J. E. (2016). Whole-Inactivated and virus-like particle vaccine strategies for Chikungunya Virus. *J. Infect. Dis.* 214(Suppl. 5), S497–S499. doi: 10.1093/infdis/jiw352

Dora, E. G., Rossi, S. L., Weaver, S. C., Tucker, S. N., and Mateo, R. (2019). An adjuvanted adenovirus 5-based vaccine elicits neutralizing antibodies and protects mice against chikungunya virus-induced footpad swelling. *Vaccine* 37, 3146–3150. doi: 10.1016/j.vaccine.2019.04.069

Elsinga, J., Gerstenbluth, I., van der Ploeg, S., Halabi, Y., Lourents, N. T., Burgerhof, J. G., et al. (2017). Long-term Chikungunya Sequelae in Curacao: burden, determinants, and a novel classification tool. *J. Infect. Dis.* 216, 573–581. doi: 10.1093/infdis/jix312

Enserink, M. (2007). Infectious diseases. Chikungunya: no longer a third world disease. *Science* 318, 1860–1861. doi: 10.1126/science.318.5858.1860

Erasmus, J. H., Auguste, A. J., Kaelber, J. T., Luo, H., Rossi, S. L., Fenton, K., et al. (2017). A chikungunya fever vaccine utilizing an insect-specific virus platform. *Nat. Med.* 23, 192–199. doi: 10.1038/nm.4253

Goyal, M., Chauhan, A., Goyal, V., Jaiswal, N., Singh, S., and Singh, M. (2018). Recent development in the strategies projected for chikungunya vaccine in humans. *Drug Des. Dev. Ther.* 12, 4195–4206. doi: 10.2147/DDDT.S181574

Harrison, V. R., Eckels, K. H., Bartelloni, P. J., and Hampton, C. (1971). Production and evaluation of a formalin-killed Chikungunya vaccine. *J. Immunol.* 107, 643–647.

Hidajat, R., Nickols, B., Forrester, N., Tretyakova, I., Weaver, S., and Pushko, P. (2016). Next generation sequencing of DNA-launched Chikungunya vaccine virus. *Virology* 490, 83–90. doi: 10.1016/j.virol.2016.01.009

Khan, M., Dhanwani, R., Rao, P. V., and Parida, M. (2012). Subunit vaccine formulations based on recombinant envelope proteins of Chikungunya virus elicit balanced Th1/Th2 response and virus-neutralizing antibodies in mice. *Virus Res.* 167, 236–246. doi: 10.1016/j.virusres.2012.05.004

Kitaoka, M. (1967). Japanese encephalitis vaccine including a preliminary report on dengue fever and chikungunya vaccines. *Jpn. J. Med. Sci. Biol.* 20(Suppl.), 41–56.

Kose, N., Fox, J. M., Sapparapu, G., Bombardi, R., Tennekoon, R. N., de Silva, A. D., et al. (2019). A lipid-encapsulated mRNA encoding a potently neutralizing human monoclonal antibody protects against chikungunya infection. *Sci. Immunol.* 4:eaaw6647. doi: 10.1126/sciimmunol.aaw6647

Kumar, M., Sudeep, A. B., and Arankalle, V. A. (2012). Evaluation of recombinant E2 protein-based and whole-virus inactivated candidate vaccines against chikungunya virus. *Vaccine* 30, 6142–6149. doi: 10.1016/j.vaccine.2012.07.072

Labadie, K., Larcher, T., Joubert, C., Mannioui, A., Delache, B., Brochard, P., et al. (2010). Chikungunya disease in nonhuman primates involves long-term viral persistence in macrophages. *J. Clin. Invest.* 120, 894–906. doi: 10.1172/JCI40104

Langsjoen, R. M., Haller, S. L., Roy, C. J., Vinet-Oliphant, H., Bergren, N. A., Erasmus, J. H., et al. (2018). Chikungunya virus strains show lineage-specific variations in virulence and cross-protective ability in murine and nonhuman primate models. *mBio* 9:e02449-17. doi: 10.1128/mBio.02449-17

Ljungberg, K., and Liljestrom, P. (2015). Self-replicating alphavirus RNA vaccines. *Expert Rev. Vaccines* 14, 177–194. doi: 10.1586/14760584.2015.965690

Lopez-Camacho, C., Kim, Y. C., Blight, J., Lazaro Moreli, M., Montoya-Diaz, E., Huiskonen, J. T., et al. (2019). Assessment of immunogenicity and neutralisation efficacy of viral-vectored vaccines against chikungunya virus. *Viruses* 11:E322. doi: 10.3390/v11040322

Metz, S. W., Geertsema, C., Martina, B. E., Andrade, P., Heldens, J. G., van Oers, M. M., et al. (2011). Functional processing and secretion of Chikungunya virus E1 and E2 glycoproteins in insect cells. *Virol. J.* 8:353. doi: 10.1186/1743-422X-8-353

Metz, S. W., Martina, B. E., van den Doel, P., Geertsema, C., Osterhaus, A. D., Vlak, J. M., et al. (2013). Chikungunya virus-like particles are more immunogenic in a lethal AG129 mouse model compared to glycoprotein E1 or E2 subunits. *Vaccine* 31, 6092–6096. doi: 10.1016/j.vaccine.2013.09.045

Muthumani, K., Block, P., Flingai, S., Muruganantham, N., Chaaithanya, I. K., Tingey, C., et al. (2016). Rapid and long-term immunity elicited by DNA-encoded antibody prophylaxis and DNA vaccination against chikungunya virus. *J. Infect. Dis.* 214, 369–378. doi: 10.1093/infdis/jiw111

Plante, K. S., Rossi, S. L., Bergren, N. A., Seymour, R. L., and Weaver, S. C. (2015). Extended preclinical safety, efficacy and stability testing of a live-attenuated chikungunya vaccine candidate. *PLoS Negl. Trop. Dis.* 9:e0004007. doi: 10.1371/journal.pntd.0004007

Powers, A. M. (2018). Vaccine and therapeutic options to control chikungunya virus. *Clin. Microbiol. Rev.* 31:e00104-16. doi: 10.1128/CMR.00104-16

Ramsauer, K., Schwameis, M., Firbas, C., Mullner, M., Putnak, R. J., Thomas, S. J., et al. (2015). Immunogenicity, safety, and tolerability of a recombinant measles-virus-based chikungunya vaccine: a randomised, double-blind, placebo-controlled, active-comparator, first-in-man trial. *Lancet Infect. Dis.* 15, 519–527. doi: 10.1016/S1473-3099(15)70043-5

Reisinger, E. C., Tschismarov, R., Beubler, E., Wiedermann, U., Firbas, C., Loebermann, M., et al. (2019). Immunogenicity, safety, and tolerability of the measles-vectored chikungunya virus vaccine MV-CHIK: a double-blind, randomised, placebo-controlled and active-controlled phase 2 trial. *Lancet* 392, 2718–2727. doi: 10.1016/S0140-6736(18)32488-7

Roques, P., Ljungberg, K., Kummerer, B. M., Gosse, L., Dereuddre-Bosquet, N., Tchitchek, N., et al. (2017). Attenuated and vectored vaccines protect nonhuman primates against chikungunya virus. *JCI Insight* 2:e83527. doi: 10.1172/jci.insight.83527

Rossi, S. L., Comer, J. E., Wang, E., Azar, S. R., Lawrence, W. S., Plante, J. A., et al. (2019). Immunogenicity and efficacy of a measles virus-vectored chikungunya vaccine in nonhuman primates. *J. Infect. Dis.* 220, 735–742. doi: 10.1093/infdis/jiz202

Rudd, P. A., Raphael, A. P., Yamada, M., Nufer, K. L., Gardner, J., Le, T. T., et al. (2015). Effective cutaneous vaccination using an inactivated chikungunya virus vaccine delivered by Foroderm. *Vaccine* 33, 5172–5180. doi: 10.1016/j.vaccine.2015.07.099

Saraswat, S., Athmaram, T. N., Parida, M., Agarwal, A., Saha, A., and Dash, P. K. (2016). Expression and characterization of yeast derived chikungunya virus like particles (CHIK-VLPs) and its evaluation as a potential vaccine candidate. *PLoS Negl. Trop. Dis.* 10:e0004782. doi: 10.1371/journal.pntd.0004782

Strauss, J. H., and Strauss, E. G. (1994). The alphaviruses: gene expression, replication, and evolution. *Microbiol. Rev.* 58, 491–562.

Taylor, A., Liu, X., Zaid, A., Goh, L. Y., Hobson-Peters, J., Hall, R. A., et al. (2017). Mutation of the N-Terminal region of chikungunya virus capsid protein: implications for vaccine design. *mBio* 8:e01970-16. doi: 10.1128/mBio.01970-16

Tiwari, M., Parida, M., Santhosh, S. R., Khan, M., Dash, P. K., and Rao, P. V. (2009). Assessment of immunogenic potential of Vero adapted formalin inactivated vaccine derived from novel ECSA genotype of chikungunya virus. *Vaccine* 27, 2513–2522. doi: 10.1016/j.vaccine.2009.02.062

Tretyakova, I., Hearn, J., Wang, E., Weaver, S., and Pushko, P. (2014). DNA vaccine initiates replication of live attenuated chikungunya virus in vitro and elicits protective immune response in mice. *J. Infect. Dis.* 209, 1882–1890. doi: 10.1093/infdis/jiu114

Tretyakova, I., Lukashevich, I. S., Glass, P., Wang, E., Weaver, S., and Pushko, P. (2013). Novel vaccine against Venezuelan equine encephalitis combines advantages of DNA immunization and a live attenuated vaccine. *Vaccine* 31, 1019–1025. doi: 10.1016/j.vaccine.2012.12.050

Vogl, T., Hartner, F. S., and Glieder, A. (2013). New opportunities by synthetic biology for biopharmaceutical production in Pichia pastoris. *Curr. Opin. Biotechnol.* 24, 1094–1101. doi: 10.1016/j.copbio.2013.02.024

Zhang, Y. N., Deng, C. L., Li, J. Q., Li, N., Zhang, Q. Y., Ye, H. Q., et al. (2019). Infectious chikungunya virus (CHIKV) with a complete capsid deletion: a new approach for a CHIKV vaccine. *J. Virol.* 93:e00504-19. doi: 10.1128/JVI.00504-19

**Conflict of Interest:** The authors declare that the research was conducted in the absence of any commercial or financial relationships that could be construed as a potential conflict of interest.

*Copyright © 2019 Gao, Song and Zhang. This is an open-access article distributed under the terms of the Creative Commons Attribution License (CC BY). The use, distribution or reproduction in other forums is permitted, provided the original author(s) and the copyright owner(s) are credited and that the original publication in this journal is cited, in accordance with accepted academic practice. No use, distribution or reproduction is permitted which does not comply with these terms.*

frontiers in Microbiology

ORIGINAL RESEARCH
published: 30 January 2020
doi: 10.3389/fmicb.2019.03079

# Montelukast, an Anti-asthmatic Drug, Inhibits Zika Virus Infection by Disrupting Viral Integrity

*Yongkang Chen†, Yuan Li†, Xiaohuan Wang and Peng Zou**

*Shanghai Public Health Clinical Center, Fudan University, Shanghai, China*

The association of Zika virus (ZIKV) infection and severe complications including neurological sequelae especially fetal microcephaly has aroused global attentions since its outbreak in 2015. Currently, there are no vaccines or therapeutic drugs clinically approved for treatments of ZIKV infection, however. And the drugs used for treating ZIKV in pregnant women require a higher safety profile. Here, we identified an anti-asthmatic drug, montelukast, which is of safety profile for pregnant women and exhibited antiviral efficacy against ZIKV infection *in vitro* and *in vivo*. And we showed that montelukast could disrupt the integrity of the virions to release the viral genomic RNA, hence irreversibly inhibiting viral infectivity. In consideration of the neuro-protective activity that montelukast possessed, which was previously reported, it is promising that montelukast could be used for patients with ZIKV infection, particularly for pregnant women.

**Keywords: Zika virus, flavivirus, montelukast, viral inactivator, viral integrity**

OPEN ACCESS

***Edited by:***
*Juan-Carlos Saiz,*
*Instituto Nacional de Investigación y Tecnología Agraria y Alimentaria (INIA), Spain*

***Reviewed by:***
*Xuping Xie,*
*The University of Texas Medical Branch at Galveston, United States*
*Cheng-Feng Qin,*
*Beijing Institute of Microbiology and Epidemiology, China*
*Antonio Mas,*
*University of Castilla–La Mancha, Spain*

***Correspondence:**
*Peng Zou*
*zoupeng@shphc.org.cn;*
*ptsou@qq.com*

*†These authors have contributed equally to this work*

***Specialty section:***
*This article was submitted to Virology, a section of the journal Frontiers in Microbiology*

***Received:*** *30 September 2019*
***Accepted:*** *19 December 2019*
***Published:*** *30 January 2020*

***Citation:***
*Chen Y, Li Y, Wang X and Zou P (2020) Montelukast, an Anti-asthmatic Drug, Inhibits Zika Virus Infection by Disrupting Viral Integrity. Front. Microbiol. 10:3079. doi: 10.3389/fmicb.2019.03079*

## INTRODUCTION

Since the first isolation in 1947 from the rhesus macaque in Zika forest, Uganda, and publication of the first human case of infection in 1952, Zika virus (ZIKV), a mosquito-borne enveloped RNA virus, has become a member of *Flavivirus* genus in the Flaviviridae family for more than 70 years together with dengue virus (DENV), yellow fever virus (YFV), Japanese encephalitis virus (JEV), and West Nile virus (WNV). The infection of ZIKV has aroused global awareness only in recent years because of some severe neurological complications such as Guillain–Barré syndrome (Brasil et al., 2016; Peixoto et al., 2019) and congenital Zika syndrome (Baud et al., 2017; Gurung et al., 2019), which consists of many clinical manifestations including intracranial calcification (ICC) and cerebellar hypoplasia (de Fatima Vasco Aragao et al., 2016; Oliveira Melo et al., 2016; Cui et al., 2017), and is remarkably typified by microcephaly found both in humans and in animal models (Cui et al., 2017), although symptoms of majority of infection with ZIKV are mild or asymptomatic. In addition, infection with ZIKV leads to impaired human spermatozoa production demonstrated by decreased sperm count in the early stage of ZIKV infection (Joguet et al., 2017). And even 1 year after ZIKV infection, abnormal spermogram results could still be observed (Avelino-Silva et al., 2018).

Since the local outbreak in Brazil and quick spread to other countries in 2015, the effort for seeking inhibitors suitable for treatment of ZIKV is ongoing till now. Targeting different stage of ZIKV life cycle, some inhibitors have been discovered (Wang et al., 2017). The first step of ZIKV infection is its attachment to the host cell membrane. A peptide derived from the stem region of E protein of ZIKV blocked the binding of virions to cells via its interaction with

E proteins to disrupt the integrity of the viral membrane (Yu et al., 2017). Erythromycin estolate was also found to effectively inhibit ZIKV infection by disrupting the integrity of the viral membrane (Wang et al., 2019). ZINC33683341 and curcumin also inhibit infection of ZIKV by disturbing the interaction between virions and cells (Delvecchio et al., 2016; Fernando et al., 2016; Li et al., 2017b; Mounce et al., 2017). Nanchangmycin, one of the antibiotics against gram-positive bacteria, inhibited ZIKV infection through blocking clathrin-mediated endocytosis (Rausch et al., 2017). A natural oxysterol, 25-hydroxycholesterol also inhibited ZIKV infection probably owing to the obstruction of the membrane fusion mediated by E protein (Li et al., 2017a). Some inhibitors can interfere with the viral RNA replication to break off the viral life cycle. For example, 7-deaza-2′-*C*-acetylene-adenosine (NITD008), an adenosine analog, inhibited ZIKV and DENV replications in a dose-dependent manner *in vitro* by terminating viral RNA synthesis and protected mice from ZIKV infection (Yin et al., 2009; Deng et al., 2016a). Emricasan, a pan-caspase inhibitor, held back the increase in caspase-3 activity induced by ZIKV infection and protected neural progenitors (Xu et al., 2016). By screening about 100 Food and Drug Administration (FDA)-approved pregnancy category B drugs, we identified montelukast, an anti-asthmatic drug. The antiviral activities of montelukast against ZIKV and other two flaviviruses, DENV and YFV, *in vitro* were evaluated. Montelukast also exhibited protective efficacy against ZIKV vertical transmission and lethal challenge. The underlying mechanisms for infectivity inhibition of flaviviruses caused by montelukast were investigated as well in this study.

# MATERIALS AND METHODS

## Cells, Viruses, and Compounds

BHK-21 cells (Baby Hamster Kidney cells), Vero E6 cells (African green monkey kidney cells), RD cells (rhabdomyosarcoma cells), and human astrocytoma cell line U-251 MG were cultured in Dulbecco's modified Eagle's medium (DMEM; Biological Industries, Israel) supplemented with 10% fetal bovine serum (FBS; Biological Industries, Israel) at 37°C and 5% $CO_2$. The C6/36 mosquito cells were grown in DMEM containing 10% FBS at 28°C with 5% $CO_2$.

ZIKV strain SZ01/2016 (GenBank number: KU866423), which was isolated from a patient who returned from Samoa and was kindly provided by Dr. Cheng-Feng Qin (Deng et al., 2016b); ZIKV strains FLR [#VR1844, American Type Culture Collection (ATCC)] and MR766 (#VR1838, ATCC) obtained from ATCC; DENV-2 kindly provided by Drs. Yunwen Hu and Zhigang Song at the Shanghai Public Health Clinical Center; and YFV strain 17D obtained from Beijing Tiantan Biological Products, Ltd., were all propagated in C6/36 cells as described previously (Yu et al., 2017). The replication-competent vesicular stomatitis virus (VSV) containing an additional viral transcriptional unit coding green fluorescent protein (VSV-GFP) was kindly provided by Dr. Nannan Wu (Wu et al., 2019) and propagated in Vero E6 cells. The enterovirus 71 (EV71) was kindly provided by Dr. Shuye Zhang (Yuan et al., 2018) and propagated in RD cells.

Montelukast sodium and chloroquine phosphate were purchased from Sigma-Aldrich (St. Louis, MO, United States). 7-Deaza-2′-*C*-acetylene-adenosine (NITD008) and curcumin were purchased from MedChemExpress (Monmouth Junction, NJ, United States). Montelukast (Mon), NITD008, and curcumin were dissolved in dimethyl sulfoxide (DMSO). Chloroquine phosphate was dissolved in sterilized water, and all of the dissolved compounds were stored at −20°C.

## Plaque Assay

Plaque assay was performed on BHK-21 cells or Vero E6 cells as previously described (Yu et al., 2017). Briefly, BHK-21 or Vero E6 cells were seeded onto cell culture plates and incubated overnight to a confluent monolayer. Virus or a mixture of virus and compounds was added into the wells and then incubated for 2 h. The supernatant was then removed, and the wells were washed and covered with an overlay of DMEM containing 0.6% low-melting-point agarose (LMP agarose, Promega, United States) and 2% FBS. The plates were then further incubated for approximately 5 days until the plaque developed. For VSV-GFP, the plates were incubated for 1 day for plaque development. After being fixed with 4% formaldehyde and stained with 1% crystal violet, the plaques were visualized, and the plaque-forming units (pfu) were counted.

## Assay for Antiviral Activity

BHK-21 cells or Vero E6 cells were seeded in six-well plates and allowed to adhere overnight. Montelukast sodium serially diluted in serum-free DMEM and 50 pfu of viruses were mixed and incubated 1 h at room temperature before being added to each well of cells. After incubation at 37°C for 2 h, the plaque assay was performed, and the plaques were visualized as described above. Curcumin, a reported antiviral drug (Mounce et al., 2017), was included as positive control. The percent inhibition by the montelukast was calculated, and the 50% inhibitory concentration (IC50) value was determined by using the software CalcuSyn (Chou and Talalay, 1984).

## Flow Cytometry Experiments

U-251 MG cells were infected with ZIKV strain SZ01 at a multiplicity of infection (MOI) of 1 after viruses incubating with serially diluted montelukast for 1 h. Then, the inoculum was removed 2 h later, and fresh DMEM containing 2% FBS and serially diluted montelukast was supplemented. Cells were trypsinized, fixed, and permeabilized with BD Fixation/Permeabilization Kit (BD Biosciences, United States) at 40 h post-infection (hpi) and then stained with anti-E mAb 4G2 (10 μg/ml); and a rabbit anti-mouse IgG, which was coupled to fluorescein isothiocyanate (FITC) (DAKO, Denmark) and diluted 1:400. Flow cytometry experiments were carried out in an LSRFortessa cell analyzer (BD Biosciences), and samples were analyzed using FlowJo software version 10 (TreeStar).

## Cytotoxicity Assay

BHK-21, Vero E6, and U-251 MG cells grown in 96-well plates ($2 \times 10^4$ cells/well) were treated with serially diluted

montelukast in DMEM containing 2% FBS for 48 h at 37°C. Cell Counting Kit-8 (CCK-8; Dojindo, Japan), a water-soluble non-radioactive reagent, allowing sensitive colorimetric assays for the determination of cell viability, was used to evaluate cytotoxicity according to the instruction manual. The absorbance at 450-nm wavelength was measured by the iMark$^{TM}$ microplate reader (Bio-Rad, United States). The percent cytotoxicity was calculated, and the 50% cytotoxicity concentration (CC50) value was determined by the CalcuSyn (Chou and Talalay, 1984).

## Time of Addition Experiments

To determine at which stage the montelukast displayed inhibitory efficiency, the time of addition assay was performed as previously described (Du et al., 2009; Liu et al., 2015). BHK-21 cells confluent in the six-well cell culture plates were infected with 50 pfu of virus; montelukast (10 μM) was added to the infected cells at 0, 1, 2, 4, and 8 hpi. Then, the supernatant was replaced with DMEM containing 0.6% LMP agarose and 2% FBS at 16 hpi. The plaque assay was performed, and the plaques were visualized and counted as described above.

## Assay for Virus Adsorption

To test whether montelukast inhibited virus attachment, the assay for virus adsorption was performed as previously described (Talarico et al., 2005). BHK-21 cells confluent in six-well plates were infected with 500 pfu of virus in the presence or absence of 10 μM of the montelukast and incubated for 1 h on ice. The curcumin (10 μM), which showed an antiviral activity at the stage of virus adsorption (Mounce et al., 2017), was included as control. Supernatant containing unadsorbed virus was discarded, cells were then washed twice with ice-cold DMEM and DMEM containing 0.6% LMP agarose, and 2% FBS was overlaid. Virus plaques were visualized and counted as described above.

## Assay for Virus Internalization

The virus internalization assay was performed as previously described (Talarico et al., 2005; Si et al., 2018). BHK-21 cells confluent in six-well plates were infected with 500 pfu of viruses on ice. After 1 h of virus adsorption, unadsorbed virus was discarded, and cells were then washed with ice-cold DMEM and transferred to 37°C in the presence or absence of 10 μM of the montelukast. The chloroquine phosphate (50 μM), which showed an antiviral activity at the stage of virus internalization (Delvecchio et al., 2016; Li et al., 2017b), was included as control. After 2 h of incubation, cells were washed with DMEM and covered with DMEM containing 0.6% LMP agarose and 2% FBS. Virus plaques were visualized and counted as described above.

## Assay for Viral RNA Replication

To test whether montelukast inhibited viral RNA replication, an assay was performed at 4 hpi, a time after entry has occurred (Rausch et al., 2017). Briefly, BHK-21 cells confluent in six-well plates were infected with 50 pfu of virus at 37°C. After 4 h of incubation, the supernatant was removed and replaced with DMEM in the presence or absence of 10 μM of the montelukast. The NITD008, which showed an antiviral activity at the stage of virus RNA replication (Deng et al., 2016a), was included as control. After incubation for additional 12 h, supernatant was removed and cells were washed with DMEM and overlaid with DMEM containing 0.6% LMP agarose and 2% FBS. Virus plaques were visualized and counted as described above.

## Infectivity Inhibition Reversibility Assay

To test whether the inhibition of montelukast on flavivirus infection is reversible, the infectivity inhibition reversibility assay was performed as previously described with some modification (Lok et al., 2012). Virus measuring 100 pfu was incubated with 10 μM of montelukast in a total volume of 10 μl of DMEM for 1 h at room temperature. Immediately before being added to BHK-21 cell monolayer, the virus/montelukast mixtures were diluted with DMEM to 1 ml, reducing the concentration of montelukast to 0.1 μM. The virus constantly treated with 10 or 0.1 μM of montelukast was included as control. The plaque assay was performed, and virus plaques were visualized and counted as described above.

## RNase Digestion Assay and Quantitative Reverse Transcription PCR

To detect whether montelukast can release the genomic RNA from the flavivirus particles, the RNase digestion assay and quantitative reverse transcription (qRT) PCR were performed as previously described (Lok et al., 2012; Yu et al., 2017). Briefly, montelukast at different concentration was incubated with ZIKV (300 pfu) at 37°C for 2 h. Then, the RNA released from virus was digested by micrococcal nuclease (New England BioLabs, Rowley, MA, United States) for 1 h at 37°C. Then, the viral genomic RNA inside the unbroken virus was extracted by using the EasyPure Viral DNA/RNA Kit (Transgen Biotech, Beijing, China) and detected by qRT-PCR using TransScript Green One-Step qRT-PCR SuperMix (Transgen Biotech, Beijing, China) and the CFX96$^{TM}$ Real-Time System (Bio-Rad, United States) in accordance with the manufacturers' instructions. The virions of ZIKV, DENV-2, and YFV were also purified for RNase digestion assay by polyethylene glycol (PEG) precipitation as described previously (Yu et al., 2017). Briefly, 50% PEG-8000 (Amresco, United States) and 5M of NaCl were added to the virus at final concentration of 10% and 0.67M, respectively. After incubation on ice overnight, the mixture was centrifuged at 20,200 *g* for 1 h. The supernatant was discarded, and the pellet containing the virions was washed with 3% PEG-8000 in PBS containing 10 mg/ml of bovine serum albumin (BSA) (Amresco, United States). After centrifugation, the pellet was resuspended in PBS, and the RNase digestion assay was performed again. The EV71, an unenveloped RNA virus, was included as negative control. The primers used to detect the RNA sequences of ZIKV, DENV-2, YFV, and EV71 were described previously (Lok et al., 2012; Fernandes-Monteiro et al., 2015; Fischer et al., 2017; Yu et al., 2017; Wu et al., 2018; Yuan et al., 2018) and listed in **Table 1**.

## Ethics Statement

All animal experiments were carried out according to ethical guidelines and approved by Shanghai Public Health

**TABLE 1 |** The primers employed to detect the viral RNA in RNase digestion assay.

| Virus | Primer name | Primer sequence (5′ → 3′) |
|---|---|---|
| ZIKV SZ01 | PrM F1 | CTTGGACAGAAACGATGCTGGG |
| | PrM R1 | TGATGGCAGGTTCCGTACACAA |
| | E F1 | TGGAGGCTGAGATGGATGG |
| | E R1 | GAACGCTGCGGTACACAAGGA |
| | Cap F1 | TCACGGCAATCAAGCCATCACT |
| | Cap R1 | GCCTCGTCTCTTCTTCTCCTT |
| DENV-2 | 5-1F | AATCCCACCAACAGCAGGGATACT |
| | 5-1R | CGCCATCACTGTTGGAATCAGCAT |
| | 5M-1F | AAGCAGAACCTCCATTCGGAGACA |
| | 5M-1R | AAACACTCCTCCCAGGGATCCAAA |
| | 3M-2F | TCACCAAATCCCACGGTAGAAGCA |
| | 3M-2R | AGGGCATGTATGGGTTGAGAACCT |
| YFV 17D | F3 | GGCAATAAACACATTTGGATTAAT |
| | R3 | CATATTGACGCCCAGGGT |
| | YFVdual-fwd-vac | GGGACTAGCGTGATCATTGA |
| | YFVdual-rv-vac | GAATAACTTTCCCGCTATCCGT |
| | F | GCACGGATGTAACAGACTGAAGA |
| | R | CCAGGCCGAACCTGTCAT |
| EV71 | F | GCAGCCCAAAACAACTTCAC |
| | R | AATTTCAGCAGCTTGGAGTGC |

*ZIKV, Zika virus; DENV, dengue virus; YFV, yellow fever virus.*

Clinical Center Laboratory Animal Welfare & Ethics Committee (2016-A021-01).

## Antiviral Efficacy of Montelukast in Pregnant C57BL/6 Mice

Antiviral efficacy of montelukast in pregnant mice was determined as previously described (Wu et al., 2016; Yu et al., 2017). Briefly, 24 pregnant C57BL/6 mice (E12–14) were randomly assigned into two groups and infected intraperitoneally (i.p.) with $1 \times 10^5$ pfu of ZIKV (SZ01). One hour later, the infected mice were i.p. administered with montelukast dissolved in PBS at 50 mg/kg of body weight ($n$ = 12) or PBS vehicle control ($n$ = 12). Mice were bled retro-orbitally to measure viremia by qRT-PCR at day 1 post-infection. Two embryos were collected randomly from each pregnant mouse, and the viral RNA loads in fetal head of each collected embryo and placenta were determined by qRT-PCR.

## Antiviral Efficacy of Montelukast in A129 Mice

To evaluate the antiviral efficacy of montelukast *in vivo*, A129 mice were used as previously described (Yin et al., 2009; Deng et al., 2016a; Shan et al., 2017; Yu et al., 2017; Tai et al., 2019). Briefly, 16 A129 mice of 4-week-old were randomly assigned into two groups and infected i.p. with ZIKV strain SZ01 at a dose of $1 \times 10^5$ pfu each mouse. One hour later, the infected A129 mice were then i.p. administered with montelukast dissolved in PBS at 50 mg/kg of body weight ($n$ = 8) or PBS vehicle control ($n$ = 8). The treatment was performed once a day for six consecutive days, followed by daily observations of mortality of mice. It was deemed to be protected if mouse survived to 21 days post-infection (dpi). The viral RNA loads of sera on 2 dpi were measured by qRT-PCR.

## Statistical Analysis

All statistical analyses were carried out by using GraphPad Prism 7.0 (GraphPad Software, Inc.). Statistical methods were listed as follows: the log-rank (Mantel–Cox) test to evaluate difference in survival; the non-parametric Mann–Whitney test to examine differences of viral RNA loads in the sera, fetal placenta, or fetal head; and Student's unpaired two-tailed $t$-test in other cases. Significant difference was defined as $P < 0.05$. $^*P < 0.05$; $^{**}P < 0.01$; $^{***}P < 0.001$; $^{****}P < 0.0001$.

# RESULTS

## Montelukast Inhibited Infection of Zika Virus Strains From the Asian and African Lineages, Dengue Virus, and Yellow Fever Virus in Different Host Cells

To identify drugs that could inhibit the infection of ZIKV, an FDA-approved drug repurposing screening was performed. BHK-21 cells were infected with mixture of ZIKV strain SZ01 and drugs at the final concentration of 10 μM. When the ZIKV-induced cytopathic effect (CPE) of BHK-21 cells was obvious, CCK-8, a highly water-soluble non-radioactive reagent like XTT, allowing sensitive colorimetric assays for the determination of cell viability, was used to detect the antiviral activity of drugs. Montelukast, showing more than 80% inhibition of ZIKV infection, was selected for further study. To confirm the antiviral activity of montelukast, whose chemical structure is shown in **Figure 1A**, against ZIKV infection, plaque reduction assay was employed in two different cell types, BHK-21 and Vero E6. First, we tested the antiviral efficacy of montelukast against infection of ZIKV strain SZ01. It showed that montelukast inhibited ZIKV strain SZ01 infection in a dose-dependent manner with a similar IC50 value of 1.14 ± 0.19 μM in BHK-21 cells (**Figure 1B** and **Table 2**) and 1.35 ± 0.17 μM in Vero E6 cells (**Figure 1E** and **Table 2**). It is known that ZIKV is classified into two distinct phylogenetic lineages, the African and the Asian lineages; and there are intrinsic differences in the pathogenicity and virulence between these two lineages of ZIKV (Simonin et al., 2017). We then further tested if montelukast could block infection by different ZIKV strains from Asian and African lineages. As shown in **Figure 1**, besides ZIKV strain SZ01 (Asian lineage), montelukast also potently inhibited infection of ZIKV strain MR766 (African lineage) and FLR (Asian lineage) with IC50 values of 1.39 ± 0.13 and 1.29 ± 0.23 μM in BHK-21 cells (**Figures 1C,D** and **Table 2**) and of 1.23 ± 0.16 and 1.88 ± 0.36 μM in Vero E6 cells (**Figures 1F,G** and **Table 2**), respectively, which indicated that montelukast was effective in blocking infection of two lineages of ZIKV strains isolated from rhesus monkeys or patients in divergent regions. Furthermore, the antiviral activity of montelukast against ZIKV strain SZ01 infection

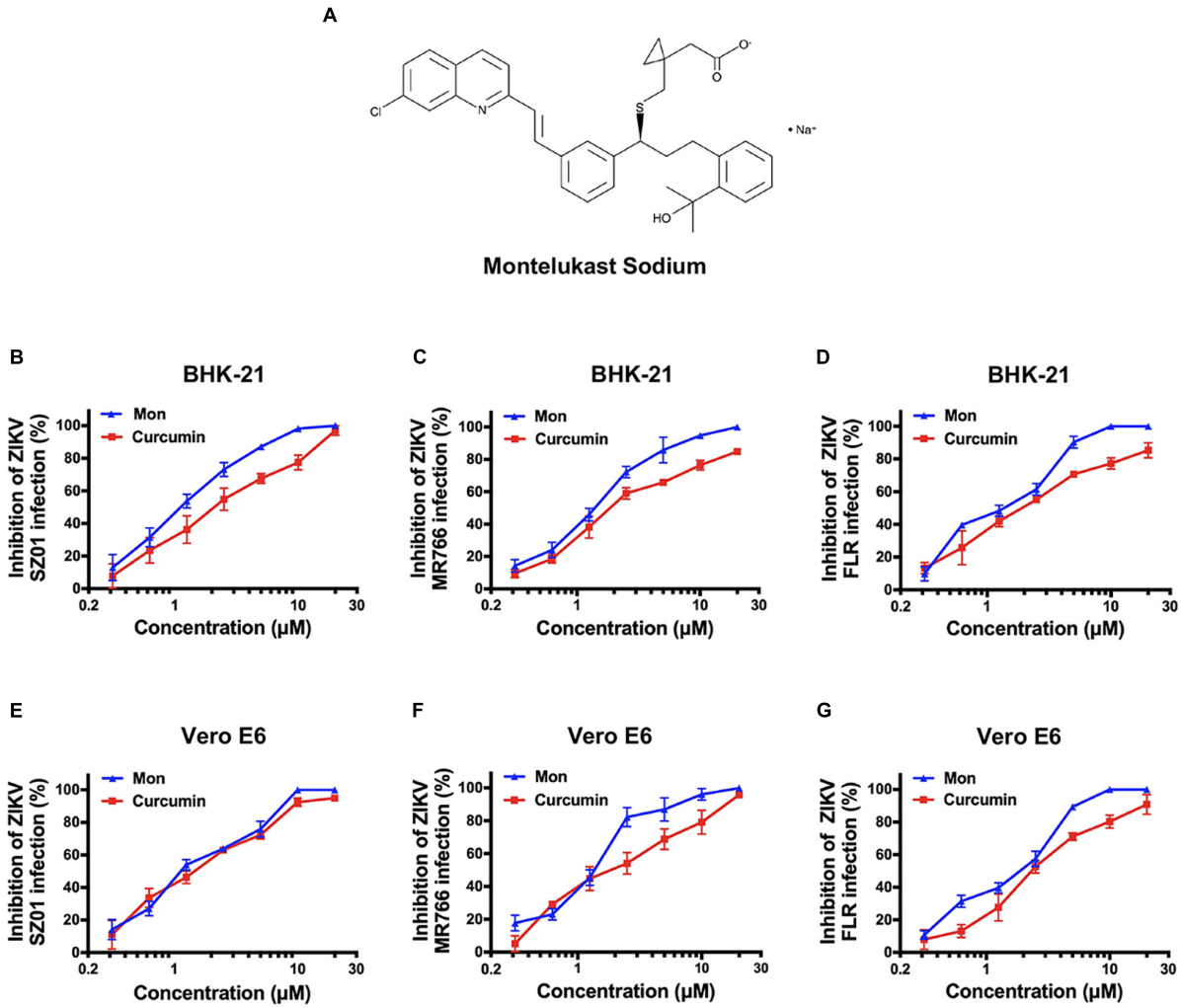


**FIGURE 1 |** The chemical structure of montelukast and its inhibitory activity against Zika virus (ZIKV) strains from Asian and African lineages in two host cells. **(A)** Chemical structure of montelukast. Dose-dependent inhibition of ZIKV strain SZ01 **(B)**, MR766 **(C)**, and FLR **(D)** infection by montelukast in BHK-21 cells and inhibition of ZIKV strain SZ01 **(E)**, MR766 **(F)**, and FLR **(G)** infection in Vero E6 cells. Curcumin, an anti-ZIKV drug, was included as positive control. All experiments were carried out in triplicate, and the error bars stand for standard deviation (SD). The 50% inhibitory concentration (IC50) is presented as means ± SD and summarized in **Table 2**.

in the human astrocytoma cells U-251 MG was tested. It showed that montelukast was also effective in inhibiting the infection of ZIKV in U-251 MG cells with IC50 value of 4.06 ± 0.13 μM (**Table 2** and **Supplementary Figure S1**). The cytotoxicity of montelukast on BHK-21 cells, Vero E6 cells, and U-251 MG cells was evaluated by using CCK-8 to exclude the possibility of cytotoxicity-induced viral reduction (**Figure 2** and **Table 3**).

Following this, we were interested in whether montelukast could inhibit infection of DENV and YFV, the other two important mosquito-borne flaviviruses circulating all around the world. It was found that montelukast could also effectively block infection of DENV-2 and YFV 17D with IC50 values of 1.03 ± 0.11 and 1.11 ± 0.07 μM in BHK-21 cells and of 0.98 ± 0.04 and 1.42 ± 0.09 μM in Vero E6 cells, respectively (**Figures 3A,B** and **Table 2**). These results suggested that montelukast may possess a broad antiviral activity against infection of a wide spectrum of flaviviruses.

## Montelukast Blocked Infection at the Early Stage of Virus Life Cycle

Montelukast is the leukotriene receptor antagonists successfully developed for treatment of asthmatic patients (Bakhireva et al., 2007; Cavero-Carbonell et al., 2017). However, little is known about its potential mechanism of the antiviral activity against ZIKV, DENV, and YFV. In order to determine at which stage of the viral life cycle the montelukast executed antiviral function, we first investigated the influence of the time of addition on plaque formation in BHK-21 cells. The montelukast was added with virus simultaneously (time 0) or at different time points after viral infection. At 16 hpi, the supernatant was discarded, and the

**TABLE 2 |** Antiviral activity of montelukast against ZIKV, DENV, and YFV in different cell lines.

| Cell type | Virus | IC50 (μM) |
|---|---|---|
| BHK-21 | ZIKV SZ01 | 1.14 ± 0.19 |
| | ZIKV MR766 | 1.39 ± 0.13 |
| | ZIKV FLR | 1.29 ± 0.23 |
| | DENV-2 | 1.03 ± 0.11 |
| | YFV 17D | 1.11 ± 0.07 |
| Vero E6 | ZIKV SZ01 | 1.35 ± 0.17 |
| | ZIKV MR766 | 1.23 ± 0.16 |
| | ZIKV FLR | 1.88 ± 0.36 |
| | DENV-2 | 0.98 ± 0.04 |
| | YFV 17D | 1.42 ± 0.09 |
| U-251 MG | ZIKV SZ01 | 4.06 ± 0.13 |

*The 50% inhibitory concentration (IC50) of montelukast was presented as means ± SD (standard deviation). ZIKV, Zika virus; DENV, dengue virus; YFV, yellow fever virus.*

**TABLE 3 |** The cytotoxicity of montelukast in different cell lines.

| Cell type | CC50 (μM) |
|---|---|
| BHK-21 | 47.78 ± 1.83 |
| Vero E6 | 46.22 ± 3.25 |
| U-251 MG | 25.05 ± 0.59 |

*The 50% cytotoxicity concentration (CC50) is presented as means ± SD (standard deviation).*

cells were then washed to perform the plaque assay for evaluating inhibitory effects of montelukast at different time points. As shown in **Figure 4A**, simultaneous addition of montelukast and ZIKV to BHK-21 cells (time 0) maximally decreased the plaque numbers. With time lapsed from 1 to 4 h, the inhibitory activity of montelukast gradually decreased. The inhibitory effect on plaque formation was barely observed if montelukast was added 8 hpi, indicating that montelukast hardly suppressed flavivirus RNA replication in the late stage. It was confirmed by the assay of viral RNA replication (**Figure 4D**) where montelukast and NITD008, an adenosine nucleoside inhibitor targeting the stage of flavivirus RNA replication (Yin et al., 2009; Deng et al., 2016a), were both added 4 hpi. The patterns of the time of addition experiment and assay of viral RNA replication were similar for DENV-2 (**Figures 4B,E**) and YFV 17D (**Figures 4C,F**), suggesting that montelukast inhibited flavivirus infection at the early stage.

As the early stage of virus infection consists of processes including viral attachment and internalization, the effect of montelukast on the virus adsorption or internalization was evaluated separately as previously described (Talarico et al., 2005; Talarico and Damonte, 2007) to ascertain the particular inhibitory step at the early stage of ZIKV life cycle. BHK-21 cells were incubated simultaneously with ZIKV and montelukast on ice, a low-temperature condition where the virus attachment to the cell is the only event of the virus life cycle that occurs (Talarico et al., 2005). As shown in **Figure 5A**, the montelukast blocked ZIKV attachment as the amount of cell-bound virus particles highly decreased in the presence of montelukast to a comparable extent caused by curcumin, a known inhibitor that suppressed ZIKV attachment to the cell (Mounce et al., 2017). The inhibitory effect of montelukast on the subsequent step, that is, virus internalization, was next analyzed. After virus adsorption on ice, the unbound virus was removed, and the montelukast was subsequently added to the cell culture. The temperature was immediately shifted to 37°C to initiate virus penetration, and plaque assay was performed thereafter. The chloroquine phosphate, a known inhibitor blocking virus internalization, was included as control. It showed that montelukast has little effect on the internalization of ZIKV (**Figure 5D**). The patterns of effect of montelukast on adsorption or internalization of DENV-2 (**Figures 5B,E**) and YFV 17D (**Figures 5C,F**) were similar to those of ZIKV. Overall, these results indicated that the antiviral action of montelukast mainly took place at the adsorption step in the early stage of virus life cycle.

## Montelukast Irreversibly Inhibited Viral Infectivity and Induced Release of Viral Genome RNA

Next, because montelukast obstructed flavivirus infection at the adsorption step, it became natural to question whether

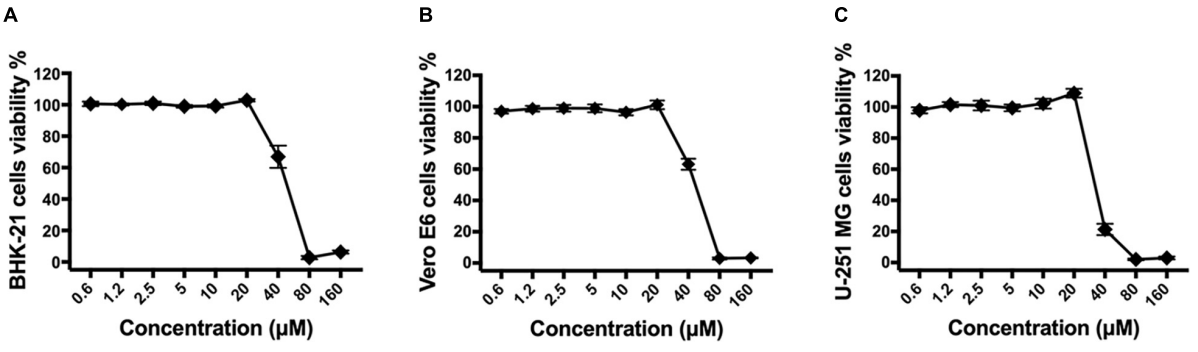


**FIGURE 2 |** The cytotoxicity of montelukast in different cell lines. BHK-21 **(A)**, Vero E6 **(B)**, or U-251 MG **(C)** cells were treated with serially diluted montelukast. Then cells viability were determined 2 days later by Cell Counting Kit-8 (CCK-8) kit according to the instruction manual. All experiments were carried out in triplicate, and the error bars stand for standard deviation (SD). The 50% cytotoxicity concentration (CC50) is presented as means ± SD and summarized in **Table 3**.

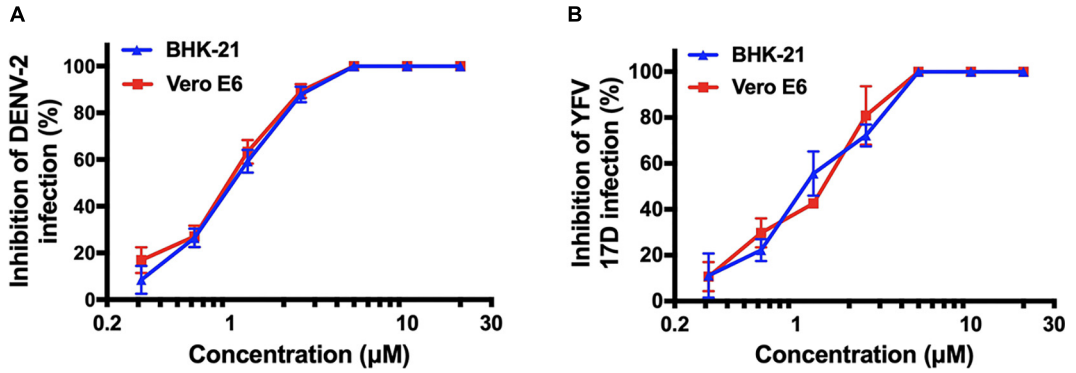


**FIGURE 3 |** Antiviral activity of montelukast against other two flaviviruses [dengue virus (DENV)-2 and yellow fever virus (YFV) 17D] in two host cells. Dose-dependent inhibition of DENV-2 **(A)** and YFV 17D **(B)** by montelukast in BHK-21 and Vero E6 cells. All experiments were carried out in triplicate, and the error bars stand for standard deviation (SD). The 50% inhibitory concentration (IC50) is presented as means ± SD and summarized in **Table 2**.

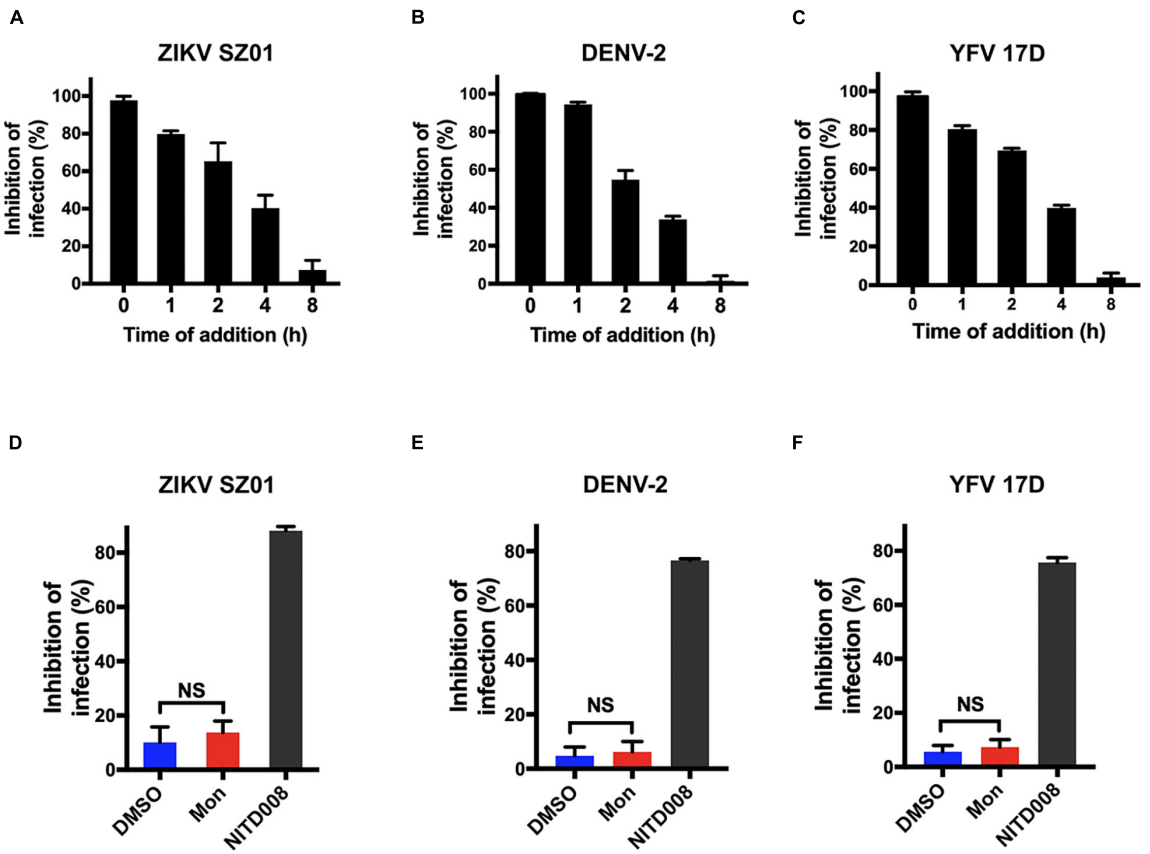


**FIGURE 4 |** Montelukast inhibited flavivirus infection at the early stage of virus life cycle. Time of addition experiment of montelukast against Zika virus (ZIKV) SZ01 **(A)**, dengue virus (DENV)-2 **(B)**, and yellow fever virus (YFV) 17D **(C)**. Montelukast hardly inhibited ZIKV SZ01 **(D)**, DENV-2 **(E)**, and YFV 17D **(F)** infection at post-entry stage. NITD008, an adenosine analog, inhibiting flaviviruses RNA replication by terminating viral RNA synthesis was included as control. All experiments were carried out in triplicate, and the error bars stand for standard deviation (SD). The data are presented as means ± SD. NS, not significant. Student's two-tailed *t*-test.

the inhibition action is reversible or not. Infectivity inhibition reversibility assay was then employed for clarification.

ZIKV was first treated with montelukast at 10 μM, a concentration sufficient to produce approximately 90% inhibition of infectivity. Then the mixture of virus and montelukast was diluted 100-fold to 0.1 μM, a concentration expected to produce negligible inhibition immediately before plaque assay was performed. ZIKV constantly treated with 10 μM

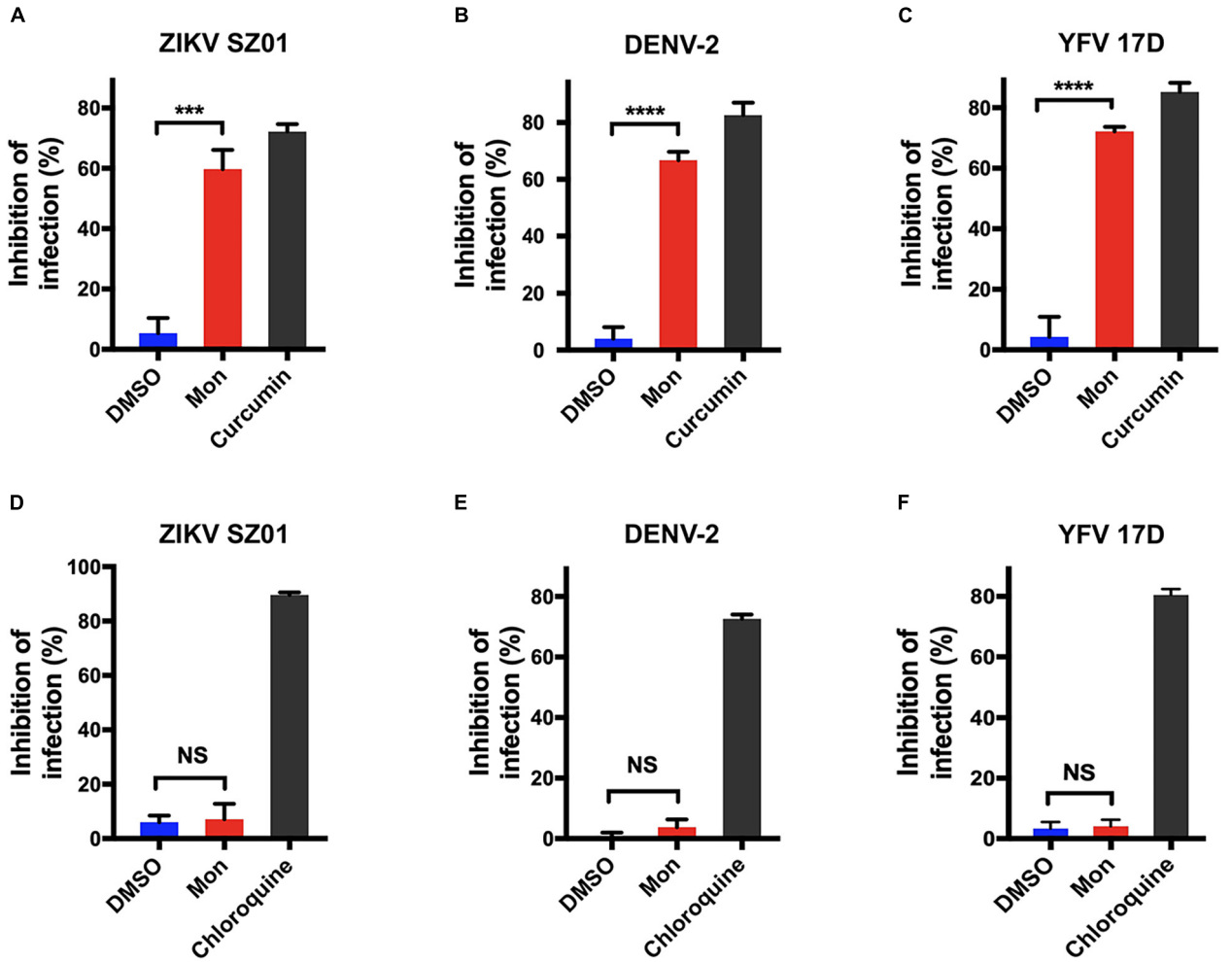


**FIGURE 5 |** Montelukast blocked flaviviruses adsorption, not internalization. Virus adsorption assay of montelukast against Zika virus (ZIKV) SZ01 **(A)**, dengue virus (DENV)-2 **(B)**, and yellow fever virus (YFV) 17D **(C)**; and curcumin, an inhibitor known to block virus adsorption, was included as control. Virus internalization assay of montelukast against ZIKV SZ01 **(D)**, DENV-2 **(E)**, and YFV 17D **(F)**, and chloroquine, an inhibitor known to block virus internalization, was included as control. All experiments were carried out in triplicate, and the error bars stand for standard deviation (SD). The data are presented as means ± SD. NS, not significant; ***$P < 0.001$; ****$P < 0.0001$, Student's two-tailed *t*-test.

or constantly treated with 0.1 μM of montelukast was also included for plaque assay. As shown in **Figure 6A**, dilution of montelukast could not abolish the inhibitory effect, indicating that the inhibition of ZIKV infectivity is irreversible. Similarly, no reversibility of inhibition was observed for DENV-2 (**Figure 6B**) and YFV 17D (**Figure 6C**).

The irreversibility of inhibitory effect of montelukast aroused our interest in whether the release of viral genome RNA is induced by montelukast. Then, the potential viral RNA release was measured by an RNase digestion assay as described previously (Lok et al., 2012; Yu et al., 2017). The RNA genomes of intact virions would be protected from RNase digestion, whereas the virions whose integrity was disrupted by treatment would be susceptible to RNA degradation by RNase digestion. As shown in **Figure 7A**, the viral genomic RNA of ZIKV treated with montelukast was digested by micrococcal nuclease in a dose-dependent manner, and almost 80% genomic RNA of ZIKV particles treated with 10 μM of montelukast was digested. Montelukast treatment caused similar RNA genome degradation upon RNase digestion for DENV-2 (**Figure 7B**), for YFV 17D (**Figure 7C**), and for purified virions of ZIKV, DENV-2, and YFV 17D (**Figures 7D–F**), which suggested that montelukast could disrupt the integrity of flaviviruses and hence irreversibly destroy the infectivity of flaviviruses.

## Montelukast Blocked Vertical Transmission of Zika Virus in Pregnant Mice

To evaluate whether montelukast could block the vertical transmission of ZIKV, pregnant C57BL/6 mice were infected with ZIKV as described previously (Wu et al., 2016; Yu et al., 2017) and were then treated with montelukast or vehicle control. As shown in **Figure 8A**, treatment with montelukast could reduce viremia

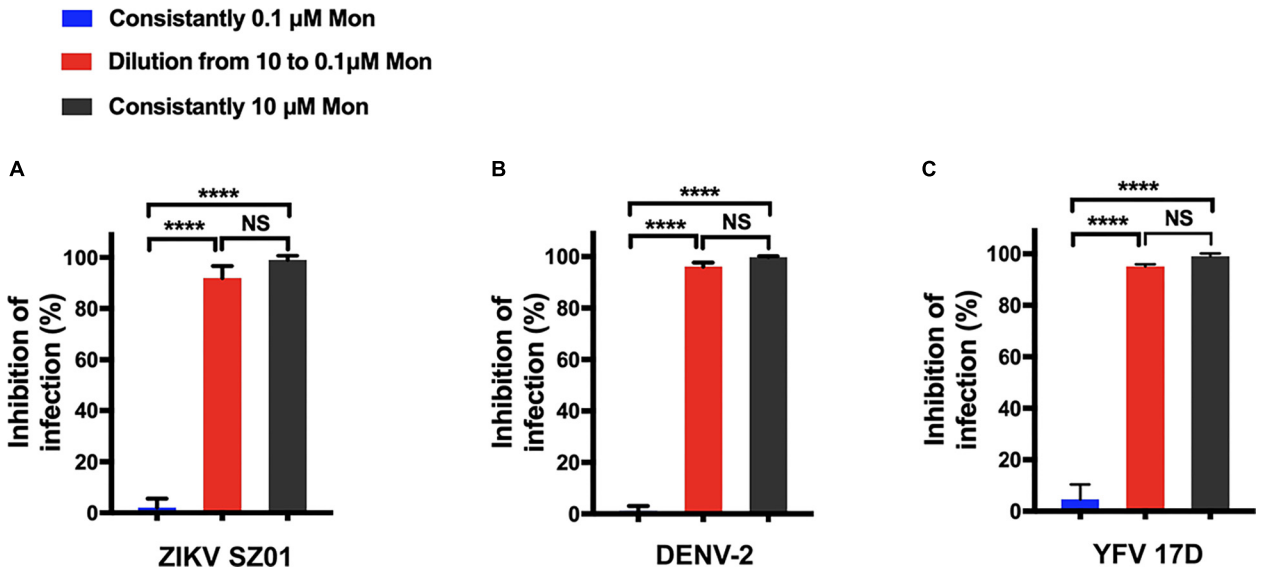


**FIGURE 6 |** Montelukast irreversibly disrupted viral infectivity. Infectivity inhibition reversibility assay of montelukast against Zika virus (ZIKV) SZ01 **(A)**, dengue virus (DENV)-2 **(B)**, and yellow fever virus (YFV) 17D **(C)**. All experiments were carried out in triplicate, and the error bars stand for standard deviation (SD). The data are presented as means ± SD. NS, not significant; ****$P < 0.0001$, Student's two-tailed *t*-test.

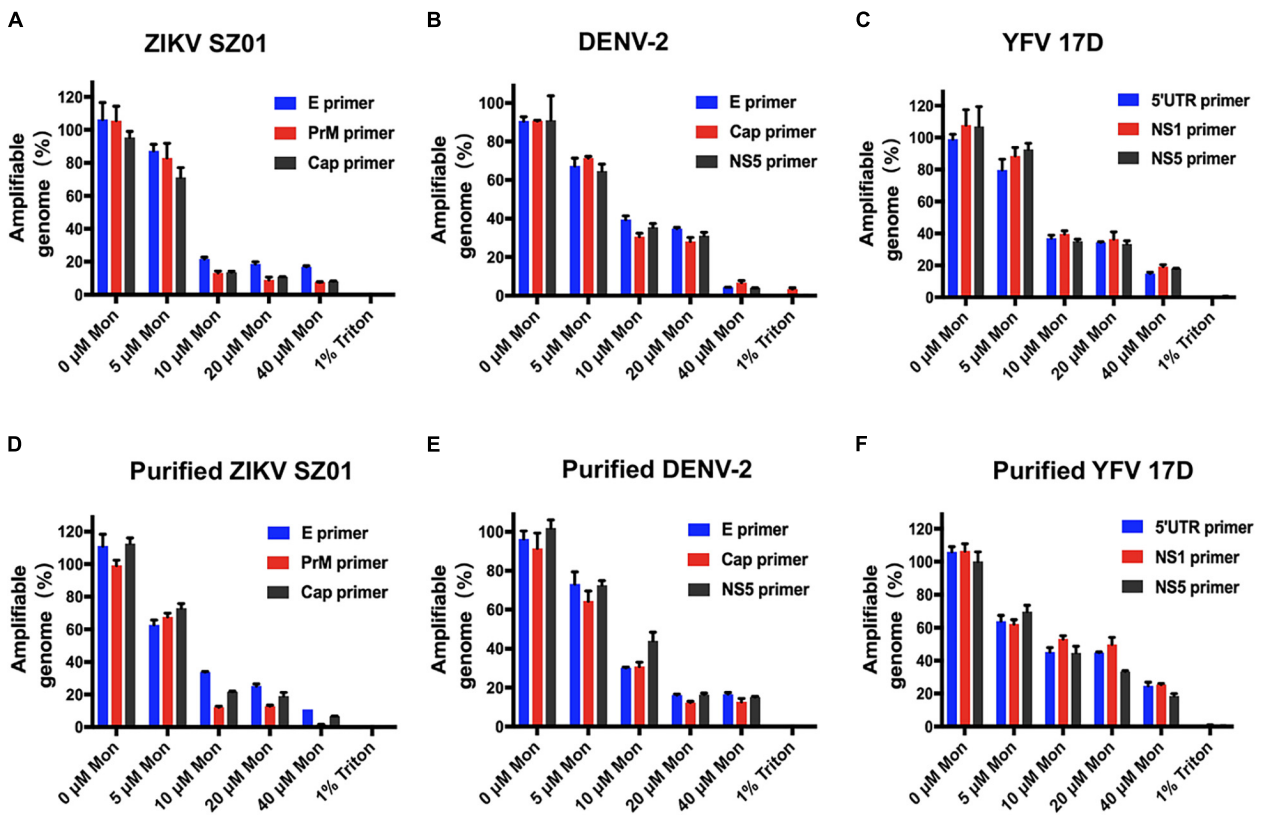


**FIGURE 7 |** Degradation of released genomic RNA of flaviviruses mediated by montelukast treatment in an RNase digestion assay. The release and degradation of genomic RNA of Zika virus (ZIKV) SZ01 **(A)**, dengue virus (DENV)-2 **(B)**, yellow fever virus (YFV) 17D **(C)**, and purified virions of ZIKV SZ01 **(D)**, DENV-2 **(E)**, and YFV 17D **(F)** were detected by using their respective primers targeting different regions in the viral genome. All experiments were carried out in triplicate, and the error bars stand for standard deviation (SD). The data are presented as means ± SD.

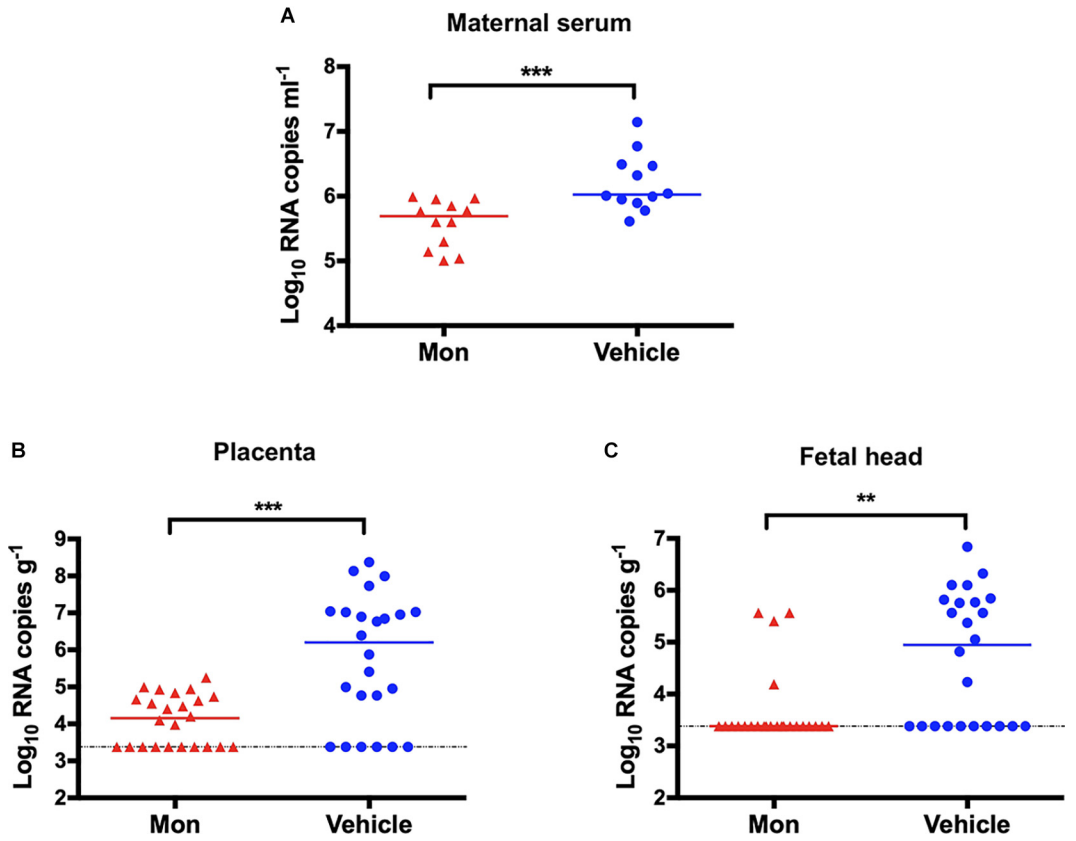


**FIGURE 8 |** Protection against vertical transmission of Zika virus (ZIKV) in montelukast-treated pregnant C57BL/6 mice. **(A)** Viremia of pregnant C57BL/6 mice ($n$ = 12 in each group). **(B)** Viral RNA loads in the placentas ($n$ = 24 in each group). Two embryos of each pregnant mouse were randomly collected, and the viral RNA load in each placenta was determined. **(C)** Viral RNA loads in the fetal heads ($n$ = 24 in each group). The viral RNA load in the fetal head of each collected embryo was determined. The bars reflect median values. The horizontal dotted lines represent limits of detection. $^{**}P < 0.01$; $^{***}P < 0.001$, Mann–Whitney test.

in the pregnant C57BL/6 mice infected with ZIKV ($P$ = 0.0006). Meanwhile, the viral RNA loads of placentas from pregnant mice treated with montelukast were greatly reduced compared with those from vehicle-treated mice ($P$ = 0.0005), and the infection rate declined from 18/24 to 14/24 (**Figure 8B**). And montelukast treatment led to significant decrease both of viral RNA load in fetal head ($P$ = 0.0014, **Figure 8C**) and of infection rate from 14/24 to 4/24. These results suggested that montelukast may lower the infection rate of the fetuses by inactivating ZIKV virions either before or after the virus invaded from the placenta to fetus, hence protecting against vertical transmission of ZIKV in pregnant mice, just like Z2, a peptide-based viral inactivator (Yu et al., 2017).

## Montelukast Protected A129 Mice From Lethal Challenge With Zika Virus

Finally, the antiviral efficacy of montelukast against ZIKV infection was evaluated in the recently established A129 (interferon alpha/beta receptor-deficient) (Dai et al., 2016; Shan et al., 2017; Yu et al., 2017; Tai et al., 2019) mouse model. The A129 mice were challenged with ZIKV i.p. and then were subsequently treated with montelukast or vehicle. The mice treated with vehicle exhibited a 100% mortality rate at 13 dpi as shown in **Figure 9A**. Instead, 75% of the A129 mice treated with montelukast were protected from death caused by ZIKV infection ($P$ = 0.0003, log-rank test). The viral loads in A129 mice treated with montelukast at 2 dpi were much lower than those of mice treated with vehicle ($P$ = 0.0002, **Figure 9B**). Although montelukast suppressed ZIKV infection at the early stage of viral life cycle, consecutive injections after ZIKV invading into cells could still render some protection possibly by irreversibly disrupting newly produced viruses and hence preventing infection of more target cells.

# DISCUSSION

ZIKV is one of the mosquito-borne flaviviruses discovered about 70 years ago and has spread all over the world in recent years, which causes Guillain–Barré syndrome, congenital Zika syndrome, and damage to testicular tissue (Brasil et al., 2016; Baud et al., 2017; Gurung et al., 2019; Peixoto et al., 2019). Currently, there are no vaccines or drugs approved for prevention and treatment of ZIKV infection, leading to the necessity and urgency of the development of anti-ZIKV therapy. Repurposing

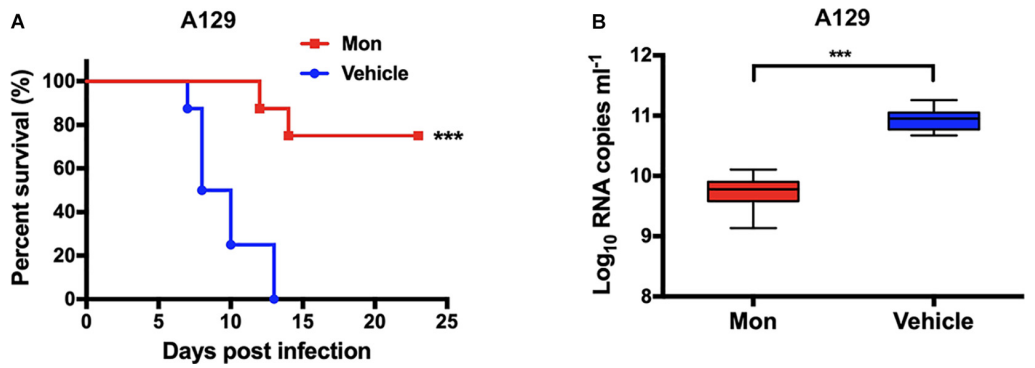


**FIGURE 9 |** Protective activity of montelukast against lethal Zika virus (ZIKV) infection in type I interferon receptor-deficient A129 mice. **(A)** Survival of ZIKV-infected A129 mice. ***$P < 0.001$, log-rank (Mantel–Cox) test. **(B)** Viral RNA loads in sera of ZIKV-infected A129 mice. Whiskers: 5th–95th percentile. ***$P < 0.001$, Mann–Whitney test.

screen of clinically approved drugs is a practical way to deal with the outbreak of emerging and reemerging infectious disease threats such as Middle East respiratory syndrome (MERS) and Ebola (Johansen et al., 2013; de Wilde et al., 2014; Dyall et al., 2014; Kouznetsova et al., 2014; Wang et al., 2017). By employing this method, some drugs have been found to be effective against ZIKV infection (Xu et al., 2016). We also identified a marketed anti-asthmatic drug, montelukast, which has not been reported as far as we know.

Montelukast, one of the leukotriene receptor antagonists, is the most prescribed cysteinyl leukotriene 1 (CysLT1) antagonist safely used in asthmatic patients for many years (Hoxha et al., 2017). It is interesting that montelukast exhibited potential antiviral efficacy against ZIKV *in vitro* and *in vivo*. Montelukast not only inhibited infections of several types of flaviviruses, including ZIKV of Asian and African lineages, DENV-2, and YFV 17D, in two kinds of cells, but also protected A129 mice from lethal ZIKV challenge and blocked vertical transmission of ZIKV in pregnant mice. The inhibition of ZIKV infectivity by montelukast is irreversible probably owing to the disruption of the integrity of ZIKV virions and the release of ZIKV genomic RNA. It should be noted that the concentration needed to cause 50% degradation of the genome was a little bit higher than the concentration required to yield 50% reduction in infectivity, which was also reported in the studies from others (Lok et al., 2012; Yu et al., 2017). Just as mentioned in their study, this might be caused by the use of more viruses in the genome degradation assay or by some virions having only partial genomes released to be still protected from degradation and to be likely non-infectious. Interestingly, montelukast has no effect on the genomic RNA release of EV71, an unenveloped RNA virus (**Supplementary Figure S3A**, and **Supplementary Figures S3B–E** show the amplicons of ZIKV SZ01, DENV-2, YFV 17D and EV71 that were resolved by agarose gel electrophoresis). Besides, montelukast also exhibited an antiviral activity against VSV-GFP (**Supplementary Figure S2**), which is an enveloped non-flavivirus, suggesting that the montelukast probably targeted to the lipid membrane of the viral shell, not to the envelope protein of the virus. On the other hand, the proven pharmacological action of montelukast could favor its antiviral effect as concomitant effects. Leukotrienes are important in mediating the vascular leakage caused by DENV infection-induced mast cell activation, leading to increased vascular permeability, which may result in hemorrhage within internal organs and leakage of plasma into the tissues, the distinctive features of dengue shock syndrome (DSS) and dengue hemorrhagic fever (DHF) (Ahmad et al., 2018). Montelukast, the leukotriene receptor antagonist, could reduce the vascular permeability and restore the vascular integrity to prevent vascular leakage and hemorrhaging (St John, 2013; St John et al., 2013). Hence, it is possible that the modulation of inflammation by montelukast would contribute to the *in vivo* anti-ZIKV effects. Certainly, other putative mechanisms underlying the antiviral action of montelukast, such as the blockage of binding of ZIKV E protein to its cell receptor, cannot be totally excluded. However, the receptor utilized by ZIKV is still controversial (Govero et al., 2016; Nowakowski et al., 2016; Retallack et al., 2016; Chen et al., 2018); therefore, more investigations will be needed in the following research.

The major sequela caused by congenital ZIKV infection is microcephaly, which is evidenced in humans and animal models (Tang et al., 2016; Cui et al., 2017), and pregnant women are the direct victims of the ZIKV infection of fetus, making it vitally important that the treatment for pregnant women infection by ZIKV should be very cautious. Luckily, montelukast is classified as category B in the FDA pregnancy category and has been successfully used for treatment of pregnant women with asthma (Bakhireva et al., 2007; Cavero-Carbonell et al., 2017). Animal studies showed no adverse effects on embryo and fetal development at oral doses up to 400 mg/kg/day in rats or up to 100 mg/kg/day in rabbits, as described in the product information of montelukast (trade name Singulair®) produced by Merck Sharp & Dohme, Ltd. With the combination of the fact that montelukast blocked vertical transmission of ZIKV in pregnant mice and its safety profile for pregnant women, it is promising that montelukast could be used for treatment of pregnant women infected with ZIKV. And more surprising and exciting to us is that montelukast displayed

neuro-protective activity in several animal models. Montelukast may improve the fiber connectivity and long-term functional recovery after brain ischemia caused by stroke, enhancing recruitment and maturation of oligodendrocyte precursor cells (Gelosa et al., 2019), and may ameliorate amyloid-β-induced memory impairment via inhibition of neuro-inflammation and apoptosis in mice (Lai et al., 2014). Moreover, treatment of old animals with montelukast reduces neuro-inflammation, elevates hippocampal neurogenesis, and improves learning and memory (Marschallinger et al., 2015). The montelukast-mediated restoration of cognitive function correlates with the increased neurogenesis. In consideration of the role of neuro-inflammation played in the occurrence and development of microcephaly induced by ZIKV infection, it is hoped that montelukast may be used for relief from neuro-inflammation.

Taken together, montelukast exhibited potent antiviral efficacy against several flaviviruses, including ZIKV of Asian and African lineages, DENV-2, and YFV 17D via the irreversible inhibition of infectivity caused by disruption of the integrity of virions, conferred protection from lethal ZIKV challenge and blocked the vertical transmission of ZIKV, indicating its potential application for treatment of ZIKV infections, especially in high-risk populations such as pregnant women considering its safety profile and neuro-protective activity.

## DATA AVAILABILITY STATEMENT

All datasets generated for this study are included in the article/**Supplementary Material**.

## ETHICS STATEMENT

The animal study was reviewed and approved by the Shanghai Public Health Clinical Center Laboratory Animal Welfare & Ethics Committee.

## AUTHOR CONTRIBUTIONS

PZ conceived and designed the experiments. YC, YL, and XW performed the experiments. YC and YL analyzed the data. YC, YL, and PZ wrote the manuscript.

## FUNDING

This work was supported by the funding from the Shanghai Public Health Clinical Center (2016-27 and KY-GW-2017-17).

## ACKNOWLEDGMENTS

We are very grateful to the staff at the Animal Experiment Department of Shanghai Public Health Clinical Center for their contribution to this study.

## SUPPLEMENTARY MATERIAL

The Supplementary Material for this article can be found online at: https://www.frontiersin.org/articles/10.3389/fmicb.2019.03079/full#supplementary-material

## REFERENCES

Ahmad, A., Waseem, T., Butt, N., Randhawa, F., Malik, U., and Shakoori, T. (2018). Montelukast reduces the risk of dengue shock syndrome in dengue patients. *Trop. Biomed.* 35, 1115–1122.

Avelino-Silva, V. I., Alvarenga, C., Abreu, C., Tozetto-Mendoza, T. R., Canto, C., Manuli, E. R., et al. (2018). Potential effect of Zika virus infection on human male fertility? *Rev. Inst. Med. Trop. Sao Paulo* 60:e64. doi: 10.1590/S1678-9946201860064

Bakhireva, L. N., Jones, K. L., Schatz, M., Klonoff-Cohen, H. S., Johnson, D., Slymen, D. J., et al. (2007). Safety of leukotriene receptor antagonists in pregnancy. *J. Allergy Clin. Immunol.* 119, 618–625. doi: 10.1016/j.jaci.2006.12.618

Baud, D., Musso, D., Vouga, M., Alves, M. P., and Vulliemoz, N. (2017). Zika virus: a new threat to human reproduction. *Am. J. Reprod. Immunol.* 77:e12614. doi: 10.1111/aji.12614

Brasil, P., Sequeira, P. C., Freitas, A. D. A., Zogbi, H. E., Calvet, G. A., de Souza, R. V., et al. (2016). Guillain-Barré syndrome associated with Zika virus infection. *Lancet* doi: 10.1016/s0140-6736(16)30058-7 [Epub ahead of print],

Cavero-Carbonell, C., Vinkel-Hansen, A., Rabanque-Hernandez, M. J., Martos, C., and Garne, E. (2017). Fetal exposure to montelukast and congenital anomalies: a population based study in Denmark. *Birth Defect. Res.* 109, 452–459. doi: 10.1002/bdra.23621

Chen, J., Yang, Y. F., Yang, Y., Zou, P., Chen, J., He, Y., et al. (2018). AXL promotes Zika virus infection in astrocytes by antagonizing type I interferon signalling. *Nat. Microbiol.* 3, 302–309. doi: 10.1038/s41564-017-0092-4

Chou, T. C., and Talalay, P. (1984). Quantitative analysis of dose-effect relationships: the combined effects of multiple drugs or enzyme inhibitors. *Adv. Enzyme Regul.* 22, 27–55. doi: 10.1016/0065-2571(84)90007-4

Cui, L., Zou, P., Chen, E., Yao, H., Zheng, H., Wang, Q., et al. (2017). Visual and motor deficits in grown-up mice with congenital Zika virus infection. *EBioMedicine* 20, 193–201. doi: 10.1016/j.ebiom.2017.04.029

Dai, L., Song, J., Lu, X., Deng, Y. Q., Musyoki, A. M., Cheng, H., et al. (2016). Structures of the Zika virus envelope protein and its complex with a flavivirus broadly protective antibody. *Cell Host Microbe* 19, 696–704. doi: 10.1016/j.chom.2016.04.013

de Fatima Vasco Aragao, M., van der Linden, V., Brainer-Lima, A. M., Coeli, R. R., Rocha, M. A., et al. (2016). Clinical features and neuroimaging (CT and MRI) findings in presumed Zika virus related congenital infection and microcephaly: retrospective case series study. *BMJ* 353:i1901. doi: 10.1136/bmj.i1901

de Wilde, A. H., Jochmans, D., Posthuma, C. C., Zevenhoven-Dobbe, J. C., van Nieuwkoop, S., Bestebroer, T. M., et al. (2014). Screening of an FDA-approved compound library identifies four small-molecule inhibitors of Middle East respiratory syndrome coronavirus replication in cell culture. *Antimicrob. Agents Chemother.* 58, 4875–4884. doi: 10.1128/aac.03011-14

Delvecchio, R., Higa, L. M., Pezzuto, P., Valadao, A. L., Garcez, P. P., Monteiro, F. L., et al. (2016). Chloroquine, an endocytosis blocking agent, inhibits Zika virus infection in different cell models. *Viruses* 8:322. doi: 10.3390/v8120322

Deng, Y. Q., Zhang, N. N., Li, C. F., Tian, M., Hao, J. N., Xie, X. P., et al. (2016a). Adenosine analog NITD008 is a potent inhibitor of Zika virus. *Open Forum Infect Dis.* 3:ofw175. doi: 10.1093/ofid/ofw175

Deng, Y. Q., Zhao, H., Li, X. F., Zhang, N. N., Liu, Z. Y., Jiang, T., et al. (2016b). Isolation, identification and genomic characterization of the Asian lineage Zika

virus imported to China. *Sci. China Life Sci.* 59, 428–430. doi: 10.1007/s11427-016-5043-4

Du, L., He, Y., Zhou, Y., Liu, S., Zheng, B. J., and Jiang, S. (2009). The spike protein of SARS-CoV–a target for vaccine and therapeutic development. *Nat. Rev. Microbiol.* 7, 226–236. doi: 10.1038/nrmicro2090

Dyall, J., Coleman, C. M., Hart, B. J., Venkataraman, T., Holbrook, M. R., Kindrachuk, J., et al. (2014). Repurposing of clinically developed drugs for treatment of Middle East respiratory syndrome coronavirus infection. *Antimicrob. Agents Chemother.* 58, 4885–4893. doi: 10.1128/aac.03036-14

Fernandes-Monteiro, A. G., Trindade, G. F., Yamamura, A. M., Moreira, O. C., de Paula, V. S., Duarte, A. C., et al. (2015). New approaches for the standardization and validation of a real-time qPCR assay using TaqMan probes for quantification of yellow fever virus on clinical samples with high quality parameters. *Hum. Vaccin Immunother.* 11, 1865–1871. doi: 10.4161/21645515.2014.990854

Fernando, S., Fernando, T., Stefanik, M., Eyer, L., and Ruzek, D. (2016). An approach for Zika virus inhibition using homology structure of the envelope protein. *Mol. Biotechnol.* 58, 801–806. doi: 10.1007/s12033-016-9979-1

Fischer, C., Torres, M. C., Patel, P., Moreira-Soto, A., Gould, E. A., Charrel, R. N., et al. (2017). Lineage-specific real-time RT-PCR for yellow fever virus outbreak surveillance, Brazil. *Emerg. Infect. Dis.* 23, 1867–1871. doi: 10.3201/eid2311.171131

Gelosa, P., Bonfanti, E., Castiglioni, L., Delgado-Garcia, J. M., Gruart, A., Fontana, L., et al. (2019). Improvement of fiber connectivity and functional recovery after stroke by montelukast, an available and safe anti-asthmatic drug. *Pharmacol. Res.* 142, 223–236. doi: 10.1016/j.phrs.2019.02.025

Govero, J., Esakky, P., Scheaffer, S. M., Fernandez, E., Drury, A., Platt, D. J., et al. (2016). Zika virus infection damages the testes in mice. *Nature* 540, 438–442. doi: 10.1038/nature20556

Gurung, S., Reuter, N., Preno, A., Dubaut, J., Nadeau, H., Hyatt, K., et al. (2019). Zika virus infection at mid-gestation results in fetal cerebral cortical injury and fetal death in the olive baboon. *PLoS Pathog.* 15:e1007507. doi: 10.1371/journal.ppat.1007507

Hoxha, M., Rovati, G. E., and Cavanillas, A. B. (2017). The leukotriene receptor antagonist montelukast and its possible role in the cardiovascular field. *Eur. J. Clin. Pharmacol.* 73, 799–809. doi: 10.1007/s00228-017-2242-2

Joguet, G., Mansuy, J. M., Matusali, G., Hamdi, S., Walschaerts, M., Pavili, L., et al. (2017). Effect of acute Zika virus infection on sperm and virus clearance in body fluids: a prospective observational study. *Lancet Infect. Dis.* 17, 1200–1208. doi: 10.1016/s1473-3099(17)30444-9

Johansen, L. M., Brannan, J. M., Delos, S. E., Shoemaker, C. J., Stossel, A., Lear, C., et al. (2013). FDA-approved selective estrogen receptor modulators inhibit Ebola virus infection. *Sci. Transl. Med.* 5:190ra179. doi: 10.1126/scitranslmed.3005471

Kouznetsova, J., Sun, W., Martinez-Romero, C., Tawa, G., Shinn, P., Chen, C. Z., et al. (2014). Identification of 53 compounds that block Ebola virus-like particle entry via a repurposing screen of approved drugs. *Emerg. Microbes Infect.* 3:e84. doi: 10.1038/emi.2014.88

Lai, J., Hu, M., Wang, H., Hu, M., Long, Y., Miao, M. X., et al. (2014). Montelukast targeting the cysteinyl leukotriene receptor 1 ameliorates Abeta1-42-induced memory impairment and neuroinflammatory and apoptotic responses in mice. *Neuropharmacology* 79, 707–714. doi: 10.1016/j.neuropharm.2014.01.011

Li, C., Deng, Y. Q., Wang, S., Ma, F., Aliyari, R., Huang, X. Y., et al. (2017a). 25-Hydroxycholesterol protects host against Zika virus infection and its associated microcephaly in a mouse model. *Immunity* 46, 446–456. doi: 10.1016/j.immuni.2017.02.012

Li, C., Zhu, X., Ji, X., Quanquin, N., Deng, Y. Q., Tian, M., et al. (2017b). Chloroquine, a FDA-approved drug, prevents zika virus infection and its associated congenital microcephaly in mice. *EBioMedicine* 24, 189–194. doi: 10.1016/j.ebiom.2017.09.034

Liu, Q., Xia, S., Sun, Z., Wang, Q., Du, L., Lu, L., et al. (2015). Testing of Middle East respiratory syndrome coronavirus replication inhibitors for the ability to block viral entry. *Antimicrob. Agents Chemother.* 59, 742–744. doi: 10.1128/AAC.03977-14

Lok, S. M., Costin, J. M., Hrobowski, Y. M., Hoffmann, A. R., Rowe, D. K., Kukkaro, P., et al. (2012). Release of dengue virus genome induced by a peptide inhibitor. *PLoS One* 7:e50995. doi: 10.1371/journal.pone.0050995

Marschallinger, J., Schaffner, I., Klein, B., Gelfert, R., Rivera, F. J., Illes, S., et al. (2015). Structural and functional rejuvenation of the aged brain by an approved anti-asthmatic drug. *Nat. Commun.* 6:8466. doi: 10.1038/ncomms9466

Mounce, B. C., Cesaro, T., Carrau, L., Vallet, T., and Vignuzzi, M. (2017). Curcumin inhibits Zika and chikungunya virus infection by inhibiting cell binding. *Antiviral Res.* 142, 148–157. doi: 10.1016/j.antiviral.2017.03.014

Nowakowski, T. J., Pollen, A. A., Di Lullo, E., Sandoval-Espinosa, C., Bershteyn, M., and Kriegstein, A. R. (2016). Expression analysis highlights AXL as a Candidate Zika virus entry receptor in neural stem cells. *Cell Stem Cell* 18, 591–596. doi: 10.1016/j.stem.2016.03.012

Oliveira Melo, A. S., Malinger, G., Ximenes, R., Szejnfeld, P. O., Alves Sampaio, S., and Bispo de Filippis, A. M. (2016). Zika virus intrauterine infection causes fetal brain abnormality and microcephaly: tip of the iceberg? *Ultrasound Obstet. Gynecol.* 47, 6–7. doi: 10.1002/uog.15831

Peixoto, H. M., Romero, G. A. S., de Araujo, W. N., and de Oliveira, M. R. F. (2019). Guillain-Barre syndrome associated with Zika virus infection in Brazil: a cost-of-illness study. *Trans. R. Soc. Trop. Med. Hyg.* 113, 252–258. doi: 10.1093/trstmh/trz010

Rausch, K., Hackett, B. A., Weinbren, N. L., Reeder, S. M., Sadovsky, Y., Hunter, C. A., et al. (2017). Screening bioactives reveals nanchangmycin as a broad spectrum antiviral active against Zika virus. *Cell Rep.* 18, 804–815. doi: 10.1016/j.celrep.2016.12.068

Retallack, H., Di Lullo, E., Arias, C., Knopp, K. A., Laurie, M. T., Sandoval-Espinosa, C., et al. (2016). Zika virus cell tropism in the developing human brain and inhibition by azithromycin. *Proc. Natl. Acad. Sci. U.S.A.* 113, 14408–14413. doi: 10.1073/pnas.1618029113

Shan, C., Muruato, A. E., Nunes, B. T. D., Luo, H., Xie, X., Medeiros, D. B. A., et al. (2017). A live-attenuated Zika virus vaccine candidate induces sterilizing immunity in mouse models. *Nat. Med.* 23, 763–767. doi: 10.1038/nm.4322

Si, L., Meng, K., Tian, Z., Sun, J., Li, H., Zhang, Z., et al. (2018). Triterpenoids manipulate a broad range of virus-host fusion via wrapping the HR2 domain prevalent in viral envelopes. *Sci. Adv.* 4:eaau8408. doi: 10.1126/sciadv.aau8408

Simonin, Y., van Riel, D., Van de Perre, P., Rockx, B., and Salinas, S. (2017). Differential virulence between Asian and African lineages of Zika virus. *PLoS Negl. Trop. Dis.* 11:e0005821. doi: 10.1371/journal.pntd.0005821

St John, A. L. (2013). Influence of mast cells on dengue protective immunity and immune pathology. *PLoS Pathog.* 9:e1003783. doi: 10.1371/journal.ppat.1003783

St John, A. L., Rathore, A. P., Raghavan, B., Ng, M. L., and Abraham, S. N. (2013). Contributions of mast cells and vasoactive products, leukotrienes and chymase, to dengue virus-induced vascular leakage. *eLife* 2:e00481. doi: 10.7554/eLife.00481

Tai, W., Voronin, D., Chen, J., Bao, W., Kessler, D. A., Shaz, B., et al. (2019). Transfusion-transmitted zika virus infection in pregnant mice leads to broad tissue tropism with severe placental damage and fetal demise. *Front. Microbiol.* 10:29. doi: 10.3389/fmicb.2019.00029

Talarico, L. B., and Damonte, E. B. (2007). Interference in dengue virus adsorption and uncoating by carrageenans. *Virology* 363, 473–485. doi: 10.1016/j.virol.2007.01.043

Talarico, L. B., Pujol, C. A., Zibetti, R. G., Faria, P. C., Noseda, M. D., Duarte, M. E., et al. (2005). The antiviral activity of sulfated polysaccharides against dengue virus is dependent on virus serotype and host cell. *Antiviral Res.* 66, 103–110. doi: 10.1016/j.antiviral.2005.02.001

Tang, H., Hammack, C., Ogden, S. C., Wen, Z., Qian, X., Li, Y., et al. (2016). Zika virus infects human cortical neural progenitors and attenuates their growth. *Cell Stem Cell* 18, 587–590. doi: 10.1016/j.stem.2016.02.016

Wang, X., Xia, S., Zou, P., and Lu, L. (2019). Erythromycin estolate inhibits Zika virus infection by blocking viral entry as a viral inactivator. *Viruses* 11:E1064. doi: 10.3390/v11111064

Wang, X., Zou, P., Wu, F., Lu, L., and Jiang, S. (2017). Development of small-molecule viral inhibitors targeting various stages of the life cycle of emerging and re-emerging viruses. *Front. Med.* 11:449–461. doi: 10.1007/s11684-017-0589-5

Wu, K. Y., Zuo, G. L., Li, X. F., Ye, Q., Deng, Y. Q., Huang, X. Y., et al. (2016). Vertical transmission of Zika virus targeting the radial glial cells affects cortex development of offspring mice. *Cell Res.* 26, 645–654. doi: 10.1038/cr.2016.58

Wu, N., Nguyen, X. N., Wang, L., Appourchaux, R., Zhang, C., Panthu, B., et al. (2019). The interferon stimulated gene 20 protein (ISG20) is an innate defense antiviral factor that discriminates self versus non-self translation. *PLoS Pathog.* 15:e1008093. doi: 10.1371/journal.ppat.1008093

Wu, W., Wang, J., Yu, N., Yan, J., Zhuo, Z., Chen, M., et al. (2018). Development of multiplex real-time reverse-transcriptase polymerase chain reaction assay for simultaneous detection of Zika, dengue, yellow fever, and chikungunya viruses in a single tube. *J. Med. Virol.* 90, 1681–1686. doi: 10.1002/jmv.25253

Xu, M., Lee, E. M., Wen, Z., Cheng, Y., Huang, W. K., Qian, X., et al. (2016). Identification of small-molecule inhibitors of Zika virus infection and induced neural cell death via a drug repurposing screen. *Nat. Med.* 22, 1101–1107. doi: 10.1038/nm.4184

Yin, Z., Chen, Y. L., Schul, W., Wang, Q. Y., Gu, F., Duraiswamy, J., et al. (2009). An adenosine nucleoside inhibitor of dengue virus. *Proc. Natl. Acad. Sci. U.S.A.* 106, 20435–20439. doi: 10.1073/pnas.0907010106

Yu, Y., Deng, Y. Q., Zou, P., Wang, Q., Dai, Y., Yu, F., et al. (2017). A peptide-based viral inactivator inhibits Zika virus infection in pregnant mice and fetuses. *Nat. Commun.* 8:15672. doi: 10.1038/ncomms15672

Yuan, M., Yan, J., Xun, J., Chen, C., Zhang, Y., Wang, M., et al. (2018). Enhanced human enterovirus 71 infection by endocytosis inhibitors reveals multiple entry pathways by enterovirus causing hand-foot-and-mouth diseases. *Virol. J.* 15:1. doi: 10.1186/s12985-017-0913-3

**Conflict of Interest:** The authors declare that the research was conducted in the absence of any commercial or financial relationships that could be construed as a potential conflict of interest.

The reviewer C-FQ declared a past co-authorship with one of the authors PZ to the handling Editor.

*Copyright © 2020 Chen, Li, Wang and Zou. This is an open-access article distributed under the terms of the Creative Commons Attribution License (CC BY). The use, distribution or reproduction in other forums is permitted, provided the original author(s) and the copyright owner(s) are credited and that the original publication in this journal is cited, in accordance with accepted academic practice. No use, distribution or reproduction is permitted which does not comply with these terms.*

frontiers in Microbiology

REVIEW
published: 30 January 2020
doi: 10.3389/fmicb.2019.02989

# Vaccines and Therapeutics Against Hantaviruses

*Rongrong Liu[1†], Hongwei Ma[1†], Jiayi Shu[2,3], Qiang Zhang[4], Mingwei Han[5], Ziyu Liu[1], Xia Jin[2*], Fanglin Zhang[1*] and Xingan Wu[1*]*

[1] Department of Microbiology, School of Basic Medicine, Fourth Military Medical University, Xi'an, China, [2] Scientific Research Center, Shanghai Public Health Clinical Center & Institutes of Biomedical Sciences, Key Laboratory of Medical Molecular Virology of Ministry of Education & Health, Shanghai Medical College, Fudan University, Shanghai, China, [3] Viral Disease and Vaccine Translational Research Unit, Institut Pasteur of Shanghai, Chinese Academy of Sciences, Shanghai, China, [4] School of Biology and Basic Medical Sciences, Soochow University, Suzhou, China, [5] Cadet Brigade, School of Basic Medicine, Fourth Military Medical University, Xi'an, China

Hantaviruses (HVs) are rodent-transmitted viruses that can cause hantavirus cardiopulmonary syndrome (HCPS) in the Americas and hemorrhagic fever with renal syndrome (HFRS) in Eurasia. Together, these viruses have annually caused approximately 200,000 human infections worldwide in recent years, with a case fatality rate of 5–15% for HFRS and up to 40% for HCPS. There is currently no effective treatment available for either HFRS or HCPS. Only whole virus inactivated vaccines against HTNV or SEOV are licensed for use in the Republic of Korea and China, but the protective efficacies of these vaccines are uncertain. To a large extent, the immune correlates of protection against hantavirus are not known. In this review, we summarized the epidemiology, virology, and pathogenesis of four HFRS-causing viruses, HTNV, SEOV, PUUV, and DOBV, and two HCPS-causing viruses, ANDV and SNV, and then discussed the existing knowledge on vaccines and therapeutics against these diseases. We think that this information will shed light on the rational development of new vaccines and treatments.

**Keywords: hantavirus, vaccine, therapeutic strategies, HFRS, HPCS**

OPEN ACCESS

***Edited by:***
*Lu Lu,*
*Fudan University, China*

***Reviewed by:***
*Gong Cheng,*
*Tsinghua University, China*
*Wei Hou,*
*Wuhan University, China*

***Correspondence:**
*Xia Jin*
*xiajin2012@outlook.com*
*Fanglin Zhang*
*flzhang@fmmu.edu.cn*
*Xingan Wu*
*wuxingan@fmmu.edu.cn*

*[†]These authors have contributed equally to this work*

***Specialty section:***
*This article was submitted to Virology, a section of the journal Frontiers in Microbiology*

***Received:*** *03 October 2019*
***Accepted:*** *10 December 2019*
***Published:*** *30 January 2020*

***Citation:***
*Liu R, Ma H, Shu J, Zhang Q, Han M, Liu Z, Jin X, Zhang F and Wu X (2020) Vaccines and Therapeutics Against Hantaviruses. Front. Microbiol. 10:2989. doi: 10.3389/fmicb.2019.02989*

## INTRODUCTION

In recent years, the repeated outbreak of hantavirus disease has caused a serious threat to human health. The spread of hantavirus from natural hosts to humans is a natural ecological process; however, the outbreak of hantavirus is driven by striped field mouse population cycle dynamics and seasonal climate change (Tian and Stenseth, 2019).

Hantavirus is a virus transmitted mainly by rodent animals, mainly through urine, feces, and saliva and the aerosols produced by them, but rarely by the bites of infected animals (Brocato and Hooper, 2019). In recent years, the infection rate of hantavirus has increased in China and Europe (Dong et al., 2019). Hantavirus disease has turned out to be a newly identified but not a "new" disease in Germany (Kruger et al., 2013). The clinical presentations may vary according to viral strains prevalence in different regions. In Asia, hantavirus infection by Hantan virus (HTNV) and Seoul virus (SEOV) targets mainly the human kidney and causes hemorrhagic fever with renal syndrome (HFRS). In North America, infection by Andes virus (ANDV) and Sin Nombre virus (SNV) manifests in mainly the lung and leads to hantavirus pulmonary syndrome (HPS) or hantavirus cardiopulmonary syndrome (HCPS), with high mortality rates; in Europe, infection by

Puumala virus (PUUV) and Dobrava-Belgrade virus (DOBV) typically causes a milder form of HFRS, nephropathia epidemica (NE) (Echterdiek et al., 2019).

Currently, there is no approved post-exposure therapeutic countermeasure against hantaviral infection, but diversified treatment strategies have been developed and applied to manage HFRS or HCPS. These strategies target viral life cycle, host immunological factors, or patient clinical symptoms. Preventive measures against hantaviral infection, especially vaccine development, are essential for future pandemics. In this paper, we reviewed the epidemiology and pathogenesis of hantavirus, and discuss the existing knowledge on vaccine and therapeutics against these diseases in order to shed light on the development of new vaccines and treatments.

# THE RE-EMERGENCE OF HANTAVIRUS

## The Epidemiology of HFRS and HCPS

China has the highest incidence and mortality of HFRS in the world, accounting for more than 90% of the total number of HFRS cases in the world (Zheng et al., 2018). In 2004, the Chinese Center for Disease Control and Prevention (China CDC) established the National Notifiable Disease Surveillance System (NNDSS) online, and HFRS cases of the whole country were reported daily through this system (Zhang et al., 2014). From 2006 to 2012, a total of 77,558 cases and 866 deaths were reported with the average annual incidence rate of 0.83 per 100,000, mortality rate of 0.01 per 100,000 and case fatality rate of 1.13% (Zhang et al., 2014), and its main causative pathogens are HTNV and SEOV (Tian and Stenseth, 2019). So far, HFRS cases have been reported in 30 out of 32 provinces in China (excluding Hong Kong, Macao, and Taiwan) (Zhang et al., 2014). In recent years, the incidence is still high in eastern China (Tian et al., 2017). The distribution map of hantavirus cases reported in recent Chinese literatures is summarized in **Figure 1**. More than 90% of the total cases were clustered in nine provinces and mainly reported in spring and autumn–winter seasons. We can observe that the annual average number of cases in Shaanxi Province was higher than 2000, ranking at the top of the list (**Figure 1**). From 2006 to 2017, Shaanxi has gradually become the province with the highest incidence in China, with approximately 4.51 cases/100,000 cases, of which more than 90% are concentrated in the central region (Xi'an, Xianyang, Baoji, and Weinan cities) (Zheng et al., 2018). By November 20 of 2017, 878 people were recorded infected in Shaanxi Province (Dong et al., 2019). We also can observe that the average annual number of cases in the cities of Shannxi, Shandong, and Jiangxi Province rank the top three (**Supplementary Figure 1**). Another place with a high incidence of HFRS is Qingdao city of Shandong Province, where HFRS incidence is three times higher than the national average, reaching 0.83/100,000 (Jiang et al., 2017).

In the US, 34 states have confirmed and recorded HCPS cases since 1993 (Prince and Lieberman, 2013). In 2008, the first locally acquired case of HFRS caused by the SEOV was confirmed. In 2017, the US CDC investigated an outbreak of SEOV infection that has infected 17 rat owners in seven states (Kerins et al., 2018). The number of hantavirus cases by year in different states is summarized in **Figure 2**. In Canada, HCPS is still very rare, but cases are recorded every year and show seasonal patterns, mainly between March and May and between September and November. A total of 64 cases have been confirmed since 2000, of which 12 were reported in 2013, most in western Canadian provinces such as Alberta, Manitoba, British Columbia, and Saskatchewan (Kerins et al., 2018). SNV and ANDV are responsible for the majority of hantavirus cases leading to HCPS.

Outside North America, individual cases and small clusters of HCPS have been reported in Balkans, northern Sweden (Bergstedt Oscarsson et al., 2016), Argentina (Pini et al., 2003), Chile (Toro et al., 1998), Poland (Gut et al., 2018), Bolivia (1998), Brazil (Suzuki et al., 2004; Limongi et al., 2009), Serbia (Stanojevic et al., 2019), United Kingdom (Duggan, 2019), Panama (Bayard et al., 2004), and Germany (Ettinger et al., 2012). Overall, in Europe, the incidence of hantavirus infections has steadily increased in recent years: In 2014, a record number of 3754 infections were registered across Europe (Vaheri et al., 2013). Chile has had an average of 67 cases per year since 1995; the disease occurs mainly in spring and summer. However, between June and October 2011, there was an increase in cases and rodent populations (Toro et al., 1998). In Paraguay, an HCPS case was first found in the Chako region in 1995. A total of 56 cases were reported in 2011, and 18 cases were reported in 2012 (Padula et al., 2007). In Panama, HCPS first appeared in 1999, with an average of 12 patients per year. However, 16 cases were reported in 2012, and 14 cases were confirmed as of 21 August 2013. For the first time since 1997, Uruguay has experienced HCPS cases, with an average of nine cases per year. The first case was recorded in northern Uruguay in 2010. In Poland, the infections are caused by mainly the PUUV and DOBV serotypes. The morbidity is not high; it ranges between 0.02 and 0.14 per 100,000 cases, but some papers suggest that the data concerning Poland is underestimated (Gut et al., 2018), because the number of infections then was higher, and it was most likely the epidemic year. In the following year, 2015, there were 6 infections, and in 2016 and 2017, there were 8 and 14 cases registered, respectively. In Germany, from 2001 to 2010, the incidence increased from 0.09 to 2.47/100,000 (Ettinger et al., 2012). In United Kingdom, the virus was first identified in laboratory rats in Scotland in 1977, and all but 1 of the 15 cases of SEOV caused acute kidney injury, which were diagnosed by the Rare and Imported Pathogens Laboratory (Duggan, 2019).

## Hantavirus Virology

Hantaviruses belong to the Family *Hantaviridae* of *Bunyavirales* and are a kind of enveloped single negative chain RNA virus (Abudurexiti et al., 2019). A maximum likelihood phylogenetic tree of the complete amino acid and CDS sequence of the M segment of hantaviruses was made based on the international Committee on Taxonomy of Viruses (ICTV) updated taxonomy of the order *Bunyavirales* in 2019 (see **Figure 3**). This phylogeny shows the modest genetic diversity of the virus family.

The diameter of hantavirus particles is 80–US210 nm, and the structure is spherical or ovoid. They are composed of 20–30%

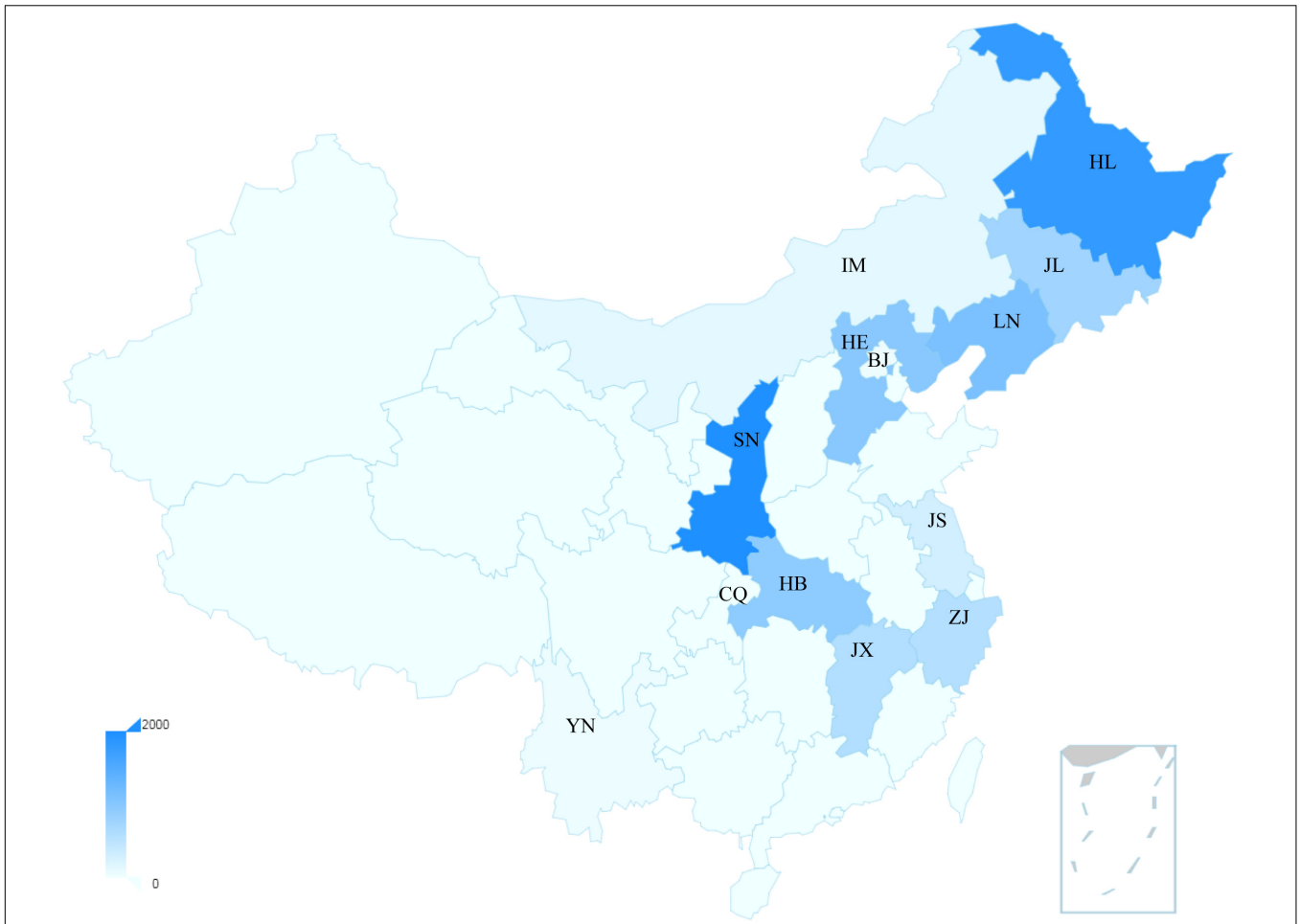


**FIGURE 1 |** The distribution map of the average hantavirus cases in China of recent years. The main provinces shown in the map were Shaanxi: SN; Heilongjiang: HL; Liaoning: LN; Hebei: HE; Hubei: HB; Jilin: JL; Jiangxi: JX; Zhejiang: ZJ; Jiangsu: JS; Inner Mongoria: IM; Beijing: BJ; Yunnan: YN; Chongqing: CQ. The bar represents the annual average number of cases. These data were published by Chinese literatures.

fat, >50% protein, 7% carbohydrates, and 2% RNA. They are very stable and can survive for more than 18 days at 4°C and −20°C and 10 days at room temperature (Vaheri et al., 2013). The genome comprises three negative sense, single-stranded RNAs that consist the small (S), medium (M), and large (L) segments that encode the nucleoprotein (Np), envelope glycoproteins (Gn and Gc), and viral RNA-dependent RNA polymerase (RdRp), respectively (Graham et al., 2019). The outer membrane of hantavirus is composed of Gn and Gc glycoprotein, which mediates the recognition of and entry into host cells. The crystal structure of HTNV Gn is very similar to that of PUUV Gn, which confirms that hantavirus Gn is conserved in hantavirus (Li et al., 2016; Rissanen et al., 2017).

## CLINICAL EVALUATION OF EXISTING VACCINES

Although there have been substantial vaccines, there is no licensed vaccine against hantavirus infection that can be widely used. Despite inactivated hantavirus vaccines being licensed for human use in China and Korea, no such vaccine has been approved in the US or Europe (Tian and Stenseth, 2019). Current clinical studies of inactivated hantavirus vaccine in China or Korea and clinical trials of DNA vaccines in the US are summarized in **Table 1**.

### Protective Efficacy of Inactivated Hantavirus Vaccines

The inactivated vaccines comprise entire virions that are inactivated physically (heat) or chemically. In Korea, Lee and An (Cho et al., 2002) first developed an inactivated HTNV vaccine (IHV), which was prepared from the HTNV strain ROK 84/105, which proliferates in the brains of lactating mice. It has been proven that it can induce protein immunization in mice and humans (Yamanishi et al., 1988). In 1990, the Korean HFRS vaccine Hantavax was put into commercial production. The total number of HFRS patients hospitalized in South Korea fell sharply from 1234 in 1991 to 415 in 1997 (Cho et al., 2002). To evaluate

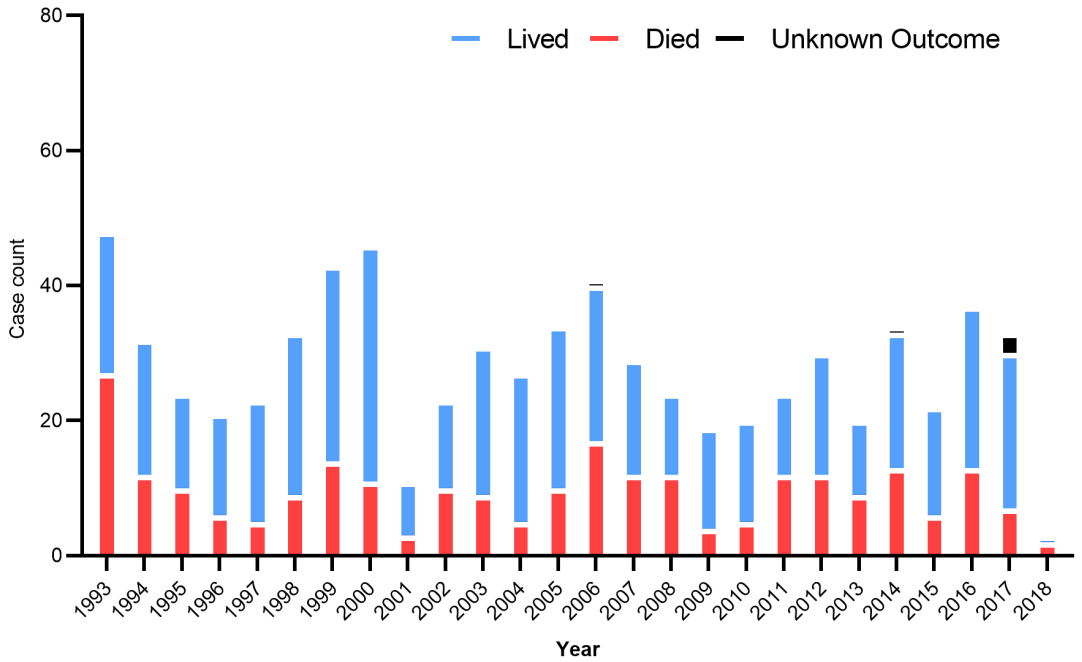


**FIGURE 2 |** US hantavirus cases from 1993 to 2018. These data were published by the Centers for Disease Control and Prevention, United States.

the immunogenicity and safety of Hantavax$^{TM}$ in healthy adults in multicenter phase III clinical trials, three dose schedules at 0, 1, and 13 months were used. The seroconversion rate was 90.14% by IFA but only 23.24% by PRNT50 after two primary doses. One month after vaccination, the positive rate of serum was 87.32 and 45.07% according to IFA and PRNT50, respectively. The neutralizing antibody response of the two initial doses of Hantavax$^{TM}$ was very poor. Therefore, it is necessary to carry out enhanced immunization within 2–6 months to provide timely protection for high-risk groups (Song et al., 2016).

From January 2011 to February 2017, the South Korean military conducted a case–control study of 100 patients to evaluate the effect of an IHV on HFRS. The vaccine effectiveness (VE) value of the IHV was 59.1%, but the VE value of HFRS high-incidence area was higher (78.7%) (Jung et al., 2018). However, in 2018, the efficacy of iHV on the progression of HFRS did not show a statistically significant protective effect. From 2009 to 2017, 18 patients inoculated with HFRS vaccine and 110 patients not vaccinated with the HFRS vaccine were recruited at Korean Army Hospital to investigate the severity (AKI) and the efficacy of dialysis events in acute renal injury. Overall, 33.3% of the effective vaccination group had three stages of AKI, compared with 54.5% for the non-vaccinated group. The curative effect of IHV on disease progression was 58.1%, but the curative effect of IHV on HFRS progress did not show a statistically significant protective effect (Yi et al., 2018).

In China, bivalent inactivated vaccines against HTNV and SEOV infection were produced in 1994 and approved by the Pharmacopoeia of China in 2005. Since 2008, the Chinese government has implemented an expanded immunization program targeting HFRS. China uses approximately 2 million doses of HFRS vaccine every year (Schmaljohn, 2012). HFRS cases have significantly dropped to less than 20,000 per year. Phase 4 clinical trials of inactivated hantavirus vaccine showed that the median OD values of IgG antibody were 0.005 (0.004–0.016), 0.116 (0.036–0.620), 0.320 (0.065–0.848), and 0.128 (0.011–0.649), and that the positivity rate was 7.7, 40.6, 62.2, and 48.2% at pre-vaccination, 1 month after the two primary doses, at the booster dose and at 18 months after the booster dose, respectively. Although two main doses can help healthy individuals develop immune responses, the three-dose series should be better than the two-dose series (Zheng et al., 2018). Another clinical study in Xian Yang city in northwest China showed that the positive rate of neutralizing antibody in the unvaccinated group was 10.0%, and the positive rate was 80.0, 90.0, 50.0, and 90%, respectively, at 1, 3, 29, and 33 months after immunization with a vaccine consisting of a mixture of inactivated HTNV and SEOV. This finding indicates that the vaccination program can induce effective humoral immunity in northwestern China and can be maintained up to 33 months after vaccination (Li et al., 2017) (**Table 1**).

## Clinical Trials of DNA Vaccines for HFRS

At present, DNA vaccines are the most popular method in the research of HFRS and HCPS vaccines, mainly focusing on the use of a hetero-expression system to produce recombinant M protein. DNA vaccines are characterized by safety because they have replication defects, cannot restore the virulence, and cannot spread from person to person or to the environment. A variety of DNA vaccines against the hantavirus envelope glycoprotein gene were developed by Hopper's group (Schmaljohn et al., 2014).

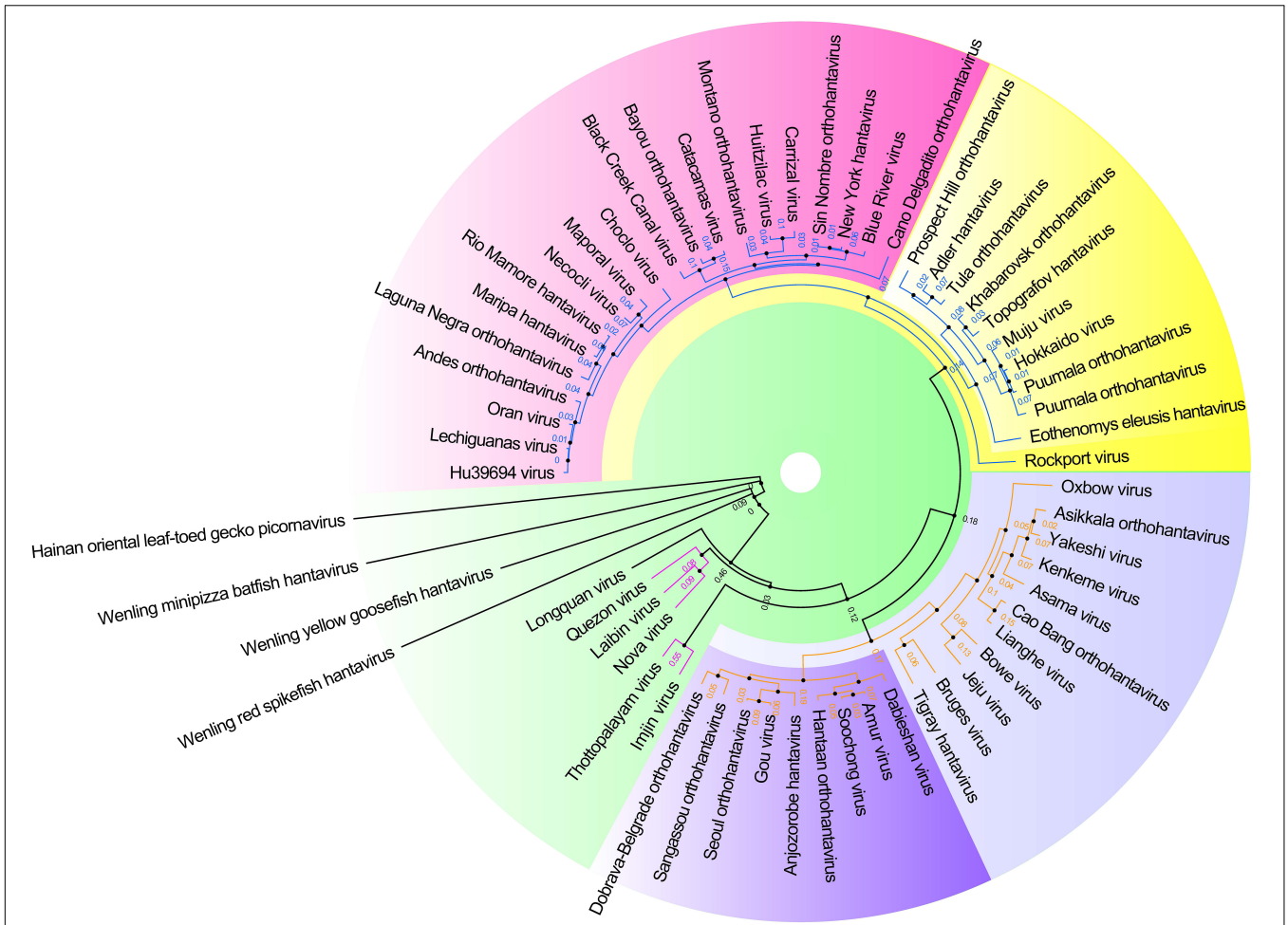


**FIGURE 3 |** Hantavirus phylogenetic tree on the basis of the M segment sequences. A maximum clade credibility tree of the complete amino acid sequence of the protein encoded by the M segment of viruses belonging to Hantavirus. Different colors represent different clade. These proteins had a high similar signature domain and highly unconserved terminal sequences, which could artificially create similarities between sequences if the alignment was not properly made. Therefore, the phylogenetic tree was made with more robust methods using T-Coffee (default parameter, removed the unconserved sites by filtering the column scores $< 4$) for multiple sequence alignment and SMS-PhyML (default parameter, bootstrap = 1000, best model = LG +G) for ML (Maximum Likelihood) tree construction.

Their studies have confirmed that these DNA vaccines produce neutralizing antibodies in multiple experimental animal species and protected hamsters from HFRS (Schmaljohn et al., 2014).

Next, they developed HFRS candidate DNA vaccines expressing HTNV or PUUV Gn and GC genes and evaluated them in an open-labeled single-center phase 1 study. The results showed that HTNV and PUUV DNA vaccines prepared by electroporation were safe. When mixed together, the response to PUUV was greater than that to the HTNV DNA vaccine, and both DNA vaccines had immunogenicity (Hooper et al., 2014).

The vaccine entered phase 2a trial in 2014 to compare the immune responses to two different doses, 1.0 and 2.0 mg, and mixed HTNV and PUUV DNA vaccines in healthy participants. All groups also received booster doses 6 months after the first vaccination to determine which doses and vaccination plans will be the best way to advance the vaccine development process. To evaluate the safety, responsiveness and immunogenicity of an ANDV DNA vaccine to prevent HPS, the first phase I clinical trials of the ANDV DNA vaccine began in February 2019[1] (**Table 1**).

## PRE-CLINICAL DEVELOPMENT OF NEW VACCINES

### DNA Vaccines

Similarly, all DNA vaccines developed against hantavirus target the M gene expressing the envelope GP (Gn and Gc) of hantaviruses (**Table 2**, part 1).

In the United States, a variety of DNA vaccines express the envelope glycoprotein gene of hantaviruses that were developed by Hopper's group (Schmaljohn et al., 2014). In 1999, HFRS candidate naked DNA vaccine was constructed by the subcloning method. The subcloned cDNA represented the medium fragment

[1]www.clinicaltrials.gov

**TABLE 1 |** Existing vaccines in clinical trials and case–control studies.

| Number | Title | Conditions | Interventions | Type | Funder Type | Age | Number Enrolled | Date | Status | References |
|---|---|---|---|---|---|---|---|---|---|---|
| AFMC-17082-IRB-17-077 | Effectiveness of inactivated hantavirus vaccine on the disease severity of hemorrhagic fever with renal syndrome | HFRS | Hantavax® | Case–control study | Korea | 20–22 | 129 | March-09 March-17 | Completed | Jung et al., 2018 |
| | Protective effectiveness of inactivated hantavirus vaccine against hemorrhagic fever with renal syndrome | HFRS | Hantavax® | Case–control study | Korea | 20–30 | 100 | January-11 February-17 | Completed | Yi et al., 2018 |
| | Persistence of immune responses to vaccine against hemorrhagic fever with renal syndrome | HFRS | Inactivated hantavirus vaccine | Phase 4 | China | 16–60 | 143 | June-11 June -13 | Completed | Zheng et al., 2018 |
| | The assessment of Hantaan virus-specific antibody responses after the immunization program for hemorrhagic fever with renal syndrome in northwest China | HFRS | HFRS inactivated vaccine [a mixture of HTNV (type I) and SEOV (type II)] | Case–control study | China | 16–60 | 100 | | Completed | Li et al., 2017 |
| NCT01502345 | Study to evaluate the safety, tolerability, and immunogenicity of Hantaan and Puumala virus DNA vaccines | HFRS | HTNV/PUUV DNA vaccine/device combination | Phase 1 | U. S. Fed \| Industry | 18–49 | 31 | January-12 January-13 | Completed | Hooper et al., 2014 |
| NCT02116205 | Phase 2a immunogenicity study of Hantaan/Puumala virus DNA vaccine for prevention of hemorrhagic fever | HFRS | HTNV/PUUV DNA vaccine | Phase 2a | V. S. Fed \| Industry | 18–49 | 132 | May-14 July-19 | Active, not recruiting | |
| NCT03682107 | Andes virus DNA vaccine for the prevention of hantavirus pulmonary syndrome using the PharmaJetStratis(R) needle-free injection delivery device | HPS | Andes virus DNA vaccine | Phase 1 | NIH | 18–49 | 48 | February-19 October-19 | Recruiting | |
| NCT03718130 | Combination HTNV and PUUV DNA vaccine | HFRS | HTNV vaccine PUUV vaccine HTNV/PUUV virus vaccines | Phase 1 | U.S. Fed | 18–49 | 72 | May-19 May-21 | Not yet recruiting | |

**TABLE 2 |** Pre-clinical development of new vaccines.

| DNA vaccine | | | | | |
|---|---|---|---|---|---|
| **Virus** | **Antigens** | **Vector** | **Delivery Methodology** | **Animal Model** | **References** |
| SEOV | M/S | pWRG7077 | I.M. | Hamsters | Hooper et al., 1999 |
| PUUV | Npeptide | HuAC/pUC19 | I.M. | BALB/c mice | Bucht et al., 2001 |
| HTNV and SEOV | M | pWRG/SEO-M,pWRG/HTN-M | I.M. | Rhesus monkeys | Hooper et al., 2001 |
| ANDV | M | pWRG/AND-M | Gene gun | Rhesus macaques | Custer et al., 2003 |
| HTNV and ANDV | M | pWRG/HA-M | Gene gun | Rhesus macaques | Hooper et al., 2006 |
| ANDV | M | pWRG/AND-M | Twin Injector electroporation device. I.M. | Hamster; rabbits | Hooper et al., 2008 |
| HTNV and PUUV | M | pWRG7077 | Gene Gun or I.M. EP | Hamsters | Spik et al., 2008 |
| PUUV | M | pWRG/PUU-M | Gene gun | Hamsters | Brocato et al., 2012 |
| ANDV | M | pWRG/AND-M | I.M. | Hamsters; ducks | Brocato et al., 2012 |
| SNV ANDV and SNV HTNV and PUUV Pan-hantavirus | M | pWRG/SN-M | Muscle electroporation (me) | Female New Zealand white rabbits (*Oryctolagus cuniculus*) | Hooper et al., 2013 |
| SNV ANDV | M | pWRG/SN-M, pWRG/AND-M | DSJI system, IM and ID needle-free devices | Rabbits and NHPs (Syrian hamsters; Rhesus macaques; Cynomolgus macaques) | Kwilas et al., 2014 |
| ANDV and SNV | Gp | pWRG/AND-M;pWRG/SN-M | Needle-free jet injection device | Syrian hamsters | Hooper et al., 2014 |
| ANDV | M | pWRG/AND-M | I.M. | Syrian hamsters | Haese et al., 2015 |
| SEOV, HTNV and PUUV | 25 Gp epitopes | pcDNA3.1-SHP pGEX-6p-1-SHP | I.M. | BALB/c mice | Zhao et al., 2012 |
| HTNV | Gn | pVAX-LAMP/Gn | I.M. | BALB/c mice | Jiang et al., 2015 |
| HTNV | Gn | pVAX-Gn, pVAX-LAMP and pVAX-LAMP/Gn; | I.M. | BALB/c mice | Jiang et al., 2017 |
| **Subunit Vaccine** | | | | | |
| **Virus** | **Antigens** | **Vector** | **Expression system** | **Results** | **References** |
| PUUV, TOPV, AMDV and DOBV | NP | pQE-32 | *Escherichia coli* cells | Immunization with NP from PUUV, TOPV, ANDV, or DOBV has cross-protection against PUUV | de Carvalho Nicacio et al., 2002 |
| PUUV | NP, G1and G2 | pBSK.K27S pWRG7079 K27 G1 pELVS K27 G2 pSC11T7 | CV-1 cells COS-7 cells | These recombinant vaccinia viruses were used to detect and clone PUUV-specific CTLs from the PBMC of NE patients. An HLA-A24-restricted CTL line recognizing the G2 protein was isolated and its 9-mer epitope was determined. | Terajima et al., 2002 |
| PUUV, DOBV, and HTNV | NP | pFX7-His6 | Yeast *Saccharomyces cerevisiae* | The yield for all nucleocapsid proteins ranged from 0.5 to 1.5 mg per g wet weight of yeast cells | Razanskiene et al., 2004 |

*(Continued)*

**TABLE 2 |** Continued

| Subunit Vaccine | | | | | |
|---|---|---|---|---|---|
| **Virus** | **Antigens** | **Vector** | **Expression system** | **Results** | **References** |
| DOBV | NP | pFX7-derived expression plasmids | Yeast *S. cerevisiae* | The antibodies induced by DOBV rN protein were highly cross-reactive to the rN proteins of HTNV and PUUV. In both mice strains, DOBV rN protein induced N-specific antibodies of all IgG sub classes, suggesting a mixed Th1/Th2 immune response. | Geldmacher et al., 2004 |
| PUUV | Gn and Gc | pTrcHis2 Topo® TA vector | COS-1 cells | The diversity between different Puumala virus: N-linked glycosylation occurs at three sites in Gn (N142, N357, and N409), and at one site in Gc (N937). Also, one possible *O*-glycosylation site was identified in Gc (T985). | Johansson et al., 2004 |
| SEOV | NP | pSTBLUE-1/SEOV-N<br>pFX7-His-SEOV-N | Yeast *S. cerevisiae* | The immunization of a rabbit with the recombinant NP resulted in the induction of a high-titered antibody response and was able to detect antibodies in sera of experimentally infected laboratory rats and in human anti-hantavirus-positive sera or serum pools of patients from different geographical origin. | Schmidt et al., 2005 |
| PUUV | NP | pFD3 | *S. cerevisiae* FH4C/pFD3-h-N–GFP | The maximal volumetric yield of N protein was 316 mg $L^{-1}$, the respective yield of h-N protein was 284 mg $L^{-1}$ | Antoniukas et al., 2006 |
| PUUV | NP | pTEXmp18 | *E. coli* mutant ICONE 200 | P40-Puu118 in particular is a good candidate for a recombinant vaccine against PUUV. All recombinant proteins linked to rP40 induced high antibody responses, indicating that rP40 is a carrier protein with potential for use in other vaccines. | Maes et al., 2008 |

*(Continued)*

**TABLE 2 |** Continued

| VLP vaccine | | | | | |
|---|---|---|---|---|---|
| **Virus** | **Antigens** | **Vector** | **Expression system** | **Results** | **References** |
| HTNV | M | pFastBacTM Dual vector | Sf9 insect cells | Chimeric HTNV VLPs containing GPI-anchored GM-CSF or CD40L induced stronger humoral immune responses and cellular immune responses compared to the HTNV VLPs and Chinese commercial inactivated hantavirus vaccine. | Cheng et al., 2016 |
| HTNV | M | pCI-neo | dhfr-deficient CHO cells | *In vitro* stimulation with CD40L or GM-CSF anchored HTNV VLP showed enhanced activation of macrophages and DCs. *In vivo*, it can induce higher level of HTNV specific antibody and neutralizing antibody in mice. Immunized mice splenocytes showed higher ability of secreting IFN-γ and IL-2, as well as enhancing CTL activity. | Ying et al., 2016 |
| HTNV | M | pCI-neo | dhfr-deficient CHO cells | GM-CSF and CD40L VLPs provided stable, long-term protection with a high titer of neutralizing antibody in mice 6 months after immunization. Furthermore, VLPs increased HTNV-specific cellular immune responses via higher expression of IFN-g and CTL responses. HTNV challenge assay results showed long-term protection against HFRS. No significant pathological alteration was observed in the organs of mice after immunization. | Dong et al., 2019 |

(M; encoding G 1 and G 2 glycoprotein) or small fragment (S; encoding nucleocapsid protein) of SEOV and was cloned into the expression vector WRG 7077. Syrian hamsters were vaccinated with the M or S vaccine with a gene gun, and hantavirus-specific antibodies were found in 5 of 5 hamsters or 4 of 5 hamsters, respectively. Evidence of infection was monitored after challenge with SEOV. Twenty-eight days later, hamsters vaccinated with M were protected hamsters from infection, but those inoculated with S were not protected (Hooper et al., 1999).

Then, HTNV M gene products G 1 and G 2 were expressed in 2001, and non-human primates were evaluated. The HTNV M gene has protective effects against HTNV, SEOV, and DOBV in hamsters. The HTNV and ANDV M genes can induce high level of neutralizing antibodies in rhesus monkeys (Hooper et al., 2001). Next, a DNA vaccine plasmid containing the

full-length M genome fragment of ANDV (pWRG/AND-M) was constructed (Hooper et al., 2008). Rhesus monkeys inoculated with pWRG/AND-M with gene guns produced very high levels of neutralizing antibodies that neutralized not only ANDV but also other HCPS-related hantavirus strains, such as SNV. On the 4th or 5th day after injection, monkey serum protected 100% of hamsters from fatal diseases (Custer et al., 2003).

Then the pWRG/HA-M plasmid containing the HTNV and ANDV M gene fragments was constructed. Rhesus monkeys were immunized with the pWRG/HA-M vaccine to produce antibodies binding to M gene products (G 1 and G 2 glycoproteins) and neutralize HTNV and ANDV. Subsequently, 1–2 years after the initial vaccination series, the neutralizing antibody titers induced by the double immunogen pWRG/HA-M or a single immunogen expressing only HTNV or ANDV Gp increased rapidly to a high level. This result is the first time that the hantavirus M gene DNA vaccine has been shown to elicit a strong memory response and stimulate an antibody response to neutralize HFRS and HCPS viruses (Hooper et al., 2006; Kwilas et al., 2014) detected the high-titer neutralizing antibody induced by an SNV/ANDV DNA vaccine encoding viral envelope Gp in laboratory animals and non-human primates (NHCPS). It can be delivered effectively using a disposable syringe injection (DSJI) system (Kwilas et al., 2014). Brocato et al. (2013) cloned codon-optimized PUUV M fragments into DNA vaccine vectors to produce the plasmid pWRG/PUU-M, which can produce high-titer neutralizing antibodies in hamsters and NHCPs. The pWRG/PUU-M vaccine protects hamsters from PUUV infection and is not affected by DOBV infection. Unexpectedly, vaccination could protect hamsters in the absence of ANDV cross-neutralizing antibodies in a lethal ANDV disease model (Brocato et al., 2013). Then, the authors tried to produce the pan-hantavirus vaccine with a mixed plasmid DNA vaccine. A study of ANDV hamster model showed that the neutralizing antibody produced by DNA vaccine technology can be used to resist the challenge of an SNV full-length M gene DNA vaccine to prevent the occurrence of HCPS. Rabbits vaccinated with SNV DNA vaccine with muscle electroporation (mEP) produced increased neutralizing antibody titers. In addition, hamsters vaccinated three times with the SNV DNA vaccine with a gene gun were completely free from SNV infection. Rabbits were vaccinated with HCPS mixture (ANDV and SNV plasmid), HFRS mixed (HTNV and PUUV plasmid), or HCPS/HFRS mixture (all four plasmids) by mEP. The results showed that the HCPS mixture and HFRS mixture produce neutralizing antibodies against ANDV/SNV and HTNV/PUUV, respectively. In addition, a mixture of HCPS/HFRS triggered neutralizing antibodies against all four viruses (Hooper et al., 2013). Spik et al. (2008) reported that PUUV and HTNV DNA vaccines should serve as separate regulators. Both vaccines produced neutralizing antibodies when injected alone, but when they were administered as mixtures, only one of the two hantavirus antibodies could be detected. In contrast, if the DNA was administered to an animal as a separate vaccine, a reaction to both was observed. To improve the use of DNA vaccine, a multihead intradermal electroporation device was developed, which can be used to vaccinate with an increased dose of DNA vaccine to the skin. The device will enable multiplasmid vaccine preparation to provide multiplasmid vaccine preparation without interference (Mackow et al., 2014).

In China, a DNA vaccine targeting hantavirus Gn merges the antigen with lysosome-associated membrane protein 1 (LAMP 1), thereby changing the antigen presentation pathway and activating CD4 T cells. The LAMP 1 targeting strategy successfully enhanced the effectiveness of the HTNV Gn vaccine. Further studies showed that pVAX-LAMP/Gn established a memory response during long-term protection (6 months) in mice. Zhao et al. constructed a multi-epitope chimeric DNA vaccine—named the SHP chimeric gene, which contains 25 glycoprotein epitopes of SEOV, HTNV, and PUUV. The humoral and cellular responses were significantly enhanced in vaccinated BALB/c mice (Zhao et al., 2012).

## Subunit Vaccines

Subunit protein vaccines not only are safe and easy to produce but also do not easily cause interference between the components of a multivalent formulation (Sun et al., 2017; Liang et al., 2018; Qu et al., 2018). Because the N protein of hantavirus circulating in different continents can provide high cross-protection in animals, the N protein is considered to be an important part of a wide range of reactive vaccines against hantavirus infection (de Carvalho Nicacio et al., 2002). Research has shown that recombinant nucleocapsid protein (rN) from PUUV, TOPV, ANDV, and DOBV could induce a cross-protective immune response to PUUV. The cross-reaction to PUUV antigen was the highest in the serum of animals immunized with ANDV rN, followed by that to TOPV and DOBV rN. In a proliferation test, T lymphocytes immunized with heterogenic rNs were effectively recalled by PUUV rN *in vitro*, as were animal T lymphocytes immunized with homologous proteins (de Carvalho Nicacio et al., 2002). In addition, recombinant vaccinia virus carrying PUUV N or the first half of the G2 gene was constructed. Detection and cloning of PUUV-specific CTLs from PBMCs of patients with NE by recombinant PUUV vaccinia virus led to the isolation of an HLA-A24-restricted CTL cell line recognizing the G2 protein, and its 9-mer epitope was determined (Terajima et al., 2002). Razanskiene et al. (2004) reported that the stability and high purity of NP of PUUV, DOBV, and HTNV ranged from 0.5 to 1.5 mg/g wet weight of yeast cells. DOBV rN protein is a promising vaccine candidate protein that can induce N-specific antibodies, and its terminal titer is as high as 1:1,000,000 in C57BL/6 mice. The antibody induced by DOBV rN protein has a high cross-reaction with rN protein of PUUV and HTNV (Geldmacher et al., 2004). It was found that there might be RNA fragment exchange between the two PUUV strains. N-linked glycosylation occurred at one site of Gn (N 142, N357, and N409) and GC (N 937), and a possible *O*-glycosylation site was identified in GC (T 985). The study of coding gene products is of great significance for the design of new vaccines (Johansson et al., 2004). Schmidt et al. (2005) reports that NP of SEOV reacts with SEOV-specific monoclonal antibodies and some HTNV- and PUUV cross-reactive monoclonal antibodies. Rabbits immunized with recombinant NP can induce a high-titer antibody response, and NP-specific antibodies were detected in

the serum of experimental infected rats and human exposed to hantavirus from different geographical sources. Yeast-expressed SEOV N protein represents a promising antigen for serological epidemiological research and vaccine development (Schmidt et al., 2005). Antoniukas et al. (2006) reported that the biomass and the expression level of recombinant PUUV NP were increased by adding plant extract to YNB medium. The maximum volume yield of the N protein was 316 mg $L^{-1}$ (Antoniukas et al., 2006) (**Table 2**, part 2).

## VLP Vaccines

Virus-like particle vaccines are similar to natural virus particles but lack infectious genetic material. They are composed of repetitive viral structural proteins with inherent self-assembly characteristics (Yong et al., 2019). How to improve the immunogenicity of VLPs is very important. It was reported that either CD40L- or GM-CSF-contained HTNV VLP expression in sf9 insect cells (Cheng et al., 2016) or CHO cells (Ying et al., 2016) could enhance the activation of macrophages and dendritic cells. CD40L/GM-CSF incorporation into VLPs induced elevated levels of HTNV-specific antibodies and neutralizing antibodies in mice. The spleen cells of immunized mice had an enhanced ability to secrete IFN-γ and IL-2, increasing CTL activity (Cheng et al., 2016). The GM-CSF and CD40L-containing VLPs expressed in a eukaryotic expression vector had a stable, long-term protective effect, with a high titer of neutralizing antibody, on mice within 6 months after immunization (Dong et al., 2019). These results suggest that CD40L/GM-CSF-containing VLPs can be used as a potential candidate vaccine (**Table 2**, part 3).

# THERAPEUTIC STRATEGIES AGAINST HANTAVIRUS INFECTION

Hantaviruses primarily infect host capillary endothelial cells of various organs, especially those of kidneys and lungs, and could spark robust immune response in humans. The basic pathological feature of both old world hantaviruses causing HFRS and new world hantaviruses leading to HCPS is dramatically increased vascular permeability, the pathogenesis of which is highly involved in viral infection and excessive immune responses of the host. Extensive capillary leakage results in multiple clinical manifestations, such as hypotensive shock in HFRS and non-cardiogenic pulmonary edema in HCPS, which might deteriorate into multisystem organ failure. Currently, there are no approved post-exposure therapeutic countermeasures against hantaviral infection, but diversified treatment strategies, which target the viral life cycle, host immunological factors or patient clinical symptoms, have been developed and applied to manage HFRS or HCPS (see **Table 3**). Virus-targeting antivirals, including classical antiviral drugs, antibodies, or novel small molecules, are tested mainly to block hantavirus entry or restrain virus replication. Although several antivirals have been proven to be protective *in vitro* or *in vivo*, there still exist some problems for their clinical application. Host-targeting medicines are designed to improve vascular function or rebuild immune homeostasis, while their curative effects are still under debate. Supportive care is universally applied for HFRS or HCPS, and the specific treatments depend on clinical findings of different disease phases.

## Virus-Targeting Antivirals

### Blocking Viral Entry

The viral entry process is composed of virus attachment or absorption on susceptible cells, penetration and subsequent uncoating, which is the first step for hantaviral life cycle. Neutralizing antibodies (NAbs) could interact with viral envelope proteins and disturb their binding with receptors on host cells, thus blocking viral attachment. During hantavirus infection, the Gn and Gc glycoproteins, but not nucleocapsid proteins (NP) are considered the major antigens in inducing NAb production (Jiang et al., 2016). High levels of NAbs could be detected in the convalescent phase of HFRS or HCPS patients, and these NAbs could protect the individual from hantaviral infection and have been used as passive immunotherapy (Manigold and Vial, 2014; Jiang et al., 2016). Presently, there are no reported clinical randomized controlled trials using NAbs in immunotherapy for HFRS or HCPS in humans. Most studies measure antibody efficacy through the focus reduction neutralization test (FRNT) and hemagglutination inhibition (HI) test at the cellular level, as well as animal experiments against lethal hantavirus challenge (sucking mice or newborn rat models for HTNV or SEOV infection and hamster models for ANDV or SNV infection) (Zhang et al., 1989; Xu et al., 2002; Manigold and Vial, 2014). For old world hantaviruses, 13 crude Fab preparations directed to the PUUV Gc protein were generated from splenic lymphocytes of a PUUV-immune individual and exhibited type-specific neutralization of PUUV, with a 44–54% reduction in FRNT (de Carvalho Nicacio et al., 2000). Anti-SR-11 (SEOV) rat serum applied 4 h before or 72 h after the challenge could protect against lethal SR-11 (SEOV) infection in newborn rats, and cross-protection effects were also found against KI-262 (SEOV) and 76-118 (HTNV) (Zhang et al., 1989). In China, 18 murine monoclonal antibodies (MAbs) targeting HTNV were prepared in our lab, among which 14 targeted NP, 4 reacted with Gc, and 1 recognized both NP and Gc. The Gc-related MAbs were active in the HI test and displayed high virus-neutralizing activity *in vitro*, and they could be regarded as HTNV NAbs. Consistently, administration of these NAbs within 48 hpi could protect suckling mice from lethal HTNV infection, indicating that NAbs might be a potentially treatment strategy for preexposure prophylaxis and postexposure therapy against HTNV infection (Xu et al., 2002). Phase I clinical pharmacology and toxicity tests for HTNV NAbs in healthy volunteers were performed, and phase II clinical trials to assess the therapeutic efficacy of these NAbs in early stages of HFRS were carried out in endemic settings in China (Xu et al., 2002, 2009). For new world hantaviruses, passive immunization with either patient-derived or vaccine-induced NAbs was capable of protecting against lethal ANDV challenge in hamsters (Manigold and Vial, 2014). A non-randomized multicenter trial using plasma from HCPS convalescent patients for the treatment of acute HCPS has been carried out in Chile, showing that plasma containing high titers of NAbs against ANDV could significantly reduce case fatality rate from 32 to

**TABLE 3 |** Potential therapeutic strategies for hantaviral infection.

| Purpose | Drugs | Type | Known/ Putative target | Virus/Evidence | Diseases | References |
|---|---|---|---|---|---|---|
| Blocking Viral Entry | MAb Fab 4G2 and 1C9 | Human MAbs Fab fragments | Gc glycoprotein | PUUV/ Vero E6 cells | HFRS | de Carvalho Nicacio et al., 2000 |
| | Anti-SR rat serum | Rat PAbs | Viral GP | SEOV/ newborn rats | | Zhang et al., 1989 |
| | 3D8, 3G1, 8G3, 8F8, 8G2 | Mice MAbs | Gc, or both NP and Gc | HTNV/Vero E6 cells/suckling mice/phase II clinical trials | | Xu et al., 2002, 2009 |
| | Patient-derived or vaccine-induced NAbs | Human PAbs | Viral GP | ANDV/hamsters | HCPS | Manigold and Vial, 2014 |
| | Human immune plasma | Human PAbs | Viral GP | ANDV/clinical trials | | Vial et al., 2015 |
| | IgY/IgYΔFc | Goose PAbs | Viral GP | ANDV/hamsters | | Haese et al., 2015 |
| | JL16 and MIB22 | Human MAbs | Viral GP | ANDV/hamsters | | Garrido et al., 2018 |
| | Lactoferin | Lactoferin | Viral GP/monocyte and NK | SEOV/ Vero E6 cell/suckling mice | HFRS | Murphy et al., 2000, 2001 |
| | Domain III and stem peptides | Peptides | Gc glycoprotein | ANDV, PUUV/Vero E6 cells | HCPS and HFRS | Barriga et al., 2016 |
| | CLVRNLAWC and CQATTARNC | Cyclic nonapeptides | Host receptor | SNV, ANDV/Vero E6 cells | HCPS | Hall et al., 2008 |
| | 012-0652, C481-1256 and G319-0078 | Peptidomimetic compounds | Host receptor | SNV, ANDV, HTNV/Vero E6 cells | HCPS and HFRS | Hall et al., 2010 |
| | Favipiravir | Pyrazine derivative | RdRp | SNV, ANDV/Vero E6 cells/hamsters | HCPS | Safronetz et al., 2013 |
| Inhibiting Viral Replication | Ribavirin | Nucleoside analogs/ mutagen/ T cell | RdRp | HTNV, PUUV, ANDV/Vero E6 cells/suckling mice (HTNV)/hamsters (ANDV) | HCPS and HFRS | Mertz et al., 2004; Safronetz et al., 2011; Kobayashi et al., 2012; Chung et al., 2013; Ogg et al., 2013; Westover et al., 2016; Malinin and Platonov, 2017 |
| | ETAR | Nucleoside analogs | RdRp | HTNV, ANDV/ Vero E6 cells/suckling mice (HTNV) | HCPS and HFRS | Chung et al., 2008 |
| | K31, K34 and 103772 | Small molecules | Viral RNA-NP interaction | SNV, ANDV/ Vero E6 cells | HCPS | Salim et al., 2016 |
| | Arbidol | Small molecules | Unclear | HTNV/Vero E6 cells/suckling mice | HFRS | Deng et al., 2009 |
| | siRNA | Small interfering RNA | S, M, and L segments | ANDV/Vero E6 cells | HCPS | Chiang et al., 2014 |
| | siRNA and 3G1-Cκ-tP | Small interfering RNA and Abs | S, M, and L segments | HTNV/Vero E6 cells/suckling mice | HFRS | Yang et al., 2017 |
| Improving Vascular Function | Pazopanib, dasatinib, PP1, bosutinib, and Src inhibitor 1 | VEGFR2 kinase inhibitor or SFK inhibitor | Vascular function/VEGF | ANDV/HUVECs | HCPS | Gorbunova et al., 2011 |
| | Vandetanib | Tyrosine-kinase inhibitor | Vascular function/VEGF | ANDV/HUVECs/ hamsters | HCPS | Bird et al., 2016 |
| | Ang-1 and S1P | Compounds | Vascular function | HTNV, ANDV, NY-1/HUVECs | HCPS and HFRS | Gavrilovskaya et al., 2008 |
| | Icatibant | Small molecules | BK type 2 receptor | PUUV/clinical case report | HFRS | Antonen et al., 2013; Laine et al., 2015 |
| Rebuilding Immune Homeostasis | Clofilium phosphate | Compounds | Alveolar macrophages | ANDV/hamsters | HCPS | Hammerbeck et al., 2016 |
| | Corticoids or methylprednisolone | Hormone | Immunotherapy | HTNV, ANDV/clinical trials | HCPS and HFRS | Vial et al., 2013; Brocato and Hooper, 2019 |

14% (Vial et al., 2015). Considering the limited availability of convalescent plasma from HCPS survivors, goose polyclonal antibodies were acquired from ANDV DNA vaccine, and the purified IgY/IgY ΔFc from egg yolks could protect hamsters from lethal ANDV infection. Recently, two NAbs, JL16 and MIB22, were developed from the ANDV GP-specific memory B cells of convalescent HCPS patients, both of which reached in a 100% protection rate against lethal ANDV challenge (Garrido et al., 2018). Although NAbs from convalescent patient or immunized animals could obviously restrain hantaviral infection and improve disease outcome, purified human or humanized NAbs against hantaviruses with increased security and efficacy should be developed for clinical experiments. Additionally, research on broadly neutralizing antibodies against hantaviruses is still lacking.

Hantaviral attachment or absorption could also be restrained by lactoferin (LF), an iron-binding glycoprotein that was reported to have broad antibacterial, antifungal, and antiviral activities. LF-pretreated Vero E6 cells showed a reduced number of SR-11 (SEOV) foci, while its antiviral effects were obviously compromised if the LF-pretreated cell monolayer was washed before SEOV infection (Murphy et al., 2000). Further, LF could suppress viral shedding within 24 hpi, the effectiveness of which failed after 48 hpi (Murphy et al., 2001). These results indicated that LF might adhere to cell surface and inhibit SEOV adsorption to host cells. Intriguingly, although LF could not inhibit the expression of NP and Gc, once hantaviral amplification was established in cells, LF contributed to higher survival rates, which might be due to LF-enhanced cytocidal function of natural killer (NK) cells (Murphy et al., 2001). Even so, the specific mechanisms of how LF inhibits SEOV absorption and influences host immune responses, as well as the effects of LF on other species of hantaviruses, remain obscure.

Hantaviral fusion with cell membrane facilitates its entry process. The Hantavirus Gc envelope glycoprotein acts as a viral fusion protein that is essential for viral entry. It has been demonstrated that Gc shares similar features with class II fusion proteins, which means that three domains of viral fusion proteins are connected by a stem region anchoring in the viral envelope (Cifuentes-Munoz et al., 2011). Exogenous protein fragments containing fusion protein domain III (DIII) and the stem region could bind to the core of the fusion protein and interfere with its conformation transition, inhibiting the membrane fusion process. Based on this effect, soluble recombinant peptides that mimic DIII and the stem region were prepared, and were proven to block both ANDV and PUUV infection in Vero E6 cells by blocking membrane fusion (Barriga et al., 2016). The strategy using viral Gc DIII and stem fragments to suppress fusion might be feasible for other hantaviruses, while the protective effects *in vivo* still need further studies to confirm.

Furthermore, antivirals targeting hantaviral receptors have been synthesized. It has been demonstrated that pathogenic hantaviruses attach to the cell surface via host-specific $\alpha_{IIb}\beta_3$ or$\alpha_v\beta_3$integrins while non-pathogenic hantaviruses initiate cellular entry relying on $\alpha_v\beta_1$ integrins (Jiang et al., 2016). Based on the structure of cyclic peptides known to bind the $\alpha_v\beta_3$ receptor, a few of cyclic peptides or small molecules were designed and screened for their antihantaviral function. The cyclic nonapeptides CLVRNLAWC and CQATTARNC could inhibit SNV and ANDV infection *in vitro* (Hall et al., 2008). After two rounds of biological screening, the peptidomimetic compounds 8012-0652, C481-1256, and G319-0078 were screened out with potency in the nanomolar range against infection of a panel of hantaviruses, including SNV, ANDV, and HTNV (Hall et al., 2010). Further studies should be performed to evaluate the safety and efficacy of these small molecules *in vivo*.

## Inhibiting Viral Replication

Viral proteins are the working molecules for viral biosynthesis, among which RdRp plays an important role in hantaviral transcription and replication and is considered a desirable drug target. The pyrazine derivative Favipiravir and the nucleoside analogs Ribavirin (RBV) and ETAR have been tested effective antihantaviral drugs that directly or indirectly affect the biological function of RdRp. Favipiravir (Avigan; T-705) was initially discovered in 2002 as an antiviral drug selectively inhibiting the RdRp of influenza virus and then reported to have a high activity against a panel of Bunyaviruses (Gowen et al., 2007; Westover et al., 2016). Favipiravir could attenuate the viral RNA replication level and decrease the progeny virus yield of SNV and ANDV *in vitro*. *In vivo* studies, including non-lethal SNV challenged and lethal ANDV challenged hamster model, demonstrated that oral administration favipiravir at the dosage of 100 mg/kg twice daily could prominently reduce viral load in hamster serum and various organs and resulted in 100% survival in the ANDV lethal infection model (Safronetz et al., 2013). Delayed favipiravir administration after the onset of viremia exerted no protective effects against ANDV infection. Notably, there is no reported clinical trial with favipiravir as an antiviral treatment in HFRS and HCPS.

RBV and ETAR are nucleoside analogs that interfere with viral replication. They can inhibit inosine monophosphate dehydrogenase and reduce the synthesis GTP *de novo*, hence affecting the function of viral RdRp. As a potent mutagen, RBV could induce RNA mutagenesis in subsequent generations of HTNV virions (Chung et al., 2013), while it is not expected that ETAR induces mutation, probably due to the lack of pseudobase pair presence (Chung et al., 2008). Additionally, RBV was reported to modulate host immune responses by suppressing interleukin-10-producing regulatory T cells (Kobayashi et al., 2012), while there is no evidence showing that ETAR could exert immunoregulatory effects (Szabo, 2017). Both *in vitro* and *in vivo* antihantaviral activity of RBV and ETAR have been confirmed by a series of studies. For HFRS therapy, RBV-treated suckling mice had a higher survival rate upon HTNV infection than the placebo control group (Huggins et al., 1986). In China, a double-blind placebo-controlled clinical trial enrolled 242 HFRS patients caused by HTNV infection. The result showed that postexposure administration of RBV could decrease mortality by sevenfold and reduce the risk of entering the oliguric phase, suggesting that RBV is effective against HTNV-induced HFRS (Huggins et al., 1991). However, a clinical trial for HFRS caused by PUUV infection in Russia showed that RBV could

not improve patient condition, especially reducing viral load, and that RBV could increase the occurrence of side effects of RBV, including rash, sinus bradycardia, hyperbilirubinemia, and reduced hemoglobin. These data suggested insufficient efficacy and safety of RBV in the treatment of HFRS caused by PUUV (Malinin and Platonov, 2017). For HCPS treatment, two studies confirmed that RBV could protect hamsters from lethally intraperitoneal or intranasal ANDV challenge without toxicity, and even abbreviated treatment regimens from 7 days to 3 days worked if therapy commenced 1 day following virus challenge (Safronetz et al., 2011; Ogg et al., 2013). Unfortunately, two clinical trials for the treatment of HCPS using RBV did not show any improvement in survival rates compared with those for patients during the same time frame or receiving placebo treatment. It is speculated that RBV treatment might be ineffective once HCPS progresses to the cardiopulmonary phase. ETAR showed an EC(50) value of 10 and 4.4 μmol/L for HTNV and ANDV in Vero E6 cells, respectively, which is much lower than its toxic dosage of 880 μmol/L (Chung et al., 2008). Moreover, ETAR administration in sucking mice with a dosage of 12.5 or 25 mg/kg at 10 days post HTNV infection could significantly increase the survival rate from 10 to 25%, an effect equal to that of RBV (Chung et al., 2008). To date, there were no studies on the antiviral activity of ETAR on other hantaviruses.

Hantaviral NP could bind to an evolutionary conserved sequence at the 5′ terminus of hantaviral genomic RNA. The interaction of NP with the viral genome could protect viral RNA from host recognition and degradation, facilitate the N-mediated viral RNA translation process, and help package the viral genome into nucleocapsids. Several compounds, namely, lead inhibitor K31, K34, and 103772, were reported to interrupt the NP-RNA interaction against SNV and ANDV infection. They could abrogate both viral RNA synthesis and translation without affecting the normal biological process of host cells, among which K31 showed antiviral activity similar to that of RBV (Salim et al., 2016). However, K31 failed to affect the replication of HIV or adenovirus, demonstrating its selectivity for hantaviruses. Arbidol, an immunomodulator developed in Russia, was also found to protect against HTNV infection both *in vivo* and *in vitro* (Deng et al., 2009).

Targeting viral RNAs is the most direct and effective way to curb hantaviral replication. Small interfering RNA (siRNA) directed against hantaviral genes could facilitate viral RNA clearance based on the RNA interfering (RNAi) mechanisms and has been tested as a potential antiviral strategy *in vitro* and *in vivo*. It has been demonstrated that siRNAs targeting the S, M, or L segment of ANDV could reduce viral replication in Vero E6 cells or human lung microvascular endothelial cells and that an S-targeted siRNA pool seemed to be more efficient in reducing viral transcription and replication than M- or L-targeted siRNA in Vero E6 cells. Importantly, these siRNAs could inhibit ANDV replication even if given after infection (Chiang et al., 2014). Although siRNAs could effectively suppress hantavirus amplification in host cells most likely through promoting viral RNA clearance, their antiviral activity might be greatly compromised considering their poor biological stability and targeting ability *in vivo*. One strategy is to combine siRNAs targeting encoding sequences of HTNV genome with recombinant antibodies (3G1-Cκ-tP) recognizing HTNV Gc, which were applied by intraperitoneal injection in an HTNV-induced encephalitis mouse model. The result indicated that through combination, siRNAs could be specifically delivered to the HTNV-infected brain cells and protect against HTNV intracranial infection (Yang et al., 2017). On all accounts, novel delivery system should be developed to ensure the stability and selectivity of siRNAs, and the efficacy and safety of these systems remained unclear for the treatment of HFRS or HCPS.

## Host-Targeting Medicines

### Improving Vascular Function

Increased capillary leakage due to hantaviral infection is the basic pathogenic feature for both HFRS and HCPS. Therefore, treatment strategies improving microvascular endothelial cell function seem to be feasible in mitigating disease severity and reducing mortality (Alkharsah, 2018). Hantavirus-disturbed vascular function is a multifactorial event whose complicated mechanisms still need to be elucidated, and two kinds of hypothesis have been developed. The vascular endothelial growth factor (VEGF) theory was first proposed and studied in depth. VEGF binding to VEGF receptor 2 (VEGFR2) could activate SFK (Src family kinases) signaling, which may result in dissociation, internalization, and degradation of VE-cadherin. Altered expression and localization of VE-cadherin contributed to impaired barrier structure of adherent junctions, which could lead to incremental cellular permeability (Jiang et al., 2016). It has been demonstrated HTNV or ANDV infection could disrupt the interaction of β3 integrin with VEGFR2 and induce VEGFR2 hyper phosphorylation, which may enhance the permeability of infected endothelial cells by sensitizing them to VEGF (Gavrilovskaya et al., 2012; Wang et al., 2012). As increased VEGF content has been noted in the plasma of HFRS and HCPS patients and is closely related to disease severity in the acute phase (Bird et al., 2016; Pal et al., 2018), it is feasible to repurpose those FDA-approved drugs targeting vasoactive mediators for use as hantaviral infection therapy. In line with this strategy, one study reported that the VEGFR2 kinase inhibitor, as well as SFK inhibitors, could obviously stabilize ANDV-induced endovascular permeability, among which the SFK inhibitors dasatinib and pazopanib blocked VE-cadherin dissociation by more 90% (Gorbunova et al., 2011). Another study also indicated that application of vandetanib, a tyrosine-kinase inhibitor preventing VEGFR2 phosphorylation, before ANDV infection could delay animal lethality and increase total survival by 23% in ANDV-challenged hamsters (Bird et al., 2016). In contrast, similar small molecules administered after the onset of viremia failed to protect hamsters from lethal ANDV challenge (Brocato and Hooper, 2019). Moreover, some other small molecules, such as angiopoietin 1 (Ang-1) and sphingosine 1-phosphate (S1P), were found to inhibit hantavirus-directed endothelial cell permeability *in vitro* (Gavrilovskaya et al., 2008), while further research *in vivo* should be performed to confirm their efficacy.

Another promising theory is increased activation of the kinin–kallikrein system (KKS) during hantavirus infection. One study using a model with co-cultured endothelial and vascular smooth muscle cells demonstrated that activation of KKS and subsequent liberation of bradykinin (BK), but not VEGF, were mainly responsible for the dramatic increase in endothelial cell permeability after hantavirus infection (Taylor et al., 2013). BK, a nonapeptide that binds BK type 2 receptor, could induce blood vessel dilatation and vascular permeability increase, resulting in collapsed blood pressure. Icatibant is a peptidomimetic drug that can block the interaction of BK with the BK type 2 receptor by binding to this receptor itself. One case reported that a 37-year-old male who once underwent splenectomy due to congenital spherocytosis manifested with severe capillary leakage syndrome caused by PUUV infection. With a single dose of icatibant, the condition of the patient stabilized, followed by gradual improvement and full recovery (Antonen et al., 2013). Another case report also confirmed the efficient treatment of icatibant in a 67-year-old female HFRS patient (Laine et al., 2015). These clinical data indicated that BK receptor antagonist might be a novel treatment strategy for hantavirus diseases. Nevertheless, it should also be noted that the foresaid two patients had spleen abnormalities, which might be related to the curative effect of icatibant. Clinical trials enrolling a large number of HFRS or HCPS patients should be performed to further identify the remedy effects of bradykinin receptor antagonists.

### Rebuilding Immune Homeostasis

It is wildly accepted that HFRS and HCPS are caused by uncontrolled systemic inflammatory responses, in which multiple inflammatory cytokines, especially TNF-α, IL-8, and RANTES, contributed to disease progression (Manigold and Vial, 2014; Schonrich and Raftery, 2017); however, immunoregulation treatment in HFRS or HCPS is undesirable. A recent study with depletion of alveolar macrophages, which are considered the main resource for proinflammatory responses, could not prevent ANDV-caused pathogenesis in hamsters (Hammerbeck et al., 2016). The immunomodulatory treatment of corticoids was firstly performed during the Korean war, but the case fatality rate was not improved (Sayer et al., 1955). In Chile, a retrospective analysis suggested that a high dose of methylprednisolone could reduce mortality in 22 HCPS patients (Brocato and Hooper, 2019). However, a double-blind clinical trial in Chile failed to observe a significantly improved outcome between methylprednisolone recipients and placebo recipients for HCPS. Similarly, another randomized prospective study did not show any benefit from corticosteroid treatment in HFRS patients (Qian et al., 1990).

## Supportive Care

The initiation of careful observation and prompt but judicious supportive treatment is crucial to improve patient survival condition for both HFRS and HCPS (Sargianou et al., 2012). It has been demonstrated that admission to the ICU and supportive treatment could greatly reduce the mortality rate of HFRS (Huggins et al., 1991). In general, the treatment principle for HFRS patients is using intravenous hydration and electrolyte therapy to maintain physiological blood pressure. Platelet transfusions can be applied to reduce the mortality in patients with severe thrombocytopenia. Intermittent hemodialysis (IHD) is the first choice to improve uremia condition and rectify kidney dysfunction in patients with acute kidney injury. Continuous renal replacement therapy (CRRT) should be applied for those critical HFRS patients, especially when they have a complication, such as multi-organ injury pulmonary edema, or cerebropathy (Jiang et al., 2016). Treatment of patients with HCPS should also be performed in the ICU with continuous cardiac monitoring and respiratory support. The palliative treatments for HCPS usually include mechanical ventilation, extracorporeal membrane oxygenation, and hemofiltration (Sargianou et al., 2012).

# DISCUSSION

HFRS and HCPS caused by hantavirus infection are reemerging infectious diseases that greatly threaten global public health. At present, there are currently no US FDA-approved treatments or vaccines available; only the whole virus-inactivated vaccine against HTNV or SEOV is available in China and Korea. With the implementation of intervention measures, the incidence of hantavirus infections seems to have shown a decline in recent years. In China and Korea, the number of HFRS cases has been drastically reduced. But the vaccines elicit suboptimal immune responses, confer inadequate protection, and may cause safety concerns. In 2017, the recurrence of global outbreak of HFRS has drawn renewed attention to this old disease, which seriously threatens human health. HFRS in China was still a natural focal disease with relatively high morbidity and fatality, and its distribution and epidemic trends had also changed. Surveillance measures, together with prevention and control strategies, should be improved and strengthened to reduce HFRS infection in China. Therefore, the best solution is to develop a functional vaccine to prevent hantavirus infection. Among the three types of vaccines discussed above, only DNA vaccine candidates have progressed to clinical trials. Subunit protein vaccines not only are safe and easy to produce but also do not easily cause interference between the components of a multivalent formulation (Sun et al., 2017; Liang et al., 2018; Qu et al., 2018). To resolve the above problems, we propose to construct a universal genetic engineering novel subunit protein vaccine against HTNV and SEOV by combining bioinformatics methods, viral surface protein structure biology knowledge, and molecular biology tools.

Antiviral treatment only works when applied during the early infection stage, possibly because uncontrolled immune responses occur and predominate the pathogenesis process post-acute infection. Immunomodulatory therapy hardly improves the patient survival rate, possibly because suppressed inflammatory responses inhibit prompt viral clearance and enhance virus-caused injury increase. Therefore, based on rapid supportive care, effectively combining antiviral treatment and immunomodulatory therapy is a potential strategy for HFRS and HPS. 3G1 and 3D8, the mice MAbs against HTNV developed

by our team, have been used for HFRS treatment and the result indicated that application of 3G1 and 3D8 at early stage of disease could significantly improve the patient condition and increase survival rates, especially for those severe or critical HFRS patients (data unpublished). Hence, NAbs might be the most promising treatment for HFRS or HPS, and the effective humanized neutralizing antibodies should be further developed.

Moreover, it is universally acknowledged that type I IFN responses are essential for hosts to defend against hantaviral infection. Multiple IFN stimulated genes (ISG) were confirmed to have antihantaviral activity. The interferon-induced MxA protein, a GTPase with extensive antiviral activity, notably against influenza viruses, was reported to inhibit HTNV and PUUV replication in Vero cells (Frese et al., 1996). The interferon-induced IFITM3 protein was able to inhibit HTNV infection in both HUVEC and A549 cells by inhibiting virus entry (Xu-Yang et al., 2016). Several studies have shown that pretreatment with type I IFN could effectively inhibit hantaviral infection. Pretreating endothelial cells (ECs) with IFNα blocks hantavirus replication, and this inhibitory effect is still observed when IFNα is added to ECs within 12 hpi; however, the addition of IFNα 15–24 h after infection had little effect on hantavirus replication. Clinical data indicated that IFN treatment is only effective prophylactically or shortly after hantavirus infection. In fact, during the natural infection process, compared with non-pathogenic hantaviruses, pathogenic hantaviruses could inhibit host IFN production at an early infection stage, but the specific mechanism remains ambiguous. Our team recently found that HTNV could induce complete autophagy at an early phase, which promotes host MAVS degradation and disturbs RIG-I-MAVS signaling-mediated IFN production. The application of autophagy inhibitors, including 3-MA and CQ, could significantly enhance type I IFN responses and inhibit HTNV replication both *in vitro* and *in vivo*. We also demonstrated that lncRNA NEAT1 could positively regulate RIG-I-DDX60-mediated IFN responses during HTNV infection and that overexpression of NEAT1 could restrain HTNV amplification both *in vitro* and *in vivo*. These results suggest that enhancing host IFN responses during the early infection phase may be a novel therapeutic strategy for HFRS and HCPS, while there is still much work to be done to translate basic medicine research to clinical practice.

## AUTHOR CONTRIBUTIONS

RL and HM wrote the manuscript. JS, MH, and ZL provided published evidence. QZ made the phylogenetic tree. XJ, FZ, and XW edited, reviewed, and approved its final version.

## FUNDING

This work was supported by grants from the National Science Foundation (Nos. 81772167, 81971563, 81602494, and 81671994) and the Key Research and Development Project of Shaanxi Province (No. 2019ZDLSF02-03).

## SUPPLEMENTARY MATERIAL

The Supplementary Material for this article can be found online at: https://www.frontiersin.org/articles/10.3389/fmicb.2019.02989/full#supplementary-material

## REFERENCES

Abudurexiti, A., Adkins, S., Alioto, D., Alkhovsky, S. V., Avsic-Zupanc, T., Ballinger, M. J., et al. (2019). Taxonomy of the order Bunyavirales: update 2019. *Arch. Virol.* 164, 1949–1965. doi: 10.1007/s00705-019-04253-6

Alkharsah, K. R. (2018). VEGF upregulation in viral infections and its possible therapeutic implications. *Int. J. Mol. Sci.* 19:E1642. doi: 10.3390/ijms19061642

Antonen, J., Leppanen, I., Tenhunen, J., Arvola, P., Makela, S., Vaheri, A., et al. (2013). A severe case of *Puumala hantavirus* infection successfully treated with bradykinin receptor antagonist icatibant. *Scand. J. Infect. Dis.* 45, 494–496. doi: 10.3109/00365548.2012.755268

Antoniukas, L., Grammel, H., and Reichl, U. (2006). Production of hantavirus *Puumala nucleocapsid* protein in *Saccharomyces cerevisiae* for vaccine and diagnostics. *J. Biotechnol.* 124, 347–362. doi: 10.1016/j.jbiotec.2005.12.028

Barriga, G. P., Villalon-Letelier, F., Marquez, C. L., Bignon, E. A., Acuna, R., Ross, B. H., et al. (2016). Inhibition of the hantavirus fusion process by predicted domain III and stem peptides from glycoprotein Gc. *PLoS Negl. Trop. Dis.* 10:e0004799. doi: 10.1371/journal.pntd.0004799

Bayard, V., Kitsutani, P. T., Barria, E. O., Ruedas, L. A., Tinnin, D. S., Muñoz, C., et al. (2004). Outbreak of hantavirus pulmonary syndrome, Los Santos, Panama, 1999–2000. *Emerg. Infect. Dis.* 10, 1635–1642. doi: 10.3201/eid1009.040143

Bergstedt Oscarsson, K., Brorstad, A., Baudin, M., Lindberg, A., Forssen, A., Evander, M., et al. (2016). Human *Puumala hantavirus* infection in northern Sweden; increased seroprevalence and association to risk and health factors. *BMC Infect. Dis.* 16:566. doi: 10.1186/s12879-016-1879-2

Bird, B. H., Shrivastava-Ranjan, P., Dodd, K. A., Erickson, B. R., and Spiropoulou, C. F. (2016). Effect of Vandetanib on *Andes virus* survival in the hamster model of Hantavirus pulmonary syndrome. *Antiviral Res.* 132, 66–69. doi: 10.1016/j.antiviral.2016.05.014

Brocato, R. L., and Hooper, J. W. (2019). Progress on the prevention and treatment of hantavirus disease. *Viruses* 11:E610. doi: 10.3390/v11070610

Brocato, R., Josleyn, M., Ballantyne, J., Vial, P., and Hooper, J. W. (2012). DNA vaccine-generated duck polyclonal antibodies as a postexposure prophylactic to prevent hantavirus pulmonary syndrome (HPS). *PLoS one* 7:e35996. doi: 10.1371/journal.pone.0035996

Brocato, R. L., Josleyn, M. J., Wahl-Jensen, V., Schmaljohn, C. S., and Hooper, J. W. (2013). Construction and nonclinical testing of a puumala virus synthetic M gene-based DNA vaccine.*Clin.Vaccine Immunol.* 20, 218–226. doi: 10.1128/CVI.00546-12

Bucht, G., Sjolander, K. B., Eriksson, S., Lindgren, L., Lundkvist, A., and Elgh, F. (2001). Modifying the cellular transport of DNA-based vaccines alters the immune response to hantavirus nucleocapsid protein. *Vaccine* 19, 3820–3829. doi: 10.1016/s0264-410x(01)00151-7

Cheng, L. F., Wang, F., Zhang, L., Yu, L., Ye, W., Liu, Z. Y., et al. (2016). Incorporation of GM-CSF or CD40L enhances the immunogenicity of *Hantaan virus*-like particles. *Front. Cell Infect. Microbiol.* 6:185. doi: 10.3389/fcimb.2016.00185

Chiang, C. F., Albarino, C. G., Lo, M. K., and Spiropoulou, C. F. (2014). Small interfering RNA inhibition of *Andes virus* replication. *PLoS One* 9:e99764. doi: 10.1371/journal.pone.0099764

Cho, H. W., Howard, C. R., and Lee, H. W. (2002). Review of an inactivated vaccine against hantaviruses. *Intervirology* 45, 328–333. doi: 10.1159/000067925

Chung, D. H., Kumarapperuma, S. C., Sun, Y., Li, Q., Chu, Y. K., Arterburn, J. B., et al. (2008). Synthesis of 1-beta-D-ribofuranosyl-3-ethynyl-[1,2,4]triazole and its *in vitro* and *in vivo* efficacy against hantavirus. *Antiviral Res.* 79, 19–27. doi: 10.1016/j.antiviral.2008.02.003

Chung, D. H., Vastermark, A., Camp, J. V., Mcallister, R., Remold, S. K., Chu, Y. K., et al. (2013). The murine model for *Hantaan virus*-induced lethal disease shows two distinct paths in viral evolutionary trajectory with and without ribavirin treatment. *J. Virol.* 87, 10997–11007. doi: 10.1128/JVI.01394-13

Cifuentes-Munoz, N., Barriga, G. P., Valenzuela, P. D., and Tischler, N. D. (2011). Aromatic and polar residues spanning the candidate fusion peptide of the *Andes virus* Gc protein are essential for membrane fusion and infection. *J. Gen. Virol.* 92, 552–563. doi: 10.1099/vir.0.027235-0

Custer, D. M., Thompson, E., Schmaljohn, C. S., Ksiazek, T. G., and Hooper, J. W. (2003). Active and passive vaccination against hantavirus pulmonary syndrome with *Andes virus* M genome segment-based DNA vaccine. *J. Virol.* 77, 9894–9905. doi: 10.1128/jvi.77.18.9894-9905.2003

de Carvalho Nicacio, C., Gonzalez Della Valle, M., Padula, P., Björling, E., Plyusnin, A., and Lundkvist, Å (2002). Cross-protection against challenge with *Puumala virus* after immunization with nucleocapsid proteins from different hantaviruses. *J. Virol.* 76, 6669–6677. doi: 10.1128/jvi.76.13.6669-6677.2002

de Carvalho Nicacio, C., Lundkvist, A., Sjolander, K. B., Plyusnin, A., Salonen, E. M., and Bjorling, E. (2000). A neutralizing recombinant human antibody Fab fragment against *Puumala hantavirus*. *J. Med. Virol.* 60, 446–454. doi: 10.1002/(sici)1096-9071(200004)60:4<446::aid-jmv13>3.0.co;2-v

Deng, H. Y., Luo, F., Shi, L. Q., Zhong, Q., Liu, Y. J., and Yang, Z. Q. (2009). Efficacy of arbidol on lethal *hantaan virus* infections in suckling mice and *in vitro*. *Acta Pharmacol. Sin.* 30, 1015–1024. doi: 10.1038/aps.2009.53

Dong, Y., Ma, T., Zhang, X., Ying, Q., Han, M., Zhang, M., et al. (2019). Incorporation of CD40 ligand or granulocyte-macrophage colony stimulating factor into *Hantaan virus* (HTNV) virus-like particles significantly enhances the long-term immunity potency against HTNV infection. *J. Med. Microbiol.* 68, 480–492. doi: 10.1099/jmm.0.000897

Duggan, J. M. (2019). Prevalence of *Seoul hantavirus* in UK wild rats: an emerging public health problem? *Vet. Rec.* 184, 523–524. doi: 10.1136/vr.l1163

Echterdiek, F., Kitterer, D., Alscher, M. D., Schwenger, V., Ruckenbrod, B., Bald, M., et al. (2019). Clinical course of hantavirus-induced nephropathia epidemica in children compared to adults in Germany—analysis of 317 patients. *Pediatr. Nephrol.* 34, 1247–1252. doi: 10.1007/s00467-019-04215-9

Ettinger, J., Hofmann, J., Enders, M., Tewald, F., Oehme, R. M., Rosenfeld, U. M., et al. (2012). Multiple synchronous outbreaks of *Puumala virus*, Germany, 2010. *Emerg. Infect. Dis.* 18, 1461–1464. doi: 10.3201/eid1809.111447

Frese, M., Kochs, G., Feldmann, H., Hertkorn, C., and Haller, O. (1996). Inhibition of bunyaviruses, phleboviruses, and hantaviruses by human MxA protein. *J. Virol.* 70, 915–923. doi: 10.1128/jvi.70.2.915-923.1996

Garrido, J. L., Prescott, J., Calvo, M., Bravo, F., Alvarez, R., Salas, A., et al. (2018). Two recombinant human monoclonal antibodies that protect against lethal *Andes hantavirus* infection *in vivo*. *Sci. Transl. Med.* 10:eaat6420. doi: 10.1126/scitranslmed.aat6420

Gavrilovskaya, I. N., Gorbunova, E. E., and Mackow, E. R. (2012). *Andes virus* infection of lymphatic endothelial cells causes giant cell and enhanced permeability responses that are rapamycin and vascular endothelial growth factor C sensitive. *J. Virol.* 86, 8765–8772. doi: 10.1128/JVI.00817-12

Gavrilovskaya, I. N., Gorbunova, E. E., Mackow, N. A., and Mackow, E. R. (2008). Hantaviruses direct endothelial cell permeability by sensitizing cells to the vascular permeability factor VEGF, while angiopoietin 1 and sphingosine 1-phosphate inhibit hantavirus-directed permeability. *J. Virol.* 82, 5797–5806. doi: 10.1128/JVI.02397-07

Geldmacher, A., Schmaler, M., Kruger, D. H., and Ulrich, R. (2004). Yeast-expressed hantavirus Dobrava nucleocapsid protein induces a strong, long-lasting, and highly cross-reactive immune response in mice. *Viral. Immunol.* 17, 115–122. doi: 10.1089/088282404322875511

Gorbunova, E. E., Gavrilovskaya, I. N., Pepini, T., and Mackow, E. R. (2011). VEGFR2 and Src kinase inhibitors suppress *Andes virus*-induced endothelial cell permeability. *J. Virol.* 85, 2296–2303. doi: 10.1128/JVI.02319-10

Gowen, B. B., Wong, M. H., Jung, K. H., Sanders, A. B., Mendenhall, M., Bailey, K. W., et al. (2007). In vitro and in vivo activities of T-705 against arenavirus and bunyavirus infections. *Antimicrob. Agents Chemother.* 51, 3168–3176. doi: 10.1128/aac.00356-07

Graham, B. S., Gilman, M. S. A., and Mclellan, J. S. (2019). Structure-based vaccine antigen design. *Annu. Rev. Med.* 70, 91–104. doi: 10.1146/annurev-med-121217-094234

Gut, A. K., Gut, R., Rymarz, A., and Wozniak-Kosek, A. (2018). Hemorrhagic fever with renal syndrome (HFRS) in Poland. *Przegl. Epidemiol.* 72, 477–485. doi: 10.32394/pe.72.4.23

Haese, N., Brocato, R. L., Henderson, T., Nilles, M. L., Kwilas, S. A., Josleyn, M. D., et al. (2015). Antiviral biologic produced in DNA vaccine/goose platform protects hamsters against hantavirus pulmonary syndrome when administered post-exposure. *PLoS Negl. Trop. Dis.* 9:e0003803. doi: 10.1371/journal.pntd.0003803

Hall, P. R., Hjelle, B., Brown, D. C., Ye, C., Bondu-Hawkins, V., Kilpatrick, K. A., et al. (2008). Multivalent presentation of antihantavirus peptides on nanoparticles enhances infection blockade. *Antimicrob. Agents Chemother.* 52, 2079–2088. doi: 10.1128/AAC.01415-07

Hall, P. R., Leitao, A., Ye, C., Kilpatrick, K., Hjelle, B., Oprea, T. I., et al. (2010). Small molecule inhibitors of hantavirus infection. *Bioorg. Med. Chem. Lett.* 20, 7085–7091. doi: 10.1016/j.bmcl.2010.09.092

Hammerbeck, C. D., Brocato, R. L., Bell, T. M., Schellhase, C. W., Mraz, S. R., Queen, L. A., et al. (2016). Depletion of alveolar macrophages does not prevent hantavirus disease pathogenesis in golden syrian hamsters. *J. Virol.* 90, 6200–6215. doi: 10.1128/jvi.00304-16

Hooper, J. W., Custer, D. M., Smith, J., and Wahl-Jensen, V. (2006). Hantaan/*Andes virus* DNA vaccine elicits a broadly cross-reactive neutralizing antibody response in nonhuman primates. *Virology* 347, 208–216. doi: 10.1016/j.virol.2005.11.035

Hooper, J. W., Custer, D. M., Thompson, E., and Schmaljohn, C. S. (2001). DNA vaccination with the *Hantaan virus* M gene protects Hamsters against three of four HFRS hantaviruses and elicits a high-titer neutralizing antibody response in Rhesus monkeys. *J. Virol.* 75, 8469–8477. doi: 10.1128/jvi.75.18.8469-8477.2001

Hooper, J. W., Ferro, A. M., and Wahl-Jensen, V. (2008). Immune serum produced by DNA vaccination protects hamsters against lethal respiratory challenge with *Andes virus*. *J. Virol.* 82, 1332–1338. doi: 10.1128/jvi.01822-07

Hooper, J. W., Josleyn, M., Ballantyne, J., and Brocato, R. (2013). A novel Sin Nombre virus DNA vaccine and its inclusion in a candidate pan-hantavirus vaccine against hantavirus pulmonary syndrome (HPS) and hemorrhagic fever with renal syndrome (HFRS). *Vaccine* 31, 4314–4321. doi: 10.1016/j.vaccine.2013.07.025

Hooper, J. W., Kamrud, K. I., Elgh, F., Custer, D., and Schmaljohn, C. S. (1999). DNA vaccination with hantavirus M segment elicits neutralizing antibodies and protects against *Seoul virus* infection. *Virology* 255, 269–278. doi: 10.1006/viro.1998.9586

Hooper, J. W., Moon, J. E., Paolino, K. M., Newcomer, R., Mclain, D. E., Josleyn, M., et al. (2014). A Phase 1 clinical trial of *Hantaan virus* and *Puumala virus* M-segment DNA vaccines for haemorrhagic fever with renal syndrome delivered by intramuscular electroporation. *Clin. Microbiol. Infect.* 20(Suppl. 5), 110–117. doi: 10.1111/1469-0691.12553

Huggins, J. W., Hsiang, C. M., Cosgriff, T. M., Guang, M. Y., Smith, J. I., Wu, Z. O., et al. (1991). Prospective, double-blind, concurrent, placebo-controlled clinical trial of intravenous ribavirin therapy of hemorrhagic fever with renal syndrome. *J. Infect. Dis.* 164, 1119–1127. doi: 10.1093/infdis/164.6.1119

Huggins, J. W., Kim, G. R., Brand, O. M., and Mckee, K. T. Jr. (1986). Ribavirin therapy for *Hantaan virus* infection in suckling mice. *J. Infect. Dis.* 153, 489–497. doi: 10.1093/infdis/153.3.489

Jiang, H., Du, H., Wang, L. M., Wang, P. Z., and Bai, X. F. (2016). Hemorrhagic fever with renal syndrome: pathogenesis and clinical picture. *Front. Cell Infect. Microbiol.* 6:1. doi: 10.3389/fcimb.2016.00001

Jiang, D., Sun, Y., Cheng, L., Zhang, G., Dong, C., and Jin, B. (2015). Construction and evaluation of DNA vaccine encoding Hantavirus glycoprotein N-terminal fused with lysosome-associated membrane protein. *Vaccine* 33, 3367–3376.doi: 10.1016/j.vaccine.2015.05.007

Jiang, F., Wang, L., Wang, S., Zhu, L., Dong, L., Zhang, Z., et al. (2017). Meteorological factors affect the epidemiology of hemorrhagic fever with renal syndrome via altering the breeding and hantavirus-carrying states of rodents and mites: a 9 years' longitudinal study. *Emerg. Microbes Infect.* 6:e104. doi: 10.1038/emi.2017.92

Johansson, P., Olsson, M., Lindgren, L., Ahlm, C., Elgh, F., Holmstrom, A., et al. (2004). Complete gene sequence of a human *Puumala hantavirus* isolate, *Puumala Umea*/hu: sequence comparison and characterisation of encoded gene products. *Virus Res.* 105, 147–155. doi: 10.1016/j.virusres.2004.05.005

Jung, J., Ko, S. J., Oh, H. S., Moon, S. M., Song, J. W., and Huh, K. (2018). Protective effectiveness of inactivated hantavirus vaccine against hemorrhagic fever with renal syndrome. *J. Infect. Dis.* 217, 1417–1420. doi: 10.1093/infdis/jiy037

Kerins, J. L., Koske, S. E., Kazmierczak, J., Austin, C., Gowdy, K., and Dibernardo, A. (2018). Outbreak of *Seoul virus* among rats and rat owners — United States and Canada, 2017. *Can. Commun. Dis. Rep.* 44, 71–74. doi: 10.14745/ccdr.v44i02a07

Kobayashi, T., Nakatsuka, K., Shimizu, M., Tamura, H., Shinya, E., Atsukawa, M., et al. (2012). Ribavirin modulates the conversion of human CD4(+) CD25(−) T cell to CD4(+) CD25(+) FOXP3(+) T cell via suppressing interleukin-10-producing regulatory T cell. *Immunology* 137, 259–270. doi: 10.1111/imm.12005

Kruger, D. H., Ulrich, R. G., and Hofmann, J. (2013). Hantaviruses as zoonotic pathogens in Germany. *Dtsch. Arztebl. Int.* 110, 461–467. doi: 10.3238/arztebl.2013.0461

Kwilas, S., Kishimori, J. M., Josleyn, M., Jerke, K., Ballantyne, J., Royals, M., et al. (2014). A hantavirus pulmonary syndrome (HPS) DNA vaccine delivered using a spring-powered jet injector elicits a potent neutralizing antibody response in rabbits and nonhuman primates. *Curr. Gene Ther.* 14, 200–210. doi: 10.2174/1566523214666140522122633

Laine, O., Leppanen, I., Koskela, S., Antonen, J., Makela, S., Sinisalo, M., et al. (2015). Severe *Puumala virus* infection in a patient with a lymphoproliferative disease treated with icatibant. *Infect. Dis.* 47, 107–111. doi: 10.3109/00365548.2014.969304

Li, S., Rissanen, I., Zeltina, A., Hepojoki, J., Raghwani, J., Harlos, K., et al. (2016). A molecular-level account of the antigenic hantaviral surface. *Cell Rep.* 15, 959–967. doi: 10.1016/j.celrep.2016.03.082

Li, Z., Zeng, H., Wang, Y., Zhang, Y., Cheng, L., Zhang, F., et al. (2017). The assessment of *Hantaan virus*-specific antibody responses after the immunization program for hemorrhagic fever with renal syndrome in northwest China. *Hum. Vaccin. Immunother.* 13, 802–807. doi: 10.1080/21645515.2016.1253645

Liang, H., Yang, R., Liu, Z., Li, M., Liu, H., and Jin, X. (2018). Recombinant *Zika virus* envelope protein elicited protective immunity against *Zika virus* in immunocompetent mice. *PLoS One* 13:e0194860. doi: 10.1371/journal.pone.0194860

Limongi, J. E., Da Costa, F. C., Pinto, R. M., De Oliveira, R. C., Bragagnolo, C., Lemos, E. R., et al. (2009). Cross-sectional survey of hantavirus infection, Brazil. *Emerg. Infect. Dis.* 15, 1981–1983. doi: 10.3201/eid1512.090229

Mackow, E. R., Dalrymple, N. A., Cimica, V., Matthys, V., Gorbunova, E., and Gavrilovskaya, I. (2014). Hantavirus interferon regulation and virulence determinants. *Virus Res.* 187, 65–71. doi: 10.1016/j.virusres.2013.12.041

Maes, P., Clement, J., Cauwe, B., Bonnet, V., Keyaerts, E., Robert, A., et al. (2008). Truncated recombinant puumala virus nucleocapsid proteins protect mice against challenge *in vivo*. *Viral Immunol.* 21, 49–60. doi: 10.1089/vim.2007.0059

Malinin, O. V., and Platonov, A. E. (2017). Insufficient efficacy and safety of intravenous ribavirin in treatment of haemorrhagic fever with renal syndrome caused by *Puumala virus*. *Infect. Dis.* 49, 514–520. doi: 10.1080/23744235.2017.1293841

Manigold, T., and Vial, P. (2014). Human hantavirus infections: epidemiology, clinical features, pathogenesis and immunology. *Swiss Med. Wkly.* 144:w13937.

Mertz, G. J., Miedzinski, L., Goade, D., Pavia, A. T., Hjelle, B., Hansbarger, C. O., et al. (2004). Placebo-controlled, double-blind trial of intravenous ribavirin for the treatment of hantavirus cardiopulmonary syndrome in North America. *Clin. Infect. Dis.* 39, 1307–1313. doi: 10.1086/425007

Murphy, M. E., Kariwa, H., Mizutani, T., Tanabe, H., Yoshimatsu, K., Arikawa, J., et al. (2001). Characterization of in vitro and in vivo antiviral activity of lactoferrin and ribavirin upon hantavirus. *J. Vet. Med. Sci.* 63, 637–645. doi: 10.1292/jvms.63.637

Murphy, M. E., Kariwa, H., Mizutani, T., Yoshimatsu, K., Arikawa, J., and Takashima, I. (2000). In vitro antiviral activity of lactoferrin and ribavirin upon hantavirus. *Arch. Virol.* 145, 1571–1582. doi: 10.1007/s007050070077

Ogg, M., Jonsson, C. B., Camp, J. V., and Hooper, J. W. (2013). Ribavirin protects Syrian hamsters against lethal hantavirus pulmonary syndrome–after intranasal exposure to *Andes virus*. *Viruses* 5, 2704–2720. doi: 10.3390/v5112704

Padula, P., Martinez, V. P., Bellomo, C., Maidana, S., San Juan, J., Tagliaferri, P., et al. (2007). Pathogenic hantaviruses, northeastern Argentina and eastern Paraguay. *Emerg. Infect. Dis.* 13, 1211–1214. doi: 10.3201/eid1308.061090

Pal, E., Korva, M., Resman Rus, K., Kejzar, N., Bogovic, P., Strle, F., et al. (2018). Relationship between circulating vascular endothelial growth factor and its soluble receptor in patients with hemorrhagic fever with renal syndrome. *Emerg. Microbes Infect.* 7:89. doi: 10.1038/s41426-018-0090-5

Pini, N., Levis, S., Calderón, G., Ramirez, J., Bravo, D., Lozano, E., et al. (2003). Hantavirus infection in humans and rodents, Northwestern Argentina. *Emerg. Infect. Dis.* 9, 1070–1076. doi: 10.3201/eid0909.020768

Prince, H. E., and Lieberman, J. M. (2013). Impact of the Yosemite hantavirus outbreak on hantavirus antibody testing at a national reference laboratory. *Clin. Vaccine Immunol.* 20, 1213–1216. doi: 10.1128/CVI.00326-13

Qian, D. Y., Ding, Y. S., Chen, G. F., Ding, J. J., Chen, Y. X., Lu, T. F., et al. (1990). A placebo-controlled clinical trial of prednisone in the treatment of early hemorrhagic fever. *J. Infect. Dis.* 162, 1213–1214. doi: 10.1093/infdis/162.5.1213

Qu, P., Zhang, W., Li, D., Zhang, C., Liu, Q., Zhang, X., et al. (2018). Insect cell-produced recombinant protein subunit vaccines protect against *Zika virus* infection. *Antivir. Res.* 154, 97–103. doi: 10.1016/j.antiviral.2018.04.010

Razanskiene, A., Schmidt, J., Geldmacher, A., Ritzi, A., Niedrig, M., Lundkvist, Å, et al. (2004). High yields of stable and highly pure nucleocapsid proteins of different hantaviruses can be generated in the yeast *Saccharomyces cerevisiae*. *J. Biotechnol.* 111, 319–333. doi: 10.1016/j.jbiotec.2004.04.010

Rissanen, I., Stass, R., Zeltina, A., Li, S., Hepojoki, J., Harlos, K., et al. (2017). Structural transitions of the conserved and metastable hantaviral glycoprotein envelope. *J. Virol.* 91:e378-17. doi: 10.1128/JVI.00378-17

Safronetz, D., Falzarano, D., Scott, D. P., Furuta, Y., Feldmann, H., and Gowen, B. B. (2013). Antiviral efficacy of favipiravir against two prominent etiological agents of hantavirus pulmonary syndrome. *Antimicrob. Agents Chemother.* 57, 4673–4680. doi: 10.1128/AAC.00886-13

Safronetz, D., Haddock, E., Feldmann, F., Ebihara, H., and Feldmann, H. (2011). In vitro and in vivo activity of ribavirin against *Andes virus* infection. *PLoS One* 6:e23560. doi: 10.1371/journal.pone.0023560

Salim, N. N., Ganaie, S. S., Roy, A., Jeeva, S., and Mir, M. A. (2016). Targeting a novel RNA-protein interaction for therapeutic intervention of Hantavirus disease. *J. Biol. Chem.* 291, 24702–24714. doi: 10.1074/jbc.m116.750729

Sargianou, M., Watson, D. C., Chra, P., Papa, A., Starakis, I., Gogos, C., et al. (2012). Hantavirus infections for the clinician: from case presentation to diagnosis and treatment. *Crit. Rev. Microbiol.* 38, 317–329. doi: 10.3109/1040841X.2012.673553

Sayer, W. J., Entwhisle, G., Uyeno, B., and Bignall, R. C. (1955). Cortisone therapy of early epidemic hemorrhagic fever: a preliminary report. *Ann. Intern. Med.* 42, 839–851.

Schmaljohn, C. S. (2012). Vaccines for hantaviruses: progress and issues. *Expert Rev. Vaccines* 11, 511–513. doi: 10.1586/erv.12.15

Schmaljohn, C. S., Spik, K. W., and Hooper, J. W. (2014). DNA vaccines for HFRS: laboratory and clinical studies. *Virus Res.* 187, 91–96. doi: 10.1016/j.virusres.2013.12.020

Schmidt, J., Jandrig, B., Klempa, B., Yoshimatsu, K., Arikawa, J., Meisel, H., et al. (2005). Nucleocapsid protein of cell culture-adapted *Seoul virus* strain 80-39: analysis of its encoding sequence, expression in yeast and immuno-reactivity. *Virus Genes* 30, 37–48. doi: 10.1007/s11262-004-4580-2

Schonrich, G., and Raftery, M. J. (2017). Exploring the immunopathogenesis of viral hemorrhagic fever in mice with a humanized immune system. *Front. Immunol.* 8:1202. doi: 10.3389/fimmu.2017.01202

Song, J. Y., Woo, H. J., Cheong, H. J., Noh, J. Y., Baek, L. J., and Kim, W. J. (2016). Long-term immunogenicity and safety of inactivated *Hantaan virus* vaccine (Hantavax) in healthy adults. *Vaccine* 34, 1289–1295. doi: 10.1016/j.vaccine.2016.01.031

Spik, K. W., Badger, C., Mathiessen, I., Tjelle, T., Hooper, J. W., and Schmaljohn, C. (2008). Mixing of M segment DNA vaccines to Hantaan virus and Puumala virus reduces their immunogenicity in hamsters. *Vaccine* 26, 5177–5181.doi: 10.1016/j.vaccine.2008.03.097

Stanojevic, M., Cirkovic, V., Siljic, M., Gligic, A., and Stamenkovic, G. (2019). Molecular characterization of Dobrava-Belgrade hantavirus in Serbia, 2007-2011. *J. Infect. Public Health* 12, 645–649. doi: 10.1016/j.jiph.2019.02.021

Sun, J., Li, M., Wang, Y., Hao, P., and Jin, X. (2017). Elaboration of tetravalent antibody responses against dengue viruses using a subunit vaccine comprised

of a single consensus dengue envelope sequence. *Vaccine* 35, 6308–6320. doi: 10.1016/j.vaccine.2017.09.063

Suzuki, A., Bisordi, I., Levis, S., Garcia, J., Pereira, L. E., Souza, R. P., et al. (2004). Identifying rodent hantavirus reservoirs, Brazil. *Emerg. Infect. Dis.* 10, 2127–2134. doi: 10.3201/eid1012.040295

Szabo, R. (2017). Antiviral therapy and prevention against hantavirus infections. *Acta Virol.* 61, 3–12. doi: 10.4149/av_2017_01_3

Taylor, S. L., Wahl-Jensen, V., Copeland, A. M., Jahrling, P. B., and Schmaljohn, C. S. (2013). Endothelial cell permeability during hantavirus infection involves factor XII-dependent increased activation of the kallikrein-kinin system. *PLoS Pathog.* 9:e1003470. doi: 10.1371/journal.ppat.1003470

Terajima, M., Van Epps, H. L., Li, D., Leporati, A. M., Juhlin, S. E., Mustonen, J., et al. (2002). Generation of recombinant vaccinia viruses expressing *Puumala virus* proteins and use in isolating cytotoxic T cells specific for *Puumala virus*. *Virus Res.* 84, 67–77. doi: 10.1016/s0168-1702(01)00416-6

Tian, H., and Stenseth, N. C. (2019). The ecological dynamics of hantavirus diseases: from environmental variability to disease prevention largely based on data from China. *PLoS Negl. Trop. Dis.* 13:e0006901. doi: 10.1371/journal.pntd.0006901

Tian, H., Yu, P., Cazelles, B., Xu, L., Tan, H., Yang, J., et al. (2017). Interannual cycles of *Hantaan virus* outbreaks at the human-animal interface in Central China are controlled by temperature and rainfall. *Proc. Natl. Acad. Sci. U.S.A.* 114, 8041–8046. doi: 10.1073/pnas.1701777114

Toro, J., Vega, J. D., Khan, A. S., Mills, J. N., Padula, P., Terry, W., et al. (1998). An outbreak of hantavirus pulmonary syndrome, Chile, 1997. *Emerg. Infect. Dis.* 4, 687–694. doi: 10.3201/eid0404.980425

Vaheri, A., Henttonen, H., Voutilainen, L., Mustonen, J., Sironen, T., and Vapalahti, O. (2013). Hantavirus infections in Europe and their impact on public health. *Rev. Med. Virol.* 23, 35–49. doi: 10.1002/rmv.1722

Vial, P. A., Valdivieso, F., Calvo, M., Rioseco, M. L., Riquelme, R., Araneda, A., et al. (2015). A non-randomized multicentre trial of human immune plasma for treatment of hantavirus cardiopulmonary syndrome caused by *Andes virus*. *Antivir. Ther.* 20, 377–386. doi: 10.3851/IMP2875

Vial, P. A., Valdivieso, F., Ferres, M., Riquelme, R., Rioseco, M. L., Calvo, M., et al. (2013). High-dose intravenous methylprednisolone for hantavirus cardiopulmonary syndrome in Chile: a double-blind, randomized controlled clinical trial. *Clin. Infect. Dis.* 57, 943–951. doi: 10.1093/cid/cit394

Wang, W., Zhang, Y., Li, Y., Pan, L., Bai, L., Zhuang, Y., et al. (2012). Dysregulation of the beta3 integrin-VEGFR2 complex in *Hantaan virus*-directed hyperpermeability upon treatment with VEGF. *Arch. Virol.* 157, 1051–1061. doi: 10.1007/s00705-012-1245-7

Westover, J. B., Sefing, E. J., Bailey, K. W., Van Wettere, A. J., Jung, K. H., Dagley, A., et al. (2016). Low-dose ribavirin potentiates the antiviral activity of favipiravir against hemorrhagic fever viruses. *Antivir. Res.* 126, 62–68. doi: 10.1016/j.antiviral.2015.12.006

Xu, R., Yang, X. Y., Yang, D. F., Zou, C. Y., Gong, P. L., and Zeng, F. D. (2009). Phase I evaluation of the safety and pharmacokinetics of a single-dose intravenous injection of a murine monoclonal antibody against *Hantaan virus* in healthy volunteers. *Antimicrob. Agents Chemother.* 53, 5055–5059. doi: 10.1128/AAC.00728-09

Xu, Z., Wei, L., Wang, L., Wang, H., and Jiang, S. (2002). The *in vitro* and *in vivo* protective activity of monoclonal antibodies directed against *Hantaan virus*: potential application for immunotherapy and passive immunization. *Biochem. Biophys. Res. Commun.* 298, 552–558. doi: 10.1016/s0006-291x(02)02491-9

Xu-Yang, Z., Pei-Yu, B., Chuan-Tao, Y., Wei, Y., Hong-Wei, M., Kang, T., et al. (2016). Interferon-induced transmembrane protein 3 inhibits *Hantaan virus* infection, and its single nucleotide polymorphism rs12252 influences the severity of hemorrhagic fever with renal syndrome. *Front. Immunol.* 7:535. doi: 10.3389/fimmu.2016.00535

Yamanishi, K., Tanishita, O., Tamura, M., Asada, H., Kondo, K., Takagi, M., et al. (1988). Development of inactivated vaccine against virus causing haemorrhagic fever with renal syndrome. *Vaccine* 6, 278–282. doi: 10.1016/0264-410x(88)90224-1

Yang, J., Sun, J. F., Wang, T. T., Guo, X. H., Wei, J. X., Jia, L. T., et al. (2017). Targeted inhibition of hantavirus replication and intracranial pathogenesis by a chimeric protein-delivered siRNA. *Antivir. Res.* 147, 107–115. doi: 10.1016/j.antiviral.2017.10.005

Yi, Y., Park, H., and Jung, J. (2018). Effectiveness of inactivated hantavirus vaccine on the disease severity of hemorrhagic fever with renal syndrome. *Kidney Res. Clin. Pract.* 37, 366–372. doi: 10.23876/j.krcp.18.0044

Ying, Q., Ma, T., Cheng, L., Zhang, X., Truax, A. D., Ma, R., et al. (2016). Construction and immunological characterization of CD40L or GM-CSF incorporated *Hantaan virus* like particle. *Oncotarget* 7, 63488–63503. doi: 10.18632/oncotarget.11329

Yong, C. Y., Ong, H. K., Yeap, S. K., Ho, K. L., and Tan, W. S. (2019). Recent advances in the vaccine development against middle east respiratory syndrome-coronavirus. *Front. Microbiol.* 10:1781. doi: 10.3389/fmicb.2019.01781

Zhang, S., Wang, S., Yin, W., Liang, M., Li, J., Zhang, Q., et al. (2014). Epidemic characteristics of hemorrhagic fever with renal syndrome in China, 2006-2012. *BMC Infect. Dis* 14:384. doi: 10.1186/1471-2334-14-384

Zhang, X. K., Takashima, I., and Hashimoto, N. (1989). Characteristics of passive immunity against hantavirus infection in rats. *Arch. Virol.* 105, 235–246. doi: 10.1007/bf01311360

Zhao, C., Sun, Y., Zhao, Y., Wang, S., Yu, T., Du, F., et al. (2012). Immunogenicity of a multi-epitope DNA vaccine against hantavirus. *Hum. Vaccin. Immunother.* 8, 208–215. doi: 10.4161/hv.18389

Zheng, Y., Zhou, B. Y., Wei, J., Xu, Y., Dong, J. H., Guan, L. Y., et al. (2018). Persistence of immune responses to vaccine against haemorrhagic fever with renal syndrome in healthy adults aged 16-60 years: results from an open-label2-year follow-up study. *Infect. Dis.* 50, 21–26. doi: 10.1080/23744235.2017.1353704

**Conflict of Interest:** The authors declare that the research was conducted in the absence of any commercial or financial relationships that could be construed as a potential conflict of interest.

*Copyright © 2020 Liu, Ma, Shu, Zhang, Han, Liu, Jin, Zhang and Wu. This is an open-access article distributed under the terms of the Creative Commons Attribution License (CC BY). The use, distribution or reproduction in other forums is permitted, provided the original author(s) and the copyright owner(s) are credited and that the original publication in this journal is cited, in accordance with accepted academic practice. No use, distribution or reproduction is permitted which does not comply with these terms.*

frontiers in Microbiology

REVIEW
published: 07 February 2020
doi: 10.3389/fmicb.2020.00135

# Broadly Protective Strategies Against Influenza Viruses: Universal Vaccines and Therapeutics

*Olivia A. Vogel*[1] *and Balaji Manicassamy*[2]*

[1]*Department of Microbiology, The University of Chicago, Chicago, IL, United States,* [2]*Department of Microbiology and Immunology, The University of Iowa, Iowa City, IA, United States*

Influenza virus is a respiratory pathogen that can cause disease in humans, with symptoms ranging from mild to life-threatening. The vast majority of influenza virus infections in humans are observed during seasonal epidemics and occasional pandemics. Given the substantial public health burden associated with influenza virus infection, yearly vaccination is recommended for protection against seasonal influenza viruses. Despite vigilant surveillance for new variants and careful selection of seasonal vaccine strains, the efficacy of seasonal vaccines can vary widely from year to year. This often results in lowered protection within the population, regardless of vaccination status. In order to broaden the protection afforded by seasonal influenza vaccines, the National Institute of Allergy and Infectious Diseases (NIAID) has deemed the development of a universal influenza virus vaccine to be a priority in influenza virus vaccine research. This universal vaccine would provide protection against all influenza virus strains, eliminating the need for the yearly reformulations of seasonal influenza vaccines. In addition to universal influenza vaccine efforts, substantial progress has been made in developing novel influenza virus therapeutics that utilize broadly neutralizing antibodies to provide protection against influenza virus infection and to mitigate disease outcomes during infection. In this review, we discuss various approaches toward the goal of improving influenza virus vaccine efficacy through a universal influenza virus vaccine. We also address the novel methods of discovery and utilization of broadly neutralizing antibodies to improve influenza disease outcomes.

**Keywords: influenza, universal influenza vaccine, vaccine, influenza therapeutics, immunization**

OPEN ACCESS

***Edited by:***
*Lijun Rong,*
*University of Illinois at Chicago, United States*

***Reviewed by:***
*Rong Hai,*
*University of California, Riverside, United States*
*Randy A. Albrecht,*
*Icahn School of Medicine at Mount Sinai, United States*

****Correspondence:***
*Balaji Manicassamy*
*balaji-manicassamy@uiowa.edu*

***Specialty section:***
*This article was submitted to Virology, a section of the journal Frontiers in Microbiology*

***Received:*** *05 December 2019*
***Accepted:*** *21 January 2020*
***Published:*** *07 February 2020*

***Citation:***
*Vogel OA and Manicassamy B (2020) Broadly Protective Strategies Against Influenza Viruses: Universal Vaccines and Therapeutics. Front. Microbiol. 11:135. doi: 10.3389/fmicb.2020.00135*

## INTRODUCTION

Influenza viruses are a significant public health burden worldwide, causing yearly epidemics and occasional pandemics. Infection with influenza virus causes acute upper respiratory disease in humans that can potentially lead to hospitalization or death. In addition to the morbidity and mortality associated with influenza virus infection, the yearly economic burden of influenza virus infections in the United States is estimated to be around $11.2 billion (Putri et al., 2018). Given the considerable impact of influenza virus infection in communities worldwide, significant attention has been focused on preventing influenza virus infection and spread of the virus through vaccination within the population as well as with other public health measures.

Influenza viruses are members of the *Orthomyxoviridae* family of viruses, which are characterized by segmented, negative sense, single-stranded RNA genome. Of the influenza virus types, influenza A and B are the only types that are known to cause disease in humans. In addition to humans, influenza A viruses can infect a broad variety of species including pigs, horses, and birds (Webster et al., 1995). In nature, influenza A viruses are maintained in water fowls, which are the main reservoir for influenza A (Webster et al., 1995). Influenza A viruses can be further classified into different subtypes based on the two major viral surface glycoproteins, hemagglutinin (HA) and neuraminidase (NA) (Fields et al., 2013). For influenza A viruses, there are 18 known HA subtypes that fall into two phylogenetic groups (Group 1 or Group 2); like HA, the 11 NA subtypes also fall within two phylogenetic groups. These phylogenetic groups are composed of viruses that are derived from a common ancestor. Unlike influenza A viruses, the diversity of influenza B viruses is limited and is categorized into two lineages, B/Yamagata and B/Victoria (Rota et al., 1990). Despite the limited diversity, influenza B viruses evolve to escape immunity and remain in circulation in humans; thus, necessitating yearly updates of the influenza B virus strains included in the seasonal vaccine.

## IMMUNOLOGICAL RESPONSES TO INFLUENZA VIRUS INFECTION

Influenza viruses predominantly infect and replicate in the epithelial cells lining the upper respiratory tract. Viral infection is initiated by the binding of viral surface glycoprotein HA to host sialic acid residues followed by internalization of the virus through endocytosis (Fields et al., 2013). Subsequently, the fusion of the viral membrane with the endosomal membrane releases the viral genomic RNA into the cytoplasm, and the RNA is then imported into the nucleus for replication (Fields et al., 2013). The initial innate immune responses against influenza virus infection are activated by the sensing of viral RNA by pattern recognition receptors such as the retinoic acid-inducible gene-I (RIG-I) and Toll-Like Receptor 7 (TLR7) (Iwasaki and Pillai, 2014). Additional innate sensing pathways also contribute to robust innate responses against influenza virus infection (Iwasaki and Pillai, 2014). Ultimately, the activation of these innate sensing pathways leads to the production of interferon and cytokines/chemokines critical for efficient activation of adaptive immune responses (B- and T-cell responses) that help control and clear infection.

Studies in humans and mice demonstrate the importance of T-cell responses in clearing primary influenza virus infection and mounting robust recall responses in subsequent infection. The importance of T-cell responses was highlighted by a study following 342 healthy adults in the UK during the 2009 H1N1 pandemic, which determined that illness was less severe in individuals with higher frequencies of pre-existing T cells to conserved CD8 epitopes (Sridhar et al., 2013). The importance of $CD8^+$ T cells during influenza virus infection was further highlighted in adoptive transfer experiments in which mice were given $CD8^+$ effector cells. After infection, viral replication was reduced in the lungs of recipient mice compared to mice that did not receive $CD8^+$ T cells (Yap et al., 1978; Lukacher et al., 1984; Hamada et al., 2009, 2013). Additionally, mice receiving $CD8^+$ T cells also displayed increased recruitment of NK cells, macrophages, and B cells after infection (Hamada et al., 2013). These results further highlight the importance of mounting $CD8^+$ immune responses during infection. More recently, $CD4^+$ T cells have also been shown to have an important role in clearing influenza infection, with the lack of $CD4^+$ T cells correlating with reduced viral clearance (Belz et al., 2002). As with $CD8^+$ T cells, adoptive transfer of $CD4^+$ memory T cells in mice was associated with greater protection during influenza infection (McKinstry et al., 2012).

The mucosal antibody response is an important feature in determining the ability of the host to efficiently clear viral infections. Mucosal antibody responses are more effective in preventing subsequent infection rather than primary viral infection. The three main immunoglobulin (Ig) isotypes induced during influenza infection are IgG, IgA, and IgM. Secretory IgA antibodies are generated early during infection and can act as an indicator of acute influenza infection (Rothbarth et al., 1999). Additionally, secretory IgA antibodies have been associated with greater protection in the upper respiratory tract while also providing cross-reactive protection against different influenza virus strains (Tamura et al., 1990; Asahi et al., 2002; Renegar et al., 2004; Ainai et al., 2013). IgM antibodies are also generated during primary infection and have been shown to have a role in complement mediated virus neutralization (Rothbarth et al., 1999; Fernandez Gonzalez et al., 2008). In contrast to serum IgA antibodies, serum IgG antibodies are associated with protection in the lower respiratory tract as well as providing strain-specific protection (Tamura et al., 1990).

## CURRENT SEASONAL INFLUENZA VACCINES

The composition of seasonal influenza virus vaccines is based on the strains currently propagating in the human population. Presently, there are two influenza A virus strains (H1N1 and H3N2) and two influenza B virus lineages circulating in humans, with only one influenza B strain from each type circulating as the predominant strain during influenza season. However, as it is impossible to predict the predominant strain for a given season, the majority of the current seasonal influenza vaccines are composed of all four strains. The selection of influenza strains for incorporation into seasonal vaccines is based on surveillance of circulating strains by WHO influenza centers as well as on an assessment of which strains will likely become the predominant strain in human populations (Gerdil, 2003). Once the vaccine strains have been selected by the WHO committee, seasonal vaccine production can begin and requires roughly 6 months for the commonly used inactivated vaccine to be produced and distributed (Gerdil, 2003).

There are four types of seasonal influenza virus vaccines currently licensed for use in humans: inactivated, live attenuated,

recombinant protein, and cell-based vaccines. A vast majority of the influenza virus vaccines administered in humans are split inactivated vaccines, which are produced in embryonated chicken eggs. For split inactivated vaccines, vaccine strains are individually grown in the allantoic cavity of embryonated chicken eggs and inactivated by treatment with formalin or β-propriolactone (Gerdil, 2003). Once purified, virus particles are then split using ether and detergent to reduce the level of viral ribonucleoproteins, which cause reactogenicity at the site of injection (Gerdil, 2003). The individual vaccine components are mixed in a standardized manner to ensure an inclusion of 15 μg of HA per strain (Sridhar et al., 2015). Inactivated vaccine is administered intramuscularly to stimulate the systemic immune response, producing mainly IgG antibodies and low amounts of IgA antibodies (Clements et al., 1986). Similar to inactivated vaccines, live attenuated influenza vaccines (LAIVs) are grown in embryonated eggs. LAIV strains are generated using a reverse genetics approach to incorporate HA and NA genes from circulating influenza strains into a cold-adapted, attenuated influenza virus backbone (Sridhar et al., 2015). Cold adaption of the LAIV backbone ensures that the replication of the vaccine strain does not occur at temperatures above 33°C, allowing for replication in the upper respiratory tract but not in the lower respiratory tract (Sridhar et al., 2015). LAIV, which is administered intranasally to mimic natural infection, stimulates robust IgA and IgG responses in the upper respiratory tract (Clements et al., 1986). LAIV has also been shown to elicit T-cell mediated responses in vaccinated children (He et al., 2006; Hoft et al., 2011). While both inactivated vaccine virus strains and LAIV viruses are grown in embryonated eggs, this poses a challenge in the event of egg shortages and for immunization of individuals with egg allergies. Recombinant protein vaccines and cell culture-based influenza vaccines have been developed to overcome limitations of egg-based vaccines. Currently, there is only one recombinant vaccine, named Flublok®, approved for use by the US Food and Drug Administration (FDA). Flublok® still contains HA protein antigens representing the selected influenza strains for the current season, but it is produced in insect cells (Cox and Hollister, 2009). In contrast to embryonated egg-based vaccines, manufacturing of Flublok® takes approximately 2 months and can be administered in individuals with egg allergies, providing an advantage over traditional seasonal egg-based vaccines (Cox and Hollister, 2009). In regard to cell-based vaccines, Flucelvax® is a licensed quadrivalent inactivated vaccine that is grown in a mammalian cell line and can avoid any potential egg-based mutations (Lamb, 2019). As with Flublok®, Flucelvax® can be administered to individuals with egg allergies and requires a shorter production time than egg-grown vaccines.

## CHALLENGES FOR CURRENT SEASONAL VACCINES

Yearly vaccination with split, inactivated influenza vaccines is still one of the most popular and efficient means of protection against seasonal influenza viruses. Prior to 2012, influenza vaccines were trivalent and contained only one influenza B virus in the vaccine. This often resulted in inadequate protection against influenza B virus, due to mismatches between the circulating influenza B virus lineage and the influenza B virus lineage chosen for vaccine incorporation (Tisa et al., 2016). To avoid issues with influenza B virus lineage mismatches, a quadrivalent inactivated vaccine that contains both influenza B virus lineages was developed (Tisa et al., 2016). Despite these improvements to the seasonal influenza virus vaccines, the effectiveness of seasonal influenza vaccines can vary greatly, depending on how closely the vaccine strains match the circulating strains. In fact, there are several instances in the recent past where seasonal vaccines failed to provide protection against antigenically drifted strains (David et al., 2005; Halloran et al., 2007; Skowronski et al., 2007). Furthermore, yearly vaccines do not provide protection against novel influenza virus strains introduced from zoonotic reservoirs, causing significant morbidity and mortality due to lack of immunity in the general population.

The types of immune responses elicited by different seasonal influenza vaccines also impact the degree and the longevity of protection. As mentioned previously, inactivated vaccines administered intramuscularly elicit production of serum IgG antibodies but fail to induce antibody and T-cell responses in the respiratory mucosa. As such, this type of vaccine provides strain-specific protection but can leave individuals vulnerable to infection by new variant strains. Preclinical studies indicate that intranasal administration of inactivated vaccines induces robust responses in the respiratory mucosa. LAIV administered intranasally closely mimics natural infection and stimulates robust IgA and IgG antibody responses; however, this vaccine failed to provide adequate protection against influenza A(H1N1) pdm09 during the 2013–2014 and 2015–2016 seasons (Grohskopf et al., 2016, 2018). This inadequate protection prompted the Advisory Committee on Immunization Practices (ACIP) to recommend against administration of this vaccine for the 2016–2017 and 2017–2018 seasons (Grohskopf et al., 2016, 2017). Later, the manufacturer determined that the reduced protection associated with the LAIV was most likely due to reduced replicative fitness of the A/California and A/Bolivia (H1N1)pdm09 LAIV strains (Ambrose et al., 2016). Currently, the quadrivalent LAIV has incorporated a new influenza A(H1N1)pdm09-like virus that provides better protection and is recommended again for use (Grohskopf et al., 2018). While the LAIV has been demonstrated to provide robust protection in younger children, responses to LAIV vaccination in preimmune adults are likely limited due to immune-mediated restriction of LAIV replication prior to induction of effective immunity.

A vast majority of seasonal influenza vaccines are manufactured in eggs. Occasionally, during vaccine production, egg adaptive mutations can arise that alter the antigenicity of the virus and, as a result, can reduce vaccine effectiveness against circulating strains. H3N2 strains in particular have been associated with increased egg-based mutations that result in reduced antigenicity of the vaccine strain, negatively impacting the protection afforded by the vaccine (Skowronski et al., 2014; Wu et al., 2017, 2019; Zost et al., 2017). Consequently, egg grown vaccines must be monitored to ensure that the vaccine strain incorporated into the vaccine matches the seed strain

chosen at the start of manufacturing. The risk of adaptive mutations and reduced antigenicity is mitigated in recombinant protein vaccines, which are grown in insect cells, or by producing the vaccine strains in mammalian cell lines. However, the cost associated with large-scale production of cell-culture grown vaccine strains remains high as compared to ones produced in eggs (Barr et al., 2018).

Another alternative to egg grown vaccine approaches involves the use of DNA and mRNA vaccines. While none are currently approved for use, DNA and mRNA vaccines can be manufactured synthetically, allowing for quicker production times than egg and cell-culture grown vaccines (Stachyra et al., 2014; Kanekiyo et al., 2019) Furthermore, DNA and mRNA vaccine approaches do not induce the anti-vector immune responses that can be elicited with viral vector-based vaccine approaches (Kanekiyo et al., 2019). DNA vaccines have also shown promise as a method of vaccine priming (Ledgerwood et al., 2011). In fact, several of the universal vaccination methods described in this review utilize DNA prime-boost vaccination to improve immune responses. Likewise, mRNA-based vaccines show potential as an alternative vaccination approach. An example of an mRNA-based approach includes RNActive® vaccines. RNActive® vaccines are mRNA vaccines complexed with protamine, which allow for the mRNA to acts as a "self-adjuvant" through interaction with TLR7 (Kallen et al., 2013). An RNActive® vaccine encoding the full-length PR8 HA has been shown to induce IgG antibodies against PR8 HA and provide protection against homologous PR8 viral challenge (Petsch et al., 2012). Furthermore, transfer of serum from PR8 HA mRNA-vaccinated mice to unvaccinated recipient mice provided protection against PR8 infection (Petsch et al., 2012). Together, these different vaccination approaches have the potential for improving upon yearly influenza virus vaccines as well as in the development of universal influenza virus vaccines.

An additional consideration for seasonal influenza vaccines is the ability to provide protection among older adults, who are often at higher risk for influenza infection. The usual dosage of 15 μg HA antigen per vaccine strain in seasonal inactivated vaccines is insufficient to induce protection in older adults. To address this concern, a new vaccine named Fluzone® was developed to improve serum antibody responses in older adults. Fluzone® is a trivalent, inactivated split-virus vaccine that contains 60 μg of HA for each influenza strain included in the vaccine (Robertson et al., 2016). This dosage is four times that of standard inactivated vaccines and has been shown to increase protection in older adults, providing a promising alternative for this high-risk group (Robertson et al., 2016).

The most significant challenge for the seasonal influenza vaccine production strategy involves ensuring that the vaccine strains match the dominant circulating strains in the population. There have been significant efforts to improve upon methods of monitoring and identifying newly evolved influenza strains worldwide, including the incorporation of modeling techniques such as antigenic cartography (Ampofo et al., 2015). Despite these efforts, the screening process is imperfect, and as result, it is not unusual to see the emergence of a variant strain after selection of another strain for vaccine production. Neutralizing antibodies induced upon vaccination predominantly target the highly immunogenic head domain of HA and provide potent protection against matching strains by blocking virus attachment to cells (Knossow et al., 2002). Consequently, these highly immunogenic regions in the head domain are prone to high mutation rates due to immune selection pressure from neutralizing antibodies. In a circulating strain, accumulation of mutations in the head domain over time leads to changes in antigenic properties (antigenic drift) and can render vaccine-induced immunity ineffective against them. In addition, these variant strains can cause epidemics in populations lacking immunity to the newly evolved strain (Fields et al., 2013). Antigenic drift is the major driving force behind the need to reformulate influenza vaccines each year and poses a significant challenge for vaccine development. Furthermore, seasonal influenza virus vaccines fail to provide protection against the novel strains transmitted from zoonotic reservoirs.

Given the considerable public health consequences associated with a lack of sufficient protection against seasonal and pandemic influenza stains, the National Institute of Allergy and Infectious Diseases (NIAID) has prioritized the development of a universal influenza vaccine that can afford protection against a broad variety of influenza viruses (Erbelding et al., 2018). Currently, the majority of universal influenza vaccine research efforts are aimed at inducing immunity against the highly conserved regions on the influenza surface proteins or internal proteins of influenza viruses as means to induce universal protection against all influenza virus strains (**Figure 1**).

## UNIVERSAL INFLUENZA VACCINE APPROACHES

### Hemagglutinin-Directed

The influenza virus surface protein HA is one of the major targets of the immune system. HA is synthesized as a precursor HA0 that is proteolytically processed into HA1 and HA2 subunits, which remain attached through a disulfide bond. Three HA molecules form a trimeric rod-shaped molecule that is composed of a long fibrous stem formed by the HA2 trimer and a globular head formed by the HA1 trimer (Fields et al., 2013). The globular head domain of HA contains the receptor binding pocket, which facilitates virus attachment to the host cell surface sialic acids (Wilson et al., 1981; Rogers et al., 1983). Once the bound virus is internalized through endocytosis, HA undergoes conformational changes under low pH conditions that allow HA2 to initiate the fusion of the viral and endosomal membranes (Skehel et al., 1982; Bullough et al., 1994). This process enables the release of the viral genomic contents into the cytoplasm. The HA1 region is highly immunogenic, more flexible to accommodate mutations than HA2 and displays a high degree of variability among influenza virus strains. Conversely, the HA2 region is highly conserved among different influenza virus subtypes and is more structurally constrained in its ability to accommodate mutations.

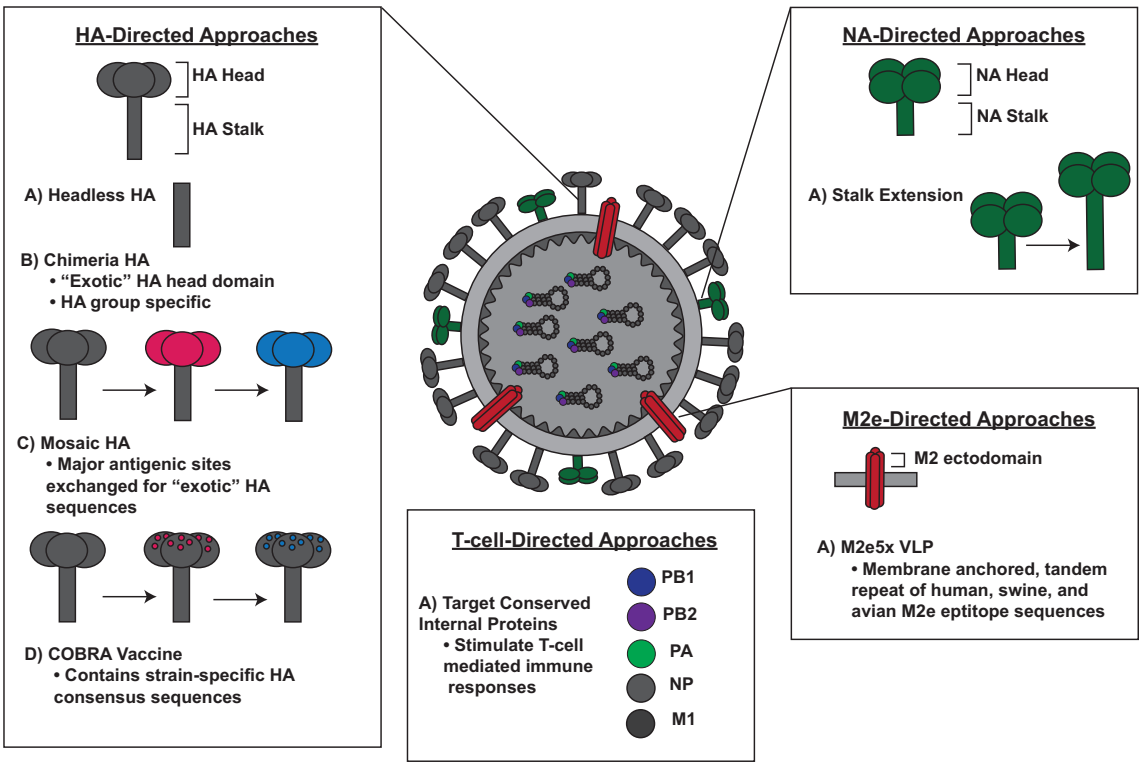


**FIGURE 1** | A schematic representation of various preclinical approaches for a universal influenza vaccine.

As described above, the antigenic variation of the HA1 domain and its resulting antigenic drift is the major reason for reformulating seasonal influenza vaccines with new strains every year. To address this challenge, several vaccine strategies based on conserved sequences in HA have been developed. Once such approach involves a novel computational-based antigen design methodology. This approach, termed computationally optimized broadly reactive antigen (COBRA), was used to generate a consensus H5 HA sequence by aligning 129 unique HA sequences from clade 2 H5N1 viruses isolated from 2004 to 2006 (Giles and Ross, 2011). Following alignment, the most common amino acid at each position was selected to generate a consensus sequence for the COBRA H5 HA (Giles and Ross, 2011). This newly generated COBRA H5 HA was confirmed to exhibit normal HA activity, including receptor binding and particle fusion (Giles and Ross, 2011). The efficacy of this COBRA H5 HA was evaluated in virus-like particle (VLP) based vaccination and challenge studies (Giles and Ross, 2011). Following vaccination of mice and ferrets, the COBRA H5N1 VLP vaccines induced increased hemagglutinin inhibition titers and provided enhanced protection against lethal challenge with different clade 2 H5N1 viruses when compared to a VLP vaccine containing an HA derived from a primary isolate (Giles and Ross, 2011). The improved efficacy of COBRA vaccine approaches have been supported by studies in a non-human primate model (cynomolgus macaques) with the COBRA HA H5N1 VLPs (Giles et al., 2012). The sera from vaccinated macaques demonstrated hemagglutinin inhibition titers against a wider range of H5N1 strains than animals vaccinated with contemporary H5N1 HA VLPs (Giles et al., 2012). In addition, vaccinated macaques were protected against viral challenge as well as exhibiting reduced lung inflammation (Giles et al., 2012). Following the same methodology used for the generation of COBRA HA H5N1 VLPs, COBRA HA H3N2 and COBRA HA H1N1 VLPS have been generated using consensus sequences from both modern and historical H3N2 and H1N1 strains. These COBRA VLP vaccines provided broad protection against a wide range of H3N2 and H1N1 strains (Carter et al., 2016; Wong et al., 2017). Recently, the COBRA H1 and H3 antigens, along with the AF03 adjuvant (squalene-in-water emulsion), induced protective responses in ferrets, with ferrets exhibiting decreased viral shedding (Allen et al., 2018). By generating more broadly reactive HAs, the COBRA approach provides an intriguing solution to overcome the challenges posed by antigenic drift of circulating strains, as COBRA-based seasonal vaccine has the potential to provide protection even during mismatch. However, as protection afforded by COBRA vaccines is only against specific HA subtypes, COBRA vaccines still fall short of serving as a true universal influenza vaccine.

To generate broadly protective immune responses against multiple influenza virus strains, several research groups developing universal influenza vaccines have targeted the highly

conserved stalk domain of HA. Antibodies directed against the HA stalk domain have been shown to be protective in both mice and humans (Okuno et al., 1993; Throsby et al., 2008; Ekiert et al., 2009). The stalk-specific antibodies provide protection by various mechanisms, including by directly preventing HA-mediated fusion or by inducing antibody-dependent cellular cytotoxicity (ADCC; Ekiert et al., 2009; DiLillo et al., 2014; He et al., 2016). Importantly, antibodies directed toward the HA stalk domain have been shown to provide cross-reactive protection against multiple influenza virus strains (Throsby et al., 2008; Sui et al., 2009). However, this cross-reactive protection is typically restricted to HAs from the same group, Group 1 HA-specific stem-directed antibodies are unable to neutralize infection by viruses carrying Group 2 HAs (Sui et al., 2009).

A major hurdle in developing effective vaccine strategies targeting the HA stalk domain is overcoming the poor immunogenicity of the HA stalk domain, as in the context of full-length HA, antibodies are mainly produced toward the highly immunogenic HA head domain (Vareckova et al., 1993). Studies performed in the 1980s with monoclonal antibodies that were cross reactive against H1 and H2 subtypes of HA demonstrated that a vaccine approach targeting the stem region of HA can provide broad protection and overcome the limitation of antigenic drift (Graves et al., 1983). This was further confirmed in a 1996 study in which mice were immunized with cells overexpressing an HA that lacked the globular head domain (Sagawa et al., 1996). Following challenge with H1N1, mice that were immunized with the headless HA exhibited increased survival compared to mice immunized with full length HA expressing cells (Sagawa et al., 1996). These studies underscore the potential immunogenicity of the HA stalk in the absence of the HA head domain.

In recent years, vaccine approaches have attempted to enhance exposure of the HA stalk domain to the immune system using HAs that lack the dominant head domain (Steel et al., 2010; Impagliazzo et al., 2015). These "headless" HAs were incorporated onto VLPs for vaccination (Steel et al., 2010; Impagliazzo et al., 2015). Nanoparticles have also been used as a method to improve HA stalk exposure during vaccination, using either HAs lacking the head domain or full-length HAs (Kanekiyo et al., 2013; Yassine et al., 2015). Vaccination in mice and ferrets demonstrated that these nanoparticle-based approaches provided cross-reactive protection following viral challenge with different influenza A virus strains (Kanekiyo et al., 2013; Yassine et al., 2015). Interestingly, when ferrets were immunized with the nanoparticle vaccine containing a full-length HA fused to ferritin, both HA stem and receptor binding site-specific antibodies were detected, demonstrating the utility of this approach in generating more broadly immunogenic HA-based vaccines (Kanekiyo et al., 2013).

Another method of improving exposure of the HA stalk domain involves the generation of chimeric HAs (cHA) that express the head domain from one virus strain and the stalk domain of another. This method involves sequential immunization with constructs that express the same stalk domain but different "exotic" head domains, thereby specifically stimulating stalk-directed antibody responses to induce broader protection than strain-specific HA head directed antibodies generated by seasonal vaccines (Hai et al., 2012; Pica et al., 2012; Krammer et al., 2013; Margine et al., 2013; Nachbagauer et al., 2017; Liu et al., 2019). Sequential vaccination of mice with cHA containing the same H1 stem but different heads demonstrated protection against challenge from Group 1 viruses but not Group 2 viruses (Krammer et al., 2013). In a recent preclinical study, ferrets were immunized with a LAIV virus expressing a cHA composed of an H8 head and a H1 stalk (cH8/1) as well as the N1 NA from the 2009 H1N1 pandemic virus (Nachbagauer et al., 2018). Subsequently, ferrets received a boost with a split virus vaccine containing a cHA with a H5 head and H1 stalk (cH5/1 IIV) (Nachbagauer et al., 2018). Ferrets vaccinated with cHA demonstrated greater protection against the pandemic H1N1 challenge as compared to ferrets immunized with two doses of a seasonal trivalent influenza vaccine, demonstrating improved protection elicited by the cHA vaccination approach (Nachbagauer et al., 2018). Despite the lack of protection across different HA groups, the cHA approach shows promise for human vaccination and has been recently evaluated in human clinical trials. The outcome of the human clinical trials is still being evaluated (Bernstein et al., 2019).

Recently, the cHA vaccine has been further improved upon through the development of mosaic HAs (mHA), in which only the major antigenic sites in the HA head domain are exchanged with "exotic HA" sequences (Broecker et al., 2019a). This strategy was developed to generate antibodies against both the stalk domain and epitopes in the head domain that fall outside the major antigenic sites (Broecker et al., 2019a). Sequential vaccination with inactivated mHA viruses induced cross-reactive antibodies to both the stalk domain and the head domain (Broecker et al., 2019a). Additionally, transfer of sera from vaccinated mice into naïve mice provided protection against viral challenge with reassortment viruses containing PR8 internal proteins with HA and NA from different H3N2 strains as compared to the seasonal inactivated quadrivalent vaccine (Broecker et al., 2019a). These results indicate that the mHA approach also has potential to provide broader protection than current seasonal vaccines.

An important challenge for HA stalk-directed vaccines is whether these vaccine strategies are capable of providing protection against strains from both HA groups. As described above, HA stalk-directed antibodies often provide HA group-specific protection. While the ability to provide protection against a broad range of influenza virus strains within a given HA subtype is a vast improvement over approved seasonal vaccines, this still falls short of providing universal influenza virus protection. Another important consideration involves providing protection for both influenza A and B virus strains. While the HA stalk-directed approaches described above demonstrate protection against influenza A viruses, protection against influenza B strains is not always addressed. A truly universal vaccine should be able to provide protection against both influenza A and B strains. Therefore, current universal vaccine research should be cognizant of the need to elicit protection for both types of influenza viruses. Antibodies targeting the HA stalk domain have been shown to be protective

against influenza B strains, with the human monoclonal antibody CR9114 demonstrating protection against lethal challenge from both influenza A and B strains (Dreyfus et al., 2012). Recently, the mHA approach was used in an attempt to generate a universal influenza B vaccine that could provide protection against a wide range of influenza B virus lineages (Sun et al., 2019). To generate the influenza B mHA, the major antigenic sites were replaced with "exotic" influenza A sequences (Sun et al., 2019). Immunization of mice involved a DNA primer followed by two mHA protein boosts (Sun et al., 2019). Importantly, mice vaccinated with the influenza B mHA demonstrated improved survival following lethal challenge with different influenza B strains (Sun et al., 2019). While this study does not provide evidence for protection against influenza A strains, it further serves to highlight the potential for vaccination approaches that improve upon the breadth of protection provided by the current seasonal vaccination strategies. It would be interesting to examine whether combining influenza A mHAs and influenza B mHAs into a single vaccine might provide even greater protection for both influenza A and B strains than the current inactivated quadrivalent vaccine.

## Neuraminidase-Directed

The second major surface protein for influenza A virus is the NA protein, which has an important role in facilitating virus release from the host cell. The sialidase or neuraminidase activity of NA helps cleave the terminal sialic acids from glycans and thereby facilitate virion release from infected cells (Fields et al., 2013). NA has been an important target for the development of antiviral drugs, such as oseltamivir (Tamiflu®) and zanamivir, both of which target the enzymatic activity of NA and are effective against both influenza A and B virus strains. Mutations that render NA resistant to the aforementioned drugs have been reported. While NA is also capable of undergoing antigenic changes, these changes occur at a much slower rate than those observed with HA (Kilbourne et al., 1990). Given the relatively conserved nature of NA, there have been several potential vaccine candidates developed that target NA in order to generate improved influenza vaccines.

Unlike HA antibodies, NA antibodies do not neutralize infection, but they have been shown to inhibit NA enzymatic activity as well as reduce viral titers in mouse models (Rott et al., 1974). In addition, NA antibodies have been shown to be protective in both chickens and humans (Murphy et al., 1972; Clements et al., 1986; Webster et al., 1988). In humans, antibodies against NA have been associated with decreased viral shedding and shortened duration of symptoms (Maier et al., 2019). Recent studies have highlighted the importance of examining neuraminidase inhibition titers as well as hemagglutinin inhibition titers as a measure of influenza disease severity, suggesting that NA-based protection should be an important consideration when developing new influenza vaccines (Monto et al., 2015; Memoli et al., 2016).

There have been several approaches taken to develop NA-based vaccines, including use of recombinant NA proteins, DNA plasmid-based NA expression, and NA incorporation onto VLPs to boost NA-directed antibody responses (Sandbulte et al., 2007; Easterbrook et al., 2012; Liu et al., 2015; Job et al., 2018). Recently, a recombinant modified vaccinia virus Ankara (MVA) vector was used to express either HA or NA from three different H7 viruses. Following vaccination with a MVA vector expressing N3 NA, mice were protected against challenge with H7N3 (Meseda et al., 2018). Likewise, a passive transfer of sera from MVA-N3 vaccinated mice into naive mice demonstrated protection against H7N3 infection (Meseda et al., 2018) In contrast, mice that received sera from the MVA-N7 vaccine were not protected against challenge with H7N3 despite the vaccine containing an NA from the same subtype as N3, suggesting that further optimization of this vaccine approach is required to elicit broader NA-based protection (Meseda et al., 2018). Another NA vaccine approach involved the use of recombinant baculovirus VLPs expressing the N1 NA from A/California/04/2009 (N1 VLP) (Kim et al., 2019). The N1 VLP vaccine elicited NA inhibition activity for H1N1, H5N1, and H3N2 (Kim et al., 2019). Additionally, the N1 VLP vaccine provided protection in mice against challenge with H1N1, H5N1, and H3N2 (Kim et al., 2019). This suggests that the N1 VLP vaccine has the potential to confer protection against different influenza strains with different N1 subtype NAs (Kim et al., 2019). Additional studies in animal models that more closely recapitulate human influenza infection, like ferrets, are necessary to further examine the efficacy of this vaccine, but this study does provide more evidence for the importance of considering NA-based immune responses for influenza vaccines.

An important challenge in inducing NA directed immune responses involves overcoming the immunodominance of HA over NA. In an attempt to subvert the HA immunodominance, a recent study generated two recombinant influenza viruses based on the H1N1 stain A/Puerto Rico/8/1934 (PR8) in which the NA stalk domain was extended by 15–30 amino acids (Broecker et al., 2019b). Using formalin-inactivated viruses expressing wildtype NA or the extended NA, the authors demonstrated that the extended NA stalk induced higher anti-NA IgG responses than the unmodified NA in mice (Broecker et al., 2019b). Similarly, extension of the NA stalk from H3N2 virus increased NA-specific antibody responses (Broecker et al., 2019b). While additional challenge studies need to be performed, the NA stalk extension approach offers an interesting solution to improving the immunogenicity of NA.

As with HA-directed vaccination approaches, these NA-directed approaches do not always demonstrate that protection elicited by the vaccine extends to both NA groups. Another consideration for NA-directed vaccines involves whether these approaches can provide robust protection in humans. As stated previously, NA-directed antibodies do not neutralize infection, and antibodies against NA have been shown to reduce the duration of symptoms in humans. As a result, more studies demonstrating protection in humans or models that more accurately reflect human influenza virus infection are necessary to demonstrate the protection these NA-based methods can provide.

## M2 Ectodomain-Directed

The third surface protein on the influenza virion is the M2 protein. M2 is encoded by the M segment, which encodes

M1 from unspliced mRNA and M2 protein by mRNA splicing (Fields et al., 2013). M2 forms homotetramers and possesses ion channel activity that allows for acidification of the inside of the virion during endocytosis and facilitates the dissociation of the matrix protein M1 from viral ribonucleoprotein complexes (Fields et al., 2013). The M2 ectodomain (M2e), which is the exposed portion of the M2 protein found on the virion membrane, is highly conserved among influenza strains (Ito et al., 1991). Additionally, M2e-directed antibodies have been detected during influenza infection and have been shown to be protective in both mice and ferrets (Black et al., 1993; Neirynck et al., 1999; Zharikova et al., 2005; El Bakkouri et al., 2011). Importantly, like NA-directed antibodies, M2 antibodies do not prevent infection but instead reduce disease severity and control the spread of infection (Mozdzanowska et al., 1999; Grandea et al., 2010). Given the conserved nature of M2e and the protection demonstrated with M2e-directed antibodies, M2e has become a target for universal influenza vaccine approaches.

As with NA and the HA stalk, M2e-directed immune responses must overcome the highly immunogenic HA head domain. In addition, while M2 is abundantly expressed on the cell surface of infected cells, M2 is less abundant on the virion itself, a challenge for eliciting robust immune responses in LAIV approaches due to the reduced availability of M2 on the LAIV virion (Lamb et al., 1985; Zebedee and Lamb, 1988). Previous attempts to improve M2e-directed immune responses involved the use of several viral vectors including papaya mosaic virus (PapMV) carrying M2e, HPV VLPs conjugated to the M2 protein, or VLPs derived from the RNA phage Qβ that display the M2e protein (Ionescu et al., 2006; Bessa et al., 2008; Denis et al., 2008). These M2e-based vaccines elicited M2 specific antibody responses and protected mice against influenza A virus challenge, highlighting the importance of M2e mediated protection and the importance of considering the M2e protein when formulating universal influenza vaccines (Ionescu et al., 2006; Bessa et al., 2008; Denis et al., 2008). Another approach to improve M2e antibody responses involved expressing a membrane anchored tandem repeat of M2e epitope sequences of human, swine, and avian origin on recombinant baculovirus VLPs (M2e5x VLP) (Kim et al., 2013; Kang et al., 2019). The M2e5x VLPs induced M2e-specific antibody responses against H1N1, H3N2, and H5N1 and conferred protection in mice against both H1N1 and H3N2 challenges (Kim et al., 2013). Recently, combinatorial vaccination with both M2e5x VLPs and HA-VLPs generated higher antibody titers, reduced lung inflammation, and provided improved protection against lethal challenge with H5N1 as compared to M2e5x VLP alone (Kang et al., 2019). While this study did not address whether these responses were greater than with HA-VLP vaccination alone, this study demonstrated the utility of combinatorial vaccination approaches to induce broader protection. The M2e5x approach was taken a step further by supplementing an attenuated pandemic A/Netherlands/602/09 LAIV with M2e5x VLPs (Lee et al., 2019). This strategy showed improved protection from morbidity and mortality in mice following viral challenge as compared to vaccination with LAIV alone (Lee et al., 2019). Importantly, incorporating LAIV into this approach allowed for induction of T-cell responses, providing an additional layer of protection against influenza viruses in the respiratory tract (Lee et al., 2019). As with NA-directed approaches, the question remains whether M2e vaccines are able to provide meaningful protection in humans when M2e directed antibodies are only shown to reduce disease severity. Likewise, the modest protection provided by M2e vaccines is a limitation for this vaccination approach as is the breadth of influenza strain protection. While M2e vaccination approaches may not provide as strong of protection as other methods, an exciting possibility for M2e approaches involves the inclusion of M2e into other vaccine strategies. This approach should be considered in the development of other vaccines to enhance the immunogenicity and protection against a broader range of influenza viruses.

## T-Cell-Directed

In comparison to the surface glycoproteins of influenza virus, the internal proteins show higher degrees of conservation among influenza viruses and are often targeted by the antigen-specific $CD8^+$ cytotoxic T cells and $CD4^+$ helper T lymphocytes. Given the importance of T cells in protection against influenza virus infection, vaccines stimulating influenza specific T-cell immunity have been explored as a promising avenue for improving influenza vaccine efficacy and developing a universal influenza vaccine.

Most T-cell-directed vaccine approaches involve targeting conserved internal influenza proteins or other highly conserved epitopes that stimulate T-cell-mediated immune responses. One such vaccine approach involved recombinantly expressing one B-cell epitope and two T-cell epitopes from H3 influenza strains in the flagellin of the *Salmonella* vaccine strain (Ben-Yedidia et al., 1999). After demonstrating the majority of the transplanted human cells in their human/mouse radiation chimeras were $CD8^+$ and $CD4^+$ cells, the recombinant vaccine was shown to elicit virus-specific antibodies and improved viral clearance after lethal challenge (Ben-Yedidia et al., 1999). In order to develop a more broadly protective vaccine, another study sought to identify conserved T-cell reactive regions by analyzing sequences from human and zoonotic influenza A and B viral proteins (Stoloff and Caparros-Wanderley, 2007). The internal proteins M1, NP, and PB1 and the surface protein M2 were found to contain conserved T-cell reactive regions, with M2 and PB1 sharing conserved sequences in both influenza A and B isolates (Stoloff and Caparros-Wanderley, 2007). Mice immunized with an antigen preparation comprised of the six conserved T-cell reactive regions, named FLU-v displayed increased $CD8^+$ T-cell responses and improved survival following challenge with PR8 (Stoloff and Caparros-Wanderley, 2007). While this study did not determine whether the vaccine provides protection against challenge with influenza B infection, it does further demonstrate the importance of stimulating $CD8^+$ T cells to generate protection against influenza infection. This vaccine is currently undergoing phase 2 clinical trials (Bernstein et al., 2019). Another conserved epitope vaccine

undergoing clinical trials involving conserved T-cell and B-cell epitopes is the Multimeric-001 vaccine, which consists of nine conserved epitopes of HA, NP, and M1 from influenza A and B viruses (Atsmon et al., 2012). Healthy human volunteers vaccinated with the Multimeric-001 vaccine exhibited increased IgG titers against the Multimeric-001 vaccine component as well as increased IL-2 and IFNγ secretion (Atsmon et al., 2012). Additionally, sera from vaccinated subjects showed increased complement mediated lysis of infected MDCK cells (Atsmon et al., 2012). This measure was incorporated as an alternative to the hemagglutinin inhibition assay, which they were unable to use because the vaccine lacked the antigenic sites for neutralizing antibodies (Atsmon et al., 2012). While this study shows promise for inducing broad protection in humans, further challenge studies are needed to determine the efficacy of this vaccine.

As with the other vaccine approaches, there have been attempts to generate T-cell-based influenza vaccines through the use of viral vectors. One approach currently in clinical trials involves the use of a modified vaccinia virus Ankara (MVA) that encodes influenza proteins NP and M1 (MVA – NP + M1) (Berthoud et al., 2011; Lillie et al., 2012). A phase 1 clinical trial demonstrated that individuals vaccinated with the MVA – NP + M1 vaccine exhibited increased T-cell responses as measured by IFNγ ELISPOT, with the majority of them being antigen-specific T cells (Berthoud et al., 2011). Next, a phase 2a clinical trial was conducted in which volunteers vaccinated with the MVA – NP + M1 exhibited less severe symptoms and reduced viral shedding after challenge with A/Wisconsin/67/2005 (H3N2) (Lillie et al., 2012). This study was performed with a limited number of human volunteers, but it does highlight another promising avenue for stimulating T-cell-based protection against influenza.

Recently, another viral vector-based vaccine approach has been described using the live-attenuated vaccinia Wyeth backbone expressing HA, NA, M1, M2, and NP from H5N1 along with IL-15 as an adjuvant (Poon et al., 2009). In a mouse model, this vaccine was shown to be protective against both Group 1 and Group 2 HA viruses, including H7N9, H3N2, H1N1, and H7N7 (Valkenburg et al., 2014). Following depletion of $CD4^+$ T cells at the time of vaccination or challenge, vaccinated mice showed reduced survival, suggesting that $CD4^+$ T cells are required for this vaccine-mediated protection (Valkenburg et al., 2018). This vaccine also stimulated increased production of H5-specific $CD4^+$ and $CD8^+$ T cells from human PBMCs, highlighting its potential for protection in humans as well (Valkenburg et al., 2018). Together, these studies illustrate the importance of stimulating T-cell-based immunity for influenza virus protection.

### Challenges to Universal Vaccine Development

An important question when discussing universal vaccine development involves defining the criteria for a successful universal influenza vaccine. Would a universal vaccine provide protection against all influenza A and B strains? Only influenza A or B? Or would the vaccine only provide universal protection within particular HA or NA subtypes? The route of administration should also be considered, especially when determining the durability of protection provided by the vaccine. Furthermore, many of the universal vaccine strategies described above require sequential vaccinations or boosters in order to achieve protection. Considering that individuals may be less likely to return to complete their vaccination regimens, this approach may have a negative impact on vaccine effectiveness from a public health standpoint. Likewise, sequential vaccination regimens with components that change at each booster vaccination may increase the likelihood of error during administration.

While the universal vaccine approaches described above demonstrate novel methods of improving protection against influenza virus infection, a concern that is often overlooked involves the degree to which pre-existing immunity impacts the antibody response to influenza infection and vaccination. This is true for all of the vaccination approaches, including HA, NA, M2e, and T-cell-directed approaches. This concept, referred to as "original antigenic sin," suggests that the first influenza virus variant an individual encounters impacts the immune response to subsequent influenza virus variants (Henry et al., 2018). While controversial, the concept that previous influenza virus exposure impacts antibody responses to influenza vaccination remains an important consideration for vaccine development (Henry et al., 2018). This can also be an important determinant in LAIV approaches, where pre-existing immunity can impact LAIV replication. It is important to note that most of the animal studies done to validate these vaccination approaches are done in naïve animals that lack any previous influenza virus exposure. While unavoidable, this serves to highlight the importance of experiments that more accurately recapitulate the complexity of pre-existing antibody responses in humans as well as thorough clinical trials in order to fully assess the potential for new vaccines to provide broad and long-lasting protection within the population.

## THERAPEUTIC APPROACH: BROADLY NEUTRALIZING ANTIBODIES

While vaccination remains the most efficient method to provide protection against influenza virus infection, there is also significant interest in developing more broadly protective therapeutic methods for prevention and treatment of influenza virus infection. A growing area of interest involves utilizing broadly neutralizing antibodies to protect against influenza virus infection. As with influenza vaccines, a significant focus on broadly neutralizing antibody research revolves around the development of HA stem targeting antibodies, in particular antibodies that neutralize both Group 1 and Group 2 influenza virus HAs. Despite the fact that the majority of neutralizing antibodies targeting the HA stem only protect against Group 1 or Group 2 HAs, HA targeting antibodies capable of neutralizing

both phylogenetic groups have been identified (Corti et al., 2011; Joyce et al., 2016). Further improvements in broadly neutralizing antibody discovery have enabled the development of novel therapies, several of which are currently in different stages of clinical trials. For example, one study was able to identify four broadly neutralizing influenza A antibodies through the activation and enrichment of human peripheral blood mononuclear cells from vaccinated donors (Nakamura et al., 2013). Of these four antibodies, two were able to neutralize both Group 1 and Group 2 influenza A viruses while also improving the survival of mice and ferrets that received the antibody 72 h post infection (Nakamura et al., 2013). Interestingly, co-administration of oseltamivir and the antibody after lethal challenge significantly improved the survival of mice as compared to either therapy alone, demonstrating a potential avenue for improving current therapies through co-administration of both antivirals and neutralizing antibodies (Nakamura et al., 2013). Using a novel antibody design approach, another broadly neutralizing HA antibody, VIS410, was engineered and shown to bind both Group 1 and Group 2 HAs (Tharakaraman et al., 2015). Experiments in mice demonstrated that VIS410 improved survival when administered either prophylactically or 48 h post infection (Tharakaraman et al., 2015). These studies also demonstrated improved protection when co-administered with oseltamivir (Tharakaraman et al., 2015). When administered post infection, VIS401-treated mice showed reduced clinical symptoms of influenza virus infection, including decreased viral spread and reduced damage in the lungs (Baranovich et al., 2016). VIS401 is currently under clinical trials. MEDI8852 is another broadly neutralizing antibody targeting the HA stem that has been shown to interact with both Group 1 and Group 2 HAs (Kallewaard et al., 2016). Even when administered 4 days post lethal virus challenge, MEDI8852 treatment improved survival of mice and protected against several different influenza A virus strains (Kallewaard et al., 2016). Similar results were observed in ferrets, with MEDI8852 providing protection against lethal challenge when administered up to 3 days post infection, further underscoring the therapeutic potential of this antibody (Kallewaard et al., 2016). In addition to several HA targeting monoclonal antibodies, a M2e targeting antibody, TCN-032, is currently in clinical trials (Ramos et al., 2015). Healthy human volunteers infected with H3N2 and treated with TCN-032 exhibited reduced viral shedding and reduced clinical symptoms (Ramos et al., 2015). While the broadly neutralizing antibodies in these studies show promise in providing protection in humans, the studies fail to address the potential for the development of escape mutants that are able to evade antibody neutralization following treatment with these antibodies. Studies examining whether prolonged treatment with these antibodies leads to resistance are important in determining whether these therapeutics can truly provide meaningful protection for a wide range of individuals. Together, these studies underscore the potential for utilizing broadly neutralizing antibodies to improve clinical outcomes of influenza virus infection.

## CONCLUSIONS

Significant resources have been invested into the development of universal influenza virus vaccines and improved therapeutics for the treatment of influenza virus infection. Many universal influenza virus vaccine candidates focus on targeting conserved epitopes of influenza, including either the three influenza surface proteins or highly conserved internal proteins. In doing so, these approaches attempt to elicit broader protection against several strains of influenza as opposed to the strain-specific protection provided by current seasonal influenza vaccines. In attempting to generate a truly universal vaccine, which would offer protection against all influenza strains, these approaches have also highlighted innovative methods for improving current vaccination approaches. By providing protection for a broader range of influenza strains, these approaches have the potential to reduce the need for yearly vaccine reformulations. While influenza strains should still be closely monitored, broader protection against more influenza strains could aid in improving yearly vaccine efficacy. The development and discovery of broadly neutralizing antibodies also illustrate the important contributions these therapeutics can offer in preventing and improving disease outcomes associated with influenza virus infection. Additionally, these studies have provided an insight into novel combinatorial approaches, as seen with studies combining M2e5x VLPs and HA-VLPs to improve vaccine immunogenicity or by combining broadly neutralizing antibodies with current antivirals to improve recovery from influenza virus infection (Nakamura et al., 2013; Tharakaraman et al., 2015; Kang et al., 2019). While the ultimate goal of developing a truly universal influenza virus vaccine has yet to be achieved, the progress made in pursuit of this goal shows the exciting promise of these new approaches for improving influenza disease outcomes and as well as the public health burden associated with inefficient protection against influenza virus infection.

## AUTHOR CONTRIBUTIONS

All authors listed have made a substantial, direct and intellectual contribution to the work, and approved it for publication.

## FUNDING

OV is supported by the NIH Molecular and Cellular Biology training program at the University of Chicago (T32GM007183). BM is supported by NIAID grants (R01AI123359 and R01AI127775).

## ACKNOWLEDGMENTS

We would like to thank Dr. Michael Rebagliati for critical reading of the manuscript.

## REFERENCES


Ainai, A., Tamura, S., Suzuki, T., van Riet, E., Ito, R., Odagiri, T., et al. (2013). Intranasal vaccination with an inactivated whole influenza virus vaccine induces strong antibody responses in serum and nasal mucus of healthy adults. *Hum. Vaccin. Immunother.* 9, 1962–1970. doi: 10.4161/hv.25458

Allen, J. D., Ray, S., and Ross, T. M. (2018). Split inactivated COBRA vaccine elicits protective antibodies against H1N1 and H3N2 influenza viruses. *PLoS One* 13:e0204284. doi: 10.1371/journal.pone.0210043

Ambrose, C. S., Bright, H., and Mallory, R. (2016). Letter to the editor: potential causes of the decreased effectiveness of the influenza A(H1N1)pdm09 strain in live attenuated influenza vaccines. *Euro Surveill.* 21, pii: 30394. doi: 10.2807/1560-7917.ES.2016.21.45.30394

Ampofo, W. K., Azziz-Baumgartner, E., Bashir, U., Cox, N. J., Fasce, R., Giovanni, M., et al. (2015). Strengthening the influenza vaccine virus selection and development process: report of the 3rd WHO informal consultation for improving influenza vaccine virus selection held at WHO headquarters, Geneva, Switzerland, 1-3 April 2014. *Vaccine* 33, 4368–4382. doi: 10.1016/j.vaccine.2015.06.090

Asahi, Y., Yoshikawa, T., Watanabe, I., Iwasaki, T., Hasegawa, H., Sato, Y., et al. (2002). Protection against influenza virus infection in polymeric Ig receptor knockout mice immunized intranasally with adjuvant-combined vaccines. *J. Immunol.* 168, 2930–2938. doi: 10.4049/jimmunol.168.6.2930

Atsmon, J., Kate-Ilovitz, E., Shaikevich, D., Singer, Y., Volokhov, I., Haim, K. Y., et al. (2012). Safety and immunogenicity of multimeric-001--a novel universal influenza vaccine. *J. Clin. Immunol.* 32, 595–603. doi: 10.1007/s10875-011-9632-5

Baranovich, T., Jones, J. C., Russier, M., Vogel, P., Szretter, K. J., Sloan, S. E., et al. (2016). The Hemagglutinin stem-binding monoclonal antibody VIS410 controls influenza virus-induced acute respiratory distress syndrome. *Antimicrob. Agents Chemother.* 60, 2118–2131. doi: 10.1128/AAC.02457-15

Barr, I. G., Donis, R. O., Katz, J. M., McCauley, J. W., Odagiri, T., Trusheim, H., et al. (2018). Cell culture-derived influenza vaccines in the severe 2017–2018 epidemic season: a step towards improved influenza vaccine effectiveness. *NPJ Vaccines* 3, 1–5. doi: 10.1038/s41541-018-0079-z

Belz, G. T., Wodarz, D., Diaz, G., Nowak, M. A., and Doherty, P. C. (2002). Compromised influenza virus-specific CD8(+)-T-cell memory in CD4(+)-T-cell-deficient mice. *J. Virol.* 76, 12388–12393. doi: 10.1128/JVI.76.23.12388-12393.2002

Ben-Yedidia, T., Marcus, H., Reisner, Y., and Arnon, R. (1999). Intranasal administration of peptide vaccine protects human/mouse radiation chimera from influenza infection. *Int. Immunol.* 11, 1043–1051. doi: 10.1093/intimm/11.7.1043

Bernstein, D. I., Guptill, J., Naficy, A., Nachbagauer, R., Berlanda-Scorza, F., Feser, J., et al. (2019). Immunogenicity of chimeric haemagglutinin-based, universal influenza virus vaccine candidates: interim results of a randomised, placebo-controlled, phase 1 clinical trial. *Lancet Infect. Dis.* 20, 80–92. doi: 10.1016/S1473-3099(19)30393-7

Berthoud, T. K., Hamill, M., Lillie, P. J., Hwenda, L., Collins, K. A., Ewer, K. J., et al. (2011). Potent CD8+ T-cell immunogenicity in humans of a novel heterosubtypic influenza A vaccine, MVA-NP+M1. *Clin. Infect. Dis.* 52, 1–7. doi: 10.1093/cid/ciq015

Bessa, J., Schmitz, N., Hinton, H. J., Schwarz, K., Jegerlehner, A., and Bachmann, M. F. (2008). Efficient induction of mucosal and systemic immune responses by virus-like particles administered intranasally: implications for vaccine design. *Eur. J. Immunol.* 38, 114–126. doi: 10.1002/eji.200636959

Black, R. A., Rota, P. A., Gorodkova, N., Klenk, H. D., and Kendal, A. P. (1993). Antibody response to the M2 protein of influenza A virus expressed in insect cells. *J. Gen. Virol.* 74, 143–146. doi: 10.1099/0022-1317-74-1-143

Broecker, F., Liu, S. T. H., Suntronwong, N., Sun, W., Bailey, M. J., Nachbagauer, R., et al. (2019a). A mosaic hemagglutinin-based influenza virus vaccine candidate protects mice from challenge with divergent H3N2 strains. *NPJ Vaccines* 31, 1–9. doi: 10.1038/s41541-019-0126-4

Broecker, F., Zheng, A., Suntrongwong, N., Sun, W., Bailey, M. J., Krammer, F., et al. (2019b). Extending the stalk enhances immunogenicity of the influenza virus neuraminidase. *J. Virol.* 93, 1–12. doi: 10.1128/JVI.00840-19

Bullough, P. A., Hughson, F. M., Skehel, J. J., and Wiley, D. C. (1994). Structure of influenza haemagglutinin at the pH of membrane fusion. *Nature* 371, 37–43. doi: 10.1038/371037a0

Carter, D. M., Darby, C. A., Lefoley, B. C., Crevar, C. J., Alefantis, T., Oomen, R., et al. (2016). Design and characterization of a computationally optimized broadly reactive hemagglutinin vaccine for H1N1 influenza viruses. *J. Virol.* 90, 4720–4734. doi: 10.1128/JVI.03152-15

Clements, M. L., Betts, R. F., Tierney, E. L., and Murphy, B. R. (1986). Serum and nasal wash antibodies associated with resistance to experimental challenge with influenza A wild-type virus. *J. Clin. Microbiol.* 24, 157–160. doi: 10.1128/JCM.24.1.157-160.1986

Corti, D., Voss, J., Gamblin, S. J., Codoni, G., Macagno, A., Jarrossay, D., et al. (2011). A neutralizing antibody selected from plasma cells that binds to group 1 and group 2 influenza A hemagglutinins. *Science* 333, 850–856. doi: 10.1126/science.1205669

Cox, M. M., and Hollister, J. R. (2009). FluBlok, a next generation influenza vaccine manufactured in insect cells. *Biologicals* 37, 182–189. doi: 10.1016/j.biologicals.2009.02.014

David, S., Skowronski, D., Tweed, S., Tuk, T., Danderfer, G., Li, Y., et al. (2005). Epidemiologic profile of a new H3N2 variant of influenza A mismatched to vaccine, 2003-2004 influenza season. *Can. Commun. Dis. Rep.* 31, 21–31. Available at: https://www.canada.ca/en/public-health/services/reports-publications/canada-communicable-disease-report-ccdr/monthly-issue/2005-31/epidemiologic-profile-a-new-h3n2-variant-influenza-a-mismatched-vaccine-2003-2004-influenza-season.html

Denis, J., Acosta-Ramirez, E., Zhao, Y., Hamelin, M. E., Koukavica, I., Baz, M., et al. (2008). Development of a universal influenza A vaccine based on the M2e peptide fused to the papaya mosaic virus (PapMV) vaccine platform. *Vaccine* 26, 3395–3403. doi: 10.1016/j.vaccine.2008.04.052

DiLillo, D. J., Tan, G. S., Palese, P., and Ravetch, J. V. (2014). Broadly neutralizing hemagglutinin stalk-specific antibodies require FcγR interactions for protection against influenza virus in vivo. *Nat. Med.* 20, 143–151. doi: 10.1038/nm.3443

Dreyfus, C., Laursen, N. S., Kwaks, T., Zuijdgeest, D., Khayat, R., Ekiert, D. C., et al. (2012). Highly conserved protective epitopes on influenza B viruses. *Science* 337, 1343–1348. doi: 10.1126/science.1222908

Easterbrook, J. D., Schwartzman, L. M., Gao, J., Kash, J. C., Morens, D. M., Couzens, L., et al. (2012). Protection against a lethal H5N1 influenza challenge by intranasal immunization with virus-like particles containing 2009 pandemic H1N1 neuraminidase in mice. *Virology* 432, 39–44. doi: 10.1016/j.virol.2012.06.003

Ekiert, D. C., Bhabha, G., Elsliger, M. A., Friesen, R. H., Jongeneelen, M., Throsby, M., et al. (2009). Antibody recognition of a highly conserved influenza virus epitope. *Science* 324, 246–251. doi: 10.1126/science.1171491

El Bakkouri, K., Descamps, F., De Filette, M., Smet, A., Festjens, E., Birkett, A., et al. (2011). Universal vaccine based on ectodomain of matrix protein 2 of influenza A: Fc receptors and alveolar macrophages mediate protection. *J. Immunol.* 186, 1022–1031. doi: 10.4049/jimmunol.0902147

Erbelding, E. J., Post, D. J., Stemmy, E. J., Roberts, P. C., Augustine, A. D., Ferguson, S., et al. (2018). A universal influenza vaccine: the strategic plan for the National Institute of Allergy and Infectious Diseases. *J. Infect. Dis.* 218, 347–354. doi: 10.1093/infdis/jiy103

Fernandez Gonzalez, S., Jayasekera, J. P., and Carroll, M. C. (2008). Complement and natural antibody are required in the long-term memory response to influenza virus. *Vaccine* 26(Suppl. 8), I86–I93. doi: 10.1016/j.vaccine.2008.11.057

Fields, B. N., Knipe, D. M., and Howley, P. M. (2013). *Fields virology*. Philadelphia: Lippincott-Raven Publishers.

Gerdil, C. (2003). The annual production cycle for influenza vaccine. *Vaccine* 21, 1776–1779. doi: 10.1016/S0264-410X(03)00071-9

Giles, B. M., Crevar, C. J., Carter, D. M., Bissel, S. J., Schultz-Cherry, S., Wiley, C. A., et al. (2012). A computationally optimized hemagglutinin virus-like particle vaccine elicits broadly reactive antibodies that protect nonhuman primates from H5N1 infection. *J. Infect. Dis.* 205, 1562–1570. doi: 10.1093/infdis/jis232

Giles, B. M., and Ross, T. M. (2011). A computationally optimized broadly reactive antigen (COBRA) based H5N1 VLP vaccine elicits broadly reactive antibodies in mice and ferrets. *Vaccine* 29, 3043–3054. doi: 10.1016/j.vaccine.2011.01.100

Grandea, A. G. III, Olsen, O. A., Cox, T. C., Renshaw, M., Hammond, P. W., Chan-Hui, P. Y., et al. (2010). Human antibodies reveal a protective epitope that is highly conserved among human and nonhuman influenza A viruses. *Proc. Natl. Acad. Sci. USA* 107, 12658–12663. doi: 10.1073/pnas.0911806107

Graves, P. N., Schulman, J. L., Young, J. F., and Palese, P. (1983). Preparation of influenza virus subviral particles lacking the HA1 subunit of hemagglutinin: unmasking of cross-reactive HA2 determinants. *Virology* 126, 106–116. doi: 10.1016/0042-6822(83)90465-8

Grohskopf, L. A., Sokolow, L. Z., Broder, K. R., Olsen, S. J., Karron, R. A., Jernigan, D. B., et al. (2016). Prevention and control of seasonal influenza with vaccines. *MMWR Recomm. Rep.* 65, 1–54. doi: 10.15585/mmwr.rr6505a1

Grohskopf, L. A., Sokolow, L. Z., Broder, K. R., Walter, E. B., Bresee, J. S., Fry, A. M., et al. (2017). Prevention and control of seasonal influenza with vaccines: recommendations of the advisory committee on immunization practices — United States, 2017–18 influenza season. *MMWR Recomm. Rep.* 66, 1–20. doi: 10.15585/mmwr.rr6602a1

Grohskopf, L. A., Sokolow, L. Z., Fry, A. M., Walter, E. B., and Jernigan, D. B. (2018). Update: ACIP recommendations for the use of quadrivalent live attenuated influenza vaccine (LAIV4) - United States, 2018-19 influenza season. *MMWR Morb. Mortal. Wkly Rep.* 67, 643–645. doi: 10.15585/mmwr.mm6722a5

Hai, R., Krammer, F., Tan, G. S., Pica, N., Eggink, D., Maamary, J., et al. (2012). Influenza viruses expressing chimeric hemagglutinins: globular head and stalk domains derived from different subtypes. *J. Virol.* 86, 5774–5781. doi: 10.1128/JVI.00137-12

Halloran, M. E., Piedra, P. A., Longini, I. M. Jr., Gaglani, M. J., Schmotzer, B., Fewlass, C., et al. (2007). Efficacy of trivalent, cold-adapted, influenza virus vaccine against influenza A (Fujian), a drift variant, during 2003-2004. *Vaccine* 25, 4038–4045. doi: 10.1016/j.vaccine.2007.02.060

Hamada, H., Bassity, E., Flies, A., Strutt, T. M., Garcia-Hernandez Mde, L., McKinstry, K. K., et al. (2013). Multiple redundant effector mechanisms of CD8+ T cells protect against influenza infection. *J. Immunol.* 190, 296–306. doi: 10.4049/jimmunol.1200571

Hamada, H., Garcia-Hernandez Mde, L., Reome, J. B., Misra, S. K., Strutt, T. M., McKinstry, K. K., et al. (2009). Tc17, a unique subset of CD8 T cells that can protect against lethal influenza challenge. *J. Immunol.* 182, 3469–3481. doi: 10.4049/jimmunol.0801814

He, X. S., Holmes, T. H., Zhang, C., Mahmood, K., Kemble, G. W., Lewis, D. B., et al. (2006). Cellular immune responses in children and adults receiving inactivated or live attenuated influenza vaccines. *J. Virol.* 80, 11756–11766. doi: 10.1128/JVI.01460-06

He, W., Tan, G. S., Mullarkey, C. E., Lee, A. J., Lam, M. M. W., Krammer, F., et al. (2016). Epitope specificity plays a critical role in regulating antibody-dependent cell-mediated cytotoxicity against influenza A virus. *Proc. Natl. Acad. Sci. USA* 113, 11931–11936. doi: 10.1073/pnas.1609316113

Henry, C., Palm, A. E., Krammer, F., and Wilson, P. C. (2018). From original antigenic sin to the universal influenza virus vaccine. *Trends Immunol.* 39, 70–79. doi: 10.1016/j.it.2017.08.003

Hoft, D. F., Babusis, E., Worku, S., Spencer, C. T., Lottenbach, K., Truscott, S. M., et al. (2011). Live and inactivated influenza vaccines induce similar humoral responses, but only live vaccines induce diverse T-cell responses in young children. *J. Infect. Dis.* 204, 845–853. doi: 10.1093/infdis/jir436

Impagliazzo, A., Milder, F., Kuipers, H., Wagner, M. V., Zhu, X., Hoffman, R. M., et al. (2015). A stable trimeric influenza hemagglutinin stem as a broadly protective immunogen. *Science* 349, 1301–1306. doi: 10.1126/science.aac7263

Ionescu, R. M., Przysiecki, C. T., Liang, X., Garsky, V. M., Fan, J., Wang, B., et al. (2006). Pharmaceutical and immunological evaluation of human papillomavirus viruslike particle as an antigen carrier. *J. Pharm. Sci.* 95, 70–79. doi: 10.1002/jps.20493

Ito, T., Gorman, O. T., Kawaoka, Y., Bean, W. J., and Webster, R. G. (1991). Evolutionary analysis of the influenza A virus M gene with comparison of the M1 and M2 proteins. *J. Virol.* 65, 5491–5498. doi: 10.1128/JVI.65.10.5491-5498.1991

Iwasaki, A., and Pillai, P. S. (2014). Innate immunity to influenza virus infection. *Nat. Rev. Immunol.* 14, 315–328. doi: 10.1038/nri3665

Job, E. R., Ysenbaert, T., Smet, A., Christopoulou, I., Strugnell, T., Oloo, E. O., et al. (2018). Broadened immunity against influenza by vaccination with computationally designed influenza virus N1 neuraminidase constructs. *NPJ Vaccines* 3:55. doi: 10.1038/s41541-018-0093-1

Joyce, M. G., Wheatley, A. K., Thomas, P. V., Chuang, G. Y., Soto, C., Bailer, R. T., et al. (2016). Vaccine-induced antibodies that neutralize group 1 and group 2 influenza A viruses. *Cell* 166, 609–623. doi: 10.1016/j.cell.2016.06.043

Kallen, K. J., Heidenreich, R., Schnee, M., Petsch, B., Schlake, T., Thess, A., et al. (2013). A novel, disruptive vaccination technology: self-adjuvanted RNActive((R)) vaccines. *Hum. Vaccin. Immunother.* 9, 2263–2276. doi: 10.4161/hv.25181

Kallewaard, N. L., Corti, D., Collins, P. J., Neu, U., McAuliffe, J. M., Benjamin, E., et al. (2016). Structure and function analysis of an antibody recognizing all influenza A subtypes. *Cell* 166, 596–608. doi: 10.1016/j.cell.2016.05.073

Kanekiyo, M., Ellis, D., and King, N. P. (2019). New vaccine design and delivery technologies. *J. Infect. Dis.* 219, S88–S96. doi: 10.1093/infdis/jiy745

Kanekiyo, M., Wei, C. J., Yassine, H. M., McTamney, P. M., Boyington, J. C., Whittle, J. R., et al. (2013). Self-assembling influenza nanoparticle vaccines elicit broadly neutralizing H1N1 antibodies. *Nature* 499, 102–106. doi: 10.1038/nature12202

Kang, H. J., Chu, K. B., Lee, D. H., Lee, S. H., Park, B. R., Kim, M. C., et al. (2019). Influenza M2 virus-like particle vaccination enhances protection in combination with avian influenza HA VLPs. *PLoS One* 14:e0216871. doi: 10.1371/journal.pone.0216871

Kilbourne, E. D., Johansson, B. E., and Grajower, B. (1990). Independent and disparate evolution in nature of influenza A virus hemagglutinin and neuraminidase glycoproteins. *Proc. Natl. Acad. Sci. USA* 87, 786–790.

Kim, K. H., Lee, Y. T., Park, S., Jung, Y. J., Lee, Y., Ko, E. J., et al. (2019). Neuraminidase expressing virus-like particle vaccine provides effective cross protection against influenza virus. *Virology* 535, 179–188. doi: 10.1016/j.virol.2019.07.008

Kim, M. C., Song, J. M., Eunjo, O., Kwon, Y. M., Lee, Y. J., Compans, R. W., et al. (2013). Virus-like particles containing multiple M2 extracellular domains confer improved cross-protection against various subtypes of influenza virus. *Mol. Ther.* 21, 485–492. doi: 10.1038/mt.2012.246

Knossow, M., Gaudier, M., Douglas, A., Barrere, B., Bizebard, T., Barbey, C., et al. (2002). Mechanism of neutralization of influenza virus infectivity by antibodies. *Virology* 302, 294–298. doi: 10.1006/viro.2002.1625

Krammer, F., Pica, N., Hai, R., Margine, I., and Palese, P. (2013). Chimeric hemagglutinin influenza virus vaccine constructs elicit broadly protective stalk-specific antibodies. *J. Virol.* 87, 6542–6550. doi: 10.1128/JVI.00641-13

Lamb, Y. N. (2019). Cell-based quadrivalent inactivated influenza virus vaccine (flucelvax((R)) tetra/flucelvax quadrivalent((R))): a review in the prevention of influenza. *Drugs* 79, 1337–1348. doi: 10.1007/s40265-019-01176-z

Lamb, R. A., Zebedee, S. L., and Richardson, C. D. (1985). Influenza virus M2 protein is an integral membrane protein expressed on the infected-cell surface. *Cell* 40, 627–633. doi: 10.1016/0092-8674(85)90211-9

Ledgerwood, J. E., Wei, C. J., Hu, Z., Gordon, I. J., Enama, M. E., Hendel, C. S., et al. (2011). DNA priming and influenza vaccine immunogenicity: two phase 1 open label randomised clinical trials. *Lancet Infect. Dis.* 11, 916–924. doi: 10.1016/S1473-3099(11)70240-7

Lee, Y. T., Kim, K. H., Ko, E. J., Kim, M. C., Lee, Y. N., Hwang, H. S., et al. (2019). Enhancing the cross protective efficacy of live attenuated influenza virus vaccine by supplemented vaccination with M2 ectodomain virus-like particles. *Virology* 529, 111–121. doi: 10.1016/j.virol.2019.01.017

Lillie, P. J., Berthoud, T. K., Powell, T. J., Lambe, T., Mullarkey, C., Spencer, A. J., et al. (2012). Preliminary assessment of the efficacy of a T-cell-based influenza vaccine, MVA-NP+M1, in humans. *Clin. Infect. Dis.* 55, 19–25. doi: 10.1093/cid/cis327

Liu, W. C., Lin, C. Y., Tsou, Y. T., Jan, J. T., and Wu, S. C. (2015). Cross-reactive neuraminidase-inhibiting antibodies elicited by immunization with recombinant neuraminidase proteins of H5N1 and pandemic H1N1 influenza A viruses. *J. Virol.* 89, 7224–7234. doi: 10.1128/JVI.00585-15

Liu, W. C., Nachbagauer, R., Stadlbauer, D., Solorzano, A., Berlanda-Scorza, F., Garcia-Sastre, A., et al. (2019). Sequential immunization with live-attenuated chimeric Hemagglutinin-based vaccines confers Heterosubtypic immunity against influenza A viruses in a preclinical ferret model. *Front. Immunol.* 10:756. doi: 10.3389/fimmu.2019.00756

Lukacher, A. E., Braciale, V. L., and Braciale, T. J. (1984). In vivo effector function of influenza virus-specific cytotoxic T lymphocyte clones is highly specific. *J. Exp. Med.* 160, 814–826. doi: 10.1084/jem.160.3.814

Maier, H. E., Nachbagauer, R., Kuan, G., Ng, S., Lopez, R., Sanchez, N., et al. (2019). Pre-existing anti-neuraminidase antibodies are associated with shortened duration of influenza A (H1N1)pdm virus shedding and illness in naturally infected adults. *Clin. Infect. Dis.* 1–8. doi: 10.1093/cid/ciz639 [Epub ahead of print].

Margine, I., Krammer, F., Hai, R., Heaton, N. S., Tan, G. S., Andrews, S. A., et al. (2013). Hemagglutinin stalk-based universal vaccine constructs protect

against group 2 influenza A viruses. *J. Virol.* 87, 10435–10446. doi: 10.1128/JVI.01715-13

McKinstry, K. K., Strutt, T. M., Kuang, Y., Brown, D. M., Sell, S., Dutton, R. W., et al. (2012). Memory CD4+ T cells protect against influenza through multiple synergizing mechanisms. *J. Clin. Invest.* 122, 2847–2856. doi: 10.1172/JCI63689

Memoli, M. J., Shaw, P. A., Han, A., Czajkowski, L., Reed, S., Athota, R., et al. (2016). Evaluation of antihemagglutinin and antineuraminidase antibodies as correlates of protection in an influenza A/H1N1 virus healthy human challenge model. *MBio* 7:e00417-16. doi: 10.1128/mBio.00417-16

Meseda, C. A., Atukorale, V., Soto, J., Eichelberger, M. C., Gao, J., Wang, W., et al. (2018). Immunogenicity and protection against influenza H7N3 in mice by modified vaccinia virus ankara vectors expressing influenza virus hemagglutinin or neuraminidase. *Sci. Rep.* 8:5364. doi: 10.1038/s41598-018-23712-9

Monto, A. S., Petrie, J. G., Cross, R. T., Johnson, E., Liu, M., Zhong, W., et al. (2015). Antibody to influenza virus neuraminidase: an independent correlate of protection. *J. Infect. Dis.* 212, 1191–1199. doi: 10.1093/infdis/jiv195

Mozdzanowska, K., Maiese, K., Furchner, M., and Gerhard, W. (1999). Treatment of influenza virus-infected SCID mice with nonneutralizing antibodies specific for the transmembrane proteins matrix 2 and neuraminidase reduces the pulmonary virus titer but fails to clear the infection. *Virology* 254, 138–146. doi: 10.1006/viro.1998.9534

Murphy, B. R., Kasel, J. A., and Chanock, R. M. (1972). Association of serum anti-neuraminidase antibody with resistance to influenza in man. *N. Engl. J. Med.* 286, 1329–1332. doi: 10.1056/NEJM197206222862502

Nachbagauer, R., Krammer, F., and Albrecht, R. A. (2018). A live-attenuated prime, inactivated boost vaccination strategy with chimeric hemagglutinin-based universal influenza virus vaccines provides protection in ferrets: a confirmatory study. *Vaccines* 6, 1–11. doi: 10.3390/vaccines6030047

Nachbagauer, R., Liu, W. C., Choi, A., Wohlbold, T. J., Atlas, T., Rajendran, M., et al. (2017). A universal influenza virus vaccine candidate confers protection against pandemic H1N1 infection in preclinical ferret studies. *NPJ Vaccines* 2:26. doi: 10.1038/s41541-017-0026-4

Nakamura, G., Chai, N., Park, S., Chiang, N., Lin, Z., Chiu, H., et al. (2013). An in vivo human-plasmablast enrichment technique allows rapid identification of therapeutic influenza A antibodies. *Cell Host Microbe* 14, 93–103. doi: 10.1016/j.chom.2013.06.004

Neirynck, S., Deroo, T., Saelens, X., Vanlandschoot, P., Jou, W. M., and Fiers, W. (1999). A universal influenza A vaccine based on the extracellular domain of the M2 protein. *Nat. Med.* 5, 1157–1163. doi: 10.1038/13484

Okuno, Y., Isegawa, Y., Sasao, F., and Ueda, S. (1993). A common neutralizing epitope conserved between the hemagglutinins of influenza A virus H1 and H2 strains. *J. Virol.* 67, 2552–2558. doi: 10.1128/JVI.67.5.2552-2558.1993

Petsch, B., Schnee, M., Vogel, A. B., Lange, E., Hoffmann, B., Voss, D., et al. (2012). Protective efficacy of in vitro synthesized, specific mRNA vaccines against influenza A virus infection. *Nat. Biotechnol.* 30, 1210–1216. doi: 10.1038/nbt.2436

Pica, N., Hai, R., Krammer, F., Wang, T. T., Maamary, J., Eggink, D., et al. (2012). Hemagglutinin stalk antibodies elicited by the 2009 pandemic influenza virus as a mechanism for the extinction of seasonal H1N1 viruses. *Proc. Natl. Acad. Sci. USA* 109, 2573–2578. doi: 10.1073/pnas.1200039109

Poon, L. L., Leung, Y. H., Nicholls, J. M., Perera, P. Y., Lichy, J. H., Yamamoto, M., et al. (2009). Vaccinia virus-based multivalent H5N1 avian influenza vaccines adjuvanted with IL-15 confer sterile cross-clade protection in mice. *J. Immunol.* 182, 3063–3071. doi: 10.4049/jimmunol.0803467

Putri, W., Muscatello, D. J., Stockwell, M. S., and Newall, A. T. (2018). Economic burden of seasonal influenza in the United States. *Vaccine* 36, 3960–3966. doi: 10.1016/j.vaccine.2018.05.057

Ramos, E. L., Mitcham, J. L., Koller, T. D., Bonavia, A., Usner, D. W., Balaratnam, G., et al. (2015). Efficacy and safety of treatment with an anti-m2e monoclonal antibody in experimental human influenza. *J. Infect. Dis.* 211, 1038–1044. doi: 10.1093/infdis/jiu539

Renegar, K. B., Small, P. A. Jr., Boykins, L. G., and Wright, P. F. (2004). Role of IgA versus IgG in the control of influenza viral infection in the murine respiratory tract. *J. Immunol.* 173, 1978–1986. doi: 10.4049/jimmunol.173.3.1978

Robertson, C. A., DiazGranados, C. A., Decker, M. D., Chit, A., Mercer, M., and Greenberg, D. P. (2016). Fluzone(R) high-dose influenza vaccine. *Expert Rev. Vaccines* 15, 1495–1505. doi: 10.1080/14760584.2016.1254044

Rogers, G. N., Paulson, J. C., Daniels, R. S., Skehel, J. J., Wilson, I. A., and Wiley, D. C. (1983). Single amino acid substitutions in influenza haemagglutinin change receptor binding specificity. *Nature* 304, 76–78. doi: 10.1038/304076a0

Rota, P. A., Wallis, T. R., Harmon, M. W., Rota, J. S., Kendal, A. P., and Nerome, K. (1990). Cocirculation of two distinct evolutionary lineages of influenza type B virus since 1983. *Virology* 175, 59–68. doi: 10.1016/0042-6822(90)90186-U

Rothbarth, P. H., Groen, J., Bohnen, A. M., de Groot, R., and Osterhaus, A. D. (1999). Influenza virus serology--a comparative study. *J. Virol. Methods* 78, 163–169. doi: 10.1016/S0166-0934(98)00174-8

Rott, R., Becht, H., and Orlich, M. (1974). The significance of influenza virus neuraminidase in immunity. *J. Gen. Virol.* 22, 35–41. doi: 10.1099/0022-1317-22-1-35

Sagawa, H., Ohshima, A., Kato, I., Okuno, Y., and Isegawa, Y. (1996). The immunological activity of a deletion mutant of influenza virus haemagglutinin lacking the globular region. *J. Gen. Virol.* 77, 1483–1487. doi: 10.1099/0022-1317-77-7-1483

Sandbulte, M. R., Jimenez, G. S., Boon, A. C., Smith, L. R., Treanor, J. J., and Webby, R. J. (2007). Cross-reactive neuraminidase antibodies afford partial protection against H5N1 in mice and are present in unexposed humans. *PLoS Med.* 4:e59. doi: 10.1371/journal.pmed.0040059

Skehel, J. J., Bayley, P. M., Brown, E. B., Martin, S. R., Waterfield, M. D., White, J. M., et al. (1982). Changes in the conformation of influenza virus hemagglutinin at the pH optimum of virus-mediated membrane fusion. *Proc. Natl. Acad. Sci. USA* 79, 968–972.

Skowronski, D. M., Janjua, N. Z., De Serres, G., Sabaiduc, S., Eshaghi, A., Dickinson, J. A., et al. (2014). Low 2012-13 influenza vaccine effectiveness associated with mutation in the egg-adapted H3N2 vaccine strain not antigenic drift in circulating viruses. *PLoS One* 9:e92153. doi: 10.1371/journal.pone.0092153

Skowronski, D. M., Masaro, C., Kwindt, T. L., Mak, A., Petric, M., Li, Y., et al. (2007). Estimating vaccine effectiveness against laboratory-confirmed influenza using a sentinel physician network: results from the 2005-2006 season of dual A and B vaccine mismatch in Canada. *Vaccine* 25, 2842–2851. doi: 10.1016/j.vaccine.2006.10.002

Sridhar, S., Begom, S., Bermingham, A., Hoschler, K., Adamson, W., Carman, W., et al. (2013). Cellular immune correlates of protection against symptomatic pandemic influenza. *Nat. Med.* 19, 1305–1312. doi: 10.1038/nm.3350

Sridhar, S., Brokstad, K. A., and Cox, R. J. (2015). Influenza vaccination strategies: comparing inactivated and live attenuated influenza vaccines. *Vaccines* 3, 373–389. doi: 10.3390/vaccines3020373

Stachyra, A., Gora-Sochacka, A., and Sirko, A. (2014). DNA vaccines against influenza. *Acta Biochim. Pol.* 61, 515–522. doi: 10.18388/abp.2014_1873

Steel, J., Lowen, A. C., Wang, T. T., Yondola, M., Gao, Q., Haye, K., et al. (2010). Influenza virus vaccine based on the conserved hemagglutinin stalk domain. *MBio* 1, 1–9. doi: 10.1128/mBio.00018-10

Stoloff, G. A., and Caparros-Wanderley, W. (2007). Synthetic multi-epitope peptides identified in silico induce protective immunity against multiple influenza serotypes. *Eur. J. Immunol.* 37, 2441–2449. doi: 10.1002/eji.200737254

Sui, J., Hwang, W. C., Perez, S., Wei, G., Aird, D., Chen, L. M., et al. (2009). Structural and functional bases for broad-spectrum neutralization of avian and human influenza A viruses. *Nat. Struct. Mol. Biol.* 16, 265–273. doi: 10.1038/nsmb.1566

Sun, W., Kirkpatrick, E., Ermler, M., Nachbagauer, R., Broecker, F., Krammer, F., et al. (2019). Development of influenza B universal vaccine candidates using the "mosaic" Hemagglutinin approach. *J. Virol.* 93, 1–17. doi: 10.1128/JVI.00333-19

Tamura, S., Funato, H., Hirabayashi, Y., Kikuta, K., Suzuki, Y., Nagamine, T., et al. (1990). Functional role of respiratory tract haemagglutinin-specific IgA antibodies in protection against influenza. *Vaccine* 8, 479–485. doi: 10.1016/0264-410X(90)90250-P

Tharakaraman, K., Subramanian, V., Viswanathan, K., Sloan, S., Yen, H. L., Barnard, D. L., et al. (2015). A broadly neutralizing human monoclonal antibody is effective against H7N9. *Proc. Natl. Acad. Sci. USA* 112, 10890–10895. doi: 10.1073/pnas.1502374112

Throsby, M., van den Brink, E., Jongeneelen, M., Poon, L. L., Alard, P., Cornelissen, L., et al. (2008). Heterosubtypic neutralizing monoclonal antibodies cross-protective against H5N1 and H1N1 recovered from human IgM+ memory B cells. *PLoS One* 3:e3942. doi: 10.1371/journal.pone.0003942

Tisa, V., Barberis, I., Faccio, V., Paganino, C., Trucchi, C., Martini, M., et al. (2016). Quadrivalent influenza vaccine: a new opportunity to reduce the influenza burden. *J. Prev. Med. Hyg.* 57, E28–E33. doi: 10.15167/2421-4248/jpmh2016.57.1.600

Valkenburg, S. A., Li, O. T. W., Li, A., Bull, M., Waldmann, T. A., Perera, L. P., et al. (2018). Protection by universal influenza vaccine is mediated by memory CD4 T cells. *Vaccine* 36, 4198–4206. doi: 10.1016/j.vaccine.2018.06.007

Valkenburg, S. A., Li, O. T., Mak, P. W., Mok, C. K., Nicholls, J. M., Guan, Y., et al. (2014). IL-15 adjuvanted multivalent vaccinia-based universal influenza vaccine requires CD4+ T cells for heterosubtypic protection. *Proc. Natl. Acad. Sci. USA* 111, 5676–5681. doi: 10.1073/pnas.1403684111

Vareckova, E., Mucha, V., Ciampor, F., Betakova, T., and Russ, G. (1993). Monoclonal antibodies demonstrate accessible HA2 epitopes in minor subpopulation of native influenza virus haemagglutinin molecules. *Arch. Virol.* 130, 45–56. doi: 10.1007/BF01318995

Webster, R. G., Reay, P. A., and Laver, W. G. (1988). Protection against lethal influenza with neuraminidase. *Virology* 164, 230–237. doi: 10.1016/0042-6822(88)90640-X

Webster, R. G., Sharp, G. B., and Claas, E. C. (1995). Interspecies transmission of influenza viruses. *Am. J. Respir. Crit. Care Med.* 152, S25–S30. doi: 10.1164/ajrccm/152.4_Pt_2.S25

Wilson, I. A., Skehel, J. J., and Wiley, D. C. (1981). Structure of the haemagglutinin membrane glycoprotein of influenza virus at 3 A resolution. *Nature* 289, 366–373. doi: 10.1038/289366a0

Wong, T. M., Allen, J. D., Bebin-Blackwell, A. G., Carter, D. M., Alefantis, T., DiNapoli, J., et al. (2017). Computationally optimized broadly reactive hemagglutinin elicits hemagglutination inhibition antibodies against a panel of H3N2 influenza virus cocirculating variants. *J. Virol.* 91, 1–19. doi: 10.1128/JVI.01581-17

Wu, N. C., Lv, H., Thompson, A. J., Wu, D. C., Ng, W. W. S., Kadam, R. U., et al. (2019). Preventing an antigenically disruptive mutation in egg-based H3N2 seasonal influenza vaccines by mutational incompatibility. *Cell Host Microbe* 25, 836–844.e5. doi: 10.1016/j.chom.2019.04.013

Wu, N. C., Zost, S. J., Thompson, A. J., Oyen, D., Nycholat, C. M., McBride, R., et al. (2017). A structural explanation for the low effectiveness of the seasonal influenza H3N2 vaccine. *PLoS Pathog.* 13:e1006682. doi: 10.1371/journal.ppat.1006682

Yap, K. L., Ada, G. L., and McKenzie, I. F. (1978). Transfer of specific cytotoxic T lymphocytes protects mice inoculated with influenza virus. *Nature* 273, 238–239. doi: 10.1038/273238a0

Yassine, H. M., Boyington, J. C., McTamney, P. M., Wei, C. J., Kanekiyo, M., Kong, W. P., et al. (2015). Hemagglutinin-stem nanoparticles generate heterosubtypic influenza protection. *Nat. Med.* 21, 1065–1070. doi: 10.1038/nm.3927

Zebedee, S. L., and Lamb, R. A. (1988). Influenza A virus M2 protein: monoclonal antibody restriction of virus growth and detection of M2 in virions. *J. Virol.* 62, 2762–2772. doi: 10.1128/JVI.62.8.2762-2772.1988

Zharikova, D., Mozdzanowska, K., Feng, J., Zhang, M., and Gerhard, W. (2005). Influenza type A virus escape mutants emerge in vivo in the presence of antibodies to the ectodomain of matrix protein 2. *J. Virol.* 79, 6644–6654. doi: 10.1128/JVI.79.11.6644-6654.2005

Zost, S. J., Parkhouse, K., Gumina, M. E., Kim, K., Diaz Perez, S., Wilson, P. C., et al. (2017). Contemporary H3N2 influenza viruses have a glycosylation site that alters binding of antibodies elicited by egg-adapted vaccine strains. *Proc. Natl. Acad. Sci. USA* 114, 12578–12583. doi: 10.1073/pnas.1712377114

**Conflict of Interest:** The authors declare that the research was conducted in the absence of any commercial or financial relationships that could be construed as a potential conflict of interest.

*Copyright © 2020 Vogel and Manicassamy. This is an open-access article distributed under the terms of the Creative Commons Attribution License (CC BY). The use, distribution or reproduction in other forums is permitted, provided the original author(s) and the copyright owner(s) are credited and that the original publication in this journal is cited, in accordance with accepted academic practice. No use, distribution or reproduction is permitted which does not comply with these terms.*

frontiers in Microbiology

REVIEW
published: 11 February 2020
doi: 10.3389/fmicb.2020.00150

# Antiviral Drugs Against Severe Fever With Thrombocytopenia Syndrome Virus Infection

*Mutsuyo Takayama-Ito and Masayuki Saijo**

*Department of Virology I, National Institute of Infectious Diseases, Tokyo, Japan*

Severe fever with thrombocytopenia syndrome (SFTS) is an emerging tick-borne infectious disease caused by SFTS virus (SFTSV), which is a novel bunyavirus. SFTSV was first isolated from patients who presented with fever, thrombocytopenia, leukocytopenia, and multiorgan dysfunction in China. Subsequently, it was found to be widely distributed in Southeast Asia (Korea, Japan, and Vietnam). SFTSV can be transmitted not only from ticks but also from domestic animals, companion animals, and humans. Because the case fatality rate of SFTS is high (6–30%), development of specific and effective treatment for SFTS is required. Studies of potential antiviral drugs for SFTS-specific therapy have been conducted on existing or newly discovered agents *in vitro* and *in vivo*, with ribavirin and favipiravir being the most promising candidates. While animal experiments and retrospective studies have demonstrated the limited efficacy of ribavirin, it was also speculated that ribavirin would be effective in patients with a viral load $<1 \times 10^6$ copies/mL. Favipiravir showed higher efficacy than ribavirin against SFTSV in *in vitro* assays and greater efficacy in animal models, even administrated 3 days after the virus inoculation. Although clinical trials evaluating the efficacy of favipiravir in SFTS patients in Japan are underway, this has yet to be confirmed. Other drugs, including hexachlorophene, calcium channel blockers, 2′-fluoro-2′-deoxycytidine, caffeic acid, amodiaquine, and interferons, have also been evaluated for their inhibitory efficacy against SFTSV. Among them, calcium channel blockers are promising because in addition to their efficacy *in vitro* and *in vivo*, retrospective clinical data have indicated that nifedipine, one of the calcium channel blockers, reduced the case fatality rate by >5-fold. Although further research is necessary to develop SFTS-specific therapy, considerable progress has been achieved in this area. Here we summarize and discuss recent advances in antiviral drugs against SFTSV.

**Keywords: severe fever with thrombocytopenia syndrome, severe fever with thrombocytopenia syndrome virus, antiviral, ribavirin, favipiravir**

OPEN ACCESS

***Edited by:***
*Lijun Rong,*
*The University of Illinois at Chicago, United States*

***Reviewed by:***
*Takashi Irie,*
*Hiroshima University, Japan*
*Alexander Freiberg,*
*The University of Texas Medical Branch at Galveston, United States*

****Correspondence:***
*Masayuki Saijo*
*msaijo@nih.go.jp*

***Specialty section:***
*This article was submitted to Virology, a section of the journal Frontiers in Microbiology*

***Received:*** *30 September 2019*
***Accepted:*** *22 January 2020*
***Published:*** *11 February 2020*

***Citation:***
*Takayama-Ito M and Saijo M (2020) Antiviral Drugs Against Severe Fever With Thrombocytopenia Syndrome Virus Infection. Front. Microbiol. 11:150. doi: 10.3389/fmicb.2020.00150*

## INTRODUCTION

Severe fever with thrombocytopenia syndrome (SFTS) is an emerging tick-borne infectious disease caused by SFTS virus (SFTSV), a novel bunyavirus classified into the genus *Phlebovirus* and family *Bunyaviridae* according to the previous nomenclature by the International Committee of Taxonomy of Viruses (ICTV). However, according to the nomenclature by the ICTV, SFTSV has

been classified into the Genus *Banyangvirus*, Family *Phenuiviridae* and re-named as *Huaiyangshan banyangvirus*. In this review article, we have referred to it as "SFTSV." SFTSV is a negative-stranded RNA virus and its genome comprises of three segments, designated as large (L), medium (M), and small (S). The L and M segments encode the RNA dependent RNA polymerase (RdRp) and glycoprotein precursors (Gn and Gc), respectively, and S segment encodes nucleoprotein and nonstructural proteins. The RdRp of SFTSV is responsible for viral replication and is a major target of nucleoside analogs, which are used as therapeutic antiviral drugs. The Gn and Gc are presented on the surface of the virion and are the main targets of neutralizing antibodies. SFTSV was first isolated from patients who presented with fever, thrombocytopenia, leukocytopenia, and multiorgan dysfunction in Hubei and Henan provinces in Central China (Yu et al., 2011). Subsequently, the virus was isolated from sick patients in Japan and South Korea, indicating that SFTSV was endemic not only to China, but also to South Korea and Japan (Kim et al., 2013; Takahashi et al., 2014). In addition, recent studies have reported SFTS as endemic to Vietnam (Tran et al., 2019) and Xinjiang, China (Zhu et al., 2019), indicating that the distribution of SFTSV in Southeast Asia might be much more extensive than expected. Humans become infected mainly via tick-bites, but through close contact with animals such as cats, and dogs and human-to-human transmission has also been reported (Gai et al., 2012; Niu et al., 2013; Kida et al., 2019). The case fatality rate of SFTS is found to vary between 6 and 30% in Japan and South Korea, with a fatality rate of approximately 30% (Choi et al., 2016; Kato et al., 2016). Although World Health Organization listed SFTS as a disease requiring urgent research and development (World Health Organization, 2017), there is no available effective SFTS treatment.

The development of vaccines against SFTSV infection has been attempted (Dong et al., 2019; Kwak et al., 2019). The development of specific treatment for SFTS is crucial because SFTSV infection is relatively rare and the affected patients are mainly elderly. Some proposed treatments for SFTS include steroid pulse therapy (Nakamura et al., 2018), plasma exchange (Oh et al., 2014; Yoo et al., 2019), and antiviral drugs (Saijo, 2018); however, their effectiveness remains unclear.

SFTSV infects a variety of cultured cells, including L929, Vero E6, Vero, and DH82 cells (Yu et al., 2011). Several studies have been conducted to identify effective antiviral agents against SFTSV by screening compound libraries or testing agents that are effective against other viruses (**Table 1**). Because it has been suggested that antiviral drugs may potentially be effective in treatment of multiple viral infections, testing approved drugs is considered as a reasonable strategy (De Clercq and Li, 2016).

Sufficient animal models are required to evaluate the efficacy of antiviral drugs in the treatment of SFTSV infections. However, adult mice and hamsters are not susceptible to SFTSV infection (Jin et al., 2012) and non-human primate models show only mild symptoms similar to those of SFTS in humans (Jin et al., 2015). Only several immunodeficient or immature animal models are available (Gowen and Hickerson, 2017). Mice deficient in α/β interferon receptor ($IFNAR^{-/-}$) (Liu et al., 2014; Tani et al., 2016) and mice and Syrian hamsters deficient for the gene encoding signal transducer and the activator of transcription 2 ($STAT2^{-/-}$) (Gowen et al., 2017; Yoshikawa et al., 2019) were found to be susceptible to SFTSV infection following subcutaneous inoculation, and newborn mice and rats were susceptible to SFTSV infection when inoculated intracerebrally (Chen et al., 2012; Zivcec et al., 2013; Ning et al., 2019). **Table 2** presents animal models that have been used to determine the efficacy of antiviral drugs against SFTSV infections.

In this review article, we summarize and discuss recent advancements made in SFTSV treatment using antiviral drugs.

## POTENTIAL THERAPEUTIC DRUGS AGAINST SFTS

### Ribavirin

Ribavirin, a nucleotide analog, exerts a broad spectrum of antiviral activity against various viruses, such as respiratory syncytial virus, influenza, measles, herpesvirus, human immunodeficiency virus, Lassa virus, and [in combination with interferon (IFN)-α] hepatitis C virus. Ribavirin can be administered orally, intravenously, or via a nebulizer (Snell, 2001). The proposed mechanisms of action of ribavirin against viruses are indirect (inosine monophosphate dehydrogenase inhibition and immunomodulatory effects) as well as direct (interference with RNA capping, polymerase inhibition, and lethal mutagenesis) (Graci and Cameron, 2006).

Shimojima et al. (2014) first reported the efficacy of ribavirin *in vitro* using three cell lines: monkey kidney-derived Vero, human hepatoma-derived Huh7, and human osteosarcoma-derived U2OS cells. When treated with ribavirin before and during infection with SFTSV, the 99% inhibitory concentration ($IC_{99}$) of ribavirin was 263, 83, and 78 μM in Vero, Huh7, and U2OS cells, respectively (**Table 1**). However, when Vero cells were treated with ribavirin 3 days after the inoculation, the inhibitory effect was dramatically decreased, suggesting that ribavirin could be used as post-exposure prophylaxis for the prevention of SFTS and also mentioned that ribavirin could be effective as part of a combination therapy to treat SFTS patients (Shimojima et al., 2014). The efficacy of ribavirin against SFTSV replication was also observed in another study, where Vero cells infected with a Korean SFTSV strain were treated at 24 and 48 h post inoculation, and the 50% inhibitory concentration ($IC_{50}$) range was 3.69–8.72 μg/mL (Lee et al., 2017) (**Table 1**). Despite several differences in viral strains and treatment procedure, ribavirin suppressed SFTS replication, suggesting that it was effective against various SFTSVs for at least 48 h after SFTSV inoculation.

Shimojima et al. (2015) investigated the improvement in efficacy when ribavirin was used in combination with IFNs. All IFNs showed dose-dependent inhibitory effects when used alone. The $IC_{90}$ of IFNα, IFNβ, and IFNγ was 29 U/ml, 24 U/ml, and 12 ng/ml, respectively, and that of ribavirin was 43 μg/mL (**Table 1**). When IFNs were combined with ribavirin at $IC_{90}$, significant inhibitory effects were observed, with reductions of $>3\ \log_{10}$ in viral titers. This study suggested that the combination

**TABLE 1 |** Efficacy of anti-SFTSV drugs *in vitro*.

| Agent | Cells | Study design | Strain of SFTSV | $IC_{50/90/99}$ | $CC_{50}$ | References |
|---|---|---|---|---|---|---|
| Ribavirin | Vero | Yield reduction | Chinese strain (HB29) | $IC_{99} = 263\,\mu M$ | >1,929 μM | Shimojima et al., 2014 |
| | Huh7 | | | $IC_{99} = 83\,\mu M$ | | |
| | U2OS | | | $IC_{99} = 78\,\mu M$ | | |
| | Vero | Yield reduction | Japanese strain (SPL030) | $IC_{99} = 424\,\mu M$ | >1,929 μM | |
| | Huh7 | | | $IC_{99} = 63\,\mu M$ | | |
| | U2OS | | | $IC_{99} = 73\,\mu M$ | | |
| | Vero | Yield reduction | Japanese strain (SPL030) | $IC_{90} = 176\,\mu M$* | >2,000 μM | Shimojima et al., 2015 |
| | | Yield reduction | Korean isolate strain | $IC_{50} = 15.1–35.7\,\mu M$ | >128 μM | Lee et al., 2017 |
| | | Yield reduction** | Japanese isolate strain | $IC_{50} = 40.1\,\mu M$ | >100 μM | Baba et al., 2017 |
| | | Yield reduction | Chinese strain (HB29) | $IC_{50} = 49.7\,\mu M$ | >320 μM | Smee et al., 2018 |
| Favipiravir | Vero | Yield reduction | Japanese strain (SPL010) | $IC_{50} = 6\,\mu M$, $IC_{90} = 22\,\mu M$ | >1,000 μM | Tani et al., 2016 |
| | | Yield reduction** | Japanese isolate strain | $IC_{50} = 25\,\mu M$ | >100 μM | Baba et al., 2017 |
| Hexachlorophene | Vero, Huh7 | Yield reduction** | Chinese strain (HB29) | $IC_{50} = 1.3\,\mu M$ | 24.3 μM | Yuan et al., 2019 |
| | | | | $IC^{99} = 7.5\,\mu M$ | | |
| Benidipine | Vero | Yield reduction** | Chinese strain | $IC_{50} = 1.412\,\mu M$ | 96.92 μM | Li et al., 2019 |
| Nifedipine | Vero | Yield reduction** | Chinese strain | $IC_{50} = 98\,\mu M$ | >250 μM | |
| 2′-Fluoro-2′-deoxycytidine | Vero | Yield reduction | Chinese strain (HB29) | $IC_{90} = 3.7\,\mu M$ | >320 μM | Smee et al., 2018 |
| Caffeic acid | Huh7.5.1–8 | Yield reduction** | Chinese strain (HB29) | $IC_{50} = 48\,\mu M$ | 7.6 mM | Ogawa et al., 2018 |
| Amodiaquine | Vero | Yield reduction** | Japanese isolates strain | $IC_{50} = 19.1\,\mu M$ | >100 μM | Baba et al., 2017 |
| IFNα | Vero | Yield reduction | Japanese strain (SPL030) | $IC_{90} = 29$ U/ml | >5,000 U/mL | Shimojima et al., 2015 |
| IFNβ | | | | $IC_{90} = 24$ U/ml | >5,000 U/mL | |
| IFNγ | | | | $IC_{90} = 12$ ng/ml | >2,000 ng/mL | |

**Combination with ribavirin and IFNs, virus titers were reduced from 3.2–3.6 log.*
***Titers were determined by RT-PCR of the virus genome.*

of ribavirin with IFNs or other agents that function via different mechanisms might be useful in treating patients with SFTS. Ribavirin has shown a limited protective effect in lethal SFTSV challenges in animal experiments (Tani et al., 2016; Gowen et al., 2017) (**Table 2**). The Chinese Ministry of Health initially approved the use of ribavirin to treat SFTS based on the results of *in vitro* studies (Ministry of Health People's Republic of China, 2011). However, a clinical study in China showed that the case fatality rate was similar between patients who received ribavirin and those who did not (Liu et al., 2013). This study included 311 patients, of whom 54 died; in those who received ribavirin therapy, the platelet counts did not increase and the viral loads did not decrease in comparison with those who did not receive the therapy. Furthermore, although the differences were not statistically significant, it was unexpectedly observed that the patients who received ribavirin therapy had lower platelet counts than those who did not.

Another study reported that two patients, in whom plasma exchange and ribavirin treatment were initiated early, recovered from rapidly progressing SFTS (Oh et al., 2014). In these patients, the platelet counts began to gradually recover after initiating ribavirin treatment. Furthermore, according to a large-scale epidemiological study in China including 2096 patients with laboratory-confirmed SFTS between 2011 and 2017, ribavirin therapy was effective in reducing the case fatality rate from 6.25% (15/240 patients) to 1.16% (2/173 patients) in patients with viral loads of $<1 \times 10^6$ copies/mL (Li et al., 2018). However, no effect was observed among those with a viral load of $>1 \times 10^6$ copies/mL.

## Favipiravir

Favipiravir (T-705), which was discovered and synthesized by Toyama Chemical Co., Ltd., exerts a broad spectrum of activity against various RNA viruses, including the influenza virus, arenaviruses, bunyaviruses, West Nile virus, yellow fever virus, and foot-and-mouth disease virus (Furuta et al., 2009). Favipiravir is converted to its active form, ribofuranosyl-5-triphosphate, by host enzymes and inhibits viral RNA polymerase in the host cells. Only a few reports have indicated resistance to favipiravir *in vitro* (Delang et al., 2014; Goldhill et al., 2018). As shown in **Tables 1**, **2** favipiravir significantly inhibits SFTSV replication *in vitro* (Tani et al., 2016; Baba et al., 2017) and *in vivo* (Tani et al., 2016, 2018; Gowen et al., 2017; Smee et al., 2018). Furthermore, the $IC_{90}$ of favipiravir (22 μM) in Vero cells (Tani et al., 2016) was lower than that of ribavirin (263 μM) (Shimojima et al., 2014).

The efficacy of favipiravir *in vivo* has been examined using animal models (**Table 2**). The intraperitoneal (i.p.) administration of favipiravir at a dose of 60 or 300 mg/kg/day for 5 days completely protected mice from death upon SFTSV infection, causing only a slight reduction in weight (Tani et al., 2016). On the other hand, ∼40% of the mice treated with

**TABLE 2 |** Efficacy of anti-SFTSV drugs *in vivo* animal model.

| Agent | Animals | Dose of agent (times/day) | Route | Treatment | Strain | Dose of virus | Route | Survival (%) | References |
|---|---|---|---|---|---|---|---|---|---|
| Ribavirin | STAT2$^{-/-}$hamster | 75 mg/kg/day (twice) | p.o. | Day 1–11 | Chinese strain (HB29) | 50 PFU | s.c. | 0 | Gowen et al., 2017 |
| | IFNAR$^{-/-}$C57BL/6 | 25 mg/kg/day (once) | i.p. | Day 0–5 | Japanese strain (SPL010) | $10^6$ $TCID_{50}$ | s.c. | 70 | Tani et al., 2016 |
| | | 100 mg/kg/day (once) | | Day 0–5 | | | | 66 | |
| Favipiravir | IFNAR$^{-/-}$C57BL/6 | 60 mg/kg/day (once) | i.p. | Day 0–5 | Japanese strain (SPL010) | $10^6$ $TCID_{50}$ | s.c. | 100 | Tani et al., 2016 |
| | | 300 mg/kg/day (once) | | | | | | 100 | |
| | | 60 mg/kg/day (once) | p.o. | | | | | 100 | |
| | | 300 mg/kg/day (once) | | | | | | 100 | |
| | | 300 mg/kg/day (once) | p.o. | Day 1–6 | | | | 100 | |
| | | | | Day 2–7 | | | | 100 | |
| | | | | Day 3–8 | | | | 100 | |
| | | | | Day 4–9 | | | | 83 | |
| | | | | Day 5–10 | | | | 50 | |
| | | 120 mg/kg/day (twice) | p.o. | Day 0–4 | Japanese strain (SPL010) | $10^6$ $TCID_{50}$ | s.c. | 100 | Tani et al., 2018 |
| | | | | Day 1–5 | | | | 100 | |
| | | | | Day 2–6 | | | | 100 | |
| | | | | Day 3–7 | | | | 100 | |
| | | | | Day 4–8 | | | | 67 | |
| | | | | Day 5–9 | | | | 0 | |
| | | 200 mg/kg/day (twice) | p.o. | Day 0–4 | | | | 100 | |
| | | | | Day 1–5 | | | | 100 | |
| | | | | Day 2–6 | | | | 100 | |
| | | | | Day 3–7 | | | | 100 | |
| | | | | Day 4–8 | | | | 100 | |
| | | | | Day 5–9 | | | | 20 | |
| | | 100 mg/kg/day (twice) | i.p. | Day 0–8 | Chinese strain (HB29) | 3 PFU | s.c. | 90 | Smee et al., 2018 |
| | STAT2$^{-/-}$hamster | 300 mg/kg/day (twice) | p.o. | Day 1–11 | Chinese strain (HB29) | 50 PFU | s.c. | 100 | Gowen et al., 2017 |
| | | 150 mg/kg/day (twice) | | | | | | 100 | |
| Benidipine | C57BL/6 | 15 mg/kg/day (once) | i.g. | Day 0–7 | Chinese strain | $10^5$ $TCID_{50}$ | i.p. | 100* | Li et al., 2019 |
| | Humanized mouse | | | Day 0–10 | | | | 83.3** | |
| Nifedipine | C57BL/6 | 100 mg/kg/day (once) | i.g. | Day 0–7 | Chinese strain | $10^5$ $TCID_{50}$ | i.p. | 100* | |
| | Humanized mice | | | Day 0–10 | | | | 100** | |
| 2′-FdC*** | IFNAR$^{-/-}$C57BL/6 | 50 mg/kg/day (twice) | i.p. | Day 0–8 | Chinese strain (HB29) | 3 PFU | s.c. | 80 | Smee et al., 2018 |
| | | 100 mg/kg/day (twice) | | Day 0–8 | | | | 100 | |
| | | 200 mg/kg/day (twice) | | Day 0–8 | | | | 80 | |
| IFN-γ | 3 days old ICR | 0.5 μg/animal (once) | i.p. | Day −1 | unknown | $1.5 \times 10^3$ $TCID_{50}$ | i.c. | 25 | Ning et al., 2019 |
| | | 0.05 μg/animal (once) | | | | | | 25 | |
| | | 0.5 μg/animal (once) | | Day +1 | unknown | $1.5 \times 10^3$ $TCID_{50}$ | | 0 | |
| | | 0.05 μg/animal (once) | | | | | | | 0 |

**Non-lethal model. The viral loads in spleen and serum were significantly reduced.*

***The fatality rate of the vehicle control group was 57.1%.*

****2′-Fluoro-2′-deoxycytidine.*

*i.g., inguinal; i.p., intraperitoneal; PFU, plaque-forming unit; p.o., oral; s.c., subcutaneous; TCID, tissue culture infective dose.*

ribavirin (i.p.) at a dose of 25 or 100 mg/kg/day lost body weight and died from SFTSV infection with reduction of the case fatality rate. All favipiravir-treated mice survived when the treatment was initiated on or earlier than 3 days post infection, whereas the mice treated at 4 and 5 days post infection exhibited 83% and 50% survival, respectively (Tani et al., 2016). These results demonstrated that favipiravir would be potentially effective for prophylactic use and also for treating of SFTSV infections.

Generally, favipiravir is orally administrated to humans. The oral administration (p.o.) of favipiravir showed similar efficacy to that of i.p. administration in a mouse model (Tani et al., 2016). Furthermore, treatment with favipiravir (300 or 150 mg/kg/day) provided complete protection against a lethal SFTSV challenge in a STAT2 knockout golden Syrian hamster model (Gowen et al., 2017). Additionally, the efficacy of favipiravir at practical dosages of 120 and 200 mg/kg/day p.o. was investigated in a mouse infection model, and all the mice survived when the treatment was initiated at no later than 4 days post infection (Tani et al., 2018).

## Hexachlorophene

Yuan et al. (2019) screened an FDA-approved drug library that contained 1,528 drug compounds and identified five that inhibited SFTSV replication at concentrations of $<10\,\mu M$, including two antibacterial and antifungal disinfectants (hexachlorophene and triclosan), a multi-kinase inhibitor for the treatment of advanced solid organ tumors (regorafenib), a small molecule agonist of the C-mannosylation of thrombopoietin receptor (c-Mpl) for the treatment of immune thrombocytopenic purpura and aplastic anemia (eltrombopag), and an antiprotozoal agent (broxyquinoline). Of them, hexachlorophene was the most potent, with an $IC_{50}$ of $1.3 \pm 0.3\,\mu M$ (RNA load) and $2.6 \pm 0.14\,\mu M$ (plaque reduction) and the highest selectivity index (50% cytotoxic concentration [$CC_{50}$]/$IC_{50}$, 18.7), which was lower than that of the other four antiviral drugs identified (**Table 1**). Furthermore, the results indicated that hexachlorophene treatment interfered with SFTSV entry without affecting virus-host cell attachment to the cells and virus infectivity (Yuan et al., 2019). It was predicted that hexachlorophene would bind to the deep hydrophobic pocket between domains I and III of the SFTSV Gc glycoprotein and would interfere with cell membrane fusion.

Hexachlorophene is an antibacterial compound, a common constituent of soaps and scrubs and is experimentally used as a cholinesterase inhibitor (Hsu et al., 2004). It was reported that hexachlorophene inhibited the viral replication of severe acute respiratory syndrome-related coronavirus *in vitro* by inhibiting 3C-like protease, which is essential for its lifecycle (Hsu et al., 2004).

## Calcium Channel Blockers

Calcium channel blockers (CCBs) reduce the intracellular $Ca^{2+}$ level and are widely used for treating various cardiovascular diseases, including hypertension, angina, and supraventricular arrhythmias. Recently, the antiviral activity of CCBs against ebolavirus (Sakurai et al., 2015), marburgvirus (Dewald et al., 2018), Junín virus (Lavanya et al., 2013), West Nile virus (Scherbik and Brinton, 2010), and Japanese encephalitis virus (Wang et al., 2017) has been reported.

Screening a library of 700 FDA-approved drugs identified the CCBs benidipine hydrochloride and nifedipine as inhibitors of SFTSV replication *in vitro* by impairing virus internalization and reducing genome replication during the post-entry phase (Li et al., 2019). This mechanism did not affect viral binding, fusion, and budding. The results of *in vitro* study suggested that treatment with benidipine hydrochloride or nifedipine inhibited SFTSV replication by reducing virus induced $Ca^{2+}$ influx. The anti-SFTSV effect of these two CCBs was further analyzed in C57BL/6 mice and humanized mouse models (**Table 2**), revealing treatment effects of a reduced viral load, increased platelet count, and decreased fatality rate in the humanized mouse model.

Notably, nifedipine is one of the most widely used drugs for treating hypertension and atherosclerosis in China. Thus, Li et al. (2019) performed a retrospective clinical investigation on a large cohort of 2087 patients with SFTS comprising 83 nifedipine-treated, who received nifedipine before admission and during hospitalization, 48 non-nifedipine-treated ones who received nifedipine before admission but not during hospitalization, and 249 general SFTS patients who did not receive nifedipine at all. The case fatality rate was decreased by >5-fold in the nifedipine-treated group (3.6%) compared with the general SFTS group (19.7%) or non-nifedipine treated group (20.8%) (Li et al., 2019). In contrast with ribavirin, a significant decrease in the case fatality rate was also observed in the nifedipine-treated patients (2.4%) with a high viral load ($>10^6$ copies/mL) when compared with the general SFTS patients (29.0%) and non-nifedipine-treated patients (34.5%). Hematemesis, one of the hemorrhagic manifestations that are closely related to death, was found to occur less frequently in the nifedipine-treated group. In this article, the authors clearly showed the inhibitory effect of benidipine hydrochloride or nifedipine in cultured cells and an animal model. Most importantly, it was found that the nifedipine administration enhanced virus clearance and improved clinical recovery.

## 2′-Fluoro-2′-deoxycytidine

2′-Fluoro-2′-deoxycytidine (2′-FdC) is a nucleoside inhibitor used in anticancer drugs. It inhibits various RNA and DNA viruses *in vitro*, such as Borna virus (Bajramovic et al., 2004), Lassa virus (Welch et al., 2016), Crimean-Congo hemorrhagic fever virus (Welch et al., 2017), influenza virus (Kumaki et al., 2011), and herpesviruses (Wohlrab et al., 1985).

Smee et al. (2018) has shown the antiviral activity of 2′-FdC against various bunyaviruses, such as La Crosse virus, Maporal virus, Punta Toro virus, Rift Valley fever virus, San Angelo virus, Heartland virus, and SFTSV. The $IC_{90}$ of 2′-FdC against SFTSV was $3.7\,\mu M$ in an *in vitro* assay (**Table 1**). This value was much lower than that of ribavirin ($49.7\,\mu M$) in the same study and favipiravir ($22\,\mu M$) in the study conducted by Tani et al. (2016). In an *in vivo* study using $IFNAR^{-/-}$ mice, a 100 mg/kg/day treatment with 2′-FdC was 100% protective against death caused by SFTSV (**Table 2**). However, all the mice treated with 2′-FdC experienced substantial weight loss after SFTSV inoculation, whereas the favipiravir-treated mice displayed very little weight

loss, suggesting that favipiravir was more effective than 2′-FdC in controlling morbidity during the infection (Smee et al., 2018). It was also found that treatments with 100 mg/kg/day of either 2′-FdC or favipiravir significantly reduced the viral titers in the serum. Furthermore, there was a slight discrepancy both in the survival rates and virus titers between mice treated with 100 mg/kg/day of 2′-FdC and those with 200 mg/kg/day of 2′-FdC. The survival rate was 80 vs. 100% for 200- and 100-mg/kg/day treatments, respectively; and the virus titer in the serum of 200 mg/kg/day-treated mice was higher than that of mice receiving the 100-mg/kg/day treatment. It was speculated that this was caused by the limited sample size ($n = 4$ or 5).

## Caffeic Acid

Caffeic Acid (CA) is a coffee-related polyphenol organic compound that can be found in various plants, including coffee beans. Single cup of coffee contains 70–350 mg chlorogenic acid, the ester of caffeic acid (Clifford, 1999). It exerts a variety of biological effects, including the suppression of cancer cells (Tang et al., 2017; Bułdak et al., 2018) and antiviral properties (Wang et al., 2009; Utsunomiya et al., 2014; Ding et al., 2017; Langland et al., 2018).

Ogawa et al. (2018) showed that CA dose-dependently inhibited SFTSV replication in an *in vitro* assay using Huh7.5.1-8 cells, a highly permissive derivative of human hepatoma Huh7 cells. The $IC_{50}$ of CA against SFTSV was 48 μM, and its $CC_{50}$ was 7.6 mM (**Table 1**). Interestingly, pretreatment of SFTSV with CA prior to inoculation effectively reduced the virus copy number in the supernatant of infected cells at 72 h post infection, and the inhibitory effect was significantly reduced when the cells were treated with CA after SFTSV inoculation. Thus, the authors speculated that CA mainly acted on the viral particles or influenced the early stages of SFTSV infection, although it could act on the host cells to inhibit viral genome replication.

## Amodiaquine

Amodiaquine is a novel compound that is routinely prescribed as an antimalarial drug is reported to show antiviral effects against ebolavirus (Gignoux et al., 2016; Sakurai et al., 2018), dengue virus (Boonyasuppayakorn et al., 2014), and zika virus (Balasubramanian et al., 2017). The mechanism of inhibitory activity of amodiaquine against malaria and those viruses remains unclear.

Baba et al. (2017) investigated the effect of amodiaquine and other halogen molecules (fluorine, bromine, and iodine) against the replication of SFTSV *in vitro*. All the derivatives also displayed anti-SFTSV activity, and the $IC_{50}$ was 36.6, 31.1, and 15.6 μM for fluorine bromine, and iodine, respectively (**Table 1**). Among the compounds tested, amodiaquine was identified as a selective inhibitor against SFTSV replication. The $CC_{50}$ and the $IC_{50}$ of amodiaquine was >100 and 19.1 μM, respectively. The $IC_{50}$ of amodiaquine was lower than those of ribavirin (40.1 μM) and favipiravir (25.0 μM).

## IFN-γ

IFN-γ is the only member of type II IFNs. It stimulates macrophage and dendritic cells to induce direct antimicrobial activities by regulating antigen processing and presentation pathways. It was initially thought that activated T cells and activated natural killer cells were the only relevant source of IFN-γ; however, macrophages and dendritic cells can also be stimulated to produce IFN-γ *in vitro* under certain conditions (Thäle and Kiderlen, 2005). Because IFN-γ can directly stimulate the expression of some potential antiviral IFN-stimulating proteins by the STAT1 signaling, it plays an important role in viral infection.

Ning et al. (2019) used enzyme-linked immunosorbent assays to demonstrate that SFTSV infection caused a substantial production of serum IFN-γ in patients with SFTS. In turn, IFN-γ exhibited a robust anti-SFTSV activity in cultured cells. Thereafter, they evaluated the efficacy of IFN-γ as an anti-SFTSV drug *in vivo* in a suckling mouse model, which showed that IFN-γ treatment prior to SFTSV infection significantly reduced mortality, protecting ∼25% of animals from death, whereas all the untreated mice died within 13 days of the SFTSV challenge. When IFN-γ was administrated post SFTSV infection, 100% of the mice died from the virus.

# DISCUSSION

Since then, a considerable number of studies regarding its epidemiological and virological characteristics have been conducted. Ribavirin, one of a broad-spectrum antiviral drug (Beaucourt and Vignuzzi, 2014), is recommended for patients with SFTS in China, and it has been used to treat a considerable number of patients (Ministry of Health People's Republic of China, 2011). The *in vitro* and *in vivo* studies on ribavirin (Shimojima et al., 2014, 2015; Tani et al., 2016; Gowen et al., 2017; Lee et al., 2017) showed the considerable effect. The results of the clinical study conducted by Liu et al. (2013), which showed that ribavirin did not reduce the fatality rate of patients with SFTS, discouraged us from considering ribavirin treatment for treating patients with SFTS. However, Li et al. (2018) reported that ribavirin is effective for early-stage patients with a low viral titer or for the pretreatment of exposed individuals. Nevertheless, in cases of ribavirin administration, patients should be intensely monitored because of the possible adverse events induced by ribavirin such as anemia and hyperamylasemia (Lu et al., 2015).

Favipiravir exhibited higher effectiveness than ribavirin in *in vitro* and *in vivo* studies (Tani et al., 2016, 2018). Meanwhile, favipiravir remained effective when it was used following SFTSV infection in animal models (Tani et al., 2016, 2018; Gowen et al., 2017) indicating its potential as an effective drug for treating SFTS patient. Currently, clinical trials are underway to evaluate the efficacy of favipiravir for treating patients with SFTS in Japan (Cyranoski, 2018; Spengler et al., 2018). Besides, it would be desirable to use intravenous administration because SFTS patients with severe symptoms could have difficulty in taking drugs orally.

Hexachlorophene, an antibacterial compound, was found to be effective for SFTSV in *in vitro* screening using an FDA-approved drug library (Yuan et al., 2019). Because hexachlorophene can cause acute and subacute neurotoxicity

in laboratory animals and humans (Kimbrough, 1973; Ramu et al., 2016), further *in vitro* and *in vivo* studies must be conducted.

CCBs, which are used to control cardiovascular diseases, have demonstrated significant effects against SFTSV replication both *in vitro* and *in vivo* (Li et al., 2019). Notably, retrospectively conducted clinical study suggested that nifedipine remarkably reduced the case fatality rate in SFTS patients (Li et al., 2019). Although nifedipine is administrated consistently for patients with cardiac disease, these findings are valuable for developing potential CCB-based therapeutics for SFTS. It is considered that the efficacy of nifedipine in treating patients with SFTS should be evaluated in a prospective manner. For clinical use, careful consideration of the risk-to-benefit value to the patient would be required because an overdose of CCBs has a high-risk of side effects, such as edema, liver damage, and death. The dose used for *in vivo* mouse study (100 mg/kg/day) was extremely higher than the dose generally used for humans (∼0.2–1.5 mg/kg/day). Still, these findings indicated the potential therapeutic effect of CCB treatment in patients with SFTS.

2′-FdC is considered a viable candidate therapeutic agent against SFTS. Although, 2′-FdC was more effective than favipiravir *in vitro*, *in vivo* efficacy was less than that of favipiravir (Smee et al., 2018). The administration protocol of 2′-FdC should be considered in future studies.

CA shows inhibitory effects against SFTSV *in vitro*. Little is known about the mechanism of the action, but it was considered that CA interacts with the viral particles, showing inhibitory effects (Ogawa et al., 2018). Because there are limited reports regarding antiviral effects of CA or chlorogenic acid *in vivo* (Wang et al., 2009; Ding et al., 2017), further studies are needed.

Baba et al. (2017) showed that amodiaquine and other halogen molecules effectively inhibited the propagation of SFTSV *in vitro*. Amodiaquine is widely used as an antimalarial drug and can be administered at a low cost. The efficacy of amodiaquine *in vivo* should be evaluated.

The anti-SFTSV efficacy of IFN-γ both *in vitro* and *in vivo* (Ning et al., 2019) was reported. Because IFN-γ is an FDA-approved drug, it has been suggested as a candidate antiviral drug for SFTSV alone or in combination with other drugs (Shimojima et al., 2015).

The efficacy of antibody-based treatment has been studied against SFTS disease. Generally, antibodies play a critical role in the treating a wide variety of viral diseases; such as acquired immunodeficiency syndrome (Ferrari et al., 2016), diseases caused by ebola virus (Mendoza et al., 2017) and influenza (Nachbagauer and Krammer, 2017). Antibody drugs neutralize viruses or bind to the virion to enhance antigen uptake by cytotoxic T cells, making them highly specific for the target virus. It was reported that antiserum of a patient recovered from SFTS completely protected mice from the lethal infection of SFTSV (Shimada et al., 2015). It was also shown that antibodies against SFTSV Gn protein significantly reduced the fatality rate in mice infected with SFTSV, even when treatment was initiated from 3 days post inoculation (Kim et al., 2019). These reports suggested that antibodies alone or in combination with antiviral drugs could be used to treat patients with SFTS.

There are two studies for developing vaccines against SFTSV infection (Dong et al., 2019; Kwak et al., 2019). A recombinant vesicular stomatitis virus expressing SFTSV antigen completely protected mice from SFTSV infection (Dong et al., 2019). A DNA vaccine expressing antigens of SFTSV, elicited both neutralizing antibody response and SFTSV-specific T cell response and protected aged-ferrets from the lethal SFTSV infection (Kwak et al., 2019). Safe and effective vaccines against SFTS should be developed.

Because all these mentioned drugs have inhibitory effect on SFTSV replication, combination therapies with some drugs, which have different mechanisms of action should be considered. Although, it should be considered that an antiviral drug against SFTS would be administrated to a pre-symptomatic exposed individual, the main targets of these drugs are certainly patients with suggestive symptoms of SFTS. SFTSV circulates between mammals and ticks in Southeast Asia, indicating that we cannot escape the risk of being infected with SFTSV. SFTS is classified in a disease category of viral hemorrhagic fever with high case fatality rate. Recently, cases of SFTS have been reported, wherein the patients were infected with SFTSV from cats, which might be infected with SFTSV from tick (Kida et al., 2019). Therefore, we are hopeful that specific treatments with antiviral agents will be developed and approved for patients with SFTS as early as possible.

## AUTHOR CONTRIBUTIONS

MS and MT-I conceptualized and designed the study. MT-I collected and assembled the data and drafted the manuscript. MS critically revised the manuscript.

## FUNDING

Some part of this review article was obtained through the studies financially supported from the Ministry of Health, Labour, and Welfare (grant number H25-Shinko-Shitei-009), Japan Agency for Medical Research and Development (AMED, 16fk0108002j, 17fk0108202j, 18fk0108002j, 19fk0108081j, 19fk0108072). The funders had no role in study design, data collection and analysis, decision to publish, or preparation of the manuscript.

## ACKNOWLEDGMENTS

We thank all the staff members working for the research project for SFTS in Japan, especially, Dr. Hideki Tani, Dr. Masayuki Shimojima, Dr. Takeshi Kurosu, Dr. Tomoki Yoshikawa, Dr. Hirofumi Kato, Dr. Masaaki Satoh, Department of Virology 1, National Institute of Infectious Diseases, Tokyo, Japan. The present affiliate of Dr. Hideki Tani is the Department of Virology, Graduate School of Medicine and Pharmaceutical Sciences, University of Toyama, Toyama, Japan.

## REFERENCES


Baba, M., Toyama, M., Sakakibara, N., Okamoto, M., Arima, N., and Saijo, M. (2017). Establishment of an antiviral assay system and identification of severe fever with thrombocytopenia syndrome virus inhibitors. *Antivir. Chem. Chemother.* 25, 83–89. doi: 10.1177/2040206617740303

Bajramovic, J. J., Volmer, R., Syan, S., Pochet, S., and Gonzalez-Dunia, D. (2004). 2'-fluoro-2'-deoxycytidine inhibits Borna disease virus replication and spread. *Antimicrob. Agents Chemother.* 48, 1422–1425. doi: 10.1128/AAC.48.4.1422-1425.2004

Balasubramanian, A., Teramoto, T., Kulkarni, A. A., Bhattacharjee, A. K., and Padmanabhan, R. (2017). Antiviral activities of selected antimalarials against dengue virus type 2 and Zika virus. *Antiviral Res.* 137, 141–150 doi: 10.1016/j.antiviral.2016.11.015

Beaucourt, S., and Vignuzzi, M. (2014). Ribavirin: a drug active against many viruses with multiple effects on virus replication and propagation. Molecular basis of ribavirin resistance. *Curr. Opin. Virol.* 8, 10–15. doi: 10.1016/j.coviro.2014.04.011

Boonyasuppayakorn, S., Reichert, E. D., Manzano, M., Nagarajan, K., and Padmanabhan, R. (2014). Amodiaquine, an antimalarial drug, inhibits dengue virus type 2 replication and infectivity. *Antiviral Res.* 106, 125–134. doi: 10.1016/j.antiviral.2014.03.014

Bułdak, R. J., Hejmo, T., Osowski, M., Bułdak, Ł., Kukla, M., Polaniak, R., et al. (2018). The impact of coffee and its selected bioactive compounds on the development and progression of colorectal cancer *in vivo* and *in vitro*. *Molecules* 23:E3309. doi: 10.3390/molecules23123309

Chen, X. P., Cong, M. L., Li, M. H., Kang, Y. J., Feng, Y. M., Plyusnin, A., et al. (2012). Infection and pathogenesis of Huaiyangshan virus (a novel tick-borne bunyavirus) in laboratory rodents. *J. Gen. Virol.* 93, 1288–1293. doi: 10.1099/vir.0.041053-0

Choi, S. J., Park, S. W., Bae, I. G., Kim, S. H., Ryu, S. Y., Kim, H. A., et al. (2016). Severe fever with thrombocytopenia syndrome in South Korea, 2013-2015. *PLoS Negl. Trop. Dis.* 10:e0005264. doi: 10.1371/journal.pntd.0005264

Clifford, M. N. (1999). Chlorogenic acids and other cinnamates– nature, occurrence and dietary burden. *J. Sci. Food. Agric.* 79:362–372. doi: 10.1002/(SICI)1097-0010(19990301)79:3<362::AID-JSFA256>3.0.CO;2-D

Cyranoski, D. (2018). East Asia braces for surge in deadly tick-borne virus news. *Nature* 556, 282–283. doi: 10.1038/d41586-018-04486-6

De Clercq, E., and Li, G. (2016). Approved antiviral drugs over the past 50 years. *Clin. Microbiol. Rev.* 29, 695–747. doi: 10.1128/CMR.00102-15

Delang, L., Guerrero, N. S., Tas, A., Quérat, G., Pastorino, B., Froeyen, M., et al. (2014). Mutations in the chikungunya virus non-structural proteins cause resistance to favipiravir (T-705), a broad-spectrum antiviral. *J. Antimicrob. Chemother.* 69, 2770–2784. doi: 10.1093/jac/dku209

Dewald, L. E., Dyall, J., Sword, J. M., Torzewski, L., Zhou, H., Postnikova, E., et al. (2018). The calcium channel blocker bepridil demonstrates efficacy in the murine model of marburg virus disease. *J. Infect. Dis.* 22, S588–S591. doi: 10.1093/infdis/jiy332

Ding, Y., Cao, Z., Cao, L., Ding, G., Wang, Z., and Xiao, W. (2017). Antiviral activity of chlorogenic acid against influenza A (H1N1/H3N2) virus and its inhibition of neuraminidase. *Sci. Rep.* 7, 1–11. doi: 10.1038/srep45723

Dong, F., Li, D., Wen, D., Li, S., Zhao, C., Qi, Y., et al. (2019). Single dose of a rVSV-based vaccine elicits complete protection against severe fever with thrombocytopenia syndrome virus. *NPJ Vaccines* 4:5. doi: 10.1038/s41541-018-0096-y

Ferrari, G., Haynes, B. F., Koenig, S., Nordstrom, J. L., Margolis, D. M., and Tomaras, G. D. (2016). Envelope-specific antibodies and antibody-derived molecules for treating and curing HIV infection. *Nat. Rev. Drug Discov.* 15, 823–834. doi: 10.1038/nrd.2016.173

Furuta, Y., Takahashi, K., Shiraki, K., Sakamoto, K., Smee, D. F., Barnard, D. L., et al. (2009). T-705 (favipiravir) and related compounds: novel broad-spectrum inhibitors of RNA viral infections. *Antiviral Res.* 82, 95–102. doi: 10.1016/j.antiviral.2009.02.198

Gai, Z., Liang, M., Zhang, Y., Zhang, S., Jin, C., Wang, S. W., et al. (2012). Person-to-person transmission of severe fever with thrombocytopenia syndrome bunyavirus through blood contact. *Clin. Infect. Dis.* 54, 249–252. doi: 10.1093/cid/cir776

Gignoux, E., Azman, A. S., De Smet, M., Azuma, P., Massaquoi, M., Job, D., et al. (2016). Effect of artesunate.amodiaquine on mortality related to Ebola virus disease. *N. Engl. J. Med.* 374, 23–32. doi: 10.1056/NEJMoa1504605

Goldhill, D. H., Te Velthuis, A. J. W., Fletcher, R. A., Langat, P., Zambon, M., Lackenby, A., et al. (2018). The mechanism of resistance to favipiravir in influenza. *Proc. Natl. Acad. Sci. U.S.A.* 115, 11613–11618. doi: 10.1073/pnas.1811345115

Gowen, B. B., and Hickerson, B. T. (2017). Hemorrhagic fever of bunyavirus etiology: disease models and progress towards new therapies. *J. Microbiol.* 55, 183–195. doi: 10.1007/s12275-017-7029-8

Gowen, B. B., Westover, J. B., Miao, J., Van Wettere, A. J., Rigas, J. D., Hickerson, B. T., et al. (2017). Modeling severe fever with thrombocytopenia syndrome virus infection in golden syrian hamsters: importance of STAT2 in preventing disease and effective treatment with favipiravir. *J. Virol.* 91, e01942–e01916. doi: 10.1128/JVI.01942-16

Graci, J. D., and Cameron, C. E. (2006). Mechanisms of action of ribavirin against distinct viruses. *Rev. Med. Virol.* 16, 37–48. doi: 10.1002/rmv.483

Hsu, J. T. A., Kuo, C. J., Hsieh, H. P., Wang, Y. C., Huang, K. K., Lin, C. P. C., et al. (2004). Evaluation of metal-conjugated compounds as inhibitors of 3CL protease of SARS-CoV. *FEBS Lett.* 574, 116–120. doi: 10.1016/j.febslet.2004.08.015

Jin, C., Jiang, H., Liang, M., Han, Y., Gu, W., Zhang, F., et al. (2015). SFTS virus infection in nonhuman primates. *J. Infect. Dis.* 211, 915–925. doi: 10.1093/infdis/jiu564

Jin, C., Liang, M., Ning, J., Gu, W., Jiang, H., Wu, W., et al. (2012). Pathogenesis of emerging severe fever with thrombocytopenia syndrome virus in C57/BL6 mouse model. *Proc. Natl. Acad. Sci. U.S.A.* 109, 10053–10058. doi: 10.1073/pnas.1120246109

Kato, H., Yamagishi, T., Shimada, T., Matsui, T., Shimojima, M., Saijo, M., et al. (2016). Epidemiological and clinical features of severe fever with thrombocytopenia syndrome in Japan, 2013-2014. *PLoS ONE* 11:e0165207. doi: 10.1371/journal.pone.0165207

Kida, K., Matsuoka, Y., Shimoda, T., Matsuoka, H., Yamada, H., Saito, T., et al. (2019). A case of cat-to-human transmission of severe fever with thrombocytopenia syndrome virus. *Jpn. J. Infect. Dis.* 72, 356–358. doi: 10.7883/yoken.JJID.2018.526

Kim, K. H., Kim, J., Ko, M., Chun, J. Y., Kim, H., Kim, S., et al. (2019). An anti-Gn glycoprotein antibody from a convalescent patient potently inhibits the infection of severe fever with thrombocytopenia syndrome virus. *PLoS Pathog.* 15:e1007375. doi: 10.1371/journal.ppat.1007375

Kim, K. H., Yi, J., Kim, G., Choi, S. J., Jun, K. I., Kim, N. H., et al. (2013). Severe fever with thrombocytopenia syndrome, South Korea, 2012. *Emerg. Infect. Dis.* 19, 1892–1894 doi: 10.3201/eid1911.130792

Kimbrough, R. D. (1973). Review of the toxicity of hexachlorophene, including its neurotoxicity. *J. Clini. Pharmacol.* 13, 439–444. doi: 10.1002/j.1552-4604.1973.tb00196.x

Kumaki, Y., Day, C. W., Smee, D. F., Morrey, J. D., and Barnard, D. L. (2011). *In vitro* and *in vivo* efficacy of fluorodeoxycytidine analogs against highly pathogenic avian influenza H5N1, seasonal, and pandemic H1N1 virus infections. *Antiviral Res.* 92, 329–340. doi: 10.1016/j.antiviral.2011.09.001

Kwak, J. E., Kim, Y. I., Park, S. J., Yu, M. A., Kwon, H. I., Eo, S., et al. (2019). Development of a SFTSV DNA vaccine that confers complete protection against lethal infection in ferrets. *Nat. Commun.* 10, 1–11. doi: 10.1038/s41467-019-11815-4

Langland, J., Jacobs, B., Wagner, C. E., Ruiz, G., and Cahill, T. M. (2018). Antiviral activity of metal chelates of caffeic acid and similar compounds towards herpes simplex, VSV-Ebola pseudotyped and vaccinia viruses. *Antiviral Res.* 160, 143–150. doi: 10.1016/j.antiviral.2018.10.021

Lavanya, M., Cuevas, C. D., Thomas, M., Cherry, S., and Ross, S. R. (2013). siRNA screen for genes that affect Junín virus entry uncovers voltage-gated calcium channels as a therapeutic target. *Sci. Transl. Med.* 5:204ra131. doi: 10.1126/scitranslmed.3006827

Lee, M. J., Kim, K. H., Yi, J., Choi, S. J., Choe, P. G., Park, W. B., et al. (2017). *In vitro* antiviral activity of ribavirin against severe fever with thrombocytopenia syndrome virus. *Korean J. Intern. Med.* 32, 731–737. doi: 10.3904/kjim.2016.109

Li, H., Lu, Q., Bin, X. B., Zhang, S. F., Liu, K., Du, J., et al. (2018). Epidemiological and clinical features of laboratory-diagnosed severe fever with

thrombocytopenia syndrome in China, 2011–17: a prospective observational study. *Lancet Infect. Dis.* 18, 1127–1137. doi: 10.1016/S1473-3099(18)30293-7

Li, H., Zhang, L. K., Li, S. F., Zhang, S. F., Wan, W. W., Zhang, Y. L., et al. (2019). Calcium channel blockers reduce severe fever with thrombocytopenia syndrome virus (SFTSV) related fatality. *Cell Res.* 29, 739–753. doi: 10.1038/s41422-019-0214-z

Liu, W., Lu, Q. B., Cui, N., Li, H., Wang, L. Y., Liu, K., et al. (2013). Case-fatality ratio and effectiveness of ribavirin therapy among hospitalized patients in china who had severe fever with thrombocytopenia syndrome. *Clin. Infect. Dis.* 57, 1292–1299. doi: 10.1093/cid/cit530

Liu, Y., Wu, B., Paessler, S., Walker, D. H., Tesh, R. B., and Yu, X. J. (2014). The pathogenesis of severe fever with thrombocytopenia syndrome virus infection in alpha/beta interferon knockout mice: insights into the pathologic mechanisms of a new viral hemorrhagic fever. *J. Virol.* 88, 1781–1786. doi: 10.1128/JVI.02277-13

Lu, Q. B., Zhang, S. Y., Cui, N., Hu, J. G., Fan, Y. D., Guo, C. T., et al. (2015). Common adverse events associated with ribavirin therapy for Severe fever with thrombocytopenia syndrome. *Antiviral Res.* 119, 19–22. doi: 10.1016/j.antiviral.2015.04.006

Mendoza, E. J., Racine, T., and Kobinger, G. P. (2017). The ongoing evolution of antibody-based treatments for Ebola virus infection. *Immunotherapy*. 9, 435–450. doi: 10.2217/imt-2017-0010

Ministry of Health and People's Republic of China (2011). Guideline for prevention and treatment of severe fever with thrombocytopenia syndrome (2010 version). *Chinese J. Clin. Infect. Dis.* 4, 193—194.

Nachbagauer, R., and Krammer, F. (2017). Universal influenza virus vaccines and therapeutic antibodies. *Clin. Microbiol. Infect.* 23, 222–228. doi: 10.1016/j.cmi.2017.02.009

Nakamura, S., Azuma, M., Maruhashi, T., Sogabe, K., Sumitani, R., Uemura, M., et al. (2018). Steroid pulse therapy in patients with encephalopathy associated with severe fever with thrombocytopenia syndrome. *J. Infect. Chemother.* 24, 389–392. doi: 10.1016/j.jiac.2017.11.004

Ning, Y., Mo, Q., Feng, K., Min, Y. Q., Li, M., Hou, D., et al. (2019). Interferon-γ-directed inhibition of a novel high-pathogenic phlebovirus and viral antagonism of the antiviral signaling by targeting STAT1. *Front. Immunol.* 10:1182. doi: 10.3389/fimmu.2019.01182

Niu, G., Li, J., Liang, M., Jiang, X., Jiang, M., Yin, H., et al. (2013). Severe fever with thrombocytopenia syndrome virus among domesticated animals, China. *Emerg. Infect. Dis.* 19, 756–763. doi: 10.3201/eid1905.120245

Ogawa, M., Shirasago, Y., Ando, S., Shimojima, M., Saijo, M., and Fukasawa, M. (2018). Caffeic acid, a coffee-related organic acid, inhibits infection by severe fever with thrombocytopenia syndrome virus *in vitro*. *J. Infect. Chemother.* 24, 597–601. doi: 10.1016/j.jiac.2018.03.005

Oh, W. S., Heo, S. T., Kim, S. H., Choi, W. J., Han, M. G., and Kim, J. Y. (2014). Plasma exchange and ribavirin for rapidly progressive severe fever with thrombocytopenia syndrome. *Int. J. Infect. Dis.* 18, 84–86. doi: 10.1016/j.ijid.2013.08.011

Ramu, J., Konak, T., Paule, M. G., Hanig, J. P., and Liachenko, S. (2016). Longitudinal diffusion tensor imaging of the rat brain after hexachlorophene exposure. *Neurotoxicology* 56, 225–232. doi: 10.1016/j.neuro.2016.08.011

Saijo, M. (2018). Pathophysiology of severe fever with thrombocytopenia syndrome and development of specific antiviral therapy. *J. Infect. Chemother.* 24, 773–781. doi: 10.1016/j.jiac.2018.07.009

Sakurai, Y., Kolokoltsov, A. A., Chen, C. C., Tidwell, M. W., Bauta, W. E., Klugbauer, N., et al. (2015). Two-pore channels control Ebola virus host cell entry and are drug targets for disease treatment. *Science*. 347, 995–998. doi: 10.1126/science.1258758

Sakurai, Y., Sakakibara, N., Toyama, M., Baba, M., and Davey, R. A. (2018). Novel amodiaquine derivatives potently inhibit Ebola virus infection. *Antiviral Res.* 160, 175–182. doi: 10.1016/j.antiviral.2018.10.025

Scherbik, S. V., and Brinton, M. A. (2010). Virus-induced $Ca^{2+}$ influx extends survival of west nile virus-infected cells. *J. Virol.* 84, 8721–8731. doi: 10.1128/JVI.00144-10

Shimada, S., Posadas, H. G., Aoki, K., Morita, K., and Hayasaka, D. (2015). Therapeutic effect of post-exposure treatment with antiserum on severe fever with thrombocytopenia syndrome (SFTS) in a mouse model of SFTS virus infection. *Virology* 482, 19–27. doi: 10.1016/j.virol.2015.03.010

Shimojima, M., Fukushi, S., Tani, H., Taniguchi, S., Fukuma, A., and Saijo, M. (2015). Combination effects of ribavirin and interferons on severe fever with thrombocytopenia syndrome virus infection. *Virol. J.* 12:181. doi: 10.1186/s12985-015-0412-3

Shimojima, M., Fukushi, S., Tani, H., Yoshikawa, T., Fukuma, A., Taniguchi, S., et al. (2014). Effects of ribavirin on severe fever with thrombocytopenia syndrome virus *in vitro*. *Jpn. J. Infect. Dis.* 67, 423–427. doi: 10.7883/yoken.67.423

Smee, D. F., Jung, K. H., Westover, J., and Gowen, B. B. (2018). 2′-Fluoro-2′-deoxycytidine is a broad-spectrum inhibitor of bunyaviruses *in vitro* and in phleboviral disease mouse models. *Antiviral Res.* 160, 48–54. doi: 10.1016/j.antiviral.2018.10.013

Snell, N. J. (2001). Ribavirin - current status of a broad spectrum antiviral agent. *Expert Opin. Pharmacother.* 2, 1317–1324. doi: 10.1517/14656566.2.8.1317

Spengler, J. R., Bente, D. A., Bray, M., Burt, F., Hewson, R., Korukluoglu, G., et al. (2018). Second international conference on Crimean-Congo hemorrhagic fever. *Antiviral Res.* 150, 137–147. doi: 10.1016/j.antiviral.2017.11.019

Takahashi, T., Maeda, K., Suzuki, T., Ishido, A., Shigeoka, T., Tominaga, T., et al. (2014). The first identification and retrospective study of severe fever with thrombocytopenia syndrome in Japan. *J. Infect. Dis.* 209, 816–827. doi: 10.1093/infdis/jit603

Tang, H., Yao, X., Yao, C., Zhao, X., Zuo, H., and Li, Z. (2017). Anti-colon cancer effect of caffeic acid p-nitro-phenethyl ester *in vitro* and *in vivo* and detection of its metabolites. *Sci. Rep.* 7:7599. doi: 10.1038/s41598-017-07953-8

Tani, H., Fukuma, A., Fukushi, S., Taniguchi, S., Yoshikawa, T., Iwata-yoshikawa, N., et al. (2016). Efficacy of T-705 (Favipiravir) in the treatment of infections with lethal severe fever with thrombocytopenia syndrome virus. *mSphere* 1, e00061–e00015. doi: 10.1128/mSphere.00061-15

Tani, H., Komeno, T., Fukuma, A., Fukushi, S., Taniguchi, S., Shimojima, M., et al. (2018). Therapeutic effects of favipiravir against severe fever with thrombocytopenia syndrome virus infection in a lethal mouse model: dose-efficacy studies upon oral administration. *PLoS ONE* 13:e0206416. doi: 10.1371/journal.pone.0206416

Thäle, C., and Kiderlen, A. F. (2005). Sources of interferon-gamma (IFN-γ) in early immune response to Listeria monocytogenes. *Immunobiology* 210, 673–683. doi: 10.1016/j.imbio.2005.07.003

Tran, X. C., Yun, Y., An,L., Van, Kim, S. H., Thao, N. T. P., Man, P. K. C., et al. (2019). Endemic severe fever with thrombocytopenia syndrome, Vietnam. *Emerg. Infect. Dis.* 25, 1029–1031. doi: 10.3201/eid2505.181463

Utsunomiya, H., Ichinose, M., Ikeda, K., Uozaki, M., Morishita, J., Kuwahara, T., et al. (2014). Inhibition by caffeic acid of the influenza a virus multiplication *in vitro*. *Int. J. Mol. Med.* 34, 1020–1024. doi: 10.3892/ijmm.2014.1859

Wang, G. F., Shi, L. P., Ren, Y. D., Liu, Q. F., Liu, H. F., Zhang, R. J., et al. (2009). Anti-hepatitis B virus activity of chlorogenic acid, quinic acid and caffeic acid *in vivo* and *in vitro*. *Antiviral Res.* 83, 186–190. doi: 10.1016/j.antiviral.2009.05.002

Wang, S., Liu, Y., Guo, J., Wang, P., Zhang, L., Xiao, G., et al. (2017). Screening of FDA-approved drugs for inhibitors of Japanese encephalitis virus infection. *J. Virol.* 91, e01055–e01017. doi: 10.1128/JVI.01055-17

Welch, S. R., Guerrero, L. W., Chakrabarti, A. K., McMullan, L. K., Flint, M., Bluemling, G. R., et al. (2016). Lassa and Ebola virus inhibitors identified using minigenome and recombinant virus reporter systems. *Antiviral Res.* 136, 9–18. doi: 10.1016/j.antiviral.2016.10.007

Welch, S. R., Scholte, F. E. M., Flint, M., Chatterjee, P., Nichol, S. T., Bergeron, É., et al. (2017). Identification of 2′-deoxy-2′-fluorocytidine as a potent inhibitor of Crimean-Congo hemorrhagic fever virus replication using a recombinant fluorescent reporter virus. *Antiviral Res.* 147, 91–99. doi: 10.1016/j.antiviral.2017.10.008

Wohlrab, F., Jamieson, A. T., Hay, J., Mengel, R., and Guschlbauer, W. (1985). The effect of 2′-fluoro-2′-deoxycytidine on herpes virus growth. *Biochim. Biophys. Acta* 824, 233–242. doi: 10.1016/0167-4781(85)90053-3

World Health Organization (2017). *Annual Review of Diseases Prioritized Under the Research and Development Blueprint, 2017*. Available online at: http://www.who.int/blueprint/what/research-development/2017-Prioritization-Long-Report.pdf?ua=1 (accessed February 7, 2020).

Yoo, J. R., Kim, S. H., Kim, Y. R., Lee, K. H., Oh, W. S., and Heo, S. T. (2019). Application of therapeutic plasma exchange in patients having severe fever with thrombocytopenia syndrome. *Korean J. Intern. Med.* 34, 902–909. doi: 10.3904/kjim.2016.194

Yoshikawa, R., Sakabe, S., Urata, S., and Yasuda, J. (2019). Species-specific pathogenicity of severe fever with thrombocytopenia syndrome virus is determined by anti-STAT2 activity of NSs. *J. Virol.* 93, e02226–e02218. doi: 10.1128/JVI.02226-18

Yu, X. J., Liang, M. F., Zhang, S. Y., Liu, Y., Li, J. D., Sun, Y. L., et al. (2011). Fever with thrombocytopenia associated with a novel bunyavirus in China. *N. Engl. J. Med.* 364, 1523–1532. doi: 10.1056/NEJMoa1010095

Yuan, S., Chan, J. F. W., Ye, Z. W., Wen, L., Tsang, T. G. W., Cao, J., et al. (2019). Screening of an FDA-approved drug library with a two-tier system identifies an entry inhibitor of severe fever with thrombocytopenia syndrome virus. *Viruses* 11:E385. doi: 10.3390/v11040385

Zhu, L., Yin, F., Moming, A., Zhang, J., Wang, B., Gao, L., et al. (2019). First case of laboratory-confirmed severe fever with thrombocytopenia syndrome disease revealed the risk of SFTSV infection in Xinjiang, China. *Emerg. Microbes Infect.* 8, 1122–1125. doi: 10.1080/22221751.2019.1645573

Zivcec, M., Safronetz, D., and Feldmann, H. (2013). Animal models of tick-borne hemorrhagic fever viruses. *Pathogens* 2, 402–421. doi: 10.3390/pathogens2020402

**Conflict of Interest:** The authors declare that the research was conducted in the absence of any commercial or financial relationships that could be construed as a potential conflict of interest.

*Copyright © 2020 Takayama-Ito and Saijo. This is an open-access article distributed under the terms of the Creative Commons Attribution License (CC BY). The use, distribution or reproduction in other forums is permitted, provided the original author(s) and the copyright owner(s) are credited and that the original publication in this journal is cited, in accordance with accepted academic practice. No use, distribution or reproduction is permitted which does not comply with these terms.*

frontiers in Microbiology

ORIGINAL RESEARCH
published: 27 February 2020
doi: 10.3389/fmicb.2020.00304

# Intradermal Immunization of EBOV VLPs in Guinea Pigs Induces Broader Antibody Responses Against GP Than Intramuscular Injection

*Ying Liu[1,2], Zhiyuan Wen[2,3], Ricardo Carrion Jr.[4], Jerritt Nunneley[4], Hilary Staples[4], Anysha Ticer[4], Jean L. Patterson[4], Richard W. Compans[2], Ling Ye[2]* and Chinglai Yang[2]**

[1] State Key Laboratory of Food Nutrition and Safety, Institute of Health Biotechnology, College of Biotechnology, Tianjin University of Science and Technology, Tianjin, China, [2] Department of Microbiology and Immunology and Emory Vaccine Center, School of Medicine, Emory University, Atlanta, GA, United States, [3] Harbin Veterinary Research Institute, Harbin, China, [4] Texas Biomedical Research Institute, San Antonio, TX, United States

OPEN ACCESS

**Edited by:**
*Lu Lu,*
*Fudan University, China*

**Reviewed by:**
*Asuka Nanbo,*
*Nagasaki University, Japan*
*Zhong Huang,*
*Institut Pasteur of Shanghai (CAS), China*

***Correspondence:**
*Ling Ye*
*yling@emory.edu*
*Chinglai Yang*
*chyang@emory.edu*

**Specialty section:**
*This article was submitted to Virology, a section of the journal Frontiers in Microbiology*

**Received:** *29 September 2019*
**Accepted:** *11 February 2020*
**Published:** *27 February 2020*

**Citation:**
*Liu Y, Wen Z, Carrion R Jr, Nunneley J, Staples H, Ticer A, Patterson JL, Compans RW, Ye L and Yang C (2020) Intradermal Immunization of EBOV VLPs in Guinea Pigs Induces Broader Antibody Responses Against GP Than Intramuscular Injection. Front. Microbiol. 11:304. doi: 10.3389/fmicb.2020.00304*

Ebolavirus (EBOV) infection in humans causes severe hemorrhagic fevers with high mortality rates that range from 30 to 80% as shown in different outbreaks. Thus the development of safe and efficacious EBOV vaccines remains an important goal for biomedical research. We have shown in early studies that immunization with insect cell-produced EBOV virus-like particles (VLPs) is able to induce protect vaccinated mice against lethal EBOV challenge. In the present study, we investigated immune responses induced by Ebola VLPs via two different routes, intramuscular and intradermal immunizations, in guinea pigs. Analyses of antibody responses revealed that similar levels of total IgG antibodies against the EBOV glycoprotein (GP) were induced by the two different immunization methods. However, further characterization showed that the EBOV GP-specific antibodies induced by intramuscular immunization were mainly of the IgG2 subtype whereas both IgG1 and IgG2 antibodies against EBOV GP were induced by intradermal immunization. In contrast, antibody responses against the EBOV matrix protein VP40 induced by intramuscular or intradermal immunizations exhibited similar IgG1 and IgG2 profiles. More interestingly, we found that the sites that the IgG1 antibodies induced by intradermal immunizations bind to in GP are different from those that bind to the IgG2 antibodies induced by intramuscular immunization. Further analyses revealed that sera from all vaccinated guinea pigs exhibited neutralizing activity against Ebola GP-mediated HIV pseudovirion infection at high levels. Moreover, all EBOV VLP-vaccinated guinea pigs survived the challenge by a high dose (1000 pfu) of guinea pig-adapted EBOV, while all control guinea pigs immunized with irrelevant VLPs succumbed to the challenge. The induction of both IgG1 and IgG2 antibody responses that recognized broader sites in GP by intradermal immunization of EBOV VLPs indicates that this approach may represent a more advantageous route of vaccination against virus infection.

**Keywords: ebola, vaccine, intradermal immunization, antibody response, VLP**

## INTRODUCTION

Ebolavirus is a member of the filoviridae family, and infection by ebolavirus in humans and non-human primates (NHPs) results in onset of severe hemorrhagic fevers with high mortality rates (Feldmann and Geisbert, 2011; Li H. et al., 2015; Ye and Yang, 2015). Since their first identification in 1976, five different ebolavirus species have been isolated from outbreaks in humans or NHPs including Ebola virus (EBOV), Sudan virus (SUDV), Bundibugyo virus (BDBV), Tai Forest virus (TAFV), and Reston virus (RESTV), and these viruses differ significantly in their amino acid sequences by as much as 40% (Towner et al., 2008). Notably, the RESTV has been found only in non-human primates from the Philippines, whereas the other four filovirus species are only detected in tropical areas of the equator Africa, and studies in recent years have shown that the African green fruit bats may serve as the natural reservoir of these ebolaviruses (Leroy et al., 2005; Groseth et al., 2007). It is noted that in recent years ebolavirus infection of humans has become more frequent (Chowell and Nishiura, 2014). Of particular concern, the 2013–2016 EBOV outbreak that infected over 28000 human infections and resulted in over 11000 deaths. Moreover, the current ongoing 2018 Kivu outbreak has a mortality rate around 67% and has thus far resulted in over 2000 individuals killed. These large-scale outbreaks demonstrates that the serious threat of EOBV infection to public health is urgent and real. Furthermore, evidence also suggests that EBOV may also infect dogs during outbreaks in addition to infect humans and NHPs (Allela et al., 2005). On the other hand, RESTV has also been indicated to infect domestic pigs in Asia based on serological analyses (Barrette et al., 2009). Further, EBOV has been demonstrated to infect pigs in experimental settings with causing pathogenesis, and virus from infected pigs were shown to transmit to NHPs with no direct contact, demonstrating that this highly lethal virus may be capable of aerosol transmission from a infected host to another susceptible host (Reed et al., 2011; Weingartl et al., 2012). The potential of EBOV to cause non-pathogenic infection in domestic pigs poses a grave danger for these viruses to become endemic and infect humans through zoonotic transmission.

The high mortality rate of EBOV infection underscores the urgent need for an effective EBOV vaccine. A number of EBOV vaccine approaches have been explored in past studies, many of these vaccine strategies have been shown to be able to protect vaccinated animals against lethal EBOV challenge in small laboratory animal models with various efficacies (Yang et al., 2008; Marzi and Feldmann, 2014). Moreover, promising results have also been obtained with viral vector-based vaccine strategies in the NHP model for protection against lethal EBOV challenge, which include recombinant adenovirus replicons (Sullivan et al., 2006), VSV (Jones et al., 2005), parainfluenza virus (Bukreyev et al., 2007), Rabies virus (Blaney et al., 2013), VRP (Herbert et al., 2013), as well as a replication defective EBOV (Marzi et al., 2015) vaccines. In addition to viral vector-based vaccines, EBOV virus-like particles (VLPs) and other protein-based subunit vaccines have been shown to induce protective immune responses against lethal EBOV infection of NHPs (Warfield et al., 2007; Swenson et al., 2008). Of these, recombinant adenovirus replicons and recombinant VSV based vaccines have been evaluated in a number of Phase I clinical trials and shown to be safe and immunogenic (Ewer et al., 2016; Regules et al., 2017). More recently, a Phase III clinical trial was conducted in Guinea with a the recombinant VSV-based vaccine that expresses EBOV GP, and this vaccine was found to be highly effective in preventing EBOV infection of people with high risks to EBOV infections (Henao-Restrepo et al., 2015). The success of the recombinant VSV/EBOV vaccine in the Phase III trial showed that an effective vaccine can control the EBOV epidemics. Nonetheless, the efficacy of viral vector-based EBOV vaccines may be hampered by the pre-existing immunity in the affected area to these viral vectors. Further, immunization by such vaccines may also induce strong immune responses against the vector and therefore dampen their ability to induce immune responses in boosting immunizations for achieving durable protection or in subsequent vaccination of high risk personnel against another filovirus in future outbreaks. Thus, development of vaccine strategies to overcome the limitations of viral vector-based vaccines is still in need.

Among the different EBOV vaccine strategies, VLPs are a subunit vaccine platform that has been shown to protect EBOV infection in NHPs. In early studies, both EBOV and Marburg virus VLPs have been evaluated in different animal models and shown to be effective in eliciting protecting vaccinated animals against lethal challenge (Warfield and Aman, 2011), demonstrating that this vaccine strategy is able to control and prevent filovirus infection. We have shown in our previous studies that EBOV VLPs produced in insect cells by the recombinant baculovirus expression system are able to stimulate dendritic cells to secret various cytokines, and neutralizing antibodies against infection mediated by the EBOV GP are induced in vaccinated animals immunized with these VLPs (Ye et al., 2006). We further demonstrated that immunization with the EBOV VLP vaccines produced from insect cells completely protected mice against lethal challenge by a high dose of mouse-adapted EBOV (Sun et al., 2009). In this study, we investigated immune responses elicited by EBOV VLPs in guinea pigs via different routes, through intramuscular (IM) and intradermal (ID) injection respectively, and showed that immunization by EBOV VLPs produced in insect cells effectively induced neutralizing antibodies against EBOV GP and conferred complete protection against lethal challenge by guinea pig-adapted EBOV. Further, we found that by IM immunization, the EBOV VLPs induced both IgG1 and IgG2 antibodies against EBOV GP in guinea pigs, as compared to the dominant IgG2 antibody responses induced by IM immunizations. More interestingly, we show that the IgG1 antibodies induced by ID immunizations against GP bind to different targets from those recognized by the IgG2 antibodies induced by IM immunizations, demonstrating the potential advantage of ID immunization in eliciting broader antibody responses against infection by EBOV.

# MATERIALS AND METHODS

## Virus and Biosafety

The stock for guinea pig-adapted EBOV was produced and titered in Vero E6 cells. All experiments with live EBOV were conducted in the BSL-4 facility at the Texas Biomedical Research Institute (TxBiomed), San Antonio, TX, United States.

## Cells and Antibodies

*Spodoptera frugiperda* Sf9 cells were maintained in SF-900 II serum-free medium with penicillin/streptomycin. The polyclonal rabbit serum against EBOV was a gift from Dr. P. Rollin (CDC). JC53BL cells (Wei et al., 2003), which express β-galactosidase and luciferase under a *tat*-activated promoter, was obtained from NIH AID Reagents and Reference Program, and maintained in DMEM plus 10% fetal calf serum (FCS). HeLa cells and 293T cells were obtained from ATCC and maintained in DMEM plus 10% FCS.

## Production and Characterization of Ebola VLPs Produced in Insect Cells

Construction and production of recombinant baculoviruses (rBVs) that express EBOV GP and VP40 (designated as rBV-GP and rBV-VP40 respectively) has been described previously (Ye et al., 2006; Sun et al., 2009). For VLP production, Sf9 cells were grown in suspension and then infected with by rBV-GP and rBV-VP40 at the MOIs (multiplicity of infection) of 5 and 2 per cell for each virus. Cell culture medium was harvested at 48 h post-infection and clarified by centrifugating at 1500 RPM for 10 min in a 50 ml conical tube, and the supernatant was then concentrated through Quickstand filtration system (GE). Subsequently, VLPs were further purified through a discontinuous sucrose gradient (10–50%), concentrated again by ultra-centrifugation, and then resuspended in PBS with a concentration of 1 ug/ul (protein/volume) (Ye et al., 2006). Purified EBOV VLPs were analyzed by Western blot using rabbit serum against EBOV to detect viral VP40 and GP proteins, analyzed by electron microscopy to examine the morphology and integrity of VLPs, and analyzed by quantitative enzyme-linked immunosorbent assay (ELISA) to quantify the levels of GP proteins in VLP preparations (Sun et al., 2009). As a control antigen for vaccination, SIVgag VLPs were produced by expressing the SIV Gag protein in Sf9 cells using the recombinant baculovirus expression system and SIVgag VLPs were purified through a sucrose gradient similarly as described above and characterized as shown in previous studies (Ye et al., 2006).

## Immunization of Guinea Pigs and Sample Collection

Female Hartley guinea pigs (∼250 g in body weight) were obtained from the Charles River Laboratory and housed at the Division of Animal Research of Emory University. Twelve guinea pigs were divided into three groups with four animals per group. Two groups of guinea pigs were vaccinated by IM or ID injection first with 50 ug of EBOV VLPs two times and then boosted again with 200 ug EBOV VLPs at 4-week intervals. The control group guinea pigs were vaccinated with SIVgag VLPs ($n = 4$) of the same dose as an irrelevant VLP control. For ID injection, VLPs were delivered by using the Mantoux method to four sites (25 to 50 ul per site based on vaccine dose) of the shaved posterior-abdomen skin of guinea pigs under kentamine/xylazine anaesthetization. Blood samples were collected from cranial vena cava under anesthesia at 1 week prior to the first immunization and 2 weeks after the second and third immunizations, and stored at −80°C until being used in analyses.

## Detection of GP and VP40 Antigen-Specific Antibodies

Antibodies against EBOV GP and VP40 antigens were detected in serum samples from each guinea pig by ELISA. The His-tagged EBOV GP was produced by infecting HeLa cells with a recombinant vaccinia virus that expresses the EBOV GP-histag protein, and the GP-histag protein secreted into the medium of infected HeLa cells was purified using a Ni-NTA agarose bead-based higtag protein purification kit following established protocols (Sun et al., 2009). The His-tagged EBOV VP40 (VP40-histag) was expressed in bacteria DH5a using plasmid DNA vector pBlusscript IIKS under the T7 promoter, and purified using Ni-NTA agarose bead-based histag protein purification kit following manufacturer's protocols. For ELISA analysis of serum samples, a microtiter plate (Maxisorb, Nunc) was coated overnight at 4°C with purified His-tagged EBOV GP or VP40 at a concentration of 2 ug/ml. Plates were then washed with PBST prior to blocking with 200 ul per well 2% BSA/PBST for 1 h at 37°C. Serum samples from vaccinated guinea pigs were serially diluted and then added to the wells of the microtiter plates that were coated and blocked and then incubated at room temperature for 2 h, and the bound antibodies specific for EBOV proteins were detected with horseradish peroxidase-labeled goat against guinea pig IgG, IgG1, or IgG2 antibodies (Bethyl Lab, Inc.). The wells were then washed and added with TMB (Sigma) at 50 ul per well to develop color, and the enzymatic reaction was stopped with addition of 50 ul per well of hydrochloric acid (0.2N), and afterward the absorbance value at 450 nm of each well was read in an ELISA reader (Bio-Tek Instruments, Inc., Winooski, VT, United States). Serial dilutions of purified guinea pig IgG (EQUITECH-BIO, Inc.) with known concentrations were used to generate a standard curve, which was used to calculate the concentrations of EBOV GP or VP40-specific antibodies in serum samples and the antibody concentrations of these antibodies were expressed as the amount of antibodies in 1 ml of serum (ng/ml).

## Blocking ELISA

Blocking ELISA was employed to investigate whether IgG2 antibodies induced by IM injection of EBOV VLPs will affect binding of IgG1 antibodies induced by ID injection of EBOV VLPs to GP. Briefly, microtiter plates were coated o/n at 4°C with purified His-tagged GP as coating antigens at a reduced concentration of 0.5 ug/ml. Plates were then washed with PBST prior to blocking with 200 ul per well 2% BSA/PBST for 1 h at 37°C, and then added with 1:400 dilution of sera from

each individual guinea pig vaccinated by IM injection of EBOV VLPs, sera from naïve guinea pigs, or PBST only for 2 h at room temperature. This serum dilution (1:400) has been predetermined to saturate binding of the amount of coated His-tagged GP antigens. The plates were then washed again and then incubated with sera from individual guinea pigs that had been vaccinated by ID injection of EBOV VLPs or SIVgag VLPs (Control). After incubation for 2 h at room temperature, the plates were washed and the bound IgG1 antibodies were detected with horseradish peroxidase-labeled goat against guinea pig IgG1 secondary antibodies (Bethyl Lab, Inc.). The wells were added with 50 ul per well of TMB (Sigma) to develop color and the color reaction was stopped with addition of 50 ul per well of hydrochloric acid (0.2N), and afterward the absorbance value at 450 nm of each well was read in an ELISA reader (Bio-Tek Instruments, Inc., Winooski, VT, United States).

## Analysis of Sera Neutralizing Activity With Pseudovirus

The levels of neutralizing antibodies against EBOV GP were detected by a single-round infectivity assay that we have developed in early studies (Mohan et al., 2012, 2015). Briefly, EBOV GP-HIV pseudovirions were produced by transfecting 293T-cells with and HIV backbone plasmid (Env-defective) and together with a DNA plasmid expressing EBOV GP in pCAGGS using the transfection reagent Fugene HD (Roche). At 48 h post-transfection, pseudovirions in the medium from transfected cells were harvested, clarified, and filtered using a 0.45 micron filter, and then titrated in JC53BL cells (Wei et al., 2003), which express β-galactosidase and luciferase under a *tat*-activated promoter. Neutralization assays were then carried out as described in our previous studies (Li W. et al., 2015). Briefly, pseudoviruses were fisrt incubated with serial dilutions of heat-inactivated serum samples for 1 h at 37°C, which were supplemented with heat-inactivated sera from naïve mouse (Innovative Research) to 5% of the total volume. The serum-pseudovirion mixtures were then added to JC53 cells that have been grown to 50% confluenvy in a 96-well plate and incubated at 37°C for 48 h. Afterward, the level of luciferase activity in each well were detected by a kit (Sigma), neutralization was calculated by measuring the percent decrease in luciferase activity in sample wells compared to virus-only control wells. The serum neutralizing activity is calculated with the formula: [(luciferase activity in control well – luciferase activity in sample well)/luciferase activity in control well × 100%], and is expressed as the percentage reduction of virus titers in sample wells compared to the titers in control wells. Statistical analysis of serum antibody responses between ID and IM vaccinated guinea pigs was performed by a Student's *t*-test.

## Lethal Challenge by Guinea Pig-Adapted EBOV

EBOV challenge study was conducted in the ABSL-4 facility at Texas Biomedical Research Institute (San Antonio, TX, United States). Guinea pigs were challenged at 22 weeks after the third vaccination by intraperitoneal injection with 1000 plaque-forming units (pfu) of guinea pig-adapted EBOV. After challenge, guinea pigs were monitored at least twice daily for weight loss and disease symptoms, and animals that exhibited severe disease signs and lost significant levels of body weight (over 25%) were sacrificed in compliance with IACUC guidelines.

# RESULTS

## Comparison of Antibody Responses Induced by EBOV VLPs Through Intradermal and Intramuscular Immunization Routes

In our previous studies, we showed that mice were effectively protected by two intramuscular immunizations with 50 ug EBOV VLPs produced in insect cells (Sun et al., 2009). To investigate the immunogenicity of insect cell-produced EBOV VLPs in guinea pigs via different immunization routes, we first vaccinated guinea pigs (groups of 4) with 50 ug EBOV VLPs by IM or ID injection as outlined in **Figure 1A**. The control group animals received immunization by 50 ug SIVgag VLPs that were similarly produced in insect cells by IM or ID injection (2 animals each route). As outlined in **Figure 1A**, blood samples were first collected at 2 weeks after the second immunization and then analyzed for antibodies against EBOV GP. As shown in **Figure 1B** (gray columns), antibodies against EBOV GP were readily detected in sera from guinea pigs after two immunizations with 50 ug EBOV VLPs by both IM and ID injections. However, the levels of anti-GP antibodies were relatively low at about 3000 ng/ml for the IM group and 2500 ng/ml for the ID groups respectively. Further, analysis of sera neutralizing activity showed that these sera failed to reduce GP-pseudovirion infection by more than 50% at 1:100 dilution (data not shown).

Based on these results, we decided to give one additional boosting immunization using 200 ug EBOV VLPs or SIVgag VLPs for the control group by IM or ID injection respectively as outlined in **Figure 1A**, and collected blood samples at 2 weeks after the third immunization to analyze the levels of antibodies against GP. As shown in **Figure 1B** (black columns), the levels of antibody responses against GP increased significantly to about 25000 ng/ml by more than eightfold for both IM and ID immunization groups after the additional boosting immunization. The neutralizing activity of sera from vaccinated guinea pigs was then determined by a pseudovirion neutralization assay. As shown in **Figure 2**, sera from guinea pigs vaccinated by EBOV VLPs via either IM or ID injection exhibited significant levels of neutralizing activity against EBOV GP mediated pseudovirion infection, with the average 50% neutralization titers reaching above 1:800 and 1:1600 dilutions for the IM and ID immunization groups respectively. However, analysis by a Student's *t*-test showed that the differences in neutralizing activity between serum samples from guinea pigs in the IM and ID immunization groups at all four serum dilutions (1:200, 1:400, 1:800, and 1:1600) are not statistically significant ($p > 0.05$).

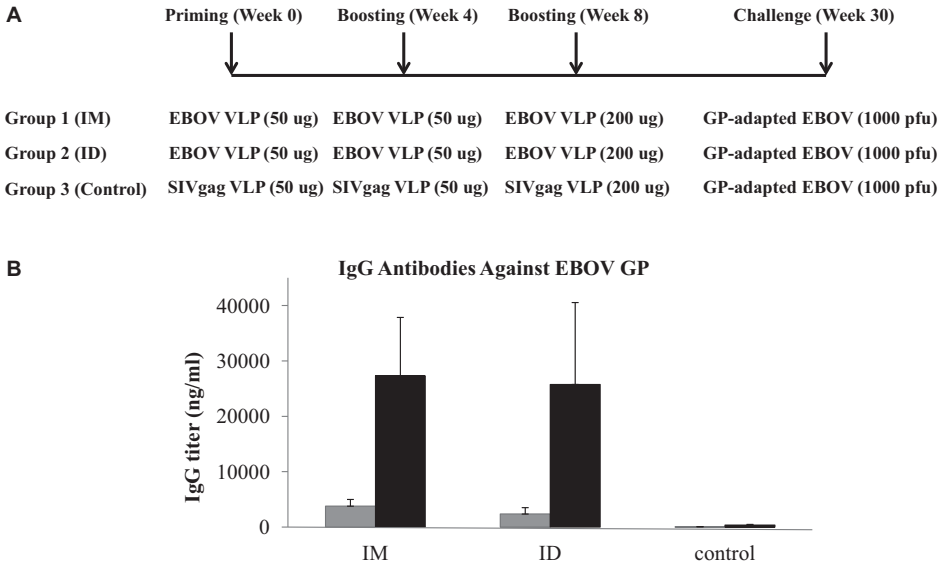


**FIGURE 1 | (A)** Schematic diagram of immunization and challenge study design. Female Hartley guinea pigs (groups of 4) were vaccinated with EBOV VLPs or control SIVgag VLPs at 4-week intervals via different immunization routes as presented. Blood samples were collected at 2 weeks after the second and third immunizations and guinea pigs were challenged at 22 weeks after the final immunization by 1000 pfu of guinea pig-adapted EBOV. **(B)** Antibody responses against GP induced by IM or ID injection of EBOV VLPs. The levels of antibody response against EBOV GP induced by VLP vaccines in guinea pigs were measured by ELISA using purified His-tagged GP as coating antigen. Antibody concentration was determined from a standard curve and expressed as ng/ml of IgG against GP in serum samples collected after the second and third immunizations. Results reported are the means and standard deviations for samples from individual animals of each group. Gray columns, antibody levels in sera from vaccinated collected at 2 weeks after the second immunization; black columns, antibody levels in sera from vaccinated collected at 2 weeks after the third immunization.

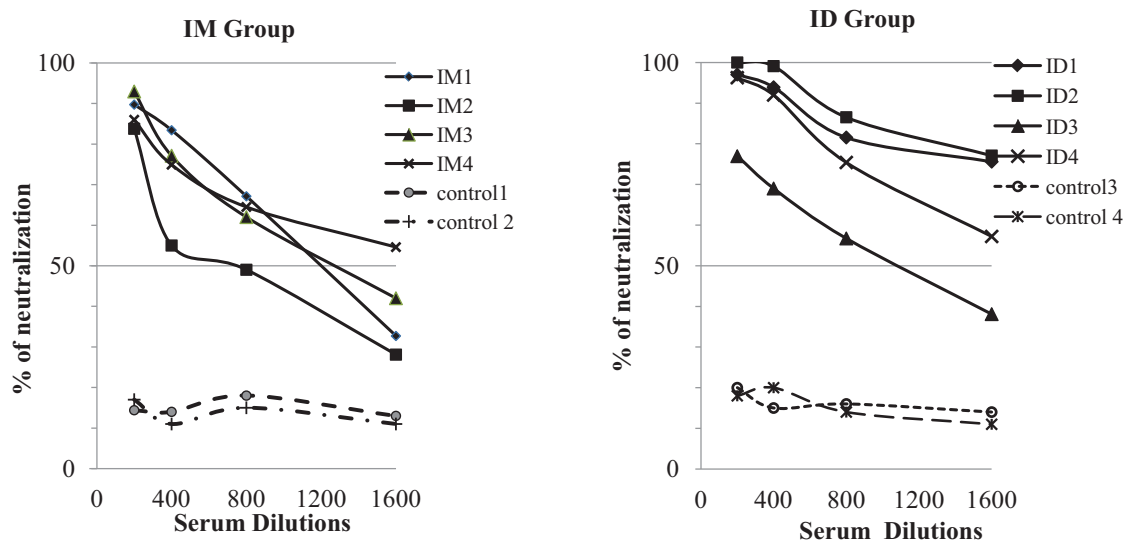


**FIGURE 2 |** Neutralization of GP-mediated pseudovirion infection by sera from vaccinated guinea pigs. Neutralizing activity of immune sera collected after the third immunization was determined by a pseudovirion neutralization assay. Serial twofold dilutions of sera were inbubated with 500 pfu of GP-pseudotyped virus at 37°C for 1 h, the mixtures were then added to JC53 cells seeded in a 96-well plate and incubated at 37°C for 2 days. Neutralization was measured as decrease in luciferase expression compared to virus-only controls after 48 h as described in Materials and Methods. Results reported are the percentage of pseudovirion neutralization by samples from individual animals of each group at the indicated dilutions. Statistical comparison of serum neutralizing activities at each dilution was performed by a Student's *t*-test, and was found to be not statistically significant ($p > 0.05$).

## Immunization Routes Affect the Profiles of Antibody Responses Against GP Induced by EBOV VLPs

We further characterized the levels of IgG1 and IgG2 subclass antibodies against GP induced by IM or ID immunization with EBOV VLPs for comparison. As shown in **Figure 3**, immunization by IM or ID injection of EBOV VLPs induced similar levels of IgG2 antibodies against GP in guinea pigs ($p > 0.05$). On the other hand, ID immunization by EBOV VLPs induced significantly higher levels of IgG1 antibodies against GP than IM immunization ($p < 0.05$). To investigate whether such differences might also be observed for other vaccine antigens in EBOV VLPs, we further determined the levels of IgG1 and IgG2 antibodies against EBOV matrix protein VP40 in EBOV VLPs for comparison. As shown in **Figure 4**, similar levels of both IgG1 and IgG2 antibodies against EBOV VP40 were induced by immunization through IM or ID injection of EBOV VLPs in guinea pigs ($p > 0.05$). Further, it is also notable that the levels of IgG1 antibodies against GP are only about one-third of the levels of IgG2 antibodies by ID immunization and about one-tenth of the levels of IgG2 antibodies by IM injection. In contrast, the levels of IgG1 and IgG2 antibodies against VP40 are similar in both IM and ID immunization groups. Taken together, these results show that the antibody profiles induced by IM and ID immunization of EBOV VLPs in guinea pigs are different only for the GP antigen but not for VP40.

Based on the different levels of IgG1 antibodies against GP induced by ID and IM injection, we carried out blocking ELISA to determine whether the IgG1 and IgG2 antibodies against GP may target similar or different epitopes. Briefly, microtiter plates were coated with a limited amount of purified His-tagged GP protein at 0.05 ug per well. After blocking, the wells were treated with sera from guinea pigs vaccinated by IM injection of EBOV VLPs at 1:400 dilutions, a dilution that has been pre-determined to saturate binding of the amount of coated GP antigen. The controls were added with the same dilution of sera from control group guinea pigs or no sera as indicated. After incubating with the first antibody, the plate was washed and then added with sera from guinea pigs vaccinated by ID injection of EBOV VLPs or from control group guinea pigs at 1:400 dilutions as indicated, followed by addition of HRP-conjugated secondary antibody against guinea pig IgG1 to determine the levels of IgG1 antibodies bound to GP for comparison. The results in **Figure 5** show that pre-incubation with sera from IM-vaccinated guinea pigs did not affect the binding of IgG1 antibodies in sera from ID-vaccinated guinea pigs to GP as compared to pre-incubation with sera from control guinea pigs or no sera. Further, without the addition of sera from ID-vaccinated guinea pigs, only low levels of IgG1 antibodies against GP in sera from IM-vaccinated guinea pigs were detected. These results suggest that the interaction of IgG1 antibodies to EBOV GP elicited by ID injection of EBOV VLPs is not affected by pre-blocking of the GP antigen by GP-specific antibodies from IM-vaccinated guinea pigs that are predominantly of the IgG2 subclass, suggesting that the IgG1 antibodies induced by ID immunization may target different epitopes in GP from those targeted by IgG2 antibodies induced by IM immunization with EBOV VLPs.

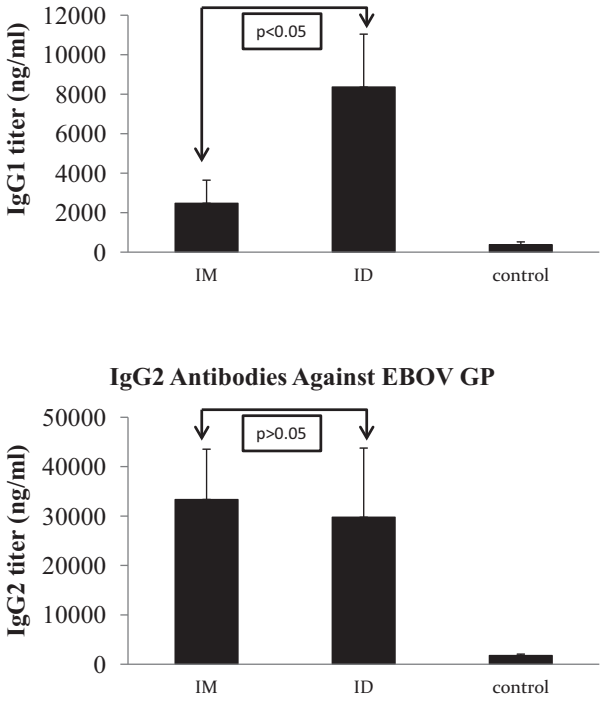


**FIGURE 3 |** Analysis of IgG1 and IgG2 subclass antibody responses against GP induced by IM and ID injection of EBOV VLPs in guinea pigs. Guinea pig sera collected after the third immunization were analyzed for IgG1 and IgG2 subclass antibody responses against GP by ELISA using purified His-tagged GP as coating antigen. The concentrations of IgG1 and IgG2 antibodies against GP were determined from a standard curve and expressed as ng/ml of GP-specific antibodies in sera. Results reported are the means and standard deviations for samples from individual animals of each group. Statistical comparison of antibody levels against EBOV GP was performed by a Student's *t*-test, and shown in each graph.

## Protection of Guinea Pigs Against Lethal EBOV Challenge

After the third immunization, the guinea pigs were transferred to the Texas Biomedical Research Institute to evaluate the protective efficacy of EBOV VLP vaccination against lethal EBOV challenge in the ABSL-4 facility. As shown in **Figure 1**, vaccinated guinea pigs as well as the control group were infected by 1000 pfu of guinea pig-adapted EBOV at 22 weeks after the final immunization, and then observed daily for disease symptoms, weight changes, and body temperatures. As shown in **Figure 6**, all control group animals that received SIV Gag VLPs by either IM or ID injection succumbed to challenge with progressive weight losses and died by day 6 post-challenge. In contrast, all animals that had been vaccinated by EBOV VLPs by either IM or ID injection survived the challenge with no significant change in body weight over 24 days post-challenge. These results show that immunization by either IM or ID injection of EBOV VLPs

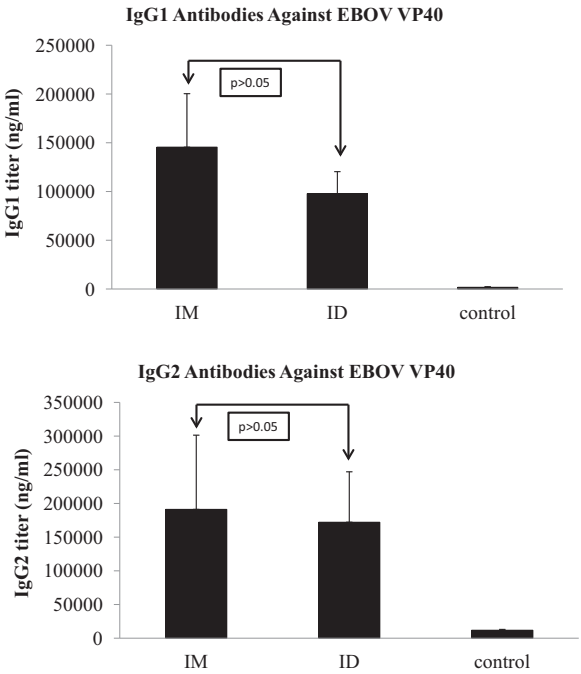


**FIGURE 4 |** Induction of similar levels of IgG1 and IgG2 subclass antibody responses against VP40 induced by IM and ID injection of EBOV VLPs in guinea pigs. Guinea pig sera collected after the third immunization were analyzed for IgG1 and IgG2 subclass antibody responses against VP40 by ELISA using purified His-tagged VP40 as coating antigen. The concentrations of IgG1 and IgG2 antibodies against VP40 were determined from a standard curve and expressed as ng/ml of VP40-specific antibodies in sera. Results reported are the means and standard deviations for samples from individual animals of each group. Statistical comparison of antibody levels against EBOV GP was performed by a Student's *t*-test, and shown in each graph.

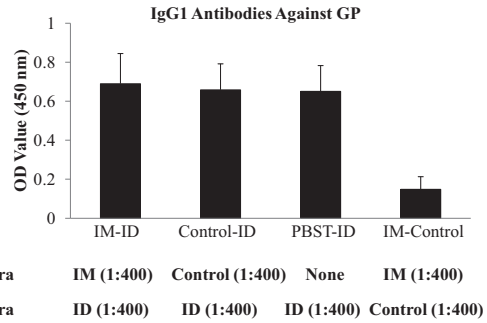


**FIGURE 5 |** Binding of IgG1 from ID immunized guinea pigs to GP was not affected by pre-incubation with sera from IM immunized guinea pigs. Microtiter plates coated with His-tagged GP were first incubated with 1:400 dilutions of sera from guinea pigs vaccinated by IM injection of EBOV VLPs (IM-ID and IM-Control), IM or ID injection of SIVgag VLPs (Control-ID), or PBST with no sera (Control-ID) as indicated for 2 h at room temperature. The plates were then washed and incubated with 1:400 dilution of sera from guinea pigs vaccinated by ID injection of EBOV VLPs (IM-ID, Control-ID, and PBST-ID) or SIVgag VLPs (IM-Control) for 2 h at room temperature. The plates were washed again and the levels of IgG1 antibodies bound to each well were determined by incubating with horseradish peroxidase-labeled goat against guinea pig IgG1 antibodies and expressed as OD values for comparison. Results reported are the means and standard deviations for samples from paired animals of each group.

effectively protected vaccinated animals against a high dose lethal challenge by guinea pig-adapted EBOV.

## DISCUSSION

In the present study, we compared the effect of two different immunization routes, IM and ID injections respectively, on the immunogenicity and protective efficacy of insect cell-derived EBOV VLPs in the guinea pig model. Our results showed that EBOV VLPs administered via both IM and ID routes induced similar levels of antibody responses against EBOV GP and vaccinated were completely protected against a high dose lethal challenge by guinea pig-adapted EBOV. Of particular interest, we observed that while immunization with EBOV VLPs by IM or ID injection induced similar levels of IgG2 subclass antibodies against GP, the levels of IgG1 subclass antibodies against EBOV GP induced by ID immunization were significantly higher than the levels induced by IM immunizations. In contrast, immunization by both IM and ID routes induced similar levels of IgG1 and IgG2 antibody responses against VP40, the EBOV matrix protein in VLPs. Moreover, by further analyses, we observed that binding of IgG1 antibodies induced by ID injection of EBOV VLPs was not blocked by sera from IM-vaccinated animals, indicating that such IgG1 antibodies may react to different epitopes in GP from those recognized by antibodies induced by IM immunization, which are predominantly of the IgG2 subclass.

In addition to serving as a protective barrier, skin has also long been known to be an important part of the immune system (Bos and Kapsenberg, 1993). The first human vaccine, vaccinia, is administered by the ID route. Skin dermis is enriched with dermal DCs as well as Langerhans cells that are professional antigen presenting cells for immune surveillance (Flacher et al., 2006). In early studies, it has also been shown that influenza vaccines delivered by ID injection are safe and immunogenic in children (Rendtorff et al., 1959). However, due to the technical difficulty of ID injection by the conventional Mantoux method as well as the small volume of vaccines that can be delivered by this route, ID injection is not widely practiced for current vaccine delivery with the exception of the BCG vaccination against Tuberculosis. More recent studies showed that administration of influenza vaccines through ID immunization required reduced vaccine doses for eliciting similar levels of immune responses as IM delivery of influenza vaccines (Kenney et al., 2004; Chiu et al., 2007). In recent studies, new technologies are being development for vaccine delivery through the ID route. A new needle-syringe device that only exposed the tip of the needle has recently been designed for easier ID injection of influenza vaccines (Laurent et al., 2007; Holland et al., 2008), and this approach has now been approved for ID delivery of seasonal influenza vaccines. Moreover, microneedles are also under development for ID delivery of vaccines (Gill et al., 2014). Recent studies have shown that ID delivery of influenza vaccines using microneedles is

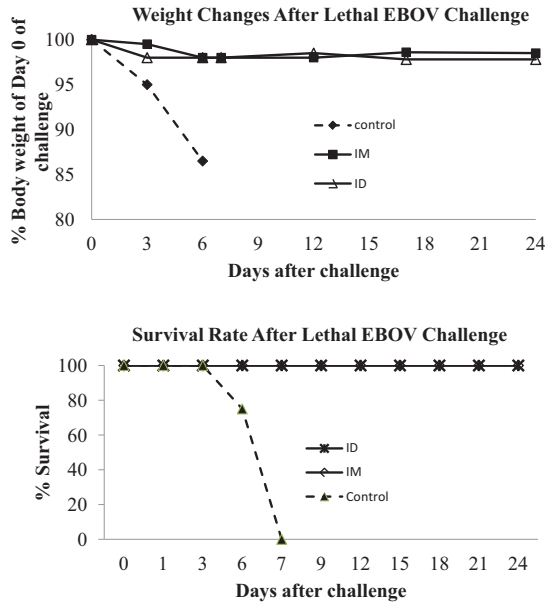


**FIGURE 6 |** Guinea pigs immunized by EBOV VLPs are protected against a high dose lethal challenge. As outlined in **Figure 1**, guinea pigs were challenged by i.p. injection of 1000 pfu guinea pig-adapted EBOV at 22 weeks after the third immunization. Guinea pigs were monitored daily and weighed on indicated days post-challenge for recording of weight changes after challenge, and animals that exhibit substantial weight loss and signs of severe disease were sacrificed in accordance with IACUC guidelines.

superior to the conventional IM immunization approach for inducing antibody responses to confer long lasting protection against influenza virus infection in mice (Koutsonanos et al., 2012). We have in recent studies shown that ID delivery of adjuvanted EBOV GP or sGP protein subunit vaccines by microneedles was able to induce strong antibody responses against EBOV GP similarly to IM immunizations, and provided complete protection against lethal challenge in mice (Liu et al., 2018a,b). Our results from this study demonstrated that ID injection of EBOV VLPs is as effective as IM injection for eliciting immune responses in guinea pigs that are protective against lethal EBOV challenge. Further, by analyzing antibody responses after immunizations, we found that while similar levels of IgG2 antibodies against GP were induced by both IM and ID injections, ID immunization of EBOV VLPs induced significantly higher levels of IgG1 antibodies against GP than IM immunization. Moreover, our results from blocking ELISA studies show that the IgG1 antibodies induced by ID injection recognize different epitopes from the IgG2 antibodies induced by IM injection. These findings indicate that antigens delivered to dermal sites may be processed differently by local antigen presenting cells that leads to more comprehensive presentation of different epitopes for induction of immune responses. Future studies to determine the targets in GP recognized by IgG1 antibodies induced by ID immunization will reveal whether such antibodies may contribute to the control of virus infection either directly or in synergy with IgG2 antibodies and provide more effective protection against EBOV infection.

In contrast to antibody responses against GP, we found that the immunization by IM or ID injection of EBOV VLPs induced similar levels of both IgG1 and IgG2 antibodies against VP40, the EBOV matrix protein that directs the formation of VLPs. Further, the levels of IgG1 and IgG2 antibody subclasses against VP40 are also similar in animals vaccinated by EBOV VLPs through either IM or ID injection, whereas antibodies against GP are predominantly of the IgG2 subclass regardless of the immunization routes. These results indicate that induction of enhanced IgG1 antibody responses by ID immunization of EBOV VLPs is specific for the GP antigen but not the VP40 antigen, even when these antigens are delivered in the same VLP vaccine complex. The functional properties of guinea pig IgG1 and IgG2 antibodies are still poorly understood. However, in an early study, it was found that the IgG2 antibodies activate complement through the classical pathway whereas the IgG1 antibodies activate complement through the alternative pathway (Togashi and Tozawa, 1982). In this respect, it seems that guinea IgG1 and IgG2 antibodies resemble more closely to mouse IgG1 or IgG2a antibodies respectively (Lucisano Valim and Lachmann, 1991; Seino et al., 1993). As such, by comparing the IgG1/IgG2 antibody ratios induced by EBOV VLPs in guinea pigs in this study, it seems that the antibody response against GP is biased toward to the Th1 type whereas the antibody response against VP40 would suggest a balanced Th1/Th2 type. These results indicate that the Th1/Th2 paradigm as demonstrated by IgG1 and IgG2 antibody ratios after vaccination may be antigen specific, underscoring the need of more comprehensive analyses for understanding the mechanism as well as correlates of vaccine-induced immune response against virus infection.

## CONCLUSION

We show in this study that the EBOV VLPs produced by the recombinant baculoviruses from insect cells are able to provide effective protection against lethal challenge in the guinea pig model by both IM and ID immunizations. In comparison to IM immunization, ID immunization of EBOV VLPs was able to elicit enhanced IgG1 antibodies against epitopes in EBOV GP that were not recognized by the IgG2 antibodies induced by IM immunization. However, additional studies are needed to understand the underlying mechanism for this observation and to identify the targets recognized by the IgG1 antibodies induced by ID immunizations. Moreover, studies to determine the targets of the antibodies of different IgG subclasses induced by vaccination through different routes will further advance our understanding of the protection against EBOV infection by vaccine-induced immune responses. It will also be of interest to determine the effect of different adjuvant on the epitope breadth as well as subclass switching of antibody responses induced by ID immunizations in comparison with the conventional IM immunization approach. In particular, it will be of interest to determine if the use of an adjuvant will enhance or suppress induction of antibody responses to the subdominant epitopes in a vaccine antigen, and if subclass switching for dominant and

subdominant epitopes will be similarly or differently affected by the use of an adjuvant. Moreover, optimization of EBOV VLPs or other subunit vaccines by ID immunization using novel microneedle vaccine delivery technologies will further reveal the potential of this vaccination approach for protection against infection by EBOV as well as other viral pathogens.

## DATA AVAILABILITY STATEMENT

All datasets generated for this study are included in the article/supplementary material.

## ETHICS STATEMENT

The animal study was reviewed and approved by the Institutional Animal Care and Usage Committee (IACUC) of Emory University and the Institutional Animal Care and Usage Committee (IACUC) of TxBiomed Research Institute.

## AUTHOR CONTRIBUTIONS

YL, LY, and ZW conducted production and characterization of EBOV VLP vaccines, immunization studies, and analyses of immune responses. RC, JN, HS, AT, and JP conducted EBOV challenge studies. LY, RWC, and CY contributed to experimental design and data analysis. YL, LY, and CY contributed to manuscript preparation.

## FUNDING

This study was supported by Public Service Grant AI093406 from the National Institutes of Health.

## REFERENCES

Allela, L., Boury, O., Pouillot, R., Delicat, A., Yaba, P., Kumulungui, B., et al. (2005). Ebola virus antibody prevalence in dogs and human risk. *Emerg. Infect. Dis.* 11, 385–390. doi: 10.3201/eid1103.040981

Barrette, R. W., Metwally, S. A., Rowland, J. M., Xu, L., Zaki, S. R., Nichol, S. T., et al. (2009). Discovery of swine as a host for the *Reston ebolavirus*. *Science* 325, 204–206. doi: 10.1126/science.1172705

Blaney, J. E., Marzi, A., Willet, M., Papaneri, A. B., Wirblich, C., Feldmann, F., et al. (2013). Antibody quality and protection from lethal Ebola virus challenge in nonhuman primates immunized with rabies virus based bivalent vaccine. *PLoS Pathog.* 9:e1003389. doi: 10.1371/journal.ppat.1003389

Bos, J. D., and Kapsenberg, M. L. (1993). The skin immune system: progress in cutaneous biology. *Immunol. Today* 14, 75–78. doi: 10.1016/0167-5699(93)90062-p

Bukreyev, A., Rollin, P. E., Tate, M. K., Yang, L., Zaki, S. R., Shieh, W. J., et al. (2007). Successful topical respiratory tract immunization of primates against Ebola virus. *J. Virol.* 81, 6379–6388. doi: 10.1128/jvi.00105-07

Chiu, S. S., Peiris, J. S., Chan, K. H., Wong, W. H., and Lau, Y. L. (2007). Immunogenicity and safety of intradermal influenza immunization at a reduced dose in healthy children. *Pediatrics* 119, 1076–1082. doi: 10.1542/peds.2006-3176

Chowell, G., and Nishiura, H. (2014). Transmission dynamics and control of Ebola virus disease (EVD): a review. *BMC Med.* 12:196. doi: 10.1186/s12916-014-0196-0

Ewer, K., Rampling, T., Venkatraman, N., Bowyer, G., Wright, D., and Lambe, T. (2016). A monovalent chimpanzee adenovirus Ebola vaccine boosted with MVA. *N. Engl. J. Med.* 374, 1635–1646. doi: 10.1056/NEJMoa1411627

Feldmann, H., and Geisbert, T. W. (2011). Ebola haemorrhagic fever. *Lancet* 377, 849–862. doi: 10.1016/S0140-6736(10)60667-8

Flacher, V., Bouschbacher, M., Verronese, E., Massacrier, C., Sisirak, V., Berthier-Vergnes, O., et al. (2006). Human Langerhans cells express a specific TLR profile and differentially respond to viruses and Gram-positive bacteria. *J. Immunol.* 177, 7959–7967. doi: 10.4049/jimmunol.177.11.7959

Gill, H. S., Kang, S. M., Quan, F. S., and Compans, R. W. (2014). Cutaneous immunization: an evolving paradigm in influenza vaccines. *Expert Opin. Drug Deliv.* 11, 615–627. doi: 10.1517/17425247.2014.885947

Groseth, A., Feldmann, H., and Strong, J. E. (2007). The ecology of Ebola virus. *Trends Microbiol.* 15, 408–416.

Henao-Restrepo, A. M., Longini, I. M., Egger, M., Dean, N. E., Edmunds, W. J., Camacho, A., et al. (2015). Efficacy and effectiveness of an rVSV-vectored vaccine expressing Ebola surface glycoprotein: interim results from the Guinea ring vaccination cluster-randomised trial. *Lancet* 386, 857–866. doi: 10.1016/S0140-6736(15)61117-5

Herbert, A. S., Kuehne, A. I., Barth, J. F., Ortiz, R. A., Nichols, D. K., Zak, S. E., et al. (2013). Venezuelan equine encephalitis virus replicon particle vaccine protects nonhuman primates from intramuscular and aerosol challenge with *Ebolavirus*. *J. Virol.* 87, 4952–4964. doi: 10.1128/JVI.03361-12

Holland, D., Booy, R., De Looze, F., Eizenberg, P., McDonald, J., Karrasch, J., et al. (2008). Intradermal influenza vaccine administered using a new microinjection system produces superior immunogenicity in elderly adults: a randomized controlled trial. *J. Infect. Dis.* 198, 650–658. doi: 10.1086/590434

Jones, S. M., Feldmann, H., Stroher, U., Geisbert, J. B., Fernando, L., Grolla, A., et al. (2005). Live attenuated recombinant vaccine protects nonhuman primates against Ebola and Marburg viruses. *Nat. Med.* 11, 786–790. doi: 10.1038/nm1258

Kenney, R. T., Frech, S. A., Muenz, L. R., Villar, C. P., and Glenn, G. M. (2004). Dose sparing with intradermal injection of influenza vaccine. *N. Engl. J. Med.* 351, 2295–2301. doi: 10.1056/nejmoa043540

Koutsonanos, D. G., Vassilieva, E. V., Stavropoulou, A., Zarnitsyn, V. G., Esser, E. S., Taherbhai, M. T., et al. (2012). Delivery of subunit influenza vaccine to skin with microneedles improves immunogenicity and long-lived protection. *Sci. Rep.* 2:357. doi: 10.1038/srep00357

Laurent, P. E., Bonnet, S., Alchas, P., Regolini, P., Mikszta, J. A., Pettis, R., et al. (2007). Evaluation of the clinical performance of a new intradermal vaccine administration technique and associated delivery system. *Vaccine* 25, 8833–8842. doi: 10.1016/j.vaccine.2007.10.020

Leroy, E. M., Kumulungui, B., Pourrut, X., Rouquet, P., Hassanin, A., Yaba, P., et al. (2005). Fruit bats as reservoirs of Ebola virus. *Nature* 438, 575–576. doi: 10.1038/438575a

Li, H., Ying, T., Yu, F., Lu, L., and Jiang, S. (2015). Development of therapeutics for treatment of Ebola virus infection. *Microbes Infect.* 17, 109–117. doi: 10.1016/j.micinf.2014.11.012

Li, W., Ye, L., Carrion, R. Jr., Mohan, G. S., Nunneley, J., Staples, H., et al. (2015). Characterization of immune responses induced by Ebola virus glycoprotein (GP) and truncated GP isoform DNA vaccines and protection against lethal Ebola virus challenge in mice. *J. Infect. Dis.* 212(Suppl. 2), S398–S403. doi: 10.1093/infdis/jiv186

Liu, Y., Ye, L., Lin, F., Gomaa, Y., Flyer, D., and Carrion, R. (2018a). Intradermal immunization by Ebola virus GP subunit vaccines using microneedle patches protects mice against lethal EBOV challenge. *Sci. Rep* 8:11193. doi: 10.1038/s41598-018-29135-w

Liu, Y., Ye, L., Lin, F., Gomaa, Y., Flyer, D., and Carrion, R. (2018b). Intradermal vaccination with adjuvanted Ebola virus soluble glycoprotein subunit vaccine by microneedle patches protects mice against lethal Ebola virus challenge. *J. Infect. Dis* 218, S545–S552. doi: 10.1093/infdis/jiy267

Lucisano Valim, Y. M., and Lachmann, P. J. (1991). The effect of antibody isotype and antigenic epitope density on the complement-fixing activity of immune complexes: a systematic study using chimaeric anti-NIP antibodies

with human Fc regions. *Clin. Exp. Immunol.* 84, 1–8. doi: 10.1111/j.1365-2249.1991.tb08115.x

Marzi, A., and Feldmann, H. (2014). Ebola virus vaccines: an overview of current approaches. *Expert Rev. Vaccines* 13, 521–531. doi: 10.1586/14760584.2014.885841

Marzi, A., Halfmann, P., Hill-Batorski, L., Feldmann, F., Shupert, W. L., Neumann, G., et al. (2015). Vaccines. An Ebola whole-virus vaccine is protective in nonhuman primates. *Science* 348, 439–442. doi: 10.1126/science.aaa4919

Mohan, G. S., Li, W., Ye, L., Compans, R. W., and Yang, C. (2012). Antigenic subversion: a novel mechanism of host immune evasion by Ebola virus. *PLoS Pathog.* 8:e1003065. doi: 10.1371/journal.ppat.1003065

Mohan, G. S., Ye, L., Li, W., Monteiro, A., Lin, X., Sapkota, B., et al. (2015). Less is more: Ebola virus surface glycoprotein expression levels regulate virus production and infectivity. *J. Virol.* 89, 1205–1217. doi: 10.1128/JVI.01810-14

Reed, D. S., Lackemeyer, M. G., Garza, N. L., Sullivan, L. J., and Nichols, D. K. (2011). Aerosol exposure to *Zaire ebolavirus* in three nonhuman primate species: differences in disease course and clinical pathology. *Microbes Infect.* 13, 930–936. doi: 10.1016/j.micinf.2011.05.002

Regules, J. A., Beigel, J. H., Paolino, K. M., Voell, J., Castellano, A. R., Hu, Z., et al. (2017). A recombinant vesicular stomatitis virus Ebola vaccine. *N. Engl. J. Med.* 376, 330–341. doi: 10.1056/NEJMoa1414216

Rendtorff, R. C., Walker, L. C., Rowland, M. E., and Packer, H. (1959). Intradermal immunization against Asian influenza in children. *J. Am. Med. Assoc.* 170, 524–528.

Seino, J., Eveleigh, P., Warnaar, S., van Haarlem, L. J., van Es, L. A., and Daha, M. R. (1993). Activation of human complement by mouse and mouse/human chimeric monoclonal antibodies. *Clin. Exp. Immunol.* 94, 291–296. doi: 10.1111/j.1365-2249.1993.tb03446.x

Sullivan, N. J., Geisbert, T. W., Geisbert, J. B., Shedlock, D. J., Xu, L., Lamoreaux, L., et al. (2006). Immune protection of nonhuman primates against Ebola virus with single low-dose adenovirus vectors encoding modified GPs. *PLoS Med.* 3:e177. doi: 10.1371/journal.pmed.0030177

Sun, Y., Carrion, R. Jr., Ye, L., Wen, Z., Ro, Y. T., and Brasky, K. (2009). Protection against lethal challenge by Ebola virus-like particles produced in insect cells. *Virology* 383, 12–21. doi: 10.1016/j.virol.2008.09.020

Swenson, D. L., Wang, D., Luo, M., Warfield, K. L., Woraratanadharm, J., Holman, D. H., et al. (2008). Vaccine to confer to nonhuman primates complete protection against multistrain Ebola and Marburg virus infections. *Clin. Vaccine Immunol.* 15, 460–467. doi: 10.1128/CVI.00431-07

Togashi, H., and Tozawa, H. (1982). Neutralization of sendai virus by the IgG subclass antibodies of the guinea pig. *Microbiol. Immunol.* 26, 821–829. doi: 10.1111/j.1348-0421.1982.tb00228.x

Towner, J. S., Sealy, T. K., Khristova, M. L., Albarino, C. G., Conlan, S., Reeder, S. A., et al. (2008). Newly discovered Ebola virus associated with hemorrhagic fever outbreak in Uganda. *PLoS Pathog.* 4:e1000212. doi: 10.1371/journal.ppat.1000212

Warfield, K. L., and Aman, M. J. (2011). Advances in virus-like particle vaccines for filoviruses. *J. Infect. Dis.* 204(Suppl. 3), S1053–S1059. doi: 10.1093/infdis/jir346

Warfield, K. L., Swenson, D. L., Olinger, G. G., Kalina, W. V., Aman, M. J., and Bavari, S. (2007). Ebola virus-like particle-based vaccine protects nonhuman primates against lethal Ebola virus challenge. *J. Infect. Dis.* 196(Suppl. 2), S430–S437.

Wei, X., Decker, J. M., Wang, S., Hui, H., Kappes, J. C., Wu, X., et al. (2003). Antibody neutralization and escape by HIV-1. *Nature* 422, 307–312.

Weingartl, H. M., Embury-Hyatt, C., Nfon, C., Leung, A., Smith, G., and Kobinger, G. (2012). Transmission of Ebola virus from pigs to non-human primates. *Sci. Rep.* 2:811. doi: 10.1038/srep00811

Yang, C., Ye, L., and Compans, R. W. (2008). Protection against filovirus infection: virus-like particle vaccines. *Expert Rev. Vaccines* 7, 333–344. doi: 10.1586/14760584.7.3.333

Ye, L., Lin, J., Sun, Y., Bennouna, S., Lo, M., Wu, Q., et al. (2006). Ebola virus-like particles produced in insect cells exhibit dendritic cell stimulating activity and induce neutralizing antibodies. *Virology* 351, 260–270. doi: 10.1016/j.virol.2006.03.021

Ye, L., and Yang, C. (2015). Development of vaccines for prevention of Ebola virus infection. *Microbes Infect.* 17, 98–108. doi: 10.1016/j.micinf.2014.12.004

**Conflict of Interest:** The authors declare that the research was conducted in the absence of any commercial or financial relationships that could be construed as a potential conflict of interest.

*Copyright © 2020 Liu, Wen, Carrion, Nunneley, Staples, Ticer, Patterson, Compans, Ye and Yang. This is an open-access article distributed under the terms of the Creative Commons Attribution License (CC BY). The use, distribution or reproduction in other forums is permitted, provided the original author(s) and the copyright owner(s) are credited and that the original publication in this journal is cited, in accordance with accepted academic practice. No use, distribution or reproduction is permitted which does not comply with these terms.*

frontiers in Microbiology

REVIEW
published: 28 February 2020
doi: 10.3389/fmicb.2020.00298

# Subunit Vaccines Against Emerging Pathogenic Human Coronaviruses

*Ning Wang[1], Jian Shang[2], Shibo Jiang[1,3]* and Lanying Du[1]**

[1] *Lindsley F. Kimball Research Institute, New York Blood Center, New York, NY, United States,* [2] *Department of Veterinary and Biomedical Sciences, College of Veterinary Medicine, University of Minnesota, Saint Paul, MN, United States,* [3] *Key Laboratory of Medical Molecular Virology (MOE/NHC/CAMS), School of Basic Medical Sciences, Shanghai Medical College, Fudan University, Shanghai, China*

Seven coronaviruses (CoVs) have been isolated from humans so far. Among them, three emerging pathogenic CoVs, including severe acute respiratory syndrome coronavirus (SARS-CoV), Middle East respiratory syndrome coronavirus (MERS-CoV), and a newly identified CoV (2019-nCoV), once caused or continue to cause severe infections in humans, posing significant threats to global public health. SARS-CoV infection in humans (with about 10% case fatality rate) was first reported from China in 2002, while MERS-CoV infection in humans (with about 34.4% case fatality rate) was first reported from Saudi Arabia in June 2012. 2019-nCoV was first reported from China in December 2019, and is currently infecting more than 70000 people (with about 2.7% case fatality rate). Both SARS-CoV and MERS-CoV are zoonotic viruses, using bats as their natural reservoirs, and then transmitting through intermediate hosts, leading to human infections. Nevertheless, the intermediate host for 2019-nCoV is still under investigation and the vaccines against this new CoV have not been available. Although a variety of vaccines have been developed against infections of SARS-CoV and MERS-CoV, none of them has been approved for use in humans. In this review, we have described the structure and function of key proteins of emerging human CoVs, overviewed the current vaccine types to be developed against SARS-CoV and MERS-CoV, and summarized recent advances in subunit vaccines against these two pathogenic human CoVs. These subunit vaccines are introduced on the basis of full-length spike (S) protein, receptor-binding domain (RBD), non-RBD S protein fragments, and non-S structural proteins, and the potential factors affecting these subunit vaccines are also illustrated. Overall, this review will be helpful for rapid design and development of vaccines against the new 2019-nCoV and any future CoVs with pandemic potential. This review was written for the topic of *Antivirals for Emerging Viruses: Vaccines and Therapeutics* in the *Virology* section of *Frontiers in Microbiology*.

**Keywords: human coronaviruses, pathogenesis, SARS-CoV, MERS-CoV, 2019-nCoV, subunit vaccines**

OPEN ACCESS

***Edited by:***
*Lijun Rong,*
*The University of Illinois at Chicago, United States*

***Reviewed by:***
*Ahmed Mohamed Kandeil, National Research Centre, Egypt*
*Liang Qiao, Loyola University Chicago, United States*

****Correspondence:***
*Shibo Jiang*
*shibojiang@fudan.edu.cn*
*Lanying Du*
*ldu@nybc.org*

***Specialty section:***
*This article was submitted to Virology, a section of the journal Frontiers in Microbiology*

***Received:*** *28 November 2019*
***Accepted:*** *10 February 2020*
***Published:*** *28 February 2020*

***Citation:***
*Wang N, Shang J, Jiang S and Du L (2020) Subunit Vaccines Against Emerging Pathogenic Human Coronaviruses. Front. Microbiol. 11:298. doi: 10.3389/fmicb.2020.00298*

## INTRODUCTION

Coronaviruses (CoVs) belong to the subfamily *Othocoronavirinae*, in the family *Coronaviridae* of the order *Nidovirales*. According to the 10th Report on Virus Taxonomy from the International Committee on Taxonomy of Viruses (ICTV), the *Othocoronavirinae* is comprised of four genera, including *alphacoronavirus (alpha-CoV)*, *betacoronavirus (beta-CoV)*, *gammacoronavirus*

*(gamma-CoV)*, and *deltacoronavirus (delta-CoV)* (King et al., 2018). Alpha- and beta-CoVs can infect mammals, including but not limited to bats, pigs, cats, mice, and humans (Kusanagi et al., 1992; Li et al., 2005b; Poon et al., 2005; Drexler et al., 2014; Pedersen, 2014; Kudelova et al., 2015; Cui et al., 2019). Gamma- and delta-CoVs usually infect birds, while some of them could infect mammals (Woo et al., 2009a, 2012, 2014; Ma et al., 2015). Since the late sixties, CoVs have been recognized as one of the viral sources responsible for the common cold. Among all CoVs identified so far, seven have the ability to infect humans, including human coronavirus 229E (HCoV-229E) and human coronavirus NL63 (HCoV-NL63), which belong to alpha-CoVs (Hamre and Procknow, 1966; Chiu et al., 2005), as well as human coronavirus OC43 (HCoV-OC43), human coronavirus HKU1 (HCoV-HKU1), severe acute respiratory syndrome coronavirus (SARS-CoV), Middle East respiratory syndrome coronavirus (MERS-CoV), and the newly emerged coronavirus (2019-nCoV), which are known to be beta-CoVs (Drosten et al., 2003; Ksiazek et al., 2003; Vabret et al., 2003; Woo et al., 2005; Zaki et al., 2012; Du et al., 2016b; Zhang et al., 2020; Zhu et al., 2020) (**Figure 1**).

Four human CoVs, including HCoV-229E, HCoV-NL63, HCoV-OC43, and HCoV-HKU1, have been identified in humans, but without causing severe infections. HCoV-229E was isolated from nasal secretions of medical students with minor upper respiratory disease. This virus was an original isolate, and was first reported in the 1960s (Hamre and Procknow, 1966). In addition to HCoV-229E, several studies have reported the recovery of HCoV-OC43 from patients with upper respiratory tract illness (Tyrrell and Bynoe, 1965; Hamre et al., 1967; McIntosh et al., 1967; Kapikian et al., 1969). In 2004, HCoV-NL63 was isolated from clinical species of infants suffering from pneumonia or bronchiolitis, and characterized for its ability to infect human respiratory tract (Fouchier et al., 2004; van der Hoek et al., 2004). The subsequent study in 2005 identified a new member of CoVs, named HCoV-HKU1, from a 71-year-old man with pneumonia (Woo et al., 2005). Generally, these four viruses are the most common pathogens causing mild upper respiratory infection or asymptomatic infection, and count for about 30% of all colds (Myint, 1994; Lau et al., 2006; Kim et al., 2017). In the serological surveillance on healthy adults, HCoV-229E, HCoV-NL63, and HCoV-OC43 demonstrated more than 90% seropositive with the immunological assay. It appears common for these CoVs to infect children (Mourez et al., 2007; Shao et al., 2007; Severance et al., 2008). In contrast to the above three human CoVs, HCoV-HKU1 has around 50% seropositive in healthy individuals and a relatively low exposure rate in children (Lehmann et al., 2008; Severance et al., 2008). Although the prevalence of various CoVs is different, the incidence among these viruses shows no significant difference (Woo et al., 2009b). The afore-mentioned four CoVs have been detected in 2.1–17.9% of clinical specimens (Esper et al., 2006; Lau et al., 2006; Gerna et al., 2007; Regamey et al., 2008; Matoba et al., 2015; Killerby et al., 2018). These viruses have also been associated with lower respiratory tract illness in children, elders, and immunodeficient individuals (Falsey et al., 2002; Fouchier et al., 2004; Woo et al., 2005; Gerna et al., 2006). HCoV-229E and HCoV-OC43 may lead to central nervous system infection since viral RNAs are detected in the brain of some patients (Arbour et al., 2000; Desforges et al., 2014).

Unlike the above four human CoVs, SARS-CoV, MERS-CoV, and 2019-nCoV have caused severe pneumonia and/or failure of other organs, even death, among infected populations (Nicholls et al., 2003; Zhong et al., 2003; Zaki et al., 2012; Zhu et al., 2020). The epidemic outbreak of SARS-CoV began in the Guangdong Province of China in November 2002, and spread through human-to-human transmission to other parts of the world within a few months (Ksiazek et al., 2003). From November 2002 to August 2003, SARS-CoV infected more than 8,098 people in 29 counties, resulting in over 774 deaths with ∼10% fatality rate (Du et al., 2009a). Palm civets serving as a potential intermediate host of this virus were traced immediately (Tu et al., 2004). Chinese horseshoe bats (*Rhinolophus sinicus*) are the natural reservoir of SARS-CoV (Li et al., 2005b). Various bat SARS-related CoVs (SARSr-CoV) have been identified in Yunnan, China, several of which can infect human cells, and have been further characterized (Ge et al., 2013; Hu et al., 2017). These discoveries indicate the threat of re-emergence of SARS-CoV or SARSr-CoV.

A decade later, another highly pathogenic human CoV, MERS-CoV, emerged, and the first patient with MERS-CoV infection was reported in Saudi Arabia in June 2012 (Zaki et al., 2012). By December 26, 2019, a total of 2,494 laboratory-confirmed cases of MERS, including 858 associated deaths in 27 countries (fatality rate 34.4%), were reported to the WHO[1]. Globally, the majority (about 80%) of human cases have been reported in Saudi Arabia, where people get infected through direct contact with infected dromedary camels or persons[2] (Zaki et al., 2012). Isolation of MERS-CoV and detection of neutralizing antibodies from dromedary camels suggest that these camels are potentially an important intermediate host (Reusken et al., 2013; Azhar et al., 2014). Similar to SARS-CoV, MERS-CoV is also an emerging zoonotic virus (Li and Du, 2019). Bats habituate several CoVs phylogenetically related to MERS-CoV, and some of them are identical to MERS-CoVs, suggesting that MERS-CoV may originate from bats (Annan et al., 2013; Lelli et al., 2013; Lau et al., 2018; Luo et al., 2018a). Different from SARS-CoV, which has not caused infections in humans since 2004 (Du et al., 2009a), the transmission of MERS-CoV has not been interrupted, and the infected human cases continue increasing[1] (Mobaraki and Ahmadzadeh, 2019). Currently, human-to-human transmission of MERS-CoV is limited.

A new CoV, 2019-nCoV, has caught worldwide attention (Liu and Saif, 2020; Zhang et al., 2020). It was first identified in Wuhan, China in December 2019, from patients with pneumonia (Zhu et al., 2020), and has infected more than 70000 people globally, including 2,009 deaths (∼2.7% fatality

[1]https://www.who.int/emergencies/mers-cov/en/

[2]https://www.who.int/docs/default-source/coronaviruse/situation-reports/20200219-sitrep-30-covid-19.pdf?sfvrsn=6e50645_2

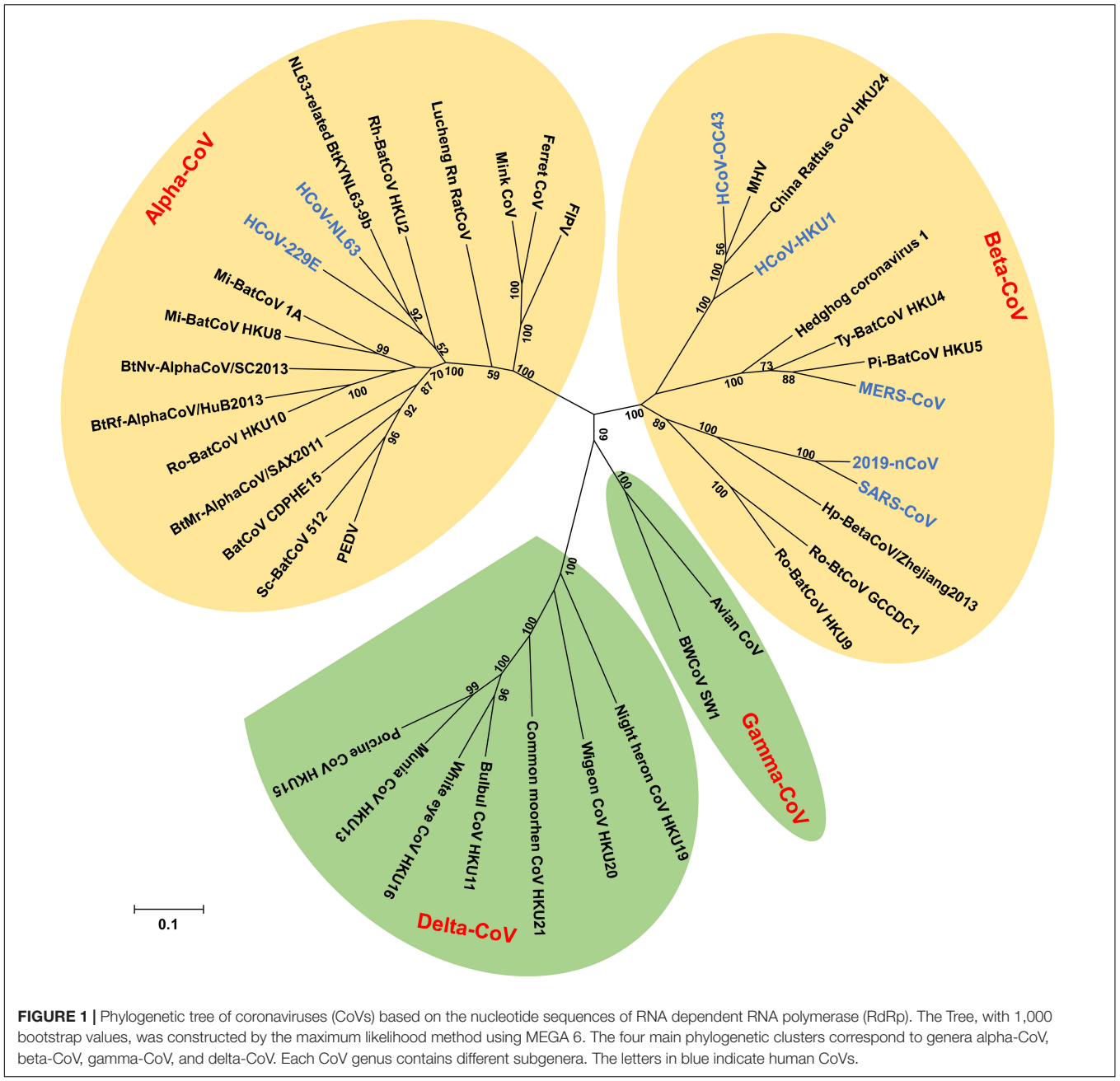


**FIGURE 1 |** Phylogenetic tree of coronaviruses (CoVs) based on the nucleotide sequences of RNA dependent RNA polymerase (RdRp). The Tree, with 1,000 bootstrap values, was constructed by the maximum likelihood method using MEGA 6. The four main phylogenetic clusters correspond to genera alpha-CoV, beta-CoV, gamma-CoV, and delta-CoV. Each CoV genus contains different subgenera. The letters in blue indicate human CoVs.

rate), as of February 19, 2020, particularly in China, and the other parts of the world, including Australia, Japan, Malaysia, Singapore, South Korea, Viet Nam, Cambodia, Philippines, Thailand, Nepal, Sri Lanka, India, United States, Canada, France, Finland, Germany, Italy, Russian Federation, Spain, Sweden, United Kingdom, Belgium, Egypt, and United Arab Emirates[3]. Different from MERS-CoV but similar to SARS-CoV, 2019-nCoV can cause human-to-human transmission, and its intermediate host that leads to the current human infection and outbreak is still under investigation.

[3]https://www.who.int/docs/default-source/coronaviruse/situation-reports/20200204-sitrep-15-ncov.pdf?sfvrsn=88fe8ad6_2

## GENOME OF EMERGING HUMAN CORONAVIRUSES, AS WELL AS STRUCTURE AND FUNCTION OF THEIR KEY PROTEINS

The human CoVs are enveloped viruses with a positive-sense, single-stranded RNA genome. They are 80–160 nm in diameter. Like other CoVs, human CoVs contain the largest viral genome [27–32 kilobase pairs (kb)] among the RNA viruses, and they share similar genome organization (Fehr and Perlman, 2015). Two large overlapping open reading frames (ORFs), *ORF 1a* and *ORF 1b*, occupy two-thirds of the genome at the 5′-terminus, and

a third of the genome at the 3′-terminus encodes four common structural proteins in the gene order of spike (S), envelope (E), membrane (M), and nucleocapsid (N) (5′–3′) (Fehr and Perlman, 2015). The large *ORF 1ab* is a replicase gene encoding polyproteins 1a (pp1a) and pp1b/1ab, which can be cleaved into 15–16 non-structural proteins (nsp2-nsp16 or nsp1-nsp16) by 3C-like proteinase ($3CL^{pro}$, nsp5) and papain-like proteinase ($PL^{pro}$, nsp3) (Bailey-Elkin et al., 2014; Fehr and Perlman, 2015; Tomar et al., 2015; Snijder et al., 2016). In addition to the genes encoding the above structural proteins, the genes encoding accessory proteins have also been detected in the 3′ region between *S–E–M–N* (Fehr and Perlman, 2015). Some beta-CoVs, such as HCoV-OC43 and HCoV-HKU1, contain hemagglutinin-esterase *(HE*) gene located between *ORF 1ab* and *S* gene encoding an additional structural protein, HE (De Groot et al., 2011; Desforges et al., 2013; Huang et al., 2015). Similar to other human CoVs, SARS-CoV possesses a ∼29-kb genome, which encodes pp1a and pp1ab, four main structural proteins (S, E, M, and N), and eight accessory proteins, such as 3a, 3b, 6, 7a, 7b, 8a, 8b, and 9b (**Figure 2A**) (Marra et al., 2003; Snijder et al., 2003). The MERS-CoV genome is about 30 kb in length and encodes pp1a, pp1ab, four structural proteins (S, E, M, and N), and five accessory proteins (3, 4a, 4b, 5, and 8b) (**Figure 2A**) (van Boheemen et al., 2012). The genomic RNA of SARS-CoV and MERS-CoV is packed inside capsid formed by the N protein, while the M, E, and S proteins form the envelope surrounding the capsid (**Figure 2B**). Accessory genes may incorporate into virions at low levels (Liu et al., 2014). Nevertheless, neither SARS-CoV nor MERS-CoV appears to contain the *HE* gene (Rota et al., 2003; Zaki et al., 2012).

Several proteins of human CoVs are important for viral infection and/or pathogenesis. For example, most nsps participate in viral RNA replication and/or transcription (Snijder et al., 2016). The accessory proteins interact with host cells, potentially helping the viruses to evade the immune system and increase their virulence (Menachery et al., 2017). The HE protein assists in the attachment of virus–host cells, thus playing a key role in the production of infectious virions, as in the case of HCoV-OC43 (Desforges et al., 2013). The M and E proteins are responsible for virus assembly or promote virulence (Scobey et al., 2013; DeDiego et al., 2014). Different from the above proteins, the S protein of human CoVs mediates viral entry into host cells and subsequent membrane fusion, enabling viral infection (Du et al., 2009a; Lu et al., 2014). The S protein is a class I viral protein, which can be cleaved into two functional subunits, an amino-terminal S1 subunit and a carboxyl-terminal S2 subunit. The S1 subunit is responsible for virus–host cell receptor binding, whereas the S2 subunit is involved in virus–host membrane fusion (Li et al., 2005a; Lu et al., 2014). The S1 contains two major domains, an N-terminal domain (NTD) and a C-terminal domain (CTD). In general, NTDs mediate sugar binding (Li, 2016; Li et al., 2017; Ou et al., 2017; Hulswit et al., 2019; Tortorici et al., 2019), whereas CTDs facilitate protein receptor recognition (Wong et al., 2004; Hofmann et al., 2006; Lu et al., 2013). The NTDs and CTDs of the S1 subunit can bind host receptors or function as receptor-binding domains (RBDs) (Lu et al., 2013; Hulswit et al., 2019). The entry of human CoVs relies on the interaction between viral and cellular membrane proteins. Recognition of S1 subunit with a receptor and/or sugar on the cell surface initiates the infection (Li, 2015). After the initial recognition and binding, the S protein undergoes conformational changes, followed by membrane fusion through the S2 region (Li, 2015, 2016; Du et al., 2017). Consequently, the viral genetic materials are delivered into the host cell through the fusion core (Du et al., 2009a).

Similar to HCoV-NL63 (Hofmann et al., 2005; Li, 2015), SARS-CoV recognizes, through the RBD in the CTD region of its S1 subunit, angiotensin-converting enzyme 2 (ACE2) as the receptor on the target cell (Li et al., 2003). The RBD (CTD) in two states (standing or lying) has been observed in the trimeric S protein. ACE2 binds to standing RBD, specifically in the receptor-binding motif (RBM), keeping the RBD in the "standing" state (Yuan et al., 2017). In addition to human ACE2, SARS-CoV S protein could also bind to palm civet and mouse ACE2s (Li et al., 2004; Li, 2008). Mutations in the RBD of S1 subunit are required for cross-species transmission of SARS-CoV (Li et al., 2005c; Li, 2008, 2016). Several bat SARSr-CoVs have been identified, and these CoVs can utilize human ACE2 as their receptor to bind the target cells (Ge et al., 2013; Hu et al., 2017). The structure of SARS-CoV S trimer and RBD binding to the ACE2 receptor is shown in **Supplementary Figures S1A,B**.

MERS-CoV RBD shares a structure similar to that of the homology domain of SARS-CoV (Wang et al., 2013). However, antibodies induced by SARS-CoV RBD have no cross-reactivity and/or cross-neutralizing activity to MERS-CoV (Du et al., 2013b). Moreover, MERS-CoV utilizes dipeptidyl peptidase 4 (DPP4) as a receptor through the RBD (CTD) region (Raj et al., 2013), which is distinct from the SARS-CoV receptor ACE2. Although the core regions of SARS-CoV and MERS-CoV RBDs are similar, their RBM regions are significantly different, which explains why they recognize different receptors (Li, 2015). MERS-CoV S trimer also maintains a structure similar to that of SARS-CoV S trimer. Both standing and lying states can be detected in the MERS-CoV RBDs, whereas DPP4 only binds to the standing RBD (Pallesen et al., 2017; Yuan et al., 2017). MERS-CoV is clustered with Ty-BatCoV HKU4 and Pi-BatCoV HKU5 in the subgenus *Merbecovirus*. Ty-BatCoV HKU4, but not Pi-BatCoV HKU5, could use human DPP4 as a receptor (Yang et al., 2014b). Recently, some MERS-related CoVs (MERSr-CoVs) have been discovered from bats that can enter human DPP4-expressing cells (Lau et al., 2018; Luo et al., 2018a). These findings suggest that the emergence of MERSr-CoV may threaten human health owing to their potential for cross-species transmission. The MERS-CoV S protein and RBD and their complexes, along with the DPP4 receptor, are shown in **Supplementary Figures S1C,D**.

Recent studies have found that the new human CoV, 2019-nCoV, which belongs to the species of SARSr-CoV, shares high sequence identify (about 79.5%) to SARS-CoV (Zhou et al., 2020). The genome of 2019-nCoV encodes pp1ab (translated from ORF 1ab), four structural proteins (S, E, M, and N), and six accessory proteins (3a, 6, 7a, 7b, 8, and 10) (**Figure 2A**). Same as SARS-CoV and MERS-CoV, 2019-nCoV appears to have no *HE* gene. The virion of 2019-nCoV consists of similar structure as SARS-CoV and MERS-CoV (**Figure 2B**). Like SARS-CoV, 2019-nCoV

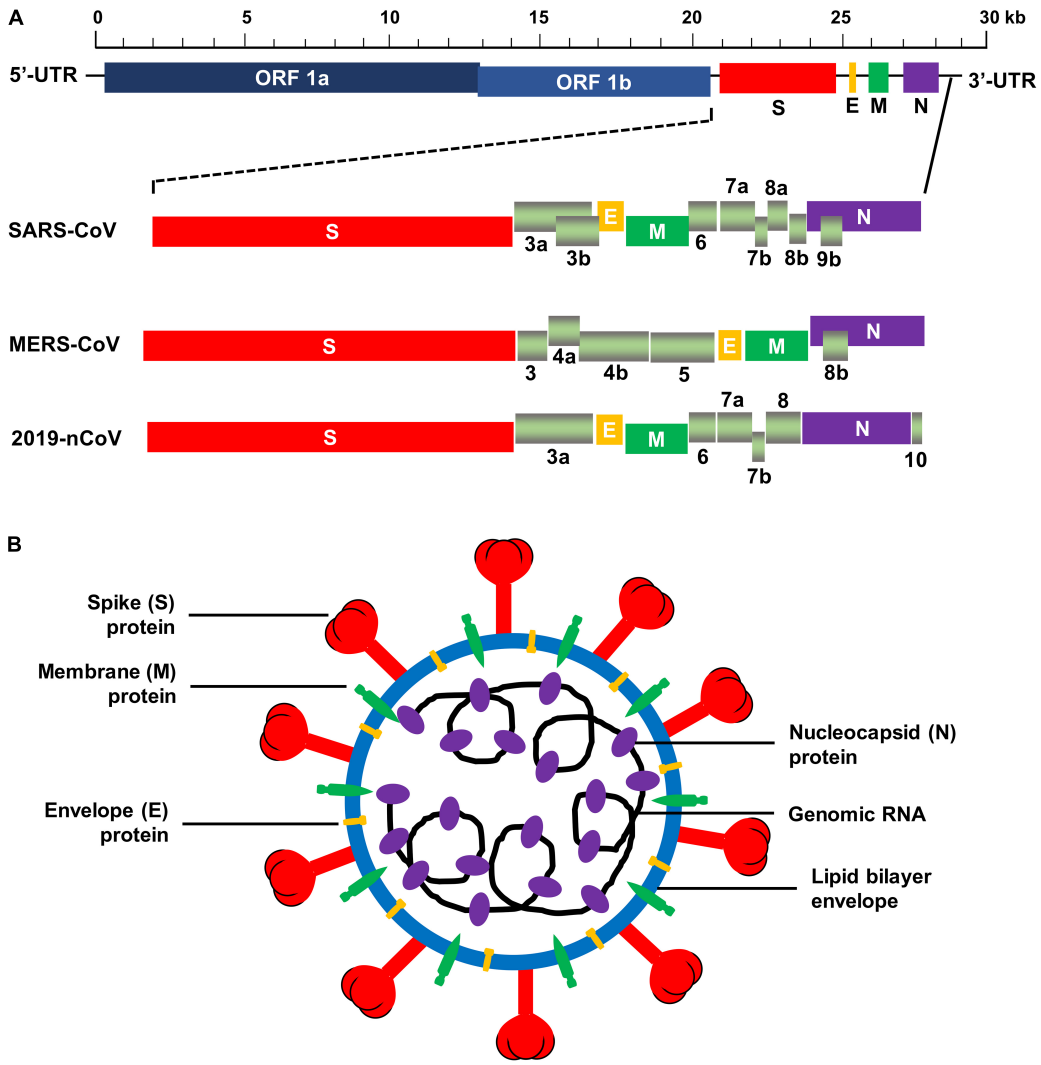


**FIGURE 2 |** Schematic structure of SARS-CoV, MERS-CoV, and 2019-nCoV. **(A)** Schematic diagram of genomic organization of SARS-CoV, MERS-CoV, and 2019-nCoV. The genomic regions or open-reading frames (ORFs) are compared. Structural proteins, including spike (S), envelope (E), membrane (M) and nucleocapsid (N) proteins, as well as non-structural proteins translated from ORF 1a and ORF 1b and accessory proteins, including 3a, 3b, 6, 7a, 7b, 8a, 8b, and 9b (for SARS-CoV), 3, 4a, 4b, 5, and 8b (for MERS-CoV), and 3a, 6, 7a, 7b, 8, and 10 (for 2019-nCoV) are indicated. 5′-UTR and 3′-UTR, untranslated regions at the N- and C-terminal regions, respectively. Kb, kilobase pair. **(B)** Schematic structure of virion of SARS-CoV, MERS-CoV, and 2019-nCoV and its major structural proteins.

also uses ACE2 as its cellular receptor to enter host cells (Zhou et al., 2020). Currently, the structure of 2019-nCoV RBD and/or its binding with the viral receptor has not yet been available.

## OVERVIEW OF VACCINES AGAINST EMERGING PATHOGENIC HUMAN CORONAVIRUSES

Unlike the four low pathogenic human CoVs, including HCoV-229E, HCoV-NL63, HCoV-OC43, and HCoV-HKU1, which cause mild to no pathogenesis in humans, SARS-CoV, MERS-CoV, and 2019-CoV are three highly pathogenic human CoVs (Channappanavar and Perlman, 2017; Cui et al., 2019; Zhu et al., 2020). With the increasing numbers of 2019-nCoV and MERS-CoV infections and continuous threat of re-emergence of SARS-CoV, as well as the potential of SARS- and MERS-related CoVs to cause human infections, it is critical to develop vaccines with strong efficacy and safety targeting these viruses to prevent their infections in humans. Since the vaccines against 2019-nCoV have not been available, the rest of the review will focus on the vaccines against SARS-CoV and MERS-CoV.

Although a variety of vaccines have been developed against SARS-CoV and MERS-CoV, most of them are in the preclinical studies, and only several have been tested in clinical trials[4,5] (Du et al., 2016b; Cho et al., 2018). Nevertheless, no vaccines

[4]https://clinicaltrials.gov/ct2/show/NCT03615911
[5]https://clinicaltrials.gov/ct2/show/NCT03399578

have been approved for the prevention of SARS and MERS in humans, demonstrating the need to develop effective and safe vaccines to control current MERS-CoV infection, or to be stockpiled for potential use against re-emerged SARS-CoV or SARSr-CoV. Particularly, effective and safe vaccines are urgently needed to prevent and control the current outbreak of 2019-nCoV.

Most SARS-CoV and MERS-CoV vaccines developed thus far are based on the inactivated or live attenuated viruses, DNAs, proteins, nanoparticles, viral vectors, including virus-like particles (VLPs) (Zeng et al., 2004; Jiang et al., 2005; Liu et al., 2005; Du et al., 2009a, 2016b; Pimentel et al., 2009; Al-Amri et al., 2017). Each vaccine type has different advantages and disadvantages. For instance, inactivated and live-attenuated virus-based vaccines are vaccine types developed using the most traditional approaches. Although they generally induce highly potent immune responses and/or protection, the possibility for incomplete inactivation of viruses or recovering virulence exists, resulting in significant safety concerns (Zhang et al., 2014). Also, these traditional vaccines may induce the antibody-dependent enhancement (ADE) effect, as in the case of SARS-CoV infection (Luo et al., 2018b). Similarly, some viral-vectored vaccines can elicit specific antibody and cellular immune responses with neutralizing activity and protection, but they might also induce anti-vector immunity or present pre-existing immunity, causing some harmful immune responses. Instead, DNA and nanoparticle vaccines maintain strong safety profile; however, the immunogenicity of these vaccines is usually lower than that of virus- or viral vector-based vaccines, often requiring optimization of sequences, components, or immunization routes, inclusion of appropriate adjuvants, or application of combinational immunization approaches (Zhang et al., 2014).

## SUBUNIT VACCINES AGAINST SARS-CoV AND MERS-CoV

Subunit vaccines are vaccines developed based on the synthetic peptides or recombinant proteins. Unlike inactivated or live-attenuated virus and some viral vectored vaccines, this vaccine type mainly contains specific viral antigenic fragments, but without including any components of infectious viruses, eliminating the concerns of incomplete inactivation, virulence recovery, or pre-existing immunity (Du et al., 2008; Deng et al., 2012). Similar to DNA or VLP-based vaccines, subunit vaccines are generally safe without causing potential harmful immune responses, making them promising vaccine candidates. Moreover, subunit vaccines may target specific, well-defined neutralizing epitopes with improved immunogenicity and/or efficacy (Du et al., 2008; Zhang et al., 2014).

A number of subunit vaccines against SARS-CoV and MERS-CoV have been developed, and these are described in detail in the next paragraphs. The targets used for the development of SARS-CoV and MERS-CoV subunit vaccines are also be discussed.

### Potential Targets for Development of SARS-CoV and MERS-CoV Subunit Vaccines

The S protein of SARS-CoV and MERS-CoV plays a vital role in receptor binding and membrane fusion. Thus, the S protein, but not other structural proteins, is the major antigen to induce protective neutralizing antibodies to block viruses from binding their respective receptor and thus inhibit viral infection (Bisht et al., 2004; Buchholz et al., 2004; Bukreyev et al., 2004; Yang et al., 2004). As a result, the S protein is also a major target for the development of subunit vaccines against SARS-CoV and MERS-CoV. Both full-length S protein and its antigenic fragments, including S1 subunit, NTD, RBD, and S2 subunit, can serve as important targets for the development of subunit vaccines (Guo et al., 2005; Mou et al., 2013; Wang et al., 2015; Jiaming et al., 2017; Zhou et al., 2018).

Although subunit vaccines based on the full-length S protein may elicit potent immune responses and/or protection, studies have found that antibodies induced by some of these vaccines mediate enhancement of viral infection *in vitro*, as in the case of SARS-CoV (Kam et al., 2007; Jaume et al., 2012), raising safety concerns for the development of full-length S protein-based subunit vaccines against SARS-CoV and MERS-CoV. In contrast, RBD-based subunit vaccines comprise the major critical neutralizing domain (Du and Jiang, 2015; Zhou et al., 2019). Therefore, these vaccines may generate potent neutralizing antibodies with strong protective immunity against viral infection. S1 subunit, for example, is much shorter than the full-length S protein, but it is no less able to induce strong immune responses and/or protection against viral infection (Li et al., 2013; Adney et al., 2019). Thus, this fragment can be used as an alternative target for subunit vaccine development. Despite their ability to induce immune responses and/or neutralizing antibodies, NTD and S2 as the targets of subunit vaccines are less immunogenic, eliciting significantly lower antibody titers, cellular immune responses, and/or protection than the other regions, such as full-length, S1, and RBD (Guo et al., 2005; Jiaming et al., 2017). Therefore, in terms of safety and efficacy, the RBD and/or S1 of S protein could be applied as critical targets for the development of subunit vaccine candidates against SARS-CoV, MERS-CoV, SARSr-CoV, and MERSr-CoV. Because of its conserved amino acid sequences and high homology among different virus strains (Elshabrawy et al., 2012; Zhou et al., 2018), the S2 subunit has potential to be used as a target for the development of universal vaccines against divergent virus strains.

In addition to the S protein, the N protein of SARS-CoV and MERS-CoV may serve as an additional target for the development of subunit vaccines. Unlike S protein, the N protein has no ability to elicit neutralizing antibodies to block virus-receptor interaction and neutralize viral infection, but it may induce specific antibody and cellular immune responses (Liu et al., 2006; Zheng et al., 2009). Several immunodominant B-cell and T-cell epitopes have been identified in the N protein of SARS-CoV and MERS-CoV, some of which are conserved in mice, non-human primates, and humans (Liu et al., 2006; Chan et al., 2011; Veit et al., 2018). Other proteins, such as M protein, can be

used as potential targets of SARS-CoV and MERS-CoV subunit vaccines. Notably, SARS-CoV M protein-derived peptides have immunogenicity to induce high-titer antibody responses in the immunized animals (He et al., 2005b), suggesting the potential for utilizing this protein to develop subunit vaccines.

## Subunit Vaccines Against SARS-CoV

Numerous subunit vaccines against SARS-CoV have been developed since the outbreak of SARS, the majority of which use the S protein and/or its antigenic fragments, in particular, RBD, as the vaccine target (**Table 1**).

### SARS-CoV Subunit Vaccines Based on Full-Length S Protein

Subunit vaccines based on SARS-CoV S protein, including full-length or trimeric S protein, are immunogenic with protection against SARS-CoV infection (He et al., 2006a; Kam et al., 2007; Li et al., 2013). Either insect cell-expressed full-length (FL-S) or extracellular domain (EC-S) SARS-CoV S protein developed high-titer S-specific antibodies with neutralizing activity against pseudotyped SARS-CoV expressing S protein of representative SARS-CoV human and palm civet strains (Tor2, GD03, and SZ3) isolated during the 2002 and 2003 or 2003 and 2004 outbreaks (He et al., 2006a). In addition, full-length S-ectodomain proteins fused with or without a foldon trimeric motif (S or S-foldon) could elicit specific antibody responses and neutralizing antibodies, protecting immunized mice against SARS-CoV challenge with undetectable virus titers in the lungs (Li et al., 2013). Moreover, a subunit vaccine (triSpike) based on a full-length S protein trimer induced specific serum and mucosal antibody responses and efficient neutralizing antibodies against SARS-CoV infection (Kam et al., 2007). Nevertheless, this vaccine also resulted in Fcγ receptor II (FcγRII)-dependent and ACE2-independent ADE, particularly in human monocytic or lymphoblastic cell lines infected with pseudotyped SARS-CoV expressing viral S protein, or in Raji B cells (B-cell lymphoma line) infected with live SARS-CoV (Kam et al., 2007; Jaume et al., 2012), raising significant concerns over the use of full-length S protein as a SARS vaccine target.

### SARS-CoV Subunit Vaccines Based on RBD

SARS-CoV RBD contains multiple conformation-dependent epitopes capable of eliciting high-titer neutralizing antibodies; thus, it is a major target for the development of SARS vaccines (He et al., 2004, 2005a; Jiang et al., 2012; Zhu et al., 2013). Subunit vaccines based on the SARS-CoV RBD have been extensively explored. Studies have found that a fusion protein containing RBD and the fragment crystallizable (Fc) region of human IgG1 (RBD-Fc) elicited highly potent neutralizing antibodies against SARS-CoV in the immunized rabbits and mice, which strongly blocked the binding between S1 protein and SARS-CoV receptor ACE2 (He et al., 2004). This RBD protein induced long-term, high-level SARS-CoV S-specific antibodies and neutralizing antibodies that could be maintained for 12 months after immunization, protecting most of the vaccinated mice against SARS-CoV infection (Du et al., 2007). In addition, recombinant RBDs (residues 318–510 or 318–536) stably or transiently expressed in Chinese hamster ovary (CHO) cells bound strongly to RBD-specific monoclonal antibodies (mAbs), elicited high-titer anti-SARS-CoV neutralizing antibodies, and protected most, or all, of the SARS-CoV-challenged mice, with undetectable viral RNA and undetectable or significantly reduced viral load (Du et al., 2009c, 2010). Significantly, a 293T cell-expressed RBD protein maintains excellent conformation and good antigenicity to bind SARS-CoV RBD-specific neutralizing mAbs. It elicited highly potent neutralizing antibodies that completely protected immunized mice against SARS-CoV challenge (Du et al., 2009b). Particularly, RBDs from the S proteins of Tor2, GD03, and SZ3, representative strains of SARS-CoV isolated from human 2002–2003, 2003–2004, and palm civet strains, can induce high-titer cross-neutralizing antibodies against pseudotyped SARS-CoV expressing respective S proteins (He et al., 2006c). Different from the full-length S protein-based SARS subunit vaccines, no obvious pathogenic effects have been identified in the RBD-based SARS subunit vaccines (Kam et al., 2007; Jaume et al., 2012).

### SARS-CoV Subunit Vaccines Based on Non-RBD S Protein Fragments

SARS subunit vaccines based on S protein fragments (S1 and S2), other than the RBD, have shown immunogenicity and/or protective efficacy against SARS-CoV infection (Guo et al., 2005; Li et al., 2013). For example, recombinant S1 proteins fused with or without foldon elicited specific antibodies with neutralizing activity that protected immunized mice against high-dose SARS-CoV challenge (Li et al., 2013). Although some studies have demonstrated that recombinant SARS-CoV S2 (residues 681–980) protein elicits specific non-neutralizing antibody response in mice (Guo et al., 2005), others have indicated that mAbs targeting highly conserved heptad repeat 1 (HR1) and HR2 domains of SARS-CoV S protein have broad neutralizing activity against pseudotyped SARS-CoV expressing S protein of divergent strains (Elshabrawy et al., 2012), indicating the potential of utilizing the S2 region as a broad-spectrum anti-SARS-CoV vaccine target (Zheng et al., 2009).

### SARS-CoV Subunit Vaccines Based on Non-S Structural Proteins

Subunit vaccines based on the N and M proteins of SARS-CoV have shown immunogenicity in vaccinated animals (Liu et al., 2006; Zheng et al., 2009). Studies have revealed that a plant-expressed SARS-CoV N protein conjugated with Freund's adjuvant elicited specific IgG antibodies, including IgG1 and IgG2a subtypes, and cellular immune responses in mice, whereas another *E. coli*-expressed N protein conjugated with Montanide ISA-51 and cysteine-phosphate-guanine (CpG) adjuvants induced specific IgG antibodies toward a Th1 (IgG2a)-type response in mice (Liu et al., 2006; Zheng et al., 2009). Although N-specific antibodies have been detected in convalescent-phase SARS patient and immunized rabbit sera, they have no neutralizing activity against SARS-CoV infection (Qiu et al., 2005). In addition, immunodominant M protein peptides (M1-31 and M132-161) identified using convalescent-phase sera of SARS patients and immunized mouse and rabbit sera have immunogenicity to elicit specific IgG antibodies in

**TABLE 1 |** Subunit Vaccines against SARS-CoV[a].

| Name | Antigenicity and functionality | Adjuvant | Route | Animal models | Antibody response | Cellular immune response | Protection | References |
|---|---|---|---|---|---|---|---|---|
| **Subunit vaccines based on SARS-CoV full-length or trimeric S protein** | | | | | | | | |
| FL-S and EC-S proteins | Bind to SARS-CoV S1, NTD, RBD, and S2-specific mAbs | MPL + TDM | S.C. | BALB/c mice | Elicit SARS-CoV S-specific Abs (IgG, > 1: $2 \times 10^5$), neutralizing (> 1:$2.4 \times 10^4$) pseudotyped SARS-CoV (Tor2, GD03, and SZ3 strains) | N/A | N/A | He et al., 2006a |
| S andS-foldon proteins | N/A | TiterMax Gold; Alum Hydro + MPL | S.C. or I.M. | BALB/c mice | Elicit SARS-CoV S-specific Abs (IgG, > 1:$10^4$) in mice, neutralizing (~$2.4 \times 10^2$ for S; ~$1:7 \times 10^2$ for S-foldon) live SARS-CoV (Urbani strain) | N/A | Protect vaccinated mice from challenge of SARS-CoV (Urbani strain, $10^5$ $TCID_{50}$) with undetectable viral load in lungs | Li et al., 2013 |
| triSpike protein | N/A | Alum hydro | I.P. or S.C. | BALB/c mice; Hamsters | Elicits SARS-CoV S-specific mucosal and serum Abs (IgA and IgG) in mice and hamsters, blocking S-ACE2 receptor binding and neutralizing live SARS-CoV (HKU-39849 strain); induces ADE | N/A | Protects vaccinated hamsters from challenge of SARS-CoV (Urbani strain, $10^3$ $TCID_{50}$) with undetectable or reduced viral load in lungs | Kam et al., 2007; Jaume et al., 2012 |
| **Subunit vaccines based on SARS-CoV RBD protein** | | | | | | | | |
| RBD-Fc protein | N/A | Freund's | I.D. orI.M. | BALB/c mice; Rabbits | Elicits SARS-CoV S/RBD-specific Abs (IgG) in mice and rabbits, neutralizing pseudotyped (rabbits: ≥ $7.3 \times 10^4$) and live (mice: $1:4 \times 10^3$; rabbits: > $1:1.5 \times 10^4$) SARS-CoV (BJ01 strain) | N/A | Protects majority (4/5) of vaccinated mice from challenge of SARS-CoV (BJ01 strain, $10^6$ $TCID_{50}$), with one mouse showing mild alveolar damage in lungs | He et al., 2004; Du et al., 2007 |
| RBD193-CHO; RBD219-CHO proteins | Binds to SARS-CoV RBD-specific mAbs (neutralizing 24H8, 31H12, 35B5, 33G4, 19B2; non-neutralizing 17H9) | Freund's | S.C. | BALB/c mice | Elicit SARS-CoV RBD-specific Abs, neutralizing pseudotyped (< 1:$10^4$ for RBD193-CHO; $1:5.8 \times 10^4$ for RBD219-CHO) and live (< 1:$10^3$ for RBD193-CHO; 1:$10^3$ for RBD219-CHO) SARS-CoV (GZ50 strain) | Induce SARS-CoV RBD-specific cellular immune responses (IFN-γ, IL-2, IL-4, IL-10) in mice | Protect all (for RBD219-CHO) or majority (3/5, for RBD219-CHO) of vaccinated mice from challenge of SARS-CoV (GZ50 strain, 100 $TCID_{50}$ for RBD193-CHO; $5 \times 10^5$ $TCID_{50}$ for RBD219-CHO) with undetectable viral RNA or no, to reduced, viral load in lungs | Du et al., 2009c, 2010 |

*(Continued)*

**TABLE 1 |** Continued

| Name | Antigenicity and functionality | Adjuvant | Route | Animal models | Antibody response | Cellular immune response | Protection | References |
|---|---|---|---|---|---|---|---|---|
| RBD-293T protein | Binds to SARS-CoV RBD-specific mAbs (neutralizing 24H8, 31H12, 35B5, 33G4, 19B2; non-neutralizing 17H9) | SAS | S.C. | BALB/c mice | Elicits SARS-CoV RBD-specific Abs (IgG), neutralizing pseudotyped (1:6.9 × $10^5$) and live (1:1.6 × $10^3$) SARS-CoV (GZ50 strain) | N/A | Protects all vaccinated mice from challenge of SARS-CoV (GZ50 strain, 100 $TCID_{50}$) with undetectable viral RNA and viral load in lungs | Du et al., 2009b |
| S318-510 protein | N/A | Alum; Alum + CpG | S.C. | 129S6/SvEv mice | Elicits SARS-CoV-specific Abs (IgG, IgG1, and IgG2a) in mice. Reduces neutralization after removing glycosylation | Induces SARS-CoV S-specific cellular immune responses (IFN-γ) in mice | N/A | Zakhartchouk et al., 2007 |
| **Subunit vaccines based on non-RBD SARS-CoV S protein fragments** | | | | | | | | |
| S1 and S1-foldon proteins | N/A | TiterMax Gold; Alum Hydro + MPL | S.C. or I.M. | BALB/c mice | Elicit SARS-CoV S-specific Abs (IgG, > 1:$10^4$) in mice, neutralizing (1:1.7 × $10^2$ for S1; 1:90 for S1-foldon) live SARS-CoV (Urbani strain) | N/A | Protect vaccinated mice from challenge of SARS-CoV (Urbani strain, $10^5$ $TCID_{50}$) with undetectable viral load in lungs | Li et al., 2013 |
| S2 protein | N/A | Freund's | S.C. | BALB/c mice | Elicits SARS-CoV S2-specific Abs (IgG, 1:1.6 × $10^3$) in mice with no neutralizing activity | Induces SARS-CoV S2-specific cellular immune responses (IFN-γ and IL-4) in mice | N/A | Guo et al., 2005 |
| **Subunit vaccines based on SARS-CoV non-S structural proteins (i.e. N and M)** | | | | | | | | |
| rN protein | N/A | Freund's | I.P. | BALB/c mice | Elicits SARS-CoV N-specific Abs (IgG (1:1.8 × $10^3$), IgG1, and IgG2a) in mice | Induces cellular immune responses with up-regulated IFN-γ and IL-10 cytokines in mice | N/A | Zheng et al., 2009 |
| rN protein | N/A | Montanide + CpG; Freund's | S.C. | BALB/c mice | Elicits SARS-CoV N-specific Abs (IgG) in mice | Induces SARS-CoV N-specific cellular immune responses (IFN- γ) in mice | N/A | Liu et al., 2006 |
| M1-31 and M132-161 peptides | Bind to sera from SARS patients or immunized mice and rabbits | Freund's | I.D. | BALB/c mice; NZW rabbits | Induce SARS-CoV M-specific Abs (IgG) in rabbits | N/A | N/A | He et al., 2005b |

[a]*Abs, antibodies; ADE, antibody-dependent enhancement; Alum hydro, aluminum hydroxide; CHO, Chinese hamster ovary; CpG, cysteine-phosphate-guanine; I.D., intradermal; I.M., intramuscular; IFN-γ, interferon gamma; IL-2, interleukin 2; IL-4, interleukin 4; IL-10, Interleukin 10; I.P., intraperitoneal; mAbs, monoclonal antibodies; Montanide, Montanide ISA-51; MPL + TDM, monophosphoryl lipid A and trehalose dicorynomycolate; N/A, not reported; NTD, N-terminal domain; NZW rabbits, New Zealand White rabbits; RBD, receptor-binding domain; SAS, Sigma adjuvant system; S.C., subcutaneous; $TCID_{50}$, median tissue culture infectious dose.*

rabbits (He et al., 2005b). In spite of their immunogenicity, it appears that these N- and M-based SARS subunit vaccines have not been investigated for their protective efficacy against SARS-CoV infection. Thus, it is unclear whether these non-S structural protein-based SARS subunit vaccines can prevent SARS-CoV infection.

### Potential Factors Affecting SARS-CoV Subunit Vaccines

A number of factors may affect the expression of proteins to be used as SARS subunit vaccines; apart from their immunogenicity and/or protective efficacy. Understanding of these factors is important to generate subunit vaccines with good quality, high immunogenicity, and excellent protection against SARS-CoV infection.

The expression of recombinant protein-based SARS subunit vaccines may be changed by the following factors. First, addition of an intron splicing enhancer to the truncated SARS-CoV S protein fragments results in better enhancement of protein expression in mammalian cells than the exon splicing enhancers, and different cells may result in different fold increase of protein expression (Chang et al., 2006). Second, inclusion of a post-transcriptional gene silencing suppressor p19 protein from tomato bushy stunt virus to a SARS-CoV N protein may significantly increase its transient expression in tobacco (Zheng et al., 2009).

The following factors may affect the immunogenicity and protective efficacy of protein-based SARS subunit vaccines, including same proteins expressed in different expression systems, and same proteins with various lengths, amino acid mutations, or deletions (He et al., 2006b; Du et al., 2009b). For example, RBD proteins containing different lengths (193-mer: RBD193-CHO or 219-mer: RBD219-CHO) elicited different immune responses and protective efficacy against SARS-CoV challenge (Du et al., 2009c, 2010). A recombinant SARS-CoV RBD (RBD-293T) protein expressed in mammalian cell system was able to induce stronger neutralizing antibody response than those expressed in insect cells (RBD-Sf9) and *E. coli* (RBD-Ec) (Du et al., 2009b), suggesting that RBD purified from mammalian cells has preference for further development due to its ability to maintain native conformation. Notably, a single mutation (R441A) in the RBD of SARS-CoV disrupted its major neutralizing epitopes and affinity to bind viral receptor ACE2, thus abolishing the vaccine's immunogenicity, and hence, its ability to induce neutralizing antibodies in immunized animals (He et al., 2006b). Additionally, deletion of a particular amino acid by changing a glycosylation site in the SARS-CoV RBD (RBD219-N1) also resulted in the alteration of subunit vaccine's immunogenicity (Chen et al., 2014).

Other factors that potentially affect the immunogenicity of SARS subunit vaccines include immunization routes and adjuvants (Zakhartchouk et al., 2007; Li et al., 2013). Significantly high-titer antibodies were induced by monomeric or trimeric SARS-CoV S and S1 proteins through the intramuscular (I.M.) route compared to the subcutaneous (S.C.) route (Li et al., 2013). Moreover, a SARS-CoV RBD subunit vaccine conjugated with Alum plus CpG adjuvants elicited a higher level of IgG2a antibody and interferon gamma (IFN-γ) secretion than the RBD with Alum alone (Zakhartchouk et al., 2007).

## Subunit Vaccines Against MERS-CoV

Subunit vaccines against MERS-CoV have been developed extensively, almost all of which are based on the S protein, including full-length S timer, NTD, S1, and S2, particularly RBD. These subunit vaccines, including their antigenicity, functionality, immunogenicity, and protective efficacy in different animal models, are summarized in **Table 2**.

### MERS-CoV Subunit Vaccines Based on Full-Length S Protein

Subunit vaccines based on the full-length S protein cover both RBD and non-RBD neutralizing epitopes, some of which may be located in the conserved S2 subunit; thus this type of subunit vaccines are expected to induce high-titer neutralizing antibodies. Although several MERS-CoV full-length S protein-based vaccines have been reported in other vaccine types, including viral vectors and DNAs (Wang et al., 2015; Wang C. et al., 2017; Haagmans et al., 2016; Zhou et al., 2018), only a few subunit vaccines have been developed that rely on the full-length S protein. For example, a recombinant MERS-CoV S protein trimer (MERS S-2P) in prefusion conformation binds to the DPP4 receptor, as well as to the MERS-CoV NTD, RBD, and S2-specific neutralizing mAbs (Pallesen et al., 2017). Whereas this protein induces neutralizing antibodies in mice against divergent pseudotyped MERS-CoV *in vitro*, its *in vivo* protective activity against MERS-CoV infection is unknown (Pallesen et al., 2017). Therefore, more studies are needed to elucidate the potential for the development of MERS-CoV full-length S-based subunit vaccines, including understanding their protective efficacy and identifying possible harmful immune responses.

### MERS-CoV Subunit Vaccines Based on RBD

Numerous MERS-CoV RBD-based subunit vaccines have been developed and extensively evaluated in available animal models since the emergence of MERS-CoV (**Table 2**) (Du et al., 2013c; Tai et al., 2017; Zhou et al., 2018). In general, these subunit vaccines have strong immunogenicity and are capable of inducing high neutralizing antibodies and/or protection against MERS-CoV infection (Ma et al., 2014b; Zhang et al., 2016; Tai et al., 2017; Wang Y. et al., 2017). Most subunit vaccines based on the MERS-CoV RBD have been described in detail in a previous review article (Zhou et al., 2019). In this section, we will briefly introduce these RBD-targeting MERS vaccines, and compare their functionality, antigenicity, immunogenicity, and protection against MERS-CoV infection.

Co-crystallographic analyses of MERS-CoV RBD and/or RBD/DPP4 complexes have confirmed that the RBD is attributed to residues 367–588 (Chen et al., 2013) or 367–606 (Lu et al., 2013) in the MERS-CoV S1 subunit. Indeed, a recombinant MERS-CoV RBD (rRBD) fragment (residues 367–606) elicits RBD-specific antibody and cellular immune responses and neutralizing antibodies in mice and/or non-human primates (NHPs) (Lan et al., 2014, 2015). However, it only partially protects

**TABLE 2 |** Subunit Vaccines against MERS-CoV[a].

| Name | Functionality and antigenicity | Adjuvant | Route | Animal models | Antibody response | Cellular immune response | Protective efficacy | References |
|---|---|---|---|---|---|---|---|---|
| **Subunit vaccines based on MERS-CoV full-length S protein** | | | | | | | | |
| MERS S-2P protein | Binds to DPP4 receptor and MERS-CoV S-NTD, RBD, and S2-specific neutralizing mAbs (G2, D12, and G4, respectively) | SAS | I.M. | BALB/c mice | Elicits neutralizing Abs in mice, neutralizing 7 pseudotyped MERS-CoV | N/A | N/A | Pallesen et al., 2017 |
| **Subunit vaccines based on MERS-CoV RBD protein** | | | | | | | | |
| rRBD (S367-606) protein | N/A | Alum<br>Hydro + CpG or poly(I:C);<br>IFA + CpG (mouse);<br>Alum (NHPs) | I.M. or S.C. | BALB/c mice; NHPs | Elicits MERS-CoV RBD-specific Abs in mice (IgG, IgG1, IgG2a, and IgG2b) and NHPs (IgG), neutralizing pseudotyped (mouse: $< 1{:}5 \times 10^2$) and live (NHPs: $< 1{:}5 \times 10^2$) MERS-CoV (EMC2012 strain) | Induces MERS-CoV RBD-specific cellular immune responses (IFN-γ, TNF-α, IL-2, IL-4, IL-6, and IL-10) in mice and/or monkeys | Partially protects vaccinated NHPs from challenge of MERS-CoV (EMC2012 strain, $6.5 \times 10^7$ $TCID_{50}$) with alleviated pneumonia and decreased viral load | Lan et al., 2014, 2015 |
| RBD (S377-662)-Fc protein | Binds to DPP4 receptor | Poly(I:C);<br>Montanide | I.N. or S.C. | BALB/c mice | Elicits MERS-CoV S1- and RBD-specific Abs (IgA, IgG ($> 1{:}10^4$), IgG1, IgG2a, and IgG3) in mice, neutralizing ($\geq 1{:}2.4 \times 10^2$) live MERS-CoV (EMC2012 strain) | Induces MERS-CoV S1-specific cellular immune responses (IFN-γ and IL-2) in mice | N/A | Du et al., 2013c; Ma et al., 2014b |
| RBD (S377-588)-Fc protein | Binds to DPP4 receptor and MERS-CoV RBD specific neutralizing mAbs (Mersmab1, m336, m337, and m338) | Montanide;<br>MF59;<br>AddaVax | I.M. or S.C. | BALB/c mice;<br>hDPP4-Tg mice;<br>Rabbits | Elicits MERS-CoV S1 and RBD-specific Abs in mice (IgG ($> 1{:}10^5$), IgG1, and IgG2a) and rabbits (IgG), neutralizing 17 pseudotyped ($\geq 1{:}10^4$) and 2 live ($\geq 1{:}10^3$) MERS-CoV (EMC2012 and London1-2012 strains) | Induces MERS-CoV S1-specific cellular immune responses (IFN-γ and IL-2) in mice | Protects vaccinated Ad5/hDPP4-transduced BALB/c mice and majority (4/6) of vaccinated hDPP4-Tg mice from MERS-CoV (EMC2012 strain, $10^5$ PFU for BALB/c; $10^{3-4}$ $TCID_{50}$ for Tg) challenge, without immunological toxicity or eosinophilic immune enhancement | Du et al., 2013a; Ma et al., 2014b; Tang et al., 2015; Zhang et al., 2016; Nyon et al., 2018 |
| RBD-Fd protein | Binds to DPP4 receptor and MERS-CoV RBD-specific neutralizing mAbs (Mersmab1, m336, m337, and m338) | MF59;<br>Alum | I.M. or S.C. | BALB/c mice;<br>hDPP4-Tg mice | Elicits MERS-CoV S1-specific Abs (IgG ($> 1{:}10^5$), IgG1, and IgG2a) in mice, neutralizing at least 9 pseudotyped ($> 1{:}10^4$) and live ($> 1{:}10^3$) MERS-CoV (EMC2012 strain) | N/A | Protects majority (5/6) of vaccinated hDPP4-Tg mice from challenge of MERS-CoV (EMC2012 strain, $10^4$ $TCID_{50}$) | Tai et al., 2016 |

*(Continued)*

**TABLE 2 |** Continued

| Name | Functionality and antigenicity | Adjuvant | Route | Animal models | Antibody response | Cellular immune response | Protective efficacy | References |
|---|---|---|---|---|---|---|---|---|
| RBD (T579N) protein | Binds to receptor DPP4 and MERS-CoV RBD-specific neutralizing mAbs (hMS-1, m336, m337, and m338) | Montanide; Alum | I.M. or S.C. | BALB/c mice; hDPP4-Tg mice | Elicits neutralizing Abs ($> 1:3 \times 10^3$) in mice against live MERS-CoV (EMC2012 strain) | N/A | Protects all vaccinated hDPP4-Tg mice from challenge of MERS-CoV (EMC2012 strain, $10^4$ $TCID_{50}$) | Du et al., 2016a |
| **Subunit vaccines based on non-RBD MERS-CoV S protein fragments** | | | | | | | | |
| S1 protein | N/A | Ribi; Alum pho | I.M. | BALB/c mice; NHPs | Elicits MERS-CoV S1-specific Abs in mice (IgG and IgG1) and NHPs (IgG), neutralizing 8 pseudotyped and live MERS-CoV (JordanN3 strain) | N/A | Protects vaccinated NHPs from challenge of MERS-CoV (JordanN3 strain, $5 \times 10^6$ PFU) with reduced abnormalities on chest CT | Wang et al., 2015 |
| S1 protein | N/A | Advax + SAS | I.M. | Dromedary camels; Alpacas | Elicits neutralizing Abs in dromedary camels ($\geq$ 1:80) and alpacas ($\geq 1:6.4 \times 10^2$) against live MERS-CoV (EMC2012 strain) | N/A | Protects vaccinated dromedary camels and alpacas from challenge of MERS-CoV (EMC2012 strain, $10^7$ $TCID_{50}$) with reduced and delayed viral shedding in the upper airways (in camels) or complete protection (in alpacas) | Adney et al., 2019 |
| rNTD protein | N/A | Alum pho + CpG | I.M. | BALB/c mice; Ad5-hDPP4 mice | Elicits MERS-CoV S-NTD-specific Abs (IgG, $\geq 1:10^4$) in mice, neutralizing pseudotyped and live (1:40) MERS-CoV (EMC2012 strain) | Induces MERS-CoV S-NTD-specific cellular immune responses (IFN-γ, IL-2, IL-6, IL-10, and IL-17A) in mice | Protects vaccinated Ad5-hDPP4-transduced mice from challenge of MERS-CoV (EMC2012 strain, $10^5$ PFU) with reduced lung abnormalities and respiratory tract pathology | Jiaming et al., 2017 |
| SP3 peptide (aa736-761) | N/A | Freund's | N/A | BALB/c mice; NZW rabbits | Elicits MERS-CoV S-specific Abs (IgG, $1:10^4$) in rabbits, neutralizing pseudotyped MERS-CoV | N/A | N/A | Yang et al., 2014a |

[a]*aa, amino acid; Abs, antibodies; Ad5, adenovirus serotype 5; Ad5-hDPP4 mice, Ad5-hDPP4-transuced mice; Alum hydro, aluminum hydroxide; Alum pho, Aluminum phosphate; hDPP4, human dipeptidyl peptidase 4; hDPP4-Tg mice, transgenic mice expressing MERS-CoV receptor human DPP4; IFA, incomplete Freund's adjuvant; I.M., intramuscular; I.N., intranasal; mAbs, monoclonal antibodies; Montanide, Montanide ISA51; N/A, not reported; NHPs, non-human primates; NZW, rabbits, New Zealand White rabbits; PFU, plaque-forming unit; rRBD, recombinant RBD; SAS, Sigma Adjuvant System; S.C., subcutaneous; $TCID_{50}$, median tissue culture infectious dose; TNF-α, tumor necrosis factor (TNF)-alpha.*

NHPs from MERS-CoV infection by alleviating pneumonia and clinical manifestations, as well as decreasing viral load (Lan et al., 2015). In addition, an RBD protein fragment containing MERS-CoV S residues 377–622 fused with the Fc tag of human IgG can induce MERS-CoV S1- and/or RBD-specific humoral and cellular immune responses in the immunized mice with neutralizing activity against MERS-CoV infection (Du et al., 2013c; Jiang et al., 2013). However, after comparing several versions of MERS-CoV RBD fragments with different lengths, it was found that a truncated RBD (residues 377–588) had the highest DPP4-binding affinity and induced the highest-titer IgG antibodies and neutralizing antibodies against MERS-CoV, identifying its role as a critical neutralizing domain (Ma et al., 2014b).

Subsequently, several MERS-CoV subunit vaccines have been designed based on the identified critical neutralizing domain of RBD fragment, including those expressed in a stable CHO cell line (S377-588-Fc), fusing with a trimeric motif foldon (RBD-Fd), or containing single or multiple mutations in the RBD of representative human and camel strains from the 2012–2015 MERS outbreaks (Tai et al., 2016, 2017; Nyon et al., 2018). These RBD proteins maintain good conformation, functionality, antigenicity, and immunogenicity, with ability to bind the DPP4 receptor and RBD-specific neutralizing mAbs and to elicit robust neutralizing antibodies cross-neutralizing multiple strains of MERS pseudoviruses and live MERS-CoV (Tai et al., 2016, 2017; Nyon et al., 2018). It is noted that the wild-type MERS-CoV RBD proteins consisting of the identified critical neutralizing domain confer partial protection of hDPP4-transgenic (hDPP4-Tg) mice from MERS-CoV infection without causing immunological toxicity or eosinophilic immune enhancement (Tai et al., 2016; Wang Y. et al., 2017; Nyon et al., 2018); nevertheless, a structurally designed mutant version of such RBD protein with a non-neutralizing epitope masked (T579N) preserves intact conformation and significantly improves overall neutralizing activity and protective efficacy, resulting in the full protection of hDPP4-Tg mice against high-dose MERS-CoV challenge (Du et al., 2016a).

The above studies indicate that protein lengths to be chosen as MERS-CoV subunit vaccines and/or structure-based vaccine design can impact on the immunogenicity and/or protection of RBD-based subunit vaccines.

## MERS-CoV Subunit Vaccines Based on Non-RBD S Protein Fragments

MERS vaccines targeting non-RBD regions of S protein have been developed and investigated in mice and NHPs. It has been shown that a MERS-CoV S1 protein formulated with Ribi (for mice) or aluminum phosphate (for NHPs) adjuvant elicited robust neutralizing antibodies in mice and NHPs against divergent strains of pseudotyped and live MERS-CoV, protecting NHPs from MERS-CoV infection (Wang et al., 2015). In addition, MERS-CoV S1 protein adjuvanted with Advax and Sigma Adjuvant System induced low-titer neutralizing antibodies in dromedary camels with reduced and delayed viral shedding after MERS-CoV challenge, but high-titer neutralizing antibodies in alpacas with complete protection of viral shedding from viral infection, indicating that protection of MERS-CoV infection is positively correlated with serum neutralizing antibody titers (Adney et al., 2019). Moreover, immunization with a recombinant MERS-CoV NTD protein (rNTD) can induce neutralizing antibodies and cell-mediated responses, protecting Ad-hDPP4-transduced mice against MERS-CoV challenge (Jiaming et al., 2017). Notably, specific antibodies with neutralizing activity have been elicited by a S2 peptide sequence (residues 736–761) of MERS-CoV in rabbits (Yang et al., 2014a), but the protective efficacy of this peptide vaccine is unknown. The above reports demonstrate the potential for the development of MERS subunit vaccines based on the non-RBD fragments of MERS-CoV S protein.

## MERS-CoV Subunit Vaccines Based on Non-S Structural Proteins

Unlike SARS subunit vaccines which have been designed based on viral N and M proteins, it appears that very few subunit vaccines have been developed based on the non-S structural protein(s) of MERS-CoV. One study reports the induction of specific antibodies by MERS-CoV N peptides (Yang et al., 2014a), and another report shows that N protein is used for development of vaccines based on viral vector Vaccinia virus, modified Vaccinia Ankara (MVA) (Veit et al., 2018). This may be potentially a consequence of the weak immunogenicity and/or protective efficacy of non-S structural proteins, further confirming the role of MERS-CoV S protein as the key target for the development of MERS vaccines, including subunit vaccines.

## Potential Factors Affecting MERS-CoV Subunit Vaccines

Similar to SARS-CoV subunit vaccines, the immunogenicity and/or protection of MERS-CoV subunit vaccines may also be affected by a number of factors, such as antigen sequences, fragment lengths, adjuvants, vaccination pathways, antigen doses, immunization doses and intervals used.

As described above, MERS-CoV subunit vaccines containing different antigens or fragment lengths, particularly those based on the RBD, have apparently variable immunogenicity and/or protective efficacy, and a critical neutralizing domain that contains an RBD fragment corresponding to residues 377–588 of S protein elicits the highest neutralizing antibodies among several fragments tested (Ma et al., 2014b; Zhang et al., 2015).

Adjuvants play an essential role in enhancing host immune responses to MERS-CoV subunit vaccines, including those based on the RBD, and different adjuvants can promote host immune responses to variant levels (Lan et al., 2014; Zhang et al., 2016). For example, while a MERS-CoV RBD subunit vaccine (S377-588 protein fused with Fc) alone induced detectable neutralizing antibody and T-cell responses in immunized mice, inclusion of an adjuvant enhanced its immunogenicity. Particularly, among the adjuvants (Freund's, aluminum, Monophosphoryl lipid A, Montanide ISA51 and MF59) conjugated with this RBD protein, MF59 could best potentiate the protein to induce the highest-titer anti-S antibodies and neutralizing antibodies, protecting mice against MERS-CoV infection (Zhang et al., 2016). Moreover, a

recombinant RBD (rRBD) protein plus alum and CpG adjuvants elicited the highest neutralizing antibodies against pseudotyped MERS-CoV infection, whereas the strongest T-cell responses were induced by this protein plus Freund's and CpG adjuvants (Lan et al., 2014).

Vaccination pathways are important in inducing efficient immune responses, and different immunization routes may elicit different immune responses to the same protein antigens. For example, immunization of mice with a MERS-CoV subunit vaccine (RBD-Fc) via the intranasal route induced higher levels of cellular immune responses and stronger local mucosal neutralizing antibody responses against MERS-CoV infection than those induced by the same vaccine via the S.C. pathway (Ma et al., 2014a). In addition, while Freund's and CpG-adjuvanted rRBD protein elicited higher-level systematic and local IFN-γ-producing T cells via the S.C. route, this protein adjuvanted with Alum and CpG induced higher-level tumor necrosis factor-alpha (TNF-α) and interleukin 4 (IL-4)-secreting T cells via the I.M. route (Lan et al., 2014).

Antigen dosage, immunization doses, and intervals may significantly affect the immunogenicity of MERS-CoV subunit vaccines. Notably, a MERS-CoV RBD (S377-588-Fc) subunit vaccine immunized at 1 μg elicited strong humoral and cellular immune responses and neutralizing antibodies in mice although the one immunized at 5 and 20 μg elicited a higher level of S1-specific antibodies (Tang et al., 2015). In addition, among the regimens at one dose and two doses at 1-, 2-, and 3-week intervals, 2 doses of this protein boosted at 4 weeks resulted in the highest antibodies and neutralizing antibodies against MERS-CoV infection (Wang Y. et al., 2017).

## POTENTIAL CHALLENGES AND FUTURE PERSPECTIVES FOR SARS-CoV AND MERS-CoV SUBUNIT VACCINES

Compared with other vaccine types such as inactivated virus and viral-vectored vaccines, SARS and MERS subunit vaccines are much safer and do not cause obvious side effects. However, these subunit vaccines may face some important challenges, mostly arising from their relatively low immunogenicity, which must be combined with appropriate adjuvants or optimized for suitable protein sequences, fragment lengths, and immunization schedules. In addition, structure and epitope-based vaccine design has become a promising strategy to improve the efficacy of subunit vaccines. This is evidenced by a structurally designed MERS-CoV RBD-based protein which has significantly improved neutralizing activity and protection against MERS-CoV infection (Du et al., 2016a). It is prospected that more structure-guided novel strategies will be developed to improve the overall immunogenicity and efficacy of subunit vaccines against emerging pathogenic human coronaviruses, including those targeting SARS-CoV and MERS-CoV. Although a large number of SARS and MERS subunit vaccines have been developed with potent immunogenicity and/or protection in available animal models, virtually all remain in the preclinical stage. It is thus expected that one or several of these promising subunit vaccines can be further processed into clinical trials to confirm their immunogenicity against viral infections in humans.

## RAPID DEVELOPMENT OF SUBUNIT VACCINES AGAINST THE NEW PATHOGENIC HUMAN CORONAVIRUS

Currently, the newly identified 2019-nCoV is spreading to infect people, resulting in significant global concerns. It is critical to rapidly design and develop effective vaccines to prevent infection of this new coronavirus. Since S protein and its fragments, such as RBD, of SARS-CoV, and MERS-CoV are prime targets for developing subunit vaccines against these two highly pathogenic human CoVs, it is expected that similar regions of 2019-nCoV can also be used as key targets for developing vaccines against this new coronavirus (Jiang et al., 2020). Similarly, other regions of 2019-nCoV, including S1 and S2 subunits of S protein and N protein, can be applied as alternative targets for vaccine development. Taken together, the approaches and strategies in the development of subunit vaccines against SARS and MERS described in this review will provide important information for the rapid design and development of safe and effective subunit vaccines against 2019-nCoV infection.

## AUTHOR CONTRIBUTIONS

SJ and LD conceived the idea and revised and edited the manuscript. NW and LD collected information and drafted the manuscript. JS performed the structural analysis. All authors read and made final approval of the manuscript.

## FUNDING

This work was supported by the NIH grants R01AI137472 and R01AI139092.

## SUPPLEMENTARY MATERIAL

The Supplementary Material for this article can be found online at: https://www.frontiersin.org/articles/10.3389/fmicb.2020.00298/full#supplementary-material

**FIGURE S1 |** Structures of SARS-CoV and MERS-CoV S proteins, RBDs, and their complexes with respective receptor. Trimeric S proteins of SARS-CoV (PDB: 5×5b) **(A)** and MERS-CoV (PDB: 5×5f) **(C)** are colored differently for each monomer. Two conformations of the RBD in each trimeric S protein are labeled as standing and lying states. The RBDs of each S protein are shown as light blue on the right panel. ACE2 and DPP4 receptors are respectively modeled to the trimeric S proteins by match-alignment of SARS-CoV RBD-ACE2 complex (PDB: 2AJF) to SARS-CoV S trimer **(B)** or MERS-CoV RBD-DPP4 complex (PDB: 4kr0) to MERS-CoV S trimer **(D)**. Each of the RBD-receptor complexes is shown on the right panel. ACE2, angiotensin-converting enzyme 2; DPP4, dipeptidyl peptidase 4; RBD, receptor-binding domain; S, spike.

## REFERENCES


Adney, D. R., Wang, L., van Doremalen, N., Shi, W., Zhang, Y., Kong, W. P., et al. (2019). Efficacy of an adjuvanted Middle East respiratory syndrome coronavirus spike protein vaccine in dromedary camels and alpacas. *Viruses* 11:E212. doi: 10.3390/v11030212

Al-Amri, S. S., Abbas, A. T., Siddiq, L. A., Alghamdi, A., Sanki, M. A., Al-Muhanna, M. K., et al. (2017). Immunogenicity of candidate MERS-CoV DNA vaccines based on the spike protein. *Sci. Rep.* 7:44875. doi: 10.1038/srep44875

Annan, A., Baldwin, H. J., Corman, V. M., Klose, S. M., Owusu, M., Nkrumah, E. E., et al. (2013). Human betacoronavirus 2c EMC/2012-related viruses in Bats, Ghana and Europe. *Emerg. Infect. Dis.* 19, 456–459. doi: 10.3201/eid1903.121503

Arbour, N., Day, R., Newcombe, J., and Talbot, P. J. (2000). Neuroinvasion by human respiratory coronaviruses. *J. Virol.* 74, 8913–8921. doi: 10.1128/jvi.74.19.8913-8921.2000

Azhar, E. I., El-Kafrawy, S. A., Farraj, S. A., Hassan, A. M., Al-Saeed, M. S., Hashem, A. M., et al. (2014). Evidence for camel-to-human transmission of MERS coronavirus. *N. Engl. J. Med.* 370, 2499–2505. doi: 10.1056/NEJMoa1401505

Bailey-Elkin, B. A., Knaap, R. C., Johnson, G. G., Dalebout, T. J., Ninaber, D. K., van Kasteren, P. B., et al. (2014). Crystal structure of the Middle East respiratory syndrome coronavirus (MERS-CoV) papain-like protease bound to ubiquitin facilitates targeted disruption of deubiquitinating activity to demonstrate its role in innate immune suppression. *J. Biol. Chem.* 289, 34667–34682. doi: 10.1074/jbc.M114.609644

Bisht, H., Roberts, A., Vogel, L., Bukreyev, A., Collins, P. L., Murphy, B. R., et al. (2004). Severe acute respiratory syndrome coronavirus spike protein expressed by attenuated vaccinia virus protectively immunizes mice. *Proc. Natl. Acad. Sci. U.S.A.* 101, 6641–6646. doi: 10.1073/pnas.0401939101

Buchholz, U. J., Bukreyev, A., Yang, L. J., Lamirande, E. W., Murphy, B. R., Subbarao, K., et al. (2004). Contributions of the structural proteins of severe acute respiratory syndrome coronavirus to protective immunity. *Proc. Natl. Acad. Sci. U.S.A.* 101, 9804–9809. doi: 10.1073/pnas.0403492101

Bukreyev, A., Lamirande, E. W., Buchholz, U. J., Vogel, L. N., Elkins, W. R., St Claire, M., et al. (2004). Mucosal immunisation of African green monkeys (*Cercopithecus aethiops*) with an attenuated parainfluenza virus expressing the SARS coronavirus spike protein for the prevention of SARS. *Lancet* 363, 2122–2127. doi: 10.1016/s0140-6736(04)16501-x

Chan, P. K., Ma, S., and Ngai, S. M. (2011). Identification of T-cell epitopes of SARS-coronavirus for development of peptide-based vaccines and cellular immunity assessment methods. *Hong Kong Med. J.* 17(Suppl. 6), 26–30.

Chang, C. Y., Hong, W. W., Chong, P., and Wu, S. C. (2006). Influence of intron and exon splicing enhancers on mammalian cell expression of a truncated spike protein of SARS-CoV and its implication for subunit vaccine development. *Vaccine* 24, 1132–1141. doi: 10.1016/j.vaccine.2005.09.011

Channappanavar, R., and Perlman, S. (2017). Pathogenic human coronavirus infections: causes and consequences of cytokine storm and immunopathology. *Semin. Immunopathol.* 39, 529–539. doi: 10.1007/s00281-017-0629-x

Chen, W. H., Du, L., Chag, S. M., Ma, C., Tricoche, N., Tao, X., et al. (2014). Yeast-expressed recombinant protein of the receptor-binding domain in SARS-CoV spike protein with deglycosylated forms as a SARS vaccine candidate. *Hum. Vaccin. Immunother.* 10, 648–658. doi: 10.4161/hv.27464

Chen, Y., Rajashankar, K. R., Yang, Y., Agnihothram, S. S., Liu, C., Lin, Y. L., et al. (2013). Crystal structure of the receptor-binding domain from newly emerged Middle East respiratory syndrome coronavirus. *J. Virol.* 87, 10777–10783. doi: 10.1128/jvi.01756-13

Chiu, S. S., Chan, K. H., Chu, K. W., Kwan, S. W., Guan, Y., Poon, L. L., et al. (2005). Human coronavirus NL63 infection and other coronavirus infections in children hospitalized with acute respiratory disease in Hong Kong, China. *Clin. Infect. Dis.* 40, 1721–1729. doi: 10.1086/430301

Cho, H., Excler, J. L., Kim, J. H., and Yoon, I. K. (2018). Development of Middle East respiratory syndrome coronavirus vaccines - advances and challenges. *Hum. Vaccin. Immunother.* 14, 304–313. doi: 10.1080/21645515.2017.1389362

Cui, J., Li, F., and Shi, Z. L. (2019). Origin and evolution of pathogenic coronaviruses. *Nat. Rev. Microbiol.* 17, 181–192. doi: 10.1038/s41579-018-0118-9

De Groot, R. J., Baker, S., Baric, R., Enjuanes, L., Gorbalenya, A., Holmes, K. V., et al. (2011). "Family *Coronaviridae*, virus taxomomy: classification and nomenclature of viruses," in *Ninth Report of the International Committee on Taxonomy of Viruses*, eds A. M. Q. King, M. J. Adams, E. B. Carstens, and E. J. Lefkowitz (Amsterdam: Elsevier Academic Press), 806–826.

DeDiego, M. L., Nieto-Torres, J. L., Jimenez-Guardeno, J. M., Regla-Nava, J. A., Castano-Rodriguez, C., Fernandez-Delgado, R., et al. (2014). Coronavirus virulence genes with main focus on SARS-CoV envelope gene. *Virus. Res.* 194, 124–137. doi: 10.1016/j.virusres.2014.07.024

Deng, M. P., Hu, Z. H., Wang, H. L., and Deng, F. (2012). Developments of subunit and VLP vaccines against influenza A virus. *Virol. Sin.* 27, 145–153. doi: 10.1007/s12250-012-3241-1

Desforges, M., Desjardins, J., Zhang, C., and Talbot, P. J. (2013). The acetyl-esterase activity of the hemagglutinin-esterase protein of human coronavirus OC43 strongly enhances the production of infectious virus. *J. Virol.* 87, 3097–3107. doi: 10.1128/jvi.02699-12

Desforges, M., Le Coupanec, A., Brison, E., Meessen-Pinard, M., and Talbot, P. J. (2014). Neuroinvasive and neurotropic human respiratory coronaviruses: potential neurovirulent agents in humans. *Adv. Exp. Med. Biol.* 807, 75–96. doi: 10.1007/978-81-322-1777-0_6

Drexler, J. F., Corman, V. M., and Drosten, C. (2014). Ecology, evolution and classification of bat coronaviruses in the aftermath of SARS. *Antiviral Res.* 101, 45–56. doi: 10.1016/j.antiviral.2013.10.013

Drosten, C., Gunther, S., Preiser, W., van der Werf, S., Brodt, H. R., Becker, S., et al. (2003). Identification of a novel coronavirus in patients with severe acute respiratory syndrome. *N. Engl. J. Med.* 348, 1967–1976. doi: 10.1056/NEJMoa030747

Du, L., He, Y., Jiang, S., and Zheng, B. J. (2008). Development of subunit vaccines against severe acute respiratory syndrome. *Drugs Today* 44, 63–73. doi: 10.1358/dot.2008.44.1.1131830

Du, L., He, Y., Zhou, Y., Liu, S., Zheng, B. J., and Jiang, S. (2009a). The spike protein of SARS-CoV - a target for vaccine and therapeutic development. *Nat. Rev. Microbiol.* 7, 226–236. doi: 10.1038/nrmicro2090

Du, L., and Jiang, S. (2015). Middle East respiratory syndrome: current status and future prospects for vaccine development. *Expert Opin. Biol. Ther.* 15, 1647–1651. doi: 10.1517/14712598.2015.1092518

Du, L., Kou, Z., Ma, C., Tao, X., Wang, L., Zhao, G., et al. (2013a). A truncated receptor-binding domain of MERS-CoV Spike protein potently inhibits MERS-CoV infection and induces strong neutralizing antibody responses: implication for developing therapeutics and vaccines. *PLoS One* 8:e81587. doi: 10.1371/journal.pone.0081587

Du, L., Ma, C., and Jiang, S. (2013b). Antibodies induced by receptor-binding domain in spike protein of SARS-CoV do not cross-neutralize the novel human coronavirus hCoV-EMC. *J. Infect.* 67, 348–350. doi: 10.1016/j.jinf.2013.05.002

Du, L., Tai, W., Yang, Y., Zhao, G., Zhu, Q., Sun, S., et al. (2016a). Introduction of neutralizing immunogenicity index to the rational design of MERS coronavirus subunit vaccines. *Nat. Commun.* 7:13473. doi: 10.1038/ncomms13473

Du, L., Tai, W., Zhou, Y., and Jiang, S. (2016b). Vaccines for the prevention against the threat of MERS-CoV. *Expert Rev. Vaccines* 15, 1123–1134. doi: 10.1586/14760584.2016.1167603

Du, L., Yang, Y., Zhou, Y., Lu, L., Li, F., and Jiang, S. (2017). MERS-CoV spike protein: a key target for antivirals. *Expert Opin. Ther. Targets* 21, 131–143. doi: 10.1080/14728222.2017.1271415

Du, L., Zhao, G., Chan, C. C., Li, L., He, Y., Zhou, Y., et al. (2010). A 219-mer CHO-expressing receptor-binding domain of SARS-CoV S protein induces potent immune responses and protective immunity. *Viral. Immunol.* 23, 211–219. doi: 10.1089/vim.2009.0090

Du, L., Zhao, G., Chan, C. C., Sun, S., Chen, M., Liu, Z., et al. (2009b). Recombinant receptor-binding domain of SARS-CoV spike protein expressed in mammalian, insect and *E. coli* cells elicits potent neutralizing antibody and protective immunity. *Virology* 393, 144–150. doi: 10.1016/j.virol.2009.07.018

Du, L., Zhao, G., He, Y., Guo, Y., Zheng, B. J., Jiang, S., et al. (2007). Receptor-binding domain of SARS-CoV spike protein induces long-term protective immunity in an animal model. *Vaccine* 25, 2832–2838. doi: 10.1016/j.vaccine.2006.10.031

Du, L., Zhao, G., Kou, Z., Ma, C., Sun, S., Poon, V. K., et al. (2013c). Identification of a receptor-binding domain in the S protein of the novel human coronavirus

Middle East Respiratory Syndrome coronavirus as an essential target for vaccine development. *J. Virol.* 87, 9939–9942. doi: 10.1128/jvi.01048-13

Du, L., Zhao, G., Li, L., He, Y., Zhou, Y., Zheng, B. J., et al. (2009c). Antigenicity and immunogenicity of SARS-CoV S protein receptor-binding domain stably expressed in CHO cells. *Biochem. Biophys. Res. Commun.* 384, 486–490. doi: 10.1016/j.bbre.2009.05.003

Elshabrawy, H. A., Coughlin, M. M., Baker, S. C., and Prabhakar, B. S. (2012). Human monoclonal antibodies against highly conserved HR1 and HR2 domains of the SARS-CoV spike protein are more broadly neutralizing. *PLoS One* 7:e50366. doi: 10.1371/journal.pone.0050366

Esper, F., Weibel, C., Ferguson, D., Landry, M. L., and Kahn, J. S. (2006). Coronavirus HKU1 infection in the United States. *Emerg. Infect. Dis.* 12, 775–779. doi: 10.3201/eid1205.051316

Falsey, A. R., Walsh, E. E., and Hayden, F. G. (2002). Rhinovirus and coronavirus infection-associated hospitalizations among older adults. *J. Infect. Dis.* 185, 1338–1341. doi: 10.1086/339881

Fehr, A. R., and Perlman, S. (2015). Coronaviruses: an overview of their replication and pathogenesis. *Methods Mol. Biol.* 1282, 1–23. doi: 10.1007/978-1-4939-2438-7_1

Fouchier, R. A. M., Hartwig, N. G., Bestebroer, T. M., Niemeyer, B., de Jong, J. C., Simon, J. H., et al. (2004). A previously undescribed coronavirus associated with respiratory disease in humans. *Proc. Natl. Acad. Sci. U.S.A.* 101, 6212–6216. doi: 10.1073/pnas.0400762101

Ge, X. Y., Li, J. L., Yang, X. L., Chmura, A. A., Zhu, G., Epstein, J. H., et al. (2013). Isolation and characterization of a bat SARS-like coronavirus that uses the ACE2 receptor. *Nature* 503, 535–538. doi: 10.1038/nature12711

Gerna, G., Campanini, G., Rovida, F., Percivalle, E., Sarasini, A., Marchi, A., et al. (2006). Genetic variability of human coronavirus OC43-, 229E-, and NL63-like strains and their association with lower respiratory tract infections of hospitalized infants and immunocompromised patients. *J. Med. Virol.* 78, 938–949. doi: 10.1002/jmv.20645

Gerna, G., Percivalle, E., Sarasini, A., Campanini, G., Piralla, A., Rovida, F., et al. (2007). Human respiratory coronavirus HKU1 versus other coronavirus infections in Italian hospitalised patients. *J. Clin. Virol.* 38, 244–250. doi: 10.1016/j.jcv.2006.12.008

Guo, Y., Sun, S., Wang, K., Zhang, S., Zhu, W., and Chen, Z. (2005). Elicitation of immunity in mice after immunization with the S2 subunit of the severe acute respiratory syndrome coronavirus. *DNA Cell Biol.* 24, 510–515. doi: 10.1089/dna.2005.24.510

Haagmans, B. L., van den Brand, J. M., Raj, V. S., Volz, A., Wohlsein, P., Smits, S. L., et al. (2016). An orthopoxvirus-based vaccine reduces virus excretion after MERS-CoV infection in dromedary camels. *Science* 351, 77–81. doi: 10.1126/science.aad1283

Hamre, D., Kindig, D. A., and Mann, J. (1967). Growth and intracellular development of a new respiratory virus. *J. Virol.* 1, 810–816. doi: 10.1128/jvi.1.4.810-816.1967

Hamre, D., and Procknow, J. J. (1966). A new virus isolated from human respiratory tract. *Proc. Soc. Exp. Biol. Med.* 121, 190–193. doi: 10.3181/00379727-121-30734

He, Y., Li, J., Heck, S., Lustigman, S., and Jiang, S. (2006a). Antigenic and immunogenic characterization of recombinant baculovirus-expressed severe acute respiratory syndrome coronavirus spike protein: implication for vaccine design. *J. Virol.* 80, 5757–5767. doi: 10.1128/jvi.00083-06

He, Y., Li, J., and Jiang, S. (2006b). A single amino acid substitution (R441A) in the receptor-binding domain of SARS coronavirus spike protein disrupts the antigenic structure and binding activity. *Biochem. Biophys. Res. Commun.* 344, 106–113. doi: 10.1016/j.bbrc.2006.03.139

He, Y., Li, J., Li, W., Lustigman, S., Farzan, M., and Jiang, S. (2006c). Cross-neutralization of human and palm civet severe acute respiratory syndrome coronaviruses by antibodies targeting the receptor-binding domain of spike protein. *J. Immunol.* 176, 6085–6092. doi: 10.4049/jimmunol.176.10.6085

He, Y., Lu, H., Siddiqui, P., Zhou, Y., and Jiang, S. (2005a). Receptor-binding domain of severe acute respiratory syndrome coronavirus spike protein contains multiple conformation-dependent epitopes that induce highly potent neutralizing antibodies. *J. Immunol.* 174, 4908–4915. doi: 10.4049/jimmunol.174.8.4908

He, Y., Zhou, Y., Liu, S., Kou, Z., Li, W., Farzan, M., et al. (2004). Receptor-binding domain of SARS-CoV spike protein induces highly potent neutralizing antibodies: implication for developing subunit vaccine. *Biochem. Biophys. Res. Commun.* 324, 773–781. doi: 10.1016/j.bbrc.2004.09.106

He, Y., Zhou, Y., Siddiqui, P., Niu, J., and Jiang, S. (2005b). Identification of immunodominant epitopes on the membrane protein of the severe acute respiratory syndrome-associated coronavirus. *J. Clin. Microbiol.* 43, 3718–3726. doi: 10.1128/jcm.43.8.3718-3726.2005

Hofmann, H., Pyrc, K., van der Hoek, L., Geier, M., Berkhout, B., and Pohlmann, S. (2005). Human coronavirus NL63 employs the severe acute respiratory syndrome coronavirus receptor for cellular entry. *Proc. Natl. Acad. Sci. U.S.A.* 102, 7988–7993. doi: 10.1073/pnas.0409465102

Hofmann, H., Simmons, G., Rennekamp, A. J., Chaipan, C., Gramberg, T., Heck, E., et al. (2006). Highly conserved regions within the spike proteins of human coronaviruses 229E and NL63 determine recognition of their respective cellular receptors. *J. Virol.* 80, 8639–8652. doi: 10.1128/jvi.00560-06

Hu, B., Zeng, L. P., Yang, X. L., Ge, X. Y., Zhang, W., Li, B., et al. (2017). Discovery of a rich gene pool of bat SARS-related coronaviruses provides new insights into the origin of SARS coronavirus. *PLoS Pathog.* 13:e1006698. doi: 10.1371/journal.ppat.1006698

Huang, X., Dong, W., Milewska, A., Golda, A., Qi, Y., Zhu, Q. K., et al. (2015). Human coronavirus HKU1 spike protein uses O-Acetylated sialic acid as an attachment receptor determinant and employs hemagglutinin-esterase protein as a receptor-destroying enzyme. *J. Virol.* 89, 7202–7213. doi: 10.1128/jvi.00854-15

Hulswit, R. J. G., Lang, Y., Bakkers, M. J. G., Li, W., Li, Z., Schouten, A., et al. (2019). Human coronaviruses OC43 and HKU1 bind to 9-O-acetylated sialic acids via a conserved receptor-binding site in spike protein domain A. *Proc. Natl Acad. Sci. U.S.A.* 116, 2681–2690. doi: 10.1073/pnas.1809667116

Jaume, M., Yip, M. S., Kam, Y. W., Cheung, C. Y., Kien, F., Roberts, A., et al. (2012). SARS CoV subunit vaccine: antibody-mediated neutralisation and enhancement. *Hong Kong Med. J.* 18(Suppl. 2), 31–36.

Jiaming, L., Yanfeng, Y., Yao, D., Yawei, H., Linlin, B., Baoying, H., et al. (2017). The recombinant N-terminal domain of spike proteins is a potential vaccine against Middle East respiratory syndrome coronavirus (MERS-CoV) infection. *Vaccine* 35, 10–18. doi: 10.1016/j.vaccine.2016.11.064

Jiang, S., Bottazzi, M. E., Du, L., Lustigman, S., Tseng, C. T., Curti, E., et al. (2012). Roadmap to developing a recombinant coronavirus S protein receptor-binding domain vaccine for severe acute respiratory syndrome. *Expert Rev. Vaccines* 11, 1405–1413. doi: 10.1586/erv.12.126

Jiang, S., Du, L., and Shi, Z. (2020). An emerging coronavirus causing pneumonia outbreak in Wuhan, China: calling for developing therapeutic and prophylactic strategies. *Emerg Microbes Infect.* 9, 275–277. doi: 10.1080/22221751.2020.1723441

Jiang, S., He, Y., and Liu, S. (2005). SARS vaccine development. *Emerg. Infect. Dis.* 11, 1016–1020. doi: 10.3201/1107.050219

Jiang, S., Lu, L., Du, L., and Debnath, A. K. (2013). A predicted receptor-binding and critical neutralizing domain in S protein of the novel human coronavirus HCoV-EMC. *J. Infect.* 66, 464–466. doi: 10.1016/j.jinf.2012.12.003

Kam, Y. W., Kien, F., Roberts, A., Cheung, Y. C., Lamirande, E. W., Vogel, L., et al. (2007). Antibodies against trimeric S glycoprotein protect hamsters against SARS-CoV challenge despite their capacity to mediate FcgammaRII-dependent entry into B cells in vitro. *Vaccine* 25, 729–740. doi: 10.1016/j.vaccine.2006.08.011

Kapikian, A. Z., James, H. D., Kelly, S. J., Dees, J. H., Turner, H. C., McIntosh, K., et al. (1969). Isolation from man of avian infectious bronchitis virus-like viruses (coronavirus) similar to 229E virus with some epidemiological observations. *J. Infect. Dis.* 119, 282–290. doi: 10.1093/infdis/119.3.282

Killerby, M. E., Biggs, H. M., Haynes, A., Dahl, R. M., Mustaquim, D., Gerber, S. I., et al. (2018). Human coronavirus circulation in the United States 2014-2017. *J. Clin. Virol.* 101, 52–56. doi: 10.1016/j.jcv.2018.01.019

Kim, K. Y., Han, S. Y., Kim, H. S., Cheong, H. M., Kim, S. S., and Kim, D. S. (2017). Human coronavirus in the 2014 winter season as a cause of lower respiratory tract infection. *Yonsei Med. J.* 58, 174–179. doi: 10.3349/ymj.2017.58.1.174

King, A. M. Q., Lefkowitz, E. J., Mushegian, A. R., Adams, M. J., Dutilh, B. E., Gorbalenya, A. E., et al. (2018). Changes to taxonomy and the international code of virus classification and nomenclature ratified by the international committee on taxonomy of viruses (2018). *Arch. Virol.* 163, 2601–2631. doi: 10.1007/s00705-018-3847-1

Ksiazek, T. G., Erdman, D., Goldsmith, C. S., Zaki, S. R., Peret, T., Emery, S., et al. (2003). A novel coronavirus associated with severe acute respiratory syndrome. *N. Engl. J. Med.* 348, 1953–1966. doi: 10.1056/NEJMoa030781

Kudelova, M., Belvoncikova, P., Vrbova, M., Kovalova, A., Stibraniova, I., Kocakova, P., et al. (2015). Detection of murine herpesvirus 68 (MHV-68) in dermacentor reticulatus ticks. *Microb. Ecol.* 70, 785–794. doi: 10.1007/s00248-015-0622-7

Kusanagi, K., Kuwahara, H., Katoh, T., Nunoya, T., Ishikawa, Y., Samejima, T., et al. (1992). Isolation and serial propagation of porcine epidemic diarrhea virus in cell-cultures and partial characterization of the isolate. *J. Vet. Med. Sci.* 54, 313–318. doi: 10.1292/jvms.54.313

Lan, J., Deng, Y., Chen, H., Lu, G., Wang, W., Guo, X., et al. (2014). Tailoring subunit vaccine immunity with adjuvant combinations and delivery routes using the Middle East respiratory coronavirus (MERS-CoV) receptor-binding domain as an antigen. *PLoS One* 9:e112602. doi: 10.1371/journal.pone.0112602

Lan, J., Yao, Y., Deng, Y., Chen, H., Lu, G., Wang, W., et al. (2015). Recombinant receptor binding domain protein induces partial protective immunity in rhesus macaques against Middle East respiratory syndrome coronavirus challenge. *EBioMedicine* 2, 1438–1446. doi: 10.1016/j.ebiom.2015.08.031

Lau, S. K., Woo, P. C., Yip, C. C., Tse, H., Tsoi, H. W., Cheng, V. C., et al. (2006). Coronavirus HKU1 and other coronavirus infections in Hong Kong. *J. Clin. Microbiol.* 44, 2063–2071. doi: 10.1128/jcm.02614-05

Lau, S. K. P., Zhang, L., Luk, H. K. H., Xiong, L., Peng, X., Li, K. S. M., et al. (2018). Receptor usage of a novel bat lineage C betacoronavirus reveals evolution of Middle East respiratory syndrome-related coronavirus spike proteins for human dipeptidyl peptidase 4 binding. *J. Infect. Dis.* 218, 197–207. doi: 10.1093/infdis/jiy018

Lehmann, C., Wolf, H., Xu, J. G., Zhao, Q. B., Shao, Y. M., Motz, M., et al. (2008). A line immunoassay utilizing recombinant nucleocapsid proteins for detection of antibodies to human coronaviruses. *Diagn. Microbiol. Infect. Dis.* 61, 40–48. doi: 10.1016/j.diagmicrobio.2007.12.002

Lelli, D., Papetti, A., Sabelli, C., Rosti, E., Moreno, A., and Boniotti, M. B. (2013). Detection of coronaviruses in bats of various species in Italy. *Viruses* 5, 2679–2689. doi: 10.3390/v5112679

Li, F. (2008). Structural analysis of major species barriers between humans and palm civets for severe acute respiratory syndrome coronavirus infections. *J. Virol.* 82, 6984–6991. doi: 10.1128/jvi.00442-08

Li, F. (2015). Receptor recognition mechanisms of coronaviruses: a decade of structural studies. *J. Virol.* 89, 1954–1964. doi: 10.1128/jvi.02615-14

Li, F. (2016). Structure, function, and evolution of coronavirus spike proteins. *Annu. Rev. Virol.* 3, 237–261. doi: 10.1146/annurev-virology-110615-042301

Li, F., and Du, L. (2019). MERS coronavirus: an emerging zoonotic virus. *Viruses* 11:E663. doi: 10.3390/v11070663

Li, F., Li, W., Farzan, M., and Harrison, S. C. (2005a). Structure of SARS coronavirus spike receptor-binding domain complexed with receptor. *Science* 309, 1864–1868. doi: 10.1126/science.1116480

Li, W., Shi, Z., Yu, M., Ren, W., Smith, C., Epstein, J. H., et al. (2005b). Bats are natural reservoirs of SARS-like coronaviruses. *Science* 310, 676–679. doi: 10.1126/science.1118391

Li, W., Zhang, C., Sui, J., Kuhn, J. H., Moore, M. J., Luo, S., et al. (2005c). Receptor and viral determinants of SARS-coronavirus adaptation to human ACE2. *EMBO J.* 24, 1634–1643. doi: 10.1038/sj.emboj.7600640

Li, J., Ulitzky, L., Silberstein, E., Taylor, D. R., and Viscidi, R. (2013). Immunogenicity and protection efficacy of monomeric and trimeric recombinant SARS coronavirus spike protein subunit vaccine candidates. *Viral. Immunol.* 26, 126–132. doi: 10.1089/vim.2012.0076

Li, W., Greenough, T. C., Moore, M. J., Vasilieva, N., Somasundaran, M., Sullivan, J. L., et al. (2004). Efficient replication of severe acute respiratory syndrome coronavirus in mouse cells is limited by murine angiotensin-converting enzyme 2. *J. Virol.* 78, 11429–11433. doi: 10.1128/jvi.78.20.11429-11433.2004

Li, W., Hulswit, R. J. G., Widjaja, I., Raj, V. S., McBride, R., Peng, W., et al. (2017). Identification of sialic acid-binding function for the Middle East respiratory syndrome coronavirus spike glycoprotein. *Proc. Natl Acad. Sci. U.S.A.* 114, E8508–E8517. doi: 10.1073/pnas.1712592114

Li, W., Moore, M. J., Vasilieva, N., Sui, J., Wong, S. K., Berne, M. A., et al. (2003). Angiotensin-converting enzyme 2 is a functional receptor for the SARS coronavirus. *Nature* 426, 450–454. doi: 10.1038/nature02145

Liu, D. X., Fung, T. S., Chong, K. K., Shukla, A., and Hilgenfeld, R. (2014). Accessory proteins of SARS-CoV and other coronaviruses. *Antiviral Res.* 109, 97–109. doi: 10.1016/j.antiviral.2014.06.013

Liu, R. Y., Wu, L. Z., Huang, B. J., Huang, J. L., Zhang, Y. L., Ke, M. L., et al. (2005). Adenoviral expression of a truncated S1 subunit of SARS-CoV spike protein results in specific humoral immune responses against SARS-CoV in rats. *Virus Res.* 112, 24–31. doi: 10.1016/j.virusres.2005.02.009

Liu, S. J., Leng, C. H., Lien, S. P., Chi, H. Y., Huang, C. Y., Lin, C. L., et al. (2006). Immunological characterizations of the nucleocapsid protein based SARS vaccine candidates. *Vaccine* 24, 3100–3108. doi: 10.1016/j.vaccine.2006.01.058

Liu, S. L., and Saif, L. (2020). Emerging viruses without borders: the Wuhan coronavirus. *Viruses* 12:E130. doi: 10.3390/v12020130

Lu, G., Hu, Y., Wang, Q., Qi, J., Gao, F., Li, Y., et al. (2013). Molecular basis of binding between novel human coronavirus MERS-CoV and its receptor CD26. *Nature* 500, 227–231. doi: 10.1038/nature12328

Lu, L., Liu, Q., Zhu, Y., Chan, K. H., Qin, L., Li, Y., et al. (2014). Structure-based discovery of Middle East respiratory syndrome coronavirus fusion inhibitor. *Nat. Commun.* 5:3067. doi: 10.1038/ncomms4067

Luo, C. M., Wang, N., Yang, X. L., Liu, H. Z., Zhang, W., Li, B., et al. (2018a). Discovery of novel bat coronaviruses in south China that use the same receptor as MERS coronavirus. *J. Virol.* 92, e116–e118. doi: 10.1128/jvi.00116-18

Luo, F., Liao, F. L., Wang, H., Tang, H. B., Yang, Z. Q., and Hou, W. (2018b). Evaluation of antibody-dependent enhancement of SARS-CoV infection in rhesus macaques immunized with an inactivated SARS-CoV vaccine. *Virol. Sin.* 33, 201–204. doi: 10.1007/s12250-018-0009-2

Ma, C., Li, Y., Wang, L., Zhao, G., Tao, X. R., Tseng, C. T., et al. (2014a). Intranasal vaccination with recombinant receptor-binding domain of MERS-CoV spike protein induces much stronger local mucosal immune responses than subcutaneous immunization: implication for designing novel mucosal MERS vaccines. *Vaccine* 32, 2100–2108. doi: 10.1016/j.vaccine.2014.02.004

Ma, C., Wang, L., Tao, X., Zhang, N., Yang, Y., Tseng, C. T., et al. (2014b). Searching for an ideal vaccine candidate among different MERS coronavirus receptor-binding fragments - The importance of immunofocusing in subunit vaccine design. *Vaccine* 32, 6170–6176. doi: 10.1016/j.vaccine.2014.08.086

Ma, Y., Zhang, Y., Liang, X., Lou, F., Oglesbee, M., Krakowka, S., et al. (2015). Origin, evolution, and virulence of porcine deltacoronaviruses in the United States. *mBio* 6:e00064. doi: 10.1128/mBio.00064-15

Marra, M. A., Jones, S. J., Astell, C. R., Holt, R. A., Brooks-Wilson, A., Butterfield, Y. S., et al. (2003). The genome sequence of the SARS-associated coronavirus. *Science* 300, 1399–1404. doi: 10.1126/science.1085953

Matoba, Y., Abiko, C., Ikeda, T., Aoki, Y., Suzuki, Y., Yahagi, K., et al. (2015). Detection of the human coronavirus 229E, HKU1, NL63, and OC43 between 2010 and 2013 in Yamagata, Japan. *Jpn. J. Infect. Dis.* 68, 138–141. doi: 10.7883/yoken.JJID.2014.266

McIntosh, K., Becker, W. B., and Chanock, R. M. (1967). Growth in suckling-mouse brain of IBV-like viruses from patients with upper respiratory tract disease. *Proc. Natl. Acad. Sci. U.S.A.* 58, 2268–2273. doi: 10.1073/pnas.58.6.2268

Menachery, V. D., Mitchell, H. D., Cockrell, A. S., Gralinski, L. E., Yount, BL Jr, Graham, R. L., et al. (2017). MERS-CoV accessory ORFs play key role for infection and pathogenesis. *mBio* 8:e00665-17. doi: 10.1128/mBio.00665-17

Mobaraki, K., and Ahmadzadeh, J. (2019). Current epidemiological status of Middle East respiratory syndrome coronavirus in the world from 1.1.2017 to 17.1.2018: a cross-sectional study. *BMC Infect. Dis.* 19:351. doi: 10.1186/s12879-019-3987-2

Mou, H., Raj, V. S., van Kuppeveld, F. J., Rottier, P. J., Haagmans, B. L., and Bosch, B. J. (2013). The receptor binding domain of the new Middle East Respiratory Syndrome coronavirus maps to a 231-residue region in the spike protein that efficiently elicits neutralizing antibodies. *J. Virol.* 87, 9379–9383. doi: 10.1128/jvi.01277-13

Mourez, T., Vabret, A., Han, Y., Dina, J., Legrand, L., Corbet, S., et al. (2007). Baculovirus expression of HCoV-OC43 nucleocapsid protein and development of a Western blot assay for detection of human antibodies against HCoV-OC43. *J. Virol. Methods* 139, 175–180. doi: 10.1016/j.jviromet.2006.09.024

Myint, S. H. (1994). Human coronaviruses - A brief review. *Rev. Med. Virol.* 4, 35–46. doi: 10.1002/rmv.1980040108

Nicholls, J. M., Poon, L. L., Lee, K. C., Ng, W. F., Lai, S. T., Leung, C. Y., et al. (2003). Lung pathology of fatal severe acute respiratory syndrome. *Lancet* 361, 1773–1778. doi: 10.1016/s0140-6736(03)13413-7

Nyon, M. P., Du, L., Tseng, C. K., Seid, C. A., Pollet, J., Naceanceno, K. S., et al. (2018). Engineering a stable CHO cell line for the expression of a MERS-coronavirus vaccine antigen. *Vaccine* 36, 1853–1862. doi: 10.1016/j.vaccine.2018.02.065

Ou, X., Guan, H., Qin, B., Mu, Z., Wojdyla, J. A., Wang, M., et al. (2017). Crystal structure of the receptor binding domain of the spike glycoprotein of human betacoronavirus HKU1. *Nat. Commun.* 8:2529. doi: 10.1038/ncomms15216

Pallesen, J., Wang, N., Corbett, K. S., Wrapp, D., Kirchdoerfer, R. N., Turner, H. L., et al. (2017). Immunogenicity and structures of a rationally designed prefusion MERS-CoV spike antigen. *Proc. Natl. Acad. Sci. U.S.A.* 114, E7348–E7357. doi: 10.1073/pnas.1707304114

Pedersen, N. C. (2014). An update on feline infectious peritonitis: virology and immunopathogenesis. *Vet. J.* 201, 123–132. doi: 10.1016/j.tvjl.2014.04.017

Pimentel, T. A., Yan, Z., Jeffers, S. A., Holmes, K. V., Hodges, R. S., and Burkhard, P. (2009). Peptide nanoparticles as novel immunogens: design and analysis of a prototypic severe acute respiratory syndrome vaccine. *Chem. Biol. Drug Des.* 73, 53–61. doi: 10.1111/j.1747-0285.2008.00746.x

Poon, L. L., Chu, D. K., Chan, K. H., Wong, O. K., Ellis, T. M., Leung, Y. H., et al. (2005). Identification of a novel coronavirus in bats. *J. Virol.* 79, 2001–2009. doi: 10.1128/jvi.79.4.2001-2009.2005

Qiu, M., Shi, Y., Guo, Z., Chen, Z., He, R., Chen, R., et al. (2005). Antibody responses to individual proteins of SARS coronavirus and their neutralization activities. *Microbes Infect.* 7, 882–889. doi: 10.1016/j.micinf.2005.02.006

Raj, V. S., Mou, H., Smits, S. L., Dekkers, D. H., Muller, M. A., Dijkman, R., et al. (2013). Dipeptidyl peptidase 4 is a functional receptor for the emerging human coronavirus-EMC. *Nature* 495, 251–254. doi: 10.1038/nature12005

Regamey, N., Kaiser, L., Roiha, H. L., Deffernez, C., Kuehni, C. E., Latzin, P., et al. (2008). Viral etiology of acute respiratory infections with cough in infancy - A community-based birth cohort study. *Pediatr. Infect. Dis. J.* 27, 100–105. doi: 10.1097/INF.0b013e31815922c8

Reusken, C. B., Haagmans, B. L., Muller, M. A., Gutierrez, C., Godeke, G. J., Meyer, B., et al. (2013). Middle East respiratory syndrome coronavirus neutralising serum antibodies in dromedary camels: a comparative serological study. *Lancet Infect. Dis.* 13, 859–866. doi: 10.1016/s1473-3099(13)70164-6

Rota, P. A., Oberste, M. S., Monroe, S. S., Nix, W. A., Campagnoli, R., Icenogle, J. P., et al. (2003). Characterization of a novel coronavirus associated with severe acute respiratory syndrome. *Science* 300, 1394–1399. doi: 10.1126/science.1085952

Scobey, T., Yount, B. L., Sims, A. C., Donaldson, E. F., Agnihothram, S. S., Menachery, V. D., et al. (2013). Reverse genetics with a full-length infectious cDNA of the Middle East respiratory syndrome coronavirus. *Proc. Natl. Acad. Sci. U.S.A.* 110, 16157–16162. doi: 10.1073/pnas.1311542110

Severance, E. G., Bossis, I., Dickerson, F. B., Stallings, C. R., Origoni, A. E., Sullens, A., et al. (2008). Development of a nucleocapsid-based human coronavirus immunoassay and estimates of individuals exposed to coronavirus in a US metropolitan population. *Clin. Vaccine Immunol.* 15, 1805–1810. doi: 10.1128/cvi.00124-08

Shao, X., Guo, X., Esper, F., Weibel, C., and Kahn, J. S. (2007). Seroepidemiology of group I human coronaviruses in children. *J. Clin. Virol.* 40, 207–213. doi: 10.1016/j.jcv.2007.08.007

Snijder, E. J., Bredenbeek, P. J., Dobbe, J. C., Thiel, V., Ziebuhr, J., Poon, L. L., et al. (2003). Unique and conserved features of genome and proteome of SARS-coronavirus, an early split-off from the coronavirus group 2 lineage. *J. Mol. Biol.* 331, 991–1004. doi: 10.1016/s0022-2836(03)00865-9

Snijder, E. J., Decroly, E., and Ziebuhr, J. (2016). The nonstructural proteins directing coronavirus RNA synthesis and processing. *Adv. Virus Res.* 96, 59–126. doi: 10.1016/bs.aivir.2016.08.008

Tai, W., Wang, Y., Fett, C. A., Zhao, G., Li, F., Perlman, S., et al. (2017). Recombinant receptor-binding domains of multiple middle east respiratory syndrome coronaviruses (MERS-CoVs) induce cross-neutralizing antibodies against divergent human and camel MERS-CoVs and antibody escape mutants. *J. Virol* 91:e01651-16. doi: 10.1128/jvi.01651-16

Tai, W., Zhao, G., Sun, S., Guo, Y., Wang, Y., Tao, X., et al. (2016). A recombinant receptor-binding domain of MERS-CoV in trimeric form protects human dipeptidyl peptidase 4 (hDPP4) transgenic mice from MERS-CoV infection. *Virology* 499, 375–382. doi: 10.1016/j.virol.2016.10.005

Tang, J., Zhang, N., Tao, X., Zhao, G., Guo, Y., Tseng, C. T., et al. (2015). Optimization of antigen dose for a receptor-binding domain-based subunit vaccine against MERS coronavirus. *Hum. Vaccin. Immunother.* 11, 1244–1250. doi: 10.1080/21645515.2015.1021527

Tomar, S., Johnston, M. L., St John, S. E., Osswald, H. L., Nyalapatla, P. R., Paul, L. N., et al. (2015). Ligand-induced dimerization of Middle East respiratory syndrome (MERS) coronavirus nsp5 protease (3CLpro): implifications for nsp5 regulation and the development of antivirals. *J. Biol. Chem.* 290, 19403–19422. doi: 10.1074/jbc.M115.651463

Tortorici, M. A., Walls, A. C., Lang, Y., Wang, C., Li, Z., Koerhuis, D., et al. (2019). Structural basis for human coronavirus attachment to sialic acid receptors. *Nat. Struct. Mol. Biol.* 26, 481–489. doi: 10.1038/s41594-019-0233-y

Tu, C., Crameri, G., Kong, X., Chen, J., Sun, Y., Yu, M., et al. (2004). Antibodies to SARS coronavirus in civets. *Emerg. Infect. Dis.* 10, 2244–2248. doi: 10.3201/eid1012.040520

Tyrrell, D. A., and Bynoe, M. L. (1965). Cultivation of a novel type of common-cold virus in organ cultures. *Br. Med. J.* 1, 1467–1470. doi: 10.1136/bmj.1.5448.1467

Vabret, A., Mourez, T., Gouarin, S., Petitjean, J., and Freymuth, F. (2003). An outbreak of coronavirus OC43 respiratory infection in Normandy, France. *Clin. Infect. Dis.* 36, 985–989. doi: 10.1086/374222

van Boheemen, S., de Graaf, M., Lauber, C., Bestebroer, T. M., Raj, V. S., Zaki, A. M., et al. (2012). Genomic characterization of a newly discovered coronavirus associated with acute respiratory distress syndrome in humans. *mBio* 3:e00473-12. doi: 10.1128/mBio.00473-12

van der Hoek, L., Pyrc, K., Jebbink, M. F., Vermeulen-Oost, W., Berkhout, R. J., Wolthers, K. C., et al. (2004). Identification of a new human coronavirus. *Nat. Med.* 10, 368–373. doi: 10.1038/nm1024

Veit, S., Jany, S., Fux, R., Sutter, G., and Volz, A. (2018). CD8+ T cells responding to the Middle East Respiratory Syndrome coronavirus nucleocapsid protein delivered by vaccinia virus MVA in mice. *Viruses* 10:E718. doi: 10.3390/v10120718

Wang, C., Zheng, X., Gai, W., Zhao, Y., Wang, H., Wang, H., et al. (2017). MERS-CoV virus-like particles produced in insect cells induce specific humoural and cellular imminity in rhesus macaques. *Oncotarget* 8, 12686–12694. doi: 10.18632/oncotarget.8475

Wang, L., Shi, W., Joyce, M. G., Modjarrad, K., Zhang, Y., Leung, K., et al. (2015). Evaluation of candidate vaccine approaches for MERS-CoV. *Nat. Commun.* 6:7712. doi: 10.1038/ncomms8712

Wang, N., Shi, X., Jiang, L., Zhang, S., Wang, D., Tong, P., et al. (2013). Structure of MERS-CoV spike receptor-binding domain complexed with human receptor DPP4. *Cell Res.* 23, 986–993. doi: 10.1038/cr.2013.92

Wang, Y., Tai, W., Yang, J., Zhao, G., Sun, S., Tseng, C. K., et al. (2017). Receptor-binding domain of MERS-CoV with optimal immunogen dosage and immunization interval protects human transgenic mice from MERS-CoV infection. *Hum. Vaccin. Immunother.* 13, 1615–1624. doi: 10.1080/21645515.2017.1296994

Wong, S. K., Li, W., Moore, M. J., Choe, H., and Farzan, M. (2004). A 193-amino acid fragment of the SARS coronavirus S protein efficiently binds angiotensin-converting enzyme 2. *J. Biol. Chem.* 279, 3197–3201. doi: 10.1074/jbc.C300520200

Woo, P. C., Lau, S. K., Chu, C. M., Chan, K. H., Tsoi, H. W., Huang, Y., et al. (2005). Characterization and complete genome sequence of a novel coronavirus, coronavirus HKU1, from patients with pneumonia. *J. Virol.* 79, 884–895. doi: 10.1128/jvi.79.2.884-895.2005

Woo, P. C., Lau, S. K., Lam, C. S., Lai, K. K., Huang, Y., Lee, P., et al. (2009a). Comparative analysis of complete genome sequences of three avian coronaviruses reveals a novel group 3c coronavirus. *J. Virol.* 83, 908–917. doi: 10.1128/jvi.01977-08

Woo, P. C., Lau, S. K., Lam, C. S., Lau, C. C., Tsang, A. K., Lau, J. H., et al. (2012). Discovery of seven novel mammalian and avian coronaviruses in the genus deltacoronavirus supports bat coronaviruses as the gene source of alphacoronavirus and betacoronavirus and avian coronaviruses as the gene source of gammacoronavirus and deltacoronavirus. *J. Virol.* 86, 3995–4008. doi: 10.1128/jvi.06540-11

Woo, P. C., Lau, S. K., Lam, C. S., Tsang, A. K., Hui, S. W., Fan, R. Y., et al. (2014). Discovery of a novel bottlenose dolphin coronavirus reveals a distinct species of marine mammal coronavirus in gammacoronavirus. *J. Virol.* 88, 1318–1331. doi: 10.1128/jvi.02351-13

Woo, P. C., Lau, S. K., Yip, C. C., Huang, Y., and Yuen, K. Y. (2009b). More and more coronaviruses: human coronavirus HKU1. *Viruses* 1, 57–71. doi: 10.3390/v1010057

Yang, Y., Deng, Y., Wen, B., Wang, H., Meng, X., Lan, J., et al. (2014a). The amino acids 736-761 of the MERS-CoV spike protein induce neutralizing antibodies: implications for the development of vaccines and antiviral agents. *Viral Immunol.* 27, 543–550. doi: 10.1089/vim.2014.0080

Yang, Y., Du, L., Liu, C., Wang, L., Ma, C., Tang, J., et al. (2014b). Receptor usage and cell entry of bat coronavirus HKU4 provide insight into bat-to-human transmission of MERS coronavirus. *Proc. Natl. Acad. Sci. U.S.A.* 111, 12516–12521. doi: 10.1073/pnas.1405889111

Yang, Z. Y., Kong, W. P., Huang, Y., Roberts, A., Murphy, B. R., Subbarao, K., et al. (2004). A DNA vaccine induces SARS coronavirus neutralization and protective immunity in mice. *Nature* 428, 561–564. doi: 10.1038/nature02463

Yuan, Y., Cao, D., Zhang, Y., Ma, J., Qi, J., Wang, Q., et al. (2017). Cryo-EM structures of MERS-CoV and SARS-CoV spike glycoproteins reveal the dynamic receptor binding domains. *Nat. Commun.* 8:15092. doi: 10.1038/ncomms15092

Zakhartchouk, A. N., Sharon, C., Satkunarajah, M., Auperin, T., Viswanathan, S., Mutwiri, G., et al. (2007). Immunogenicity of a receptor-binding domain of SARS coronavirus spike protein in mice: implications for a subunit vaccine. *Vaccine* 25, 136–143. doi: 10.1016/j.vaccine.2006.06.084

Zaki, A. M., van Boheemen, S., Bestebroer, T. M., Osterhaus, A. D., and Fouchier, R. A. (2012). Isolation of a novel coronavirus from a man with pneumonia in Saudi Arabia. *N. Engl. J. Med.* 367, 1814–1820. doi: 10.1056/NEJMoa1211721

Zeng, F., Chow, K. Y., Hon, C. C., Law, K. M., Yip, C. W., Chan, K. H., et al. (2004). Characterization of humoral responses in mice immunized with plasmid DNAs encoding SARS-CoV spike gene fragments. *Biochem. Biophys. Res. Commun.* 315, 1134–1139. doi: 10.1016/j.bbrc.2004.01.166

Zhang, N., Channappanavar, R., Ma, C., Wang, L., Tang, J., Garron, T., et al. (2016). Identification of an ideal adjuvant for receptor-binding domain-based subunit vaccines against Middle East respiratory syndrome coronavirus. *Cell. Mol. Immunol.* 13, 180–190. doi: 10.1038/cmi.2015.03

Zhang, N., Jiang, S., and Du, L. (2014). Current advancements and potential strategies in the development of MERS-CoV vaccines. *Expert Rev. Vaccines* 13, 761–774. doi: 10.1586/14760584.2014.912134

Zhang, N., Tang, J., Lu, L., Jiang, S., and Du, L. (2015). Receptor-binding domain-based subunit vaccines against MERS-CoV. *Virus Res.* 202, 151–159. doi: 10.1016/j.virusres.2014.11.013

Zhang, N., Wang, L., Deng, X., Liang, R., Su, M., He, C., et al. (2020). Recent advances in the detection of respiratory virus infection in humans. *J. Med. Virol.* [Epub ahead of print].

Zheng, N., Xia, R., Yang, C., Yin, B., Li, Y., Duan, C., et al. (2009). Boosted expression of the SARS-CoV nucleocapsid protein in tobacco and its immunogenicity in mice. *Vaccine* 27, 5001–5007. doi: 10.1016/j.vaccine.2009.05.073

Zhong, N. S., Zheng, B. J., Li, Y. M., Poon, L. L., Xie, Z. H., Chan, K. H., et al. (2003). Epidemiology and cause of severe acute respiratory syndrome (SARS) in Guangdong, People's Republic of China, in February, 2003. *Lancet* 362, 1353–1358. doi: 10.1016/s0140-6736(03)14630-2

Zhou, P., Yang, X. L., Wang, X. G., Hu, B., Zhang, L., Zhang, W., et al. (2020). A pneumonia outbreak associated with a new coronavirus of probable bat origin. *Nature* [Epub ahead of print].

Zhou, Y., Jiang, S., and Du, L. (2018). Prospects for a MERS-CoV spike vaccine. *Expert Rev. Vaccines* 17, 677–686. doi: 10.1080/14760584.2018.1506702

Zhou, Y., Yang, Y., Huang, J., Jiang, S., and Du, L. (2019). Advances in MERS-CoV vaccines and therapeutics based on the receptor-binding domain. *Viruses* 11:E60. doi: 10.3390/v11010060

Zhu, N., Zhang, D., Wang, W., Li, X., Yang, B., Song, J., et al. (2020). A novel coronavirus from patients with pneumonia in China, 2019. *N. Engl. J. Med.* [Epub ahead of print].

Zhu, X., Liu, Q., Du, L., Lu, L., and Jiang, S. (2013). Receptor-binding domain as a target for developing SARS vaccines. *J. Thoracic Dis.* 5, S142–S148. doi: 10.3978/j.issn.2072-1439.2013.06.06

**Conflict of Interest:** The authors declare that the research was conducted in the absence of any commercial or financial relationships that could be construed as a potential conflict of interest.

*Copyright © 2020 Wang, Shang, Jiang and Du. This is an open-access article distributed under the terms of the Creative Commons Attribution License (CC BY). The use, distribution or reproduction in other forums is permitted, provided the original author(s) and the copyright owner(s) are credited and that the original publication in this journal is cited, in accordance with accepted academic practice. No use, distribution or reproduction is permitted which does not comply with these terms.*

frontiers in Microbiology

ORIGINAL RESEARCH
published: 28 February 2020
doi: 10.3389/fmicb.2020.00182

# Identification of Chebulinic Acid and Chebulagic Acid as Novel Influenza Viral Neuraminidase Inhibitors

*Ping Li[1†], Ruikun Du[1,2,3†], Yanyan Wang[1], Xuewen Hou[1], Lin Wang[1], Xiujuan Zhao[1], Peng Zhan[4], Xinyong Liu[4], Lijun Rong[5]* and Qinghua Cui[1,2,3]**

[1] College of Pharmacy, Shandong University of Traditional Chinese Medicine, Jinan, China, [2] Qingdao Academy of Chinese Medicinal Sciences, Shandong University of Traditional Chinese Medicine, Qingdao, China, [3] Research Center, College of Chinese Medicine, Shandong University of Traditional Chinese Medicine, Jinan, China, [4] Department of Medicinal Chemistry, Key Laboratory of Chemical Biology (Ministry of Education), School of Pharmaceutical Sciences, Shandong University, Jinan, China, [5] Department of Microbiology and Immunology, College of Medicine, University of Illinois at Chicago, Chicago, IL, United States

OPEN ACCESS

**Edited by:**
Chunfu Zheng,
Fujian Medical University, China

**Reviewed by:**
Qi Wang,
Harbin Veterinary Research Institute (CAAS), China
Jun Wang,
The University of Arizona, United States

***Correspondence:**
Lijun Rong
Lijun@uic.edu
Qinghua Cui
cuiqinghua1122@163.com

[†] These authors have contributed equally to this work

**Specialty section:**
This article was submitted to Virology, a section of the journal Frontiers in Microbiology

**Received:** 20 November 2019
**Accepted:** 24 January 2020
**Published:** 28 February 2020

**Citation:**
Li P, Du R, Wang Y, Hou X, Wang L, Zhao X, Zhan P, Liu X, Rong L and Cui Q (2020) Identification of Chebulinic Acid and Chebulagic Acid as Novel Influenza Viral Neuraminidase Inhibitors. Front. Microbiol. 11:182. doi: 10.3389/fmicb.2020.00182

The influenza A virus (IAV) causes seasonal epidemics and occasional but devastating pandemics, which are of a major public health concern. Although several antiviral drugs are currently available, there is an urgent need to develop novel antiviral therapies with different mechanisms of action due to emergence of drug resistance. In this study, two related compounds, chebulagic acid (CHLA) and chebulinic acid (CHLI), were identified as novel inhibitors against IAV replication. A reporter virus-based infection assay demonstrated that CHLA and CHLI exhibit no inhibitory effect on IAV entry or RNA replication during the virus replication cycle. Results of viral release inhibition assay and neuraminidase (NA) inhibition assay indicated that CHLA and CHLI exert their inhibitory effect on the NA-mediated viral release. Moreover, oseltamivir-resistance mutation NA/H274Y of NA is susceptible to CHLA or CHLI, suggesting a different mechanism of action for CHLA and CHLI. In summary, CHLA and CHLI are promising new NA inhibitors that may be further developed as novel antivirals against IAVs.

**Keywords: influenza A virus, chebulinic acid, chebulagic acid, neuraminidase, neuraminidase inhibitor**

## INTRODUCTION

Influenza vaccines and antiviral drugs are effective in preventing infection or ameliorating disease severity (Vasileiou et al., 2017). However, influenza infection, as an acute respiratory disease caused by seasonal outbreaks and, periodically, pandemics of influenza viruses and accounting for up to 650,000 annual deaths globally (World Health Organization [WHO], 2018), remains a serious public health concern. This is partly due to the fact that current influenza vaccines can target only selected strains based on annual surveillance and prediction, which does not always match the circulating strains, leading to a sharp drop in vaccine efficacy (de Jong et al., 2000; Nachbagauer and Krammer, 2017). Moreover, emergence of drug resistance strains of influenza A viruses (IAVs) reduces the effectiveness of the current anti-influenza therapies. The three clinically available classes of antivirals for treatment and prevention of influenza infections are the viral ion channel M2 blockers (amantadine and rimantadine), neuraminidase (NA) inhibitors (oseltamivir, zanamivir, peramivir, and laninamivir), and most recently the licensed baloxavir marboxil, which is an oral cap-dependent endonuclease inhibitor of influenza virus polymerase inhibitor

(Alves Galvao et al., 2014; Alame et al., 2016; Kashiwagi et al., 2016; Heo, 2018; Noshi et al., 2018). However, high levels of resistance to M2 channel blockers and NA inhibitors have emerged, undermining the efficacy of these drugs (Hata et al., 2007; Samson et al., 2013; van der Vries et al., 2013; Lackenby et al., 2018). Moreover, mutations responsible for reduced susceptibility of influenza A/H3N2 virus to baloxavir have been detected already (Takashita et al., 2019). Therefore, the development of antiviral drugs with different mechanisms of action is urgently needed against influenza viruses.

Natural products contain structurally diversified bioactive chemicals, which are valuable sources for new drug discovery. Among the new medicines approved by the U.S. Food and Drug Administration (FDA) between 1981 and 2010, natural products or their direct derivatives account for 34% (Harvey et al., 2015). In the present study, 352 natural product samples were screened for anti-IAV activity using a phenotypic screening approach based on a recombinant IAV expressing Gaussia luciferase (Zhao et al., 2019). The extracts from both unripe and ripe pods of *Terminalia chebula* Retz. display potent anti-IAV activity. Further, two constitutes of *T. chebula*, chebulagic acid (CHLA) and chebulinic acid (CHLI), were identified as novel antivirals against IAV. Detailed studies revealed that both compounds specifically block progeny virus release by inhibiting IAV NA activity. Moreover, CHLA and CHLI showed highly inhibitory efficacy against an oseltamivir-resistant IAV strain, suggesting their potential as novel cost-effective NA inhibitors for controlling influenza virus infections.

# MATERIALS AND METHODS

## Library of Natural Product Samples

Dispensing granules of 352 natural product samples were purchased from EFONG Pharmaceutical Company (Foshan, Guangdong, China) and arrayed in 96-well plates at a 20-mg/mL stock concentration in DMSO. All of the sample plates were stored at −80°C until use.

## Cells, Viruses, and Compounds

Madin–Darby canine kidney (MDCK) epithelial cells were grown in Dulbecco's modified Eagle's medium (DMEM; Cellgro, Manassas, VA, United States) supplemented with 10% fetal bovine serum (FBS; Gibco, Carlsbad, CA, United States), 1000 units/mL of penicillin, and 100 μg/mL of streptomycin (Invitrogen, Carlsbad, CA, United States). Infections were performed in Opti-MEM containing 2 μg/mL *N*-tosyl-L-phenylalanine chloromethyl ketone (TPCK)–trypsin (Sigma–Aldrich, St. Louis, MO, United States). All cells were grown at 37°C in 5% $CO_2$.

Recombinant reporter virus PR8-PB2-Gluc and influenza strains A/Puerto Rico/8/1934 (H1N1, A/H1N1/PR8) and A/Wyoming/3/03 (H3N2, A/H3N2/NY) were prepared and stocked in our lab as previously described (Zhao et al., 2018; Wang et al., 2019). Oseltamivir-resistant influenza A/H1N1/pdm(09) virus containing NA/H274Y was provided by Beijing CDC, China, influenza A/Brisbane/10/2007(H3N2) was provided by Chinese Academy of Medical Sciences, and influenza B-Yamagata-like and B-Victoria-like strains were provided by Shandong CDC (Jinan, China).

Fifteen chemical components (> 98% purity) from *T. chebula* were purchased from the National Institutes for Food and Drug Control (Beijing, China).

## High-Throughput Screen

The library of natural product samples was screened using a phenotypic screening approach described previously (Zhao et al., 2019). Briefly, MDCK cells were seeded in 96-well plates at a density of 5000 cells/well 24 h before infection. In the presence of natural product samples (final concentration of 25 μg/mL), MDCK cells were challenged with recombinant reporter virus PR8-PB2-Gluc at an MOI of 0.01. Infection was quantified after 36 h of incubation by measuring the luciferase activity with PierceTM Gaussia Luciferase Glow Assay kit (Thermo Fisher, Hillsboro, OR, United States) according to the manufacturer's instructions. Data were normalized to signals from the negative controls (virus alone with DMSO), and an average of > 90% inhibition for duplicates was applied for picking hits.

The selected active samples were then reformatted into new 96-well plates and tested against PR8-PB2-Gluc at 25 μg/mL in 0.125% DMSO (v/v) to confirm the primary results. Cell cytotoxicity was examined 48 h post-treatment using the CellTiter-Glo® Luminescent Cell Viability Assay (Promega, Madison, WI, United States), treated for the antiviral screen.

The confirmed hit samples were twofold serially diluted, respectively, for dose–response analysis, and the $IC_{50}$ and $CC_{50}$ values were determined by fitting dose–response curves with a four-parameter logistic regression to the data in GraphPad Prism software (version 5.02, La Jolla, CA, United States).

## One-Cycle Infection Inhibition Assay

To determine whether the hit natural product samples or its derivatives were target to viral entry or genome replication steps, a one-cycle infection inhibition assay was carried out using the reporter virus PR8-PB2-Gluc. Briefly, MDCK cells growing in a 96-well plate were infected with PR8-PB2-Gluc at an MOI of 0.1 in the presence of various concentrations of test samples/compounds. After 1 h of incubation, unabsorbed viruses were removed, and the cells were treated with the tested samples. In order to prevent the second round of infection, DMEM containing 10% FBS, instead of Opti-MEM containing 2 μg/mL of TPCK–trypsin, was used during infection to avoid HA cleavage and infectious virus production. After 24 h, infections were quantified by measuring the luciferase activity with PierceTM Gaussia Luciferase Glow Assay kit (Thermo Fisher, Hillsboro, OR, United States). Meanwhile, in the presence of the reporter virus PR8-PB2-Gluc, cell cytotoxicity for the test compounds was determined.

## Virus Release Inhibition Assay

To determine whether the hit natural product samples or the derivatives target to the release of progeny viruses, MDCK cells were infected with the reporter virus PR8-PB2-Gluc at an MOI of 0.1. At 20 h post-infection (p.i.), the culture medium was

removed, and the cells were washed with PBS three times. Fresh Opti-MEM containing 2 μg/mL of TPCK–trypsin was added and cultured for 2 h in the presence of various concentrations of test samples/compounds. The culture medium was harvested and titrated using luciferase assay.

## Neuraminidase (NA) Inhibition Assay

Neuraminidase inhibition assay was performed using Neuraminidase Inhibitors Screening kit (Beyotime Biotechnology, Shanghai, China) according to manufacturer's instructions. Briefly, NA and various concentrations of test samples/compounds were added to each well of 96-well plates. In order to fully interact between the compounds and NA, the 96-well plates were mixed for 1 min and incubated at 37°C for 2 min. Then fluorescent substrates were added, mixed, and incubated. After incubation for 1 h, the decrease in fluorescence was monitored to reflect NA inhibition efficacy.

## Viral Yield Reduction Assay

Viral yield reduction assay was performed as previously described (Zhu et al., 2011). Briefly, MDCK cells growing in 24-well plates were infected with A/H1N1/PR8, A/H3N2/NY, oseltamivir-resistant influenza A/H1N1/pdm(09), A/H3N2/Brisbane, B-Yamagata-like, and B-Victoria-like strains at an MOI of 0.01 with or without various concentrations of test samples/compounds. The culture supernatants were harvested at 24 h p.i., and virus titers ($TCID_{50}$/mL) in the culture supernatants were determined using MDCK cells.

# RESULTS

## Extracts of *T. chebula* Inhibit IAV Replication

To discover novel antiviral actives against IAV, a library consisting of 352 natural product samples was prepared and screened using a phenotypic screening approach based on a reporter influenza A PR8-PB2-Gluc virus (Zhao et al., 2019) in a primary screen and confirmation screen. As a result, 12 hit samples were identified to inhibit IAV infection (**Supplementary Table S1**).

Among the most potent anti-IAV natural product samples, both unripe and ripe pods of *T. chebula* significantly inhibited IAV replication with $IC_{50}$s of 5.8 ± 1.4 and 7.0 ± 1.0 μg/mL, respectively (**Figures 1A,B**). Since unripe pods of *T. chebula* exhibited a $CC_{50}$ to MDCK cells of 255.1 ± 1.3 μg/mL, while ripe pods of *T. chebula* showed no obvious cytotoxicity at a high concentration as 500 μg/mL, it is likely that there is some difference between the compositions of the two natural product sample preparations.

## CHLA and CHLI Inhibit IAV Replication

Considering the close relation between unripe and ripe pods of *T. chebula*, the chemical compositions of the two samples were compared based on spectroscopic data with previously reported literature. Fifteen overlapped constituents were subsequently shortlisted and subjected to antiviral evaluation. As shown in **Figure 2A**, at a concentration of 12.5 μM, corilagin and ellagic acid showed about 40% inhibition, while CHLA, CHLI, and 1,2,3,4,6-pentagalloyllucose (PGG) showed > 90% inhibition. Since corilagin, ellagic acid, and PGG have been well characterized for their antiviral activity against IAV (Liu et al., 2011; Chen et al., 2015; Zu et al., 2015), CHLA and CHLI, which are structurally related, were chosen for further analysis.

High-performance liquid chromatography was performed to further demonstrate that unripe and ripe pods of *T. chebula* share the constituents of CHLA and CHLI (**Supplementary Figure S1**), of which the dose–response effects against IAV replication were subsequently determined. As shown in **Figures 2B,C**, the $IC_{50}$ values against IAV replication of CHLA and CHLI were 1.36 ± 0.36 and 1.86 ± 0.98 μM, respectively, while the $CC_{50}$ values of both compounds were greater than 100 μM. These results show that CHLA and CHLI are potent anti-IAV inhibitors.

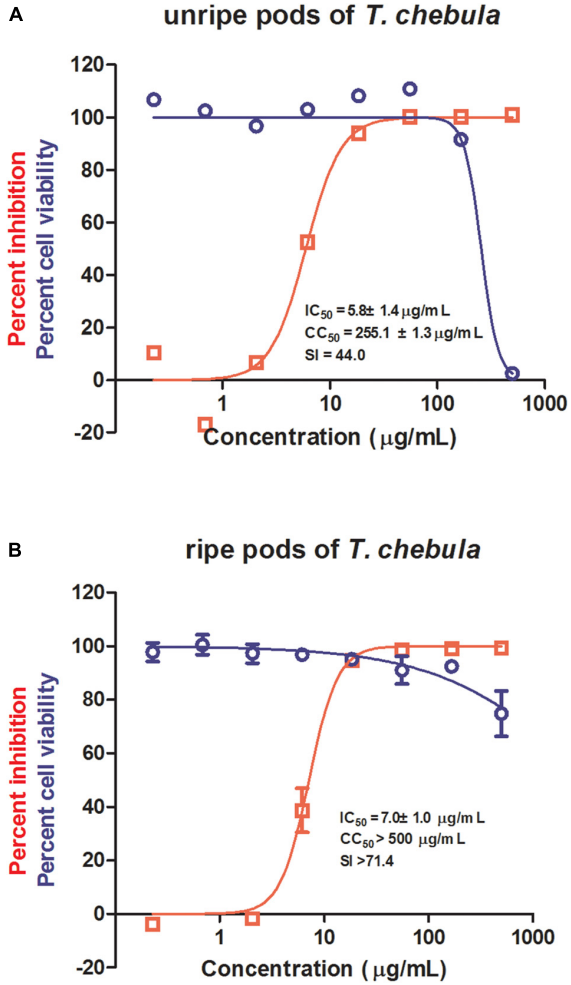


**FIGURE 1 |** Antiviral activities of unripe and ripe pods of *Terminalia chebula* on influenza virus. The *in vitro* dose–response curves against influenza A virus (IAV) (red) and cytotoxicity in Madin–Darby canine kidney (MDCK) cells (blue) of unripe **(A)** and ripe **(B)** pods of *T. chebula*. Data are means ± SD from three independent experiments.

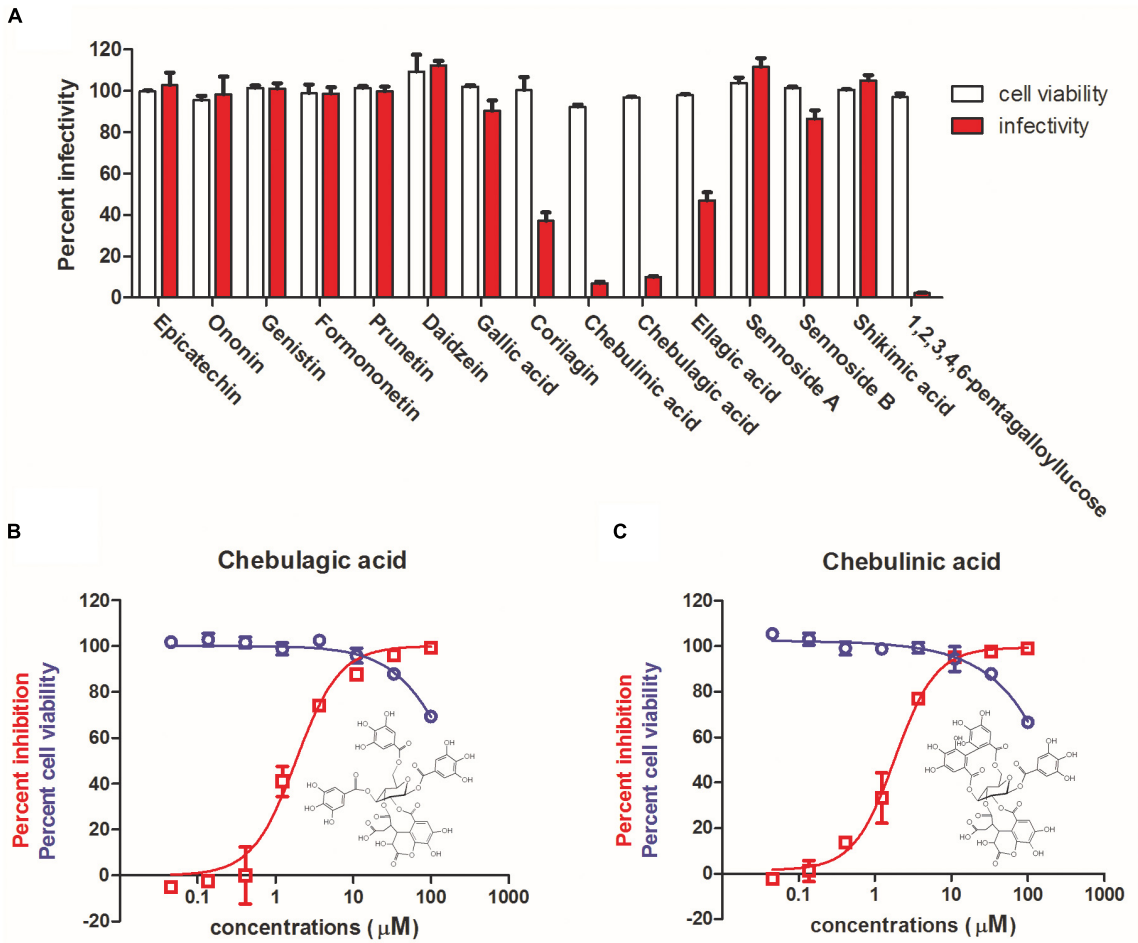


**FIGURE 2 |** Identification of chebulagic acid (CHLA) and chebulinic acid (CHLI) as novel antiviral actives against influenza virus infection. **(A)** Antiviral determination of 15 overlapped components of unripe and ripe pods of *T. chebula* at 12.5 μM. **(B)** CHLA and **(C)** CHLI were examined against influenza virus in MDCK cells *in vitro* for dose–response evaluation (red) and cytotoxicity assay (blue). Insets: molecular structures of **(B)** CHLA and **(C)** CHLI. Data are means ± SD from three independent experiments.

## CHLA and CHLI Do Not Inhibit Virus Entry or RNA Replication of IAV

To identify the target(s) and possible mechanism of action for CHLA and CHLI on IAV replication, a reporter IAV-based one-cycle infection assay was performed. Briefly, MDCK cells were infected by the reporter IAV PR8-PB2-Gluc in the absence or presence of test compounds, without the addition of TPCK–trypsin in the culture medium. Without exogenous trypsin-mediated HA cleavage, the progeny viruses are non-infectious and could not initiate a second round of infection. In this context, decreased expression of the reporter luciferase would be expected upon treatment with inhibitors targeting virus entry or RNA replication.

As shown in **Figure 3**, neither CHLA nor CHLI reduced Gluc expression. Note that the slight decrease in Gluc levels at 100 μM of CHLA and CHLI might be due to cytotoxicity (**Supplementary Figure S2**). These results suggest that CHLA and CHLI do not interfere with IAV entry or RNA replication.

## CHLA and CHLI Target NA to Block Viral Release

The effects of CHLA and CHLI on viral release were next investigated by a viral release inhibition assay. Briefly, infected cells were washed and cultured in an infection medium for another 2 h, in the absence or presence of different concentrations of test compounds. The progeny viruses were then harvested and titrated. Both CHLA and CHLI inhibited virus release in a dose-dependent manner, like the positive control oseltamivir phosphate (**Figure 4A**).

It has been well documented that the influenza viral NA activity contributes to progeny virus release from an infected cell surface (Du et al., 2019). We therefore examined whether CHLA and CHLI blocked viral release of IAV by inhibiting viral NA activity. A standard fluorimetric method was used (Li et al., 2016), and the results showed that both CHLA and CHLI inhibited viral NA activity in a dose-dependent manner (**Figure 4B**).

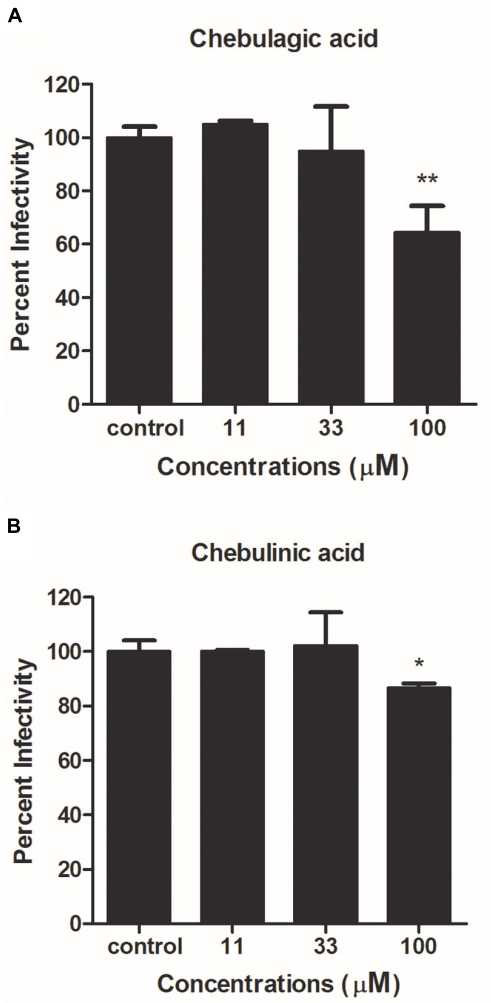


**FIGURE 3 |** Reporter luciferase-based one-cycle infection inhibition assay. MDCK cells growing in 96-well plates were infected with reporter influenza PR8-PB2-Gluc virus at an MOI of 0.1, in the absence or presence of increasing concentrations of **(A)** CHLA and **(B)** CHLI. Dulbecco's modified Eagle's medium (DMEM) supplemented with 4% fetal bovine serum (FBS) were used as culture medium during infection to avoid generation of infectious progeny viruses. At 24 h post infection (p.i.), Gluc expression was determined, and viral infectivities were evaluated. Data are means ± SD from three independent experiments. $^{*}p < 0.05$; $^{**}p < 0.01$; Student's *t*-test.

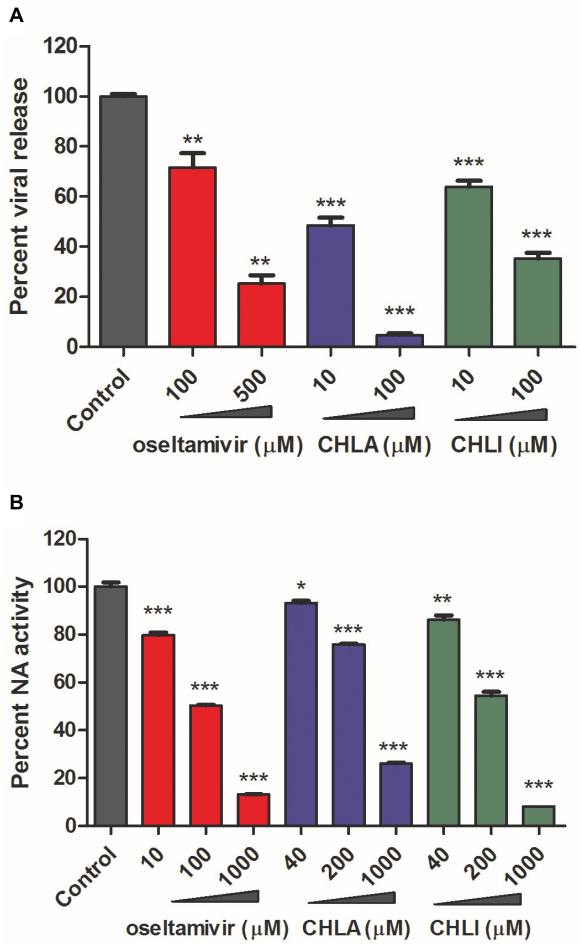


**FIGURE 4 |** CHLA and CHLI block neuraminidase (NA)-mediated virus release. **(A)** Virus release inhibition assay. MDCK cells were infected with reporter influenza PR8-PB2-Gluc virus at an MOI of 0.1. At 20 h p.i., infected cells were washed three times, and fresh Opti-MEM containing 2 μg/mL of *N*-tosyl-L-phenylalanine chloromethyl ketone (TPCK)–trypsin was added for another 2-h incubation, in the absence or presence of indicated compounds. The supernatants were harvested, and progeny viruses were titrated by luciferase assay. Data are means ± SD from three independent experiments. $^{**}p < 0.01$; $^{***}p < 0.001$; Student's *t*-test. **(B)** NA inhibition assay. The NA was incubated with fluorimetric substrates in the absence or presence of indicated compounds. The intensity of fluorescence was detected to reflect NA activities. Data are means ± SD from three independent experiments. $^{*}p < 0.05$; $^{**}p < 0.01$; $^{***}p < 0.001$; Student's *t*-test.

Together, these results indicate that CHLA and CHLI inhibit IAV replication by preventing the viral NA-mediated progeny virus release.

## CHLA and CHLI Are Effective to Inhibit an Oseltamivir-Resistant IAV

To compare the antiviral potency of CHLA and CHLI with the marketed NA inhibitor oseltamivir carboxylate, a yield reduction assay was performed with six influenza virus strains, including A/H1N1/PR8, A/H3N2/NY, A/H3N2/Brisbane, B-Yamagate, B-Victoria, and an oseltamivir-resistant A/H1N1pdm(09), which contains the NA/H274Y substitution. As a result, CHLA and CHLI showed significant inhibition against all influenza virus strains (**Figure 5**). Note that the $IC_{90}$s of CHLA (1.26 μM) and CHLI (1.58 μM) upon A/H1N1/PR8 were lower than that of oseltamivir carboxylate (3.92 μM), suggesting their comparable activities (**Figure 5A**).While compared to IAVs (**Figures 5A–C**), IBVs showed less sensitivity to CHLA and CHLI (**Figures 5D,E**).Interestingly, NA/H274Y in A/H1N1/pdm(09) virus conferred resistance to oseltamivir carboxylate, but the potency of CHLA and CHLI was not affected by the substitution (**Figure 5F**).

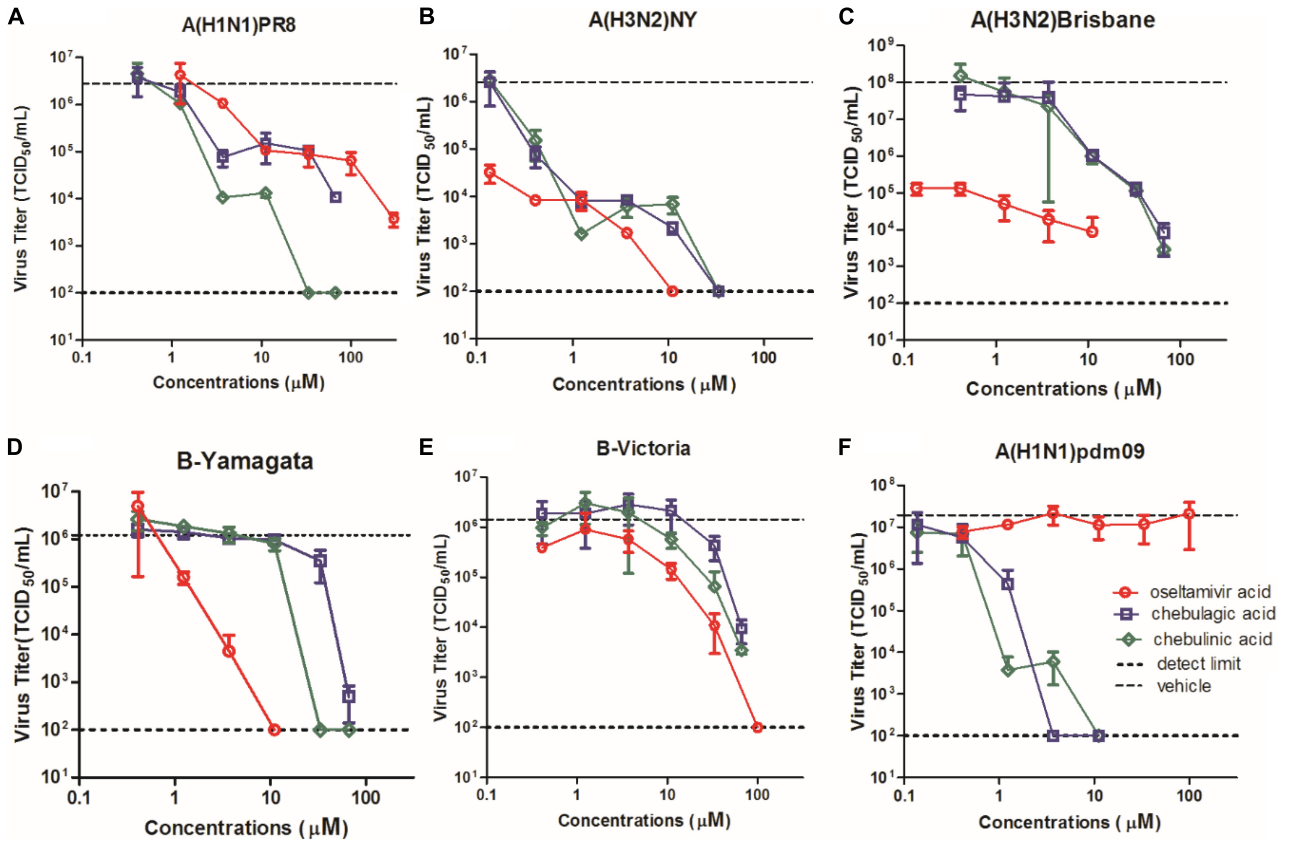


**FIGURE 5 |** Dose–response curves of CHLA, CHLI, and reference compound oseltamivir acid against virus replication in a yield reduction assay. MDCK cells in 24-well plates were infected with **(A)** A/H1N1/PR8, **(B)** A/H3N2/NY, **(C)** oseltamivir-resistant influenza virus A/H1N1/pdm(09), **(D)** A/H3N2/Brisbane, **(E)** B-Yamagata, and **(F)** B-Victoria at an MOI of 0.01. The culture supernatants were collected at 24 h p.i., and virus titers ($TCID_{50}$/mL) in the culture supernatants were determined using MDCK cells. Each point represents the mean and standard deviation of three independent experiments.

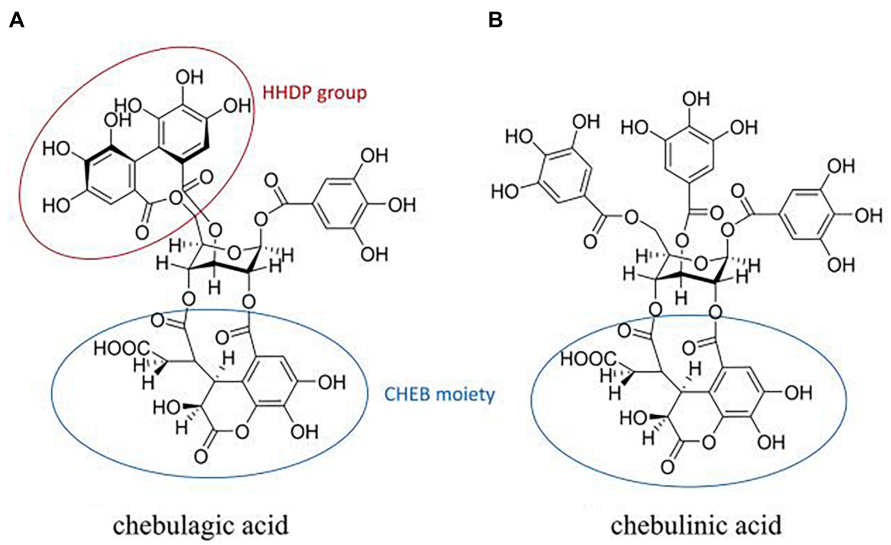


**FIGURE 6 |** Structures of chebulagic acid **(A)** and chebulinic acid **(B)**. Circles are framed hexahydrodiphenoyl (HHDP) and chebuloyl (CHEB) moieties.

## DISCUSSION

In this study, a phenotypic screening approach was initially used to evaluate 352 natural product samples for activity against IAV infection, and 12 natural product samples were identified as putative hits with high anti-IAV potency. Among these hit natural product samples, unripe and ripe pods of *T. chebula* displayed the most potent anti-IAV activity.

Unripe and ripe pods of *T. chebula* are two different medical materials usually prescribed in Traditional Chinese Medicine formula. However, the compositions of unripe pods and ripe pods of *T. chebula* are highly overlapping, and our study showed that CHLA and CHLI, two overlapped tannin constituents of the two samples, exhibit highly inhibitory effects against IAV replication, with $IC_{50}$s of 1.36 and 1.86 μM, respectively (**Figure 2**). Moreover, the SIs of CHLA and CHLI against IAV replication in MDCK cells are > 74 and > 54, respectively, suggesting that the two compounds are good candidates for novel antivirals against IAV (**Figure 2**).

Previous studies reported that CHLA and CHLI exhibit broad-spectrum antiviral activities by targeting viral glycoprotein–glycosaminoglycan interactions (Lin et al., 2011, 2013; Kesharwani et al., 2017). However, our data demonstrated that CHLA and CHLI do not interfere with influenza virus entry or RNA replication, but act as NA inhibitors targeting virus release.

Neuraminidase is a major surface glycoprotein with a sialidase activity, which contributes to the release of newly formed virions from infected cells and facilitates propagation of the virus (Du et al., 2019). For the purpose of antiviral development, NA is considered one of the major targets (Colman, 1994; Grienke et al., 2012). Currently, four NA inhibitors are available for the prophylaxis and treatment of influenza virus infections, including oseltamivir (Shobugawa et al., 2012), zanamivir (von Itzstein et al., 1993), peramivir (Alame et al., 2016), and laninamivir (Kashiwagi et al., 2016). Among these drugs, oseltamivir remains a first-line therapy since it was approved in 1999. However, resistance to oseltamivir has constantly been reported due to its wide use in clinic, and various mutants with resistance to the other NA inhibitors have also appeared (Samson et al., 2013; van der Vries et al., 2013; Lackenby et al., 2018). Therefore, it is imperative to discover novel NA inhibitors with different structures and mechanisms of action.

There are 11 NA subtypes of IAV, of which N10 and N11 were recently identified in bat IAV genomes (Tong et al., 2012, 2013). The N1–N9 subtypes can be phylogenetically divided into two groups. Group I includes N1, N4, N5, and N8, while group II is comprised of N2, N3, N6, N7, and N9 (Russell et al., 2006). Crystallographic studies show that group 1 NAs (except NA of A/H1N1pdm[09]) possess a large cavity termed 150-cavity adjacent to the catalytic site, but the 150-cavity was not observed in group 2 NAs (Li et al., 2010; Air, 2012). Upon binding of oseltamivir or zanamivir, the open 150-loop of group 1 NAs would adopt a closed conformation (Russell et al., 2006). Besides, inhibitors targeting the 150-cavity may also effectively target group 2 influenza NAs, perhaps by inducing the rigid closed 150-loop of group-2 NAs into a half-open one (Wu et al., 2013). The structure of A/H1N1pdm(09) NA presents a deficient 150-cavity in its crystal structure, conferring resistance to oseltamivir (Li et al., 2010). In addition, another auxiliary binding site adjacent to the sialic acid binding site called "430-cavity" has also been implicated and exploited for the design of new antivirals (Amaro et al., 2007; Swaminathan et al., 2013; Jia et al., 2019).

CHLA (1-*O*-galloyl-2,4-*O*-chebuloyl-3,6-*O*-hexahydroxydiphenoyl-β-D-glucose) (**Figure 6A**) and CHLI (1,3,6-tri-*O*-galloyl-2,4-*O*-chebuloyl-β-D-glucopyranoside) (**Figure 6B**) share the same molecular backbone of a β-D-glucose residue linked to a chebuloyl moiety. The difference is that CHLI has three free galloyl groups attached to the β-D-glucose residue, while CHLA contains only one galloyl group and a hexahydrodiphenoyl (HHDP) group, which is assumed to be a substitution for the two galloyl groups (Olennikov et al., 2015). The presence of the constrained HHDP group in CHLA is considered to result in larger spatial hindrance and less molecular flexibility. Thus, CHLI shows more broad-spectrum and potent biological activities due to the more favorable structure for entering the binding cavities or catalytic pockets of target proteases or enzymes. However, in our screening of anti-influenza activity described above, both of them showed excellent biological activity. The $IC_{90}$ of CHLI is even better. It can be inferred that the active site is related to its common CHEB structure. Although the mechanism of action of CHLA and CHLI on NA is not clear yet, we predict that they bind to the active site(s) of NA, either one single interaction with the 430-cavity or multiple interactions to both 150- and 430-cavities.

## CONCLUSION

In summary, we demonstrate that CHLA and CHLI can effectively inhibit IAV replication. These compounds act as NA inhibitors and show antiviral potency to both wild-type and oseltamivir-resistant IAV strains. Therefore, they may be further developed as a potential therapy against IAVs.

## DATA AVAILABILITY STATEMENT

The raw data supporting the conclusions of this article will be made available by the authors, without undue reservation, to any qualified researcher.

## AUTHOR CONTRIBUTIONS

RD, LR, and QC conceived and designed the experiments. PL, YW, XH, XZ, LW, and RD performed the experiments. PL, PZ, and XL analyzed the data. RD, LR, and QC wrote the manuscript. All authors contributed to the final version.

## FUNDING

This research was funded by (1) The Drug Innovation Major Project (Grant No. 2018ZX09711001); (2) the Key Research and Development Projects of Science and Technology Department of Shandong Province (Grant No. 2017CXGC1309); (3) Shandong

Provincial Natural Science Foundation, China (Grant No. ZR2019MH078); (4) Project for function implementation of advanced equipment, SDUTCM (Grant No. 2018yq22); and (5) Project for development of TCM Science and Technology in Shandong Province (Grant No. 2019-0031).

## SUPPLEMENTARY MATERIAL

The Supplementary Material for this article can be found online at: https://www.frontiersin.org/articles/10.3389/fmicb.2020.00182/full#supplementary-material

## REFERENCES


Air, G. M. (2012). Influenza neuraminidase. *Influenza Other Respir. Viruses* 6, 245–256. doi: 10.1111/j.1750-2659.2011.00304.x

Alame, M. M., Massaad, E., and Zaraket, H. (2016). Peramivir: a novel intravenous neuraminidase inhibitor for treatment of acute influenza infections. *Front. Microbiol.* 7:450. doi: 10.3389/fmicb.2016.00450

Alves Galvao, M. G., Rocha Crispino Santos, M. A., Alves, and da Cunha, A. J. (2014). Amantadine and rimantadine for influenza A in children and the elderly. *Cochrane Database Syst. Rev.* 11:CD002745. doi: 10.1002/14651858.CD002745.pub4

Amaro, R. E., Minh, D. D., Cheng, L. S., Lindstrom, W. M. Jr., Olson, A. J., Lin, J. H., et al. (2007). Remarkable loop flexibility in avian influenza N1 and its implications for antiviral drug design. *J. Am. Chem. Soc.* 129, 7764–7765. doi: 10.1021/ja0723535

Chen, G. H., Lin, Y. L., Hsu, W. L., Hsieh, S. K., and Tzen, J. T. C. (2015). Significant elevation of antiviral activity of strictinin from Pu′er tea after thermal degradation to ellagic acid and gallic acid. *J. Food Drug Anal.* 23, 116–123. doi: 10.1016/j.jfda.2014.07.007

Colman, P. M. (1994). Influenza virus neuraminidase: structure, antibodies, and inhibitors. *Protein Sci.* 3, 1687–1696. doi: 10.1002/pro.5560031007

de Jong, J. C., Beyer, W. E., Palache, A. M., Rimmelzwaan, G. F., and Osterhaus, A. D. (2000). Mismatch between the 1997/1998 influenza vaccine and the major epidemic A(H3N2) virus strain as the cause of an inadequate vaccine-induced antibody response to this strain in the elderly. *J. Med. Virol.* 61, 94–99. doi: 10.1002/(sici)1096-9071(200005)61:1<94::aid-jmv15>3.0.co;2-c

Du, R., Cui, Q., and Rong, L. (2019). Competitive cooperation of hemagglutinin and neuraminidase during influenza a virus entry. *Viruses* 11:E458. doi: 10.3390/v11050458

Grienke, U., Schmidtke, M., von Grafenstein, S., Kirchmair, J., Liedl, K. R., and Rollinger, J. M. (2012). Influenza neuraminidase: a druggable target for natural products. *Nat. Prod. Rep.* 29, 11–36. doi: 10.1039/c1np00053e

Harvey, A. L., Edrada-Ebel, R., and Quinn, R. J. (2015). The re-emergence of natural products for drug discovery in the genomics era. *Nat. Rev. Drug Discov.* 14, 111–129. doi: 10.1038/nrd4510

Hata, M., Tsuzuki, M., Goto, Y., Kumagai, N., Harada, M., Hashimoto, M., et al. (2007). High frequency of amantadine-resistant influenza A (H3N2) viruses in the 2005-2006 season and rapid detection of amantadine-resistant influenza A (H3N2) viruses by MAMA-PCR. *Jpn. J. Infect. Dis.* 60, 202–204. doi: 10.1097/QAI.0b013e318068d233

Heo, Y. A. (2018). Baloxavir: first global approval. *Drugs* 78, 693–697. doi: 10.1007/s40265-018-0899-1

Jia, R., Zhang, J., Ai, W., Ding, X., Desta, S., Sun, L., et al. (2019). Design, synthesis and biological evaluation of "Multi-Site"-binding influenza virus neuraminidase inhibitors. *Eur. J. Med. Chem.* 178, 64–80. doi: 10.1016/j.ejmech.2019.05.076

Kashiwagi, S., Watanabe, A., Ikematsu, H., Uemori, M., and Awamura, S. (2016). Long-acting neuraminidase inhibitor laninamivir octanoate as post-exposure prophylaxis for influenza. *Clin. Infect. Dis.* 63, 330–337. doi: 10.1093/cid/ciw255

Kesharwani, A., Polachira, S. K., Nair, R., Agarwal, A., Mishra, N. N., and Gupta, S. K. (2017). Anti-HSV-2 activity of Terminalia chebula Retz extract and its constituents, chebulagic and chebulinic acids. *BMC Complement. Altern. Med.* 17:110. doi: 10.1186/s12906-017-1620-8

Lackenby, A., Besselaar, T. G., Daniels, R. S., Fry, A., Gregory, V., Gubareva, L. V., et al. (2018). Global update on the susceptibility of human influenza viruses to neuraminidase inhibitors and status of novel antivirals, 2016-2017. *Antiviral Res.* 157, 38–46. doi: 10.1016/j.antiviral.2018.07.001

Li, J., Yang, X., and Huang, L. (2016). Anti-influenza virus activity and constituents. characterization of *Paeonia delavayi* extracts. *Molecules* 21:E1133. doi: 10.3390/molecules21091133

Li, Q., Qi, J., Zhang, W., Vavricka, C. J., Shi, Y., Wei, J., et al. (2010). The 2009 pandemic H1N1 neuraminidase N1 lacks the 150-cavity in its active site. *Nat. Struct. Mol. Biol.* 17, 1266–1268. doi: 10.1038/nsmb.1909

Lin, L. T., Chen, T. Y., Chung, C. Y., Noyce, R. S., Grindley, T. B., McCormick, C., et al. (2011). Hydrolyzable tannins (chebulagic acid and punicalagin) target viral glycoprotein-glycosaminoglycan interactions to inhibit herpes simplex virus 1 entry and cell-to-cell spread. *J. Virol.* 85, 4386–4398. doi: 10.1128/jvi.01492-10

Lin, L. T., Chen, T. Y., Lin, S. C., Chung, C. Y., Lin, T. C., Wang, G. H., et al. (2013). Broad-spectrum antiviral activity of chebulagic acid and punicalagin against viruses that use glycosaminoglycans for entry. *BMC Microbiol.* 13:187. doi: 10.1186/1471-2180-13-187

Liu, G., Xiong, S., Xiang, Y. F., Guo, C. W., Ge, F., Yang, C. R., et al. (2011). Antiviral activity and possible mechanisms of action of pentagalloylglucose (PGG) against influenza A virus. *Arch. Virol.* 156, 1359–1369. doi: 10.1007/s00705-011-0989-9

Nachbagauer, R., and Krammer, F. (2017). Universal influenza virus vaccines and therapeutic antibodies. *Clin. Microbiol. Infect.* 23, 222–228. doi: 10.1016/j.cmi.2017.02.009

Noshi, T., Kitano, M., Taniguchi, K., Yamamoto, A., Omoto, S., Baba, K., et al. (2018). In vitro characterization of baloxavir acid, a first-in-class cap-dependent endonuclease inhibitor of the influenza virus polymerase PA subunit. *Antivir. Res.* 160, 109–117. doi: 10.1016/j.antiviral.2018.10.008

Olennikov, D., Kashchenko, N., and Chirikova, N. (2015). *In vitro* bioaccessibility, human gut microbiota metabolites and hepatoprotective potential of chebulic ellagitannins: a case of padma hepaten® formulation. *Nutrients* 7, 8456–8477. doi: 10.3390/nu7105406

Russell, R. J., Haire, L. F., Stevens, D. J., Collins, P. J., Lin, Y. P., Blackburn, G. M., et al. (2006). The structure of H5N1 avian influenza neuraminidase suggests new opportunities for drug design. *Nature* 443, 45–49. doi: 10.1038/nature05114

Samson, M., Pizzorno, A., Abed, Y., and Boivin, G. (2013). Influenza virus resistance to neuraminidase inhibitors. *Antivir. Res.* 98, 174–185. doi: 10.1016/j.antiviral.2013.03.014

Shobugawa, Y., Saito, R., Sato, I., Kawashima, T., Dapat, C., Dapat, I. C., et al., (2012). Clinical effectiveness of neuraminidase inhibitors—oseltamivir, zanamivir, laninamivir, and peramivir—for treatment of influenza A(H3N2) and A(H1N1)pdm09 infection: an observational study in the 2010–2011 influenza season in Japan. *J. Infect. Chemother.* 18, 858–864. doi: 10.1007/s10156-012-0428-1

Swaminathan, K., Dyason, J. C., Maggioni, A., von Itzstein, M., and Downard, K. M. (2013). Binding of a natural anthocyanin inhibitor to influenza neuraminidase by mass spectrometry. *Anal. Bioanal. Chem.* 405, 6563–6572. doi: 10.1007/s00216-013-7068-x

Takashita, E., Kawakami, C., Ogawa, R., Morita, H., Fujisaki, S., Shirakura, M., et al. (2019). Influenza A(H3N2) virus exhibiting reduced susceptibility to baloxavir due to a polymerase acidic subunit I38T substitution detected from a hospitalised child without prior baloxavir treatment, Japan, January 2019. *Euro Surveill.* 24:1900170. doi: 10.2807/1560-7917.es.2019.24.12.1900170

Tong, S., Li, Y., Rivailler, P., Conrardy, C., Castillo, D. A., Chen, L. M., et al. (2012). A distinct lineage of influenza A virus from bats. *Proc. Natl. Acad. Sci. U.S.A.* 109, 4269–4274. doi: 10.1073/pnas.1116200109

Tong, S., Zhu, X., Li, Y., Shi, M., Zhang, J., Bourgeois, M., et al. (2013). New world bats harbor diverse influenza A viruses. *PLoS Pathog.* 9:e1003657. doi: 10.1371/journal.ppat.1003657

van der Vries, E., Schutten, M., Fraaij, P., Boucher, C., and Osterhaus, A. (2013). Influenza virus resistance to antiviral therapy. *Adv. Pharmacol.* 67, 217–246. doi: 10.1016/b978-0-12-405880-4.00006-8

Vasileiou, E., Sheikh, A., Butler, C., El Ferkh, K., von Wissmann, B., McMenamin, J., et al. (2017). Effectiveness of influenza vaccines in asthma: a systematic review and meta-analysis. *Clin. Infect. Dis.* 65, 1388–1395. doi: 10.1093/cid/cix524

von Itzstein, M., Wu, W. Y., Kok, G. B., Pegg, M. S., Dyason, J. C., Jin, B., et al. (1993). Rational design of potent sialidase-based inhibitors of influenza virus replication. *Nature* 363, 418–423. doi: 10.1038/363418a0

Wang, L., Cui, Q., Zhao, X., Li, P., Wang, Y., Rong, L., et al. (2019). Generation of a reassortant influenza a subtype H3N2 virus expressing gaussia luciferase. *Viruses* 11:665. doi: 10.3390/v11070665

World Health Organization [WHO] (2018). *2018 Influenza (seasonal) Fact Sheet*. Geneva: WHO.

Wu, Y., Qin, G., Gao, F., Liu, Y., Vavricka, C. J., Qi, J., et al. (2013). Induced opening of influenza virus neuraminidase N2 150-loop suggests an important role in inhibitor binding. *Sci. Rep.* 3:1551. doi: 10.1038/srep01551

Zhao, X., Wang, L., Cui, Q., Li, P., Wang, Y., Zhang, Y., et al. (2018). A mechanism underlying attenuation of recombinant influenza a viruses carrying reporter genes. *Viruses* 10:679. doi: 10.3390/v10120679

Zhao, X., Wang, Y., Cui, Q., Li, P., Wang, L., Chen, Z., et al. (2019). A parallel phenotypic versus target-based screening strategy for RNA-dependent RNA polymerase inhibitors of the influenza a virus. *Viruses* 11:826. doi: 10.3390/v11090826

Zhu, L., Li, Y., Li, S., Li, H., Qiu, Z., Lee, C., et al., (2011). Inhibition of influenza A virus (H1N1) fusion by benzenesulfonamide derivatives targeting viral hemagglutinin. *PLoS One*. 6:e29120. doi: 10.1371/journal.pone.0029120

Zu, M., Li, C., Fang, J. S., Lian, W. W., Liu, A. L., Zheng, L. S., et al. (2015). Drug discovery of host CLK1 inhibitors for influenza treatment. *Molecules* 20, 19735–19747. doi: 10.3390/molecules201119653

**Conflict of Interest:** The authors declare that the research was conducted in the absence of any commercial or financial relationships that could be construed as a potential conflict of interest.

*Copyright © 2020 Li, Du, Wang, Hou, Wang, Zhao, Zhan, Liu, Rong and Cui. This is an open-access article distributed under the terms of the Creative Commons Attribution License (CC BY). The use, distribution or reproduction in other forums is permitted, provided the original author(s) and the copyright owner(s) are credited and that the original publication in this journal is cited, in accordance with accepted academic practice. No use, distribution or reproduction is permitted which does not comply with these terms.*

frontiers in Microbiology

ORIGINAL RESEARCH
published: 19 March 2020
doi: 10.3389/fmicb.2020.00357

# Does Mucosal B1 Activation Result in the Accumulation of Peak IgM During Chronic Intrarectal SIVmac239 Exposure to Protect Chinese-Origin Rhesus Macaques From Disease Progression?

*Zhe Cong[1†], Ling Tong[1†], Yuhong Wang[2], Aihua Su[1], Ting Chen[1], Qiang Wei[1], Jing Xue[1*] and Chuan Qin[1*]*

[1] *Beijing Key Laboratory for Animal Models of Emerging and Remerging Infectious Diseases, NHC Key Laboratory of Human Disease Comparative Medicine, Institute of Laboratory Animal Science, Chinese Academy of Medical Sciences and Comparative Medicine Center, Peking Union Medical College, Beijing, China,* [2] *Department of Gerontology and Geriatrics, The First Affiliated Hospital of Harbin Medical University, Harbin, China*

OPEN ACCESS

**Edited by:**
*Lijun Rong,*
*University of Illinois at Chicago, United States*

**Reviewed by:**
*John Zaunders,*
*St Vincent's Hospital Sydney, Australia*
*Teiichiro Shiino,*
*National Institute of Infectious Diseases (NIID), Japan*
*Fan Wu,*
*Fudan University, China*

***Correspondence:**
*Jing Xue*
*xuejing@cnilas.org;*
*jessie830817@163.com*
*Chuan Qin*
*qinchuan@pumc.edu.cn*

*† These authors have contributed equally to this work*

**Specialty section:**
*This article was submitted to Virology, a section of the journal Frontiers in Microbiology*

**Received:** *17 November 2019*
**Accepted:** *18 February 2020*
**Published:** *19 March 2020*

**Citation:**
*Cong Z, Tong L, Wang Y, Su A, Chen T, Wei Q, Xue J and Qin C (2020) Does Mucosal B1 Activation Result in the Accumulation of Peak IgM During Chronic Intrarectal SIVmac239 Exposure to Protect Chinese-Origin Rhesus Macaques From Disease Progression? Front. Microbiol. 11:357. doi: 10.3389/fmicb.2020.00357*

Human immunodeficiency virus (HIV) infection is characterized by a dynamic process and highly variable progression. Although extensive comparisons have been reported between the minority of non-progressors (NPGs) and the majority of progressors (PGs), the underlying mechanism is still unclear. One reason for this is that the initial onset of infection is very difficult to track, particularly when men who have sex with men (MSM) are predominantly responsible for the transmission of human HIV. To find potential early protection strategies against later progression during chronic mucosal exposure, 10 Chinese-origin rhesus macaques (ChRhs) that underwent repetitive simian immunodeficiency virus (SIV) intrarectal exposure were longitudinally tracked. The results of the periodic detection of peripheral blood mononuclear cells (PBMCs) and colorectal mucosal lamina propria mononuclear cells (LPMCs) with immunoglobulins in rectal fluid were compared between non-progressive and progressive subgroups, which were classified based on their circulating viral loads. As a result, four NPGs and six PGs were observed after disease onset for 2 months. Upon comparing the mucosal and systemic immune responses, the PBMC response did not differ between the two subgroups. Regarding LPMCs, the increased activation of B1a/B1 cells among B cells and a peak in IgM in rectal fluid was observed approximately 10 days after the first exposure, followed by consistently low viremia in the four non-progressive ChRhs. In the six progressive ChRhs, neither B cell activation nor a peak in IgM was observed, while a robust elevation in IgG was observed, followed by consistently high viremia post exposure. Based on the PBMC-LPMC disparity between the subgroups of monkeys, we hypothesize that

early B1 activation in LPMCs that result in an IgM peak might attenuate the entry and acquisition of SIV in the mucosa, resulting in very low dissemination into blood. Our models have suggested that the use of early surveillance both systemically and in the mucosa to comprehensively determine virus–host interactions would be informative for mucosal vaccine development.

**Keywords: PBMC, LPMC, SIV, IgM, B1 cells, Chinese-origin rhesus macaques, disease progression**

## INTRODUCTION

A tiny proportion of humans exposed to human immunodeficiency virus (HIV) retain a long-term non-progressive status and are known as "long-term non-progressors" (LTNPs) or "elite controllers" (ECs). Compared to the majority of those infected with HIV, who produce a strong virus-specific immune response and show obvious disease characteristics, LTNPs demonstrate extraordinarily low viral loads and do not progress to illness despite a lack of antiretroviral treatment (Sahu et al., 2001, 2005). More than 90% of new HIV infections occur by sexual transmission through mucosal contact (Tebit et al., 2012). Men who have sex with men (MSM) have the highest risk of HIV transmission and continue to transmit new HIV infections worldwide. Repetitive mucosal exposures in MSM could substantially enhance the frequency of mucosal immunity (Hladik and McElrath, 2008). Therefore, spontaneous LTNPs or ECs who are also MSM could provide a natural model of HIV-host immunity interactions. However, despite intensive studies comparing "dichotomized" infectors (Bendenoun et al., 2018), the mechanisms of "natural" protective mechanisms have not been clarified (Gurdasani et al., 2014). When considering the scenario, mucosal immunity as the first barrier (Miller et al., 1989; Xu et al., 2013) is the primary step in HIV infection, even in cases where infection occurs by the intravenous route (Bolton et al., 2012; Sutton et al., 2016). Therefore, early mucosal immunity, which could potentially confer some protection to non-progressed MSM infectors, has not been revealed because it is extremely difficult to detect the primary response to mucosal exposure during HIV transmission. In the present study, we employed Chinese-origin rhesus macaques (ChRhs) to generate spontaneous viral controllers with repeated low-dose simian immunodeficiency virus (SIV) exposure by the mucosal route. The animals were observed and the number of SIV RNA copies was detected periodically. NHP monkeys were divided into non-progressors (NPGs) and progressors (PGs) based on the degree of viral replication. By tracking primary mucosal immunity, immune responses occurring from the entry point in the rectal mucosa to the peripheral blood were compared in parallel to find some informative clues about how the first barrier of mucosal immunity performs in future non-progressive controllers.

## MATERIALS AND METHODS

### Animals and Ethics Statement

Two- to 4-year-old male and female ChRhs (*Macaca mulatta*) were housed and cared for in accordance with the Care and Use of Laboratory Animals of the Institute of Laboratory Animal Science and the recommendations of the welfare report for the use of non-human primates in research[1] in an Association for the Assessment and Accreditation of Laboratory Animal Care (AAALAC)-accredited facility. All macaques used in this study tested negative for the major histocompatibility complex class I (MHC-I) Mamu-A*01, Mamu-A*02, Mamu-B*08, and Mamu-B*17 alleles (Silver and Watkins, 2017) to reduce the bias introduced by MHC-enhanced control on SIV replication (Silver and Watkins, 2017). All animal procedures and experiments were performed according to protocols approved by the Institutional Animal Care and Use Committee (IACUC) of the Institute of Laboratory Animal Science, Chinese Academy of Medical Sciences (No. ILAS-VL-2012-002 and No. ILAS-VL-2015-003). All animals were anesthetized with an intramuscular injection of 10 mg/kg ketamine hydrochloride prior to sample collection, and the experiments were performed in the biosafety level 3 laboratory.

### Animal Model and Longitudinal Tracing

Ten ChRhs were exposed intrarectally to SIVmac239 at a median tissue culture infectious dose ($TCID_{50}$) of 100 twice a week for 5 weeks. The SIVmac239 strain used was kindly gifted by Dr. Preston Marx at the Aaron Diamond AIDS Research Center of the United States. For the longitudinal tracking of virus-host immunity, peripheral blood, intestinal biopsy specimens, and rectal fluid were collected prior to and after the designated virus exposure. The animal model and longitudinal sampling schedule are shown in **Figure 1**. During the 60-day observation period, peripheral blood mononuclear cells (PBMCs) were collected at four time points. Colorectal mucosal lamina propria mononuclear cells (LPMCs) were biopsied by using an endoscope four times before or after PBMCs collection for the sake of animal welfare (McGary et al., 2017). Rectal fluid was collected at eight time points. The viral load in peripheral blood was intensively detected at twelve time points in each exposed monkey.

### qRT-PCR Assay

Plasma RNA was extracted and purified using a QIAamp Viral RNA Mini Kit (Qiagen, Valencia, CA, United States). The quantification of plasma viral RNA in each sample was performed by quantitative real-time reverse transcription-PCR (qRT-PCR) using primers specific to a conserved region in the SIVmac239

[1]http://www.acmedsci.ac.uk/more/news/the-use-of-non-human-primates-in-research/

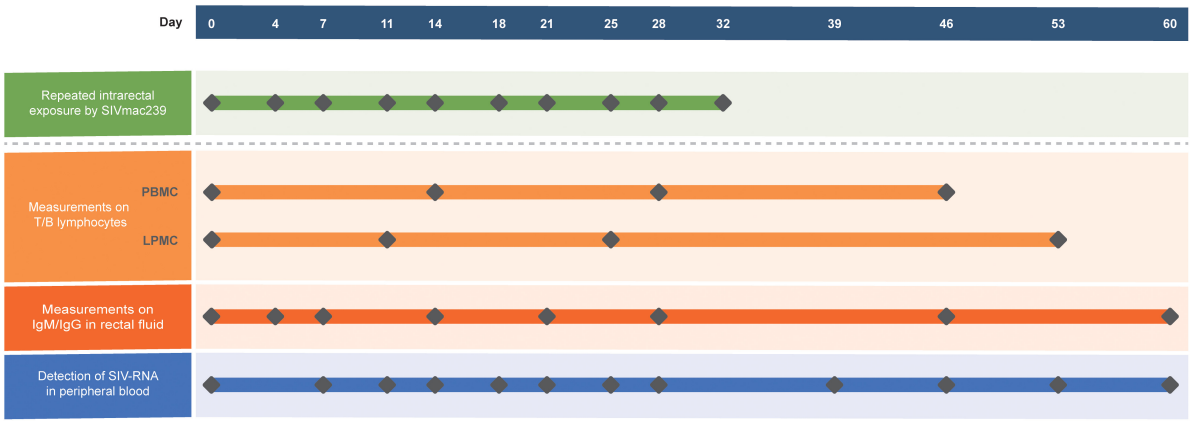


**FIGURE 1 |** Generation of the model using 10 ChRhs with periodical detection in the circulation and gut. Ten ChRhs were intrarectally exposed to low doses of SIVmac239 twice a week 10 times (along the green bar). T and B lymphocytes were measured at four time points in PBMCs or LPMCs at a short interval to minimize the impairment of the animals (along the light orange bar). Eight measurements of IgM and IgG were carried out in rectal fluid (along the dark orange bar). The plasma viral loads were detected 10 times (along the blue bar).

genome. The primers and probes used for vRNA amplification were gag91 forward (GCAGAGGAGGAAATTACCCAGTAC), gag91 reverse (CAATTTTACCCAGGCATTTAATGTT), and pSIVgag91-1 (5′-FAM-ACCTGCCATTAAGCCCGA-MGB-3′) (Chong et al., 2018). The limit of detection was 100 copy equivalents of RNA per ml of plasma. Three test reactions were performed for each sample.

## Flow Cytometry to Measure T/B Cell Shifting in PBMCs/LPMCs

Gut biopsies were performed as previously described (Xue et al., 2013), and the biopsy tissue was then treated with 5 mM EDTA and 60 U/ml collagenase. LPMCs were enriched for lymphocytes by Percoll density gradient centrifugation, and PBMCs were isolated using conventional Ficoll Hypaque density gradient centrifugation (GE Healthcare, Uppsala, Sweden). Polychromatic flow cytometry was performed to stain the T lymphocyte panel or B lymphocyte panel. For the T lymphocyte panel, 50 μl of EDTA-anticoagulated whole blood or $1 \times 10^6$ primary cells derived from the lamina propria were stained with the monoclonal antibodies CD3-PE/Cy7 (SP34-2), CD4-Percp/Cy5.5 (L200), and CD8-APC/Cy7 (RPA-T8) from BD Biosciences (San Jose, CA, United States). The $CD4^+$ T cell counts were determined with BD Truecount tubes according to the manufacturer's instructions (BD, San Jose, CA, United States). For the B lymphocyte panel, PBMCs or LPMCs were incubated with CD3-PE/Cy7 (SP34-2) from BD Biosciences (San Jose, CA, United States); CD20-FITC (2H7), CD43-APC (10G7), and CD27-APC/Cy7 (O323) from Biolegend (San Diego, CA, United States); and CD5- PerCP/Cy5.5 (5D7) from Invitrogen (Carlsbad, CA, United States) to determine the following B cell subsets (Brocca-Cofano et al., 2017): B cells, $CD3^-CD20^+$; B1 cells, $CD3^-CD20^+CD43^+CD27^+$; and B1a cells, $CD3^-CD20^+CD43^+CD27^+CD5^+$. All the samples were analyzed by flow cytometry (FACSAria; BD, CA, United States).

## Purification of IgM and IgG in Rectal Fluid

IgM in rectal fluid was purified with HiTrap™ IgM Purification HP according to the manufacturer's instructions (GE, Boston, MA, United States) (Hara et al., 2013). IgG in rectal fluid was purified with Protein A agarose resin. Briefly, the Protein A agarose resin was washed and equilibrated with PBS at pH 7.5. Then, filtered rectal fluid from each monkey was loaded onto the column at a flow rate of 0.2 ml/min. The adsorbed materials were eluted with 0.1 M glycine buffer at pH 2.5 after washing the column with PBS at a flow rate of 1 ml/min. The eluted fractions were neutralized with phosphate buffer at pH 8.5 and the effluents were monitored by UV spectrometry at 280 nm.

## Statistical Analysis

Mann–Whitney *U*-tests were used to compare the plasma viral loads of non-progressive and progressive monkeys. Comparisons between two subgroups were determined using the unpaired *t*-test (Welch). Correlations between two variables were assessed by the Spearman correlation. All statistical analyses were performed with GraphPad Prism 6.0 software (GraphPad Software Inc., San Diego, CA, United States).

# RESULTS

## Generation of a Chronic Progression-Dichotomized Model Using 10 Homogenous ChRhs

To track the immune responses of monkey models between NPGs and PGs in parallel, 10 ChRhs were inoculated intrarectally with SIV (McDermott et al., 2004). The age, weight, white blood cell count in peripheral blood, and daily function score (Deng et al., 2019) were comparable to those at baseline (data

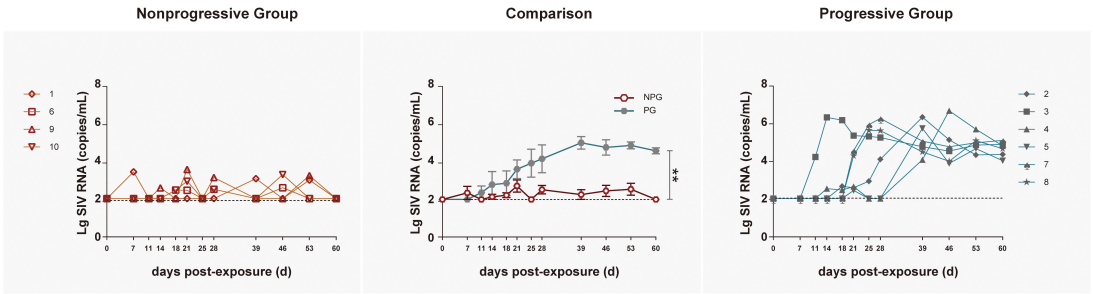


**FIGURE 2 |** Tracking plasma viral loads by detecting SIV RNA in non-progressive and progressive monkeys. The log of the geometric mean of the number of plasma SIVmac239 copies was compared between four non-progressive monkeys (orange line) and six progressive monkeys (blue line). The plasma viral loads are shown as log10 copies/ml. The assay had a sensitivity of 100 viral RNA copies per ml of plasma (black dotted lines). According to the Mann–Whitney *U*-test, the viral load in progressive monkeys was significantly increased compared with that in non-progressive monkeys (**$P < 0.01$).

not shown). The methods of repetitive mucosal exposure and sampling of peripheral blood, gut tissue, and rectal fluid were carried out on schedule (**Figure 1**). According to viral copy detection in peripheral blood, six ChRhs (Nos. 2, 3, 4, 5, 7, and 8) developed into chronic SIV PGs with stable high viremia and mild variation. By using peak plasma viremia to determine the degree of viral replication, the average number of copies was determined to be approximately $10^6$ copies/ml with a range from 5.55 to 6.59 $\log_{10}$ RNA copies/ml. The remaining ChRhs (Nos. 1, 6, 9, and 10) were found to be NPGs, as the peak plasma viremia of SIVmac239 in these monkeys was consistently lower than $10^4$ copies/ml throughout the entire observation period (**Figure 2**). During the follow-up observation period of 1 year, viremia in the four non-progressive monkeys remained as low as approximately 2–4 $\log_{10}$ RNA copies/ml (data not shown). Therefore, the non-progressive monkeys successfully mimicked the "long-term HIV controllers," and the progressive monkeys mimicked the chronic HIV infectors.

## T/B Lymphocyte Activation in PBMCs and LPMCs in Non-Progressive and Progressive Monkeys

Longitudinal changes in the $CD4^+$ T cell counts, $CD8^+$ T cell counts, and $CD4^+/CD8^+$ T cell ratios in peripheral blood were demonstrated in the four non-progressive monkeys and six progressive monkeys (**Figure 3**). Comparisons between the two subgroups revealed no changes in the $CD4^+$ T cell counts, $CD8^+$ T cell counts, or $CD4^+/CD8^+$ T cell ratios at any of the four detection times between NPGs and PGs ($P > 0.05$). A notably higher average $CD4^+/CD8^+$ T cell ratio was observed in NPGs at baseline, although statistical significance was not maintained ($P = 0.068$), indicating that measurement of the baseline T lymphocytes in peripheral blood could not be used to predict the outcome of the shift in T lymphocyte activation. For LPMCs, four monkeys among the NPGs and six monkeys among the PGs also showed a similar tendency in terms of the T lymphocyte shift after repeated low-dose SIV challenge (**Figure 4**). The percentages of $CD4^+$ T cells, percentages of $CD8^+$ T cells, and $CD4^+/CD8^+$ T cell ratios were comparable between NPGs and PGs at each observation point ($P > 0.05$).

Next, the activation of B lymphocytes was examined between the two subgroups. In PBMCs, the B cell subset shift remained stable, including that of B1 cells among B cells and B1a cells among B1 cells, between NPGs and PGs. In addition, compared to the shifting of T cell subsets, the longitudinal shifting of B cell subsets was more stable, indicating that B lymphocyte activation in PBMCs was minimally impacted during SIV mucosal exposure in ChRhs (**Figure 5**). However, in LPMCs, the percentage of B1a cells among B1 cells and that of B1 cells among B cells from mucosa was significantly increased in non-progressive monkeys compared with progressive monkeys at the first detection. Additionally, dramatically increased B1/B and B1a/B1 cell ratios were observed in the early stage (approximately 11 days after the initial challenge) in the NPGs compared to the PGs (**Figure 6**). The increased numbers of B1a/B1 cells in LPMCs from NPGs were observed for 25 days after the initial exposure. At 53 days post exposure, a non-significant difference in the B cell shift was shown between the two progression-distinct subgroups. Longitudinally, the peaks in the increased B1 and B1a cells indicated the transient activation of B lymphocytes in LPMCs during the early stage in the four non-progressive monkeys.

## Expression of IgM and IgG in Rectal Fluid From 10 Monkeys

In NPGs, IgM in rectal fluid precipitously increased to an average of 0.56 mg/ml with a range of 0.397–0.958 mg/ml at 14 days postexposure and gradually decreased to baseline levels at 21 days postexposure. Undetectably low IgM levels were observed during the entire observation period in the six PGs. An elevated IgG level in rectal fluid was shown at 46 days postexposure, and this level plateaued until 60 days (**Figure 7**).

B1 cells have been identified as a major source of infection-induced local IgM (Choi and Baumgarth, 2008; Baumgarth, 2011). To reveal the correlation between B cell activation in LPMCs, at 14 days postexposure the level of IgM in rectal fluid, viral replication in peripheral blood, B1a/B1 ratio, and IgM levels were individually correlated with the peak viral load in ten monkeys, including both NPGs and PGs. A temporally significant correlation was observed between the B1a/B1 ratio in LPMCs ($P < 0.05$, $R = -0.6848$) or the level of IgM in rectal

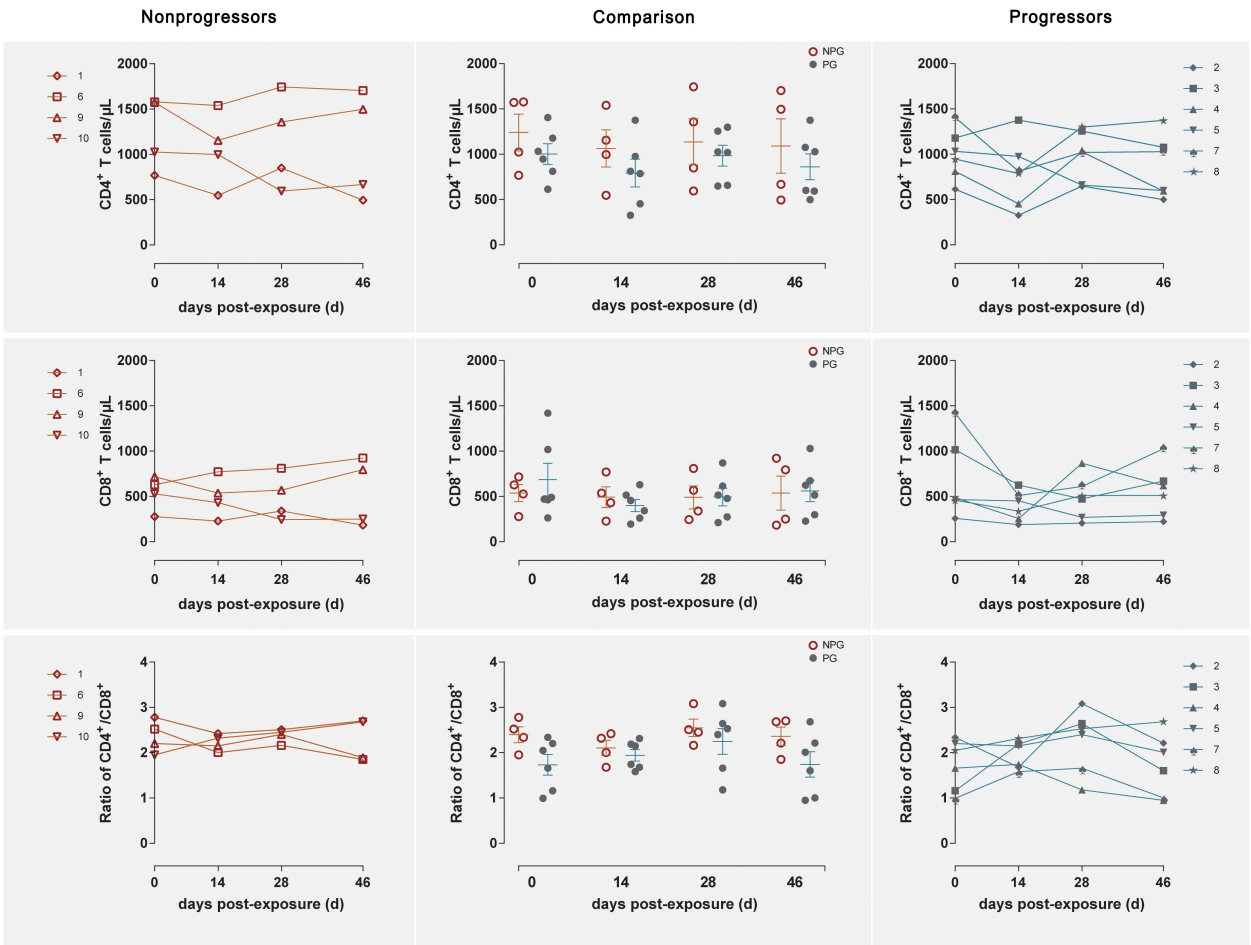


**FIGURE 3 |** Changes in T lymphocytes among PBMCs between non-progressive and progressive monkeys. The $CD4^+$ T cell counts, $CD8^+$ T cell counts, and $CD4^+/CD8^+$ ratios were measured in peripheral blood at four time points in four non-progressive monkeys and six progressive monkeys. No significant differences were found between the two subgroups at any time point, indicating that no notable T cell changes occurred in PBMCs from ChRhs subjected to repetitive SIV mucosal exposure (unpaired *t*-test, Welch's correction, $P > 0.05$).

fluid ($P < 0.05$, $R = -0.7781$) at 14 days postexposure and the peak viral load during the observation (**Figure 8**). As B1 cells contribute substantially to mucosal defense against pathogens, the presence of both negative correlations indicated that stepwise activation of B1 cells with subsequent peak IgM production in LPMCs might be responsible for the suppressed viral load in non-progressive monkeys. Therefore, we hypothesized that transient mucosal B1 cell activation along with peak IgM production in LPMCs impeded viral progression in SIV-infected monkeys.

## DISCUSSION

We tracked the stepwise progression/non-progression of chronic mucosal exposure to SIV in ChRhs, which could mimic the most prevalent route of HIV transmission. It has been documented that ChRhs are relatively resistant to SIV-related progression, with approximately 30% of infected monkeys maintaining very low viral loads for several years (Ling et al., 2002). Therefore, the progression-dichotomized statuses of these homogenous monkeys could be easily predicted. In the present study, monkeys with genes highly associated with SIV spontaneous controllers, such as the MHC-I alleles Mamu-A*01 (Pal et al., 2002; Lim et al., 2010), Mamu-A*02 (Loffredo et al., 2004), Mamu-B*08 (Loffredo et al., 2007), and Mamu-B*17 (Yant et al., 2006), were removed from the study. Therefore, the MHC-dependent disparity has been minimized. As no well-acknowledged criteria for the viral load defining ECs/LTNPs/PGs status have been established in the ChRh model, as they have in HIV-infected humans, we simply classified the monkeys as either NPGs or PGs in the ChRh model. The dose used in this study could be considered low according to our experience. Indeed, even a $TCID_{50}$ of 50,000 could produce non-progressive controllers. As low- and high-dose challenges produced a similar PG/controller ratio (McDermott et al., 2004; Tasca et al., 2007; Xiao et al., 2012; Greene et al., 2014), the initial acquisition very likely played a predominant role in later outcomes. Based on the longitudinal viral load trajectories, four monkeys were observed

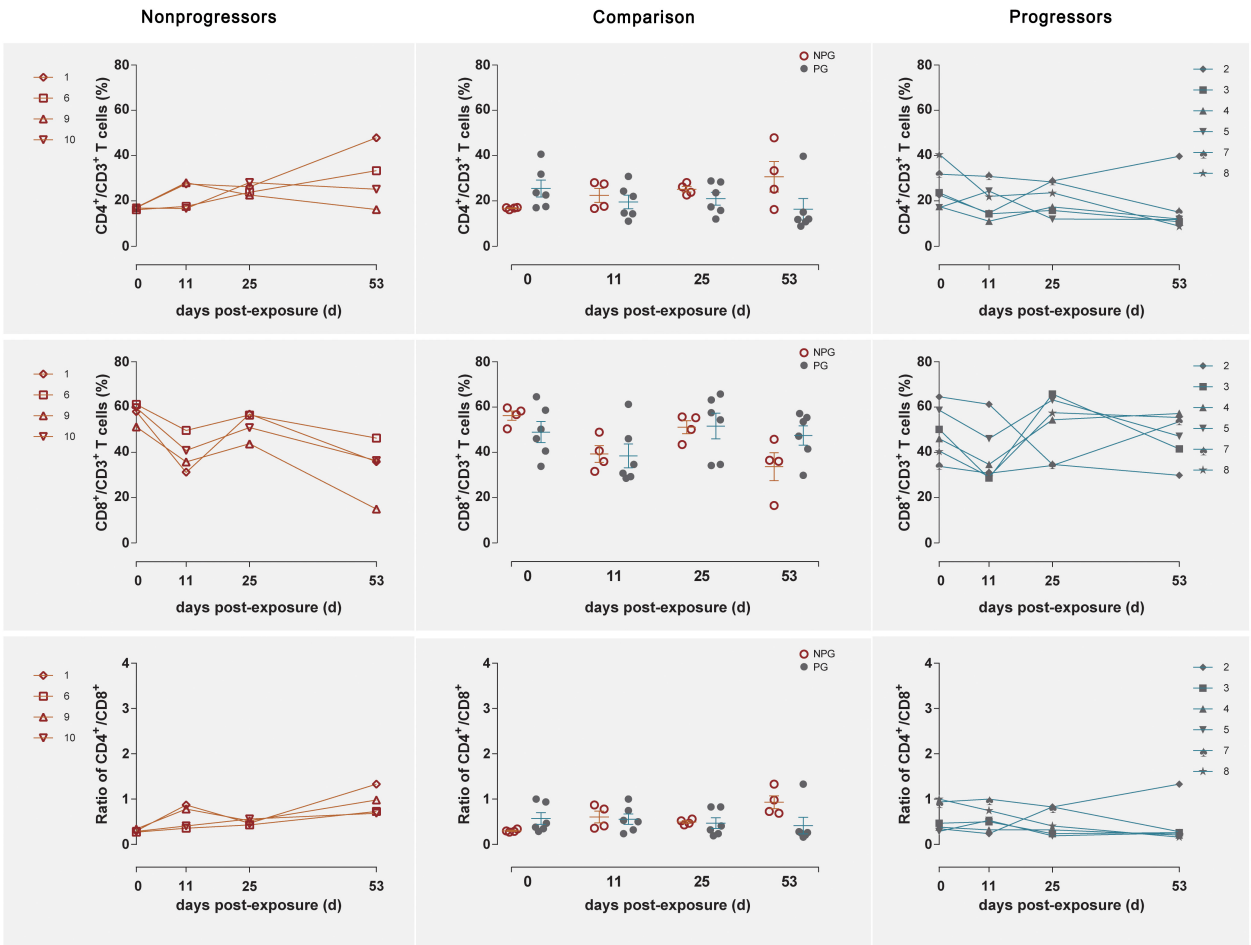


**FIGURE 4 |** Changes in T lymphocytes among LPMCs in non-progressive and progressive monkeys. The $CD4^+$ T cell percentages, $CD8^+$ T cell percentages, and $CD4^+/CD8^+$ ratios were measured in LPMCs obtained at four time points in four non-progressive monkeys and six progressive monkeys. No significant differences were found between the two subgroups at any time point, indicating that no notable T cell changes occurred in LPMCs from ten ChRhs subjected to repetitive SIV mucosal exposure (unpaired *t*-test, Welch's correction, $P > 0.05$).

to be NPGs, while six monkeys were classified as PGs among the 10 ChRhs. Therefore, we could use the present SIV ChRh model to mimic the general immunity disparity between the minority of NPGs/ECs and the majority of PGs in humans with HIV. Another characteristic of our model was that it could be used to track the very early stage of chronic mucosal infection with parallel detection in LPMCs and PBMCs. In humans, it is very difficult to track the onset of a chronic infection by observing both systemic and mucosal immunity (Lama et al., 2016). Here, we intensively tracked both PBMCs and LPMCs for T and B cell activation as well as IgM and IgG expression from rectal fluid, as it has been shown that the levels of immunoglobins in rectal fluid could robustly reflect the concentrations in mucosal tissues (Cottrell et al., 2016). A notable limitation was that IgA could not be detected despite numerous attempts to purify IgA from monkeys.

Our tracking observation resulted in an interesting difference between NPGs and PGs in the early stage post exposure. B1 cell activation (Choi and Baumgarth, 2008; Baumgarth, 2011), along with a precipitous increase in IgM, was observed in LPMCs at only approximately 9–11 days after the initial exposure in the four non-progressive monkeys. Our results are consistent with the phenomenon that early treatment with anti-HIV neutralizing antibodies potently induces sustainable immunity and subsequent progression (Nishimura et al., 2017). Although neutralizing antibodies showed a superior ability to block viral infection compared to that of non-neutralizing antibodies (Cheeseman et al., 2017), a paradoxical phenomenon showed that non-neutralizing antibodies were much more commonly detected in HIV ECs than neutralizing antibodies (Theze et al., 2011). In addition, a mucosal vaccine was found to have protective efficacy independent of anti-HIV neutralizing antibodies (Sui et al., 2019). Therefore, determination of the extent to which the early IgM peak contributes to the substantial suppression of viral dissemination within the mucosa in NPGs requires further experiments. As a non-specific antibody, natural IgM has been shown to robustly neutralize viruses within the mucosal epithelial barrier *in vitro* (Devito et al., 2018).

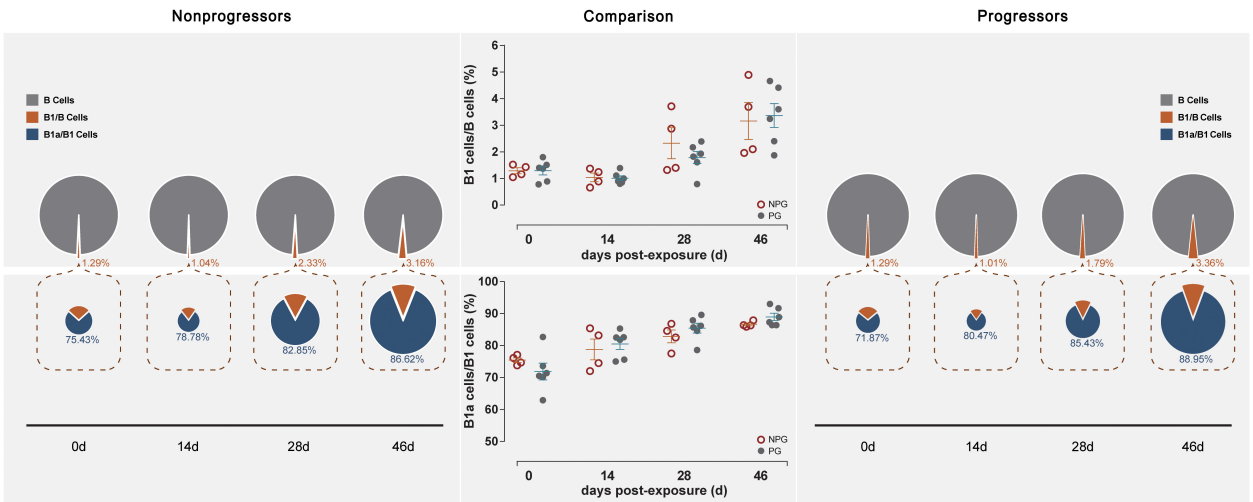


**FIGURE 5 |** Changes in B lymphocytes in PBMCs between non-progressive and progressive monkeys. B cell subsets, including B1/B and B1a/B1, were measured from PBMCs at four time points in four non-progressive monkeys and six progressive monkeys. The percentages of B1/B and B1a/B1 cells were compared between the two subgroups at each time point. No significant changes in B cells occurred in PBMCs in ten ChRhs under repetitive SIV mucosal exposure (unpaired *t*-test, Welch's correction, $P > 0.05$).

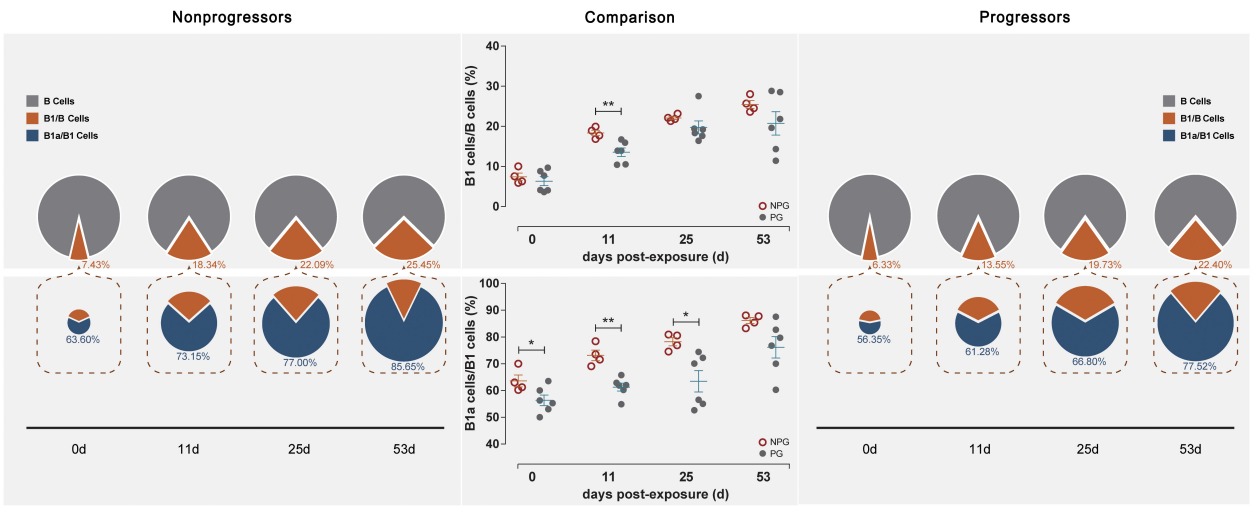


**FIGURE 6 |** Changes in B lymphocytes among LPMCs in non-progressive and progressive monkeys. B cell subsets, including B1/B and B1a/B1 cells, were measured among LPMCs obtained at four time points in four non-progressive monkeys and six progressive monkeys. The percentages of B1/B and B1a/B1 cells were compared between the two subgroups at each time point. Notably, increased ratios of B1/B and B1a/B1 cells were found in the four non-progressive monkeys during the early stage after initial exposure (unpaired *t*-test, Welch's correction, $^{*}P < 0.05$, $^{**}P < 0.01$).

After a peak in IgM was induced in LPMCs, viremia remained consistently low in the four NPGs, and the timing was consistent with that of the viremia peak during infection via the intrarectal route (Haseltine, 1989). Over 14 days, a stepwise route of infection from the mucosal epithelial barrier to the peripheral blood via profound mucosal immunity was observed (Miller et al., 2005; Haase, 2010). In this scenario, we supposed that the peak in IgM that occurred after approximately 10 days might have been an accumulative response to repetitive SIV exposure. Within the mucosa, gut-associated lymphoid tissue (GALT) made up of organized lymphoid nodules and multifunctional LPMCs could mount profound immunity responses both cellularly and humorally. Therefore, the LPMC response showed a sufficiently high efficacy to produce an EC without this response being mirrored in the blood (Shacklett and Ferre, 2011). Moreover, colorectal tissue was proven to be a consistent viral reservoir in long-term non-progressive ChRhs (Ling et al., 2010). Therefore, the disparity between the responses of NPGs and PGs has strongly demonstrated the fact that "outcomes depend on a race between expansion of infection and the immune response generated to contain it" (Li et al., 2009) in the early stages of viral infection.

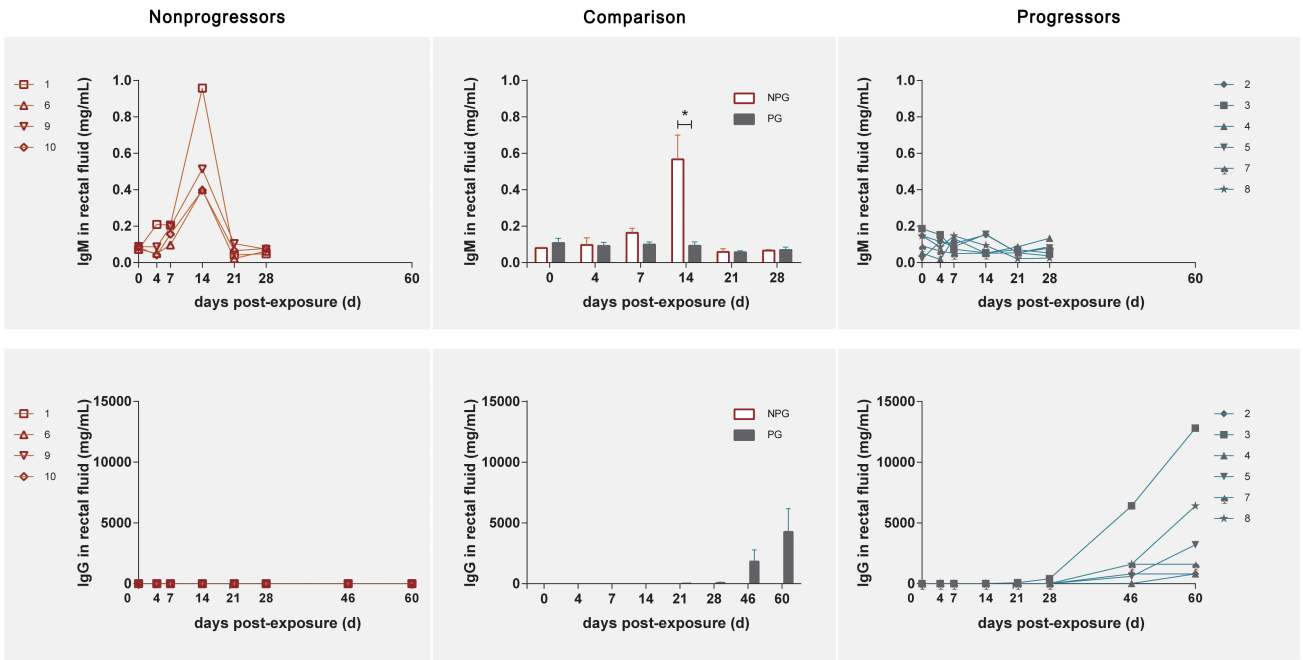


**FIGURE 7 |** Levels of IgM and IgG in rectal fluid in non-progressive and progressive monkeys. The levels of IgM and IgG were detected after initial exposure. A precipitously elevated IgM level in rectal fluid was found in four non-progressive monkeys during the early stage after initial exposure. In six progressive monkeys, a gradual increase in IgG was observed during the late stage 2 weeks after the first exposure. According to unpaired t test results, the level of IgM in the four non-progressive monkeys was significantly higher than that in the six progressive monkeys, whereas the level of IgG in the six progressive monkeys was significantly higher than that in the four non-progressive monkeys (*$P < 0.01$).

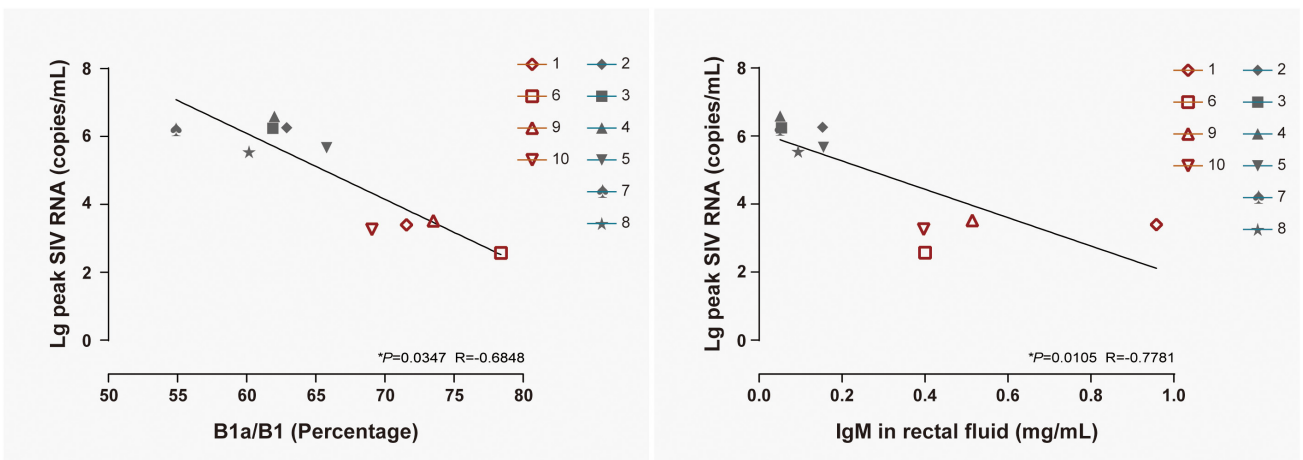


**FIGURE 8 |** Correlation of the B1a/B1 cell ratio among LPMCs and the IgM level in rectal fluid with peak viremia in 10 ChRhs. The correlations of peak viremia with the B1a/B1 cell ratio among LPMCs detected on day 11 post infection (left panel) and the level of IgM in rectal fluid detected at day 14 post infection (right panel) are shown. Using the Spearman correlation, strong significant linear correlations were observed between the B1a/B1 cell ratio and peak viremia ($R = -0.6848$) and between the level of IgM in rectal fluid and peak viremia ($R = -0.7781$) in 10 ChRhs with mucosal SIV exposure (*$P < 0.05$).

Taken together, our results support the hypothesis that an accumulative mucosal immune response induced by repetitive antigenic stimulation results in a peak IgM response in LPMCs. This mechanism may be the reason that ∼30% of ChRhs were protected from dissemination and led to their becoming NPGs. The exposure-dependent immune response was mild yet accumulative and produced a robust non-specific IgM to neutralize insufficient antigens, followed by the blockage of dissemination. We hypothesize that early B1 cell activation along with the IgM peak in LPMCs might exert a "decapacitating effect" to protect ChRhs from progression. The primary cause of this result was the characterized

genotypes, which were characterized as central to the PG. On the other hand, susceptible animals who acquired SIV infection, albeit at a low dose, gradually developed an antigen-specific IgG response, and subsequent viral dissemination could not be avoided. The heterogeneity between individuals whose minority could be initiated with minimal acquisition of the virus might be the determining cause of the remaining NPGs. Additional studies will be needed to explore the effect of the interaction between individual genotypes on the GALT-IgM response in ChRhs to determine the underlying mechanism.

## DATA AVAILABILITY STATEMENT

All datasets generated for this study are included in the article/supplementary material.

## ETHICS STATEMENT

The animal study was reviewed and approved by the Institutional Animal Care and Use Committee (IACUC) at the Institute of Laboratory Animal Science, Chinese Academy of Medical Sciences (No. ILAS-VL-2012-002 and No. ILAS-VL-2015-003).

## AUTHOR CONTRIBUTIONS

JX and CQ contributed to conceptualization, resources, and supervision. ZC and LT contributed to methodology. ZC, LT, AS, and TC contributed to investigation. LT, YW, and JX contributed to writing the original draft. YW and JX contributed to writing—review and editing. ZC, JX, and QW contributed to funding acquisition.

## FUNDING

This work was supported by the National Natural Science Foundation of China (81971944 to JX), the National Mega Projects of China for Major Infectious Diseases (2017ZX10304402 and 2018ZX10101001 to JX and 2018ZX10301103 to ZC), and the CAMS Innovation Fund for Medical Sciences (2017-I2M-1-014 to QW).

## REFERENCES

Baumgarth, N. (2011). The double life of a B-1 cell: self-reactivity selects for protective effector functions. *Nat. Rev. Immunol.* 11, 34–46. doi: 10.1038/nri2901

Bendenoun, M., Samri, A., Avettand-Fenoel, V., Cardinaud, S., Descours, B., Carcelain, G., et al. (2018). What is the most important for elite control: genetic background of patient, genetic background of partner, both or neither? Description of complete natural history within a couple of MSM. *EBioMedicine* 27, 51–60. doi: 10.1016/j.ebiom.2017.12.003

Bolton, D. L., Song, K., Wilson, R. L., Kozlowski, P. A., Tomaras, G. D., Keele, B. F., et al. (2012). Comparison of systemic and mucosal vaccination: impact on intravenous and rectal SIV challenge. *Mucosal Immunol.* 5, 41–52. doi: 10.1038/mi.2011.45

Brocca-Cofano, E., Kuhrt, D., Siewe, B., Xu, C., Haret-Richter, G. S., Craigo, J., et al. (2017). Pathogenic correlates of simian immunodeficiency virus-associated B cell dysfunction. *J. Virol.* 91:e1051-17. doi: 10.1128/JVI.01051-17

Cheeseman, H. M., Olejniczak, N. J., Rogers, P. M., Evans, A. B., King, D. F. L., Ziprin, P., et al. (2017). Broadly neutralizing antibodies display potential for prevention of HIV-1 infection of mucosal tissue superior to that of nonneutralizing antibodies. *J. Virol.* 91:e1762-16. doi: 10.1128/JVI.01762-16

Choi, Y. S., and Baumgarth, N. (2008). Dual role for B-1a cells in immunity to influenza virus infection. *J. Exp. Med.* 205, 3053–3064. doi: 10.1084/jem.20080979

Chong, H., Xue, J., Zhu, Y., Cong, Z., Chen, T., Guo, Y., et al. (2018). Design of novel HIV-1/2 fusion inhibitors with high therapeutic efficacy in rhesus monkey models. *J. Virol.* 92:e775-18. doi: 10.1128/JVI.00775-18

Cottrell, M. L., Prince, H. M., Allmon, A., Mollan, K. R., Hudgens, M. G., Sykes, C., et al. (2016). Cervicovaginal and rectal fluid as a surrogate marker of antiretroviral tissue concentration: implications for clinical trial design. *J. Acquir. Immune Defic. Syndr.* 72, 498–506. doi: 10.1097/QAI.0000000000000996

Deng, W., Guan, G., Xiao, C., Qu, G., Xue, J., Qin, C., et al. (2019). Construction of a comprehensive observer-based scale assessing aging-related health and functioning in captive rhesus macaques. *Aging (Albany NY)* 11, 6892–6903. doi: 10.18632/aging.102219

Devito, C., Ellegard, R., Falkeborn, T., Svensson, L., Ohlin, M., Larsson, M., et al. (2018). Human IgM monoclonal antibodies block HIV-transmission to immune cells in cervico-vaginal tissues and across polarized epithelial cells in vitro. *Sci. Rep.* 8:10180. doi: 10.1038/s41598-018-28242-y

Greene, J. M., Weiler, A. M., Reynolds, M. R., Cain, B. T., Pham, N. H., Ericsen, A. J., et al. (2014). Rapid, repeated, low-dose challenges with SIVmac239 infect animals in a condensed challenge window. *Retrovirology* 11:66. doi: 10.1186/s12977-014-0066-z

Gurdasani, D., Iles, L., Dillon, D. G., Young, E. H., Olson, A. D., Naranbhai, V., et al. (2014). A systematic review of definitions of extreme phenotypes of HIV control and progression. *AIDS* 28, 149–162. doi: 10.1097/QAD.0000000000000049

Haase, A. T. (2010). Targeting early infection to prevent HIV-1 mucosal transmission. *Nature* 464, 217–223. doi: 10.1038/nature08757

Hara, A., Furuichi, K., Higuchi, M., Iwata, Y., Sakai, N., Kaneko, S., et al. (2013). Autoantibodies to erythropoietin receptor in patients with immune-mediated diseases: relationship to anaemia with erythroid hypoplasia. *Br. J. Haematol.* 160, 244–250. doi: 10.1111/bjh.12105

Haseltine, W. A. (1989). Silent HIV infections. *N. Engl. J. Med.* 320, 1487–1489. doi: 10.1056/nejm198906013202210

Hladik, F., and McElrath, M. J. (2008). Setting the stage: host invasion by HIV. *Nat. Rev. Immunol.* 8, 447–457. doi: 10.1038/nri2302

Lama, J. R., Karuna, S. T., Grant, S. P., Swann, E. M., Ganoza, C., Segura, P., et al. (2016). Transient peripheral immune activation follows elective sigmoidoscopy or circumcision in a cohort study of MSM at risk of HIV infection. *PLoS One* 11:e0160487. doi: 10.1371/journal.pone.0160487

Li, Q., Skinner, P. J., Ha, S. J., Duan, L., Mattila, T. L., Hage, A., et al. (2009). Visualizing antigen-specific and infected cells in situ predicts outcomes in early viral infection. *Science* 323, 1726–1729. doi: 10.1126/science.1168676

Lim, S. Y., Chan, T., Gelman, R. S., Whitney, J. B., O'Brien, K. L., Barouch, D. H., et al. (2010). Contributions of Mamu-A*01 status and TRIM5 allele expression, but not CCL3L copy number variation, to the control of SIVmac251 replication in Indian-origin rhesus monkeys. *PLoS Genet.* 6:e1000997. doi: 10.1371/journal.pgen.1000997

Ling, B., Mohan, M., Lackner, A. A., Green, L. C., Marx, P. A., Doyle, L. A., et al. (2010). The large intestine as a major reservoir for simian immunodeficiency virus in macaques with long-term, nonprogressing non-progressing infection. *J. Infect. Dis.* 202, 1846–1854. doi: 10.1086/657413

Ling, B., Veazey, R. S., Luckay, A., Penedo, C., Xu, K., Lifson, J. D., et al. (2002). SIV(mac) pathogenesis in rhesus macaques of Chinese and Indian origin compared with primary HIV infections in humans. *AIDS* 16, 1489–1496. doi: 10.1097/00002030-200207260-00005

Loffredo, J. T., Maxwell, J., Qi, Y., Glidden, C. E., Borchardt, G. J., Soma, T., et al. (2007). Mamu-B*08-positive macaques control simian immunodeficiency virus replication. *J. Virol.* 81, 8827–8832. doi: 10.1128/jvi.00895-07

Loffredo, J. T., Sidney, J., Wojewoda, C., Dodds, E., Reynolds, M. R., Napoe, G., et al. (2004). Identification of seventeen new simian immunodeficiency virus-derived CD8 + T cell epitopes restricted by the high frequency molecule, Mamu-A*02, and potential escape from CTL recognition. *J. Immunol.* 173, 5064–5076. doi: 10.4049/jimmunol.173.8.5064

McDermott, A. B., Mitchen, J., Piaskowski, S., De Souza, I., Yant, L. J., Stephany, J., et al. (2004). Repeated low-dose mucosal simian immunodeficiency virus SIVmac239 challenge results in the same viral and immunological kinetics as high-dose challenge: a model for the evaluation of vaccine efficacy in nonhuman non-human primates. *J. Virol.* 78, 3140–3144. doi: 10.1128/jvi.78.6.3140-3144.2004

McGary, C. S., Alvarez, X., Harrington, S., Cervasi, B., Ryan, E. S., Iriele, R. I., et al. (2017). The loss of CCR6 (+) and CD161 (+) CD4 (+) T-cell homeostasis contributes to disease progression in SIV-infected rhesus macaques. *Mucosal Immunol.* 10, 1082–1096. doi: 10.1038/mi.2016.116

Miller, C. J., Alexander, N. J., Sutjipto, S., Lackner, A. A., Gettie, A., Hendrickx, A. G., et al. (1989). Genital mucosal transmission of simian immunodeficiency virus: animal model for heterosexual transmission of human immunodeficiency virus. *J. Virol.* 63, 4277–4284. doi: 10.1128/jvi.63.10.4277-4284.1989

Miller, C. J., Li, Q., Abel, K., Kim, E. Y., Ma, Z. M., Wietgrefe, S., et al. (2005). Propagation and dissemination of infection after vaginal transmission of simian immunodeficiency virus. *J. Virol.* 79, 9217–9227. doi: 10.1128/jvi.79.14.9217-9227.2005

Nishimura, Y., Gautam, R., Chun, T. W., Sadjadpour, R., Foulds, K. E., Shingai, M., et al. (2017). Early antibody therapy can induce long-lasting immunity to SHIV. *Nature* 543, 559–563. doi: 10.1038/nature21435

Pal, R., Venzon, D., Letvin, N. L., Santra, S., Montefiori, D. C., Miller, N. R., et al. (2002). ALVAC-SIV-gag-pol-env-based vaccination and macaque major histocompatibility complex class I (A*01) delay simian immunodeficiency virus SIVmac-induced immunodeficiency. *J. Virol.* 76, 292–302. doi: 10.1128/jvi.76.1.292-302.2002

Sahu, G. K., Chen, J. J., Huang, J. C., Ramsey, K. M., and Cloyd, M. W. (2001). Transient or occult HIV-1 infection in high-risk adults. *AIDS* 15, 1175–1177. doi: 10.1097/00002030-200106150-00013

Sahu, G. K., McNearney, T., Evans, A., Turner, A., Weaver, S., Huang, J. C., et al. (2005). Transient or occult HIV infections may occur more frequently than progressive infections: changing the paradigm about HIV persistence. *Arch. Virol. Suppl.* 19, 131–145. doi: 10.1007/3-211-29981-5_11

Shacklett, B. L., and Ferre, A. L. (2011). Mucosal immunity in HIV controllers: the right place at the right time. *Curr. Opin. HIV AIDS* 6, 202–207. doi: 10.1097/COH.0b013e3283453e2b

Silver, Z. A., and Watkins, D. I. (2017). The role of MHC class I gene products in SIV infection of macaques. *Immunogenetics* 69, 511–519. doi: 10.1007/s00251-017-0997-3

Sui, Y., Lewis, G. K., Wang, Y., Berckmueller, K., Frey, B., Dzutsev, A., et al. (2019). Mucosal vaccine efficacy against intrarectal SHIV is independent of anti-Env antibody response. *J. Clin. Invest.* 129, 1314–1328. doi: 10.1172/JCI122110

Sutton, M. S., Burns, C. M., Weiler, A. M., Balgeman, A. J., Braasch, A., Lehrer-Brey, G., et al. (2016). Vaccination with live attenuated simian immunodeficiency virus (SIV) protects from mucosal, but not necessarily intravenous, challenge with a minimally heterologous SIV. *J. Virol.* 90, 5541–5548. doi: 10.1128/JVI.00192-16

Tasca, S., Tsai, L., Trunova, N., Gettie, A., Saifuddin, M., Bohm, R., et al. (2007). Induction of potent local cellular immunity with low dose X4 SHIV(SF33A) vaginal exposure. *Virology* 367, 196–211. doi: 10.1016/j.virol.2007.05.021

Tebit, D. M., Ndembi, N., Weinberg, A., and Quinones-Mateu, M. E. (2012). Mucosal transmission of human immunodeficiency virus. *Curr. HIV Res.* 10, 3–8. doi: 10.2174/157016212799304689

Theze, J., Chakrabarti, L. A., Vingert, B., Porichis, F., and Kaufmann, D. E. (2011). HIV controllers: a multifactorial phenotype of spontaneous viral suppression. *Clin. Immunol.* 141, 15–30. doi: 10.1016/j.clim.2011.07.007

Xiao, P., Patterson, L. J., Kuate, S., Brocca-Cofano, E., Thomas, M. A., Venzon, D., et al. (2012). Replicating adenovirus-simian immunodeficiency virus (SIV) recombinant priming and envelope protein boosting elicits localized, mucosal IgA immunity in rhesus macaques correlated with delayed acquisition following a repeated low-dose rectal SIV (mac251) challenge. *J. Virol.* 86, 4644–4657. doi: 10.1128/JVI.06812-11

Xu, H., Wang, X., and Veazey, R. S. (2013). Mucosal immunology of HIV infection. *Immunol. Rev.* 254, 10–33. doi: 10.1111/imr.12072

Xue, J., Cong, Z., Xiong, J., Wang, W., Jiang, H., Chen, T., et al. (2013). Repressive effect of primary virus replication on superinfection correlated with gut-derived central memory CD4 (+) T cells in SHIV-infected Chinese rhesus macaques. *PLoS One* 8:e72295. doi: 10.1371/journal.pone.0072295

Yant, L. J., Friedrich, T. C., Johnson, R. C., May, G. E., Maness, N. J., Enz, A. M., et al. (2006). The high-frequency major histocompatibility complex class I allele Mamu-B*17 is associated with control of simian immunodeficiency virus SIVmac239 replication. *J. Virol.* 80, 5074–5077. doi: 10.1128/jvi.80.10.5074-5077.2006

**Conflict of Interest:** The authors declare that the research was conducted in the absence of any commercial or financial relationships that could be construed as a potential conflict of interest.

*Copyright © 2020 Cong, Tong, Wang, Su, Chen, Wei, Xue and Qin. This is an open-access article distributed under the terms of the Creative Commons Attribution License (CC BY). The use, distribution or reproduction in other forums is permitted, provided the original author(s) and the copyright owner(s) are credited and that the original publication in this journal is cited, in accordance with accepted academic practice. No use, distribution or reproduction is permitted which does not comply with these terms.*

frontiers in Microbiology

REVIEW
published: 20 March 2020
doi: 10.3389/fmicb.2020.00362

# Defeat Dengue and Zika Viruses With a One-Two Punch of Vaccine and Vector Blockade

*Jin Sun[1], Senyan Du[2], Zhihang Zheng[1,3], Gong Cheng[2] and Xia Jin[1,4]**

*[1] Viral Disease and Vaccine Translational Research Unit, CAS Key Laboratory of Molecular Virology and Immunology, Institut Pasteur of Shanghai, Chinese Academy of Sciences, Shanghai, China, [2] Tsinghua-Peking Center for Life Sciences, School of Medicine, Tsinghua University, Beijing, China, [3] Institut Pasteur of Shanghai, Chinese Academy of Sciences, University of Chinese Academy of Sciences, Shanghai, China, [4] Shanghai Public Health Clinical Center, Fudan University, Shanghai, China*

Dengue virus (DENV) and Zika virus (ZIKV) are two mosquito-borne flaviviruses afflicting nearly half of the world population. Human infection by these viruses can either be asymptomatic or manifest as clinical diseases from mild to severe. Despite more cases are presented as self-limiting febrile illness, severe dengue disease can be manifested as hemorrhagic fever and hemorrhagic shock syndrome, and ZIKV infection has been linked to increased incidence of peripheral neuropathy Guillain-Barre syndrome and central neural disease such as microcephaly. The current prevention and treatment of these infectious diseases are either non-satisfactory or entirely lacking. Because DENV and ZIKV have much similarities in genomic and structural features, almost identical mode of mosquito-mediated transmission, and probably the same pattern of host innate and adaptive immunity toward them, it is reasonable and often desirable to investigate these two viruses side-by-side, and thereby devise common countermeasures against both. Here, we review the existing knowledge on DENV and ZIKV regarding epidemiology, molecular virology, protective immunity and vaccine development, discuss recent new discoveries on the functions of flavivirus NS1 protein in viral pathogenesis and transmission, and propose a one-two punch strategy using vaccine and vector blockade to overcome antibody-dependent enhancement and defeat Dengue and Zika viruses.

**Keywords: dengue virus, Zika virus, epidemiology, virology, protective immunity, vaccine, mosquitoes**

OPEN ACCESS

***Edited by:***
*Lu Lu,*
*Fudan University, China*

***Reviewed by:***
*Cheng-Feng Qin,*
*Beijing Institute of Microbiology and Epidemiology, China*
*Svetlana Khaiboullina,*
*University of Nevada, Reno, United States*
*Jing An,*
*Capital Medical University, China*

***Correspondence:**
*Xia Jin*
*xjin@ips.ac.cn;*
*jinxia@shphc.org.cn*

***Specialty section:***
*This article was submitted to Virology, a section of the journal Frontiers in Microbiology*

***Received:*** *28 September 2019*
***Accepted:*** *18 February 2020*
***Published:*** *20 March 2020*

***Citation:***
*Sun J, Du S, Zheng Z, Cheng G and Jin X (2020) Defeat Dengue and Zika Viruses With a One-Two Punch of Vaccine and Vector Blockade. Front. Microbiol. 11:362. doi: 10.3389/fmicb.2020.00362*

## EPIDEMIOLOGY OF DENGUE VIRUS AND ZIKA VIRUS

Dengue virus (DENV) is the most prevalent mosquito-borne flavivirus that affects over half of the world population in 128 countries and regions (Brady et al., 2012). Zika virus (ZIKV) is another virus that has caught public attention while sweeping across 60 countries and infecting several million people during 2014–2016 (Baud et al., 2017). The transmitting vectors of DENV and ZIKV are *Aedes* mosquitoes, mainly *A. aegypti* and *A. albopictus* (Guzman et al., 2010; Weaver et al., 2016). These viruses cause human diseases that share some similar clinical manifestations but also have features that are distinct from each other.

Dengue viruses are antigenically classified into four serotypes that originate from one ancestor phylogenetically and cause common pathologies in human. Infection by any serotype of dengue

virus can be either symptomatic (∼25%) or not (Bhatt et al., 2013; St John and Rathore, 2019). The majority of symptomatic infection only develop self-limited febrile illness with manifestations of high fever, facial flushing, rash, myalgia, arthralgia, headache, retro-orbital pain, vomiting, epistaxis, or gum bleeding. Febrile phase lasts 2–7 days, during which viremia and plasma NS1 can be detected in the initial 1–4 days. Only a small percentage of the symptomatic patients (mostly children) progress to more severe forms of dengue disease, Dengue Hemorrhagic Fever (DHF) and Dengue Shock Syndrome (DSS), in which plasma leakage and hemorrhagic manifestations occur; meanwhile, leukopenia, hemoconcentration, and thrombocytopenia can be detected by laboratory tests. Severe plasma leakage that leads to metabolic acidosis and shock with occasional organ impairment is fetal without proper treatment (World Health Organization [WHO], 2009). Immune responses induced during infection by one serotype of dengue virus can confer life-long protection against homotypic viruses and provide cross-protection toward heterotypic viruses for short-term. Strikingly, such cross-reactivities have the potential to enhance disease severity of a secondary heterotypic infection, probably through a mechanism called Antibody Dependent Enhancement (ADE). Consistently, increased risk of DHF/DSS has been observed for secondary dengue virus infections in some epidemiological studies (Sangkawibha et al., 1984; Guzman et al., 2013; Katzelnick et al., 2017). Dengue like disease has been a public health problem for over two centuries. In 1780, Benjamin Rush recorded in Philadelphia an epidemic of bilious remitting fever, which is now considered as one of the earliest descriptions of dengue like diseases in America (Rush, 1951; Packard, 2016). In the following decades, such outbreaks appeared throughout Atlantic World. The name "dengue virus" appeared in the Caribbean in 1820s, it might have derived from Swahili "*Ka-dinga-pepo*" or Spanish "*denguero,*" meaning seizures caused by an evil spirit or referring to the special gait, to describe the agonizing status after infection (Barnett, 2017). Nevertheless, whether all of these early epidemics were caused by dengue virus rather than another clinically similar arbovirus, chikungunya virus, was uncertain, as disease of these outbreaks was often named as "break bone fever" and some were described as rheumatic diseases (Carey, 1971). Although it is unclear when dengue virus was first introduced to Asia, as sylvatic strains of DENV-1 (strain P72-1244), -2 (strain P8-1407), -4 (strain P73-1120 and P75-514, P75-215) were isolated from sentinel monkeys or *A. niveus* mosquitoes in the rainforest of Malaysia, and the existence of sylvatic DENV-3 is supported indirectly by monkey seroconversion against DENV-3 in Malaysia, it is suggested that the four serotype viruses evolved independently in the rainforests of southeast Asia based on the phylogenic analysis (Wang et al., 2000; Holmes and Twiddy, 2003). The huge troop deployments during the Second World War might have also exacerbated the spread of dengue viruses in Asia (Clarke, 2002). Since the beginning of twentieth century, due to the increased urbanization and lacking control of *Aedes* mosquitoes, all four serotypes of dengue viruses have been found in South Asia, causing endemics each year. Similarly, multiple serotypes of dengue virus were circulating in tropical and sub-tropical regions of America after 1950s, leading to regular outbreaks in these regions (Gubler, 1987). Coincide with this, increased DHF and DSS cases were reported in different outbreaks after World War II (Halstead, 1966; World Health Organization [WHO], 1966). Now, the four serotype viruses are co-circulating in all endemic regions (Mackenzie et al., 2004), and estimated to infect 390 million people, causing 10,000 death, and 96 million symptomatic infections in 128 countries each year (Guzman et al., 2010; Brady et al., 2012; Bhatt et al., 2013). Roughly, the world population live under the threat of dengue disease is recently predicted to increase to over 60% by 2080 (Messina et al., 2019). Although modern era of dengue research has begun since Sabin and his colleagues first isolated the virus in 1944 (Sabin, 1952), the dissemination of dengue viruses are still continuing, as no antiviral drugs are available and the only licensed vaccine is far from satisfactory.

In comparison, Zika virus emerged more recently as a public health concern. The historical documents of Zika virus started as its first isolation from a monkey in Zika forest of Uganda in 1947 (Dick et al., 1952). In the following decades, only a few sporadic outbreaks were reported in Africa and South Asia, the number of cases during each outbreak never exceeded a few dozen before 2007 (Duffy et al., 2009; Grard et al., 2014). Symptoms of ZIKV infection including fever, arthralgia, rash and conjunctivitis were presented in patients during the early outbreaks, although 50–80% infections were asymptomatic (Weaver et al., 2016). Fundamental epidemic and clinical changes of the disease first appeared in an outbreak in French Polynesia in 2013, when 28,000 people were infected, and Guillain-Barre syndrome was observed for the first time to be associated with Zika virus infection, implicating the neurotropic feature of Zika virus (Musso et al., 2018); additionally, detection of viral RNA in semen and urine were also documented during this outbreak. Nevertheless, the threat of Zika virus was not recognized until 2015–2016 when it caused much larger outbreaks in South America, most pronounced in Brazil (Campos et al., 2015). In this outbreak, 40% notified Brazilian cases were from northeast region of Brazil (Faria et al., 2017), where Zika virus infected 63% peoples in Salvador. The virus spread to most countries in Americas (Netto et al., 2017), and then further expanded into a pandemic with several outbreaks in South Asia and pacific islands (Baud et al., 2017). In Europe, travel-associated ZIKV cases were reported in most EU (European Union) countries during 2015–2016, with the largest number of cases in France, and largest percentage related to the Caribbean (Spiteri et al., 2017). During the Brazil outbreak, ZIKV has been suspected to persistently replicate in multiple organs for months, and confirmed to be capable of sexual and vertical transmission; and found to be associated with increased ratios of microcephaly and congenital diseases in newborn babies (Weaver et al., 2016). Soon after, the association between Zika virus infection and microcephaly was confirmed by extensive studies in mice (Li et al., 2016; Yockey et al., 2016; Vermillion et al., 2017; Szaba et al., 2018). Furthermore, *in vivo* replication of ZIKV in neuron, placenta and fetus was also verified by using autopsy samples (Martines et al., 2016; Mlakar et al., 2016). Since early 2016, WHO has declared Zika virus disease as a public health emergency of global concern.

It should be noted that ZIKV and DENV spread through the same *Aedes* mosquito vectors in overlapping epidemic areas, and cross-reactivity of their adaptive immune responses are also often observed, therefore, inspecting their similarity in viral and genomic structures should be of value.

## VIROLOGICAL FEATURES OF DENGUE VIRUS AND ZIKA VIRUS

Both Dengue virus and Zika virus belong to the genus of *flavivirus* in the *flaviviridae* family, and they have similar genome organization and virion morphology. They both have one single-stranded positive RNA as genome, which contain an open reading frame (ORF) of ∼11,000 nucleotides, flanked by 100 nucleotides at the 5′UTR and 400–500 nucleotides at the 3′UTR. The single ORF encodes a polyprotein of 3000-amino acid that is translationally or post-translationally processed into three structural proteins (C, prM, E) and seven non-structural proteins (NS1, NS2A, NS2B, NS3, NS4A, NS5). Generally, the sequence homology between DENV and ZIKV polyprotein is 55–56%, whereas the homology among four serotype dengue virus polyproteins is 69–72%. The three structural proteins and phospholipid bilayers derived from ER of infected cells form the major architecture of viral particles of ZIKV and DENV, whereas the non-structural proteins (except for NS1) mainly retain intracellular location and participate in viral RNA replication and viral polyprotein processing: NS5 is RNA dependent RNA polymerase and methyltransferase, NS3 is helicase, NS2B/NS3 complex is a serine protease that processes polyprotein at C/pr, NS2A/NS2B, NS2B/NS3, NS3/NS4A, NS4A/2K, and NS4B/NS5 junctions. The NS proteins also interact with host immunity: NS2B/NS3, NS4A, NS4B, and NS5 can be antagonists of innate immune responses; NS1 can directly or indirectly cause pathology (Lindenbach et al., 2007; Ngono and Shresta, 2018). On the surface of the mature virus particles, 90 copies of E homodimers lie flat on the virus membrane, packed in a herringbone array; each E dimer is comprised of two antiparallel monomers whose c-terminal helixes are anchored into the lipid bilayer of virus envelope. As envelope protein directly mediates receptor binding and post-entry membrane fusion, it is mostly outwardly exposed and thus contains most neutralization epitopes. Underneath each dimeric E ectodomains are a pair of M proteins buried in the pockets and holes formed between two E subunits on the viral membrane. Similarly, M proteins are anchored to membrane through c-terminal tans-membrane helixes, complexed with each E protein and modulating conformational change of E to initiate membrane fusion at post-entry stage in a pH dependent manner (Zhang et al., 2013; Sirohi et al., 2016). Inside the envelope, the capsids interact with genomic RNA, forming a spherical nucleocapsid, in which ordered structure of capsid surrounding RNA has never been observed in dengue viruses; but a recent study at 9 Å resolution showed structure of immature Zika virus and demonstrated that there was a regular but broken shell of capsid inside the membrane, implying a dynamical morphological alteration during Zika virus maturation (Prasad et al., 2017). Despite minor differences, the structures of DENV and ZIKV are generally similar. A noted difference exists in a region surrounding glycosylation site at $Asn^{154}$ of ZIKV envelope protein and $Asn^{153}$ of DENV envelope protein, these sites may influence virus transmission and pathology through affecting receptor binding and cell tropism (Sirohi et al., 2016).

The precursor of M protein, prM, shields fusion peptide of E protein from acidic environment in trans-Golgi apparatus through its globular "pr" domain when newly budded virus particles transit through exocytosis pathway and thus prevents virus from fusing with Golgi apparatus prematurely. After that, the "pr" peptide is cleaved by a proprotein convertase, Furin, in Golgi apparatus and it dissociates from virus surface once particle reaches extracellular space (Gaucher et al., 2008; Yu et al., 2008, 2009). However, not only fully mature viral particles are produced during viral culture, partially mature or immature virions can also be detected in the supernatant. The immature viruses are those whose pr peptides were not fully proteolytic cleaved from all M proteins on surface. Functionally, in contrast to the mature virus, the immature DENV and ZIKV are non-infectious, however, such immature virus particle can also infect FcγR bearing cells after being bound by antibodies specific for "pr" peptides (Rodenhuis-Zybert et al., 2010; Wirawan et al., 2019), and the uptake of immature virion/antibody complexes creates mature, infectious viruses (Rodenhuis-Zybert et al., 2010).

Besides structural proteins incorporated into viral particles, another membrane associated glycoprotein NS1 can also be secreted extracellularly as hexamers, and detected in blood during acute infection. The NS1 protein can cause pathology in humans through either altering endothelial permeability or inducing antibodies that cross-react with host endothelial proteins; it can also facilitate viral transmission in mosquitoes through antagonizing mosquito innate immunity via suppressing the expression of immune-related genes involved in ROS and JAK/STAT pathways (Liu et al., 2011; Liu J. et al., 2016; Puerta-Guardo et al., 2019). Consistently, antibodies to NS1 can protect mice from lethal diseases in experimental models (Wan et al., 2017; Bailey et al., 2018).

## CELL TROPISM OF DENGUE VIRUS AND ZIKA VIRUS

Transmission of DENV and ZIKV are mainly mediated by *Aedes* mosquitoes. When human is bitten by infected mosquitoes, viruses are inoculated directly into the blood vessels or epidermis where keratinocytes, skin dendritic cells (DC) (Limon-Flores et al., 2005), monocytes and myeloid DC are probably infected and become the first virus carriers for further dissemination (Khaiboullina S. F. et al., 2019). An earlier investigation on dengue virus has indicated that immature skin DC, Langerhans cells were infected by dengue virus and then emigrated from the skin to transmit the virus to other organs (Wu et al., 2000). Our studies have demonstrated that monocyte was the principle target cell among PBMCs for both DENV and ZIKV infection, as well as the main mediators for ADE of both viruses in PBMCs (Kou et al., 2008; Li et al., 2018). Consistently, two other studies also

provided evidences that circulating CD14 + monocytes were the primary cellular targets of ZIKV infection in PBMCs (Foo et al., 2017; Michlmayr et al., 2017).

As they disseminate through the circulatory and lymphatic system, dengue virus and Zika virus spread to different tissues and organs. Dengue virus infects primary vascular endothelial cells, splenic macrophage and Kupffer cells in *ex vivo* infection assay and immunohistochemistry of autopsy specimens (Marianneau et al., 1999; Jessie et al., 2004; Blackley et al., 2007; Dalrymple and Mackow, 2012). In contrast, besides these tissues, Zika virus also replicates in uterus and many immune privileged organs, including placenta, brain and testicles (Govero et al., 2016; Quicke et al., 2016; Sanchez-San Martin et al., 2018; Khaiboullina S. F. et al., 2019), causing neuropathology, congenital disorders, and damages to reproductive organs. So far, Zika virus has been found to infect a wide range of cell types, including neural progenitor cells, mature neurons and astrocytes in brain, Sertoli cells, Leydig cells, stem-like testicular peritubular cells, primary spermatocytes and spermatogonia in testicles, vaginal epithelium and uterine fibroblast in uterus, and trophoblasts, Hofbauer cells and endothelial cells in placenta (Ma et al., 2016; Miner and Diamond, 2017; Qian et al., 2017). Several investigations indicated Zika virus infects endothelial cells, the key component of blood tissue barriers, a fact that may help to explain how Zika virus crosses blood brain barrier and placental barrier (Liu S. et al., 2016; Papa et al., 2017). However, it is still controversial as to whether Zika virus infection alters endothelial barrier integrity. A recent study showed that ZIKV infection of human umbilical vein endothelial cells (HUVECs) increased endothelial permeability (Khaiboullina S. et al., 2019), whereas some other studies have demonstrated that Zika virus directionally infected polarized epithelial cells from apical side and egressed at basolateral side without a disruption of cell monolayer integrity (Tamhankar and Patterson, 2019).

Understanding of ZIKV cell tropism and dissemination across blood tissue barriers will help to better elucidate Zika pathology, and provide opportunity for the development of efficient treatment or prevention strategy. Meanwhile, pathogenic characteristics and tissue tropism should also been considered during development of prophylactic ZIKV vaccine. Its criteria for protective efficacies need to include not only reduced viral load and neuropathology, but also inhibited vertical transmission, and decreased damages to reproductive systems in animal models (Griffin et al., 2017; Shan et al., 2017; Zou et al., 2018). Different from DENV vaccine candidates, ZIKV vaccine might have to elicit higher level of immune responses (Shan et al., 2019) to overcome the special immune status (such as immune tolerance) of recipients during pregnancy (Nancy et al., 2012), and follow-up studies of the incidence of fetal microcephaly in women received ZIKV vaccine are also necessary in clinical trials.

## THE BENEFITS AND LIMITATIONS OF THE ONLY LICENSED DENGUE VACCINE

With effort that lasted two decades, the first licensed vaccine *Dengvaxia* (called CYD-TDV before licensure) has been developed by Sanofi Pasteur. It is a live attenuated vaccine comprised of four Dengue-Yellow Fever virus chimeras in one dose at 1:1:1:1 ratios, and it has been approved to use in over 20 dengue endemic countries and European Union and USA (World Health Organization [WHO], 2017; Halstead and Dans, 2019). Each component of this vaccine was developed on the backbone of Yellow Fever 17D vaccine by replacing prM and E genes with those from each serotype of dengue viruses (Guirakhoo et al., 2000; Guirakhoo et al., 2001). Through such a strategy, CYD-TDV was developed and showed to elicit neutralizing antibodies to four serotype of dengue viruses; moreover, this vaccines has high genetic stability, with limited mosquito transmission, and it is less hepatotropic (one major adverse effect of YF vaccine) (Guirakhoo et al., 2002; Brandler et al., 2005; Higgs et al., 2006; McGee et al., 2008; Mantel et al., 2011). In the large multicenter phase III trials, this vaccine had showed protective efficacies against symptomatic virologically confirmed dengue (VCD) of 54.8% in Asian, and 64.7% in Latin America; the general efficacies against hospitalization and severe dengue cases reached 80.3 and 95.5%, respectively, in Latin America (Capeding et al., 2014; Villar et al., 2015). Though not completely satisfactory, in light of the urgency and significant global demand of a dengue vaccine, CYD-TDV vaccine (*Dengvaxia*) was licensed at the end of 2015, accompanied by the WHO Strategic Advisory Group of Experts (SAGE) recommendation that this vaccine be used in all dengue-endemic counties (World Health Organization [WHO], 2017).

Despite filling in the void of dengue vaccine, its phase II and phase III trials revealed concerns regarding the vaccine's safety. First, the immunogenicity and efficacy of this vaccine varied by age and prior dengue-infections: vaccinees of seronegative and children younger than 9 years' old had increased risk of diseases (Hadinegoro et al., 2015). Vaccination of flavivirus seronegative individuals induced significant lower level of neutralizing antibodies comparing to those having pre-existing flavivirus immunity, specifically, the Geometric Mean Titer (GMTs) of seronegative groups were 47.4–90.8% lower than those of seropositive ones (Guirakhoo et al., 2006; Lanata et al., 2012; Dayan et al., 2013a; Hss et al., 2013). Notably, during long-term follow-up of participants of the two Phase III trials and one Phase IIb trial, vaccinated Asians between ages 2 and 5 years old have had an increased risk of hospitalization in the first year, with a relative risk of 7.5; and vaccinated Thai children between ages 4 and 5 had a relative risk of 2.44 in the 3rd year after vaccination. The vaccine efficacies in children younger than 9 years of age were significantly lower than those of 9 years or older according to a number of criteria (VCD:44.6% vs. 67.8%; hospitalization: 56.1% vs. 86.1%; DHF: 66.7% vs. 90.9%). Further analysis indicated that the lowest vaccine efficacy of 14.4% was in dengue seronegative children younger than 9 years of age (Hadinegoro et al., 2015). It is postulated that vaccination in dengue seronegative recipients had mimicked a course of asymptomatic primary dengue infection, which induced antibodies that enhance subsequent natural dengue infection. Consistently, after the large scale vaccination in Philippines, several vaccinated children and adults have died from lethal dengue diseases. By the time Sanofi Pasteur and WHO modified the instruction for *Dengvaxia* vaccination after those long-term

follow-up studies, limiting its use to people who has a previous dengue infection (Vannice et al., 2018), 800,000 Philippine children had already been vaccinated, among them only 100,000 were seropositive, the rest were thus placed at the increased risk of severe DHF/DSS (Fatima and Syed, 2018). Second, *Dengvaxia* has a low protective efficacy against dengue-2 viruses that are endemic in Asia. In a Phase IIb trial, *Dengvaxia* showed poor protection against dengue-2 virus, reached an efficacy of merely 9%, despite having generated decent neutralization antibodies to DENV-2, with similar GMT (Geometric Mean Titer) as those specific for other serotypes when tested at 28 days after the final immunization (Sabchareon et al., 2012). Similarly, in a Phase III trial in Latin America, the GMTs of neutralization antibodies to DENV-1,-2,-3,-4 were 395, 574, 508, and 241, respectively, at 28 days after the 3rd injection; but the corresponding protective efficacy during the 1st year were 50.3, 42.3, 74, and 77.7% for each of the four serotypes (Villar et al., 2015). Based on these large scale clinical studies, an expected correlation between efficacies and neutralizing antibody titer PRNT (Plaque Reduction Neutralizing Test) values were not found for all four serotypes. It should be noted that a waning of cross-genotype neutralization was observed for monovalent CYD-2 vaccine induced antibodies at 6 months post immunization in a Phase I trial; specifically, GMT of neutralizing antibody specific for dengue-2 clinical isolates of heterologous genotype dropped as much as 10-fold compared with those that were specific for laboratory strain 16681 of autologous genotype (Guirakhoo et al., 2006). All these may indicate that high serotype-2 specific neutralization antibodies had been elicited by CYD-TDV, but it only sustained for a short time and was restricted to a limited number of genotypes. Such unsatisfied efficacy and lower neutralizing titers toward one serotype will also increase the risk of infection by that serotype, especially in those who are seronegative at the baseline. Third, although the highest level of protection was supposed to be achieved after the 3rd vaccination, its efficacy was found to be similar with that in peoples only received the 1st dose. How to modify the immunization schedule of this live attenuated vaccine to boost immune responses is still unclear, but it will probably be helpful to improve the efficacy of vaccine itself. Last but not the least, whether the emergence of Zika virus in DENV endemic regions and prior ZIKV immunity in vaccine recipients will affect the efficacy of *Dengvaxia* is unknown, and whether vaccination by *Dengvaxia* will enhance or prevent Zika virus infection is also uncertain. As co-circulation of two viruses and complicated interference between Dengue and Zika virus-specific immunity have already been observed (Bardina et al., 2017; Fowler et al., 2018; Li et al., 2018; Leborgne et al., 2019), it is worthwhile taking the probable influence of ZIKV into consideration during dengue vaccine development. Therefore, either the currently licensed dengue vaccine *Dengvaxia* or other new vaccines must be applied judiciously in epidemic regions.

# OTHER DENGUE AND ZIKA VACCINES CURRENTLY IN CLINICAL TRIALS

## Other Dengue Vaccines in Clinical Trials

Besides the approved dengue vaccine *Dengvaxia*, several other dengue vaccine candidates have been advanced into clinical trials, these include two recombinant live attenuated vaccines, one subunit protein vaccine, and one DNA vaccine (**Table 1**).

The live attenuated dengue vaccine TAK-003 (DENVax or TDV) is developed by Takeda Vaccine Incorporated. It is comprised of one attenuated dengue-2 viruses, and three other chimeras that contain prM and E genes of other three serotypes built on the backbone of attenuated DENV-2 (Osorio et al., 2015). Here, the backbone DENV-2 in TAK-003 is derived from dengue-2 attenuated virus strain PDK-53, which was obtained through serially passaging of DENV-2 16681 in primary dog kidney cells for 53 times (Bhamarapravati et al., 1987). This tetravalent vaccine has non-structural proteins of DENV-2, and it is capable of activating DENV-2 NS1 specific T cell responses and antibodies (Sharma et al., 2019), both of which *Dengvaxia* is incapable of inducing. But among tetravalent immune responses elicited by the chimeric TDV, the immunity to DENV-4 was the lowest when testing in Phase I and Phase II studies of tetravalent TDV formulations (Osorio et al., 2014; George et al., 2015; Sirivichayakul et al., 2016). Moreover, in the released data from part 1 of its ongoing phase III study, the efficacy of TAK-003 to DENV-4 was still unclear for the insufficient case numbers of DENV-4 infection during study (Biswal et al., 2019). Irrespective of this shortfall, the merits of this vaccine warrants its further testing in several Phase III trials in endemic regions.

A second tetravalent live attenuated dengue vaccine candidate is LAVDelta30 (TV003/TV005), invented by US NIAID and under co-development with Butantan Institute. This vaccine is comprised of attenuated DENV-1, DENV-3, and DENV-4 viruses that contain a 30-nucleotide deletion or additional 31-nucleotide

**TABLE 1 |** Dengue vaccines in clinical trials.

| Name | Vaccine type | Immunogen | Developer | Current status |
|---|---|---|---|---|
| DENVax (TAK-003) | Live attenuated chimeric vaccine | Attenuated DENV-2; Substitution with DENV-1,3,4 prM and E genes on DENV-2 backbone; | Takeda Vaccine Inc. | Phase III |
| LAV Delta 30 (TV003/TV005) | Live attenuated chimeric vaccine | Attenuated DENV-1,3 and 4, through deletion in 3′UTR, DENV-2 prME on the backbone of attenuated DENV-4 | NIAID/Butantan Institute | Phase III |
| DENV subunit V180 | Subunit protein | Ectodomain (N-terminal 80%) of envelope protein, expressed in S2 cell line | Hawaii Biotech Inc./Merk | Phase I |
| D1ME100 | DNA | prM and E genes | US Naval Research Center | Phase I |

deletion in 3′ UTR regions (rDEN1delta30, rDEN3delta30/31, rDEN4delta30) (Blaney et al., 2001, 2008; Whitehead et al., 2003a). Because the same deletion of 30 nucleotides in DENV-2 failed to attenuate it sufficiently, a chimeric virus was obtained by replacing prM and E genes of rDEN4delta30 with DENV-2 prM/E and used instead (Whitehead et al., 2003b). In completed trials and released results, this vaccine was reported to produce neutralizing antibodies and multi-type specific T cell responses in both seronegative and seropositive recipients, although GMTs of neutralizing antibody in seropositive recipients are always higher than those in seronegatives (Weiskopf et al., 2015a; Kirkpatrick et al., 2016). Generally safe, but the vaccine has induced adverse effects such as rash, neutropenia and short-time viremia (Durbin et al., 2005, 2006, 2011, 2013). Its first Phase III trial has been initiated in Brazil.

In contrast to the more rapid progress of live attenuated vaccines into Phase III clinical trials, protein and DNA vaccines are lagging behind in Phase I trials. A subunit dengue vaccine V180 is developed by Hawaii Biotech Inc., and then bought by Merk & Co., Incorporated. This vaccine is comprised of four *Drosophila* S2 cell expressed N-terminal 395aa of envelope proteins (E80) representing four serotype of dengue viruses, and it has been demonstrated to produce neutralizing antibody and provide protection against challenge with multiple serotypes of DENV in murine and non-human primate models (Clements et al., 2010; Govindarajan et al., 2015). In a recent Phase I clinical trial, tetravalent E80 vaccines formulated with different adjuvants were shown to be well tolerated in seronegative recipients in Australia, and they elicited tetravalent neutralizing antibodies, albeit of short duration (Manoff et al., 2019). Use this protein vaccine in adults who previously received attenuated vaccines, TV003 or TV005, has also been tested in clinical trial, the results of which are pending (ID: NCT02450838).

A DNA vaccine under clinical development is developed by US Naval Medical Research Center, and it contains prM and E genes. Monovalent DENV-1 prM and E DNA (D1ME) vaccines showed immunogenicity in Phase I clinical trial after being demonstrated conferring protection in a monkey model (Beckett et al., 2011). The neutralizing antibody was detectable only in the vaccine group receiving higher dose of DNA, and its titer was low. Therefore, tetravalent formulations of this vaccine were tested with combination of Vaxfectin® adjuvant to improve its immunogenicity in further clinical trials (Porter et al., 2012), much of its results have not been published.

## Zika Vaccines in Clinical Trials

In contrast to Dengue vaccines, Zika vaccines have only been developed recently since the large ZIKV outbreaks in 2015–2016. Multiple candidates are under development simultaneously, including traditional inactivated vaccine, live attenuated vaccine, and genetically engineered subunit protein vaccine, DNA vaccine, and novel mRNA vaccines; among them, only the seven candidate vaccines that are in Phase I or II clinical trials will be discussed (**Table 2**).

The most advanced Zika vaccine candidates is a DNA vaccine containing Zika virus prM and E genes (VRC5283) that is being developed by NIAID and tested in Phase II clinical trial. The vaccine plasmid expresses prM and E proteins and forms non-infectious but highly antigenic virus like particles (VLP) *in vivo*. Recipients of this vaccine by needle-free injection on both arms with split-dose showed 100% seroconversion, and generated neutralizing antibody with higher GMT values than those received a single-full dose injection on one arm and those administered the vaccine via needle and syringe injection. It is probably because the needle-free injection has enhanced dispersion field and increases the contact area between antigens and dermal APC (Mitragotri, 2006). The split-dose vaccination group also elicited best CD4 + and CD8 + T cell immune responses across all groups (Gaudinski et al., 2018). Another DNA vaccine GLS-5700 (developed by GeneOne/Inovio) containing consensus sequences of ZIKV prM and E genes, delivered via intradermal injection followed by electroporation, produced neutralizing antibodies in 62% participants as measured by the Plaque Reduction Neutralizing Test (PRNT). In addition, adoptive transfer of sera from vaccine recipients protected 92% immune deficient mice from lethal ZIKV challenge (Tebas et al., 2017).

The development of inactivated Zika vaccine was started soon after the ZIKV outbreaks. There are currently two purified inactivated Zika vaccine candidates in Phase I clinical trials, they were developed by WRAIR/NIAID/Harvard University/Sanofi Pasteur (ZPIV) and Valneva Australia GmbH (VLA1601) separately. Inactivated vaccine has the advantages of easy manufacture, established platforms based on many other vaccines, such as those for Japanese Encephalitis (JE) and Polio viruses, have been developed. According to preliminary results of the WRAIR/NIAID vaccine (ZPIV) in three Phase I trials, the formalin-inactivated virus vaccine induced 95% seroconversion, had a peak neutralization antibody GMT of 286, with only moderate adverse effect. Adoptive transfer of human IgG from vaccine recipients to mice prior to challenge with ZIKV led to reduced viremia in mice, indicating its potential for protection in humans (Modjarrad et al., 2018).

Using a similar strategy for DENV-2 vaccine TV003/TV005, recombinant live attenuated Zika vaccine has been constructed with the backbone of attenuated DENV-4 of TV003 (rZIKV/D4delta30), by NIAID, wherein prM and E genes of DEN4delta30 were substituted by the corresponding genes from ZIKV. This vaccine is now in Phase I clinical trial, and might be tested in combination with DENV vaccine TV005 in the future (ID: NCT03611946) (Durbin and Wilder-Smith, 2017; Wilder-Smith et al., 2018). Other viral vectors such as Measles vaccine virus has also been adapted to construct chimeric ZIKV vaccine. One of such vaccine, MV-ZIKA, has been developed by Themis Bioscience GmbH and advanced into Phase I clinical trial (ID: NCT02996890).

Novel vaccine strategy such as lipid nanoparticle-encapsulated modified mRNA has also been used to develop Zika vaccine. An mRNA that contains prM-E genes of ZIKV and optimized 5′ and 3′ untranslated sequences with type-1 cap was obtained through enzymatically synthesis using modified nucleoside, and packaged into lipid nanoparticles (LNP). Such mRNA-LNP vaccine could efficiently produce virus like particle in cells. After intramuscular delivery, two doses of mRNA-LNP vaccine were able to elicit

**TABLE 2 |** Zika vaccines in clinical trials.

| Name | Vaccine type | Immunogen | Developers | Current status |
|---|---|---|---|---|
| VRC5283 | DNA | Wild type prM and E genes, needle-free injection | NIAID | Phase II |
| GLS-5700 | DNA | Consensus prM and E genes, injection & electroporation | GeneOne life science Inc./Inovio Pharmaceuticals | Phase I |
| ZIKV purified inactivated vaccine (ZPIV) | Inactivated vaccine | Formalin-inactivated whole virus | WRAIR/NIAID/Harvard University/Sanofi Pasteur | Phase I |
| VLA1601 | Inactivated vaccine | Formalin-inactivated whole virus | Valneva Australia GmbH | Phase I |
| rZIKV/D4delta30 | Chimeric live attenuated vaccine | ZIKV prM and E genes inserted to DEN4delta30 | NIAID | Phase I |
| MV-ZIKA | Viral vector | ZIKV prM and E genges inserted to measles virus vector | Themis Bioscience GmbH | Phase I |
| mRNA-1325 | mRNA | Lipid nanoparticle encapsulated modified mRNA of prM and E | ModernaTX, Inc. | Phase I |

high titers (∼1/100,000) of neutralizing antibodies, and conferred protection against ZIKV challenge in mice (Richner et al., 2017a). An mRNA-based vaccine is now in Phase I clinical trial (ID: NCT03014089).

Besides, other forms of ZIKV vaccine, such as protein based subunit vaccine (Medina et al., 2018; Metz et al., 2019; Slon-Campos et al., 2019) and live attenuated Zika vaccines (Richner et al., 2017b; Xie et al., 2018; Shan et al., 2019) are also under development at the pre-clinical stage. Considering the cross-reactivity and ADE between ZIKV and DENV, newly developed ZIKV vaccine should also be tested for DENV enhancement activity. This additional requirement will likely to be a huge obstacle for both ZIKV and DENV vaccines.

# PROTECTIVE IMMUNITY AGAINST DENGUE AND ZIKA VIRUSES

## Protective Antibody Response

Although various antibodies targeting different viral proteins are induced after flavivirus infection, only two types of antibodies have been documented to provide significant protection: neutralizing antibodies to viral surface E protein (Crill and Chang, 2004; Dejnirattisai et al., 2015; Stettler et al., 2016; Robbiani et al., 2017) and non-neutralizing antibodies specific for NS1 protein (Henchal et al., 1988; Beatty et al., 2015; Wan et al., 2017; Bailey et al., 2018).

The ectodomain of flavivirus envelope protein can be structurally divided into three sub-domains: Domain II is a long finger-like area lying parallel to virus surface and it contains a fusion peptide on its tip; Domain III is an immunoglobulin-like folded structure projecting slightly away from virus surface, and it is linked to the C-terminal stem region and thought to be involved in virus binding; Domain I is an eight-stranded β-barrel that connects domain II and domain III. Previous study with dengue specific mouse monoclonal antibodies indicated that E domain III was the predominant targets for DENV neutralizing antibodies, and antibodies to this region are mainly serotype specific (Lok et al., 2008); whereas antibodies specific for fusion loop epitopes (FLE) are usually highly cross-reactive with modest neutralization activities (Crill and Chang, 2004). However, in convalescent dengue patient, anti-E Domain III specific neutralizing antibodies only constitute a small proportion of DENV antibody repertoire. Mapping antibody epitope using recombinant envelope proteins, it was found that neutralizing antibody epitopes in human distributed widely across both domain III and domain I/II regions (Beltramello et al., 2010; Stettler et al., 2016), and the depletion of EDIII specific antibodies did not affect the neutralization activity of human immune sera significantly (Williams et al., 2012). Subsequent studies with human samples revealed another class of antibodies that target quaternary epitopes on virus surface, and that these antibodies do not bind to recombinant envelope proteins, but recognize epitopes spanning one dimer or two adjacent dimers of E proteins on the intact virus surface. One group of such antibodies, also called envelope dimer epitope (EDE) antibodies, usually have broad neutralizing activities to all four serotype dengue viruses (Dejnirattisai et al., 2015; Rouvinski et al., 2015).

On the contrary, the importance of ZIKV EDIII specific antibodies has been shown directly in some human studies. In one study with a panel of human mAb isolated from four convalescent patients, antibodies to E domain III and quaternary epitopes were found to be the most potent at neutralization (Stettler et al., 2016). Additionally, using two cohorts of ZIKV infected individuals from Mexico and Brazil, it was revealed that the levels of antibodies specific for the lateral ridge of ZIKV E domain III were positively correlated with sera neutralization antibody titers (Robbiani et al., 2017). Moreover, antibodies to quaternary epitopes formed between E domains II and III of Zika virus were demonstrated to be both protective and therapeutic in murine models (Sapparapu et al., 2016; Hasan et al., 2017; Collins et al., 2019).

DENV and ZIKV show high level of structure homology between their envelope proteins, and share 35, 51, and 29% amino acid identity in EDI, EDII, and EDIII, respectively. Thereby, cross-reactivities are frequently observed between antibodies targeting E domain I/II of two viruses, but less so for domain III antibodies (Stettler et al., 2016). The broadly neutralizing

EDE1 antibodies, one subset of EDE antibodies originally isolated from DENV patients, has been shown to potently neutralize Zika virus *in vitro* and provides protection against lethal challenge of Zika virus in mice. These antibodies recognize a conserved conformational region on the E dimer which prM interacts with during virus maturation. Another subset is EDE2 antibodies that have broader footprints covering N153 glycosylation site of DENV E proteins, these antibodies can also cross-neutralize ZIKV at high concentrations (Fernandez et al., 2017; Abbink et al., 2018; **Figure 1A**). In contrast, ZIKV neutralization antibodies targeting quaternary epitopes identified so far, such as ZIKV-117, A9E, and G9E, are mainly type-specific (Sapparapu et al., 2016; Hasan et al., 2017; Collins et al., 2019). Notably, cross-reactive antibodies EDE1 and EDE2 were isolated mainly from patients of acute secondary DENV infection, whereas A9E and G9E were isolated from DENV naïve ZIKV patients at 6 months after the onset of illness. Whether such cross-complex neutralizing B cell responses can sustain long time after recovery from infection is unclear, and whether its frequency increases after a heterotypic secondary infection is also unknown.

Collectively, neutralization antibodies to dengue or Zika viruses are mainly constituted of type specific EDIII antibodies, cross-reactive EDI/II antibodies, and potently neutralizing quaternary epitope antibodies that often neutralize four serotypes of dengue viruses simultaneously.

Other than antibodies to envelope proteins, there are abundant prM specific antibodies in human sera after dengue virus infection (Dejnirattisai et al., 2010). However, such antibodies are poorly neutralizing with high cross-reactivity, and induces ADE in a wide range of concentrations, probably because prM antibodies facilitate non-infectious immature virus to become mature and infectious (Rodenhuis-Zybert et al., 2010). In experimental models, immature viral particles may achieve infectivity with the help of antibody against "pr" upon entering the acidic endosome, where the "pr" peptide is cleaved together with the antibody by Furin. Even partially mature viruses that keeping pr peptides in some region on viral surface, can also obtain enhanced infection in Fcγ receptor bearing cells with the help of anti-pr antibodies (Rodenhuis-Zybert et al., 2010; Wirawan et al., 2019). Because of these reasons, prM antibody is now thought to be undesirable among vaccine induced immune responses.

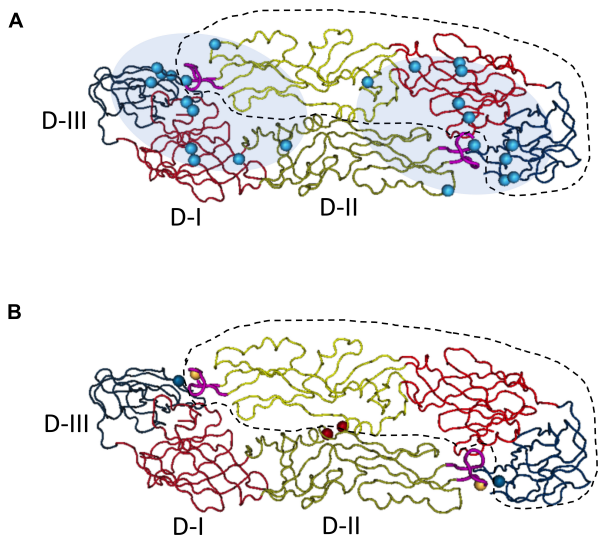


**FIGURE 1 |** Quaternary epitopes on dengue virus dimeric envelope proteins and stabilizing dimeric structure of E proteins through the addition of disulfate bonds between two monomers. Based on the published structure of DENV-2 E dimer (PDB access NO:1OAN), three domains of E monomer were denoted with different colors on backbones (D-I, red; D-II, yellow; D-III, blue). One of the E monomers in the dimeric structure was circled with dash line. On the tip of domain II, the fusion loop was labeled in pink. The structural image presented the top view, distal from virus membrane. **(A)** Epitopes distribution of EDE epitopes, the residues (cyan spheres) critical for EDE antibody binding were determined by Dejnirattisai et al. Fab binding regions of EDE antibodies were mapped to either end of the dimer (cyan shadow), covering the interface of two monomers. Figure adapted from Dejnirattisai et al. (2015) and Rouvinski et al. (2015). **(B)** Stabilization of dimeric E proteins was achieved through adding disulfate bonds, after introducing mutations into domain II, L107C (yellow spheres) A259C (red spheres) and domain III, A313C (blue spheres). Figure adapted from Rouvinski et al. (2017).

## Antibody Dependent Enhancement

One adverse characteristic of flavivirus prM or E antibodies is their ability to induce ADE. When the concentration or affinity of antibodies is too low to neutralize virus infection, the immune complexes formed by virus and antibodies tend to interact with Fcγ receptors on myeloid cell surface through Fc domains of antibodies, they do not induce Fcγ-mediated viral clearance, but aid virus infection by directly increasing virus uptake through Fcγ receptor, or boosting virus replication intracellularly via activating downstream pathway to antagonize the innate immunity (Halstead, 1988; Kliks, 1990). In the latter case, it is hypothesized that legation of Fcγ receptor transmits signals through spleen tyrosine kinase (SYK) to activate extracellular signal-regulated kinase (ERK), and subsequently enhances the transcription of genes including IL-10, which antagonizes type-I IFN pathway through stimulating members of the suppressor of cytokine signaling (SOCs) (Halstead et al., 2010). A number of *in vitro* studies have already demonstrated that most antibodies to DENV or ZIKV prM and E proteins have the potential to enhance viral infections at sub-neutralizing concentrations, irrespective of their neutralization potency (Pierson et al., 2007; Dejnirattisai et al., 2015, 2016). Two classes of antibodies are thought to induce mainly ADE effect rather than neutralization, these are antibodies to fusion-loop and antibodies specific for "pr" peptide, both of which are abundant in patient sera (Beltramello et al., 2010; Dejnirattisai et al., 2010). They are generally highly cross-reactive and marginally neutralizing (Rodenhuis-Zybert et al., 2010; de Alwis et al., 2014). Further investigation on Zika and dengue monoclonal antibodies indicates that antibody concentrations that induce peak ADE are usually negatively correlated with antibodies' neutralizing capacity (Li et al., 2017).

In addition to *in vitro* studies using human samples, ADE of heterotypic DENV infection has been more stringently demonstrated in mouse models. Administering heterotypic DENV immune sera or viral-specific monoclonal antibodies to

AG129 immune deficient mice prior to infection with non-lethal dose of DENV-2 increased viral replication and enhanced disease severity; and increased infection of liver sinusoidal endothelial cells were observed for all four serotypes of clinical isolates (Zellweger et al., 2010). Consistently, clinical evidence of ADE in DENV infection has been reported previously. Infants born to dengue immune mother had elevated risk of DHF/DSS at 6–9 months of age, due to the decay of maternal-derived DENV antibodies (Halstead, 2003). Further, the increased risk of hospitalization in younger children vaccinated with CYD-TDV in Phase III clinical trials are also suspected to have been caused by ADE, as a result of vaccine-induced poorly neutralizing antibodies. More recently, a long-term study on a Nicaragua pediatric cohort showed that the risk of severe dengue diseases was highest within a narrow range of preexisting anti-DENV antibody titers, affirming antibody concentration is a critical determinant of ADE (Katzelnick et al., 2017).

More significantly, a cross-serocomplex ADE between ZIKV and DENV has also been reproduced in mouse model. DENV and WNV immune sera were both found to enhance Zika virus infection in mice (Bardina et al., 2017). Also, the presence of DENV-specific antibodies in ZIKV-infected pregnant mice significantly enhanced viral replication in placenta, and increased placenta damage, reduced fetal growth, and accelerated fetal resorption (Leborgne et al., 2019). Reciprocally, maternally acquired Zika virus antibodies also enhanced dengue disease severity in mice (Fowler et al., 2018). In non-human primate models, the results are not as clear. Two studies did not show enhanced Zika virus infection in macaques that were infected by DENV either 420 days or 2.8 years before experiments (McCracken et al., 2017; Pantoja et al., 2017). However, it should be noted that the interval between primary and secondary DENV infections is critical for disease severity, and DENV ADE in human has only occurred within a relatively narrow range of pre-existing DENV antibody concentration (Katzelnick et al., 2017). In dengue infected patients, this interval was usually 12 months or longer, but unknown for enhancement of Zika virus infection. Limited data from a long-term cohort study in Brazil before and after the 2015 ZIKV outbreak have found that the pre-existing DENV NS1 specific IgG3 antibody within 4–6 months of infection was positively associated with the risk of subsequent ZIKV infection, but high titer of total IgG to DENV was associated with protection against the acquisition of ZIKV infection (Rodriguez-Barraquer et al., 2019). Our previous study using sera of convalescent dengue patients also revealed that stronger cross-serocomplex ADE of ZIKV infection in PBMC appeared more often in sera obtained within 3 months of DENV infection (Li et al., 2018). These results are supportive of the idea that concentrations of cross-reactive antibodies or intervals between two infections are important factors for determining cross-serocomplex enhancement between ZIKV and DENV.

Collectively, ADE is now considered to be the underlying mechanism for enhanced risk of DHF/DSS in secondary dengue virus infection, and it highlights the necessity of avoiding the induction of inadequate immune response toward any serotypes during vaccine development. Despite the impact of prior cross-serocomplex immunity for subsequent ZIKV or DENV infections are clinically unknown, candidate vaccines that provide protection and avoid ADE should be prioritized for development.

## T Cell Responses

Aside from the double-edged antibody responses, DENV and ZIKV infections also elicit strong T cell responses of dubious functions. For a long time, T cells activated during dengue virus infection was postulated to cause pathology through producing cytokines such as IFN-γ and TNF-α, which in some models directly increases vascular permeability (Rothman et al., 2014). However, in clinical studies, the appearance of T cell responses was found after the occurrence of hemoconcentration or thrombocytopenia in DHF patients (Jin, 2008; Dung et al., 2010). In mouse models, DENV-specific CD8 + T cell responses were protective and essential for virus clearance during primary infection; and CD4 + T cell responses elicited after peptide vaccination also contributed to protection, although they seemed to be dispensable for virus clearance in primary infection (Yauch et al., 2009; Yauch et al., 2010). A subsequent human cohort study further illustrated that DENV specific CD8 + T cell responses played protective roles against DENV infection in an HLA-linked manner (Weiskopf et al., 2013). DENV-1, -2, -4 specific human CD8 + T cell epitopes are distributed predominantly on NS3, NS4B and NS5 proteins (Duangchinda et al., 2010; Rivino et al., 2013; Weiskopf et al., 2013), whereas human CD4 + T cell epitopes are mainly located on C, NS3, and NS5 viral proteins (Weiskopf et al., 2016; Grifoni et al., 2017a). In some studies, DENV-3 specific CD8 + T cell responses were found to target both structural and non-structural proteins (Weiskopf et al., 2014, 2015b). Of note, all these observations were based on limited sample size and HLA types, and of unknown sequences of heterotypic infections when the subjects had experience secondary infections. These uncertainty in clinical studies might have not revealed the full scope of T cell responses toward conserved epitopes.

Similarly, ZIKV specific CD8 + T cells were also first showed to be protective in a mouse model (Elong Ngono et al., 2017; Huang et al., 2017), and human ZIKV CD8 + T cells were revealed to have cytotoxic antiviral function and bear signature transcriptional profiles (Grifoni et al., 2018). Though, CD8 + T cell infiltration into mouse brain and its antiviral cytotoxicity might be associated with neurological pathology in ZIKV infection, the pre-existence of specific CD8 + T cells did protect mice from CNS disease (Huang et al., 2017; Jurado et al., 2018). Whether ZIKV CD4 + T cell responses are necessary for virus clearance in primary infection is still controversial, but memory CD4 + T cells elicited by infection or peptide immunization have been demonstrated to protect host from subsequent ZIKV infection (Hassert et al., 2018; Elong Ngono et al., 2019). In one cohort study conducted in dengue endemic countries, ZIKV specific CD8 + T cell epitopes were found to be located mainly on C, prM, and E proteins in dengue naïve patients, but targeted broadly across the proteome, especially those conserved regions, in dengue experienced patients (Grifoni et al., 2017b). This is in accord with observations made in human HLA-transgenic mice (Wen et al., 2017b).

Cross-reactive T cell responses were often observed between DENV and ZIKV, because of their homology at amino acid level. DENV specific memory CD8 + T cells could cross-react with Zika virus and protected mice from subsequent lethal ZIKV challenge (Wen et al., 2017a). Adoptive transfer of DENV CD8 + T cells to pregnant mice inhibited Zika virus replication in placenta and increased the survival of fetus (Regla-Nava et al., 2018). In DENV convalescent patients, memory CD4 + and CD8 + T cells could be activated by peptides derived from ZIKV capsid and NS3 proteins, and the activated CD8 + T cells could kill ZIKV infected cells *in vitro* (Lim et al., 2018). Nevertheless, studies on the cross-reactive CD4 + T cells are few, evidence for ZIKV specific memory T cells cross-react with DENV antigens is still lacking.

All above demonstrate that T cell response is an important element of adaptive immunity toward dengue and Zika virus, and T cell component should be considered in the development of protective vaccines.

## B AND T CELL VACCINES OF THE NEXT-GENERATION

Based on the existing knowledge of vaccine immunology and protective immunity to DENV and ZIKV, it is predicted that an ideal dengue or Zika vaccine should induce both humoral and cellular immune response to ensure full protection.

### Universal B Cell Vaccines for DENV and ZIKV

Previous investigation on dengue and Zika vaccine mainly focused on the B cell immunity, aiming to elicit enough neutralizing antibodies for *in vivo* protection. Because of the complex interaction among antibody responses to four DENV serotypes and ZIKV, an ideal dengue vaccine should elicit long-lasting, serotype-specific neutralizing antibodies to each serotype of virus or broadly neutralizing antibodies that cross-react with all serotypes of viruses. Zika vaccines developed independently need to be able to trigger autologous neutralizing antibodies but minimal cross-reactivity with dengue viruses. Alternatively, pentavalent vaccines would be necessary, if ADE cross sero-complex is verified in epidemiological studies in the future. However, to induce long-term B cell memory response that sustains potent neutralization is not easy, and to produce adequate and relatively balanced neutralizing antibodies against each of these viruses is also difficult. The following approaches may be considered.

First, epitope selection is necessary to design vaccines that produce strong neutralizing antibody responses and minimal ADE effect. Traditional live attenuated vaccines have the advantages of strong immunogenicity and mimicry of wildtype virus. However, the antibody responses elicited by intact or recombinant dengue or Zika viruses still maintain the dual functions of neutralization and enhancement. One prominent source of antigens that induce enhancing antibodies is the immature or partially mature viral particles within the vaccine produced *in vitro* or viruses replicated *in vivo*, and the percentages of which are difficult to determine due to variability in cell cultures for different virus strains. Epitopes on "pr" peptides are probably exposed on immature ZIKV virus surface and elicit abundant ADE inducing antibodies, similar to what happened in DENV infected patients. The same issue must be dealt with for DNA or RNA vaccines that incorporate prM and E genes in order to make virus like particles *in vivo* (Beckett et al., 2011; Porter et al., 2012; Richner et al., 2017a). Similarly, *in vitro* produced virus like particle vaccines will not be ideal unless the immature virus-like particle can be eliminated through procedures such as exogenous Furin cleavage, but how to produce enough immunogens is another problem even more complicated to deal with (Urakami et al., 2017). Therefore, the exact effect and ratio of "pr" antibodies elicited by these vaccines have to be determined during development. In comparison, subunit proteins are easier for epitope selection and quality control. In most subunit candidate vaccines of DENV and ZIKV, soluble EDIII or E80 as antigens were chosen (Block et al., 2010; Liang et al., 2018; Manoff et al., 2019) to induce neutralizing antibodies that block virus attachment or/and inhibit post-entry membrane fusion. Nevertheless, fusion-loop epitope antibodies can still be induced by E80 due to the probable re-exposure of fusion-loop under acidic environment even for an envelope dimer immunogen. One study has attempted to abolish fusion loop through site-directed mutation in mRNA vaccine (Richner et al., 2017a), but both neutralization and enhancement activities were attenuated, indicating this region was probably essential for E dimeric structure on VLP surface. Alternatively, cross-linking of two E80 proteins through additional disulfate bonds in domain II and domain III could stabilize the anti-parallel structure of the soluble E80 dimer, limiting the exposure of fusion-loop, but enabling the presentation of cross-serocomplex broadly neutralizing EDE epitopes (Rouvinski et al., 2017; **Figure 1B**). Consistently, in a recent study, the covalently stabilized ZIKV E dimer has successfully elicited protective antibody responses against ZIKV infection in mice, without causing cross-reactivity to dengue viruses or ADE of DENV (Slon-Campos et al., 2019). Currently, both Zika EDIII and Dengue tetravalent EDIII vaccines are under development. The EDIII component theoretically has more serotype/complex specificity and produce less ADE effect. Whether these type-specific neutralization antibodies induced are strong enough to provide *in vivo* protection toward multiple viruses is to be determined.

Second, relatively balanced neutralization against each of the viruses is required for an ideal tetravalent dengue vaccine or pentavalent Dengue/Zika vaccine. The majority of dengue vaccine candidates are comprised of mixed antigens representing four serotypes, and they are administered to recipients simultaneously to elicit a tetravalent response. When using attenuated viruses, however, different replicative capacity of each virus may produce interference among them, leading to imbalanced neutralizing antibody responses (Dayan et al., 2013b). As for tetravalent protein or DNA vaccines, the immune dominance of specific antigens also affected the balance of neutralizing activities elicited by the vaccines (Block et al., 2010). Thus, modulation of dosage of each serotype of virus or antigen is always needed to improve the relative

balance of antibody responses induced. Because the correlation between neutralizing titers and *in vivo* protection varies among four serotypes of dengue viruses or Zika virus, to adjust the balance among immune responses in order to achieve broad protection becomes even more difficult. An alternative strategy is to elicit broadly neutralizing antibodies through a single antigen presenting conserved neutralizing epitopes. To this end, we obtained a consensus E80 sequence that contains epitopes conserved across all four serotype viruses through *in silicon* calculation with a dataset composed of 3,127 published sequences of dengue viruses, and found this single consensus E80 protein was immunogenic and capable of inducing neutralizing antibodies toward all four serotypes of DENV, with less bias than conventional tetravalent E80 vaccine (Sun et al., 2017). When administered in a DNA prime and protein boost regimen, this vaccine conferred protections against all four serotypes of viruses in a mouse model (Wang et al., 2019). This vaccine design strategy uniformly enriched all conserved epitopes on a single E80, further incorporation of consensus E80 monomers derived from both DENV and ZIKV to a stabilized dimer might help to present most cross-neutralizing epitopes on surface.

Moreover, to elicit long-term neutralizing B cell memory response is another essential aim for dengue or Zika vaccine. In clinical trial of CYD-TDV, GMT of antibody to each serotype of viruses was measured at 28 days after each immunization, significant increase of GMT level was only observed after the 1st and 2nd immunization, and protection efficacy in recipients accepted all three doses (per protocol analysis) showed no differences with those only vaccinated for the first dose (intention-to-treat analysis) (Capeding et al., 2014; Villar et al., 2015). Whether B cell memory response elicited by multiple and single doses of CYD-TDV both waned to the same level in the first year is uncertain. For obvious reasons, dengue experienced vaccine recipients have higher GMT than dengue naïve ones, and the formers were better protected from subsequent dengue infections. In an earlier Phase I clinical trial with monovalent CYD-2 vaccine, dramatic decrease of neutralizing antibodies was observed in YF naïve group from 1st to 12th month, whereas YF-immune subjects maintained higher GMTs of antibody responses to dengue virus-2 and heterotypic viruses throughout the first year after immunization, despite the vaccine specific GMT were initially similar for the two groups in the 1st month (Guirakhoo et al., 2006). More followed-up studies are needed for confirmation, but it inferred that boosting with heterologous antigens (i.e., vaccinate recipients having prior flavivirus infection) have helped host immunity to focus on a few conserved epitopes to produce stronger and longer cross-reactive broadly neutralization responses, but repetition of immunization with same antigens (i.e., various antibody responses primed in the first immunization were equally boosted in the following two repeated immunization) only elicited various antibodies of weak cross-neutralization and sustained these responses only for a short-term. In fact, this hypothesis is in line with the theory of "original antigenic sin" (Halstead et al., 1983; Kuno et al., 1993; Zompi and Harris, 2013). Therefore, to achieve long-term antibody responses by B cells toward selected epitopes corresponding to stronger and broader neutralization, heterologous prime-boost immunization to highlight conserved epitopes might be a useful approach.

In summary, through enriching conserved epitopes and selectively presenting broadly neutralizing epitopes, we should be able to construct a universal dengue and Zika B cell vaccine. Furthermore, with suitable heterologous vaccines in prime-and-boost regimens, we might have a chance to achieve the induction of potent, broadly reactive, and protective B cell immune responses that have limited ADE effect.

## T Cell Vaccines for DENV and ZIKV

In contrast to the extensive attention on B cell responses, T cell immunity produced by flavivirus vaccine had never been carefully examined until a recent retrospective study that investigated why there was a higher efficacy of CYD-TDV in dengue experienced than dengue naïve vaccine recipients. As a chimera of Dengue virus and YF-17D vaccine, CYD-TDV mainly elicited YFV specific T cell responses through YFV non-structural proteins, of which reactivity to dengue virus was limited. One hypothesis is that, with prior dengue virus infection, dengue specific memory T cell responses were boosted by YFV cross-reactive epitopes in seropositive recipients and contributed to protection. Indeed, the cross-serotype and cross-complex protection of dengue virus specific T cells has already been reported in mouse models. Specifically, memory T cells can relieve mice from lethal disease in an adoptive transfer model, avoiding ADE effect successfully (Wen et al., 2017a). Therefore, T cell vaccine is complementary to traditional B cell vaccines for defense against DENV and ZIKV.

Distinct from B cell epitopes, T cell epitopes are linear, continuous and major histocompatibility complex (MHC) antigen (human leukocyte antigen, HLA, in humans) restricted. Some HLA-linked protective epitopes have already been identified for DENV and ZIKV, it is worthwhile to study epitope distribution for more HLA allotypes. This can be initiated through predictive computational algorithms according to parameters such as MHC affinity, and followed by experimental verification (Elong Ngono et al., 2017, 2019). Viral proteins that contain most epitopes for common HLA allotypes could be included as antigens for T cell vaccines (**Figure 2**). Such an approach had been tested in a study of immunogenicity and protection efficacy of multiepitope DENV NS3 DNA vaccine in Balb/c mice, and it demonstrated that *in vivo* expression of NS3 epitopes elicited T cell responses and protective immunity against DENV-2 infection (Costa et al., 2011). Dominant epitopes from different proteins of different viruses presented by various HLA allotypes can also be integrated into a polypeptide string, which can be made into immunogens to elicit protective T cell immunity in a large population, just as what has been done for HIV CD4 + T cell vaccine (Liu H. et al., 2017).

Live attenuated vaccine has an advantage on eliciting T cell responses. TAK-003 and TV003 containing non-structural proteins of DENV have been shown to elicit both antibody responses and T cell responses. However, to avoid ADE, a flavivirus T cell vaccine without cell surface epitopes is obviously more suitable for the proof-of-concept study. To accomplish

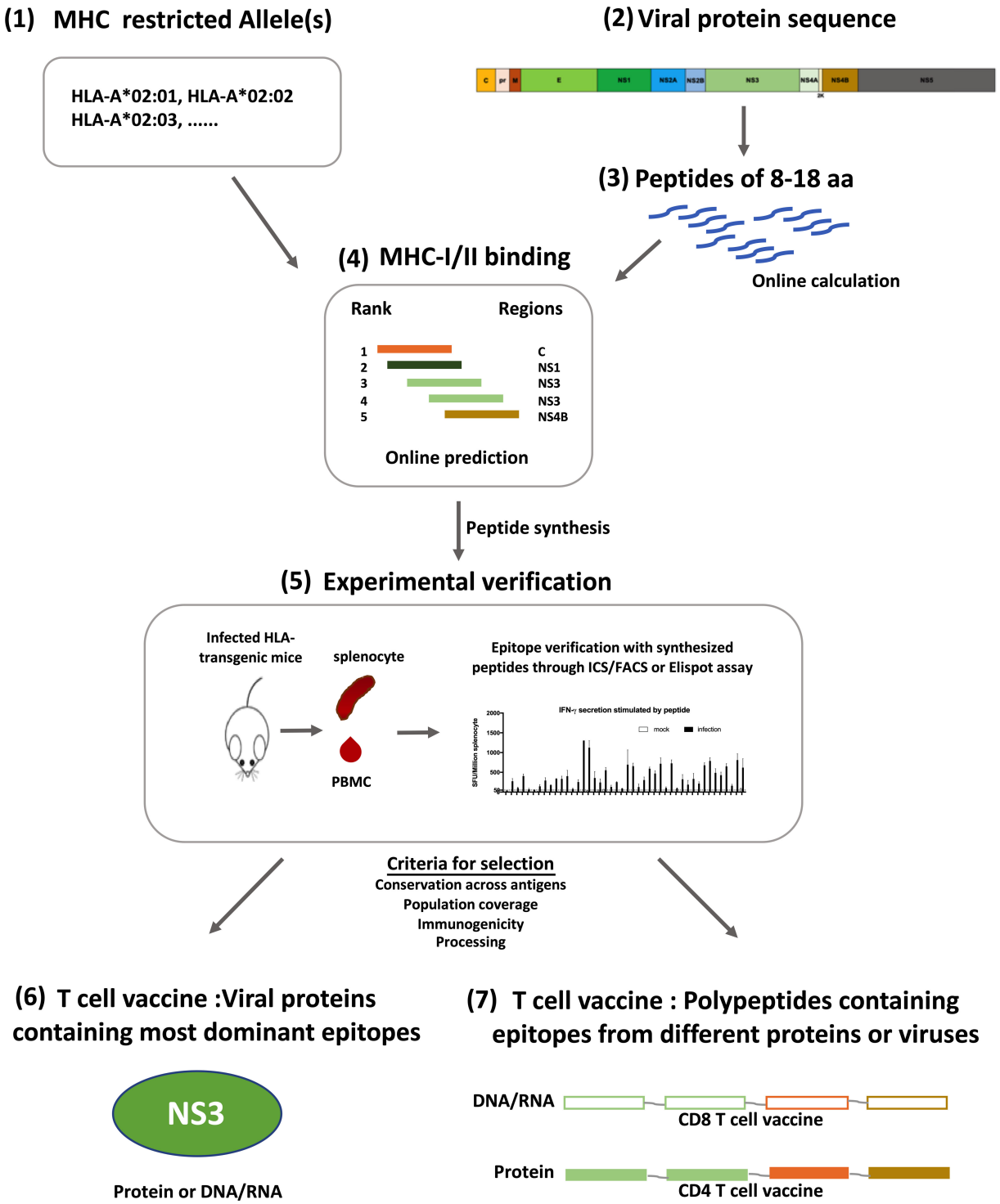


**FIGURE 2 |** Designing strategy for flavivirus T cell vaccines. Development of T cell vaccine could be initiated from the prediction of T cell epitopes on Immune Epitope Database (IEDB) (1–4). With selected HLA molecules (1) and protein sequences (2), both CD4 + and CD8 + T cell epitopes can be predicted according to the sequences of linear peptides derived from a protein (3), and the affinity of peptides to selected MHC molecules (4). Predicted epitopes were verified in HLA-transgenic mice with synthesized peptides through Elispot or Intracellular cytokine staining assay (5). Verified epitopes were further selected based on their conservation across different strains of viruses (HLA-allotype), population coverage, immunogenicity and processing efficiency, all of which could be calculated online. Some can be tested experimentally. Using these selected epitopes, T cell vaccine can be prepared with two different strategies, one is using antigens which contain most dominant epitopes and have reliable population coverage and sequence conservation (6); the other is to make immunogens with a string of peptides containing epitopes from different genes or strains, thus having higher population and antigen coverage (7). Both kinds of vaccines can be either DNA/RNA or proteins, depending on the T cell subset to be activated.

this goal, many factors affecting the immunogenicity of T cell antigens should be considered. First, immunogens activating two main subsets of T cells have to be delivered in different ways. CD4 + T cell epitopes are mainly presented through an exogenous antigen presentation pathway, whereas CD8 + T cell epitopes are presented more efficiently through an endogenous antigen presentation pathway (Cresswell et al., 2005; Roche and Furuta, 2015; Sadegh-Nasseri and Kim, 2019). Therefore, CD4 + T cell antigens should be administered either directly to extracellular space or secreted to extracellular space after *in vivo* expression. On the other hand, CD8 + T cell antigens are best delivered as DNA or RNA vaccines that have better antigen expression and retention intracellularly. Second, immune dominance of T cell epitopes might be affected by epitope composition of vaccines, and will also be influenced by prior flavivirus infection. How to induce protective T cell immunity toward four serotypes of DENV and ZIKV simultaneously, and whether cross-reactive T cell responses could be induced through heterologous prime-boost vaccination strategy, are all questions that have to be addressed during flavivirus T cell vaccine development. Finally, to achieve sterilizing immunity against viruses is extremely hard through T cell vaccine alone, as the effector T cells are only activated by processed immunogens and only target infected cells bearing linear epitopes on surface, both of which happen after cells were infected.

In summary, we propose an improvement of the strategy for dengue and Zika virus vaccine development by inclusion of T cell epitopes in order to overcome the ADE effect *in vivo*.

## VECTOR BLOCKADE THROUGH NS1 ANTIBODIES

As both DENV and ZIKV are transmitted through *Aedes* mosquitoes, countermeasures that block the transmission steps of these vectors are important adjuncts to vaccines or antiviral drugs for controlling their infections. In urban areas, through spraying insecticides and clearing up standing water in containers such as discarded tires and plant pots, adult mosquitoes and mosquito larvae can be effectively removed. These approaches had helped to eliminate dengue fever from southern United States in 1920s. However, absolute elimination of mosquitoes from cities was impossible, reintroduction occurred when global travel became frequent and the new vector, *A. albopictus,* was imported from Asia. Nowadays, investigators are trying to sterilize mosquitoes through genetically engineered endosymbiotic bacteria *Wolbachia* (Zheng et al., 2019), but debate on its long-term ecological influence is continuing.

Leaving the eco-system intact, our investigations on NS1 provided an alternative strategy to block flavivirus-mosquito transmission which is more specific and environmentally friendly. Soluble NS1 hexamers are secreted during virus infection, and a high concentration of plasma NS1 coexists with viremia during the acute phase of disease. We demonstrated that blood meal from infected mice that have NS1 antigenemia can suppress the expression of immune genes (JAK-STAT, ROS) in midgut of mosquitoes, facilitating flavivirus acquisition by mosquitoes. Although transferring NS1 antibody to AG6 mice did not affect the viremia in mice directly, it significantly inhibited DENV-2 transmission from AG6 mice to mosquitoes (Liu J. et al., 2016). Immunization generated NS1 antibodies might competitively bind to soluble NS1 in blood and prevent NS1 from suppressing the expression of immune genes in midgut of mosquitoes after a blood meal. Furthermore, we demonstrated that NS1 antigenemia also determined ZIKV infectivity in mosquitoes. Specifically, comparing with ZIKV Asian strains that were isolated before recent outbreaks, contemporary strains causing recent epidemics have an alanine-to-valine substitution at the 188th residue in NS1. This mutation results in higher level of NS1 secretion, which subsequently dampens the expression of immune genes in mosquito and is responsible for the enhanced infectivity in mosquitoes. This mechanism helps to explain how ZIKV of Asian lineage acquired the ability to rapidly spread from Asia to America (Liu Y. et al., 2017).

Besides blockade of viral transmission, NS1 antibodies have been identified to have multiple other roles in immunity and host pathology, some of which are completely opposite. Previously, soluble DENV NS1 was found to contribute directly to vascular leakage through increasing endothelial permeability and degradation of endothelial glycocalyx components, or indirectly through inducing vasoactive cytokines (TNF-α, IL-1β, and IL-6) via TLR-4 activation (Beatty et al., 2015; Modhiran et al., 2015; Glasner et al., 2017). Further study on DENV, WNV, YFV, JEV, and ZIKV revealed that the effect of NS1 on cell permeability was probably universal in flavivirus but had tissue-specificity and thus there are different disease patterns for different viruses (Puerta-Guardo et al., 2019). In addition, DENV NS1 also facilitates viral immune evasion through inhibiting complement cascade in mammals (Avirutnan et al., 2010). Therefore, blocking NS1 through specific antibodies has been shown to attenuate plasma leakage and mortality in dengue infected mice (Henchal et al., 1988; Wan et al., 2017). Because a fraction of NS1 dimer also presents on the surface of infected cells, antibodies also probably target Fcγ-receptors to mediate viral clearance by phagocytosis or initiate complement dependent cytotoxicity (CDC). Recent investigations show that transferring ZIKV NS1 antibodies from human or vaccinated mice to IFN deficient mice provided protection through Fcγ-receptor mediated pathway (Bailey et al., 2018, 2019). On the contrary, much evidence also indicated NS1 antibodies being capable of cross-react with coagulation factors and adhesin molecules on platelets and endothelial cells, causing disruption of platelet aggregation and apoptosis of endothelial cells, and thus leading to pathology in DENV infections (Falconar, 1997; Lin et al., 2005; Cheng et al., 2009; Liu et al., 2011).

Based on these evidence, we had constructed a modified DENV2 sNS1 with deletion of epitopes mimicking autoantigens (ΔNS1), and found that prior immunization with either ΔNS1 or full-length NS1 in AG6 mice significantly helped to neutralize NS1 antigenemia and block the transmission of virus to mosquitoes. Notably, unlike antibodies elicited to full-length NS1, antibodies generated against ΔNS1 did not cross-react

with human endothelial cells or human primary platelets. And after infection, viremia in mice immunized with modified-NS1 (ΔNS1) was significantly lower than those of mock or full-length NS1 immunized mice (Liu J. et al., 2016). In agreement with these results, mice immunized with ΔNS1 showed less vascular leakage and higher survival rate in AG6 mice after DENV-2 challenge, compared to mice that were immunized with full-length NS1 or PBS. Collectively, through antibodies specific to NS1 proteins that have been removed cross-reactive epitopes to autoantigens, we had successfully overcome the adverse effect of NS1 antibodies, blocked virus transmission, inhibited virus replication and protected mice from lethal diseases. Importantly, antibodies to NS1 do not have any risk of inducing ADE.

All above suggest that NS1 is an important target for blocking DENV/ZIKV human-mosquito transmission, and the modified NS1 elicits protective immunity toward ZIKV/DENV infection. Inclusion of suitable form of NS1 in human vaccine might offer a better chance for defeating DENV and ZIKV epidemics.

## SPECIAL CONCERNS IN THE DEVELOPMENT OF ZIKV AND DENV VACCINES

Because ZIKV and DENV have different pathogenic characteristics and tropism, special issues should be considered during the development of vaccines to these viruses, especially for prophylactic ZIKV vaccines which are currently under development by several research groups (Richner et al., 2017b; Tebas et al., 2017; Medina et al., 2018; Modjarrad et al., 2018; Zou et al., 2018).

At the early stage of vaccine development for these two viruses, the primary aims are to inhibit virus replication in vaccinated animals, and to reduce mortality in lethal infection murine models. However, ZIKV has the ability to infect and replicate in reproductive systems, it can disseminate through sexual and vertical transmission, and it is associated with increased incidence of microcephaly in fetus. It is still unclear what level of viral load is enough to cause vertical or sexual transmission, or induce inflammation in these tissues and placenta, or damage testicle, or contribute to fetal microcephaly. According to the literature, viral clearance might be more difficult in these organs comparing to others (Barzon et al., 2016; Govero et al., 2016; Mansuy et al., 2016; Prisant et al., 2016; Miner and Diamond, 2017). Therefore, during ZIKV vaccine development, specified criteria for protective efficacies should include reduced neuropathology in adult mice, inhibited vertical transmission to fetus in pregnant animals, and decreased damages to reproductive systems. In contrast, evaluation of DENV vaccine in disease models mainly includes blockage of vascular leakage or hemorrhagic manifestations in mouse model.

Correspondingly, in clinical trial, severe dengue (DHS/DSS), virologically confirmed dengue, and hospitalization were the three major parameters to evaluate DENV vaccine candidates (Hadinegoro et al., 2015; Biswal et al., 2019). In addition to these three parameters, for the evaluation of ZIKV vaccine, other parameters might have to be included, such as neurological diseases (Guillain-Barre syndrome, fetal brain development abnormality).

To fulfill the criteria above, ZIKV vaccine strategy should also be modified, since the characteristics and type of protective immune responses in different organs are not the same. For example, the access of T cells to maternal-fetal interface was limited during pregnancy (Nancy et al., 2012). It has been found that weaker T cell responses were elicited by a live attenuated ZIKV vaccine during pregnancy, comparing to that in non-pregnant mice. In addition, higher neutralizing antibody titers were required to protect pregnant mice and block vertical transmission of ZIKV (Shan et al., 2019). Such evidence warrants a vaccine with higher potency in eliciting T cell and B cell immunity. In another study, it is observed that CD4 + T cell mediated antibody response, but not CD8 + T cells, was essential for viral clearance in intravaginal infection model. Though further investigations are necessary, this might imply the importance of CD4 + T cell immunity in blocking sexual transmission, which should also be considered during vaccine design (Elong Ngono et al., 2019).

## A ONE-TWO PUNCH STRATEGY

After it is discovered for 70 years, we are still searching for better approaches to defeat dengue viruses. The sudden outbreaks of Zika virus has brought additional difficulties to solve the dengue problem, because the pre-existing ZIKV antibodies have the potential to enhance DENV infection, and antibodies elicited by dengue vaccines also have the potential to augment ZIKV infection. However, as for any other scientific challenges before, the large global outbreak of ZIKV has brought in extensive investigations on flavivirus virology, immunology, vaccinology, vector biology, and new tools to counteract the diseases. To combat mosquito-borne viruses, a one-two punch strategy that combines human preventive vaccine and vector blockade to cut transmission cycles at multiple steps may be necessary (as **Figure 3** shows). Compared with other approaches for vector blockade, active immunization with NS1/ΔNS1 in human, is more feasible and has less spillover effect on ecology. Application of B cell vaccines producing broadly neutralizing antibodies may efficiently block virus infection in human and inhibit both vertical and sexual transmission of ZIKV. In addition, T cell vaccine can act in synergy with B cell vaccine to elicit functional T cell responses that inhibit virus replication in human, aiding to protect human from severe disease. At a minimal, incorporating NS1 within both B cell and T cell vaccines will likely to help overcoming the effect of ADE in human, blocking transmission to mosquitos, and providing opportunities for total disease control. However, further experimental evaluation on the feasibility, efficiency and safety of these approaches are necessary.

## SUMMARY

We have reviewed the existing knowledge on epidemiology, molecular virology, and vaccine development of DENV and ZIKV; and updated our understanding on

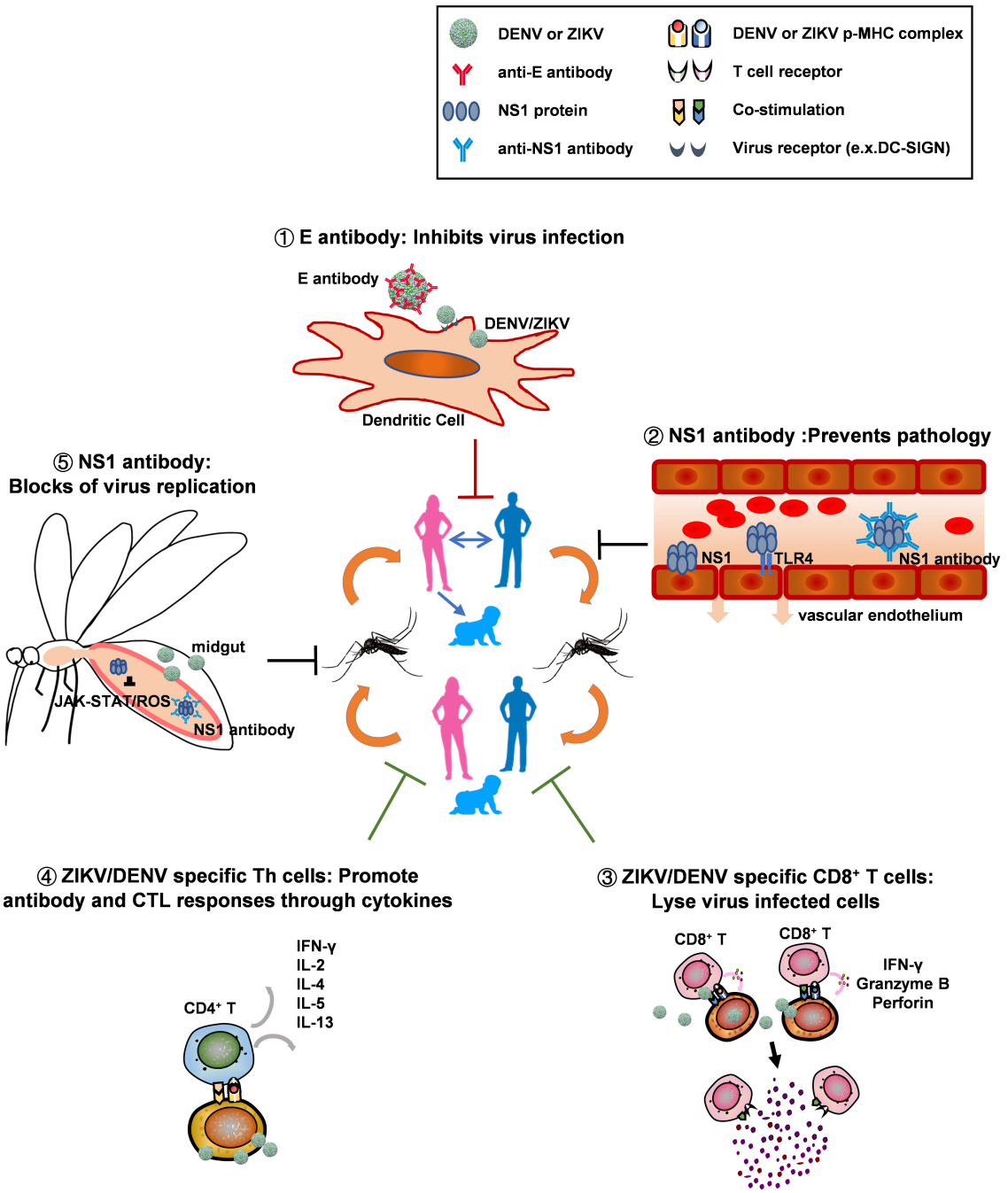


**FIGURE 3 |** Urban cycle of dengue and Zika virus transmission can be blocked at multiple steps by vaccine elicited immune responses. Both dengue and Zika viruses are transmitted between human through mosquitoes in urban areas, where prevention measures can be applied. By human immunization with universal or pentavalent vaccines that elicit both T cell and B cell responses, especially those that also target NS1antigens, viral transmission in the urban cycle may be blocked and viral diseases can be controlled at multiple steps: (1) Virus transmission to humans and virus replication *in vivo* are inhibited by broadly neutralizing antibodies specific for envelope proteins; these antibodies block virus attachment and virus entry in dendritic cells or other target cells such as monocytes and macrophages; (2) Antibodies specific for NS1 proteins; these can reduce virus induced pathology in human through preventing NS1 hexamers attachment to endothelial cells, because the attachment may trigger the degradation of endothelial glycocalyx components or activate TLR4 pathway to produce vasoactive cytokines, both of which will increase endothelium permeability; (3) Virus replication in human is inhibited by functional CD8 + T cells. Vaccine induced memory CD8 + T cells can be activated by infected cells that present DENV or ZIKV peptides in the context of MHC-I molecules, and activated CD8 + T cells directly lyse infected cells by secreting granzyme B and perforin; (4) Both CD8 + T cell and antibody-producing B cell responses are facilitated by activated CD4 + T helper (Th) cells that secret cytokines such as IFN-γ, IL-2,IL-4, IL-5, or IL-13; (5) Viral transmission to mosquitoes is inhibited by NS1 antibodies. Mosquitoes acquire both NS1 protein and virus particles during a blood meal from acutely infected patients. The NS1 antigenemia could help virus to replicate in the midgut of mosquitoes, by antagonizing mosquito immunity such as JAK-STAT and ROS pathways. The abundant NS1 antibodies in human plasma of vaccine recipients may bind to NS1 protein and thus neutralize the antagonistic effect of NS1 to mosquito immunity, resulting in restriction of virus propagation in the midgut of mosquitoes.

protective immunity against DENV and ZIKV. We have also discussed recent discoveries on the functions of flavivirus NS1 in viral pathogenesis and transmission. Based on such knowledge, we proposed a potential one-two punch strategy that overcomes ADE and defeats Dengue and Zika viruses through a combination of vaccines and vector blockade.

## AUTHOR CONTRIBUTIONS

XJ conceived, drafted, and wrote the manuscript. JS drafted and wrote the manuscript. ZZ assisted to make the tables and drew the figure. SD and GC modified the manuscript, assisted to write, and amended the sections on NS1.

## FUNDING

This work was supported by the grant: National Natural Science Foundation of China, 31670941; Ministry of Science and Technology of People's Republic of China, 2016YFC1201000; Strategic Priority Research Program of the Chinese Academy of Sciences, XDB29040000; and Science and Technology Commission of Shanghai Municipality, 19ZR1462900.

## REFERENCES

Abbink, P., Larocca, R. A., Dejnirattisai, W., Peterson, R., Nkolola, J. P., Borducchi, E. N., et al. (2018). Therapeutic and protective efficacy of a dengue antibody against Zika infection in rhesus monkeys. *Nat. Med.* 24, 721–723. doi: 10.1038/s41591-018-0056-0

Avirutnan, P., Fuchs, A., Hauhart, R. E., Somnuke, P., Youn, S., Diamond, M. S., et al. (2010). Antagonism of the complement component C4 by flavivirus nonstructural protein NS1. *J. Exp. Med.* 207, 793–806. doi: 10.1084/jem.20092545

Bailey, M. J., Broecker, F., Duehr, J., Arumemi, F., Krammer, F., Palese, P., et al. (2019). Antibodies elicited by an ns1-based vaccine protect mice against Zika Virus. *MBio* 10, e2861–e2818. doi: 10.1128/mBio.02861-18

Bailey, M. J., Duehr, J., Dulin, H., Broecker, F., Brown, J. A., Arumemi, F. O., et al. (2018). Human antibodies targeting Zika virus NS1 provide protection against disease in a mouse model. *Nat. Commun.* 9:4560. doi: 10.1038/s41467-018-07008-0

Bardina, S. V., Bunduc, P., Tripathi, S., Duehr, J., Frere, J. J., Brown, J. A., et al. (2017). Enhancement of Zika virus pathogenesis by preexisting antiflavivirus immunity. *Science* 356, 175–180. doi: 10.1126/science.aal4365

Barnett, R. (2017). Dengue. *Lancet* 390:1941. doi: 10.1016/S0140-6736(17)32651-X

Barzon, L., Pacenti, M., Franchin, E., Lavezzo, E., Trevisan, M., Sgarabotto, D., et al. (2016). Infection dynamics in a traveller with persistent shedding of Zika virus RNA in semen for six months after returning from Haiti to Italy, January 2016. *Euro Surveill* 21:30316. doi: 10.2807/1560-7917.ES.2016.21.32.30316

Baud, D., Gubler, D. J., Schaub, B., Lanteri, M. C., and Musso, D. (2017). An update on Zika virus infection. *Lancet* 390, 2099–2109. doi: 10.1016/S0140-6736(17)31450-2

Beatty, P. R., Puerta-Guardo, H., Killingbeck, S. S., Glasner, D. R., Hopkins, K., and Harris, E. (2015). Dengue virus NS1 triggers endothelial permeability and vascular leak that is prevented by NS1 vaccination. *Sci. Transl. Med.* 7:304ra141. doi: 10.1126/scitranslmed.aaa3787

Beckett, C. G., Tjaden, J., Burgess, T., Danko, J. R., Tamminga, C., Simmons, M., et al. (2011). Evaluation of a prototype dengue-1 DNA vaccine in a Phase 1 clinical trial. *Vaccine* 29, 960–968. doi: 10.1016/j.vaccine.2010.11.050

Beltramello, M., Williams, K. L., Simmons, C. P., Macagno, A., Simonelli, L., Quyen, N. T., et al. (2010). The human immune response to Dengue virus is dominated by highly cross-reactive antibodies endowed with neutralizing and enhancing activity. *Cell Host Microbe* 8, 271–283. doi: 10.1016/j.chom.2010.08.007

Bhamarapravati, N., Yoksan, S., Chayaniyayothin, T., Angsubphakorn, S., and Bunyaratvej, A. (1987). Immunization with a live attenuated dengue-2-virus candidate vaccine (16681-PDK 53): clinical, immunological and biological responses in adult volunteers. *Bull World Health Organ.* 65, 189–195.

Bhatt, S., Gething, P. W., Brady, O. J., Messina, J. P., Farlow, A. W., Moyes, C. L., et al. (2013). The global distribution and burden of dengue. *Nature* 496, 504–507. doi: 10.1038/nature12060

Biswal, S., Reynales, H., Saez-Llorens, X., Lopez, P., Borja-Tabora, C., Kosalaraksa, P., et al. (2019). Efficacy of a tetravalent dengue vaccine in healthy children and adolescents. *N. Engl. J. Med.* 381, 2009–2019. doi: 10.1056/NEJMoa1903869

Blackley, S., Kou, Z., Chen, H., Quinn, M., Rose, R. C., Schlesinger, J. J., et al. (2007). Primary human splenic macrophages, but not T or B cells, are the principal target cells for dengue virus infection in vitro. *J. Virol.* 81, 13325–13334. doi: 10.1128/JVI.01568-07

Blaney, JE Jr, Johnson, D. H., Firestone, C. Y., Hanson, C. T., Murphy, B. R., and Whitehead, S. S. (2001). Chemical mutagenesis of dengue virus type 4 yields mutant viruses which are temperature sensitive in vero cells or human liver cells and attenuated in mice. *J. Virol.* 75, 9731–9740. doi: 10.1128/JVI.75.20.9731-9740.2001

Blaney, JE Jr, Sathe, N. S., Goddard, L., Hanson, C. T., Romero, T. A., Hanley, K. A., et al. (2008). Dengue virus type 3 vaccine candidates generated by introduction of deletions in the 3′ untranslated region (3′-UTR) or by exchange of the DENV-3 3'-UTR with that of DENV-4. *Vaccine* 26, 817–828. doi: 10.1016/j.vaccine.2007.11.082

Block, O. K., Rodrigo, W. W., Quinn, M., Jin, X., Rose, R. C., and Schlesinger, J. J. (2010). A tetravalent recombinant dengue domain III protein vaccine stimulates neutralizing and enhancing antibodies in mice. *Vaccine* 28, 8085–8094. doi: 10.1016/j.vaccine.2010.10.004

Brady, O. J., Gething, P. W., Bhatt, S., Messina, J. P., Brownstein, J. S., Hoen, A. G., et al. (2012). Refining the global spatial limits of dengue virus transmission by evidence-based consensus. *PLoS Negl. Trop. Dis.* 6:e1760. doi: 10.1371/journal.pntd.0001760

Brandler, S., Brown, N., Ermak, T. H., Mitchell, F., Parsons, M., Zhang, Z., et al. (2005). Replication of chimeric yellow fever virus-dengue serotype 1-4 virus vaccine strains in dendritic and hepatic cells. *Am. J. Trop. Med. Hyg.* 72, 74–81. doi: 10.4269/ajtmh.2005.72.74

Campos, G. S., Bandeira, A. C., and Sardi, S. I. (2015). Zika virus outbreak. Bahia, Brazil. *Emerg. Infect. Dis.* 21, 1885–1886. doi: 10.3201/eid2110.150847

Capeding, M. R., Tran, N. H., Hadinegoro, S. R., Ismail, H. I., Chotpitayasunondh, T., Chua, M. N., et al. (2014). Clinical efficacy and safety of a novel tetravalent dengue vaccine in healthy children in Asia: a phase 3, randomised, observer-masked, placebo-controlled trial. *Lancet* 384, 1358–1365. doi: 10.1016/S0140-6736(14)61060-6

Carey, D. E. (1971). Chikungunya and dengue: a case of mistaken identity? *J. Hist. Med. Allied Sci.* 26, 243–262. doi: 10.1093/jhmas/xxvi.3.243

Cheng, H. J., Lei, H. Y., Lin, C. F., Luo, Y. H., Wan, S. W., Liu, H. S., et al. (2009). Anti-dengue virus nonstructural protein 1 antibodies recognize protein disulfide isomerase on platelets and inhibit platelet aggregation. *Mol. Immunol.* 47, 398–406. doi: 10.1016/j.molimm.2009.08.033

Clarke, T. (2002). Dengue virus: break-bone fever. *Nature* 416, 672–674. doi: 10.1038/416672a

Clements, D. E., Coller, B. A., Lieberman, M. M., Ogata, S., Wang, G., Harada, K. E., et al. (2010). Development of a recombinant tetravalent dengue virus vaccine: immunogenicity and efficacy studies in mice and monkeys. *Vaccine* 28, 2705–2715. doi: 10.1016/j.vaccine.2010.01.022

Collins, M. H., Tu, H. A., Gimblet-Ochieng, C., Liou, G. A., Jadi, R. S., Metz, S. W., et al. (2019). Human antibody response to Zika targets type-specific quaternary structure epitopes. *JCI Insight* 4:e123588. doi: 10.1172/jci.insight.124588

Costa, S. M., Yorio, A. P., Goncalves, A. J., Vidale, M. M., Costa, E. C., Mohana-Borges, R., et al. (2011). Induction of a protective response in mice by the dengue virus NS3 protein using DNA vaccines. *PLoS One* 6:e25685. doi: 10.1371/journal.pone.0025685

Cresswell, P., Ackerman, A. L., Giodini, A., Peaper, D. R., and Wearsch, P. A. (2005). Mechanisms of MHC class I-restricted antigen processing and cross-presentation. *Immunol. Rev.* 207, 145–157. doi: 10.1111/j.0105-2896.2005.00316.x

Crill, W. D., and Chang, G. J. (2004). Localization and characterization of flavivirus envelope glycoprotein cross-reactive epitopes. *J. Virol.* 78, 13975–13986. doi: 10.1128/JVI.78.24.13975-13986.2004

Dalrymple, N. A., and Mackow, E. R. (2012). Endothelial cells elicit immune-enhancing responses to dengue virus infection. *J. Virol.* 86, 6408–6415. doi: 10.1128/JVI.00213-12

Dayan, G. H., Garbes, P., Noriega, F., Izoton, de Sadovsky, A. D., Rodrigues, P. M., et al. (2013a). Immunogenicity and safety of a recombinant tetravalent dengue vaccine in children and adolescents ages 9-16 years in Brazil. *Am. J. Trop. Med. Hyg.* 89, 1058–1065. doi: 10.4269/ajtmh.13-0304

Dayan, G. H., Thakur, M., Boaz, M., and Johnson, C. (2013b). Safety and immunogenicity of three tetravalent dengue vaccine formulations in healthy adults in the USA. *Vaccine* 31, 5047–5054. doi: 10.1016/j.vaccine.2013.08.088

de Alwis, R., Williams, K. L., Schmid, M. A., Lai, C. Y., Patel, B., Smith, S. A., et al. (2014). Dengue viruses are enhanced by distinct populations of serotype cross-reactive antibodies in human immune sera. *PLoS Pathog.* 10:e1004386. doi: 10.1371/journal.ppat.1004386

Dejnirattisai, W., Jumnainsong, A., Onsirisakul, N., Fitton, P., Vasanawathana, S., Limpitikul, W., et al. (2010). Cross-reacting antibodies enhance dengue virus infection in humans. *Science* 328, 745–748. doi: 10.1126/science.1185181

Dejnirattisai, W., Supasa, P., Wongwiwat, W., Rouvinski, A., Barba-Spaeth, G., Duangchinda, T., et al. (2016). Dengue virus sero-cross-reactivity drives antibody-dependent enhancement of infection with zika virus. *Nat. Immunol.* 17, 1102–1108. doi: 10.1038/ni.3515

Dejnirattisai, W., Wongwiwat, W., Supasa, S., Zhang, X., Dai, X., Rouvinski, A., et al. (2015). A new class of highly potent, broadly neutralizing antibodies isolated from viremic patients infected with dengue virus. *Nat. Immunol.* 16, 170–177. doi: 10.1038/ni.3058

Dick, G. W., Kitchen, S. F., and Haddow, A. J. (1952). Zika virus. I. Isolations and serological specificity. *Trans. R Soc. Trop. Med. Hyg.* 46, 509–520. doi: 10.1016/0035-9203(52)90042-4

Duangchinda, T., Dejnirattisai, W., Vasanawathana, S., Limpitikul, W., Tangthawornchaikul, N., Malasit, P., et al. (2010). Immunodominant T-cell responses to dengue virus NS3 are associated with DHF. *Proc. Natl. Acad. Sci. U.S.A.* 107, 16922–16927. doi: 10.1073/pnas.1010867107

Duffy, M. R., Chen, T. H., Hancock, W. T., Powers, A. M., Kool, J. L., Lanciotti, R. S., et al. (2009). Zika virus outbreak on Yap Island. Federated States of Micronesia. *N. Engl. J. Med.* 360, 2536–2543. doi: 10.1056/NEJMoa0805715

Dung, N. T., Duyen, H. T., Thuy, N. T., Ngoc, T. V., Chau, N. V., Hien, T. T., et al. (2010). Timing of CD8+ T cell responses in relation to commencement of capillary leakage in children with dengue. *J. Immunol.* 184, 7281–7287. doi: 10.4049/jimmunol.0903262

Durbin, A., and Wilder-Smith, A. (2017). An update on Zika vaccine developments. *Expert Rev. Vaccines* 16, 781–787. doi: 10.1080/14760584.2017.1345309

Durbin, A. P., Kirkpatrick, B. D., Pierce, K. K., Elwood, D., Larsson, C. J., Lindow, J. C., et al. (2013). A single dose of any of four different live attenuated tetravalent dengue vaccines is safe and immunogenic in flavivirus-naive adults: a randomized, double-blind clinical trial. *J. Infect. Dis.* 207, 957–965. doi: 10.1093/infdis/jis936

Durbin, A. P., McArthur, J. H., Marron, J. A., Blaney, J. E., Thumar, B., Wanionek, K., et al. (2006). rDEN2/4Delta30(ME), a live attenuated chimeric dengue serotype 2 vaccine is safe and highly immunogenic in healthy dengue-naive adults. *Hum. Vaccin* 2, 255–260. doi: 10.4161/hv.2.6.3494

Durbin, A. P., Whitehead, S. S., McArthur, J., Perreault, J. R., Blaney, JE Jr, Thumar, B., et al. (2005). rDEN4delta30, a live attenuated dengue virus type 4 vaccine candidate, is safe, immunogenic, and highly infectious in healthy adult volunteers. *J. Infect. Dis.* 191, 710–718. doi: 10.1086/427780

Durbin, A. P., Whitehead, S. S., Shaffer, D., Elwood, D., Wanionek, K., Thumar, B., et al. (2011). A single dose of the DENV-1 candidate vaccine rDEN1Delta30 is strongly immunogenic and induces resistance to a second dose in a randomized trial. *PLoS Negl. Trop. Dis.* 5:e1267. doi: 10.1371/journal.pntd.0001267

Elong Ngono, A., Vizcarra, E. A., Tang, W. W., Sheets, N., Joo, Y., Kim, K., et al. (2017). Mapping and role of the CD8(+) T cell response during primary Zika Virus Infection in Mice. *Cell Host Microbe* 21, 35–46. doi: 10.1016/j.chom.2016.12.010

Elong Ngono, A., Young, M. P., Bunz, M., Xu, Z., Hattakam, S., Vizcarra, E., et al. (2019). CD4+ T cells promote humoral immunity and viral control during Zika virus infection. *PLoS Pathog.* 15:e1007474. doi: 10.1371/journal.ppat.1007474

Falconar, A. K. (1997). The dengue virus nonstructural-1 protein (NS1) generates antibodies to common epitopes on human blood clotting, integrin/adhesin proteins and binds to human endothelial cells: potential implications in haemorrhagic fever pathogenesis. *Arch. Virol.* 142, 897–916. doi: 10.1007/s007050050127

Faria, N. R., Quick, J., Claro, I. M., Theze, J., de Jesus, J. G., Giovanetti, M., et al. (2017). Establishment and cryptic transmission of Zika virus in Brazil and the Americas. *Nature* 546, 406–410. doi: 10.1038/nature22401

Fatima, K., and Syed, N. I. (2018). Dengvaxia controversy: impact on vaccine hesitancy. *J. Glob. Health* 8:010312. doi: 10.7189/jogh.08-020312

Fernandez, E., Dejnirattisai, W., Cao, B., Scheaffer, S. M., Supasa, P., Wongwiwat, W., et al. (2017). Human antibodies to the dengue virus E-dimer epitope have therapeutic activity against Zika virus infection. *Nat. Immunol.* 18, 1261–1269. doi: 10.1038/ni.3849

Foo, S. S., Chen, W., Chan, Y., Bowman, J. W., Chang, L. C., Choi, Y., et al. (2017). Asian Zika virus strains target CD14(+) blood monocytes and induce M2-skewed immunosuppression during pregnancy. *Nat. Microbiol.* 2, 1558–1570. doi: 10.1038/s41564-017-0016-3

Fowler, A. M., Tang, W. W., Young, M. P., Mamidi, A., Viramontes, K. M., McCauley, M. D., et al. (2018). Maternally acquired zika antibodies enhance dengue disease severity in mice. *Cell Host Microbe* 24, 743.E5–750.e5. doi: 10.1016/j.chom.2018.09.015

Gaucher, D., Therrien, R., Kettaf, N., Angermann, B. R., Boucher, G., Filali-Mouhim, A., et al. (2008). Yellow fever vaccine induces integrated multilineage and polyfunctional immune responses. *J. Exp. Med.* 205, 3119–3131. doi: 10.1084/jem.20082292

Gaudinski, M. R., Houser, K. V., Morabito, K. M., Hu, Z., Yamshchikov, G., Rothwell, R. S., et al. (2018). Safety, tolerability, and immunogenicity of two Zika virus DNA vaccine candidates in healthy adults: randomised, open-label, phase 1 clinical trials. *Lancet* 391, 552–562. doi: 10.1016/S0140-6736(17)33105-7

George, S. L., Wong, M. A., Dube, T. J., Boroughs, K. L., Stovall, J. L., Luy, B. E., et al. (2015). Safety and immunogenicity of a live attenuated tetravalent dengue vaccine candidate in flavivirus-naive adults: a Randomized, double-blinded phase 1 Clinical Trial. *J. Infect. Dis.* 212, 1032–1041. doi: 10.1093/infdis/jiv179

Glasner, D. R., Ratnasiri, K., Puerta-Guardo, H., Espinosa, D. A., Beatty, P. R., and Harris, E. (2017). Dengue virus NS1 cytokine-independent vascular leak is dependent on endothelial glycocalyx components. *PLoS Pathog.* 13:e1006673. doi: 10.1371/journal.ppat.1006673

Govero, J., Esakky, P., Scheaffer, S. M., Fernandez, E., Drury, A., Platt, D. J., et al. (2016). Zika virus infection damages the testes in mice. *Nature* 540, 438–442. doi: 10.1038/nature20556

Govindarajan, D., Meschino, S., Guan, L., Clements, D. E., ter Meulen, J. H., Casimiro, D. R., et al. (2015). Preclinical development of a dengue tetravalent recombinant subunit vaccine: Immunogenicity and protective efficacy in nonhuman primates. *Vaccine* 33, 4105–4116. doi: 10.1016/j.vaccine.2015.06.067

Grard, G., Caron, M., Mombo, I. M., Nkoghe, D., Mboui Ondo, S., Jiolle, D., et al. (2014). Zika virus in Gabon (Central Africa)–2007: a new threat from Aedes albopictus? *PLoS Negl. Trop. Dis.* 8:e2681. doi: 10.1371/journal.pntd.0002681

Griffin, B. D., Muthumani, K., Warner, B. M., Majer, A., Hagan, M., Audet, J., et al. (2017). DNA vaccination protects mice against Zika virus-induced damage to the testes. *Nat. Commun.* 8:15743. doi: 10.1038/ncomms15743

Grifoni, A., Angelo, M. A., Lopez, B., O'Rourke, P. H., Sidney, J., Cerpas, C., et al. (2017a). Global assessment of dengue virus-specific CD4(+) T cell responses in dengue-endemic areas. *Front. Immunol.* 8:1309. doi: 10.3389/fimmu.2017.01309

Grifoni, A., Pham, J., Sidney, J., O'Rourke, P. H., Paul, S., Peters, B., et al. (2017b). Prior dengue virus exposure shapes T Cell Immunity to Zika Virus in Humans. *J. Virol.* 91:e01469-17. doi: 10.1128/JVI.01469-17

Grifoni, A., Costa-Ramos, P., Pham, J., Tian, Y., Rosales, S. L., Seumois, G., et al. (2018). Cutting edge: transcriptional profiling reveals multifunctional and

cytotoxic antiviral responses of Zika Virus-Specific CD8(+) T Cells. *J. Immunol.* 201, 3487–3491. doi: 10.4049/jimmunol.1801090

Gubler, D. J. (1987). Dengue and dengue hemorrhagic fever in the Americas. *P R Health Sci. J.* 6, 107–111.

Guirakhoo, F., Arroyo, J., Pugachev, K. V., Miller, C., Zhang, Z. X., Weltzin, R., et al. (2001). Construction, safety, and immunogenicity in nonhuman primates of a chimeric yellow fever-dengue virus tetravalent vaccine. *J. Virol.* 75, 7290–7304. doi: 10.1128/JVI.75.16.7290-7304.2001

Guirakhoo, F., Kitchener, S., Morrison, D., Forrat, R., McCarthy, K., Nichols, R., et al. (2006). Live attenuated chimeric yellow fever dengue type 2 (ChimeriVax-DEN2) vaccine: phase I clinical trial for safety and immunogenicity: effect of yellow fever pre-immunity in induction of cross neutralizing antibody responses to all 4 dengue serotypes. *Hum. Vaccin* 2, 60–67. doi: 10.4161/hv.2.2.2555

Guirakhoo, F., Pugachev, K., Arroyo, J., Miller, C., Zhang, Z. X., Weltzin, R., et al. (2002). Viremia and immunogenicity in nonhuman primates of a tetravalent yellow fever-dengue chimeric vaccine: genetic reconstructions, dose adjustment, and antibody responses against wild-type dengue virus isolates. *Virology* 298, 146–159. doi: 10.1006/viro.2002.1462

Guirakhoo, F., Weltzin, R., Chambers, T. J., Zhang, Z. X., Soike, K., Ratterree, M., et al. (2000). Recombinant chimeric yellow fever-dengue type 2 virus is immunogenic and protective in nonhuman primates. *J. Virol.* 74, 5477–5485. doi: 10.1128/jvi.74.12.5477-5485.2000

Guzman, M. G., Alvarez, M., and Halstead, S. B. (2013). Secondary infection as a risk factor for dengue hemorrhagic fever/dengue shock syndrome: an historical perspective and role of antibody-dependent enhancement of infection. *Arch. Virol.* 158, 1445–1459. doi: 10.1007/s00705-013-1645-3

Guzman, M. G., Halstead, S. B., Artsob, H., Buchy, P., Farrar, J., Gubler, D. J., et al. (2010). Dengue: a continuing global threat. *Nat. Rev,. Microbiol.* 8(Suppl.), S7–S16. doi: 10.1038/nrmicro2460

Hadinegoro, S. R., Arredondo-Garcia, J. L., Capeding, M. R., Deseda, C., Chotpitayasunondh, T., Dietze, R., et al. (2015). Efficacy and long-term safety of a dengue vaccine in regions of endemic disease. *N. Engl. J. Med.* 373, 1195–1206. doi: 10.1056/NEJMoa1506223

Halstead, S. B. (1966). Mosquito-borne haemorrhagic fevers of South and South-East Asia. *Bull. World Health Organ.* 35, 3–15.

Halstead, S. B. (1988). Pathogenesis of dengue: challenges to molecular biology. *Science* 239, 476–481. doi: 10.1126/science.3277268

Halstead, S. B. (2003). Neutralization and antibody-dependent enhancement of dengue viruses. *Adv. Virus Res.* 60, 421–467. doi: 10.1016/s0065-3527(03)60011-4

Halstead, S. B., and Dans, L. F. (2019). Dengue infection and advances in dengue vaccines for children. *Lancet Child Adolesc. Health* 3, 734–741. doi: 10.1016/S2352-4642(19)30205-6

Halstead, S. B., Mahalingam, S., Marovich, M. A., Ubol, S., and Mosser, D. M. (2010). Intrinsic antibody-dependent enhancement of microbial infection in macrophages: disease regulation by immune complexes. *Lancet Infect. Dis.* 10, 712–722. doi: 10.1016/S1473-3099(10)70166-3

Halstead, S. B., Rojanasuphot, S., and Sangkawibha, N. (1983). Original antigenic sin in dengue. *Am. J. Trop. Med. Hyg.* 32, 154–156. doi: 10.4269/ajtmh.1983.32.154

Hasan, S. S., Miller, A., Sapparapu, G., Fernandez, E., Klose, T., Long, F., et al. (2017). A human antibody against Zika virus crosslinks the E protein to prevent infection. *Nat. Commun.* 8:14722. doi: 10.1038/ncomms14722

Hassert, M., Wolf, K. J., Schwetye, K. E., DiPaolo, R. J., Brien, J. D., and Pinto, A. K. (2018). CD4+T cells mediate protection against Zika associated severe disease in a mouse model of infection. *PLoS Pathog.* 14:e1007237. doi: 10.1371/journal.ppat.1007237

Henchal, E. A., Henchal, L. S., and Schlesinger, J. J. (1988). Synergistic interactions of anti-NS1 monoclonal antibodies protect passively immunized mice from lethal challenge with dengue 2 virus. *J. Gen. Virol.* 69(Pt 8), 2101–2107. doi: 10.1099/0022-1317-69-8-2101

Higgs, S., Vanlandingham, D. L., Klingler, K. A., McElroy, K. L., McGee, C. E., Harrington, L., et al. (2006). Growth characteristics of ChimeriVax-Den vaccine viruses in Aedes aegypti and Aedes albopictus from Thailand. *Am. J. Trop. Med. Hyg.* 75, 986–993. doi: 10.4269/ajtmh.2006.75.986

Holmes, E. C., and Twiddy, S. S. (2003). The origin, emergence and evolutionary genetics of dengue virus. *Infect. Genet. Evol.* 3, 19–28. doi: 10.1016/s1567-1348(03)00004-2

Hss, A. S., Koh, M. T., Tan, K. K., Chan, L. G., Zhou, L., Bouckenooghe, A., et al. (2013). Safety and immunogenicity of a tetravalent dengue vaccine in healthy children aged 2-11 years in Malaysia: a randomized, placebo-controlled. Phase III study. *Vaccine* 31, 5814–5821. doi: 10.1016/j.vaccine.2013.10.013

Huang, H., Li, S., Zhang, Y., Han, X., Jia, B., Liu, H., et al. (2017). CD8(+) T Cell Immune Response in Immunocompetent Mice during Zika Virus Infection. *J. Virol.* 91, e900–e917. doi: 10.1128/JVI.00900-17

Jessie, K., Fong, M. Y., Devi, S., Lam, S. K., and Wong, K. T. (2004). Localization of dengue virus in naturally infected human tissues, by immunohistochemistry and in situ hybridization. *J. Infect. Dis.* 189, 1411–1418. doi: 10.1086/383043

Jin, X. (2008). Cellular and molecular basis of antibody-dependent enhancement in human dengue pathogenesis. *Future Virol.* 3, 343–361. doi: 10.2217/17460794.3.4.343

Jurado, K. A., Yockey, L. J., Wong, P. W., Lee, S., Huttner, A. J., and Iwasaki, A. (2018). Antiviral CD8 T cells induce Zika-virus-associated paralysis in mice. *Nat. Microbiol.* 3, 141–147. doi: 10.1038/s41564-017-0060-z

Katzelnick, L. C., Gresh, L., Halloran, M. E., Mercado, J. C., Kuan, G., Gordon, A., et al. (2017). Antibody-dependent enhancement of severe dengue disease in humans. *Science* 358, 929–932. doi: 10.1126/science.aan6836

Khaiboullina, S., Uppal, T., Kletenkov, K., St Jeor, S. C., Garanina, E., Rizvanov, A., et al. (2019). Transcriptome profiling reveals Pro-Inflammatory cytokines and matrix metalloproteinase activation in Zika Virus infected human umbilical vein endothelial cells. *Front. Pharmacol.* 10:642. doi: 10.3389/fphar.2019.00642

Khaiboullina, S. F., Ribeiro, F. M., Uppal, T., Martynova, E. V., Rizvanov, A. A., and Verma, S. C. (2019). Zika virus transmission through blood tissue barriers. *Front. Microbiol.* 10:1465. doi: 10.3389/fmicb.2019.01465

Kirkpatrick, B. D., Whitehead, S. S., Pierce, K. K., Tibery, C. M., Grier, P. L., Hynes, N. A., et al. (2016). The live attenuated dengue vaccine TV003 elicits complete protection against dengue in a human challenge model. *Sci Transl Med 8(330), 330ra336*. doi: 119710.1126/scitranslmed.aaf1517

Kliks, S. (1990). Antibody-enhanced infection of monocytes as the pathogenetic mechanism for severe dengue illness. *AIDS Res. Hum. Retroviruses* 6, 993–998. doi: 10.1089/aid.1990.6.993

Kou, Z., Quinn, M., Chen, H., Rodrigo, W. W., Rose, R. C., Schlesinger, J. J., et al. (2008). Monocytes, but not T or B cells, are the principal target cells for dengue virus (DV) infection among human peripheral blood mononuclear cells. *J. Med. Virol.* 80, 134–146. doi: 10.1002/jmv.21051

Kuno, G., Gubler, D. J., and Oliver, A. (1993). Use of 'original antigenic sin' theory to determine the serotypes of previous dengue infections. *Trans. R Soc. Trop. Med. Hyg.* 87, 103–105. doi: 10.1016/0035-9203(93)90444-u

Lanata, C. F., Andrade, T., Gil, A. I., Terrones, C., Valladolid, O., Zambrano, B., et al. (2012). Immunogenicity and safety of tetravalent dengue vaccine in 2-11 year-olds previously vaccinated against yellow fever: randomized, controlled, phase II study in Piura. *Peru. Vaccine* 30, 5935–5941. doi: 10.1016/j.vaccine.2012.07.043

Leborgne, C., Latournerie, V., Boutin, S., Desgue, D., Quere, A., Pignot, E., et al. (2019). Prevalence and long-term monitoring of humoral immunity against adeno-associated virus in duchenne muscular dystrophy patients. *Cell Immunol.* 342:103780. doi: 10.1016/j.cellimm.2018.03.004

Li, C., Xu, D., Ye, Q., Hong, S., Jiang, Y., Liu, X., et al. (2016). Zika virus disrupts neural progenitor development and leads to microcephaly in mice. *Cell Stem Cell* 19, 120–126. doi: 10.1016/j.stem.2016.04.017

Li, M., Wang, X., Wang, Q., Yu, L., Wang, L., Yan, J., et al. (2017). Both structure and function of human monoclonal antibodies contribute to enhancement of Zika virus infectivity in vitro. *Sci. China Life Sci.* 60, 1396–1398. doi: 10.1007/s11427-017-9192-0

Li, M., Zhao, L., Zhang, C., Wang, X., Hong, W., Sun, J., et al. (2018). Dengue immune sera enhance Zika virus infection in human peripheral blood monocytes through Fc gamma receptors. *PLoS One* 13:e0200478. doi: 10.1371/journal.pone.0200478

Liang, H., Yang, R., Liu, Z., Li, M., Liu, H., and Jin, X. (2018). Recombinant Zika virus envelope protein elicited protective immunity against Zika virus in immunocompetent mice. *PLoS One* 13:e0194860. doi: 10.1371/journal.pone.0194860

Lim, M. Q., Kumaran, E. A. P., Tan, H. C., Lye, D. C., Leo, Y. S., Ooi, E. E., et al. (2018). Cross-reactivity and anti-viral function of dengue capsid and NS3-specific memory T Cells Toward Zika Virus. *Front. Immunol.* 9:2225. doi: 10.3389/fimmu.2018.02225

Limon-Flores, A. Y., Perez-Tapia, M., Estrada-Garcia, I., Vaughan, G., Escobar-Gutierrez, A., Calderon-Amador, J., et al. (2005). Dengue virus inoculation to human skin explants: an effective approach to assess in situ the early infection and the effects on cutaneous dendritic cells. *Int. J. Exp. Pathol.* 86, 323–334. doi: 10.1111/j.0959-9673.2005.00445.x

Lin, C. F., Chiu, S. C., Hsiao, Y. L., Wan, S. W., Lei, H. Y., Shiau, A. L., et al. (2005). Expression of cytokine, chemokine, and adhesion molecules during endothelial cell activation induced by antibodies against dengue virus nonstructural protein 1. *J. Immunol.* 174, 395–403. doi: 10.4049/jimmunol.174.1.395

Lindenbach, B. D., Thiel, H. J., and Rice, C. M. (2007). "Flaviviridae:the Viruses and Their replication," in *Fields Virology*, ed. P. M. H. D. M. Knipe (Philadelphia: Wolters Kluwer Health/Lippincott Williams & Wilkins), 1101–1152.

Liu, H., Shen, W., Shu, J., Kou, Z., and Jin, X. (2017). A novel polyepitope vaccine elicited HIV peptide specific CD4+ T cell responses in HLA-A2/DRB1 transgenic mice. *PLoS One* 12:e0184207. doi: 10.1371/journal.pone.0184207

Liu, Y., Liu, J., Du, S., Shan, C., Nie, K., Zhang, R., et al. (2017). Evolutionary enhancement of Zika virus infectivity in Aedes aegypti mosquitoes. *Nature* 545, 482–486. doi: 10.1038/nature22365

Liu, I. J., Chiu, C. Y., Chen, Y. C., and Wu, H. C. (2011). Molecular mimicry of human endothelial cell antigen by autoantibodies to nonstructural protein 1 of dengue virus. *J. Biol. Chem.* 286, 9726–9736. doi: 10.1074/jbc.M110.170993

Liu, J., Liu, Y., Nie, K., Du, S., Qiu, J., Pang, X., et al. (2016). Flavivirus NS1 protein in infected host sera enhances viral acquisition by mosquitoes. *Nat. Microbiol.* 1:16087. doi: 10.1038/nmicrobiol.2016.87

Liu, S., DeLalio, L. J., Isakson, B. E., and Wang, T. T. (2016). AXL-Mediated Productive Infection of Human Endothelial Cells by Zika Virus. *Circ. Res.* 119, 1183–1189. doi: 10.1161/CIRCRESAHA.116.309866

Lok, S. M., Kostyuchenko, V., Nybakken, G. E., Holdaway, H. A., Battisti, A. J., Sukupolvi-Petty, S., et al. (2008). Binding of a neutralizing antibody to dengue virus alters the arrangement of surface glycoproteins. *Nat. Struct. Mol. Biol.* 15, 312–317. doi: 10.1038/nsmb.1382

Ma, W., Li, S., Ma, S., Jia, L., Zhang, F., Zhang, Y., et al. (2016). Zika virus causes testis damage and leads to male infertility in mice. *Cell* 167, 1511.e10–1524.e10 doi: 10.1016/j.cell.2016.11.016

Mackenzie, J. S., Gubler, D. J., and Petersen, L. R. (2004). Emerging flaviviruses: the spread and resurgence of Japanese encephalitis, West Nile and dengue viruses. *Nat. Med.* 10(Suppl.), S98–S109. doi: 10.1038/nm1144

Manoff, S. B., Sausser, M., Falk Russell, A., Martin, J., Radley, D., Hyatt, D., et al. (2019). Immunogenicity and safety of an investigational tetravalent recombinant subunit vaccine for dengue: results of a Phase I randomized clinical trial in flavivirus-naive adults. *Hum. Vaccin Immunother.* 15, 2195–2204. doi: 10.1080/21645515.2018.1546523

Mansuy, J. M., Dutertre, M., Mengelle, C., Fourcade, C., Marchou, B., Delobel, P., et al. (2016). Zika virus: high infectious viral load in semen, a new sexually transmitted pathogen? *Lancet Infect Dis.* 16:405. doi: 10.1016/S1473-3099(16)00138-9

Mantel, N., Girerd, Y., Geny, C., Bernard, I., Pontvianne, J., Lang, J., et al. (2011). Genetic stability of a dengue vaccine based on chimeric yellow fever/dengue viruses. *Vaccine* 29, 6629–6635. doi: 10.1016/j.vaccine.2011.06.101

Marianneau, P., Steffan, A. M., Royer, C., Drouet, M. T., Jaeck, D., Kirn, A., et al. (1999). Infection of primary cultures of human Kupffer cells by Dengue virus: no viral progeny synthesis, but cytokine production is evident. *J. Virol.* 73, 5201–5206. doi: 10.1128/jvi.73.6.5201-5206.1999

Martines, R. B., Bhatnagar, J., de Oliveira Ramos, A. M., Davi, H. P., Iglezias, S. D., Kanamura, C. T., et al. (2016). Pathology of congenital Zika syndrome in Brazil: a case series. *Lancet* 388, 898–904. doi: 10.1016/S0140-6736(16)30883-2

McCracken, M. K., Gromowski, G. D., Friberg, H. L., Lin, X., Abbink, P., De La Barrera, R., et al. (2017). Impact of prior flavivirus immunity on Zika virus infection in rhesus macaques. *PLoS Pathog.* 13:e1006487. doi: 10.1371/journal.ppat.1006487

McGee, C. E., Tsetsarkin, K., Vanlandingham, D. L., McElroy, K. L., Lang, J., Guy, B., et al. (2008). Substitution of wild-type yellow fever Asibi sequences for 17D vaccine sequences in ChimeriVax-dengue 4 does not enhance infection of Aedes aegypti mosquitoes. *J. Infect. Dis.* 197, 686–692. doi: 10.1086/527328

Medina, L. O., To, A., Lieberman, M. M., Wong, T. A. S., Namekar, M., Nakano, E., et al. (2018). A recombinant subunit based zika virus vaccine is efficacious in Non-human primates. *Front. Immunol.* 9:2464. doi: 10.3389/fimmu.2018.02464

Messina, J. P., Brady, O. J., Golding, N., Kraemer, M. U. G., Wint, G. R. W., Ray, S. E., et al. (2019). The current and future global distribution and population at risk of dengue. *Nat. Microbiol.* 4, 1508–1515. doi: 10.1038/s41564-019-0476-8

Metz, S. W., Thomas, A., Brackbill, A., Forsberg, J., Miley, M. J., Lopez, C. A., et al. (2019). Oligomeric state of the ZIKV E protein defines protective immune responses. *Nat. Commun.* 10:4606. doi: 10.1038/s41467-019-12677-6

Michlmayr, D., Andrade, P., Gonzalez, K., Balmaseda, A., and Harris, E. (2017). CD14(+)CD16(+) monocytes are the main target of Zika virus infection in peripheral blood mononuclear cells in a paediatric study in Nicaragua. *Nat. Microbiol.* 2, 1462–1470. doi: 10.1038/s41564-017-0035-0

Miner, J. J., and Diamond, M. S. (2017). Zika virus pathogenesis and tissue tropism. *Cell Host Microbe* 21, 134–142. doi: 10.1016/j.chom.2017.01.004

Mitragotri, S. (2006). Current status and future prospects of needle-free liquid jet injectors. *Nat. Rev. Drug Discov.* 5, 543–548. doi: 10.1038/nrd2076

Mlakar, J., Korva, M., Tul, N., Popovic, M., Poljsak-Prijatelj, M., Mraz, J., et al. (2016). Zika virus associated with microcephaly. *N. Engl. J. Med* 374, 951–958. doi: 10.1056/NEJMoa1600651

Modhiran, N., Watterson, D., Muller, D. A., Panetta, A. K., Sester, D. P., Liu, L., et al. (2015). Dengue virus NS1 protein activates cells via Toll-like receptor 4 and disrupts endothelial cell monolayer integrity. *Sci. Transl. Med.* 7:304ra142. doi: 10.1126/scitranslmed.aaa3863

Modjarrad, K., Lin, L., George, S. L., Stephenson, K. E., Eckels, K. H., De La Barrera, R. A., et al. (2018). Preliminary aggregate safety and immunogenicity results from three trials of a purified inactivated Zika virus vaccine candidate: phase 1, randomised, double-blind, placebo-controlled clinical trials. *Lancet* 391, 563–571. doi: 10.1016/S0140-6736(17)33106-9

Musso, D., Bossin, H., Mallet, H. P., Besnard, M., Broult, J., Baudouin, L., et al. (2018). Zika virus in French Polynesia 2013-14: anatomy of a completed outbreak. *Lancet Infect Dis.* 18, e172–e182. doi: 10.1016/S1473-3099(17)30446-2

Nancy, P., Tagliani, E., Tay, C. S., Asp, P., Levy, D. E., and Erlebacher, A. (2012). Chemokine gene silencing in decidual stromal cells limits T cell access to the maternal-fetal interface. *Science* 336, 1317–1321. doi: 10.1126/science.1220030

Netto, E. M., Moreira-Soto, A., Pedroso, C., Hoser, C., Funk, S., Kucharski, A. J., et al. (2017). High Zika virus seroprevalence in salvador, northeastern brazil limits the potential for further outbreaks. *MBio* 8:01390-17. doi: 10.1128/mBio.01390-17

Ngono, A. E., and Shresta, S. (2018). Immune response to dengue and zika. *Annu. Rev. Immunol.* 36, 279–308. doi: 10.1146/annurev-immunol-042617-053142

Osorio, J. E., Partidos, C. D., Wallace, D., and Stinchcomb, D. T. (2015). Development of a recombinant, chimeric tetravalent dengue vaccine candidate. *Vaccine* 33, 7112–7120. doi: 10.1016/j.vaccine.2015.11.022

Osorio, J. E., Velez, I. D., Thomson, C., Lopez, L., Jimenez, A., Haller, A. A., et al. (2014). Safety and immunogenicity of a recombinant live attenuated tetravalent dengue vaccine (DENVax) in flavivirus-naive healthy adults in Colombia: a randomised, placebo-controlled, phase 1 study. *Lancet Infect Dis.* 14, 830–838. doi: 10.1016/S1473-3099(14)70811-4

Packard, R. M. (2016). The Fielding H. Garrison Lecture: "Break-Bone" Fever in Philadelphia, 1780: Reflections on the History of Disease. *Bull. Hist Med.* 90, 193–221. doi: 10.1353/bhm.2016.0041

Pantoja, P., Perez-Guzman, E. X., Rodriguez, I. V., White, L. J., Gonzalez, O., Serrano, C., et al. (2017). Zika virus pathogenesis in rhesus macaques is unaffected by pre-existing immunity to dengue virus. *Nat. Commun.* 8:15674. doi: 10.1038/ncomms15674

Papa, M. P., Meuren, L. M., Coelho, S. V. A., Lucas, C. G. O., Mustafa, Y. M., Lemos Matassoli, F., et al. (2017). Zika Virus infects, activates, and crosses brain microvascular endothelial cells, without barrier disruption. *Front. Microbiol.* 8:2557. doi: 10.3389/fmicb.2017.02557

Pierson, T. C., Xu, Q., Nelson, S., Oliphant, T., Nybakken, G. E., Fremont, D. H., et al. (2007). The stoichiometry of antibody-mediated neutralization and enhancement of West Nile virus infection. *Cell Host Microbe* 1, 135–145. doi: 10.1016/j.chom.2007.03.002

Porter, K. R., Ewing, D., Chen, L., Wu, S. J., Hayes, C. G., Ferrari, M., et al. (2012). Immunogenicity and protective efficacy of a vaxfectin-adjuvanted tetravalent dengue DNA vaccine. *Vaccine* 30, 336–341. doi: 10.1016/j.vaccine.2011.10.085

Prasad, V. M., Miller, A. S., Klose, T., Sirohi, D., Buda, G., Jiang, W., et al. (2017). Structure of the immature Zika virus at 9 A resolution. *Nat. Struct. Mol. Biol.* 24, 184–186. doi: 10.1038/nsmb.3352

Prisant, N., Bujan, L., Benichou, H., Hayot, P. H., Pavili, L., Lurel, S., et al. (2016). Zika virus in the female genital tract. *Lancet Infect Dis.* 16, 1000–1001. doi: 10.1016/S1473-3099(16)30193-1

Puerta-Guardo, H., Glasner, D. R., Espinosa, D. A., Biering, S. B., Patana, M., Ratnasiri, K., et al. (2019). Flavivirus NS1 triggers tissue-specific vascular endothelial dysfunction reflecting disease tropism. *Cell Rep.* 26, 1598.e8–1613.e8. doi: 10.1016/j.celrep.2019.01.036

Qian, X., Nguyen, H. N., Jacob, F., Song, H., and Ming, G. L. (2017). Using brain organoids to understand Zika virus-induced microcephaly. *Development* 144, 952–957. doi: 10.1242/dev.140707

Quicke, K. M., Bowen, J. R., Johnson, E. L., McDonald, C. E., Ma, H., O'Neal, J. T., et al. (2016). Zika Virus Infects Human Placental Macrophages. *Cell Host Microbe* 20, 83–90. doi: 10.1016/j.chom.2016.05.015

Regla-Nava, J. A., Elong Ngono, A., Viramontes, K. M., Huynh, A. T., Wang, Y. T., Nguyen, A. T., et al. (2018). Cross-reactive Dengue virus-specific CD8(+) T cells protect against Zika virus during pregnancy. *Nat. Commun.* 9:3042. doi: 10.1038/s41467-018-05458-0

Richner, J. M., Himansu, S., Dowd, K. A., Butler, S. L., Salazar, V., Fox, J. M., et al. (2017a). Modified mRNA vaccines protect against Zika Virus Infection. *Cell* 169:176. doi: 10.1016/j.cell.2017.03.016

Richner, J. M., Jagger, B. W., Shan, C., Fontes, C. R., Dowd, K. A., Cao, B., et al. (2017b). Vaccine mediated protection against Zika virus-induced congenital disease. *Cell* 170, 273.e12–283.e12. doi: 10.1016/j.cell.2017.06.040

Rivino, L., Tan, A. T., Chia, A., Kumaran, E. A., Grotenbreg, G. M., MacAry, P. A., et al. (2013). Defining CD8+ T cell determinants during human viral infection in populations of Asian ethnicity. *J. Immunol.* 191, 4010–4019. doi: 10.4049/jimmunol.1301507

Robbiani, D. F., Bozzacco, L., Keeffe, J. R., Khouri, R., Olsen, P. C., Gazumyan, A., et al. (2017). Recurrent potent human neutralizing antibodies to zika virus in brazil and mexico. *Cell* 169, 597.e11–609.e11. doi: 10.1016/j.cell.2017.04.024

Roche, P. A., and Furuta, K. (2015). The ins and outs of MHC class II-mediated antigen processing and presentation. *Nat. Rev. Immunol.* 15, 203–216. doi: 10.1038/nri3818

Rodenhuis-Zybert, I. A., van der Schaar, H. M., da Silva, Voorham, J. M., van der Ende-Metselaar, H., Lei, H. Y., et al. (2010). Immature dengue virus: a veiled pathogen? *PLoS Pathog.* 6:e1000718. doi: 10.1371/journal.ppat.1000718

Rodriguez-Barraquer, I., Costa, F., Nascimento, E. J. M., Nery, N. J., Castanha, P. M. S., Sacramento, G. A., et al. (2019). Impact of preexisting dengue immunity on Zika virus emergence in a dengue endemic region. *Science* 363, 607–610. doi: 10.1126/science.aav6618

Rothman, A. L., Medin, C. L., Friberg, H., and Currier, J. R. (2014). Immunopathogenesis versus protection in dengue virus infections. *Curr. Trop. Med. Rep.* 1, 13–20. doi: 10.1007/s40475-013-0009-0

Rouvinski, A., Dejnirattisai, W., Guardado-Calvo, P., Vaney, M. C., Sharma, A., Duquerroy, S., et al. (2017). Covalently linked dengue virus envelope glycoprotein dimers reduce exposure of the immunodominant fusion loop epitope. *Nat. Commun.* 8:15411. doi: 10.1038/ncomms15411

Rouvinski, A., Guardado-Calvo, P., Barba-Spaeth, G., Duquerroy, S., Vaney, M. C., Kikuti, C. M., et al. (2015). Recognition determinants of broadly neutralizing human antibodies against dengue viruses. *Nature* 520, 109–113. doi: 10.1038/nature14130

Rush, B. (1951). An account of the bilious remitting fever: as it appeared in philadelphia, in the summer and autumn of the year 1780. *Am. J. Med.* 11, 546–550. doi: 10.1016/0002-9343(51)90035-6

Sabchareon, A., Wallace, D., Sirivichayakul, C., Limkittikul, K., Chanthavanich, P., Suvannadabba, S., et al. (2012). Protective efficacy of the recombinant, live-attenuated, CYD tetravalent dengue vaccine in Thai schoolchildren: a randomised, controlled phase 2b trial. *Lancet* 380, 1559–1567. doi: 10.1016/S0140-6736(12)61428-7

Sabin, A. B. (1952). Research on dengue during World War II. *Am. J. Trop. Med. Hyg.* 1, 30–50. doi: 10.4269/ajtmh.1952.1.30

Sadegh-Nasseri, S., and Kim, A. (2019). Selection of immunodominant epitopes during antigen processing is hierarchical. *Mol. Immunol.* 113, 115–119. doi: 10.1016/j.molimm.2018.08.011

Sanchez-San Martin, C., Li, T., Bouquet, J., Streithorst, J., Yu, G., Paranjpe, A., et al. (2018). Differentiation enhances Zika virus infection of neuronal brain cells. *Sci. Rep.* 8:14543. doi: 10.1038/s41598-018-32400-7

Sangkawibha, N., Rojanasuphot, S., Ahandrik, S., Viriyapongse, S., Jatanasen, S., Salitul, V., et al. (1984). Risk factors in dengue shock syndrome: a prospective epidemiologic study in Rayong. Thailand. I. The 1980 outbreak. *Am. .J Epidemiol.* 120, 653–669. doi: 10.1093/oxfordjournals.aje.a113932

Sapparapu, G., Fernandez, E., Kose, N., Bin, C., Fox, J. M., Bombardi, R. G., et al. (2016). Neutralizing human antibodies prevent Zika virus replication and fetal disease in mice. *Nature* 540, 443–447. doi: 10.1038/nature20564

Shan, C., Muruato, A. E., Jagger, B. W., Richner, J., Nunes, B. T. D., Medeiros, D. B. A., et al. (2017). A single-dose live-attenuated vaccine prevents Zika virus pregnancy transmission and testis damage. *Nat. Commun.* 8:676. doi: 10.1038/s41467-017-00737-8

Shan, C., Xie, X., Luo, H., Muruato, A. E., Liu, Y., Wakamiya, M., et al. (2019). Maternal vaccination and protective immunity against Zika virus vertical transmission. *Nat. Commun.* 10:5677. doi: 10.1038/s41467-019-13589-1

Sharma, M., Glasner, D. R., Watkins, H., Puerta-Guardo, H., Kassa, Y., Egan, M. A., et al. (2019). Magnitude and functionality of the ns1-specific antibody response elicited by a live-attenuated tetravalent dengue vaccine candidate. *J. Infect. Dis.* 221, 867–877. doi: 10.1093/infdis/jiz081

Sirivichayakul, C., Barranco-Santana, E. A., Esquilin-Rivera, I., Oh, H. M., Raanan, M., Sariol, C. A., et al. (2016). Safety and immunogenicity of a tetravalent dengue vaccine candidate in healthy children and adults in dengue-endemic regions: a randomized, placebo-controlled phase 2 Study. *J. Infect. Dis.* 213, 1562–1572. doi: 10.1093/infdis/jiv762

Sirohi, D., Chen, Z., Sun, L., Klose, T., Pierson, T. C., Rossmann, M. G., et al. (2016). The 3.8 A resolution cryo-EM structure of Zika virus. *Science* 352, 467–470. doi: 10.1126/science.aaf5316

Slon-Campos, J. L., Dejnirattisai, W., Jagger, B. W., Lopez-Camacho, C., Wongwiwat, W., Durnell, L. A., et al. (2019). A protective Zika virus E-dimer-based subunit vaccine engineered to abrogate antibody-dependent enhancement of dengue infection. *Nat. Immunol.* 20, 1291–1298. doi: 10.1038/s41590-019-0477-z

Spiteri, G., Sudre, B., Septfons, A., Beaute, J., The European, Zika Surveillance, et al. (2017). Surveillance of Zika virus infection in the EU/EEA, June 2015 to January 2017. *Euro. Surveill* 22, 17–00254. doi: 10.2807/1560-7917.ES.2017.22.41.17-00254

St John, A. L., and Rathore, A. P. S. (2019). Adaptive immune responses to primary and secondary dengue virus infections. *Nat. Rev. Immunol.* 19, 218–230. doi: 10.1038/s41577-019-0123-x

Stettler, K., Beltramello, M., Espinosa, D. A., Graham, V., Cassotta, A., Bianchi, S., et al. (2016). Specificity, cross-reactivity, and function of antibodies elicited by Zika virus infection. *Science* 353, 823–826. doi: 10.1126/science.aaf8505

Sun, J., Li, M., Wang, Y., Hao, P., and Jin, X. (2017). Elaboration of tetravalent antibody responses against dengue viruses using a subunit vaccine comprised of a single consensus dengue envelope sequence. *Vaccine* 35, 6308–6320. doi: 10.1016/j.vaccine.2017.09.063

Szaba, F. M., Tighe, M., Kummer, L. W., Lanzer, K. G., Ward, J. M., Lanthier, P., et al. (2018). Zika virus infection in immunocompetent pregnant mice causes fetal damage and placental pathology in the absence of fetal infection. *PLoS Pathog.* 14:e1006994. doi: 10.1371/journal.ppat.1006994

Tamhankar, M., and Patterson, J. L. (2019). Directional entry and release of Zika virus from polarized epithelial cells. *Virol. J.* 16:99. doi: 10.1186/s12985-019-1200-2

Tebas, P., Roberts, C. C., Muthumani, K., Reuschel, E. L., Kudchodkar, S. B., Zaidi, F. I., et al. (2017). Safety and Immunogenicity of an Anti-Zika Virus DNA Vaccine - Preliminary Report. *N. Engl. J. Med.* doi: 10.1056/NEJMoa1708120

Urakami, A., Ngwe Tun, M. M., Moi, M. L., Sakurai, A., Ishikawa, M., Kuno, S., et al. (2017). An envelope-modified tetravalent dengue virus-like-particle vaccine has implications for flavivirus vaccine design. *J. Virol.* 91:e01181-17. doi: 10.1128/JVI.01181-17

Vannice, K. S., Wilder-Smith, A., Barrett, A. D. T., Carrijo, K., Cavaleri, M., de Silva, A., et al. (2018). Clinical development and regulatory points for consideration

for second-generation live attenuated dengue vaccines. *Vaccine* 36, 3411–3417. doi: 10.1016/j.vaccine.2018.02.062

Vermillion, M. S., Lei, J., Shabi, Y., Baxter, V. K., Crilly, N. P., McLane, M., et al. (2017). Intrauterine Zika virus infection of pregnant immunocompetent mice models transplacental transmission and adverse perinatal outcomes. *Nat. Commun.* 8:14575. doi: 10.1038/ncomms14575

Villar, L., Dayan, G. H., Arredondo-Garcia, J. L., Rivera, D. M., Cunha, R., Deseda, C., et al. (2015). Efficacy of a tetravalent dengue vaccine in children in Latin America. *N. Engl. J. Med.* 372, 113–123. doi: 10.1056/NEJMoa1411037

Wan, S. W., Chen, P. W., Chen, C. Y., Lai, Y. C., Chu, Y. T., Hung, C. Y., et al. (2017). Therapeutic effects of monoclonal antibody against dengue Virus NS1 in a STAT1 knockout mouse model of dengue infection. *J. Immunol.* 199, 2834–2844. doi: 10.4049/jimmunol.1601523

Wang, E., Ni, H., Xu, R., Barrett, A. D., Watowich, S. J., Gubler, D. J., et al. (2000). Evolutionary relationships of endemic/epidemic and sylvatic dengue viruses. *J. Virol.* 74, 3227–3234. doi: 10.1128/jvi.74.7.3227-3234.2000

Wang, R., Zheng, X., Sun, J., Feng, K., Gao, N., Fan, D., et al. (2019). Vaccination with a single consensus envelope protein ectodomain sequence administered in a heterologous regimen induces tetravalent immune responses and protection against dengue viruses in mice. *Front. Microbiol.* 10:1113. doi: 10.3389/fmicb.2019.01113

Weaver, S. C., Costa, F., Garcia-Blanco, M. A., Ko, A. I., Ribeiro, G. S., Saade, G., et al. (2016). Zika virus: History, emergence, biology, and prospects for control. *Antiviral. Res.* 130, 69–80. doi: 10.1016/j.antiviral.2016.03.010

Weiskopf, D., Angelo, M. A., Bangs, D. J., Sidney, J., Paul, S., Peters, B., et al. (2015a). The human CD8+ T cell responses induced by a live attenuated tetravalent dengue vaccine are directed against highly conserved epitopes. *J. Virol.* 89, 120–128. doi: 10.1128/JVI.02129-14

Weiskopf, D., Cerpas, C., Angelo, M. A., Bangs, D. J., Sidney, J., Paul, S., et al. (2015b). Human CD8+ T-Cell responses against the 4 dengue virus serotypes are associated with distinct patterns of protein targets. *J. Infect. Dis.* 212, 1743–1751. doi: 10.1093/infdis/jiv289

Weiskopf, D., Angelo, M. A., de Azeredo, E. L., Sidney, J., Greenbaum, J. A., Fernando, A. N., et al. (2013). Comprehensive analysis of dengue virus-specific responses supports an HLA-linked protective role for CD8+ T cells. *Proc. Natl. Acad. Sci. U.S.A.* 110, E2046–E2053. doi: 10.1073/pnas.1305227110

Weiskopf, D., Angelo, M. A., Grifoni, A., O'Rourke, P. H., Sidney, J., Paul, S., et al. (2016). HLA-DRB1 alleles are associated with different magnitudes of dengue virus-specific CD4+ T-Cell Responses. *J. Infect. Dis.* 214, 1117–1124. doi: 10.1093/infdis/jiw309

Weiskopf, D., Angelo, M. A., Sidney, J., Peters, B., Shresta, S., and Sette, A. (2014). Immunodominance changes as a function of the infecting dengue virus serotype and primary versus secondary infection. *J. Virol.* 88, 11383–11394. doi: 10.1128/JVI.01108-14

Wen, J., Elong Ngono, A., Regla-Nava, J. A., Kim, K., Gorman, M. J., Diamond, M. S., et al. (2017a). Dengue virus-reactive CD8(+) T cells mediate cross-protection against subsequent Zika virus challenge. *Nat. Commun.* 8:1459. doi: 10.1038/s41467-017-01669-z

Wen, J., Tang, W. W., Sheets, N., Ellison, J., Sette, A., Kim, K., et al. (2017b). Identification of Zika virus epitopes reveals immunodominant and protective roles for dengue virus cross-reactive CD8(+) T cells. *Nat. Microbiol,.* 2:17036. doi: 10.1038/nmicrobiol.2017.36

Whitehead, S. S., Falgout, B., Hanley, K. A., Blaney, JE Jr, Markoff, L., and Murphy, B. R. (2003a). A live, attenuated dengue virus type 1 vaccine candidate with a 30-nucleotide deletion in the 3' untranslated region is highly attenuated and immunogenic in monkeys. *J. Virol.* 77, 1653–1657. doi: 10.1128/jvi.77.2.1653-1657.2003

Whitehead, S. S., Hanley, K. A., Blaney, JE Jr, Gilmore, L. E., Elkins, W. R., and Murphy, B. R. (2003b). Substitution of the structural genes of dengue virus type 4 with those of type 2 results in chimeric vaccine candidates which are attenuated for mosquitoes, mice, and rhesus monkeys. *Vaccine* 21, 4307–4316. doi: 10.1016/s0264-410x(03)00488-2

Wilder-Smith, A., Vannice, K., Durbin, A., Hombach, J., Thomas, S. J., Thevarjan, I., et al. (2018). Zika vaccines and therapeutics: landscape analysis and challenges ahead. *BMC Med.* 16:84. doi: 10.1186/s12916-018-1067-x

Williams, K. L., Wahala, W. M., Orozco, S., de Silva, A. M., and Harris, E. (2012). Antibodies targeting dengue virus envelope domain III are not required for serotype-specific protection or prevention of enhancement in vivo. *Virology* 429, 12–20. doi: 10.1016/j.virol.2012.03.003

Wirawan, M., Fibriansah, G., Marzinek, J. K., Lim, X. X., Ng, T. S., Sim, A. Y. L., et al. (2019). Mechanism of enhanced immature dengue virus attachment to endosomal membrane induced by prm antibody. *Structure* 27, 253.e8–267.e8. doi: 10.1016/j.str.2018.10.009

World Health Organization [WHO] (1966). Mosquito-borne hemorrhagic fevers of South-East Asia and the Western Pacific. *Bull World Health Organ.* 35, 17–33.

World Health Organization [WHO] (2009). *Dengue: Guidelines for Diagnosis, Treatment, Prevention and Control: New Edition*. Geneva: WHO.

World Health Organization [WHO] (2017). Dengue vaccine: WHO position paper, July 2016 - recommendations. *Vaccine* 35, 1200–1201. doi: 10.1016/j.vaccine.2016.10.070

Wu, S. J., Grouard-Vogel, G., Sun, W., Mascola, J. R., Brachtel, E., Putvatana, R., et al. (2000). Human skin Langerhans cells are targets of dengue virus infection. *Nat. Med.* 6, 816–820. doi: 10.1038/77553

Xie, X., Kum, D. B., Xia, H., Luo, H., Shan, C., Zou, J., et al. (2018). A single-dose live-attenuated zika virus vaccine with controlled infection rounds that protects against vertical transmission. *Cell Host Microbe* 24, 487.e5–499.e5. doi: 10.1016/j.chom.2018.09.008

Yauch, L. E., Prestwood, T. R., May, M. M., Morar, M. M., Zellweger, R. M., Peters, B., et al. (2010). CD4+ T cells are not required for the induction of dengue virus-specific CD8+ T cell or antibody responses but contribute to protection after vaccination. *J. Immunol.* 185, 5405–5416. doi: 10.4049/jimmunol.1001709

Yauch, L. E., Zellweger, R. M., Kotturi, M. F., Qutubuddin, A., Sidney, J., Peters, B., et al. (2009). A protective role for dengue virus-specific CD8+ T cells. *J. Immunol.* 182, 4865–4873. doi: 10.4049/jimmunol.0801974

Yockey, L. J., Varela, L., Rakib, T., Khoury-Hanold, W., Fink, S. L., Stutz, B., et al. (2016). Vaginal exposure to zika virus during pregnancy leads to fetal brain infection. *Cell* 166, 1247.e4–1256.e4 doi: 10.1016/j.cell.2016.08.004

Yu, I. M., Holdaway, H. A., Chipman, P. R., Kuhn, R. J., Rossmann, M. G., and Chen, J. (2009). Association of the pr peptides with dengue virus at acidic pH blocks membrane fusion. *J. Virol.* 83, 12101–12107. doi: 10.1128/JVI.01637-09

Yu, I. M., Zhang, W., Holdaway, H. A., Li, L., Kostyuchenko, V. A., Chipman, P. R., et al. (2008). Structure of the immature dengue virus at low pH primes proteolytic maturation. *Science* 319, 1834–1837. doi: 10.1126/science.1153264

Zellweger, R. M., Prestwood, T. R., and Shresta, S. (2010). Enhanced infection of liver sinusoidal endothelial cells in a mouse model of antibody-induced severe dengue disease. *Cell Host Microbe* 7, 128–139. doi: 10.1016/j.chom.2010.01.004

Zhang, X., Ge, P., Yu, X., Brannan, J. M., Bi, G., Zhang, Q., et al. (2013). Cryo-EM structure of the mature dengue virus at 3.5-*A resolution*. *Nat. Struct. Mol. Biol.* 20, 105–110. doi: 10.1038/nsmb.2463

Zheng, X., Zhang, D., Li, Y., Yang, C., Wu, Y., Liang, X., et al. (2019). Incompatible and sterile insect techniques combined eliminate mosquitoes. *Nature* 572, 56–61. doi: 10.1038/s41586-019-1407-9

Zompi, S., and Harris, E. (2013). Original antigenic sin in dengue revisited. *Proc. Natl. Acad. Sci. U.S.A.* 110, 8761–8762. doi: 10.1073/pnas.1306333110

Zou, J., Xie, X., Luo, H., Shan, C., Muruato, A. E., Weaver, S. C., et al. (2018). A single-dose plasmid-launched live-attenuated Zika vaccine induces protective immunity. *EBioMedicine* 36, 92–102. doi: 10.1016/j.ebiom.2018.08.056

**Conflict of Interest:** The authors declare that the research was conducted in the absence of any commercial or financial relationships that could be construed as a potential conflict of interest.

The handling editor declared a shared affiliation, though no other collaboration, with one of the authors, XJ, at the time of review.

*Copyright © 2020 Sun, Du, Zheng, Cheng and Jin. This is an open-access article distributed under the terms of the Creative Commons Attribution License (CC BY). The use, distribution or reproduction in other forums is permitted, provided the original author(s) and the copyright owner(s) are credited and that the original publication in this journal is cited, in accordance with accepted academic practice. No use, distribution or reproduction is permitted which does not comply with these terms.*

frontiers in Microbiology

ORIGINAL RESEARCH
published: 23 April 2020
doi: 10.3389/fmicb.2020.00609

# Virus-Like Particles Derived From a Virulent Strain of Pest des Petits Ruminants Virus Elicit a More Vigorous Immune Response in Mice and Small Ruminants Than Those From a Vaccine Strain

*Feihu Yan[1†], Entao Li[1,2†], Ling Li[3†], Zachary Schiffman[4,5], Pei Huang[1,6], Shengnan Zhang[1,7], Guohua Li[1,8], Hongli Jin[1,9], Hualei Wang[9], Xinghai Zhang[1,9], Yuwei Gao[1], Na Feng[1]*, Yongkun Zhao[1]*, Chengyu Wang[1]* and Xianzhu Xia[1,2,6]*

[1] Key Laboratory of Jilin Province for Zoonosis Prevention and Control, Changchun Veterinary Research Institute, Chinese Academy of Agricultural Sciences, Changchun, China, [2] College of Veterinary Medicine, South China Agricultural University, Guangzhou, China, [3] National Research Center for Exotic Animal Diseases, China Animal Health and Epidemiology Center, Qingdao, China, [4] Department of Medical Microbiology and Infectious Diseases, University of Manitoba, Winnipeg, MB, Canada, [5] National Microbiology Laboratory, Special Pathogens Program, Public Health Agency of Canada, Winnipeg, MB, Canada, [6] College of Veterinary Medicine, Jilin Agricultural University, Changchun, China, [7] College of Wildlife Resources, Northeast Forestry University, Harbin, China, [8] College of Animal Science and Technology, Shihezi University, Shihezi, China, [9] College of Veterinary Medicine, Jilin University, Changchun, China

Peste des petits ruminants (PPRs) is highly contagious, acute or subacute disease of small ruminants caused by peste des petits ruminants virus (PPRV). To date, several studies have designed and evaluated PPRV-like particles (VLPs) as a vaccine candidate for the prevention and control of PPR, with the majority of these VLPs constructed using sequences derived from a PPRV vaccine strain due to its high immunogenicity. However, because of the lack of available genetic material and certain structural proteins and/or the alteration of posttranslational glycosylation modifications, the immunogenicity of VLPs derived from a vaccine strain is not always optimal. In this study, two PPRV VLP candidates, derived from either the lineage IV Tibet/30 virulent strain or the lineage II Nigeria 75/1 vaccine strain, were generated using a baculovirus system through the coexpression of the PPRV matrix (M), hemagglutinin (H), and fusion (F) proteins in the high expression level cell line High Five. These VLPs were then used to immunize mice, goats, and sheep followed by two boosts after primary immunization. Both VLPs were found to induce a potent humoral immune response as demonstrated by the high ratio of immunoglobulin G1 (IgG1) to IgG2a. In all animals, both VLPs induced high titers of virus-neutralizing antibodies (VNAs), as well as H- and F-specific antibodies, with the Tibet/30 VLPs yielding higher antibody titers by comparison to the Nigeria 75/1 VLPs. Studies in mice also demonstrated that the Tibet/30 VLPs induced a more robust interleukin 4 and interferon γ response than the Nigeria 75/1 VLPs. Goats and sheep immunized with both VLPs exhibited a robust humoral and cell-mediated immune response. Furthermore, our

OPEN ACCESS

**Edited by:**
*Lijun Rong,*
*The University of Illinois at Chicago, United States*

**Reviewed by:**
*Sara Louise Cosby, Agri-Food and Biosciences Institute (AFBI), United Kingdom*
*Ruikun Du, Shandong University of Traditional Chinese Medicine, China*

***Correspondence:**
*Na Feng*
*fengna0308@126.com*
*Yongkun Zhao*
*zhaoyongkun1976@126.com*
*Chengyu Wang*
*wangchengyu2019103@163.com*

*[†]These authors have contributed equally to this work*

**Specialty section:**
*This article was submitted to Virology, a section of the journal Frontiers in Microbiology*

**Received:** *27 November 2019*
**Accepted:** *19 March 2020*
**Published:** *23 April 2020*

**Citation:**
*Yan F, Li E, Li L, Schiffman Z, Huang P, Zhang S, Li G, Jin H, Wang H, Zhang X, Gao Y, Feng N, Zhao Y, Wang C and Xia X (2020) Virus-Like Particles Derived From a Virulent Strain of Pest des Petits Ruminants Virus Elicit a More Vigorous Immune Response in Mice and Small Ruminants Than Those From a Vaccine Strain. Front. Microbiol. 11:609. doi: 10.3389/fmicb.2020.00609*

results demonstrated that the VLPs derived from the virulent lineage IV Tibet/30 strain were more immunogenic, inducing a more potent and robust humoral and cell-mediated immune response in vaccinated animals by comparison to the lineage II Nigeria 75/1 vaccine strain VLPs. In addition, VNA titers were significantly higher among animals vaccinated with the Tibet/30 VLPs by comparison to the Nigeria 75/1 VLPs. Taken together, these findings suggest that VLPs derived from the virulent lineage IV Tibet/30 strain are more immunogenic by comparison to those derived from the lineage II Nigeria 75/1 vaccine strain and thus represent a promising vaccine candidate for the control and eradication of PPR.

**Keywords: peste des petits ruminants virus, virus-like particles, small ruminants, virulent strain, vaccine strain, immune response**

## INTRODUCTION

Peste des petits ruminants virus (PPRV), renamed to small ruminant morbillivirus in 2017 (referred to as PPRV throughout this study) (Amarasinghe et al., 2017), is the etiological agent of peste des petits ruminants (PPRs), a highly contagious and devastating transboundary disease, which affects nearly 30 million animals, mainly goats and sheep, annually across more than 70 countries worldwide. Peste des petits ruminants virus (genus *Morbillivirus*, family Paramyxoviridae) is a non-segmented, negative-sense RNA virus with a genome of ∼16 kb that encodes a total of six structural proteins [nucleocapsid (N), phosphoprotein (P), matrix (M), fusion (F), hemagglutinin (H), and polymerase (L)] and two non-structural proteins (V and C) (Gibbs et al., 1979; Bailey et al., 2005). Coexpression of the PPRV M, F, and H proteins results in the efficient assembly and release of virus-like particles (VLPs) (Wang et al., 2017). The M protein is the most abundant structural protein within the mature virion and plays a critical role in viral morphogenesis, acting as a driving force of virus budding (Haffar et al., 1999; Pohl et al., 2007). Proteins F and H are two surface expressed glycoproteins, which play an important role in attachment to the host cell, as well as mediating fusion of the viral envelope with the host cell membrane (Baron et al., 2016). While both the F and H proteins are potent inducers of a protective host immune response, the H protein is more immunogenic compared to F, ultimately stimulating a more robust humoral immune response, with the majority of virus-neutralizing antibodies (VNAs) being directed against the H protein (Sinnathamby et al., 2001; Renukaradhya et al., 2002; Rahman et al., 2003; Diallo et al., 2007).

Peste des petits ruminant is classified by the World Organization for Animal Health (OIE) as a notifiable terrestrial animal disease and is estimated to result in economic losses of US $1.4 million to $2.1 billion annually, mostly in Africa and Asia, mainly due to morbidity, mortality, production losses, and treatment costs. Furthermore, PPR also has severe negative impacts on food and job security, as well as livelihood, especially among women and children, exacerbating poverty and malnutrition, particularly among highly vulnerable rural communities (Kumar et al., 2014).

Following the successful global eradication of rinderpest in 2011, a global consensus was reached on the need to eradicate PPR (Taylor, 2016). In April 2015, a PPR global control and eradication strategy were endorsed during a conference in Côte d'Ivoire with the aim of eradicating PPR globally by 2030 (OIE and FAO, 2015). To implement this strategy, the Food and Agriculture Organization of the United Nations (FAO) and OIE, 2016 launched, in October 2016, an initial PPR global eradication program for 2017–2021. In accordance with this strategy, the Chinese government issued in December 2015 the National Eradication Program for PPR (2016–2020), with the goal of eradicating PPR countrywide by 2020 (Liu et al., 2018). Lessons learned from the global eradication of rinderpest in 2011 demonstrated that the use of a highly efficacious vaccine was critical to the campaign's success, and as such, vaccination has been identified as the most suitable option for the control and eradication of PPR.

Sequence-based phylogenetic analysis has classified PPRV into four distinct lineages (I, II, III, and IV) (Forsyth and Barrett, 1995; Couacy-Hymann et al., 2002), but only one serotype exists. Lineages I, II, and III are most prominent among African and Middle Eastern countries, whereas lineage IV is most prominent among Asian countries (Wu et al., 2016) and more recently several African countries previously reporting only a single lineage (Kwiatek et al., 2011; Munir, 2015). Although there is only one serotype of PPRV, there are quantitative and qualitative differences in immune responses among different lineages (Hodgson et al., 2018). While PPRV VLPs derived from lineage II vaccine strains have proven promising as a differentiating infected from vaccinated animals (DIVA) vaccine candidate, the immunogenicity of VLPs derived from virulent strains still remains largely unknown (Li et al., 2014; Liu et al., 2015; Wang et al., 2017; Yan et al., 2019).

To this effect, we constructed two VLP vaccine candidates derived from the lineage IV Tibet/30 virulent strain and lineage II–attenuated Nigeria 75/1 vaccine strain respectively using a baculovirus system for the simultaneous coexpression of the codon-optimized M, F, and H proteins in insect cells. These VLPs were subsequently used to immunize mice, goats, and sheep, and the results revealed that the Tibet/30 VLPs were highly immunogenic, eliciting a more potent humoral and cell-mediated immune response among vaccinated animals by comparison to the Nigeria 75/1 VLPs and thus represents a prospective candidate vaccine for the control and eradication of PPR.

# MATERIALS AND METHODS

## Cells and Viruses

Adherent *Spodoptera frugiperda* (Sf9) insect cells used for baculovirus rescue and propagation were maintained in Grace's Insect Medium (Life Technologies, San Diego, CA, United States) and cultured at 27°C. High Five insect cells (BTI-TN-5B1-4) used for VLP production were grown in suspension in Express Five serum-free media (Thermo Fisher Scientific, Saint Louis, MO, United States) and cultured at 27°C on a temperate orbital shaker at 200 rpm. Propagation and titration of PPRV were done on African green monkey kidney cells (Vero), which were cultured in Dulbecco modified Eagle medium supplemented with 10% heat inactivated fetal bovine serum at 37°C with 5% $CO_2$. Peste des petits ruminants virus vaccine strain Nigeria 75/1 was stored in our laboratory.

## Construction of Bacmid Transfer Plasmid

Codon optimized open reading frames for the PPRV M, F, and H genes from the PPRV virulent strain China/Tibet/Geg/07-30 (GenBank FJ905304.1) and vaccine strain Nigeria 75/1 (GenBank HQ197753.1) with restriction enzyme sequences (**Table 1**) were synthesized by Sangon Biotech (Shanghai, China) Co., Ltd. The synthetic codon optimized genes were cloned into Puc57-Simple plasmid, respectively. The M gene was inserted into a modified pFastBacDual vector under a p10 promoter flanked by *Rsr*II and *Stu*I restriction sites yielding the recombinant plasmid pFBD-M. Then the H gene was cloned into pFBD-M under a polyhedrin (pH) promoter digested with *Sal*I and *Hin*gIII to yield the recombinant plasmid pFBD-M-H. Subsequently, the F gene was cloned into the recombinant plasmid pFBD-M-H vector under the second pH promoter digested with *Nhe*I and *Sph*I yielding the recombinant transfer plasmid pFBD-M-F-H (**Figure 1A**). Bacmid transfer plasmids were transformed into *Escherichia coli* DH10TMBac competent cells (Life Technologies, United States) containing the AcMNPV baculovirus genome to obtain recombinant bacmids containing M, F, and H genes of the PPRV Tibet/30 and Nigeria 75/1 strains, respectively. Recombinant bacmids were identified by polymerase chain reaction using three pairs of gene specific primers for the two PPRV strains. The sequences of all primers used in this study are summarized in **Table 1**.

**TABLE 1** | Sequences of primers used in the present study.

| Primer | Sequence (5′–3′) | Restriction enzyme site |
|---|---|---|
| $M_{Tibet}F$ | ACACCGGTCCGATGACCGAAATCTACGACTT | *Rsr*II |
| $M_{Tibet}R$ | ACACAGGCCTTTAGAGAATTTTAAAGAGGCC | *Stu*I |
| $F_{Tibet}F$ | ACACGTCGACATGACCAGGGTTGCTATC | *Sal*I |
| $F_{Tibet}R$ | ACACAAGCTTTTACAGAGAGCGAACGTAAG | *Hin*gIII |
| $H_{Tibet}F$ | ACACGCTAGCATGTCCGCTCAAAGGGAGAG | *Nhe*I |
| $H_{Tibet}R$ | ACACGCATGCTTACACGGGATTGCAAGTGAC | *Sph*I |
| $M_{Nigeria}F$ | ACACGGTCCGATGACCGAGATCTACGAT | *Rsr*II |
| $M_{Nigeria}R$ | ATACAGGCCTTTACAGGATCTTGAACAG | *Stu*I |
| $F_{Nigeria}F$ | ACAGTCGACATGACACGGGTCGCAACC | *Sal*I |
| $F_{Nigeria}R$ | ATACAAGCTTCTACAGTGATCTCACGTA | *Hin*gIII |
| $H_{Nigeria}F$ | ACAGCTAGCATGTCCGCACAAAGGGAA | *Nhe*I |
| $H_{Nigeria}R$ | ATACGCATGCTCAGACTGGATTACATGT | *Sph*I |

[a]*Restriction enzyme sites are underlined.*

## Generation and Identification of Recombinant Baculoviruses

Recombinant baculoviruses (rBVs) expressing PPRV M, F, and H proteins from either the virulent Tibet/30 strain or vaccine Nigeria 75/1 strain were rescued using the Cellfectin II Reagent (Life Technologies, United States) as previously described (Yan et al., 2019). Briefly, Sf9 cells were seeded 24 h prior to transfection in a 6-well plate at a density of $8 \times 10^5$ cells/well to achieve a confluency of 80–90%. For transfection, 3 μg of recombinant bacmid DNA diluted in 100 μL unsupplemented Grace's Insect Medium was combined with 100 μL diluted Cellfectin II Reagent (8 μL Cellfectin II Reagent diluted in unsupplemented Grace's Medium) vortexed briefly and subsequently incubated at room temperature for 15–30 min. The DNA–lipid mixture was then added onto the Sf9 cells and incubated at 27°C. After 72 h, first-generation rBVs (P1) were harvested and subsequently passaged for several generations in order to obtain high-titer baculovirus.

To confirm expression of the M, F, and H proteins, both rBVs were subjected to immunofluorescence assay (IFA) and Western blot (WB) as previously described (Yan et al., 2019). Briefly, Sf9 cells were infected with the two rBVs, as well as wild-type baculovirus at a multiplicity of infection (MOI) of 1. Fourth-eight hours after infection, the cells were either fixed with 80% acetone and subjected to IFA analysis or lysed in sodium dodecyl sulfate–polyacrylamide gel electrophoresis sample buffer followed by WB analysis.

## Generation and Purification of PPRV VLPs

To generate PPRV VLPs, suspension High Five cells were infected with the rBVs at an MOI of 5 and the supernatants harvested at 120 h after infection and subjected to centrifugation at 7,000 rpm for 30 min to pellet cells and debris. The resulting clarified supernatant was then subjected to ultracentrifugation at a speed of 30,000 rpm for 1.5 h at 4°C to pellet the VLPs. The VLPs were then purified by ultracentrifugation at 35,000 rpm for 1.5 h at 4°C using a sucrose density gradient of 20–40–60% (wt/vol) prepared in phosphate-buffered saline (PBS). Protein bands between 20 and 40% corresponding to the purified VLPs were harvested and subsequently subjected to ultracentrifugation at 35,000 rpm for 1.5 h at 4°C to remove the sucrose. Lastly, the concentration of the VLPs was quantified using the BCA protein assay kit as per the manufacturer's protocol (Beyotime, Nanjing, China).

## Electron and Immunoelectron Microscopy

The presence and morphology of PPRV VLPs were evaluated by negative staining electron microscopy as previously described

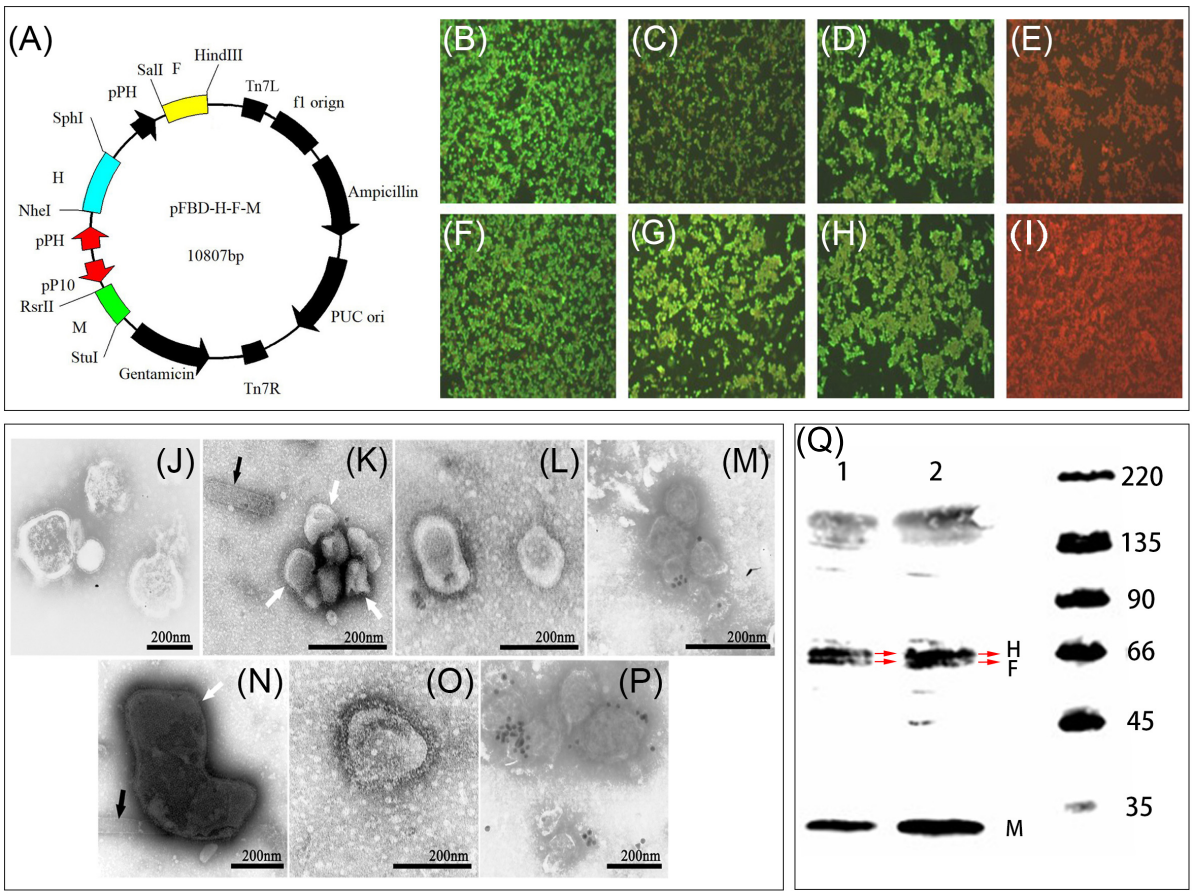


**FIGURE 1 |** Generation and characterization of PPRV VLPs. **(A)** Schematic diagram for the recombinant plasmids pFBD-M-F-H. **(B–I)** Detection of the expression of M, F, and H. Sf9 cells were mock-infected or infected with rBVs rpFBD-M-F-H or wild-type baculovirus. Expression was evaluated by IFA using mouse anti-PPRV M, F, and H polyclonal antibody, respectively. Nigeria 75/1 M protein **(B)**, Nigeria 75/1 F protein **(C)**, Nigeria 75/1 H protein **(D)**, Tibet/30 M protein **(E)**, Tibet/30 F protein **(F)**, Tibet/30 H protein **(G)**, wild-type baculovirus-infected control **(H)**, and mock-infected control **(I)**. **(J–P)** Transmission electron microscopy images of virus and VLP preparations. Native PPRV particles **(J)**, residual baculoviruses (indicated by black triangles) in preparations of Nigeria 75/1 VLPs (indicated by white arrow) **(K)**, purified Nigeria 75/1 PPRV VLPs **(L)**, and immunogold-labeled Nigeria 75/1 VLPs stained with mouse anti-PPRV H polyclonal antibody followed by gold-labeled goat anti-mouse IgG antibody **(M)**. Residual baculoviruses (indicated by black triangles) in preparations of Tibet/30 VLPs (indicated by white arrow) **(N)**, purified Tibet/30 PPRV VLPs **(O)**, and immunogold-labeled Tibet/30 VLPs stained with mouse anti-PPRV H polyclonal antibody followed by gold-labeled goat anti-mouse IgG antibody **(P)**. **(Q)** Western blot depicting (1) Nigeria 75/1 and (2) Tibet/30 VLP protein expression using sheep polyclonal antibody. However, M, F, and H proteins incorporation in both VLPs were confirmed by Western blot analysis, which demonstrated both M (38 kDa), F (59 kDa), and H (68 kDa) consistent with their respective molecular sizes.

(Qi et al., 2015). For immunoelectron microscopy, PPRV VLPs were applied to a copper–rhodium (Cu-Rh) grid and incubated at room temperature for 60 min followed by incubation with sheep anti-PPRV antibodies (1:200 dilution) at 37°C for 60 min. The copper mesh was then incubated with a 1:50 diluted 10 nm gold-labeled mouse anti-sheep immunoglobulin G (IgG) antibody at 37°C for 30 min (Abcam, Cambridge, MA, United States), and the copper mesh subsequently observed under a transmission electron microscope.

## Immunization of Mice, Goats, and Sheep and Sera Collection

All live animal work was performed in accordance with guidelines from the Animal Welfare and Ethics Committee of the Changchun Veterinary Research Institute (permit no. SCXK-2012-017). The environment and housing facilities satisfied the National Standards of Laboratory Animal Requirements (GB 14925-2001) of China.

Eight-week-old female BALB/c mice were purchased from the Changchun Institute of Biological Products Co., Ltd., China, and randomly separated into three groups of 10. Mice were vaccinated intramuscularly in the gastrocnemius muscle with 50 μg PPRV Tibet/30 or Nigeria 75/1 VLPs in 50 μL PBS mixed with 50 μL AddaVax adjuvant. Mice in the control group were given 50 μL PBS mixed with 50 μL AddaVax adjuvant. All groups received a second and third booster immunization at 2 and 4 weeks following the primary immunization. For mice, whole blood was collected 2, 4, 6, and 8 weeks following primary immunization, and

the sera subsequently separated and stored at −80°C for further analysis.

Nine outbred goats (12–24 months old) and nine outbred sheep (8–16 months old) were fed by the Zhaoyuan Gaojiatan Goat Farm (Shandong, China) and independently randomized into three groups of three animals each. Goats were multipoint vaccinated subcutaneously (s.c.) in the neck skin with 300 μg PPRV Tibet/30 or Nigeria 75/1 VLPs in 500 μ μL PBS mixed with 1 mL AddaVax adjuvant. Goats in the control group were given 500 μL PBS mixed with 1 mL AddaVax adjuvant. All groups received a second and third booster immunization at three and 6 weeks following the primary immunization. Sheep were immunized using the same exact approach as for goats. For both goats and sheep, whole blood was collected through the jugular vein at 3, 6, 9, 12, and 15 weeks after primary immunization using 10 mL vacuum blood collection tubes and the serum subsequently separated and stored at −80°C for further analysis.

## Virus Neutralization Assay

Serum samples from mice, goats, and sheep were analyzed for PPRV-specific VNA titers using a microneutralization assay. Briefly, 50 μL 2-fold serial diluted inactivated sera were combined with 50 μL PPRV Nigeria 75/1 ($100TCID_{50}$) in 96-well cell culture plate and incubated at 37°C and 5% $CO_2$ for 1 h. Virus-only control wells and uninfected-cell control wells were included. Following incubation, 100 μL ($2 \times 10^5$ cells) of Vero cell suspension was added to each well, and cytopathic effect (CPE) observed 8 days after infection. Virus neutralizing antibody titers were defined as the highest serum dilution at which the CPE was inhibited by at least 50% (Yan et al., 2019).

## Enzyme-Linked Immuneospot Assays for Cytokine Production in Mice

Mouse splenocytes were harvested 2 weeks following the second immunization and stimulated with inactivated PPRV Nigeria 75/1 (10 μ μg/mL). Cells producing interleukin 2 (IL-2), IL-4, IL-10, or interferon γ (IFN-γ) were identified using enzyme-linked immunospot assay (ELISpot) kits (Mabtech AB, Stockholm, Sweden; R&D Systems, Minneapolis, MN, United States) according to the manufacturer's instructions. Spot-forming cells (SFCs) were counted using an automated ELISpot reader (AID ELISPOT reader-iSpot, AID GmbH, GER).

## Enzyme-Linked Immunosorbent Assay for PPRV-Specific Antibody and Cytokine

Mouse sera obtained 2 weeks following the third immunization were analyzed for PPRV-specific IgG, IgG1, and IgG2a. Antibody titers were measured using an indirect enzyme-linked immunosorbent assay (ELISA), as previously described (Yan et al., 2019). Purified inactive PPRV (Nigeria 75/1) was used as the coating antigen at a concentration of 2 mg/mL, and the optical density value was recorded at 450 nm absorbance.

To determine antibody responses to the F and H protein of PPRV, an indirect ELISA was developed using purified F and H proteins produced in house from either the virulent Tibet/30 strain or Nigeria 75/1 vaccine strain. Briefly, 96-well flat-bottomed plates were coated with purified F and H proteins (0.5 μg/well) overnight at 4°C and all subsequent steps performed as previously described (Yan et al., 2019). Total IgG was detected using a similar method: 96-well plates were coated with 0.05 μg purified inactivated PPRV (Nigeria 75/1), and horseradish peroxidase (HRP)–conjugated rabbit anti-goat IgG diluted 1:10,000 in PBST (Thermo Fisher Scientific, United States) used as the secondary antibody.

Cytokine responses in goats and sheep were evaluated using commercially available ELISA kits for goat or sheep IL-2, IL-4, IL-10, and IFN-γ (Cusabio, Burlington, NC, United States). The reagents, samples, and standards were prepared according to the manufacturer's protocol.

## Data Analysis

Figures were generated using GraphPad Prism 8.0 software (GraphPad Company, SanDiego, CA, United States). Differences between means were evaluated using the one-way analysis of variance (ANOVA) or two-way ANOVA and were deemed significant at $P \leq 0.05$.

# RESULTS

## Generation and Identification of PPRV VLPs

The M, F, and H genes derived from either the PPRV virulent Tibet/30 or Nigeria 75/1 vaccine strain were cloned into a modified pFastBacDual plasmid, which could carry three exogenous genes under the control of a p10 and two pH promoters, respectively, as shown in **Figure 1A**. Recombinant bacmid was obtained after homologous reorganization in competent DH10bac cells, and rBVs were rescued in Sf9 insect cells following bacmid transfection. Subsequent infection of High Five insect cells with the two rBVs yielded PPRV VLPs derived from the virulent Tibet/30 strain and Nigeria 75/1 vaccine strain, respectively. Expression of the PPRV M, F, and H proteins was confirmed by IFA and WB (**Figures 1B–I,Q**). Furthermore, transmission electron microscopy revealed that the morphology of the VLPs resembled that of authentic PPRV containing spikes on the particle surface (**Figures 1J,K,N**). In addition, removal of residual baculovirus following purification by ultracentrifugation using a sucrose density gradient was confirmed by transmission electron microscopy (**Figures 1L,O**). Lastly, immunoelectron microscopy suggested that the two major PPRV immunogenic glycoproteins F and H, respectively, were incorporated into the VLPs (**Figures 1M,P**) and confirmed by WB (**Figure 1Q**).

## Characterization of the Humoral Immune Response to PPRV VLPs in Mice

To evaluate the immunogenicity of the PPRV VLPs, mice were vaccinated with 50 μg PPRV Tibet/30 or Nigeria 75/1 VLPs and boosted 2 and 4 weeks after primary vaccination, after which VNA titers were determined using a microneutralization assay to assess the humoral immune response. At 2 weeks

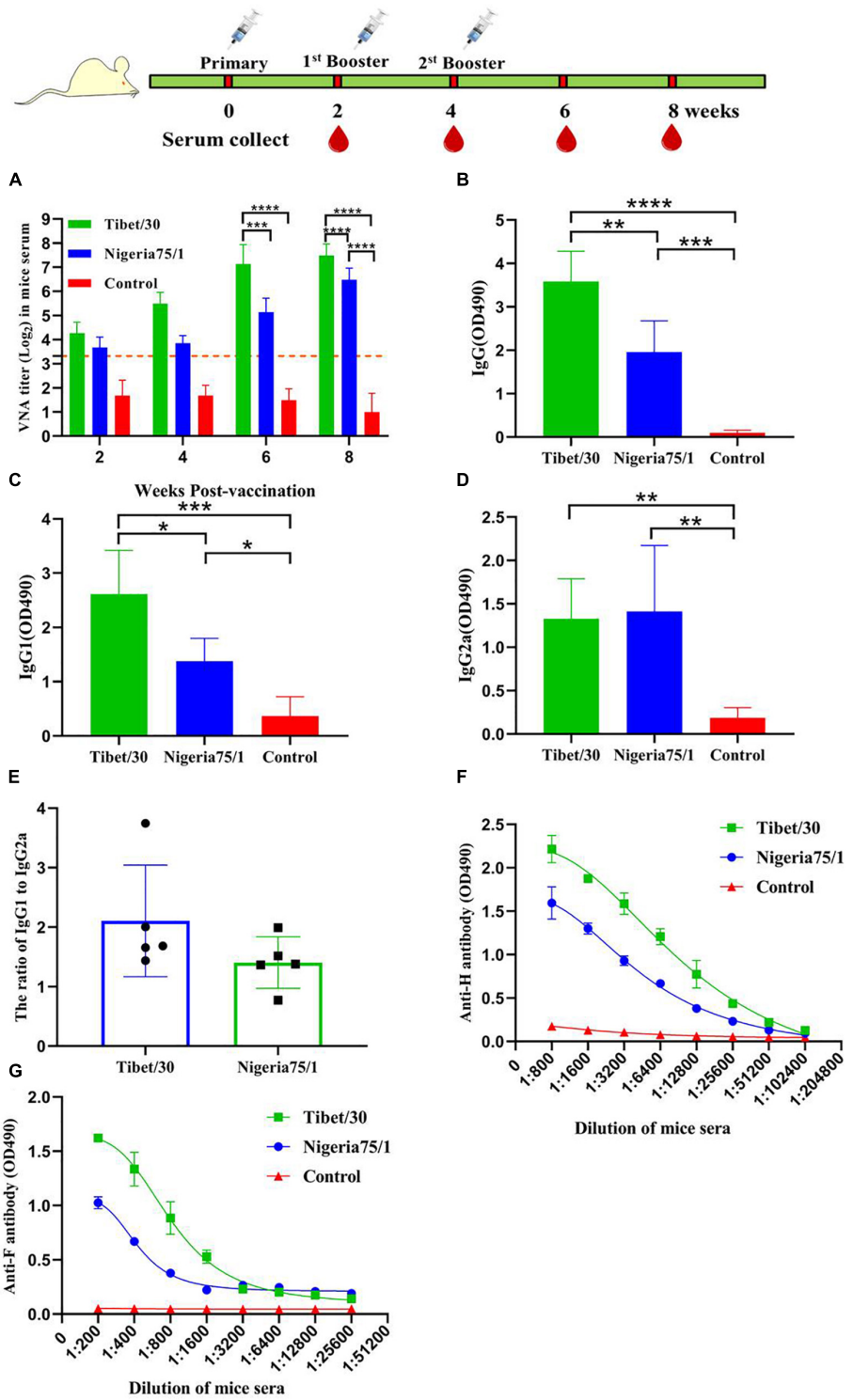


**FIGURE 2 |** Virus-like particle immunization induces humoral immune response in mice. Mice were immunized thrice via s.c. route at 2 weeks' interval with PPRV Tibet/30 VLPs, PPRV Nigeria 75/1 VLPs, or PBS, all with equal volume of adjuvant. Serum samples were collected 2, 4, 6, and 8 weeks after primary vaccination. **(A)** VNA titers were measured by virus neutralization assay. Dotted line represented antibody titers greater than 10, indicating positive serum conversion. **(B–D)** The specific anti-PPRV serum IgG and isotype responses were detected by ELISA. The serum dilution factor was 5,000. Serum IgG **(B)**, IgG1 **(C)**, and IgG2a **(D)**, responses were determined 6 weeks after the primary immunization. **(E)** The IgG1/IgG2a ratio was calculated. **(F,G)** Serum was collected from mouse 6 weeks after the primary immunization for analyzing F- and H-specific antibodies by ELISA. Data were depicted as the means ± SD for seven mice from each group and were analyzed by one- or two-way ANOVA (*$P < 0.05$, **$P < 0.01$, ***$P < 0.001$, ****$P < 0.0001$).

after primary vaccination, VNA titers from both the PPRV Tibet/30 and Nigeria 75/1 VLP-vaccinated groups exceeded 10 (**Figure 2A**), the standard minimum value as defined by the OIE, required for protection in goats immunized with live-attenuated PPRV Nigeria 75/1 (OIE, 2008; Yan et al., 2019). In the case of the Tibet/30 VLP-immunized group, VNA titers continued to increase to $2^5$–$2^6$ and $2^7$–$2^8$ at 4 and 6 weeks after primary vaccination, respectively, and those levels sustained at $2^7$–$2^8$ at 8 weeks after primary vaccination (**Figure 2A**). By comparison, VNA titers from the Nigeria 75/1 VLP-immunized group increased to $2^3$–$2^4$ and $2^5$–$2^6$ four and 6 weeks after primary vaccination respectively and those levels sustained at $2^6$–$2^7$ 8 weeks after primary vaccination (**Figure 2A**). In short, both PPRV VLPs elicited a potent humoral immune response in mice, resulting in the production of high amounts of VNAs, however, VNA titers were significantly higher at 6 and 8 weeks after vaccination in mice vaccinated with Tibet/30 VLPs by comparison to Nigeria 75/1 VLPs (**Figure 2A**).

To further evaluate the humoral immune responses induced by the two PPRV VLPs, antigen-specific total IgG and IgG1 and IgG2a titers were determined by ELISA. While both the Tibet/30 and Nigeria 75/1 VLPs induced the production of PPRV-specific IgG in mice, the Tibet/30 VLPs induced IgG titers significantly higher than Nigeria 75/1 VLPs (**Figure 2B**). Furthermore, both the PPRV Tibet/30 and Nigeria 75/1 VLP-vaccinated groups exhibited total IgG titers significantly higher than the PBS control group (**Figure 2B**). In the case of IgG1, the trend was similar to that observed for total IgG (**Figure 2C**). Both VLPs significantly upregulated IgG2a production; however, there was no significant difference among Tibet/30 and Nigeria 75/1 VLP-vaccinated groups (**Figure 2D**). The relatively high ratio of IgG1 to IgG2a for both the Tibet/30 and Nigeria 75/1 VLP-vaccinated mice suggested the activation of $T_H2$-type immune response (**Figure 2E**).

Lastly, antibodies against the two major PPRV surface glycoproteins namely H and F were measured using an established ELISA. As shown in **Figures 2F,G**, both PPRV VLPs induced high levels of antibodies toward the H and F proteins, with the Tibet/30 VLPs inducing a more potent response by comparison to Nigeria 75/1 VLPs, which is consistent with the results obtained from the VNA assay. Taken together, these data demonstrate that the PPRV Tibet/30 VLPs elicited a more significant humoral immune response in mice by comparison to the PPRV Nigeria 75/1 VLPs.

## Characterization of the Cell-Mediated Immune Response in Mice Vaccinated With PPRV VLPs

To investigate whether PPRV VLPs could elicit a cell-mediated immune response in mice, the activation of PPRV-specific IL-2, IL-4, IL-10, and IFN-γ in splenocytes were evaluated by ELISpot assays. The results demonstrated that the Tibet/30 VLPs elicited the activation of mouse splenocytes with significantly more SFCs for IL-2, IL-4, IL-10, and IFN-γ by comparison to the PBS control group (**Figure 3**). Although the Nigeria 75/1 VLPs exhibited significantly higher numbers of IL-2 and IFN-γ SFCs compared to the PBS control group, no significant difference was observed for IL-4 and IL-10 (**Figure 3**). Furthermore, the Tibet/30 VLPs appeared to be superior at eliciting IL-4 and IFN-γ production with significantly more SFCs when compared to Nigeria 75/1 VLPs (**Figures 3B,D**).

## Characterization of the Humoral Immune Response to PPRV VLPs in Goats and Sheep

Goats and sheep are among the two most susceptible hosts to PPRV infection and as such represent the ideal animal models for evaluating the immunogenicity and humoral immune response induced by PPRV VLPs. To evaluate the immunogenicity of the PPRV VLPs, both goats and sheep were vaccinated with 300 μg PPRV Tibet/30 or Nigeria 75/1 VLPs and boosted 3 and 6 weeks after primary vaccination, after which VNA titers were determined using a microneutralization assay to assess the humoral immune response. At 3 weeks after primary vaccination, VNA titers from both the PPRV Tibet/30 and Nigeria 75/1 VLP-vaccinated groups exceeded the OIE standard of 10 for both goats and sheep (**Figures 4A,B**). In goats, VNA titers gradually increased and reached statistical significance by comparison to the PBS control group at 9 weeks after primary vaccination, in the case of the Tibet/30 VLP-immunized group and remained statistically significant 12 and 15 weeks after primary vaccination (**Figure 4A**). In contrast, the Nigeria 75/1 VLP-immunized group only reached statistical significance by comparison to the PBS control group 15 weeks following primary vaccination (**Figure 4A**). In contrast, VNA titers of Tibet/30 VLP-vaccinated sheep only reached statistical significance by comparison to the PBS control group 12 weeks after primary vaccination with this significance sustained 15 weeks after primary vaccination (**Figure 4B**), whereas VNA titers for Nigeria 75/1 VLP-vaccinated sheep did not reach statistical significance by comparison to the PBS control at any point (**Figure 4B**). Furthermore, Tibet/30 VLP-immunized goats exhibited significantly higher VNA titers by comparison to Nigeria 75/1 VLP-immunized goats 9, 12, and 15 weeks after initial vaccination (**Figure 4A**), whereas in sheep this significance was only observed 12 and 15 weeks after initial vaccination (**Figure 4B**).

As in mice, the humoral immune responses in goats and sheep induced by the two PPRV VLPs were further evaluated by quantifying total antigen-specific IgG titers by ELISA. Although both the Tibet/30 and Nigeria 75/1 VLPs induced the production of PPRV-specific IgG in goats, the Tibet/30 VLPs induced IgG titers significantly higher than Nigeria 75/1 VLPs 9 weeks after initial vaccination (**Figure 4C**). In contrast, there was no statistical difference in total IgG among sheep vaccinated with either the Tibet/30 or Nigeria 75/1 PPRV VLPs, which may be attributed to the lower susceptibility of sheep to PPRV (**Figure 4D**). Additionally, in both goats and sheep, total IgG levels for both the PPRV Tibet/30 and Nigeria 75/1 VLP-vaccinated groups were significantly higher than the PBS control group (**Figures 4C,D**).

Furthermore, all animals developed high levels of PPRV-specific antibodies against the two major PPRV surface

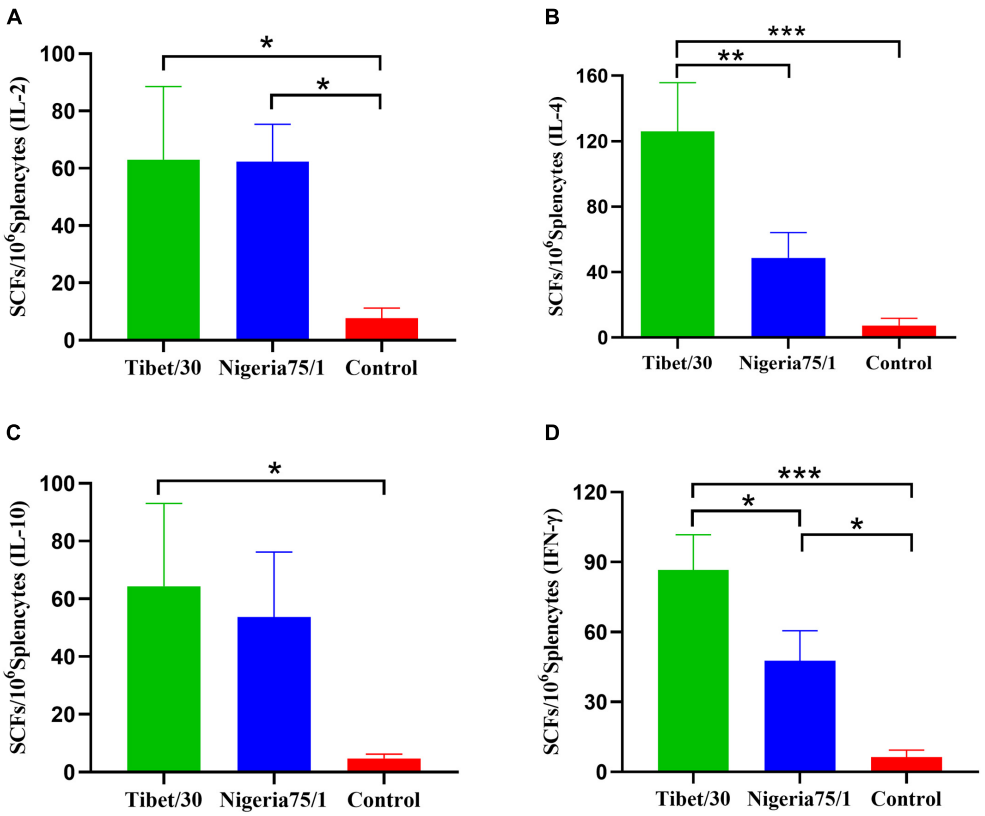


**FIGURE 3 |** Virus-like particle immunization induces cell-mediated immune response in mice. Splenocytes from mice were stimulated with inactivated PPRV 2 weeks after the third immunization. Splenocytes producing IL-2 **(A)**, IL-4 **(B)**, IL-10 **(C)**, or IFN-γ **(D)** were identified by ELISpot. Data are depicted as the means ± SD of SFCs per million splenocytes from three mice in each group and were analyzed by one-way ANOVA (*$P < 0.05$, **$P < 0.01$, ***$P < 0.001$).

glycoproteins, namely, H and F, with the Tibet/30 VLPs yielding higher titers by comparison to Nigeria 75/1 VLPs in both goats and sheep (**Figures 4E–H**). In general, the humoral immune indicators evaluated suggest that sheep mounted a less robust humoral immune response than goats, which could possibly be attributed to their reduced susceptibility to PPRV infection. Overall, these data are in agreement with those observed in mice and suggest that although both PPRV VLPs elicited a strong humoral immune response in goats and sheep, the Tibet/30 VLPs were more effective at inducing this response by comparison to Nigeria 75/1 VLPs.

## Characterization of the Cell-Mediated Immune Response in Goats and Sheep Vaccinated With PPRV VLPs

Cell-mediated immune responses were evaluated by quantifying the levels of secreted IL-2, IL-4, IL-10, and IFN-γ in the serum of PPRV VLP-vaccinated goats and sheep as well as control animals by ELISA. In both goats and sheep, all four cytokines were significantly elevated in animals vaccinated with the Tibet/30 VLPs by comparison to the PBS control group (**Figure 5**). Despite, both goats and sheep vaccinated with Nigeria 75/1 VLPs exhibiting elevated levels of all four cytokines, none with the exception of IL-2 in sheep, were significantly elevated by comparison to the PBS control group (**Figure 5**). None of the animals in either control group exhibited a pronounced cytokine response as expected (**Figure 5**). Furthermore, the levels of IL-4 and IFN-γ were significantly elevated in both goats and sheep vaccinated with Tibet/30 VLPs by comparison to Nigeria 75/1 VLPs (**Figures 5B,D**). In addition, IL-10 levels were significantly elevated in goats but not sheep vaccinated with Tibet/30 VLPs by comparison to Nigeria 75/1 VLPs (**Figure 5C**). In both animals, there was no statistical difference in the levels of IL-2 among Tibet/30 or Nigeria 75/1 VLP-vaccinated groups (**Figure 5A**). Taken together, these data indicate that both PPRV VLPs elicited a cell-mediated immune response in goats and sheep, with the Tibet/30 VLPs inducing an overall more pronounced response than Nigeria 75/1 VLPs.

# DISCUSSION

The production of VLPs using a baculovirus/insect cell expression system has proven to be an efficient strategy for vaccine development. Several VLP-based vaccines have been licensed and commercialized, such as Engerix-B®, 2012 (GSK, March 2012) and Cervarix®, 2011 (GSK, July 2011) against

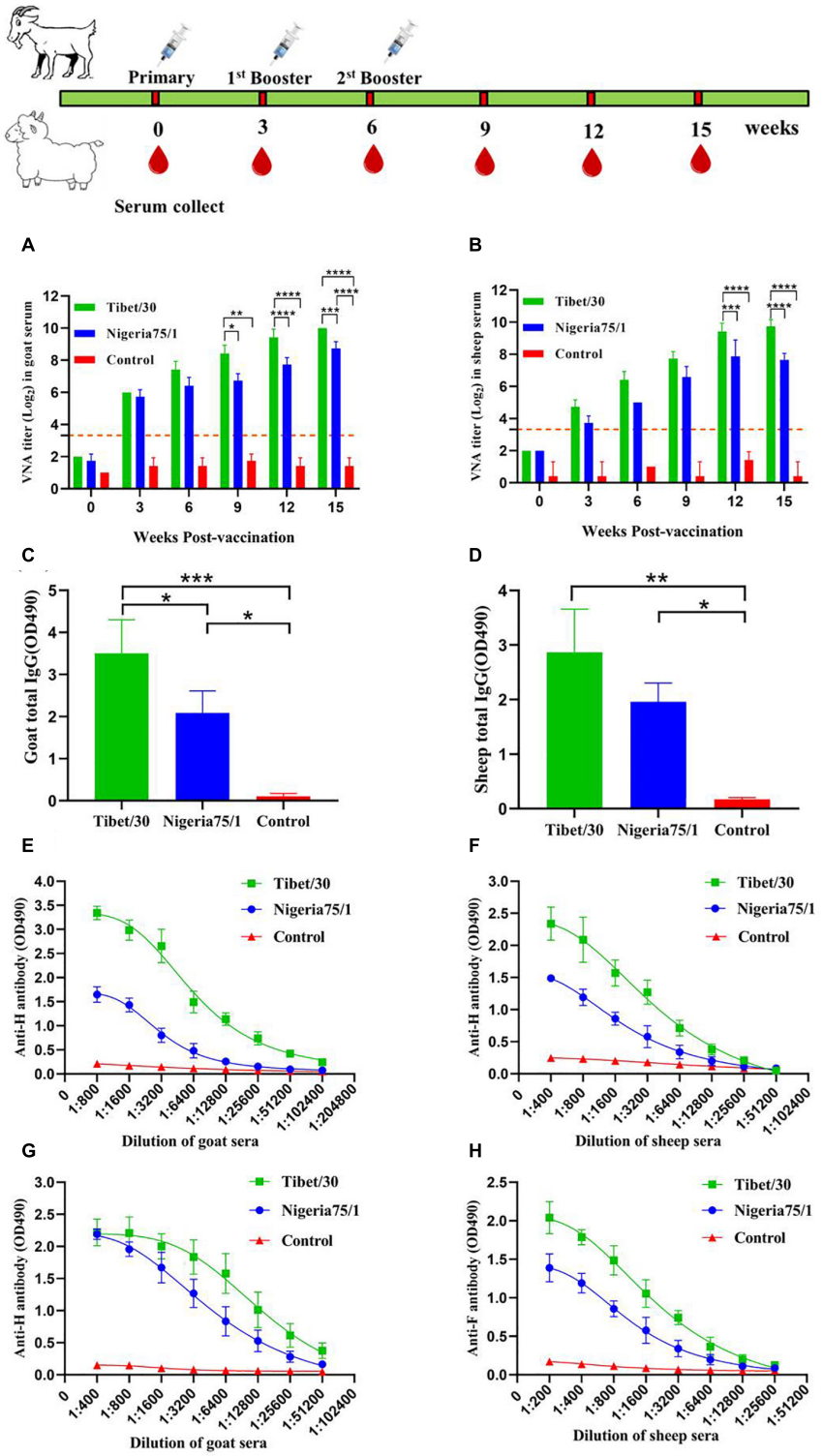


**FIGURE 4 |** Virus-like particle immunization induces humoral response in goats and sheep. Goats or sheep were immunized thrice via s.c. route at 3 weeks' interval with PPRV Tibet/30 VLPs, PPRV Nigeria 75/1 VLPs, or adjuvant. **(A,B)** VNA titers were measured at 3, 6, 9, 12, and 15 weeks after primary vaccination. Dotted lines represent antibody titers greater than 10, indicating positive serum conversion. **(C,D)** Total goat serum IgG **(C)** and total sheep serum IgG **(D)** responses were determined 9 weeks after the primary immunization. **(E–H)** Serum was collected from each goat or sheep 3 weeks after the second booster immunization for analyzing PPRV F- and H-specific antibodies by ELISA. Data are depicted as the means ± SD for three goats of sheep from each group and were analyzed by one-way or two-way ANOVA (*$P < 0.05$, **$P < 0.01$, ***$P < 0.001$, ****$P < 0.0001$).

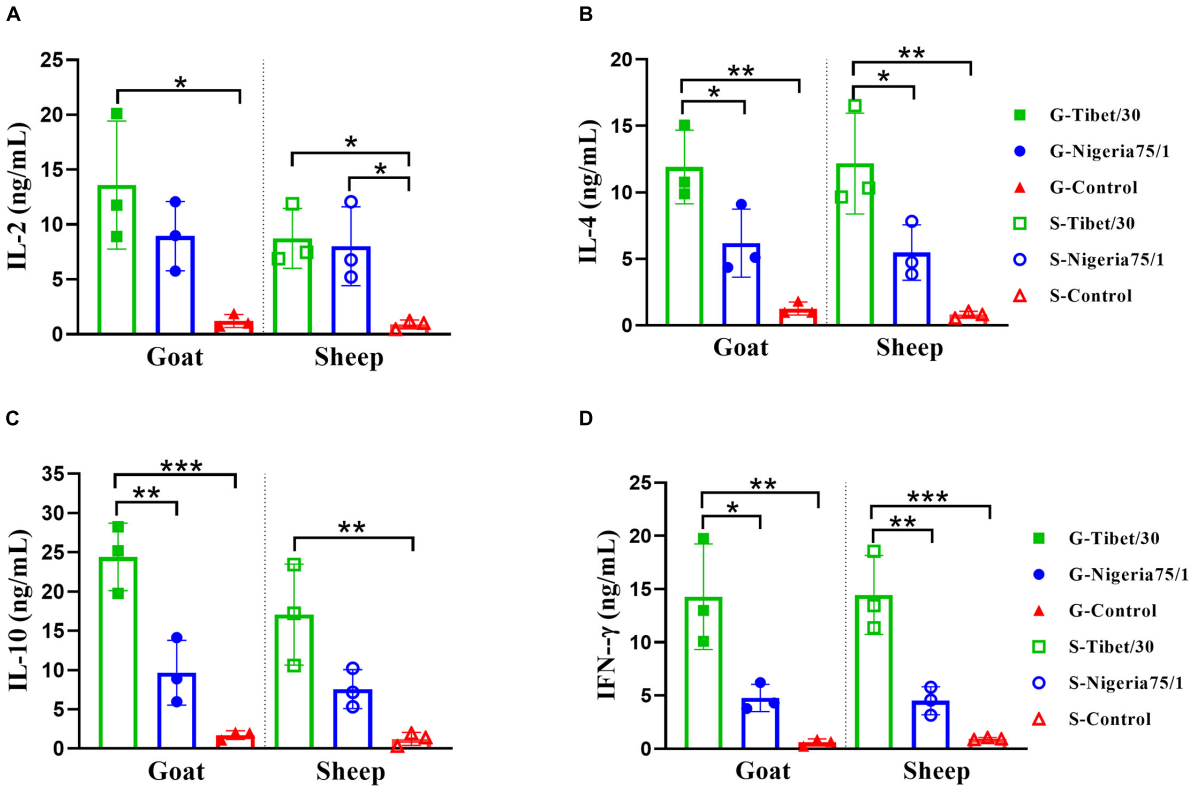


**FIGURE 5 |** Virus-like particle immunization induces significant cytokine response in goats and sheep. **(A–D)** Serum was collected 3 weeks after the second immunization from animals immunized with PPRV Tibet/30 VLPs, PPRV Nigeria 75/1 VLPs, or adjuvant and were analyzed for the production of IL-2 **(A)**, IL-4 **(B)**, IL-10 **(C)**, and IFN-γ **(D)**. Data are depicted as the means ± SD for three goats or sheep from each group and were analyzed by one-way ANOVA (*$P < 0.05$, **$P < 0.01$, ***$P < 0.001$).

hepatitis B virus and human papillomavirus, respectively, as well as the veterinary vaccine Porcilis® (Kushnir et al., 2012) against porcine circovirus type 2. Most often, VLPs are constructed using sequences derived from a virus vaccine strain due to its well-established immunogenicity. However, because of the lack of genetic material and certain structural proteins and/or the alteration of posttranslational glycosylation modifications, the immunogenicity of VLPs derived from a vaccine strain may not always be optimal. In this study, we constructed two PPRV VLP vaccine candidates derived from the sequences of either the virulent Tibet/30 or attenuated Nigeria 75/1 PPRV strains using a baculovirus system for the simultaneous coexpression of the codon-optimized M, F, and H proteins in insect cells. These VLPs were subsequently used to immunize mice, goats, and sheep and their immunogenicity compared by evaluating the magnitude of the humoral and cell-mediated immune responses they induced. Animal experiments demonstrated that both PPRV VLPs were capable of eliciting humoral and cell-mediated immune response in mice, goats, and sheep, with the Tibet/30 VLPs exhibiting a greater immunogenicity by comparison to the Nigeria 75/1 VLPs. Together, these data suggest that both PPRV VLPs represent suitable vaccine candidates for the control and eradication of PPR, with the Tibet/30 VLPs being the most promising candidate because of its greater immunogenicity. This conclusion also provides a way to improve VLP immunogenicity through the use of sequences derived from a PPRV strain rather than a vaccine strain.

A number of studies have previously explored the formation of PPRV VLPs and have demonstrated that coexpression of the PPRV M and N proteins are sufficient for the production of spikeless PPRV VLPs in insect cells. However, because of the lack of the PPRV H and F surface glycoproteins, which are the most immunological relevant determinants, these VLPs were unable to elicit an efficient protective immune response (Liu et al., 2014). On the other hand, coexpression of the N, M, F, and H proteins resulted in the successful assembly and release of PPRV VLPs in either Vero (Wang et al., 2017) or insect cells (Yan et al., 2019) and was capable of inducing strong humoral and cell-mediated immune responses in mice and goats (Yan et al., 2019). Furthermore, it has been demonstrated that expression of the M protein alone is sufficient for the assembly and release of PPRV VLPs; however, in the absence of M, no PPRV VLPs were released for any combination of N, H, and F proteins (Wang et al., 2017). While the expression of the F protein alone could support low levels of VLP assembly, no release was observed in the absence of M, further highlighting its crucial role as a structural protein in the assembly and release of VLPs (Wang et al., 2017). In

contrast to the F protein, expression of the N or H proteins alone could neither support assembly nor release of VLPs (Wang et al., 2017). In our study, we constructed PPRV VLPs through the coexpression of the M, F, and H proteins respectively, with the M protein acting as the structural protein supporting assembly and release of the VLPs and the two glycoproteins, namely, F and H acting as the main immunogenic determinants on the surface of the PPRV VLPs. We chose to omit the N protein because of its non-essential role in the assembly and release of PPRV VLPs, as well as the convenience of using commercial kits for DIVA. Through the coexpression of the M, F, and H proteins, we were successful in generating PPRV VLPs derived from both the virulent Tibet/30 and attenuated Nigeria 75/1 PPRV strains, using a baculovirus/insect cell expression system, with the morphology of these VLPs resembling authentic PPRV containing spikes protruding from the particulate surfaces (**Figure 1A**).

To simplify the production process and reduce baculovirus contamination during purification, we constructed a single rBV carrying three codon-optimized exogenous genes encoding the M, F, and H proteins, respectively. All three proteins were expressed under the control of p10 and two pH promoters, respectively (**Figure 1**). This approach of using a single rBV expressing all three viral proteins rather than three separate rBVs each expressing one viral protein reduces the amount of residual baculovirus within the harvested supernatant, thus benefiting subsequent purification.

Peste des petits ruminants virus–like particles display antigenic epitopes in the correct conformation and in a highly repetitive manner, leading to crosslinking of B-cell immunoglobulin receptors (Bachmann and Zinkernagel, 1997; Grgacic and Anderson, 2006; Kushnir et al., 2012). This reaction stimulates B-cell proliferation and upregulation of both MHC class II and costimulatory molecules that allow for subsequent interactions with T-helper cells, which trigger immunoglobulin secretion, affinity maturation, and the long-lived memory B cells (Chackerian, 2007). Our results revealed that both PPRV VLPs were capable of eliciting a humoral immune response in mice, goats, and sheep, which resulted in the production of VNAs to titers sufficient for protection against PPRV infection. These data suggest that both the virulent Tibet/30 and vaccine Nigeria 75/1 PPRV strains share common neutralizing epitopes; however, those on the Tibet/30 strain appear to be more immunogenic, ultimately eliciting a more robust humoral immune response. These findings are further supported by higher levels of H- and F-specific antibody titers among mice, goats, and sheep vaccinated with the Tibet/30 VLPs as compared to those vaccinated with the Nigeria 75/1 VLPs. Additionally, the relatively high IgG1/IgG2a ratio in mice indicated that both PPRV VLPs elicited a $T_H2$-preferred immune response favoring humoral immunity and was more pronounced among Tibet/30 VLP-vaccinated animals compared to those vaccinated with the Nigeria 75/1 VLPs. Although these findings are in agreement with those observed by Li et al. (2014), they contradict our previous findings (Yan et al., 2019) and can possibly be attributed to differences in adjuvant and/or the lack of the N protein within the VLPs, which has been found to induce a CTL response (Mitra-Kaushik et al., 2001).

A number of cytokines were elevated, modulating an antiviral immune response upon antigen recognition and presentation. Analysis of ELISpot assays detecting IL-2–, IL-4–, IL-10–, and IFN-γ–secreting mouse splenocytes showed that the Tibet/30 VLP-vaccinated group exhibited significantly increased levels of all four cytokines as compared to the PBS control group. In contrast, mice vaccinated with the Nigeria 75/1 VLPs only demonstrated significantly increased levels of IL-2 and IFN-γ as compared to the PBS control group, with the levels of

**FIGURE 6 |** Amino acid sequence alignment analyses of H protein. Homology of the PPRV H protein from PPRV Tibet/30 and Nigeria75/1 strains was analyzed using MEGA (Molecular Evolutionary Genetics Analysis) version 6.0. Capital letters represent the location of amino acid site mutations, and * represents the amino acid without difference between two strains.

IL-4 and IL-10, although slightly upregulated not reaching statistical significance. A similar trend was observed in both goats and sheep whereby all four cytokines were significantly elevated in animals vaccinated with the Tibet/30 VLPs by comparison to the PBS control group. Although both goats and sheep vaccinated with Nigeria 75/1 VLPs had elevated levels of all four cytokines, none with the exception of IL-2 in sheep were significantly elevated by comparison to the PBS control group. Interleukin 4 produced by $T_H2$ cells drives the maturation of B cells into plasma cells, resulting in antibody production, isotype switching, and affinity maturation (Fang et al., 2007). Interleukin 10, which is also secreted by $T_H2$ cells, inhibits the activation of $T_H1$ cells and ultimately their production of cytokines (Moore et al., 2001). Interestingly, IL-4 and IFN-γ levels were significantly elevated in mice, goats, and sheep vaccinated with Tibet/30 VLPs by comparison to Nigeria 75/1 VLPs. In addition, IL-10 levels were significantly elevated in goats but not sheep vaccinated with Tibet/30 VLPs by comparison to Nigeria 75/1 VLPs. Taken together, these data support the conclusion that the PPRV VLPs elicited a $T_H2$-preferred immune response favoring humoral immunity, which was more pronounced among Tibet/30 VLP-vaccinated animals compared with those vaccinated with Nigeria 75/1 VLPs. Overall the immune indicators in this study were more or less higher than those observed in our previous study and is likely due to the use of AddaVax as the adjuvant rather than Freund's complete adjuvant (Yan et al., 2019). AddaVax is a squalene-based oil-in-water nanoemulsion based on the formulation of MF95 that has been demonstrated to elicit both cellular and humoral immune responses and licensed in Europe for adjuvanted flu vaccines (Vesikari et al., 2011; Alving et al., 2012; Calabro et al., 2013).

A recent study by Hodgson et al. (2018) reported qualitative and quantitative differences in immunogenicity among PPRV lineages. To this effect, we set out to compare the immunogenicity of PPRV VLPs derived from PPRV strains of different lineages and virulence, namely, the lineage IV Tibet/30 virulent strain and the lineage II–attenuated Nigeria 75/1 vaccine strain. The PPRV lineage II Nigeria 75/1 strain was first isolated from a goat that succumbed to PPRV infection and later passaged on Vero cells to yield the first PPR-attenuated vaccine (Taylor and Abegunde, 1979; Diallo et al., 1989). The PPRV lineage IV Tibet/30 strain was isolated from a sick goat in July 2007 during the first outbreak of PPR in southwestern Tibet of China (Wang et al., 2009; Wu et al., 2016). The attenuated Nigeria 75/1 vaccine strain (lineage II) and virulent Tibet/30 strain (lineage IV) share 97, 96.5, and 92.9% similarity at the amino acid level for the M, F, and H proteins, respectively. The H protein of morbilliviruses is highly immunogenic and has been found to be a major inducer of both humoral and cell-mediated immune responses (Berhe et al., 2003). As such, the low homology in H proteins among the two PPRV strains under study could possibly account for the differences in immunogenicity observed for the two PPRV VLPs. The H protein of PPRV is a 609-residue type II integral membrane glycoprotein (Yu et al., 2017). The two PPRV strains under investigation differ by a total of 43 amino acids distributed among the N-terminal cytoplasmic tail (three mutants), stalk region (three mutants), and C-terminal globular head (37 mutants) containing the receptor binding site and immune epitopes, respectively (**Figure 6**; Colf et al., 2007; Yu et al., 2017). No mutants were observed in the transmembrane region of the PPRV H protein. B-cell epitope regions have been mapped to two discontinuous regions on the PPRV H protein from aa263-368 and aa538-609 (Renukaradhya et al., 2002). Interestingly, 11 mutants (25.6%) are located within aa263-368 and could possibly account for the differences in humoral immune responses observed among Tibet/30 and Nigeria 75/1 VLP-vaccinated animals. Frequent differences were also observed at aa163-179, the initial portion of head region N-terminal domain, and may represent a novel antigenic determinant. Lastly, differences in amino acids among the PPRV M and F proteins could also contribute to the differences in immunogenicity observed between the two PPRV VLPs by influencing the amount of antigenic proteins incorporated onto VLP surface, as well as the attachment and uptake rate of VLPs to host cells, which requires further investigation.

## DATA AVAILABILITY STATEMENT

All datasets generated for this study are included in the article/supplementary material.

## ETHICS STATEMENT

All live animal work was performed in accordance with guidelines from the Animal Welfare and Ethics Committee of the Changchun Veterinary Research Institute (Permit No. SCXK-2012-017). The environment and housing facilities satisfied the National Standards of Laboratory Animal Requirements (GB 14925-2001) of China.

## AUTHOR CONTRIBUTIONS

FY, NF, CW, and YZ conceived the study and designed experiments. FY, EL, LL, and SZ performed the animal experiments. FY, EL, HW, GL, and NF performed *in vitro* experiments and analyzed data. FY, PH, HJ, and XZ interpreted the data. FY, EL, LL, and ZS wrote the manuscript. ZS, YG, and XX reviewed the manuscript.

## FUNDING

This work was supported by grant from Wild Animal Epidemic Source Disease Surveillance Project of State Forestry Administration (21080611).

## ACKNOWLEDGMENTS

We would like to thank Ms. Qi Wang for the excellent technical assistance with animal experiments.

## REFERENCES


Alving, C. R., Peachman, K. K., Rao, M., and Reed, S. G. (2012). Adjuvants for human vaccines. *Curr. Opin. Immunol.* 24, 310–315. doi: 10.1016/j.coi.2012.03.008

Amarasinghe, G. K., Bao, Y., Basler, C. F., Bavari, S., Beer, M., Bejerman, N., et al. (2017). Taxonomy of the order Mononegavirales: update 2017. *Arch. Virol.* 162, 2493–2504. doi: 10.1007/s00705-017-3311-7

Bachmann, M. F., and Zinkernagel, R. M. (1997). Neutralizing antiviral B cell responses. *Annu. Rev. Immunol.* 15, 235–270. doi: 10.1146/annurev.immunol.15.1.235

Bailey, D., Banyard, A., Dash, P., Ozkul, A., and Barrett, T. (2005). Full genome sequence of peste des petits ruminants virus, a member of the *Morbillivirus* genus. *Virus Res.* 110, 119–124. doi: 10.1016/j.virusres.2005.01.013

Baron, M. D., Diallo, A., Lancelot, R., and Libeau, G. (2016). Peste des Petits Ruminants Virus. *Adv. Virus Res.* 95, 1–42. doi: 10.1016/bs.aivir.2016.02.001

Berhe, G., Minet, C., Le Goff, C., Barrett, T., Ngangnou, A., Grillet, C., et al. (2003). Development of a dual recombinant vaccine to protect small ruminants against peste-des-petits-ruminants virus and capripoxvirus infections. *J. Virol.* 77, 1571–1577. doi: 10.1128/jvi.77.2.1571-1577.2003

Calabro, S., Tritto, E., Pezzotti, A., Taccone, M., Muzzi, A., Bertholet, S., et al. (2013). The adjuvant effect of MF59 is due to the oil-in-water emulsion formulation, none of the individual components induce a comparable adjuvant effect. *Vaccine* 31, 3363–3369. doi: 10.1016/j.vaccine.2013.05.007

Cervarix® (2011). *Prescribing Information*. Brentford: GlaxoSmithKline.

Chackerian, B. (2007). Virus-like particles: flexible platforms for vaccine development. *Expert Rev. Vaccines* 6, 381–390. doi: 10.1586/14760584.6.3.381

Colf, L. A., Juo, Z. S., and Garcia, K. C. (2007). Structure of the measles virus hemagglutinin. *Nat. Struct. Mol. Biol.* 14, 1227–1228. doi: 10.1038/nsmb1342

Couacy-Hymann, E., Roger, F., Hurard, C., Guillou, J. P., Libeau, G., and Diallo, A. (2002). Rapid and sensitive detection of peste des petits ruminants virus by a polymerase chain reaction assay. *J. Virol. Methods* 100, 17–25. doi: 10.1016/s0166-0934(01)00386-x

Diallo, A., Barrett, T., Barbron, M., Subbarao, S. M., and Taylor, W. P. (1989). Differentiation of rinderpest and peste des petits ruminants viruses using specific cDNA clones. *J. Virol. Methods* 23, 127–136. doi: 10.1016/0166-0934(89)90126-2

Diallo, A., Minet, C., Le Goff, C., Berhe, G., Albina, E., Libeau, G., et al. (2007). The threat of peste des petits ruminants: progress in vaccine development for disease control. *Vaccine* 25, 5591–5597. doi: 10.1016/j.vaccine.2007.02.013

Engerix-B® (2012). *Prescribing Information*. Brentford: GlaxoSmithKline.

Fang, T. C., Yashiro-Ohtani, Y., Del Bianco, C., Knoblock, D. M., Blacklow, S. C., and Pear, W. S. (2007). Notch directly regulates Gata3 expression during T helper 2 cell differentiation. *Immunity* 27, 100–110. doi: 10.1016/j.immuni.2007.04.018

Forsyth, M. A., and Barrett, T. (1995). Evaluation of polymerase chain reaction for the detection and characterisation of rinderpest and peste des petits ruminants viruses for epidemiological studies. *Virus Res.* 39, 151–163. doi: 10.1016/0168-1702(95)00076-3

Gibbs, E. P., Taylor, W. P., Lawman, M. J., and Bryant, J. (1979). Classification of peste des petits ruminants virus as the fourth member of the genus *Morbillivirus*. *Intervirology* 11, 268–274. doi: 10.1159/000149044

Grgacic, E. V., and Anderson, D. A. (2006). Virus-like particles: passport to immune recognition. *Methods* 40, 60–65. doi: 10.1016/j.ymeth.2006.07.018

Haffar, A., Libeau, G., Moussa, A., Cecile, M., and Diallo, A. (1999). The matrix protein gene sequence analysis reveals close relationship between peste des petits ruminants virus (PPRV) and dolphin morbillivirus. *Virus Res.* 64, 69–75. doi: 10.1016/s0168-1702(99)00080-5

Hodgson, S., Moffat, K., Hill, H., Flannery, J. T., Graham, S. P., Baron, M. D., et al. (2018). Comparison of the immunogenicities and cross-lineage efficacies of live attenuated peste des petits ruminants virus vaccines PPRV/Nigeria/75/1 and PPRV/Sungri/96. *J. Virol.* 92:01471-18. doi: 10.1128/JVI.01471-18

Kumar, N., Maherchandani, S., Kashyap, S. K., Singh, S. V., Sharma, S., Chaubey, K. K., et al. (2014). Peste des petits ruminants virus infection of small ruminants: a comprehensive review. *Viruses* 6, 2287–2327. doi: 10.3390/v6062287

Kushnir, N., Streatfield, S. J., and Yusibov, V. (2012). Virus-like particles as a highly efficient vaccine platform: diversity of targets and production systems and advances in clinical development. *Vaccine* 31, 58–83. doi: 10.1016/j.vaccine.2012.10.083

Kwiatek, O., Ali, Y. H., Saeed, I. K., Khalafalla, A. I., Mohamed, O. I., Obeida, A. A., et al. (2011). Asian lineage of peste des petits ruminants virus Africa. *Emerg. Infect. Dis.* 17, 1223–1231. doi: 10.3201/eid1707.101216

Li, W., Jin, H., Sui, X., Zhao, Z., Yang, C., Wang, W., et al. (2014). Self-assembly and release of peste des petits ruminants virus-like particles in an insect cell-baculovirus system and their immunogenicity in mice and goats. *PLoS One* 9:e104791. doi: 10.1371/journal.pone.0104791

Liu, F., Li, J., Li, L., Liu, Y., Wu, X., and Wang, Z. (2018). Peste des petits ruminants in China since its first outbreak in 2007: a 10-year review. *Transbound Emerg. Dis.* 65, 638–648. doi: 10.1111/tbed.12808

Liu, F., Wu, X., Li, L., Liu, Z., and Wang, Z. (2014). Formation of peste des petits ruminants spikeless virus-like particles by co-expression of M and N proteins in insect cells. *Res. Vet. Sci.* 96, 213–216. doi: 10.1016/j.rvsc.2013.10.012

Liu, F., Wu, X., Zou, Y., Li, L., and Wang, Z. (2015). Peste des petits ruminants virus-like particles induce both complete virus-specific antibodies and virus neutralizing antibodies in mice. *J. Virol. Methods* 213, 45–49. doi: 10.1016/j.jviromet.2014.11.018

Mitra-Kaushik, S., Nayak, R., and Shaila, M. S. (2001). Identification of a cytotoxic T-cell epitope on the recombinant nucleocapsid proteins of Rinderpest and Peste des petits ruminants viruses presented as assembled nucleocapsids. *Virology* 279, 210–220. doi: 10.1006/viro.2000.0698

Moore, K. W., de Waal Malefyt, R., Coffman, R. L., and O'Garra, A. (2001). Interleukin-10 and the interleukin-10 receptor. *Annu. Rev. Immunol.* 19, 683–765. doi: 10.1146/annurev.immunol.19.1.683

Munir, M. (2015). *Peste des Petits Ruminants: An Introduction*. Berlin: Springer, 1–10.

OIE (2008). *Manual of Diagnostic Tests and Vaccines for Terrestrial Animals*. Paris: OIE.

OIE (2016). *Peste des Petits Ruminants Portal*. Availabe online at:https://www.oie.int/en/animal-health-in-the-world/ppr-portal/distribution/ (accessed April 9, 2019).

OIE, and FAO (2015). *Global Strategy for the Control and Eradication of PPR*. Paris: OIE.

Pohl, C., Duprex, W. P., Krohne, G., Rima, B. K., and Schneider-Schaulies, S. (2007). Measles virus M and F proteins associate with detergent-resistant membrane fractions and promote formation of virus-like particles. *J. Gen. Virol.* 88(Pt 4), 1243–1250. doi: 10.1099/vir.0.82578-0

Qi, Y., Kang, H., Zheng, X., Wang, H., Gao, Y., Yang, S., et al. (2015). Incorporation of membrane-anchored flagellin or *Escherichia coli* heat-labile enterotoxin B subunit enhances the immunogenicity of rabies virus-like particles in mice and dogs. *Front. Microbiol.* 6:169. doi: 10.3389/fmicb.2015.00169

Rahman, M. M., Shaila, M. S., and Gopinathan, K. P. (2003). Baculovirus display of fusion protein of Peste des petits ruminants virus and hemagglutination protein of Rinderpest virus and immunogenicity of the displayed proteins in mouse model. *Virology* 317, 36–49. doi: 10.1016/j.virol.2003.08.022

Renukaradhya, G. J., Sinnathamby, G., Seth, S., Rajasekhar, M., and Shaila, M. S. (2002). Mapping of B-cell epitopic sites and delineation of functional domains on the hemagglutinin-neuraminidase protein of peste des petits ruminants virus. *Virus Res.* 90, 171–185. doi: 10.1016/s0168-1702(02)00151-x

Sinnathamby, G., Renukaradhya, G. J., Rajasekhar, M., Nayak, R., and Shaila, M. S. (2001). Immune responses in goats to recombinant hemagglutinin-neuraminidase glycoprotein of Peste des petits ruminants virus: identification of a T cell determinant. *Vaccine* 19, 4816–4823. doi: 10.1016/s0264-410x(01)00210-9

Taylor, W. (2016). The global eradication of peste des petits ruminants (PPR) within 15 years–is this a pipe dream? *Trop. Anim. Health Prod.* 48, 559–567. doi: 10.1007/s11250-016-0993-x

Taylor, W. P., and Abegunde, A. (1979). The isolation of peste des petits ruminants virus from Nigerian sheep and goats. *Res. Vet. Sci.* 26, 94–96.

Vesikari, T., Knuf, M., Wutzler, P., Karvonen, A., Kieninger-Baum, D., Schmitt, H. J., et al. (2011). Oil-in-water emulsion adjuvant with influenza vaccine in young children. *N. Engl. J. Med.* 365, 1406–1416. doi: 10.1056/NEJMoa1010331

Wang, Q., Ou, C., Dou, Y., Chen, L., Meng, X., Liu, X., et al. (2017). M protein is sufficient for assembly and release of Peste des petits ruminants virus-like particles. *Microb. Pathog.* 107, 81–87. doi: 10.1016/j.micpath.2017.03.021

Wang, Z., Bao, J., Wu, X., Liu, Y., Li, L., Liu, C., et al. (2009). Peste des petits ruminants virus in Tibet, China. *Emerg. Infect. Dis.* 15, 299–301. doi: 10.3201/eid1502.080817

Wu, X., Liu, F., Li, L., Zou, Y., Liu, S., and Wang, Z. (2016). Major mutation events in structural genes of peste des petits ruminants virus through serial passages in vitro. *Virus Genes* 52, 422–427. doi: 10.1007/s11262-016-1317-y

Yan, F., Banadyga, L., Zhao, Y., Zhao, Z., Schiffman, Z., Huang, P., et al. (2019). Peste des petits ruminants virus-like particles induce a potent humoral and cellular immune response in goats. *Viruses* 11:918. doi: 10.3390/v11100918

Yu, R., Zhu, R., Gao, W., Zhang, M., Dong, S., Chen, B., et al. (2017). Fine mapping and conservation analysis of linear B-cell epitopes of peste des petits ruminants virus hemagglutinin protein. *Vet. Microbiol.* 208, 110–117. doi: 10.1016/j.vetmic.2017.07.008

**Conflict of Interest:** The authors declare that the research was conducted in the absence of any commercial or financial relationships that could be construed as a potential conflict of interest.

*Copyright © 2020 Yan, Li, Li, Schiffman, Huang, Zhang, Li, Jin, Wang, Zhang, Gao, Feng, Zhao, Wang and Xia. This is an open-access article distributed under the terms of the Creative Commons Attribution License (CC BY). The use, distribution or reproduction in other forums is permitted, provided the original author(s) and the copyright owner(s) are credited and that the original publication in this journal is cited, in accordance with accepted academic practice. No use, distribution or reproduction is permitted which does not comply with these terms.*

frontiers in Microbiology

ORIGINAL RESEARCH
published: 23 April 2020
doi: 10.3389/fmicb.2020.00603

# Discovery of Retro-1 Analogs Exhibiting Enhanced Anti-vaccinia Virus Activity

*Lalita Priyamvada[1], Philip Alabi[2], Andres Leon[2], Amrita Kumar[3], Suryaprakash Sambhara[3], Victoria A. Olson[1], Jason K. Sello[2]* and Panayampalli S. Satheshkumar[1]**

[1] Poxvirus and Rabies Branch, Centers for Disease Control and Prevention, Atlanta, GA, United States, [2] Department of Chemistry, Brown University, Providence, RI, United States, [3] Immunology and Pathogenesis Branch, Influenza Division, Centers for Disease Control and Prevention, Atlanta, GA, United States

Orthopoxviruses (OPXVs) are an increasing threat to human health due to the growing population of OPXV-naive individuals after the discontinuation of routine smallpox vaccination. Antiviral drugs that are effective as postexposure treatments against variola virus (the causative agent of smallpox) or other OPXVs are critical in the event of an OPXV outbreak or exposure. The only US Food and Drug Administration-approved drug to treat smallpox, Tecovirimat (ST-246), exerts its antiviral effect by inhibiting extracellular virus (EV) formation, thereby preventing cell–cell and long-distance spread. We and others have previously demonstrated that host Golgi-associated retrograde proteins play an important role in monkeypox virus (MPXV) and vaccinia virus (VACV) EV formation. Inhibition of the retrograde pathway by small molecules such as Retro-2 has been shown to decrease VACV infection *in vitro* and to a lesser extent *in vivo*. To identify more potent inhibitors of the retrograde pathway, we screened a large panel of compounds containing a benzodiazepine scaffold like that of Retro-1, against VACV infection. We found that a subset of these compounds displayed better anti-VACV activity, causing a reduction in EV particle formation and viral spread compared to Retro-1. PA104 emerged as the most potent analog, inhibiting 90% viral spread at 1.3 μM with a high selectivity index. In addition, PA104 strongly inhibited two distinct ST-246-resistant viruses, demonstrating its potential benefit for use in combination therapy with ST-246. These data and further characterizations of the specific protein targets and *in vivo* efficacy of PA104 may have important implications for the design of effective antivirals against OPXV.

**Keywords: viral inhibitor, poxvirus, antiviral agent, retrograde transport, vaccinia virus, Retro-1, retrograde inhibitor, ST-246**

OPEN ACCESS

***Edited by:***
*Lu Lu,*
*Fudan University, China*

***Reviewed by:***
*Chen Peng,*
*National Institute of Allergy and Infectious Diseases (NIAID), United States*
*Carlos Maluquer De Motes, University of Surrey, United Kingdom*
*Daniel Gillet, CEA Saclay, France*

****Correspondence:***
*Jason K. Sello*
*Jason_sello@brown.edu*
*Panayampalli S. Satheshkumar*
*xdv3@cdc.gov*

***Specialty section:***
*This article was submitted to Virology, a section of the journal Frontiers in Microbiology*

***Received:*** *26 November 2019*
***Accepted:*** *18 March 2020*
***Published:*** *23 April 2020*

***Citation:***
*Priyamvada L, Alabi P, Leon A, Kumar A, Sambhara S, Olson VA, Sello JK and Satheshkumar PS (2020) Discovery of Retro-1 Analogs Exhibiting Enhanced Anti-vaccinia Virus Activity. Front. Microbiol. 11:603. doi: 10.3389/fmicb.2020.00603*

## INTRODUCTION

The *Orthopoxvirus* (OPXV) genus contains several human pathogens of public health concern, including variola virus (the causative agent of smallpox), monkeypox virus (MPXV), cowpox virus, and vaccinia virus (VACV, the virus that formulates the smallpox vaccine) (Fenner and Nakano, 1988). While smallpox has been eradicated, other OPXVs continue to pose a threat to human health due to the lack of protective immunity post the cessation of routine smallpox vaccination (Durski et al., 2018). In particular, the incidence of MPXV has been on the rise due to several recent

outbreaks in West and Central Africa after a long hiatus in reported epidemics (Durski et al., 2018). There is also a risk of MPXV infections spreading outside the endemic region through travel or the importation of infected animals, as seen in several recent cases (Reed et al., 2004; Vaughan et al., 2018; Angelo et al., 2019; Erez et al., 2019). In addition, the identification of several new OPXVs over the past decade demonstrates the ongoing circulation and maintenance of these viruses in animal reservoirs, and highlights the need for surveillance and development of better diagnostic assays and therapeutics (Hoffmann et al., 2015; Vora et al., 2015; Springer et al., 2017; Lanave et al., 2018).

OPXVs are large double-stranded DNA viruses that have a complex life cycle, replicate in the cytoplasm of infected cells, and generate two distinct virion forms: mature virus (MV) and extracellular virus (EV), differentiated based on the number of membranes surrounding the central DNA core (Condit et al., 2006). Mature viruses consist of a viral core and a single viral membrane and harbor all the necessary proteins required for virus binding and entry. Although infectious, MVs remain inside an infected cell until lysis (Smith et al., 2002). A proportion of MVs undergo double-membrane wrapping to generate wrapped virus (WV), which can stay attached to the infected cell (cell-associated virus) or exit the cell (EV) (Smith et al., 2002; Moss, 2006). Although EV particles constitute only 1–10% of MVs, they are essential for cell-to-cell and long-distance viral spread and therefore play an important role in OPXV pathogenesis (Payne, 1980; Blasco and Moss, 1992; Engelstad and Smith, 1993). VACV mutants that fail to generate EVs produce small plaques *in vitro* and are attenuated *in vivo,* even in severely immunodeficient animal models (Blasco and Moss, 1991; Engelstad and Smith, 1993; Wolffe et al., 1993; Grosenbach et al., 2010).

The importance of EV formation for VACV pathogenesis is further highlighted by the fact that pharmacological intervention is efficacious in suppressing infection. At present, tecovirimat (ST-246) is the only US Food and Drug Administration-approved antiviral available for postexposure treatment against smallpox. ST-246 targets the viral envelope protein F13 required for EV formation, thereby decreasing viral spread and infection-induced pathology (Yang et al., 2005; Grosenbach et al., 2011). However, prolonged treatment of ST-246 can lead to the generation of drug-resistant viruses due to mutations in the F13L gene, as documented in a progressive vaccinia (PV) patient in 2009 (Lederman et al., 2012). A single amino acid mutation in F13L may overcome the therapeutic effect of the drug, reinforcing the need for additional therapeutic candidates that are safe and effective against OPXVs.

In our efforts to develop new therapeutic strategies, we focused on the peculiar dependence of OPXVs on the retrograde transport pathway for EV formation. While several viruses (Simian virus 40, papillomavirus, and influenza) rely on retrograde transport for entry into a cell, OPXVs require retrograde transport for EV membrane wrapping, and consequently viral egress (Spooner et al., 2006; Harrison et al., 2016; Sivan et al., 2016). We and others have previously demonstrated that impeding the retrograde pathway by targeting the Golgi-associated retrograde protein complex can greatly reduce EV yield with minimal impact on MV formation in VACV and MPXV (Harrison et al., 2016; Realegeno et al., 2017). Treatment with small molecule inhibitors of the retrograde pathway such as Retro-1 and Retro-2 significantly decreased EV formation *in vitro* by preventing the trafficking of the viral protein F13, which is required for membrane wrapping (Harrison et al., 2016; Sivan et al., 2016). However, initial characterizations of the antiviral efficacy of Retro-2 *in vivo* yielded underwhelming results, with treated mice showing marginal improvement in signs of clinical disease and comparable lung viral titers compared to untreated mice (Harrison et al., 2016). Additionally, better clinical scores were only observed in animals pretreated with Retro-2, and not in mice treated only postinfection (Harrison et al., 2016). Given the highly selective, potent anti-VACV activities of Retro-1 and Retro-2 *in vitro*, we were interested in structurally optimizing these small molecule inhibitors to identify novel antivirals with greater inhibitory effect compared to the parent compounds *in vitro,* as well as better *in vivo* therapeutic efficacy.

To this end, we screened a diverse collection of greater than 80 compounds sharing a benzodiazepine scaffold like Retro-1 for efficacy in *in vitro* anti-VACV assays. These efforts led to the identification of a potent antiviral we have named PA104. Like Retro-1 and Retro-2, PA104 can potently inhibit EV formation and VACV spread, while minimally impacting MV yield and causing little to no cytotoxicity. We also show that the reduction in viral spread by PA104 is attributable to inhibition of EV formation as evidenced by lack of virus secreted in media and impaired actin tail formation in infected cells. It is particularly noteworthy that PA104 also inhibits viral spread of two distinct ST-246-resistant viruses, establishing its potential for use in postexposure treatment in combination with ST-246. These observations warrant further investigation of PA104 and its efficacy as an antiviral agent.

# MATERIALS AND METHODS

## Viruses, Cell Lines, and Inhibitors

Vaccinia virus WR-GFP, VACV WR A4-YFP, VACV WR-Luc, and VACV IHDJ stocks were grown in BSC40 cells with Dulbecco modified eagle medium (DMEM) containing 2% fetal bovine serum (FBS). Two ST-246-resistant viruses were used in this study, each containing distinct mutations in the F13L gene: the first (A290V) was isolated from a 2009 human PV case (Lederman et al., 2012) and thereafter passaged in our laboratory, and the second (N267D) was provided by SIGA Technologies (Smith et al., 2011). These two viruses will hereby be referred to as RV1 and RV2, respectively. All viral stocks were titered by plaque assay prior to use in experiments. BSC40 and HeLa cell lines were passaged in DMEM with 10% FBS and 10 units/mL of penicillin and 100 μg/mL of streptomycin (penicillin–streptomycin). For all experiments involving viral infection, DMEM containing 2% FBS, hereby referred to as "DMEM-2," was used as a diluent or culture media.

The novel compounds in this study were synthesized in-house using diversity-oriented synthetic approaches. Our

synthetic approach involved two different six- and four-step synthetic schemes that were utilized (based on synthetic limitations: cost, the scope of reactions, readily available starting materials) at different stages of the SAR. The specific retrosynthetic disconnections that were effected to access these molecules are shown below. The exact details of these reaction modules/improvisations and navigations of synthetic constraints will be presented in a subsequent publication. Meanwhile, additional information about the compounds can be made available upon request.

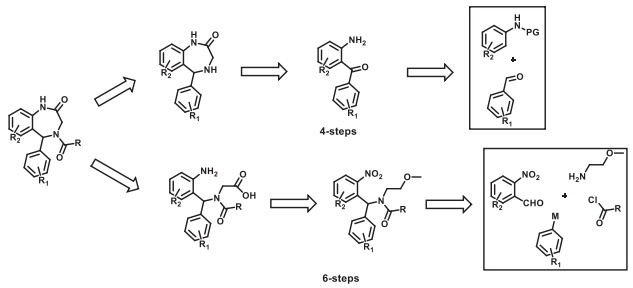


## Viral Spread Assay

The viral spread assay was performed as previously described (Cryer et al., 2017). A serial dilution series of retrograde inhibitor compounds was mixed 1:1 (vol/vol) with VACV-WR-GFP virus diluted in DMEM-2 at multiplicity of infection (MOI) 0.3. The mixture was transferred to black 96-well, clear-bottom plates (06-443-2; Corning, NY, United States) containing HeLa cells. Each plate included four to eight wells of the following controls: uninfected cells, no treatment (virus only), and virus + AraC (cytosine arabinoside, 40 μg/mL), and each dilution series was tested in duplicate. The cells were infected with the virus + compound mixture at 37°C for 24 h. Following infection, the cells were washed once with phosphate-buffered saline (PBS) and fixed with 4% paraformaldehyde for 15 min at room temperature (RT). Cells were then washed with PBS and stained with 4',6-diamidino-2-phenylindole (DAPI) for nuclei visualization for 10 min at RT. The plates were imaged using the ArrayScan XTI High Content Screen (HCS) reader, and the percentage of GFP and DAPI positive cells was quantified using the HCS Studio Cell Analysis software as previously described (Johnson et al., 2008). Total viral spread and viral spread for each compound were measured as shown below:

$$Total\ viral\ spread\ =\ \%GFP^{+}_{virus\ only} - \%GFP^{+}_{AraC}$$

$$Viral\ spread\ for\ compound\ =\ \frac{\%GFP^{+}_{Compound} - \%GFP^{+}_{AraC}}{Total\ viral\ spread}$$

Viral spread data were analyzed using a non-linear regression (curve fit) with the sigmoidal dose–response variable slope equation to determine the concentrations required for 50% inhibition ($IC_{50}$) and 90% inhibition ($IC_{90}$) of viral spread relative to the no treatment control. Analyses were performed using GraphPad Prism software (GraphPad Software, v7, San Diego, CA, United States). Values were determined based on two or more replicates from two independent experiments.

## Cytotoxicity Assay

The potential cytotoxic effects of the retrograde inhibitor compounds were tested at a range of concentrations spanning 400–0.3 μM. HeLa cells seeded in 96-well plates were infected with a mixture of VACV WR (MOI 0.01) and serially diluted compounds at 37°C for 24 h. Each concentration was tested in duplicate. Supernatants were collected, and the levels of extracellular lactate dehydrogenase (LDH) released in the supernatants were quantified using the LDH Cytotoxicity Assay Kit (88953; Thermo Scientific Pierce, Waltham, MA, United States) as per the manufacturer's instructions. Cytotoxicity data were analyzed using a non-linear regression (curve fit) with the sigmoidal dose–response variable slope equation to determine the concentrations required for 50% LDH signal ($CC_{50}$) relative to the positive control (lysed cells). This analysis was performed using GraphPad Prism software (GraphPad Software, v7). Values were determined based on two or more replicates from two independent experiments.

## Entry Assay

BSC40 cells were infected with VACV WR-Luc virus at MOI 3 for 1 h at RT. After infection, cells were washed three times with PBS to remove unbound virus. Retrograde inhibitor compounds diluted to 2.5 μM in DMEM-2 were added to cells and incubated at 37°C for 2 h. All compounds were tested in duplicate. Reporter lysis buffer was added to the wells to lyse cells, and luciferase activity was measured using the Luciferase Assay System (Promega, Madison, WI, United States) according to manufacturer's instructions. Luciferase activity was measured using an ENSPIRE plate reader (PerkinElmer, Waltham, MA, United States).

## MV and EV Quantification

BSC40 cells were infected with VACV IHDJ virus at MOI 3 for 1 h at RT. The infected cells were washed three times with DMEM-2 to remove excess virus, and retrograde inhibitor compounds were then added to the cells at a concentration of 2.5 μM. Each compound was tested in triplicate, and the cells were incubated with the compounds for 24 h at 37°C. Supernatants were collected and frozen down to determine EV yield. To measure MV yield, cells were washed three times with PBS to remove any EV particles, collected using a cell scraper, and freeze-thawed three times to release MV particles. Extracellular virus and MV yield was quantified by titering the supernatants and cells, respectively, by plaque assay. The percent EV formation and EV inhibition were determined as follows:

$$\%EV\ formation\ =\ \frac{EV\ yield}{(EV\ yield + MV\ yield)}$$

$$\%EV\ Inhibition\ for\ compound\ =\ 100 - \frac{\%EV\ formation_{Compound}}{\%EV\ formation_{Virus\ only}}$$

Statistical significance was measured using a one-way analysis of variance (ANOVA) test. MV end EV yields in the presence of the retrograde inhibitor compounds and ST-246 were compared to the virus only control using *post hoc* Sidak multiple-comparisons test.

## Effect on ST-246-Resistant Viruses

BSC40 cells seeded in 12-well plates were infected with approximately 100 plaque forming units (pfu) of VACV WR, RV1, or RV2 for 1 h at 37°C. The virus was removed and compounds PA24, PA63, and PA104 were added to the cells at a concentration of 10 μM, and ST-246 at 2 μM diluted in DMEM containing 2% carboxymethylcellulose. After a 72-h incubation with the inhibitors at 37°C, the cells were stained with crystal violet (CV) containing 4% paraformaldehyde for 15 min at RT. Post-CV staining, the plates were washed with water and imaged.

## Confocal Imaging

BSC40 cells were seeded in 24-well glass- bottom tissue culture plates (MatTek Corporation, Ashland, MA, United States) and infected with VACV WR A4-YFP (MOI 1) for 1 h at 37°C. The virus was removed, and compounds PA24, PA63, and PA104 were added to the cells at a concentration of 10 μM. After a 24-h incubation with the inhibitors at 37°C, cells were washed with PBS and fixed with 4% paraformaldehyde for 15 min at RT. Cells were stained with Alexa Flour 594 Phalloidin (ThermoFisher, Waltham, MA, United States) for actin visualization and with DAPI for nuclei visualization. After staining, cells were mounted with Prolong Gold Antifade Mounting media (Molecular Probes, Eugene, OR, United States) and imaged using the LSM 710 inverted confocal microscope (Zeiss, Oberkochen, Germany). Virus-loaded actin tails in infected cells were counted for each condition (number of cells counted per condition ranging between 5 and 9) and compared for statistical significance using a one-way ANOVA test.

## Isolation of ST246-Resistant Virus From PV Case

BSC40 cells were infected with serially diluted culture material isolated from a 2009 PV patient (Lederman et al., 2012) in the presence or absence of ST-246. Plaques observed in the presence of ST-246 were picked and reconstituted in DMEM-2. Plaque purification was performed by serially passaging single plaques grown in the presence of ST-246 four times. The isolated virus was grown in a six-well plate of BSC40 cells to create an RV1 viral

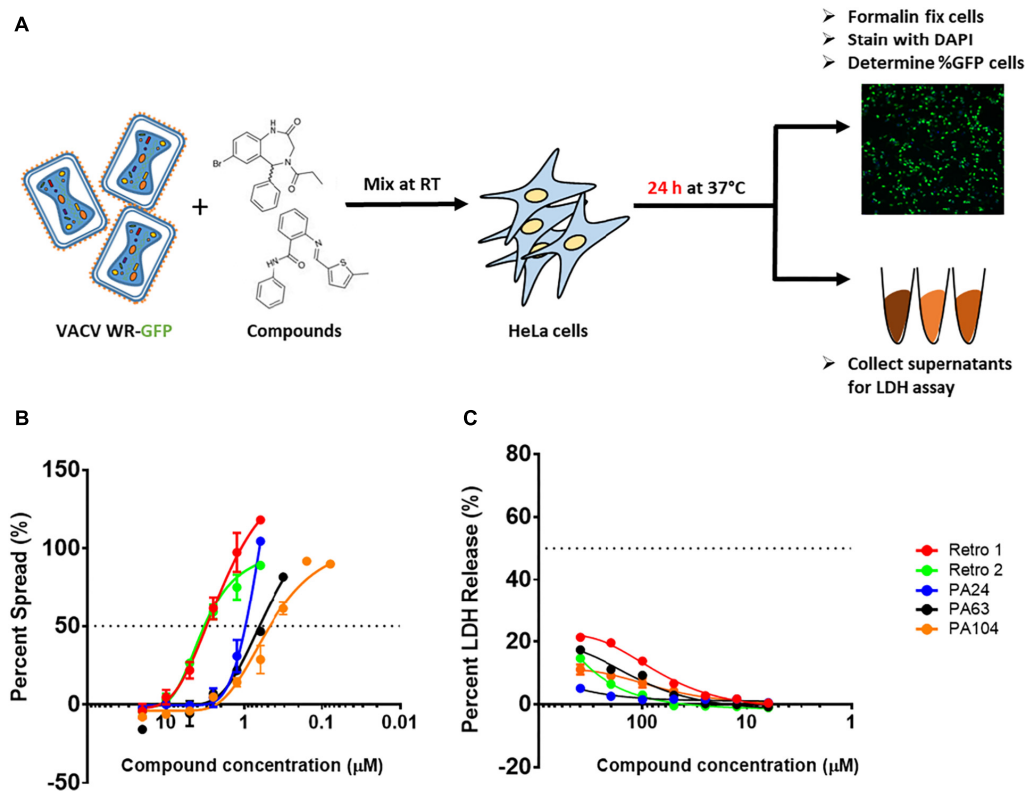


**FIGURE 1 |** Structural analogs of Retro-1 can inhibit VACV spread with minimal cytotoxicity. **(A)** Schematic representation of steps used to determine viral spread and cellular toxicity in the presence of Retro-1 analogs. The virus spread and cytotoxicity assays were performed twice for each compound, in duplicate. **(B)** Representative graph showing percent viral spread in the presence of a serial dilution series of five retrograde inhibitors. Values plotted represent the average of two independent experiments. **(C)** Representative graph showing percent LDH release in the presence of a serial dilution series of five retrograde inhibitors. Values plotted represent the average ± SEM from two independent experiments.

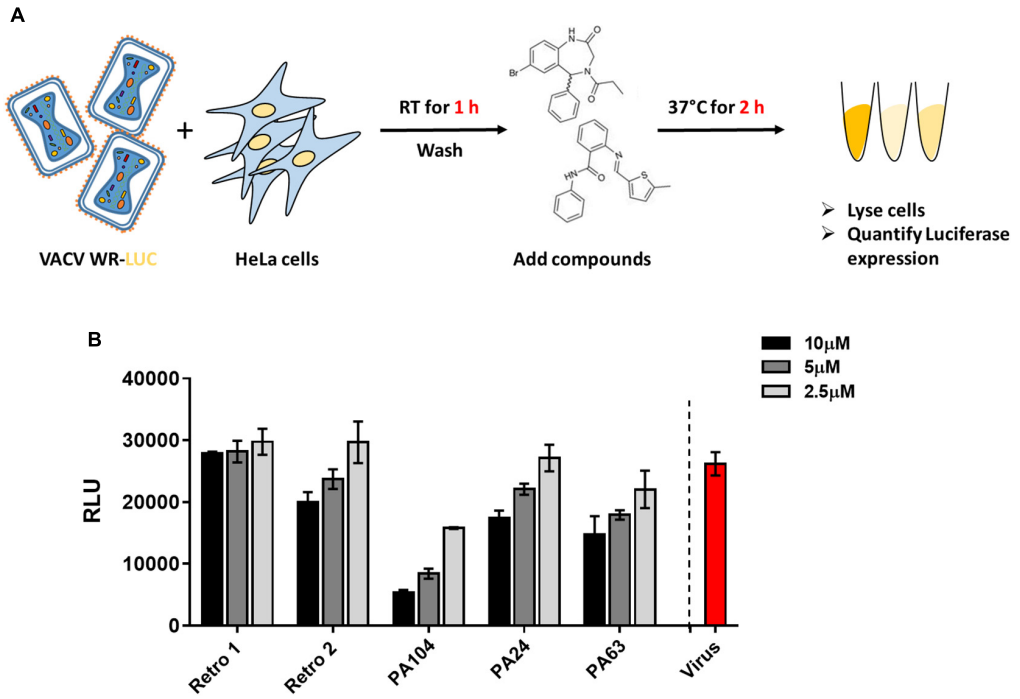


**FIGURE 2 |** Effect of Retro-1 analogs on early stages of VACV infection. **(A)** Schematic representation of VACV entry assay. **(B)** Relative light units (RLUs) in the presence of select retrograde inhibitors diluted to 2.5 μM (light gray), 5 μM (dark gray), and 10 μM (black). Values plotted represent the average of two independent experiments.

stock. To confirm the presence of the previously characterized A290V mutation in RV1, the F13L gene was sequenced by Sanger sequencing.

## RESULTS

### Screen of Benzodiazepines Yields Inhibitors of VACV Spread *in vitro*

To identify new inhibitors of VACV infection, we quantified viral spread in the presence of diverse compounds sharing a core structure with Retro-1 using VACV WR-GFP as shown in **Figure 1A**. A total of 83 compounds were tested, and the percentage of $GFP^+$ cells was determined by fluorescent imaging. We measured viral spread for each compound over a range of concentrations (**Figure 1B**) and determined the 50% inhibitory concentrations ($IC_{50}$) for all and the 90% inhibitory concentrations ($IC_{90}$) for a subset of the compounds. Of the compounds tested, 52 showed > 50% inhibition of VACV spread at concentrations ≤ 10 μM. Within this subset, 17 compounds showed greater inhibitory potency than Retro-1 and Retro-2 and had $IC_{50}$ and $IC_{90}$ values ranging between 0.5 and 2.0 μM and between 1.3 and 5.2 μM, respectively (**Table 1**, data not shown). In addition to examining their effect on viral spread, we also assessed the cellular cytotoxicity of a subset of compounds by measuring cell-released LDH levels (**Figure 1C**). We observed that a majority of potently inhibitory compounds exhibited low cytotoxicity even at 400 μM. Based on the viral spread screen of the Retro-1 like benzodiazepines, we narrowed our focus to three of the most potent VACV inhibitors: PA24, PA63, and PA104 (**Table 1**).

### Retro-1 Derivatives Inhibit VACV Infection Post-entry

Given the considerable reduction in viral spread described earlier, we checked the effect of PA24, PA63, and PA104 on VACV entry. We infected cells with VACV WR-Luc at RT, which allowed virus attachment but not entry, washed cells to remove unbound virus, and subsequently added the inhibitors (**Figure 2A**). After a 2-h incubation at 37°C, we determined luciferase expression, controlled by a synthetic early/late promoter, as a surrogate for early protein synthesis. As shown in **Supplementary Figure S1A**, input luciferase activity was very low, suggesting that the RLU values in our assay were largely attributable to viral entry and gene expression, rather than prepackaged luciferase.

**TABLE 1 |** Inhibitory and cytotoxic activities of select compounds.

| Compound | IC50 (μM) | IC90 (μM) | CC50 (μM) | SI |
|---|---|---|---|---|
| ST-246 | 0.04 | 0.1 | >400 | >10000 |
| Retro 1 | 3.0 | 7.2 | >400 | >135 |
| Retro 2 | 2.2 | 5.5 | >400 | >194 |
| PA104 | 0.5 | 1.3 | >400 | >800 |
| PA63 | 0.7 | 1.7 | >400 | >570 |
| PA24 | 1.0 | 1.8 | >400 | >400 |

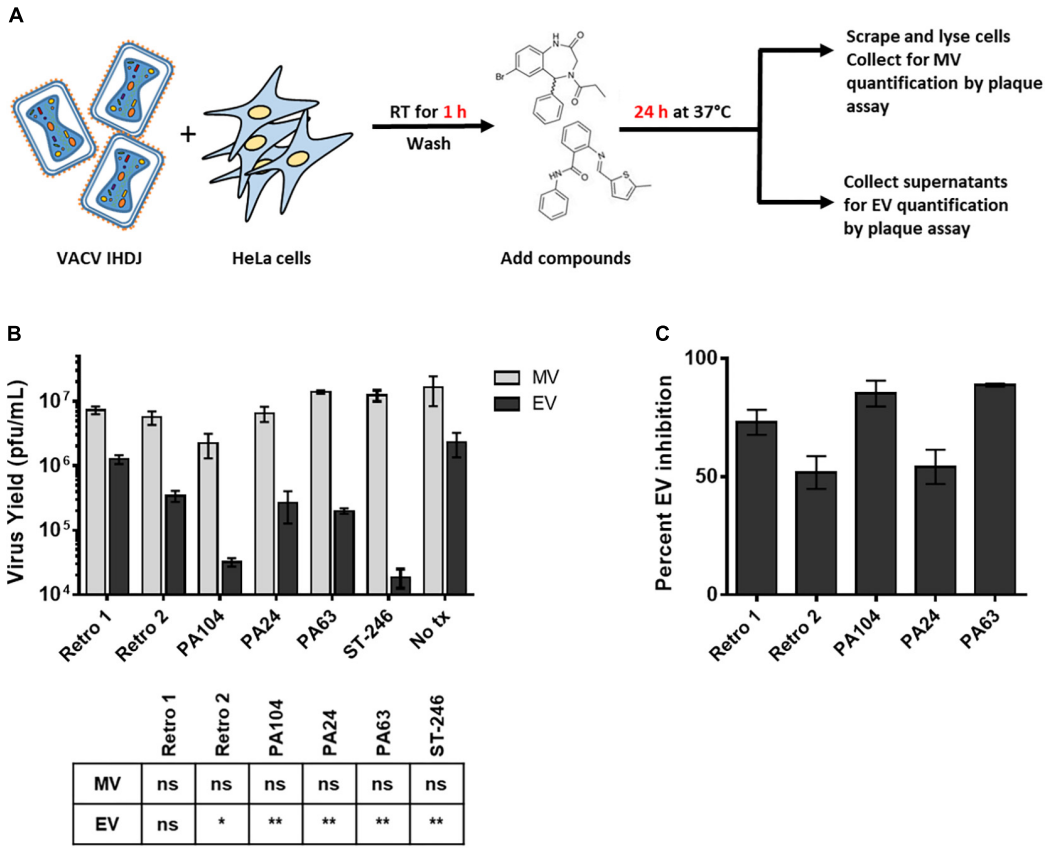


| | Retro 1 | Retro 2 | PA104 | PA24 | PA63 | ST-246 |
|---|---|---|---|---|---|---|
| MV | ns | ns | ns | ns | ns | ns |
| EV | ns | * | ** | ** | ** | ** |

**FIGURE 3 |** Reduced EV formation in the presence of Retro-1 analogs. **(A)** Schematic representation of assay used to determine MV and EV yield in the presence of Retro-2 and Retro-1 analogs. **(B)** Mature virus (light gray) and EV (black) yield (pfu/mL) in the presence of 2.5 μM retrograde inhibitors. Values represent the average of three replicates. The results of one-way analysis of variance and *post hoc* Sidak multiple-comparisons test comparing the three replicates ($n = 3$) of each compound to no treatment control are tabulated below graph: ns = not significant, $^{*}p \leq 0.05$ and $^{**}p \leq 0.005$. **(C)** Percent inhibition of EV formation in the presence of 2.5 μM retrograde inhibitors. Values calculated based upon yield data shown in **(B)**. Values in both **(B)** and **(C)** represent average ± SEM.

We observed that PA24 and PA63 did not markedly decrease viral entry at the lower concentrations tested, corroborating the findings of a previous study that tested Retro-1 and Retro-2 (Sivan et al., 2016) (**Figure 2B**). While a higher concentration (10 μM) of PA24 and PA63 reduced viral entry, for PA104 a decrease in viral entry was observed at all three concentrations tested (**Figure 2B**). To exclude the possibility that these compounds affect the enzymatic activity of luciferase, we added different concentrations of PA104 to lysed VACV WR-Luc-infected cells just before the addition of the substrate. We found no difference in luciferase activity between the treatment groups (**Supplementary Figure S1B**). Together, these data demonstrate that potent retrograde inhibitors may inhibit virus entry at high concentrations.

## Reduced EV Yield in the Presence of Retro-1 Derivatives

Previous studies have shown that Retro-1 and Retro-2 can inhibit the retrograde pathway and cause a reduction in EV particle formation during VACV and MPXV infection (Harrison et al., 2016; Sivan et al., 2016). To confirm that the decrease in viral spread observed earlier was attributable to a reduction in EV but not MV particle production, we infected cells with VACV IHDJ, a VACV strain that produces a relatively higher proportion of EV particles (**Figure 3A**). We observed that at 2.5 μM all three compounds significantly decreased EV yield compared to control (**Figure 3B**). While none of the three compounds significantly affected MV formation, a small reduction in MV yield was observed in case of PA104 (**Figure 3B**). We hypothesize that this reduction in MV production could be due to effects on viral entry (**Figure 2B**). The reduction in EV yield among the compounds tested ranged between 54 and 89% (**Figure 3C**).

## PA104 Strongly Suppresses Actin Tail Formation in VACV-Infected Cells

The double-membrane wrapping of MVs and subsequent formation of EVs in an infected cell triggers the polymerization of actin. This results in the formation of actin tails that can propel the EV particles to neighboring cells, causing cell-to-cell spread (Smith et al., 2002). Since we had observed a decrease

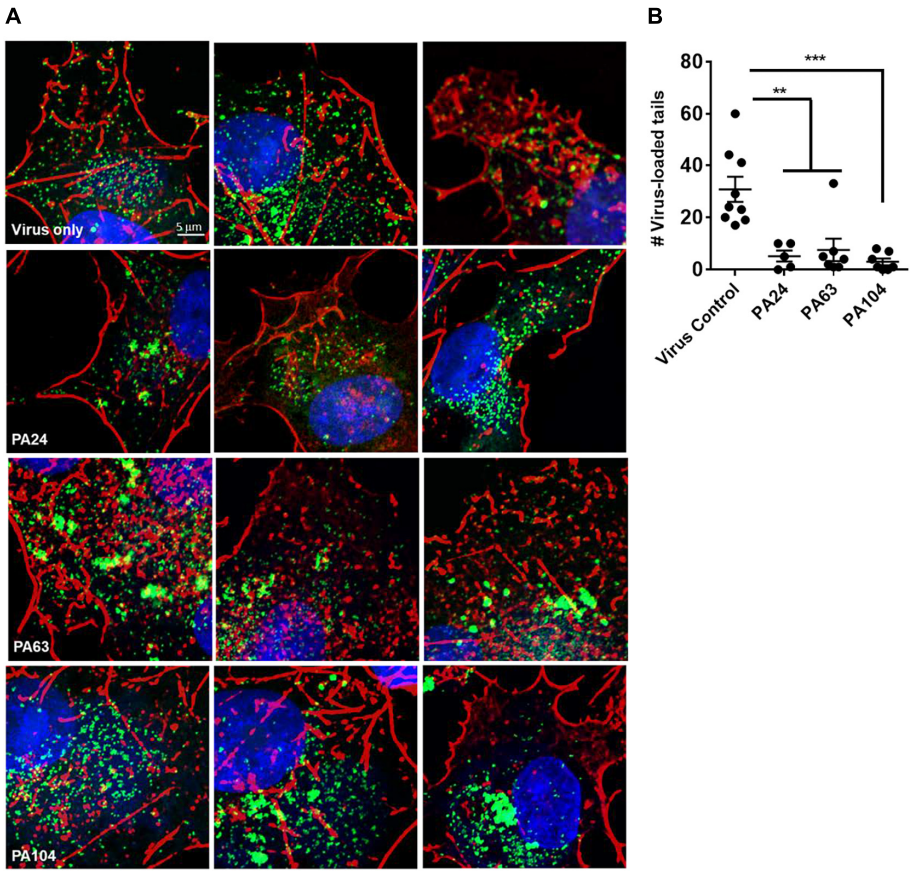


**FIGURE 4 |** Inhibition of EV formation visualized by actin staining. **(A)** Confocal microscopy images of cells infected with VACV WR A4-YFP virus in the presence or absence of Retro-1 analogs PA63, PA24, and PA104. Few to no virus-loaded actin tails observed in the presence of Retro-1 analogs in comparison to virus-only treatment. Nuclei, actin, and VACV are stained blue, red, and green, respectively. Scale bars represent 5 μm. **(B)** Average number of virus-loaded actin tails per cell for each treatment. For each condition, virus-loaded actin tails from five to nine cells were counted (virus control: 9, PA24: 5, PA63: 9, and PA104: 7). Each dot represents one cell, and the average ± SEM for all four conditions are shown. Results of one-way analysis of variance and *post hoc* Tukey multiple-comparisons test comparing the four treatments are described: $^{**}p \leq 0.005$ and $^{***}p \leq 0.0005$.

in both viral spread and EV yield in the presence of Retro-1 analogs, we were interested in testing the effect of these compounds on the appearance of virus-loaded actin tails within cells. To this end, we infected cells with VACV in the presence or absence of PA24, PA63, and PA104 and visualized actin-associated virus particles using confocal microscopy. In the absence of the Retro-1 inhibitors, infected cells had several actin tails loaded with VACV at the tips (the viral particles appear as green dots due to the fusion of GFP with the core protein A4), which is characteristic of VACV infection (**Figure 4** and **Supplementary Figure S2**). On the other hand, in all three inhibitor conditions, actin aggregates appeared shorter and did not resemble the clearly defined tails observed in the untreated control (**Figure 4A**). We enumerated the virus-loaded actin tails for each condition and found a significant decrease in virus-loaded tails in the presence of PA24, PA63, and PA104 (**Figure 4B**). In case of PA104, the reduction in actin tail staining was the most significant compared to the virus control. These data corroborate the results shown in **Figures 3B,C**, demonstrating that fewer virus-loaded actin tails appear in the presence of retrograde inhibitors, which results in a lower EV yield overall.

## PA104 Potently Inhibits the Spread of ST-246-Resistant Viruses

ST-246, targets F13, a peripheral viral membrane protein, interfering with its intracellular localization (Yang et al., 2005). However, mutations in F13L gene can cause viral resistance to ST-246 as demonstrated previously (Yang et al., 2005; Lederman et al., 2012; Duraffour et al., 2015). To investigate whether the potent anti-VACV compounds identified in this study could inhibit ST-246–resistant virus, we infected cells with two different ST-246-resistant viruses in the presence of 10 μM PA104, PA24, and PA63. The two viruses used contained distinct resistance-conferring mutations; the first, hereby referred to as RV1, was isolated from the lesions of a PV patient by serial plaque purification in the presence of ST-246 (Lederman et al., 2012). We sequenced the F13L gene of our isolated RV1 and found the previously reported resistance mutation A290V (**Figure 5A**).

A

```
ACAM    MWPFASVPAGAKCRLVETLPENMDFRSDHLTTFECFNEIITLAKKYIYIASFCCNPLSTT 60
RV1     ------------------------------------------------------------ 60
RV2     ------------------------------------------------------------ 60
        ************************************************************

ACAM    RGALIFDKLKEASEKGIKIIVLLDERGKRNLGELQSHCPDINFITVNIDKKNNVGLLLGC 120
RV1     ------------------------------------------------------------ 120
RV2     ------------------------------------------------------------ 120
        ************************************************************

ACAM    FWVSDDERCYVGNASFTGGSIHTIKTLGVYSDYPPLATDLRRRFDTFKAFNSAKNSWLNL 180
RV1     ------------------------------------------------------------ 180
RV2     ------------------------------------------------------------ 180
        ************************************************************

ACAM    CSAACCLPVSTAYHIKNPIGGVFFTDSPEHLLGYSRDLDTDVVIDKLRSAKTSIDIEHLA 240
RV1     ------------------------------------------------------------ 240
RV2     ------------------------------------------------------------ 240
        ************************************************************

ACAM    IVPTTRVDGNSYYWPDIYNSIIEAAINRGVKIRLLVGNWDKNDVYSMATARSLDALCVQN 300
RV1     -----------------------------------------V---------- 300
RV2     -----------------------D------------------------------ 300
        ************************:**********************.********** 

ACAM    DLSVKVFTIQNNTKLLIVDDEYVHITSANFDGTHYQNHGFVSFNSIDKQLVSEAKKIFER 360
RV1     ------------------------------------------------------------ 360
RV2     ------------------------------------------------------------ 360
        ************************************************************

ACAM    DWVSSHSKSLKI    372
RV1     ---------       369
RV2     ------------    369
        *********
```

B

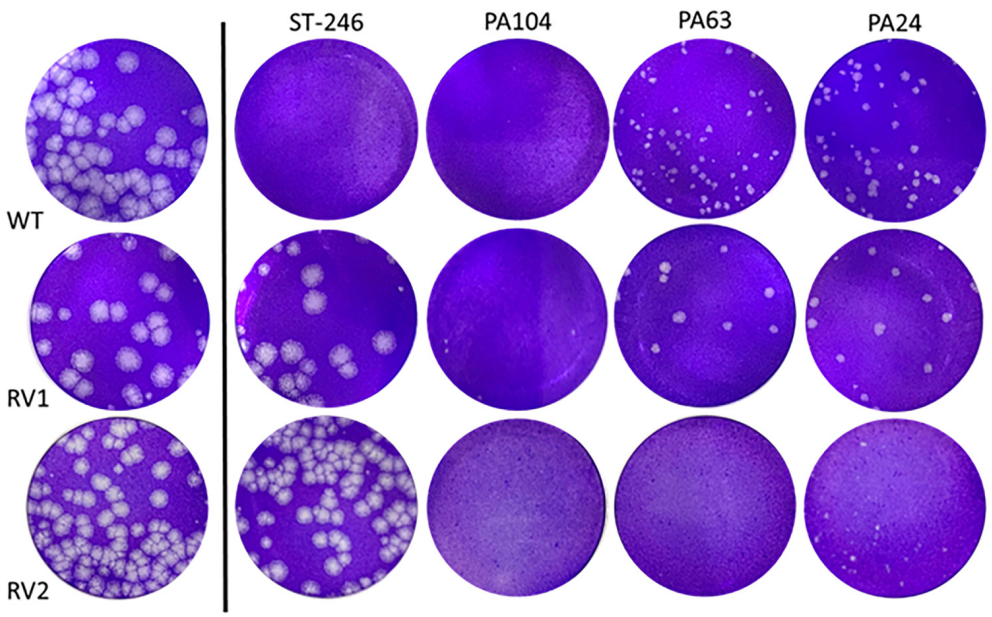


**FIGURE 5 |** Retro-1 analogs PA104, PA24, and PA63 inhibit viral spread of ST-246-resistant VACV. **(A)** RV1 and RV2 sequence alignments showing preserved A290V and N267D mutations, respectively. Amino acid alignment of F13 of lab-grown RV1 viral isolates and RV2 compared to published ACAM strain (Lederman et al., 2012). **(B)** Plaque assay images showing observable decrease in viral plaque size of RV1 and RV2 virus in the presence of 10 μM PA104, PA24, and PA63.

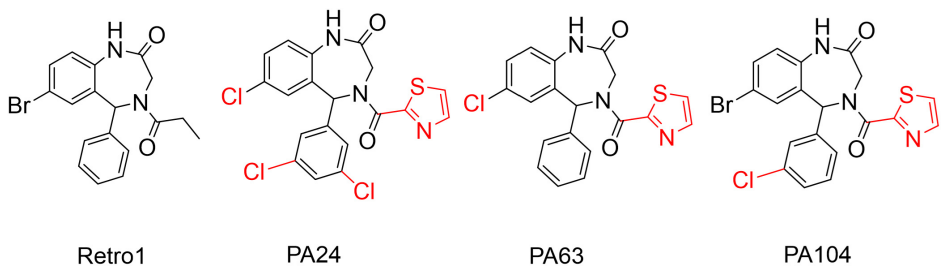


**FIGURE 6 |** Structural modifications in PA104, PA24, and PA63. All modifications made to the original Retro-1 structure shown in red.

The second virus, hereby referred to as RV2, was acquired from SIGA Technologies and contains the N267D resistance mutation (Smith et al., 2011).

While both the ST-246-resistant viruses formed large plaques in the presence or absence of 2 μM ST-246, a concentration of ST-246 over 50-fold higher than its IC50 value, treatment with PA104, PA24, and PA63 caused a considerable reduction in viral plaque size. As shown in **Figure 5B**, all three compounds substantially reduced the size of RV2 plaques. For RV1, on the other hand, PA104 was markedly more effective in reducing viral spread than PA24 and PA63 (**Figure 5B**). Overall, these data show that retrograde inhibitors can block EV formation and spread of ST-246-resistant VACV.

## DISCUSSION

In this study, we describe the screening and characterization of a panel of compounds sharing the benzodiazepine scaffold of Retro-1. These efforts resulted in the discovery of three compounds, PA24, PA63, and PA104, with impressive antiviral activity against VACV, the most potent and promising of which is PA104. The structural differences between these analogs and their parent Retro-1 have been highlighted in **Figure 6**, and nuclear magnetic resonance (NMR) and mass spectrometry (MS) data are provided in **Supplementary Data Sheets S1, S2**. We demonstrated the following: (i) Retro-1 derivatives potently inhibit VACV spread *in vitro* with minimal cytotoxicity. (ii) The inhibitory effect was predominantly at a late stage of viral replication. (iii) EV formation is the main target of the analogs, which have little impact on MV yield. (iv) Retro-1 analogs can effectively decrease viral spread of ST-246-resistant viruses. In addition, we identified the Retro-1 derivative PA104 as a promising antiviral candidate with superior anti-VACV efficacy compared to the previously characterized Retro-1 and Retro-2, low cellular toxicity, and potent activity against ST-246-resistant viruses.

In total, 83 compounds were tested for their ability to decrease VACV spread *in vitro*. We observed that 17 of these compounds had comparable or more potent anti-VACV activity than Retro-1 and Retro-2 ($IC_{50}$ and $IC_{90}$ values $\leq$ Retro-1 and Retro-2). We focused on three compounds with high potency and low cytotoxicity, PA24, PA63, and PA104, and subsequently tested their impact on VACV entry and EV/MV yield. The most potent inhibitor of VACV spread, PA104, caused an observable reduction in luciferase activity even at 2.5 μM. In contrast, PA24 and PA63 only appeared to affect entry at higher concentrations. All three compounds tested minimally impacted MV yield while considerably reducing EV yield, except for PA104, which caused a small reduction in MV yield in addition to decreasing EV formation. The spread assay, entry assay, and MV/EV yield data together suggest that while the main mechanism of viral inhibition by Retro-1 derivatives is the inhibition of EV particle formation, select compounds such as PA104 may impact viral entry when present at concentrations greater than their effective inhibitory concentrations. These findings aligned well with previous characterizations of Retro-1 and Retro-2 activity *in vitro* (Harrison et al., 2016; Sivan et al., 2016).

Vaccinia virus replicates in the cytoplasm of the infected cells, resulting in the formation of infectious, single-membrane MV particles at the site of replication (Condit et al., 2006). Although infectious, these MV particles remain intracellular unless wrapped by two additional membranes of post-Golgi or endosomal origin to form EVs. Once the outer layer of the EV double membrane fuses with the plasma membrane, an EV can be propelled out of the infected cell by actin tails (Smith et al., 2002). Because viral spread and EV yield were greatly reduced in the presence of our panel of compounds, we visualized actin tail-associated EVs in infected cells using confocal microscopy. Fewer actin tails were detected in the presence of all three compounds tested, PA104, PA63, and PA24, with the greatest reduction observed in case of PA104.

We and others have previously reported the spontaneous development of ST-246 resistance, both *in vitro* (Yang et al., 2005; Duraffour et al., 2015) and clinically in a smallpox-vaccinated PV patient receiving ST-246 as part of their treatment regimen (Lederman et al., 2012). In healthy individuals, it is possible that the immune response might overcome such resistant viruses, if they arise. However, additional interventions may be required for at-risk groups that cannot mount a protective immune response, such as individuals with immune deficiencies. For such cases, it would be beneficial to have additional antiviral candidates that can be administered in combination with ST-246 and can suppress ST-246-resistant viruses. We tested the inhibitory potential of PA104, PA63, and PA24 against two different ST-246-resistant viruses and found that all three compounds reduced viral spread of both viruses, as determined by a reduction in viral

plaque size. Interestingly, while RV2 was substantially inhibited by all three Retro-1 compounds, RV1 appeared to be less efficiently inhibited by PA24 and PA63. These differences in the levels of viral inhibition by the same compounds could potentially be caused by additional uncharacterized mutations in other genes, or strain differences between the viruses; whereas RV1 was an Acambis strain of VACV, RV2 was a Western Reserve strain. Nevertheless, PA104 treatment resulted in maximal inhibition of plaque size for wild-type as well as RV1 and RV2 ST-246-resistant viruses. We hypothesize that its superior capacity to inhibit these viruses compared to PA24 and PA63 could be due to its ability to target multiple steps of VACV infection, including viral entry and MV formation, in addition to EV formation (**Figures 2**, **3**).

In all, given its high SI (>800), submicromolar effective concentration, and potent inhibition of ST-246-resistant viruses, PA104 emerges as a promising candidate for future *in vivo* exploration. Further, PA104 targets a host-specific process rather than a viral protein, offering two additional advantages. First, the absence of a direct viral target reduces the probability of viral resistance to the compound (Lin and Gallay, 2013; Kaufmann et al., 2018). Second is the possibility of broad-range applicability to other viruses and non-viral pathogens that utilize the retrograde pathway for entry or egress. We and others have previously shown that Retro-2 and its analogs can reduce *Leishmania*, polyomavirus, and papillomavirus infections, as well as inhibit Shiga toxin trafficking in cells (Noel et al., 2013; Carney et al., 2014; Craig et al., 2017). Recent reports have also investigated the effect of Retro-2 derivatives on HSV2 infections (Dai et al., 2018). A majority of these studies have focused primarily on Retro-2 derivatives, and at present, less is understood about the antipathogenic potential of Retro-1 and its derivatives. To our knowledge, this is the first study to provide an in-depth, large-scale characterization of the inhibitory potential of compounds structurally related to Retro-1. As the retrograde pathway plays an important role for several pathogens and toxins, further characterization of compounds such as PA104 and exploration of their *in vivo* activity could have important implications for the design of broad-spectrum therapeutics that have immense public health benefits. An in-depth structure–activity relationship study of PA104 and other structural analogs of Retro-1 is in progress and will be reported in due course.

## DATA AVAILABILITY STATEMENT

The raw data supporting the conclusions of this article will be made available by the authors, without undue reservation, to any qualified researcher.

## AUTHOR CONTRIBUTIONS

LP, JS, and PS contributed to the conception and design of the study. PA, AL, and JS designed and generated the benzodiazepine scaffold-containing compounds. LP and PS performed poxvirus experiments and wrote the first draft of the manuscript. AK and SS performed confocal imaging experiments. LP, PA, VO, JS, and PS edited the manuscript. All authors contributed to the manuscript revision and read and approved the submitted version.

## FUNDING

The study was supported by the CDC Intramural Research and Biomedical Advanced Research and Developmental Authority (BARDA) and an ORISE Postdoctoral Fellowship (LP) and funding from Brown University (JS).

## ACKNOWLEDGMENTS

We thank Dr. Bernard Moss, Dr. Jan Carette, and SIGA Technologies for reagents, and Dr. Jinxin Gao for his help with F13 sequencing. The findings and conclusions in this report are those of the authors and do not necessarily represent the official position of the Centers for Disease Control and Prevention.

## SUPPLEMENTARY MATERIAL

The Supplementary Material for this article can be found online at: https://www.frontiersin.org/articles/10.3389/fmicb.2020.00603/full#supplementary-material

**FIGURE S1 |** Validation of luciferase-based viral entry assay. **(A)** Minimal input luciferase activity after 5 min infection at RT. Luciferase activity in cells infected for 5 min at RT was significantly lower than infection for 2 h at 37°C. **** indicates an unpaired *t*-test *p*-value < 0.0001. **(B)** PA104 does not impact luciferase enzyme activity. No difference observed in RLU values in the presence of three concentrations of PA104. Both graphs show mean values ± SEM.

**FIGURE S2 |** Fewer virus-loaded actin tails in the presence of Retro-1 inhibitors. Confocal microscopy images of cells infected with VACV WR A4-YFP virus in the presence or absence of Retro-1 analogs PA63, PA24, and PA104. Lower magnification images of cells pictured in **Figure 4**. Scale bars represent 10 μm and white boxes indicate the area within each cell that was magnified to create **Figure 4**.

**DATA SHEET S1 |** NMR and MS data for PA104, PA24, and PA63.

## REFERENCES

Angelo, K. M., Petersen, B. W., Hamer, D. H., Schwartz, E., and Brunette, G. (2019). Monkeypox transmission among international travellers-serious monkey business?. *J. Travel Med.* 26:taz002.

Blasco, R., and Moss, B. (1991). Extracellular vaccinia virus formation and cell-to-cell virus transmission are prevented by deletion of the gene encoding the 37,000-Dalton outer envelope protein. *J. Virol.* 65, 5910–5920.

Blasco, R., and Moss, B. (1992). Role of cell-associated enveloped vaccinia virus in cell-to-cell spread. *J. Virol.* 66, 4170–4179.

Carney, D. W., Nelson, C. D., Ferris, B. D., Stevens, J. P., Lipovsky, A., Kazakov, T., et al. (2014). Structural optimization of a retrograde trafficking inhibitor that protects cells from infections by human polyoma- and

papillomaviruses. *Bioorg. Med. Chem.* 22, 4836–4847. doi: 10.1016/j.bmc.2014.06.053

Condit, R. C., Moussatche, N., and Traktman, P. (2006). In a nutshell: structure and assembly of the vaccinia virion. *Adv. Virus Res.* 66, 31–124.

Craig, E., Huyghues-Despointes, C. E., Yu, C., Handy, E. L., Sello, J. K., and Kima, P. E. (2017). Structurally optimized analogs of the retrograde trafficking inhibitor Retro-2cycl limit Leishmania infections. *PLoS Negl. Trop. Dis.* 11:e0005556. doi: 10.1371/journal.pntd.0005556

Cryer, M., Lane, K., Greer, M., Cates, R., Burt, S., Andrus, M., et al. (2017). Isolation and identification of compounds from Kalanchoe pinnata having human alphaherpesvirus and vaccinia virus antiviral activity. *Pharm. Biol.* 55, 1586–1591. doi: 10.1080/13880209.2017.1310907

Dai, W., Wu, Y., Bi, J., Wang, J., Wang, S., Kong, W., et al. (2018). Antiviral effect of Retro-2.1 against Herpes simplex virus type 2 in vitro. *J. Microbiol. Biotechnol.* 28, 849–859. doi: 10.4014/jmb.1712.12052

Duraffour, S., Lorenzo, M. M., Zoller, G., Topalis, D., Grosenbach, D., Hruby, D. E., et al. (2015). ST-246 is a key antiviral to inhibit the viral F13L phospholipase, one of the essential proteins for orthopoxvirus wrapping. *J. Antimicrob. Chemother.* 70, 1367–1380. doi: 10.1093/jac/dku545

Durski, K. N., Mccollum, A. M., Nakazawa, Y., Petersen, B. W., Reynolds, M. G., Briand, S., et al. (2018). Emergence of Monkeypox - West and Central Africa, 1970-2017. *MMWR Morb. Mortal. Wkly. Rep.* 67, 306–310. doi: 10.15585/mmwr.mm6710a5

Engelstad, M., and Smith, G. L. (1993). The vaccinia virus 42-kDa envelope protein is required for the envelopment and egress of extracellular virus and for virus virulence. *Virology* 194, 627–637.

Erez, N., Achdout, H., Milrot, E., Schwartz, Y., Wiener-Well, Y., Paran, N., et al. (2019). Diagnosis of imported monkeypox Israel, 2018. *Emerg. Infect. Dis.* 25, 980–983. doi: 10.3201/eid2505.190076

Fenner, F., and Nakano, J. H. (1988). "Poxviridae: the poxviruses," in *Laboratory Diagnosis of Infectious Diseases Principles and Practice: VOLUME II Viral, Rickettsial, and Chlamydial Diseases*, eds E. H. Lennette, P. Halonen, and F. A. Murphy (New York, NY: Springer New York), 177–210.

Grosenbach, D. W., Berhanu, A., King, D. S., Mosier, S., Jones, K. F., Jordan, R. A., et al. (2010). Efficacy of ST-246 versus lethal poxvirus challenge in immunodeficient mice. *Proc. Natl. Acad. Sci. U.S.A.* 107, 838–843. doi: 10.1073/pnas.0912134107

Grosenbach, D. W., Jordan, R., and Hruby, D. E. (2011). Development of the small-molecule antiviral ST-246 as a smallpox therapeutic. *Future Virol.* 6, 653–671.

Harrison, K., Haga, I. R., Pechenick Jowers, T., Jasim, S., Cintrat, J. C., Gillet, D., et al. (2016). Vaccinia virus uses retromer-independent cellular retrograde transport pathways to facilitate the wrapping of intracellular mature virions during virus morphogenesis. *J. Virol.* 90, 10120–10132. doi: 10.1128/JVI.01464-16

Hoffmann, D., Franke, A., Jenckel, M., Tamosiunaite, A., Schluckebier, J., Granzow, H., et al. (2015). Out of the reservoir: phenotypic and genotypic characterization of a novel cowpox virus isolated from a common vole. *J. Virol.* 89, 10959–10969. doi: 10.1128/JVI.01195-15

Johnson, M. C., Damon, I. K., and Karem, K. L. (2008). A rapid, high-throughput vaccinia virus neutralization assay for testing smallpox vaccine efficacy based on detection of green fluorescent protein. *J. Virol. Methods* 150, 14–20. doi: 10.1016/j.jviromet.2008.02.009

Kaufmann, S. H. E., Dorhoi, A., Hotchkiss, R. S., and Bartenschlager, R. (2018). Host-directed therapies for bacterial and viral infections. *Nat. Rev. Drug Discov.* 17, 35–56. doi: 10.1038/nrd.2017.162

Lanave, G., Dowgier, G., Decaro, N., Albanese, F., Brogi, E., Parisi, A., et al. (2018). Novel Orthopoxvirus and lethal disease in cat. *Italy. Emerg. Infect. Dis* 24, 1665–1673. doi: 10.3201/eid2409.171283

Lederman, E. R., Davidson, W., Groff, H. L., Smith, S. K., Warkentien, T., Li, Y., et al. (2012). Progressive vaccinia: case description and laboratory-guided therapy with vaccinia immune globulin ST-246, and CMX001. *J. Infect. Dis.* 206, 1372–1385. doi: 10.1093/infdis/jis510

Lin, K., and Gallay, P. (2013). Curing a viral infection by targeting the host: the example of cyclophilin inhibitors. *Antiviral Res.* 99, 68–77. doi: 10.1016/j.antiviral.2013.03.020

Moss, B. (2006). Poxvirus entry and membrane fusion. *Virology* 344, 48–54.

Noel, R., Gupta, N., Pons, V., Goudet, A., Garcia-Castillo, M. D., Michau, A., et al. (2013). N-methyldihydroquinazolinone derivatives of Retro-2 with enhanced efficacy against Shiga toxin. *J. Med. Chem.* 56, 3404–3413. doi: 10.1021/jm4002346

Payne, L. G. (1980). Significance of extracellular enveloped virus in the in vitro and in vivo dissemination of vaccinia. *J. Gen. Virol.* 50, 89–100.

Realegeno, S., Puschnik, A. S., Kumar, A., Goldsmith, C., Burgado, J., Sambhara, S., et al. (2017). Monkeypox virus host factor screen using haploid cells identifies essential role of GARP complex in extracellular virus formation. *J. Virol.* 91:e00011-17.

Reed, K. D., Melski, J. W., Graham, M. B., Regnery, R. L., Sotir, M. J., Wegner, M. V., et al. (2004). The detection of monkeypox in humans in the Western Hemisphere. *N. Engl. J. Med.* 350, 342–350.

Sivan, G., Weisberg, A. S., Americo, J. L., and Moss, B. (2016). Retrograde transport from early endosomes to the trans-Golgi network enables membrane wrapping and egress of vaccinia virus virions. *J. Virol.* 90, 8891–8905. doi: 10.1128/JVI.01114-16

Smith, G. L., Vanderplasschen, A., and Law, M. (2002). The formation and function of extracellular enveloped vaccinia virus. *J. Gen. Virol.* 83, 2915–2931. doi: 10.1099/0022-1317-83-12-2915

Smith, S. K., Self, J., Weiss, S., Carroll, D., Braden, Z., Regnery, R. L., et al. (2011). Effective antiviral treatment of systemic orthopoxvirus disease: ST-246 treatment of prairie dogs infected with monkeypox virus. *J. Virol.* 85, 9176–9187. doi: 10.1128/JVI.02173-10

Spooner, R. A., Smith, D. C., Easton, A. J., Roberts, L. M., and Lord, J. M. (2006). Retrograde transport pathways utilised by viruses and protein toxins. *Virol. J.* 3:26.

Springer, Y. P., Hsu, C. H., Werle, Z. R., Olson, L. E., Cooper, M. P., Castrodale, L. J., et al. (2017). Novel Orthopoxvirus Infection in an Alaska Resident. *Clin. Infect. Dis.* 64, 1737–1741. doi: 10.1093/cid/cix219

Vaughan, A., Aarons, E., Astbury, J., Balasegaram, S., Beadsworth, M., Beck, C. R., et al. (2018). Two cases of monkeypox imported to the United Kingdom, September 2018. *Euro. Surveill.* 23, doi: 10.2807/1560-7917.ES.2018.23.38.1800509

Vora, N. M., Li, Y., Geleishvili, M., Emerson, G. L., Khmaladze, E., Maghlakelidze, G., et al. (2015). Human infection with a zoonotic orthopoxvirus in the country of Georgia. *N. Engl. J. Med.* 372, 1223–1230. doi: 10.1056/NEJMoa1407647

Wolffe, E. J., Isaacs, S. N., and Moss, B. (1993). Deletion of the vaccinia virus B5R gene encoding a 42-kilodalton membrane glycoprotein inhibits extracellular virus envelope formation and dissemination. *J. Virol.* 67, 4732–4741.

Yang, G., Pevear, D. C., Davies, M. H., Collett, M. S., Bailey, T., Rippen, S., et al. (2005). An orally bioavailable antipoxvirus compound (ST-246) inhibits extracellular virus formation and protects mice from lethal orthopoxvirus Challenge. *J. Virol.* 79, 13139–13149.

**Conflict of Interest:** The authors declare that the research was conducted in the absence of any commercial or financial relationships that could be construed as a potential conflict of interest.

*Copyright © 2020 Priyamvada, Alabi, Leon, Kumar, Sambhara, Olson, Sello and Satheshkumar. This is an open-access article distributed under the terms of the Creative Commons Attribution License (CC BY). The use, distribution or reproduction in other forums is permitted, provided the original author(s) and the copyright owner(s) are credited and that the original publication in this journal is cited, in accordance with accepted academic practice. No use, distribution or reproduction is permitted which does not comply with these terms.*

frontiers in Microbiology

REVIEW
published: 24 April 2020
doi: 10.3389/fmicb.2020.00658

# The Current and Future State of Vaccines, Antivirals and Gene Therapies Against Emerging Coronaviruses

*Longping V. Tse[1], Rita M. Meganck[2], Rachel L. Graham[1] and Ralph S. Baric[1,3]**

[1] Department of Epidemiology, The University of North Carolina at Chapel Hill, Chapel Hill, NC, United States, [2] Curriculum in Genetics and Molecular Biology, The University of North Carolina at Chapel Hill, Chapel Hill, NC, United States, [3] Department of Microbiology and Immunology, The University of North Carolina at Chapel Hill, Chapel Hill, NC, United States

Emerging coronaviruses (CoV) are constant global public health threats to society. Multiple ongoing clinical trials for vaccines and antivirals against CoVs showcase the availability of medical interventions to both prevent and treat the future emergence of highly pathogenic CoVs in human. However, given the diverse nature of CoVs and our close interactions with wild, domestic and companion animals, the next epidemic zoonotic CoV could resist the existing vaccines and antivirals developed, which are primarily focused on Severe Acute Respiratory Syndrome Coronavirus (SARS-CoV) and Middle East Respiratory Syndrome Coronavirus (MERS CoV). In late 2019, the novel CoV (SARS-CoV-2) emerged in Wuhan, China, causing global public health concern. In this review, we will summarize the key advancements of current vaccines and antivirals against SARS-CoV and MERS-CoV as well as discuss the challenge and opportunity in the current SARS-CoV-2 crisis. At the end, we advocate the development of a "plug-and-play" platform technologies that could allow quick manufacturing and administration of broad-spectrum countermeasures in an outbreak setting. We will discuss the potential of AAV-based gene therapy technology for *in vivo* therapeutic antibody delivery to combat SARS-CoV-2 outbreak and the future emergence of severe CoVs.

**Keywords: coronavirus (CoV), vaccine, antivirals, adeno-associate virus, passive immunization strategy, MERS- and SARS-CoV, 2019 nCoV**

OPEN ACCESS

***Edited by:***
*Lu Lu,*
*Fudan University, China*

***Reviewed by:***
*Jasper Fuk Woo Chan,*
*The University of Hong Kong, Hong Kong*
*Susan Baker,*
*Loyola University Chicago, United States*

***Correspondence:**
*Ralph S. Baric*
*rbaric@email.unc.edu*

***Specialty section:***
*This article was submitted to Virology, a section of the journal Frontiers in Microbiology*

***Received:*** *11 November 2019*
***Accepted:*** *23 March 2020*
***Published:*** *24 April 2020*

***Citation:***
*Tse LV, Meganck RM, Graham RL and Baric RS (2020) The Current and Future State of Vaccines, Antivirals and Gene Therapies Against Emerging Coronaviruses. Front. Microbiol. 11:658. doi: 10.3389/fmicb.2020.00658*

## INTRODUCTION

The zoonotic transmission and subsequent adaptation to humans of emerging RNA viruses is a global public health concern. In the 21st century alone, coronaviruses (CoV) have been responsible for two separate endemics, the severe acute respiratory syndrome (SARS) and Middle East Respiratory Syndrome (MERS) CoVs (de Wit et al., 2016). In late Dec 2019, a novel SARS-like CoV designated 2019 nCoV emerged in Wuhan China, causing > 60,000 cases and over 1350 deaths in an ongoing epidemic (Hui et al., 2020). Other highly pathogenic threat viruses that have emerged in the 21st century include influenza viruses, Ebola viruses, flaviviruses and paramyxoviruses (Mackenzie and Jeggo, 2013). The high mutation and recombination rate of RNA viruses

drives the emergence of new viral strains that can rapidly adapt to new and changing ecologies (Drake and Holland, 1999; Lauring and Andino, 2010). Furthermore, industrialization, globalization and traditional cultural habits potentiate the likelihood of zoonotic transmission and facilitate the spread of viruses in the human population. While new outbreaks from emergent viruses are inevitable, scientists, epidemiologists, and the health care industry are racing to develop new technologies to better predict and minimize the impact of an outbreak by employing global viral surveillance programs and developing vaccines and antivirals (Lipkin and Firth, 2013). A major challenge of vaccine and antiviral development is the elusive nature of the emerging viruses, which oftentimes emerge from highly heterogeneous populations of virus strains that circulate in animal reservoirs (Lauring and Andino, 2010). Therefore, to prepare for future outbreaks, vaccines and antivirals will need to be both potent and broadly effective against multiple potential emerging viruses within and across virus families. Additionally, in order to control and prevent viral spread, treatments must be readily available to affected populations and have a fast response time. In this review, we will focus our discussion on the challenges, as well as current development, of vaccines and antivirals for SARS-CoV and MERS-CoV. At the end, we will also discuss the potential use of AAV-based gene therapy as a quick response to prevent and treat emerging viral infections in the current SARS-CoV-2 and future outbreak situations.

## Endemic and Emerging Coronaviruses

Coronaviruses are a diverse group of positive-stranded RNA viruses which infect a wide range of animals from birds to mammals, causing a variety of diseases (Perlman and Netland, 2009; Woo et al., 2009; Peck et al., 2015). Based on sequence identity of the spike protein or the non-structural proteins (nsp), CoVs are classified into four different sub-groups, *alphacoronaviruses*, *betacoronaviruses*, *gammacoronaviruses,* and *deltacoronaviruses* (**Figure 1**). Human coronaviruses (hCoVs), such as 229E, OC43, NL-63 and HKU-1 are highly transmissible respiratory viruses which are responsible for around 10-20% of common cold cases annually (McIntosh et al., 1970; Cabeça et al., 2013). HCoV-related illness is often self-limited in immune competent individuals but may cause more severe upper and lower respiratory tract infections in the young and elderly population (Woo et al., 2005; Lau et al., 2006). In addition, highly pathogenic CoVs may emerge through zoonotic reservoirs. In the past two decades, SARS-CoV and MERS-CoV emerged from bats and spread to humans through intermediate hosts including civet cats and camels, respectively (Raj et al., 2014). SARS-CoV and MERS-CoV belong to the sub-groups 2b and 2c of the *Betacoronavirus* genus (Peck et al., 2015). The latest CoV outbreak is the SARS-CoV-2, a *Betacoronavirus* 2b which emerged from bats and spread to humans (Lu et al., 2020). The mortality rate of these viruses range from 10 to 40% but can exceed 50% in the elderly (Min et al., 2004; Li et al., 2005; Bolles et al., 2011b; Raj et al., 2014; Sharif-Yakan and Kanj, 2014; World Health Organization [WHO], 2018). The unusually high mortality rate is linked to disease progression leading to acute respiratory distress syndrome (ARDS) which causes hypoxemia, pulmonary edema, and infiltration of inflammatory immune cells in the lung (Cabeça et al., 2013; Gralinski and Baric, 2015). If unresolved, the diseases progress to late phase ARDS, leading to end-stage lung disease and death (Ding et al., 2003). Currently, no vaccines or antiviral drugs are approved to prevent or treat severe CoV infection.

## The Challenge for Vaccine Development

The CoV *S*-protein is the major envelope glycoprotein and the main determinant of protective immunity. The *S*-protein is composed of two principle subunits, S1 and S2; S1 governs receptor binding and S2 is responsible for membrane fusion (Li, 2016). Similar to other class I fusion proteins, *S*-protein undergoes a major conformational change between pre-fusion and post-fusion which also presents different antigenic epitopes. While able to bind to both conformations, Abs targeting the post-fusion form are not necessary neutralizing; in contrast, Abs targeting the pre-fusion form of the *S*-protein correlate better with neutralization. In particular, vaccines and neutralizing antibodies (nAbs) which target the receptor binding domain (RBD) of the *S*-protein can effectively neutralize the virus (Zhu et al., 2007; Tang et al., 2014). However, due to high selective pressure and tropism determinants, *S*-protein is the most diverse region of CoV. For instance, the *S*-proteins from SARS-CoV and MERS-CoV share only 44% sequence identity (Kandeel, 2018). The majority of differences between *S*-proteins is in the S1 region, which is further separated into the N-terminal Domain (NTD) and RBD. The diverse nature of the RBD between SARS-CoV and MERS-CoV is reflected in the use of different entry receptors, either angiotensin I converting enzyme 2 (ACE2) or dipeptidyl peptidase 4 (DPP4), respectively (Li et al., 2003; Raj et al., 2013). The diversity of *S*-protein also renders vaccines and nAbs unlikely to be cross-protective between existing and emerging CoVs. Surveillance and experimental data have identified multiple animal SARS- and MERS-like CoVs that have significant diversity in *S*-protein and are able to replicate in human cells without adaptation (Menachery et al., 2015, 2016; Luo et al., 2018). Once transmitted to human population, such variation between *S*-protein between the previous and the new emerging CoVs will pose a major challenge on the progress of vaccine development.

# CRITERIA FOR GENERATING EFFECTIVE VACCINE FOR CoVs

## Vaccine Criteria for SARS and MERS-CoV Viruses

The surface glycoproteins are the main target for vaccine development. In CoV infection, Abs against *S*-protein were shown to be protective in multiple animal studies. Furthermore, in a passive immunization study in camel, the nAb level is directly correlated to lung pathology and survival (Zhao et al., 2015). As such, one of the main goals for CoV vaccines in humans is the ability to elicit a strong humoral immune response against the *S*-protein. Particularly, the pre-fusion form of the *S*-protein is an attractive target for Abs to confer protective immunity.

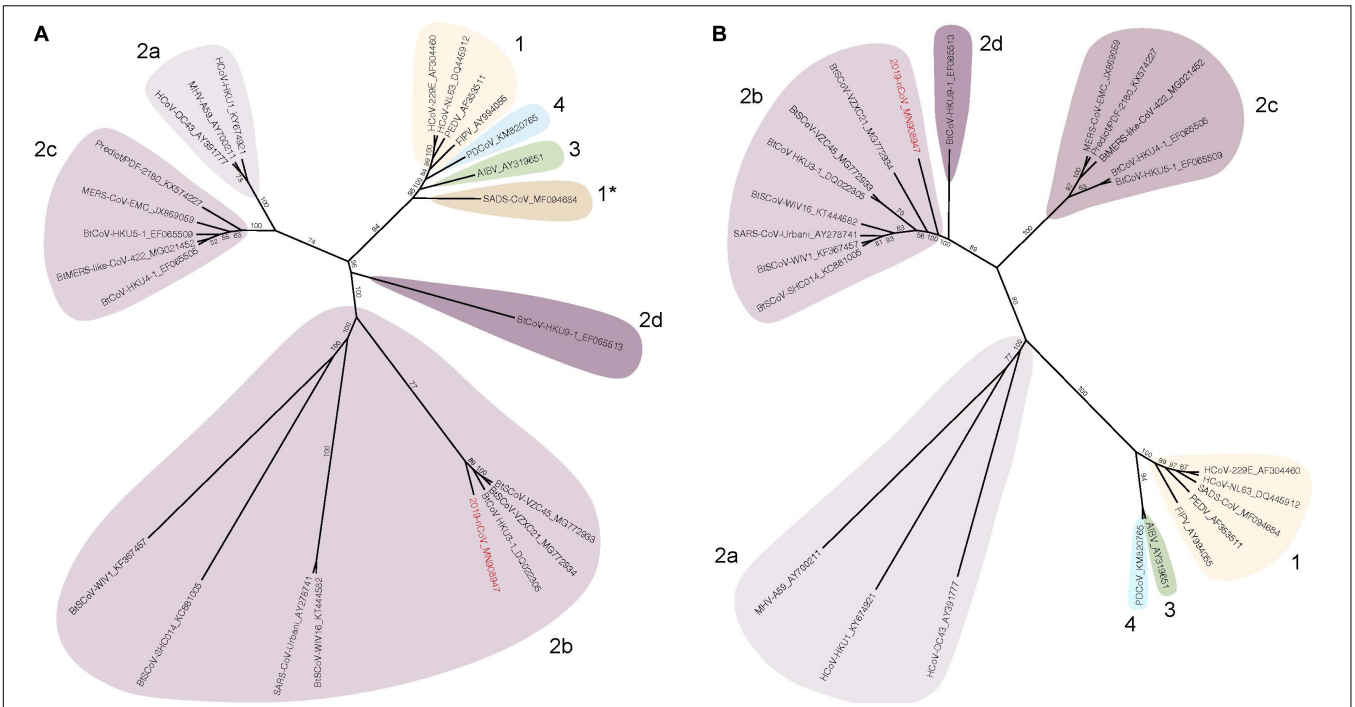


**FIGURE 1 |** Spike and nsp12 phylogeny of representative coronaviruses. The Spike **(A)** and nsp12 **(B)** protein sequences of selected coronaviruses were aligned and phylogenetically compared. Coronavirus genera are grouped by classic subgroup designations (1, 2a-d, 3, and 4). In the Spike tree in **(A)**, SADS-CoV is designated as 1* because of its distinctive grouping compared with more conserved proteins (e.g., nsp12, see **(B)**). Branches in each tree are labeled with consensus support values (in %). Sequences were aligned using free end gaps with the Blosum62 cost matrix, and the tree was constructed using the neighbor-joining method based on the multiple sequence alignment in Geneious Prime. Numbers following the underscores in each sequence correspond to the GenBank Accession number. The SARS-CoV-2 is highlighted in red. The radial phylogram was exported from Geneious and then rendered for publication using Adobe Illustrator CC 2020.

In order to "lock" the *S*-protein in its antigenic optimal pre-fusion form, two mutations, V1060P and L1061P, were introduced into the MERS-CoV *S*-protein (Pallesen et al., 2017). The resulting MERS S-2P is able to elicit both RBD and non-RBD binding nAbs (Pallesen et al., 2017). The same strategy was also shown to work in the SARS-CoV-2 *S*-protein (Wrapp et al., 2020). Other structural proteins such as E and M and the nsp N also contribute to viral protection and clearance (Channappanavar et al., 2014; Zhao et al., 2016; Deng et al., 2018). Similarly to other respiratory viruses such as influenza, mucosal IgA plays a major role in disease protection and has a synergistic effect with IgG (Belshe et al., 2000; Plotkin, 2010). In order to elicit a strong mucosal IgA immunity, the route of vaccine administration is important. Studies have shown that intranasal inoculation of a recombinant RBD vaccine can elicit greater mucosal IgA production than intramuscular or subcutaneous injection (Ma et al., 2014a). However, the duration of mucosal antibodies is typically shorter lived than systemic IgG responses and the longest longitudinal study of MERS-CoV IgA responses ended after 6 months (Hapfelmeier et al., 2010; Ma et al., 2014a). In comparison, in a natural infection case study, SARS-targeting systemic memory B cells were present up to 6 years for SARS-CoV (Oh et al., 2012; Tang et al., 2019); and up to 34 months post infection for MERS-CoV (Payne et al., 2016). Another important consideration for SARS-CoV and MERS-CoV vaccination is the T cell response against the virus, specifically the N proteins, which is important for viral clearance (Zhao et al., 2010; Channappanavar et al., 2014). A study has shown that adoptive transfer of viral specific T-cells to SCID mice enhances survival and reduces lung titer after SARS-CoV infection (Zhao et al., 2010). Moreover, intranasal vaccination of N protein using the VEEV replicon system elicits CD4+ memory T-cells responses in the airway. Upon challenge, the airway CD4+ memory T cells secrete IFN-γ, which subsequently enhances the innate immune response as well as coordinates the CD8+ T cell priming and migration which protects mice from lethal disease, but not weight loss or virus titers under carefully controlled conditions (Zhao et al., 2016). Interestingly, Rag−/− mice are able to clear SARS-CoV infection, suggesting innate immunity is sufficient for viral clearance (Zhao et al., 2010). However, the mechanism of this viral clearance is still unknown. Another important aspect of emerging CoV vaccine is the breadth of protection. As mentioned previously, the antigenic variation in the *S*-protein between CoVs limits the breadth of cross protection against multiple emerging CoVs, and is especially true for *S*-protein only vaccines (Wang et al., 2018, 2019).

Learning from natural infection, MERS-CoV specific CD4+ and CD8+ T cells are detected in PBMCs in MERS-CoV infected survivors (Zhao et al., 2017). Therefore, a balance of B cell and T cell responses is generally considered the gold standard to prevent and resolve MERS-CoV and SARS-CoV infection. Multiple strategies have been developed to elicit long lasting B and T

cell responses for SARS-CoV and MERS-CoV. These include the traditional live attenuated, inactivated, and subunit vaccines, and newer development of nanoparticles, vectorized vaccines, and RNA/DNA vaccines. In this review, we have selected only the vaccine studies that have an *in vivo* challenge model and have summarized the different parameters, including vaccine components, dosage, challenge conditions, animal models and the study outcome in **Table 1**. We will also discuss each type of vaccine strategy and focus on the finished clinical trial targeting SARS-CoV and the 3 ongoing clinical trials targeting MERS-CoV using DNA (Martin et al., 2008; Modjarrad et al., 2019) and vectorized vaccines. Other comprehensive reviews on CoV vaccine development can be found elsewhere (Zhang et al., 2014; Du and Jiang, 2015; Perlman and Vijay, 2016; Schindewolf and Menachery, 2019; Yong et al., 2019).

## Current Vaccine Strategies

Inactivated vaccines are the quickest option for vaccine development in an outbreak situation. Multiple chemical and physical methods have been applied singly or in combination to inactivate CoVs, including β-propiolactone, formalin, formaldehyde and UV. While multiple studies have shown the efficacy of inactivated vaccines in hamster, ferret and multiple mouse challenge models (Stadler et al., 2005; See et al., 2006, 2008; Spruth et al., 2006; Roberts et al., 2010), one study suggested a potential vaccine enhanced pathologies (Bolles et al., 2011a). In this study, double inactivation (DIV) of SARS-CoV using formalin and UV+alum elicits a Th2 skewed response and is only partially protective to young mice (6–8 weeks-old) and not protective to experimentally aged mice (12–14 weeks-old) (Bolles et al., 2011a). Furthermore, upon challenge, DIV vaccinated mice show increased infiltration of eosinophils, neutrophils and other inflammatory cell populations in the lung, likely due to the N specific immune response (Bolles et al., 2011a). Further studies have suggested that by replacing alum with TLR agonists such as Poly I:C, Poly U or LPS as adjuvants, the skewed Th2 responses can be alleviated and may reduce the infiltration of eosinophils in the lung (Iwata-Yoshikawa et al., 2014).

Gamma-ray inactivated whole MERS-CoV (WIV) with alum or M59 also suffers from the Th2 skewed immune response and pulmonary eosinophilia upon challenge, suggesting a potential risk of using inactive virus for CoV vaccination (Agrawal et al., 2016). Interestingly, formaldehyde inactivated MERS-CoV co-administered with alum and CpG shows a more balanced Th1/Th2 response and is able to protect mice from a challenge model (Ad5 transduced hDPP4) with reduction in lung viral titer and improved lung pathology. There is no observable vaccine-induced lung pathology or infiltration of eosinophils upon challenge (Deng et al., 2018). The difference in vaccine outcomes indicates an incomplete understanding of the effect of adjuvants on the inactivated SARS and MERS-CoV vaccines. In respiratory syncytial virus (RSV) vaccines, formalin inactivated vaccines presents the post-fusion form predominately and fail to elicit protective immune responses. Whether the same phenomenon exists in inactivated CoV is still unknown, although it could explain the discrepancy between reports. The inconsistent results from different vaccine models also underscores the host genetic elements affecting vaccine outcome. Nevertheless, inactivated vaccine is still one of the most straightforward methods for vaccine development and has the quickest response time in an outbreak situation.

Live attenuated viral vaccines are the closest mimic of natural infection and generally elicit strong B and T cell responses (Zhao et al., 2017). Multiple strategies have been used to genetically attenuate SARS-CoV and MERS-CoV by either deleting or mutating structural, non-structural or accessory proteins. Intranasal immunization of a SARS-CoV lacking E protein (rSARS-CoV-ΔE) has shown complete protection from pulmonary replication in a Golden Syrian hamster model (Lamirande et al., 2008). A similar virus has been generated in the MERS backbone, creating a conditional mutant that requires trans expression of E for productive replication (Almazán et al., 2013). Mutations of the DEDD motif of the 3′ to 5′ exonuclease (ExoN-nsp14) "proof-reading protein" on a mouse-adapted SARS-CoV attenuated the virus both *in vitro* and *in vivo*. A single intranasal immunization is able to elicit strong nAbs (>6-fold protective titers) and completely protect against lethal challenges in an aged mouse model (12 months-old BALB/c) (Graham et al., 2012). Mutations in the nsp 16 (NSP16), a 2′*O*-methyltransferase, in both SARS-CoV and MERS-CoV have also been shown to attenuate the viruses and to protect BALB/c and CRISPR-Cas humanized DPP4-288-330 mice from lethal challenge (Menachery et al., 2014, 2017, 2018). Moreover, these attenuation strategies can be multiplexed, leading to highly stable live attenuated vaccines with limited capability to undergo recombination and reversion repair (Graham et al., 2018; Menachery et al., 2018). Although the live attenuated vaccine is effective in small animal models, there remain safety concerns about potential revertants and recombination with natural CoVs which hinders their usage in the clinical setting. Furthermore, live attenuated vaccines often require greater time for development and safety testing which lessens utility in an outbreak situation.

Protein-based subunit vaccines are considered the safest format of vaccine. However, the low immunogenicity of subunit vaccines dictates a heavily reliance on adjuvants. Different forms of the *S*-protein, including the S1 RBD, RBD-Fc (RBD with human IgG Fc fusion), and N-terminal domain (NTD), have demonstrated various degrees of nAb responses and protection in multiple animal models including non-human primates (NHP) (Lan et al., 2015; Zhang et al., 2016; Jiaming et al., 2017; Wang et al., 2017; Deng et al., 2018; Nyon et al., 2018; Adney et al., 2019). For instance, the SARS-CoV S1 subunit vaccine produced from sf9 cells and with the adjuvant saponin or protollin are able to reduce lung viral titer in young or aged mice after challenge, respectively (Bisht et al., 2005; Hu et al., 2007). An RBD subunit of SARS-CoV produced from Chinese hamster ovarian (CHO) cells with Freund's adjuvant is able to protect young BALB/c mice from infection (Du et al., 2010). MERS-CoV-S1 with adjuvants MF59 or Advax HCXL is able to protect alpacas and dromedary camels against MERS-CoV challenge (Adney et al., 2019). Adjuvant selection can affect the vaccine outcome, and combinations of adjuvants can have synergistic effects on the strength of the response. For instance, rRBD with adjuvants alum and CpG ODN together elicits a stronger humoral and cellular T cell response

**TABLE 1 |** Summary of SARS-CoV and MERS-CoV vaccines studies

| SARS-CoV Vaccines | Antigens | Vaccine formulations | Dose, Time of vaccination | Animal models | Challenge dose. Virus strains, Time after last vaccination, Route | Results | References |
|---|---|---|---|---|---|---|---|
| Whole Inactivated Vaccine | Inactivated | SARS-CoV FRA (*b*-propiolactone) + MF59 | 5 μg at 0, 2, and 4 weeks, SC | BALB/c | $10^4$ TCID50 SARS-CoV Urbani, IN | Protection, no virus detected in Lung and Nasal Turbinates | Stadler et al., 2005 EID |
| | Inactivated | SARS-CoV Tor2 (*b*-propiolactone) + Alum | 50 μg at 0 and 4 weeks, SC | 6 week old 129S6/SvEv | $10^6$ pfu SARS-CoV Tor2 at week 3, IN | Protection | See et al., 2006 JGV |
| | Double Inactive | SARS-CoV (Utah) formaldehyde and UV inactivation + Al(OH)3 | 0.08 – 0.2 μg at week 0 and 2, SC | 6 – 8 weeks CD1 mice | $10^5$ TCID50 SARS-CoV Utah at week 3 or 11, IN | Protection, no virus detected in lung and trachea | Spruth et al., 2006 Vaccines |
| | Inactivated | SARS-CoV Tor2 (*b*-propiolactone) + Alum | 50 μg at 0 and 4 weeks, SC | 8 – 10 month old ferret | $10^6$ pfu SARS-CoV Tor2 at week 3, IN | Weak protection, slight reduction of viral titer in lung, BAL and nasal wash, slight improvement in lung pathology | See et al., 2008 JGV |
| | Inactivated | SARS-CoV Urbina (*b*-propiolactone) + AS01B and AS03A | 0.15 – 1.5 μg at week 0 and 3, IM | BALB/c | $10^5$ TCID50 SARS-CoV Urbani at week 3, IN | Protection, no virus detected in lung | Roberts et al., 2010 Viral Immunology |
| | Inactivated | SARS-CoV Urbina (*b*-propiolactone) + AS01B and AS03A | 2.0 μg at week 0 and 3, IM | 4 – 8 week old Golden syrian hamsters | $10^3$ TCID50 SARS-CoV Urbani at week 4 or 18, IN | Partial protection, reduce viral titer in lung | Roberts et al., 2010 Viral Immunology |
| | Double Inactive | SARS-CoV MA15 formalin and UV inactivated + Alum | 0.2 μg at week 0 and 3–4 week, footpad | 6 – 8 weeks old BALB/cAnNHsd | $10^5$ PFU SARS-CoV MA15, SZ61and GD03 at week 5, IN | Partial protection, reduce viral titer in lung and good protection from lethal challenge (MA15) | Bolles et al., 2011a JVI |
| | Double Inactive | SARS-CoV MA15 formalin and UV inactivated + Alum | 0.2 μg at week 0 and 3–4 week, footpad | 12 – 14 months old BALB/cAnNHsd | $10^5$ PFU SARS-CoV MA15, SZ61and GD03 at week 5, IN | Weak protection, small drop in viral titer in lung, weak protection from leathal challenge (MA15) | Bolles et al., 2011a JVI |
| LAV | SARS-CoV-ΔE (Urbani) | SARS-CoV-ΔE (Urbani) | $10^3$ TCID50 at 0 week, IN | 7 week old Golden syrian hamsters | $10^3$ TCID50 SARS-CoV Urbani and GD03 at week 4, IN | Protection, no virus detected in lung | Lamirande et al., 2008 JVI |
| | SARS-C0V ExoN (MA15) | SARS-CoV-ExoN (MA15) | $10^{2.5}$ or $10^4$ PFU at week | 12 months old BALB/c | $10^{2.5}$ TCID50 SARS-CoV MA15 at week 4, IN | Complete survival from lethal challenge, no virus detected in lung | Graham et al., 2012 Nat Med |
| | SARS-CoV ΔNSP16 | SARS-CoV Δ2′-*O*-Methyltransferase | $10^2$ PFU at week 0, IN | 10 weeks old BALB/c and C57BL/6 | $10^5$ PFU SARS-CoV MA15 at week 4, IN | Complete survival from lethal challenge, no viral titer performed | Menachery et al., 2014 JVI |
| | SARS-CoV ΔNSP16/ExoN | SARS-CoV Δ2′-*O*-Methyltransferase and ExoN mutation | $10^2$ PFU at week 0, IN | 12 months old BALB/c | $10^5$ PFU SARS-CoV MA15 at week 4, IN | Complete survival from lethal challenge, no virus detected in lung | Menachery et al., 2018 JVI |
| Subunit | subunit nS Sf9 | SARS-CoV S (14-762) Urbani + QS21 | 10 μg at week 0, 4, and 8, SC | 6 weeks old BALB/c | $10^5$ TCID50 SARS-CoV (Urbani) at week 4, IN | Protection, reduce viral titer in lung and nasal turbinates | Bisht et al., 2005 Virology |
| | Ectodomain Sf9 | SARS-CoV S ectodomain (Urbani) + Protollin | 10 or 30 μg at week 0, 2 and 5, IN | ∼ 1 year old BALB/c | $5x10^4$ TCID50 SARS-CoV Urbani at week 1, IN | Protection, reduce viral titer in lung | Hu et al., 2007 Vaccines |

*(Continued)*

**TABLE 1 |** Continued

| SARS-CoV Vaccines | Antigens | Vaccine formulations | Dose, Time of vaccination | Animal models | Challenge dose. Virus strains, Time after last vaccination, Route | Results | References |
|---|---|---|---|---|---|---|---|
| | Subunit RBD219 CHO | SARS-CoV RBD (318-536)Tor2 + Freund | 20 μg at week 0 and 10 μg at week 3 and 6, SC | 4 – 6 weeks old BALB/c | $5x10^5$ TCID50 SARS-CoV GZ50 at 10 day, IN | Protection, no virus detected in lung | Du et al., 2010 viral immunology |
| Subunit Trimer | Spike trimer | SARS-CoV RBD Spike Trimer Urbani + Alum | 50 μg at week 0, 3, and 6, SC | 5 weeks old Golden syrian hamsters | $10^3$ TCID50 SARS-CoV Urbani at week 2, IN | Protection, no virus detected in lung and reduce pneumonitis | Kam et al., 2007 Vaccines |
| VLP | MHV-S VLP | SARS-CoV S in MHV + Alum | 2 μg at 0 and 4 weeks | 6 – 8 week old BALB/c | $10^6$ TCID50 SARS-CoV at week 8, IN | Protect, no virus detected in Lung | Lokugamage et al., 2008 Vaccine |
| | Flu M1-S | SARS-CoV S Urbani in influenza M1 + Al(OH)3 | 0.8 or 4 μg at week 0 and 3, IM | 6 – 8 weeks old BALB/c | 2xLD50 mouse adapted SARS-CoV V2163 at week 3, IN | Complete survival from lethal challenge, no virus detected in lung | Liu et al., 2011 Vaccines |
| DNA | Plasmid *S*-Ectodomain | Plasmid expressing SARS-CoV S ΔCD or ectodomain (Urbani) | 25 μg at week 0, 3, and 6, IM | 6 – 8 week old BALB/c | $10^4$ TCID50 SARS-CoV Urbani, at Day 30, IN | Protection, reduce viral titer in lung and nasal turbinates | Yang et al., 2004 Nature |
| Vector | BHPIV3 SARS-S | SARS-CoV S or SME Urbani in parainfluenza virus type 3 vector (BHPIV3) | $10^6$ TCID50 at 0 week, IN | Golden syrian hamsters | $10^3$ TCID50 SARS-CoV Urbani at week 4, IN | Protection, no virus detected in lung | Buchholz et al., 2004 PNAS |
| | BHPIV3 SARS-S | SARS-CoV S Urbani in parainfluenza virus type 3 vector (BHPIV3) | $10^6$ TCID50 each at 0 week, IN and IT | African green monkeys | "A large dose of SARS-CoV" at week 4, IN | Protection, no virus detected in lung | Bukreyev et al., 2004 Lancet |
| | MVA-SARS-S | SARS-CoV S Urbani in MVA | $10^7$ at 0 and 4 week, IN | BALB/c | $10^4$ TCID50 SARS-CoV Urbani, at week 8, IN | Protection, reduce viral titer in lung and nasal turbinates | Bisht et al., 2004 PNAS |
| | MVA-SARS-S | SARS-CoV S Urbani in MVA | $10^7$ at 0 and 4 week, IM | BALB/c | $10^4$ TCID50 SARS-CoV Urbani, at week 8, IN | Protection, reduce viral titer in lung and nasal turbinates | Bisht et al., 2004 PNAS |
| | MVA-SARS-S | SARS-CoV S and N Tor2 in MVA | $10^8$ pfu at 0 and $5 \times 10^7$ at 2 week, IP and SC | Ferret | $10^6$ pfu SARS-CoV Tor2 at week 4, IN | No protection according to viral RNA in lung, Ab induction | Czub et al., 2005 Vaccines |
| | VSV-S | VSV-SARS-S Urbani | $1.4 \times 10^4$ pfu at week 0, IN | BALB/c | $10^4$ TCID50 SARS-CoV Urbani at month 1 and 4, IN | Protection, no virus detected in lung and nasal turbinates | Kapadia et al., 2005 Virology |
| | hAd5 (N+S) | Human Adenovirus 5 with S + Ad5 N gene | $3 \times 10^8$ pfu each at 0 and 4 weeks, IM | 6 week old 129S6/SvEv | $10^6$ pfu SARS-CoV Tor2 at week 3, IN | No protection despite strong IgG1, IgG2a Ab induction and high IFN-g secretion | See et al., 2006 JGV |
| | hAd5 (N+S) | Human Adenovirus 5 with S + Ad5 N gene | $3 \times 10^8$ pfu each at 0 and 4 weeks, IN | 6 week old 129S6/SvEv | $10^6$ pfu SARS-CoV Tor2 at week 3, IN | Partial protection, Induction of IgA | See et al., 2006 JGV |

*(Continued)*

**TABLE 1 |** Continued

| MERS-CoV Vaccines | Antigens | Vaccine formulations | Dose, Time of vaccination | Animal models | Challenge dose. Virus strains, Time after last vaccination, Route | Results | References |
|---|---|---|---|---|---|---|---|
| | VEEV-S | SARS-CoV GD03 S in VEEV | $10^6$ IU at 0 week, boost 3 – 5 weeks, footpad | 4 – 7 weeks old | $10^5$ pfu SARS-CoV GD03 and Urbani at week 7 – 8 and week 54, IN | Protection, no virus detected in lung | Deming et al., 2006 PlOS Med |
| | VEEV-S | SARS-CoV GD03 S in VEEV | $10^6$ IU at 0 week, boost 3 - 5 week, footpad | > 26 week old | $10^5$ pfu SARS-CoV GD03 and Urbani at week 7 -8 and week 54, IN | No protection | Deming et al., 2006 PlOS Med |
| | hAd5-S + AdC7-S | Human Adenovirus 5 with S + Chimpanzee AdC7 with S Tor2 | $5 \times 10^{11}$ VP/kg at 0 and 1 month, IM | 18 – 20 weeks old ferret | $10^6$ pfu SARS-CoV Tor2 at not specify, IN | Protection, reduce viral titer in lung and nasal turbinates | Kobinger et al., 2007 Vaccines |
| | hAd5 (N+S) | Human Adenovirus 5 with S + Ad5 N gene | $1 \times 10^9$ pfu each at 0 and 4 weeks, IM | 8 - 10 month old ferret | $10^6$ pfu SARS-CoV Tor2 at week 3, IN | Inconclusive, control hAd5 shows non-specific protection | See et al., 2008 JGV |
| | hAd5 (N+S) | Human Adenovirus 5 with S + Ad5 N gene | $1 \times 10^9$ pfu each at 0 and 4 weeks, IN | 8 – 10 months old ferret | $10^6$ pfu SARS-CoV Tor2 at week 3, IN | Inconclusive, control hAd5 shows non-specific protection | See et al., 2008 JGV |
| Whole Inactivaed Vaccine | Inactivated | MERS-CoV ($\gamma$-ray) + Alum or MF59 | $10^6$ TCID50 at week 0 and 3, IM | hCD26/DPP4 transgenic mice | $10^3$ TCID50 (100xLD50) MERS-CoV at week 3, IN | Protection from virus replication, no virus detected in lung, increase lung pathology | Agrawal et al., 2016 Human vaccine and immuno therapy |
| | Inactivated | MERS-CoV EMC/2012 (formaldehyde) + Alum and CpG | 1 $\mu$g at week 0, 4 and 8, IM | 14 – 16 week old BALB/c transduced with hDPP4 by Ad5 | $10^5$ PFU MERS-CoV (EMC/2012) at week 2, IN | Protection, no virus detected in lung | Deng et al., 2018 Emerging Microbes and infection |
| LAV | MERSS-CoV $\Delta$NSP16 | MERS-CoV $\Delta 2'$-*O*-Methyltransferase EMC MA1 | $10^6$ PFU at week 0, IN | 10 - 20 week old C57BL/6 288-330+/+ | $10^6$ PFU MERS-CoV EMC MA1 at week 4, IN | Complete survival from lethal challenge, reduce viral titer in lung | Menachery et al., 2017 msphere |
| Subunit | RBD | MERS-CoV RBD S367-606 (EMC/2012) + alum | 200 $\mu$g at week 0 and 100 $\mu$g at week 8 and 25, IM | Rhesus Macaque | $6.5x10^7$ TCID50 MERS-CoV (EMC/2012) at week 2, IN | Partial protection, reduce viral titer in lung and trachea | Lan et al., 2015 EBioMedicine |
| | NTD | MERS-CoV NTD S18-353 (EMC/2012) + alum and CpG | 5 or 1 $\mu$g at week 0, 4 and 8, IM | 16 – 18 weeks old BALB/c transduced with hDPP4 by Ad5 | $10^5$ PFU MERS-CoV (EMC/2012) at week 2, IN | Partial protection, reduce lung and trachea pathologies, no viral titer information | Jiaming et al., 2017 Vaccines |
| | S ectodomain | MERS-CoV EMC/2012 S ectodomain + Alum and CpG | 1 $\mu$g at week 0, 4 and 8, IM | 14 – 16 week old BALB/c transduced with hDPP4 by Ad5 | $10^5$ PFU MERS-CoV (EMC/2012) at week 2, IN | Protection, reduction in lung viral titer | Deng et al., 2018 Emerging Microbes and infection |
| | RBD-Fc | MERS-CoV RBD S377-588 Fc (EMC/2012) + MF59 | 10 $\mu$g at week 0, 3, and 6, SC | 4 – 6 weeks old BALB/c transduced with hDPP4 by Ad5 | $10^5$ PFU MERS-CoV (EMC/2012) at week 2, IN | Protection, no virus detected in lung | Zhang et al., 2016 Cellular and molecular immunology |
| | RBD-Fc | MERS-CoV RBD S377-588 Fc (EMC/2012) + Addavax | 10 $\mu$g at week 0 and 4, IM | hCD26/DPP4 transgenic mice | $10^3$ TCID50 (100xLD50) MERS-CoV (EMC/2012) at week 4, IN | Complete survival from lethal challenge, no virus detected in lung | Nyon et al., 2018 Vaccines |

*(Continued)*

**TABLE 1** | Continued

| MERS-CoV Vaccines | Antigens | Vaccine formulations | Dose, Time of vaccination | Animal models | Challenge dose. Virus strains, Time after last vaccination, Route | Results | References |
|---|---|---|---|---|---|---|---|
| | S1 | MERS-CoV ENgland1 S1 + Advax HCXL or Sigma oil-in-water emulsion | 400 μg at week 0, 4 and 15, IM | dromedary camel | $10^7$ TCID50 MERS-CoV (EMC/2012) at ∼week 4, IN | Protection, reduce viral titer in lung and nasal turbinate | Adney et al., 2019 Virus |
| | S1 | MERS-CoV ENgland1 S1 + Advax HCXL or Sigma oil-in-water emulsion | 400 μg at week 0, 4, and 15, IM | Alpaca | $10^7$ TCID50 MERS-CoV (EMC/2012) at ∼week 4, IN | Protection, no virus detected in lung, nasal turbinate and nasal swabs | Adney et al., 2019 Virus |
| Subunit Trimer | RBD Trimer | MERS-CoV RBD-Fd (Trimer) + alum | 5 μg at week 0 and 4, IM | hCD26/DPP4 transgenic mice | $10^4$ TCID50 MERS-CoV (EMC/2012) at week 12, IN | Complete survival from lethal challenge, no viral titer performed | Tai et al., 2016 Virology |
| VLP | S nanoparticles | MERS-CoV Jordan S nanoparticle + Matrix M1 | 10 μg at week 0 and 3, IM | 15 – 17 weeks old BALB/c transduced with hDPP4 by Ad5 | $2.5 \times 10^3$ PFU MERS-CoV (Jordan) at week 4, IN | Protection from chalenge, no virus detected in lung | Coleman et al., 2017 Vaccines |
| | BNSP333-S | MERS-CoV S1 Jordan fused with rabies virus G protein VLP | 10 μg at week 0, 1, and 3, IM | 15 – 17 weeks old BALB/c transduced with hDPP4 by Ad5 | $2.5 \times 10^3$ PFU MERS-CoV (Jordan) at week 4, IN | Protection, no virus detected in lung | Wirblich et al., 2017 JVI |
| DNA | Plasmid S-protein | Plasmid expressing MERS-CoV S1 (Al-Hasa_1_2013) | 0.5 or 2 mg at week 0, 3 and 6, IM | Rhesus macaques | $7 \times 10^6$ TCID50 MERS-CoV (EMC/2012) at week 5, IT, IN, oral and ocular | Protection, reduce viral titer in lung, reduce clinical pathology | Muthumani et al., 2015 STM |
| | Plasmid S1 | Plasmid expressing MERS-CoV S1 (Al-Hasa_15_2013) | 100 μg at week 0, 3 and 6, IM | 14 - 16 week old BALB/c transduced with hDPP4 by Ad5 | $10^5$ PFU MERS-CoV (EMC/2012) at Day 18, IN | Protection, reduce viral titer in lung | Chi et al., 2017 Vaccines |
| Vector | MVvca2 S or soluble S | Recombinant measles virus with MERS-CoV (EMC/2012) S or soluble S | $10^5$ TCID50 at week 0 and 4, IP | 6 – 12 week old IFNAR−/− CD46Ge transduced with hDPP4 by Ad5 | $7 \times 10^4$ TCID50 MERS-CoV (EMC/2012) at week 6, IN | Protection, reduce viral titer in lung, reduce lung pathology | Malczyk et al., 2015 JVI |
| | ChAdOx1 MERS | ChAdOx1 with MERS-CoV *S*-protein (EMC/2012) | $10^8$ IU at week 0, IN or IM | hCD26/DPP4 transgenic mice | $10^4$ TCID50 MERS-CoV (EMC/2012) at week 4, IN | Complete survival from lethal challenge, no virus detected in lung, reduce lung pathology | Munster et al., 2017 npj |
| | MVA-MERS-S | MVA with MERS-CoV *S*-protein | $10^6$, $10^7$, or $10^8$ PFU at week 0, IM or SC | 14 – 16 week old BALB/c transduced with hDPP4 by Ad5 | $7 \times 10^4$ TCID50 MERS-CoV (EMC/2012) at week 6, IN | Protection, reduce viral RNA genome in lung, reduce lung pathology | Volz et al., 2015 JVI |
| | rAd5-S1/F/CD40L | hAd5 with MERS-CoV S1 trimer fused with CD40L | $10^9$ PFU at week 0 and 4, IM | hCD26/DPP4 transgenic mice | $10^3$ TCID50 (100xLD50) MERS-CoV (EMC/2012) at week 4, IN | Complete survival from lethal challenge, no virus detected in lung, reduce lung pathology | Hashem et al., 2019 JID |

*Selection criteria: Only animal studies with a challenge model are included. LAV, live attenuated vaccine; VLP, virus like particle; RBD, receptor binding domain; IM, intramuscular; IN, intranasal; SC, subcutaneous; IP, intraperitoneal.*

(Lan et al., 2014). Additionally, rNTD with alum is able to reduce lung pathology in a non-lethal MERS-CoV challenge (Jiaming et al., 2017). Instead of adjuvants alone, immune enhancers such as an Fc fragment, which increases the protein half-life when fused with the RBD, can also elicit a stronger IgG nAb and cellular immune response in multiple experimental animals (Du et al., 2013; Ma et al., 2014b; Tang et al., 2015; Nyon et al., 2018). RBD-Fc fusion subunit vaccine is able to protect a lethal challenge of MERS-CoV in adenovirus transduced hCD26/DPP4 mice (Zhang et al., 2016; Wang et al., 2017). While a large amount of work concerning the subunit vaccines has been done in conjunction with different adjuvants, the effect of each adjuvant is not well understood and multi-adjuvant systems (combinatorial admixes) have not been rigorously tested. A more systematic method of studying the effect of different adjuvants on CoV vaccines will be valuable for vaccine development, perhaps using genetic reference populations that more accurately phenocopy human genetic variation (Leist and Baric, 2018).

Trimeric forms of the *S*-protein and RBD have been developed using the T4 trimerization domain to mimic the native conformation of the spike RBD (Kam et al., 2007; Tai et al., 2016). The trimeric RBD antigens are able to elicit a robust nAb response and protect 80% of hDPP4 transgenic mice from lethal MERS-CoV challenge, although most animals still experienced slight weight loss (Tai et al., 2016). Alternatively, the MERS-CoV *S*-protein has been structurally designed to remain in perfusion state by mutating V1060 and L1061 at the tip of the central helix to proline (S-2P) (Kirchdoerfer et al., 2016; Pallesen et al., 2017). The MERS S-2P protein retains the receptor binding properties of the wild-type S and elicits nAbs against at least 3 different S domains, including RBD, NTD, and S2. Intramuscular injection of the MERS S-2P elicits nAb responses in mice comparable to the monomeric S1 and trimeric *S*-protein antigens. (Pallesen et al., 2017).

Similar to subunit vaccines are the viral like particle (VLP) and nanoparticle vaccines. VLP and nanoparticles provide multivalent binding similar to actual viruses without the potential safety concerns. In SARS-CoV, multiple systems were used to generate *S*-protein VLPs, including the mouse hepatitis virus (MHV) and influenza matrix 1 (M1). In the chimeric MHV system, the SARS-CoV protein is co-expressed with the MHV E, M and N proteins to produce MHV-S VLP. Mice vaccinated with the MHV-S VLP and alum have inhibited viral replication in lung after a homologous strain challenge (Lokugamage et al., 2008). Instead of using MHV structural proteins, the influenza system express the SARS-CoV *S*-protein with influenza virus M1 proteins in Sf9 cells to create the M1-S VLP. Immunization of M1-S VLP with aluminum hydroxide can protect mice from a lethal challenge of SARS-CoV (Liu et al., 2011). In MERS-CoV, expression of S, E, and M proteins using the baculovirus system produces VLPs that are morphologically similar to the actual virus (Coleman et al., 2014; Wang et al., 2017b). Other methods such as CPV-based (Wang et al., 2017a), rabies virus (MV)-based (Wirblich et al., 2017), ferritin-based (Seong, 2018), and *S*-protein aggregates (Coleman et al., 2014) are all able to elicit immune responses and reduce viral replication in a mouse model when co-administered with Matrix M1 adjuvant (Coleman et al., 2017). Although all show different degree of immune response in animal, only one study showed a reduction of viral titer *in vivo* via an adenovirus transduced hCD26/DPP4 mouse model (Coleman et al., 2017).

## Clinical Trials for SARS- and MERS-CoV Vaccines

A finished phase 1 clinical trial for a SARS-CoV vaccine is a DNA vaccine that encodes the ectodomain of the SARS-CoV *S*-protein (NCT00099463). DNA vaccines rely on a continuous expression of antigen from a DNA plasmid that is injected intramuscularly and electroporated (Muthumani et al., 2015; Wang et al., 2015; Chi et al., 2017). In pre-clinical studies, 3 doses of an intramuscular plasmid injection was able to reduce viral titer in both lung and nasal turbinate in a BALB/c challenge model (Yang et al., 2004). The phase 1 trial showed favorable results; after 3 doses of DNA vaccine, all subjects showed CD4+ T cell responses, while 80% of subjects had nAbs and 20% of subjects showed CD8+ T cell responses. However, there has been no follow-up in the vaccine development, likely due to the end of the SARS-CoV outbreak (Martin et al., 2008). One MERS-CoV vaccine that is currently undergoing clinical trials (NCT03721718) is a DNA-based vaccine (Modjarrad et al., 2019). GLS-5300 is a DNA vaccine based on a consensus full-length *S*-protein from MERS-CoV under the control of a CMV promoter. In preclinical studies, the vaccine was electroporated into mice, camel and rhesus monkeys three times within 1 month. The vaccine elicited B cell responses in all animals at 1 month post vaccination, and extracted IgG was able to neutralize multiple strains of MERS-CoV including England/2/2013, and Al-Hasa/1/2013 and, surprisingly, a group 1b CoV NL63 and a group 2a CoV HKU1 using the pseudotype neutralization assay (Muthumani et al., 2015). T cell responses were assessed in mice and monkeys, with both demonstrating T cell responses as indicated by the presence of IFN-γ, TNFα and IL2-secreting CD4+ and CD8+ T cells after peptide stimulation. Rhesus monkeys were also protected from challenge of the vaccine strain with lower viral titers and lung pathology as assessed by radiography and pathology studies (Muthumani et al., 2015). Currently, GLS-5300 has completed Phase I clinical trials (safety). Three doses (0.67, 2, and 6 mg) of GLS-5300 were electroporated intramuscularly at weeks 0, 4, and 12. Ninety-four percent of subjects were seroconverted and nAbs were detected in 50% of the individuals. Seventy-six percent of subjects developed T-cell responses against peptides derived from MERS-CoV *S*-proteins (Modjarrad et al., 2019). Other than a full *S*-protein DNA vaccine, different designs also show promising results in preclinical mouse models. Notably, a DNA vaccine composed of only the S1 domain showed efficacy when paired with different adjuvants (Chi et al., 2017). Hybrid strategies using a DNA vaccine paired with a protein booster also showed promising results in eliciting more balanced Th1 and Th2 responses (Wang et al., 2015; Al-Amri et al., 2017).

## Vector-Based Vaccines

Two out of the three clinical trials for MERS vaccines are vectorized vaccines. Viral vector-based vaccines have multiple

advantages over the generic protein or DNA-based subunit vaccines. Firstly, as viral vectors utilize a defined viral entry mechanism, they are more efficient at delivering DNA into cells. Second, the vector itself can serve as an adjuvant which in turn elicits both B- and T-cell responses (Ura et al., 2014). Finally, a wide variety of vector systems including measles viruses (Malczyk et al., 2015; Bodmer et al., 2018), Venezuelan equine encephalitis virus (VEEV) replicon system (Deming et al., 2006; Agnihothram et al., 2014; Zhao et al., 2016), adeno-associated virus (AAV) (Du et al., 2008), parainfluenza type 3 (BHPIV3) (Buchholz et al., 2004; Bukreyev et al., 2004), human and chimpanzee adenovirus (hAd5 and ChAdOx1) (See et al., 2006, 2008; Kobinger et al., 2007; Kim et al., 2014; Guo et al., 2015; Hashem et al., 2019) and modified vaccinia virus Ankara (MVA) (Bisht et al., 2004; Czub et al., 2005; Kapadia et al., 2005; Haagmans et al., 2016) have been previously established for use as vaccine platforms for multiple infectious diseases. Herein, we will focus on the three systems that have been or are currently under clinical trial; all others are summarized in **Table 1**.

Replication-defective adenovirus vectors are one of the most effective choices to deliver vaccine antigens. Human adenovirus 5 (hAd5) and enteric adenovirus type 41 (Ad41) have both been used to deliver MERS-CoV S or S1 proteins. Intramuscular inoculation of the vaccine elicits both B-cell (nAb titer) and T-cell (IFN-γ secreting splenocytes and pulmonary lymphocytes) responses (Guo et al., 2015). However, pre-existing nAbs against hAd5 and 41 in the human population have limited their usage to dromedary camels instead of humans (Chirmule et al., 1999). The pre-existing nAb problem against hAd5 can be circumvented by using a chimpanzee adenovirus. One such platform is ChAdOx1, wherein the adenovirus E1 gene is replaced by a MERS-CoV *S*-protein with an N-terminal secretion peptide from human plasminogen activator (tPA) driven by a CMV promoter. Intramuscular inoculation of the vector successfully elicits nAbs against *S*-protein as quickly as 14 days post infection. Splenic CD8+ T-cells secreting IFN-γ, TNF-α and IL-17 are also present at 28 days post infection (Alharbi et al., 2017). A single intranasal or intramuscular inoculation of ChAdOx1-MERS is able to protect a human DPP4 transgenic mouse from lethal challenge by MERS-CoV, and the vaccine (Munster et al., 2017) is currently under phase 1 clinical trial (NCT03399578). CHAdOx1 has also shown effective protection for Rift Valley Fever Virus in dromedary camels (Warimwe et al., 2016).

The modified vaccinia virus Ankara (MVA) vector is another effective platform for MERS-CoV vaccine development. *S*-protein is inserted into the MAV genome at deletion site III driven by the viral P11 promoter. After a single intramuscular injection, BALB/c mice produce nAbs against both the RBD and S2, as tested *in vitro* (Song et al., 2013). A follow-up study identified IFN-γ secreting splenocytes after peptide S291 stimulation at 56 days post infection, suggesting the vaccine is able to elicit memory CD8+ T cell responses. The vaccine is also able to protect a hDDP4-transduced BALB/c mouse model. RNA genomes in the lungs and lung pathology are drastically reduced compared to mock vaccination (Volz et al., 2015). The MAV based MERS-CoV vaccine has also been tested on dromedary camels and elicits induction of nAbs in sera and nasal swabs. Vaccinated camels also show reduced RNA genomes and gross pathology. The Phase I clinical trial has just been completed and the results are pending (NCT03615911).

# ANTIVIRALS

## The Challenge for Treatment Windows

The average incubation period for SARS-CoV and MERS-CoV is around 5 days (Zumla et al., 2015; de Wit et al., 2016) and the main site of viral replication is the lower respiratory tract (Corman et al., 2015; Petrovsky, 2016). At 7–10 days after symptomatic onset, viral RNA titer peaks in the upper respiratory tract (Drosten et al., 2004; Corman et al., 2015). For terminal cases, disease lasts for an average of 12 days post symptomatic onset for MERS-CoV and 24 days for SARS-CoV (Zumla et al., 2015). Interestingly, severe symptoms begin as the viral titer is decreasing, suggesting that severe CoV pathogenesis is due to immune complications and the inability to resolve inflammation (Peiris et al., 2003a; Wang et al., 2004). SARS-CoV upregulates pro-inflammatory cytokine production in the lung, including IL1, IL6, IL8, IL10, CXCL10 and TNF-α production (Binnie et al., 2014). Compared to SARS-CoV infected patients with mild diseases, patients with ARDS fail to induce interferon (IFN) expression and the subsequent IFN-stimulated genes (ISGs) that are indicative of adaptive immune responses (Cameron et al., 2007; Binnie et al., 2014). The inability to switch from an innate immune response to the adaptive immune response may lead to uncontrollable inflammation and severe end stage lung disease. Given the rapid progression of symptoms to terminal illness, there is only approximately a 1 week treatment window after the onset of symptoms for antiviral and medical intervention (Widagdo et al., 2017). This treatment window could further compromised by delays in virus diagnosis, causing a challenge for timely medical intervention administration when the virus titers and pathological symptom are relatively mild (Corman et al., 2015; Ahmed, 2019). Unlike humans, experimental animal models have a compressed disease course (<7 days), and it is difficult to differentiate between early and late phase of infection. It would be beneficial for clinical studies to separate the early- (<10 days) and late-phase (>10 days) patients to determine differences in patient response between the groups.

## The Challenge for Therapeutic Development

Despite of the presence of a 3′ to 5′ exoribonuclease (exoN) proofreading enzyme, their large genome size (28–30 kb) means that CoVs remain in the category of highly mutating viruses (Eckerle et al., 2007, 2010; Denison et al., 2011). The high mutation rate poses a considerable challenge for antiviral development as drug resistant viruses could arise or already exist within the quasispecies in nature or from an infected individual (Briese et al., 2014). For instance, after a prolonged period of nAb or drug treatments, the CoV can acquire mutations which confer resistance to the therapeutics (Zumla et al., 2016a). The appearance of these "escape viruses" has been confirmed in multiple mouse model studies in well-contained laboratory

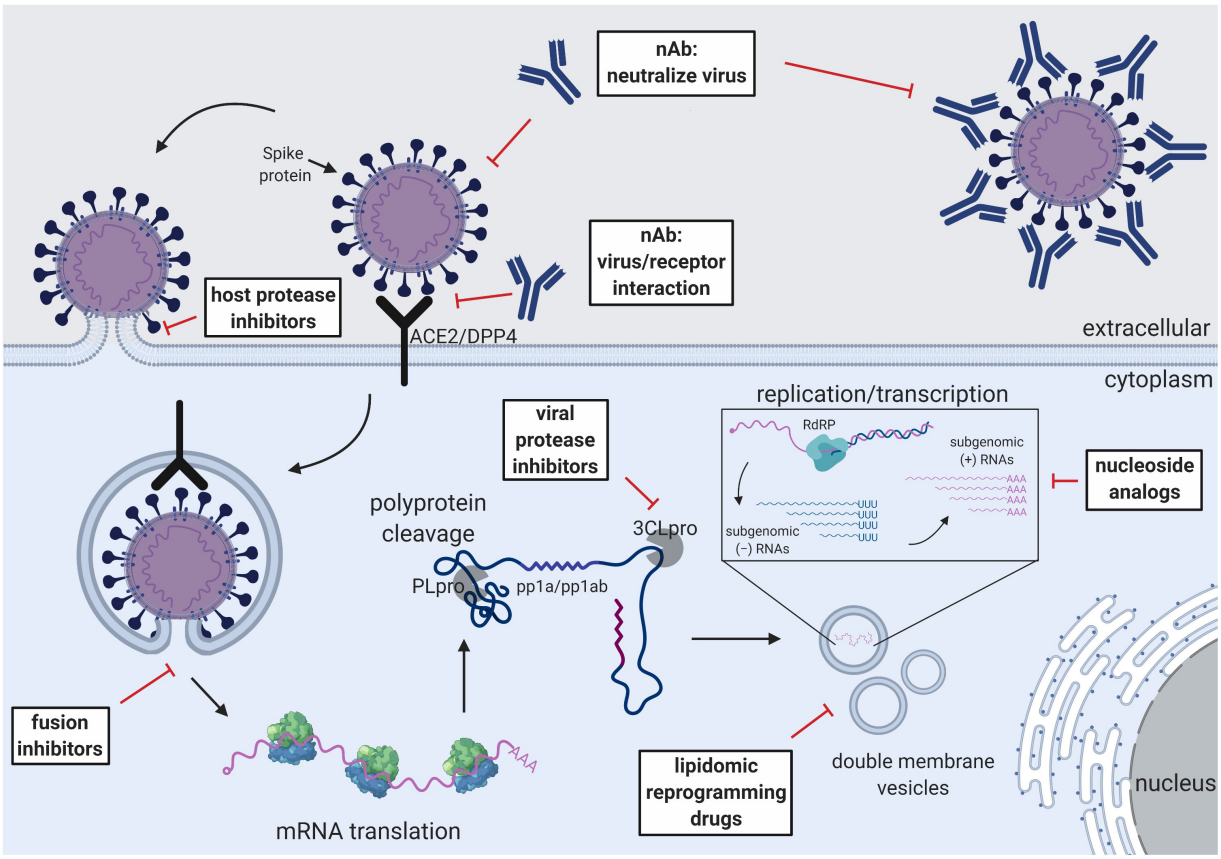


**FIGURE 2 |** Schematic of the CoV replication cycle and key steps for antiviral targets. White text boxes indicate the subtype of antivirals that work either extracellularly or intracellularly. Different steps of the CoV replication cycle are illustrated in cartoon form, including receptor binding, membrane fusion, viral RNA replication, sub-genomic RNA transcription and translation.

settings as well as in nature (Neuman et al., 2006; Ter Meulen et al., 2006; Huang et al., 2008; Jiang et al., 2014; Tang et al., 2014; Tai et al., 2017; Kleine-Weber et al., 2019). Fortunately, some of the mutations that confer drug resistance also compromise viral fitness and attenuate the virus (Deng et al., 2014; Agostini et al., 2018). Another therapeutic intervention is the use of immune modulators, such as IFN-α2a/2b, IFN-β1b and corticosteroids in treating CoVs (Loutfy et al., 2003; Peiris et al., 2003b; Sung et al., 2004). Although multiple studies have shown efficacy of IFN-α2a/2b and IFN-β1b singly or in combination with off-labeled antivirals such as ribavirin, lopinavir (LPV) and ritonavir (RTV) in treating SARS- and MERS-CoV in mouse, rhesus monkey and marmoset models (Haagmans et al., 2004; Barnard et al., 2006b; Falzarano et al., 2013b; Chan et al., 2015), clinical studies have shown inconclusive results (Momattin et al., 2013; Mo and Fisher, 2016). Currently, a randomized controlled trial is underway to determine the efficacy of a combination of LPV/RTV and IFN-β1b in treating MERS-CoV infection (NCT02845843).

## Convalescent Plasma and Monoclonal Antibodies

Although there is no approved drug to treat severe CoV infection, multiple strategies have shown promising results in an experimental setting (**Figure 2**). Convalescent plasma (CP) is derived from patients who have recovered from SARS-CoV and MERS-CoV infection and contains high titer nAbs (Hsueh et al., 2004; Al Kahlout et al., 2019; Shin et al., 2019). Some data suggest that CP use against SARS-CoV infection is safe and, when administered at an early time point, may reduce mortality (Mair-Jenkins et al., 2015). CP neutralizing titers > 1:80 may have a positive impact on infected MERS-CoV patients with respiratory failure (Ko et al., 2018). Unfortunately, CP from convalescent patients is difficult to obtain in large quantities and the Ab titer is too low to have beneficial effects, making it difficult to be used as a main stream therapeutic or for clinical testing (Arabi et al., 2016). As such, no systematic, well-designed clinical trial has formally demonstrated the efficacy of CP in emerging CoV infection. Rather, a clinical trial for testing CP against MERS-CoV infection was withdrawn prior to patient enrollment (NCT02190799).

Although CP from convalescent patients is difficult to obtain, the active component (neutralizing antibodies) can be isolated and subsequently produced in large quantity using recombinant technology (Corti et al., 2016). Passive infusion of neutralizing monoclonal Abs (mAbs) has been used for several diseases with success, including RSV and Ebola virus (Graham and Ambrosino, 2015; Zumla et al., 2016b). Numerous highly potent mAbs against

SARS-CoV and MERS-CoV have been isolated by multiple groups all over the world using different methods such as phage display and direct B cell cloning from immunized animals or convalescent patients (Sui et al., 2004; Traggiai et al., 2004; Greenough et al., 2005; van den Brink et al., 2005; Zhu et al., 2007; Corti et al., 2016). While all of them shows protecting activity *in vitro*, several of them have also shown efficacy in mouse and NHP models (Ter Meulen et al., 2004; Johnson et al., 2016; Chen et al., 2017; van Doremalen et al., 2017; de Wit et al., 2018; Xu et al., 2019). The plethora of potent nAbs have also provided insight into the major antigenic sites on which vaccine development should focus. A list of mAbs that show efficacy *in vivo* against SARS-CoV and MERS-CoV are summarized in **Table 2**. Due to the differences in testing conditions, direct comparison of mAb efficacy should be avoided. Multiple comprehensive review articles on the subject can also be found (Prabakaran et al., 2009; Coughlin and Prabhakar, 2012; Xu et al., 2019).

The binding epitopes of some well-studied mAbs provide valuable information for the neutralization mechanism and clinical implications. The majority of the mAbs target the RBD of the spike protein and prevent viral attachment. For example, mAb 80R is able to protect both *in vitro* and a 16 weeks old mouse model against SARS-CoV Urbani. However, it is unable to protect other strains due to amino acid variations in the RBD (Zhu et al., 2007). On the other hand, S230.15 mimics receptor binding and triggers conformational changes in the SARS *S*-protein, completely protecting young and old mice from SARS-CoV challenge against multiple SARS-CoV, including Urbani, GD03 and SZ16 (Rockx et al., 2008; Walls et al., 2019a). Similar to SARS-CoV, the majority of mAbs targeting MERS-CoV, such as MERS-4, MERS-27 (Jiang et al., 2014), m336 (Ying et al., 2014, 2015) and humanized Ab 4C2 and 2E6 (Li et al., 2015) all target the RBD and prevent the virus from binding to DPP4 with high potency. Interestingly, the mAb LCA60, isolated from a MERS-CoV infected patient, binds to RBD region and confers a broader neutralizing breadth, and is able to neutralize EMC2012 and London1 strains of MERS-CoV (Corti et al., 2015). Non-RBD targeting Abs G2 and G4 recognize the non-RBD region of S1 and S2 of MERS-CoV, respectively, showing cross-reactivity with multiple MERS-CoV variants and can protect hDPP4 transduced mice from challenge (Wang et al., 2015, 2018). Two nanobodies isolated from camelids, NbMS10 and HCAb-83, show potency in hDPP4 transgenic mice by reducing weight loss and increasing survival after challenge. Interestingly, NbMS10 is able to protect mice as a therapeutic treatment 3 days post infection (Raj et al., 2018; Zhao et al., 2018).

While many mAbs show promising properties for clinical use, two mAbs, REGN3048 and REGN3051, have completed phase 1 clinical trials (NCT03301090). These two mAbs were isolated from VelocImmune mice (expressing the variable regions of human Ig heavy and kappa light chain) immunized with MERS *S*-protein. Both mAbs show picomolar binding and inhibition of MERS pseudo particles transduction on Huh7 cells. REGN3048 is able to neutralize seven natural isolates of S variants, and IP injection of the mAb at 1 day before or after challenge reduces MERS-CoV RNA levels and lung pathologies in an hDPP4 transgenic mouse model (Pascal et al., 2015). Given the acute severe phase that is associated with emerging CoV infections, a major hurdle for therapeutic antibodies and drugs is that early administration will likely prove most efficacious in clinical care, as has also been shown with influenza virus, Ebola virus and RSV immunotherapeutics (Olinger et al., 2012; Qiu et al., 2012; Fry et al., 2014; Rezaee et al., 2017).

## Fusion and Viral Protease Inhibitors

Another critical step for CoV life cycle is membrane fusion and the subsequent release of the RNA genome for replication (Millet and Whittaker, 2018). Membrane fusion of CoVs is governed by the S2 domain of the *S*-protein (Pallesen et al., 2017; Tortorici and Veesler, 2019). The S2 stem undergoes a major conformational change at the two heptad repeat regions (HR1 and HR2) to bring the host and viral membrane in close proximity for fusion pore formation (Yuan et al., 2017; Walls et al., 2019b). Multiple peptidomimetic fusion inhibitors that mimic the HR1 and HR2 of either SARS-CoV or MERS-CoV block the formation of the helical core and efficiently inhibit membrane fusion in the micromolar range (Gao et al., 2013; Lu et al., 2014; Xia et al., 2019). A single report has shown treatment of HR2 peptide 5h prior to MERS-CoV challenge in an Ad5-hDPP4 transduction mouse model reduces viral lung titer (Channappanavar et al., 2015). The ability of these drugs to protect in lethal, high titer mouse models has yet to be proven.

CoV nsp3 and nsp5 genes encode the papain-like cysteine protease (PLpro) and 3C-like serine protease (3CLpro), respectively (Perlman and Netland, 2009). PLpro cleaves the polyprotein and separates it into nsp1 to 4 while 3CLpro separates nsp4 to 16 (Ziebuhr et al., 2000; Harcourt et al., 2004). Since polyprotein processing is a critical step for CoV replication and transcription, viral proteases are high priority drug targets. Originally developed as HIV protease inhibitors, LPV and RTV have low micromolar activity against 3CLpro of both SARS-CoV and MERS-CoV *in vitro* (Wu et al., 2004; De Wilde et al., 2014). Testing in SARS-CoV infected patients has shown beneficial outcomes, including lowering the viral load, reducing the onset of ARDS, and lowering mortality rates with LPV and RTV (see nucleoside analogs) treatments (Chu et al., 2004). However, most of the drug studies were performed using retrospective control, sometimes with unbalanced gender ratios, and no treatment has proven efficacious in a randomized control trial (Zumla et al., 2016a). In a marmoset model, LPV/RTV treatment suggested a modest improvement in clinical and pathological outcome as well as reduction of viral load (Chan et al., 2015). However, due to different pathological consequences of treated and untreated group, viral titers were measured at different time points post-infection and all the experiments were performed with a relatively small number ($n = 3$) of single gender (male) animals (Chan et al., 2015). SARS-CoV and MERS-CoV infection has been shown to be heavily biased by age and gender, where elders and males experience more severe complications than females in clinical cases and mouse models (Karlberg et al., 2004; Alghamdi et al., 2014; Channappanavar et al., 2017). A single subject in a case study, an elderly patient, survived a severe MERS-CoV infection using a combination therapy of LPV/RTV,

**TABLE 2 |** Summary of SAR-CoV and MERS-CoV neutralizating antibodies.

| SARS mAbs | Epitopes | Origins | Animal models | Treatment timing, Routes | Dose, route of infection, Strains | Results | References |
|---|---|---|---|---|---|---|---|
| S3.1 | Spike | EBV transformated B cell from SARS patient | 8 weeks old BALB/c | 24 h pre-infection, prophoylatic, IP | $10^4$ TCID50, IN, Urbani | Reduce viral titer (lung and nasal turbinates) | Traggiai et al., 2004 |
| 80R | RBD | Phage display on naive human antibody library | 16 weeks old BALB/c | 24 h pre-infection, prophoylatic, IP | $10^4$ TCID50, IN, Urbani | Reduce viral titer (lung) | Sui et al., 2004 |
| m396 | RBD | Naive human antibody library | 8 week old BALB/c | 24 h pre-infection, prophoylatic, IP | $10^5$ TCID50, IN, Urbani, GD03, SZ16 | Reduce viral titer (lung) | Zhu et al., 2007 |
| S230.15 | RBD | EBV transformated B cell from SARS patient | 8 weeks old BALB/c | 24 h pre-infection, prophoylatic, IP | $10^5$ TCID50, IN, Urbani, GD03, SZ16 | Reduce viral titer (lung) | Zhu et al., 2007 |
| | | | 12 months old BALB/c | 24 h pre-infection, prophoylatic, IP | $10^6$ PFU, IN, Urbani, GZ02, SZ16 | | Rockx et al., 2008 |
| | | | | Co-administration, IN | $10^6$ PFU, IN, GZ02 | Not conclusive, reduce titer | |
| | | | | 1, 2, and 3 days post-infection, theraputic | $10^6$ PFU, IN, GZ02 | Not protective | |
| CR3014 | RBD | Naive human antibody library | Ferret | 24 h pre-infection, prophoylatic, IP | $10^4$ TCID50, IT, HKU-39849 | Reduce viral titer (lung), no lung lesion | van den Brink et al., 2005 |
| | | | | Co-administration | $10^3$ and $10^4$ TCID50, IT, HKU-39849 | Reduce viral titer (lung), reduce lung lesion | Ter Meulen et al., 2004 |
| | | | 4 – 6 weeks old BALB/c | 24 h pre-infection, prophoylatic, IP | $10^5$ TCID50, IN, Urbani, GD03, SZ16 | Reduce viral titer (lung) | Greenough et al., 2005 |
| m68 | Spike (non-RBD) | Transgenic mice with human Ig gene immunized with SARS-CoV Spike | 4 – 6 weeks old BALB/c | 24 h pre-infection, prophoylatic, IP | $10^5$ TCID50, IN, Urbani, GD03, SZ16 | Reduce viral titer (lung) | Greenough et al., 2005 |
| **MERS mAbs** | **Epitopes** | **Origins** | **Animal models** | **Treatment timing, Routes** | **Dose, route of infection, Strains** | **Results** | **References** |
| 4C2 | RBD | Mice immunized with MERS-CoV RBD | 4 – 6 weeks old BALB/c transduced with hDPP4 by Ad5 | 24 h pre-infection, prophylactic, IV | $10^5$ PFU, IN, EMC/2012 | Reduce viral titer (lung) | Li et al., 2015 |
| | | | | 24 h post-infection, theraputic, IV | | | |
| Mersmab1 | RBD | Mice immunized with MERS-CoV S1 | hDPP4 transgenic mice | 24 h post-infection, theraputic, IV | $10^{4.6}$ TCID50, IN, EMC/2012 | Reduce viral titer (lung) | Du et al., 2014; Qiu et al., 2016 |
| CDC2-C2 | RBD | Single B cell cloning from MERS patients | hDPP4 transgenic mice | 24 h pre-infection, prophylactic, IP | $10^6$ TCID50, IN, EMC/2012 | Reduce viral titer (lung) | Wang et al., 2015, 2018 |
| G2 | Spike (non-RBD) | Mice primed with MERS-CoV DNA and S1 protein | hDPP4 transgenic mice | 24 h pre-infection, prophylactic, IP | $10^6$ TCID50, IN, EMC/2012 | Reduce viral titer (lung) | Wang et al., 2015, 2018 |
| G4 | S2 | Mice primed with MERS-CoV DNA and S1 protein | hDPP4 transgenic mice | 24 h pre-infection, prophylactic, IP | $10^6$ TCID50, IN, EMC/2012 | Reduce viral titer (lung) | Wang et al., 2015, 2018 |
| MCA1 | RBD | Phage display on naive human antibody library | 2 years old common marmosets | 24 h pre-infection, prophylactic, IP | $5 \times 10^6$ PFU, IT, EMC/2012 | Reduce viral titer (lung), weight loss and patholicical scores | Chen et al., 2017 |
| | | | | 2 or 12 h post-infection, theraputic, IP | | | |

*(Continued)*

**TABLE 2 |** Continued

| MERS mAbs | Epitopes | Origins | Animal models | Treatment timing, Routes | Dose, route of infection, Strains | Results | References |
|---|---|---|---|---|---|---|---|
| LCA60 | RBD | Single B cell cloning from MERS patients | 4 – 6 weeks old BALB/c transduced with hDPP4 by Ad5 | 24 h pre-infection, prophylactic, IP | $10^5$ PFU, IN, EMC/2012 and London1/2012 | Reduce viral titer (lung), weight loss and pathology | Corti et al., 2015 |
| | | | | 24 h post-infection, theraputic, IP | | | Corti et al., 2015 |
| | | | 2 – 6 years old common marmosets | 24 h pre-infection, prophylactic, IP | $5.2 \times 10^6$ PFU, IN + IT + ocular + orally, EMC/2012 | Moderately protective, reduce weight loss and pathology | de Wit et al., 2019 |
| m336 | RBD | Phage display on navie human antibody library | hDPP4 transgenic mice | 12h pre-infection, prophylactic, IP | $10^4$ TCID50, IN, EMC/2012 | reduce viral titer (lung), weight loss and patholicical scores | Ying et al., 2014, 2015 |
| | | | | 12h post-infection, theraputic, IP | | | Agrawal et al., 2016 |
| | | | 5 – 7 months old Australian white rabbit | 24 h pre-infection, prophylactic, IV and IN | $10^5$ TCID50, IN, EMC/2012 | Reduce viral RNA titer and lung inflammation | Houser et al., 2016 |
| | | | Common marmosets | 6 h (IV) and 48 h (SC) post-infection, theraputic | $5.2 \times 10^6$ PFU, IN + IT + ocular + orally, EMC/2012 | Moderately protective, reduce clinical diseases and gross pathology | van Doremalen et al., 2017 |
| NbMS10 | RBD | llama immunized with MERS-CoV RBD | hDPP4 transgenic mice | 3 days pre-infection, prophylactic, IP | $10^{5.3}$ TCID50, IN, EMC/2012 | Reduce weight loss and increase survival | Zhao et al., 2018 |
| | | | | 1 or 3 days post-infection, theraputic, IP | | | Zhao et al., 2018 |
| HCAb-83 | RBD | Dromedary camel immunized with MERS-CoV DNA and Spike protein | hDPP4 transgenic mice | 6 h pre-infection, prophylactic, IP | $10^5$ TCID50, IN, EMC/2012 | Reduce viral titer (lung), weight loss and increase survival | Raj et al., 2018 |

*IV, intravenous; IN, intranasal; IT, intratracheal; SC, subcutaneous; IP, intraperitoneal.*

IFN1α, and ribavirin (Kim et al., 2016). An ongoing clinical trial in Saudi Arabia has begun to use a combination of LPV/RTV and IFNβ-1b for laboratory-confirmed MERS-CoV infection (NCT02845843). Given the importance of 3CLpro I viral life cycle, it is an attractive target for novel drug development (Kumar et al., 2017).

## Nucleoside Analogs and RdRp Inhibitors

Ribavirin is a guanosine analog that targets RNA dependent RNA polymerases (RdRp) and has a broad efficacy against RNA viruses (Loustaud-Ratti et al., 2016). The drug inhibits viral RNA synthesis and has shown efficacy against HCV and RSV (De Clercq et al., 2016). Ribavirin inhibits SARS-CoV and MERS-CoV replication at high concentration *in vitro* (Tan et al., 2004; Falzarano et al., 2013a), However, ribavirin enhances viral replication in the mouse lung and prolongs viral persistence in a SARS-CoV mouse model (Barnard et al., 2006a). Although not effective as a monotherapy, ribavirin shows a synergistic effect against SARS-CoV and MERS-CoV when combine with IFN (Momattin et al., 2013). In a rhesus macaque model, MERS-CoV infected monkeys show improvement after treating with ribavirin and IFN-α2b (Falzarano et al., 2013b). Furthermore, ribavirin has been used in clinical settings during SARS-CoV and MERS-CoV outbreaks (Omrani et al., 2014; Khalid et al., 2015; Shalhoub et al., 2015). While some studies report positive outcome after treatment with ribavirin + IFN, others suggest no significant improvement (Dicaro et al., 2004; Khalid et al., 2015). Due to the variation in dosage and time of administration and the lack of control, the efficacy of using ribavirin in patients is inconclusive. Mechanistically, studies show that recombinant CoV with a deleted proof-reading exonucleases N (ExoN) shows higher sensitivity toward ribavirin. These results indirectly suggest that the low activity of ribavirin in CoV could be explained by the presence of a proofreading exonucleases N (ExoN, nsp14) which can excise the drug from the viral mRNA in CoVs (Smith et al., 2013; Ferron et al., 2017).

Two nucleoside analogs, β-D-N4-Hydroxycytidine (NHC) and GS-5734 (remdesivir), have shown high efficacy against CoVs and are less sensitive to ExoN (Sheahan et al., 2017, 2020; Agostini et al., 2018, 2019). NHC is a cytidine analog and has recently been shown to inhibit multiple viruses, including influenza virus, RSV and Ebola virus (Reynard et al., 2015; Urakova et al., 2017;

Yoon et al., 2018). It has micro-molar EC50 against both alpha and beta CoVs including SARS-CoV and MERS-CoV (Barnard et al., 2004; Pyrc et al., 2006; Agostini et al., 2019). Currently under clinical development for Ebola viruses, remdesivir is a nucleoside prodrug that is effective against multiple other RNA viruses including Nipah viruses, RSV, and CoVs (Lo et al., 2017; Sheahan et al., 2017). Remdesivir has sub-micromolar inhibition concentrations in a broad range of CoVs including SARS-CoV, MERS-CoV, and hCoV-NL63, as well as pre-pandemic bat-CoVs WIV1 and SHC014 in an *in vitro* human airway epithelial (HAE) model (Sheahan et al., 2017; Agostini et al., 2018). Prophylactic administration (one day pre-infection) of remdesivir can mitigate disease by reducing the viral titer and lung pathology in lethal mouse models challenged with a mouse adapted SARS-CoV MA15. Remdesivir also shows therapeutic activity when administered early at one day post-infection (corresponding to 7–10 days after the onset of symptoms in human infection). However, treatment initiated two days post infection does not improve disease outcomes, although the murine disease model is more compressed than in humans (Sheahan et al., 2017). Importantly, remdesivir shows excellent prophylactic protection. Rhesus macaques are completely protected from MERS-CoV infection as scored by lung pathology and clinical score as well as inhibited viral growth. Therapeutic treatment 12-h post infection shows moderate improvement of clinical outcomes on NHPs (de Wit et al., 2020). The parental nucleoside of remdesivir, GS-441524, has also shown to be effective for treating FIP, a disease caused by the α-CoV FIPV (Murphy et al., 2018; Pedersen et al., 2019). Currently, NHC and remdesivir are the only broadly effective antiviral drugs against all SARS-like, MERS-like, human contemporary, and animal CoVs (Sheahan et al., 2017; Agostini et al., 2018; Murphy et al., 2018; Pedersen et al., 2019). Some antiviral drugs, such as chloroquine and T-705, also show efficacy *in vitro* and are under consideration for the current COVID-19 outbreak (Wang et al., 2020).

# HOST FACTOR INHIBITORS AND IMMUNO-MODULATORS

## Host Protease Inhibitors

Like all class I viral fusion proteins, CoV S glycoproteins require proteolytic cleavage by host proteases for membrane fusion and viral entry (Belouzard et al., 2012; White and Whittaker, 2016; Millet and Whittaker, 2018). Two cleavage events have been characterized in SARS-CoV and MERS-CoV. The first cleavage event separates the head (S1) and the fusion stem (S2) by cutting the S1/S2 junction (Millet and Whittaker, 2015). The second cleavage event occurs at the S2' site which is usually located immediately upstream of the fusion peptide (Belouzard et al., 2009). Multiple proteases have been shown to be involved in the cleavage events, including cathepsin-L, trypsin-like serine proteases, transmembrane serine proteases (TTSP) and proprotein convertases such as furin (Millet and Whittaker, 2015). Cathepsin-L inhibitors MDL28170 and SSAA09E1 block SARS-CoV pseudotyped particle infection in pre-treated 293T cells (Simmons et al., 2005; Adedeji et al., 2013). While a peptidomimetic furin substrate, decanoyl-RVKR-chloromethylketone, has been shown to inhibit cleavage of MERS *S*-protein and block infection in multiple cell lines including normal human bronchial epithelial cells (NHBE), the *in vivo* potency of this approach is less certain (Gierer et al., 2014; Millet and Whittaker, 2014; Matsuyama et al., 2018).

## Host Receptor Inhibitors

The blocking of receptor interactions is also a target of antiviral development. *N*-(2-aminoethyl)-1 aziridine-ethanamine (NAAE) blocks the interaction of SARS *S*-protein and ACE2 and inhibits S-mediated cell-to-cell fusion at millimolar concentrations (Huentelman et al., 2004). Similarly, an Ab blocking DPP4 can also inhibit MERS-CoV infection on primary bronchial epithelial cells (Raj et al., 2013). Importantly, the *S*-proteins of SARS-CoVs and MERS-CoV interact with their receptors outside of the active sites. Therefore, it would be of interest to develop inhibitors that do not affect the normal function of the host proteins but abolish the interaction of the CoV and receptor. Otherwise, long term inhibition of cellular proteins could have adverse effects on the host. For instance, inhibition of ACE2 may cause hypertension (Danilczyk and Penninger, 2006). Additionally, DPP4 is also responsible for multiple cellular functions including immune homeostasis, stem cell development, metabolism and T-cell regulation, and hence is not an ideal target for MERS-CoV infection (Matteucci and Giampietro, 2016; Ou et al., 2019).

## Other Host Factor Inhibitors

Another attractive target to inhibit CoV infection is the host metabolic pathways essential for CoV life cycles. CoVs replicate and transcribe in membrane-bound vesicles derived from the host's rough ER (Snijder et al., 2006; Stertz et al., 2007; Reggiori et al., 2010). MERS-CoV infection upregulates the biosynthetic pathways of multiple major lipogenic enzymes, including fatty acid synthase (FAS), acetyl-CoA carboxylase (ACC) and HMG-CoA synthase (HMGCS) (Yuan et al., 2019). AM580, which targets the major lipid biosynthesis transactivator n-SREBPs by interfering with and downregulating global lipid synthesis (Goldstein et al., 2006; Yuan et al., 2019), inhibits the replication of multiple viruses including influenza virus, Zika virus, Enterovirus-A71 and MERS-CoV (Yuan et al., 2019). Remarkably, MERS-CoV viral titer is reduced by 1,000- to 1,000,000-fold in the presence of AM580 in Huh7 cells or a human intestinal organoid model, respectively, and IP injection of AM580 for 3 days protects a human hDPP4 transgenic mouse model from MERS-CoV lethal challenge (Yuan et al., 2019).

## Immune Modulators

### Corticosteroids

SARS-CoV and MERS-CoV both cause lung inflammation and can progress into severe respiratory syndrome. Lacking direct antiviral effect, corticosteroids are an immune suppressor which is administrated to severe patients to alleviate lung inflammation. However, immune suppression could also facilitate viral replication. Therefore, corticosteroids are often administrated with antiviral or other immune modulators, such as IFN which

can activate the immune system. Retrospective and prospective clinical studies have shown mixed observation in treating SARS-CoV and MERS-CoV patients with corticosteroids, IFN and ribavirin; while some showed a positive effect, others showed no difference.

### IFNs

SARS-CoV and MERS-CoV are able to suppress the induction of IFN synthesis by multiple mechanisms including inhibition of the IFN signal transduction pathways and evading detection by pattern recognition receptors (PRRs) and toll-like receptors (TLRs) (Frieman et al., 2008; Lim et al., 2016; Mubarak et al., 2019). Therefore, external administration of IFN regiments could re-initiate the antiviral immune response in the host. During the SARS-CoV and MERS-CoV outbreaks, IFN-α, IFN-β, and IFN-γ were used in combination with various antiviral drugs, including LPV/RTV, ribavirin, corticosteroids and poly I:C (Zumla et al., 2016a). Although most of the clinical reports are positive, there is no consensus on the efficacy of IFN treatment in CoV infection. In animal model studies, IFN treatment is only effective when administrated at early time point for both SARS-CoV and MERS-CoV (Channappanavar et al., 2016, 2019). Furthermore, many of the clinical studies were confounded by multiple factors, including IFN dosages, combination of different antivirals, and the stage of infection (Mo and Fisher, 2016). For instance, some studies targeted patients in the late stage of infection and show a worse survival rate than average (Al-Tawfiq et al., 2014; Khalid et al., 2014). Based on multiple research reports, IFN-β shows the best efficacy in treating MERS-CoV infection (Chan et al., 2013; Hart et al., 2014; Kim et al., 2016). Currently, an open labeled, well controlled clinical study is aiming to test a set dose of LPV/RTV and IFN-β in treating MERS-CoV. The trial will probably provide insight into treating MERS-CoV infection in human population.

## THE CURRENT SARS-CoV-2 OUTBREAK: A CHALLENGE, AN OPPORTUNITY

In December 2019, a new CoV outbreak started in Wuhan, China, a megacity with a population of 11 million. With an estimated basic reproduction number ($R_0$) of 1.4 – 2.5, SARS-CoV-2 quickly spread to every province in China and began to spread globally by the end of January 2020 (Zhou et al., 2020), and was declared a worldwide pandemic in March 2020 by the World Health Organization. SARS-CoV-2 is capable of human-to-human transmission via either symptomatic or asymptomatic patients (Rothe et al., 2020). The high mutation rate of CoVs and the possibility of super-spreader could potentiate the continuous spreading globally. Originally from bat, the SARS-CoV-2 Is 96% identical to a bat CoV designated RaTG13, isolated from a cave in Yunnan Province, China and belongs to the betacoronavirus 2b family, as does SARS-CoV (Zhou et al., 2020). However, the *S*-proteins between SARS-CoV and 2019 nCoV share only 76–78% sequence similarity, rendering the current experimental vaccines and antivirals unlikely to be fully protective against SARS-CoV-2. As many group 2b SARS-like CoV have pre-epidemic potential, vaccines and countermeasures should be targeted against all of these strains to maximally protect against current and future threats to the global health and economy (Menachery et al., 2015, 2016).

After two CoV outbreaks in the last two decades, the public health officials and clinicians have experience in preventing spread and treating SARS-CoV-2 patients. Prompt communication between governments, quick quarantine procedures, and rapid viral detection assays have helped minimize SARS-CoV-2 cases in other countries thus far. Additionally, the scientific community has developed novel vaccine strategies and experimental antivirals to fight emerging CoV. New vaccines that specifically targeting SARS-CoV-2 are under development. Moderna had started a phase 1 clinical trial on an RNA vaccine (mRNA-1273) that encodes the prefusion stabilized form of SARS-CoV-2 *S*-protein (NCT04283461). Although there are no published studies of a RNA vaccine platform against CoV, the RNA platform has shown efficacy against multiple other viral infectious diseases including influenza, rabies, Flavivirus, and Ebola viruses in experimental animal models (Zhang et al., 2019). Furthermore, pre-clinical data of the Zika virus mRNA vaccine (mRNA-1893) from Moderna has shown protection against Zika virus and abrogated maternal transmission of Zika virus in pregnant mice (Richner et al., 2017; Jagger et al., 2019). Broad-spectrum antivirals which have shown efficacy against multiple CoVs have the potential to treat SARS-CoV-2 (Sheahan et al., 2017, 2020). Given the high number of infected patients and at risk individuals, the current situation provides an opportunity to initiate clinical trials for (a) vaccine formulation designed to protect uninfected people, (b) broad spectrum antivirals to treat infected individuals and (c) formulation of immune modulators to alleviate clinical pathologies. A well-designed clinical trial could not only ameliorate the current situation, but also lay the foundation for future CoV outbreaks. Supported by a recent study on SARS-CoV-2 (Wang et al., 2020) and multiple research studies on SARS and MERS-CoVs (Sheahan et al., 2017, 2020; de Wit et al., 2020) and a single clinical report (Holshue et al., 2020), remdesivir hold promises as treatment for SARS-CoV-2. The Chinese government has started a clinical trial using remdesivir for treating SARS-CoV-2 patients with mild to severe symptoms (NCT04252664, NCT04257656). On the clinical side, if time and resources permit, a centralized repository that records and digitizes infection cases would aid future medical and epidemiology studies through machine learning programs. Finally, the current situation also provides an opportunity to develop unconventional treatments, such as gene therapy, to target infectious diseases.

## UNCONVENTIONAL VACCINES AND THERAPEUTICS – GENE THERAPIES

The field of gene therapy has undergone rapid growth in the last 10 years. Although mainly focused on rare genetic diseases, its potential in treating infectious diseases should not be discounted. One of the leading vectors, adeno-associated virus (AAV), has

proven to be safe for human use and multiple AAV-based gene therapy drugs are approved by the FDA and the EMA (Kay et al., 2000; Kaplitt et al., 2007). So far, the only report of use of AAV in CoV is as a DNA vaccine to deliver SARS-CoV spike protein for immunization (Du et al., 2008). Given the recent developments in human antibody cloning technologies, AAV holds a promising potential to be a hybrid of vaccine and therapeutic which acts as a passive immunization vector to provide protection for the outbreak and as a therapeutic in early time scales.

## AAV as a Vector for Passive Immunization Against Emerging CoV

### The Vectors – Safety

AAV is a non-pathogenic, non-enveloped, 4.7 kb single-stranded DNA virus belonging to the *Dependoparvovirus* genus within the family *Parvoviridae* (Cotmore et al., 2014). AAV infects a wide variety of animals, from bearded dragons to humans. Natural AAV isolates have different tissue tropisms in humans and can be reverse engineered to better fulfill various medical needs. To target SARS-CoV, MERS-CoV and other respiratory virus infections, a human airway tropic AAV is needed. Multiple reports have demonstrated that natural isolates AAV5 (Zabner et al., 2000), AAV6 (Limberis et al., 2009), and AAV9 (Adam et al., 2014) as well as engineered vectors AAV2.5 (Li et al., 2009) and AAV2.5T (Excoffon et al., 2009) are able to transduce human lung epithelial cells, including primary human airway epithelial (HAE) cultures. Although there is a high prevalence of nAbs against AAVs in the human population, new technologies have been developed to engineer AAV to evade humoral immune responses (Tse et al., 2015, 2017). These developments potentially allow for the delivery of CoV vaccines or immunotherapeutic directly to the mucosal compartments of the lung.

### The Package – Flexibility

Passive immunization of AAV can be developed as a platform technology in which the nAb can be quickly exchanged to target specific pathogens. Multiple studies have shown passive immunization using AAV is effective against viral infectious diseases such as HIV, (Balazs et al., 2012; Lin and Balazs, 2018) Ebola, (Limberis et al., 2016) influenza, (Balazs et al., 2013; Laursen et al., 2018), and others (Nieto and Salvetti, 2014). The package for delivery is extremely flexible, from authentic immunoglobulins (IgG) to immunoadhesins (IA) to single chain variable fragments (scFv) to bi-specific antibodies (Naso et al., 2017). Furthermore, a combination of Abs, small antiviral peptides and immuno-modulators can be co-delivered at the same time to achieve multidimensional therapy. Although AAV-based passive immunization has not yet been tested as therapeutic, it could serve as a fast-acting prophylactic alternative to traditional vaccines.

### The Timing – Quick

The most important aspect to control an outbreak is to reduce the spread by protecting the population from infection. However, there is a lag time between the beginning of an outbreak and the development of an effective vaccine in which the population is completely vulnerable. Prophylactic treatments, such as infusion of Abs and antivirals, could protect individual for a short duration. However, these prophylactic treatments require constant intake to stay effective and are toxic as well as financially impractical for long-term use (Hansel et al., 2010). AAV-based passive immunization could perfectly fill the vacuum by protecting the population before the arrival of a vaccine. Since AAV is a platform technology, anti-viral packages can be swapped and tested quickly, within a month (Strobel et al., 2019). After administration in animals, protection can be achieved in less than a week, faster than any vaccine strategies. In an influenza study, AAV9 delivery of IA via intranasal inoculation protected animals from lethal influenza challenges including H5N1, H1N1 and H1N1 1918 within 3 days of AAV administration (Limberis et al., 2013). Unlike traditional gene therapy in which the transgene lasts for long periods of time, the natural turnover rate of airway epithelia means that the nAb introduction is not permanent, reducing the chance that the host will produce antibodies targeting the therapeutic antibody delivered by AAV (anti-drug antibody responses) (Nieto and Salvetti, 2014). Therefore, AAV-based passive immunization is a quick and excellent option to deploy in an outbreak situation for emerging infectious diseases.

## The Challenges

AAV-based gene therapy has great potential for treating viral infectious diseases. However, there are multiple hurdles for AAV-based gene therapy to achieve its full potential. (1) Low transduction efficiency, (2) pre-existing nAb against AAVs, (3) transgene toxicity and loss of expression, and (4) extremely high price tag (Colella et al., 2018; Kaemmerer, 2018). Fortunately, multiple strategies have been developed to address these hurdles (Tse et al., 2015). For instance, through vector engineering, a new generation of AAV vectors can evade pre-existing nAbs while retaining a good transduction profile in the respiratory system (Li et al., 2009; Tse et al., 2017). For rare genetic diseases, life-long gene expression is important for therapeutic purposes but could cause toxicity. On the contrary, for emerging CoVs, the goal is a short-term protection from the virus. Therefore, AAV can target epithelial cells that have a regular turn-over rate, hence providing short-term protection and preventing transgene toxicity. AAV-based therapies are known for their extremely high prices, sometime up to a million US dollar per treatment. However, the prices are inflated due to the small market size of rare genetic diseases and the cost for drug development. Given the huge market size of infectious diseases, the price for AAV-based therapy for infectious diseases should be more reasonable. Unlike rare genetic diseases and other infectious diseases, an emerging CoV outbreak is uniquely suitable for AAV-based passive immunization as a short-term protection therapy before vaccine deployment.

# CONCLUSION

The continuous development of vaccines, antivirals, and hopefully gene therapies will provide an arsenal for combating and controlling emerging CoV diseases. For vaccine development, understanding the antigenicity and neutralizing

antibody footprints of different CoVs could aid the development of broad-spectrum vaccines and, ultimately, the possibility of a universal CoV vaccine. Vaccine formulation, including dosage and adjuvants, should be tested systemically and, if possible, on animal models that reflects the genetic variation of the human population. A deeper understanding of the basic biology of CoV and host-virus interaction can lead to the discovery of druggable targets. Importantly, we should not overlook the potential of the existing broad-spectrum antivirals and should start clinical trials on these drugs in a timely fashion. Prevention is always the best treatment, and constant viral surveillance of wild animals for potential emerging CoVs is extremely important. Testing the outbreak potential of heterologous SARS- and MERS-like viruses with different spike proteins could better prepare society from the next outbreak. A centralized digital database that collect public health and clinical information of the current outbreak would allow global retrospective studies in the future using machine learning and other big data analysis. On the research side, quick, reliable and easily employed viral testing kits should be developed. Innovative technologies such as gene therapy should be adequately explored for their potential to combat CoVs and act as another line of defense against elusive emerging viral diseases. The current SARS-CoV-2 poses a huge challenge for society; however, given experience with emerging CoVs and global effort, it is hoped that the impact of the outbreak will be minimal.

## AUTHOR CONTRIBUTIONS

LT wrote the review. RM, RG, and RB reviewed and revised the final version.

## FUNDING

The manuscript presented here were supported by grants from the National Institute of Allergy and Infectious Disease of the United States National Institutes of Health (NIH) by awards AI108197, AI110700, AI132178, and AI149644 (RB). **Figure 2** is generated using biorender (https://biorender.com/).

## ACKNOWLEDGMENTS

We thank Dr. Timothy Sheahan and Dr. Yixuan Hou for critical reading of this manuscript and all members in the RB laboratory for helpful discussions.

## REFERENCES

Adam, V. S., Crosariol, M., Kumar, S., Ge, M. Q., Czack, S. E., Roy, S., et al. (2014). Adeno-associated virus 9-mediated airway expression of antibody protects old and immunodeficient mice against influenza virus. *Clin. Vaccine Immunol.* 21, 1528–1533. doi: 10.1128/CVI.00572-514

Adedeji, A. O., Severson, W., Jonsson, C., Singh, K., Weiss, S. R., and Sarafianos, S. G. (2013). Novel inhibitors of severe acute respiratory syndrome coronavirus entry that act by three distinct mechanisms. *J. Virol.* 87, 8017–8028. doi: 10.1128/jvi.00998-913

Adney, D. R., Wang, L., Van Doremalen, N., Shi, W., Zhang, Y., Kong, W., et al. (2019). Efficacy of an adjuvanted middle east respiratory syndrome coronavirus spike protein vaccine in dromedary camels and alpacas. *Viruses* 11:212. doi: 10.3390/v11030212

Agnihothram, S., Gopal, R., Yount, B. L. J., Donaldson, E. F., Menachery, V. D., Graham, R. L., et al. (2014). Evaluation of serologic and antigenic relationships between middle eastern respiratory syndrome coronavirus and other coronaviruses to develop vaccine platforms for the rapid response to emerging coronaviruses. *J. Infect. Dis.* 209, 995–1006. doi: 10.1093/infdis/jit609

Agostini, M. L., Andres, E. L., Sims, A. C., Graham, R. L., Sheahan, T. P., Lu, X., et al. (2018). Coronavirus susceptibility to the antiviral remdesivir (GS-5734) is mediated by the viral polymerase and the proofreading exoribonuclease. *mBio* 9, 1–15. doi: 10.1128/mBio.00221-218

Agostini, M. L., Pruijssers, A. J., Chappell, J. D., Gribble, J., Lu, X., Andres, E. L., et al. (2019). Small-molecule antiviral β-d-N4-hydroxycytidine inhibits a proofreading-intact coronavirus with a high genetic barrier to resistance. *J. Virol.* 93:e01348-19. doi: 10.1128/JVI.01348-1319

Agrawal, A. S., Tao, X., Algaissi, A., Garron, T., Narayanan, K., Peng, B. H., et al. (2016). Immunization with inactivated Middle East Respiratory Syndrome coronavirus vaccine leads to lung immunopathology on challenge with live virus. *Hum. Vaccines Immunother.* 12, 2351–2356. doi: 10.1080/21645515.2016.1177688

Ahmed, A. E. (2019). Diagnostic delays in Middle East respiratory syndrome coronavirus patients and health systems. *J. Infect. Public Health* 12, 767–771. doi: 10.1016/j.jiph.2019.04.002

Al Kahlout, R. A., Nasrallah, G. K., Farag, E. A., Wang, L., Lattwein, E., Müller, M. A., et al. (2019). Comparative serological study for the prevalence of Anti-MERS coronavirus antibodies in high- and low-risk groups in qatar. *J. Immunol. Res.* 2019:1386740. doi: 10.1155/2019/1386740

Al-Amri, S. S., Abbas, A. T., Siddiq, L. A., Alghamdi, A., Sanki, M. A., Al-Muhanna, M. K., et al. (2017). Immunogenicity of candidate MERS-CoV DNA vaccines based on the spike protein. *Sci. Rep.* 7:44875. doi: 10.1038/srep44875

Alghamdi, I. G., Hussain, I. I., Almalki, S. S., Alghamdi, M. S., Alghamdi, M. M., and El-Sheemy, M. A. (2014). The pattern of Middle East respiratory syndrome coronavirus in Saudi Arabia: a descriptive epidemiological analysis of data from the Saudi Ministry of Health. *Int. J. Gen. Med.* 7, 417–423. doi: 10.2147/IJGM.S67061

Alharbi, N. K., Padron-Regalado, E., Thompson, C. P., Kupke, A., Wells, D., Sloan, M. A., et al. (2017). ChAdOx1 and MVA based vaccine candidates against MERS-CoV elicit neutralising antibodies and cellular immune responses in mice. *Vaccine* 35, 3780–3788. doi: 10.1016/j.vaccine.2017.05.032

Almazán, F., Dediego, M. L., Sola, I., Zuñiga, S., Nieto-torres, J. L., Marquez-jurado, S., et al. (2013). A Vaccine candidate east respiratory syndrome coronavirus as a vaccine candidate. *mBio* 4, 1–11. doi: 10.1128/mBio.00650-13.Editor

Al-Tawfiq, J. A., Momattin, H., Dib, J., and Memish, Z. A. (2014). Ribavirin and interferon therapy in patients infected with the Middle East respiratory syndrome coronavirus: an observational study. *Int. J. Infect. Dis.* 20, 42–46. doi: 10.1016/j.ijid.2013.12.003

Arabi, Y. M., Hajeer, A. H., Luke, T., Raviprakash, K., Balkhy, H., Johani, S., et al. (2016). Feasibility of using convalescent plasma immunotherapy for MERS-CoV infection, Saudi Arabia. *Emerg. Infect. Dis.* 22, 1554–1561. doi: 10.3201/eid2209.151164

Balazs, A. B., Bloom, J. D., Hong, C. M., Rao, D. S., and Baltimore, D. (2013). Broad protection against influenza infection by vectored immunoprophylaxis in mice. *Nat. Biotechnol.* 31:647. doi: 10.1038/nbt.2618

Balazs, A. B., Chen, J., Hong, C. M., Rao, D. S., Yang, L., and Baltimore, D. (2012). Antibody-based protection against HIV infection by vectored immunoprophylaxis. *Nature* 481, 81–84. doi: 10.1038/nature10660

Barnard, D. L., Day, C. W., Bailey, K., Heiner, M., Montgomery, R., Lauridsen, L., et al. (2006a). Enhancement of the infectivity of SARS-CoV in BALB/c mice by IMP dehydrogenase inhibitors, including ribavirin. *Antiviral Res.* 71, 53–63. doi: 10.1016/j.antiviral.2006.03.001

Barnard, D. L., Day, C. W., Bailey, K., Heiner, M., Montgomery, R., Lauridsen, L., et al. (2006b). Evaluation of immunomodulators, interferons and known in vitro SARS-CoV inhibitors for inhibition of SARS-CoV replication in BALB/c mice. *Antivir. Chem. Chemother.* 17, 275–284. doi: 10.1177/095632020601700505

Barnard, D. L., Hubbard, V. D., Burton, J., Smee, D. F., Morrey, J. D., Otto, M. J., et al. (2004). Inhibition of severe acute respiratory syndrome-associated coronavirus (SARSCoV) by calpain inhibitors and β-D-N4-hydroxycytidine. *Antivir. Chem. Chemother.* 15, 15–22. doi: 10.1177/095632020401500102

Belouzard, S., Chu, V. C., and Whittaker, G. R. (2009). Activation of the SARS coronavirus spike protein via sequential proteolytic cleavage at two distinct sites. *Proc. Natl. Acad. Sci. U.S.A.* 106, 5871–5876. doi: 10.1073/pnas.0809524106

Belouzard, S., Millet, J. K., Licitra, B. N., and Whittaker, G. R. (2012). Mechanisms of coronavirus cell entry mediated by the viral spike protein. *Viruses* 4, 1011–1033. doi: 10.3390/v4061011

Belshe, R. B., Gruber, W. C., Mendelman, P. M., Mehta, H. B., Mahmood, K., Reisinger, K., et al. (2000). Correlates of immune protection induced by live, attenuated, cold-adapted, trivalent, intranasal influenza virus vaccine. *J. Infect. Dis.* 181, 1133–1137. doi: 10.1086/315323

Binnie, A., Tsang, J. L. Y., and Dos Santos, C. C. (2014). Biomarkers in acute respiratory distress syndrome. *Curr. Opin. Crit. Care* 20, 47–55. doi: 10.1097/MCC.0000000000000048

Bisht, H., Roberts, A., Vogel, L., Bukreyev, A., Collins, P. L., Murphy, B. R., et al. (2004). Severe acute respiratory syndrome coronavirus spike protein expressed by attenuated vaccinia virus protectively immunizes mice. *Proc. Natl. Acad. Sci. U.S.A.* 101, 6641–6646. doi: 10.1073/pnas.0401939101

Bisht, H., Roberts, A., Vogel, L., Subbarao, K., and Moss, B. (2005). Neutralizing antibody and protective immunity to SARS coronavirus infection of mice induced by a soluble recombinant polypeptide containing an N-terminal segment of the spike glycoprotein. *Virology* 334, 160–165. doi: 10.1016/j.virol.2005.01.042

Bodmer, B. S., Fiedler, A. H., Hanauer, J. R. H., and Mühlebach, M. D. (2018). Live-attenuated bivalent measles virus-derived vaccines targeting Middle East respiratory syndrome coronavirus induce robust and multifunctional T cell responses against both viruses in an appropriate mouse model. *Virology* 521, 99–107. doi: 10.1016/j.virol.2018.05.028

Bolles, M., Deming, D., Long, K., Agnihothram, S., Whitmore, A., Ferris, M., et al. (2011a). A double-inactivated severe acute respiratory syndrome coronavirus vaccine provides incomplete protection in mice and induces increased eosinophilic proinflammatory pulmonary response upon challenge. *J. Virol.* 85, 12201–12215. doi: 10.1128/jvi.06048-6011

Bolles, M., Donaldson, E., and Baric, R. (2011b). SARS-CoV and emergent coronaviruses: viral determinants of interspecies transmission. *Curr. Opin. Virol.* 1, 624–634. doi: 10.1016/j.coviro.2011.10.012

Briese, T., Mishra, N., Jain, K., East, M., Syndrome, R., Quasispecies, C., et al. (2014). Dromedary camels in Saudi Arabia include homologues of human isolates revealed through whole-genome analysis etc. *mBio* 5, 1–5. doi: 10.1128/mBio.01146-14.Editor

Buchholz, U. J., Bukreyev, A., Yang, L., Lamirande, E. W., Murphy, B. R., Subbarao, K., et al. (2004). Contributions of the structural proteins of severe respiratory syndrome coronavirus to protective immunity. *Proc. Natl. Acad. Sci. U.S.A.* 101, 9804–9809. doi: 10.1073/pnas.0403492101

Bukreyev, A., Lamirande, E. W., Buchholz, U. J., Vogel, L. N., Elkins, W. R., St Claire, M., et al. (2004). Mucosal immunisation of African green monkeys (*Cercopithecus aethiops*) with an attenuated parainfluenza virus expressing the SARS coronavirus spike protein for the prevention of SARS. *Lancet* 363, 2122–2127. doi: 10.1016/S0140-6736(04)16501-X

Cabeça, T. K., Granato, C., and Bellei, N. (2013). Epidemiological and clinical features of human coronavirus infections among different subsets of patients. *Influenza Other Respir. Viruses* 7, 1040–1047. doi: 10.1111/irv.12101

Cameron, M. J., Ran, L., Xu, L., Danesh, A., Bermejo-Martin, J. F., Cameron, C. M., et al. (2007). Interferon-mediated immunopathological events are associated with atypical innate and adaptive immune responses in patients with severe acute respiratory syndrome. *J. Virol.* 81, 8692–8706. doi: 10.1128/jvi.00527-527

Chan, J. F. W., Chan, K. H., Kao, R. Y. T., To, K. K. W., Zheng, B. J., Li, C. P. Y., et al. (2013). Broad-spectrum antivirals for the emerging Middle East respiratory syndrome coronavirus. *J. Infect.* 67, 606–616. doi: 10.1016/j.jinf.2013.09.029

Chan, J. F. W., Yao, Y., Yeung, M. L., Deng, W., Bao, L., Jia, L., et al. (2015). Treatment with lopinavir/ritonavir or interferon-β1b improves outcome of MERSCoV infection in a nonhuman primate model of common marmoset. *J. Infect. Dis.* 212, 1904–1913. doi: 10.1093/infdis/jiv392

Channappanavar, R., Fehr, A. R., Vijay, R., Mack, M., Zhao, J., Meyerholz, D. K., et al. (2016). Dysregulated type I interferon and inflammatory monocyte-macrophage responses cause lethal pneumonia in SARS-CoV-infected mice. *Cell Host Microbe* 19, 181–193. doi: 10.1016/j.chom.2016.01.007

Channappanavar, R., Fehr, A. R., Zheng, J., Wohlford-Lenane, C., Abrahante, J. E., Mack, M., et al. (2019). IFN-I response timing relative to virus replication determines MERS coronavirus infection outcomes. *J. Clin. Invest.* 129, 3625–3639. doi: 10.1172/JCI126363

Channappanavar, R., Fett, C., Mack, M., Ten Eyck, P. P., Meyerholz, D. K., and Perlman, S. (2017). Sex-based differences in susceptibility to severe acute respiratory syndrome coronavirus infection. *J. Immunol.* 198, 4046–4053. doi: 10.4049/jimmunol.1601896

Channappanavar, R., Lu, L., Xia, S., Du, L., Meyerholz, D. K., Perlman, S., et al. (2015). Protective effect of intranasal regimens containing peptidic middle east respiratory syndrome coronavirus fusion Inhibitor against MERS-CoV infection. *J. Infect. Dis.* 212, 1894–1903. doi: 10.1093/infdis/jiv325

Channappanavar, R., Zhao, J., and Perlman, S. (2014). T cell-mediated immune response to respiratory coronaviruses. *Immunol. Res.* 59, 118–128. doi: 10.1007/s12026-014-8534-z

Chen, Z., Bao, L., Chen, C., Zou, T., Xue, Y., Li, F., et al. (2017). Human neutralizing monoclonal antibody inhibition of Middle East respiratory syndrome coronavirus replication in the common marmoset. *J. Infect. Dis.* 215, 1807–1815. doi: 10.1093/infdis/jix209

Chi, H., Zheng, X., Wang, X., Wang, C., Wang, H., Gai, W., et al. (2017). DNA vaccine encoding Middle East respiratory syndrome coronavirus S1 protein induces protective immune responses in mice. *Vaccine* 35, 2069–2075. doi: 10.1016/j.vaccine.2017.02.063

Chirmule, N., Propert, K. J., Magosin, S. A., Qian, Y., Qian, R., and Wilson, J. M. (1999). Immune responses to adenovirus and adeno-associated virus in humans. *Gene Ther.* 6, 1574–1583. doi: 10.1038/sj.gt.3300994

Chu, C. M., Cheng, V. C. C., Hung, I. F. N., Wong, M. M. L., Chan, K. H., Chan, K. S., et al. (2004). Role of lopinavir/ritonavir in the treatment of SARS: initial virological and clinical findings. *Thorax* 59, 252–256. doi: 10.1136/thorax.2003.012658

Colella, P., Ronzitti, G., and Mingozzi, F. (2018). Emerging Issues in AAV-Mediated In Vivo Gene Therapy. *Mol. Ther. Methods Clin. Dev.* 8, 87–104. doi: 10.1016/j.omtm.2017.11.007

Coleman, C. M., Liu, Y. V., Mu, H., Taylor, J. K., Massare, M., Flyer, D. C., et al. (2014). Purified coronavirus spike protein nanoparticles induce coronavirus neutralizing antibodies in mice. *Vaccine* 32, 3169–3174. doi: 10.1016/j.vaccine.2014.04.016

Coleman, C. M., Venkataraman, T., Liu, Y. V., Glenn, G. M., Smith, G. E., Flyer, D. C., et al. (2017). MERS-CoV spike nanoparticles protect mice from MERS-CoV infection. *Vaccine* 35, 1586–1589. doi: 10.1016/j.vaccine.2017.02.012

Corman, V. M., Albarrak, A. M., Omrani, A. S., Albarrak, M. M., Farah, M. E., Almasri, M., et al. (2015). Viral shedding and antibody response in 37 patients with Middle East respiratory syndrome coronavirus infection. *Clin. Infect. Dis.* 62, 477–483. doi: 10.1093/cid/civ951

Corti, D., Passini, N., Lanzavecchia, A., and Zambon, M. (2016). Rapid generation of a human monoclonal antibody to combat Middle East respiratory syndrome. *J. Infect. Public Health* 9, 231–235. doi: 10.1016/j.jiph.2016.04.003

Corti, D., Zhao, J., Pedotti, M., Simonelli, L., Agnihothram, S., Fett, C., et al. (2015). Prophylactic and postexposure efficacy of a potent human monoclonal antibody against MERS coronavirus. *Proc. Natl. Acad. Sci. U.S.A.* 112, 10473–10478. doi: 10.1073/pnas.1510199112

Cotmore, S. F., Agbandje-McKenna, M., Chiorini, J. A., Mukha, D. V., Pintel, D. J., Qiu, J., et al. (2014). The family Parvoviridae. *Arch. Virol.* 159, 1239–1247. doi: 10.1007/s00705-013-1914-1911

Coughlin, M. M., and Prabhakar, B. S. (2012). Neutralizing human monoclonal antibodies to severe acute respiratory syndrome coronavirus: target, mechanism of action, and therapeutic potential. *Rev. Med. Virol.* 22, 2–17. doi: 10.1002/rmv.706

Czub, M., Weingartl, H., Czub, S., He, R., and Cao, J. (2005). Evaluation of modified vaccinia virus Ankara based recombinant SARS vaccine in ferrets. *Vaccine* 23, 2273–2279. doi: 10.1016/j.vaccine.2005.01.033

Danilczyk, U., and Penninger, J. M. (2006). Angiotensin-converting enzyme II in the heart and the kidney. *Circ. Res.* 98, 463–471. doi: 10.1161/01.RES.0000205761.22353.5f

De Clercq, E., Li, G., Clercq, E., and De. (2016). Approved antiviral drugs over the past 50 years. *Clin. Microbiol. Rev.* 29, 695–747. doi: 10.1128/CMR.00102-15. Address

De Wilde, A. H., Jochmans, D., Posthuma, C. C., Zevenhoven-Dobbe, J. C., Van Nieuwkoop, S., Bestebroer, T. M., et al. (2014). Screening of an FDA-approved compound library identifies four small-molecule inhibitors of Middle East respiratory syndrome coronavirus replication in cell culture. *Antimicrob. Agents Chemother.* 58, 4875–4884. doi: 10.1128/AAC.03011-3014

de Wit, E., Feldmann, F., Cronin, J., Jordan, R., Okumura, A., Thomas, T., et al. (2020). Prophylactic and therapeutic remdesivir (GS-5734) treatment in the rhesus macaque model of MERS-CoV infection. *Proc. Natl. Acad. Sci. U.S.A.* 117, 6771–6776. doi: 10.1073/pnas.1922083117

de Wit, E., Feldmann, F., Horne, E., Okumura, A., Cameroni, E., Haddock, E., et al. (2019). Prophylactic efficacy of a human monoclonal antibody against MERS-CoV in the common marmoset. *Antiviral Res.* 163, 70–74. doi: 10.1016/j.antiviral.2019.01.016

de Wit, E., Feldmann, F., Okumura, A., Horne, E., Haddock, E., Saturday, G., et al. (2018). Prophylactic and therapeutic efficacy of mAb treatment against MERS-CoV in common marmosets. *Antiviral Res.* 156, 64–71. doi: 10.1016/j.antiviral.2018.06.006

de Wit, E., Van Doremalen, N., Falzarano, D., and Munster, V. J. (2016). SARS and MERS: Recent insights into emerging coronaviruses. *Nat. Rev. Microbiol.* 14, 523–534. doi: 10.1038/nrmicro.2016.81

Deming, D., Sheahan, T., Heise, M., Yount, B., Davis, N., Sims, A., et al. (2006). Vaccine efficacy in senescent mice challenged with recombinant SARS-CoV bearing epidemic and zoonotic spike variants. *PLoS Med.* 3:e0030525. doi: 10.1371/journal.pmed.0030525

Deng, X., StJohn, S. E., Osswald, H. L., O'Brien, A., Banach, B. S., Sleeman, K., et al. (2014). Coronaviruses resistant to a 3C-like protease inhibitor are attenuated for replication and pathogenesis, revealing a low genetic barrier but high fitness cost of resistance. *J. Virol.* 88, 11886–11898. doi: 10.1128/jvi.01528-1514

Deng, Y., Lan, J., Bao, L., Huang, B., Ye, F., Chen, Y., et al. (2018). Enhanced protection in mice induced by immunization with inactivated whole viruses compare to spike protein of middle east respiratory syndrome coronavirus. *Emerg. Microbes Infect.* 7:60. doi: 10.1038/s41426-018-0056-57

Denison, M. R., Graham, R. L., Donaldson, E. F., Eckerle, L. D., and Baric, R. S. (2011). Coronaviruses: an RNA proofreading machine regulates replication fidelity and diversity. *RNA Biol.* 8, 270–279. doi: 10.4161/rna.8.2.15013

Dicaro, A., Li, Y., Strong, J. E., Aoki, F., Plummer, F., Jones, S. M., et al. (2004). Severe acute respiratory syndrome - related coronavirus is inhibited by interferon- a. *J. Infect. Dis.* 189, 1164–1167. doi: 10.1086/382597

Ding, Y., Wang, H., Shen, H., Li, Z., Geng, J., Han, H., et al. (2003). The clinical pathology of severe acute respiratory syndrome (SARS): a report from China. *J. Pathol.* 200, 282–289. doi: 10.1002/path.1440

Drake, J. W., and Holland, J. J. (1999). Mutation rates among RNA viruses. *Proc. Natl. Acad. Sci. U.S.A.* 96, 13910–13913. doi: 10.1073/pnas.96.24.13910

Drosten, C., Chiu, L. L., Panning, M., Leong, H. N., Preiser, W., Tam, J. S., et al. (2004). Evaluation of advanced reverse transcription-PCR assays and an alternative PCR target region for detection of severe acute respiratory syndrome-associated Coronavirus. *J. Clin. Microbiol.* 42, 2043–2047. doi: 10.1128/JCM.42.5.2043-2047.2004

Du, L., and Jiang, S. (2015). Middle East respiratory syndrome: current status and future prospects for vaccine development. *Expert Opin. Biol. Ther.* 15, 1647–1651. doi: 10.1517/14712598.2015.1092518

Du, L., Kou, Z., Ma, C., Tao, X., Wang, L., Zhao, G., et al. (2013). A truncated receptor-binding domain of MERS-CoV spike protein potently inhibits MERS-CoV infection and induces strong neutralizing antibody responses?: implication for developing therapeutics and vaccines. *PLoS One* 8:e0081587. doi: 10.1371/journal.pone.0081587

Du, L., Zhao, G., Chan, C. C. S., and Li, L. (2010). A 219-mer CHO-Expressing Receptor-Binding Domain. *Viral Immunol.* 23, 211–219. doi: 10.1089/vim.2009.0090

Du, L., Zhao, G., Lin, Y., Sui, H., Chan, C., Ma, S., et al. (2008). Intranasal vaccination of recombinant adeno-associated virus encoding receptor-binding domain of severe acute respiratory syndrome coronavirus (SARS-CoV) spike protein induces strong mucosal immune responses and provides long-term protection against SARS-. *J. Immunol.* 180, 948–956. doi: 10.4049/jimmunol.180.2.948

Du, L., Zhao, G., Yang, Y., Qiu, H., Wang, L., Kou, Z., et al. (2014). A conformation-dependent neutralizing monoclonal antibody specifically targeting receptor-binding domain in Middle East respiratory syndrome coronavirus spike protein. *J. Virol.* 88, 7045–7053. doi: 10.1128/jvi.00433-14

Eckerle, L. D., Becker, M. M., Halpin, R. A., Li, K., Venter, E., Lu, X., et al. (2010). Infidelity of SARS-CoV Nsp14-exonuclease mutant virus replication is revealed by complete genome sequencing. *PLoS Pathog.* 6:e1000896. doi: 10.1371/journal.ppat.1000896

Eckerle, L. D., Lu, X., Sperry, S. M., Choi, L., and Denison, M. R. (2007). High fidelity of murine hepatitis virus replication is decreased in nsp14 exoribonuclease mutants. *J. Virol.* 81, 12135–12144. doi: 10.1128/jvi.01296-1297

Excoffon, K. J. D. A., Koerber, J. T., Dickey, D. D., Murtha, M., Keshavjee, S., Kaspar, B. K., et al. (2009). Directed evolution of adeno-associated virus to an infectious respiratory virus. *Proc. Natl. Acad. Sci. U.S.A.* 106, 3865–3870. doi: 10.1073/pnas.0813365106

Falzarano, D., De Wit, E., Martellaro, C., Callison, J., Munster, V. J., and Feldmann, H. (2013a). Inhibition of novel β coronavirus replication by a combination of interferon-α2b and ribavirin. *Sci. Rep.* 3, 1–6. doi: 10.1038/srep01686

Falzarano, D., de Wit, E., Rasmussen, A. L., Feldmann, F., Okumura, A., Scott, D. P., et al. (2013b). Treatment with interferon-α2b and ribavirin improves outcome in MERS-CoV-infected rhesus macaques. *Nat. Med.* 19, 1313–1317. doi: 10.1038/nm.3362

Ferron, F., Subissi, L., Theresa, A., Morais, S. De, Thi, N., Le, T., et al. (2017). Structural and molecular basis of mismatch correction and ribavirin excision from coronavirus RNA. *Proc. Natl. Acad. Sci. U.S.A.* 115, E162–E171. doi: 10.1073/pnas.1718806115

Frieman, M., Heise, M., and Baric, R. (2008). SARS coronavirus and innate immunity. *Virus Res.* 133, 101–112. doi: 10.1016/j.virusres.2007.03.015

Fry, A. M., Goswami, D., Nahar, K., Sharmin, A. T., Rahman, M., Gubareva, L., et al. (2014). Efficacy of oseltamivir treatment started within 5 days of symptom onset to reduce infl uenza illness duration and virus shedding in an urban setting in Bangladesh?: a randomised placebo-controlled trial. *Lancet Infect. Dis.* 14, 109–118. doi: 10.1016/S1473-3099(13)70267-70266

Gao, J., Lu, G., Qi, J., Li, Y., Wu, Y., Deng, Y., et al. (2013). Structure of the fusion core and inhibition of fusion by a heptad repeat peptide derived from the S protein of middle east respiratory syndrome coronavirus. *J. Virol.* 87, 13134–13140. doi: 10.1128/jvi.02433-2413

Gierer, S., Müller, M. A., Heurich, A., Ritz, D., Springstein, B. L., Karsten, C. B., et al. (2014). Inhibition of proprotein convertases abrogates processing of the middle eastern respiratory syndrome coronavirus spike protein in infected cells but does not reduce viral infectivity. *J. Infect. Dis.* 211, 889–897. doi: 10.1093/infdis/jiu407

Goldstein, J. L., DeBose-Boyd, R. A., and Brown, M. S. (2006). Protein sensors for membrane sterols. *Cell* 124, 35–46. doi: 10.1016/j.cell.2005.12.022

Graham, B. S., and Ambrosino, D. M. (2015). History of passive antibody administration for prevention and treatment of infectious diseases. *Curr. Opin. HIV AIDS* 10, 129–134. doi: 10.1097/COH.0000000000000154

Graham, R. L., Becker, M. M., Eckerle, L. D., Bolles, M., Denison, M. R., and Baric, R. S. (2012). A live, impaired-fidelity coronavirus vaccine protects in an aged, immunocompromised mouse model of lethal disease. *Nat. Med.* 18, 1820–1826. doi: 10.1038/nm.2972

Graham, R. L., Deming, D. J., Deming, M. E., Yount, B. L., and Baric, R. S. (2018). Evaluation of a recombination-resistant coronavirus as a broadly applicable, rapidly implementable vaccine platform. *Commun. Biol.* 1:179. doi: 10.1038/s42003-018-0175-177

Gralinski, L. E., and Baric, R. S. (2015). Molecular pathology of emerging coronavirus infections. *J. Pathol.* 235, 185–195. doi: 10.1002/path.4454

Greenough, T. C., Babcock, G. J., Roberts, A., Hernandez, H. J., and Thomas, W. D. Jr. (2005). Development and characterization of a severe acute respiratory syndrome-associated coronavirus-neutralizing human monoclonal antibody

that provides effective immunoprophylaxis in mice. *J. Infect. Dis.* 191, 507–514. doi: 10.1086/427242

Guo, X., Deng, Y., Chen, H., Lan, J., Wang, W., Zou, X., et al. (2015). Systemic and mucosal immunity in mice elicited by a single immunization with human adenovirus type 5 or 41 vector-based vaccines carrying the spike protein of Middle East respiratory syndrome coronavirus. *Immunology* 145, 476–484. doi: 10.1111/imm.12462

Haagmans, B. L., Kuiken, T., Martina, B. E., Fouchier, R. A. M., Rimmelzwaan, G. F., van Amerongen, G., et al. (2004). Pegylated interferon-α protects type 1 pneumocytes against SARS coronavirus infection in macaques. *Nat. Med.* 10, 290–293. doi: 10.1038/nm1001

Haagmans, B. L., van den Brand, J. M. A., Raj, V. S., Volz, A., Wohlsein, P., Smits, S. L., et al. (2016). An orthopoxvirus-based vaccine reduces virus excretion after MERS-CoV infection in dromedary camels. *Science* 351, 77–81. doi: 10.1126/science.aad1283

Hansel, T. T., Kropshofer, H., Singer, T., Mitchell, J. A., and George, A. J. T. (2010). The safety and side effects of monoclonal antibodies. *Nat. Rev. Drug Discov.* 9, 325–338. doi: 10.1038/nrd3003

Hapfelmeier, S., Lawson, M. A. E., Slack, E., Kirundi, J. K., Stoel, M., Heikenwalder, M., et al. (2010). Reversible microbial colonization of germ-free mice reveals the dynamics of IgA immune responses. *Science* 328, 1705–1709. doi: 10.1126/science.1188454

Harcourt, B. H., Jukneliene, D., Kanjanahaluethai, A., Bechill, J., Severson, K. M., Smith, C. M., et al. (2004). Identification of severe acute respiratory syndrome coronavirus replicase products and characterization of papain-like protease activity. *J. Virol.* 78, 13600–13612. doi: 10.1128/JVI.78.24.13600

Hart, B. J., Dyall, J., Postnikova, E., Zhou, H., Kindrachuk, J., Johnson, R. F., et al. (2014). Interferon-β and mycophenolic acid are potent inhibitors of middle east respiratory syndrome coronavirus in cell-based assays. *J. Gen. Virol.* 95, 571–577. doi: 10.1099/vir.0.061911-61910

Hashem, A. M., Algaissi, A., Agrawal, A. S., Al-Amri, S. S., Alhabbab, R. Y., Sohrab, S. S., et al. (2019). A highly immunogenic, protective, and safe adenovirus-based vaccine expressing middle east respiratory syndrome coronavirus S1-CD40L fusion protein in a transgenic human dipeptidyl peptidase 4 mouse model. *J. Infect. Dis.* 220, 1558–1567. doi: 10.1093/infdis/jiz137

Holshue, M. L., DeBolt, C., Lindquist, S., Lofy, K. H., Wiesman, J., Bruce, H., et al. (2020). First case of 2019 novel coronavirus in the United States. *N. Engl. J. Med.* 382, 929–936. doi: 10.1056/nejmoa2001191

Houser, K. V., Gretebeck, L., Ying, T., Wang, Y., Vogel, L., Lamirande, E. W., et al. (2016). Prophylaxis with a Middle East respiratory syndrome coronavirus (MERS-CoV)-specific human monoclonal antibody protects rabbits from MERS-CoV infection. *J. Infect. Dis.* 213, 1557–1561. doi: 10.1093/infdis/jiw080

Hsueh, P. R., Huang, L. M., Chen, P. J., Kao, C. L., and Yang, P. C. (2004). Chronological evolution of IgM, IgA, IgG and neutralisation antibodies after infection with SARS-associated coronavirus. *Clin. Microbiol. Infect.* 10, 1062–1066. doi: 10.1111/j.1469-0691.2004.01009.x

Hu, M. C., Jones, T., Kenney, R. T., Barnard, D. L., Burt, D. S., and Lowell, G. H. (2007). Intranasal Protollin-formulated recombinant SARS S-protein elicits respiratory and serum neutralizing antibodies and protection in mice. *Vaccine* 25, 6334–6340. doi: 10.1016/j.vaccine.2007.06.017

Huang, J. D., Zheng, B. J., and Sun, H. Z. (2008). Helicases as antiviral drug targets. *Hong Kong Med. J.* 14, 36–38.

Huentelman, M. J., Zubcevic, J., Hernández Prada, J. A., Xiao, X., Dimitrov, D. S., Raizada, M. K., et al. (2004). Sructure-based discovery of a novel angiotensin-converting enzyme 2 inhibitor. *Hypertension* 44, 903–906. doi: 10.1161/01.HYP.0000146120.29648.36

Hui, D. S., Azhar, I. E., Madani, T. A., Ntoumi, F., Kock, R., Dar, O., et al. (2020). The continuing 2019-nCoV epidemic threat of novel coronaviruses to global health — The latest 2019 novel coronavirus outbreak in Wuhan. *China Int. J. Infect. Dis.* 91, 264–266. doi: 10.1016/j.ijid.2020.01.009

Iwata-Yoshikawa, N., Uda, A., Suzuki, T., Tsunetsugu-Yokota, Y., Sato, Y., Morikawa, S., et al. (2014). Effects of toll-like receptor stimulation on eosinophilic infiltration in lungs of BALB/c mice immunized with UV-inactivated severe acute respiratory syndrome-related coronavirus vaccine. *J. Virol.* 88, 8597–8614. doi: 10.1128/jvi.00983-914

Jagger, B. W., Dowd, K. A., Chen, R. E., Desai, P., Foreman, B., Burgomaster, K. E., et al. (2019). Protective efficacy of nucleic acid vaccines against transmission of zika virus during pregnancy in mice. *J. Infect. Dis.* 220, 1577–1588. doi: 10.1093/infdis/jiz338

Jiaming, L., Yanfeng, Y., Yao, D., Yawei, H., Linlin, B., Baoying, H., et al. (2017). The recombinant N-terminal domain of spike proteins is a potential vaccine against Middle East respiratory syndrome coronavirus (MERS-CoV) infection. *Vaccine* 35, 10–18. doi: 10.1016/j.vaccine.2016.11.064

Jiang, L., Wang, N., Zuo, T., Shi, X., Poon, K.-M. M. V., Wu, Y., et al. (2014). Potent neutralization of MERS-CoV by human neutralizing monoclonal antibodies to the viral spike glycoprotein. *Sci. Transl. Med.* 6:234ra59. doi: 10.1126/scitranslmed.3008140

Johnson, R. F., Bagci, U., Keith, L., Tang, X., Mollura, D. J., Zeitlin, L., et al. (2016). 3B11-N, a monoclonal antibody against MERS-CoV, reduces lung pathology in rhesus monkeys following intratracheal inoculation of MERS-CoV Jordan-n3/2012. *Virology* 490, 49–58. doi: 10.1016/j.virol.2016.01.004

Kaemmerer, W. F. (2018). How will the field of gene therapy survive its success? *Bioeng. Transl. Med.* 3, 166–177. doi: 10.1002/btm2.10090

Kam, Y. W., Kien, F., Roberts, A., Cheung, Y. C., Lamirande, E. W., Vogel, L., et al. (2007). Antibodies against trimeric S glycoprotein protect hamsters against SARS-CoV challenge despite their capacity to mediate FcgammaRII-dependent entry into B cells *in vitro*. *Vaccine* 25, 729–740. doi: 10.1016/j.vaccine.2006.08.011

Kandeel, M. (2018). Bioinformatics analysis of the recent MERS-CoV with special reference to the virus-encoded Spike protein. *Mol. Enzymol. Drug Targets* 01, 1–10. doi: 10.21767/2572-5475.10001

Kapadia, S. U., Rose, J. K., Lamirande, E., Vogel, L., Subbarao, K., and Roberts, A. (2005). Long-term protection from SARS coronavirus infection conferred by a single immunization with an attenuated VSV-based vaccine. *Virology* 340, 174–182. doi: 10.1016/j.virol.2005.06.016

Kaplitt, M. G., Feigin, A., Tang, C., Fitzsimons, H. L., Mattis, P., Lawlor, P. A., et al. (2007). Safety and tolerability of gene therapy with an adeno-associated virus (AAV) borne GAD gene for Parkinson's disease: an open label, phase I trial. *Lancet* 369, 2097–2105. doi: 10.1016/S0140-6736(07)60982-60989

Karlberg, J., Chong, D. S. Y., and Lai, W. Y. Y. (2004). Do men have a higher case fatality rate of severe acute respiratory syndrome than women do? *Am. J. Epidemiol.* 159, 229–231. doi: 10.1093/aje/kwh056

Kay, M. A., Manno, C. S., Ragni, M. V., Larson, P. J., Couto, L. B., McClelland, A., et al. (2000). Evidence for gene transfer and expression of factor IX in haemophilia B patients treated with an AAV vector. *Nat. Genet.* 24, 257–261. doi: 10.1038/73464

Khalid, M., Al Rabiah, F., Khan, B., Al Mobeireek, A., Butt, T. S., and Al Mutairy, E. (2015). Ribavirin and interferon-alpha2b as primary and preventive treatment for Middle East respiratory syndrome coronavirus: a preliminary report of two cases. *Antivir. Ther.* 20, 87–91. doi: 10.3851/IMP2792

Khalid, M., Khan, B., Al Rabiah, F., Alismaili, R., Saleemi, S., Rehan-Khaliq, A. M., et al. (2014). Middle eastern respiratory syndrome corona virus (MERS CoV): case reports from a tertiary care hospital in Saudi Arabia. *Ann. Saudi Med.* 34, 396–400. doi: 10.5144/0256-4947.2014.396

Kim, E., Okada, K., Kenniston, T., Raj, V. S., AlHajri, M. M., Farag, E. A. B. A. B. A., et al. (2014). Immunogenicity of an adenoviral-based Middle East Respiratory syndrome coronavirus vaccine in BALB/c mice. *Vaccine* 32, 5975–5982. doi: 10.1016/j.vaccine.2014.08.058

Kim, U. J., Won, E.-J., Kee, S.-J., Jung, S.-I., and Jang, H.-C. (2016). Combination therapy with lopinavir/ritonavir, ribavirin and interferon-alpha for Middle East respiratory syndrome. *Antivir. Ther.* 21, 455–459. doi: 10.3851/IMP3002

Kirchdoerfer, R. N., Cottrell, C. A., Wang, N., Pallesen, J., Yassine, H. M., Turner, H. L., et al. (2016). Pre-fusion structure of a human coronavirus spike protein. *Nature* 531, 118–121. doi: 10.1038/nature17200

Kleine-Weber, H., Elzayat, T., Wang, L., Elzayat, M. T., Wang, L., Graham, B. S., et al. (2019). Mutations in the spike protein of Middle East respiratory syndrome coronavirus transmitted in Korea increase. *J. Virol.* 93, 1–14. doi: 10.1128/JVI.01381-1318

Ko, J.-H., Seok, H., Cho, S. Y., Ha, Y. E., Baek, J. Y., Kim, S. H., et al. (2018). Challenges of convalescent plasma infusion therapy in Middle East respiratory coronavirus infection: a single centre experience. *Antivir. Ther.* 23, 617–622. doi: 10.3851/IMP3243

Kobinger, G. P., Figueredo, J. M., Rowe, T., Zhi, Y., Gao, G., Sanmiguel, J. C., et al. (2007). Adenovirus-based vaccine prevents pneumonia in ferrets challenged

with the SARS coronavirus and stimulates robust immune responses in macaques. *Vaccine* 25, 5220–5231. doi: 10.1016/j.vaccine.2007.04.065

Kumar, V., Shin, J. S., Shie, J. J., Ku, K. B., Kim, C., Go, Y. Y., et al. (2017). Identification and evaluation of potent Middle East respiratory syndrome coronavirus (MERS-CoV) 3CLPro inhibitors. *Antiviral Res.* 141, 101–106. doi: 10.1016/j.antiviral.2017.02.007

Lamirande, E. W., DeDiego, M. L., Roberts, A., Jackson, J. P., Alvarez, E., Sheahan, T., et al. (2008). A live attenuated severe acute respiratory syndrome coronavirus is immunogenic and efficacious in golden syrian hamsters. *J. Virol.* 82, 7721–7724. doi: 10.1128/jvi.00304-308

Lan, J., Deng, Y., Chen, H., Lu, G., Wang, W., Guo, X., et al. (2014). Tailoring subunit vaccine immunity with adjuvant combinations and delivery routes using the middle east respiratory coronavirus (MERS-CoV) receptor-binding domain as an antigen. *PLoS One* 9:e0112602. doi: 10.1371/journal.pone.0112602

Lan, J., Yao, Y., Deng, Y., Chen, H., Lu, G., Wang, W., et al. (2015). Recombinant receptor binding domain protein induces partial protective immunity in rhesus macaques against Middle East respiratory syndrome coronavirus challenge. *EBioMedicine* 2, 1438–1446. doi: 10.1016/j.ebiom.2015.08.031

Lau, S. K. P., Woo, P. C. Y., Yip, C. C. Y., Tse, H., Tsoi, H. W., Cheng, V. C. C., et al. (2006). Coronavirus HKU1 and other coronavirus infections in Hong Kong. *J. Clin. Microbiol.* 44, 2063–2071. doi: 10.1128/JCM.02614-2615

Lauring, A. S., and Andino, R. (2010). Quasispecies theory and the behavior of RNA viruses. *PLoS Pathog.* 6:e1001005. doi: 10.1371/journal.ppat.1001005

Laursen, N. S., Friesen, R. H. E., Zhu, X., Jongeneelen, M., Blokland, S., Vermond, J., et al. (2018). Universal protection against influenza infection by a multidomain antibody to influenza hemagglutinin. *Science* 362, 598–602. doi: 10.1126/science.aaq0620

Leist, S. R., and Baric, R. S. (2018). Giving the genes a shuffle: using natural variation to understand host genetic contributions to viral infections. *Trends Genet.* 34, 777–789. doi: 10.1016/j.tig.2018.07.005

Li, F. (2016). Structure, function, and evolution of coronavirus spike proteins. *Annu. Rev. Virol.* 3, 237–261. doi: 10.1146/annurev-virology-110615-142301

Li, W., Moore, M. J., Vasilieva, N., Sui, J., Wong, S. K., Berne, M. A., et al. (2003). Angiotensin-converting enzyme 2 is a functional receptor for the SARS coronavirus. *Nature* 426, 450–454. doi: 10.1038/nature02145

Li, W., Shi, Z., Yu, M., Ren, W., Smith, C., Epstein, J. H., et al. (2005). Bats are natural reservoirs of SARS-like coronaviruses. *Science* 310, 676–680. doi: 10.1126/science.1118391

Li, W., Zhang, L., Johnson, J. S., Zhijian, W., Grieger, J. C., Ping-Jie, X., et al. (2009). Generation of novel aav variants by directed evolution for improved cftr delivery to human ciliated airway epithelium. *Mol. Ther.* 17, 2067–2077. doi: 10.1038/mt.2009.155

Li, Y., Wan, Y., Liu, P., Zhao, J., Lu, G., Qi, J., et al. (2015). A humanized neutralizing antibody against MERS-CoV targeting the receptor-binding domain of the spike protein. *Cell Res.* 25, 1237–1249. doi: 10.1038/cr.2015.113

Lim, Y., Ng, Y., Tam, J., and Liu, D. (2016). Human coronaviruses: a review of virus-host interactions. *Diseases* 4, 26. doi: 10.3390/diseases4030026

Limberis, M. P., Adam, V. S., Wong, G., Gren, J., Kobasa, D., Ross, T. M., et al. (2013). Intranasal antibody gene transfer in mice and ferrets elicits broad protection against pandemic influenza. *Sci. Transl. Med.* 5:187ra72. doi: 10.1126/scitranslmed.3006729

Limberis, M. P., Tretiakova, A., Nambiar, K., Wong, G., Racine, T., Crosariol, M., et al. (2016). Adeno-associated virus serotype 9-expressed zmapp in mice confers protection against systemic and airway-acquired ebola virus infection. *J. Infect. Dis.* 214, 1975–1979. doi: 10.1093/infdis/jiw460

Limberis, M. P., Vandenberghe, L. H., Zhang, L., Pickles, R. J., and Wilson, J. M. (2009). Transduction efficiencies of novel AAV vectors in mouse airway epithelium in vivo and human ciliated airway epithelium *in vitro*. *Mol. Ther.* 17, 294–301. doi: 10.1038/mt.2008.261

Lin, A., and Balazs, A. B. (2018). Adeno-associated virus gene delivery of broadly neutralizing antibodies as prevention and therapy against hiv-1 11 medical and health sciences 1103 clinical sciences 11 medical and health sciences 1108 medical microbiology marit van Gils, m.j.vangils@amc. *Retrovirology* 15, 1–17. doi: 10.1186/s12977-018-0449-447

Lipkin, W. I., and Firth, C. (2013). Viral surveillance and discovery. *Curr. Opin. Virol.* 3, 199–204. doi: 10.1016/j.coviro.2013.03.010

Liu, Y. V., Massare, M. J., Barnard, D. L., Kort, T., Nathan, M., Wang, L., et al. (2011). Chimeric severe acute respiratory syndrome coronavirus (SARS-CoV) S glycoprotein and influenza matrix 1 efficiently form virus-like particles (VLPs) that protect mice against challenge with SARS-CoV. *Vaccine* 29, 6606–6613. doi: 10.1016/j.vaccine.2011.06.111

Lo, M. K., Jordan, R., Arvey, A., Sudhamsu, J., Shrivastava-Ranjan, P., Hotard, A. L., et al. (2017). GS-5734 and its parent nucleoside analog inhibit Filo-, Pneumo-, and Paramyxoviruses. *Sci. Rep.* 7, 1–7. doi: 10.1038/srep43395

Lokugamage, K. G., Yoshikawa-Iwata, N., Ito, N., Watts, D. M., Wyde, P. R., Wang, N., et al. (2008). Chimeric coronavirus-like particles carrying severe acute respiratory syndrome coronavirus (SCoV) S protein protect mice against challenge with SCoV. *Vaccine* 26, 797–808. doi: 10.1016/j.vaccine.2007.11.092

Loustaud-Ratti, V., Debette-Gratien, M., Jacques, J., Alain, S., Marquet, P., Sautereau, D., et al. (2016). Ribavirin: Past, present and future. *World J. Hepatol.* 8, 123–130. doi: 10.4254/wjh.v8.i2.123

Loutfy, M. R., Blatt, L. M., Siminovitch, K. A., Ward, S., Wolff, B., Lho, H., et al. (2003). Interferon alfacon-1 plus corticosteroids in severe acute respiratory syndrome: a preliminary study. *JAMA* 290, 3222–3228. doi: 10.1001/jama.290.24.3222

Lu, L., Liu, Q., Zhu, Y., Chan, K. H., Qin, L., Li, Y., et al. (2014). Structure-based discovery of Middle East respiratory syndrome coronavirus fusion inhibitor. *Nat. Commun.* 5:3067. doi: 10.1038/ncomms4067

Lu, R., Zhao, X., Li, J., Niu, P., Yang, B., Wu, H., et al. (2020). Genomic characterisation and epidemiology of 2019 novel coronavirus: implications for virus origins and receptor binding. *Lancet* 6736, 1–10. doi: 10.1016/S0140-6736(20)30251-30258

Luo, C.-M., Wang, N., Yang, X.-L., Liu, H.-Z., Zhang, W., Li, B., et al. (2018). Discovery of novel bat coronaviruses in south china that use the same receptor as middle east respiratory syndrome coronavirus. *J. Virol.* 92:e00116-18. doi: 10.1128/JVI.00116-118

Ma, C., Li, Y., Wang, L., Zhao, G., Tao, X., Tseng, C.-T. K., et al. (2014a). Intranasal vaccination with recombinant receptor-binding domain of MERS-CoV spike protein induces much stronger local mucosal immune responses than subcutaneous immunization: implication for designing novel mucosal MERS vaccines. *Vaccine* 32, 2100–2108. doi: 10.1016/j.vaccine.2014.02.004

Ma, C., Wang, L., Tao, X., Zhang, N., Yang, Y., Tseng, C.-T. K., et al. (2014b). Searching for an ideal vaccine candidate among different MERS coronavirus receptor-binding fragments—The importance of immunofocusing in subunit vaccine design. *Vaccine* 32, 6170–6176. doi: 10.1016/j.vaccine.2014.08.086

Mackenzie, J. S., and Jeggo, M. (2013). Reservoirs and vectors of emerging viruses. *Curr. Opin. Virol.* 3, 170–179. doi: 10.1016/j.coviro.2013.02.002

Mair-Jenkins, J., Saavedra-Campos, M., Baillie, J. K., Cleary, P., Khaw, F. M., Lim, W. S., et al. (2015). The effectiveness of convalescent plasma and hyperimmune immunoglobulin for the treatment of severe acute respiratory infections of viral etiology: a systematic review and exploratory meta-analysis. *J. Infect. Dis.* 211, 80–90. doi: 10.1093/infdis/jiu396

Malczyk, A. H., Kupke, A., Prüfer, S., Scheuplein, V. A., Hutzler, S., Kreuz, D., et al. (2015). A highly immunogenic and protective Middle East respiratory syndrome coronavirus vaccine based on a recombinant measles virus vaccine platform. *J. Virol.* 89, 11654–11667. doi: 10.1128/jvi.01815-15

Martin, J. E., Louder, M. K., Holman, L. S. A., Gordon, I. J., Enama, M. E., Larkin, B. D., et al. (2008). A SARS DNA vaccine induces neutralizing antibody and cellular immune responses in healthy adults in a Phase I clinical trial. *Vaccine* 26, 6338–6343. doi: 10.1016/j.vaccine.2008.09.026

Matsuyama, S., Shirato, K., Kawase, M., Terada, Y., Kawachi, K., Fukushi, S., et al. (2018). Middle East Respiratory syndrome coronavirus spike protein is not activated directly by cellular furin during viral entry into target cells. *J. Virol.* 92:e00683-18. doi: 10.1128/JVI.00683-618

Matteucci, E., and Giampietro, O. (2016). Dipeptidyl peptidase-4 (CD26): knowing the function before inhibiting the enzyme. *Curr. Med. Chem.* 4, 80–102. doi: 10.2174/9781681082493116090005

McIntosh, K., Kapikian, A. Z., Turner, H. C., Hartley, J. W., Parrott, R. H., and Chanock, R. M. (1970). Seroepidemiologic studies of coronavirus infection in adults and children. *Am. J. Epidemiol.* 91, 585–592. doi: 10.1093/oxfordjournals.aje.a121171

Menachery, V. D., Gralinski, L. E., Mitchell, H. D., Dinnon, K. H., Leist, S. R., Yount, B. L., et al. (2017). Middle East respiratory syndrome coronavirus

nonstructural protein 16 is necessary for interferon resistance and viral pathogenesis. *mSphere* 2, 1–12. doi: 10.1128/msphere.00346-317

Menachery, V. D., Gralinski, L. E., Mitchell, H. D., Dinnon, K. H., Leist, S. R., Yount, B. L., et al. (2018). Combination attenuation offers strategy for live attenuated coronavirus vaccines. *J. Virol.* 92, 1–15. doi: 10.1128/jvi.00710-718

Menachery, V. D., Yount, B. L., Debbink, K., Agnihothram, S., Gralinski, L. E., Plante, J. A., et al. (2015). A SARS-like cluster of circulating bat coronaviruses shows potential for human emergence. *Nat. Med.* 21, 1508–1513. doi: 10.1038/nm.3985

Menachery, V. D., Yount, B. L., Josset, L., Gralinski, L. E., Scobey, T., Agnihothram, S., et al. (2014). Attenuation and restoration of severe acute respiratory syndrome coronavirus mutant lacking 2'-o-methyltransferase activity. *J. Virol.* 88, 4251–4264. doi: 10.1128/jvi.03571-3513

Menachery, V. D., Yount, B. L., Sims, A. C., Debbink, K., Agnihothram, S. S., Gralinski, L. E., et al. (2016). SARS-like WIV1-CoV poised for human emergence. *Proc. Natl. Acad. Sci. U.S.A.* 113, 3048–3053. doi: 10.1073/pnas.1517719113

Millet, J. K., and Whittaker, G. R. (2014). Host cell entry of Middle East respiratory syndrome coronavirus after two-step, furin-mediated activation of the spike protein. *Proc. Natl. Acad. Sci. U.S.A.* 111, 15214–15219. doi: 10.1073/pnas.1407087111

Millet, J. K., and Whittaker, G. R. (2015). Host cell proteases: critical determinants of coronavirus tropism and pathogenesis. *Virus Res.* 202, 120–134. doi: 10.1016/j.virusres.2014.11.021

Millet, J. K., and Whittaker, G. R. (2018). Physiological and molecular triggers for SARS-CoV membrane fusion and entry into host cells. *Virology* 517, 3–8. doi: 10.1016/j.virol.2017.12.015

Min, J., Yu, D., Liang, W., Xu, R., Wang, Z., Fang, L., et al. (2004). Molecular evolution of the SARS coronavirus during the course of the SARS epidemic in China. *Science* 303, 1666–1669. doi: 10.1126/science.1092002

Mo, Y., and Fisher, D. (2016). A review of treatment modalities for Middle East Respiratory Syndrome. *J. Antimicrob. Chemother.* 71, 3340–3350. doi: 10.1093/jac/dkw338

Modjarrad, K., Roberts, C. C., Mills, K. T., Castellano, A. R., Paolino, K., Muthumani, K., et al. (2019). Safety and immunogenicity of an anti-Middle East respiratory syndrome coronavirus DNA vaccine: a phase 1, open-label, single-arm, dose-escalation trial. *Lancet Infect. Dis.* 19, 1013–1022. doi: 10.1016/S1473-3099(19)30266-X

Momattin, H., Mohammed, K., Zumla, A., Memish, Z. A., and Al-Tawfiq, J. A. (2013). Therapeutic Options for Middle East respiratory syndrome coronavirus (MERS-CoV) - possible lessons from a systematic review of SARS-CoV therapy. *Int. J. Infect. Dis.* 17, e792–e798. doi: 10.1016/j.ijid.2013.07.002

Mubarak, A., Alturaiki, W., and Hemida, M. G. (2019). Middle east respiratory syndrome coronavirus (mers-cov): infection, immunological response, and vaccine development. *J. Immunol. Res.* 2019, 1–11. doi: 10.1155/2019/6491738

Munster, V. J., Wells, D., Lambe, T., Wright, D., Fischer, R. J., Bushmaker, T., et al. (2017). Protective efficacy of a novel simian adenovirus vaccine against lethal MERS-CoV challenge in a transgenic human DPP4 mouse model. *NPJ Vaccines* 2, 1–3. doi: 10.1038/s41541-017-0029-21

Murphy, B. G., Perron, M., Murakami, E., Bauer, K., Park, Y., Eckstrand, C., et al. (2018). The nucleoside analog GS-441524 strongly inhibits feline infectious peritonitis (FIP) virus in tissue culture and experimental cat infection studies. *Vet. Microbiol.* 219, 226–233. doi: 10.1016/j.vetmic.2018.04.026

Muthumani, K., Falzarano, D., Reuschel, E. L., Tingey, C., Flingai, S., Villarreal, D. O., et al. (2015). A synthetic consensus anti-spike protein DNA vaccine induces protective immunity against Middle East respiratory syndrome coronavirus in nonhuman primates. *Sci. Transl. Med.* 7:301ra132. doi: 10.1126/scitranslmed.aac7462

Naso, M. F., Tomkowicz, B., Perry, W. L., and Strohl, W. R. (2017). Adeno-associated virus (AAV) as a vector for gene therapy. *BioDrugs* 31, 317–334. doi: 10.1007/s40259-017-0234-235

Neuman, B. W., Stein, D. A., Kroeker, A. D., Bestwick, R. K., Iversen, P. L., Moulton, H. M., et al. (2006). Inhibition and escape of SARS-CoV treated with antisense morpholino oligomers. *Adv. Exp. Med. Biol.* 581, 567–571. doi: 10.1007/978-0-387-33012-9_103

Nieto, K., and Salvetti, A. (2014). AAV vectors vaccines against infectious diseases. *Front. Immunol.* 5:5. doi: 10.3389/fimmu.2014.00005

Nyon, M. P., Du, L., Tseng, C.-T. K. T. K., Seid, C. A., Pollet, J., Naceanceno, K. S., et al. (2018). Engineering a stable CHO cell line for the expression of a MERS-coronavirus vaccine antigen. *Vaccine* 36, 1853–1862. doi: 10.1016/j.vaccine.2018.02.065

Oh, H. J., Gan, S. K., Bertoletti, A., and Tan, Y. (2012). Understanding the T cell immune response in SARS coronavirus infection. *Emerg. Microbes Infect.* 1:e23. doi: 10.1038/emi.2012.26

Olinger, G. G., Pettitt, J., Kim, D., Working, C., Bohorov, O., Bratcher, B., et al. (2012). Delayed treatment of Ebola virus infection with plant-derived monoclonal antibodies provides protection in rhesus macaques. *Proc. Natl. Acad. Sci. U.S.A.* 109, 18030–18035. doi: 10.1073/pnas.1213709109

Omrani, A. S., Saad, M. M., Baig, K., Bahloul, A., Abdul-Matin, M., Alaidaroos, A. Y., et al. (2014). Ribavirin and interferon alfa-2a for severe Middle East respiratory syndrome coronavirus infection: a retrospective cohort study. *Lancet Infect. Dis.* 14, 1090–1095. doi: 10.1016/S1473-3099(14)70920-X

Ou, X., Leary, H. A. O., and Broxmeyer, H. E. (2019). Review Article Implications of DPP4 modi fi cation of proteins that regulate stem / progenitor and more mature cell types. *Blood* 122, 161–170. doi: 10.1182/blood-2013-02-487470.X.O

Pallesen, J., Wang, N., Corbett, K. S., Wrapp, D., Kirchdoerfer, R. N., Turner, H. L., et al. (2017). Immunogenicity and structures of a rationally designed prefusion MERS-CoV spike antigen. *Proc. Natl. Acad. Sci. U.S.A.* 114, E7348–E7357. doi: 10.1073/pnas.1707304114

Pascal, K. E., Coleman, C. M., Mujica, A. O., Kamat, V., Badithe, A., Fairhurst, J., et al. (2015). Pre- and postexposure efficacy of fully human antibodies against Spike protein in a novel humanized mouse model of MERS-CoV infection. *Proc. Natl. Acad. Sci. U.S.A.* 112, 8738–8743. doi: 10.1073/pnas.1510830112

Payne, D. C., Iblan, I., Rha, B., Alqasrawi, S., Haddadin, A., Nsour, M., et al. (2016). Persistence of antibodies against Middle East respiratory syndrome coronavirus. *Emerg. Infect. Dis.* 22, 1824–1826.

Peck, K. M., Burch, C. L., Heise, M. T., and Baric, R. S. (2015). Coronavirus host range expansion and middle east respiratory syndrome coronavirus emergence: biochemical mechanisms and evolutionary perspectives. *Annu. Rev. Virol.* 2, 95–117. doi: 10.1146/annurev-virology-100114-155029

Pedersen, N. C., Perron, M., Bannasch, M., Montgomery, E., Murakami, E., Liepnieks, M., et al. (2019). Efficacy and safety of the nucleoside analog GS-441524 for treatment of cats with naturally occurring feline infectious peritonitis. *J. Feline Med. Surg.* 21, 271–281. doi: 10.1177/1098612X19825701

Peiris, J. S. M., Chu, C. M., Cheng, V. C. C., Chan, K. S. H., Hung, I. F. N., Poon, L. L. M., et al. (2003a). Clinical progression and viral load in a community outbreak of coronavirus-associated SARS pneumonia: a prospective study. *Lancet* 361, 1767–1772. doi: 10.1016/S0140-6736(03)13412-13415

Peiris, J. S. M., Lai, S. T., Poon, L. L. M., Guan, Y., Yam, L. Y. C., Lim, W., et al. (2003b). Coronavirus as a possible cause of severe acute respiratory syndrome. *Lancet* 361, 1319–1325. doi: 10.1016/S0140-6736(03)13077-13072

Perlman, S., and Netland, J. (2009). Coronaviruses post-SARS: update on replication and pathogenesis. *Nat. Rev. Microbiol.* 7, 439–450. doi: 10.1038/nrmicro2147

Perlman, S., and Vijay, R. (2016). Middle East respiratory syndrome vaccines. *Int. J. Infect. Dis.* 47, 23–28. doi: 10.1016/j.ijid.2016.04.008

Petrovsky, N. (2016). SARS coronavirus infections of the lower respiratory tract and their prevention. *Microbiol. Respir. Syst. Infect.* 2016, 45–53. doi: 10.1016/B978-0-12-804543-5.00003-8

Plotkin, S. A. (2010). Correlates of protection induced by vaccination. *Clin. Vaccine Immunol.* 17, 1055–1065. doi: 10.1128/CVI.00131-110

Prabakaran, P., Zhu, Z., Xiao, X., Biragyn, A., Dimitrov, A. S., Broder, C. C., et al. (2009). Potent human monoclonal antibodies against SARS CoV, Nipah and Hendra viruses. *Expert Opin. Biol. Ther.* 9, 355–368. doi: 10.1517/14712590902763755

Pyrc, K., Bosch, B. J., Berkhout, B., Jebbink, M. F., Dijkman, R., Rottier, P., et al. (2006). Inhibition of human coronavirus NL63 infection at early stages of the replication cycle. *Antimicrob. Agents Chemother.* 50, 2000–2008. doi: 10.1128/AAC.01598-1595

Qiu, H., Sun, S., Xiao, H., Feng, J., Guo, Y., Tai, W., et al. (2016). Single-dose treatment with a humanized neutralizing antibody affords full protection of a human transgenic mouse model from lethal Middle East respiratory syndrome (MERS)-coronavirus infection. *Antiviral Res.* 132, 141–148. doi: 10.1016/j.antiviral.2016.06.003

Qiu, X., Audet, J., Wong, G., Pillet, S., Bello, A., Cabral, T., et al. (2012). Successful treatment of ebola virus - infected cynomolgus macaques with monoclonal antibodies. *Sci. Transl. Med.* 4, 1–12.

Raj, V. S., Mou, H., Smits, S. L., Dekkers, D. H. W., Müller, M. A., Dijkman, R., et al. (2013). Dipeptidyl peptidase 4 is a functional receptor for the emerging human coronavirus-EMC. *Nature* 495, 251–254. doi: 10.1038/nature 12005

Raj, V. S., Okba, N. M. A., Gutierrez-Alvarez, J., Drabek, D., van Dieren, B., Widagdo, W., et al. (2018). Chimeric camel/human heavy-chain antibodies protect against MERS-CoV infection. *Sci. Adv.* 4, 1–10. doi: 10.1126/sciadv. aas9667

Raj, V. S., Osterhaus, A. D. M. E., Fouchier, R. A. M., and Haagmans, B. L. (2014). MERS: emergence of a novel human coronavirus. *Curr. Opin. Virol.* 5, 58–62. doi: 10.1016/j.coviro.2014.01.010

Reggiori, F., Monastyrska, I., Verheije, M. H., Calì, T., Ulasli, M., Bianchi, S., et al. (2010). Coronaviruses hijack the LC3-I-positive EDEMosomes, ER-derived vesicles exporting short-lived ERAD regulators, for replication. *Cell Host Microbe* 7, 500–508. doi: 10.1016/j.chom.2010.05.013

Reynard, O., Nguyen, X. N., Alazard-Dany, N., Barateau, V., Cimarelli, A., and Volchkov, V. E. (2015). Identification of a new ribonucleoside inhibitor of ebola virus replication. *Viruses* 7, 6233–6240. doi: 10.3390/v7122934

Rezaee, F., Linfield, D. T., Harford, T. J., and Piedimonte, G. (2017). Ongoing developments in RSV prophylaxis?: a clinician's analysis. *Curr. Opin. Virol.* 112781, 70–78. doi: 10.1016/j.coviro.2017.03.015

Richner, J. M., Himansu, S., Dowd, K. A., Butler, S. L., Salazar, V., Fox, J. M., et al. (2017). Modified mRNA vaccines protect against zika virus infection. *Cell* 168, 1114.e10–1125.e10. doi: 10.1016/j.cell.2017.02.017

Roberts, A., Lamirande, E. W., Vogel, L., Baras, B., Goossens, G., Knott, I., et al. (2010). Immunogenicity and protective efficacy in mice and hamsters of a β-propiolactone inactivated whole virus SARS-CoV vaccine. *Viral Immunol.* 23, 509–519. doi: 10.1089/vim.2010.0028

Rockx, B., Corti, D., Donaldson, E., Sheahan, T., Stadler, K., Lanzavecchia, A., et al. (2008). Structural basis for potent cross-neutralizing human monoclonal antibody protection against lethal human and zoonotic severe acute respiratory syndrome coronavirus challenge. *J. Virol.* 82, 3220–3235. doi: 10.1128/jvi. 02377-2377

Rothe, C., Schunk, M., Sothmann, P., Bretzel, G., Froeschl, G., Wallrauch, C., et al. (2020). Transmission of 2019-nCoV infection from an asymptomatic contact in Germany. *N. Engl. J. Med.* 382, 970–971. doi: 10.1056/nejmc2001468

Schindewolf, C., and Menachery, V. D. (2019). Middle east respiratory syndrome vaccine candidates: cautious optimism. *Viruses* 11:74. doi: 10.3390/v11010074

See, R. H., Petric, M., Lawrence, D. J., Mok, C. P. Y., Rowe, T., Zitzow, L. A., et al. (2008). Severe acute respiratory syndrome vaccine efficacy in ferrets: whole killed virus and adenovirus-vectored vaccines. *J. Gen. Virol.* 89, 2136–2146. doi: 10.1099/vir.0.2008/001891-1890

See, R. H., Zakhartchouk, A. N., Petric, M., Lawrence, D. J., Mok, C. P. Y., Hogan, R. J., et al. (2006). Comparative evaluation of two severe acute respiratory syndrome (SARS) vaccine candidates in mice challenged with SARS coronavirus. *J. Gen. Virol.* 87, 641–650. doi: 10.1099/vir.0.81579-81570

Seong, B. L. (2018). Chaperna-mediated assembly of ferritin-based middle east respiratory syndrome-coronavirus nanoparticles. *Front. Immunol.* 9:1093. doi: 10.3389/fimmu.2018.01093

Shalhoub, S., Farahat, F., Al-Jiffri, A., Simhairi, R., Shamma, O., Siddiqi, N., et al. (2015). IFN-α2a or IFN-β1a in combination with ribavirin to treat Middle East respiratory syndrome coronavirus pneumonia: a retrospective study. *J. Antimicrob. Chemother.* 70, 2129–2132. doi: 10.1093/jac/ dkv085

Sharif-Yakan, A., and Kanj, S. S. (2014). Emergence of MERS-CoV in the middle east: origins, transmission, treatment, and perspectives. *PLoS Pathog.* 10:e1004457. doi: 10.1371/journal.ppat.1004457

Sheahan, T. P., Sims, A. C., Graham, R. L., Menachery, V. D., Gralinski, L. E., Case, J. B., et al. (2017). Broad-spectrum antiviral GS-5734 inhibits both epidemic and zoonotic coronaviruses. *Sci. Transl. Med.* 9, 1–11. doi: 10.1126/scitranslmed. aal3653

Sheahan, T. P., Sims, A. C., Leist, S. R., Schäfer, A., Won, J., Brown, A. J., et al. (2020). Comparative therapeutic efficacy of remdesivir and combination lopinavir, ritonavir, and interferon beta against MERS-CoV. *Nat. Commun.* 11:222. doi: 10.1038/s41467-019-13940-13946

Shin, H. S., Kim, Y., Kim, G., Lee, J. Y., Jeong, I., Joh, J. S., et al. (2019). Immune responses to middle east respiratory syndrome coronavirus during the acute and convalescent phases of human infection. *Clin. Infect. Dis.* 68, 984–992. doi: 10.1093/cid/ciy595

Simmons, G., Gosalia, D. N., Rennekamp, A. J., Reeves, J. D., Diamond, S. L., and Bates, P. (2005). Inhibitors of cathepsin L prevent severe acute respiratory syndrome coronavirus entry. *Proc. Natl. Acad. Sci. U.S.A.* 102, 11876–11881. doi: 10.1073/pnas.0505577102

Smith, E. C., Blanc, H., Surdel, M. C., Vignuzzi, M., and Denison, M. R. (2013). Coronaviruses lacking exoribonuclease activity are susceptible to lethal mutagenesis: evidence for proofreading and potential therapeutics. *PLoS Pathog.* 9:e1003565. doi: 10.1371/journal.ppat.1003565

Snijder, E. J., van der Meer, Y., Zevenhoven-Dobbe, J., Onderwater, J. J. M., van der Meulen, J., Koerten, H. K., et al. (2006). Ultrastructure and origin of membrane vesicles associated with the severe acute respiratory syndrome coronavirus replication complex. *J. Virol.* 80, 5927–5940. doi: 10.1128/jvi.02501-2505

Song, F., Fux, R., Provacia, L. B., Volz, A., Eickmann, M., Becker, S., et al. (2013). Middle east respiratory syndrome coronavirus spike protein delivered by modified vaccinia virus ankara efficiently induces virus-neutralizing antibodies. *J. Virol.* 87, 11950–11954. doi: 10.1128/jvi.01672-1613

Spruth, M., Kistner, O., Savidis-Dacho, H., Hitter, E., Crowe, B., Gerencer, M., et al. (2006). A double-inactivated whole virus candidate SARS coronavirus vaccine stimulates neutralising and protective antibody responses. *Vaccine* 24, 652–661. doi: 10.1016/j.vaccine.2005.08.055

Stadler, K., Roberts, A., Becker, S., Vogel, L., Eickmann, M., Kolesnikova, L., et al. (2005). SARS vaccine protective in mice [2]. *Emerg. Infect. Dis.* 11, 1312–1314. doi: 10.3201/eid1108.041003

Stertz, S., Reichelt, M., Spiegel, M., Kuri, T., Martínez-Sobrido, L., García-Sastre, A., et al. (2007). The intracellular sites of early replication and budding of SARS-coronavirus. *Virology* 361, 304–315. doi: 10.1016/j.virol.2006.11.027

Strobel, B., Zuckschwerdt, K., Zimmermann, G., Mayer, C., Eytner, R., Rechtsteiner, P., et al. (2019). Standardized, Scalable, and Timely Flexible Adeno-Associated Virus Vector Production Using Frozen High-Density HEK-293 Cell Stocks and CELLdiscs. *Hum. Gene Ther. Methods* 30, 23–33. doi: 10.1089/hgtb.20 18.228

Sui, J., Li, W., Murakami, A., Tamin, A., Matthews, L. J., Wong, S. K., et al. (2004). Potent neutralization of severe acute respiratory syndrome (SARS) coronavirus by a human mAb to S1 protein that blocks receptor association. *Proc. Natl. Acad. Sci. U.S.A.* 101, 2536–2541. doi: 10.1073/pnas.0307140101

Sung, J. J. Y., Wu, A., Joynt, G. M., Yuen, K. Y., Lee, N., Chan, P. K. S., et al. (2004). Severe acute respiratory syndrome: report of treatment and outcome after a major outbreak. *Thorax* 59, 414–420. doi: 10.1136/thx.2003.014076

Tai, W., Wang, Y., Fett, C. A., Zhao, G., Li, F., Perlman, S., et al. (2017). Recombinant receptor-binding domains of multiple middle east respiratory syndrome coronaviruses (MERS-CoVs) induce cross-neutralizing antibodies against divergent human and camel MERS-CoVs and antibody escape mutants. *J. Virol.* 91:e01651-16. doi: 10.1128/JVI.01651-1616

Tai, W., Zhao, G., Sun, S., Guo, Y., Wang, Y., Tao, X., et al. (2016). A recombinant receptor-binding domain of MERS-CoV in trimeric form protects human dipeptidyl peptidase 4 (hDPP4) transgenic mice from MERS-CoV infection. *Virology* 499, 375–382. doi: 10.1016/j.virol.2016.10.005

Tan, E. L. C., Ooi, E. E., Lin, C. Y., Tan, H. C., Ling, A. E., Lim, B., et al. (2004). Inhibition of SARS coronavirus infection in vitro with clinically approved antiviral drugs. *Emerg. Infect. Dis.* 10, 581–586. doi: 10.3201/eid1004.030458

Tang, F., Quan, Y., Xin, Z., Wrammert, J., Ma, M., Lv, H., et al. (2019). Lack of peripheral memory B cell responses in recovered patients with severe acute respiratory syndrome: a six-year follow-up study. *J. Immunol.* 186, 7264–7268. doi: 10.4049/jimmunol.0903490

Tang, J., Zhang, N., Tao, X., Zhao, G., Guo, Y., Tseng, C. K., et al. (2015). Optimization of antigen dose for a receptor- binding domain-based subunit vaccine against MERS coronavirus. *Hum. Vaccines Immunother.* 11, 1244–1250. doi: 10.1080/21645515.2015.1021527

Tang, X. C., Agnihothram, S. S., Jiao, Y., Stanhope, J., Graham, R. L., Peterson, E. C., et al. (2014). Identification of human neutralizing antibodies against MERS-CoV and their role in virus adaptive evolution. *Proc. Natl. Acad. Sci. U.S.A.* 111, E2018–E2026. doi: 10.1073/pnas.1402074111

Ter Meulen, J., Bakker, A. B. H., Van Den Brink, E. N., Weverling, G. J., Martina, B. E. E., Haagmans, B. L., et al. (2004). Human monoclonal antibody as

prophylaxis for SARS coronavirus infection in ferrets. *Lancet* 363, 2139–2141. doi: 10.1016/S0140-6736(04)16506-16509

Ter Meulen, J., Van Den Brink, E. N., Poon, L. L. M., Marissen, W. E., Leung, C. S. W., Cox, F., et al. (2006). Human monoclonal antibody combination against SARS coronavirus: synergy and coverage of escape mutants. *PLoS Med.* 3:e237. doi: 10.1371/journal.pmed.0030237

Tortorici, M. A., and Veesler, D. (2019). *Structural Insights into Coronavirus Entry*, 1st Edn. Amsterdam: Elsevier.

Traggiai, E., Becker, S., Subbarao, K., Kolesnikova, L., Uematsu, Y., Gismondo, M. R., et al. (2004). An efficient method to make human monoclonal antibodies from memory B cells: potent neutralization of SARS coronavirus. *Nat. Med.* 10, 871–875. doi: 10.1038/nm1080

Tse, L. V., Klinc, K. A., Madigan, V. J., Castellanos Rivera, R. M., Wells, L. F., Havlik, L. P., et al. (2017). Structure-guided evolution of antigenically distinct adeno-associated virus variants for immune evasion. *Proc. Natl. Acad. Sci. U.S.A.* 114, E4812–E4821. doi: 10.1073/pnas.1704766114

Tse, L. V., Moller-Tank, S., and Asokan, A. (2015). Strategies to circumvent humoral immunity to adeno-associated viral vectors. *Expert Opin. Biol. Ther.* 15, 845–855. doi: 10.1517/14712598.2015.1035645

Ura, T., Okuda, K., and Shimada, M. (2014). Developments in viral vector-based vaccines. *Vaccines* 2, 624–641. doi: 10.3390/vaccines2030624

Urakova, N., Kuznetsova, V., Crossman, D. K., Sokratian, A., Guthrie, D. B., Kolykhalov, A. A., et al. (2017). β-D- N 4 -hydroxycytidine is a potent anti-alphavirus compound that induces a high level of mutations in the viral genome. *J. Virol.* 92, 1–22. doi: 10.1128/jvi.01965-1917

van den Brink, E. N., ter Meulen, J., Cox, F., Jongeneelen, M. A. C., Thijsse, A., Throsby, M., et al. (2005). Molecular and biological characterization of human monoclonal antibodies binding to the spike and nucleocapsid proteins of severe acute respiratory syndrome coronavirus. *J. Virol.* 79, 1635–1644. doi: 10.1128/jvi.79.3.1635-1644.2005

van Doremalen, N., Falzarano, D., Ying, T., de Wit, E., Bushmaker, T., Feldmann, F., et al. (2017). Efficacy of antibody-based therapies against Middle East respiratory syndrome coronavirus (MERS-CoV) in common marmosets. *Antiviral Res.* 143, 30–37. doi: 10.1016/j.antiviral.2017.03.025

Volz, A., Kupke, A., Song, F., Jany, S., Fux, R., Shams-Eldin, H., et al. (2015). Protective efficacy of recombinant modified vaccinia virus ankara delivering middle east respiratory syndrome coronavirus spike glycoprotein. *J. Virol.* 89, 8651–8656. doi: 10.1128/jvi.00614-615

Walls, A. C., Xiong, X., Park, Y. J., Tortorici, M. A., Snijder, J., Quispe, J., et al. (2019a). Unexpected receptor functional mimicry elucidates activation of coronavirus fusion. *Cell* 176, 1026.e15–1039.e15. doi: 10.1016/j.cell.2018.12.028

Walls, A. C., Xiong, X., Rey, A., Park, Y., Corti, D., Veesler, D., et al. (2019b). Activation of coronavirus fusion unexpected receptor functional mimicry elucidates activation of coronavirus fusion. *Cell* 176, 1026–1039.

Wang, C., Zheng, X., Gai, W., Wong, G., Wang, H., Jin, H., et al. (2017a). Novel chimeric virus-like particles vaccine displaying MERS-CoV receptor-binding domain induce specific humoral and cellular immune response in mice. *Antiviral Res.* 140, 55–61. doi: 10.1016/j.antiviral.2016.12.019

Wang, C., Zheng, X., Gai, W., Zhao, Y., Gao, Y., Yang, S., et al. (2017b). MERS-CoV virus-like particles produced in insect cells induce specific humoural and cellular imminity in rhesus macaques. *Oncotarget* 8, 12686–12694.

Wang, Y., Tai, W., Yang, J., Zhao, G., Sun, S., Tseng, C.-T. K., et al. (2017). Receptor-binding domain of MERS-CoV with optimal immunogen dosage and immunization interval protects human transgenic mice from MERS-CoV infection. *Hum. Vaccin. Immunother.* 13, 1615–1624. doi: 10.1080/21645515.2017.1296994

Wang, L., Shi, W., Chappell, J. D., Joyce, M. G., Zhang, Y., Kanekiyo, M., et al. (2018). Importance of neutralizing monoclonal antibodies targeting multiple antigenic sites on the middle east respiratory syndrome coronavirus spike glycoprotein to avoid neutralization escape. *J. Virol.* 92, 1–21. doi: 10.1128/jvi.02002-2017

Wang, L., Shi, W., Joyce, M. G., Modjarrad, K., Zhang, Y., Leung, K., et al. (2015). Evaluation of candidate vaccine approaches for MERS-CoV. *Nat. Commun.* 6, 1–11. doi: 10.1038/ncomms8712

Wang, M., Cao, R., Zhang, L., Yang, X., Liu, J., Xu, M., et al. (2020). Remdesivir and chloroquine effectively inhibit the recently emerged novel coronavirus (2019-nCoV) *in vitro*. *Cell Res.* 30, 269–271. doi: 10.1038/s41422-020-0282-280

Wang, N., Rosen, O., Wang, L., Turner, H. L., Stevens, L. J., Corbett, K. S., et al. (2019). Structural Definition of a Neutralization-Sensitive Epitope on the MERS-CoV S1-NTD. *Cell Rep.* 28, 3395.e6–3405.e6. doi: 10.1016/j.celrep.2019.08.052

Wang, W., Chen, S., Liu, I., Kao, C., Chen, H., Chiang, B., et al. (2004). Temporal relationship of viral load, ribavirin, interleukin (IL)-6, IL-8, and clinical progression in patients with severe acute respiratory syndrome. *Clin. Infect. Dis.* 39, 1071–1075. doi: 10.1086/423808

Warimwe, G. M., Gesharisha, J., Carr, B. V., Otieno, S., Otingah, K., Wright, D., et al. (2016). Chimpanzee adenovirus vaccine provides multispecies protection against rift valley fever. *Sci. Rep.* 6, 1–7. doi: 10.1038/srep20617

White, J. M., and Whittaker, G. R. (2016). Fusion of enveloped viruses in endosomes. *Traffic* 17, 593–614. doi: 10.1111/tra.12389

Widagdo, W., Okba, N. M. A., Stalin Raj, V., and Haagmans, B. L. (2017). MERS-coronavirus: from discovery to intervention. *One Heal.* 3, 11–16. doi: 10.1016/j.onehlt.2016.12.001

Wirblich, C., Coleman, C. M., Kurup, D., Abraham, T. S., Bernbaum, J. G., Jahrling, P. B., et al. (2017). One-health: a safe, efficient, dual-use vaccine for humans and animals against middle east respiratory syndrome coronavirus and rabies virus. *J. Virol.* 91, 1–15.

Woo, P. C. Y., Lau, S. K. P., Huang, Y., and Yuen, K. Y. (2009). Coronavirus diversity, phylogeny and interspecies jumping. *Exp. Biol. Med.* 234, 1117–1127. doi: 10.3181/0903-MR-94

Woo, P. C. Y., Lau, S. K. P., Tsoi, H., Huang, Y., Poon, R. W. S., Chu, C., et al. (2005). Clinical and molecular epidemiological features of coronavirus HKU1-associated community-acquired pneumonia. *J. Infect. Dis.* 192, 1898–1907. doi: 10.1086/497151

World Health Organization [WHO] (2018). *WHO MERS Global Summary and Assessment of Risk*. Geneva: WHO.

Wrapp, D., Wang, N., Corbett, K. S., Goldsmith, J. A., Hsieh, C.-L., Abiona, O., et al. (2020). Cryo-EM structure of the 2019-nCoV spike in the prefusion conformation. *Science* 1263, 1260–1263. doi: 10.1126/science.abb2507

Wu, C. Y., Jan, J. T., Ma, S. H., Kuo, C. J., Juan, H. F., Cheng, Y. S. E., et al. (2004). Small molecules targeting severe acute respiratory syndrome human coronavirus. *Proc. Natl. Acad. Sci. U.S.A.* 101, 10012–10017. doi: 10.1073/pnas.0403596101

Xia, S., Yan, L., Xu, W., Agrawal, A. S., Algaissi, A., Tseng, C. T. K., et al. (2019). A pan-coronavirus fusion inhibitor targeting the HR1 domain of human coronavirus spike. *Sci. Adv.* 5:eaav4580. doi: 10.1126/sciadv.aav4580

Xu, J., Jia, W., Wang, P., Zhang, S., Shi, X., Wang, X., et al. (2019). Antibodies and vaccines against Middle East respiratory syndrome coronavirus. *Emerg. Microbes Infect.* 8, 841–856. doi: 10.1080/22221751.2019.1624482

Yang, Z. Y., Kong, W. P., Huang, Y., Roberts, A., Murphy, B. R., Subbarao, K., et al. (2004). A DNA vaccine induces SARS coronavirus neutralization and protective immunity in mice. *Nature* 428, 561–564. doi: 10.1038/nature02463

Ying, T., Du, L., Ju, T. W., Prabakaran, P., Lau, C. C. Y., Lu, L., et al. (2014). Exceptionally potent neutralization of middle east respiratory syndrome coronavirus by human monoclonal antibodies. *J. Virol.* 88, 7796–7805. doi: 10.1128/jvi.00912-914

Ying, T., Prabakaran, P., Du, L., Shi, W., Feng, Y., Wang, Y., et al. (2015). Junctional and allele-specific residues are critical for MERS-CoV neutralization by an exceptionally potent germline-like antibody. *Nat. Commun.* 6:8223. doi: 10.1038/ncomms9223

Yong, C. Y., Ong, H. K., Yeap, S. K., Ho, K. L., and Tan, W. S. (2019). Recent advances in the vaccine development against middle east respiratory syndrome-coronavirus. *Front. Microbiol.* 10:1781. doi: 10.3389/fmicb.2019.01781

Yoon, J. J., Toots, M., Lee, S., Lee, M. E., Ludeke, B., Luczo, J. M., et al. (2018). Orally efficacious broad-spectrum ribonucleoside analog inhibitor of influenza and respiratory syncytial viruses. *Antimicrob. Agents Chemother.* 62, 1–18. doi: 10.1128/AAC.00766-718

Yuan, S., Chu, H., Chan, J. F. W., Ye, Z. W., Wen, L., Yan, B., et al. (2019). SREBP-dependent lipidomic reprogramming as a broad-spectrum antiviral target. *Nat. Commun.* 10:120. doi: 10.1038/s41467-018-08015-x

Yuan, Y., Cao, D., Zhang, Y., Ma, J., Qi, J., Wang, Q., et al. (2017). Cryo-EM structures of MERS-CoV and SARS-CoV spike glycoproteins reveal the dynamic receptor binding domains. *Nat. Commun.* 8:15092. doi: 10.1038/ncomms15092

Zabner, J., Seiler, M., Walters, R., Kotin, R. M., Fulgeras, W., Davidson, B. L., et al. (2000). Adeno-associated virus type 5 (AAV5) but not AAV2 binds to the apical surfaces of airway epithelia and facilitates gene transfer. *J. Virol.* 74, 3852–3858. doi: 10.1128/JVI.74.8.3852-3858.2000

Zhang, C., Maruggi, G., Shan, H., and Li, J. (2019). Advances in mRNA vaccines for infectious diseases. *Front. Immunol.* 10:594. doi: 10.3389/fimmu.2019.00594

Zhang, N., Channappanavar, R., Ma, C., Wang, L., Tang, J., Garron, T., et al. (2016). Identification of an ideal adjuvant for receptor-binding domain-based subunit vaccines against Middle East respiratory syndrome coronavirus. *Cell. Mol. Immunol.* 13, 180–190. doi: 10.1038/cmi.2015.03

Zhang, N., Jiang, S., and Du, L. (2014). Current advancements and potential strategies in the development of MERS-CoV vaccines. *Expert Rev. Vaccines* 13, 761–774. doi: 10.1586/14760584.2014.912134

Zhao, G., He, L., Sun, S., Qiu, H., Tai, W., Chen, J., et al. (2018). A novel nanobody targeting middle east respiratory syndrome coronavirus (MERS-CoV) receptor-binding domain has potent cross-neutralizing activity and protective efficacy against MERS-CoV. *J. Virol.* 92:e00837-18. doi: 10.1128/JVI.00837-818

Zhao, J., Alshukairi, A. N., Baharoon, S. A., Ahmed, W. A., Bokhari, A. A., Nehdi, A. M., et al. (2017). Recovery from the Middle East respiratory syndrome is associated with antibody and T cell responses. *Sci. Immunol.* 5393, 1–11.

Zhao, J., Perera, R. A. P. M., Kayali, G., Meyerholz, D., Perlman, S., and Peiris, M. (2015). Passive immunotherapy with dromedary immune serum in an experimental animal model for middle east respiratory syndrome. *J. Virol.* 89, 6117–6120. doi: 10.1128/JVI.00446-415

Zhao, J., Zhao, J., and Perlman, S. (2010). T cell responses are required for protection from clinical disease and for virus clearance in severe acute respiratory syndrome coronavirus-infected mice ?. *J. Virol.* 84, 9318–9325. doi: 10.1128/JVI.01049-1010

Zhao, J. J. J., Zhao, J. J. J., Mangalam, A. K., Channappanavar, R., Fett, C., Meyerholz, D. K., et al. (2016). Airway memory CD4+ T cells mediate protective immunity against emerging respiratory coronaviruses. *Immunity* 44, 1379–1391. doi: 10.1016/j.immuni.2016.05.006

Zhou, P., Yang, X.-L., Wang, X.-G., Hu, B., Zhang, L., Zhang, W., et al. (2020). A pneumonia outbreak associated with a new coronavirus of probable bat origin. *Nature* 579, 270–273. doi: 10.1038/s41586-020-2012-2017

Zhu, Z., Chakraborti, S., He, Y., Roberts, A., Sheahan, T., Xiao, X., et al. (2007). Potent cross-reactive neutralization of SARS coronavirus isolates by human monoclonal antibodies. *Proc. Natl. Acad. Sci. U.S.A.* 104, 12123–12128. doi: 10.1073/pnas.0701000104

Ziebuhr, J., Snijder, E. J., and Gorbalenya, A. E. (2000). Virus-encoded proteinases and proteolytic processing in the nidovirales. *J. Gen. Virol.* 81(Pt 4), 853–879.

Zumla, A., Chan, J. F. W. W., Azhar, E. I., Hui, D. S. C. C., and Yuen, K. Y. (2016a). Coronaviruses-drug discovery and therapeutic options. *Nat. Rev. Drug Discov.* 15, 327–347. doi: 10.1038/nrd.2015.37

Zumla, A., Hui, D. S., Perlman, S., To, C., and Stanley, P. (2015). Middle east respiratory syndrome HHS public access. *Lancet* 386, 995–1007. doi: 10.1016/S0140-6736(15)60454-60458

Zumla, A., Rao, M., Wallis, R. S., Kaufmann, S. H. E., Rustomjee, R., Mwaba, P., et al. (2016b). Host-directed therapies for infectious diseases: current status, recent progress, and future prospects. *Lancet Infect. Dis.* 16, e47–e63. doi: 10.1016/S1473-3099(16)00078-75

**Conflict of Interest:** The authors declare that the research was conducted in the absence of any commercial or financial relationships that could be construed as a potential conflict of interest.

*Copyright © 2020 Tse, Meganck, Graham and Baric. This is an open-access article distributed under the terms of the Creative Commons Attribution License (CC BY). The use, distribution or reproduction in other forums is permitted, provided the original author(s) and the copyright owner(s) are credited and that the original publication in this journal is cited, in accordance with accepted academic practice. No use, distribution or reproduction is permitted which does not comply with these terms.*

frontiers in Microbiology

ORIGINAL RESEARCH
published: 30 April 2020
doi: 10.3389/fmicb.2020.00504

# Tolcapone Potently Inhibits Seminal Amyloid Fibrils Formation and Blocks Entry of Ebola Pseudoviruses

*Mengjie Qiu[1], Zhaofeng Li[1], Yuliu Chen[1], Jiayin Guo[1], Wei Xu[1], Tao Qi[2], Yurong Qiu[2], Jianxin Pang[1], Lin Li[1,3], Shuwen Liu[1]* and Suiyi Tan[1]**

[1] Guangdong Provincial Key Laboratory of New Drug Screening, School of Pharmaceutical Sciences, Southern Medical University, Guangzhou, China, [2] Laboratory Medicine Center, Nanfang Hospital, Southern Medical University, Guangzhou, China, [3] School of Pharmacy, Guangdong Medical University, Dongguan, China

Ebola virus (EBOV), the causative pathogen of the deadly EBOV disease (EVD), can be transmitted *via* sexual transmission. Seminal amyloid fibrils have been found enhancers of EBOV infection. Currently, limited preventive vaccine or therapeutic is available to block EBOV infection through sexual intercourse. In this study, we repurpose tolcapone, a US Food and Drug Administration (FDA)-approved agent for Parkinson's disease, as a potent inhibitor of seminal amyloid fibrils, among which semen-derived enhancer of viral infection (SEVI) is the best-characterized. Tolcapone binds to the amyloidogenic region of the SEVI precursor peptide (PAP248–286) and inhibits PAP248–286 aggregation by disrupting PAP248–286 oligomerization. In addition, tolcapone interacts with preformed SEVI fibrils and influences the activity of SEVI in promoting infection of pseudovirus (PsV) carrying the envelope glycoprotein (GP) of the EBOV Zaire or Sudan species (Zaire PsV and Sudan PsV, respectively). Tolcapone significantly antagonizes SEVI-mediated enhancement of both Zaire PsV and Sudan PsV binding to and subsequent internalization in HeLa cells. Of note, tolcapone is also effective in inhibiting the entry of both Zaire PsV and Sudan PsV. Tolcapone inhibits viral entry possibly through binding with critical residues in EBOV GP. Moreover, the combination of tolcapone with two small-molecule entry inhibitors, including bepridil and sertraline, exhibited synergistic anti-EBOV effects in semen. Collectively, as a bifunctional agent targeting the viral infection-enhancing amyloid and the virus itself during sexual intercourse, tolcapone can act as either a prophylactic topical agent to prevent the sexual transmission of EBOV or a therapeutic to treat EBOV infection.

**Keywords: Ebola virus, tolcapone, semen-derived enhancer of viral infection (SEVI), sexual transmission, entry inhibitor**

OPEN ACCESS

***Edited by:***
*Christopher C. Broder, Uniformed Services University of the Health Sciences, United States*

***Reviewed by:***
*Asuka Nanbo, Nagasaki University, Japan*
*Masfique Mehedi, University of North Dakota, United States*

***Correspondence:**
*Suiyi Tan*
*suiyitan@smu.edu.cn*
*Shuwen Liu*
*liusw@smu.edu.cn*

***Specialty section:***
*This article was submitted to Virology, a section of the journal Frontiers in Microbiology*

***Received:*** *30 November 2019*
***Accepted:*** *09 March 2020*
***Published:*** *30 April 2020*

***Citation:***
*Qiu M, Li Z, Chen Y, Guo J, Xu W, Qi T, Qiu Y, Pang J, Li L, Liu S and Tan S (2020) Tolcapone Potently Inhibits Seminal Amyloid Fibrils Formation and Blocks Entry of Ebola Pseudoviruses. Front. Microbiol. 11:504. doi: 10.3389/fmicb.2020.00504*

## INTRODUCTION

Ebola virus (EBOV) is the causative pathogen of the deadly EBOV disease (EVD). It belongs to the *Filoviridae* family and can be classified into six distinct species, including *Zaire ebolavirus* (ZEBOV), *Sudan ebolavirus* (SUDV), *Tai Forest ebolavirus* (TAFV), *Bundibugyo ebolavirus* (BDBV), *Reston ebolavirus* (RESTV), and the newly identified *Bombali ebolavirus* (BOMV) (Van Kerkhove et al., 2015; Goldstein et al., 2018). Among them, ZEBOV have the highest case-fatality rates

(60–90%) followed by those for the SUDV (40–60%). Other EBOVs have been associated with rates of mortality of 0–25% (Weyer et al., 2015; Thorson et al., 2016). After the first recognized outbreak in 1976, numerous EBOV outbreaks have occurred over the years. However, it was only until the recent outbreak of EBOV in 2014–2016, which caused approximately 28,200 cases and 11,300 deaths, highlighted the danger and global impact of this pathogen. Although the epidemic has now subsided, the increase in outbreak frequency, number of cases, and associated social and economic cost necessitates the need for effective vaccines and drugs to combat this pandemic threat (Dhama et al., 2018).

EBOVs are usually transmitted through direct contact with EVD patients, whose body fluids contain high titers of viruses (Lanini et al., 2015). The shedding of infectious virus and virus genome in semen has been documented since 1976 (Rodriguez et al., 1999; Bausch et al., 2007; Mate et al., 2015; Barnes et al., 2017). However, sexual transmission of EBOV was only recently confirmed during the 2014–2016 outbreaks in West Africa (Mate et al., 2015; Keita et al., 2016; Thorson et al., 2016). Several follow-up studies have shown that EBOV could persist in semen up to 2 years after the onset of disease (Barnes et al., 2017; Deen et al., 2017; Keita et al., 2017), which raises a critical concern for the increasing risk of sexual transmission of EBOVs by asymptomatic survivors (Fischer et al., 2017). Although WHO recommends safe sexual practices, including abstinence or condom use, for at least 1 year after the onset of symptoms (Thorson et al., 2016; Keita et al., 2017), it might be too short based on the fact of long-term persistence of virus genome in semen (Fischer et al., 2017) and not practicable because 74% of male EVD survivors were reported to not prefer to use condoms during sexual intercourse. Therefore, an effective and safe microbicide, administered vaginally by women without the need for approval and cooperation from sexual partners in the low-income countries to prevent EBOV sexual transmission before the next outbreak, is urgently needed.

Human semen contains amyloid fibrils that could greatly enhance infection of pathogens of sexually transmitted infections (STIs), including HIV-1, herpes simplex virus (HSV), cytomegalovirus (CMV) (Tang et al., 2013; Torres et al., 2015), etc. Among them, the well-documented pathogen is HIV-1 (Münch et al., 2007; Roan et al., 2009, 2011; Kim et al., 2010). Seminal amyloid fibrils are highly cationic and are made up of naturally occurring peptide fragments, including prostatic acid phosphatase (PAP248–286 and PAP85–120) and the homologous proteins semenogelin 1 (SEM1) and semenogelin 2 (SEM2) (Arnold et al., 2012). Semen-derived enhancer of viral infection (SEVI), formed by PAP248–286 self-aggregating, is the best-characterized seminal amyloid (Lee and Ramamoorthy, 2018). Recently, infection by EBOV with sexual transmission routes has been found to also be enhanced by SEVI (Bart et al., 2018). These seminal fibrils act in a conformation- and charge-dependent manner to increase infection by promoting viral entry into target cells, which is similar with that reported for HIV-1 (Roan et al., 2009; Bart et al., 2018). SEVI specifically enhances EBOV binding to and subsequent internalization and macropinocytotic uptake into target cells (Bart et al., 2018). More importantly, seminal amyloid fibrils establish a microenvironment that might be beneficial for EBOV persistence (Bart et al., 2018). Of note, the potency of antiretroviral agents decreases in the presence of seminal amyloids/semen (Zirafi et al., 2014). Therefore, seminal amyloid fibril serves as a novel drug target for sexually transmitted EBOV. Although there are five compassionate-use investigational therapeutics for treatment of EVD, including the antivirals favipiravir (Sissoko et al., 2016) and GS-5734 (Warren et al., 2016) and antibody therapeutics mAb114 (Corti et al., 2016), Zmapp (Qiu et al., 2014), and REGN3470-3471-3479 (Sivapalasingam et al., 2018), none of these are US Food and Drug Administration (FDA)-approved or have been tested effective in the context of EBOV sexual transmission. Seeking a time-saving, cost-saving, and multifunctional candidate microbicide is of particular importance.

During our review of the amyloid inhibitors in the literature in our previous study (Lump et al., 2015; Xun et al., 2015; Ren et al., 2018; Zhang et al., 2018; Li et al., 2019; Tan et al., 2019), we noticed that tolcapone, an active catechol-*O*-methyltransferase (COMT) inhibitor clinically used as an adjunct to levodopa/carbidopa for Parkinson's disease (Olanow and Watkins, 2007; Müller, 2015), possessed inhibitory activity against transthyretin (TTR) amyloidosis, which is a plasma homotetrameric protein associated with fatal systemic amyloidoses. Tolcapone was also shown to be effective in treating amyloid transthyretin (ATTR) amyloidosis *in vivo* (Gamez et al., 2019). It shows high binding affinity to the thyroxine binding sites of the native tetrameric form of TTR, preventing its dissociation into monomers. The drug also exhibits fibril disruption activity *in vitro* (Sant'Anna et al., 2016). More importantly, tolcapone displays inhibitory activity against EBOV infection by targeting the interaction between viral protein 35 (VP35) and nucleoprotein (NP) at the late stage of viral infection (Liu et al., 2017). Therefore, we questioned whether tolcapone could be a repositioned compound with simultaneously inhibitory effects on seminal amyloidogenic peptide fibrillogenesis and EBOV infection to stop the sexual transmission of EBOV.

In the current study, we sought to elucidate the inhibitory effects of tolcapone on the seminal amyloid fibrils and the underlying mode of action. We also reported for the first time that tolcapone was a potent EBOV entry inhibitor. It exhibited a synergistic effect in combination with other entry inhibitor-based antiviral agents. As well, the safety profile of tolcapone *in vitro* was explored.

# MATERIALS AND METHODS

## Reagents

Congo red, ammonium persulfate, DL-dithiothreitol (DTT), tris (2, 2-bipyridyl) dichlororuthenium (II) [Ru $(bpy)_3^{2+}$], 3-(4,5-dimethylthiazol-2-yl)-2,5-diphenyltetrazolium bromide (MTT), polyethyleneimine (PEI), Triton, thioflavin T (ThT), and SYPRO Orange Protein dye were purchased from Sigma (St. Louis,

MO, United States). Chemicals, including tolcapone, bepridil hydrochloride (bepridil), sertraline hydrochloride (sertraline), and favipiravir, were bought from TargetMol (United States). PAP248-286, PAP248-286(Ala), and SEM1 86-107 (>95% purity) were synthesized by Scilight-Peptide (Beijing, China). Peptides PAP 248–286 and SEM1 86–107 were first dissolved in phosphate buffered saline (PBS) at the concentration of 1 mM, and fibril formation was promoted by agitation at 37°C for 24–72 h at 1,400 rpm by using an Eppendorf Thermomixer. Semen (SE) samples were obtained from healthy lab members with written informed consent in accordance with the Declaration of Helsinki, and the study was approved by the Human Ethics Committee of Southern Medical University, China. Ejaculates were liquefied as soon as collected for 30 min at room temperature. Seminal fluid (SE-F), representing the cell-free supernatant of SE, was collected by centrifugation of 1 ml SE for 15 min at 10,000 rpm and stored in 1-ml aliquots at −20°C. HEK-293T cells, Huh-7 cells, and HeLa cells were grown in Dulbecco's modified Eagle's medium (DMEM) supplemented with 10% fetal bovine serum (FBS; ExCell Bio) and 1% penicillin/streptomycin at 37°C and 5% carbon dioxide ($CO_2$). A549 cells and THP-1 cells were maintained in RPMI 1640 medium supplemented with 10% FBS and 1% penicillin/streptomycin at 37°C and 5% $CO_2$. Human monocyte-derived THP-1 cells were differentiated into macrophages by using phorbol-12-myristate-13-acetate (PMA; Sigma) before they were used as target cells (Johnson et al., 2014). Plasmids of HIV-1HXB2 (X4 strain), HIV-1 JR-FL (R5 strain), vesicular stomatitis virus-G (VSV-G), pNL4-3.Luc.$R^-E^-$, and anti-p24 monoclonal antibody (183-12H-5C) were obtained from the National Institutes of Health AIDS Research and Reference Reagent Program. Plasmids of glycoproteins (GPs) of ZEBOV and SUDV were prepared as described elsewhere (Li et al., 2017). The soluble Zaire GP [without the mucin-like domain (MLD) and the transmembrane (TM) domain] that possesses the native trimer conformation of GP is a gift from Dr. Lu Lu of Fudan University, China.

## Congo Red Staining Assay

Peptide PAP248–286 or PAP248–286(Ala) at 220 μM in PBS was mixed with inhibitor at various concentrations and then agitated at 1,400 rpm at 37°C by using an Eppendorf Thermomixer. To monitor the reaction kinetics, 10-μl aliquot of the reaction mixture were withdrawn from each tube at different time points and detected by a Congo red kit as previously described (Tan et al., 2019). The Congo red staining measurements were plotted as a function of time and fitted by a sigmoidal curve using Origin data analysis software to determine lag time ($t_{lag}$) (Nakka et al., 2018).

## Thioflavin T Fluorescence Assay

Ten microliters of sample prepared as described above was mixed with 190 μl of thioflavin T (ThT) working solution (50 μM) (Nilsson, 2004). The fluorescence of the mixture was measured using an RF-5301 PC spectrofluorophotometer (Shimadzu) at an excitation wavelength of 440 nm and an emission of 485 nm.

## Transmission Electron Microscopy Analysis

Fibrils were generated as described in the Congo red staining section. At indicated time points, aliquots were removed from respective reactions and subjected to transmission electron microscopy (TEM) analysis (Tan et al., 2013). The morphology of SEVI or seminal fibrils in the presence and absence of tolcapone (the final concentration of PAP248–286 was 66 μM, and the final dilution of SE-F was 1:5) was visualized using an H-7650 TEM (Hitachi Limited, Tokyo, Japan).

## Circular Dichroism Spectroscopy

PAP248–286 at 220 μM was incubated with or without tolcapone at various concentrations and agitated at 1,400 rpm at 37°C, after which circular dichroism (CD) measurements were performed using a J-715 spectrometer (Jasco, Japan). The CD spectra were recorded in the 190–280-nm region at a scan speed of 50 nm·$min^{-1}$, with a bandwidth of 1 nm and a time constant of 2 s. All measurements were done at room temperature, and the final concentration of each sample was 66 μM. The baseline was corrected to values for the buffer content with different concentrations of tolcapone. The CD curves were smoothed using GraphPad Prism software.

## Tricine-Sodium Dodecyl Sulfate-Polyacrylamide Gel Electrophoresis

PAP248–286 was incubated with tolcapone at indicated concentrations at 37°C for 30 min. Mixtures were then centrifuged at 5,000 rpm for 5 min. The free PAP248–286 in the supernatant was mixed with loading buffer and boiled at 100°C for 10 min. Then, the samples were separated by 16% gradient tricine-sodium dodecyl sulfate-polyacrylamide gel electrophoresis (SDS-PAGE). Peptides were visualized by Coomassie blue staining as indicated elsewhere (Tan et al., 2013).

## Photo-Induced Cross-Linking of Unmodified Proteins

Samples were chemically cross-linked using photo-induced cross-linking of unmodified proteins (PICUPs) as previously reported (Ren et al., 2018). Firstly, PAP248–286 monomer at 220 μM was incubated with various concentrations of tolcapone or suramin (15, 20, and 30 μM) at 37°C for 30 min. Next, 1 μl of 40 mM tris (2,2-bipyridyl)dichlororuthenium (II) [Ru (bpy) 32+] and 1 μl of 800 mM ammonium persulfate were added to 18 μl of the mixed sample. The mixture was then exposed to visible light for 8 s, and the cross-linking reaction was terminated by the addition of 2 μl of 5 M DTT. Non-cross-linked PAP248–286 monomer served as a negative control. The samples were separated by 16% gradient tricine-SDS-PAGE, and Coomassie blue staining was used to determine the frequency distribution of monomers and oligomers of PAP248–286.

## Preparation of Pseudoviruses and Viral Infection Assay

Pseudoviruses were prepared as previously described (Chan et al., 2000; Xun et al., 2015; Li et al., 2017; Qiu et al., 2019). Briefly, HEK-293T cells were co-transfected with a pNL4-3.Luc.$R^-E^-$ plasmid and different EBOVs Env-encoding plasmids derived from Zaire pseudovirus (Zaire PsV), Sudan pseudovirus (Sudan PsV), HIV-1 Env-encoding plasmids derived from HIV-1HXB2 (X4 strain), HIV-1JR-FL (R5 strain), and VSV-G Env-encoding plasmids by using a PEI transfection reagent. Cell culture supernatants containing pseudoviruses were collected 72 h after transfection and centrifuged at 3,500 rpm for 15 min to remove detached cells and cell debris and then stored in a -80°C refrigerator. The pseudoviruses were quantitated by determination of the level of p24 antigen by ELISA as described elsewhere (Li et al., 2010). In detail, 5 μg/ml of 183-12H-5C diluted in sodium carbonate buffer (0.05 M, pH = 9.6) was coated onto all wells of a 96-well polystyrene plate (Corning, United States) at 4°C overnight. After blocking with 2% skimmed milk powder, the lyzed pseudovirus serially diluted in PBS was added to the wells, and the plate was incubated at 37°C for 1 h. Rabbit polyclonal to HIV-1 p24 antibody (Abcam, United Kingdom) at a 1:2,000 dilution was added into the wells, and the plate was incubated at 37°C for 1 h and then further incubated with peroxidase affinipure goat anti-rabbit IgG (H+L) (Abcam, United Kingdom) at a 1:3,000 dilution ratio for one more hour at 37°C. The absorbance of the wells was measured after reacting with tetramethylbenzidine (Sigma, United States). When stored at −80°C in 6 months, the luciferase values in HeLa, A549, THP-1, and Huh-7 cells showed no significant difference compared with that at 0 months, indicating that the activity of pseudovirions was relatively stable at −80°C for 6 months.

PAP248–286 or whole SE-F was agitated to allow fibril formation with or without tolcapone as described in the Congo red staining section. Samples at indicated time points were collected and centrifuged to pellet the fibrils at 12,000 rpm for 5 min to remove the remaining free tolcapone. The pellets were resuspended in culture medium and used to determine their abilities to enhance Ebola pseudoviruses infection as described previously (Xun et al., 2015). Briefly, the pellets were mixed with Ebola pseudovirus (10 ng p24) for 10 min at room temperature. The pseudovirus–fibril mixtures were then used to infect various target cells ($10^4$/well) that have been cultured overnight. Luciferase activity in triplicate well was measured 72 h postinfection using luciferase assay kit (Promega) according to the manufacturer's instruction. The enhancement of viral infection was shown relative to those measured in the absence of peptide (Tan et al., 2019). The final concentration of PAP248–286 and SE-F in the infection assay was 11 μM and 5%, respectively.

To confirm that tolcapone could diminish the mature fibril-mediated enhancement of viral infection, SEVI or whole SE-F, which has been agitated for 8 h, was incubated with graded concentration of tolcapone at 37°C for 15 min. To eliminate the anti-EBOV activity of tolcapone itself as much as possible, the SEVI or SE-F and tolcapone mixtures were centrifuged at 12,000 rpm for 5 min to discard the free tolcapone. Then, the pellets were dissolved in fresh medium and were tested on their abilities to enhance EBOV infection as described above. SEVI was tested at a final concentration of 11 μM, and SE-F was used at a final concentration of 5%.

## Measurement of the Entry Inhibition Activity of Tolcapone Individually and in Combination With Entry-Inhibitory Antivirals in Semen

A pseudo-EBOV inhibition assay was performed in HeLa, A549, THP-1, and Huh-7 cells as previously described (Li et al., 2017). Briefly, cells were seeded at $10^4$ cells/well into a 96-well plate and incubated overnight at 37°C. EBOV PsV (60 ng p24) was incubated with a serially diluted inhibitor for 30 min at 37°C, followed by the addition of cultured cells. The cells were incubated with or without pseudovirus as virus control and cell control, respectively. The culture was replaced with fresh medium 14 h post-infection, and luciferase activity was detected 72 h later. The effective 50% inhibitory concentration ($IC_{50}$) was calculated using the Compusyn software (Xu et al., 2014).

For the inhibitor combination assay, tolcapone was mixed with entry inhibitor at the indicated molar concentration ratio, while tolcapone and each entry inhibitor were included as controls. The mixtures were serially diluted, incubated with SE-F, and tested for their inhibitory activities on Zaire PsV infection in HeLa cells as described above. SE-F was used at a final dilution of 1:20 to avoid cytotoxicity. Each sample was tested in triplicate, and data were analyzed for synergistic effect by calculating the combination index (CI), using the CalcuSyn program. CI values of $<1$ and $>1$ indicate synergy and antagonism, respectively, and synergy was divided into different strengths, according to CI values, as follows: $<0.1$ indicates very strong synergism; 0.1–0.3 indicates strong synergism; 0.3–0.7 indicates synergism; 0.7–0.85 indicates moderate synergism; and 0.85–0.90 indicates slight synergism (Qi et al., 2017). Fold of potency enhancement was calculated with the ratio of concentrations of inhibitor tested alone and in combination.

## Binding/Internalization Assays

SEVI was incubated with or without tolcapone at 37°C for 15 min, and the pellets were collected by centrifugation at 12,000 rpm for 5 min to remove free tolcapone. Afterward, the fibril pellets were resuspended and further incubated with Zaire-PsV (30 ng p24) at 37°C for 15 min and then added to HeLa cells on ice and either lysed in 1% Triton after 1 h (binding) or warmed to 37°C for an additional 1 h to allow internalization, then washed, trypsinized, and lysed (internalization) (Bart et al., 2018). The amounts of binding or internalized virus were determined by Western blotting.

## Mass Spectrometric Analysis

Mass spectrometric detection was performed on an AB Sciex API4000 Triple Quad rupole mass spectrometer running in positive ionization mode. Electrospray (ESI) voltage was set at 5.5 kV, source temperature at 0°C. Ion source gas 1 (desolvation gas-nitrogen) pressure was set at 15 psig, ion source gas 2

(nebulizer gas-nitrogen) at 10 psig, and curtain gas flow at 10 psig. Electron multiplier CEM was set at 2,000 V, and entrance potential was fixed at 10 V. The final concentration of PAP248–286 is 2 μg/ml, and tolcapone is 20 μg/ml. The mixture of PAP248–286 and tolcapone above was agitated at 1,400 rpm at 37°C in an Eppendorf Thermomixer before being detected by mass spectrometry.

## Zeta Potential Measurement

SEVI at 220 μM was treated with tolcapone at indicated concentrations. Mixtures were centrifuged for 10 min at 10,000 rpm. The pellets were resuspended in 1 ml of 1 mM potassium chloride (KCl). Zeta potential measurements were taken on a Zeta Nanosizer (Malvern, United Kingdom).

## Differential Scanning Fluorimetry

Zaire GP (after the deletion of MLD and TM domain) at 10 μM, buffered by the addition of 10 μl PBS at pH 4.0, was mixed with 5 μl of SYPRO Orange dye (Sigma) at a 1:200 dilution, along with 10 μl of tolcapone or favipiravir (1, 10, and 40 μM) in 10% dimethyl sulfoxide (DMSO) or just 10% DMSO. The mixture was made up to a total volume of 25 μl. Samples were placed in a semi skirted 96-well PCR plate, sealed, and heated on an LightCycler 480 instrument (Roche) from 37°C to 95°C at a rate of 1°C $\cdot min^{-1}$. Fluorescence changes were monitored with excitation and emission wavelengths at 465 and 580 nm, respectively. Reference wells, i.e., solutions without inhibitors, but with the same amount of DMSO, were used to compare the melting temperature ($T_m$). Experiments were carried out in triplicate. The data were processed by LightCycler® Thermal Shift Analysis.

## Cytotoxicity Assay

The cytotoxicity of tolcapone toward HeLa, A549, THP-1, and Huh-7 cells was evaluated using MTT assays (Tan et al., 2013). Briefly, approximately 90% confluent cells were plated in 96-well plates at $1 \times 10^5$/ml, and the plates were incubated at 37°C overnight. Different concentrations of tolcapone were added, and the cells were incubated for an additional 48 h at 37°C. Then, the culture supernatant was discarded, and 100 μl of 0.5 mg/ml MTT solution was added to the cells. After incubating the cells for an additional 4 h at 37°C, the supernatant was removed, and the formazan crystals formed were dissolved in 150 μl of DMSO. The absorbance of the resulting solution at 570 or 450 nm was measured using an ELISA reader. The 50% cytotoxicity concentration ($CC_{50}$) values were calculated.

## Computational Docking Analysis

Molecular docking calculations were conducted using the Vina protocol in Yinfo Cloud Platform[1]. The three-dimensional (3D) structure of compound tolcapone was constructed with energy minimization in MMFF94 force field. The crystal/NMR structure of PAP248–286 [RCSB Protein Data Bank (PDB) No. 2L3H] and Ebola GP [RCSB Protein Data Bank (PDB) No. 5JQ3] was downloaded from the RCSB Protein Data Bank[2]. The crystal ligand was separated and used to define the binding pocket. AutoDockVina (Trott and Olson, 2010) program was utilized to perform semi-flexible docking with maximum nine poses output after internal clustering.

[1]http://cloud.yinfotek.com/

[2]http://www.rcsb.org/

## Statistics Analysis

Statistical analysis of the experimental data was performed using a one-way or two-way analysis of variance (ANOVA) test in GraphPad Prism 5.0 (San Diego, CA, United States); $p$-values $< 0.05$ was considered as statistically significant; the probability level is indicated by single or multiple asterisks (*) (*$p < 0.05$; **$p < 0.01$; ***$p < 0.001$). All results were expressed as means ± standard deviation (SD) of three independent experiments.

# RESULTS

## Tolcapone Inhibits the Assembly of Semen-Derived Enhancer of Viral Infection Amyloid Fibrils

Tolcapone was firstly assessed for its effects on inhibiting the spontaneous amyloidogenesis of PAP248–286, the well-characterized seminal amyloidogenic peptide. The aggregation kinetics of PAP248–286 alone or in the presence of tolcapone was analyzed by Congo red binding assay. Congo red is an amyloid-binding specific dye. It can specifically bind with amyloid fibrils, resulting in increased optical absorbance proportional to the amount of fibrils (Nilsson, 2004). The amyloid fibrils growing curve should indicate three phases, including a lag phase, a fast growth phase, and a steady equilibrium phase. For the pure PAP248–286, the lag phase was negligible ($t_{lag}$ was around 0.06 h), and the growth phase remarkably turned to the equilibrium phase after 12 h (**Figure 1A**). However, co-incubation with different concentrations of tolcapone greatly increased the lag phase and lowered the maximum of optical absorbance compared to that of the PAP248–286 control (**Figure 1A**). The values of $t_{lag}$ were 6.20 h (tolcapone at 660 μM), 10.86 h (tolcapone at 1,320 μM), and 44.15 h (tolcapone at 2,640 μM). The results demonstrate that tolcapone could effectively inhibit PAP248–286 aggregation.

The conformational conversion of PAP248–286 in the absence or presence of tolcapone was analyzed by far-UV CD spectroscopy. As shown in **Figure 1B**, the CD spectrum of PAP248–286 with or without tolcapone at the time point of 4 h (left panel) presented a major negative peak at around 200 nm, implying a mainly random coil structure (Sarr et al., 2018). At the time point of 24 h (middle panel) and 48 h (right panel), the CD spectrum of PAP248–286 presented a major positive peak at ∼202 nm and a minor negative peak at ∼222 nm, which is a typical spectrum of the β-sheet-rich conformation. However, for the PAP248–286 sample that was co-incubated with tolcapone, the CD spectrum was much the same as that at the 4 h, a mainly random coil structure. The results suggest that tolcapone inhibits the structural transition of PAP248–286 from random coil to cross β-sheet structure.

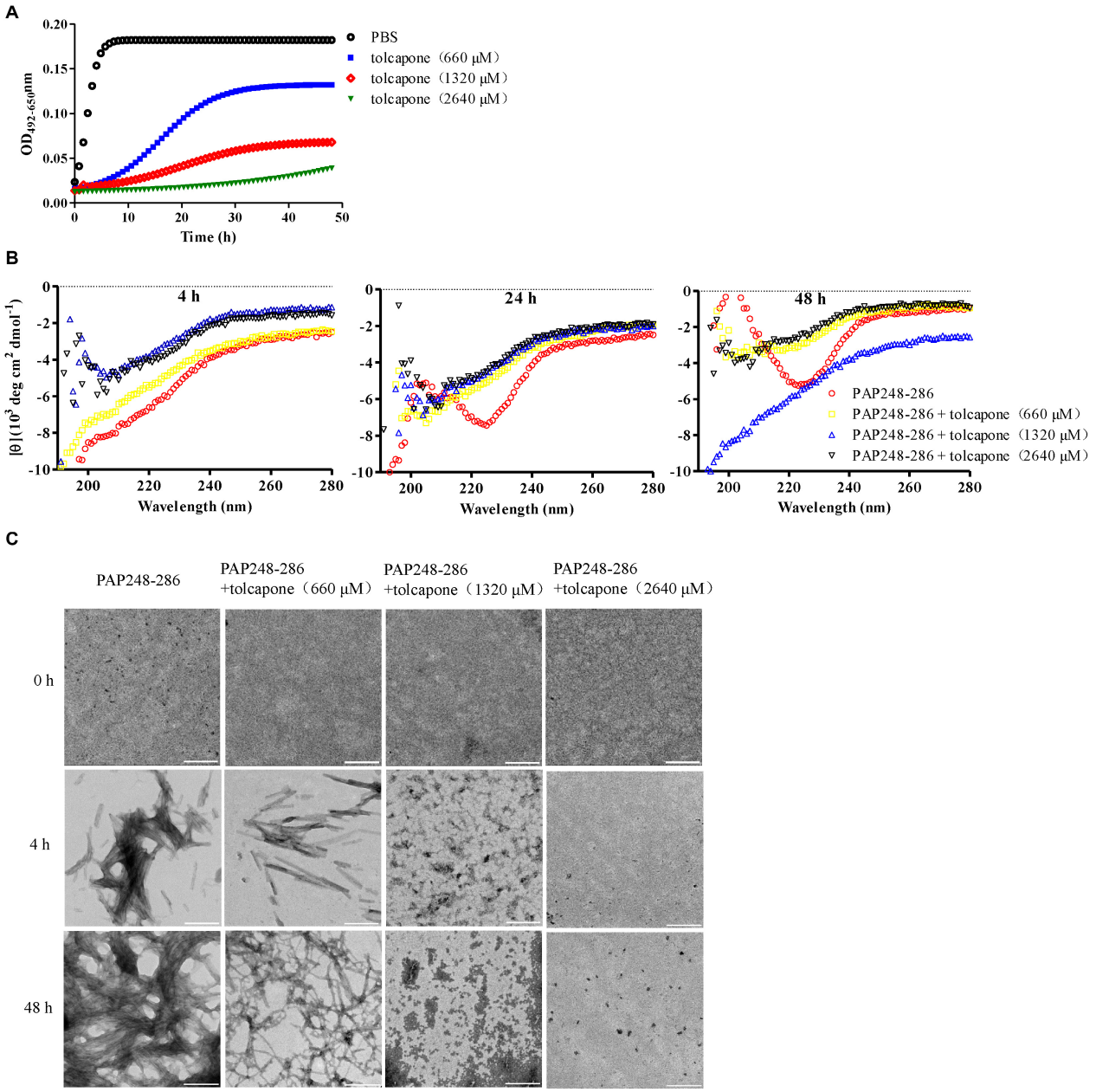


**FIGURE 1 |** Tolcapone inhibits the assembly of semen-derived enhancer of viral infection (SEVI) amyloid fibrils. **(A)** PAP248–286 (220 μM) was incubated with tolcapone (660, 1320, 2640 μM), and the mixture was agitated at 1,400 rpm at 37°C. Fibril formation was detected by Congo red staining at the indicated time points (0, 2, 4, 8, 12, 24, 48 h). The Congo red staining measurements were plotted as a function of time and fitted by a sigmoidal curve using Origin data analysis software to determine lag time ($t_{lag}$). **(B)** β-Sheet formation of SEVI fibrils was monitored by circular dichroism (CD) spectroscopy at the time point of 4, 24, and 48 h. SEVI was tested at 66 μM. The experiment was repeated once, and a similar result was obtained. **(C)** SEVI fibrils in the presence or absence of tolcapone at 0, 4, and 48 h were visualized by transmission electron microscopy (TEM). Scale bars indicate 200 nm.

In order to further investigate the inhibitory effect of tolcapone on PAP248–286 aggregation, the morphological changes of PAP248–286 fibers in the presence or absence of tolcapone were observed using TEM. Robust, abundant, and mature fibrils formed by PAP248–286 were identified after agitation for 48 h. However, after co-incubation with tolcapone, the aggregation products were only short and thinner protofibrils and amorphous aggregates. When incubated with 2,640 μM tolcapone, limited amyloid fibrils were visualized even after agitation for 48 h (**Figure 1C**).

Besides PAP248–286, other amyloidogenic peptides derived from semenogelins (SEMs), including SEM1 86–107, have also been reported to enhance HIV-1 and EBOV infection

(Roan et al., 2014; Bart et al., 2018). To investigate whether tolcapone also inhibits SEM1 86–107 aggregation, SEM1 86–107 was agitated in the presence of tolcapone, and the changes of absorbance of Congo red during incubation were monitored. Compared to PAP248–286, tolcapone could inhibit SEM1 86–107 fibrillogenesis at higher concentration compared to that for PAP248–286. Amyloid fibril formation of SEM1 86–107 could be partially inhibited by 15 times of tolcapone (**Supplementary Figure S1**). Taken together, the above results suggest that tolcapone effectively obstructed the fibrillogenesis of PAP248–286.

## Tolcapone Attenuates the Ability of Semen-Derived Enhancer of Viral Infection Fibrils to Enhance Pseudo-Ebola Virus Infection

It is reported that the fibrillar form of PAP248–286 aggregates, but not the monomer, possesses the ability to enhance EBOV infection (Bart et al., 2018). Therefore, we intended to determine whether enhancement of EBOV infection by PAP248–286 is lost in the presence of tolcapone, resulting from the inability of PAP248–286 to form fibrils. We first verified that mature SEVI fibrils could enhance EBOV infection in our EBOV/HIV-1_(NL4-3)Luc pseudoviral system, which is real mimicry of EBOV entry process and allowed to be used in a BSL-2 environment. The enhancement ability of SEVI on infection against Zaire PsV and Sudan PsV to various target cells during sexual transmission, including epithelium-derived HeLa and A549 cells, monocyte-derived THP1 cells, was examined. Human hepatocyte-derived Huh-7 cells, which represent the severely damaged target cell by EBOV infection, were also tested. Experiments were done with a low titer of virus to achieve optimal enhancing effect of SEVI. Our data demonstrated that SEVI enhanced both Zaire PsV (**Figure 2A**, left panel) and Sudan PsV (**Figure 2A**, right panel) infection of various cells lines. Next, we investigated whether tolcapone inhibited PAP248–286 fibril formation and, therefore, attenuated SEVI-induced enhancement of Ebola PsV infection. To eliminate the potential anti-EBOV activity of tolcapone itself, all the tolcapone-treated samples were centrifuged at 12,000 rpm for 5 min to remove the remaining free tolcapone. As expected, after agitating for 2–48 h, PAP248–286 effectively enhanced both Zaire PsV and Sudan PsV infection to various cell lines in a time-dependent manner, indicating an increase in fibril formation over time. In contrast, the PAP248–286 lost its ability to enhance pseudo-EBOV infection after agitation in the presence of various concentrations of tolcapone, and the effect was dose-dependent (**Figures 2B–E**).

SEVI has been well-documented to enhance HIV-1 infection. We also tested the antagonizing effects of tolcapone on SEVI-mediated HIV-1 infection. As shown in **Supplementary Figure S2**, tolcapone-treated PAP248–286 lost the ability to enhance both HIV-1 NL4-3 (X4-tropic) and HIV-1 SF162 (R5-tropic) infection even after agitation for 48 h. The results verify that tolcapone could effectively inhibit the conversion of PAP248–286 monomers to infection-promoting amyloids.

## Tolcapone Antagonizes the Assembly of Seminal Amyloid Fibrils

The effect of tolcapone on the fibrillogenesis of fresh semen, in which endogenous amyloid fibrils have been removed by centrifugation, was detected *via* the enhancement of fluorescence intensity upon the binding of the commonly used amyloid-specific ThT dye (Nilsson, 2004). We found that SE-F alone displayed a slight increase in fluorescence intensity, suggesting the presence of newly formed seminal fibrils. Of note, tolcapone dose-dependently inhibited the new formation of seminal fibrils in SE-F (**Figure 3A**). We further confirmed the inhibitory effects using TEM assay. Consistent with the results of the ThT assay, fresh SE-F could form amyloid fibrils. However, in the presence of tolcapone, limited newly formed amyloid fibrils could be found in SE-F after 8-h agitation (**Figure 3B**). We further examined whether tolcapone inhibited the infection-enhancing properties of human SE-F. To eliminate the potential anti-EBOV activity of tolcapone itself, all the tolcapone-treated samples were centrifuged at 12,000 rpm for 5 min to remove the remaining free tolcapone. SE-F samples could enhance the infection by Zaire PsV and Sudan PsV to HeLa cells. However, incubated with tolcapone, SE-F gradually lost the ability to enhance Zaire PsV and Sudan PsV infection (**Figure 3C**). The results show that tolcapone could inhibit the newly formed seminal amyloid fibrils of human SE.

## Tolcapone Inhibits Oligomerization of PAP248–286 Monomers

Seminal amyloid fibrils are distinct from other amyloid fibrils due to its positive charges. We found that tolcapone failed to inhibit the fibril formation of PAP248–286(Ala), a mutant peptide in which the positively charged lysines and arginines were replaced with neutral alanines (**Figure 4A**). The results suggested that the tolcapone might target the positive charged residues in PAP248–286 to prevent PAP248–286 aggregation. We next investigated whether a potential interaction between tolcapone and PAP248–286 might account for tolcapone's inhibitory activity on PAP248–286 aggregation. We found that after the co-incubation of tolcapone with PAP248–286, the level of PAP248–286 in the supernatant gradually decreased with increasing amounts of tolcapone, suggesting a binding of tolcapone with PAP248–286 (**Figure 4B**). Suramin, which has been shown to interact with PAP248–286 (Tan et al., 2019), was served as a positive control. We further applied mass spectrometry to examine the potential interaction between PAP248–286 and tolcapone. The parent ion of tolcapone has been detected at m/z 274.2 (**Supplementary Figure S3A**), and the parent ion of PAP248–286 was obtained at m/z 526.0 (**Supplementary Figure S3B**). When tolcapone was mixed with PAP248–286 at the molar ratio of 10:1, the parent ion for tolcapone alone or PAP248–286 alone could not be detected in the mass spectrometry of the mixture (**Supplementary Figure S3C**), which suggests a potential interaction between PAP248–286 and tolcapone.

In order to further validate the interaction between tolcapone and PAP248–286 at the atomic level, computational molecular docking analysis was conducted. The result showed that

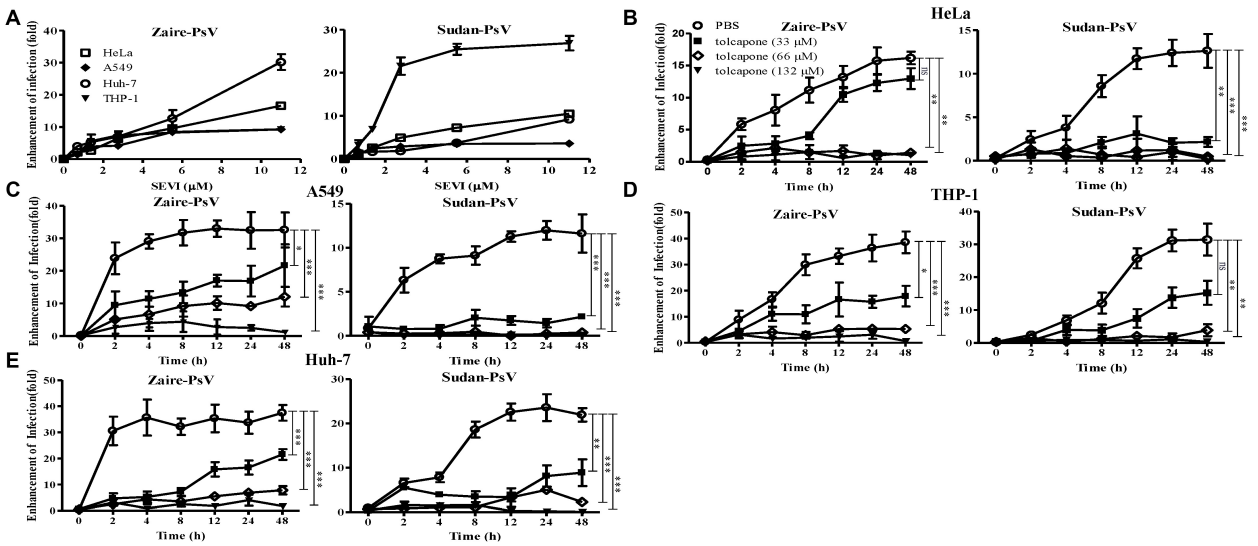


**FIGURE 2 |** Tolcapone attenuates the ability of semen-derived enhancer of viral infection (SEVI) fibrils to enhance pseudo-EBOV infection. **(A)** Increasing concentrations of mature SEVI fibrils were mixed with Zaire-pseudovirus (PsV) (left panel) and Sudan-PsV (right panel) at room temperature for 10 min, respectively. The mixtures were used to infect HeLa, A549, Huh-7, and THP-1 cells. Luciferase activities were determined 72 h later, and results are reported as *n*-fold enhancement of infection relative to that without SEVI. The data are represented as the mean ± SD of three independent experiments. **(B–E)** In the presence of tolcapone, PAP248–286 lost the ability to enhance Zaire-PsV (left panel) and Sudan-PsV (right panel) infection in various cells after agitation. PAP248–286 was agitated with tolcapone at various concentrations as described above. Pellets were collected at the indicated time points by centrifugation, which were then mixed with Zaire-PsV (left panel) and Sudan-PsV (right panel). Mixtures were then used to infect HeLa **(B)**, A549 **(C),** THP-1 **(D),** and Huh-7 **(E)** cells. Luciferase activities were determined 72 h later. The final concentration of SEVI was 11 μM. The data represent the mean ± SD of three independent experiments. $^{*}p < 0.05$; $^{**}p < 0.01$; $^{***}p < 0.001$; one-way ANOVA.

tolcapone binds to PAP248–286 and forms hydrogen bonds *via* ASN265 and ASN269 (**Figure 4C**). Besides, π–π interactions also existed in the PAP248–286–tolcapone complexes *via* LYS272, LEU258, and LEU268 (**Figure 4C**), forming strong electrostatic interactions. Of note, PAP248–253, PAP260–270, and PAP279–286 have been shown to be the amyloidogenic region with high fibril-forming propensity (Castellano and Shorter, 2012; Elias et al., 2014; Li et al., 2019). Tolcapone interacts with PAP248–286 by occupying the key residues in the amyloidogenic region of PAP248–286 and positive residue (**Figures 4A,C**), which might be responsible for the inhibitory effects of tolcapone on PAP248–286 aggregation.

The presence of low-n-order oligomers during the early stages of fibril assembly suggests a lag phase in fibril formation. Preventing the protein oligomerization has been shown a treatment option to inhibit amyloidogensis. We therefore used PICUPs to determine whether tolcapone prevents PAP248–286 monomer oligomerization. It was found that tolcapone significantly inhibited oligomerization of PAP248–286 dose-dependently. In the presence of cross-linking chemicals, the PAP248–286 monomer, which was used as a positive control, predominantly existed as a mixture of oligomers on the order of 2–10. The oligomerization of PAP248–286 (220 μM) did not proceed to completion in the presence of 30 μM of tolcapone (**Figure 4D**). As a negative control, suramin did not inhibit the early oligomerization of PAP248–286 (**Figure 4E**). The result suggests that tolcapone targeted the monomeric PAP248–286 and prevented its assembly into any sized oligomer.

## Tolcapone Modifies the Surface Charge of Semen-Derived Enhancer of Viral Infection and Blocks Amyloid-Induced Enhancement of Viral Infection

The positive surface charge of SEVI fibril contributes to the facilitation of virion attachment to target cells and enhancement of viral infection. Thus, we investigated whether negatively charged tolcapone attenuates the interaction between SEVI fibrils and viruses. Zeta potential could be applied to determine the surface charge of a particle in solution. Tolcapone neutralized SEVI's surface positive charge due to the fact that tolcapone significantly decreased the zeta potential of SEVI fibrils in a dose-dependent manner (**Figure 5A**). Tolcapone significantly influenced SEVI's activity in enhancing infection of Zaire PsV and Sudan PsV by blocking the formation of virion–amyloid complexes. Mature SEVI fibrils were pretreated with tolcapone at 37°C for 15 min. Pellets were collected by centrifugation to remove the free tolcapone and then subjected to viral infection experiments. With increasing concentrations of tolcapone, mature SEVI fibrils gradually lost the ability to enhance Zaire PsV and Sudan PsV infection (**Figure 5B**). We next determined whether tolcapone inhibited the activity of endogenous mature fibrils in semen. The fresh SE-F was agitated at 37°C for 2 h to allow the newly formed amyloid fibrils. Then, the agitated SE-F was mixed with tolcapone at 37°C for 15 min. Mixtures were then centrifuged at 12,000 rpm for 5 min to collect the fibrils, which were

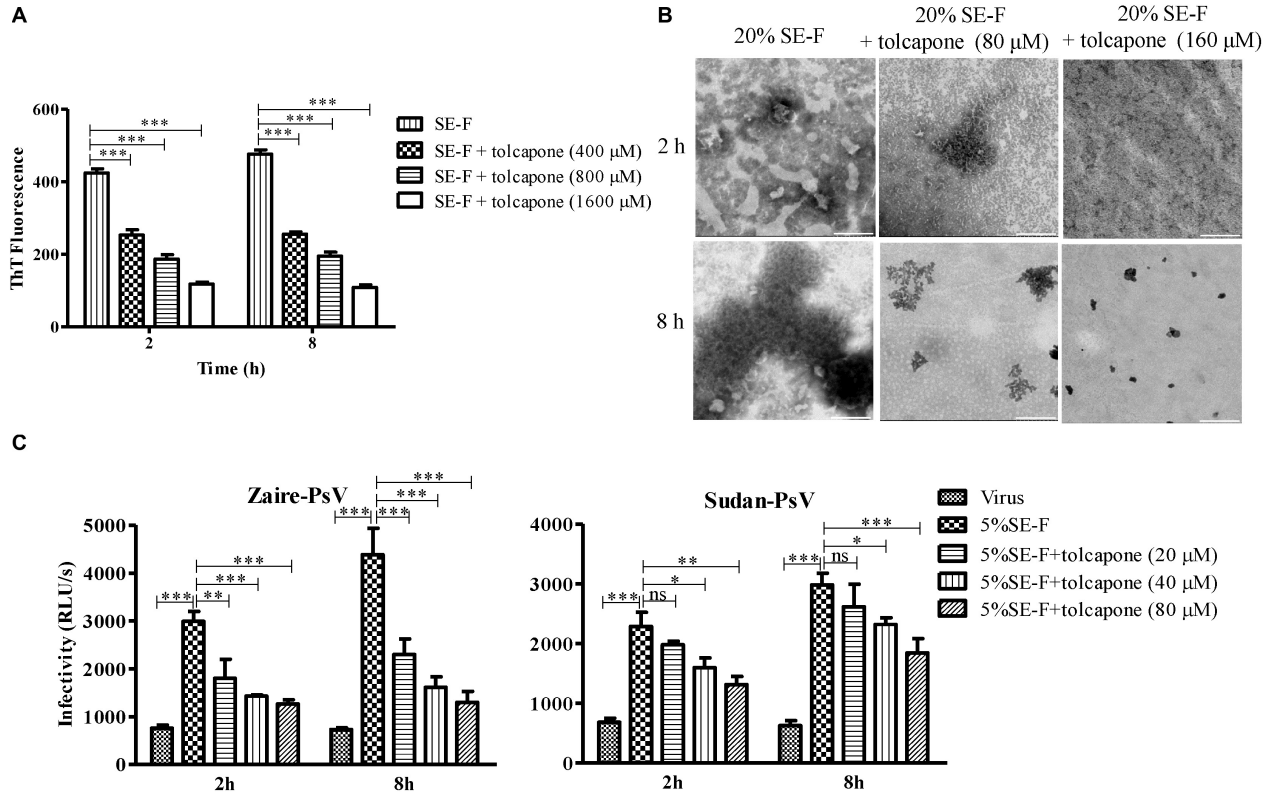


**FIGURE 3 |** Tolcapone antagonizes the assembly of endogenous seminal amyloid fibrils. **(A)** Seminal amyloid fibril formation was antagonized by tolcapone in a dose-dependent manner. Fresh seminal fluid (SE-F) samples with tolcapone (0, 400, 800, and 1,600 μM) were agitated at 1,400 rpm at 37°C for 8 h. Fibril integrity at 2 and 8 h was detected by thioflavin T (ThT) assay. The data represent the mean ± SD of three independent experiments. *$p < 0.05$; **$p < 0.01$; ***$p < 0.001$; two-way ANOVA. **(B)** Samples of seminal fibrils (1:5 dilutions) in the presence or absence of tolcapone (80 and 160 μM) after agitation for 2 and 8 h were visualized by transmission electron microscopy (TEM). Scale bars indicate 200 nm. **(C)** SE-F in the presence of tolcapone at the graded concentrations was agitated to allow fibril formation. The fibrils in the pellet were tested on their abilities to infect Zaire-PsV (left panel) and Sudan-PsV (right panel) in HeLa after 72 h. SE-F was finally diluted 20-fold. Shown are means ± SD of three independent experiments. *$p < 0.05$; **$p < 0.01$; ***$p < 0.001$; two-way ANOVA.

used to determine their abilities to enhance Zaire PsV and Sudan PsV infection. It was shown that the newly formed amyloid fibrils in SE-F could greatly enhance both Zaire PsV (**Figure 5C**, left panel) and Sudan-PsV (**Figure 5C**, right panel) infection to HeLa cell. However, tolcapone significantly blocked endogenous seminal fibril-mediated enhancement of Zaire PsV (**Figure 5C**, left panel) and Sudan-PsV (**Figure 5C**, right panel) infection to HeLa cell.

## Tolcapone Antagonizes Semen-Derived Enhancer of Viral Infection-Induced Enhancement of Zaire Pseudovirus Binding and Internalization in HeLa Cells

It is reported that SEVI-mediated enhancement of EBOV infection was involved in the promotion of viral binding and internalization (Bart et al., 2018). We first confirmed whether SEVI could enhance Zaire PsV binding and internalization in HeLa cells. Zaire PsV was pre-incubated with SEVI before binding to HeLa cells on ice for 1 h to test the binding ability or shifted to 37°C for an additional hour to permit internalization. Lysates were analyzed by Western blotting, and signal in the presence of SEVI was compared with Zaire PsV binding/internalization in the absence of SEVI. When incubated at 4°C, in which Ebola pseudoviruses could only bind to cells but not be internalized in cells because of deficiency of energy required for entry, SEVI could dose-dependently enhance Zaire PsV binding to HeLa cells (**Figure 6A**). Similarly, when incubated at 37°C after binding, the internalization of Zaire PsV in HeLa cells was dose-dependently increased (**Figure 6B**). The result confirmed that SEVI enhanced EBOV binding and internalization of HeLa cells.

Then, we determined whether tolcapone could antagonize SEVI-mediated enhancement of viral binding and internalization. Tolcapone was incubated with mature SEVI at 37°C for 15 min, and the tolcapone-bound fibrils were collected by centrifugation, which were then used to test their abilities to bind and internalize virus as described above. Tolcapone could dose-dependently decrease the enhancement of Zaire PsV binding (**Figure 6C** and **Supplementary Figure S4**) to HeLa cells and subsequent internalization (**Figure 6D** and **Supplementary Figure S5**) in HeLa cells.

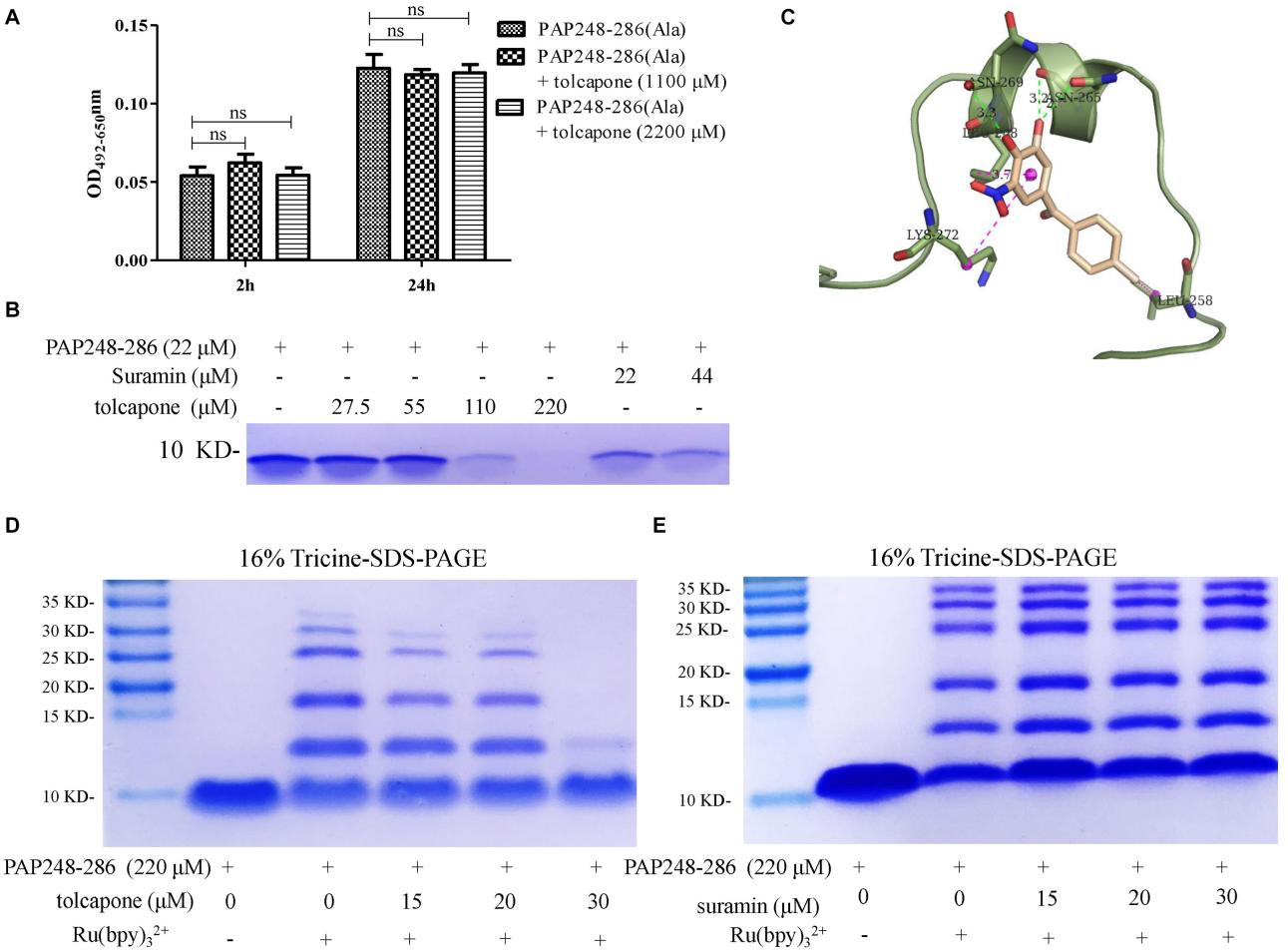


**FIGURE 4 |** Tolcapone inhibits oligomerization of PAP248–286 monomers. **(A)** PAP248–286(Ala) (220 μM) were agitated with or without tolcapone. Fibril formation was detected by Congo red staining at 2 and 24 h. The data represent means ± SD of three independent experiments. **(B)** PAP248–286 at 22 μM was incubated with tolcapone or suramin at different concentrations at 37°C for 30 min. The remaining free PAP248–286 in the supernatants after centrifugation at 5,000 rpm for 10 min was recognized by Coomassic blue. **(C)** Presumed binding sites of tolcapone to PAP248–286. According to the computational docking results, tolcapone formed hydrogen bonds with ASN265 and ASN269, and it bound to LYS272, LEU258, and LEU268 by π–π interactions. **(D)** The effects of tolcapone on the oligomerization of PAP248–286 were assessed using 16% tricine-sodium dodecyl sulfate (SDS)-polyacrylamide gel electrophoresis (PAGE) and Coomassie blue staining. PAP248–286 monomer at 220 μM with or without cross-linking served as the control. **(E)** Suramin showed no ability to inhibit the oligomerization of PAP248–286.

## Tolcapone Is a Potent Entry Inhibitor of Both Zaire Pseudovirus and Sudan Pseudovirus

Interestingly, when we tested tolcapone alone with the pseudoviruses, we found that tolcapone had anti-EBOV entry activity. Pseudoparticles were exposed to tolcapone and then added to various cells. Infection rates were measured 72 h later by quantifying luciferase activity. The results showed that tolcapone efficiently blocked infection by both tested pseudoparticles in various cell lines. The half-maximal inhibitory concentrations ($IC_{50}$) of tolcapone against the two pesudoviruses were similar and ranged between 1.41 and 8.76 μM for Sudan PsV and 2.99 and 4.33 μM for Zaire PsV (**Figures 7A–D** and **Table 1**). In contrast, a VSV-G pseudotyped virus expressing the VSV-G envelope and HIV-1 Env pseudotyped viruses, including HIV-1 HXB2 (X4 strain) and HIV-1 JR-FL (R5 strain), were used as negative control to evaluate the specificity of tolcapone for the EBOV envelope. Tolcapone could not effectively inhibit the infection against VSV-G pseudovirus and HIV-1 pseudoviruses at concentrations below 100 μM (**Figure 7E**), which suggested that tolcapone might be an EBOV entry inhibitor that targets EBOV envelope proteins specifically.

EBOV has a membrane envelope decorated by trimers of a GP (cleaved by furin to form GP1 and GP2 subunits) which is solely responsible for host cell attachment, endosomal entry, and membrane fusion. GP is thus a primary target for the development of antiviral drugs. Differential scanning fluorimetry (DSF) was performed to evaluate the potential

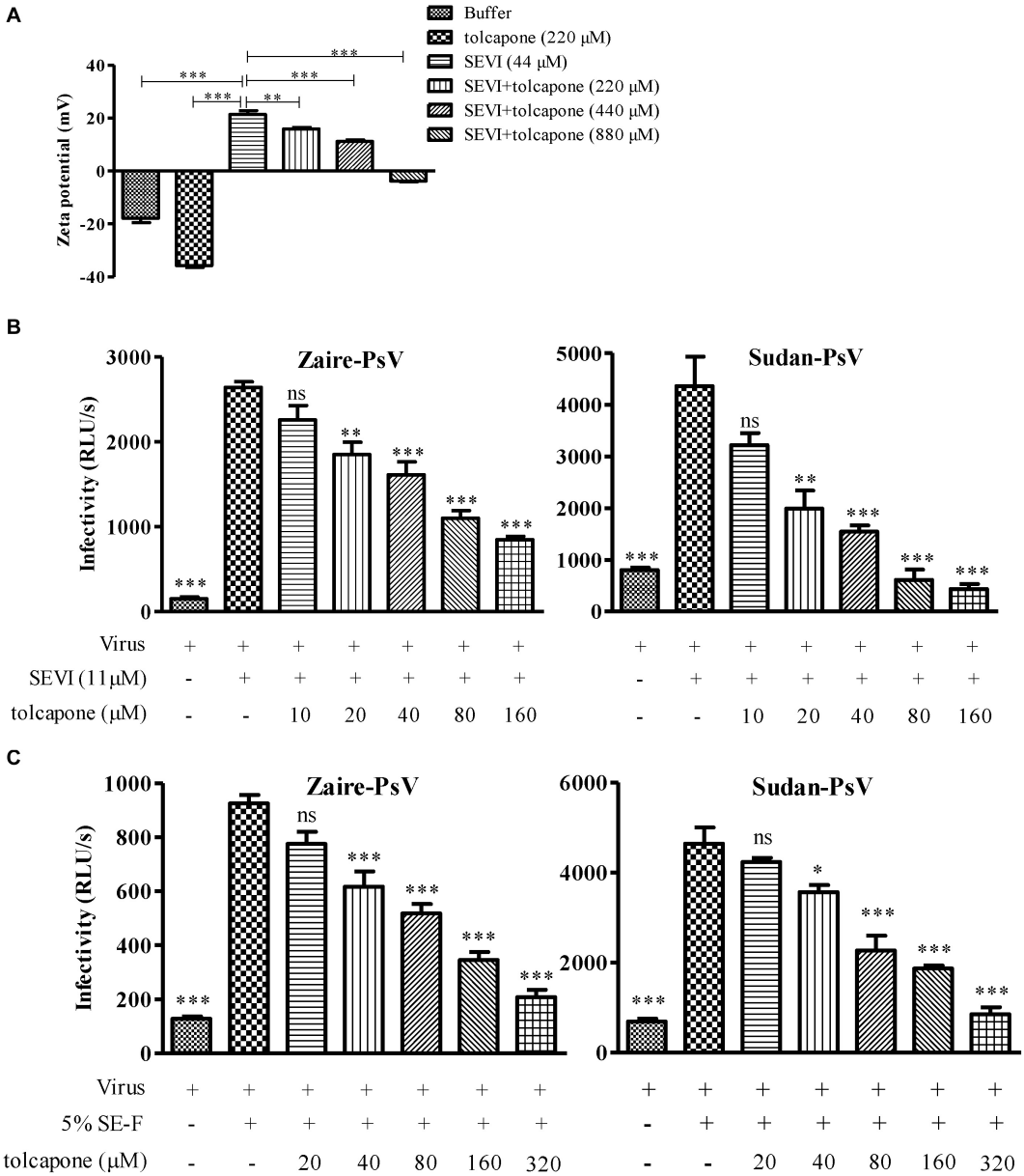


**FIGURE 5 |** Tolcapone modifies the surface charge of semen-derived enhancer of viral infection (SEVI) and blocks amyloid-induced enhancement of viral infection. **(A)** Zeta potential of SEVI fibrils in the presence or absence of tolcapone. The results are the average values ± SD ($n = 3$). *$p < 0.05$; **$p < 0.01$; ***$p < 0.001$; one-way ANOVA. SEVI **(B)** or agitated seminal fluid (SE-F) **(C)** was incubated with tolcapone at the indicated concentrations or phosphate buffered saline (PBS) for 15 min at 37°C. The mixtures were centrifuged, and the pellets were then incubated with Zaire-pseudovirus (PsV) (left panel) or Sudan-PsV (right panel), respectively. Infection of HeLa cells by measuring luciferase activity as described above 72 h post-infection. The data represent the mean ± SD of three independent experiments. *$p < 0.05$; **$p < 0.01$; ***$p < 0.001$; one-way ANOVA.

interaction between tolcapone and EBOV GP trimer. DSF is a commonly used approach for detecting protein–ligand interactions. Upon binding to a folded protein, ligands stabilize the protein; thus, detecting an increase in the temperature at which the protein unfolds as a function of ligand concentration can serve as evidence of a direct interaction (Bai et al., 2019; Forneris et al., 2009). As shown in **Supplementary Figure S6A**, binding of 40 μM tolcapone to Zaire GP led to a shift of the $T_m$ by 4.75°C. In contrast, the $T_m$ of the mixture of favipiravir (RNA-dependent RNA polymerase inhibitor) and Zaire GP (after the deletion of MLD and TM domain) had no significant change (**Supplementary Figure S6B**).

To further explore the binding mode of tolcapone with Zaire GP, we used computational molecular docking to simulate the binding of tolcapone to EBOV GP and analyzed

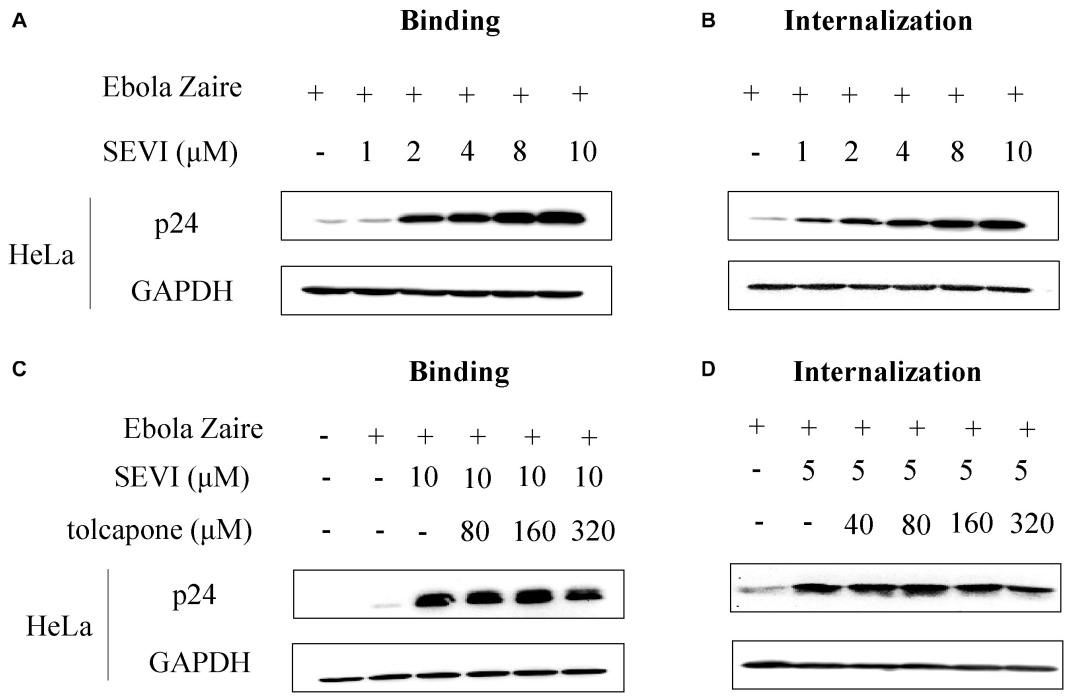


**FIGURE 6 |** Tolcapone inhibits semen-derived enhancer of viral infection (SEVI)-induced enhancement of binding and internalization of Zaire-pseudovirus (PsV) to HeLa cells. Zaire-PsV was incubated with SEVI **(A,B)** or tolcapone-treated SEVI **(C,D)** then bound to HeLa cells on ice. Cells were either lysed in 1% Triton for 10 min on ice after 1 h (binding) **(A,C)** or warmed to 37°C for 1 h to allow viral internalization, washed with phosphate buffered saline (PBS), trypsinized, and lysed with 1% Triton (internalization) **(B,D)**. Lysates were used for determination of the level of p24 by Western blotting.

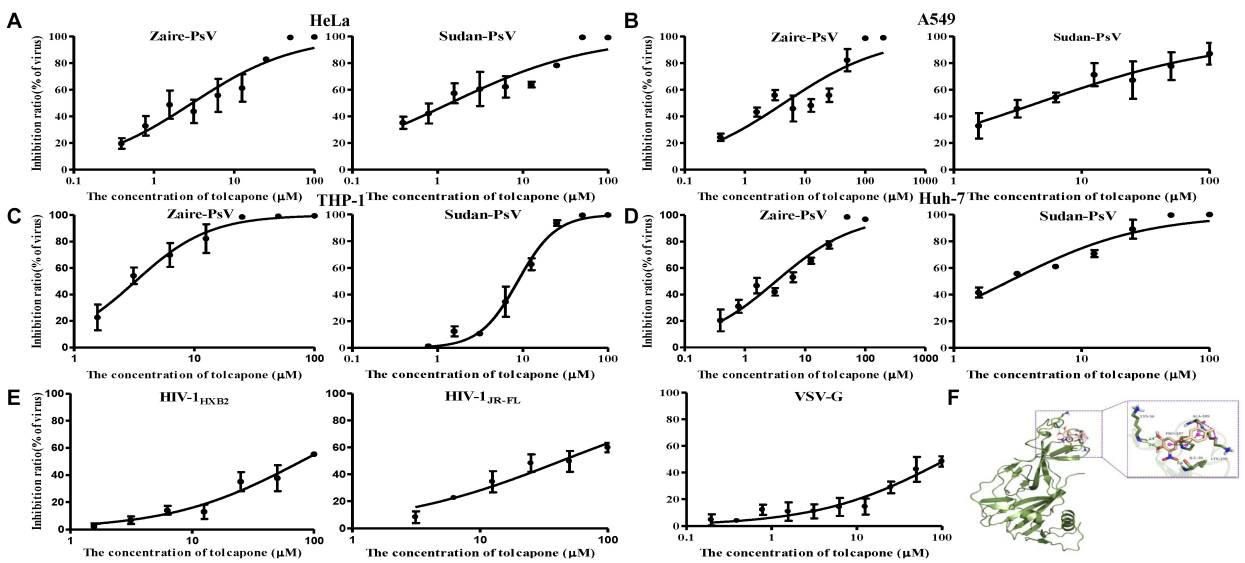


**FIGURE 7 |** Tolcapone was a potent entry inhibitor of both Zaire PsV and Sudan PsV. The indicated concentrations of tolcapone were incubated with Zaire-PsV (left panel) or Sudan-PsV (right panel), respectively, for 30 min at room temperature. The mixtures were then added to prepared **(A)** HeLa, **(B)** A549, **(C)** THP-1, and **(D)** Huh-7 cells. Luciferase activities were measured at 72 h post-infection. Each sample was tested in triplicate, and the data are presented as the mean ± SD. **(E)** % Inhibition of HIV-1HXB2 (left panel), HIV-1JR-FL (middle panel), and VSV-G (right panel) infection by tolcapone. **(F)** Presumed binding sites of tolcapone to Ebola glycoprotein. According to the computational docking results, tolcapone formed hydrogen bonds with LYS56 and ILE38, and it bound to LYS190, ALA189, and PRO187 by hydrophobic interactions.

its possible binding sites. As shown in **Figure 7F**, tolcapone binds to EBOV GP, and they form hydrogen bonds *via* LYS56 and ILE38, and it bound to LYS190, ALA189, and PRO187 by hydrophobic interactions, which were consistent with the binding sites of inhibitors in related studies (Zhao et al., 2016).

## Tolcapone Exhibited a Synergistic Effect in Combination With Other Entry Inhibitor-Based Antivirals Against Zaire Pseudovirus Infection in Semen

Two FDA-approved drugs, sertraline (Zoloft) and bepridil (Vascor), have been shown to have both strong *in vitro* and *in vivo* anti-EBOV activity (Johansen et al., 2015). Sertraline is a selective serotonin reuptake inhibitor, and bepridil is a calcium channel blocker, both of which affect the fusion process late in the entry pathway. As shown in **Table 2** and **Supplementary Figure S7**, combining tolcapone and bepridil in SE resulted in synergistic inhibitory activity against Zaire PsV infection in HeLa cells with CI values of 0.372 for 50% inhibition, including potency enhancement of 40.72-fold for bepridil and 2.88-fold for tolcapone. Combining tolcapone and sertraline resulted in strong synergistic inhibitory activity against Zaire PsV infection with CI values of 0.151 for 50% inhibition, including potency enhancement of 61.69-fold for sertraline and 7.4-fold for tolcapone. These results suggest that tolcapone and other entry inhibitors could be used in combination to enhance anti-EBOV activity.

**TABLE 1 |** Entry-inhibitory activity of tolcapone against Zaire PsV and Sudan PsV in various cell lines[a].

| Cell lines | Zaire PsV Sudan PsV |
|---|---|
| | $IC_{50}$ (μM) $IC_{50}$ (μM) |
| HeLa | 2.99 ± 1.33 1.41 ± 0.74 |
| A549 | 4.33 ± 2.26 4.49 ± 1.70 |
| THP-1 | 3.24 ± 0.78 8.76 ± 1.23 |
| HuH-7 | 3.29 ± 0.99 2.72 ± 0.61 |

[a]*Each sample was tested in triplicate, and the experiment was repeated three times. Data are presented as the mean ± SD.*

## Tolcapone Showed Low Cytotoxicity *in vitro*

The potential cytotoxic effects of tolcapone on EBOV target cells (Huh-7 cell, THP-1, and A549 cells) and reproductive tract epithelial cells (HeLa cell) were evaluated using MTT assays. Tolcapone displayed low cytotoxicity *in vitro* toward all cells lines tested, with 50% cytotoxic concentration ($CC_{50}$) values ranging from 169.3 to 324.8 μM (**Figure 8** and **Table 3**). The selectivity index ($SI = CC_{50}/IC_{50}$) ranged from 52 to 98 (**Table 3**), suggesting that tolcapone might be safe for use *in vivo*.

# DISCUSSION

Outbreaks of EVD are responsible for recent global health threats by causing many thousands of deaths and widespread disruption in the regions where the virus emerges. EBOV burden is directly associated with the rate of transmission. Although virus persisting in the semen has been well documented (Rodriguez et al., 1999; Bausch et al., 2007), little was known of its infectiousness. The role of sexual transmission of EBOV was recently confirmed in 2015 with the fact that at least one fatal case of EVD was contracted through sexual intercourse from a male survivor (Mate et al., 2015), and half of the Ebola outbreak flare-ups reported between 2015 and 2016 was likely associated with sexual transmission (Subissi et al., 2018). Recently, seminal amyloid fibrils, potential important host factors that facilitate EBOV sexual transmission, have been identified (Bart et al., 2018). Seminal amyloids greatly enhance EBOV infection and stabilize viral infectivity, thus, they are potential targets for intervention to prevent EBOV sexual transmission. Long-term persistence of infectious virus (Crozier, 2016; Diallo et al., 2016; Sow et al., 2016; Deen et al., 2017) and the infection-enhancing amyloids in semen underscore the critical need to develop rapid antiviral and anti-amyloid countermeasures to prevent virus transmission during unprotected sexual intercourse.

Although there has been great progress in developing anti-EBOV agents, to date, limited countermeasures were available to block EBOV sexual transmission. In this study, we found that tolcapone was a novel bifunctional topical

**TABLE 2 |** Combination index and dose reduction values for entry inhibition of Zaire-PsV infection by combining tolcapone with entry-inhibitory antivirals in semen.

| Drug combination, %Inhibitory Conc. (Molar ratio) | CI[a] | Tolcapone | | | Entry-inhibitory antivirals | | |
|---|---|---|---|---|---|---|---|
| | | $IC_{50}$(nM)[b] Alone | Mixture | Dose reduction (Fold) | $IC_{50}$(nM)[b] Alone | Mixture | Dose reduction (Fold) |
| **Tolcapone:Bepridil (133:1)** | | | | | | | |
| 50 | 0.372 | 2637.62 | 915.67 | 2.88 | 279.74 | 6.87 | 40.72 |
| 90 | 0.216 | 29044.10 | 5619.65 | 5.17 | 1844.83 | 42.15 | 43.77 |
| **Tolcapone:Sertraline (100:1)** | | | | | | | |
| 50 | 0.151 | 2637.62 | 356.26 | 7.40 | 219.63 | 3.56 | 61.69 |
| 90 | 0.534 | 29044.10 | 13009.00 | 2.23 | 1514.23 | 130.09 | 11.64 |

[a]*CI, combination index.* [b]*Data are the means of two independent experiments performed in triplicate.*

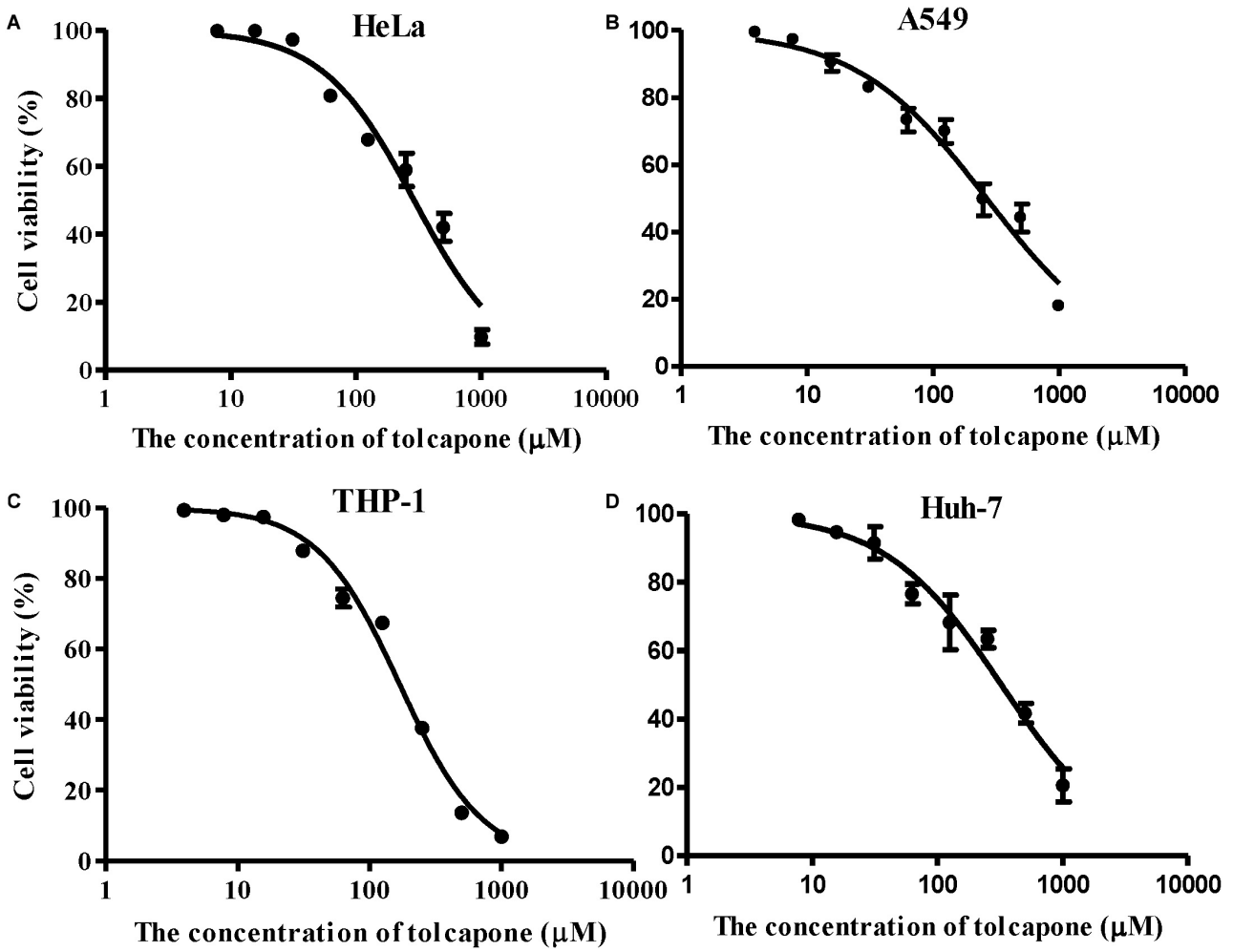


**FIGURE 8 |** Cytotoxicity of tolcapone *in vitro*. **(A)** HeLa, **(B)** A549, **(C)** THP-1, and **(D)** Huh-7 cells. The concentrations of tolcapone were double diluted from 1,000 to 7.81 μM. Cytotoxicity was evaluated by 3-(4,5-dimethylthiazol-2-yl)-2,5-diphenyltetrazolium bromide (MTT) assay.

agent counteracting sexual EBOV transmission both through targeting the infection-enhancing effects of amyloids in semen and by inhibiting virus entry. Tolcapone binds with amyloidogenic PAP248–286 and inhibits SEVI fibril formation (**Figures 1**, **4B**), which results in the deficiency of PAP248–286 and fresh SE-F to enhance pseudo-EBOV infection (**Figures 2**, **3**). Tolcapone also interacts with the mature amyloid fibrils and blocks fibril-mediated enhancement of pseudo-EBOV infection (**Figure 5**). More importantly, tolcapone antagonizes fibril-induced increase in binding and internalization of Zaire PsV in HeLa cells (**Figures 6C,D**). Tolcapone was found here to possess a dual mechanism of action on semen-derived amyloid fibrils and prevent the enhancement of EBOV sexual transmission by seminal fibrils.

Although tolcapone was found previously to have anti-EBOV activity by interfering with complex of the viral protein 35 (VP35) and nucleoprotein (NP), which is critical for viral RNA synthesis (Liu et al., 2017), we report here for the first time that tolcapone is also an effective EBOV entry inhibitor. Viral entry inhibitors are valuable as treatment options since blocking infection early in the life cycle will reduce cellular and tissue damage associated with the replication of incoming viruses. Tolcapone was shown to exhibit inhibitory activities against two pseudotyped viruses with values of $IC_{50}$ ranging from 1.41 to 8.76 μM in various cell lines

**TABLE 3 |** Cytotoxicity *in vitro* and selective index values of tolcapone against all tested cells[a].

| Cell lines | Category | $CC_{50}$ (μM) | $IC_{50}$ (μM) | SI |
|---|---|---|---|---|
| HeLa | Reproductive cancer cells | 292.6 ± 41.6 | 2.99 ± 1.33 | 97.86 |
| A549 | Lung carcinoma cells | 266.1 ± 34.3 | 4.33 ± 2.26 | 61.45 |
| THP-1 | Human macrophages | 169.3 ± 14.5 | 3.24 ± 0.78 | 52.25 |
| HuH-7 | Hepatoma cells | 324.8 ± 48.8 | 3.29 ± 0.99 | 98.72 |

[a] *The assay was performed in triplicate; Data are presented as the mean ± SD.*

(**Table 1** and **Figure 7**). Among several pseudotyped virions with different envelopes, tolcapone specifically inhibits pseudo-EBOV infection (**Figure 7E**). The GP of EBOV has been considered the only viral factor that mediates viral entry (Hunt et al., 2012). Our results showed that tolcapone binds with the GP trimer and inhibits viral entry (**Supplementary Figure S6** and **Figure 7F**). Of note, tolcapone also exhibited synergistic effects with two small-molecule entry inhibitors of EBOV (**Table 2**) in semen, suggesting that tolcapone could be used alone or in combination to augment the antiviral potency and increase barriers against the development of drug resistance. Moreover, we evaluated the potential safety of tolcapone as a candidate microbicide. Our results showed that tolcapone displayed little cytotoxicity toward all tested cell lines *in vitro* (**Table 3**).

Several agents have been found in the past decade to minimize the viral infection-enhancing activity of semen amyloids in the context of stopping HIV-1 sexual transmission (Capule et al., 2012; Lump et al., 2015; Xun et al., 2015; LoRicco et al., 2016; Tan et al., 2019). However, most of them are at the stage of preclinical research. Tolcapone, shown in this study, is a repositioned compound with a newly identified activity as a potent SEVI fibril inhibitor and an EBOV entry inhibitor. It has been used in human and confirmed *in vivo* safety (Olanow and Watkins, 2007; Eggert et al., 2014). As a repositioned drug, tolcapone can bypass much of the early cost and time required to bring a drug to market. Compared to suramin, another repositioned compound that has been demonstrated to have anti-SEVI activity by us previously (Tan et al., 2019), tolcapone requires higher concentrations to inhibit PAP248–286 aggregation, which might potentially result from the fact that it possesses lower number and density of negatively charged residues. However, the abundant negative charge might imply non-specific binding in the human body and decrease the suitability for *in vivo* use. Moreover, our PICUP studies revealed that tolcapone inhibited PAP248–286 aggregation by the mechanism of disrupting PAP248–286 oligomerization at the early stage of fibrillogenesis, while suramin did not interfere with PAP248–286 oligomerization (**Figures 4D,E**). Suramin only coats on PAP248–286 and creates a steric barrier to block PAP248–286 interaction. It would therefore be expected that the most efficacious therapeutic agents would be those that block the early assembly processes associated with amyloid protein oligomerization.

Considering EVD outbreak and HIV-1, another important sexually transmitted pathogen, both prevalent in Africa, exploring bifunctional agent by targeting EBOV and seminal amyloids is of particular importance. The interplay between HIV and EBOV is not exactly known. However, the available literature verifies that EVD outbreak adversely affects the diagnosis and treatment of HIV/AIDS. Due to the interruption of routine health delivery services during the EBOV outbreak (Hira and Piot, 2016; Nagel et al., 2019), the chance of transmission and the number of prevalence and deaths caused by HIV/AIDS increased (Hira and Piot, 2016; Jacobs et al., 2017; Leno et al., 2018; Subissi et al., 2018; Nagel et al., 2019). Furthermore, HIV-positive EVD survivors have been documented and HIV-1 might play a role in supporting EBOV persistence in semen (Purpura et al., 2017). The situation of co-infection of HIV-1 and EBOV might be neglected due to the incomplete medical record. Seminal amyloids could enhance both HIV-1 and EBOV infection. Bifunctional agent by targeting EBOV and seminal amyloids might simultaneously inhibit EBOV and HIV-1 sexual transmission. Our results show that tolcapone could antagonize SEVI-mediated enhancement of EBOV and HIV-1 infection (**Figure 2** and **Supplementary Figure S2**).

An important limitation of the present study is the inability to study the inhibitory effects with infectious EBOV. Because of its lethality, EBOV can only be handled in laboratories with biosecurity level-4 containment. Therefore, only few laboratories in the world can conduct EBOV research using the authentic virus (Dhama et al., 2018). Evaluation of the inhibitory effects of tolcapone on semen-mediated enhancement of infection against infectious EBOV strain is warranted.

## CONCLUSION

Exhibiting both excellent anti-amyloid and anti-EBOV effects, tolcapone might represent a prophylactic supplement or a lead product for the design of combination microbicide candidates to reduce the sexual transmission of EBOV.

## DATA AVAILABILITY STATEMENT

All datasets generated for this study are included in the article/**Supplementary Material**.

## ETHICS STATEMENT

Semen (SE) samples were obtained from healthy lab members with written informed consent in accordance with the Declaration of Helsinki and the study was approved by the Human Ethics Committee of Southern Medical University, China. The patients/participants provided their written informed consent to participate in this study.

## AUTHOR CONTRIBUTIONS

ST and SL conceived and designed the project. MQ, ZL, and YC performed the experiments and analyzed the data. JG and JP performed the mass spectrometric analysis. TQ and YQ collected semen samples. ZL and WX performed the DSF. LL and SL discussed the results and commented on the manuscript. ST and MQ wrote the manuscript.

## FUNDING

This work was supported by grants from the National Natural Science Foundation of China (81772194 to ST and

81773787 to SL), the Natural Science Foundation of Guangdong Province (2017A030313598 to ST, 2015A030313241 to ST and 2018A030313056 to WX), the National S&T Key Special Foundation (2018ZX10301101 to SL), and Guangzhou Science and Technology Program (201904010477 to WX).

## SUPPLEMENTARY MATERIAL

The Supplementary Material for this article can be found online at: https://www.frontiersin.org/articles/10.3389/fmicb.2020.00504/full#supplementary-material

## REFERENCES


Arnold, F., Schnell, J., Zirafi, O., Stürzel, C., Meier, C., Weil, T., et al. (2012). Naturally occurring fragments from two distinct regions of the prostatic acid phosphatase form amyloidogenic enhancers of HIV infection. *J. Virol.* 86, 1244–1249. doi: 10.1128/JVI.06121-6111

Bai, N., Roder, H., Dickson, A., and Karanicolas, J. (2019). Isothermal analysis of thermofluor data can readily provide quantitative binding affinities. *Sci. Rep.* 9:2650. doi: 10.1038/s41598-018-37072-x

Barnes, K. G., Kindrachuk, J., Lin, A. E., Wohl, S., Qu, J., Tostenson, S. D., et al. (2017). Evidence of ebola virus replication and high concentration in semen of a patient during recovery. *Clin. Infect. Dis.* 65, 1400–1403. doi: 10.1093/cid/cix518

Bart, S. M., Cohen, C., Dye, J. M., Shorter, J., and Bates, P. (2018). Enhancement of Ebola virus infection by seminal amyloid fibrils. *Proc. Natl. Acad. Sci. U.S.A.* 115, 7410–7415. doi: 10.1073/pnas.1721646115

Bausch, D. G., Towner, J. S., Dowell, S. F., Kaducu, F., Lukwiya, M., Sanchez, A., et al. (2007). Assessment of the risk of Ebola virus transmission from bodily fluids and fomites. *J. Infect Dis.* 196(Suppl. 2), S142–S147. doi: 10.1086/520545

Capule, C. C., Brown, C., Olsen, J. S., Dewhurst, S., and Yang, J. (2012). Oligovalent amyloid-binding agents reduce SEVI-mediated enhancement of HIV-1 infection. *J. Am. Chem. Soc.* 134, 905–908. doi: 10.1021/ja210931b

Castellano, L. M., and Shorter, J. (2012). The surprising role of amyloid fibrils in HIV infection. *Biology* 1, 58–80. doi: 10.3390/biology1010058

Chan, S. Y., Speck, R. F., Ma, M. C., and Goldsmith, M. A. (2000). Distinct mechanisms of entry by envelope glycoproteins of Marburg and Ebola (Zaire) viruses. *J. Virol.* 74, 4933–4937. doi: 10.1128/jvi.74.10.4933-4937.2000

Corti, D., Misasi, J., Mulangu, S., Stanley, D. A., Kanekiyo, M., Wollen, S., et al. (2016). Protective monotherapy against lethal Ebola virus infection by a potently neutralizing antibody. *Science* 351, 1339–1342. doi: 10.1126/science.aad5224

Crozier, I. (2016). Ebola virus RNA in the semen of male survivors of ebola virus disease: the uncertain gravitas of a privileged persistence. *J. Infect. Dis.* 214, 1467–1469. doi: 10.1093/infdis/jiw079

Deen, G. F., Broutet, N., Xu, W., Knust, B., Sesay, F. R., McDonald, S. L. R., et al. (2017). Ebola RNA persistence in semen of ebola virus disease survivors - final report. *N. Engl. J. Med.* 377, 1428–1437. doi: 10.1056/NEJMoa1511410

Dhama, K., Karthik, K., Khandia, R., Chakraborty, S., Munjal, A., Latheef, S. K., et al. (2018). Advances in designing and developing vaccines, drugs, and therapies to counter ebola virus. *Front. Immunol.* 9:1803. doi: 10.3389/fimmu.2018.01803

Diallo, B., Sissoko, D., Loman, N. J., Bah, H. A., Bah, H., Worrell, M. C., et al. (2016). Resurgence of ebola virus disease in guinea linked to a survivor with virus persistence in seminal fluid for more than 500 days. *Clin. Infect. Dis.* 63, 1353–1356. doi: 10.1093/cid/ciw601

Eggert, K., Oertel, W. H., Lees, A. J., and German Competence Network on Parkinson's disease (2014). Safety and efficacy of tolcapone in the long-term use in Parkinson disease: an observational study. *Clin. Neuropharmacol.* 37, 1–5. doi: 10.1097/WNF.0000000000000008

Elias, A. K., Scanlon, D., Musgrave, I. F., and Carver, J. A. (2014). SEVI, the semen enhancer of HIV infection along with fragments from its central region, form amyloid fibrils that are toxic to neuronal cells. *Biochim. Biophys. Acta* 1844, 1591–1598. doi: 10.1016/j.bbapap.2014.06.006

Fischer, W. A., Brown, J., Wohl, D. A., Loftis, A. J., Tozay, S., Reeves, E., et al. (2017). Ebola virus ribonucleic acid detection in semen more than two years after resolution of acute ebola virus infection. *Open Forum Infect Dis.* 4:ofx155. doi: 10.1093/ofid/ofx155

Forneris, F., Orru, R., Bonivento, D., Chiarelli, L. R., and Mattevi, A. (2009). ThermoFAD, a thermofluor-adapted flavin ad hoc detection system for protein folding and ligand binding. *FEBS J.* 276, 2833–2840. doi: 10.1111/j.1742-4658.2009.07006.x

Gamez, J., Salvado, M., Reig, N., Sune, P., Casasnovas, C., Rojas-Garcia, R., et al. (2019). Transthyretin stabilization activity of the catechol-O-methyltransferase inhibitor tolcapone (SOM0226) in hereditary ATTR amyloidosis patients and asymptomatic carriers: proof-of-concept study. *Amyloid* 26, 74–84. doi: 10.1080/13506129.2019.1597702

Goldstein, T., Anthony, S. J., Gbakima, A., Bird, B. H., Bangura, J., Tremeau-Bravard, A., et al. (2018). The discovery of Bombali virus adds further support for bats as hosts of ebolaviruses. *Nat. Microbiol.* 3, 1084–1089. doi: 10.1038/s41564-018-0227-222

Hira, S., and Piot, P. (2016). The counter effects of the Ebola epidemic on control and treatment of HIV/AIDS, tuberculosis, and malaria in West Africa. *AIDS* 30, 2555–2559. doi: 10.1097/QAD.0000000000001231

Hunt, C. L., Lennemann, N. J., and Maury, W. (2012). Filovirus entry: a novelty in the viral fusion world. *Viruses* 4, 258–275. doi: 10.3390/v4020258

Jacobs, G. P., Bhat, P., Owiti, P., Edwards, J. K., Tweya, H., and Najjemba, R. (2017). Did the 2014 Ebola outbreak in Liberia affect HIV testing, linkage to care and ART initiation? *Public Health Action* 7(Suppl. 1), S70–S75. doi: 10.5588/pha.16.0101

Johansen, L. M., DeWald, L. E., Shoemaker, C. J., Hoffstrom, B. G., Lear-Rooney, C. M., Stossel, A., et al. (2015). A screen of approved drugs and molecular probes identifies therapeutics with anti-Ebola virus activity. *Sci. Transl. Med.* 7:290ra289. doi: 10.1126/scitranslmed.aaa5597

Johnson, J. C., Martinez, O., Honko, A. N., Hensley, L. E., Olinger, G. G., and Basler, C. F. (2014). Pyridinyl imidazole inhibitors of p38 MAP kinase impair viral entry and reduce cytokine induction by Zaire ebolavirus in human dendritic cells. *Antiviral Res.* 107, 102–109. doi: 10.1016/j.antiviral.2014.04.014

Keita, A. K., Toure, A., Sow, M. S., Raoul, H., Magassouba, N., Delaporte, E., et al. (2017). Extraordinary long-term and fluctuating persistence of Ebola virus RNA in semen of survivors in Guinea: implications for public health. *Clin. Microbiol. Infect.* 23, 412–413. doi: 10.1016/j.cmi.2016.11.005

Keita, M., Duraffour, S., Loman, N. J., Rambaut, A., Diallo, B., Magassouba, N., et al. (2016). Unusual ebola virus chain of transmission, conakry, Guinea, 2014-2015. *Emerg. Infect. Dis.* 22, 2149–2152. doi: 10.3201/eid2212.160847

Kim, K. A., Yolamanova, M., Zirafi, O., Roan, N. R., Staendker, L., Forssmann, W. G., et al. (2010). Semen-mediated enhancement of HIV infection is donor-dependent and correlates with the levels of SEVI. *Retrovirology* 7:55. doi: 10.1186/1742-4690-7-55

Lanini, S., Portella, G., Vairo, F., Kobinger, G. P., Pesenti, A., Langer, M., et al. (2015). Blood kinetics of Ebola virus in survivors and nonsurvivors. *J. Clin. Invest.* 125, 4692–4698. doi: 10.1172/JCI83111

Lee, Y. H., and Ramamoorthy, A. (2018). Semen-derived amyloidogenic peptides-Key players of HIV infection. *Protein Sci.* 27, 1151–1165. doi: 10.1002/pro.3395

Leno, N. N., Delamou, A., Koita, Y., Diallo, T. S., Kaba, A., Delvaux, T., et al. (2018). Ebola virus disease outbreak in Guinea: what effects on prevention of mother-to-child transmission of HIV services? *Reprod. Health* 15:60. doi: 10.1186/s12978-018-0502-y

Li, H., Yu, F., Xia, S., Yu, Y., Wang, Q., Lv, M., et al. (2017). Chemically modified human serum albumin potently blocks entry of ebola pseudoviruses and viruslike particles. *Antimicrob. Agents Chemother.* 61:e02168-16. doi: 10.1128/AAC.02168-2116

Li, J., Yang, Z., Liu, H., Qiu, M., Zhang, T., Li, W., et al. (2019). ADS-J1 disaggregates semen-derived amyloid fibrils. *Biochem. J.* 476, 1021–1035. doi: 10.1042/BCJ20180886

Li, L., Qiao, P., Yang, J., Lu, L., Tan, S., Lu, H., et al. (2010). Maleic anhydride-modified chicken ovalbumin as an effective and inexpensive anti-HIV microbicide candidate for prevention of HIV sexual transmission. *Retrovirology* 7:37. doi: 10.1186/1742-4690-7-37

Liu, G., Nash, P. J., Johnson, B., Pietzsch, C., Ilagan, M. X., Bukreyev, A., et al. (2017). A sensitive *in vitro* high-throughput screen to identify pan-filoviral replication inhibitors targeting the VP35-NP interface. *ACS Infect. Dis.* 3, 190–198. doi: 10.1021/acsinfecdis.6b00209

LoRicco, J. G., Xu, C. S., Neidleman, J., Bergkvist, M., Greene, W. C., Roan, N. R., et al. (2016). Gallic Acid is an Antagonist of Semen Amyloid Fibrils that Enhance HIV-1 Infection. *J. Biol. Chem.* 291, 14045–14055. doi: 10.1074/jbc.M116.718684

Lump, E., Castellano, L. M., Meier, C., Seeliger, J., Erwin, N., Sperlich, B., et al. (2015). A molecular tweezer antagonizes seminal amyloids and HIV infection. *eLife* 4:e05397. doi: 10.7554/eLife.05397

Mate, S. E., Kugelman, J. R., Nyenswah, T. G., Ladner, J. T., Wiley, M. R., Cordier-Lassalle, T., et al. (2015). Molecular evidence of sexual transmission of ebola virus. *N. Engl. J. Med.* 373, 2448–2454. doi: 10.1056/NEJMoa1509773

Müller, T. (2015). Catechol-O-methyltransferase inhibitors in Parkinson's disease. *Drugs* 75, 157–174. doi: 10.1007/s40265-014-0343-340

Münch, J., Rucker, E., Standker, L., Adermann, K., Goffinet, C., Schindler, M., et al. (2007). Semen-derived amyloid fibrils drastically enhance HIV infection. *Cell* 131, 1059–1071. doi: 10.1016/j.cell.2007.10.014

Nagel, E., Blackowicz, M. J., Sahr, F., and Jarrett, O. D. (2019). Impact of the Ebola epidemic on clinical outcomes of HIV-infected soldiers and their dependents in Sierra Leone. *Int. J. STD AIDS* 30, 106–112. doi: 10.1177/0956462418797843

Nakka, P. P., Li, K., and Forciniti, D. (2018). Effect of differences in the primary structure of the a-chain on the aggregation of insulin fragments. *ACS Omega* 3, 9636–9647. doi: 10.1021/acsomega.8b00500

Nilsson, M. R. (2004). Techniques to study amyloid fibril formation *in vitro*. *Methods* 34, 151–160. doi: 10.1016/j.ymeth.2004.03.012

Olanow, C. W., and Watkins, P. B. (2007). Tolcapone: an efficacy and safety review (2007). *Clin. Neuropharmacol.* 30, 287–294. doi: 10.1097/wnf.0b013e318038d2b6

Purpura, L. J., Rogers, E., Baller, A., White, S., Soka, M., Choi, M. J., et al. (2017). Ebola virus RNA in semen from an HIV-positive survivor of Ebola. *Emerg. Infect. Dis.* 23, 714–715. doi: 10.3201/eid2304.161743

Qi, Q., Wang, Q., Chen, W., Yu, F., Du, L., Dimitrov, D. S., et al. (2017). Anti-HIV antibody and drug combinations exhibit synergistic activity against drug-resistant HIV-1 strains. *J. Infect.* 75, 68–71. doi: 10.1016/j.jinf.2017.03.006

Qiu, J., Liang, T., Wu, J., Yu, F., He, X., Tian, Y., et al. (2019). N-substituted pyrrole derivative 12m inhibits HIV-1 entry by targeting Gp41 of HIV-1 envelope glycoprotein. *Front. Pharmacol.* 10:859. doi: 10.3389/fphar.2019.00859

Qiu, X., Wong, G., Audet, J., Bello, A., Fernando, L., Alimonti, J. B., et al. (2014). Reversion of advanced Ebola virus disease in nonhuman primates with ZMapp. *Nature* 514, 47–53. doi: 10.1038/nature13777

Ren, R., Yin, S., Lai, B., Ma, L., Wen, J., Zhang, X., et al. (2018). Myricetin antagonizes semen-derived enhancer of viral infection (SEVI) formation and influences its infection-enhancing activity. *Retrovirology* 15:49. doi: 10.1186/s12977-018-0432-433

Roan, N. R., Liu, H., Usmani, S. M., Neidleman, J., Muller, J. A., Avila-Herrera, A., et al. (2014). Liquefaction of semen generates and later degrades a conserved semenogelin peptide that enhances HIV infection. *J. Virol.* 88, 7221–7234. doi: 10.1128/JVI.00269-214

Roan, N. R., Muller, J. A., Liu, H., Chu, S., Arnold, F., Sturzel, C. M., et al. (2011). Peptides released by physiological cleavage of semen coagulum proteins form amyloids that enhance HIV infection. *Cell Host Microbe* 10, 541–550. doi: 10.1016/j.chom.2011.10.010

Roan, N. R., Münch, J., Arhel, N., Mothes, W., Neidleman, J., Kobayashi, A., et al. (2009). The cationic properties of SEVI underlie its ability to enhance human immunodeficiency virus infection. *J. Virol.* 83, 73–80. doi: 10.1128/JVI.01366-1368

Rodriguez, L. L., De Roo, A., Guimard, Y., Trappier, S. G., Sanchez, A., Bressler, D., et al. (1999). Persistence and genetic stability of Ebola virus during the outbreak in Kikwit, Democratic Republic of the Congo, 1995. *J. Infect. Dis.* 179(Suppl. 1), S170–S176. doi: 10.1086/514291

Sant'Anna, R., Gallego, P., Robinson, L. Z., Pereira-Henriques, A., Ferreira, N., Pinheiro, F., et al. (2016). Repositioning tolcapone as a potent inhibitor of transthyretin amyloidogenesis and associated cellular toxicity. *Nat. Commun.* 7:10787. doi: 10.1038/ncomms10787

Sarr, M., Kronqvist, N., Chen, G., Aleksis, R., Purhonen, P., Hebert, H., et al. (2018). A spidroin-derived solubility tag enables controlled aggregation of a designed amyloid protein. *FEBS J.* 285, 1873–1885. doi: 10.1111/febs.14451

Sissoko, D., Laouenan, C., Folkesson, E., M'Lebing, A. B., Beavogui, A. H., Baize, S., et al. (2016). Experimental treatment with favipiravir for ebola virus disease (the JIKI Trial): a historically controlled, single-arm proof-of-concept trial in Guinea. *PLoS Med.* 13:e1001967. doi: 10.1371/journal.pmed.1001967

Sivapalasingam, S., Kamal, M., Slim, R., Hosain, R., Shao, W., Stoltz, R., et al. (2018). Safety, pharmacokinetics, and immunogenicity of a co-formulated cocktail of three human monoclonal antibodies targeting Ebola virus glycoprotein in healthy adults: a randomised, first-in-human phase 1 study. *Lancet Infect. Dis.* 18, 884–893. doi: 10.1016/S1473-3099(18)30397-30399

Sow, M. S., Etard, J. F., Baize, S., Magassouba, N., Faye, O., Msellati, P., et al. (2016). New evidence of long-lasting persistence of ebola virus genetic material in semen of survivors. *J. Infect. Dis.* 214, 1475–1476. doi: 10.1093/infdis/jiw078

Subissi, L., Keita, M., Mesfin, S., Rezza, G., Diallo, B., Van Gucht, S., et al. (2018). Ebola virus transmission caused by persistently infected survivors of the 2014-2016 outbreak in West Africa. *J. Infect. Dis.* 218(Suppl._5), S287–S291. doi: 10.1093/infdis/jiy280

Tan, S., Li, J. Q., Cheng, H., Li, Z., Lan, Y., Zhang, T. T., et al. (2019). The anti-parasitic drug suramin potently inhibits formation of seminal amyloid fibrils and their interaction with HIV-1. *J. Biol. Chem.* 294, 13740–13754. doi: 10.1074/jbc.RA118.006797

Tan, S., Lu, L., Li, L., Liu, J., Oksov, Y., Lu, H., et al. (2013). Polyanionic candidate microbicides accelerate the formation of semen-derived amyloid fibrils to enhance HIV-1 infection. *PLoS One* 8:e59777. doi: 10.1371/journal.pone.0059777

Tang, Q., Roan, N. R., and Yamamura, Y. (2013). Seminal plasma and semen amyloids enhance cytomegalovirus infection in cell culture. *J. Virol.* 87, 12583–12591. doi: 10.1128/JVI.02083-2013

Thorson, A., Formenty, P., Lofthouse, C., and Broutet, N. (2016). Systematic review of the literature on viral persistence and sexual transmission from recovered Ebola survivors: evidence and recommendations. *BMJ Open* 6:e008859. doi: 10.1136/bmjopen-2015-008859

Torres, L., Ortiz, T., and Tang, Q. (2015). Enhancement of herpes simplex virus (HSV) infection by seminal plasma and semen amyloids implicates a new target for the prevention of HSV infection. *Viruses* 7, 2057–2073. doi: 10.3390/v7042057

Trott, O., and Olson, A. J. (2010). AutoDock Vina: improving the speed and accuracy of docking with a new scoring function, efficient optimization, and multithreading. *J. Comput. Chem.* 31, 455–461. doi: 10.1002/jcc.21334

Van Kerkhove, M. D., Bento, A. I., Mills, H. L., Ferguson, N. M., and Donnelly, C. A. (2015). A review of epidemiological parameters from Ebola outbreaks to inform early public health decision-making. *Sci. Data* 2:150019. doi: 10.1038/sdata.2015.19

Warren, T. K., Jordan, R., Lo, M. K., Ray, A. S., Mackman, R. L., Soloveva, V., et al. (2016). Therapeutic efficacy of the small molecule GS-5734 against Ebola virus in rhesus monkeys. *Nature* 531, 381–385. doi: 10.1038/nature17180

Weyer, J., Grobbelaar, A., and Blumberg, L. (2015). Ebola virus disease: history, epidemiology and outbreaks. *Curr. Infect. Dis. Rep.* 17:480. doi: 10.1007/s11908-015-0480-y

Xu, W., Wang, Q., Yu, F., Lu, L., and Jiang, S. (2014). Synergistic effect resulting from combinations of a bifunctional HIV-1 antagonist with antiretroviral drugs. *J. Acquir. Immune Defic. Syndr.* 67, 1–6. doi: 10.1097/QAI.0000000000000265

Xun, T., Li, W., Chen, J., Yu, F., Xu, W., Wang, Q., et al. (2015). ADS-J1 inhibits semen-derived amyloid fibril formation and blocks fibril-mediated enhancement of HIV-1 infection. *Antimicrob. Agents Chemother.* 59, 5123–5134. doi: 10.1128/AAC.00385-315

Zhang, X., Chen, J., Yu, F., Wang, C., Ren, R., Wang, Q., et al. (2018). 3-hydroxyphthalic anhydride- modified rabbit anti-PAP IgG as a potential bifunctional HIV-1 entry inhibitor. *Front. Microbiol.* 9:1330. doi: 10.3389/fmicb.2018.01330

Zhao, Y., Ren, J., Harlos, K., Jones, D. M., Zeltina, A., Bowden, T. A., et al. (2016). Toremifene interacts with and destabilizes the Ebola virus glycoprotein. *Nature* 535, 169–172. doi: 10.1038/nature18615

Zirafi, O., Kim, K. A., Roan, N. R., Kluge, S. F., Muller, J. A., Jiang, S., et al. (2014). Semen enhances HIV infectivity and impairs the antiviral efficacy of microbicides. *Sci. Transl. Med.* 6:262ra157. doi: 10.1126/scitranslmed.3009634

**Conflict of Interest:** The authors declare that the research was conducted in the absence of any commercial or financial relationships that could be construed as a potential conflict of interest.

*Copyright © 2020 Qiu, Li, Chen, Guo, Xu, Qi, Qiu, Pang, Li, Liu and Tan. This is an open-access article distributed under the terms of the Creative Commons Attribution License (CC BY). The use, distribution or reproduction in other forums is permitted, provided the original author(s) and the copyright owner(s) are credited and that the original publication in this journal is cited, in accordance with accepted academic practice. No use, distribution or reproduction is permitted which does not comply with these terms.*

frontiers in Microbiology

REVIEW
published: 25 May 2020
doi: 10.3389/fmicb.2020.01063

# Protein- and Peptide-Based Virus Inactivators: Inactivating Viruses Before Their Entry Into Cells

*Xiaojie Su[1†], Qian Wang[1†], Yumei Wen[1], Shibo Jiang[1,2*†] and Lu Lu[1*†]*

[1] Key Laboratory of Medical Molecular Virology (MOE/NHC/CAMS), School of Basic Medical Sciences, Fudan University, Shanghai, China, [2] Lindsley F. Kimball Research Institute, New York Blood Center, New York, NY, United States

OPEN ACCESS

**Edited by:**
Nejat Duzgunes,
University of the Pacific, United States

**Reviewed by:**
Doina Atanasiu,
University of Pennsylvania, United States
Konstantin Kousoulas,
Louisiana State University, United States

***Correspondence:**
Shibo Jiang
shibojiang@fudan.edu.cn
Lu Lu
lul@fudan.edu.cn

**†ORCID:**
Xiaojie Su
orcid.org/0000-0002-5175-9370
Qian Wang
orcid.org/0000-0002-6149-5057
Shibo Jiang
orcid.org/0000-0001-8283-7135
Lu Lu
orcid.org/0000-0002-2255-0391

**Specialty section:**
This article was submitted to Virology, a section of the journal Frontiers in Microbiology

**Received:** 30 November 2019
**Accepted:** 29 April 2020
**Published:** 25 May 2020

**Citation:**
Su X, Wang Q, Wen Y, Jiang S and Lu L (2020) Protein- and Peptide-Based Virus Inactivators: Inactivating Viruses Before Their Entry Into Cells. Front. Microbiol. 11:1063. doi: 10.3389/fmicb.2020.01063

Infectious diseases caused by human immunodeficiency virus (HIV) and other highly pathogenic enveloped viruses, have threatened the global public health. Most antiviral drugs act as passive defenders to inhibit viral replication inside the cell, while a few of them function as gate keepers to combat viruses outside the cell, including fusion inhibitors, e.g., enfuvirtide, and receptor antagonists, e.g., maraviroc, as well as virus inactivators (including attachment inhibitors). Different from fusion inhibitors and receptor antagonists that must act in the presence of target cells, virus inactivators can actively inactivate cell-free virions in the blood, through interaction with one or more sites in the envelope glycoproteins (Envs) on virions. Notably, a number of protein- and peptide-based virus inactivators (PPVIs) under development are expected to have a better utilization rate than the current antiviral drugs and be safer for *in vivo* human application than the chemical-based virus inactivators. Here we have highlighted recent progress in developing PPVIs against several important enveloped viruses, including HIV, influenza virus, Zika virus (ZIKV), dengue virus (DENV), and herpes simplex virus (HSV), and the potential use of PPVIs for urgent treatment of infection by newly emerging or re-emerging viruses.

**Keywords: enveloped virus, envelope proteins, inactivation, virus inactivator, emerging viruses**

## INTRODUCTION

Human immunodeficiency virus (HIV), influenza virus and many other viruses are enveloped viruses (Harrison, 2008). In most cases, viral envelope derives from the host cell membrane, while in some cases, it derives from the organelle membrane. For example, the envelope of both DENV and ZIKV derives from the endoplasmic reticulum membrane (Kuhn et al., 2002). One or more envelope glycoproteins (Envs) are expressed on the surface of the viral envelope and can play important roles in viral entry into the target cell, including attaching the virus to surface receptor of the host cell and mediating virus-cell membrane fusion, allowing the viral genome to enter the host cell for replication (Vigant et al., 2015; Lu et al., 2016).

The outbreak of infectious diseases caused by highly pathogenic enveloped viruses, such as HIV, has posed threat to public health worldwide. Thus, it is essential to develop safe and effective antiviral drugs to combat these infectious diseases (Wang et al., 2017). Since the first antiviral drug for treatment of HIV infection, zidovudine, was approved for clinical use in 1987, the United States FDA has approved >80 antiviral drugs so far. They are mainly applied to treat and prevent infection

of HIV, herpes simplex virus (HSV), influenza virus, hepatitis B virus (HBV), and hepatitis C virus (HCV) (Chaudhuri et al., 2018). However, most of these antiviral drugs are considered as "passive defenders" because they have to enter the virus-infected cells to inhibit viral replication in the cells (**Figure 1A**). Therefore, these drugs must possess the ability to penetrate the cell membranes without affecting the normal function of the intracellular proteins. Consequently, they have the weakness of relatively low utilization rate because most part of a drug remaining outside the infected cells does not participate in inhibition of viral infection.

In contrast to "passive defenders," some antiviral agents used in clinics or under development serve as "gate keepers" to combat viruses outside cells. As mentioned above, viral entry can be divided into two steps: viral attachment to cell receptor(s) and then viral fusion with the target cell. Therefore, "gate keepers" can be classified into three groups: attachment inhibitors that inhibiting the attachment of virions to the target cell by blocking binding of viral Env (e.g., gp120) to cellular the receptor (e.g., soluble CD4) (Deen et al., 1988), receptor antagonists that bind to the cell surface receptor to prevent binding of virions to the receptor (e.g., maraviroc) (Fatkenheuer et al., 2005), and fusion inhibitors that inhibit fusion between viral and target cell membranes (e.g., enfuvirtide) (Jiang et al., 1993a,b; Wild et al., 1994; Lalezari et al., 2003). In general, attachment inhibitors possess some virus inactivation abilities in mechanism, more or less, due to their ability to block the receptor-binding site (RBS) on viral Envs (Lu et al., 2012; Qi et al., 2017). Therefore, attachment inhibitors belong to virus inactivators here; and "gate keepers" includes virus inactivators, receptor antagonists, and fusion inhibitors (**Figure 1A**).

Different from fusion inhibitors and receptor antagonist blockers that must act in the presence of target cells, virus inactivators can actively attack and inactivate cell-free virions in the blood, through interaction with one or more sites in Envs on virions. The mechanisms of virus inactivators vary: they can bind and block the RBS on viral Envs (Chen et al., 2014), or induce the conformational change of Env, causing virions to lose the ability to enter the host cell (Lu et al., 2012). Some other inactivators may bind to the Env stem or the viral lipid membrane, to disrupt the integrity of the viral envelope or lead to the release of viral genetic materials (Yu et al., 2017) (**Figure 1B**). Because they can actively attack and then inactivate cell-free virions anywhere they meet in the blood, they should have higher utilization rate than the current antiviral drugs. They are expected to be much safer for *in vivo* human application than the chemical-based virus inactivators (e.g., detergents), most of which can non-specifically lyse lipid membranes of viruses and cells (Polsky et al., 1988; Phillips et al., 2000). PPVIs also have potential for further development as novel antiviral drugs for the urgent treatment of infection by the highly pathogenic emerging and re-emerging viruses.

In this review, we focus on an update of recent developments of PPVIs against several important enveloped viruses, including HIV, ZIKV, influenza virus, DENV, and HSV, and their mechanisms of action. We have also discussed their advantages and disadvantages, compared with the traditional antiviral drugs and the potential application for urgent treatment of infection by newly emerging and re-emerging viruses.

## Protein- and Peptide-Based HIV Inactivators

Human immunodeficiency virus primarily targets the immune system, including $CD4^+$ T cells and macrophages. After sexual transmission, HIV enters into $CD4^+$ cells in the mucosal tissues and then spreads to the lymphoid organs within days (Haase, 2005; Moir et al., 2011). The immune system of the HIV-infected patient is gradually destroyed, eventually resulting in acquired immunodeficiency syndrome (AIDS) and death (Moir et al., 2011). More than 40 anti-HIV drugs have been approved by the United States FDA, most of which are reverse transcriptase inhibitors (RTIs, including NRTIs and NNRTIs), protease inhibitors (PIs) and integrase inhibitors (INIs) (Deeks et al., 2015). They must enter HIV-infected cells to inhibit viral replication. The only peptide-based HIV fusion inhibitor, enfuvirtide (also known as T20) (Jiang et al., 1993a; Wild et al., 1994; Lalezari et al., 2003), and a small-molecule CCR5 antagonist, maraviroc (Fatkenheuer et al., 2005), must act on the cell surface where the virus binds to the cellular receptor (Lu et al., 2016). These drugs have shown good effects in combating HIV; however, they cannot attack the cell-free virions in the blood, thus also having the problem of low utilization rate.

Human immunodeficiency virus type 1 (HIV-1) envelope glycoprotein is originally expressed as the gp160 glycoprotein precursor, approximately 850 amino acids in length (**Figure 2A**), which is cleaved by viral protease to form a highly glycosylated trimer of heterodimers, non-covalently associated by three gp120 and three gp41 subunits (Liu et al., 2008) (**Figure 2C**). The surface subunit gp120 is approximately 500 amino acids in length, composed of several variable regions V1–V5 and the remaining more conserved regions (Starcich et al., 1986). A conserved binding site to the cellular receptor CD4 (CD4bs) is found on the surface of the gp120 subunit, which contains the conserved hydrophobic Phe-43 pocket (residues 362–372). The transmembrane subunit gp41, approximately 350 amino acids in length, is comprised of the fusion peptide (FP), N-terminal heptad repeat (NHR), C-terminal heptad repeat (CHR), membrane-proximal external region (MPER), transmembrane region (TM), and cytoplasmic region (CP). As shown in **Figure 2B**, HIV-1 entry is originated by gp120 binding to the CD4 molecule on the target cell, resulting in its conformational change to expose the coreceptor-binding site (CoRbs) on gp120, further allowing gp120 binding to the coreceptor CCR5 or CXCR4 (Chan and Kim, 1998). Subsequently, gp41 also changes conformation by inserting its FP into the target cell membrane to form a prehairpin fusion intermediate conformation (PFI) (Melikyan, 2008). Then, NHRs and CHRs of the three gp41 subunits interact with each other to form a six-helix bundle (6-HB) core structure, bringing the viral envelope and cell membrane into close proximity to achieve fusion (Su et al., 2017). Therefore, the HIV-1 Env composed of gp120 and gp41 subunits is a key component responsible for

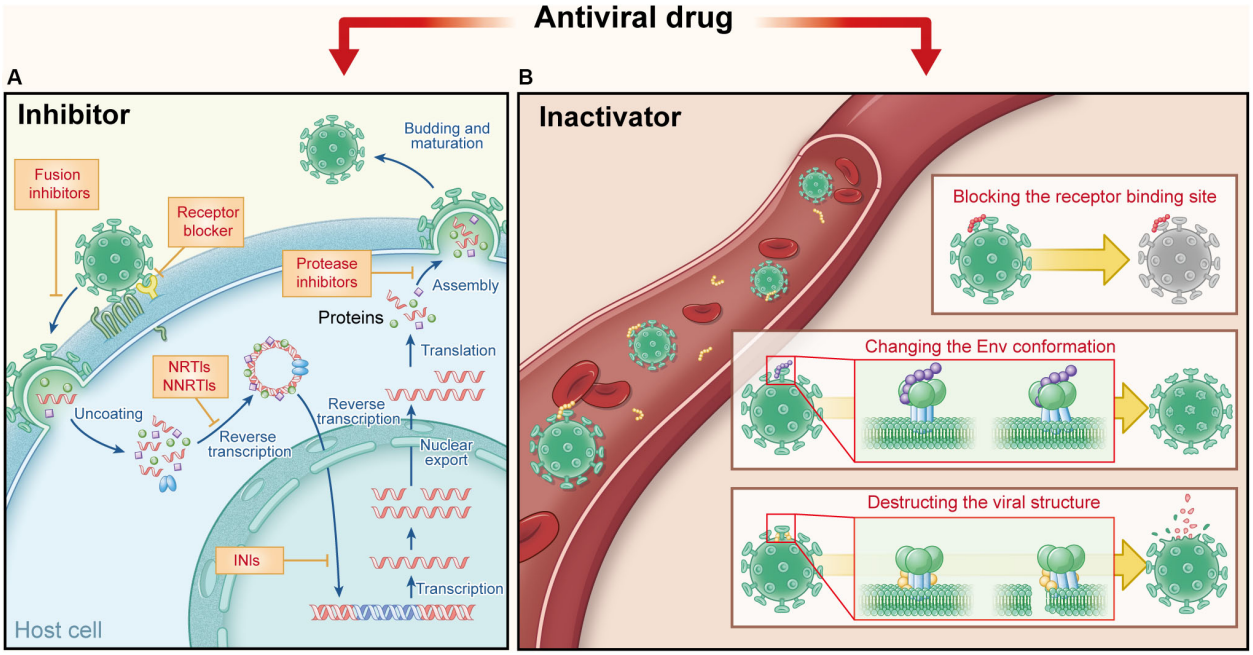


**FIGURE 1 |** Comparison of current antiviral drugs and the protein- and peptide-based inactivators, taking HIV as the example. **(A)** Major targets and mechanisms of the current anti-HIV drugs. They must act in the presence of target cells: receptor antagonists bind the cell surface receptor to prevent the virus binding and fusion inhibitors target the fusion process, while other inhibitors target viral replication in HIV-infected cells, including nucleoside transcriptase inhibitors (NRTIs) and nucleoside transcriptase inhibitors (NNRTIs), integrase inhibitors (INIs), and protease inhibitors (PIs). **(B)** Targets and action mechanisms of the protein- and peptide-based HIV inactivators. They can actively attack and inactivate cell-free virions that they meet in the blood, by blocking the RBS on viral Envs, changing the Env conformation or destructing the viral structure.

mediating entry of the virion into the target cell, and also an important target for development of the protein- and peptide-based HIV-1 inactivators (D'Souza et al., 2000).

Lu et al. (2012) proposed, for the first time, the strategy of designing and developing a protein-based HIV-1 inactivator, 2DLT, for inactivating cell-free HIV-1 virions in the absence of target cells (Sanders, 2013). 2DLT, a bivalent recombinant protein, consists of three parts: (1) the D1D2 domain of CD4 (2D), (2) a 35-amino acid linker (L), and (3) T1144 (T), a peptide-based HIV fusion inhibitor (Dwyer et al., 2007; Pan et al., 2009). Binding of D1D2 in 2DLT to the CD4-binding site (CD4bs) in HIV-1 gp120 triggers the formation of a gp120/gp41 pre-fusion intermediate (PFI), in which gp41 NHR is partially exposed (Haim et al., 2009). The T1144 portion in 2DLT then binds the exposed NHR, resulting in the destabilization of PFI thus inactivation of the cell-free virions (**Figure 2C**). The results from the virus inactivation assay indicated that 2DLT could effectively inactivate cell-free HIV-1 virions, including laboratory-adapted strains and primary isolates of different subtypes with an EC50 (Half maximal effective concentration causing virus inactivation) between 17.3 and 78.6 nM, which is about two–six fold more potent than D1D2 alone, while T1144 alone had no virus inactivation activity (Lu et al., 2012). Therefore, this bivalent protein can actively attack the cell-free virions anywhere in blood when they meet and irreversibly inactivate the cell-free virions through a double hit by targeting gp120 and gp41 simultaneously or sequentially (Lu et al., 2012; Sanders, 2013). Subsequently, the antiviral effects of 2DLT in combination with different anti-HIV drugs were explored, including HIV entry inhibitors, NRTIs, NNRTIs and protease inhibitors. The results indicated that the combination of 2DLT with these drugs brought about synergism or strong synergism against infection of both X4 and R5 HIV-1 strains (Xu et al., 2014).

Actually, several anti-HIV proteins or peptides with HIV inactivation activity similar to that of 2DLT had already been studied before 2011, but without assessing their virus inactivation effects. The first one was soluble CD4 (sCD4) (Deen et al., 1988; Traunecker et al., 1988). Theoretically, sCD4 could interact with the CD4bs in gp120 on HIV-1 and inactivate the cell-free virions in the absence of host cells because virions would lose their ability to bind with the cellular receptor CD4, making it impossible for them to enter the CD4 T cell for replication. Indeed, *in vitro* studies indicated that sCD4 could inhibit HIV-1 infection with IC50 (half maximal inhibitory concentration) values between 40 and 700 nM (Daar et al., 1990; Orloff et al., 1993). The results from phases I–II clinical trials showed that intravenously administered sCD4 effectively reduced viral titers in sera without causing obvious toxicity. However, the half-life of sCD4 is short, leading to viral relapse within a short time after treatment (Kahn et al., 1990; Schooley et al., 1990). At low concentrations (<1 μg/ml or 20 nM), sCD4 could not effectively inhibit HIV-1 infection, but rather enhanced the infection of some HIV-1 clinical isolates in host cells, including some CD4-CCR5+ cells. This is because sCD4 binding to CD4bs in gp120

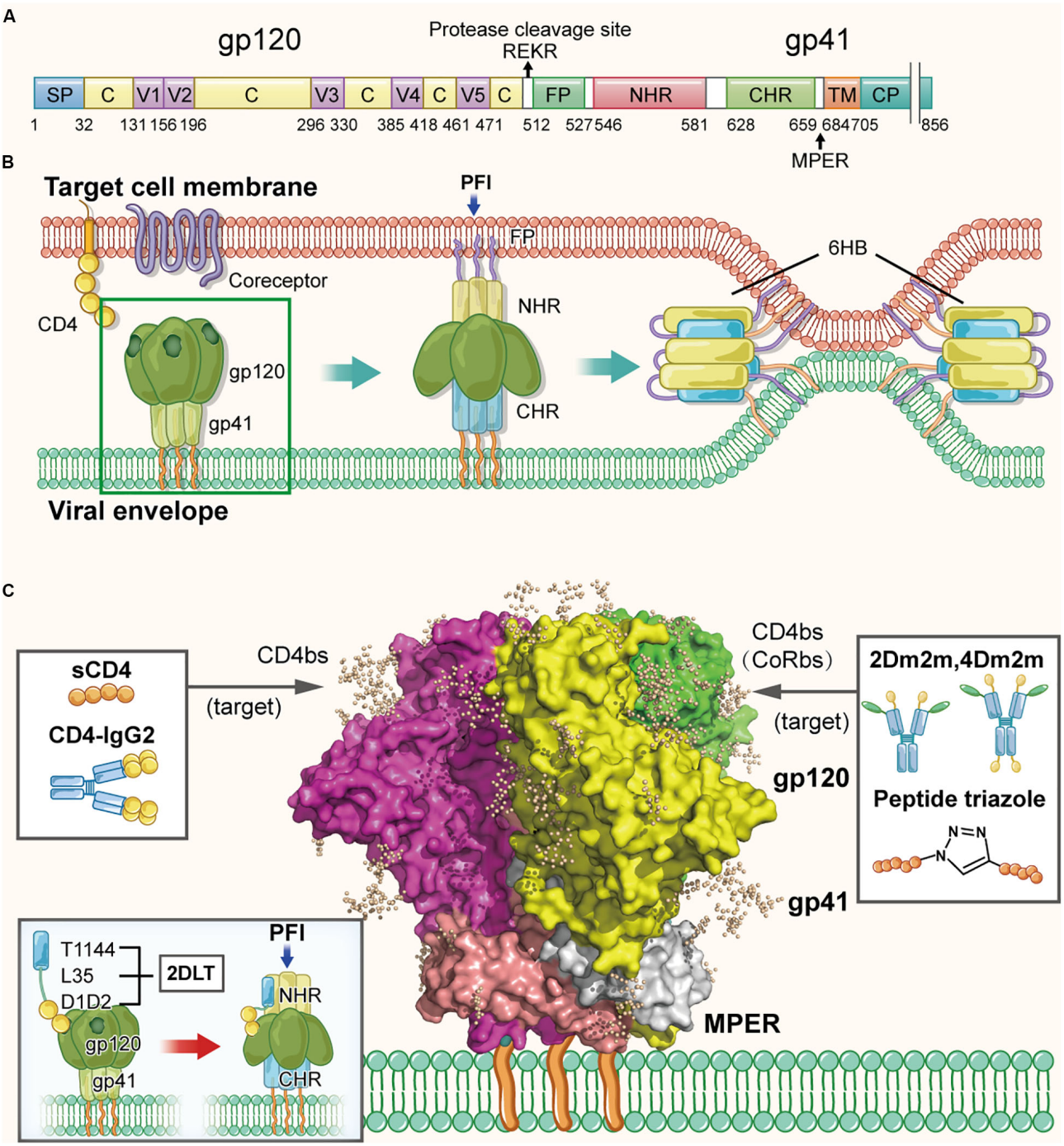


**FIGURE 2 |** Structure of HIV-1 Env in the native and fusion-intermediate states, which serve as targets for protein- and peptide-based HIV inactivators. **(A)** Schematic representation of HIV-1 Env composition, including the surface subunit gp120 and the transmembrane subunit gp41. Key residues of CD4bs are located in the region of residues 362–372 in gp120. Amino acid residues are numbered according to those of BG505 SOSIP.664 trimer (PDB ID: 5V8M). **(B)** Attachment of the HIV-1 Env to the cellular receptor(s) and fusion of viral envelope with the target cell membrane. Binding of gp120 with CD4 on the target cell surface triggers conformational change of gp120 with the exposure of the CoRbs, allowing gp120 binding to its coreceptor CCR5 or CXCR4. Subsequently, gp41 changes its conformation, resulting in the insertion of fusion peptide (FP) of gp41 into the target cell membrane and formation of the pre-fusion intermediate (PFI) state. The N- and C-terminal heptad repeats (NHRs and CHRs) of the three gp41 subunits interact with each other to form a six-helix bundle (6-HB) structure, which brings the viral envelope and target cell membrane together to achieve fusion. The pre-fusion trimer is highlighted in a green box, which is shown in more detail in **(C)**. **(C)** Side view of the pre-fusion, trimeric conformation of the Env present on the virion surface, which is presented as the glycan-shielded crystal structure (modified from PDB ID: 5V8M). Names and illustrations of inactivators are drawn in the three boxes, and the arrows depict their target sites, including CD4bs, CD4bs plus CoRbs or PFI induced by D1D2 binding to CD4bs.

triggers the exposure of CoRbs in gp120 and NHR in gp41, facilitating the interaction between CoRbs in gp120 and the CCR5 coreceptor on the host cell and, hence, fusion between the viral envelope and host cell membrane (Sullivan et al., 1998). Since CD4 is an important immune molecule that exerts its function through interaction with a number of human proteins, *in vivo* application of sCD4, an anti-HIV drug, may cause some adverse effects to the immune system. Therefore, development of sCD4 for clinical use has been discontinued, but the important information from the research on sCD4 has promoted studies of HIV inactivators containing part(s) of CD4 molecule.

Allaway et al. (1995) constructed a fusion protein CD4-IgG2 comprised of human IgG2 in which the Fv portions of both heavy and light chains were replaced by D1D2 domains of CD4. They found that CD4-IgG2 bound gp120 with high affinity and was much more potent than sCD4 to inhibit HIV-1 fusion and infection. Unlike sCD4, CD4-IgG2 could not enhance HIV-1 infection in CD4- CCR5+ cells. Like the broadly neutralizing antibodies (bnAbs), IgG1b12, 2G12, and 2F5, CD4-IgG2 could effectively neutralize a panel of laboratory-adapted strains and primary isolates of HIV-1 with different subtypes with IC50s from 5 to 80 nM (Trkola et al., 1995), and it was capable of reducing viral titers in rodent models (Gauduin et al., 1998). The results from clinical trials showed that CD4-IgG2 was well-tolerated at doses of 0.2–10 mg/kg with a half-life of 3–4 days *in vivo*, which was much longer than that of sCD4 (Jacobson et al., 2000). In advanced disease, an 80% response rate and ∼0.5 log10 mean reductions in viral load for 4–6 weeks after treatment were mediated by CD4-IgG2 (Jacobson et al., 2004). However, the concern about the enhancement of infection of some HIV-1 strains caused by sCD4- or CD4-containing molecule, like CD4-IgG2, cannot be excluded since no such study has been reported so far.

According to the structural similarity between CD4's the CDR2-like loop in CD4 and scyllatoxin's the β-hairpin region of scyllatoxin, a short scorpion toxin, the side chains of nine residues in CD4 that are critical for, central in the gp120 binding to HIV-1 gp120, was transferred to the structurally homologous region in the scorpion toxin scaffold (Vita et al., 1999). The resulting miniprotein (27 residues), CD4M9 inhibited CD4 binding to gp120 with an IC50 of 40 μM and suppressed the infection of HIV-1 X4 and R5 strains with IC50s ranging from 0.4 to 5 μM. Subsequently, they designed bivalent and trivalent CD4-mimetic miniproteins based on CD4M9 and tested their antiviral activity *in vitro*. Results showed that though their antiviral activity was improved, it was still much weaker than that of sCD4 (Li et al., 2004, 2007). Theoretically, these recombinant fusion proteins are expected to possess HIV-1 inactivation activity if a virus inactivation assay is performed.

Since the single D1 domain of CD4 is unstable and has low gp120-binding affinity, Sharma et al. (2005) and Chen et al. (2011) constructed two mutants of the CD4 D1 domain, CD4D1 and CD4PEP1, using mutagenesis. They demonstrated that both CD4D1 and CD4PEP1 could interact with gp120 with KD values of 40 and 26 nM, respectively. However, their virus inhibition or inactivation activities have not been detected and reported. Chen et al. (2011) identified two monomeric D1 mutants with high stability, solubility and gp120-binding affinity, designated mD1.1 and mD1.2, through screening a large D1 mutant library and found that both mD1.1 and mD1.2 could effectively neutralize HIV-1 primary isolates (Sharma et al., 2005). Subsequently, they identified an mD1.2 mutant, mD1.22, which had higher thermostability, better solubility and stronger gp120-binding affinity compared to mD1.2. *In vitro* studies showed that mD1.22 was several folds more potent than D1D2 and mD1.2 in inhibiting R5-tropic HIV-1 primary isolates, Bal and JRFL (Chen et al., 2014). To further improve its anti-HIV-1 activity and breadth, mD1.22 was fused with m36.4, an engineered human antibody domain targeting a CD4-induced (CD4i) epitope, which overlaps the HIV-1 coreceptor-binding site (CoRbs) on gp120 (Chen et al., 2008). This resulted in the generation of two bispecific multivalent fusion proteins, 2Dm2m and 4Dm2m, which could inhibit infection by all HIV-1 strains tested, including 41 HIV-1 isolates circulating predominantly in China, with an average IC50 of 1.7 and 0.2 nM, respectively (Chen et al., 2014). Most recently, the virus inactivation assay was utilized to compare the ability of 2Dm2m and 4Dm2m to inactivate cell-free HIV-1 IIIB virions against full-length sCD4, D1D2 (Sharma et al., 2005; Chen et al., 2011), and mD1.22 (Chen et al., 2014). The results implied that mD1.22, 2Dm2m, and 4Dm2m were highly effective in inactivating HIV-1 with EC50s of 3.1, 1.1, and 0.3 nM, respectively, which are much more potent than those of sCD4 (EC50: 153 nM) and D1D2 (EC50: 64.7 nM) (Qi et al., 2017). These results indicate that the single-domain protein mD1.22 and the bispecific multivalent proteins 2Dm2m and 4Dm2m are important HIV inactivators and are promising to be further developed into new anti-HIV drugs for treatment and prevention of HIV infection.

By screening phage display libraries of random 12-mer peptides, Ferrer and Harrison (1999) and Biorn et al. (2004) identified a 12 amino-acid peptide, 12p1 (RINNIPWSEAMM), which could inhibit gp120 interaction with sCD4 and mAb 17b, a neutralizing antibody that targets the CoRbs on gp120, indicating that 12p1 could simultaneously bind to CD4bs and CoRbs. Later, Ferrer and Harrison (1999) and Biorn et al. (2004) demonstrated that 12p1 could preferentially bind gp120 before gp120engagement of CD4, thus limiting the interaction of gp120 with the receptor CD4 and the coreceptor CCR5, both of which are crucial for viral entry. Therefore, 12p1 may act as an HIV-1 attachment inhibitor and/or inactivator. By optimizing the structure and activity of 12p1, Chaiken and Rashad (2015) designed and synthesized a class of peptide triazoles which could simultaneously bind CD4bs and CoRbs on gp120 with higher affinity than that of 12p1, causing gp120 shedding from the viral particles, and thereby irreversibly inactivating the virions (Aneja et al., 2015). This group has designed and synthesized a new peptide triazole denoted KR13 which can simultaneously induce the shedding of gp120 and the release of capsid protein p24 from HIV-1 pseudoviruses (Bastian et al., 2011, 2013). Later, they found that gold nanoparticle-conjugated KR13 (AuNP-KR13) exhibited more potent virus-inactivating effect than that of peptide KR13 alone because AuNP-KR13 had many more gp120-binding sites than KR13 (Rosemary Bastian et al., 2015).

Most recently, Chaiken and Rashad (2015) designed and engineered a recombinant chimera, denoted DAVEI (dual-acting virucidal entry inhibitor), composed of the lectin cyanovirin-N (CVN) and the HIV-1 gp41 MPER sequence, which could effectively inactivate the HIV-1 pseudovirus Bal.01 with an EC50 value of 28.3 nM. They found that DAVEI exhibited potent and irreversible inactivation of HIV-1 virions by dual engagement of gp120 and gp41, while CVN or MPER alone had no HIV-1 inactivation activity (Parajuli et al., 2016, 2018). These studies provided rational approaches for the design and development of specific HIV-1 inactivators with improved antiviral activity for treatment and prevention of HIV-1 infection.

The CD4bs on gp120 appear to be the most important target of protein- and peptide-based HIV inactivators. Most of those that are under preclinical and clinical development target CD4bs alone, CD4bs plus co-receptor-binding site (CoRbs) on gp120, or CD4bs plus some region(s) in the HIV-1 gp41 (**Figure 2C**). These strategies can also be applied to design and develop virus inactivators against other enveloped viruses, such as those described below.

## Protein- and Peptide-Based Influenza Virus Inactivators

Influenza viruses belong to the *Orthomyxoviridae* family having segmented negative-sense, single-stranded RNA genomes (Palese and Shaw, 2007). Influenza virus infection can lead to a high fever, cough, headache, sore throat etc. after 1–3-day incubation period. Influenza viruses are classified as types A, B, C, and D, on the basis of antigenic properties of the viral nucleoprotein (NP) and matrix protein (M). Since most annual influenza epidemics in humans are caused by influenza A viruses (IAVs) (Dou et al., 2018), we mainly discuss IAVs here. A vital challenge in combating IAVs is the constant evolution of the surface antigens, hemagglutinin (HA) and neuraminidase (NA), to resist pressure from the host immune system, which is described as antigenic drift and antigenic shift. Therefore, IAVs are classified into subtypes based on the genetic and antigenic differences of HA and NA, including 18 subtypes of HA (H1–H18) and 11 subtypes of NA (N1–N11) (Gamblin and Skehel, 2010).

At present, there are mainly two types of anti-influenza drugs used in clinics, including (1) M2 ion channel inhibitors, such as amantadine (Bright et al., 2006) and rimantadine, which block viral uncoating, and (2) neuraminidase inhibitors (NAIs), including oseltamivir (de Jong et al., 2005), zanamivir, peramivir, and laninamivir octanoate, which inhibit viral release. However, the continual emergence of drug resistance seriously limits their effectiveness and clinical applications (Zeng et al., 2017). In 2018, a new antiviral drug, baloxavir marboxil (trade name Xofluza), which can inhibit viral replication in cells, was approved by Japanese and United States FDA and proved effective against infection by influenza virus strains resistant to current anti-influenza drugs (Ng, 2019). Still, several cases of drug resistance to baloxavir marboxil have been reported recently (Takashita et al., 2019; Sato et al., 2020). Also, these drugs mentioned above must inhibit viral infection in the presence of target cells, instead of inactivating cell-free influenza virions.

As mentioned above, two envelope glycoproteins, HA and NA, are on the surface of the influenza virion. HA is originally translated as the HA0 precursor, about 560 amino acids (**Figure 3A**). Subsequently, it undergoes proteolytic cleavage and glycosylation to form a heterodimerized trimer composed of three HA1 and three HA2 subunits, and approximately 350–400 trimers are found on the surface of a virion (Skehel and Wiley, 2000). On the surface of HA1 globular head, it is the RBS (residues 116–261), composed of a β-barrel motif and α-helices, which resembles a shallow pocket. The key receptor binding residues are highly conserved among different HA subtypes (Priyadarzini et al., 2012). The C-terminus of HA2 subunit is the conserved stem, which is the target of multiple neutralizing antibodies (Ekiert et al., 2009; Sui et al., 2009). As shown in **Figure 3B**, to initiate the entry process, the RBS on HA attaches the virus to cell surface receptors that contain terminal sialic-acid residues, which triggers the virion entering an endosome via endocytosis (Sun and Whittaker, 2013). The acidic environment in the endosome induces conformational change of HA, enabling the exposure of the fusion peptide on the N-terminus of HA2. Subsequently, the fusion peptide inserts into the endosomal membrane with the C-terminal transmembrane domain (TMD) anchoring HA2 in the viral envelope, to create a pre-hairpin conformation (Bullough et al., 1994). Afterward, the HA2 subunit fold back on itself to form a hairpin that brings the two membranes closer. The hairpin further collapses into a six-helix bundle, which enables the formation of the lipid stalk and the subsequent fusion of the two membranes (Harrison, 2008, 2015).

Because HA plays a key role in viral attachment and membrane fusion, it is the promising target for the development of protein- and peptide-based IAV inactivators. Recently, Holthausen et al. (2017) isolated an amphibian special host defense peptide (HDP), urumin, from skin secretions of a frog native to southern India. This is a 27-amino acid peptide with net positive charges. Different from most HDPs that exert their virucidal activity by non-specific interaction with the viral lipid membranes, urumin could specifically interact with the conserved stalk region of H1N1 HA and then destroy the influenza virions. Interestingly, *in vivo* application of urumin could protect naive mice from challenge with a lethal dose of IAV infection, suggesting that urumin has good potential for further development into a first-line antiviral treatment during influenza outbreaks.

Using a computer-aided strategy based on the structural information of the binding site of neutralizing antibodies (Ekiert et al., 2009; Sui et al., 2009), Baker and colleagues designed proteins named HB36 and HB80, which could bind to a conserved surface patch of the HA stem from the 1918 H1N1 pandemic virus (Fleishman et al., 2011). Results showed HB36 and HB80 bound H1 and H5 HAs with low nanomolar (nM) affinity. Based on their mechanism of action, proteins designed in this way are expected to possess viral inactivation abilities; however, a viral inactivation experiment was not performed in this study. Therefore, the actual inactivation activities of HB36 and HB80 were uncertain, which requires further investigation.

In addition to the conserved stem of HA, the receptor-binding pocket mentioned above is also a promising target of IAV

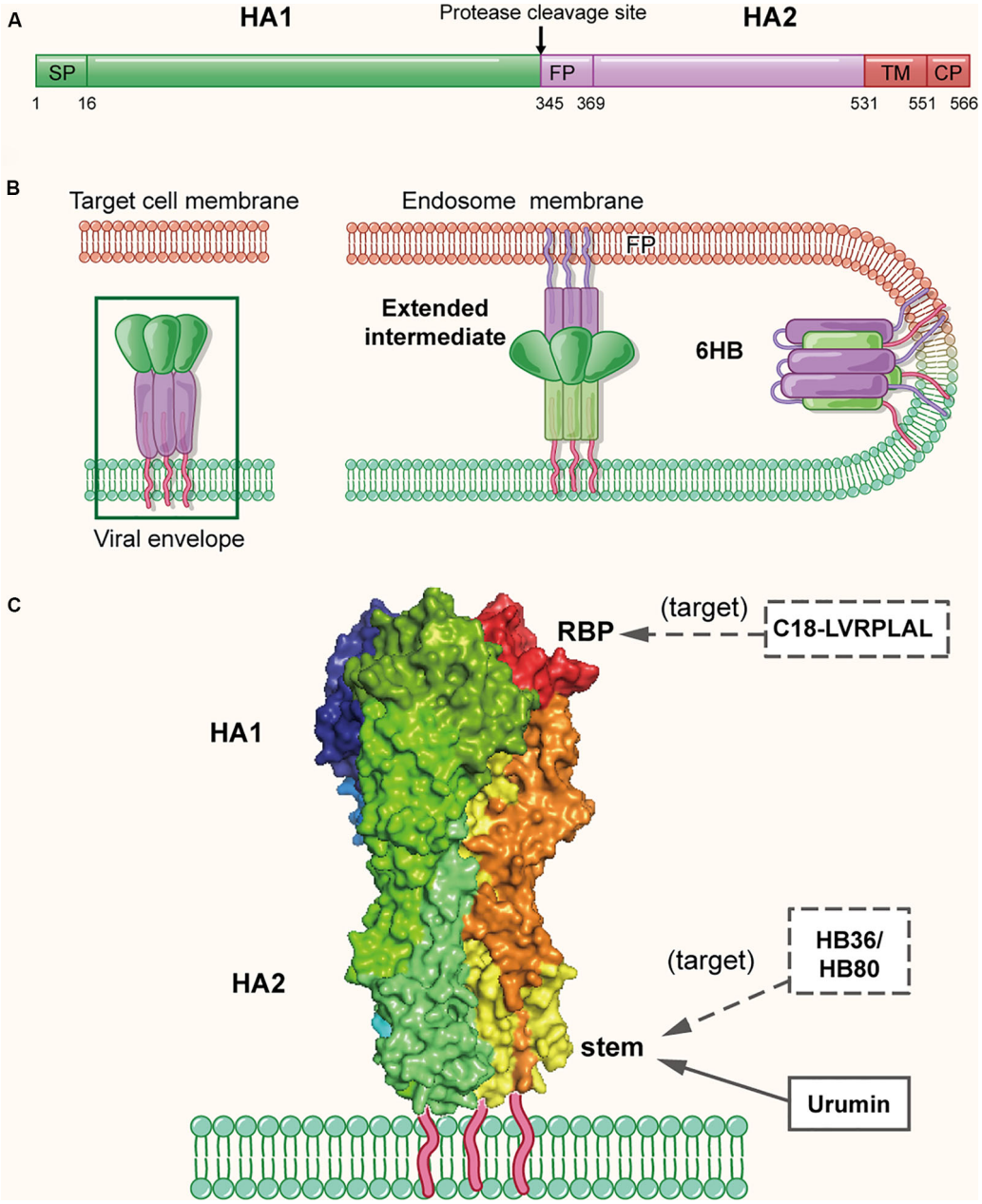


**FIGURE 3 |** The structure of influenza virus HA protein in the native and fusion-intermediate states, which serve as the target of the protein- and peptide-based influenza virus inactivators. **(A)** Schematic representation of HA composition, including surface subunit HA1 and transmembrane subunit HA2. **(B)** Attachment of HA protein to the cellular receptor(s) and fusion of viral envelope with endosomal membrane. To initiate the entry process, the RBS on HA attaches the virus to cell surface receptors that contain terminal sialic-acid residues, followed by entry of the virion into an endosome of the host cell via endocytosis. The acidic environment in the endosome induces conformational change of HA, enabling the exposure of the fusion peptide on the N-terminus of HA2. Subsequently, the fusion peptide inserts into the endosomal membrane with the C-terminal transmembrane domain (TMD) anchoring HA2 in the viral envelope, creating a pre-hairpin conformation (extended intermediate). Afterward, the HA2 trimers fold back on themselves forming a hairpin conformation, which then further collapses into a six-helix bundle, bringing the viral envelope and endosomal membrane together for fusion. The pre-fusion trimer is highlighted in a green box, which is shown in more detail in **(C)**. **(C)** Side view of the pre-fusion, trimeric conformation of HA protein present on the virion surface (modified from PDB ID: 4FNK). The heads of HA1 subunits are colored with dark tints, showing the receptor-binding pockets (RBPs). Names of inactivators are listed in the three boxes, and the arrows depict their target sites, including the conserved stem and RBP. Notably, potential inactivators remaining to be tested are listed in the box with dashed lines and arrow.

inactivators (Whittle et al., 2011; Ekiert et al., 2012; Yang et al., 2013) (**Figure 3C**). Through screening a phage-displayed random peptide library, Matsubara et al. (2010) identified several 15-mer sialic acid-mimic peptides that could bind the RBSs in H1 and H3 HAs and inhibit infection by the A/Puerto Rico/8/34 (H1N1) and A/Aichi/2/68 (H3N2) strains of IAV with IC50 at low μM level.

Later, they identified a series of 7-mer sialic acid-mimic peptides (Matsubara et al., 2016) by screening another phage-displayed random peptide library. They found that these peptides could also bind H1 and H3 HAs and that the binding could be inhibited in the presence of sialic acid. Plaque assays indicated that one of these peptides, C18-LVRPLAL, could strongly inhibit infection by the A/Aichi/2/68 (H3N2) strain with an IC50 value of 6.4 μM. However, none of the above peptides have been tested for their virus inactivation activities using a virus inactivation assay.

In sum, two conserved sites on HA protein, including the receptor-binding pocket and the conserved stem, have been the promising targets of influenza virus inactivators. Although HA protein itself does not belong to the range of inactivators we discuss here for not acting on cell-free virions, it can function through other two ways. It can be the possible receptor antagonist, which binds to the cell receptor to inhibit viral infection. Also, it has been the key immunogen of currently licensed influenza vaccines (Bosch et al., 2010; Houser and Subbarao, 2015; Yamada et al., 2019), which could elicit strain-specific anti-HA antibodies to neutralize the virus and prevent or control infection. Moreover, since most agents mentioned above have not been testified to possess inactivation activities against influenza virus with a standard assay, there still remains a long way to put them into practice.

## Protein- and Peptide-Based ZIKV and DENV Inactivators

Flaviviruses, with a positive-sense single-stranded RNA genome, are enveloped viruses transmitted by hematophagous mosquito vectors. Flavivirus infection may cause neurological, viscerotrophic or hemorrhagic diseases (Slon Campos et al., 2018). The *Flavivirus* genus (Flaviviridae family) is comprised of a variety of human pathogens, including DENV, ZIKV, yellow fever virus (YFV), West Nile virus (WNV), and so on (Kuno et al., 1998).

Zika virus infection usually causes mild symptoms, such as rash, fever, headache, and joint pain, but severe symptoms in some cases, such as Guillain-Barré syndrome, meningo-encephalitis and myelitis. ZIKV infection of pregnant women may cause microcephaly in their fetuses and newborns (Cui et al., 2017; Culshaw et al., 2018). Currently, with repurposing approaches, several FDA-approved drugs with anti-ZIKV activities have been identified, such as Sofosbuvir (Xu et al., 2016), but no drug has been licensed for clinical use (Wang et al., 2017; Han and Mesplede, 2018). Four serotypes of DENV (DENV-1, 2, 3, and 4) constitute the primary mosquito-borne viral pathogen. DENV is endemic in more than 100 countries worldwide, and infects ∼390 million people each year, of which 96 million people exhibit disease symptoms (Bhatt et al., 2013). After DENV infection, some individuals exhibit mild symptoms like flu, while others might suffer from more severe diseases, such as dengue hemorrhagic fever and shock syndrome (DHF/DSS) (Halstead, 2007). Till now, only several small molecule anti-DENV drugs such as UV-4B (Warfield et al., 2016) have entered Phase I or Phase II clinical trials (Tian et al., 2018), and no specific anti-DENV drugs have been approved for clinical use yet.

The particle structure and genomic organization are similar among all flaviviruses, with 180 E proteins and 180 M proteins forming 90 heterodimers, covering most surface area of a virion (Slon Campos et al., 2018). Taking DENV as an example, the ectodomain of each E protein monomer consists of three domains I, II, and III. Domain II contains a highly hydrophobic fusion loop capable of mediating fusion, and domain III contains RBSs. The C-terminus of domain III is the stem, a membrane anchoring region (**Figure 4A**), which is highly conserved in flaviviruses and forms a helix-loop-helix structure located below the E protein ectodomain and partially embedded in the viral envelope (**Figure 4C**) (Zhang et al., 2013). The M protein, consisting of 75 amino acids, includes a 40-amino acid ectodomain and a 35-amino acid transmembrane region. The ectodomain includes a hydrophobic loop structure, followed by an amphipathic helix, which may interact with the E protein on the virion surface (Zhang et al., 2013). Analysis of the interaction between E and M proteins on the DENV surface revealed that M protein, functioning as a pH-sensitive chaperone, plays a vital role during the process of viral infection and maturation (Li et al., 2008). As shown in **Figure 4B**, DENV infection is initiated by binding of domain III of E protein to the receptors on the target cell (Huerta et al., 2008), followed by entry of the virion into the endosome in the host cell via endocytosis. Under the acidic environment in the endosome, the E protein dimer dissociates, resulting in the individual subunits swinging outward. The exposed fusion loops insert into the endosomal membrane, promoting reassembly of the subunits to form the extended, trimeric intermediate. Subsequently, domain III in each subunit is reversely folded, bringing the viral envelope and the endosomal membrane into close proximity for fusion (Harrison, 2008; Klein et al., 2013).

Since E protein plays an significant role in receptor binding and membrane fusion, it is considered as a promising source and target for development of protein- and peptide-based DENV inactivators. In recent years, the structure of DENV E protein has been well determined using X-ray crystallography and cryo-electron microscopy (Cryo-EM) (Zhang et al., 2013), which has allowed researchers to rationally design DENV inactivators (Chew et al., 2017). Using a physiochemical algorithm, the Wimley-White interfacial hydrophobicity scale (WWIHS), together with the known structural information of DENV E protein, Hrobowski et al. (2005) designed four peptides (DN80, DN57, DN81, and DN59) derived from different regions of DENV E protein. They found that DN59, derived from the helix-loop-helix sequence of the DENV-2 E protein stem region (residues 692–724) with amphipathicity and membrane-binding ability, could inhibit infection of all four serotypes of DENV with IC50 values in the range of 2–5 μM. It was also effective against some other flaviviruses, such as yellow fever virus (YFV) (Lok et al., 2012). Further studies of its mechanism of action have shown that it can irreversibly inactivate virions by directly interacting with viral lipid membranes and forming holes at the five-fold vertices in the viral envelope, allowing the release of viral genomic RNA (Schmidt et al., 2010a,b; Lok et al., 2012).

Since the stem of flavivirus E protein is highly conserved, results of the above studies imply that protein- and peptide-based

ZIKV inactivators can also originate from the stem sequence. Accordingly, peptide Z2 was designed and synthesized, which is derived from the stem of ZIKV E protein (residues 421–453), and similarly Z2 was shown to inhibit infection by different strains of ZIKV and other flaviviruses, including YFV and DENV with IC50 values between 1 and 14 μM. Animal studies indicated that Z2 could protect A129 and AG6 mice from lethal ZIKV challenge; Z2 was also found to cross the placental barrier and prohibit vertical transmission of ZIKV in pregnant mice. The mechanism studies suggested that Z2 could interact with E protein and inactivate the virions, with an EC50 value of ∼2.5 μM, by forming pores in the viral envelope, allowing the release of the viral RNA genome (Yu et al., 2017). Although Z2 could not cross the blood–brain barrier (BBB) to enter the fetal brain, it was able to inactivate virions in the placenta or umbilical cord, thus effectively reducing the viral titers in the fetal brain.

In addition to the conserved stem, other regions in E protein may also serve as sources of DENV inactivators. Based on the native dimeric E structure, Costin et al. (2010) designed a set of anti-DENV peptides using predictive strategies together with computational optimization. The two most active peptides, DN57opt and 1OAN1, derived from the domain II hinge region (residues 205–232) and the first domain I/domain II beta sheet connection (residues 41–60), respectively, could inhibit DENV-2 infection with IC50 values of 8 and 7 μM, respectively. The biolayer interferometry study demonstrated that both DN57opt and 1OAN1 could bind to soluble DENV-2 E protein, and Cryo-EM analysis revealed that the surface of virions treated with DN57opt or 1OAN1 became rough, suggesting that the viral envelope may have been damaged (Costin et al., 2010). However, the virus inactivation abilities of these peptides were not reported, and their specific mechanism of action needs to be further explored.

Apart from being the source of DENV inactivators, other regions of E protein can also be potential targets. A previous study reported the existence of a hydrophobic pocket between domain I and II, which acted as a hinge of the E protein structural rearrangement and could interact with the detergent β-*N*-octyl-glucoside (Modis et al., 2003). By molecular docking analysis, Panya et al. (2014) identified several short peptides targeting the hydrophobic pocket. They found that the dipeptide Glu-Phe (EF for short) could inhibit the infection of all four DENV serotypes, but it was the most effective against DENV-2 with an IC50 value of 96 μM. Different inhibitory effect for the four serotypes of DENV was possible because of the different amino acid sequence of their hydrophobic pockets. Inferred from its mechanism of action, EF peptide can be considered as a DENV inactivator, as potentially confirmed by performing a virus inactivation assay. In addition, the lateral loop of domain III has been verified to play an important role in virus-cell receptor interaction, thus making it another feasible target of protein- and peptide-based DENV inactivators (Hung et al., 2004; Mazumder et al., 2007). Using the BioMoDroid algorithm, Alhoot et al. (2013) screened for anti-DENV peptides targeting a short sequence (residues 380–389) in the lateral loop of DENV-2 E protein domain III. They found that peptides DET2 and DET4 could inhibit DENV-2 infection with IC50 values of 500 and 35 μM, respectively. Observed with transmission electron microscopy, the surface of virions was found to become irregular and have rough edges, suggesting that these peptides could inactivate virions by disrupting integrity of the viral envelope.

Other studies showed that M protein of DENV could interact with native E protein to trigger the conformation of DENV E protein, suggesting that peptides derived from M protein may act as DENV inactivators. Panya et al. (2015) designed a novel anti-DENV peptide, MLH40, derived from the conserved ectodomain of M protein, and found that it could inhibit infection of four serotypes of DENV with IC50 values ranging from 24 to 31 μM. Molecular docking analysis suggested that the N-terminal loop of MLH40 could interact with DENV E protein to alter its native dimeric conformation. However, its inactivation activity has not been tested and reported.

In sum, the studies on DENV and ZIKV inactivators are not as comprehensive as those on HIV inactivators (**Figure 4C**). Almost all of them are peptides, not proteins; some important targets including the RBS in domain III have not been utilized adequately like CD4bs in HIV gp120 (Huerta et al., 2008). In addition, the viral inactivation activities of many peptides have not been verified with the virus inactivation assay, and specific targets and action mechanisms of most peptide-based inactivators have not been clearly elucidated. Despite of these deficiencies, the design and development of DENV and ZIKV inactivators can be referential paradigms for those of newly emerging or re-emerging viruses.

## Protein- and Peptide-Based HSV Inactivators

Herpesviruses, a large and diverse family of enveloped viruses with double-stranded DNA genomes, can bring about lifelong, latent infections (Pellet and Roizman, 2013). These viruses are classified as three subfamilies, alpha-, beta-, and gamma-, on the basis of their genome sequences and biological properties (Davison et al., 2009). In alpha-herpesviruses, herpes simplex virus types 1 and 2 (HSV-1 and HSV-2) and varicella-zoster virus (VZV) are human pathogens, which routinely infect humans (Roizman et al., 2013). HSV, among the most widespread pathogenic agents in the human population, causes varieties of diseases, ranging from oral and genital ulcers to devastating encephalitis. Following the initial infection at a peripheral site, it will establish a lifetime latency in sensory neurons, which can be reactivated by some internal or external stimuli, including fever, immunosuppression, trauma, etc. (Roizman et al., 2013). So far, three categories of drugs have got approval for the treatment of HSV infection, including (1) the nucleoside analogs such as acyclovir (ACV), (2) the acyclic nucleotide analog cidofovir and (3) the pyrophosphate analog foscarnet (Kimberlin and Whitley, 2007). Till now, ACV remains the prototypic antiviral agent and the reference for treating HSV infection. However, viral resistance to ACV has become a critical clinical problem, especially concerning immunocompromised patients undergoing long-term therapy (Englund et al., 1990). Although the other two drugs also have been proven to be effective for treating HSV infection, they are reserved for confirmed cases of ACV resistance

due to their nephrotoxicity (Galdiero et al., 2013). In addition, these drugs all exert antiviral effects by targeting viral DNA polymerase in target cells, therefore no antiviral drugs targeting HSV entry are available currently, let alone inactivating virions (Galdiero et al., 2013).

Different from most of other enveloped viruses using a single Env to mediate viral fusion process, HSV utilize a set of surface glycoproteins including gD, gH/gL, and gB as the core fusion components. Therein gD acts as the receptor-binding protein, gH/gL as the fusion regulator and gB as the class III fusogen (Heldwein et al., 2006; Arii and Kawaguchi, 2018). Taking HSV-1 as the example, HSV-1 gD (369-amino acids) is a type I membrane glycoprotein with a short cytoplasmic tail and an ectodomain with an immunoglobulin-like core flanked by N- and C-terminal extensions (Carfi et al., 2001). As shown in **Figure 5A**, HSV-1 gH is an 838-amino acid type I membrane glycoprotein comprised of a single pass transmembrane domain, a short cytoplasmic tail and an ectodomain (Gompels and Minson, 1986). Its ectodomain can be subdivided into domains H1 (H1A and H1B), H2 and H3, and the N-terminal H1 domain binds gL to form a non-covalent heterodimer (Gompels and Minson, 1986; Chowdary et al., 2010). Results showed the crystal structure of gH/gL complex does not resemble any other known viral fusogen structure. Therefore, the gB-gH/gL complex is key for fusion and can be inhibited by neutralizing antibody to gH, implying that the gH/gL complex activates gB through direct binding (Chowdary et al., 2010). Furthermore, a recent study confirmed the C-terminal domain H3 of HSV-1 is important for interaction with gB (Bohm et al., 2016). HSV-1 gB, is a 904-amino acid glycoprotein with an extended rodlike ectodomain, transmembrane domain (TM) and cytoplasmic domain (CP) (**Figure 5A**). The ectodomain has five distinct parts, domains I–V, and domain IV is fully exposed with neutralizing epitopes on it and possibly interacts with cellular receptors (Heldwein et al., 2006).

Herpes simplex virus may enter cells through endocytosis or direct fusion of the viral envelope with cellular membrane, relying on the target cell type (Nicola, 2016); notably, both routes require the same set of viral glycoproteins (Nicola and Straus, 2004). HSV entry through direct fusion is a coordinated process that involves a cascade of events, which can be briefly divided into (1) binding to specific cell receptors, (2) intracellular signaling, and (3) fusion of the viral envelope with host cell membrane (Connolly et al., 2011). At the beginning of entry process, binding of glycoprotein D to one of its cognate receptors is significant. Four gD receptors of HSV-1 and HSV-2 have been confirmed: a member of the tumor necrosis factor (TNF) receptor family, herpesvirus entry mediator (HVEM); the poliovirus receptor family, including nectin-1 and nectin-2, belonging to the immunoglobulin superfamily; and a modified form of heparan sulfate, 3-*O*-sulfated heparan sulfate, 3-*O*-HS (Weed and Nicola, 2017). Binding of gD to either receptor results in its C-terminus movement, which exposes the profusion domain of gD (residues 260–285) (Cocchi et al., 2004; Krummenacher et al., 2005; Gallagher et al., 2013). Recent studies demonstrated gB may also bind to specific cell receptors, such as paired immunoglobulin-like type 2 receptor (PILR)α (Satoh et al., 2008), myelin-associated glycoprotein (MAG) (Suenaga et al., 2010), non-muscle myosin heavy chain IIA (NMHC-IIA) (Arii et al., 2010) or non-muscle myosin heavy chain IIB (NMHC-IIB) (Arii et al., 2015). Meanwhile, gH/gL may be facilitated by the activated form of gD to convert into a conformation able to interact with gB (Atanasiu et al., 2007, 2010a,b, 2016), triggering the prefusion form of gB transforming into a fusogenic state. Next, Akt (protein kinase B) may be triggered to translocate to the outer leaflet microdomains of the plasma membrane to interact with gB (Cheshenko et al., 2013, 2018), which further induces Akt phosphorylation and intracellular calcium release. Subsequently gB inserts the fusion loop into the target cell membrane (Zeev-Ben-Mordehai et al., 2016) to form the extended, trimeric intermediate, which results in fusion of the two membranes and release of the capsid into the cell (**Figure 5B**) (Eisenberg et al., 2012; Arii and Kawaguchi, 2018).

Since the direct fusion is governed by gD, gH/gL, and gB, they are potential sources and targets of protein- and peptide-based HSV inactivators (Galdiero et al., 2013). Akkarawongsa et al. (2009) identified three antiviral peptides, gB94, gB122, and gB131, from the peptide library of HIV-1 gB-1 ectodomain (**Figure 5C**). The peptides gB94 (residues 496–510) and gB122 (residues 636–650) could inactivate cell-free virions with EC50 of 125 and 138 μM, respectively, although their detailed mechanism of action has not been reported. However, while peptide gB131 (residues 681–695) exhibited no virus inactivation, it did show inhibitory activity (IC50: ∼12 μM). More recently, Cetina-Corona et al. (2016) created a library of continuous 15-25 residue stretches (CRSs) located on the surface of HSV-2 gH and HSV-1 gB through bioinformatics analysis. According to the flexibility, charged residues and conservatism of the CRS sequence, they selected and synthesized peptides CB-1 and CB-2 derived from gH and peptides U-1 and U-2 derived from gB (**Figure 5C**). Results showed that peptides U-1 and U-2 at 100 μM could inactivate more than 80% of HSV-1 and HSV-2 virions, while peptides CB-1 and CB-2 at 100 μM could only inactivate less than 50% of these virions. However, the detailed mechanism of action showing how these peptides inactivate cell-free HSV virions has not been clarified. Meanwhile, the viral inactivation activities of these peptide inactivators are relatively weak, requiring further optimization.

As mentioned above, the fusion process is mediated by a set of interactions between gD, gH/gL, and gB, and between these glycoproteins and their receptors (Azab and Osterrieder, 2017; Weed and Nicola, 2017), thus multiple glycoprotein or RBSs are potential to be targets of HSV inactivators. Taking the potent gH/gL-specific neutralizing antibody as the example, it could inhibit the formation of the gB-gH/gL complex, suggesting that the gB binding site in gH/gL may locate in the vicinity of the neutralizing epitope (Chowdary et al., 2010; Bohm et al., 2016). Therefore, the neutralizing epitope in gH/gL may serve as one of the targets. Similarly, glycoprotein-binding sites or RBSs on gD (Di Giovine et al., 2011; Lee et al., 2013; Cairns et al., 2019) also prompt the design of HSV inactivators, just like the CD4bs in HIV gp120. Therefore, more comprehensive studies on the crystal structures of these glycoproteins and the mechanism of the fusion process

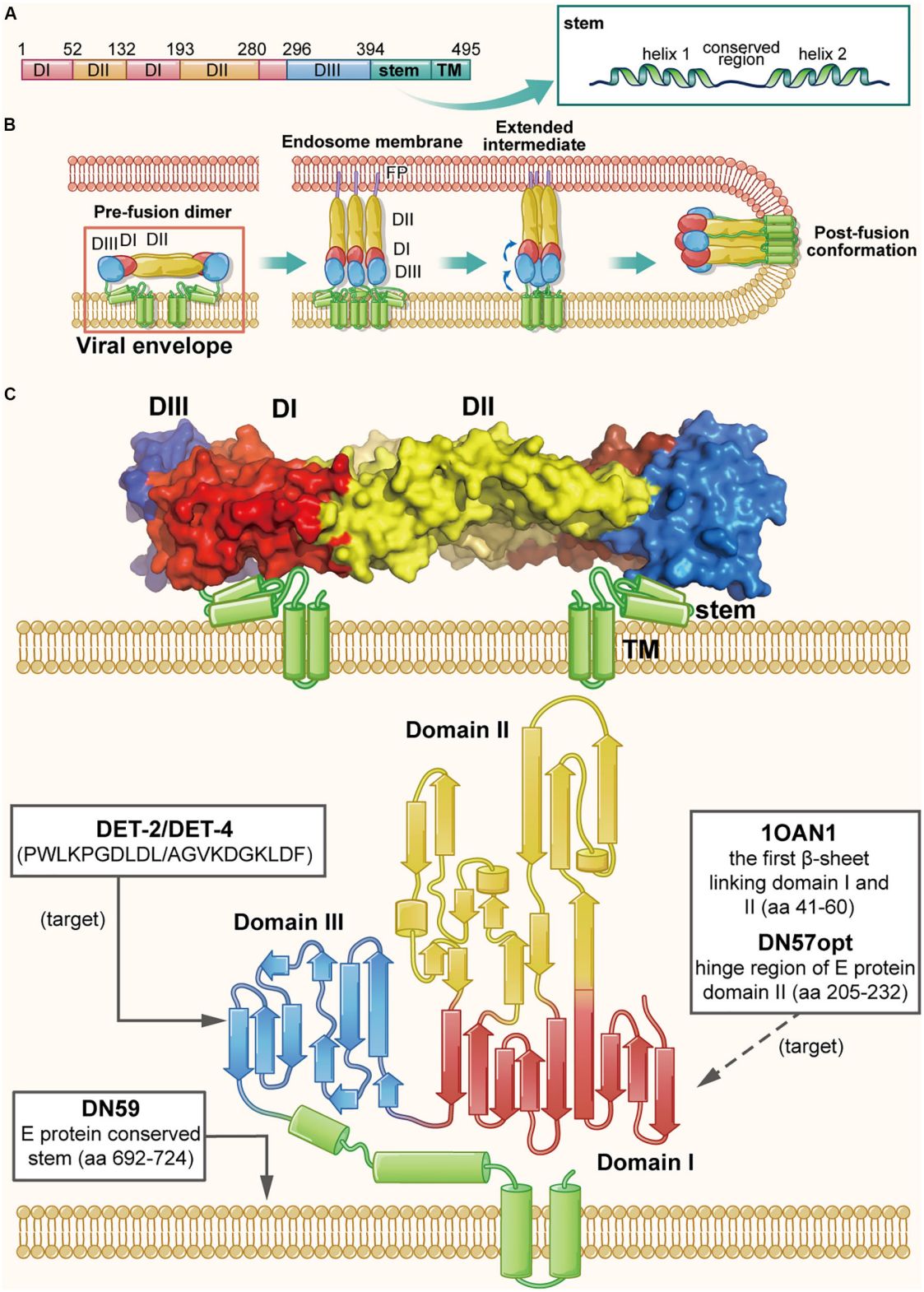


**FIGURE 4 |** The structure of DENV E protein in the native and fusion-intermediate states, which serve as sources and targets of the protein- and peptide-based DENV inactivators. **(A)** Schematic representation of E protein composition, including domains I–III (colored red, yellow and blue, respectively), stem and transmembrane region (TM). **(B)** Attachment of DENV E protein to the cellular receptor(s) and fusion of viral envelope with the endosome membrane. Binding of E

*(Continued)*

**FIGURE 4 |** Continued
protein domain III with the receptor on the target cell is followed by entry of the virion into endosomes of the host cell via endocytosis. Under the acidic environment in the endosome, E protein dimer dissociates, resulting in the individual subunits swinging outward. The exposed fusion loops insert into the endosomal membrane, which facilitates the reassembling of the subunits to form the extended, trimeric intermediate. Subsequently, domain III in each subunit is reversely folded to promote the viral envelope and the endosomal membrane into close proximity for fusion. The pre-fusion dimer is highlighted in a red box, which is shown in more detail in **(C)**. **(C)** Side view of the pre-fusion, dimeric conformation of E protein present on the virion surface (modified from PDB ID: 1OAN). Names and sequences of inactivators are listed in the three boxes, and the arrows depict their target sites, including the lateral loop of domain III and the viral lipid membrane. Notably, potential inactivators remaining to be tested are listed in the box with a dashed arrow.

are essential for the design of protein- and peptide-based HSV inactivators.

## DISCUSSION

The lower eukaryotic organisms, such as invertebrates and plants, only possess the innate immunity system, including some antimicrobial peptides (AMPs) that can non-specifically destroy the viral envelope and inactivate the cell-free virions (Ganz, 2003; Seo et al., 2012). After long evolution, higher vertebrates have gained an advanced adaptive immune system that can specifically attack and inactivate pathogenic viruses. Neutralizing antibodies are a vital component of the adaptive immune system. According to our definition of virus inactivators described before, many of the viral neutralizing antibodies with the ability to irreversibly inactivate cell-free virions can be considered as protein-based virus inactivators. The development of neutralizing antibodies during the evolutionary process may also reflect the fact that protein-based virus inactivators able to actively attack and inactivate cell-free virions have certain advantages against viral infections (Burton, 2002). Nonetheless, how these neutralizing antibodies inactivate cell-free virions is still unclear, and for this reason, they were not discussed in detail in this review.

Viral fusion proteins in different oligomeric states and structures can be classified into three different classes (classes I, II, and III) (Weissenhorn et al., 2007; Harrison, 2008). Here we reviewed the development of PPVIs against the following representative enveloped viruses: HIV and influenza virus (with class I membrane fusion), ZIKV and DENV (with class II membrane fusion), and HSV (with class III membrane fusion). Although their fusion/entry processes vary from each other, some common technologies can be used for identifying or designing and evaluating PPVIs, including those (1) for constructing recombinant fusion proteins, such as those applied to design the potent protein-based HIV-1 inactivators 2DLT and 2Dm2m (Lu et al., 2012; Chen et al., 2014); (2) for constructing phage display peptide libraries, such as the one utilized to screen for the peptide 12p1, from which the peptide-based HIV-1 inactivator Triazole KR13 was designed (Bastian et al., 2011, 2013); (3) for performing computer-aided design of proteins or peptides targeting the RBS, such as the CD4bs in HIV-1 gp120 and sialic-acid binding site in influenza virus HA1, or the conserved stem regions, such as those in DENV and ZIKV E protein; and (4) for performing viral inactivation assays, such as those for evaluating inactivation activities of the PPVIs against HIV-1 and ZIKV (Lu et al., 2012; Yu et al., 2017). In general, these techniques and strategies have been successfully applied to design a variety of virus inactivators targeting viral Envs, and they can also be used for the design of virus inactivators against other enveloped viruses, particularly the newly emerging and re-emerging viruses with potential to cause global pandemics (**Table 1**).

Moreover, by learning from the design strategies of inactivators against enveloped viruses, we can now design and develop viral inactivators targeting key proteins involved in the entry process of non-enveloped viruses. The entry process of a non-enveloped virion is initiated by binding of the viral capsid protein to the cell receptor, followed by entry of the virion into endosomes in the host cell through clathrin- or caveolae-mediated endocytosis or macropinocytosis. The low pH environment causes conformational change of the virus capsid, leading to the externalization of membrane-penetrating peptides (MPPs) in endosomal compartments. Finally, MPPs are integrated or associated with endosomal membranes, leading to distortion and disruption of the membrane and allowing the release of nucleocapsid or genome into the cytosol (Kumar et al., 2018). Considering that most complicated fusion steps occur in the cell endosome, the receptor-binding domains in the viral capsid protein seem to be the best targets for design of PPVIs against non-enveloped viruses. However, the structure and function of the receptor-binding domains in their capsid proteins have not been well studied (Day and Schelhaas, 2014). Therefore, the design of virus inactivators against non-enveloped viruses still has a long way to go.

At present, development of PPVIs has become a topic of strong interest in the field of antiviral drugs. Different from "passive defenders," and fusion inhibitors and receptor antagonists in "gate keepers," protein- and peptide-based inactivators have been found to actively attack and inactivate cell-free virions anywhere they meet in the blood by specifically interacting with one or more sites in Env on the virion, thus they are expected to have higher utilization rate than the current antiviral drugs. The action mechanisms of PPVIs include (1) blocking the RBS on viral Envs, (2) inducing conformational changes of viral Env, causing the virion to lose the ability to enter the host cell, or (3) binding to the Env stem or the viral lipid membrane, to disrupt the integrity of the viral envelope or lead to the release of viral genetic materials. Apart from these, exact mechanisms of some PPVIs still remain to be explored.

In general, protein and peptide drugs are safer for humans than small-molecule chemical drugs because these big molecules do not enter the host cells, thus having no adverse effect on the functions of intracellular proteins. However, the effect of long-term use of PPVIs, especially those mimicking human proteins,

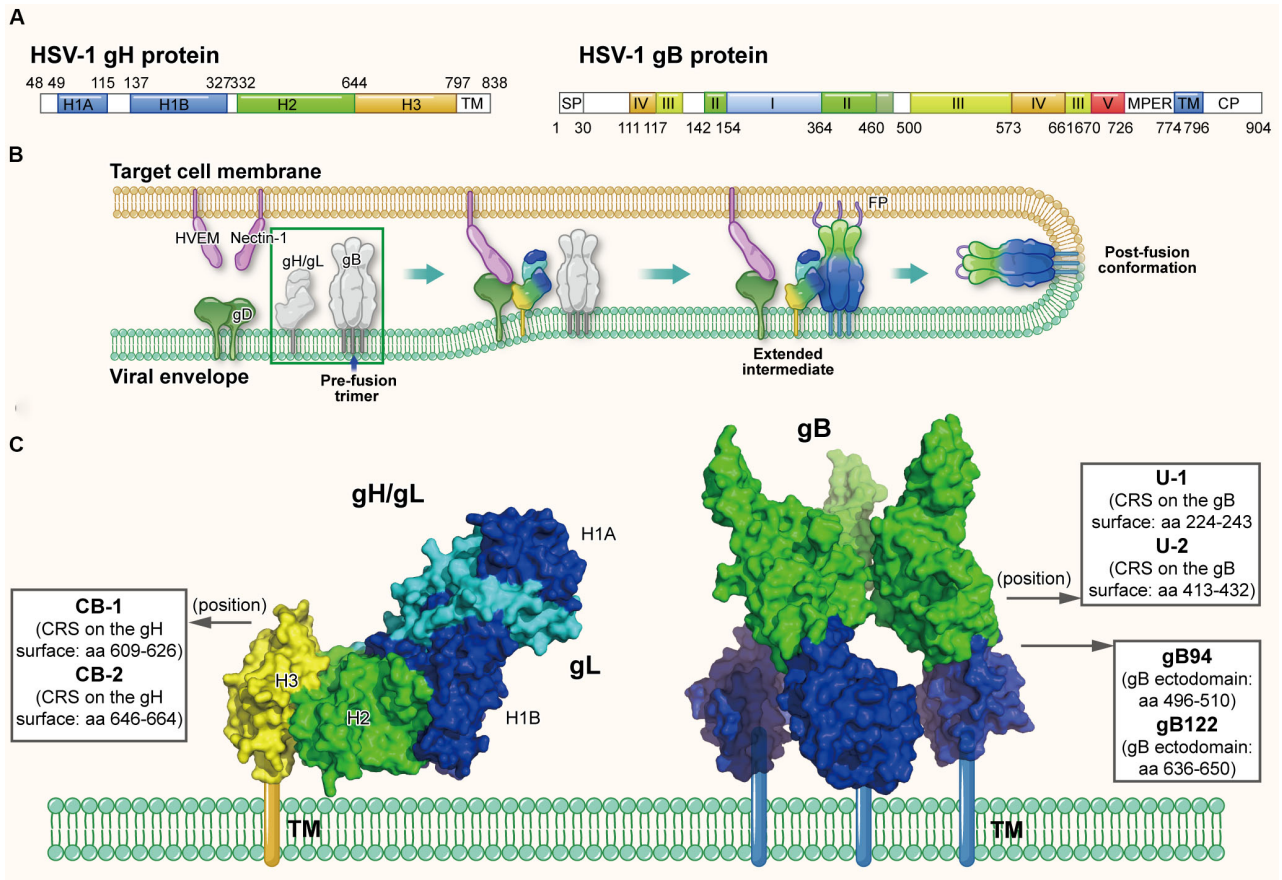


**FIGURE 5 |** The structures of HSV gH and gB protein in the native and fusion-intermediate states, which serve as sources of protein- and peptide-based HSV inactivators. **(A)** Schematic representation of HSV-1 gH and gB composition. gH is composed of the ectodomain (H1, H2, and H3 domains, colored mazarine blue, green, and yellow, respectively), transmembrane domain (TM) and cytoplasmic tail (CP). gB is composed of domains I–V, transmembrane region (TM) and cytoplasmic domain (CP). **(B)** The HSV entry process orchestrated by a set of glycoproteins, including receptor-binding gD, fusion-regulating gH/gL and the fusogen gB. gD binding to either receptor, such as HVEM and nectin-1, causes its conformational change to expose the profusion domain. gB may also bind to specific cell receptors, such as (PILR)α and NMHC-II. Meanwhile, gH/gL may be facilitated by the activated form of gD to convert into a form able to interact with gB, triggering the transformation of the prefusion form of gB into a fusogenic state. Next, Akt (protein kinase B) may be triggered to translocate to the outer leaflet microdomains of the plasma membrane to interact with gB, which further induces Akt phosphorylation and intracellular calcium release. Subsequently gB inserts the fusion loop into the target cell membrane to form the extended, trimeric intermediate, which allows fusion of the two membranes. The pre-fusion conformation of gH/gL and gB are highlighted in a green box, which is shown in more detail in **(C)**. **(C)** Side view of the pre-fusion conformation of the native gH/gL complex (modified from PDB ID: 3M1C) and gB (modified from PDB ID: 5FZ2). Names and sequences of inactivators are listed in the three boxes, and the arrows depict their positions on gH/gL and gB. Target sites of these inactivators have not been defined clearly, thus not shown here.

such as the CD4 receptor, on the normal function of human body are still unknown, since many of these drug candidates have not been tested in clinics. To solve this problem, maybe we can design binding analogs of human proteins, like CD4M9 (Vita et al., 1999), or only select the core domain of natural structures, like mD1.22 mentioned above (Chen et al., 2014). Another potential problem is the immunogenicity of the protein- and peptide-based inactivators. After long-term use in humans, these exogenous proteins and peptides may induce specific antibodies against them, which may attenuate their inactivation activities. Therefore, immunogenicity of these drug candidates to humans should be assessed and reduced before further development. In recent years, strategies to remove the immunogenicity of the protein-based drug candidates are increasingly diverse and mature. In fact, they mainly focus on the T-cell epitope of the candidate, since T cell plays a key role in activating B cells to transform into antibody-producing plasma cells (Moise et al., 2016) and the linear T-cell epitope is more prone to predict than the steric B-cell epitope. One method adopted widely is to calculate the T-cell epitope with a forecasting software, such as Epimatrix developed by EpiVax Inc. (De Groot et al., 2008), validate the T-cell epitope with experiments (such as T-cell proliferation assay) and mutate its amino-acid sequence to remove the immunogenicity (Weber et al., 2009).

Besides these two disadvantages, compared with chemical-based virus inactivators, PPVIs usually have a shorter half-life and lack oral availability thus require several times of injection a week. In terms of their higher production cost, PPVIs are

**TABLE 1 |** Summary of protein- and peptide-based virus inactivators.

| Name | Sequence | Target | EC50* (virus tested) | Reference |
|---|---|---|---|---|
| **HIV inactivators** | | | | |
| sCD4 | Extracellular D1–D4 or D1D2 domain | gp120 CD4bs | 153 and 297 nM (HIV-1 IIIB and Bal, respectively) | Deen et al., 1988; Traunecker et al., 1988; Daar et al., 1990; Orloff et al., 1993 |
| 2DLT | D1D2 domain-L35-T1144 | gp120 CD4bs + gp41 PFI | 17.3–78.6 nM (multiple HIV-1 strains) | Lu et al., 2012 |
| 2Dm2m/4Dm2m | 2 or 4 mD1.22 with 2 m36.4 | gp120 CD4bs + CoRbs | 0.3–1.1 nM (HIV-1 IIIB) | Chen et al., 2014; Qi et al., 2017 |
| Triazole KR13 | Modified peptide derived from 12p1 (RINNIPWSEAMM) | gp120 CD4bs + CoRbs | 0.5–25.6 μM (multiple HIV-1 strains) | Bastian et al., 2011, 2013 |
| DAVEI | CVN + gp41 MPER | gp120 glycan sites + gp41 | 28.3 nM (HIV-1 Bal.01 pseudovirus) | Parajuli et al., 2018 |
| **Influenza virus inactivators** | | | | |
| Urumin | IPLRGAFINGRWDSQCHRFSNGAIACA | H1 HA conserved stem | HNBD# | Holthausen et al., 2017 |
| **ZIKV inactivators** | | | | |
| DN59 | E protein stem (aa 692–724): MAILDDTAWDFGSLGGVFTSIGKALHQ VFGAIY | DENV lipid membrane | 4.8 μM (DENV-2) | Schmidt et al., 2010a,b; Lok et al., 2012 |
| Z2 | E protein stem (aa 421–453): MAVLGDTAWDFGSVGGALNSLGKGIH QIFGAAF | ZIKV lipid membrane | 2.52 μM | Yu et al., 2017 |
| **HSV inactivators** | | | | |
| gB94 | gB ectodomain (aa 496–510): KTTSSIEFARLQFTY | HSV-1 | 125 μM | Akkarawongsa et al., 2009 |
| gB122 | gB ectodomain (aa 636–650): GHRRYFTFGGGYVYF | HSV-1 and 2 | 118 μM | Akkarawongsa et al., 2009 |
| U-1 | CRS on gB surface (aa 224–243): HRDDHETDMELKPANAATRT | HSV-1 and 2 | HNBD# | Cetina-Corona et al., 2016 |
| U-2 | CRS on gB surface (aa 413–432): CIGKDARDAMDRIFARRYNA | HSV-1 and 2 | HNBD# | Cetina-Corona et al., 2016 |
| CB-1 | CRS on gH surface (aa 609–626): QATRSETPVEVLAQQTHG | HSV-1 and 2 | HNBD# | Cetina-Corona et al., 2016 |
| CB-2 | CRS on gH surface (aa 646–664): PEASHRCGGQSANVEPRIL | HSV-1 and 2 | HNBD# | Cetina-Corona et al., 2016) |

**EC50, half maximal effective concentration causing virus inactivation. #HNBD, has not been defined. CD4bs, CD4-binding site; CoRbs, coreceptor-binding site.*

generally more expensive for long-term treatment of chronic viral infection. Lentiviral vector-based gene therapy to secret a PPVI continuously can be one choice to lower the cost (Perez et al., 2005; Egerer et al., 2011; Falkenhagen et al., 2014, 2017). For example, Falkenhagen et al. (2014) designed lentiviral vectors encoding secreted anti-HIV proteins including sCD4, which could prohibit the infection of both gene-modified and unmodified cells. They further investigated the *in vivo* application of this approach by injecting gene-modified hematopoietic stem/progenitor cells (HSPCs) into humanized mice. The results demonstrated a reduction of viral load over time in humanized mice capable of secreting sCD4, upon challenge with HIV (Falkenhagen et al., 2017). Therefore, continuous delivery of secreted PPVIs via gene therapy is also a potential way apart from oral administration of chemical-based virus inactivators or frequent injection of PPVIs.

In particular, the disadvantages of PPVIs mentioned above may not be the problems for the urgent treatment of the highly pathogenic emerging and re-emerging virus infections, e.g., Ebola virus or Middle East respiratory syndrome coronavirus (MERS-CoV) infection. Drugs are especially key in the first aid, when several days later, protective antibodies are produced in the body to combat viruses, but lives may be taken away at any time (Baseler et al., 2017; Mubarak et al., 2019). In fact, characteristics of medication against these viral infections are short-term use (1–3 weeks), rapid application and high safety for the infirm patients, therefore the cost may not be a problem to consider. Besides, the need of rapid application parallels to the injection requirement of PPVIs, which takes effect faster than oral administration. Also, protein-based drugs are intrinsically safe (Zaman et al., 2019), and in this circumstance, their short half-lives become an advantage instead because they will not accumulate in the body. In sum, PPVIs may be a good choice when facing the pandemic of the highly pathogenic newly emerging and re-emerging viruses.

Nowadays, a variety of protein and peptide drugs, including antibody drugs, have been approved for clinical use. Because of their advantages mentioned above, we believe that more and

more PPVIs will be developed for treatment and prevention of viral infections, particularly useful for combating the pandemics or epidemics of newly emerging and re-emerging virus infections.

## AUTHOR CONTRIBUTIONS

YW organized the manuscript. XS and QW collected related literatures, drew the table, and wrote the manuscript. LL revised the introduction, HIV, and influenza virus part of the manuscript. SJ revised the ZIKV and DENV, HSV, and the discussion part of the manuscript.

## FUNDING

This study was supported by grants from the National Mega-Projects of China for Major Infectious Diseases (2018ZX10301403 to LL) and the National Natural Science Foundation of China (81661128041, 81672019, and 81822045 to LL, 81630090 to SJ, and 81701998 to QW).

## ACKNOWLEDGMENTS

We thank Guangzhou Sagene Biotech Co., LTD. for the assistance in preparing the figures with high quality.

## REFERENCES

Akkarawongsa, R., Pocaro, N. E., Case, G., Kolb, A. W., and Brandt, C. R. (2009). Multiple peptides homologous to herpes simplex virus type 1 glycoprotein B inhibit viral infection. *Antimicrob. Agents Chemother.* 53, 987–996. doi: 10.1128/AAC.00793-08

Alhoot, M. A., Rathinam, A. K., Wang, S. M., Manikam, R., and Sekaran, S. D. (2013). Inhibition of dengue virus entry into target cells using synthetic antiviral peptides. *Int. J. Med. Sci.* 10, 719–729. doi: 10.7150/ijms.5037

Allaway, G. P., Davis-Bruno, K. L., Beaudry, G. A., Garcia, E. B., Wong, E. L., Ryder, A. M., et al. (1995). Expression and characterization of CD4-IgG2, a novel heterotetramer that neutralizes primary HIV type 1 isolates. *AIDS Res. Hum. Retroviruses* 11, 533–539. doi: 10.1089/aid.1995.11.533

Aneja, R., Rashad, A. A., Li, H., Kalyana Sundaram, R. V., Duffy, C., Bailey, L. D., et al. (2015). Peptide triazole inactivators of HIV-1 utilize a conserved two-cavity binding site at the junction of the inner and outer domains of Env gp120. *J. Med. Chem.* 58, 3843–3858. doi: 10.1021/acs.jmedchem.5b00073

Arii, J., Goto, H., Suenaga, T., Oyama, M., Kozuka-Hata, H., Imai, T., et al. (2010). Non-muscle myosin IIA is a functional entry receptor for herpes simplex virus-1. *Nature* 467, 859–862. doi: 10.1038/nature09420

Arii, J., Hirohata, Y., Kato, A., and Kawaguchi, Y. (2015). Nonmuscle myosin heavy chain IIb mediates herpes simplex virus 1 entry. *J. Virol.* 89, 1879–1888. doi: 10.1128/JVI.03079-14

Arii, J., and Kawaguchi, Y. (2018). The role of HSV glycoproteins in mediating cell entry. *Adv. Exp. Med. Biol.* 1045, 3–21. doi: 10.1007/978-981-10-7230-7_1

Atanasiu, D., Saw, W. T., Cohen, G. H., and Eisenberg, R. J. (2010a). Cascade of events governing cell-cell fusion induced by herpes simplex virus glycoproteins gD, gH/gL, and gB. *J. Virol.* 84, 12292–12299. doi: 10.1128/JVI.01700-10

Atanasiu, D., Saw, W. T., Eisenberg, R. J., and Cohen, G. H. (2016). Regulation of herpes simplex virus glycoprotein-induced cascade of events governing cell-cell fusion. *J. Virol.* 90, 10535–10544. doi: 10.1128/JVI.01501-16

Atanasiu, D., Whitbeck, J. C., Cairns, T. M., Reilly, B., Cohen, G. H., and Eisenberg, R. J. (2007). Bimolecular complementation reveals that glycoproteins gB and gH/gL of herpes simplex virus interact with each other during cell fusion. *Proc. Natl. Acad. Sci. U.S.A.* 104, 18718–18723. doi: 10.1073/pnas.0707452104

Atanasiu, D., Whitbeck, J. C., de Leon, M. P., Lou, H., Hannah, B. P., Cohen, G. H., et al. (2010b). Bimolecular complementation defines functional regions of Herpes simplex virus gB that are involved with gH/gL as a necessary step leading to cell fusion. *J. Virol.* 84, 3825–3834. doi: 10.1128/JVI.02687-09

Azab, W., and Osterrieder, K. (2017). Initial contact: the first steps in herpesvirus entry. *Adv. Anat. Embryol. Cell Biol.* 223, 1–27. doi: 10.1007/978-3-319-53168-7_1

Baseler, L., Chertow, D. S., Johnson, K. M., Feldmann, H., and Morens, D. M. (2017). The pathogenesis of ebola virus disease. *Annu. Rev. Pathol.* 12, 387–418. doi: 10.1146/annurev-pathol-052016-100506

Bastian, A. R., Contarino, M., Bailey, L. D., Aneja, R., Moreira, D. R., Freedman, K., et al. (2013). Interactions of peptide triazole thiols with Env gp120 induce irreversible breakdown and inactivation of HIV-1 virions. *Retrovirology* 10:153. doi: 10.1186/1742-4690-10-153

Bastian, A. R., Kantharaju, McFadden, K., Duffy, C., Rajagopal, S., Contarino, M. R., et al. (2011). Cell-free HIV-1 virucidal action by modified peptide triazole inhibitors of Env gp120. *ChemMedChem* 6, 1335–1339, 1318. doi: 10.1002/cmdc.201100177

Bhatt, S., Gething, P. W., Brady, O. J., Messina, J. P., Farlow, A. W., Moyes, C. L., et al. (2013). The global distribution and burden of dengue. *Nature* 496, 504–507. doi: 10.1038/nature12060

Biorn, A. C., Cocklin, S., Madani, N., Si, Z., Ivanovic, T., Samanen, J., et al. (2004). Mode of action for linear peptide inhibitors of HIV-1 gp120 interactions. *Biochemistry* 43, 1928–1938. doi: 10.1021/bi035088i

Bohm, S. W., Backovic, M., Klupp, B. G., Rey, F. A., Mettenleiter, T. C., and Fuchs, W. (2016). Functional characterization of glycoprotein H chimeras composed of conserved domains of the pseudorabies virus and herpes simplex virus 1 homologs. *J. Virol.* 90, 421–432. doi: 10.1128/JVI.01985-15

Bosch, B. J., Bodewes, R., de Vries, R. P., Kreijtz, J. H., Bartelink, W., van Amerongen, G., et al. (2010). Recombinant soluble, multimeric HA and NA exhibit distinctive types of protection against pandemic swine-origin 2009 A(H1N1) influenza virus infection in ferrets. *J. Virol.* 84, 10366–10374. doi: 10.1128/JVI.01035-10

Bright, R. A., Shay, D. K., Shu, B., Cox, N. J., and Klimov, A. I. (2006). Adamantane resistance among influenza A viruses isolated early during the 2005-2006 influenza season in the United States. *JAMA* 295, 891–894. doi: 10.1001/jama.295.8.joc60020

Bullough, P. A., Hughson, F. M., Skehel, J. J., and Wiley, D. C. (1994). Structure of influenza haemagglutinin at the pH of membrane fusion. *Nature* 371, 37–43. doi: 10.1038/371037a0

Burton, D. R. (2002). Antibodies, viruses and vaccines. *Nat. Rev. Immunol.* 2, 706–713. doi: 10.1038/nri891

Cairns, T. M., Ditto, N. T., Atanasiu, D., Lou, H., Brooks, B. D., Saw, W. T., et al. (2019). Surface plasmon resonance reveals direct binding of herpes simplex virus glycoproteins gH/gL to gD and locates a gH/gl binding site on gD. *J. Virol.* 93:e00289-19. doi: 10.1128/JVI.00289-19

Carfi, A., Willis, S. H., Whitbeck, J. C., Krummenacher, C., Cohen, G. H., Eisenberg, R. J., et al. (2001). Herpes simplex virus glycoprotein D bound to the human receptor HveA. *Mol. Cell* 8, 169–179. doi: 10.1016/s1097-2765(01)00298-2

Cetina-Corona, A., Lopez-Sanchez, U., Salinas-Trujano, J., Mendez-Tenorio, A., Barron, B. L., and Torres-Flores, J. (2016). Peptides derived from glycoproteins H and B of herpes simplex virus type 1 and herpes simplex virus type 2 are capable of blocking herpetic infection *in vitro*. *Intervirology* 59, 235–242. doi: 10.1159/000464134

Chaiken, I., and Rashad, A. A. (2015). Peptide triazole inactivators of HIV-1: how do they work and what is their potential? *Future Med. Chem.* 7, 2305–2310. doi: 10.4155/fmc.15.152

Chan, D. C., and Kim, P. S. (1998). HIV entry and its inhibition. *Cell* 93, 681–684. doi: 10.1016/s0092-8674(00)81430-0

Chaudhuri, S., Symons, J. A., and Deval, J. (2018). Innovation and trends in the development and approval of antiviral medicines: 1987-2017 and beyond. *Antiviral Res.* 155, 76–88. doi: 10.1016/j.antiviral.2018.05.005

Chen, W., Feng, Y., Gong, R., Zhu, Z., Wang, Y., Zhao, Q., et al. (2011). Engineered single human CD4 domains as potent HIV-1 inhibitors and components of vaccine immunogens. *J. Virol.* 85, 9395–9405. doi: 10.1128/JVI.05119-11

Chen, W., Feng, Y., Prabakaran, P., Ying, T., Wang, Y., Sun, J., et al. (2014). Exceptionally potent and broadly cross-reactive, bispecific multivalent HIV-1 inhibitors based on single human CD4 and antibody domains. *J. Virol.* 88, 1125–1139. doi: 10.1128/JVI.02566-13

Chen, W., Zhu, Z., Feng, Y., and Dimitrov, D. S. (2008). Human domain antibodies to conserved sterically restricted regions on gp120 as exceptionally potent cross-reactive HIV-1 neutralizers. *Proc. Natl. Acad. Sci. U.S.A.* 105, 17121–17126. doi: 10.1073/pnas.0805297105

Cheshenko, N., Pierce, C., and Herold, B. C. (2018). Herpes simplex viruses activate phospholipid scramblase to redistribute phosphatidylserines and Akt to the outer leaflet of the plasma membrane and promote viral entry. *PLoS Pathog.* 14:e1006766. doi: 10.1371/journal.ppat.1006766

Cheshenko, N., Trepanier, J. B., Stefanidou, M., Buckley, N., Gonzalez, P., Jacobs, W., et al. (2013). HSV activates Akt to trigger calcium release and promote viral entry: novel candidate target for treatment and suppression. *FASEB J.* 27, 2584–2599. doi: 10.1096/fj.12-220285

Chew, M. F., Poh, K. S., and Poh, C. L. (2017). Peptides as therapeutic agents for dengue virus. *Int. J. Med. Sci.* 14, 1342–1359. doi: 10.7150/ijms.21875

Chowdary, T. K., Cairns, T. M., Atanasiu, D., Cohen, G. H., Eisenberg, R. J., and Heldwein, E. E. (2010). Crystal structure of the conserved herpesvirus fusion regulator complex gH-gL. *Nat. Struct. Mol. Biol.* 17, 882–888. doi: 10.1038/nsmb.1837

Cocchi, F., Fusco, D., Menotti, L., Gianni, T., Eisenberg, R. J., Cohen, G. H., et al. (2004). The soluble ectodomain of herpes simplex virus gD contains a membrane-proximal pro-fusion domain and suffices to mediate virus entry. *Proc. Natl. Acad. Sci. U.S.A.* 101, 7445–7450. doi: 10.1073/pnas.0401883101

Connolly, S. A., Jackson, J. O., Jardetzky, T. S., and Longnecker, R. (2011). Fusing structure and function: a structural view of the herpesvirus entry machinery. *Nat. Rev. Microbiol.* 9, 369–381. doi: 10.1038/nrmicro2548

Costin, J. M., Jenwitheesuk, E., Lok, S. M., Hunsperger, E., Conrads, K. A., Fontaine, K. A., et al. (2010). Structural optimization and de novo design of dengue virus entry inhibitory peptides. *PLoS Negl. Trop. Dis.* 4:e721. doi: 10.1371/journal.pntd.0000721

Cui, L., Zou, P., Chen, E., Yao, H., Zheng, H., Wang, Q., et al. (2017). Visual and motor deficits in grown-up mice with congenital zika virus infection. *EBioMedicine* 20, 193–201. doi: 10.1016/j.ebiom.2017.04.029

Culshaw, A., Mongkolsapaya, J., and Screaton, G. (2018). The immunology of Zika Virus. *F1000Res.* 7:203. doi: 10.12688/f1000research.12271.1

Daar, E. S., Li, X. L., Moudgil, T., and Ho, D. D. (1990). High concentrations of recombinant soluble CD4 are required to neutralize primary human immunodeficiency virus type 1 isolates. *Proc. Natl. Acad. Sci. U.S.A.* 87, 6574–6578. doi: 10.1073/pnas.87.17.6574

Davison, A. J., Eberle, R., Ehlers, B., Hayward, G. S., McGeoch, D. J., Minson, A. C., et al. (2009). The order Herpesvirales. *Arch. Virol.* 154, 171–177. doi: 10.1007/s00705-008-0278-4

Day, P. M., and Schelhaas, M. (2014). Concepts of papillomavirus entry into host cells. *Curr. Opin. Virol.* 4, 24–31. doi: 10.1016/j.coviro.2013.11.002

De Groot, A. S., Moise, L., Mcmurry, J. A., Wambre, E., Van Overtvelt, L., and Moingeon, P. (2008). Activation of natural regulatory T cells by IgG Fc-derived peptide \"Tregitopes\". *Blood* 112, 3303–3311. doi: 10.1182/blood-2008-02-138073

de Jong, M. D., Tran, T. T., Truong, H. K., Vo, M. H., Smith, G. J., Nguyen, V. C., et al. (2005). Oseltamivir resistance during treatment of influenza A (H5N1) infection. *N. Engl. J. Med.* 353, 2667–2672. doi: 10.1056/NEJMoa054512

Deeks, S. G., Overbaugh, J., Phillips, A., and Buchbinder, S. (2015). HIV infection. *Nat. Rev. Dis. Primers* 1:15035. doi: 10.1038/nrdp.2015.35

Deen, K. C., McDougal, J. S., Inacker, R., Folena-Wasserman, G., Arthos, J., Rosenberg, J., et al. (1988). A soluble form of CD4 (T4) protein inhibits AIDS virus infection. *Nature* 331, 82–84. doi: 10.1038/331082a0

Di Giovine, P., Settembre, E. C., Bhargava, A. K., Luftig, M. A., Lou, H., Cohen, G. H., et al. (2011). Structure of herpes simplex virus glycoprotein D bound to the human receptor nectin-1. *PLoS Pathog.* 7:e1002277. doi: 10.1371/journal.ppat.1002277

Dou, D., Revol, R., Ostbye, H., Wang, H., and Daniels, R. (2018). Influenza A virus cell entry, replication, virion assembly and movement. *Front. Immunol.* 9:1581. doi: 10.3389/fimmu.2018.01581

D'Souza, M. P., Cairns, J. S., and Plaeger, S. F. (2000). Current evidence and future directions for targeting HIV entry: therapeutic and prophylactic strategies. *JAMA* 284, 215–222. doi: 10.1001/jama.284.2.215

Dwyer, J. J., Wilson, K. L., Davison, D. K., Freel, S. A., Seedorff, J. E., Wring, S. A., et al. (2007). Design of helical, oligomeric HIV-1 fusion inhibitor peptides with potent activity against enfuvirtide-resistant virus. *Proc. Natl. Acad. Sci. U.S.A.* 104, 12772–12777. doi: 10.1073/pnas.0701478104

Egerer, L., Volk, A., Kahle, J., Kimpel, J., Brauer, F., Hermann, F. G., et al. (2011). Secreted antiviral entry inhibitory (SAVE) peptides for gene therapy of HIV infection. *Mol. Ther.* 19, 1236–1244. doi: 10.1038/mt.2011.30

Eisenberg, R. J., Atanasiu, D., Cairns, T. M., Gallagher, J. R., Krummenacher, C., and Cohen, G. H. (2012). Herpes virus fusion and entry: a story with many characters. *Viruses* 4, 800–832. doi: 10.3390/v4050800

Ekiert, D. C., Bhabha, G., Elsliger, M. A., Friesen, R. H., Jongeneelen, M., Throsby, M., et al. (2009). Antibody recognition of a highly conserved influenza virus epitope. *Science* 324, 246–251. doi: 10.1126/science.1171491

Ekiert, D. C., Kashyap, A. K., Steel, J., Rubrum, A., Bhabha, G., Khayat, R., et al. (2012). Cross-neutralization of influenza A viruses mediated by a single antibody loop. *Nature* 489, 526–532. doi: 10.1038/nature11414

Englund, J. A., Zimmerman, M. E., Swierkosz, E. M., Goodman, J. L., Scholl, D. R., and Balfour, H. H. Jr. (1990). Herpes simplex virus resistant to acyclovir. A study in a tertiary care center. *Ann. Intern. Med.* 112, 416–422. doi: 10.7326/0003-4819-76-3-112-6-416

Falkenhagen, A., Ameli, M., Asad, S., Read, S. E., and Joshi, S. (2014). A novel gene therapy strategy using secreted multifunctional anti-HIV proteins to confer protection to gene-modified and unmodified target cells. *Gene Ther.* 21, 175–187. doi: 10.1038/gt.2013.70

Falkenhagen, A., Singh, J., Asad, S., Leontyev, D., Read, S., Zuniga-Pflucker, J. C., et al. (2017). Control of HIV infection *in vivo* using gene therapy with a secreted entry inhibitor. *Mol. Ther. Nucleic Acids* 9, 132–144. doi: 10.1016/j.omtn.2017.08.017

Fatkenheuer, G., Pozniak, A. L., Johnson, M. A., Plettenberg, A., Staszewski, S., Hoepelman, A. I., et al. (2005). Efficacy of short-term monotherapy with maraviroc, a new CCR5 antagonist, in patients infected with HIV-1. *Nat. Med.* 11, 1170–1172. doi: 10.1038/nm1319

Ferrer, M., and Harrison, S. C. (1999). Peptide ligands to human immunodeficiency virus type 1 gp120 identified from phage display libraries. *J. Virol.* 73, 5795–5802.

Fleishman, S. J., Whitehead, T. A., Ekiert, D. C., Dreyfus, C., Corn, J. E., Strauch, E. M., et al. (2011). Computational design of proteins targeting the conserved stem region of influenza hemagglutinin. *Science* 332, 816–821. doi: 10.1126/science.1202617

Galdiero, S., Falanga, A., Tarallo, R., Russo, L., Galdiero, E., Cantisani, M., et al. (2013). Peptide inhibitors against herpes simplex virus infections. *J. Pept. Sci.* 19, 148–158. doi: 10.1002/psc.2489

Gallagher, J. R., Saw, W. T., Atanasiu, D., Lou, H., Eisenberg, R. J., and Cohen, G. H. (2013). Displacement of the C terminus of herpes simplex virus gD is sufficient to expose the fusion-activating interfaces on gD. *J. Virol.* 87, 12656–12666. doi: 10.1128/JVI.01727-13

Gamblin, S. J., and Skehel, J. J. (2010). Influenza hemagglutinin and neuraminidase membrane glycoproteins. *J. Biol. Chem.* 285, 28403–28409. doi: 10.1074/jbc.R110.129809

Ganz, T. (2003). The role of antimicrobial peptides in innate immunity. *Integr. Comp. Biol.* 43, 300–304. doi: 10.1093/icb/43.2.300

Gauduin, M. C., Allaway, G. P., Olson, W. C., Weir, R., Maddon, P. J., and Koup, R. A. (1998). CD4-immunoglobulin G2 protects Hu-PBL-SCID mice against challenge by primary human immunodeficiency virus type 1 isolates. *J. Virol.* 72, 3475–3478.

Gompels, U., and Minson, A. (1986). The properties and sequence of glycoprotein H of herpes simplex virus type 1. *Virology* 153, 230–247. doi: 10.1016/0042-6822(86)90026-7

Haase, A. T. (2005). Perils at mucosal front lines for HIV and SIV and their hosts. *Nat. Rev. Immunol.* 5, 783–792. doi: 10.1038/nri1706

Haim, H., Si, Z., Madani, N., Wang, L., Courter, J. R., Princiotto, A., et al. (2009). Soluble CD4 and CD4-mimetic compounds inhibit HIV-1 infection

by induction of a short-lived activated state. *PLoS Pathog.* 5:e1000360. doi: 10.1371/journal.ppat.1000360

Halstead, S. B. (2007). Dengue. *Lancet* 370, 1644–1652. doi: 10.1016/S0140-6736(07)61687-0

Han, Y., and Mesplede, T. (2018). Investigational drugs for the treatment of Zika virus infection: a preclinical and clinical update. *Expert Opin. Investig. Drugs* 27, 951–962. doi: 10.1080/13543784.2018.1548609

Harrison, S. C. (2008). Viral membrane fusion. *Nat. Struct. Mol. Biol.* 15, 690–698. doi: 10.1038/nsmb.1456

Harrison, S. C. (2015). Viral membrane fusion. *Virology* 47, 498–507. doi: 10.1016/j.virol.2015.03.043

Heldwein, E. E., Lou, H., Bender, F. C., Cohen, G. H., Eisenberg, R. J., and Harrison, S. C. (2006). Crystal structure of glycoprotein B from herpes simplex virus 1. *Science* 313, 217–220. doi: 10.1126/science.1126548

Holthausen, D. J., Lee, S. H., Kumar, V. T., Bouvier, N. M., Krammer, F., Ellebedy, A. H., et al. (2017). An amphibian host defense peptide is virucidal for human H1 hemagglutinin-bearing influenza viruses. *Immunity* 46, 587–595. doi: 10.1016/j.immuni.2017.03.018

Houser, K., and Subbarao, K. (2015). Influenza vaccines: challenges and solutions. *Cell Host Microbe* 17, 295–300. doi: 10.1016/j.chom.2015.02.012

Hrobowski, Y. M., Garry, R. F., and Michael, S. F. (2005). Peptide inhibitors of dengue virus and West Nile virus infectivity. *Virol. J.* 2:49. doi: 10.1186/1743-422X-2-49

Huerta, V., Chinea, G., Fleitas, N., Sarria, M., Sanchez, J., Toledo, P., et al. (2008). Characterization of the interaction of domain III of the envelope protein of dengue virus with putative receptors from CHO cells. *Virus Res.* 137, 225–234. doi: 10.1016/j.virusres.2008.07.022

Hung, J. J., Hsieh, M. T., Young, M. J., Kao, C. L., King, C. C., and Chang, W. (2004). An external loop region of domain III of dengue virus type 2 envelope protein is involved in serotype-specific binding to mosquito but not mammalian cells. *J. Virol.* 78, 378–388. doi: 10.1128/jvi.78.1.378-388.2004

Jacobson, J. M., Israel, R. J., Lowy, I., Ostrow, N. A., Vassilatos, L. S., Barish, M., et al. (2004). Treatment of advanced human immunodeficiency virus type 1 disease with the viral entry inhibitor PRO 542. *Antimicrob. Agents Chemother.* 48, 423–429. doi: 10.1128/aac.48.2.423-429.2004

Jacobson, J. M., Lowy, I., Fletcher, C. V., O'Neill, T. J., Tran, D. N., Ketas, T. J., et al. (2000). Single-dose safety, pharmacology, and antiviral activity of the human immunodeficiency virus (HIV) type 1 entry inhibitor PRO 542 in HIV-infected adults. *J. Infect. Dis.* 182, 326–329. doi: 10.1086/315698

Jiang, S., Lin, K., Strick, N., and Neurath, A. R. (1993a). HIV-1 inhibition by a peptide. *Nature* 365:113. doi: 10.1038/365113a0

Jiang, S., Lin, K., Strick, N., and Neurath, A. R. (1993b). Inhibition of HIV-1 infection by a fusion domain binding peptide from the HIV-1 envelope glycoprotein GP41. *Biochem. Biophys. Res. Commun.* 195, 533–538. doi: 10.1006/bbrc.1993.2078

Kahn, J. O., Allan, J. D., Hodges, T. L., Kaplan, L. D., Arri, C. J., Fitch, H. F., et al. (1990). The safety and pharmacokinetics of recombinant soluble CD4 (rCD4) in subjects with the acquired immunodeficiency syndrome (AIDS) and AIDS-related complex. A phase 1 study. *Ann. Intern. Med.* 112, 254–261. doi: 10.7326/0003-4819-112-4-

Kimberlin, D. W., and Whitley, R. J. (2007). ""Antiviral therapy of HSV-1 and -2,"," in *Human Herpesviruses: Biology, Therapy, and Immunoprophylaxis*, eds A. Arvin, G. Campadelli-Fiume, E. Mocarski, P. S. Moore, B. Roizman, R. Whitley, et al. (Cambridge: Cambridge University Press).

Klein, D. E., Choi, J. L., and Harrison, S. C. (2013). Structure of a dengue virus envelope protein late-stage fusion intermediate. *J. Virol.* 87, 2287–2293. doi: 10.1128/JVI.02957-12

Krummenacher, C., Supekar, V. M., Whitbeck, J. C., Lazear, E., Connolly, S. A., Eisenberg, R. J., et al. (2005). Structure of unliganded HSV gD reveals a mechanism for receptor-mediated activation of virus entry. *EMBO J.* 24, 4144–4153. doi: 10.1038/sj.emboj.7600875

Kuhn, R. J., Zhang, W., Rossmann, M. G., Pletnev, S. V., Corver, J., Lenches, E., et al. (2002). Structure of dengue virus: implications for flavivirus organization, maturation, and fusion. *Cell* 108, 717–725. doi: 10.1016/s0092-8674(02)00660-8

Kumar, C. S., Dey, D., Ghosh, S., and Banerjee, M. (2018). Breach: host membrane penetration and entry by nonenveloped viruses. *Trends Microbiol.* 26, 525–537. doi: 10.1016/j.tim.2017.09.010

Kuno, G., Chang, G. J., Tsuchiya, K. R., Karabatsos, N., and Cropp, C. B. (1998). Phylogeny of the genus Flavivirus. *J. Virol.* 72, 73–83.

Lalezari, J. P., Henry, K., O'Hearn, M., Montaner, J. S., Piliero, P. J., Trottier, B., et al. (2003). Enfuvirtide, an HIV-1 fusion inhibitor, for drug-resistant HIV infection in North and South America. *N. Engl. J. Med.* 348, 2175–2185. doi: 10.1056/NEJMoa035026

Lee, C. C., Lin, L. L., Chan, W. E., Ko, T. P., Lai, J. S., and Wang, A. H. (2013). Structural basis for the antibody neutralization of herpes simplex virus. *Acta Crystallogr. D Biol. Crystallogr.* 69(Pt 10), 1935–1945. doi: 10.1107/S0907444913016776

Li, H., Guan, Y., Szczepanska, A., Moreno-Vargas, A. J., Carmona, A. T., Robina, I., et al. (2007). Synthesis and anti-HIV activity of trivalent CD4-mimetic miniproteins. *Bioorg. Med. Chem.* 15, 4220–4228. doi: 10.1016/j.bmc.2007.03.064

Li, H., Song, H., Heredia, A., Le, N., Redfield, R., Lewis, G. K., et al. (2004). Synthetic bivalent CD4-mimetic miniproteins show enhanced anti-HIV activity over the monovalent miniprotein. *Bioconjug. Chem.* 15, 783–789. doi: 10.1021/bc049960r

Li, L., Lok, S. M., Yu, I. M., Zhang, Y., Kuhn, R. J., Chen, J., et al. (2008). The flavivirus precursor membrane-envelope protein complex: structure and maturation. *Science* 319, 1830–1834. doi: 10.1126/science.1153263

Liu, J., Bartesaghi, A., Borgnia, M. J., Sapiro, G., and Subramaniam, S. (2008). Molecular architecture of native HIV-1 gp120 trimers. *Nature* 455, 109–113. doi: 10.1038/nature07159

Lok, S. M., Costin, J. M., Hrobowski, Y. M., Hoffmann, A. R., Rowe, D. K., Kukkaro, P., et al. (2012). Release of dengue virus genome induced by a peptide inhibitor. *PLoS One* 7:e50995. doi: 10.1371/journal.pone.0050995

Lu, L., Pan, C., Li, Y., Lu, H., He, W., and Jiang, S. (2012). A bivalent recombinant protein inactivates HIV-1 by targeting the gp41 prehairpin fusion intermediate induced by CD4 D1D2 domains. *Retrovirology* 9:104. doi: 10.1186/1742-4690-9-104

Lu, L., Yu, F., Cai, L., Debnath, A. K., and Jiang, S. (2016). Development of small-molecule HIV entry inhibitors specifically targeting gp120 or gp41. *Curr. Top. Med. Chem.* 16, 1074–1090. doi: 10.2174/1568026615666150901114527

Matsubara, T., Onishi, A., Saito, T., Shimada, A., Inoue, H., Taki, T., et al. (2010). Sialic acid-mimic peptides as hemagglutinin inhibitors for anti-influenza therapy. *J. Med. Chem.* 53, 4441–4449. doi: 10.1021/jm1002183

Matsubara, T., Onishi, A., Yamaguchi, D., and Sato, T. (2016). Heptapeptide ligands against receptor-binding sites of influenza hemagglutinin toward anti-influenza therapy. *Bioorg. Med. Chem.* 24, 1106–1114. doi: 10.1016/j.bmc.2016.01.039

Mazumder, R., Hu, Z. Z., Vinayaka, C. R., Sagripanti, J. L., Frost, S. D., Kosakovsky Pond, S. L., et al. (2007). Computational analysis and identification of amino acid sites in dengue E proteins relevant to development of diagnostics and vaccines. *Virus Genes* 35, 175–186. doi: 10.1007/s11262-007-0103-2

Melikyan, G. B. (2008). Common principles and intermediates of viral protein-mediated fusion: the HIV-1 paradigm. *Retrovirology* 5:111. doi: 10.1186/1742-4690-5-111

Modis, Y., Ogata, S., Clements, D., and Harrison, S. C. (2003). A ligand-binding pocket in the dengue virus envelope glycoprotein. *Proc. Natl. Acad. Sci. U.S.A.* 100, 6986–6991. doi: 10.1073/pnas.0832193100

Moir, S., Chun, T. W., and Fauci, A. S. (2011). Pathogenic mechanisms of HIV disease. *Annu. Rev. Pathol.* 6, 223–248. doi: 10.1146/annurev-pathol-011110-130254

Moise, L., Beseme, S., Tassone, R., Liu, R., Kibria, F., Terry, F., et al. (2016). T cell epitope redundancy: cross-conservation of the TCR face between pathogens and self and its implications for vaccines and autoimmunity. *Expert Rev. Vaccines* 15, 607–617. doi: 10.1586/14760584.2016.1123098

Mubarak, A., Alturaiki, W., and Hemida, M. G. (2019). Middle east respiratory syndrome coronavirus (MERS-CoV): infection, immunological response, and vaccine development. *J. Immunol. Res.* 2019:6491738. doi: 10.1155/2019/6491738

Ng, K. E. (2019). Xofluza (Baloxavir Marboxil) for the treatment of acute uncomplicated influenza. *P T* 44, 9–11.

Nicola, A. V. (2016). Herpesvirus entry into host cells mediated by endosomal low pH. *Traffic* 17, 965–975. doi: 10.1111/tra.12408

Nicola, A. V., and Straus, S. E. (2004). Cellular and viral requirements for rapid endocytic entry of herpes simplex virus. *J. Virol.* 78, 7508–7517. doi: 10.1128/JVI.78.14.7508-7517.2004

Orloff, S. L., Kennedy, M. S., Belperron, A. A., Maddon, P. J., and McDougal, J. S. (1993). Two mechanisms of soluble CD4 (sCD4)-mediated inhibition of human immunodeficiency virus type 1 (HIV-1) infectivity and their relation to primary HIV-1 isolates with reduced sensitivity to sCD4. *J. Virol.* 67, 1461–1471.

Palese, P., and Shaw, M. L. (2007). "Orthomyxoviridae: the viruses and their replication," in *Fields Virology*, 5th Edn, eds D. M. Knipe and P. M. Howley (Philadelphia, PA: Lippincott Williams & Wilkins), 1647–1689.

Pan, C., Cai, L., Lu, H., Qi, Z., and Jiang, S. (2009). Combinations of the first and next generations of human immunodeficiency virus (HIV) fusion inhibitors exhibit a highly potent synergistic effect against enfuvirtide- sensitive and -resistant HIV type 1 strains. *J. Virol.* 83, 7862–7872. doi: 10.1128/JVI.00168-09

Panya, A., Bangphoomi, K., Choowongkomon, K., and Yenchitsomanus, P. T. (2014). Peptide inhibitors against dengue virus infection. *Chem. Biol. Drug Des.* 84, 148–157. doi: 10.1111/cbdd.12309

Panya, A., Sawasdee, N., Junking, M., Srisawat, C., Choowongkomon, K., and Yenchitsomanus, P. T. (2015). A peptide inhibitor derived from the conserved ectodomain region of DENV membrane (M) protein with activity against dengue virus infection. *Chem. Biol. Drug Des.* 86, 1093–1104. doi: 10.1111/cbdd.12576

Parajuli, B., Acharya, K., Bach, H. C., Parajuli, B., Zhang, S., Smith, A. B., et al. (2018). Restricted HIV-1 Env glycan engagement by lectin-reengineered DAVEI protein chimera is sufficient for lytic inactivation of the virus. *Biochem. J.* 475, 931–957. doi: 10.1042/BCJ20170662

Parajuli, B., Acharya, K., Yu, R., Ngo, B., Rashad, A. A., Abrams, C. F., et al. (2016). Lytic inactivation of human immunodeficiency virus by dual engagement of gp120 and gp41 domains in the virus Env protein trimer. *Biochemistry* 55, 6100–6114. doi: 10.1021/acs.biochem.6b00570

Pellet, P. E., and Roizman, B. (2013). "Herpesviridae," in *Fields Virology*, 6th Edn, eds D. M. Knipe and P. M. Howley (Philadelphia, PA: Lippincott-Williams & Wilkins), 1802–1822.

Perez, E. E., Riley, J. L., Carroll, R. G., von Laer, D., and June, C. H. (2005). Suppression of HIV-1 infection in primary CD4 T cells transduced with a self-inactivating lentiviral vector encoding a membrane expressed gp41-derived fusion inhibitor. *Clin. Immunol.* 115, 26–32. doi: 10.1016/j.clim.2005.02.019

Phillips, D. M., Taylor, C. L., Zacharopoulos, V. R., and Maguire, R. A. (2000). Nonoxynol-9 causes rapid exfoliation of sheets of rectal epithelium. *Contraception* 62, 149–154. doi: 10.1016/s0010-7824(00)00156-6

Polsky, B., Baron, P. A., Gold, J. W., Smith, J. L., Jensen, R. H., and Armstrong, D. (1988). *In vitro* inactivation of HIV-1 by contraceptive sponge containing nonoxynol-9. *Lancet* 1:1456. doi: 10.1016/s0140-6736(88)92261-1

Priyadarzini, T. R., Selvin, J. F., Gromiha, M. M., Fukui, K., and Veluraja, K. (2012). Theoretical investigation on the binding specificity of sialyldisaccharides with hemagglutinins of influenza A virus by molecular dynamics simulations. *J. Biol. Chem.* 287, 34547–34557. doi: 10.1074/jbc.M112.357061

Qi, Q., Wang, Q., Chen, W., Du, L., Dimitrov, D. S., Lu, L., et al. (2017). HIV-1 gp41-targeting fusion inhibitory peptides enhance the gp120-targeting protein-mediated inactivation of HIV-1 virions. *Emerg. Microbes Infect.* 6:e59. doi: 10.1038/emi.2017.46

Roizman, B., Knipe, D. M., and Whitley, R. J. (2013). "Herpes simplex viruses," in *Fields Virology*, 6th Edn, eds D. M. Knipe and P. M. Howley (Philadelphia, PA: Lippincott-Williams & Wilkins), 1823–1897.

Rosemary Bastian, A., Nangarlia, A., Bailey, L. D., Holmes, A., Kalyana Sundaram, R. V., Ang, C., et al. (2015). Mechanism of multivalent nanoparticle encounter with HIV-1 for potency enhancement of peptide triazole virus inactivation. *J. Biol. Chem.* 290, 529–543. doi: 10.1074/jbc.M114.608315

Sanders, R. W. (2013). HIV takes double hit before entry. *BMC Biol.* 10:99. doi: 10.1186/1741-7007-10-99

Sato, M., Takashita, E., Katayose, M., Nemoto, K., Sakai, N., Hashimoto, K., et al. (2020). Detection of variants with reduced baloxavir marboxil susceptibility after treatment of children with influenza A during the 2018/2019 influenza season. *J. Infect. Dis.* doi: 10.1093/infdis/jiaa061 [Epub ahead of print].

Satoh, T., Arii, J., Suenaga, T., Wang, J., Kogure, A., Uehori, J., et al. (2008). PILRalpha is a herpes simplex virus-1 entry coreceptor that associates with glycoprotein B. *Cell* 132, 935–944. doi: 10.1016/j.cell.2008.01.043

Schmidt, A. G., Yang, P. L., and Harrison, S. C. (2010a). Peptide inhibitors of dengue-virus entry target a late-stage fusion intermediate. *PLoS Pathog.* 6:e1000851. doi: 10.1371/journal.ppat.1000851

Schmidt, A. G., Yang, P. L., and Harrison, S. C. (2010b). Peptide inhibitors of flavivirus entry derived from the E protein stem. *J. Virol.* 84, 12549–12554. doi: 10.1128/JVI.01440-10

Schooley, R. T., Merigan, T. C., Gaut, P., Hirsch, M. S., Holodniy, M., Flynn, T., et al. (1990). Recombinant soluble CD4 therapy in patients with the acquired immunodeficiency syndrome (AIDS) and AIDS-related complex. A phase I-II escalating dosage trial. *Ann. Intern. Med.* 112, 247–253. doi: 10.7326/0003-4819-112-4-247

Seo, M. D., Won, H. S., Kim, J. H., Mishig-Ochir, T., and Lee, B. J. (2012). Antimicrobial peptides for therapeutic applications: a review. *Molecules* 17, 12276–12286. doi: 10.3390/molecules171012276

Sharma, D., Balamurali, M. M., Chakraborty, K., Kumaran, S., Jeganathan, S., Rashid, U., et al. (2005). Protein minimization of the gp120 binding region of human CD4. *Biochemistry* 44, 16192–16202. doi: 10.1021/bi051120s

Skehel, J. J., and Wiley, D. C. (2000). Receptor binding and membrane fusion in virus entry: the influenza hemagglutinin. *Annu. Rev. Biochem.* 69, 531–569. doi: 10.1146/annurev.biochem.69.1.531

Slon Campos, J. L., Mongkolsapaya, J., and Screaton, G. R. (2018). The immune response against flaviviruses. *Nat. Immunol.* 19, 1189–1198. doi: 10.1038/s41590-018-0210-3

Starcich, B. R., Hahn, B. H., Shaw, G. M., McNeely, P. D., Modrow, S., Wolf, H., et al. (1986). Identification and characterization of conserved and variable regions in the envelope gene of HTLV-III/LAV, the retrovirus of AIDS. *Cell* 45, 637–648. doi: 10.1016/0092-8674(86)90778-6

Su, S., Wang, Q., Xu, W., Yu, F., Hua, C., Zhu, Y., et al. (2017). A novel HIV-1 gp41 tripartite model for rational design of HIV-1 fusion inhibitors with improved antiviral activity. *AIDS* 31, 885–894. doi: 10.1097/QAD.0000000000001415

Suenaga, T., Satoh, T., Somboonthum, P., Kawaguchi, Y., Mori, Y., and Arase, H. (2010). Myelin-associated glycoprotein mediates membrane fusion and entry of neurotropic herpesviruses. *Proc. Natl. Acad. Sci. U.S.A.* 107, 866–871. doi: 10.1073/pnas.0913351107

Sui, J., Hwang, W. C., Perez, S., Wei, G., Aird, D., Chen, L. M., et al. (2009). Structural and functional bases for broad-spectrum neutralization of avian and human influenza A viruses. *Nat. Struct. Mol. Biol.* 16, 265–273. doi: 10.1038/nsmb.1566

Sullivan, N., Sun, Y., Binley, J., Lee, J., Barbas, C. F. III, Parren, P. W., et al. (1998). Determinants of human immunodeficiency virus type 1 envelope glycoprotein activation by soluble CD4 and monoclonal antibodies. *J. Virol.* 72, 6332–6338.

Sun, X., and Whittaker, G. R. (2013). Entry of influenza virus. *Adv. Exp. Med. Biol.* 790, 72–82. doi: 10.1007/978-1-4614-7651-1_4

Takashita, E., Kawakami, C., Ogawa, R., Morita, H., Fujisaki, S., Shirakura, M., et al. (2019). Influenza A(H3N2) virus exhibiting reduced susceptibility to baloxavir due to a polymerase acidic subunit I38T substitution detected from a hospitalised child without prior baloxavir treatment, Japan, January 2019. *Euro Surveill.* 24:1900170. doi: 10.2807/1560-7917.ES.2019.24.12.1900170

Tian, Y. S., Zhou, Y., Takagi, T., Kameoka, M., and Kawashita, N. (2018). Dengue virus and its inhibitors: a brief review. *Chem. Pharm. Bull.* 66, 191–206. doi: 10.1248/cpb.c17-00794

Traunecker, A., Luke, W., and Karjalainen, K. (1988). Soluble CD4 molecules neutralize human immunodeficiency virus type 1. *Nature* 331, 84–86. doi: 10.1038/331084a0

Trkola, A., Pomales, A. B., Yuan, H., Korber, B., Maddon, P. J., Allaway, G. P., et al. (1995). Cross-clade neutralization of primary isolates of human immunodeficiency virus type 1 by human monoclonal antibodies and tetrameric CD4-IgG. *J. Virol.* 69, 6609–6617.

Vigant, F., Santos, N. C., and Lee, B. (2015). Broad-spectrum antivirals against viral fusion. *Nat. Rev. Microbiol.* 13, 426–437. doi: 10.1038/nrmicro3475

Vita, C., Drakopoulou, E., Vizzavona, J., Rochette, S., Martin, L., Menez, A., et al. (1999). Rational engineering of a miniprotein that reproduces the core of the CD4 site interacting with HIV-1 envelope glycoprotein. *Proc. Natl. Acad. Sci. U.S.A.* 96, 13091–13096. doi: 10.1073/pnas.96.23.13091

Wang, X., Zou, P., Wu, F., Lu, L., and Jiang, S. (2017). Development of small-molecule viral inhibitors targeting various stages of the life cycle of emerging and re-emerging viruses. *Front. Med.* 11:449–461. doi: 10.1007/s11684-017-0589-5

Warfield, K. L., Plummer, E. M., Sayce, A. C., Alonzi, D. S., Tang, W., Tyrrell, B. E., et al. (2016). Inhibition of endoplasmic reticulum glucosidases is required for

in vitro and *in vivo* dengue antiviral activity by the iminosugar UV-4. *Antiviral Res.* 129, 93–98. doi: 10.1016/j.antiviral.2016.03.001

Weber, C. A., Mehta, P. J., Ardito, M., Moise, L., Martin, B., and De Groot, A. S. (2009). T cell epitope: friend or foe? Immunogenicity of biologics in context. *Adv. Drug Deliv. Rev.* 61, 965–976. doi: 10.1016/j.addr.2009.07.001

Weed, D. J., and Nicola, A. V. (2017). Herpes simplex virus membrane fusion. *Adv. Anat. Embryol. Cell Biol.* 223, 29–47. doi: 10.1007/978-3-319-53168-7_2

Weissenhorn, W., Hinz, A., and Gaudin, Y. (2007). Virus membrane fusion. *FEBS Lett.* 581, 2150–2155. doi: 10.1016/j.febslet.2007.01.093

Whittle, J. R., Zhang, R., Khurana, S., King, L. R., Manischewitz, J., Golding, H., et al. (2011). Broadly neutralizing human antibody that recognizes the receptor-binding pocket of influenza virus hemagglutinin. *Proc. Natl. Acad. Sci. U.S.A.* 108, 14216–14221. doi: 10.1073/pnas.1111497108

Wild, C. T., Shugars, D. C., Greenwell, T. K., McDanal, C. B., and Matthews, T. J. (1994). Peptides corresponding to a predictive alpha-helical domain of human immunodeficiency virus type 1 gp41 are potent inhibitors of virus infection. *Proc. Natl. Acad. Sci. U.S.A.* 91, 9770–9774. doi: 10.1073/pnas.91.21.9770

Xu, M., Lee, E. M., Wen, Z., Cheng, Y., Huang, W. K., Qian, X., et al. (2016). Identification of small-molecule inhibitors of Zika virus infection and induced neural cell death via a drug repurposing screen. *Nat. Med.* 22, 1101–1107. doi: 10.1038/nm.4184

Xu, W., Wang, Q., Yu, F., Lu, L., and Jiang, S. (2014). Synergistic effect resulting from combinations of a bifunctional HIV-1 antagonist with antiretroviral drugs. *J. Acquir. Immune Defic. Syndr.* 67, 1–6. doi: 10.1097/QAI.0000000000000265

Yamada, S., Yasuhara, A., and Kawaoka, Y. (2019). Soluble recombinant hemagglutinin protein of H1N1pdm09 influenza virus elicits cross-protection against a lethal H5N1 challenge in mice. *Front. Microbiol.* 10:2031. doi: 10.3389/fmicb.2019.02031

Yang, J., Li, M., Shen, X., and Liu, S. (2013). Influenza A virus entry inhibitors targeting the hemagglutinin. *Viruses* 5, 352–373. doi: 10.3390/v5010352

Yu, Y., Deng, Y. Q., Zou, P., Wang, Q., Dai, Y., Yu, F., et al. (2017). A peptide-based viral inactivator inhibits Zika virus infection in pregnant mice and fetuses. *Nat. Commun.* 8:15672. doi: 10.1038/ncomms15672

Zaman, R., Islam, R. A., Ibnat, N., Othman, I., Zaini, A., Lee, C. Y., et al. (2019). Current strategies in extending half-lives of therapeutic proteins. *J. Control. Release* 301, 176–189. doi: 10.1016/j.jconrel.2019.02.016

Zeev-Ben-Mordehai, T., Vasishtan, D., Hernandez Duran, A., Vollmer, B., White, P., Prasad Pandurangan, A., et al. (2016). Two distinct trimeric conformations of natively membrane-anchored full-length herpes simplex virus 1 glycoprotein B. *Proc. Natl. Acad. Sci. U.S.A.* 113, 4176–4181. doi: 10.1073/pnas.1523234113

Zeng, L. Y., Yang, J., and Liu, S. (2017). Investigational hemagglutinin-targeted influenza virus inhibitors. *Expert Opin. Investig. Drugs* 26, 63–73. doi: 10.1080/13543784.2017.1269170

Zhang, X., Ge, P., Yu, X., Brannan, J. M., Bi, G., Zhang, Q., et al. (2013). Cryo-EM structure of the mature dengue virus at 3.5-A resolution. *Nat. Struct. Mol. Biol.* 20, 105–110. doi: 10.1038/nsmb.2463

**Conflict of Interest:** The authors declare that the research was conducted in the absence of any commercial or financial relationships that could be construed as a potential conflict of interest.

*Copyright © 2020 Su, Wang, Wen, Jiang and Lu. This is an open-access article distributed under the terms of the Creative Commons Attribution License (CC BY). The use, distribution or reproduction in other forums is permitted, provided the original author(s) and the copyright owner(s) are credited and that the original publication in this journal is cited, in accordance with accepted academic practice. No use, distribution or reproduction is permitted which does not comply with these terms.*

frontiers in Microbiology

ORIGINAL RESEARCH
published: 05 June 2020
doi: 10.3389/fmicb.2020.01085

# Contributions of HA1 and HA2 Subunits of Highly Pathogenic Avian Influenza Virus in Induction of Neutralizing Antibodies and Protection in Chickens

*Edris Shirvani, Anandan Paldurai, Berin P. Varghese and Siba K. Samal**

*Virginia-Maryland College of Veterinary Medicine, University of Maryland, College Park, College Park, MD, United States*

Highly pathogenic avian influenza virus (HPAIV) subtype H5N1 causes a devastating disease in poultry. Vaccination is an effective method of controlling avian influenza virus (AIV) infection in poultry. The hemagglutinin (HA) protein is the major determinant recognized by the immune system of the host. Cleavage of the HA precursor HA0 into HA1 and HA2 subunits is required for infectivity of the AIV. We evaluated the individual contributions of HA1 and HA2 subunits to the induction of HPAIV serum neutralizing antibodies and protective immunity in chickens. Using reverse genetics, recombinant Newcastle disease viruses (rNDVs) were generated, each expressing HA1, HA2, or HA protein of H5N1 HPAIV. Chickens were immunized with rNDVs expressing HA1, HA2, or HA. Immunization with HA induced high titers of serum neutralizing antibodies and prevented death following challenge. Immunization with HA1 or HA2 alone neither induced serum neutralizing antibodies nor prevented death following challenge. Our results suggest that interaction of HA1 and HA2 subunits is necessary for the display of epitopes on HA protein involved in the induction of neutralizing antibodies and protection. These epitopes are lost when the two subunits are separated. Therefore, vaccination with either a HA1 or HA2 subunit may not provide protection against HPAIV.

**Keywords: highly pathogenic avian influenza virus, hemagglutinin subunits, protective epitopes, native conformation, poultry vaccines, natural host model**

OPEN ACCESS

***Edited by:***
*Lijun Rong,*
*University of Illinois at Chicago, United States*

***Reviewed by:***
*Jae-Keun Park,*
*National Institutes of Health (NIH), United States*
*Wei Zou,*
*University of Michigan, United States*
*Daniela Rajao,*
*University of Georgia, United States*

***Correspondence:**
*Siba K. Samal*
*ssamal@umd.edu*

***Specialty section:***
*This article was submitted to Virology, a section of the journal Frontiers in Microbiology*

***Received:*** *11 November 2019*
***Accepted:*** *30 April 2020*
***Published:*** *05 June 2020*

***Citation:***
*Shirvani E, Paldurai A, Varghese BP and Samal SK (2020) Contributions of HA1 and HA2 Subunits of Highly Pathogenic Avian Influenza Virus in Induction of Neutralizing Antibodies and Protection in Chickens. Front. Microbiol. 11:1085. doi: 10.3389/fmicb.2020.01085*

## INTRODUCTION

Avian influenza (AI) is a serious disease in poultry. Avian influenza virus (AIV) belongs to the genus *Alphainfluenzavirus* in the family *Orthomyxoviridae* (International Committee on Taxonomy of Viruses [ICTV], 2018). Avian influenza viruses are divided into subtypes based on antigenic differences in the two major surface glycoproteins, hemagglutinin (HA) and neuraminidase (NA) (Palese and Shaw, 2013). Currently, 16 HA subtypes (H1–H16) and 11 NA subtypes (N1–N11) in different combinations have been found in avian populations. Avian influenza viruses are classified into highly pathogenic avian influenza (HPAI) and low pathogenic avian influenza (LPAI) viruses. Highly pathogenic avian influenza viruses in poultry are of H5 and H7 subtypes (Palese and Shaw, 2013; OIE, 2018b). Furthermore, in recent years, H5, H7, H9, and H10 subtypes of AIVs have caused

human infections, with H5 and H7 causing serious disease in humans (Chen et al., 2014; Sutton, 2018; Peacock et al., 2019).

Vaccination is considered a practical method to control AI in endemic countries (Swayne, 2012; OIE, 2018b). However, live vaccines against AIV are not recommended for use in poultry, because of the potential risk of genome segment reassortment between vaccine and field strains that can lead to the emergence of viral variants with different antigenic properties (OIE, 2018b). The vast majority of AIV vaccines (95.5%) currently used in the field are inactivated vaccines (Swayne, 2012). However, they do not elicit strong immune responses. The process of production and administration of this type of vaccine are expensive, labor intensive, and time consuming. Furthermore, vaccination programs with inactivated vaccines cause difficulty as it is hard to differentiate vaccinated birds from infected ones, which can result in trade restrictions (Swayne, 2006; Swayne et al., 2011). Therefore, viral vectored vaccines containing the HA protein of highly pathogenic avian influenza virus (HPAIV) have been developed and licensed in some countries (OIE, 2018b; Suarez and Pantin-Jackwood, 2017).

Hemagglutinin is an important multifunctional protein in influenza virus. The HA protein mediates binding of the virus to the host cell receptor. It is the major antigen against which neutralizing antibodies are induced during infection (Palese and Shaw, 2013). Each HA monomer is synthesized as an inactive precursor protein HA0. The cleavage of HA0 protein into HA1 and HA2 subunits by a cellular protease is a prerequisite for viral infectivity (Klenk et al., 1975; Lazarowitz and Choppin, 1975). Following cleavage, the HA1 and HA2 subunits are held together by disulfide bonds. The HA1 binds to sialic acid receptors on cell surfaces and initiates virus entry by endocytosis. Due to acidic pH-induced conformational change of HA2 in endosomes, the fusion of viral and endosomal membranes occurs (Palese and Shaw, 2013). The HA1 subunit, which forms the globular head, is highly variable among subtypes and contains major neutralizing epitopes. The HA2 subunit, which forms most of the stalk domain, is considerably conserved among subtypes and contains few but cross-reactive neutralizing epitopes (Palese and Shaw, 2013; Kirkpatrick et al., 2018; Koutsakos et al., 2019).

The presence of subtype-specific neutralizing epitopes on a HA1 subunit and the presence of broad neutralizing epitopes on a HA2 subunit makes them potential candidates to develop subtype-specific and universal vaccines against influenza viruses, respectively (Palese and Shaw, 2013; Koutsakos et al., 2019). To date, several head-based and stalk-based vaccine candidates against human influenza viruses have been evaluated in mice and/or ferret models, but an effective vaccine is not yet available (Gao et al., 2006; Steel et al., 2010; Krammer et al., 2014; Mallajosyula et al., 2014; Yassine et al., 2015; Sutton et al., 2017; Krammer and Palese, 2019). Some promising outcomes from mice and/or ferret model challenge studies keep these approaches attractive (Gao et al., 2006; Steel et al., 2010; Mallajosyula et al., 2014; Yassine et al., 2015). Although mice and ferrets represent invaluable animal models to study human influenza virus pathogenesis, they may not accurately reflect the disease pathogenesis in humans (Thangavel and Bouvier, 2014; Zeng et al., 2019); hence, mice and ferrets may not be suitable animal models to evaluate the protective efficacies of HA1 and HA2 subunit vaccines against an influenza virus challenge. Therefore, there is a need to clearly evaluate the contributions of HA1 and HA2 subunits in a natural host model. Chickens are highly susceptible to H5N1 HPAIV infection and play a critical role in the spread of the virus. Hence, chickens provide a natural model to determine the contributions of HA1 and HA2 subunits of H5N1 HPAIV in the induction of neutralizing antibodies and protection. Viral vectored vaccines containing the intact HA protein of H5N1 HPAIV have been investigated in chickens in several studies (Kim and Samal, 2016, 2019; Suarez and Pantin-Jackwood, 2017). However, the individual contributions of HA1 and HA2 subunits of HPAIV HA protein in the induction of neutralizing antibodies and protection has not been investigated in chickens.

Newcastle disease virus (NDV) (Veits et al., 2006; Kim and Samal, 2016, 2019), turkey herpesvirus (HVT) (Balzli et al., 2018), fowl pox virus (FPV) (Bublot et al., 2007), adenovirus (Toro and Tang, 2009; Steel et al., 2010), infectious laryngotracheitis virus (ILTV) (Pavlova et al., 2009), and Marek's disease virus (MDV) (Cui et al., 2013) have been used as live recombinant vaccine vectors against HPAIV in chickens. Among these vectors, NDV is most promising, because it infects chickens through the respiratory tract as HPAIV, resulting in eliciting robust local and systemic immune responses (Perez et al., 2019). Newcastle disease virus belongs to the genus *Orthoavulavirus* in the family *Paramyxoviridae* (International Committee on Taxonomy of Viruses [ICTV], 2018). A virulent NDV strain, LaSota, has been used as a safe and effective live vaccine for more than 60 years (Samal, 2019). In this study, we have used reverse genetics techniques to generate recombinant NDVs (rNDVs) expressing HA1, HA2, or HA protein of H5N1 HPAIV. The individual contributions of HA1 and HA2 subunits of HPAIV HA protein in the induction of neutralizing antibodies and protection were evaluated in chickens. Our results showed that when the HA1 and HA2 subunits were separated neither provided protection nor induced neutralizing antibodies. Therefore, rNDVs expressing HA1 or HA2 subunits were not protective in chickens against HPAIV challenge, while rNDV expressing the intact HA protein provided complete protection. These results may have implications in the development of vaccines against all influenza viruses.

# MATERIALS AND METHODS

## Cells and Viruses

Human epidermoid carcinoma (HEp-2) cells, chicken embryo fibroblast (DF1) cells, and Madin-Darby canine kidney (MDCK) cells purchased from the American Type Culture Collection (ATCC, Manassas, VA), were used to recover rNDVs, to determine *in vitro* characteristics of rNDVs, and to assess neutralizing antibodies induced against AIV, respectively. HEp-2 and DF1 cells were grown in Dulbecco's minimal essential medium (DMEM) containing 10% fetal bovine serum (FBS). Madin-Darby canine kidney cells were grown

in DMEM containing 5% FBS. The rNDV strain LaSota and rNDVs expressing HA1, HA2, or HA protein of H5N1 HPAIV, recovered by reverse genetic technique, were grown in 10-day-old embryonated specific pathogen free (SPF) chicken eggs (Charles Rivers, MA) at 99.5°F. The HPAIV strain A/Vietnam/1203/2004 (H5N1) and the LPAIV strain A/Mallard/Pennsylvania/10218/1984 (H5N2) viruses were propagated in 10-day-old SPF embryonated chicken eggs in Biosafety level-3 plus and Biosafety level-2 facilities, respectively. The 50% endpoint titers of H5N1 HPAIV and H5N2 LPAIV in allantoic fluid harvested from eggs were determined by 50% embryo infectious dose ($EID_{50}$) and tissue culture 50% infectious dose ($TCID_{50}$) methods, respectively. The titers of viruses were calculated using a formula derived from Reed and Muench and Spearman–Karber methods (Ramakrishnan, 2016). The modified vaccinia virus strain Ankara, expressing T7 RNA polymerase (MVA-T7), was propagated using primary chicken embryo fibroblast cells.

## Generation of rNDVs Expressing HA1, HA2, or HA Protein of HPAIV (H5N1)

A plasmid pBR322 containing full-length antigenomic cDNA of NDV strain LaSota had been constructed previously (Huang et al., 2001). A previously constructed plasmid of full-length antigenomic cDNA of NDV strain LaSota containing the transcription cassette of HPAIV A/Vietnam/1203/2004 (H5N1) HA gene between NDV P and M genes also was used in this study (Kim et al., 2014). The polybasic cleavage site (PQRERRRKKR'G) of HPAIV strain A/Vietnam/1203/2004 (H5N1) was modified to the monobasic cleavage site (PQRETR'G) of LPAIV strain A/Mexico/31381/94 (H5N2). The HA1, HA2, and HA genes were codon optimized for higher levels of expression. Four transcription cassettes were designed: (i) a transcription cassette containing the HA1 subunit (1020 nt) to determine the contribution of the HA1 subunit in the induction of neutralizing antibodies and protection, (ii) a transcription cassette containing the HA1 subunit (1020 nt) fused with TM and CT of NDV F gene (171 nt) for incorporation into NDV envelope, (iii) a transcription cassette containing the signal sequence of the HA gene (48 nt) fused with the HA2 gene (660 nt) to determine the contribution of the HA2 subunit in the induction of neutralizing antibodies and protection, and (iv) a transcription cassette containing the HA gene, constructed previously (Kim et al., 2014), to evaluate the contributions of HA1 and HA2 subunits in comparison with intact HA in the induction of protection and immunity. The transcription cassettes of codon optimized HA1 and HA2 genes were amplified from the plasmid containing the codon optimized HA gene of HPAIV A/Vietnam/1203/2004 (H5N1). The amplified fragments were cloned into individual pGEM®-T Easy Vectors (Promega Corporation). The correct sequence of the genes introduced into the pGEM®-T vectors was confirmed by nucleotide sequence analysis. Then, they were re-cloned into complete individual plasmids containing cDNA of NDV strain LaSota at P and M genes junction using *Pme*I site, following digestion of transcription cassettes from shuttle vectors using *Pme*I restriction enzyme (**Figure 1**). Recombinant Newcastle disease viruses containing the HA1 gene, the HA1 gene fused with TM and CT of NDV F gene, signal peptide fused with the HA2 gene, and the intact HA gene were recovered by reverse genetics as described previously (Huang et al., 2001). The presence of transcription cassettes containing HPAIV genes in rNDVs genomes was confirmed by RT-PCR. Briefly, a primer pair set (NDV strain LaSota P gene 2899 forward primer: 5′ TTAAACCCGCCACTGCATGCGG 3′ and NDV strain LaSota M gene 3297 reverse primer: 5′ CAGCCCAATTGTCCTAGATG 3′) was used to amplify the transcription cassettes containing HPAIV genes from cDNA synthesized from extracted rNDVs genome. Thirty-five cycles of PCR at 94°C for 30 s of denaturation, 56°C for 30 s of annealing, and 68°C for 150 s of elongation using the TAKARA LA Tag polymerase was used to amplify the fragments.

## Expression of HA1, HA2, and HA Proteins of H5N1 HPAIV

The expression of HA1, HA2, and HA proteins were detected in DF1 cells by Western blot analysis. DF1 cells were infected with rLaSota, rLaSota/HA1, rLaSota/HA1 + NDV F TM&CT, rLaSota/HA2, and rLaSota/HA at a multiplicity of infection (MOI) of 0.1 in presence of 10% fresh allantoic fluid, harvested from embryonated SPF chicken eggs. DF1 cell lysates and supernatants were collected 30 h post-infection. A polyclonal chicken anti H5N1 HPAIV and a monoclonal anti NDV HN protein sera were used to detect the expression of HA1, HA2, and HA proteins of HPAIV and HN protein of NDV by Western blot analysis, respectively. The surface expression of HA1, HA2, and HA proteins by NDV vectors was confirmed by an indirect immunofluorescence assay (IFA). Monolayer of DF1 cells on four-well chamber slides were infected with rNDVs. The cells were fixed and blocked on the slide surface 24 h post infection using 3% paraformaldehyde and 3% goat serum, respectively. The expression of HPAIV on the cell surface was detected using the above polyclonal chicken anti H5N1 HPAIV primary antibody and a goat anti chicken fluorescent conjugated secondary antibody (KPL). The expression of HA1, HA2, and HA proteins in embryonated chicken eggs and the incorporation of HA1, HA2, and HA proteins into an NDV envelope were assessed by Western blot analysis. Ten-days-old embryonated SPF chicken eggs were infected with rLaSota, rLaSota/HA1, rLaSota/HA1 + NDV F TM&CT, rLaSota/HA2, or rLaSota/HA. Allantoic fluids were harvested from infected eggs three days after infection. Allantoic fluid also was collected from uninfected eggs as control. The allantoic fluids were centrifuged at 1500 rpm for 10 min, then were centrifuged through 30% sucrose cushion (SW41rotor) at 25,000 rpm for 2.5 h at 4°C. Then pellets were dissolved in 50 μl PBS, lysed, and analyzed by Western blot using the two above antisera.

## Growth Characteristics of rNDVs Expressing HA1, HA2, or HA Protein of H5N1 HPAIV

Recombinant Newcastle disease viruses expressing HPAIV HA1, HA2, or HA protein were passaged in eggs. The allantoic fluids

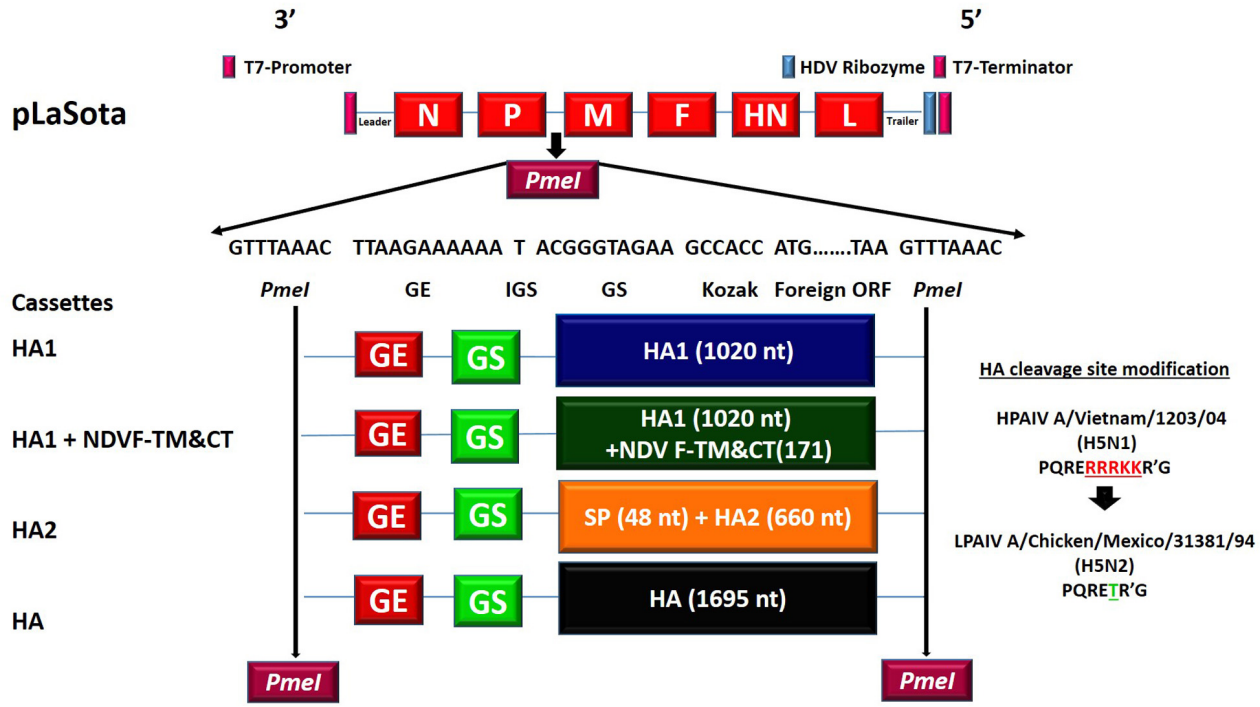


**FIGURE 1 |** Construction of recombinant NDVs containing H5N1 HPAIV HA1, HA2, or HA gene. The following four transcription cassettes were inserted into individual plasmids containing cDNA of LaSota between P and M genes using *Pme*I site: (i) codon optimized HA1 subunit of HA gene of H5N1 HPAIV (1,020 nt), (ii) codon optimized HA1 subunit of HA gene of H5N1 HPAIV (1,020 nt) fused with N-terminus of transmembrane and cytoplasmic tail of F gene of NDV (171 nt), (iii) the N-terminus of codon optimized HA2 subunit of HA gene of H5N1 HPAIV (660 nt) fused with C-terminus of signal peptide sequence of HA gene of H5N1 HPAIV(48 nt), and (iv) the codon optimized HA gene of H5N1 HPAIV (1;1695 nt). Each transcription cassette contains; *Pme*I restriction enzyme site sequence at two ends of the transcription cassette plus in the constant order; 3′-GE signal of NDV, one T nucleotide as intergenic sequence (IGS), GS signal of NDV, Kozak sequence (In order to follow the rule of six ACC and GCCACC were used for HA construct and other constructs, respectively.), and foreign gene ORF sequence-5′.

containing high titers ($2^8$ HAU/50 μl) of each recombinant virus were aliquoted in vials and stored at −70°C. The titer of each virus was determined by plaque forming unit (PFU) assay on DF1 cells in the presence of 10% fresh allantoic fluid. Monolayer DF1 cells in 6-well tissue culture plates were washed with DMEM and infected at an MOI of 0.1 with parental rLaSota, rLaSota strains expressing HA1, HA1 + NDV F TM&CT, HA2, or HA protein. After 90 min adsorption at 37°C, cells were washed with DMEM, then incubated with DMEM containing 10% fresh SPF chicken egg allantoic fluid at 37°C in presence of 5% $CO_2$. At intervals of 8 h until 64 h post-infection, volumes of 200 μl of supernatant from infected cells were collected and replaced with equal volumes of fresh DMEM containing 10% fresh allantoic fluid. The titer of rNDVs in collected supernatants was determined by $TCID_{50}$ method on DF1 cells. The titers were calculated using a formula derived from Reed and Muench and Spearman–Karber methods (Ramakrishnan, 2016).

## The Protective Efficacies of rNDVs Expressing HA1, HA2, or HA Protein Against H5N1 HPAIV Challenge

The protective efficacies of rNDVs expressing HA1, HA2, or HA protein of H5N1 HPAIV were evaluated in SPF chicks immunized at one day old and challenged against H5N1 HPAIV at 3 weeks after immunization. A total of 50 one-day-old SPF White Leghorn chicks, obtained from Charles Rivers, were divided into five groups of 10 each in Biosafety level-2. Chicks of groups one to five were immunized with $10^6$ PFU, 200 μl in volume, of rLaSota as empty vector control, rLaSota/HA1, rLaSota/HA1 + NDV F TM&CT, rLaSota/HA2, and rLaSota/HA, respectively, via the oculonasal route. Three weeks after immunization, blood was collected from all chickens. Then, they were moved into the Biosafety level-3 plus facility and were challenged with $10^6$ $EID_{50}$, 200 μl in volume, of HPAIV A/Vietnam/1203/2004 (H5N1) via the oculonasal route (OIE, 2018b). The infected birds were observed daily for 10 days after challenge. The mortality rate was recorded for each group daily. We conducted all experiments involving avirulent NDV strain LaSota in our USDA approved Biosafety level-2 and Biosafety level-2 plus facilities and the experiment involving HPAIV in our USDA approved Biosafety level-3 plus facility following the guidelines and approval of the Institutional Animal Care and Use Committee (IACUC), University of Maryland.

## Serological Assays

The sera were collected from all chickens three weeks after immunization. The humoral antibodies induced against NDV

and HPAIV in sera of immunized chickens were assessed. Hemagglutination inhibition (HI) assay using the protocol of OIE was used to assess the level of antibody titers mounted against a LPAIV A/Mallard (H5N2) in chickens immunized with rNDVs (OIE, 2018b). To confirm the result, we repeated the HI assay four times and we calculated the titers as the mean of four experiments. The virus neutralization assay was used to measure neutralizing antibodies induced against a LPAIV A/Mallard (H5N2) in chickens immunized by rNDVs. Briefly, serum samples of all immunized chickens were incubated at 56°C for 30 min. The titer of LPAIV (H5N2) was determined by $TCID_{50}$ on MDCK cells in the presence of DMEM containing 1μg/ml N-tosyl-l-phenylalanine chloromethyl ketone (TPCK)-treated trypsin. 100 $TCID_{50}$ of H5N2 LPAIV was mixed with 2-fold dilutions of antiserum and incubated for 90 min at 37°C. 100 μl of each serum and virus mixture was added into the monolayer of MDCK cells, three wells of 96-well tissue culture plate per dilution and incubated at 37°C. One hour after incubation, the supernatant of wells were removed and wells were washed with DMEM. Hundred microliter of DMEM containing 1 μg/ml TPCK-treated trypsin were added to each well. The plates were incubated at 37°C in the presence of 5% $CO_2$. Three days after infection, 50 μl of supernatant of each well were transferred to HA assay plate. The presence of H5N2 LPAIV in supernatants were detected by HA assay using 1% chicken RBC. The serum titers were calculated using a formula derived from Reed and Muench and Spearman–Karber methods (Ramakrishnan, 2016). Hemagglutination inhibition assay using the protocol of OIE was used to assess the level of antibody titers mounted against NDV strain LaSota in chickens immunized with rNDVs (OIE, 2018a).

## Statistical Analysis

The data for antibody response against LPAIV was analyzed by paired *t*-test between each two groups. The data for antibody response against NDV was analyzed among groups by One-Way-ANOVA analysis (Tukey test). To avoid bias, HPAIV challenge experiment was designed as a blinded study.

# RESULTS

## Generation rNDVs Expressing HA1, HA2, or HA Protein of H5N1 HPAIV

The expression cassettes of HPAIV HA gene subunits were constructed and inserted between P and M genes of NDV in individual plasmids containing full length antigenomic cDNA of NDV strain LaSota (**Figure 1**). The correct sequence of transcription cassettes containing HPAIV HA subunits and flanking regions was confirmed by sequence analysis. Infectious rNDVs containing the HA1 subunit, HA1 subunit fused with NDV-F TM and CT domains, the HA2 subunit, and the HA gene of HPAIV were recovered from all cDNAs by reverse genetics technique using HEp-2 cells. They were named rLaSota/HA1, rLaSota/HA1 + NDV F TM&CT, rLaSota/HA2, and rLaSota/HA, respectively. The presence of HA1, HA2, and HA genes in rNDVs were confirmed by RT-PCR.

## Expression of HA1, HA2, and HA Proteins of H5N1 HPAIV

The expression of HA1, HA2, and HA proteins of HPAIV was detected by Western blot analysis of infected DF1 cell lysates (**Figure 2A**, upper panel). The HA protein was expressed efficiently (**Figure 2A**, lane 5), a ∼70 kDa band representing uncleaved HA protein (HA0), a ∼64 kDa band representing HA1 subunit, and a ∼25 kDa band representing HA2 subunit. The expression of HA1 subunit fused with NDV F protein TM and CT was much higher than that of HA1 subunit alone, a ∼60 kDa band represents HA1 subunit fused with NDV F protein TM and CT (**Figure 2A**, lane 4), and a ∼55 kDa band represents HA1 subunit (**Figure 2A**, lane 3). In the case of HA2 expressed by rLaSota/HA2, there is a band (∼25 kDa) on the bottom of the gel (**Figure 2A**, lane 6). Lanes 1 and 2 of **Figure 2A** represent DF1 cells and rNDV, respectively, as controls. A monoclonal anti-NDV HN antibody was used to detect a ∼70 kDa of the HN protein of NDV in cell lysates (**Figure 2A**, lower panel). We also evaluated expression of HPAIV HA1, HA2, and HA proteins in eggs and their incorporation into an NDV envelope (**Figure 2B**). Our results showed that the HA protein was expressed in eggs and incorporated into an NDV envelope, efficiently. The ∼60and ∼25 kDa bands represent cleaved HA1 and HA2 subunits, respectively (**Figure 2B**, lane 1). The HA2 subunit was expressed in eggs and incorporated into the NDV envelope, inefficiently. A ∼25 kDa band shows HA2 subunit (**Figure 2B**, lane 2). The HA1 subunit fused with NDVF protein TM and CT showed very little expression in the egg and incorporation into NDV envelope. A very weak ∼60 kDa band represents HA1 subunit fused with NDV F protein TM and CT (**Figure 2B**, lane 3). Lane 4 of **Figure 2B** shows that HA1 without TM and CT did not express in the egg and did not get incorporated into the NDV envelope. Lanes 5 and 6 of **Figure 2B** represents partially purified NDV particles and allantoic fluid as control. The ∼50-55 kDa bands in lanes 1–5 were as a result of a non-specific interaction of antibodies with NDV proteins. A monoclonal anti-NDV HN antibody was used to detect the ∼70 kDa HN protein of NDV (**Figure 2B**, lower panel). The surface expression of HA1, HA2, and HA proteins by NDV vectors were detected by IFA. HA1 fused with NDV F TM and CT domains, HA2 and HA proteins were expressed at a high level on the surface of DF1 cells, whereas HA1 alone was not expressed on the cells' surface (**Figure 2C**). In order to determine the conformational structure of expressed proteins, the expression of HA1, HA2, and HA proteins by rNDVs was detected using western blot analysis under non-reducing non-denaturing conditions. Both HA1 and HA2 in DF1 cell lysates infected with rNDVs (**Supplementary Figures 2A,B**) and in chicken eggs and purified NDV particles (**Supplementary Figures 2C,D**) were detected at sizes that were larger than our predictions. The oligomerization of HA1, HA2, and HA proteins were also determined by Western blot analysis (**Supplementary Figure 3**). The oligomer forms were detected for HA1, HA2, and HA proteins under non-reducing and denaturing conditions (**Supplementary Figure 3A**).

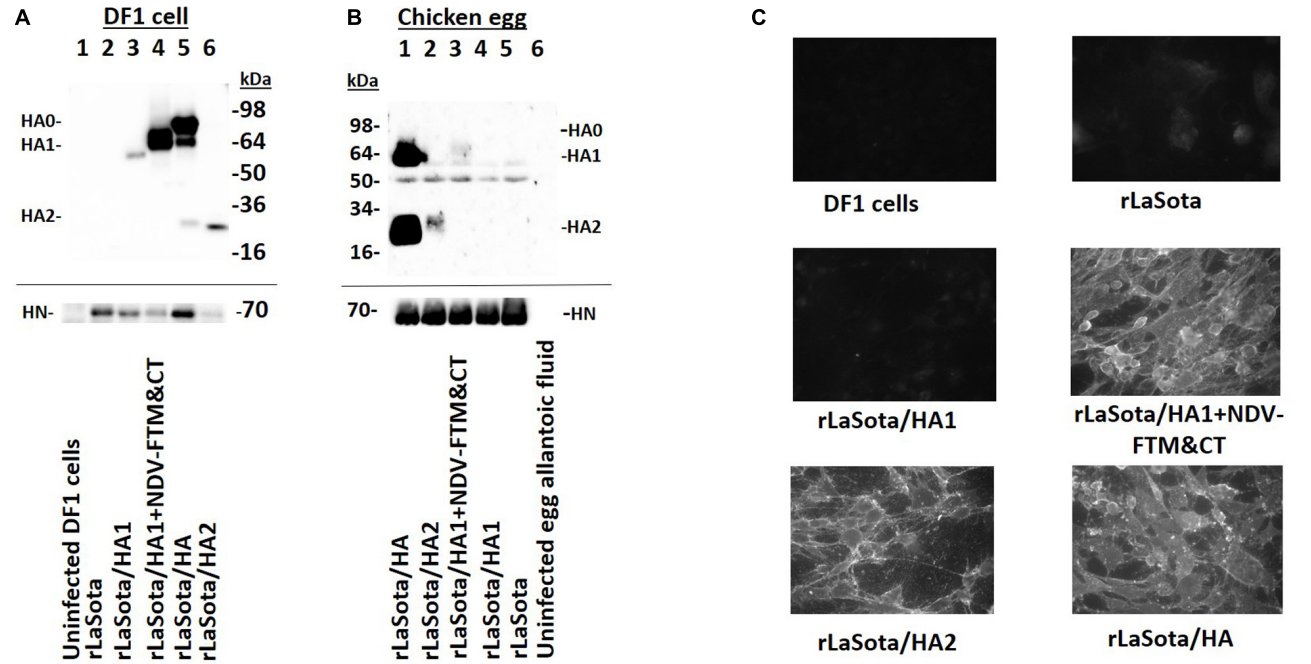


**FIGURE 2 |** The expression of HA1, HA2, and HA proteins of HPAIV by rNDVs. **(A)** The expression of HA1, HA2, and HA proteins were detected in infected DF1 cell lysates by Western blot analysis using a chicken polyclonal anti H5N1 HPAIV serum **(upper panel)**; uninfected DF1 cells (lane 1), rLaSota (lane 2), rLaSota/HA1 (lane 3), rLaSota/HA1 + NDV F TM&CT (lane 4), rLaSota/HA (lane 5), and rLaSota/HA2 (lane 6). A monoclonal anti NDV HN antibody was used to detect the 70 kDa HN protein of NDV in DF1 cell lysates **(lower panel)**; uninfected DF1 cells (lane 1), rLaSota (lane 2), rLaSota/HA1 (lane 3), rLaSota/HA1 + NDVF TM&CT (lane 4), rLaSota/HA (lane 5) and rLaSota/HA2 (lane 6). The full length of cropped gels is presented in **Supplementary Figure 1**. **(B)** The expression of HA1, HA2 and HA proteins of HPAIV in embryonated chicken eggs and the incorporation of these proteins into NDV particles were detected by Western blot using a chicken polyclonal anti H5N1 HPAIV serum **(upper panel)**; rLaSota/HA (lane 1), rLaSota/HA 2(lane 2), rLaSota/HA1 + NDVF TM&CT (lane 3), rLaSota/HA1 (lane 4), rLaSota (lane 5) and uninfected allantoic fluid (lane 6). A monoclonal anti NDV HN antibody was used to detect the 70 kDa HN protein of NDV **(lower panel)**; rLaSota/HA (lane 1), rLaSota/HA 2(lane 2), rLaSota/HA1 + NDV F TM&CT (lane 3), rLaSota/HA1 (lane 4), rLaSota (lane 5) and uninfected allantoic fluid (lane 6). **(C)** DF1 cells were infected with rNDVs at MOI of 0.1. The cells were fixed with 3% paraformaldehyde 24 h post-infection, then were blocked with 3% goat serum. The florescence signals on the surface of cells were observed by immunofluorescence microscope after interacting the cells with a primary chicken polyclonal anti H5N1 HPAIV serum and a secondary FITC conjugated goat anti chicken antibody.

## Growth Characteristics of rNDVs Expressing HA1, HA2, or HA Protein of H5N1 HPAIV

The rNDVs expressing HA1, HA2, or HA protein were passaged in 10-day-old embryonated SPF chicken eggs. All rNDVs replicated in eggs efficiently with titers of $2^8$ $HAU/_{50}$ μl (parental rNDV strain LaSota usually replicates in eggs with titer of $2^9$ $HAU/_{50}$μl). The multicycle growth kinetics of rNDVs in the presence of fresh allantoic fluid, as a source of protease, in DF1 cells showed that rNDVs expressing HA1, HA2, or HA protein grew at similar levels compared to the parental rNDV. Compared to parental rNDV, other rNDVs grew slightly slower at first, but viruses reached similar titers after 32 h. However, there was no statistical significance among groups (**Figure 3**).

## The Protective Efficacies of rNDVs Expressing HA1, HA2, or HA Protein in Chickens Against H5N1 HPAIV Challenge

The protective efficacies of rNDVs expressing HA1, HA2, or HA protein were evaluated in one-day-old SPF chicks immunized at one day old and challenged with H5N1 HPAIV at three weeks post immunization. The survival rates against HPAIV were recorded daily for ten days after challenge (**Figure 4**). The results showed an 100% survival rate for chickens immunized with rLaSota/HA until ten days post-challenge, while an 100% mortality was observed for chickens immunized with empty LaSota vector and chicks immunized with rLaSota/HA1 at day two post-challenge. The mortality rate for chickens immunized with rLaSota/HA2 was nine out of ten chickens at day two post-challenge. One out of ten chickens immunized with rLaSota/HA2 survived until ten days post-challenge. In the case of chickens immunized with rLaSota/HA1 + NDV F TM&CT, results showed eight out of ten chickens died at day two post-challenge and the remaining two chickens died at day three post-challenge. In this study, virus shedding from infected birds was not evaluated, because all chickens immunized with empty LaSota vector, rLaSota/HA1, or rLaSota/HA2 died before day four post-challenge. However, in another challenge, we evaluated the protective efficacy of rLaSota/HA in preventing post-challenge oropharyngeal viral load in SPF chickens (Shirvani et al., 2020).

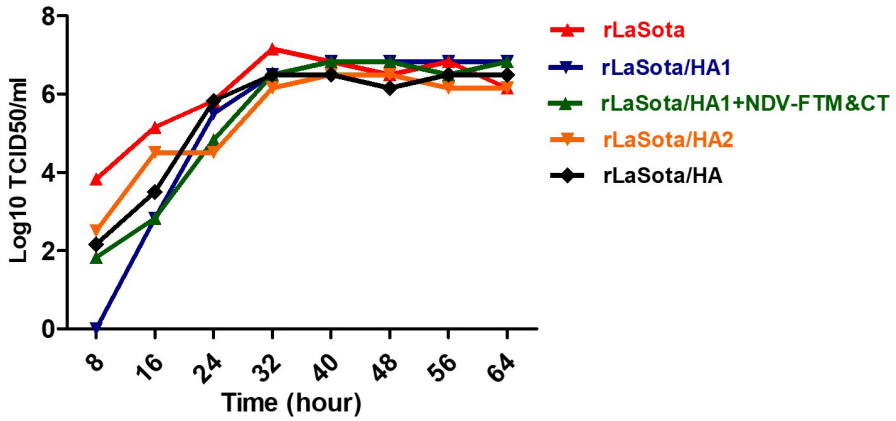


**FIGURE 3 |** Growth kinetics of rNDVs expressing HA1, HA2, or HA protein in DF1 cells. The monolayers of DF1 cells in six-well plate tissue culture were infected with rNDVs at an MOI of 0.1. The over layered media containing the virus were removed after one-hour adsorption and replaced with fresh DMEM containing 10% allantoic fluid. The titer of viruses in volumes of supernatants collected in 8 h intervals were detected by $TCID_{50}$ using DF1 cells.

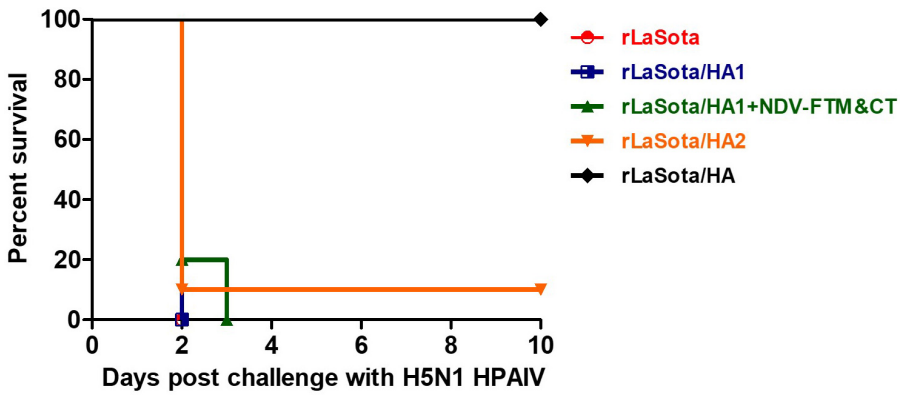


**FIGURE 4 |** Survival rate of immunized chickens with rNDVs expressing HA1, HA2, or HA protein of HPAIV against H5N1 HPAIV challenge. Groups of ten SPF chicks were immunized with $10^6$ PFU of rLaSota, rLaSota/HA1, rLaSota/HA1 + NDV F TM&CT, rLaSota/HA2, or rLaSota/HA via the oculonasal route at one day old. Three weeks after immunization, chickens were challenged with $10^6$ $EID_{50}$ of HPAIV A/Vietnam/1203/2004 (H5N1) through oculanasal route. Chickens were observed daily for ten days after challenge. The percent of survival rate was recorded for each group.

## Antibody Response Against AIV

Neutralizing antibodies induced against LPAIV (H5N2) in serum samples of chickens at 21 days after immunization were assessed by a micro-virus neutralization assay on MDCK cells. The results showed that compared to rLaSota group, the significant level of neutralizing antibodies against LPAIV (H5N2) were detected only in serum samples of chickens immunized with rLaSota expressing intact HA protein ($P < 0.05$). However, compared to the rLaSota group, insignificant titers of neutralizing antibodies against LPAIV (H5N2) were detected in serum samples of chickens immunized with rLaSota/HA2 and rLaSota/HA1 + NDV F TM&CT ($P > 0.05$) (**Figure 5A**). The data were statistically analyzed by the paired *t*-test between the rLaSota group and each vaccinated group.

The HI titers of antibodies induced against a heterologous H5N2 LPAIV were assessed in sera of chickens 21 days after immunization by HI assay using the protocol of OIE (repeated four times). The results showed that, compared to groups immunized with rLaSota, rLaSota/HA1, rLaSota/HA1 + NDV F TM&CT, or rLaSota/HA2, HI titers against H5N2 LPAIV was detected at a significantly higher level only in serum samples of chickens immunized with rLaSota expressing intact HA protein ($P < 0.05$) (**Figure 5B**). The data were statistically analyzed by the paired *t*-test between each two groups.

The results showed that comparable HI titers against NDV strain LaSota were detected in sera collected from chickens of five groups ($P > 0.05$) (**Figure 6**). The data were statistically analyzed by the One-Way-ANOVA analysis (Tukey test) among five groups.

## DISCUSSION

This study aimed to determine the individual contributions of HA1 and HA2 subunits of H5N1 HPAIV HA protein in the induction of neutralizing antibodies and protection in

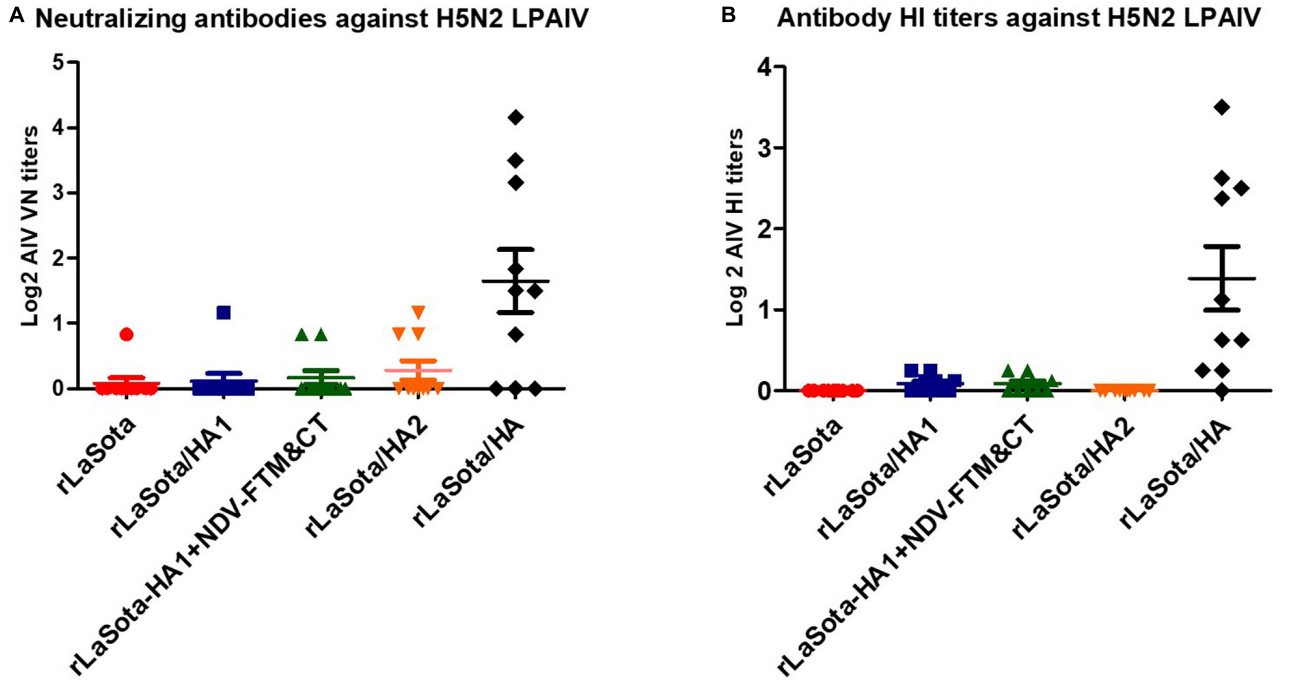


**FIGURE 5 |** Antibody response against AIV. SPF chicks were immunized at one day old and sera were collected at day 21 after immunization. Neutralizing antibodies against a heterologous H5N2 LPAIV in collected sera were assessed by a micro-virus neutralization assay on MDCK cells using a standard protocol **(A)**. Symbols and horizontal lines represent individual titers of each sample and mean titers of each group, respectively. HI antibody titers were assessed against a heterologous H5N2 LPAIV by HI assay (repeated four times) using the protocol of OIE **(B)**. Each symbol represents mean titers of four HI assays for individual samples and horizontal lines represent mean titers of each group, respectively. Serum titers were expressed as reciprocals Log2 dilution.

chickens. rNDV was used as the expression vector, because NDV infects the respiratory tract just as HPAIV does and has been previously used to express HPAIV HA protein (Veits et al., 2006; Nayak et al., 2009; Kim and Samal, 2016). Chickens are highly susceptible to HPAIV infection; therefore, are an ideal system for this study. Our results showed that the intact HA protein induced a neutralizing antibody response and provided complete protection against death following a lethal homologous challenge. Whereas, HA1 or HA2 subunit neither induced significant levels of a neutralizing antibody response nor provided protection following a lethal homologous challenge. These results suggest that the epitopes responsible for the induction of protective immunity are present on both the HA subunits in their native conformation, but their native conformation is lost when the two subunits are separated.

The intact HA protein and HA1 fused with NDV F TM and CT domains were detected at high levels in DF1 cells by both Western blot and IFA. The HA2 protein was also detected in DF1 cells by IFA at a high level and by Western blot at a lower level, but the HA1 protein was not detected in DF1 cells by IFA and detected by Western blot at a very low level. We also evaluated expression of these proteins in the egg and incorporation of them into NDV particles. Among the four proteins, the intact HA protein was detected in the egg at a high level and incorporated into the NDV envelope efficiently; the HA2 protein was detected in eggs at a low level and incorporated into the NDV envelope inefficiently. HA1 with NDV F TM and CT was detected at very low level in the egg and showed very little incorporation, and HA1 was not detected in the egg and did not incorporate into the NDV virion. Furthermore, the size of detected HA1 and HA2 proteins either in cell or in egg are different from the size of detected bands for the cleaved HA1 and HA2 from whole HA protein, respectively. Therefore, among HPAIV antigens, only whole HA was detected at a high level by anti HPAIV serum regardless the environment of expression and incorporated efficiently into NDV envelop. These results suggest that separation of HA1 and HA2 subunits led to a change in the conformational structure of immunoreactive epitopes on HA1 and HA2 subunits. The addition of NDV F TM and CT domains might have restored the conformation of some of the immunoreactive epitopes when protein was expressed in DF1 cells, but not in the egg, which may be because some cellular factors needed for folding are absent in the egg. Oligomerization studies also showed that HA1, HA2, and HA proteins formed oligomers, suggesting that the inability of HA1 to react with H5N1 antiserum was not due to absence of oligomerization (**Supplementary Figure 3**).

The result of the protective efficacies of rNDVs expressing HA1, HA2, or HA protein in one-day-old chicks showed that rNDV expressing the intact HA protein provided complete protection against HPAIV infection in chickens, while rNDV expressing HA1 or HA2 subunit were not protective. Our finding that the HA provided complete protection from lethal challenge was not unexpected, because it is well established that the HA protein contains the major protective antigens of HPAIV

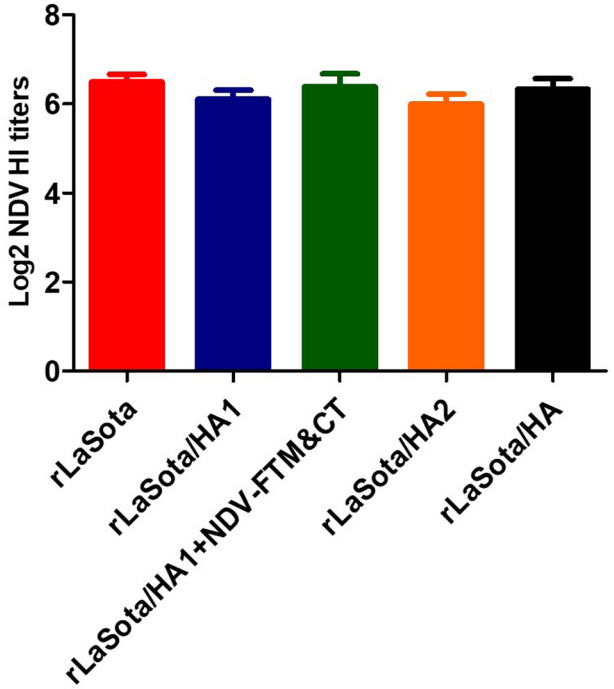


**FIGURE 6 |** Antibody response against NDV. SPF chicks were immunized at one day old and sera were collected at day 21 after immunization. HI antibody titers induced against NDV strain LaSota in collected sera were assessed by HI assay using the protocol of OIE. Serum titers are expressed as reciprocal Log2 dilution.

(Veits et al., 2006; Nayak et al., 2009). However, our results showed that when separated the HA1 or HA2 subunit alone does not provide protection in chickens. These results suggest that the native conformation of HA is maintained when the HA1 and HA2 subunits are held together by disulfide bonds. The important protective epitopes are only present on HA in its native conformation. But when HA1 and HA2 subunits are separated, the conformations of these two proteins are changed, leading to the loss of the protective epitopes. It is also possible that some protective epitopes on HA protein are formed by residues from both HA1 and HA2 subunits and hence these epitopes are lost when the two subunits are separated.

The neutralizing antibodies against a H5N2 LPAIV were detected only in serum samples of chickens immunized with rNDV expressing the whole HA protein. Our results showed that the HA1 and HA2 subunits, when separated, failed to induce neutralizing antibodies. These results suggest that the conformational changes caused by the separation of HA1 and HA2 subunits might be the reason for the loss of neutralizing epitopes located on HA1 and HA2 subunits. Our results provide indirect evidence that the disulfide bond between HA1 and HA2 or some other interactions between key residues of HA1 and HA2 is necessary to maintain the native conformation of HA protein (Palese and Shaw, 2013; Wang et al., 2015). This is consistent with outcomes of an earlier study which showed that the interaction between HA1 and HA2 subunits affects HA protein stability and AIV infectivity (Wang et al., 2015). Interestingly, rNDV expressing HA1 subunit fused with NDV F TM and CT also did not induce neutralizing antibodies or provide protection, but somehow resulted in high levels of expression of HA1 detected by Western blot analysis and IFA only in DF1 cells. This result suggests that the addition of NDV F TM and CT leads to conformational change of HA1 and exposure of non-neutralizing epitopes, which were recognized by AIV antibodies in Western blot and IFA. However, the presence of NDV F TM and CT was not able to compensate for the lack of HA2 subunit required for correct folding, incorporation into the NDV envelope, and induction of protective immunity. Previous studies have shown that HA1 and HA2 subunits of H5N1 HPAIV (Gao et al., 2006) and stem fragment of H1N1 (Steel et al., 2010; Mallajosyula et al., 2014; Yassine et al., 2015) provided protection and induced antibodies in mouse and/or ferret models. Although mice and ferrets are excellent animal models to study human influenza virus pathogenesis and transmission, they may not be sufficiently permissive to evaluate the protective efficacy of human influenza virus vaccines (Thangavel and Bouvier, 2014; Zeng et al., 2019).

The antibodies against NDV were detected at similar levels in immunized chickens of all groups, indicating that all the recombinant viruses grew at the same level in chickens. The level of antibodies induced against the NDV backbone was higher than antibodies detected against AIV for two reasons. Firstly, for NDV, a homologous virus was used in HI assay for the detection of antibodies against NDV, while for HPAIV, a heterologous LPAIV (H5N2), with about 90% amino acid identity with the HA protein of recombinant vaccine, was utilized to detect HI and neutralizing antibody titers against H5N1 HPAIV. Previous studies have shown that the antibody titers assayed against a heterologous H5 HPAIV were lower compared to the homologous H5 HPAIV virus (Swayne et al., 2015; Jang et al., 2018). Secondly, for HPAIV, antibodies induced against HA protein contribute to HI and VN assays. But for NDV, the antibodies induced against heamagglutininin–neuraminidase (HN) protein are detected by HI test and antibodies induced against F and HN proteins contribute to the VN assay (Samal, 2019).

## CONCLUSION

Therefore, a H5N1 vaccine construct incorporating either HA1 or HA2 subunit may not provide protection against HPAIV challenge in chickens. Our results showed that immunization with HA1 or HA2 alone neither induced serum neutralizing antibodies nor prevented death following challenge. Immunization with HA protein is necessary for complete protection against HPAIV.

## DATA AVAILABILITY STATEMENT

All datasets generated for this study are included in the article/**Supplementary Material**.

## ETHICS STATEMENT

The animal study was reviewed and approved by Institutional Animal Care and Use Committee (IACUC), University of Maryland.

## AUTHOR CONTRIBUTIONS

SS and ES conceived and designed the experiments, analyzed the data, and wrote the manuscript. ES built the constructs and *in vitro* characterization experiments and performed the immunization and animal experiments in Biosafety level 2 facilities. AP and BV performed the HPAIV challenge and animal experiments in Biosafety level 3 plus facilities. SS contributed reagents, materials, and analysis tools. All the authors reviewed the manuscript.

## ACKNOWLEDGMENTS

We would like to thank all our laboratory members for their technical assistance and help.

## SUPPLEMENTARY MATERIAL

The Supplementary Material for this article can be found online at: https://www.frontiersin.org/articles/10.3389/fmicb.2020.01085/full#supplementary-material

## REFERENCES


Balzli, C. L., Bertran, K., Lee, D. H., Killmaster, L., Pritchard, N., Linz, P., et al. (2018). The efficacy of recombinant turkey herpesvirus vaccines targeting the H5 of highly pathogenic avian influenza virus from the 2014–2015 North American outbreak. *Vaccine* 36, 84–90. doi: 10.1016/j.vaccine.2017.11.026

Bublot, M., Pritchard, N., Cruz, J. S., Mickle, T. R., Selleck, P., and Swayne, D. E. (2007). Efficacy of a fowl pox-vectored avian influenza H5 vaccine against Asian H5N1 highly pathogenic avian influenza virus challenge. *Avian. Dis.* 51, 498–500. doi: 10.1637/7624-042706r.1

Chen, H., Yuan, H., Gao, R., Zhang, J., and Wang, D. (2014). Clinical and epidemiological characteristics of a fatal case of avian influenza A H10N8 virus infection: a descriptive study. *Lancet* 383, 714–721.

Cui, H., Gao, H., Cui, X., Zhao, Y., Shi, X., Li, Q., et al. (2013). Avirulent Marek's disease virus type 1 strain 814 vectored vaccine expressing avian influenza (AI) virus H5 haemagglutinin induced better protection than turkey herpesvirus vectored AI vaccine. *PLoS One* 8:e53340. doi: 10.1371/journal.pone.0053340

Gao, W., Soloff, A. C., Lu, X., Montecalvo, A., Nguyen, D. C., Matsuoka, Y., et al. (2006). Protection of mice and poultry from Lethal H5N1 avian influenza virus through adenovirus-based immunization. *J. Virol.* 80, 1959–1964. doi: 10.1128/jvi.80.4.1959-1964.2006

Huang, Z., Krishnamurthy, S., Panda, A., and Samal, S. K. (2001). High-level expression of a foreign gene from the most 39-proximal locus of a recombinant Newcastle disease virus. *J. Gen. Virol.* 82, 1729–1736. doi: 10.1099/0022-1317-82-7-1729

International Committee on Taxonomy of Viruses [ICTV] (2018). Available online at: https://talk.ictvonline.org/taxonomy/

Jang, H., Elaish, M., Mahesh, K. C., Abundo, M. C., Ghorbani, A., Ngunjiri, J. M., et al. (2018). Efficacy and synergy of live-attenuated and inactivated influenza vaccines in young chickens. *PLoS One* 13:e195285. doi: 10.1371/journal.pone.0195285

Kim, S. H., Paldurai, A., Xiao, S., Collins, P. L., and Samal, S. K. (2014). Modified Newcastle disease virus vectors expressing the H5 hemagglutinin induce enhanced protection against highly pathogenic H5N1 avian influenza virus in chickens. *Vaccine* 32, 4428–4435. doi: 10.1016/j.vaccine.2014.06.061

Kim, S. H., and Samal, S. K. (2016). Newcastle disease virus as a vaccine vector for development of human and veterinary vaccines. *Viruses* 7:183. doi: 10.3390/v8070183

Kim, S. H., and Samal, S. K. (2019). Innovation in newcastle disease virus vectored avian influenza vaccines. *Viruses* 11:3. doi: 10.3390/v11030300

Kirkpatrick, E., Qiu, X., Wilson, P. C., Bahl, J., and Krammer, F. (2018). The influenza virus hemagglutinin head evolves faster than the stalk Domain. *Sci. Rep.* 8:1. doi: 10.1038/s41598-018-28706-1

Klenk, H. D., Rott, R., Orlich, M., and Blodorn, J. (1975). Activation of influenza A viruses by trypsin treatment. *Virology* 68, 426–439. doi: 10.1016/0042-6822(75)90284-6

Koutsakos, M., Kedzierska, K., and Subbarao, K. (2019). Immune responses to avian influenza viruses. *J. Immunol.* 202, 382–391. doi: 10.4049/jimmunol.1801070

Krammer, F., Hai, R., Yondola, M., Tan, G. S., Leyva-Grado, V. H., Ryder, A. B., et al. (2014). Assessment of influenza virus hemagglutinin stalk-based immunity in ferrets. *J. Virol.* 88, 3432–3442. doi: 10.1128/jvi.03004-13

Krammer, F., and Palese, P. (2019). Universal influenza virus vaccines that target the conserved hemagglutinin stalk and conserved sites in head domain. *J. Infect. Dis.* 219, S62–S67. doi: 10.1093/infdis/jiy711

Lazarowitz, S. G., and Choppin, W. (1975). Enhancement of the infectivity of influenza A and B viruses by proteolytic cleavage of the hemagglutinin polypeptide. *Virology* 68, 440–454. doi: 10.1016/0042-6822(75)90285-8

Mallajosyula, V. V. A., Citron, M., Ferrara, F., Lu, X., Callahan, C., Heidecker, G. J., et al. (2014). Influenza hemagglutinin stem-fragment immunogen elicits broadly neutralizing antibodies and confers heterologous protection. *PNAS* 111:25. doi: 10.1073/pnas.1402766111

Nayak, B., Rout, S. N., Kumar, S., Khalil, M. S., Fouda, M. M., Ahmed, L. E., et al. (2009). Immunization of chickens with Newcastle disease virus expressing H5 hemagglutinin protects against highly pathogenic H5N1 avian influenza viruses. *PLoS One* 4:e6509. doi: 10.1371/journal.pone.0006509

OIE (2018a). *(World Organization for Animal Health) Newcastle disease, In OIE Terrestrial Manual, Chapter 2.3.14*. Available online at: https://www.oie.int/fileadmin/Home/eng/Health_standards/tahm/3.03.14_NEWCASTLE_DIS.pdf

OIE (2018b). *(World Organization for Animal Health) Avian Influenza. In OIE Terrestrial Manual, Chapter 3.3.4*. Available online at: https://www.oie.int/fileadmin/Home/eng/Health_standards/tahm/3.03.04_AI.pdf

Palese, P., and Shaw, M. L. (2013). "Orthomyxoviridae: the viruses and their replication," in *Fields Virology*, eds D. M. Knipe and P. M. Holey (Philadelphia: Lippincott Williams & Wilkins), 1151–1186.

Pavlova, S. P., Veits, J., Mettenleiter, T. C., and Fuchs, W. (2009). Live vaccination with an H5-hemagglutinin-expressing infectious laryngotracheitis virus recombinant protects chickens against different highly pathogenic avian influenza viruses of the H5 subtype. *Vaccine* 27, 5085–5090. doi: 10.1016/j.vaccine.2009.06.048

Peacock, T. P., James, J., Sealy, J. E., and Iqbal, M. (2019). A Global Perspective on H9N2 Avian Influenza Virus. *Viruses* 11:7. doi: 10.3390/v11070620

Perez, D. R., Carnaccini, S., Cardenas-Garsia, S., Ferreri, L. M., Santos, J., and Rajao, D. S. (2019). "Avian Influenza Virus," in *Avian Virology-Current Research and Future Trends*, ed. S. K. Samal (Norfolk: Caister Academic Press), 1–41.

Ramakrishnan, M. A. (2016). Determination of 50% endpoint titer using a simple formula. *World J Virol.* 5, 85–86.

Samal, S. K. (2019). "Newcastle Disease Virus," in *Avian Virology-Current Research and Future Trends*, ed. S. K. Samal (Norfolk: Caister Academic Press), 43–85.

Shirvani, E., Varghese, B. P., Paldouri, A., and Samal, S. K. (2020). A recombinant avian paramyxovirus type-3 (APMV-3) expressing HA protein of highly pathogenic avian influenza virus (HPAIV) protects chickens against HPAIV. *Sci. Rep.* 10:2221.

Steel, J., Lowen, A. C., Wang, T. T., Yondola, M., Gao, Q., Haye, K., et al. (2010). Influenza virus vaccine based on the conserved hemagglutinin stalk domain. *mBio* 1:e00018-10. doi: 10.1128/mBio.00018-10

Suarez, D. L., and Pantin-Jackwood, M. P. (2017). Recombinant viral-vectored vaccines for the control of avian influenza in poultry. *Vet. Microbiol.* 206, 144–151. doi: 10.1016/j.vetmic.2016.11.025

Sutton, T. C. (2018). The pandemic threat of emerging H5 and H7 avian influenza viruses. *Viruses* 10:9. doi: 10.3390/v10090461

Sutton, T. C., Chakraborty, S., Mallajosyula, V. V. A., Lamirande, E. W., Ganti, K., Bock, K. B., et al. (2017). Protective efficacy of influenza group 2 hemagglutinin stem-fragment immunogen vaccines. *NPJ Vaccines* 2:35. doi: 10.1038/s41541-017-0036-2

Swayne, D. E. (2006). Principles for vaccine protection in chickens and domestic waterfowl against avian influenza emphasis on Asian H5N1 high pathogenicity Avian Influenza. *Ann. N.Y. Acad. Sci.* 1081, 174–181. doi: 10.1196/annals.1373.021

Swayne, D. E. (2012). Impact of vaccines and vaccination on global control of avian influenza. *Avian Dis.* 56, 818–828. doi: 10.1637/10183-041012-review.1

Swayne, D. E., Pavade, G., Hamilton, K., Vallat, B., and Miyagishima, K. (2011). Assessment of national strategies for control of high-pathogenicity avian influenza and low-pathogenicity notifiable avian influenza in poultry, with emphasis on vaccines and vaccination. *Rev. Sci. Tech.* 30, 839–870.

Swayne, D. E., Suarez, D. L., Spackman, E., Jadhao, S., Dauphin, G., Torchetti, M. K., et al. (2015). Antibody Titer Has Positive Predictive Value for Vaccine Protection against Challenge with Natural Antigenic-Drift Variants of H5N1 High-Pathogenicity Avian Influenza Viruses from Indonesia. *J. Virol.* 89:7. doi: 10.1128/JVI.00025-15

Thangavel, R. R., and Bouvier, N. M. (2014). Animal models for influenza virus pathogenesis, transmission, and immunology. *J. Immunol. Methods* 0, 60–79. doi: 10.1016/j.jim.2014.03.023

Toro, H., and Tang, D. C. (2009). Protection of chickens against avian influenza with non-replicating adenovirus-vectored vaccine. *Poul. Sci.* 88, 867–871. doi: 10.3382/ps.2008-00333

Veits, J., Wiesner, D., Fuchs, W., Hoffmann, B., Granzow, H., Starick, E., et al. (2006). Newcastle disease virus expressing H5 hemagglutinin gene protects chickens against Newcastle disease and avian influenza. *Proc. Natl. Acad. Sci. U.S.A.* 103, 8197–8202. doi: 10.1073/pnas.0602461103

Wang, W., Christopher, J. D. F., Alvarado-Facundo, E., Vassell, R., and Weiss, C. D. (2015). Intermonomer Interactions in Hemagglutinin Subunits HA1 and HA2Affecting Hemagglutinin stability and influenza virus infectivity. *J. Virol.* 89:20. doi: 10.1128/JVI.00939-15

Yassine, H. M., Boyington, J. F., McTamney, P. M., Wei, C. J., Kanekiyo, M., Kong, W. P., et al. (2015). Hemagglutinin-stem nanoparticles generate heterosubtypic influenza protection. *Nat. Med.* 21:9. doi: 10.1038/nm.3927

Zeng, H., Goldsmith, C. S., Kumar, A., Belser, J. A., Sun, X., Pappas, C., et al. (2019). Tropism and infectivity of a seasonal A(H1N1) and a highly pathogenic avian A(H5N1) influenza virus in primary differentiated ferret nasal epithelial cell cultures. *J. Virol.* 93:10. doi: 10.1128/JVI.00080-19

**Conflict of Interest:** The authors declare that the research was conducted in the absence of any commercial or financial relationships that could be construed as a potential conflict of interest.

The reviewer, DR, declared a past co-authorship with one of the authors, SS, to the handling editor.

*Copyright © 2020 Shirvani, Paldurai, Varghese and Samal. This is an open-access article distributed under the terms of the Creative Commons Attribution License (CC BY). The use, distribution or reproduction in other forums is permitted, provided the original author(s) and the copyright owner(s) are credited and that the original publication in this journal is cited, in accordance with accepted academic practice. No use, distribution or reproduction is permitted which does not comply with these terms.*

frontiers in Microbiology

ORIGINAL RESEARCH
published: 14 August 2020
doi: 10.3389/fmicb.2020.01961

# Self-Assembly M2e-Based Peptide Nanovaccine Confers Broad Protection Against Influenza Viruses

*Qimin Wang[1†], Yuling Zhang[1†], Peng Zou[1], Meixiang Wang[1], Weihui Fu[1], Jialei She[1], Zhigang Song[1], Jianqing Xu[1], Jinghe Huang[2]* and Fan Wu[1]**

[1] Shanghai Public Health Clinical Center, Fudan University, Shanghai, China, [2] Key Laboratory of Medical Molecular Virology (MOE/NHC/CAMS), School of Basic Medical Sciences and Shanghai Public Health Clinical Center, Fudan University, Shanghai, China

The extracellular domain of influenza M2 protein (M2e) is highly conserved and is a promising target for development of universal influenza vaccines. Here, we synthesized a peptide vaccine consisting of M2e epitope linked to a fibrillizing peptide, which could self-assemble into nanoparticle in physiological salt solutions. When administrated into mice without additional adjuvant, the influenza A M2e epitope-bearing nanoparticles induced antibodies against M2e of different influenza subtypes. Comparing with other M2e-based vaccine, these M2e nanoparticles did not induce immune response against the fibrillizing peptide, demonstrating minimal immunogenicity of vaccine carrier. Furthermore, vaccination with M2e-based nanoparticles did not only protect mice against homologous challenge of influenza PR8 H1N1 virus, but also provide protection against heterologous challenge of highly pathogenic avian influenza H7N9 virus. These results indicated that M2e-based self-assembled nanoparticle vaccine is safe and can elicit cross-protection, therefore is a promising candidate of universal influenza vaccines.

**Keywords: influenza, M2e, peptide, self-assembly, nanoparticle**

OPEN ACCESS

***Edited by:***
*Lijun Rong,*
*University of Illinois at Chicago, United States*

***Reviewed by:***
*Randy A. Albrecht,*
*Icahn School of Medicine at Mount Sinai, United States*
*Lanying Du,*
*New York Blood Center, United States*

****Correspondence:***
*Jinghe Huang*
*jinghehuang@fudan.edu.cn*
*Fan Wu*
*wufan@fudan.edu.cn;*
*wufan@shphc.org.cn*

*† These authors have contributed equally to this work*

***Specialty section:***
*This article was submitted to Virology, a section of the journal Frontiers in Microbiology*

***Received:*** *22 November 2019*
***Accepted:*** *24 July 2020*
***Published:*** *14 August 2020*

***Citation:***
*Wang Q, Zhang Y, Zou P, Wang M, Fu W, She J, Song Z, Xu J, Huang J and Wu F (2020) Self-Assembly M2e-Based Peptide Nanovaccine Confers Broad Protection Against Influenza Viruses. Front. Microbiol. 11:1961. doi: 10.3389/fmicb.2020.01961*

## INTRODUCTION

Influenza remains as a great threat to public health despite that it has been studied for over 100 years since 1918. The seasonal flu epidemics cause about 3–5 million cases of severe illness and 290,000 to 650,000 deaths around the world annually (World Health Organization [WHO], 2018). Current seasonal influenza vaccines, including inactivated and live-attenuated influenza vaccines, provide protection by inducing neutralizing antibodies against the influenza hemagglutinin protein (HA) (Caton et al., 1982). Viruses could escape from the protection by rapid antigenic drift due to the accumulation of mutations on the antibody binding site of HA protein and make vaccine ineffective (Ilyushina et al., 2019). The antigenic components of influenza vaccine need to be updated every year to catch up with the change of epidemic viruses (Krammer and Palese, 2015). The viral antigen components in seasonal vaccines are selected based on the influenza surveillance data and epidemic prediction (Auladell et al., 2019). Seasonal flu vaccine efficacy is determined by the similarity between the vaccine strains and circulating viruses (Estrada and Schultz-Cherry, 2019). The vaccine may not be able to provide enough protection when mismatched with the circulating strains (Belongia et al., 2016), resulting in the outbreak of influenza infection. It has been suggested that the ineffectiveness of seasonal flu vaccine caused significant morbidity and mortality

worldwide during the 2017–2018 flu season (Barr et al., 2018). Furthermore, the appearance of highly pathogenic avian influenza viruses, including H5N1 and H7N9 viruses, poses challenges on the current strategy of influenza vaccine by emerging novel influenza strains. Avian influenza viruses may cause worldwide influenza pandemic if they acquire efficient transmission between humans. Current seasonal influenza vaccine could not provide efficient protection against avian influenza viruses (Stephenson et al., 2004; Zhou et al., 2013). There is an urgent need to improve vaccine strategy against influenza and to develop universal influenza vaccines that could provide cross-protection against different influenza strains.

The ectodomain of influenza M2 protein (M2e) is a promising target for developing universal influenza vaccines (Estrada and Schultz-Cherry, 2019). M2e contains 23 amino acids and is highly conserved across multiple influenza strains. Passive administration of M2e-specific monoclonal antibodies was able to provide protection against influenza challenge in experimental animals (Zebedee and Lamb, 1988; Liu et al., 2004). A M2e-specific human monoclonal antibody could reduce clinical symptoms and viral loads when given to volunteers who were challenged with influenza epidemic strains (Ramos et al., 2015). M2e-elicited protective immunity has been achieved in animals by vaccination with different types of M2e-based influenza vaccines including M2e peptide conjugates, recombinant M2e fusion proteins, M2e-based DNA vaccines and others. Several M2e influenza vaccines have been evaluated in phase I/II clinical trials, yet there has not been M2e-based influenza vaccine available for clinical use (Kolpe et al., 2017).

Due to the poor immunogenicity of the pure M2e protein, most of M2e-based vaccines used carrier proteins, chemically or genetically fused with M2e, to enhance the immunogenicity of M2e vaccines (Estrada and Schultz-Cherry, 2019; Mezhenskaya et al., 2019). These vaccines did not only successfully provoke M2e-specific immune responses but also induced strong immune responses to the carrier proteins, which may cause unexpected side effect when used in humans. For example, an M2e-based influenza vaccine VAX102, which is a recombinant M2e–flagellin fusion protein, caused strong local and systemic adverse reactions when given in high dose to humans (Turley et al., 2011). Strong carrier-specific immune response may also cause carrier-induced epitopic suppression and so attenuate M2e-specific immune response (Heinen et al., 2002). Another M2e-based vaccine ACAM-FLU-A, which consists of three tandem copies of M2e epitope fused to hepatitis B core protein, induced M2e-specific antibodies in a phase I clinical trial (ClinicalTrials.gov Identifier No. NCT00819013). However, the titers of M2e-specific antibodies decreased rapidly over time in the volunteers (Kolpe et al., 2017). Although the detailed results and underlying mechanisms have not been published yet, we speculated that the decrease of M2e-specific antibodies may be due to the strong immunogenicity of HBV core protein since carrier-induced epitopic suppression was previously observed in epitope conjugate vaccines (Jegerlehner et al., 2010).

In this study, we performed proof-of-concept research and evaluated the safety and effectiveness of a novel method to enhance the immunogenicity of M2e epitope. We synthesized a peptide that consists of M2e epitope linked to a fibrillized peptide Q11. The Q11 peptide could self-assemble into a nanofiber in physiological pH condition and act as immune adjuvant to enhance the immunogenicity of the linked antigenic epitopes (Rudra et al., 2010, 2012a,b). We validated that the M2e-Q11 peptide could self-assemble into nanoparticles and provoke M2e-specific antibody response in mice without additional adjuvant. Furthermore, M2e-Q11 nanoparticles did not induce immune responses against the fibrillizing Q11 peptide, reducing the potential side effects that could be caused by the immunogenicity of the vaccine carrier. Vaccination with M2e-Q11 nanoparticles was also able to protect mice against lethal does challenge of different influenza subtypes, suggesting that the self-assembly of M2e-Q11 nanoparticles is a promising strategy for developing universal influenza vaccine.

# MATERIALS AND METHODS

## Peptides and Virus

Peptides were synthesized by solid phase method in Synpeptide Co. (Shanghai, China). M2e peptide, N-SLLTEVETPIRN EWGCRCNDSSD, is a conserved M2e domain of human influenza A virus. Q11 peptide, N-QQKFQFQFEQQ, is a self-assembly peptide which forms into fibril in physiological pH conditions. M2e-Q11 peptide, N-SLLTEVETPIRNEW GCRCNDSSDSGSGQQKFQFQFEQQ, is the M2e peptide covalently linked to Q11 peptide with spacer sequence GSGS. Avian M2e peptide, N-SLLTEVETPTRTGWECNCSGSSD, is a peptide containing M2e sequence from avian H7N9 virus. Swine M2e peptide, N-SLLTEVETPTRSEWECRCSGSSD, is a peptide containing M2e sequence from swine H1N1 influenza virus. All the peptides were purified by HPLC and analyzed by mass spectrometry. The purity of the peptides was above 90%. Stock solution of the peptides was prepared at the concentration of 8 mM in distilled water and stored at −20°C.

Mouse-adapted influenza viruses, A/Purto Rico/8/34 (PR8, H1N1) and avian influenza virus A/Shanghai/4664T/2013 (H7N9) were propagated in MDCK cells. The TCID50 and plague forming units (PFU) of viruses were evaluated on MDCK cell monolayer. The lethal doses of viruses was titrated on mice and calculated by Reed–Muench method. The experiments involved avian H7N9 influenza virus were conducted in ABSL-3 lab in Shanghai public health center and under protocols approved by the institutional biosafety committee.

## Nanoparticle Size Determination

Peptides M2e-Q11, Q11, and M2e were diluted from the stocking concentration (8 mM) to 1mM with PBS and incubated at room temperature for 4 h to allow fibrilization. The solutions were further incubated overnight at 4°C before being diluted with PBS to a final concentration of 0.25 mM. Peptide solutions were adsorbed onto carbon-coated 200 mesh copper grids and negatively stained with 2% uranyl acetate and imaged with a FEI Tecnai G2 Spirit transmission electron Microscope. The size distributions of nanoparticles were analyzed by dynamic light scattering with Zetasizer ZEN3600 (Malvern Panalytical Ltd.).

## Immunization

Female Balb/C mice (6–8 weeks old) were divided into four groups and intraperitoneally immunized with 10 nM of M2e-Q11 peptide, Q11 peptide and M2e peptide, respectively. Prior to immunization, M2e-Q11and Q11 peptides were diluted into sterile PBS solution at the concentration of 2 mM and incubated at room temperature for fibrilization. M2e peptide was diluted into 200 μM and 1:1 mixed with aluminum adjuvant (InvivoGen 5200). Mice were intraperitoneally immunized for 10 nM nanoparticle or peptide each. Boosting immunization was given with the same vaccine formula 2 weeks post the first immunization. Sera were collected 14 days after the booster. Sera from mice immunized with PBS were collected as negative controls.

## Antibody Detection

M2e and Q11 specific antibodies were measured by Enzyme-linked Immunosorbent Assay (ELISA). Briefly, Nunc-immuno plates (Nunc 442404) were coated with 50 μL PBS-diluted human M2e peptide, avian M2e peptide, or swine M2e peptide, 5 μg/mL, at 4°C for overnight. Unspecific binding was blocked with 200 μL of 0.25% gelatin in PBST solution (0.5% Tween-20 in PBS). 50 μL of the serially diluted sera was added to each well and incubated at 37°C for one and half hours. After extensive washing with PBST solution, binding antibodies were detected by HRP labeled goat anti-mouse IgG antibody (BioLegend B243363) and TMB substrate (Biosharp 0759), accordingly to manufacturer's instructions.

The isotypes of M2e-specific antibodies were determined by ELISA with Mouse Monoclonal Antibody Isotyping Reagents (Sigma, ISO-2) following the manufacturer's instructions.

## Influenza Virus Challenge

Mice were anesthetized by isoflurane (Baxter CN2L9100) and intranasally challenged with 5 LD50 of mouse-adapted PR8 ($5 \times 10^3$ $TCID_{50}$) and avian H7N9 ($1.75 \times 10^4$ $TCID_{50}$) influenza viruses, 3 weeks post the final immunization. Mouse body weight and survival rates were monitored daily for 2 weeks post infection.

## Detection of Pulmonary Virus Titers by RT-qPCR

At the 14th day of challenge, the surviving mice were deeply anesthetized and decapitated, and their lung tissues were taken for RNA extraction (Tiangen DP431). Primers and probe targeting the M gene of influenza and the β-actin of mouse were used for RT-qPCR with the following sequences: 1012FluA-Fv1 GGARTGGMTAAAGACAAGAC CAATC; 1012FluA-Rv1 GGCRTTYTGGACAAASCGTCTAC; 1012FluA-Pv1 5′ ROX-AGTCCTCGCTCACTGGGCACGGT-3′ BHQ2; b-actin Forward GAGATTACTGCTCTGGCTCCTA; b-actin Reverse GGACTCATCGTACTCCTGCTTG; b-actin P 5′VIC- CCTGAGCGCAAGTACTCTGTGTGGATC-3′ BHQ. RT-qPCR was performed using the ABI 7500 detection system in One Step PrimeScript™ RT-PCR Kit (Perfect Real Time) (Takara RR064A) with the following conditions: 42°C for 10 min, 95°C for 2 min, and 40 cycles of 95°C for 10 s and 60°C for 1 min. Threshold cycle (CT) values representing viral genomes were analyzed with CFX Manager software, and the data were shown as genome equivalents (GEq) per microliter.

## Statistical Analysis

Antibody titers, viral titers, and body weights between groups were compared by 1- or 2-way ANOVA. The survival rate was compared by Log-rank test. *P*-value of less than 0.05 was considered as significant. All the statistical analysis was performed by GraphPad Prism version 7.00 (GraphPad Software, San Diego, CA, United States).

# RESULTS

## M2e-Q11 Peptide Assembled Into Nanostructure in PBS Solution

Influenza M2e epitope consists of only 23 amino acids and is poorly immunogenic when administered alone. We previously reported that a 23-mer M2e peptide could partially self-assemble into polymer through intra-peptide disulfide bonds and induce M2e-specific immune response with adjuvants in experimental mice (Wu et al., 2007; Zou et al., 2017). In this study, we synthesized a 38-mer M2e-Q11 peptide, SLLT EVETPIRNEWGCRCNDSSDSGSGQQKFQFQFEQQ, consists of human influenza M2e epitope linked to a fibrillizing peptide Q11 domain (QQKFQFQFEQQ) with four amino acid Ser-Gly-Ser-Gly as spacer. The Q11 peptide was used to promote the peptide assembly into nanoparticle since it has been successfully used as immune adjuvant to enhance immunogenicity of ovalbumin and malaria epitopes. The M2e and Q11 peptides were also synthesized as controls. All the peptides dissolved in water at 10 mg/ml without precipitation. When diluted into PBS solution, M2e-Q11 and Q11 peptides assembled into different nanostructure, which were observed under TEM and shown in **Figure 1**. Q11 peptide self-assembled into fibrous structure as previously described (Rudra et al., 2010). However, M2e-Q11 peptide did not form long nanofibers as the Q11 peptide did, but assembled into branched nano sticks instead. The branched nano sticks were about 100 nm in length and 15 nm in width. Despite that the M2e peptide could form peptide polymer by intra-peptide disulfide interaction, it did not form detectable nanostructure under TEM. The size distributions of the nanoparticles were analyzed by dynamic light scattering analysis and shown in **Figure 2A**. The average hydrodynamic diameter was 776 ± 147 nm for Q11 peptide nanoparticles and 238 ± 25 nm for M2e-Q11 peptide nanoparticles.

Next, we used an M2e-specific monoclonal antibody 8C6 to evaluate whether M2e epitope was correctly presented on the M2e-Q11 nanoparticles. 8C6 was isolated from M2e-immunized mouse and could protect against lethal dose of influenza challenge when passively administered into mice (Liu et al., 2004). The interaction of mAb 8C6 with M2e-Q11, Q11 nanoparticles and M2e peptides were evaluated by ELISA. As shown in **Figure 2**, 8C6 efficiently recognized M2e-Q11 nanoparticles and M2e peptide, but was not able to bind the

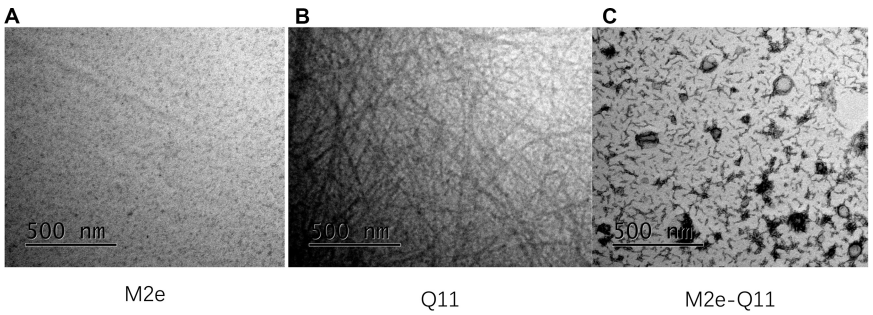


**FIGURE 1 |** Nanostructure of self-assembly peptides by Transmission electron microscope (TEM). Peptides were diluted into PBS solution and incubated overnight to assemble into nanostructure. Peptide solutions were adsorbed onto carbon-coated copper grids and negatively stained with uranyl acetate and imaged with a FEI Tecnai G2 Spirit TEM. **(A)** M2e peptide; **(B)** Q11 peptide; **(C)** M2e-Q11 peptide.

Q11 nanofibers. These results suggested that the protective M2e epitope was correctly presented on M2e-Q11 nanoparticles and accessible to protective antibodies.

## M2e-Q11 Nanoparticles Induced Antibodies Recognizing M2e Epitopes of Human, Swine, and Avian Influenza Viruses

We evaluated whether M2e-Q11 nanoparticles were able to induce M2e-specific immune response. Balb/c mice were intraperitoneally immunized with M2e-Q11 nanoparticles or Q11 nanofiber without adjuvants. Mice were also intraperitoneally immunized of M2e peptide with aluminum adjuvant as positive control. Mouse sera were collected 14 days after the boosting immunization. M2e-specific and Q11-specific antibodies were evaluated by ELISA. As shown in **Figure 3A**, M2e-specific antibodies were induced in mice immunized with M2e-Q11 nanoparticles. The titers of M2e-specific antibody in mice immunized with M2e-Q11 nanoparticles were about 1:1600, which were lower than those in mice immunized with aluminum-adjuvant-M2e peptide. As expected, M2e-specific antibodies were not detected in mice immunized with Q11 nanofiber or PBS solution. Consistent with previous reports, neither M2e-Q11 nanoparticles nor Q11 nanofiber was able to induce Q11-specific antibodies (**Figure 3B**). Comparing to aluminum-adjuvant-M2e peptide which induced multiple isotype of M2e-specific antibodies (**Figure 3C**), M2e-Q11 nanoparticles mainly induced IgG1 and IgM isotypes of M2e-specific antibodies (**Figure 3D**).

We further evaluated whether antibodies induced by M2e-Q11 nanoparticles could cross-react with M2e proteins of other influenza subtypes. We synthesized M2e peptides according to M2e sequences from swine H1N1 and avian H7N9 influenza viruses and tested the cross-reactivity of antisera to these peptides by ELISA. There are six amino acid substitutions among human M2e, swine H1N1 and avian H7N9 M2e sequences (**Figure 4A**). As shown in **Figures 4B–D**, sera from M2e-Q11 vaccinated mice efficiently bind to M2e peptides from avian H7N9 and swine H1N1 influenza virus despite that there were six amino acid substitutions in human M2e versus swine and avian M2e sequences. The titers of antibodies from M2e-Q11 immunized mice were about 1024 against avian and swine M2e, which were similar to the titers against human influenza M2e. We observed that aluminum-adjuvant-M2e peptide vaccine also induced antibodies against avian and swine M2e peptide but antibody titers against swine and avian influenza M2e peptides were about fourfold lower than that against human M2e peptide.

## Vaccinated With M2e-Q11 Nanoparticle Protected Mice Against H1N1 and Avian H7N9 Influenza Challenge

We evaluated the protective efficacy of vaccination with M2e-Q11 nanoparticles against homologous influenza virus in mice. Mice were challenged with lethal dose of mouse-adapted influenza PR8 H1N1 virus after the prime-boost immunization. All the mice showed signs of influenza disease such as huddling, ruffled fur from 3-day post-infection. As shown in **Figure 5A**, seven of eight mice in Q11-immunized group died after influenza virus infection. The median survival time in this group is 8 days. In contrast, five of eight M2e-Q11 vaccinated mice survived from influenza PR8 challenge. The survival rate is significantly higher than mice immunized with Q11 nanofiber ($P = 0.0222$, Log-rank test). M2e-Q11 immunized mice also exhibited less body weight loss than mice immunized with Q11 nanofiber (**Figure 5B**, $P = 0.0249$, two-way ANOVA). As a positive control, six of eight mice immunized with aluminum-adjuvant M2e peptide survived from influenza challenge. However, neither survival rates or body weight change differ significantly between the mice immunized with aluminum-adjuvant M2e peptide and M2e-Q11 nanoparticles. The pulmonary viral titers in survivors of M2e-Q11 immunized group were lower than those of aluminum-adjuvant M2e peptide but the difference was not significant (**Figure 5C**, $p = 0.4875$, $t$-test).

We next evaluated whether the M2e-Q11 nanoparticle could provide cross-protection against heterologous influenza viruses. Mice were challenged with highly pathogenic avian H7N9 influenza virus after the prime-boost immunization. As shown in **Figure 5D**, five of eight mice in Q11 immunized group died from avian H7N9 influenza infection. The median survival time in this group was 12 days. However, all the mice immunized with

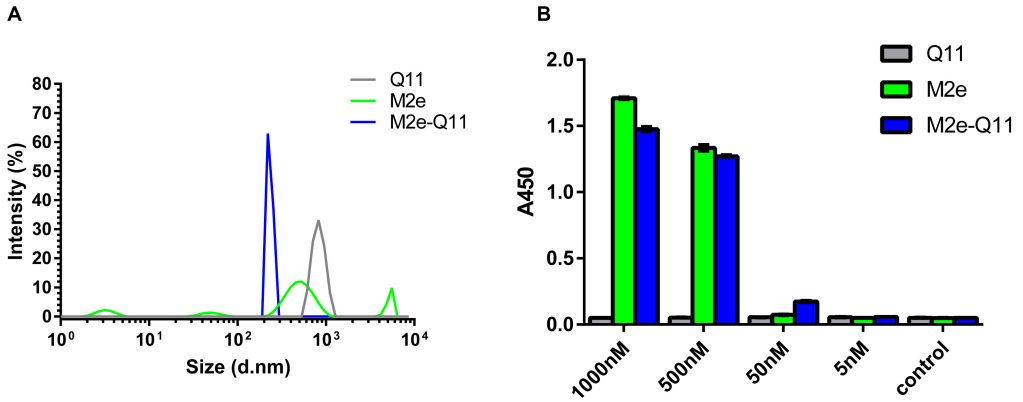


**FIGURE 2 |** Characterization of M2e-Q11 nanoparticles. **(A)** Size distribution of Q11, M2e-Q11 peptide nanoparticles and M2e peptide. **(B)** Reactivity of protective anti-M2e mAb 8C6 to self-assembly nanoparticles. Plates were coated with peptide or peptide-formed nanoparticles at different concentrations. Binding of 8C6 to peptide or nanoparticles were measured by ELISA. Each sample was tested in triplicate and mean values of absorbance at 450 nm (A450) are shown.

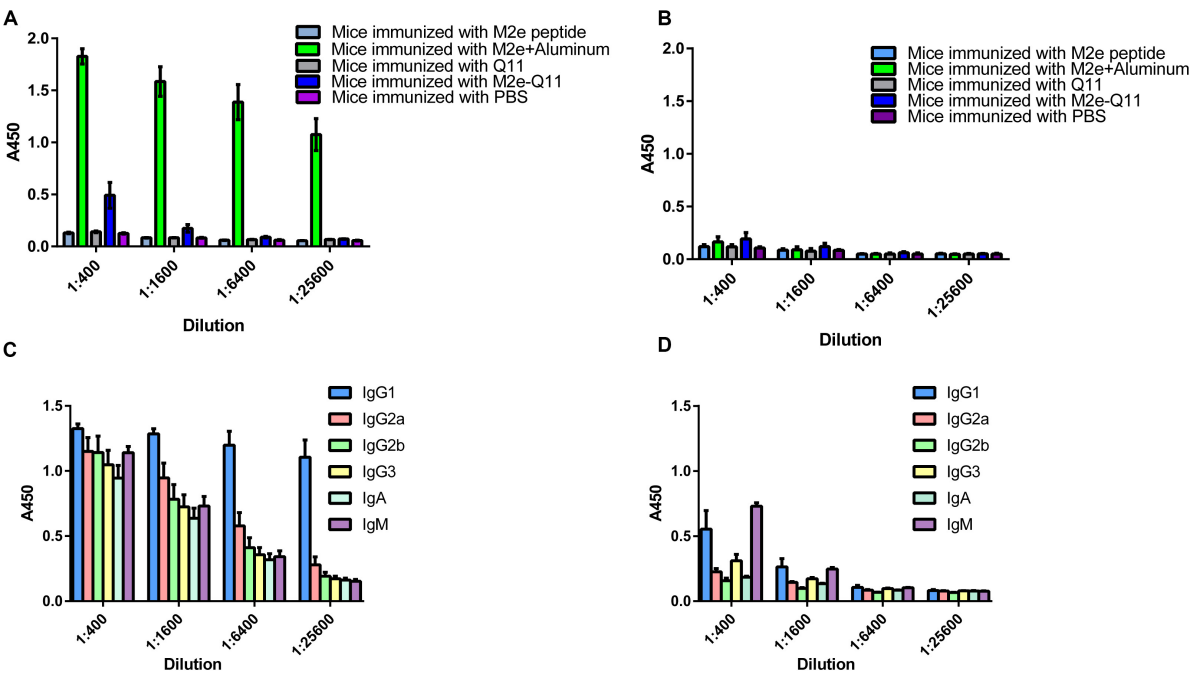


**FIGURE 3 |** M2e-specific and Q11-secific antibodies were determined by ELISA. Mice were immunized with M2e-Q11 nanoparticle, aluminum-adjuvant M2e peptide, Q11 nanofiber, M2e peptide or PBS alone. Sera were collected 14 days after twice immunization. Antibodies specific for human influenza M2e peptide **(A)** or Q11 peptide **(B)** were tested by ELISA. Average values of absorbance at 450 nm (A450) of eight mice in each group are shown. The isotypes of M2e-specific antibodies in mice immunized with aluminum-adjuvant M2e peptide **(C)** and M2e-Q11 peptide nanoparticles **(D)** are shown.

M2e-Q11 or aluminum-adjuvant M2e peptide survived from avian H7N9 influenza infection. The survival rates in these two groups were significantly higher than Q11-immunized group ($P$ = 0.0004, Log-rank test). The mice immunized with M2e-Q11 nanoparticles and aluminum-adjuvant M2e peptide also showed loss of body weight, but significantly less than mice immunized with Q11 nanofiber (**Figure 5E**, $P < 0.0001$, two-way ANOVA). However, no significant difference was observed in the pulmonary viral titers among the survivors of the three groups (**Figure 5F**, $P$ = 0.6505, one-way ANOVA).

## DISCUSSION

The application of nanotechnology is a promising strategy for development of effective vaccines against infectious viruses (Chen et al., 2013). Multiple nanotechnology platforms including polymeric nanoparticles, self-assembly proteins and peptides, inorganic gold nanoparticles have been investigated for the development of influenza vaccines (Al-Halifa et al., 2019). Here, we used the fibrillizing peptide Q11 to form an influenza M2e-based nanoparticle vaccine. The M2e-Q11 peptide

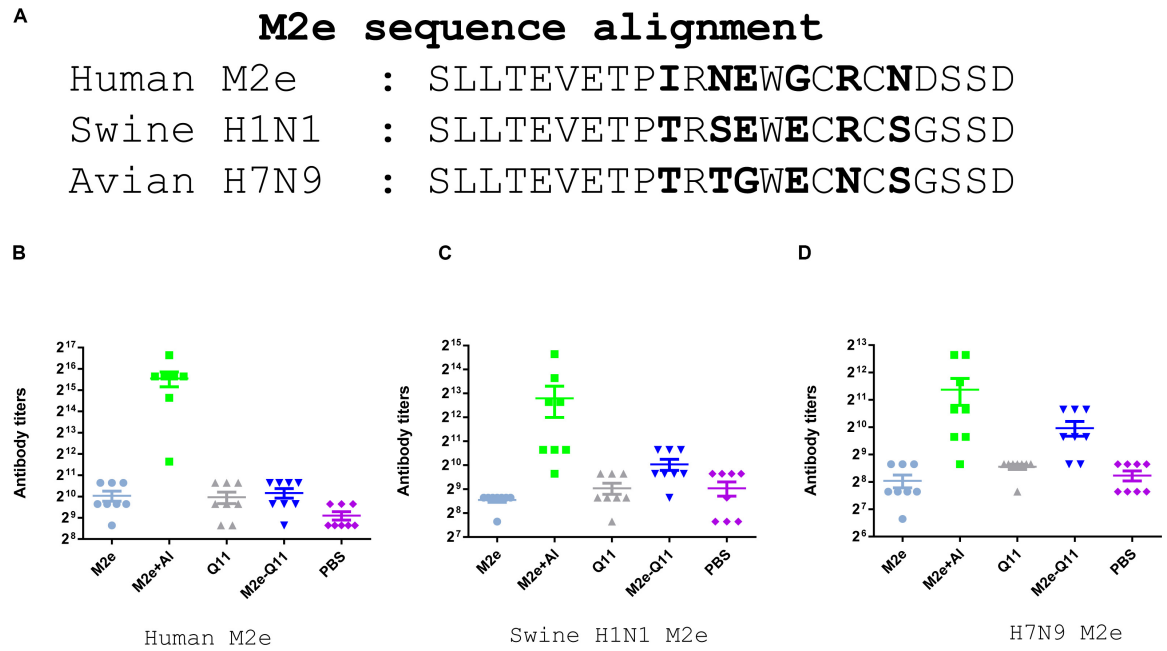


**FIGURE 4 |** Evaluation of antibodies cross-reactive with swine H1N1 and Avian H7N9 M2e peptide. **(A)** Sequence alignment of human influenza, swine H1N1 and avian H7N9 M2e sequences. The amino acid substitutions were highlighted in bold. Antibodies titers specific for human M2e **(B)**, swine H1N1 influenza M2e **(C)** and avian H7N9 M2e **(D)** are shown.

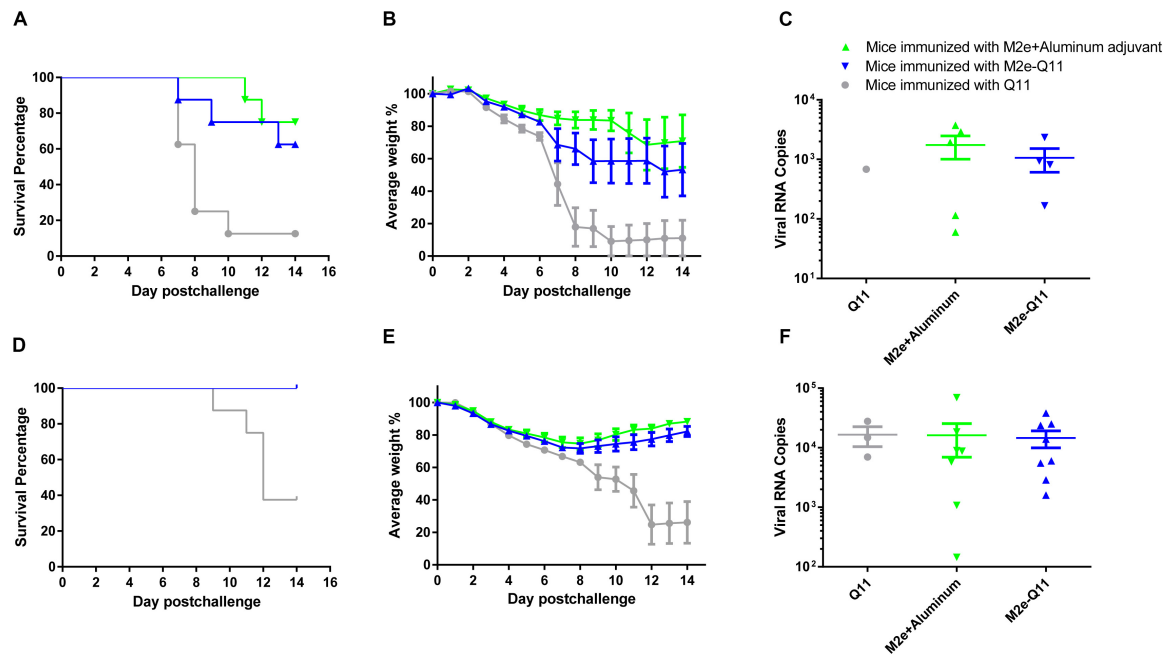


**FIGURE 5 |** Vaccination with M2e-Q11 nanoparticle conferred protection against PR8 and avian H7N9 influenza challenge. **(A)** Mice were immunized with M2e-Q11 nanoparticle, aluminum-adjuvant M2e peptide or Q11 nanofiber and challenged with 5 $LD_{50}$ ($5 \times 10^3$ TCID50) of mouse-adapted influenza PR8 virus (A/Purto Rico/8/34, H1N1). The survival curves were analyzed by Kaplan–Meier methods ($N = 8$ in each group). **(B)** Average weight of eight mice challenged with influenza PR8 virus in each group are shown. **(C)** Viral RNA copies in the lung tissues of survivors in each group challenged with influenza PR8 virus are shown. **(D)** Mice were immunized with M2e-Q11 nanoparticle, aluminum-adjuvant M2e peptide or Q11 nanofiber and challenged with 5$LD_{50}$ (1.75 × 10^4TCID50) of avian influenza H7N9 virus (A/Shanghai/4664T/2013). The survival curves were analyzed by Kaplan–Meier methods ($N = 8$ in each group). **(E)** Average weight of eight mice challenged with avian influenza H7N9 virus in each group are shown. **(F)** Viral RNA copies in the lung tissues of survivors in each group challenged with influenza H7N9 virus are shown.

successfully self-assemble into nanoparticles in physiological salt solution and induced antibody responses against different subtypes of influenza M2e peptides in experimental mice. This self-assembling M2e nanovaccine also protected mice against multiple subtypes of influenza viruses, include both group 1 (mouse-adapted H1N1 PR8) and group 2 (avian influenza H7N9) influenza viruses.

One advantage of using self-assembling peptide vaccine over protein-based peptide vaccines is the low immunogenicity of the carriers. Self-assembling peptides usually do not induce immune responses (Chen et al., 2013). In our study, neither M2e-Q11 nor Q11 nanoparticle induced detectable Q11-specific antibodies in mice after a prime-boost immunization. The low immunogenicity of carriers may avoid potential side effects or carrier-induced epitopic suppression in clinical use. Another advantage of peptide-based nanovaccines is that peptides can be synthesized in high purity by current solid-phase peptide synthesis method without downstream purification (Rudra et al., 2010). It does not only reduce the production cost, but also lower the risk of potential side effects caused by the contamination of bacterial endotoxin or mammalian cell components during protein expression.

In research reported in this paper, we used the self-assembling Q11 domain to promote the formation of nanoparticles because it has been successfully used to enhance the immunogenicity of several antigenic epitopes (Rudra et al., 2010, 2012a,b). Other self-assembling peptides may also have similar adjuvant activities. However, the ability of forming nanoparticles of self-assembling peptides needs to be evaluated when linked to antigenic epitopes. Q11 conjugates successfully self-assembled into nanofiber and induced strong humoral and T cell immune responses when incorporated with short antigenic epitopes such as ova, malaria and influenza T cell epitopes (Rudra et al., 2010, 2012a,b; Si et al., 2018). While M2e-Q11 conjugate in this study failed to form nanofibers, it assembled into short nanosticks instead. The M2e epitope consists of 23 amino acids, which is longer than ova, malaria, and influenza T cell epitopes (Mezhenskaya et al., 2019). The structure of M2e peptide may prevent Q11 from forming long nanofibers. In a previous report, a conjugate of Q11 peptide linked with a 29-mer B cell epitope J14 from streptococcus, failed to form nanostructure and did not induce specific immune responses (Azmi et al., 2014). These results indicated that the adjuvant activity of fibrilized peptide is dependent on its ability of forming nanoparticles. How the differences of nanoparticle size and structure influence the antigen presentation and immune responses is still under investigation.

Comparing with traditional inactivated or live-attenuated influenza vaccines, immune response induced by M2e-based vaccines were not able to prevent influenza infection (Heinen et al., 2002). Mice immunized with M2e-Q11 nanoparticles or aluminum-adjuvant M2e peptide still got infected and showed signs of disease such as huddling, ruffled fur and weight loss after challenge with influenza viruses. However, M2e-Q11 nanoparticle could provide cross-protection and significantly reduced the mortality of mice after infection with either group 1 or group 2 influenza subtypes. The protective mechanism(s) mediated by M2e-Q11 nanoparticles is still under investigation. Previous studies showed that M2e-sepcific antibodies contributed to protection induced by M2e-based vaccines (Deng et al., 2015; Rappazzo et al., 2016). However, M2e-Q11 nanoparticles induced comparable protection against PR8 virus as aluminum-adjuvant M2e peptide despite that it induced lower titers of anti-M2e antibodies than aluminum-adjuvant M2e peptide. Furthermore, although there were more than 25% (6/23) amino acid substitutions between the M2e antigen and influenza H7N9 M2e sequences, M2e-Q11 nanoparticle still provided complete protection against avian influenza H7N9 virus. These results indicated that M2e-Q11 nanoparticles induced immune responses against the conserved regions of M2e domain and so could be a promising candidate for universal influenza vaccine.

## DATA AVAILABILITY STATEMENT

All datasets generated for this study are included in the article/supplementary material.

## ETHICS STATEMENT

The animal study was reviewed and approved by Institutional Animal Care and Use Committee of Shanghai Public Health Clinical Center.

## AUTHOR CONTRIBUTIONS

FW, JH, QW, and YZ conceived and designed the experiments. QW, YZ, PZ, MW, WF, JS, and ZS performed the experiments. FW, JH, QW, YZ, and JX analyzed the data. FW, JH, QW, and YZ wrote the manuscript. All authors contributed to the article and approved the submitted version.

## FUNDING

This work was supported by the National Megaprojects of China for Major Infectious Diseases (2018ZX10301403 to FW and 2017ZX10202102 to JH), National Natural Science Foundation of China (31771008 to JH), Hundred Talent Program of Shanghai Municipal Health Commission (2018BR08 to JH), Chinese Academy of Medical Sciences (2019PT350002 to JH), and grants from the Shanghai Public Health Clinical Center (KY-GW-2018-07 to QW and KY-GW-2018-15 to YZ).

## ACKNOWLEDGMENTS

We thank Dr. Weishan Huang in Department of Pathobiological Sciences, School of Veterinary Medicine, Louisiana State University for reviewing the manuscript and Dr. Min Luo and Kaiyue Wu in Fudan University for the analysis of size distributions of nanoparticles.

## REFERENCES


Al-Halifa, S., Gauthier, L., Arpin, D., Bourgault, S., and Archambault, D. (2019). Nanoparticle-based vaccines against respiratory viruses. *Front. Immunol.* 10:22. doi: 10.3389/fimmu.2019.00022

Auladell, M., Jia, X., Hensen, L., Chua, B., Fox, A., Nguyen, T. H. O., et al. (2019). Recalling the future: immunological memory toward unpredictable influenza viruses. *Front. Immunol.* 10:1400. doi: 10.3389/fimmu.2019.01400

Azmi, F., Ahmad Fuaad, A. A., Giddam, A. K., Batzloff, M. R., Good, M. F., Skwarczynski, M., et al. (2014). Self-adjuvanting vaccine against group A streptococcus: application of fibrillized peptide and immunostimulatory lipid as adjuvant. *Bioorg. Med. Chem.* 22, 6401–6408. doi: 10.1016/j.bmc.2014.09.042

Barr, I. G., Donis, R. O., Katz, J. M., Mccauley, J. W., Odagiri, T., Trusheim, H., et al. (2018). Cell culture-derived influenza vaccines in the severe 2017-2018 epidemic season: a step towards improved influenza vaccine effectiveness. *NPJ Vaccines* 3:44.

Belongia, E. A., Simpson, M. D., King, J. P., Sundaram, M. E., Kelley, N. S., Osterholm, M. T., et al. (2016). Variable influenza vaccine effectiveness by subtype: a systematic review and meta-analysis of test-negative design studies. *Lancet Infect. Dis.* 16, 942–951. doi: 10.1016/s1473-3099(16)00129-8

Caton, A. J., Brownlee, G. G., Yewdell, J. W., and Gerhard, W. (1982). The antigenic structure of the influenza virus A/PR/8/34 hemagglutinin (H1 subtype). *Cell* 31, 417–427. doi: 10.1016/0092-8674(82)90135-0

Chen, J., Pompano, R. R., Santiago, F. W., Maillat, L., Sciammas, R., Sun, T., et al. (2013). The use of self-adjuvanting nanofiber vaccines to elicit high-affinity B cell responses to peptide antigens without inflammation. *Biomaterials* 34, 8776–8785. doi: 10.1016/j.biomaterials.2013.07.063

Deng, L., Cho, K. J., Fiers, W., and Saelens, X. (2015). M2e-based universal influenza A vaccines. *Vaccines* 3, 105–136. doi: 10.3390/vaccines3010105

Estrada, L. D., and Schultz-Cherry, S. (2019). Development of a universal influenza vaccine. *J. Immunol.* 202, 392–398.

Heinen, P. P., Rijsewijk, F. A., De Boer-Luijtze, E. A., and Bianchi, A. T. J. (2002). Vaccination of pigs with a DNA construct expressing an influenza virus M2-nucleoprotein fusion protein exacerbates disease after challenge with influenza A virus. *J. Gen. Virol.* 83, 1851–1859. doi: 10.1099/0022-1317-83-8-1851

Ilyushina, N. A., Komatsu, T. E., Ince, W. L., Donaldson, E. F., Lee, N., O'rear, J. J., et al. (2019). Influenza A virus hemagglutinin mutations associated with use of neuraminidase inhibitors correlate with decreased inhibition by anti-influenza antibodies. *Virol. J.* 16:149.

Jegerlehner, A., Wiesel, M., Dietmeier, K., Zabel, F., Gatto, D., Saudan, P., et al. (2010). Carrier induced epitopic suppression of antibody responses induced by virus-like particles is a dynamic phenomenon caused by carrier-specific antibodies. *Vaccine* 28, 5503–5512. doi: 10.1016/j.vaccine.2010.02.103

Kolpe, A., Schepens, B., Fiers, W., and Saelens, X. (2017). M2-based influenza vaccines: recent advances and clinical potential. *Expert Rev. Vaccines* 16, 123–136. doi: 10.1080/14760584.2017.1240041

Krammer, F., and Palese, P. (2015). Advances in the development of influenza virus vaccines. *Nat. Rev. Drug Discov.* 14, 167–182.

Liu, W., Zou, P., and Chen, Y. H. (2004). Monoclonal antibodies recognizing EVETPIRN epitope of influenza A virus M2 protein could protect mice from lethal influenza A virus challenge. *Immunol. Lett.* 93, 131–136. doi: 10.1016/j.imlet.2004.03.003

Mezhenskaya, D., Isakova-Sivak, I., and Rudenko, L. (2019). M2e-based universal influenza vaccines: a historical overview and new approaches to development. *J. Biomed. Sci.* 26:76.

Ramos, E. L., Mitcham, J. L., Koller, T. D., Bonavia, A., Usner, D. W., Balaratnam, G., et al. (2015). Efficacy and safety of treatment with an anti-m2e monoclonal antibody in experimental human influenza. *J. Infect. Dis.* 211, 1038–1044. doi: 10.1093/infdis/jiu539

Rappazzo, C. G., Watkins, H. C., Guarino, C. M., Chau, A., Lopez, J. L., Delisa, M. P., et al. (2016). Recombinant M2e outer membrane vesicle vaccines protect against lethal influenza A challenge in BALB/c mice. *Vaccine* 34, 1252–1258. doi: 10.1016/j.vaccine.2016.01.028

Rudra, J. S., Mishra, S., Chong, A. S., Mitchell, R. A., Nardin, E. H., Nussenzweig, V., et al. (2012a). Self-assembled peptide nanofibers raising durable antibody responses against a malaria epitope. *Biomaterials* 33, 6476–6484. doi: 10.1016/j.biomaterials.2012.05.041

Rudra, J. S., Sun, T., Bird, K. C., Daniels, M. D., Gasiorowski, J. Z., Chong, A. S., et al. (2012b). Modulating adaptive immune responses to peptide self-assemblies. *ACS Nano.* 6, 1557–1564. doi: 10.1021/nn204530r

Rudra, J. S., Tian, Y. F., Jung, J. P., and Collier, J. H. (2010). A self-assembling peptide acting as an immune adjuvant. *Proc. Natl. Acad. Sci. U.S.A.* 107, 622–627. doi: 10.1073/pnas.0912124107

Si, Y., Wen, Y., Kelly, S. H., Chong, A. S., and Collier, J. H. (2018). Intranasal delivery of adjuvant-free peptide nanofibers elicits resident CD8(+) T cell responses. *J. Control. Release* 282, 120–130. doi: 10.1016/j.jconrel.2018.04.031

Stephenson, I., Nicholson, K. G., Wood, J. M., Zambon, M. C., and Katz, J. M. (2004). Confronting the avian influenza threat: vaccine development for a potential pandemic. *Lancet Infect. Dis.* 4, 499–509. doi: 10.1016/s1473-3099(04)01105-3

Turley, C. B., Rupp, R. E., Johnson, C., Taylor, D. N., Wolfson, J., Tussey, L., et al. (2011). Safety and immunogenicity of a recombinant M2e-flagellin influenza vaccine (STF2.4xM2e) in healthy adults. *Vaccine* 29, 5145–5152. doi: 10.1016/j.vaccine.2011.05.041

World Health Organization [WHO] (2018). *Fact Sheets Influenza (Seasonal)*. Available online at: https://www.who.int/news-room/fact-sheets/detail/influenza-(seasonal) (accessed May 22, 2020).

Wu, F., Huang, J. H., Yuan, X. Y., Huang, W. S., and Chen, Y. H. (2007). Characterization of immunity induced by M2e of influenza virus. *Vaccine* 25, 8868–8873. doi: 10.1016/j.vaccine.2007.09.056

Zebedee, S. L., and Lamb, R. A. (1988). Influenza A virus M2 protein: monoclonal antibody restriction of virus growth and detection of M2 in virions. *J. Virol.* 62, 2762–2772. doi: 10.1128/jvi.62.8.2762-2772.1988

Zhou, J., Wang, D., Gao, R., Zhao, B., Song, J., Qi, X., et al. (2013). Biological features of novel avian influenza A (H7N9) virus. *Nature* 499, 500–503.

Zou, P., Li, Y., Huang, J., and Wu, F. (2017). Self-assembly polymerization enhances the immunogenicity of influenza M2e peptide. *Microbes Infect.* 19, 648–654. doi: 10.1016/j.micinf.2017.09.004


**Conflict of Interest:** The authors declare that the research was conducted in the absence of any commercial or financial relationships that could be construed as a potential conflict of interest.

*Copyright © 2020 Wang, Zhang, Zou, Wang, Fu, She, Song, Xu, Huang and Wu. This is an open-access article distributed under the terms of the Creative Commons Attribution License (CC BY). The use, distribution or reproduction in other forums is permitted, provided the original author(s) and the copyright owner(s) are credited and that the original publication in this journal is cited, in accordance with accepted academic practice. No use, distribution or reproduction is permitted which does not comply with these terms.*

# Advantages of publishing in Frontiers

**OPEN ACCESS**
Articles are free to read for greatest visibility and readership

**FAST PUBLICATION**
Around 90 days from submission to decision

**HIGH QUALITY PEER-REVIEW**
Rigorous, collaborative, and constructive peer-review

**TRANSPARENT PEER-REVIEW**
Editors and reviewers acknowledged by name on published articles

**Frontiers**
Avenue du Tribunal-Fédéral 34
1005 Lausanne | Switzerland

**Visit us:** www.frontiersin.org
**Contact us:** info@frontiersin.org | +41 21 510 17 00

**REPRODUCIBILITY OF RESEARCH**
Support open data and methods to enhance research reproducibility

**DIGITAL PUBLISHING**
Articles designed for optimal readership across devices

**FOLLOW US**
@frontiersin

**IMPACT METRICS**
Advanced article metrics track visibility across digital media

**EXTENSIVE PROMOTION**
Marketing and promotion of impactful research

**LOOP RESEARCH NETWORK**
Our network increases your article's readership